VOLUME 29 / NUMBER 15
AUGUST 8, 1991
ACC. NOS. N91-23073 TO N91-24086

STAR

AN ABSTRACT JOURNAL

Scientific and Technical Aerospace Reports

PRODUCED BY THE
SCIENTIFIC AND TECHNICAL
INFORMATION
DIVISION

NASA

NATIONAL AERONAUTICS AND SPACE ADMINISTRATION

***Scientific and Technical Aerospace Reports* (*STAR*)** is an abstract journal that provides comprehensive coverage of worldwide aerospace-related reports. It is a major product of the International Aerospace Database managed by the NASA Scientific and Technical Information (STI) Program. The coverage includes reports on aeronautics, space, and supporting disciplines. *STAR* lists current, publicly available reports entered into the NASA STI Database during the 2-week period preceding publication. An explanation of items that appear in each citation is given on the last page of each volume.

NASA sponsors a companion journal, *International Aerospace Abstracts* (*IAA*), that lists abstracts of the open literature on aerospace subjects available worldwide. *IAA* is available through the American Institute of Aeronautics and Astronautics.

Entries found in *STAR* and *IAA* are available through NASA's online service, RECON, as the International Aerospace Database and through DIALOG as the Aerospace Database.

Information on aerospace and related subjects is gathered by the NASA STI Program through national and international agreements and exchanges and is made available to the NASA community as well as to the public in many forms through various outlets. The section on NASA STI Program Products and Services contains additional information.

US ISSN 0036-8741

Volume 29 Number 15 / August 8, 1991

TABLE OF CONTENTS

AERONAUTICS For related information see also *Astronautics.*

01 AERONAUTICS (GENERAL) **2363**

02 AERODYNAMICS **2363**
Includes aerodynamics of bodies, combinations, wings, rotors, and control surfaces; and internal flow in ducts and turbomachinery. For related information see also *34 Fluid Mechanics and Heat Transfer.*

03 AIR TRANSPORTATION AND SAFETY **2367**
Includes passenger and cargo air transport operations; and aircraft accidents. For related information see also *16 Space Transportation* and *85 Urban Technology and Transportation.*

04 AIRCRAFT COMMUNICATIONS AND NAVIGATION **2368**
Includes digital and voice communication with aircraft; air navigation systems (satellite and ground based); and air traffic control. For related information see also *17 Space Communications, Spacecraft Communications, Command and Tracking* and *32 Communications and Radar.*

05 AIRCRAFT DESIGN, TESTING AND PERFORMANCE **2369**
Includes aircraft simulation technology. For related information see also *18 Spacecraft Design, Testing and Performance* and *39 Structural Mechanics.* For land transportation vehicles see *85 Urban Technology and Transportation.*

06 AIRCRAFT INSTRUMENTATION **2375**
Includes cockpit and cabin display devices; and flight instruments. For related information see also *19 Space craft Instrumentation* and *35 Instrumentation and Photography.*

07 AIRCRAFT PROPULSION AND POWER **2375**
Includes prime propulsion systems and systems components, e.g., gas turbine engines and compressors; and onboard auxiliary power plants for aircraft. For related information see also *20 Spacecraft Propulsion and Power, 28 Propellants and Fuels,* and *44 Energy Production and Conversion.*

08 AIRCRAFT STABILITY AND CONTROL **2383**
Includes aircraft handling qualities; piloting; flight controls; and autopilots. For related information see also *05 Aircraft Design, Testing and Performance.*

09 RESEARCH AND SUPPORT FACILITIES (AIR) **2384**
Includes airports, hangars and runways; aircraft repair and overhaul facilities; wind tunnels; shock tubes; and aircraft engine test stands. For related information see also *14 Ground Support Systems and Facilities (Space).*

ASTRONAUTICS For related information see also *Aeronautics.*

12 ASTRONAUTICS (GENERAL) **2385**
For extraterrestrial exploration see *91 Lunar and Planetary Exploration.*

13 ASTRODYNAMICS **2386**
Includes powered and free-flight trajectories; and orbital and launching dynamics.

14 GROUND SUPPORT SYSTEMS AND FACILITIES (SPACE) **2386**
Includes launch complexes, research and production facilities; ground support equipment, e.g., mobile transporters; and simulators. For related information see also *09 Research and Support Facilities (Air).*

15 LAUNCH VEHICLES AND SPACE VEHICLES **2386**
Includes boosters; operating problems of launch/space vehicle systems; and reusable vehicles. For related information see also *20 Spacecraft Propulsion and Power.*

16 SPACE TRANSPORTATION **2386**
Includes passenger and cargo space transportation, e.g., shuttle operations; and space rescue techniques. For related information see also *03 Air Transportation and Safety* and *18 Spacecraft Design, Testing and Performance.* For space suits see *54 Man/System Technology and Life Support.*

17 SPACE COMMUNICATIONS, SPACECRAFT COMMUNICATIONS, COMMAND AND TRACKING . **2387**
Includes telemetry; space communications networks; astronavigation and guidance; and radio blackout. For related information see also *04 Aircraft Communications and Navigation* and *32 Communications and Radar.*

N.A.—no abstracts were assigned to this category for this issue.

18 SPACECRAFT DESIGN, TESTING AND PERFORMANCE **2387**
Includes satellites; space platforms; space stations; spacecraft systems and components such as thermal and environmental controls; and attitude controls. For life support systems see *54 Man/System Technology and Life Support.* For related information see also *05 Aircraft Design, Testing and Performance, 39 Structural Mechanics,* and *16 Space Transportation.*

19 SPACECRAFT INSTRUMENTATION **2390**
For related information see also *06 Aircraft Instrumentation* and *35 Instrumentation and Photography.*

20 SPACECRAFT PROPULSION AND POWER **2390**
Includes main propulsion systems and components, e.g., rocket engines; and spacecraft auxiliary power sources. For related information see also *07 Aircraft Propulsion and Power, 28 Propellants and Fuels, 44 Energy Production and Conversion,* and *15 Launch Vehicles and Space Vehicles.*

CHEMISTRY AND MATERIALS

23 CHEMISTRY AND MATERIALS (GENERAL) **2391**

24 COMPOSITE MATERIALS **2392**
Includes physical, chemical, and mechanical properties of laminates and other composite materials. For ceramic materials see *27 Nonmetallic Materials.*

25 INORGANIC AND PHYSICAL CHEMISTRY **2397**
Includes chemical analysis, e.g., chromatography; combustion theory; electrochemistry; and photochemistry. For related information see also *77 Thermodynamics and Statistical Physics.*

26 METALLIC MATERIALS **2400**
Includes physical, chemical, and mechanical properties of metals, e.g., corrosion; and metallurgy.

27 NONMETALLIC MATERIALS **2403**
Includes physical, chemical, and mechanical properties of plastics, elastomers, lubricants, polymers, textiles, adhesives, and ceramic materials. For composite materials see *24 Composite Materials.*

28 PROPELLANTS AND FUELS **2408**
Includes rocket propellants, igniters and oxidizers; their storage and handling procedures; and aircraft fuels. For related information see also *07 Aircraft Propulsion and Power, 20 Spacecraft Propulsion and Power,* and *44 Energy Production and Conversion.*

29 MATERIALS PROCESSING ..... **N.A.**
Includes space-based development of products and processes for commercial application. For biological materials see *55 Space Biology.*

ENGINEERING For related information see also *Physics.*

31 ENGINEERING (GENERAL) **2409**
Includes vacuum technology; control engineering; display engineering; cryogenics; and fire prevention.

32 COMMUNICATIONS AND RADAR **2410**
Includes radar; land and global communications; communications theory; and optical communications. For related information see also *04 Aircraft Communications and Navigation* and *17 Space Communications, Spacecraft Communications, Command and Tracking.* For search and rescue see *03 Air Transportation and Safety,* and *16 Space Transportation.*

33 ELECTRONICS AND ELECTRICAL ENGINEERING **2416**
Includes test equipment and maintainability; components, e.g., tunnel diodes and transistors; microminiaturization; and integrated circuitry. For related information see also *60 Computer Operations and Hardware* and *76 Solid-State Physics.*

34 FLUID MECHANICS AND HEAT TRANSFER **2420**
Includes boundary layers; hydrodynamics; fluidics; mass transfer and ablation cooling. For related information see also *02 Aerodynamics* and *77 Thermodynamics and Statistical Physics.*

35 INSTRUMENTATION AND PHOTOGRAPHY **2430**
Includes remote sensors; measuring instruments and gauges; detectors; cameras and photographic supplies; and holography. For aerial photography see *43 Earth Resources and Remote Sensing.* For related information see also *06 Aircraft Instrumentation* and *19 Spacecraft Instrumentation.*

36 LASERS AND MASERS **2432**
Includes parametric amplifiers. For related information see also *76 Solid-State Physics.*

37 MECHANICAL ENGINEERING **2434**
Includes auxiliary systems (nonpower); machine elements and processes; and mechanical equipment.

38 QUALITY ASSURANCE AND RELIABILITY **2441**
Includes product sampling procedures and techniques; and quality control.

39 STRUCTURAL MECHANICS **2441**
Includes structural element design and weight analysis; fatigue; and thermal stress. For applications see *05 Aircraft Design, Testing and Performance* and *18 Spacecraft Design, Testing and Performance.*

GEOSCIENCES For related information see also *Space Sciences.*

42 GEOSCIENCES (GENERAL) **2448**

43 EARTH RESOURCES AND REMOTE SENSING **2456**
Includes remote sensing of earth resources by aircraft and spacecraft; photogrammetry; and aerial photography. For instrumentation see *35 Instrumentation and Photography.*

44 ENERGY PRODUCTION AND CONVERSION **2457**
Includes specific energy conversion systems, e.g., fuel cells; global sources of energy; geophysical conversion; and windpower. For related information see also *07 Aircraft Propulsion and Power, 20 Spacecraft Propulsion and Power,* and *28 Propellants and Fuels.*

45 ENVIRONMENT POLLUTION **2458**
Includes atmospheric, noise, thermal, and water pollution.

46 GEOPHYSICS **2460**
Includes aeronomy; upper and lower atmosphere studies; ionospheric and magnetospheric physics; and geomagnetism. For space radiation see *93 Space Radiation.*

47 METEOROLOGY AND CLIMATOLOGY **2465**
Includes weather forecasting and modification.

48 OCEANOGRAPHY **2470**
Includes biological, dynamic, and physical oceanography; and marine resources. For related information see also *43 Earth Resources and Remote Sensing.*

LIFE SCIENCES

51 LIFE SCIENCES (GENERAL) **2472**

52 AEROSPACE MEDICINE **2473**
Includes physiological factors; biological effects of radiation; and effects of weightlessness on man and animals.

53 BEHAVIORAL SCIENCES **2476**
Includes psychological factors; individual and group behavior; crew training and evaluation; and psychiatric research.

54 MAN/SYSTEM TECHNOLOGY AND LIFE SUPPORT **2477**
Includes human engineering; biotechnology; and space suits and protective clothing. For related information see also *16 Space Transportation.*

55 SPACE BIOLOGY ..... **N.A.**
Includes exobiology; planetary biology; and extraterrestrial life.

MATHEMATICAL AND COMPUTER SCIENCES

59 MATHEMATICAL AND COMPUTER SCIENCES (GENERAL) ..... **N.A.**

60 COMPUTER OPERATIONS AND HARDWARE **2480**
Includes hardware for computer graphics, firmware, and data processing. For components see *33 Electronics and Electrical Engineering.*

61 COMPUTER PROGRAMMING AND SOFTWARE **2481**
Includes computer programs, routines, algorithms, and specific applications, e.g., CAD/CAM.

62 COMPUTER SYSTEMS **2488**
Includes computer networks and special application computer systems.

63 CYBERNETICS **2489**
Includes feedback and control theory, artificial intelligence, robotics and expert systems. For related information see also *54 Man/System Technology and Life Support.*

64 NUMERICAL ANALYSIS **2493**
Includes iteration, difference equations, and numerical approximation.

65 STATISTICS AND PROBABILITY **2495**
Includes data sampling and smoothing; Monte Carlo method; and stochastic processes.

66 SYSTEMS ANALYSIS **2496**
Includes mathematical modeling; network analysis; and operations research.

67 THEORETICAL MATHEMATICS ..... **N.A.**
Includes topology and number theory.

PHYSICS For related information see also *Engineering.*

70 PHYSICS (GENERAL) **2497**
For precision time and time interval (PTTI) see *35 Instrumentation and Photography;* for geophysics, astrophysics or solar physics see *46 Geophysics, 90 Astrophysics,* or *92 Solar Physics.*

71 ACOUSTICS **2500**
Includes sound generation, transmission, and attenuation. For noise pollution see *45 Environment Pollution.*

72 ATOMIC AND MOLECULAR PHYSICS **2502**
Includes atomic structure, electron properties, and molecular spectra.

73 NUCLEAR AND HIGH-ENERGY PHYSICS **2506**
Includes elementary and nuclear particles; and reactor theory. For space radiation see *93 Space Radiation.*

74 OPTICS **2507**
Includes light phenomena and optical devices. For lasers see *36 Lasers and Masers.*

75 PLASMA PHYSICS **2510**
Includes magnetohydrodynamics and plasma fusion. For ionospheric plasmas see *46 Geophysics.* For space plasmas see *90 Astrophysics.*

76 SOLID-STATE PHYSICS **2514**
Includes superconductivity. For related information see also *33 Electronics and Electrical Engineering* and *36 Lasers and Masers.*

77 THERMODYNAMICS AND STATISTICAL PHYSICS **2520**
Includes quantum mechanics; theoretical physics; and Bose and Fermi statistics. For related information see also *25 Inorganic and Physical Chemistry* and *34 Fluid Mechanics and Heat Transfer.*

SOCIAL SCIENCES

80 SOCIAL SCIENCES (GENERAL) ..... **N.A.**
Includes educational matters.

81 ADMINISTRATION AND MANAGEMENT **2520**
Includes management planning and research.

82 DOCUMENTATION AND INFORMATION SCIENCE **2521**
Includes information management; information storage and retrieval technology; technical writing; graphic arts; and micrography. For computer documentation see *61 Computer Programming and Software.*

83 ECONOMICS AND COST ANALYSIS ..... **N.A.**
Includes cost effectiveness studies.

84 LAW, POLITICAL SCIENCE AND SPACE POLICY **2526**
Includes NASA appropriation hearings; aviation law; space law and policy; international law; international cooperation; and patent policy.

85 URBAN TECHNOLOGY AND TRANSPORTATION **2526**
Includes applications of space technology to urban problems; technology transfer; technology assessment; and surface and mass transportation. For related information see *03 Air Transportation and Safety, 16 Space Transportation,* and *44 Energy Production and Conversion.*

SPACE SCIENCES For related information see also *Geosciences.*

88 SPACE SCIENCES (GENERAL) ..... **N.A.**

89 ASTRONOMY **2526**
Includes radio, gamma-ray, and infrared astronomy; and astrometry.

90 ASTROPHYSICS **2529**
Includes cosmology; celestial mechanics; space plasmas; and interstellar and interplanetary gases and dust. For related information see also *75 Plasma Physics.*

91 LUNAR AND PLANETARY EXPLORATION **2533**
Includes planetology; and manned and unmanned flights. For spacecraft design or space stations see *18 Spacecraft Design, Testing and Performance.*

92 SOLAR PHYSICS **2534**
Includes solar activity, solar flares, solar radiation and sunspots. For related information see *93 Space Radiation.*

93 SPACE RADIATION **2534**
Includes cosmic radiation; and inner and outer earth's radiation belts. For biological effects of radiation see *52 Aerospace Medicine.* For theory see *73 Nuclear and High-Energy Physics.*

GENERAL

Includes aeronautical, astronautical, and space science related histories, biographies, and pertinent reports too broad for categorization; histories or broad overviews of NASA programs.

99 GENERAL **2535**

SUBJECT INDEX **I-1**

PERSONAL AUTHOR INDEX **I-71**

CORPORATE SOURCE INDEX **I-79**

CONTRACT NUMBER INDEX **I-91**

REPORT/ACCESSION NUMBER INDEX **I-95**

APPENDIX **A-1**

TYPICAL CITATION AND ABSTRACT

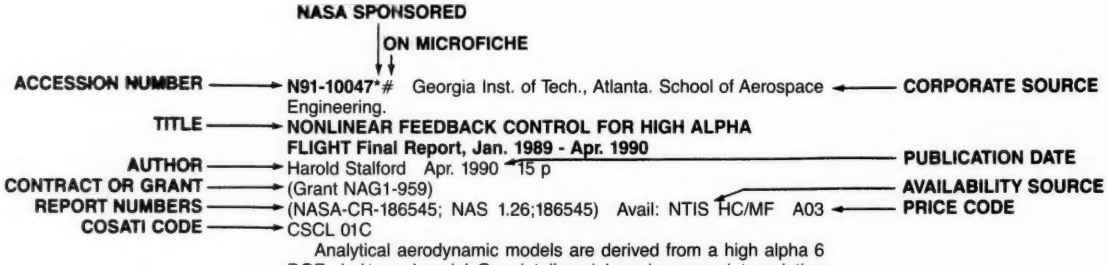

Analytical aerodynamic models are derived from a high alpha 6 DOF wind tunnel model. One detail model requires some interpolation between nonlinear functions of alpha. One analytical model requires no interpolation and as such is a completely continuous model. Flight path optimization is conducted on the basic maneuvers: half-loop, 90 degree pitch-up, and level turn. The optimal control analysis uses the derived analytical model in the equations of motion and is based on both moment and force equations. The maximum principle solution for the half-loop is poststall trajectory performing the half-loop in 13.6 seconds. The agility induced by thrust vectoring capability provided a minimum effect on reducing the maneuver time. By means of thrust vectoring control the 90 degrees pitch-up maneuver can be executed in a small place over a short time interval. The agility capability of thrust vectoring is quite beneficial for pitch-up maneuvers. The level turn results are based currently on only outer layer solutions of singular pertrubation. Poststall solutions provide high turn rates but generate higher losses of energy than that of classical sustained solutions.

Author

VOLUME 29 NUMBER 15 / AUGUST 8, 1991

Scientific and Technical Aerospace Reports

A Semimonthly Publication of the National Aeronautics and Space Administration

01 AERONAUTICS (GENERAL)

N91-23073* National Aeronautics and Space Administration, Washington, DC.
AERONAUTICAL ENGINEERING: A CUMULATIVE INDEX TO A CONTINUING BIBLIOGRAPHY (SUPPLEMENT 261)
Feb. 1991 562 p
(NASA-SP-7037(261); NAS 1.21:7037(261)) Avail: NTIS HC A24; NTIS standing order as PB90-914100, $17.75 domestic, $35.50 foreign CSCL 01B

This publication is a cummulative index to the abstracts contained in Supplements 249 through 260 of Aeronautical Engineering: A Continuing Bibliography. The bibliographic series is compiled through the cooperative efforts of the American Institute of Aeronautics and Astronautics (AIAA) and the National Aeronautics and Space Administration (NASA). Seven indexes are included -- subject, personal author, corporate source, foreign technology, contract number, report number and accession number. Author

N91-23074* National Aeronautics and Space Administration, Washington, DC.
AERONAUTICAL ENGINEERING: A CONTINUING BIBLIOGRAPHY WITH INDEXES (SUPPLEMENT 262)
Feb. 1991 142 p
(NASA-SP-7037(262); NAS 1.21:7037(262)) Avail: NTIS HC A07; NTIS standing order as PB91-914100, $17.00 domestic, $34.00 foreign CSCL 01B

This bibliography lists 474 reports, articles, and other documents introduced into the NASA scientific and technical information system in Jan. 1991. Subject coverage includes: design, construction and testing of aircraft and aircraft engines; aircraft components, equipment and systems; ground support systems; and theoretical and applied aspects of aerodynamics and general fluid dynamics. Author

N91-23075# Federal Aviation Administration, Atlantic City, NJ.
NAS OPERATIONAL TEST AND EVALUATION/INTEGRATION OF THE MAINTENANCE MANAGEMENT SYSTEM (MMS) TEST PLAN
Frances M. Bayne, Cheryl Krouse, Corey Bolling, Edward Palka, Joseph Pointkowski, and Edward Xzydlowski May 1991 160 p
(DOT/FAA/CT-TN90/41) Avail: NTIS HC/MF A08

Given here is the test plan for the National Airspace System (NAS) Operational Test and Evaluation (OT and E)/Integration of the Maintenance Management System (MMS) performed on the ACN-230 Maintenance Processor Subsystem (MPS) located at the Federal Aviation Administration (FAA) Technical Center. The MMS versions to be tested are A03, A03.01, A03.1, and A03.2. Author

N91-23076# Institute for Defense Analyses, Alexandria, VA.
THE COSTS AND BENEFITS OF AIRCRAFT AVAILABILITY Final Report, Jan. - Sep. 1990
Matthew S. Goldberg and Karen W. Tyson Mar. 1991 45 p
(AD-A232660; AD-E501359; IDA-P-2462; IDA/HQ-90-35834)
Avail: NTIS HC/MF A03 CSCL 01/2

This paper contains estimates of the effects of research and development costs (through initial operational capability) and unit procurement costs on the mission-capable (MC) rates of eleven tactical aircraft models. These estimates are transformed into estimates of the marginal cost of increasing MC rates through, respectively, increased development or increased procurement expenditures. The benefits of higher MC rates are also computed. One benefit is that, with more reliable aircraft, the procurement quantity may be reduced. A second benefit is that more reliable aircraft have lower operations and maintenance (O and M) costs in the field. The magnitudes of these effects are also estimated. Finally, the costs and benefits are combined to compute optimal levels of investment in reliability, both for hypothetical aircraft models and for the eleven aircraft models used in the statistical analysis. GRA

N91-23077# Institute for Defense Analyses, Alexandria, VA.
ESTIMATING FIXED AND VARIABLE COSTS OF AIRFRAME MANUFACTURERS Final Report, Dec. 1988 - Dec. 1990
Stephen J. Balut, Thomas P. Frazier, and James Bui Mar. 1991 42 p
(AD-A232661; AD-E501360; IDA-P-2401; IDA/HQ-90-35536)
Avail: NTIS HC/MF A03 CSCL 05/3

This report presents a model for separating annual costs at airframe manufacturing plants into fixed and variable components. The use of the model is to aid defense analysts in estimating the cost to manufacture aircraft systems when the manufacturer has not yet been determined or when proprietary models for the specific firms are not available. The material is unclassified and non-proprietary. GRA

02 AERODYNAMICS

Includes aerodynamics of bodies, combinations, wings, rotors, and control surfaces; and internal flow in ducts and turbomachinery.

For related information see also *34 Fluid Mechanics and Heat Transfer.*

N91-23078# Old Dominion Univ., Norfolk, VA.
AN EXPERIMENTAL STUDY OF AN AXISYMMETRIC TURBULENT BOUNDARY LAYER DISTURBED BY A PERIODIC FREESTREAM Ph.D. Thesis
Chithrabhanu Koodalattupuram Apr. 1990 212 p
Avail: NTIS HC/MF A10

Behavior of an axisymmetric equilibrium turbulent boundary layer disturbed by a propeller wake in the freestream was investigated experimentally. Tests were conducted in a low speed wind tunnel and measurements of turbulence quantities were made using an x wire probe and a constant temperature anemometer. The boundary layer flow on a cylindrical body was characterized by measuring its gross parameters and comparing them with classical values. Propeller speed was measured using an electronic circuit whose output signal was also used to trigger the hot wire probe. Gross boundary layer characteristics of the disturbed boundary layer did not deviate appreciably from the classical two dimensional turbulent boundary layer except immediately behind the propeller. From conditional sampling, it was found that the near wall periodic Reynolds stress approached 30 percent of the conventional time averaged Reynolds stress. Turbulent kinetic

energy, kinetic energy of the organized field, and various kinetic energy production terms responsible for exchange of turbulent kinetic energy between different flow fields were calculated from the experimental data. It was found that kinetic energy was being transferred from the organized flow field to the random turbulent flow field, as expected. The variation of both periodic and turbulent kinetic energy were governed by similar equations. A mechanism for the transport of turbulent kinetic energy was suggested.
Dissert. Abstr.

N91-23079# Federal Aviation Administration, Cambridge, MA.
AIRCRAFT WAKE VORTICES: AN ASSESSMENT OF THE CURRENT SITUATION Final Report, Mar. - Aug. 1990
J. N. Hallock Jan. 1991 67 p
(AD-A231658; DOT-VNTSC-FAA-90-6; DOT/FAA/RD-90/29)
Avail: NTIS HC/MF A04 CSCL 01/1

The state of knowledge about aircraft wake vortices in the summer of 1990 is summarized. With the advent of a new FAA wake vortex program, the current situation was assessed by answering five questions: (1) what is known about wake vortices, (2) what isn't known about wake vortices, (3) what are the requirements and limitations for operational systems to solve the wake vortex problems, (4) where does one go from here, and (5) why is there a need to collect more wake vortex data. GRA

N91-23080*# Rockwell International Corp., Los Angeles, CA.
AERODYNAMIC PRELIMINARY ANALYSIS SYSTEM 2. PART 1: THEORY
E. Bonner, W. Clever, and K. Dunn Apr. 1991 144 p
(Contract NAS1-18015)
(NASA-CR-182076; NAS 1.26:182076) Avail: NTIS HC/MF A07 CSCL 01A

An aerodynamic analysis system based on potential theory at subsonic and/or supersonic speeds and impact type finite element solutions at hypersonic conditions is described. Three dimensional configurations having multiple nonplanar surfaces of arbitrary planform and bodies of noncircular contour may be analyzed. Static, rotary, and control longitudinal and lateral directional characteristics may be generated. The analysis was implemented on a time sharing system in conjunction with an input tablet digitizer and an interactive graphics input/output display and editing terminal to maximize its responsiveness to the preliminary analysis problem. The program provides an efficient analysis for systematically performing various aerodynamic configuration tradeoff and evaluation studies.
Author

N91-23081*# Rockwell International Corp., Los Angeles, CA.
AERODYNAMIC PRELIMINARY ANALYSIS SYSTEM 2. PART 2: USER'S MANUAL
G. Sova, P. Divan, and L. Spacht Apr. 1991 339 p
(Contract NAS1-18015)
(NASA-CR-182077; NAS 1.26:182077) Avail: NTIS HC/MF A15 CSCL 01A

An aerodynamic analysis system based on potential theory at subsonic and/or supersonic speeds and impact type finite element solutions at hypersonic conditions is described. Three dimensional configurations have multiple nonplanar surfaces of arbitrary planforms and bodies of noncircular contour may be analyzed. Static, rotary, and control longitudinal and lateral-directional characteristics may be generated. The analysis was implemented on a time sharing system in conjunction with an input tablet digitizer and an interactive graphics input/output display and editing terminal to maximize its responsiveness to the preliminary analysis. Computation times on an IBM 3081 are typically less than one minute of CPU/Mach number at subsonic, supersonic, or hypersonic speeds. This is a user manual for the computer programming. Author

N91-23082 California Univ., Berkeley.
INTERFEROMETRIC INVESTIGATION OF SUPERSONIC FLOW FIELDS WITH SHOCK-SHOCK INTERACTIONS Ph.D. Thesis
Mark Paul Loomis 1990 127 p
Avail: Univ. Microfilms Order No. DA9103798

An experimental investigation of the two-dimensional interaction between an oblique shock wave generated by a wedge and the bow shock upstream of an cylinder placed in cross flow is presented. New interferometric techniques to provide density information on the entire flow field were compared to previous investigations. Results were compared with a concurrent numerical investigation. The data obtained are useful in documenting and understanding such complex flow fields as that occurring when oblique shocks impinge on the cowl inlet of a vehicle such as the National Aerospace Plane. Depending on the position of the impinging shock with respect to the bow shock, type 1, 2, and 3 interactions as defined by Edney were obtained. The experiments were performed in a 14 by 14 cm supersonic wind tunnel with a nominal Mach number of 2.4. The primary experimental emphasis was the development of interferometric techniques and the application of these techniques to provide interferometric data for the different types of interactions. Since the flow field was two dimensional, the global density was deduced from the interferograms. Two types of interferometers were constructed and used, holographic interferometry and dark central ground interferometry. Using holographic interferometry, interferograms were made by storing holographically two images of the test section, one at test conditions and one with no flow in the tunnel. By comparing the two images an interferogram was constructed after the test had taken place. The second interferometer used a relatively new technique called dark central ground interferometry. The method involved placing a spatial filter at the focal point of the system after the beam has passed through the test section. Since the technique produces real time interferograms it was found to have many advantages over holographic interferometry. The current study represents one of the first applications of this technique in routine wind tunnel testing. Dissert. Abstr.

N91-23083*# National Aeronautics and Space Administration. Lewis Research Center, Cleveland, OH.
NASA AEROPROPULSION RESEARCH IN SUPPORT OF PROPULSION SYSTEMS OF THE 21ST CENTURY
Joseph A. Ziemianski and Edward A. Willis (Sverdrup Technology, Inc., Brook Park, OH.) 1991 26 p Presented at the 36th International Gas Turbine and Aeroengine Congress and Exposition, Orlando, FL, 3-6 Jun. 1991; sponsored by ASME
(NASA-TM-104403; E-6226; NAS 1.15:104403) Avail: NTIS HC/MF A03 CSCL 01A

A review is given of the NASA's ongoing and planned research and technology programs leading to advanced air breathing propulsion systems of the next century. The primary focus is on efforts being performed or sponsored by NASA-Lewis, with emphasis on civil, subsonic, and supersonic transportation systems which should begin to enter service within 10 to 20 years. Subsonic transport propulsion program elements, including ducted UltraHigh Bypass (UHB) engines and high efficiency cores are discussed in terms of goals, technical issues and problems, approaches and plans. Similarly, The Supersonic Cruise Propulsion Program is reviewed via discussion of near term and far term goals; barrier issues such as NOx and noise reduction and the consequent Phase 1 (near term) research plans are described; and finally, emerging technologies such as the supersonic through-flow fan are considered for their potential long term impact. Author

N91-23084*# Minnesota Univ., Minneapolis. Dept. of Aerospace Engineering and Mechanics.
A STUDY OF THE NOISE MECHANISMS OF TRANSONIC BLADE-VORTEX INTERACTIONS Semiannual Technical Report
Anastasios S. Lyrintzis and Y. Xue 1990 37 p Presented at the AHS 46th Annual Forum, Washington, DC, 21-23 May 1990
(Grants NAG2-588; NAG2-646)
(NASA-CR-188199; NAS 1.26:188199) Avail: NTIS HC/MF A03 CSCL 01A

Transonic blade-vortex interactions (BVI) are simulated numerically and the noise mechanisms are investigated. The two-dimensional high frequency transonic small disturbance equation is solved numerically (VTRAN2 code). An ADI scheme

with monotone switches is used; viscous effects are included on the boundary, and the vortex is simulated by the cloud in cell method. The Kirchhoff method is used for the extension of the numerical two-dimensional near-field aerodynamic results to the linear acoustic three dimensional far field. The viscous effects (shock/boundary layer interactions) on BVI is investigated. The different types of shock motion are identified and compared. Two important disturbances with different directivity exist in the pressure signal and are believed to be related to the fluctuating lift and drag forces. Noise directivity for different cases is shown. The maximum radiation occurs at an angle between 60 and 90 degrees below the horizontal for an airfoil-fixed coordinate system and depends on the details of the airfoil shape. Different airfoil shapes are studied and classified according to the BVI noise produced.
Author

N91-23085# Sandia National Labs., Albuquerque, NM.
A VORTEX PANEL METHOD FOR CALCULATING AIRCRAFT DOWNWASH ON PARACHUTE TRAJECTORIES
T. L. Fullerton, J. H. Strickland, and W. D. Sundberg 1991 8 p Presented at the 11th AIAA Aerodynamic Decelerator Systems Technology Conference, San Diego, 9-11 Apr. 1991
(Contract DE-AC04-76DP-00789)
(DE91-009764; SAND-90-2178C; CONF-9104171-7) Avail: NTIS HC/MF A02

A discussion is presented of a methodology of the paneled wing method for calculating aircraft induced wake velocities. This discussion includes a description of how an aircraft and its wake are represented by finite length vortex filaments, how the strength and location of these filaments are determined based upon aircraft characteristics and trajectory data, and how the induced velocity values are determined once the location and strength of the vortex filaments are known. Examples are presented showing comparisons between induced velocity values calculated using both the paneled wing method and Strickland's lifting line method. Comparison is also made between calculated results from the paneled wing method and wind tunnel data collected in the wake of a scale model aircraft. Additional examples show the effect of including aircraft downwash calculations in a trajectory analysis for a parachute-retarded store delivered via aircraft.
DOE

N91-23086*# National Aeronautics and Space Administration. Lewis Research Center, Cleveland, OH.
SIMULATION OF ICED WING AERODYNAMICS
M. G. Potapczuk, M. B. Bragg, O. J. Kwon, and L. N. Sankar (Georgia Inst. of Tech., Atlanta.) 1991 17 p Presented at the 68th Fluid Dynamics Panel Specialists Meeting, Toulouse, France, 29 Apr. - 1 May 1991; sponsored by AGARD
(NASA-TM-104362; E-6158; NAS 1.15:104362) Avail: NTIS HC/MF A03 CSCL 01A

The sectional and total aerodynamic load characteristics of moderate aspect ratio wings with and without simulated glaze leading edge ice were studied both computationally, using a three dimensional, compressible Navier-Stokes solver, and experimentally. The wing has an untwisted, untapered planform shape with NACA 0012 airfoil section. The wing has an unswept and swept configuration with aspect ratios of 4.06 and 5.0. Comparisons of computed surface pressures and sectional loads with experimental data for identical configurations are given. The abrupt decrease in stall angle of attack for the wing, as a result of the leading edge ice formation, was demonstrated numerically and experimentally.
Author

N91-23087*# National Aeronautics and Space Administration. Lewis Research Center, Cleveland, OH.
ICING SIMULATION: A SURVEY OF COMPUTER MODELS AND EXPERIMENTAL FACILITIES
M. G. Potapczuk and J. J. Reinmann 1991 29 p Presented at the 68th Fluid Dynamics Panel Specialists Meeting, Toulouse, France, 29 Apr. - 1 May 1991; sponsored by AGARD
(NASA-TM-104366; E-6164; NAS 1.15:104366) Avail: NTIS HC/MF A03 CSCL 01A

A survey of the current methods for simulation of the response of an aircraft or aircraft subsystem to an icing encounter is presented. The topics discussed include a computer code modeling of aircraft icing and performance degradation, an evaluation of experimental facility simulation capabilities, and ice protection system evaluation tests in simulated icing conditions. Current research focussed on upgrading simulation fidelity of both experimental and computational methods is discussed. The need for increased understanding of the physical processes governing ice accretion, ice shedding, and iced airfoil aerodynamics is examined.
Author

N91-23088# Deutsche Forschungsanstalt fuer Luft- und Raumfahrt, Goettingen (Germany, F.R.). Hauptabt. Windkanaele.
PROCEDURE FOR DETERMINATION OF THREE-DIMENSIONAL WIND TUNNEL WALL INTERFERENCES AND WALL ADAPTATION IN COMPRESSIBLE SUBSONIC FLOW USING MEASURED WALL PRESSURES Thesis - Technische Univ.
Harmut Holst 11 Dec. 1990 171 p In GERMAN; ENGLISH summary
(DLR-FB-90-46; ISSN-0171-1342; ETN-91-99067) Avail: NTIS HC/MF A08; DLR, Wissenschaftliches Berichtswesen, VB-PL-DO, Postfach 90 60 58, 5000 Cologne, Fed. Republic of Germany, HC 60 DM

Green's Theorem is applied to the problem of wall interferences in wind tunnels. The velocity components at the boundaries of the test section are the data required for the calculation. The computation of the wall adaptation is performed in a single step. Measurements in an adaptive test section show that the method can be used for the determination of wall interferences, wall adaptation, and residual interferences. Computations demonstrate that optimization of slot widths in test sections with longitudinally slotted walls and calculation of residual interferences can be performed using this method. The limitations of the method are discussed.
ESA

N91-23089*# National Aeronautics and Space Administration. Lewis Research Center, Cleveland, OH.
A STUDY OF THREE DIMENSIONAL TURBULENT BOUNDARY LAYER SEPARATION AND VORTEX FLOW CONTROL USING THE REDUCED NAVIER STOKES EQUATIONS
Bernhard H. Anderson and Saeed Farokhi (Kansas Univ., Lawrence.) 1991 8 p Presented at the Turbulent Shear Flow Symposium, Munich, Fed. Republic of Germany, 9-11 Sep. 1991
(NASA-TM-104407; E-6233; NAS 1.15:104407) Avail: NTIS HC/MF A02 CSCL 01A

A reduced Navier Stokes (RNS) initial value space marching solution technique was applied to vortex generator and separated flow problems and demonstrated good predictions of the engine face flow field. This RNS solution technique using FLARE approximations can adequately describe the topological and topographical structure flow separation associated with vortex liftoff, and this conclusion led to the concept of a subclass of separations which can be called vorticity separations: separations dominated by the transport of vorticity. Adequate near wall resolution of vorticity separations appears necessary for good predictions of these flows.
Author

N91-23090# Messerschmitt-Boelkow-Blohm G.m.b.H., Munich (Germany, F.R.). Hubschrauber und Flugzeuge.
PROBLEMS OF HYPERSONIC AEROTHERMODYNAMICS [PROBLEME DER HYPERSCHALL-AEROTHERMODYNAMIK]
E. H. Hirschel 15 Jan. 1991 18 p In GERMAN Presented at 7th DGLR-Fachsymposium Stroemungen mit Ablosung, Aachen, Fed. Republic of Germany, 7-9 Nov. 1990
(MBB-FE202/5/PUB/436; ETN-91-99249) Copyright Avail: NTIS HC/MF A03

Derived from basic problems of the aerothermodynamical project for hypersonic range flight equipments configurative aspects of such flight equipments, are represented using the Saenger space transportation systems. The Saenger lower stage is in the center of the examinations, as it is dominated by friction effects, whereas the upper stage is dominated by reentry pressure forces. The

flow phenomena occurring in the lower stage, and in particular heat loads are discussed. Wind tunnel and numerical simulation aspects are represented. ESA

N91-23091# Aerospatiale, Toulouse (France). Direction Hypersonique.
HYPERSONIC NUMERICAL SIMULATION: PROBLEMS AND PERSPECTIVES. HYPERSONIC VEHICLES AND NUMERICAL SIMULATION IN STRUCTURAL ANALYSIS [LA SIMULATION NUMERIQUE EN HYPERSONIQUE: PROBLEMES ET PERSPECTIVES. LES VEHICULES HYPERSONIQUES ET LA SIMULATION NUMERIQUE EN ANALYSE STRUCTURALE]
J. M. Thomas 1991 30 p In FRENCH Presented at Congres ONERA: Evolution du Calculateur Aeronautique, 9 Oct. 1990, and Journees SAMCEF 90: L'Analyse Structurale, Liege, Belgium, 18 Oct. 1990
(Rept-911-111-106; ETN-91-99270) Copyright Avail: NTIS HC/MF A03

The thermal behavior of motor structures is reported. Cooling techniques are described. Supercomputer and numerical simulation operations are presented. Complex composite structure examples are given. It is shown that structural problems can be divided into two groups: those which are in common with all possible structures, such as hypersonic transportation, space launcher, missiles, military aircraft, and those which are specific to each possible architecture. Specific problems and problems in common with all architectures are enumerated. Research work in structures are presented. Temperature range, stress cycles, utilization time, component dimensions, damage tolerance aspects are determining parameters for materials. New industrial materials are tabulated. ESA

N91-23092# Cranfield Inst. of Tech., Bedford (England). Dept. of Aerodynamics.
THE PERFORMANCE OF 60 DEG DELTA WINGS: THE EFFECTS OF LEADING EDGE RADIUS ON VORTEX FLAPS AND THE WING
B. K. Hu and J. L. Stollery Mar. 1990 35 p
(Cranfield-Aero-9004; ISBN-1-871564-05-0; ETN-91-99333)
Avail: NTIS HC/MF A03

Low speed wind tunnel tests were conducted on 60 degree delta wings. The wings were tested with well rounded and sharp leading edge vortex flaps to estimate the effects of leading edge radius on the aerodynamic performance. The Reynolds number based on root chord was approx. 800,000. Results indicate that leading edge radius has little effect on the contribution of the vortex flap to lift/drag ratio on the 60 deg delta wing. The 60 deg delta wing with a well rounded leading edge and no vortex flap deflection has a higher lift/drag ratio over almost the entire lift coefficient range tested. ESA

N91-23093# Universal Energy Systems, Inc., Dayton, OH.
COMPUTATION OF VISCOUS SHOCK/SHOCK HYPERSONIC INTERACTIONS WITH AN IMPLICIT FLUX SPLIT SCHEME Final Report, Sep. 1989 - Sep. 1990
Datta Gaitonde Dec. 1990 61 p
(Contract F33615-88-C-2908)
(AD-A232405; WRDC-TR-90-3076) Avail: NTIS HC/MF A04 CSCL 20/4

The interaction of an impinging shock with the bow shock generated by a blunt geometry is examined numerically for hypersonic (Mach 8, perfect gas) flows with modified Steger-Warming flux split scheme. The modifications are designed to reduce numerical dissipation in the boundary layer thus improving the resolution and accuracy of the resulting algorithm. The full 2-D Navier-Stokes equations are solved in finite volume formulation with central differencing for viscous terms and residual driven line Gauss-Seidel relaxation for time advancement. Grid resolution studies are performed. For a Type IV interaction, comparison with surface pressure and heat transfer rates display good overall agreement with experimental values. For a Type III+ interaction, a detailed comparison is made with experimental surface quantities and a computation with Van Leer's flux splitting algorithm. The peak amplification of pressure is modestly overpredicted with the current algorithm. The computed peak heat transfer is comparable to that obtained in previous research with Van Leer's splitting, although anomalous behavior is observed in the vicinity of the stagnation point. This behavior may be eliminated with appropriate corrections. GRA

N91-23094# Lehigh Univ., Bethlehem, PA.
UNSTEADY FLOW STRUCTURE FROM SWEPT EDGES SUBJECTED TO CONTROLLED MOTION Final Report, 1 May 1986 - 31 Oct. 1990
Donald Rockwell 26 Dec. 1990 89 p
(Grant AF-AFOSR-0177-86; AF Proj. 2307)
(AD-A232714; LU-AFOSR-FR-90; AFOSR-91-0139TR) Avail: NTIS HC/MF A05 CSCL 01/1

This program addresses the unsteady flow structure and loading of delta wings subjected to controlled pitching motion. Efforts are focussed on three primary areas: generation of computer-aided techniques for quantitative interpretation of flow structure; development of new types of experimental instrumental and facilities; and characterization of the unsteady flow structure on delta wings. Computer applications for quantitative visualization of the vortex structure involve tracking of hydrogen bubble timelines and particles illuminated by scanning lasers. These techniques are integrated with active control systems that generate prescribed pitching motion of delta wings. Characterization of the unsteady flow structure is concerned with the response of the vortex breakdown to the motion of the wing and with preliminary consideration of the instantaneous cross-sectional structure of the leading edge vortices. The phase lag of these features of the flow structure, relative to the wing motion, is a central consideration. GRA

N91-23161# Cranfield Inst. of Tech., Bedford (England). Coll. of Aeronautics.
SOME ASPECTS OF SHOCK-WAVE BOUNDARY LAYER INTERACTION RELEVANT TO INTAKE FLOWS
J. L. Stollery *In* AGARD, Hypersonic Combined Cycle Propulsion Dec. 1990 14 p (For primary document see N91-23147 15-07)
Copyright Avail: NTIS HC/MF A20; Non-NATO Nationals requests available only from AGARD/Scientific Publications Executive

N91-23162*# National Aeronautics and Space Administration. Lewis Research Center, Cleveland, OH.
COMPUTATIONAL MODELING AND VALIDATION FOR HYPERSONIC INLETS
Louis A. Povinelli *In* AGARD, Hypersonic Combined Cycle Propulsion Dec. 1990 10 p Previously announced as N90-22011 (For primary document see N91-23147 15-07)
Copyright Avail: NTIS HC/MF A20; Non-NATO Nationals requests available only from AGARD/Scientific Publications Executive CSCL 01A

N91-23164# Deutsche Forschungsanstalt fuer Luft- und Raumfahrt, Cologne (Germany, F.R.). Inst. fuer Antriebstechnik.
AERODYNAMICS AND STABILIZATION OF COMBUSTION OF HYDROGEN JETS INJECTED INTO SUBSONIC AIRFLOW
J. Koopman, M. Rachner, H. Wiegand, and H. Eickhoff *In* AGARD, Hypersonic Combined Cycle Propulsion Dec. 1990 16 p (For primary document see N91-23147 15-07)
Copyright Avail: NTIS HC/MF A20; Non-NATO Nationals requests available only from AGARD/Scientific Publications Executive

N91-23174# Rome Univ. (Italy). Dipt. di Meccanica e Aeronautica.
REACTING SHOCK WAVES IN HYPERSONIC PROPULSION APPLICATIONS
M. Onofri *In* AGARD, Hypersonic Combined Cycle Propulsion Dec. 1990 10 p (For primary document see N91-23147 15-07)
Copyright Avail: NTIS HC/MF A20; Non-NATO Nationals requests available only from AGARD/Scientific Publications Executive

N91-23175*# Sverdrup Technology, Inc., Cleveland, OH.
VISCOUS THREE-DIMENSIONAL ANALYSES FOR NOZZLES FOR HYPERSONIC PROPULSION
G. J. Harloff, D. R. Reddy, and H. T. Lai *In* AGARD, Hypersonic Combined Cycle Propulsion Dec. 1990 18 p Previously announced as N90-17635 (For primary document see N91-23147 15-07)
Copyright Avail: NTIS HC/MF A20; Non-NATO Nationals requests available only from AGARD/Scientific Publications Executive CSCL 01A

03 AIR TRANSPORTATION AND SAFETY

Includes passenger and cargo air transport operations; and aircraft accidents.

For related information see also *16 Space Transportation* and *85 Urban Technology and Transportation.*

N91-23095*# National Aeronautics and Space Administration. Ames Research Center, Moffett Field, CA.
AIRBORNE RESCUE SYSTEM Patent Application
Leonard A. Haslim, inventor (to NASA) 6 Oct. 1989 17 p
(NASA-Case-ARC-11909-1; NAS 1.71:ARC-11909-1; US-Patent-Appl-SN-418320) Avail: NTIS HC/MF A03 CSCL 01C

The airborne rescue system includes a boom with telescoping members for extending a line and collar to a rescue victim. The boom extends beyond the tip of the helicopter rotor so that the victim may avoid the rotor downwash. The rescue line is played out and reeled in by winch. The line is temporarily retained under the boom. When the boom is extended, the rescue line passes through clips. When the victim dons the collar and the tension in the line reaches a predetermined level, the clips open and release the line from the boom. Then the rescue line can form a straight line between the victim and the winch, and the victim can be lifted to the helicopter. A translator is utilized to push out or pull in the telescoping members. The translator comprises a tape and a rope. Inside the telescoping members the tape is curled around the rope and the tape has a tube-like configuration. The tape and rope are provided from supply spools. NASA

N91-23096 California Univ., Berkeley.
NEAR MIDAIR COLLISIONS AS AN INDICATOR OF GENERAL AVIATION COLLISION RISK Ph.D. Thesis
H. Paul Shuch 1990 225 p
Avail: Univ. Microfilms Order No. DA9103873

Conventional wisdom suggests aircraft midair collisions to be random events, governed by the laws of Brownian Motion, and best analyzed by stochastic methods. An alternative hypothesis, that such accidents are deterministic in nature, and that specific factors leading to midair collisions can be identified and mitigated, is discussed. A predictive model using case control theory is developed for assessing Risk Index, a criterion measure of midair collision likelihood, for any General Aviation flight, actual or hypothetical. Generating the model requires statistical validation of two independent near midair collision data bases, and identifying within them those aircraft, aircrew and airspace characteristics most closely associated with collision risk. Dissert. Abstr.

N91-23097# Boeing Commercial Airplane Co., Seattle, WA. Advanced Programs-Payloads.
AIRCRAFT COMMAND IN EMERGENCY SITUATIONS (ACES). PHASE 1: CONCEPT DEVELOPMENT Final Report
Thomas L. Reynolds, Gregory E. Grimstad, and Charles D. Anderson Apr. 1991 136 p
(Contract DTFA03-89-C-00061)
(DOT/FAA/CT-90/21) Avail: NTIS HC/MF A07

Two conceptual approaches for an advanced smoke/fire detection system for commercial passenger jet aircraft are defined that would provide for accurate, timely guidance to the flight crew for their use in responding to possible and/or actual inflight smoke and fire events within the pressurized fuselage. The motivation for this was the computerization of the modern commercial jet aircraft flight deck, the evolution toward the two-man crew, and documented times taken to locate and implement the appropriate emergency procedure. The primary objective of the Aircraft Command in Emergency Situations (ACES) System concepts are to provide the capability to reduce the time required for the flight deck crew to make a decision to land the aircraft. Author

N91-23098*# National Aeronautics and Space Administration. Lewis Research Center, Cleveland, OH.
ENGINE TECHNOLOGY CHALLENGES FOR A 21ST CENTURY HIGH SPEED CIVIL TRANSPORT
Robert J. Shaw 1991 13 p Proposed for presentation at the 10th International Symposium on Air Breathing Engines, Nottingham, England, 1-6 Sep. 1991; sponsored by AIAA
(NASA-TM-104363; E-6159; NAS 1.15:104363) Avail: NTIS HC/MF A03 CSCL 01C

Recent NASA funded studies by Boeing and Douglas suggest an opportunity exists for a 21st Century High Speed Civil Transport (HSCT) to become part of the international air transportation system. However, before this opportunity for high speed travel can be realized, certain environmental and and economic barrier issues must be overcome. These challenges are outlined. Research activities which NASA has planned to address these barrier issues and to provide a technology base to allow U.S. manufacturers to make an informed go/no go decision on developing the HSCT are discussed. Author

N91-23099*# National Aeronautics and Space Administration. Ames Research Center, Moffett Field, CA.
MICROWAVE LANDING SYSTEM MODELING WITH APPLICATION TO AIR TRAFFIC CONTROL
M. M. Poulose Apr. 1991 23 p
(NASA-TM-102832; A-90184; NAS 1.15:102832) Avail: NTIS HC/MF A03 CSCL 01C

Compared to the current instrument landing system, the microwave landing system (MLS), which is in the advanced stage of implementation, can potentially provide significant fuel and time savings as well as more flexibility in approach and landing functions. However, the expanded coverage and increased accuracy requirements of the MLS make it more susceptible to the features of the site in which it is located. An analytical approach is presented for evaluating the multipath effects of scatterers that are commonly found in airport environments. The approach combines a multiplane model with a ray-tracing technique and a formulation for estimating the electromagnetic fields caused by the antenna array in the presence of scatterers. The model is applied to several airport scenarios. The reduced computational burden enables the scattering effects on MLS position information to be evaluated in near real time. Evaluation in near real time would permit the incorporation of the modeling scheme into air traffic control automation; it would adaptively delineate zones of reduced accuracy within the MLS coverage volume, and help establish safe approach and takeoff trajectories in the presence of uneven terrain and other scatterers. Author

N91-23100# Army Aeromedical Research Lab., Fort Rucker, AL.
A TEST OF THE AMERICAN SAFETY FLIGHT SYSTEMS, INC. PREBREATHER/PORTABLE OXYGEN SYSTEM Final Report
Robert L. Stephens, Francis S. Knox, Robert A. Mitchell, and Vadankumar M. Patel Jan. 1991 27 p
(DA Proj. 3E1-62787-A-878)
(AD-A232723; USAARL-91-5) Avail: NTIS HC/MF A03 CSCL 14/2

In response to a request from the Aviation Life Support Equipment Product Manager (ALSE-PM) of the Aviation Systems Command (AVSCOM), the U.S. Army Aeromedical Research Laboratory (USAARL) conducted an investigation and evaluation of the Prebreather/Portable Oxygen System (P/POS) manufactured by American Safety Flight Systems, Inc. A test of the P/POS was conducted in the hypobaric chamber at the U.S. Army School of

Aviation Medicine. Four crews of four subjects each and one crew of three (the last crew had only three because one subject had a middle ear infection) prebreathed 100 percent chamber oxygen for 30 minutes. Then they switched to the P/POS while the chamber was depressurized to 18,000 feet MSL at a rate of 500 fpm. They remained at this altitude pressure until they reduced the P/POS pressure from 1800 psi to 200 psi. Following this, the chamber was repressurized to sea level at a rate of 4000 fpm. Mission durations, percent oxygen saturation and cognitive performance were measured for each subject. The average mission duration was 2 hr 28 min with a standard deviation of 13.9 min. The study indicated the P/POS will meet the needs of all helicopter missions for the Army that do not require prebreathing. GRA

04 AIRCRAFT COMMUNICATIONS AND NAVIGATION

Includes digital and voice communication with aircraft; air navigation systems (satellite and ground based); and air traffic control.

For related information see also *17 Space Communications, Spacecraft Communications, Command and Tracking* and *Communications and Radar.*

N91-23101 Texas Univ., Austin.
TARGET MANEUVER MODELS FOR IMPROVED HOMING GUIDANCE Ph.D. Thesis
Kevin Donghuan Kim 1990 204 p
Avail: Univ. Microfilms Order No. DA9105584

The development of a guidance law for a homing missile using angle-only measurements and where the target is highly maneuverable is considered. A new stochastic dynamic target model is proposed on the assumption that certain targets execute evasive maneuvers orthogonal to their velocity vector. Along with this new acceleration dynamic model, the orthogonality is also enforced by the addition of a fictitious auxiliary measurements. The target states are estimated by the modified gain extended Kalman filter, and the angular target maneuver rate is constructed on-line. A guidance law that minimizes a quadratic performance index subject to the assumed stochastic engagement dynamics that includes state dependent noise is derived. Dissert. Abstr.

N91-23102*# National Aeronautics and Space Administration. Lewis Research Center, Cleveland, OH.
CHARACTERISTICS OF A FUTURE AERONAUTICAL SATELLITE COMMUNICATIONS SYSTEM
Philip Y. Sohn, Alan Stern, and Fred Schmidt (Ball Corp., Bloomfield, CO.) 1991 30 p Presented at the Advanced Network and Technology Concepts for Mobile, Micro, and Personal Communications, Pasadena, CA, 30-31 May 1991; sponsored by JPL
(NASA-TM-104389; E-6200; NAS 1.15:104389) Avail: NTIS HC/MF A03 CSCL 17G

A possible operational system scenario for providing satellite communications services to the future aviation community was analyzed. The system concept relies on a Ka-band (20/30 GHz) satellite that utilizes multibeam antenna (MBA) technology. The aircraft terminal uses an extremely small aperture antenna as a result of using this higher spectrum at Ka-band. The satellite functions as a relay between the aircraft and the ground stations. The ground stations function as interfaces to the existing terrestrial networks such as the Public Service Telephone Network (PSTN). Various system tradeoffs are first examined to ensure optimized system parameters. High level performance specifications and design approaches are generated for the space, ground, and aeronautical elements in the system. Both technical and economical issues affecting the feasibility of the studied concept are addressed with the 1995 timeframe in mind. Author

N91-23103# Deutsche Forschungsanstalt fuer Luft- und Raumfahrt, Cologne (Germany, F.R.). Forschungsbereich Flugmechanik/Flugfuehrung.
FLIGHT MECHANICS/AIR NAVIGATION RESEARCH FIELD. A 1990 SCIENTIFIC REPORT OF THE GERMAN AIR AND SPACE RESEARCH ORGANIZATION Annual Report, 1990 [FORSCHUNGSBEREICH FLUGMECHNIK/FLUGFUEHRUNG, WISSENSCHAFTLICHER BERICHT, STAND 1990]
Dorothea Koch-Peters, Marianne Salein, and Adalbert Timme 1990 143 p In GERMAN Original contains color illustrations
(ISSN-0720-7808; ETN-91-99079) Avail: NTIS HC/MF A07

The tasks and aims of both institutes are defined and presented. Flight test data acquisition and analysis, system identification, wind tunnel simulation, real time signal processing are focused upon. The pilot/automatic systems relationship, the design of automatic systems and the improvement of the required sensors are the main concern of air navigation research. The flight safety problems are considered to be solved only when the different navigation aspects on board and on the ground are fully integrated. The Institute of Flight Medicine is described and its aims defined, as well as the Department of Traffic Research, and the Institute for the Dynamics of Flight Systems. ESA

N91-23104 Max-Planck-Inst. fuer Physik und Astrophysik, Garching (Germany, F.R.). Inst. fuer Extraterrestrische Physik.
HIGH RESOLUTION IMAGING FOR BRACKETT GAMMA AND H2 1-0 S(1) EMISSION IN THE SEYFERT GALAXY NGC 1068
V. Rotaciuc, A. Krabbe, M. Cameron, S. Drapatz, R. Genzel, A. Sternberg, and J. W. V. Storey Oct. 1990 22 p Submitted for publication Sponsored in part by Minerva Society and Alexander von Humboldt Society
(MPE-Preprint-192; ETN-91-99080) Copyright Avail: Fachinformationszentrum Karlsruhe, 7514 Leopoldshafen-Eggenstein 2, Fed. Republic of Germany

One inch resolution imaging of 2 micron HI Brackett gamma and H2 1-0 S(1) line emission toward the nucleus of the Seyfert 2 galaxy NGC 1068 is reported. The data, taken with a new imaging Fabry-Perot, shows that the emission in both infrared lines originates from within 2 inches (170 pc) of the peak of radio, near infrared and visible continuum radiation. The vibrational molecular emission has a double lobed shape, with a minimum toward the nucleus and two peaks about 1.3 inches on either side of the nucleus along position angle 70 deg east of north. In contrast, the Brackett gamma emission is peaked on the nucleus, similar to the central radio continuum structure and the Narrow-Line Region (NLR) in the visible. The Brackett gamma emission has an approximate one inch (FWHM (Full Width at Half Maximum)) diameter, and is more compact than the distributions of various visible NLR tracers. The H2 emission is probably produced in hot gas with mass a few 1000 of the solar mass. However, the total molecular mass in the circumnuclear region hydrogen may approach 10(exp 8) of the solar mass. The H2 emission is not produced in a 1 pc size obscuring torus, but probably comes from a system of molecular clouds in the vincinity of the NLR. The molecular clouds probably contributed significantly to the extinction of the nuclear source. The circumnuclear Brackett gamma and H2 emission lines are proposed as being excited by UV or X-ray photons emitted by a central nonstellar source. ESA

N91-23105# Technische Univ., Brunswick (Germany, F.R.). Inst. fuer Verkehr, Eisenbahnwesen und Verkehrssicherung.
AIRBORNE COLLISION AVOIDANCE SYSTEM (ACAS) IN CONTROLLED AIR TRAFFIC. ASPECTS OF RECIPROCAL INFLUENCE IN SECONDARY SURVEILLANCE RADAR (SSR) RADIO LOADS [BORDKOLLISIONSSCHUTZSYSTEME IM KRONTROLLIERTEN LUFTVERKEHR ASPEKTE GEGENSEITIGER BEEINFLUSSUNG IM SSR FUNKFELD]
Andreas Herber and Roland Mallwitz Nov. 1990 45 p In GERMAN
(ETN-91-99253) Avail: NTIS HC/MF A03

The aim was a qualitative and quantitative evaluation of potential reciprocal influences in secondary surveillance radar (SSR) radio loads. This was made possible by an interpretation of the results

of the radio load measurements and by an analysis of existing specifications for the various airborne collision avoidance system (ACAS). Definitive statements are impossible on account of the continuously changing boundary conditions, such as the number of active ground stations. It was shown by the algorithms contained in all II/III ACAS for interference limitations, that the performance realized additionally in the radio loads by all instruments for a maximum of 280 interrogations is limited within a perimeter of 30 nautical miles. It appears differently for ACAS I instruments, where this system is hardly active on account of high interrogation numbers. The observation area is limited to 5 nautical miles. It was concluded that the actions of ACAS II/III on the air traffic control are possible with secondary radar. ESA

N91-23106# Federal Aviation Administration, Atlantic City, NJ.
DIFFERENTIAL GPS TERMINAL AREA TEST RESULTS Technical Report, Nov. 1989 - Nov. 1990
L. F. Persello Nov. 1990 61 p
(AD-A232668; DOT/FAA/CT-TN90/48) Avail: NTIS HC/MF A04 CSCL 17/7

This report describes flight tests conducted by the Federal Aviation Administration (FAA) Technical Center to examine the performance of the Differential Global Positioning System (DGPS) in the terminal area. The tests employed a Convair 580 (CV-580) and a pair of Motorola Eagle Mini Rangers. With the advent of a maturing Global Positioning System (GPS) constellation, the FAA is assuming a more intensive stance in addressing the many questions/problems associated with GPS. These DGPS tests investigated the obtainable accuracy under static and dynamic conditions. The static tests employed survey points as a baseline. The dynamic tests incorporated terminal area flight profiles and nonprecision approaches using a laser tracker as a base line. The accuracy performance of DGPS showed an order of magnitude improvement in the static environment and a 4 to 5 fold improvement in the dynamic environment over stand alone GPS. The DGPS tests were conducted in an effort to build an FAA DGPS data base to aid in addressing GPS questions/problems. GRA

N91-23150# Honeywell, Inc., Minneapolis, MN. Systems and Research Center.
NAVIGATION, GUIDANCE, AND TRAJECTORY OPTIMIZATION FOR HYPERSONIC VEHICLES
R. L. Schultz, M. J. Hoffman, A. M. Case, and S. I. Sheikh *In* AGARD, Hypersonic Combined Cycle Propulsion Dec. 1990 22 p Sponsored in part by AF (For primary document see N91-23147 15-07)
Copyright Avail: NTIS HC/MF A20; Non-NATO Nationals requests available only from AGARD/Scientific Publications Executive

N91-24073*# Jet Propulsion Lab., California Inst. of Tech., Pasadena.
HIGH PRECISION APPLICATIONS OF THE GLOBAL POSITIONING SYSTEM
Stephen M. Lichten *In* NASA, Washington, Technology 2000, Volume 2 1991 p 276-284 (For primary document see N91-24041 15-99)
Avail: NTIS HC/MF A16 CSCL 17G

05 AIRCRAFT DESIGN, TESTING AND PERFORMANCE

Includes aircraft simulation technology.

For related information see also *18 Spacecraft Design, Testing and Performance* and *39 Structural Mechanics*.For land transportation vehicles see *85 Urban Technology and Transportation*.

N91-23107# Israel Aircraft Industries Ltd., Ben-Gurion Airport. Engineering Div.
REAL TIME ESTIMATION OF AIRCRAFT ANGULAR ATTITUDE
G. Shadmon Apr. 1987 16 p
(IAITIC-87-1004; ITN-88-85003) Avail: NTIS HC/MF A03

A new method is presented for estimating aircraft angular attitude under real time conditions. The basis for the estimation is the requirement of best possible compatibility between the current estimate and the time history of the past measurements. The characteristics of the estimation technique are: (1) use of the quaternion formalism on characterizing the rotational motion; (2) adoption of the Least Square (LS) method as the tool of extracting the estimated quaternion out of the foregoing requirement; and (3) incorporation of the fading memory technique as a means of reducing the sensitivity to modelling errors. The main advantage of that method is its extremely small computation burden. This is reflected by a lack of the usual operations of matrix inversion and matrix propagation in time. Included are the review of the pertinent quaternion properties, the derivation of the estimation method, and the application to a real case. ISA

N91-23108# Advisory Group for Aerospace Research and Development, Neuilly-Sur-Seine (France). Flight Mechanics Panel.
FLYING QUALITIES
Feb. 1991 379 p In ENGLISH and FRENCH Symposium held in Quebec City, Quebec, 15-18 Oct. 1990
(AGARD-CP-508; ISBN-92-835-0602-2) Copyright Avail: NTIS HC/MF A17; Non-NATO Nationals requests available only from AGARD/Scientific Publications Executive

The purpose of this symposium was to review flying quality issues of today and to report progress towards their resolution. The following topic areas were covered: (1) flying qualities experiences and contemporary aircraft; (2) application of flying qualities specifications; (3) flying qualities research; and (4) flying qualities at high incidence. For individual titles, see N91-23109 through N91-23131.

N91-23109# Thomas (Dieter), Fuerstenfeldbruck (Germany, F.R.).
THE ART OF FLYING QUALITIES TESTING
Dieter Thomas *In* AGARD, Flying Qualities Feb. 1991 12 p (For primary document see N91-23108 15-05)
Copyright Avail: NTIS HC/MF A17; Non-NATO Nationals requests available only from AGARD/Scientific Publications Executive

A veteran test pilot discusses the need for flight test engineers to listen to test pilot opinion in designing cockpits and flight control systems. Through personal experiences, the test pilot illustrates the practical evaluation of good flying qualities and techniqes used in this evaluation for the promotion of air safety through the expression of pilot opinion. K.S.

N91-23110# McDonnell-Douglas Helicopter Co., Mesa, AZ.
ADFCS AND NOTAR (TRADEMARK): TWO WAYS TO FIX FLYING QUALITIES
Channing S. Morse *In* AGARD, Flying Qualities Feb. 1991 13 p (For primary document see N91-23108 15-05)
Copyright Avail: NTIS HC/MF A17; Non-NATO Nationals requests available only from AGARD/Scientific Publications Executive

The development, flight tests, and flying qualities of the Advanced Digital Flight Control System (ADFCS) and No Tail Rotor (NOTAR) System for military helicopters are reviewed. Emphasis is placed on some of the directional control problems faced on the ADFCS program in left sideward flight and the potential for the NOTAR system to improve the flying qualities of an advanced, highly augmented rotorcraft. Author

N91-23111# Air Force Flight Dynamics Lab., Wright-Patterson AFB, OH.
MIL-STD-1797 IS NOT A COOKBOOK
David B. Leggett and G. Thomas Black (Aeronautical Systems Div., Wright-Patterson AFB, OH.) *In* AGARD, Flying Qualities Feb. 1991 19 p (For primary document see N91-23108 15-05)
Copyright Avail: NTIS HC/MF A17; Non-NATO Nationals requests available only from AGARD/Scientific Publications Executive

Despite many years of experience, some confusion still exists concerning the nature, purpose, and application of the flying qualities specifications. Much of this confusion stems from the form of the requirements themselves. A question frequently raised is whether flying qualities are pilot-oriented properties or whether they are the parameters defined in the requirements of the flying qualities specification. This question arises from the fact that most of the objective criteria in the specification are not closed-loop (pilot-in-the-loop) performance criteria or pilot acceptance criteria, but rather are criteria on open-loop (pilot-out-of-the loop) characteristics of the augmented aircraft. Another source of confusion concerns the role of the specification itself: is it only a contractual document, or is it also a design guide. If the latter, is it equally effective in both roles. Consideration of the above questions leads to yet another. If the specification is intended as a design guide and the criteria are open-loop properties instead of closed-loop properties, which is more important: pilot satisfaction with closed-loop performance or compliance with the open-loop requirements? These questions are addressed by reviewing the background of the United States military flying qualities specifications. The advantages and disadvantages of different types of requirements are discussed. The way the specification is used by the USAF Aeronautical Systems Division Program offices is described. Author

N91-23112# Aeritalia S.p.A., Turin (Italy). Flight Mechanics Group.

FLYING QUALITIES EXPERIENCE ON THE AMX AIRCRAFT

Bava Renzo *In* AGARD, Flying Qualities Feb. 1991 20 p (For primary document see N91-23108 15-05)

Copyright Avail: NTIS HC/MF A17; Non-NATO Nationals requests available only from AGARD/Scientific Publications Executive

The AMX is a subsonic ground attack aircraft with a fly-by-wire flight control system (FCS) built into a digital flight control computer. From the flight mechanics point of view, it was designed against the MIL-F87985-C requirement. For some specific flight tasks, the need of more demanding requirements was envisaged. Modern handling qualities criteria were applied in the area of longitudinal and lateral-directional precision tracking task and pilot-induced oscillation (PIO) tendencies to cope with operational problems. High incidence criteria were used in the design and evaluation of control modifications which improve the flying qualities in the stall and post stall regions. Comparisons between analytical predictions, manned simulation, and in-flight results were made. Indications of agreement or disagreement with data and new criteria are presented. Author

N91-23113# British Aerospace Public Ltd. Co., Preston (England). Military Aircraft Div.

THE DEVELOPMENT OF ALTERNATE CRITERIA FOR FBW HANDLING QUALITIES **c08**

J. C. Gibson *In* AGARD, Flying Qualities Feb. 1991 13 p (For primary document see N91-23108 15-05)

Copyright Avail: NTIS HC/MF A17; Non-NATO Nationals requests available only from AGARD/Scientific Publications Executive

Provision of robust flight control systems and structural mode stability margins and carefree handling in highly unstable combat aircraft with a wide range of store loading requires new methods for handling qualities optimization. The possibilities for new control modes and task-tailored handling were greatly enhanced by modern controls. This has led to development of many alternate criteria which were tried and tested in two digital fly by wire (FBW) research aircraft, the Experimental Aircraft Program (EAP) and Jaguar FBW, and were further developed for use in European fighter aircraft (EFA). They cover the field of flight path and attitude bandwidth, tracking dynamics and sensitivity, pilot-induced oscillation (PIO) prevention, and enhanced lateral directional damping. Derived as design guidelines with the facility to design for optimum rather than merely acceptable handling, more research is needed into formal boundaries for levels 1, 2, and 3 specifications. The criteria are reviewed and some are illustrated by example. Author

N91-23114# Deutsche Forschungsanstalt fuer Luft- und Raumfahrt, Brunswick (Germany, F.R.). Inst. fuer Flugmechanik.

DEVELOPMENT OF MIL-8785C INTO A HANDLING QUALITIES SPECIFICATION FOR A NEW EUROPEAN FIGHTER AIRCRAFT **c08**

E. Buchacker, H. Galleithner, R. Koehler, and M. Marchand *In* AGARD, Flying Qualities Feb. 1991 16 p (For primary document see N91-23108 15-05)

Copyright Avail: NTIS HC/MF A17; Non-NATO Nationals requests available only from AGARD/Scientific Publications Executive

For the development of the Tornado, which started in the sixties, a draft version of MIL 8785B was used as a guideline and specification for the flying qualities the airplane should have. No consideration was given at that time to the fact that requirements, which were based on mathematical models of the airplane, only considered the flight mechanics of the bare airframe. In most cases, a new airplane is sold on performance promises. The fact that a pilot has to be able to fly an airplane safely and efficiently in order to achieve full performance, especially in a combat airplane, is often forgotten. The Armed Forces are repeatedly disappointed with their aircraft when it becomes clear that it is impossible to achieve the promised performance for reasons of conflicting flying qualities issues which demand other than performance optimal trim schedules. This, coupled with the fact that there was not a lot of flying qualities research within the nations participating in the Tornado program, led to the situation that it is was more or less only during flight tests that the user realized the problems involved with full authority full time flight control systems. In the meantime, however, some research efforts have been initiated by government and industry that have provided some second thoughts on flying qualities requirements for highly augmented airplanes with a basically unstable pitch axis. Together with industry, the four nations involved in the European Fighter Aircraft (EFA) Program decided to initiate an effort to generate a flying qualities specification for EFA based on the MIL-F-8785C. Some of the issues discussed include the following: the equivalent system approach, high order requirements for the pitch axis, the carefree handling issue, roll performance, small lateral directional inputs, air combat, and stall and spin. Author

N91-23115# Aeronautical Systems Div., Wright-Patterson AFB, OH.

DO CIVIL FLYING QUALITIES REQUIREMENTS ADDRESS MILITARY MISSIONS FOR OFF-THE-SHELF PROCUREMENT

G. Thomas Black, Walter A. Grady (Test Wing, 4950th, Wright-Patterson AFB, OH), and Dann C. McDonald *In* AGARD, Flying Qualities Feb. 1991 8 p (For primary document see N91-23108 15-05)

Copyright Avail: NTIS HC/MF A17; Non-NATO Nationals requests available only from AGARD/Scientific Publications Executive

Off-the-shelf procurement of civil aircraft for use by the military services is a tradition dating back to the earliest days of aviation. This relieves the military of the responsibility for development costs, takes advantage of civil designs already in existence, and has resulted in the development of many capable military aircraft. However, while civil aircraft missions have remained relatively unchanged for over half a century, new military mission have continued to evolve. Yet, the military services still procure civil certified aircraft to accomplish these demanding missions. In the United States, Federal Aviation Regulations 23 and 25 and their predecessors are the certification standards for civil aircraft. The primary objective of these regulations is to insure a minimum standard of airworthiness. Flying qualities requirements make up only a small portion of these regulations, and address primarily static stability characteristics. This has sometimes led to undesirable flying qualities when attempting to perform demanding military mission with civil certificated aircraft. The unique military missions are addressed in the U. S. military flying qualities specification, MIL-STD-1797A, and its predecessors (MIL-F-8785 series). These military specification requirements are compared to the civil requirements to substantiate their applicability to off-the-shelf procurement. Specifically, where military and civil missions differ, military flying qualities requirements should be

invoked. To illustrate this, several examples are examined. Finally, the future of off-the-shelf procurement is contemplated, some implications discussed, and recommendations made. Author

N91-23116# Dornier System G.m.b.H., Friedrichshafen (Germany, F.R.).
HANDLING QUALITIES OF HIGHLY AUGMENTED UNSTABLE AIRCRAFT SUMMARY OF AN AGARD-FMP WORKING GROUP EFFORT **c08**
Horst Wuennenberg *In* AGARD, Flying Qualities Feb. 1991 6 p (For primary document see N91-23108 15-05)
Copyright Avail: NTIS HC/MF A17; Non-NATO Nationals requests available only from AGARD/Scientific Publications Executive

Methods and criteria which were found to be useful as design guides and for the evaluation of handling qualities of highly augmented aircraft are presented. It was the unanimous opinion of the members of the working group that no one method or criterion is adequate by itself, and that several or even all of the recommended criteria should be checked. Experience has shown that one metric may not show a deficiency that will be exposed by other criteria. Alternately, a configuration that passes several of the proposed criteria has a high probability of being accepted as desirable by most pilots. The major topics covered by the working group's report are listed. Author

N91-23117# Wright Research Development Center, Wright-Patterson AFB, OH.
THE HANDLING QUALITIES OF THE STOL AND MANEUVER TECHNOLOGY DEMONSTRATOR FROM SPECIFICATION TO FLIGHT TEST **c08**
David J. Moorhouse, Kevin D. Citurs, Richard W. Thomas, and Mark R. Crawford (Air Force Flight Test Center, Edwards AFB, CA.) *In* AGARD, Flying Qualities Feb. 1991 9 p (For primary document see N91-23108 15-05)
Copyright Avail: NTIS HC/MF A17; Non-NATO Nationals requests available only from AGARD/Scientific Publications Executive

The STOL and Maneuver Technology Demonstrator (S/MTD) development from the initial specification through current flight test results is discussed. Lessons learned with respect to individual specification criteria and design methodology are presented. Two areas are identified in which it is considered that the current criteria are inadequate: pitch axis requirements as a function of touchdown dispersion and the directional axis requirement for target tracking. Author

N91-23118# Pisa Univ. (Italy). Dipartimento di Ingregneria Aerospaziale.
METRICS FOR ROLL RESPONSE FLYING QUALITIES
Mario Innocenti *In* AGARD, Flying Qualities Feb. 1991 11 p (For primary document see N91-23108 15-05)
Copyright Avail: NTIS HC/MF A17; Non-NATO Nationals requests available only from AGARD/Scientific Publications Executive

Roll characteristics of highly augmented aircraft during compensating tasks such as tracking and landing are shown to present degraded flying qualities and unstable oscillations similar to those observed in the pitch axis. The ideas behind Gibson's method are extended to develop handling qualities criteria for the roll axis control system. The analysis is performed using an existing data base for highly augmented class IV aircraft and parameters such as roll time constant, systems delay, and loop sensitivity are considered for designing for good handling qualities and to evaluate control systems performance. Levels of flying qualities are determined in the time domain as well as in the frequency domain for both tracking and landing tasks. The presence of pilot induced oscillations and roll ratcheting are identified. Author

N91-23119# Royal Aerospace Establishment, Bedford (England).
HANDLING QUALITIES GUIDELINES FOR THE DESIGN OF FLY-BY-WIRE FLIGHT CONTROL SYSTEMS FOR TRANSPORT AIRCRAFT **c08**
O. P. Nicholas, H. T. Huynh, W. P. deBoer, J. A. J. vanEngelen, and D. Shafranek (Deutsche Forschungsanstalt fuer Luft- und Raumfahrt, Brunswick, Germany, F.R.) *In* AGARD, Flying Qualities Feb. 1991 12 p (For primary document see N91-23108 15-05)
Copyright Avail: NTIS HC/MF A17; Non-NATO Nationals requests available only from AGARD/Scientific Publications Executive

The work of the GARTEUR Flight Mechanics Action Group 01 is summarized. The objectives, which concentrated on longitudinal control, are outlined. The flight control systems and the simulator trials are discussed. Existing handling qualities criteria and the Action Group's tentative proposals for handling qualities measures which can be applied to flight path control and system changeover are assessed. Finally, the Group's guidelines and recommendations for further work are reviewed. Author

N91-23120# Calspan Advanced Technology Center, Buffalo, NY. Flight Research Dept.
THE FLYING QUALITIES INFLUENCE OF DELAY IN THE FIGHTER PILOT'S CUING ENVIRONMENT
Randall E. Bailey *In* AGARD, Flying Qualities Feb. 1991 25 p (For primary document see N91-23108 15-05)
(Contract F33615-83-C-3603)
Copyright Avail: NTIS HC/MF A17; Non-NATO Nationals requests available only from AGARD/Scientific Publications Executive

Flight testing has amply demonstrated the serious flying qualities deficiencies that can occur from excessive control system delay. Delay outside of the control system, yet within the pilot's cuing environment, can be potentially as deleterious as control system delay effects. Summarized here are the results of flight tests to evaluate the effect on flying qualities on time delay in the pilot's cuing environment introduced outside the flight control system. These delays were introduced in the tactile cuing, head-up display visual cuing, and the motion and visual cuing during the simulation of fighter aircraft. Author

N91-23121# Systems Technology, Inc., Hawthorne, CA.
ESTIMATION OF PILOT RATINGS VIA PILOT MODELING
Duane McRuer *In* AGARD, Flying Qualities Feb. 1991 24 p (For primary document see N91-23108 15-05)
Copyright Avail: NTIS HC/MF A17; Non-NATO Nationals requests available only from AGARD/Scientific Publications Executive

In well-designed flying qualities experiments, pilot ratings and commentaries become fundamental indicators of pilot and system dynamic behavior, system performance, and pilot workload. Accordingly, they are intrinsically associated with pilot models. Some of these connections are summarized. A brief review of appropriate pilot dynamic models is followed by an introduction to pilot ratings in general. One approach that has been used to connect the pilot's assessments to pilot and pilot-vehicle system dynamics, is to associate pilot and system dynamic and performance characteristics with ratings using functional relationships. Representative forms of pilot rating functionals are given and illustrated by an extensive cross section of examples. A means of combining single axis ratings into a multi-axis estimate is developed. The development relies on workload and attentional demand concepts, although the ultimate combination rules have a validity based on experiment which transcends any such basis. Also covered is a clinical approach to rating estimates, which is more general and does not rely directly on empirical correlations. Author

N91-23122# National Aeronautical Establishment, Ottawa (Ontario). Flight Research Lab.
AN INITIAL STUDY INTO THE INFLUENCE OF CONTROL STICK CHARACTERISTICS ON THE HANDLING QUALITIES OF A FLY-BY-WIRE HELICOPTER
J. Murray Morgan *In* AGARD, Flying Qualities Feb. 1991 13 p Sponsored in part by Department of National Defence, Ottawa, Ontario (For primary document see N91-23108 15-05)
Copyright Avail: NTIS HC/MF A17; Non-NATO Nationals requests available only from AGARD/Scientific Publications Executive

A piloted experiment was flown using the Institute for Aerospace Research Bell 205A variable stability helicopter. The experimental

variables were the static and dynamic characteristics of a conventional center-mounted cyclic controller. The cyclic controller characteristics were changed by varying the mass and spring gradient to provide five basic cases, while for each case the dynamics of the stick were varied to provide critically damped, underdamped, and overdamped models. Two pilots were asked to fly a variety of tasks designed to exercise three fundamental modes of helicopter flight, high frequency stabilization, gross single axis tasks with off axis stabilization and simultaneous multi axis control. The stick sensitivity was adjusted in proportion to the spring gradient to give constant static sensitivity with respect to applied force. A first order filter was incorporated on an optional basis to reduce the command response bandwidth of the roll channel to the Level 1/Level 2 boundary of the ADS-33C criterion for divided attention operation. The results achieved indicate that cyclic stick characteristics are of considerably less importance than had been previously thought, that large values of overdamping can be tolerated even in low frequency sticks, but that underdamped sticks should be avoided especially if the resonant frequency of the stick is close to an undesirable and easily excited aircraft mode. There was a suggestion that a boundary based on undamped natural frequency also existed. The results did not support the contention that inertia alone is enough to specify an acceptable/unacceptable boundary for stick design. Author

N91-23123# National Aeronautical Establishment, Ottawa (Ontario). Flight Research Lab.

AN INVESTIGATION INTO THE USE OF SIDE-ARM CONTROL FOR CIVIL ROTORCRAFT APPLICATIONS **c08**

S. W. Baillie and S. Kereliuk *In* AGARD, Flying Qualities Feb. 1991 12 p Prepared in cooperation with FAA, Atlantic City, NJ (For primary document see N91-23108 15-05)

Copyright Avail: NTIS HC/MF A17; Non-NATO Nationals requests available only from AGARD/Scientific Publications Executive

An evaluation of the handling qualities of civil rotorcraft incorporating force or displacement sensing side-arm controllers with varying degrees of control integration was carried out on the NAE Bell 205 Airborne Simulator. Evaluators were certification pilots from the FAA and Transport Canada. The results indicate that integrated 4-axis side-arm control is a viable option for civil rotorcraft operations, even when used in conjunction with very low levels of stability and control augmentation. Author

N91-23124# National Aeronautical Establishment, Ottawa (Ontario).

DETERMINATION OF DECISION-HEIGHT WINDOWS FOR DECELERATING IMC APPROACHES IN HELICOPTERS **c08**

Roger H. Hoh (Hoh Aeronautics, Inc., Lomita, CA.), S. W. Baillie, S. Kereliuk, and Joseph J. Traybar *In* AGARD, Flying, Qualities Feb. 1991 17 p Prepared in cooperation with Federal Aviation Administration, Atlantic City, NJ (For primary document see N91-23108 15-05)

Copyright Avail: NTIS HC/MF A17; Non-NATO Nationals requests available only from AGARD/Scientific Publications Executive

The basic limitations were defined of the pilot plus rotorcraft in making the transition from a very low decision height to a steady hover over the helipad. The term 'decision-height window' is defined as the limits of glideslope/localizer tracking errors, and groundspeed variations, that can exist at breakout to allow a safe visual transition to hover. The dimensions of the decision-height window can have a significant impact on the required rotorcraft handling qualities, and for setting autopilot coupler and flight director performance standards for decelerating instrument approaches in rotorcraft. Author

N91-23125# Dornier System G.m.b.H., Friedrichshafen (Germany, F.R.).

INTEGRATION OF HANDLING QUALITY ASPECTS INTO THE AERODYNAMIC DESIGN OF MODERN UNSTABLE FIGHTERS **c08**

Peter Mangold *In* AGARD, Flying Qualities Feb. 1991 30 p (For primary document see N91-23108 15-05)

Copyright Avail: NTIS HC/MF A17; Non-NATO Nationals requests available only from AGARD/Scientific Publications Executive

The following subject areas are covered: flightmechanical design of unaugmented stable configurations; design criteria for modern configurations with unstable characteristics in pitch; development of specific criteria for modern fighter configurations; and aerodynamic/flightmechanical pecularities of configurations. Author

N91-23126# Test Squadron (6510th), Edwards AFB, CA.

B-1B HIGH AOA TESTING IN THE EVALUATION OF A STALL INHIBITOR SYSTEM

Mark S. Sobota *In* AGARD, Flying Qualities Feb. 1991 21 p (For primary document see N91-23108 15-05)

Copyright Avail: NTIS HC/MF A17; Non-NATO Nationals requests available only from AGARD/Scientific Publications Executive

High angle-of-attack (AOA) B-1B flight tests were conducted to evaluate a flight control Stall Inhibitor System/Stability Enhancement Function (SIS/SEF). The SIS/SEF system was integrated into the basic B-1B flight control system because of an inherent stability problem in the B-1 aircraft design. The problem lies in the fact that aerodynamically the B-1 was stability limited and not lift limited. This resulted in a lack of longitudinal stability while operating at high AOA conditions with no warning or natural cues to the pilot that the aircraft was approaching an unstable region. To safely utilize all the available AOA at the higher gross weights demanded, some means of providing 'apparent' stability was essential to provide cues to the pilot of these stability limitations. Significant test results of the SIS/SEF flight test program are presented. Author

N91-23127*# National Aeronautics and Space Administration. Hugh L. Dryden Flight Research Facility, Edwards, CA.

FLYING QUALITIES OF THE X-29 FORWARD SWEPT WING AIRCRAFT

Lawrence A. Walchli (Wright Research Development Center, Wright-Patterson AFB, OH.) and Rogers E. Smith *In* AGARD, Flying Qualities Feb. 1991 13 p (For primary document see N91-23108 15-05)

Copyright Avail: NTIS HC/MF A17; Non-NATO Nationals requests available only from AGARD/Scientific Publications Executive CSCL 01C

An overview of the X-29 Forward Swept Wing Technology Demonstrator traces its development and test path during past years. Brief descriptions of the aircraft and its flight control system provide insight for evaluating this unique vehicle. The baseline flight control system provided a starting point for safe concept evaluation and envelope expansion for the aircraft. Subsequent up-dates resulted in performance levels favorably comparable to current fighter aircraft. Efforts are described for the current expansion of the X-29's capabilities into the high angle-of-attack (AOA) regime of flight. Control law changes have permitted all axis maneuvering to 40 deg AOA with pitch excursions to 66 deg, thereby exploiting the full potential of the X-29 forward swept wing configuration. Author

N91-23128# Deutsche Forschungsanstalt fuer Luft- und Raumfahrt, Brunswick (Germany, F.R.). Inst. fuer Flugmechanik.

HANDLING QUALITIES EVALUATION FOR HIGHLY AUGMENTED HELICOPTERS

Heinz-Juergen Pausder and Wolfgang vonGruenhagen *In* AGARD, Flying Qualities Feb. 1991 14 p (For primary document see N91-23108 15-05)

Copyright Avail: NTIS HC/MF A17; Non-NATO Nationals requests available only from AGARD/Scientific Publications Executive

The realization and utilization of the helicopter airborne simulator ATTHeS (Advanced Technology Testing Helicopter System) are described. The explicit model following control system which is designed for ATTHeS is briefly presented. The potential is reviewed of the simulation system which is illustrated by the overall system performance identified from flight test data. Due to the implemented explicit model following systems, the in-flight simulation facility is provided with the capability of a flexible and broad variation of

stability and control characteristics. Finally, results of a bandwidth phase delay study are presented and the influence of coupling on handling qualities evaluation is discussed. Author

N91-23129# Naval Air Development Center, Warminster, PA. Flight Dynamics Branch.
AGILITY: A RATIONAL DEVELOPMENT OF FUNDAMENTAL METRICS AND THEIR RELATIONSHIP TO FLYING QUALITIES
C. J. Mazza *In* AGARD, Flying Qualities Feb. 1991 7 p (For primary document see N91-23108 15-05)
Copyright Avail: NTIS HC/MF A17; Non-NATO Nationals requests available only from AGARD/Scientific Publications Executive

The results of the first phase of a three year agility program are presented. A highly valuable approach was produced for developing a rational concept of agility and for relating agility to the flight dynamics, maneuvering performance, and to the design of the aircraft. The flight mechanics of a rigid aircraft in three-space maneuvering flight are examined with respect to total velocity, acceleration, and the time-rate-of-change of accleration. The terms of the expanded 'agility vector' are interpreted with regard to their potential for providing a rational basis for the evaluation of any given set of agility metrics and for suggesting, directly, a new set of metrics. A potential form of agility is offered for which a readily acceptable relationship is traced to both flying qualities and maneuvering performance. Author

N91-23130# British Aerospace Public Ltd. Co., Preston (England). Military Aircraft Div.
A REVIEW OF HIGH ANGLE OF ATTACK REQUIREMENTS FOR COMBAT AIRCRAFT
K. McKay and M. J. Walker *In* AGARD, Flying Qualities Feb. 1991 12 p (For primary document see N91-23108 15-05)
Copyright Avail: NTIS HC/MF A17; Non-NATO Nationals requests available only from AGARD/Scientific Publications Executive

Design of an aircraft for use at high angles of attack can have major implications on the configuration which is chosen. The objective is to review the implications of designing for high angle of attack on configuration. This naturally leads onto consideration of agility and the criteria which could be used in the early design stages to ensure an aircraft is adequately agile. Author

N91-23131# Messerschmitt-Boelkow-Blohm G.m.b.H., Munich (Germany, F.R.).
X-31A AT FIRST FLIGHT
W. B. Herbst *In* AGARD, Flying Qualities Feb. 1991 8 p (For primary document see N91-23108 15-05)
Copyright Avail: NTIS HC/MF A17; Non-NATO Nationals requests available only from AGARD/Scientific Publications Executive

The X-31A accomplished its first flight on October 11, 1990. A summary is presented about objectives of this international experimental flight test development program, its status, and follow-on planning. Author

N91-23132 Stanford Univ., CA.
A NEW ARCHITECTURE AND EXPERT SYSTEM FOR AIRCRAFT DESIGN SYNTHESIS Ph.D. Thesis
Masami Takai 1990 223 p
Avail: Univ. Microfilms Order No. DA9102359

Described here is a new program architecture which satisfies the requirement that preliminary design tools accommodate unprecedented extendability in both the sets of variables used to describe the design and the set of analysis routines. In this architecture, a set of procedural modules are compiled separately and linked with the main executive program. Unlike conventional programs, the subroutines and order of execution are selected by the system during the computation, based on the desired output and on the currently available results in the database. The method can greatly improve the efficiency of aircraft design optimization by generating the computational path for a given objective function and avoiding redundant calculations made by conventional methods with rigid program structures. The quasi-procedural architecture is enhanced by a rule-based expert system. The expert system warns of problems with the current design and suggests solutions to make the design feasible. For design optimization, the expert system can identify the active constraints and suggest a set of design variables to satisfy the constraints while best retaining the objective value. Dissert. Abstr.

N91-23133*# National Aeronautics and Space Administration. Hugh L. Dryden Flight Research Facility, Edwards, CA.
BUFFET INDUCED STRUCTURAL/FLIGHT-CONTROL SYSTEM INTERACTION OF THE X-29A AIRCRAFT
David F. Voracek and Robert Clarke Apr. 1991 15 p Presented at the 32nd AIAA Structures, Structural Dynamics, and Materials Conference, Baltimore, MD, 8-10 Apr. 1991 Previously announced in IAA as A91-32012
(NASA-TM-101735; H-1687; NAS 1.15:101735; Paper-91-1053)
Avail: NTIS HC/MF A03 CSCL 01C

High angle-of-attack flight regime research is currently being conducted for modern fighter aircraft at the NASA Ames Research Center's Dryden Flight Research Facility. This flight regime provides enhanced maneuverability to fighter pilots in combat situations. Flight research data are being acquired to compare and validate advanced computational fluid dynamic solutions and wind-tunnel models. High angle-of-attack flight creates unique aerodynamic phenomena including wing rock and buffet on the airframe. These phenomena increase the level of excitation of the structural modes, especially on the vertical and horizontal stabilizers. With high gain digital flight-control systems, this structural response may result in an aeroservoelastic interaction. A structural interaction on the X-29A aircraft was observed during high angle-of-attack flight testing. The roll and yaw rate gyros sensed the aircraft's structural modes at 11, 13, and 16 Hz. The rate gyro output signals were then amplified through the flight-control laws and sent as commands to the flaperons and rudder. The flight data indicated that as the angle of attack increased, the amplitude of the buffet on the vertical stabilizer increased, which resulted in more excitation to the structural modes. The flight-control system sensors and command signals showed this increase in modal power at the structural frequencies up to a 30 degree angle-of-attack. Beyond a 30 degree angle-of-attack, the vertical stabilizer response, the feedback sensor amplitude, and control surface command signal amplitude remained relatively constant. Data are presented that show the increased modal power in the aircraft structural accelerometers, the feedback sensors, and the command signals as a function of angle of attack. This structural interaction is traced from the aerodynamic buffet to the flight-control surfaces.
Author

N91-23134# Systems Control Technology, Inc., Arlington, VA.
AIR AMBULANCE HELICOPTER OPERATIONAL ANALYSIS Final Report
Robert Newman May 1991 168 p
(Contract DTFA01-87-C-00014)
(DOT/FAA/RD-91/7) Avail: NTIS HC/MF A08

This study of visual flight rules (VFR) weather minimums and operational areas for helicopter emergency medical service operators is based on operator responses to a questionnaire. The national average VFR operational weather minimums for all respondents was determined. Also, an estimate of the percentage of time that each respondent can not fly because of ceiling and/or visibility below their VFR operating minimums was determined, as was the average percentage of time all responders can not fly. Analysis of the data indicated that on the average the operators have voluntarily adopted stricter minimums than recommended in the current FAA Advisory Circular (AC) 135-14, 'Emergency Medical Services/Helicopter (EMS/H).' Furthermore, the analysis indicated that on the average the operators have more restrictive daylight minimums than those in the proposed change to AC 135-14 and less restrictive night minimums than those in the proposed change. Some general observations about minimums for operations in mountainous areas are also provided. The coverage areas reported by the operators were plotted on two maps of the United States, one for the local coverage areas and one for the cross country coverage areas. From these maps, the percentage of coverage for the conterminous United States, each FAA region, and each

state were determined. The weather data were also averaged over each state and used to determine the percentage of time that coverage is available in areas where EMS/H service is provided. The FAA is in the process of determining if there is an economic justification for the improvement of low altitude communication, navigation, and surveillance services within the National Airspace System (NAS). A recent FAA survey, Rotorcraft Low Altitude CNS Benefit/Cost Analysis (DOT/FAA/DS-89-11, Sept. 1989) found that the helicopter ambulance mission is a source of significant social benefit. The results of the Air Ambulance Helicopter Operational Analysis provides data which will support further analysis of the benefits of air ambulance helicopters in an IFR environment. Author

N91-23135*# National Aeronautics and Space Administration. Langley Research Center, Hampton, VA.
APPLICATION OF MULTIDISCIPLINARY OPTIMIZATION METHODS TO THE DESIGN OF A SUPERSONIC TRANSPORT
J.-F. M. Barthelemy, P. G. Coen, Gregory A. Wrenn, M. F. Riley, Augustine R. Dovi, and L. E. Hall (Unisys Corp., Detroit, MI.) Mar. 1991 7 p Presented at the North Atlantic Treaty Organization-AGARD Structures and Materials Panel Meeting, Bath, England, 1-2 May 1991
(NASA-TM-104073; NAS 1.15:104073) Avail: NTIS HC/MF A02 CSCL 01C

An optimization design method is discussed. This method is based on integrating existing disciplinary analysis and sensitivity analysis techniques by means of generalized sensitivity equations. A generic design system implementing this method is described. The system is being used to design the configuration and internal structure of a supersonic transport wing for optimum performance. This problem combines the disciplines of linear aerodynamics, structures, and performance. Initial results which include the disciplines of aerodynamics and structures in a conventional minimum weight design under static aeroelastic constraints are presented. Author

N91-23136*# McDonnell-Douglas Helicopter Co., Mesa, AZ.
TECHNOLOGY NEEDS FOR HIGH-SPEED ROTORCRAFT
John Rutherford, Matthew ORourke, Christopher Martin, Marc Lovenguth, and Clark Mitchell Apr. 1991 245 p
(Contract NAS2-13070)
(NASA-CR-177578; NAS 1.26:177578; L9KVAE-FR-91001) Avail: NTIS HC/MF A11 CSCL 01C

A study to determine the technology development required for high-speed rotorcraft development was conducted. The study begins with an initial assessment of six concepts capable of flight at, or greater than 450 knots with helicopter-like hover efficiency (disk loading less than 50 pfs). These concepts were sized and evaluated based on measures of effectiveness and operational considerations. Additionally, an initial assessment of the impact of technology advances on the vehicles attributes was made. From these initial concepts a tilt wing and rotor/wing concepts were selected for further evaluation. A more detailed examination of conversion and technology trade studies were conducted on these two vehicles, each sized for a different mission. Author

N91-23137# Deutsche Forschungsanstalt fuer Luft- und Raumfahrt, Cologne (Germany, F.R.). Hauptabt. Verkehrsforschung.
THE LIMITS OF THE LANDING PROCESS OF AIRCRAFT
Hanns-Juergen Peters Apr. 1990 120 p In GERMAN; ENGLISH summary
(DLR-FB-90-49; ISSN-0939-2963; ETN-91-99069) Avail: NTIS HC/MF A06; DLR, Wissenschaftliches Berichtswesen, VB-PL-DO, Postfach 90 60 58, 5000 Cologne, Fed. Republic of Germany, HC 45 DM

A Monte Carlo model is used for examining the aircraft landing process. Distributions of arrivals in Terminal Maneuvering Area (TMA) and admissible minimal distances in final approach are the input data. The arrival distribution of some airports are replaced by the Poisson distribution, which is modified by variation of its parameter lambda. In the model, the aircraft distances can be changed by integer steps of one minute. Different distances are necessary to meet German special safety rules, with respect to air vortices caused by preflying aircraft. Results yielded are the maximal numbers of aircrafts in final approach, average rates of landings per hour depending on lambda, and aircraft distances. ESA

N91-23138# Aeronautical Research Inst. of Sweden, Stockholm. Structures Dept.
LONG TIME MEASUREMENTS OF LANDING GEAR LOADS ON SAAB SF-340 COMMUTER AIRCRAFT
A. I. Gustavsson, A. F. Blom, and L. Helmersson (Saab-Scania, Linkoping, Sweden) Dec. 1990 27 p Sponsored by Swedish Board for Technical Development; Swedish Civil Aviation Administration; and Saab-Scania, Linkoeping, Sweden
(FFA-TN-1990-53; ETN-91-99107) Avail: NTIS HC/MF A03

Strain gauge measurements of forces acting on the nose gear and main gears of the commuter aircraft SAAB SF-340 are reported. During initial flight tests, forces in the longitudinal, transversal, and vertical directions were measured for various maneuvers such as takeoff, landing, taxiing, and towing. The investigation revealed high transversal loads at the main gears at touch down. The nose gear is most severely strained when steering during taxiing run and when the aircraft is towed connected to a tractor with a tow bar. The results from such initial measurements formed the basis for a subsequent investigation with on line data acquisition of landing gear loads on a commuter aircraft in service at Swedair AB. The data acquisition system and the data analysis methods are described. The data acquisition was continuously carried out during nearly six months including various parameters such as different aircraft weight and static landing gear loads. Results from these measurements are presented as cumulative exceedances of longitudinal, transversal, and vertical loads obtained from the rainflow count analyses performed online during the measurements. ESA

N91-23139# Aerospatiale, Chatillon (France). Div. Engins Tactiques.
PYROTECHNICAL SAFETY OF AEROSPATIALE TACTICAL MISSILES: APPLICATION TO CONVENTIONAL WARHEAD
Alain Grave 1991 7 p
(Rept-911-320-101; ETN-91-99272) Avail: NTIS HC/MF A02

A qualitative review of some past safety tests done on various in service conventional warheads is given. The diversity of tests configurations, fuel fire, bullet impact and sympathetic detonation is shown, and despite the difficulty of comparison with current standard tests, the situation is resumed. Work on the second generation Exocet anti-ship warhead, for which safety specifications were defined, is described. The use of composite (PBX) explosive loading was able to satisfy the safety requirements. Some aspects of current studies and developments from a safety point of view are given. ESA

N91-23140# Cranfield Inst. of Tech., Bedford (England). Dept. of Aerodynamics.
THE PERFORMANCE OF 60 DEG DELTA WINGS: THE EFFECTS OF LEADING EDGE RADIUS AND VORTEX FLAPS
B. K. Hu and J. L. Stollery Nov. 1989 24 p
(Cranfield-Aero-9002; ISBN-1-871564-03-4; ETN-91-99332)
Avail: NTIS HC/MF A03

Low speed wind tunnel tests were conducted on sharp edge flat 60 deg delta wing, the wing with leading edge vortex flap deflected 30 deg and 60 deg delta wing with well rounded leading edge to estimate the effects of leading edge vortex flap and leading edge radius on the aerodynamic performance of 60 deg delta wings. Results indicate that the leading edge vortex flap can increase lift/drag ratio of up to 19 pct., well rounded leading edge can increase further lift/drag ratio of up to 39 pct. ESA

N91-23141# Army Engineer Waterways Experiment Station, Vicksburg, MS. Environmental Lab.
ANALYTICAL STUDY OF THE EFFECTS OF WEIGHT ON LIGHT HELICOPTER (LH) EXPOSURE TO GROUND-BASED WEAPONS Final Report, Aug. 1989 - Apr. 1990
Charles D. Hahn and Ken G. Hall Jan. 1991 151 p
(AD-A232024; WES/TR/EL-91-2) Avail: NTIS HC/MF A08 CSCL 01/3

In support of the U.S. Army Light Helicopter (LH) Program, the U.S. Army Engineer Waterways Experiment Station (WES) was directed by the U.S. Army Laboratory Command Survivability Management Office (SMO) to simulate typical LH missions using the WES Helicopter Mission Survivability (HELMS) Model and to determine the effect of increasing weight on aircraft exposure to ground-based weapons. This report describes the HELMS model and the missions simulated as well as the terrain used for the simulations. Simulation data are presented as well as the results of the study. GRA

N91-23142# General Accounting Office, Washington, DC. National Security and International Affairs Div.
STRATEGIC MISSILES: UNCERTAINTIES PERSIST IN THE ADVANCED CRUISE MISSILE (ACM) PROGRAM
Nov. 1990 7 p
(AD-A232058; GAO/NSIAD-91-35) Avail: NTIS HC/MF A02 CSCL 05/1

The Advanced Cruise Missile (ACM) program has been delayed for several years because of various cost, schedule, and performance problems. As a result of these problems and the resulting risk that additional production commitments would create in significant additional costs to repair and retrofit missiles, the Congress directed changes in the program in each of the last four years. Because of continued concern about the ACM's progress, the Chairman House Committee on Armed Services, asked GAO to evaluate the program. Specifically, GAO reviewed the ACM's procurement quantity, acquisition strategy, technical performance, production readiness, and cost. GRA

N91-23143# Naval Postgraduate School, Monterey, CA.
DESIGN AND CONSTRUCTION OF A COMPOSITE AIRFRAME FOR UAV RESEARCH M.S. Thesis
Jeffrey L. Ellwood Jun. 1990 86 p
(AD-A232422) Avail: NTIS HC/MF A05 CSCL 01/3

A half-scale Unmanned Aerial Vehicle (UAV) was designed and constructed from composite materials for the Flight Research Lab at the Naval Postgraduate School. The vehicle was designed as a technology demonstrator for two studies. First, the Tilted Ducted Fan (TDF) vertical flight capability engine and its stability and control systems, and second, for the tail configuration testing for longitudinal and lateral-directional stability enhancement of an existing tailless Unmanned Aerial Vehicle. Completion of these research and test objectives should provide the configuration requirements for a full-scale development vehicle with vertical takeoff and landing with transition to the forward flight mode. GRA

N91-23144# Wright State Univ., Dayton, OH.
A COMPUTER AIDED MULTIVARIABLE CONTROL SYSTEMS DESIGN TECHNIQUE WITH APPLICATION TO AIRCRAFT FLYING QUALITIES Final Report, Aug. 1987 - Aug. 1990
L. R. Pujara Jan. 1991 175 p
(Contract F33615-87-C-3615)
(AD-A232549; WRDC-TR-90-3069) Avail: NTIS HC/MF A08 CSCL 01/3

A computer aided multivariable control system design technique is developed for matching the frequency response of a compensated loop system with a given desired transfer function matrix over a frequency interval of interest. Two examples of application of the technique are provided as well as a simple robustness analysis of one the application examples. GRA

06 AIRCRAFT INSTRUMENTATION

Includes cockpit and cabin display devices; and flight instruments.

For related information see also *19 Spacecraft Instrumentation* and *35 Instrumentation and Photography.*

N91-23145# Naval Postgraduate School, Monterey, CA.
AN ENGINEERING STUDY OF ALTITUDE DETERMINATION DEFICIENCIES OF THE SERVICE AIRCRAFT INSTRUMENTATION PACKAGE (SAIP) M.S. Thesis
Steven R. Eastburg 1991 125 p
(AD-A232055) Avail: NTIS HC/MF A06 CSCL 01/4

Altitude determination errors of the U.S. Navy's Service Aircraft Instrumentation Package (SAIP), an airborne positioning pod, were examined in a multifaceted study involving in-flight evaluations, wind tunnel testing, and pressure sensitivity experiments. The original objectives of the research related to identifying aerodynamic sources of pod static pressure inaccuracies and recommending specific remedies to alleviate these errors. After an extensive evaluation, results revealed that the problem exists not in the aerodynamic measurement performance of the probe, but in the electronic circuitry residing within the Air Data Unit (ADU). The ADU houses multiple pressure transducers, each associated with different static and dynamic pressure ports, in a single module. This circuit configuration leads to electrical interference and an attendant degradation of the static pressure output voltage. Accurate static pressure voltages, which can be subsequently converted into appropriate SAIP barometric altitudes, are obtained by electrically isolating the three ADU dynamic pressure transducers from the single operative static pressure transducer and remaining ADU circuitry. GRA

N91-23146# United Technologies Corp., West Palm Beach, FL. Sikorsky Aircraft Div.
MECHANICAL COMPONENT DIAGNOSTIC SYSTEM Final Report, Oct. 1987 - May 1990
R. A. Sewersky Jan. 1991 56 p
(Contract DAAJ02-87-C-0015)
(AD-A232126; SER-701-640; AVSCOM-TR-90-D-24) Avail: NTIS HC/MF A04 CSCL 01/3

The Mechanical Component Diagnostic System (MCDS) research and development (R and D) program was designed to investigate and demonstrate the benefits of onboard data recording/processing and rotor tuning equipment for monitoring and diagnosis of mechanical subsystems on rotorcraft. The payoffs for such a concept include reduced aircraft vibration levels (with extended MTBF of electronics and mechanical systems as well as reduced crew fatigue), reduced maintenance flights, and early warning of component failures. This program demonstrates an approach to a practical, automated system which monitors certain mechanical subsystems, provides inflight vibration and control system status, and prescribes corrective actions to the maintainer. Various monitoring components were developed and integrated to demonstrate the concept. GRA

07 AIRCRAFT PROPULSION AND POWER

Includes prime propulsion systems and systems components, e.g., gas turbine engines and compressors; and onboard auxilliary power plants for aircraft.

For related information see also *20 Spacecraft Propulsion and Power, 28 Propellants and Fuels,* and *44 Energy Production and Conversion.*

N91-23147# Advisory Group for Aerospace Research and Development, Neuilly-Sur-Seine (France). Propulsion and Energetics Panel.
HYPERSONIC COMBINED CYCLE PROPULSION
Dec. 1990 474 p In ENGLISH and FRENCH Symposium held in Madrid, Spain, 28 May - 1 Jun. 1990

(AGARD-CP-479; ISBN-92-835-0594-8) Copyright Avail: NTIS HC/MF A20; Non-NATO Nationals requests available only from AGARD/Scientific Publications Executive

The proceedings of the symposium are presented. The symposium was arranged in the following sessions: (1) Technical review of hypersonic propulsion/mission requirements; (2) Propulsion concepts; (3) Air intake flow; (4) Turbomachinery; (5) Combustion and ram/scramjets; (6) Nozzle flow; and (7) High temperature materials. The present status in the broad subject of contributing to hypersonic combined cycle propulsion is discussed. Considerable progress in design and analysis, using computational fluid dynamics techniques are reported. For individual titles, see N91-23148 through N91-23178.

N91-23148# Sener S.A., Madrid (Spain).
HYPERSONIC PROPULSION: PAST AND PRESENT
C. SanchezTarifa *In* AGARD, Hypersonic Combined Cycle Propulsion Dec. 1990 24 p (For primary document see N91-23147 15-07)
Copyright Avail: NTIS HC/MF A20; Non-NATO Nationals requests available only from AGARD/Scientific Publications Executive

The change in the concept of hypersonic speed with time is briefly discussed. The evolution of the hypersonic propulsion is restricted to the history of the ramjets. Considering the abundance of literature on the subject, only the most remarkable achievements are reviewed. Less divulged historical events, such as the propulsion of helicopters by ramjets, are discussed in more detail, and special attention is given to the contributions of Spain to supersonic combustion. The present state of the hypersonic propulsion is examined. Some of the most demanding problems facing the propulsion system of the Aerospace Plane and the Hypersonic Cruise Aircraft are reviewed. Author

N91-23149# Office National d'Etudes et de Recherches Aerospatiales, Modane (France).
A STUDY OF SUPERSONIC AND HYPERSONIC RAMJET ENGINES IN FRANCE FROM 1950 TO 1974 (APPLICATION ON COMBINED CYCLE AIRCRAFT ENGINES) [L'ETUDE DU STATOREACTEUR SUPERSONIQUE ET HYPERSONIQUE EN FRANCE DE 1950 A 1974 (APPLICATION AUX MOTEURS COMBINES AEROBIES)]
Roger Marguet, Pierre Berton, and Francis Hirsinger *In* AGARD, Hypersonic Combined Cycle Propulsion Dec. 1990 16 p In FRENCH (For primary document see N91-23147 15-07)
Copyright Avail: NTIS HC/MF A20; Non-NATO Nationals requests available only from AGARD/Scientific Publications Executive

France has the potential for theoretical and experimental research on the ramjet engine which would allow its operational programs such as ASMP (Air Surface Medium Range by nuclear stress). The direction of these studies evolved trends for the future, especially in the area of very high speed and the use of combined engines. This is due in large part to significant national action on the ramjet engine during the period of 1951 to 1972, during which a number of flight tests or ground tests has proven the concepts of the conventional ramjet engine and the combined turbo-ramjet, as well as the dual mode hypersonic ramjet, the latter comes from a subsonic combustion after supersonic. These fixed point tests, on a large scale, were done in the ONERA wind tunnel at Modane. At the request of the organizers of the symposium, the status, main work, and results are reviewed which was conducted during this period in France. An analysis is made of the data. It is hoped that it will lead to more research on the hypersonic propulsion ramjet engine. Transl. by E.R.

N91-23150# Honeywell, Inc., Minneapolis, MN. Systems and Research Center.
NAVIGATION, GUIDANCE, AND TRAJECTORY OPTIMIZATION FOR HYPERSONIC VEHICLES **c04**
R. L. Schultz, M. J. Hoffman, A. M. Case, and S. I. Sheikh *In* AGARD, Hypersonic Combined Cycle Propulsion Dec. 1990 22 p Sponsored in part by AF (For primary document see N91-23147 15-07)
Copyright Avail: NTIS HC/MF A20; Non-NATO Nationals requests available only from AGARD/Scientific Publications Executive

A computationally efficient, real time trajectory optimization and guidance approach for hypersonic aircraft is described. The optimization algorithms compute, in-flight, minimum fuel trajectories within constraints from the current aircraft position to its final destination. In-flight trajectory computation can provide a high degree of vehicle autonomy which could greatly reduce aircraft ground support costs. The optimization approach is based on Euler-Lagrange theory and energy state approximations. A 3-D, spherical earth, aircraft motion model, with constraints on temperature, dynamic pressure and stall, is used. An exact optimal iterative solution and an approx. closed form feedback solution method are developed. In the exact approach, solutions are computed by iteration on adjoint constants. Each iteration requires a complete forward trajectory integration. In the approx. closed form feedback approach, the adjoint constants are expressed in terms of the states. No forward trajectory calculations are required, thus, the computations are minimal. Minimum fuel climb to orbit, powered abort, and unpowered abort trajectories are computed with both methods. The approx. closed form feedback solution closely matches the optimal iterative solution. A computationally efficient method for generating unpowered descent footprints is also described. Footprints are used to identify candidate landing sites under an engine failure or other emergency conditions, and to initiate final descent. A hypersonic vehicle guidance, navigation, and control configuration using the optimal closed form feedback guidance and the footprint generator is described. Author

N91-23151# Deutsche Forschungsanstalt fuer Luft- und Raumfahrt, Cologne (Germany, F.R.). Inst. fuer Antriebstechnik.
TRAJECTORY OPTIMIZATION CONSIDERATIONS FOR RAMJET ENGINES
Frans G. J. Kremer *In* AGARD, Hypersonic Combined Cycle Propulsion Dec. 1990 12 p (For primary document see N91-23147 15-07)
Copyright Avail: NTIS HC/MF A20; Non-NATO Nationals requests available only from AGARD/Scientific Publications Executive

For supersonic and hypersonic flight conditions with ramjets, trajectory calculations have to be coupled with the engine performances. In space transportation systems ramjet will be used in a relatively wide range of Mach numbers, and therefore not always near the optimum design point. Optimization of several physical parameters along the trajectory will be inevitable. Some of these parameters are discussed along with their importance for an ascent trajectory, having a minimum fuel requirement. Author

N91-23152# Societe Europeenne de Propulsion, Suresnes (France).
COMPARATIVE STUDY OF DIFFERENT SYSTEMS OF COMBINED CYCLE PROPULSION
Philippe Ramette, Dominique Scherrer, and Michel Doublier (Societe Nationale d'Etude et de Construction de Moteurs d'Aviation, Suresnes, France) *In* AGARD, Hypersonic Combined Cycle Propulsion Dec. 1990 11 p In FRENCH; ENGLISH summary (For primary document see N91-23147 15-07)
Copyright Avail: NTIS HC/MF A20; Non-NATO Nationals requests available only from AGARD/Scientific Publications Executive

Since 1986 the French Space Agency, CNES, is sponsoring some comparative studies of different concepts of combined cycle engines made jointly by SNECMA, SEP, and ONERA. SNECMA and SEP recently joined their efforts in combined cycle propulsion by creating a common Joint Venture named HYPERSPACE. The recent progress of comparative studies of different combined cycle engine systems is presented focusing on the following concepts: (1) the turborocket family including the turbo rocket-ramjet and the turbo expander-ramjet; (2) the turbojet family with the turbofan-ramjet and the turboramjet; (3) the rocket-ramjet; (4) the liquefied air rocket; (4) the cooled air rocket; and (5) the scramjet which is also presently in progress. The comparison of these concepts include their theoretical performance, some design considerations and an approximate evaluation of the technological difficulties with each concept. Author

N91-23153*# National Aeronautics and Space Administration. Langley Research Center, Hampton, VA.
HYPERSONIC PROPULSION: STATUS AND CHALLENGE
R. Wayne Guy *In* AGARD, Hypersonic Combined Cycle Propulsion Dec. 1990 19 p (For primary document see N91-23147 15-07)
Copyright Avail: NTIS HC/MF A20; Non-NATO Nationals requests available only from AGARD/Scientific Publications Executive CSCL 21E

Scientists in the U.S. are again focusing on the challenge of hypersonic flight with the proposed National Aerospace Plane (NASP). This renewed interest has led to an expansion of research related to high speed airbreathing propulsion, in particular, the supersonic combustion ramjet, or scramjet. The history is briefly traced of scramjet research in the U.S., with emphasis on NASA sponsored efforts, from the Hypersonic Research Engine (HRE) to the current status of today's airframe integrated scramjets. The challenges of scramjet technology development from takeover to orbital speeds are outlined. Existing scramjet test facilities such as NASA Langley's Scramjet Test Complex as well as new high Mach number pulse facilities are discussed. The important partnership role of experimental methods and computational fluid dynamics is emphasized for the successful design of single stage to orbit vehicles. Author

N91-23154# Industrieanlagen-Betriebsgesellschaft m.b.H., Ottobrunn (Germany, F.R.).
AIRBREATHING PROPULSION FOR SPACE TRANSPORT: NEW CONCEPTS, SPECIAL PROBLEMS AND ATTEMPTS AT SOLUTIONS
H. Kuenkler *In* AGARD, Hypersonic Combined Cycle Propulsion Dec. 1990 14 p (For primary document see N91-23147 15-07)
Copyright Avail: NTIS HC/MF A20; Non-NATO Nationals requests available only from AGARD/Scientific Publications Executive

The design requirements of airbreathing propulsion for space transport application strongly depend on the particular mission demands and differ markedly from those of conventional airbreathing propulsion systems. Especially the low thrust densities and high thermal loads at high Mach numbers demands a systematic approach to design and selection of possible propulsion concepts. Main problems of propulsion system concepts and of their development as well as to present attempts for possible solutions are discussed. Author

N91-23155# Wright Research Development Center, Wright-Patterson AFB, OH. Turbine Engine Div.
TURBOJET POTENTIAL FOR HYPERSONIC FLIGHT
Jeffrey M. Stricker and Douglas J. Essman *In* AGARD, Hypersonic Combined Cycle Propulsion Dec. 1990 11 p (For primary document see N91-23147 15-07)
Copyright Avail: NTIS HC/MF A20; Non-NATO Nationals requests available only from AGARD/Scientific Publications Executive

Over the past few years, interest in manned hypersonic flight has increased significantly. The disadvantages of a three mode propulsion system (turbojet/ramjet/scramjet) are the complexity, weight, and costs which accompany it. Inlet and exhaust geometry variations required for proper integration play a major role. The utilization is explored of the turbine engine for aircraft propulsion up to the scramjet transition. Examination of the uninstalled cycle performance is presented as well as an assessment of installed engine operation in a hydrogen fueled aircraft. Both non-afterburning and afterburning turbine engines are compared to turboramjet and air turboramjet (ATR) engines for a Mach 5 long duration cruise mission along with a pure acceleration mission, i.e., the turbomachinery is used to accelerate the vehicle to a Mach number where the scramjet can take over. From this assessment, a baseline engine configuration/cycle is defined for feasibility studies and critical technology identification. A discussion of the feasibility of the perferred concept from an engine component by component standpoint is provided as well as a discussion of technology risk compared to the state of the art. Author

N91-23156# Fiat Aviazione S.p.A., Turin (Italy).
AIRBREATHING PROPULSION FOR TRANSATMOSPHERIC FLIGHT
G. Andrei, U. Borio, and M. Maiurano *In* AGARD, Hypersonic Combined Cycle Propulsion Dec. 1990 11 p (For primary document see N91-23147 15-07)
Copyright Avail: NTIS HC/MF A20; Non-NATO Nationals requests available only from AGARD/Scientific Publications Executive

The application of airbreathing propulsion systems to winged launchers is examined. The characteristics of ramjet based, LH2 fueled, powerplants are analyzed. The main ramjet design parameters are highlighted. Options (rockets, turboengines) for the boost phase from takeoff to ramjet mode transition are described, and their potential applicability to Single Stage to Orbit (SSTO) and Two Stage to Orbit (TSTO) launcher is discussed. Author

N91-23157# Office National d'Etudes et de Recherches Aerospatiales, Paris (France).
COMPACT HEAT EXCHANGER FOR AN INVERSE COMPONENTS ENGINE [ECHANGEUR COMPACT POUR MONTEUR A COMPOSANTS INVERSES (MCI)]
Yves Ribaud *In* AGARD, Hypersonic Combined Cycle Propulsion Dec. 1990 10 p In FRENCH; ENGLISH summary (For primary document see N91-23147 15-07)
Copyright Avail: NTIS HC/MF A20; Non-NATO Nationals requests available only from AGARD/Scientific Publications Executive

A presizing study on a counter current heat exchanger fitted for the inverse components engine (ICE) was performed first using analytical calculations and then with a calculation code. The first calculation results show that the heat exchanger integration on the engine axis seems to be possible without a too great penalty on weight and length. The future main research purpose will be directed towards the reduction of the turbine exhaust section. Author

N91-23158# Aerojet TechSystems Co., Sacramento, CA. Aeropropulsion.
DESIGN CONSIDERATIONS FOR COMBINED AIR BREATHING-ROCKET PROPULSION SYSTEMS
David L. Kors *In* AGARD, Hypersonic Combined Cycle Propulsion Dec. 1990 13 p Previously announced in IAA as A91-14442 (For primary document see N91-23147 15-07)
(AIAA-90-0098) Copyright Avail: NTIS HC/MF A20; Non-NATO Nationals requests available only from AGARD/Scientific Publications Executive

Combined air breathing rocket propulsion systems have been studied and carried through proof of principle demonstrations during the last three decades. Currently, a number of countries are studying and in some cases actually starting development of demonstrator vehicles for hypersonic flight which use combinations of air breathing and rocket propulsion. A summary of this activity including the propulsion options being studied is discussed. This type of propulsion is much more revolutionary in nature than most previous propulsion developments and thus results in technology challenges that are even more severe than those faced by either conventional air breathing propulsion or rocket designers. These include: (1) propulsion/vehicle integration; (2) engine stability over a wide operating range; (3) high performance over a wide operating range; (4) system level thermal management; and (5) advanced materials. A discussion of these technical issues including the impact of underachieved development goals on system level performance is also included. Author

N91-23159*# National Aeronautics and Space Administration, Washington, DC.
CRYOGENIC HYDROGEN-INDUCED AIR-LIQUEFACTION TECHNOLOGIES
William J. D. Escher *In* AGARD, Hypersonic Combined Cycle Propulsion Dec. 1990 13 p (For primary document see N91-23147 15-07)
Copyright Avail: NTIS HC/MF A20; Non-NATO Nationals requests available only from AGARD/Scientific Publications Executive CSCL 21E

Extensive use of a special advanced airbreathing propulsion archives data base, as well as direct contacts with individuals who were active in the field in previous years, a technical assessment of cryogenic hydrogen induced air liquefaction, as a prospective onboard aerospace vehicle process, was performed and documented in 1986. The resulting assessment report is summarized. Technical findings relating the status of air liquefaction technology are presented both as a singular technical area, and also as that of a cluster of collateral technical areas including: Compact lightweight cryogenic heat exchangers; Heat exchanger atmospheric constituents fouling alleviation; Para/ortho hydrogen shift conversion catalysts; Hydrogen turbine expanders, cryogenic air compressors and liquid air pumps; Hydrogen recycling using slush hydrogen as heat sinks; Liquid hydrogen/liquid air rocket type combustion devices; Air Collection and Enrichment System (ACES); and Technically related engine concepts. Author

N91-23160# Office National d'Etudes et de Recherches Aerospatiales, Paris (France).
SUPERSONIC-HYPERSONIC INLET STUDIES FOR AEROSPACEPLANE
C. Sans, P. Champigny, P. Duveau, and C. Ginovart *In* AGARD, Hypersonic Combined Cycle Propulsion Dec. 1990 11 p In FRENCH; ENGLISH summary (For primary document see N91-23147 15-07)
Copyright Avail: NTIS HC/MF A20; Non-NATO Nationals requests available only from AGARD/Scientific Publications Executive

Recent improvements in technology have allowed the design of rockets to launch satellites. Reusable shuttles were then used to limit launch costs. A new stage is needed for horizontal takeoff and landing aerospace planes. These single or two stage vehicles will need new propulsion systems, able to provide enough thrust in the whole flight corridor. Mixed propulsion systems seem to be well adapted to this need. During atmospheric flight air breathing engines are necessary to improve performances. Thus inlets will have to be installed. The success of this project will depend on the choice of the inlets, for which mass flow ratios is a paramount objective. Pressure recovery seems to be of less importance at high Mach numbers because of structural stresses. Current design methods are examined which are based on: (1) semiempirical predictions, using experimental data bases, shock boundary layer interaction laws, shock and side overflow losses; (2) 2-D and 3-D Euler codes taking into account the internal bleed effects; and (3) Navier-Stokes codes for specific problems. Some examples of inlet design are presented for rocket ramrocket engines. Problems of inlet integration are presented. Author

N91-23161# Cranfield Inst. of Tech., Bedford (England). Coll. of Aeronautics.
SOME ASPECTS OF SHOCK-WAVE BOUNDARY LAYER INTERACTION RELEVANT TO INTAKE FLOWS **c02**
J. L. Stollery *In* AGARD, Hypersonic Combined Cycle Propulsion Dec. 1990 14 p (For primary document see N91-23147 15-07)
Copyright Avail: NTIS HC/MF A20; Non-NATO Nationals requests available only from AGARD/Scientific Publications Executive

Four main topics are discussed: (1) 2-D shock induced separation; (2) 3-D glancing interaction; (3) shock/shock boundary layer interaction; and (4) hypersonic viscous interaction. Wherever possible both laminar and turbulent flows are considered and reference is made to experimental data and to the results of mathematical modeling. Some thoughts on future research topics are presented along with the facilities needed to pursue them. Author

N91-23162*# National Aeronautics and Space Administration. Lewis Research Center, Cleveland, OH.
COMPUTATIONAL MODELING AND VALIDATION FOR HYPERSONIC INLETS **c02**
Louis A. Povinelli *In* AGARD, Hypersonic Combined Cycle Propulsion Dec. 1990 10 p Previously announced as N90-22011 (For primary document see N91-23147 15-07)
Copyright Avail: NTIS HC/MF A20; Non-NATO Nationals requests available only from AGARD/Scientific Publications Executive CSCL 01A

Hypersonic inlet research activity at NASA is reviewed. The basis is the experimental tests performed with three inlets: the NASA-Lewis Mach 5, the McDonnell Douglas Mach 12, and the NASA-Langley Mach 18. Both 3-D parabolized Navier-Stokes and Navier-Stokes codes were used to compute the flow within the three inlets. Modeling assumptions in the codes involve the turbulence model, the nature of the boundary layer, shock wave boundary layer interaction, and the flow spilled to the outside of the inlet. Use of the codes in conjunction with the experimental data are helping to develop a clearer knowledge of the inlet flow physics and to focus on the modeling improvements required in order to arrive at validated codes. Author

N91-23163# Rolls-Royce Ltd., Bristol (England). Turbine Technology Dept.
DESIGN CONSIDERATIONS OF A HIGH EXPANSION RATIO HYDROGEN TURBINE
A. T. Holmes and R. Varvill *In* AGARD, Hypersonic Combined Cycle Propulsion 8 p(SEE N91-23147 15-07) Dec. 1990 (For primary document see N91-23147 15-07)
Copyright Avail: NTIS HC/MF A20; Non-NATO Nationals requests available only from AGARD/Scientific Publications Executive

The high specific heat of hydrogen compared with air leads to turbine stages which have low pressure ratios for comparable levels of specific work. In high speed propulsion systems designed for reusable space launch vehicles, the choice of scantlings is influenced by the need to minimize weight consistent with the achievement of the required efficiency. The effect of unit increase of mass in a component is, typically, to increase the takeoff weight by approximately five units, and efficiencies significantly lower than those of normal aero-gas turbine practice are adopted. A multi-stage turbine design with overall pressure ratio of 7.6 and overall loading delta H/ u squared = 31.4 is described. A parametric study covering a range of mean diameters and number of stages was performed, in which the aim was to establish the trends of efficiency against weight. The final design has ten stages with a common hub diameter. Author

N91-23164# Deutsche Forschungsanstalt fuer Luft- und Raumfahrt, Cologne (Germany, F.R.). Inst. fuer Antriebstechnik.
AERODYNAMICS AND STABILIZATION OF COMBUSTION OF HYDROGEN JETS INJECTED INTO SUBSONIC AIRFLOW **c02**
J. Koopman, M. Rachner, H. Wiegand, and H. Eickhoff *In* AGARD, Hypersonic Combined Cycle Propulsion Dec. 1990 16 p (For primary document see N91-23147 15-07)
Copyright Avail: NTIS HC/MF A20; Non-NATO Nationals requests available only from AGARD/Scientific Publications Executive

The aerodynamics and stabilization of burning hydrogen jets, injected transversally into a subsonic airstream, were investigated. The structural behavior of deflecting cold and burning jets were studied by flow visualization. Experiments and numerical analysis on jet penetration were performed. Flame extinction limits of 'wake stabilized' flames were established and correlated. Author

N91-23165# Technische Univ., Munich (Germany, F.R.).
EXPERIMENTAL INVESTIGATIONS ON THE TRANSITION FROM STABLE TO UNSTABLE COMBUSTION BY MEANS OF ACTIVE INSTABILITY CONTROL **c25**
S. Gleis, D. Vortmeyer, and W. Rau *In* AGARD, Hypersonic Combined Cycle Propulsion 7 p(SEE N91-23147 15-07) Dec. 1990 (For primary document see N91-23147 15-07)
Copyright Avail: NTIS HC/MF A20; Non-NATO Nationals requests available only from AGARD/Scientific Publications Executive

The interaction of numerous parameters affect excitation and development of combustion instabilities, and determine the excited acoustic modes. Therefore, to avoid combustion stabilities, it is essential to make out the sources of disturbances and to interrupt the feedback loop. The newly developed method of 'Active Instability Control' (AIC) opens experimental opportunities for this kind of diagnostics, because after having stabilized the oscillating

system it starts to oscillate again if the AIC-system is switched off. It takes about 300 msec until the oscillation is again fully developed. During this transition period the combustion chamber pressure was registered, the intensity of chemical reaction and the flame contours time resolved by high-speed/Schlieren-cinematography. Experiments with a laboratory combustor showed, that during the onset of instability various mechanisms of excitation can be observed. Further investigations pointed out that although vortex shedding is an important driving force for oscillations, it is not the origin for instability. Author

N91-23166# Johns Hopkins Univ., Laurel, MD. Applied Physics Lab.

DESIGN TECHNIQUES FOR DUAL MODE RAM-SCRAMJET COMBUSTORS

F. S. Billig, S. Corda, and P. P. Pandolfini *In* AGARD, Hypersonic Combined Cycle Propulsion Dec. 1990 20 p (For primary document see N91-23147 15-07)

Copyright Avail: NTIS HC/MF A20; Non-NATO Nationals requests available only from AGARD/Scientific Publications Executive

A disciplined analytical method that describes the different engine operating modes and internal flow structures in dual mode ram-scramjet combustors is presented. Solutions for physical systems are dependent on empirical data bases from unit process experiments which include shock trains, jet penetration, and mixing. A synopsis of an experimental data base is presented and the method by which it is embodied in the analytical models is discussed. The models are then applied to develop design procedures for combustor-inlet isolators, discrete hole injectors, controlled shear layer mixing, and establishes the efficacy of sudden expansion steps for anchoring shock trains. Author

N91-23167# Rockwell International Corp., Canoga Park, CA. Rocketdyne Div.

USE OF SECONDARY FLOWS FOR RAPID MIXING IN SCRAMJET COMBUSTORS

G. V. R. Rao and A. A. Heiba *In* AGARD, Hypersoic Combined Cycle Propulsion Dec. 1990 7 p (For primary document see N91-23147 15-07)

Copyright Avail: NTIS HC/MF A20; Non-NATO Nationals requests available only from AGARD/Scientific Publications Executive

An efficient scramjet combustor requires rapid mixing of parallel supersonic streams of air and injected fuel. The velocity differential between the two streams may not be enough for spreading the mixing layer. To augment the mixing process, secondary flows can be generated by a skewed supersonic nozzle for the fuel. A conical ramp that shields the injector can provide large lateral gradients in the airflow. The Unified Solution Algorithm (USA) code developed by Rockwell International was used to compute inviscid flow fields over typical configurations. The results are presented. The interaction of the pressure and density gradients in the air and fuel streams at the injector exit appears to be the major source of rapid mixing of the stream. Author

N91-23168# Toronto Univ., Downsview (Ontario). Inst. for Aerospace Studies.

PERFORMANCE CHARACTERISTICS OF HYPERSONIC DETONATION WAVE RAMJETS

T. M. Atamanchuk and J. P. Sislian *In* AGARD, Hypersonic Combined Cycle Propulsion Dec. 1990 13 p Previously announced in IAA as A90-42188 (For primary document see N91-23147 15-07)

Copyright Avail: NTIS HC/MF A20; Non-NATO Nationals requests available only from AGARD/Scientific Publications Executive

One method of heat addition to a supersonic flow is by means of shock-induced combustion or in this particular study a detonation wave. In order to assess the performance potential of a propulsion utilizing such a mode of heat addition a first order inviscid computational scheme based on Godunov's method was developed. This computational method was chosen since it allows the tracking of flow-field discontinuities such as shocks and slipstreams, thus making it possible to generate a vehicle geometry operating at design conditions for given freestream conditions. This same code was also used to determine the flow-field generated by a given body geometry at off-design conditions. Pressures acting on these planar and axisymmetric bodies were calculated and used to determine various performance parameters over a range of Mach numbers. Two configurations consisting of multiple shock external and internal inlet compression, followed by an oblique Chapman-Jouguet detonation wave, were considered. Aerodynamic performance of planar multiple external shock inlet compression vehicles acting as lifting-propulsive bodies (integrated engine-airframe configurations) were also investigated. Off-design performance of these geometries was evaluated by varying the heat addition to the flow in order to obtain the desired thrust-to-dray ratio. For most body geometries operating at flight Mach numbers less than the design Mach number, it was found that no value of heat addition would maintain the design thrust-to-drag ratio. However, for flight Mach numbers greater than the design Mach number it was found that there usually existed at least two values, and in some cases three, of heat addition which would give the design thrust-to-drag ratio. Author

N91-23169*# National Aeronautics and Space Administration. Ames Research Center, Moffett Field, CA.

ANALYTICAL AND EXPERIMENTAL INVESTIGATIONS OF THE OBLIQUE DETONATION WAVE ENGINE CONCEPT

Gene P. Menees, Henry G. Adelman, and Jean-Luc Cambier (Eloret Corp., Moffett Field, CA.) *In* AGARD, Hypersonic Combined Cycle Propulsion Dec. 1990 15 p (For primary document see N91-23147 15-07)

Copyright Avail: NTIS HC/MF A20; Non-NATO Nationals requests available only from AGARD/Scientific Publications Executive CSCL 21E

Wave combustors, which include the oblique detonation wave engine (ODWE), are attractive propulsion concepts for hypersonic flight. These engines utilize oblique shock or detonation waves to rapidly mix, ignite, and combust the air-fuel mixture in thin zones in the combustion chamber. Benefits of these combustion systems include shorter and lighter engines which require less cooling and can provide thrust at higher Mach numbers than conventional scramjets. The wave combustor's ability to operate at lower combustor inlet pressures may allow the vehicle to operate at lower dynamic pressures which could lessen the heating loads on the airframe. The research program at NASA-Ames includes analytical studies of the ODWE combustor using Computational Fluid Dynamics (CFD) codes which fully couple finite rate chemistry with fluid dynamics. In addition, experimental proof-of-concept studies are being performed in an arc heated hypersonic wind tunnel. Several fuel injection design were studied analytically and experimentally. In-stream strut fuel injectors were chosen to provide good mixing with minimal stagnation pressure losses. Measurements of flow field properties behind the oblique wave are compared to analytical predictions. Author

N91-23170# Prins Maurits Lab. TNO, Rijswijk (Netherlands).

THEORETICAL AND EXPERIMENTAL PERFORMANCE OF A SOLID FUEL RAMJET COMBUSTION CYCLE FOR HYPERSONIC FLIGHT CONDITIONS

P. J. M. Elands, P. A. O. G. Korting, R. G. Veraar, and P. Dijkstra (Technische Univ., Delft, Netherlands) *In* AGARD, Hypersonic Combined Cycle Propulsion Dec. 1990 11 p (For primary document see N91-23147 15-07)

Copyright Avail: NTIS HC/MF A20; Non-NATO Nationals requests available only from AGARD/Scientific Publications Executive

A research program was performed to validate a numerical simulation of the flow and combustion process in the combustion chamber of a solid fuel ramjet with experimental results. Operating conditions were chosen to represent a sustained missile flight at Mach 4 at an altitude of 13 km. Experimental data were obtained by burning cylindrical fuel grains made of polyethylene and hydroxyl terminated polybutadiene in a solid fuel ramjet using a connected pipe facility. For numerical simulation a computer code was developed, describing rotational symmetric steady-state turbulent reacting flows through channels with and without a sudden

expansion. Calculations were performed using polyethylene as a fuel. For the validation emphasis was laid on the regression rate. The results show that the computer code predicts the mean regression rate with reasonable accuracy. The value for the effective heat of gasification is found to be very important. The experiments and the calculations performed show the feasibility to apply a solid fuel ramjet for sustained hypersonic flight at these conditions. Author

N91-23171# Messerschmitt-Boelkow-Blohm G.m.b.H., Munich (Germany, F.R.).

HIGHLY INTEGRATED DUCTED ROCKET PROPULSION MODULES FOR FUTURE HYPERSONIC TACTICAL MISSILES **c20**

Hermann-L. Weinreich *In* AGARD, Hypersonic Combined Cycle Propulsion Dec. 1990 13 p (For primary document see N91-23147 15-07)

Copyright Avail: NTIS HC/MF A20; Non-NATO Nationals requests available only from AGARD/Scientific Publications Executive

Integrated airbreathing propulsion systems for future hypersonic tactical missiles were studied under funding of the German MOD. A 30 km range (Mach 5) antiradiation mission was selected for more detailed investigations. Main aspects for the missile/propulsion design are simple design with no or minimum geometrical variability, no ejecta during boost/sustain transition, and high average velocity (transition Mach number well above 3). To minimize the mass fraction of the required booster propellant an optimum, common (non-ejectable) boost/sustain nozzle must be adopted; the booster pressure should be optimized to use the strength potential of the ramcombustor structure; and the intake must be closed during boost to reudce drag and to avoid dangerous buzz. A special two position intake concept permits intake closure during boost, strating of the internal shock system, and cruisé flight with minimum external drag and high pressure recovery at transition Mach numbers. Based on promising test results of the DLR/Cologne obtained with a comparable intake model a new family of intakes with different internal compression ratio and lip-bluntness was designed. A boron loaded ducted rocket with subsonic self throttling gas generator flow was selected for cruise flight propulsion due to its simple design, excellent combustion stability, and the high level of existing experience. Even at combustor temperatures above the condensation temperature of boron-oxide, the volumetric impulse of boron loaded propellants remains attractive. The ducted rocket gas generator can be integrated within the missile freebody which also contains seeker, warhead, electric compartment, and missile controls. The missile flight control system is based on jet reaction using minirockets during boost and high pressure intake tap air during cruise. C/C material was adopted for the structural design. The superiority of the ducted rocket powered medium range antiradiation missile was demonstrated by comparison with a rocket powered missile having the same diameter and payload. For short range (6 to 12 km) low level missions the solid fuel ramjet with integral boost is an attractive propulsion concept. Author

N91-23172# Oxford Univ. (England). Dept. of Engineering Science.

PITOT SURVEYS OF TWO MODERATELY UNDER-EXPANDED JETS

T. M. Cain and T. V. Jones *In* AGARD, Hypersonic Combined Cycle Propulsion Dec. 1990 15 p (For primary document see N91-23147 15-07)

Copyright Avail: NTIS HC/MF A20; Non-NATO Nationals requests available only from AGARD/Scientific Publications Executive

In the free expansion of the exhaust gases of engines flying at altitudes suitable for air-breathing launchers, the turbulent shear layers interact with the jet shock structure, posing a challenge for CFD. A series of experiments in this flow regime is performed to provide data suitable for code validation. Angular and axial Pitot surveys of heated, high pressure, nitrogen jets exhausted from a Mach 3 conical nozzle into a low pressure tank are presented. The results indicate that there is strong turbulent mixing throughout the flow field downstream of the first Mach disk in addition to a repetitive shock cell structure. Author

N91-23173# Rockwell International Corp., Canoga Park, CA. Rocketdyne Div.

THE EFFECT OF COMBUSTOR FLOW NONUNIFORMITY ON THE PERFORMANCE OF HYPERSONIC NOZZLES

P. Goel, S. L. Barson, and S. D. Halloran *In* AGARD, Hypersonic Combined Cycle Propulsion Dec. 1990 18 p (For primary document see N91-23147 15-07)

(Contract F33657-87-C-2214)

Copyright Avail: NTIS HC/MF A20; Non-NATO Nationals requests available only from AGARD/Scientific Publications Executive

A parametric, 3-D Euler, CFD study was performed on a hypersonic vehicle engine nozzle. The configuration analyzed, though generic, is representative of those being considered for current generation vehicles. A series of flow profiles ranging from completely uniform to highly distorted were developed and introduced at the inflow plane of the nozzle in an effort to understand the associated impact on nozzle performance. Nozzle performance is quantified for each case and a qualitative rationale for the performance impact is developed. Author

N91-23174# Rome Univ. (Italy). Dipt. di Meccanica e Aeronautica.

REACTING SHOCK WAVES IN HYPERSONIC PROPULSION APPLICATIONS **c02**

M. Onofri *In* AGARD, Hypersonic Combined Cycle Propulsion Dec. 1990 10 p (For primary document see N91-23147 15-07)

Copyright Avail: NTIS HC/MF A20; Non-NATO Nationals requests available only from AGARD/Scientific Publications Executive

Problems connected to the occurrence of finite rate chemical processes behind shock waves in hypersonic flow fields are analyzed and a numerical technique is proposed for their solution. The computational difficulties connected with the presence of large gradients of the species concentrations are considered. A method is proposed, based on a shock-fitting technique for the gas dynamic model and a variable step integration along the streamlines for the energy and species conservation equations. This approach provides the needed resolution where it is actually required, without becoming cumbersome elsewhere, and the relaxation layer behind shocks can be computed efficiently and precisely. Author

N91-23175*# Sverdrup Technology, Inc., Cleveland, OH.

VISCOUS THREE-DIMENSIONAL ANALYSES FOR NOZZLES FOR HYPERSONIC PROPULSION **c02**

G. J. Harloff, D. R. Reddy, and H. T. Lai *In* AGARD, Hypersonic Combined Cycle Propulsion Dec. 1990 18 p Previously announced as N90-17635 (For primary document see N91-23147 15-07)

Copyright Avail: NTIS HC/MF A20; Non-NATO Nationals requests available only from AGARD/Scientific Publications Executive CSCL 01A

A Navier-Stokes computer code was validated using a number of two- and three-dimensional configurations for both laminar and turbulent flows. The validation data covers a range of freestream Mach numbers from 3 to 14, including wall pressures, velocity pressure, and skin friction. Nozzle flow fields computed for a generic scramjet nozzle from Mach 3 to 20, wall pressures, wall skin friction values, heat transfer values, and overall performance are presented. In addition, three-dimensional solutions obtained for two asymmetric, single expansion ramp nozzles at a pressure ratio of 10 consists of the internal expansion region in the converging/diverging sections and the external superonic exhaust in a quiescent ambient environment. The fundamental characteristics that were captured successfully include expansion fans; Mach wave reflections; mixing layers; and nonsymmetrical, multiple inviscid cell, supersonic exhausts. Comparison with experimental data for wall pressure distributions at the center planes shows good agreement. Author

N91-23176# Motoren- und Turbinen-Union Muenchen G.m.b.H. (Germany, F.R.).
THE 2-D SUPERSONIC NOZZLE DESIGN
Michael Goeing and Joerg Heyse *In* AGARD, Hypersonic Combined Cycle Propulsion Dec. 1990 10 p (For primary document see N91-23147 15-07)
Copyright Avail: NTIS HC/MF A20; Non-NATO Nationals requests available only from AGARD/Scientific Publications Executive

A method based on the theory of characteristics is presented for two-dimensional, supersonic nozzle design. Individual nozzle configurations for different applications are obtained by combining the geometric attributes of the symmetric, single expansion ramp, and Prandtl-Meyer type expansion nozzles. Corresponding to the design criteria, such as minimum length and optimum thrust efficiency, relations between desired properties of the flow field and nozzle geometry parameters are found, and a family of length-optimized, two-dimensional, supersonic nozzles is defined. The method can be applied for the design of wind tunnel and steam turbine nozzles as well as for thrust nozzle design of high Mach number aircraft. Author

N91-23177# Air Force Materials Lab., Wright-Patterson AFB, OH. Materials Technology.
MATERIALS FOR HYPERSONIC ENGINES
Terence M. F. Ronald *In* AGARD, Hypersonic Combined Cycle Propulsion 4 p(SEE N91-23147 15-07) Dec. 1990 (For primary document see N91-23147 15-07)
Copyright Avail: NTIS HC/MF A20; Non-NATO Nationals requests available only from AGARD/Scientific Publications Executive

The structural materials development program for the National AeroSpace Plane (NASP) is described. It indicates the materials studied, the approaches followed, and the general properties being developed. The major materials include titanium-aluminides, titanium-aluminide metal matrix composites, carbon-carbon composites, ceramic-matrix composites, beryllium alloys, and copper-matrix composites. Author

N91-23178# Societe Europeenne de Propulsion, Saint-Medard-en-Jalles (France).
MATERIALS AND MATERIAL SYSTEMS FOR COMBINED CYCLE ENGINES [MATERIAUX ET SYSTEMES DE MATERIAUX POUR LA PROPULSION COMBINEE]
D. Boury, A. Beaurain, A. LaSalmonie, and Y. Honnorat (Societe Nationale d'Etude et de Construction de Moteurs d'Aviation, Evry Cedex, France) *In* AGARD, Hypersonic Combined Cycle Propulsion Dec. 1990 18 p In FRENCH; ENGLISH summary (For primary document see N91-23147 15-07)
Copyright Avail: NTIS HC/MF A20; Non-NATO Nationals requests available only from AGARD/Scientific Publications Executive

The different categories of materials which can be considered for the engineering and production of the future hypersonic combined cycle engines are reviewed. The large size of the parts associated with the non-current conditions of temperature and environment makes new problems, the solution of which require programs of very large extent. The non-metallic reinforced materials have a potential place as large as that of the metallic materials on these developments. The assembly of such dissimilar parts goes through specific solution of mechanical assembly and the solving of a great deal of tribological problems. Author

N91-23179*# National Aeronautics and Space Administration. Lewis Research Center, Cleveland, OH.
EFFECTS OF INLET DISTORTION ON THE DEVELOPMENT OF SECONDARY FLOWS IN A SUBSONIC AXIAL INLET COMPRESSOR ROTOR Ph.D. Thesis - Toledo Univ., OH
Albert K. Owen Apr. 1991 340 p Prepared in cooperation with Army Aviation Systems Command, Cleveland, OH Original contains color illustrations
(DA Proj. 1L1-61102-AH-45)
(NASA-TM-104356; E-5583; NAS 1.15:104356; AVSCOM-TR-90-C-012) Avail: NTIS HC/MF A15; 16 functional color pages CSCL 21E

Detailed flow measurements were taken inside an isolated axial compressor rotor operating subsonically near peak efficiency. Laser anemometer measurements were made with two inlet velocity profiles. One profile consisted of an unmodified baseline flow, and the second profile was distorted by placing axisymmetric screens on the hub and shroud well upstream of the rotor. A primary flow is defined in the rotor and deviations from this primary flow for each inlet flow condition identified. A comparison between the two flow deviations is made to assess the development of a passage vortex due to the distortion of the inlet flow. A comparison of experimental results with computational predictions from a Navier-Stokes solver showed good agreement between predicted and measured flow. Measured results indicate that a distorted inlet profile has minimal effect on the development of the flow in the rotor passage and the resulting passage vortex. Author

N91-23180*# National Aeronautics and Space Administration. Lewis Research Center, Cleveland, OH.
MULTI-HEAT ADDITION TURBINE ENGINE Patent Application
Leo C. Franciscus, inventor (to NASA) and Theodore A. Brabbs, inventor (to NASA) (Sverdrup Technology, Inc., Brook Park, OH.) 30 Jan. 1991 12 p
(NASA-Case-LEW-15094-1; NAS 1.71:LEW-15094-1; US-Patent-Appl-SN-647902) Avail: NTIS HC/MF A03 CSCL 21E

A multi-heat addition turbine engine (MHATE) incorporates a plurality of heat addition devices to transfer energy to air and a plurality of turbines to extract energy from the air while converting it to work. The MHATE provides dry power and lower fuel consumption or lower combustor exit temperatures. NASA

N91-23181*# State Univ. of New York, Buffalo. Dept. of Mechanical and Aerospace Engineering.
MIXING AND NON-EQUILIBRIUM CHEMICAL REACTION IN A COMPRESSIBLE MIXING LAYER M.S. Thesis Final Report
Craig J. Steinberger May 1991 76 p Sponsored in cooperation with the American Chemical Society
(Grants NAG3-1011; NAG1-1122)
(NASA-CR-187084; NAS 1.26:187084) Avail: NTIS HC/MF A05 CSCL 21E

The effects of compressibility, chemical reaction exothermicity, and non-equilibrium chemical modeling in a reacting plane mixing layer were investigated by means of two dimensional direct numerical simulations. The chemical reaction was irreversible and second order of the type A + B yields Products + Heat. The general governing fluid equations of a compressible reacting flow field were solved by means of high order finite difference methods. Physical effects were then determined by examining the response of the mixing layer to variation of the relevant non-dimensionalized parameters. The simulations show that increased compressibility generally results in a suppressed mixing, and consequently a reduced chemical reaction conversion rate. Reaction heat release was found to enhance mixing at the initial stages of the layer growth, but had a stabilizing effect at later times. The increased stability manifested itself in the suppression or delay of the formation of large coherent structures within the flow. Calculations were performed for a constant rate chemical kinetics model and an Arrhenius type kinetic prototype. The choice of the model was shown to have an effect on the development of the flow. The Arrhenius model caused a greater temperature increase due to reaction than the constant kinetic model. This had the same effect as increasing the exothermicity of the reaction. Localized flame quenching was also observed when the Zeldovich number was relatively large. Author

N91-23182# National Aerospace Lab., Tokyo (Japan).
RESEARCH ON AERODYNAMIC CONTROL OF BLADE TIP CLEARANCE FLOW IN AIR-COOLED TURBINE
H. Usui, S. Inoue, M. Minoda, and H. Nose May 1990 20 p In JAPANESE
(DE91-764223; NAL-TM-620) Avail: NTIS HC/MF A03

Nowadays, cooling measurements are being made of the increase in inlet temperature. In order to increase the gas turbine efficiency, it is necessary to take into consideration the influence

of cooling air outlet, which cools the turbine blade, on the main flow. A newly designed rotating unit is used to test the aerodynamics of the air-cooled turbine. The influence of cooling the air outlet from the shroud ring at the moving blade tip on the performance was investigated. Also, the influence of the outlet angle, moving blade tip clearance, etc. were investigated. Some of the conclusions made from the results are as follows: (1) with increase in blade tip clearance, the flow rate at the turbine entrance almost uniformly increases at an arbitrary expansion ratio; (2) the thermal isolation efficiency, as defined by use of main flow only, uniformly increases at an arbitrary expansion ratio, in the case where cooling air exists; and (3) the thermal isolation efficiency, where cooling air is also regarded as an operating fluid, is equal regardless of whether or not cooling air exists, while the existence of the cooling air outlet produced a similar effect given the reduction in blade tip clearance. DOE

N91-23183*# National Aeronautics and Space Administration. Lewis Research Center, Cleveland, OH.

ADVANCED ICE PROTECTION SYSTEMS TEST IN THE NASA LEWIS ICING RESEARCH TUNNEL

Thomas H. Bond, Jaiwon Shin, and Geert A. Mesander (Oklahoma City Air Logistics Center, Tinker AFB, OK.) 1991 12 p Presented at the 47th Annual Forum and Technology Display, Phoenix, AZ, 6-8 May 1991; sponsored by American Helicopter Society
(NASA-TM-103757; E-6013; NAS 1.15:103757) Avail: NTIS HC/MF A03 CSCL 21E

Tests of eight different deicing systems based on variations of three different technologies were conducted in the NASA Lewis Research Center Icing Research Tunnel (IRT) in June and July 1990. The systems used pneumatic, eddy current repulsive, and electro-expulsive means to shed ice. The tests were conducted on a 1.83 m span, 0.53 m chord NACA 0012 airfoil operated at a 4 degree angle of attack. The models were tested at two temperatures: a glaze condition at minus 3.9 C and a rime condition at minus 17.2 C. The systems were tested through a range of icing spray times and cycling rates. Characterization of the deicers was accomplished by monitoring power consumption, ice shed particle size, and residual ice. High speed video motion analysis was performed to quantify ice particle size. Author

N91-23184*# National Aeronautics and Space Administration. Lewis Research Center, Cleveland, OH.

MODEL ROTOR ICING TESTS IN THE NASA LEWIS ICING RESEARCH TUNNEL

Robert J. Flemming, Randall K. Britton (Sverdrup Technology, Inc., Brook Park, OH.), and Thomas H. Bond 1991 27 p Presented at the 68th Meeting of the Fluid Dynamic Panel Specialists Meeting on the Effects of Adverse Weather on Aerodynamics, Toulouse, France, 29 Apr. - 1 May 1991; sponsored by AGARD
(NASA-TM-104351; E-6136; NAS 1.15:104351) Avail: NTIS HC/MF A03 CSCL 21E

Tests of a lightly instrumented two-bladed teetering rotor and a heavily instrumented sub-scale articulated main rotor were conducted in the NASA Lewis Research Center Icing Research Tunnel (IRT) in August 1988 and September and November 1989. The first was an OH-58 tail rotor which had a diameter of 1.575 m and a blade chord of 0.133 m, and was mounted on a NASA designed test rig. The second, a four bladed articulated rotor, had a diameter of 1.83 m with 0.124 m chord blades specially fabricated for the experiment. This rotor was mounted on a Sikorsky Aircraft Powered Force Model, which enclosed a rotor balance and other measurement systems. The models were exposed to variations in temperature, liquid water content, and medium droplet diameter, and were operated over ranges of advance ratio, shaft angle, tip Mach number (rotor speed), and weight coefficient to determine the effect of these parameters on ice accretion. In addition to strain gage and balance data, the test was documented with still, video, and high speed photography, ice profile tracing, and ice molds. Presented here are the sensitivity of the model rotors to the test parameters and a comparison of the results to theoretical predictions. Author

N91-23185*# National Aeronautics and Space Administration. Lewis Research Center, Cleveland, OH.

A CFD STUDY OF JET MIXING IN REDUCED FLOW AREAS FOR LOWER COMBUSTOR EMISSIONS

C. E. Smith, M. V. Talpallikar (CFD Research Corp., Huntsville, AL.), and J. D. Holdeman 1991 17 p Presented at the 27th Joint Propulsion Conference, Sacramento, CA, 24-27 Jun. 1991; sponsored by AIAA, SAE, ASME, and ASEE Original contains color illustrations
(Contract NAS3-25967)
(NASA-TM-104411; E-6238; NAS 1.15:104411; AIAA-91-2460)
Avail: NTIS HC/MF A03; 2 functional color pages CSCL 21E

The Rich-burn/Quick-mix/Lean-burn (RQL) combustor has the potential of significantly reducing NO(x) emissions in combustion chambers of High Speed Civil Transport aircraft. Previous work on RQL combustors for industrial applications suggested the benefit of necking down the mixing section. A 3-D numerical investigation was performed to study the effects of neckdown on NO(x) emissions and to develop a correlation for optimum mixing designs in terms of neckdown area ratio. The results of the study showed that jet mixing in reduced flow areas does not enhance mixing, but does decrease residence time at high flame temperatures, thus reducing NO(x) formation. By necking down the mixing flow area by 4, a potential NO(x) reduction of 16:1 is possible for annual combustors. However, there is a penalty that accompanies the mixing neckdown: reduced pressure drop across the combustor swirler. At conventional combustor loading parameters, the pressure drop penalty does not appear to be excessive. Author

N91-23186*# National Aeronautics and Space Administration. Lewis Research Center, Cleveland, OH.

A THREE-DIMENSIONAL NAVIER-STOKES STAGE ANALYSIS OF THE FLOW THROUGH A COMPACT RADIAL TURBINE

James D. Heidmann 1991 13 p Presented at the 27th Joint Propulsion Conference, Sacramento, CA, 24-27 Jun. 1991; sponsored by AIAA, SAE, ASME, and American Society for Electrical Engineers
(NASA-TM-104420; E-6254; NAS 1.15:104420) Avail: NTIS HC/MF A03 CSCL 21E

A steady, three dimensional Navier-Stokes average passage computer code is used to analyze the flow through a compact radial turbine stage. The code is based upon the average passage set of equations for turbomachinery, whereby the flow fields for all passages in a given blade row are assumed to be identical while retaining their three-dimensionality. A stage solution is achieved by alternating between stator and rotor calculations, while coupling the two solutions by means of a set of axisymmetric body forces which model the absent blade row. Results from the stage calculation are compared with experimental data and with results from an isolated rotor solution having axisymmetric inlet flow quantities upstream of the vacated stator space. Although the mass-averaged loss through the rotor is comparable for both solutions, the details of the loss distribution differ due to stator effects. The stage calculation predicts smaller spanwise variations in efficiency, in closer agreement with the data. The results of the study indicate that stage analyses hold promise for improved prediction of loss mechanisms in multi-blade row turbomachinery, which could lead to improved designs through the reduction of these losses. Author

N91-23187# Aerospatiale, Toulouse (France).

INTEGRATION OF PROPULSIVE SYSTEMS: SELECTION AND COMPROMISE [INTEGRATION DES SYSTEMES PROPULSIFS: CHOIX ET COMPROMIS]

Alain Garcia 1991 36 p In FRENCH Presented at AAF-ONERA Colloque Aeropropulsion, Paris, France, 20-21-May 1990
(Rept-911-111-101; ETN-91-99265) Avail: NTIS HC/MF A03

Emphasis is on a high percentage of dilute ion engines. It is shown that a solution allowing the best performances may be conflicting, particularly for the motor position in the plane, the safety, and the acoustic nuisances. Motor manufacturers have to consistently exchange their views, while taking into account their own interests, in order to reach the best compromise. Original

solutions result from economic necessity. More and more performing design tools are being developed in order to meet with the requirements of program leaders. Computer aided design plays an important part in shape creation. Composite materials are widely used. Airborne computer operated jet engines are being introduced. It is shown that competition is a factor of progress, with the example of thrust inverters. Improvements were realized in the integration of high dilution engines, with regard to mass, fuel consumption, power plant drag and acoustic nuisance. ESA

N91-23188# Aerospatiale, Toulouse (France).
THE CERTIFICATION OF THE AIRCRAFT INTEGRATED PROPULSIVE SYSTEM [LA CERTIFICATION DU SYSTEME PROPULSIF INTEGRE SUR AVION]
Philippe Martin and Martine Sainte-Marie 1991 35 p In FRENCH Presented at AAF-ONERA Colloque Aeropropulsion 90, Paris, France, 20-21 Mar. 1990
(Rept-911-111-102; ETN-91-99266) Avail: NTIS HC/MF A03

The propulsive system of an Airbus type aircraft is described. It includes the Full Authority Digital Electronic Control (FADEC) which is integrated with the aircraft, in order to realize the automatic control for thrust level, starting sequence, and thrust reversal sequence. The global certification process is presented, which includes the propulsive system certification. Airworthiness certification is given by the authorities for the aircraft. Differences between engine and aircraft regulations are outlined for various aspects such as motor fatigue, composite materials, thunder, and electromagnetic radiation protection. Engine and aircraft regulations are sometimes interpreted differently for subjects like icing protection and motor bursting. It is concluded that a better harmonization of such regulations is desired, while maintaining present safety levels. ESA

08 AIRCRAFT STABILITY AND CONTROL

Includes aircraft handling qualities; piloting; flight controls; and autopilots.

For related information see also *05 Aircraft Design, Testing and Performance.*

N91-23189 Michigan Univ., Ann Arbor.
REAL-TIME SIMULATION OF CONSTRAINED DYNAMIC SYSTEMS Ph.D. Thesis
Sugjoon Yoon 1990 232 p
Avail: Univ. Microfilms Order No. DA9034550

A new, convenient, and effective energy constraint control is developed from a geometric interpretation of the relation between the controls of geometric and energy constraint violations. Test simulations show that the combination of geometric and energy controls yields improved accuracy, not only in the constraints, but also in the state variables. A study is made of truncation errors and their modeling in the continuous time domain. This model can be used to determine the effectiveness of various constraint controls and integration methods in reducing the errors in the solution due to truncation errors. Several new methods are developed for effective control of constraints violations.
Dissert. Abstr.

N91-23190 California Univ., Los Angeles.
INTEGRATED MULTIDISCIPLINARY OPTIMIZATION OF ACTIVELY CONTROLLED FIBER COMPOSITE WINGS Ph.D. Thesis
Eliezer Livne 1990 432 p
Avail: Univ. Microfilms Order No. DA9105834

The synthesis of actively controlled fiber composite wings is formulated as a multidisciplinary design optimization problem. An integration of analysis techniques spanning the disciplines of structures, aerodynamics, and controls is described. A rich variety of behavior constraints can be treated including stress, displacement, control surface travel and hinge moment, natural frequency, aeroservoelastic stability, gust response, and handling quality constraints as well as performance measures in terms of drag/lift coefficients, drag polar shape, required load factor on roll rate, and wing mass. The design space includes a simultaneous treatment of structural, aerodynamic, and control system design variables. Capabilities and accuracy of the analysis and related behavior sensitivity analysis are discussed. Applicability of approximation concepts to the multidisciplinary optimization problem is examined by studying typical aeroservoelastic stability, gust response, and performance related constraints. The high computational efficiency of the combined analysis and sensitivity as well as the good quality of key behavior constraint approximations set the stage for the optimization of actively controlled fiber composite wings in a practical preliminary design context. Design studies of different wing configurations demonstrate the power of the new technology and offer better understanding of the multidisciplinary interactions inherent to this complex problem. Author

N91-23191# Deutsche Forschungsanstalt fuer Luft- und Raumfahrt, Brunswick (Germany, F.R.). Abt. Flaechenflugzeuge.
EVALUATION TECHNIQUES FOR HIGHLY AUGMENTED AIRCRAFT
Knut Wilhelm and Anton M. H. Nieuwpoort (Fokker B.V., Schipol-Oost, Netherlands) Nov. 1990 51 p
(DLR-FB-90-35; ISSN-0939-2963; ETN-91-99063) Avail: NTIS HC/MF A04; DLR, Wissenschaftliches Berichtswesen, VB-PL-DO, Postfach 90 60 58, 5000 Cologne, Fed. Republic of Germany, HC 20.50 DM

The handling qualities evaluation is a very important part of the overall flight control system development process. For determining the flight characteristics of highly augmented aircraft there are basically two methods: evaluation using pilots under operational conditions and numerical handling qualities evaluation using mathematical models of the aircraft. Both methods are addressed with main emphasis laid on those techniques suitable for handling qualities analysis of highly augmented aircraft. The important role of system identification in the handling qualities evaluation process is presented. ESA

N91-23192# Aerospatiale, Toulouse (France).
THE ELECTRICAL FLIGHT CONTROL SYSTEM OF A320 AIRBUS: A FAULT TOLERANT SYSTEM [LES COMMANDES DE VOL ELECTRIQUES DE L'AIRBUS A320: UN SYSTEME TOLERANT AUX FAUTES]
Dominique Briere and Pascal Traverse 1991 6 p In FRENCH; ENGLISH summary Presented at 7th International Conference on Reliability and Maintenance, Brest, France, 1990
(Rept-911-111-103; ETN-91-99267) Avail: NTIS HC/MF A02

The A 320 Airbus is the first civil aircraft equipped with an electrical flight control system. This system is based on very stringent dependability constraints, both in terms of safety and availability. The basic building blocks are control and monitoring computers. The control channel is in charge of the function of the computer, for instance, to slave a control surface. The monitoring channel is used to detect a possible failure of the control channel. A high level of redundancy is built in the system. Particular attention is drawn to possible external stresses. The system is built to tolerate both hardware and software design faults. ESA

N91-23193# Army Missile Command, Redstone Arsenal, AL. Guidance and Control Directorate.
ANALYSIS OF THE FLUTTER CHARACTERISTICS OF THE ADVANCED KINETIC ENERGY MISSILE (ADKEM) CONTROL SURFACE Final Technical Report, Oct. 1989 - Feb. 1990
Stephen C. Cayson and Roger P. Berry Aug. 1990 66 p
(AD-A232377; AD-E951621; AMSMI/TR-RD-GC-90-10) Avail: NTIS HC/MF A04 CSCL 16/2

This report describes the analysis of the flutter characteristics of the control fin for the Advanced Kinetic Energy Missile (ADKEM). First of all, the control fin stability equation is determined from the two-degree-of-freedom equations of motion for the fin. This equation is a function of the fin bending stiffness and the actuator

dynamic stiffness, which are then found. The fin bending stiffness is found by assuming that there is a distributed load on the fin and solving for the bending moment and angular deflection using numerical integration. The actuator dynamic stiffness is solved for by applying a torque disturbance to the second order actuator equation of motion and calculating the resulting fin angular deflection. This data is then compared to the existing third order model and non-linear model data to check for validity. Knowing these values, the possibility of fin flutter may be determined.
Author (GRA)

N91-23113# British Aerospace Public Ltd. Co., Preston (England). Military Aircraft Div.
THE DEVELOPMENT OF ALTERNATE CRITERIA FOR FBW HANDLING QUALITIES
J. C. Gibson *In* AGARD, Flying Qualities Feb. 1991 13 p (For primary document see N91-23108 15-05)
Copyright Avail: NTIS HC/MF A17; Non-NATO Nationals requests available only from AGARD/Scientific Publications Executive

N91-23114# Deutsche Forschungsanstalt fuer Luft- und Raumfahrt, Brunswick (Germany, F.R.). Inst. fuer Flugmechanik.
DEVELOPMENT OF MIL-8785C INTO A HANDLING QUALITIES SPECIFICATION FOR A NEW EUROPEAN FIGHTER AIRCRAFT
E. Buchacker, H. Galleithner, R. Koehler, and M. Marchand *In* AGARD, Flying Qualities Feb. 1991 16 p (For primary document see N91-23108 15-05)
Copyright Avail: NTIS HC/MF A17; Non-NATO Nationals requests available only from AGARD/Scientific Publications Executive

N91-23116# Dornier System G.m.b.H., Friedrichshafen (Germany, F.R.).
HANDLING QUALITIES OF HIGHLY AUGMENTED UNSTABLE AIRCRAFT SUMMARY OF AN AGARD-FMP WORKING GROUP EFFORT
Horst Wuennenberg *In* AGARD, Flying Qualities Feb. 1991 6 p (For primary document see N91-23108 15-05)
Copyright Avail: NTIS HC/MF A17; Non-NATO Nationals requests available only from AGARD/Scientific Publications Executive

N91-23117# Wright Research Development Center, Wright-Patterson AFB, OH.
THE HANDLING QUALITIES OF THE STOL AND MANEUVER TECHNOLOGY DEMONSTRATOR FROM SPECIFICATION TO FLIGHT TEST
David J. Moorhouse, Kevin D. Citurs, Richard W. Thomas, and Mark R. Crawford (Air Force Flight Test Center, Edwards AFB, CA.) *In* AGARD, Flying Qualities Feb. 1991 9 p (For primary document see N91-23108 15-05)
Copyright Avail: NTIS HC/MF A17; Non-NATO Nationals requests available only from AGARD/Scientific Publications Executive

N91-23119# Royal Aerospace Establishment, Bedford (England).
HANDLING QUALITIES GUIDELINES FOR THE DESIGN OF FLY-BY-WIRE FLIGHT CONTROL SYSTEMS FOR TRANSPORT AIRCRAFT
O. P. Nicholas, H. T. Huynh, W. P. deBoer, J. A. J. vanEngelen, and D. Shafranek (Deutsche Forschungsanstalt fuer Luft- und Raumfahrt, Brunswick, Germany, F.R.) *In* AGARD, Flying Qualities Feb. 1991 12 p (For primary document see N91-23108 15-05)
Copyright Avail: NTIS HC/MF A17; Non-NATO Nationals requests available only from AGARD/Scientific Publications Executive

N91-23123# National Aeronautical Establishment, Ottawa (Ontario). Flight Research Lab.
AN INVESTIGATION INTO THE USE OF SIDE-ARM CONTROL FOR CIVIL ROTORCRAFT APPLICATIONS
S. W. Baillie and S. Kereliuk *In* AGARD, Flying Qualities Feb. 1991 12 p Prepared in cooperation with FAA, Atlantic City, NJ (For primary document see N91-23108 15-05)
Copyright Avail: NTIS HC/MF A17; Non-NATO Nationals requests available only from AGARD/Scientific Publications Executive

N91-23124# National Aeronautical Establishment, Ottawa (Ontario).
DETERMINATION OF DECISION-HEIGHT WINDOWS FOR DECELERATING IMC APPROACHES IN HELICOPTERS
Roger H. Hoh (Hoh Aeronautics, Inc., Lomita, CA.), S. W. Baillie, S. Kereliuk, and Joseph J. Traybar *In* AGARD, Flying, Qualities Feb. 1991 17 p Prepared in cooperation with Federal Aviation Administration, Atlantic City, NJ (For primary document see N91-23108 15-05)
Copyright Avail: NTIS HC/MF A17; Non-NATO Nationals requests available only from AGARD/Scientific Publications Executive

N91-23125# Dornier System G.m.b.H., Friedrichshafen (Germany, F.R.).
INTEGRATION OF HANDLING QUALITY ASPECTS INTO THE AERODYNAMIC DESIGN OF MODERN UNSTABLE FIGHTERS
Peter Mangold *In* AGARD, Flying Qualities Feb. 1991 30 p (For primary document see N91-23108 15-05)
Copyright Avail: NTIS HC/MF A17; Non-NATO Nationals requests available only from AGARD/Scientific Publications Executive

09 RESEARCH AND SUPPORT FACILITIES (AIR)

Includes airports, hangars and runways; aircraft repair and overhaul facilities; wind tunnels; shock tubes; and aircraft engine test stands.

For related information see also *14 Ground Support Systems and Facilities (Space).*

N91-23194# Israel Aircraft Industries Ltd., Ben-Gurion Airport. Materials and Process Engineering.
IAI HYPERSONIC WIND TUNNEL
L. Y. Jacobi and M. Zilberman May 1987 18 p Presented at the 67th Semiannual STA Meeting, Arnold AFS, TN, 13-15 Apr. 1987; sponsored by Calspan Corp./AEDC Div.
(IAITIC-87-1006; ITN-88-85005) Avail: NTIS HC/MF A03

IAI (Israel Aircraft Industries) has initiated a program to have its own capability in experimental hypersonic aerodynamics. It is planning to reconstruct and operate the Hypersonic Wind Tunnel, purchased in 1978 from General Dynamics, together with its Tri-sonic Wind Tunnel to complement its Low Speed and High Speed Wind Tunnels. The air supply system, air heater, by-pass valve, nozzles, test chamber and diffuser-ejector system of the Hypersonic Wind Tunnel are described and its operational characteristics and experience presented. The purpose of the presentation is to invite participants' suggestions for future development of hypersonic vehicles. ISA

N91-23195*# MCAT Inst., San Jose, CA.
DEVELOPMENT OF A QUIET SUPERSONIC WIND TUNNEL WITH A CRYOGENIC ADAPTIVE NOZZLE Annual Progress Report, May 1990 - Apr. 1991
Stephen D. Wolf Feb. 1991 106 p
(Contract NCC2-604)
(NASA-CR-186769; NAS 1.26:186769) Avail: NTIS HC/MF A06 CSCL 14B

The main objectives of this work is to demonstrate the potential of a cryogenic adaptive nozzle to generate quiet (low disturbance) supersonic flow. A drive system was researched for the Fluid Mechanics Laboratory (FML) Laminar Flow Supersonic Wind Tunnel (LFSWT) using a pilot tunnel. A supportive effort for ongoing Proof of Concept (PoC) research leading to the design of critical components of the LFSWT was maintained. The state-of-the-art in quiet supersonic wind tunnel design was investigated. A supersonic research capability was developed within the FML.
Author

N91-23196# Von Karman Inst. for Fluid Dynamics, Rhode-Saint-Genese (Belgium).
THE VKI HYPERSONIC WIND TUNNELS AND ASSOCIATED MEASUREMENT TECHNIQUES
G. Simeonides Nov. 1990 177 p
(VKI-TM-46; ETN-91-99111) Avail: NTIS HC/MF A09

A description of the two hypersonic facilities at the Belgian Von Karman Institute (VKI), providing details of their performance capabilities and operation, as well as measurement techniques currently employed is presented. The two wind tunnels are described with emphasis being placed on the Longshot intermittent tunnel which is capable of Mach/Reynolds number simulation of lifting reentry flight. The analysis of its performance and the efforts undertaken since 1982 to modernize the facility are summarized. Measurement techniques employed in two tunnels, emphasizing the measurement of heat transfer by various intrusive or non intrusive methods, are given. The instrumentation/acquisition systems are discussed together with the accuracy of various measurements, particularly in the Longshot facility. ESA

N91-23197# Aerospatiale Aquitaine, Saint-Medard en Jalles (France). Lab. Materiaux et Structures Composites.
EXPERIMENTATION FACILITIES FOR THERMOMECHANICAL STATIC TESTS WITH ANALYTIC TEST SPECIMENS AT AEROSPATIALE [MOYENS D'ESSAIS THERMOMECANIQUES STATIQUES SUR EPROUVETTE ANALYTIQUE A AEROSPATIALE]
J. M. Lequertier 1991 33 p In FRENCH Presented at Journee de la Societe des Hautes Temperatures sur Les Mesures Mecaniques Haute Temperature, Orleans, France, 22 Nov. 1990
(Rept-911-430-108; ETN-91-99280) Avail: NTIS HC/MF A03

The aim is to determine the strain/stress macroscopic curve at a given temperature. Thermostructural composites are developed from fiber and matrix components having a brittle mechanical behavior. These materials are prepared at very high temperatures. Materials being currently developed in civil aviation are presented with regard to their thermochemical performance. The static analytic thermomechanical tests are described. Cold and hot chops are used and compared. Tensile test specimens, compression tests specimens, and shearing test specimens are outlined. High temperature, optical, and interferential extensometers are used for these tests. ESA

N91-23198# Federal Aviation Administration, Washington, DC. Systems Research and Development Service.
PRECISION RUNWAY MONITOR DEMONSTRATION REPORT Final Report
Feb. 1991 133 p
(AD-A232671; DOT/FAA/RD-91/5) Avail: NTIS HC/MF A07 CSCL 01/5

This report is prepared as the result of a development and demonstration project to increase landing capacity on closely spaced parallel runways. The project developed new equipment and procedures, and demonstrated them in a variety of ways at two different airports. The new monitoring equipment consists of radars and displays. The systems installed at Raleigh, NC included an electronically scanned antenna capable of half-second update intervals, while the Memphis, TN installation provided a mechanically rotating back-to-back antenna with a 2.4-second update interval. In addition, both sites provided enhanced high-resolution color ATC display systems. The purpose of the report is to present findings relevant to a decision concerning whether or not the current standard for runway separation of 4,300 ft can be reduced to 3,400 ft when the precision runway monitor equipment is utilized. The 3,400-ft separation was the spacing demonstrated most often in both simulations and flight tests. The demonstration produced a broad recognition that both systems could be used to monitor parallel runways spaced at 3400 feet apart. GRA

N91-23199# Army Engineer Waterways Experiment Station, Vicksburg, MS. Geotechnical Lab.
LITERATURE REVIEW ON GEOTEXTILES TO IMPROVE PAVEMENTS FOR GENERAL AVIATION AIRPORTS Final Report
Dewey W. White, Jr. Feb. 1991 61 p
(AD-A232871; WES/MP/GL-91-3) Avail: NTIS HC/MF A04 CSCL 13/2

This report covers a literature search and review to obtain information on geotextile applications related to pavement construction. Applicable information from this study would be used to prepare guidelines on design application, material specifications, performance criteria, and construction procedures for improving subgrade support with geotextiles in general aviation airport pavements. The study revealed that there are numerous design procedures available for using geotextiles in aggregate surfaced pavements and flexible pavement road construction. However, there is no generally accepted procedure for either type construction. The state-of-the-art has not advanced to the point where design procedures for using geotextiles in paved airport construction are available. Construction/installation procedures are available for using geotextiles in aggregate surfaced pavements and flexible pavements for roads, and these may be used as an aid in recommending procedures for airport construction. GRA

12 ASTRONAUTICS (GENERAL)

For extraterrestrial exploration see *91 Lunar and Planetary Exploration.*

N91-23200*# Boeing Aerospace Co., Huntsville, AL. Advanced Civil Space Systems.
PILOTED ROVER TECHNOLOGY STUDY Final Report
D. L. Thrasher 10 Aug. 1990 192 p
(Contract NAS8-37857)
(NASA-CR-186989; NAS 1.26:186989; D615-10014) Avail: NTIS HC/MF A09 CSCL 22A

This is the May 25, 1990 summary report for Space Transfer Concepts and Analyses (STCA) Study, special study task 9.1, Piloted Rovers Technology Study. Piloted rover concepts, mission scenarios, and the requirements necessary for completion of these missions resulting in the establishment of a lunar base. These tasks were intended to lead to a logical conclusion concerning which piloted rovers technologies are needed to accomplish the various missions, along with a recommended schedule for the development of these technologies. Author

N91-23201# Synthesis Group, Arlington, VA.
AMER!CA AT THE THRESHOLD
1991 191 p Prepared for the Executive Office of the President, Washington, DC Original contains color illustrations Contains poster as supplement
Avail: NTIS HC/MF A09; also available SOD HC $13.00 as 033-000-01097-4

The Space Exploration Initiative is a challenge issued by President Bush that will return America to the Moon to stay and onward to Mars by 2019. In doing this, six 'visions' guide and direct the space efforts. These efforts are: Knowledge of the universe; Advancement in science and engineering; U.S. leadership; Technologies for Earth; Commercialization of space; and Strengthened U.S. economy. Why the Moon and Mars were chosen as the objects of exploration is examined. Ten recommendations are provided for the effective implementation of the SPI, along with a detailed examination of each. Author

13 ASTRODYNAMICS

Includes powered and free-flight trajectories; and orbital and launching dynamics.

N91-23202 Texas Univ., Austin.
PRECISION ORBIT DETERMINATION OF GLOBAL POSITIONING SYSTEM SATELLITES Ph.D. Thesis
Ching-Shun Ho 1990 182 p
Avail: Univ. Microfilms Order No. DA9105568

Precise geodetic measurement can provide an excellent study of plate tectonic motion. The potential of Global Positioning System (GPS) was shown in determining the precise baseline. The precise GPS satellite orbit is one key to high-accuracy long baseline (greater than 200 km) solutions. GPS orbit determination is examined using two L-band signals transmitted by GPS satellites. The analysis of the pseudo-range and phase data collected during the CASA UNO campaign is discussed. The fidelity of the applied forces and derived observation models were tested by processing the tracking data from the campaign with the unconstrained batch estimation approach. The orbit accuracy was assessed through the baseline solution and the orbit comparison. Dissert. Abstr.

N91-23203# GKSS-Forschungszentrum Geesthacht (Germany, F.R.). Inst. fuer Physik.
HIGHER ACCURACY REQUIREMENTS FOR THE SATISFACTORY POSITION CALCULATION OF AN ARTIFICIAL SATELLITE
J. Straka and H. Grassl (Max-Planck-Inst. fuer Meteorologie, Hamburg, Germany, F.R.) 1990 56 p In GERMAN; ENGLISH summary
(GKSS-90/E/25; ISSN-0344-9629; ETN-91-99191) Copyright Avail: NTIS HC/MF A04

The development of a program for computing the position of an artificial satellite of the Earth was discussed under the assumption of higher accuracy. It was shown that the numerical integration of the equations of motion of a satellite gives higher accuracy than the conventional analytical treatment of these equations. It was possible to obtain the coordinates of the SEASAT satellite with an accuracy between 80 and 250 m, by integrating over 0.5 till 3 days, if the Earth gravity potential up to order 20 and possibly 28 and the disturbances caused by Sun and Moon were considered. Problems with the acquisition of input data for satellite navigation were discussed. ESA

14 GROUND SUPPORT SYSTEMS AND FACILITIES (SPACE)

Includes launch complexes, research and production facilities; ground support equipment, e.g., mobile transporters; and simulators.

For related information see also *09 Research and Support Facilities (Air).*

N91-23204 Prins Maurits Lab. TNO, Rijswijk (Netherlands).
ON THE EFFICIENCY OF RAIL ACCELERATORS Final Report
W. A. deZeeuw and W. J. Kolbert Jul. 1990 12 p Sponsored by DWOO; HDO-TNO; and DOD
(PML-1990-64; TD-90-2723; ETN-91-99092) Copyright Avail: TNO Prins Maurits Lab., P.O. Box 45, 2280 AA Rijswijk ZH, Netherlands

A general definition of the launch efficiency for electromagnetic rail launchers, which is based on a formal analysis of a generalization of Faraday's law in differential form, is presented. The launch efficiency is deduced by consideration of inductive and resistive contributions to the enregy delivered to a rail accelerator. ESA

N91-23587# Fokker Space and Systems, Amsterdam (Netherlands).
BUILDING REAL-TIME SIMULATORS FOR SPACE APPLICATIONS
J. A. Hoogstraten *In* ESA, Space and Sea Dec. 1990 p 179-186 (For primary document see N91-23563 15-42) Copyright Avail: NTIS HC/MF A13

15 LAUNCH VEHICLES AND SPACE VEHICLES

Includes boosters; operating problems of launch/space vehicle systems; and reusable vehicles.

For related information see also *20 Spacecraft Propulsion and Power.*

N91-23205*# Sverdrup Technology, Inc., Brook Park, OH.
THE APPLICATION OF NEURAL NETWORKS TO THE SSME STARTUP TRANSIENT Final Report
Claudia M. Meyer and William A. Maul Jun. 1991 16 p Presented at the 27th Joint Propulsion Conference, Sacramento, CA, 24-27 Jun. 1991; sponsored by AIAA, SAE, ASME, and American Society for Electrical Engineers
(Contract NAS3-25266)
(NASA-CR-187138; E-6268; NAS 1.26:187138) Avail: NTIS HC/MF A03 CSCL 22D

Feedforward neural networks were used to model three parameters during the Space Shuttle Main Engine startup transient. The three parameters were the main combustion chamber pressure, a controlled parameter, the high pressure oxidizer turbine discharge temperature, a redlined parameter, and the high pressure fuel pump discharge pressure, a failure-indicating performance parameter. Network inputs consisted of time windows of data from engine measurements that correlated highly to the modeled parameter. A standard backpropagation algorithm was used to train the feedforward networks on two nominal firings. Each trained network was validated with four additional nominal firings. For all three parameters, the neural networks were able to accurately predict the data in the validation sets as well as the training set. Author

16 SPACE TRANSPORTATION

Includes passenger and cargo space transportation, e.g., shuttle operations; and space rescue techniques.

For related information see also *03 Air Transportation and Safety* and *18 Spacecraft Design, Testing and Performance.* For space suits see *54 Man/System Technology and Life Support.*

N91-23206*# Computer Technology Associates, Inc., Rockville, MD.
ASTROMAG PHASE A ASSEMBLY AND SERVICING OPERATIONS REPORT Final Report, Aug. - Dec. 1989
Link A. Parikh 31 Dec. 1989 64 p
(Contract NAS5-30546)
(NASA-CR-186262; NAS 1.26:186262) Avail: NTIS HC/MF A04 CSCL 22B

Operations concepts for the assembly and servicing of the Astromag Attached Payload on the Space Station Freedom (SSF) are presented. Scenario scripts and graphical representations of the installation of the core facility (CF) on the SSF, installation of experiment hardware on the CF, and the changeout of experiments on the CF are also presented. Author

N91-23207*# National Aeronautics and Space Administration. Ames Research Center, Moffett Field, CA.
TECHNOLOGIES FOR AEROBRAKING
David M. Cooper and James O. Arnold Mar. 1991 19 p Presented at the 41st Congress of the International Astronautical Federation, Dresden, German D.R., 6-13 Oct. 1990
(NASA-TM-102854; A-90250; NAS 1.15:102854) Avail: NTIS HC/MF A03 CSCL 22B

Aerobraking is one of the largest contributors to making both lunar and Mars missions affordable. The use of

aerobraking/aeroassist over all propulsive approaches saves as much as 60 percent of the initial mass required in low earth orbit (LEO); thus, the number and size of earth to orbit launch vehicles is reduced. Lunar transfer vehicles (LTV), which will be used to transport personnel and materials from LEO to lunar outpost, will aerobrake into earth's atmosphere at approximately 11 km/sec on return from the lunar surface. Current plans for both manned and robotic missions to Mars use aerocapture during arrival at Mars and at return to Earth. At Mars, the entry velocities will range from about 6 to 9.5 km/sec, and at Earth the return velocity will be about 12.5 to 14 km/sec. These entry velocities depend on trajectories, flight dates, and mission scenarios and bound the range of velocities required for the current studies. In order to successfully design aerobrakes to withstand the aerodynamic forces and heating associated with these entry velocities, as well as to make them efficient, several critical technologies must be developed. These are vehicle concepts and configurations, aerothermodynamics, thermal protection system materials, and guidance, navigation, and control systems. The status of each of these technologies are described, and what must be accomplished in each area to meet the requirements of the Space Exploration Initiative is outlined. Author

N91-23208# Aerospatiale Aquitaine, Saint-Medard en Jalles (France). Div. Systemes Strategiques et Spatiaux.
SIMOUN: A HIGH TEMPERATURE AND LOW PRESSURE TESTING FACILITY FOR MATERIAL CHARACTERIZATION [SIMOUN: MOYEN D'ESSAIS HAUTE TEMPERATURE ET BASSE PRESSION POUR LA CARACTERISATION DES MATERIAUX]
R. Leroux 1991 6 p In FRENCH; ENGLISH summary
(Rept-911-430-121; ETN-91-99293) Avail: NTIS HC/MF A02

A technical description of the SIMOUN testing facility is given, including its general characteristics. The steam vacuum system is reviewed. SIMOUN is shown as one of the most important experimentation systems used for the development of the thermal protections of the Hermes Spaceplane. The plasma generation and the vacuum system allow control of the temperature and pressure conditions required for material test specimens. ESA

N91-23209# Aerospatiale Aquitaine, Saint-Medard en Jalles (France). Strategic and Space Div.
SIMOUN: A NEW TEST APPLIANCE FOR THE DEVELOPMENT OF HERMES THERMAL PROTECTIONS [SIMOUN: UN NOUVEAU MOYEN D'ESSAIS POUR LE DEVELOPPEMENT DES PROTECTIONS THERMIQUES D'HERMES]
P. Charpentier and R. Leroux 1991 8 p In FRENCH
(Rept-911-430-129; ETN-91-99301) Avail: NTIS HC/MF A02

The development of the European space aircraft Hermes requires new materials capable to resist the severe conditions of atmospheric reentry, with high temperature, from 1100 to 1900 C, and low pressure during about half an hour. SIMOUN is one of the testing appliances developed by ESA to test these materials in conditions of reentry as representative as possible, while submitting them to a very hot air flow created by a plasma generator. The main characteristics of the testing appliance, its possible different configurations, the types of measurement carried out, and the organization of its operation are successively presented. ESA

17 SPACE COMM., SPACECRAFT COMM., COMMAND & TRACKING

Includes telemetry; space communications networks; astronavigation and guidance; and radio blackout.

For related information see also *04 Aircraft Communications and Navigation* and *32 Communications and Radar.*

N91-23210*# National Aeronautics and Space Administration. Lyndon B. Johnson Space Center, Houston, TX.
SIMULATION AND ANALYSES OF THE AEROASSIST FLIGHT EXPERIMENT ATTITUDE UPDATE METHOD
J. R. Carpenter Jun. 1991 70 p
(NASA-TM-102174; S-623; NAS 1.15:102174) Avail: NTIS HC/MF A04 CSCL 09F

A method which will be used to update the alignment of the Aeroassist Flight Experiment's Inertial Measuring Unit is simulated and analyzed. This method, the Star Line Maneuver, uses measurements from the Space Shuttle Orbiter star trackers along with an extended Kalman filter to estimate a correction to the attitude quaternion maintained by an Inertial Measuring Unit in the Orbiter's payload bay. This quaternion is corrupted by on-orbit bending of the Orbiter payload bay with respect to the Orbiter navigation base, which is incorporated into the payload quaternion when it is initialized via a direct transfer of the Orbiter attitude state. The method of updating this quaternion is examined through verification of baseline cases and Monte Carlo analysis using a simplified simulation, The simulation uses nominal state dynamics and measurement models from the Kalman filter as its real world models, and is programmed on Microvax minicomputer using Matlab, and interactive matrix analysis tool. Results are presented which confirm and augment previous performance studies, thereby enhancing confidence in the Star Line Maneuver design methodology. Author

18 SPACECRAFT DESIGN, TESTING AND PERFORMANCE

Includes satellites; space platforms; space stations; spacecraft systems and components such as thermal and environmental controls; and attitude controls.

For life support systems see *54 Man/System Technology and Life Support.* For related information see also *05 Aircraft Design, Testing and Performance, 39 Structural Mechanics,* and *16 Space Transportation.*

N91-23211*# Computer Technology Associates, Inc., Rockville, MD.
ASTROMAG DATA SYSTEM CONCEPT Final Report, Aug. - Dec. 1989
Darrell Roos, Chieh-San Cheng, Penny Newsome, and Nitya Nath 29 Dec. 1989 45 p
(Contract NAS5-30546)
(NASA-CR-186341; NAS 1.26:186341) Avail: NTIS HC/MF A03 CSCL 22B

A feasible, top-level data system is defined that could accomplish and support the Astromag Data System functions and interfaces necessary to support the scientific objectives of Astromag. This data system must also be able to function in the environment of the Space Station Freedom Manned Base (SSFMB) and other anticipated NASA elements. Author

N91-23212*# Smithsonian Astrophysical Observatory, Cambridge, MA.
SMALL EXPLORER PROJECT: SUBMILLIMETER WAVE ASTRONOMY SATELLITE (SWAS). MISSION OPERATIONS AND DATA ANALYSIS PLAN
Gary J. Melnick Jul. 1990 44 p
(Contract NAS5-30702)
(NASA-CR-186954; NAS 1.26:186954) Avail: NTIS HC/MF A03 CSCL 22B

The Mission Operations and Data Analysis Plan is presented for the Submillimeter Wave Astronomy Satellite (SWAS) Project. It defines organizational responsibilities, discusses target selection and navigation, specifies instrument command and data requirements, defines data reduction and analysis hardware and software requirements, and discusses mission operations center staffing requirements. Author

N91-23213*# National Aeronautics and Space Administration, Washington, DC.
THE COMBINED RELEASE AND RADIATION EFFECTS SATELLITE PROGRAM (CRRES): A UNIQUE SERIES OF SCIENTIFIC EXPERIMENTS

1991 28 p Original contains color illustrations
(NASA-TM-104957; NAS 1.15:104957) Avail: NTIS HC/MF A03; 20 functional color pages CSCL 22B

CRRES is a program to study the space environment which surrounds Earth and the effects of space radiation on modern satellite electronic systems. The satellite will carry an array of active experiments including chemical releases and a complement of sophisticated scientific instruments to accomplish these objectives. Other chemical release active experiments will be performed with suborbital rocket probes. These chemical releases will paint the magnetic and electric fields in Earthspace with clouds of glowing ions. Earthspace will be a laboratory, and the releases will be studied with an extensive network of ground-, aircraft-, and satellite-based diagnostic instruments. Author

N91-23214*# National Aeronautics and Space Administration, Washington, DC.
ROSAT: AN INTERNATIONAL MISSION EXPLORING THE HIGH ENERGY UNIVERSE
1991 25 p Original contains color illustrations
(NASA-TM-104958; NAS 1.15:104958) Avail: NTIS HC/MF A03; 19 functional color pages CSCL 22B

ROSAT was designed specifically to detect high energy radiation, by using its telescopes to study x ray and ultraviolet emissions, regions of the electromagnetic spectrum that cannot be seen and that cannot penetrate the Earth's atmosphere. ROSAT is an international astronomical observatory project. ROSAT's science mission is divided into two phases. With its in-orbit checkout period complete, ROSAT has begun phase one of its mission, an all sky survey to map the heavens. When the 6 month mapping survey is complete, the satellite will begin phase two and be pointed at selected objects, studying individual targets, for the remainder of its mission. Author

N91-23215*# National Aeronautics and Space Administration. Marshall Space Flight Center, Huntsville, AL.
ATMOSPHERIC TURBULENCE REVIEW OF SPACE SHUTTLE LAUNCHES
Michael Susko Washington May 1991 69 p
(NASA-TM-4289; NAS 1.15:4289) Avail: NTIS HC/MF A04 CSCL 22C

Research and analysis on the identification of turbulent regions from the surface to 16 km during Space Shuttle launches are discussed. It was demonstrated that the results from the FPS-16 radar/jimsphere balloon system in measuring winds can indeed indicate the presence or conditions ripe for turbulence in the troposphere and lower stratosphere. It was further demonstrated that atmospheric data obtained during the shuttle launches by the rawinsonde in conjunction with the jimsphere provides the necessary meteorological data to compute aerodynamic parameters to identify turbulence, such as Reynolds number drag coefficient, turbulent stresses, total energy, stability parameter, vertical gradient of kinetic energy, Richardson number, and the turbulence probability index. Enhanced temperature lapse rates and inversion rates, strong vector wind shears, and large changes in wind direction identify the occurrence of turbulence at the troposphere. When any two of the above conditions occur simultaneously, a significant probability of turbulence can occur. Author

N91-23216# Aerospatiale, Toulouse (France).
SATELLITE UTILIZATION BY CIVIL AVIATION [UTILISATION DES SATELLITES PAR L'AVIATION CIVILE]
M. J. Grossin 20 Oct. 1989 38 p In FRENCH Presented at Symposium International sur l'Evolution des Telecommunications, 1989
(Rept-911-111-105; ETN-91-99269) Avail: NTIS HC/MF A03

International work carried out in this field is presented. The space segment of the International Maritime Satellite (INMARSAT) organization is described. Eight geostationary satellites are in service for the main three oceanic regions. Spot beam satellites are to be used at the end of the nineties. The ground segment measures the liaison between satellites and the international telecommunication network. Satellite communication antennas are presented. Satellite navigation systems, GPS (Global Positioning System) for the U.S. and GLONASS (Global Navigation Satellite System) for the USSR are reported. ESA

N91-23217# Aerospatiale Aquitaine, Saint-Medard en Jalles (France).
AEROCOAT THERMAL PROTECTIONS [PROTECTIONS THERMIQUES AEROCOAT]
Guy Metivaud 1991 9 p In FRENCH
(Rept-911-430-102; ETN-91-99274) Avail: NTIS HC/MF A02

Aerocoat (French trademark) thermal protections allow very efficient thermal barriers to be made using small thicknesses. The operating principle of these insulating materials used for space vehicles is described. The mechanical, physical, and chemical characteristics of Aerocoat materials are given. Tests carried out are reported. Thermal insulation characteristics are given. The Aerocoat insulation process is explained. ESA

N91-23218# Aerospatiale, Cannes (France).
COMMUNICATION AND BROADCASTING SATELLITES PAYLOAD RECONFIGURATION TECHNOLOGIES
Philippe Vizier 1991 8 p
(Rept-911-440-102; CA-2/90; ETN-91-99304) Avail: NTIS HC/MF A02

Payload configuration capability to match evolutive missions over the operational lifetime of communication and broadcasting satellites is addressed. The operational requirements for which payload reconfiguration is necessary, the different technical solutions for obtaining such reconfigurable payloads and the critical hardware to be developed and space qualified prior to being carried on board the spacecraft are presented. Reconfigurable payloads are concluced to be a promising alternative to conventional ones. They correspond to a cost effective solution through optimized missions and extended lifetime capability. ESA

N91-23219# Aerospatiale, Cannes (France).
CONFERENCE ON SPACE TECHNOLOGY: SATELLITE APPLICATION DEVELOPMENT
Jean Jacques Bloch, Charles Carton, and Philippe Vizier 1991 5 p Conference held in Manama, Bahrain, 6-7 Mar. 1990; sponsored by Bahrain Centre for Studies and Research, Ministry for Studies and Research, and Aerospatiale
(Rept-911-440-103; Rept-218-CA/IS/T; ETN-91-99305) Avail: NTIS HC/MF A01

Subjects mentioned in the program were new technologies for commercial satellites, satellite applications and future prospects, existing satellite application systems and new generation systems. An important participation of Eurospatiale in the fields of remote sensing and telecommunication is noted. Regional coordination in the Persian Gulf is desired in the field of Earth observation. ESA

N91-23220# Aerospatiale, Cannes (France).
A NEW GENERATION OF RADIATORS
M. Amidieu, V. Berthon, and T. Maciazsek (Centre National d'Etudes Spatiales, Toulouse, France) 1991 9 p Presented at the 20th International Conference on Environmental Systems, Williamsburg, VA, 9-12 Jul. 1990
(Rept-911-440-105; CA-4/90; ETN-91-99307) Avail: NTIS HC/MF A02

Activities in the field of active thermal control which led to the definition, manufacture, and testing of a new generation of radiators are discussed. The fluid loop radiator study, engaged under the Hermes program requirements resulted in the definition of large radiative panels that have low mass, low manufacturing cost constraints and various possible shapes. The hybrid radiator study, with respect to the heat exchanger, provided a data base of results on the wet and dry concepts. A prototype model was defined after a trade off analysis and the choice of the dry contact solution was selected. With respect to the two phase active thermal control concept, a complete loop is under development studies. The problems of on ground testing were analyzed, particularly on the

condenser section, the goal being the flight performance prediction of a space radiator. ESA

N91-23221# Aerospatiale, Cannes (France). Artificial Intelligence Dept.
REACTIVE PROCEDURE BASED DECISION MAKING FOR SATELLITE CONTROL
J. C. Chautard and C. Honnorat 1991 20 p Sponsored in part by European Economic Community; CNES; and SATEXPERT
(Rept-911-440-106; CA-7/90; ETN-91-99308) Avail: NTIS HC/MF A03

In the space field, the ever growing complexity of satellites led to a significant increase in the amount of data to be processed from the ground, and to a critical need to react safely in case of contingency. Moreover, since the life cycle of satellites of the new generation often exceeds 10 years, maintaining a full team of trained engineers and experts along this period of time is too constraining and costly. In this context work on specifying and prototyping what will be the new family of ground based centers for automated satellite control was undertaken. A survey of the techniques involved in these systems with specific focus on the decision making aspect is presented. Knowledge based techniqes are shown to be a natural answer to the main requirements of the problems and, through the reactivity question, the concepts of the procedural command module are introduced. A demonstrator implementing a procedural expert system coupled to a satellite simulator is described. ESA

N91-23222# Aerospatiale, Cannes (France).
DESIGN RULES AND SYSTEM TESTING METHODS
Daniel Dodi 1991 21 p
(Rept-911-440-107; CA-10/90; ETN-91-99309) Avail: NTIS HC/MF A03

Deep verification that the charging risk is minimized and implementation of adequate protection against remaining satellite discharge effects (ESD) are now common practices. Those prevention rules have insured nominal operations in flight (with reference to ESD) for the past ten years. For the quite seldom anomalies reported, (two identical anomalies for the TELE-X and TDF-1 over two years in orbit) simulation on ground (on TDF-2, for instance) have always attributed the default to unsatisfactory implementation of preventive methods. The still pending area is the test method to verify the satellite withstanding to ESD phenomenon. At the moment, classical test methods derived from US MIL STD 1541 are adjusted to favor the magnetic coupling with external cablers. An approach, more representative of ESD effects because it depends on satellite configuration is developed. ESA

N91-23223# Aerospatiale, Cannes (France).
THE EUTELSAT 2 PROGRAMME
Claude Burgio and Jean-Jacques Dumesnil (Eutelsat, Paris, France) 1991 4 p
(Rept-911-440-108; CA-1/90; ETN-91-99310) Avail: NTIS HC/MF A01

The Eutelsat 2 spacecraft is a spacebus 100 B model, three axis stabilized, with a launch weight of 1800 kilograms, designed to be operational during eclipse and to be compatible with Ariane 4 and Atlas Centaur launch vehicles. The predicted in orbit lifetime is above seven years. The Eutelsat 2 mission is reviewed and a technical description including the communications payload, of the satellite is given. The program schedule and future prospects are discussed. ESA

N91-23224# Aerospatiale, Cannes (France).
PREDICTIONS AND VERIFICATION OF ESD TESTS MADE WITH SPHERE INJECTIONS ON A FLIGHT REPRESENTATIVE TELECOMMUNICATION SATELLITE: ARABSAT STM
Daniel Dodi 1991 18 p
(Rept-911-440-109; ETN-91-99311) Avail: NTIS HC/MF A03

ESD (discharge effects) tests performed on the flight representative (in terms of structure, coatings, cable routing) Arabsat STM satellite with the Nucletudes sphere injector are reported. The spherical injector aimed at better simulating the blow off effect, was applied onto different locations of the satellite skins (structure and MLI (thermal coating)), and the resulting coupling effects on inside and outside cables were measured. An associated modelization of the satellite including thermal coatings and cables was developed based on separate elementary characterizations as well as on measurements performed on the satellite. Predictions results present a good correlation with tests and evidence the predominance of the magnetic coupling. ESA

N91-23225# Naval Postgraduate School, Monterey, CA.
AN ARTIFICIAL NEURAL NETWORK CONTROL SYSTEM FOR SPACECRAFT ATTITUDE STABILIZATION M.S. Thesis
Clement M. Segura Jun. 1990 77 p
(AD-A232013) Avail: NTIS HC/MF A05 CSCL 22/5

This document reports the results of research into the application of artificial neural networks to controlling dynamic systems. The network used is a feed-forward, fully-connected, 3-layer perception. Two methods of training neural networks via error back-propagation were used. Pattern matching training is a direct method that teaches the basic response. Performance index training is a new technique that refines the response. Performance index training is based on the concept of enforced performance. A neural network will learn to meet a specific performance goal if the performance standard is the only solution to a problem. Performance index training is devised to teach the neural network the time-optimal control law for the system. Real-time adaptation of a neural network in closed loop control of the Crew/Equipment Retriever was demonstrated in computer simulations. GRA

N91-23226# Naval Postgraduate School, Monterey, CA.
SATELLITE MANEUVER EVALUATION TOOL M.S. Thesis
Carlos I. Noriega Sep. 1990 138 p
(AD-A232016) Avail: NTIS HC/MF A07 CSCL 22/1

When first introduced to orbital mechanics, students often experience difficulty in visualizing a satellite's actual path through space. The Satellite Maneuver Evaluation Tool (SMET) seeks to alleviate that problem. SMET is a three-dimensional color graphics simulation of satellites in flight. It allows a student to interactively modify a satellite's orbital parameters and see the effects as the satellites' positions are updated continuously with respect to time. The user can change parameters by defining a maneuver or by directly entering a change through keyboard or dial inputs. SMET offers the user the capability to demonstrate difficult concepts, as well as a method to simulate actual satellite maneuvers. Instructors can videotape SMET sessions for classroom demonstrations. Instantaneous images can also be saved for redisplay or for printout. This thesis provides a background on the mathematical formulas modeled by SMET. It also includes a detailed user's guide for SMET. GRA

N91-23227# Army Construction Engineering Research Lab., Champaign, IL.
LARGE SPACE STRUCTURES FIELDING PLAN Final Technical Report
Charles C. Lozar, Alvin Smith, and Andre N. Brackens Jan. 1991 56 p
(DA Proj. 4A1-62731-AT-41)
(AD-A232097; CERL-TR-M-91/14) Avail: NTIS HC/MF A04 CSCL 22/1

As the U.S. space program advances, there will be a need for large space structures (LSS) to support different space missions. Construction of extraterrestrial base or extraterrestrial LSS, whether in orbit or on the surface of another body, requires the preparation and execution of exquisitely detailed plans. Requirements for the LSS - the high degree of reliability, the interface with other nodes of the overall operation, and effective contingency plans -- all point to the many integration activities that must occur before and during construction. This study develops the preliminary plan for identifying efforts that will be required for LSS construction to support future Army initiatives in space (including space defense systems). It provides a logical sequence of steps that can be followed whether the LSS are to be platforms (unmanned) or

Stations (unmanned). The complexity of this fielding plan suggested that an automated version would make it easier to implement. Such computer programs should consist of a hierarchical, multiple-track format and should be designed to serve developers at the top level (overall management scheme) to lower levels (detailed, engineer usable information). GRA

N91-23228# Air Force Geophysics Lab., Hanscom AFB, MA.
LABORATORY STUDY OF THE THERMOCHEMICAL PROPERTIES OF MATERIALS USED IN SPACECRAFT Interim Report
Terry L. Thiem, Lyn R. Watson, Rainer A. Dressler, Richard H. Salter, and Edmond Murad 4 Sep. 1990 31 p
(AD-A232124; GL-TR-90-0224; ERP-1072) Avail: NTIS HC/MF A03 CSCL 22/5

A high temperature mass spectrometer used to obtain laboratory data on the thermochemical properties of materials encountered in space research is described in detail. The experimental procedures and data analysis necessary to obtain thermochemical constants from the mass spectrometer data are also described. The present experimental arrangement allows cell temperatures of up to 2100 K. Reliable measurements at signal levels below 10 ion counts/s can be made because of the very low background signal and the entirely automated data acquisition and averaging system. In preliminary studies of osmium and its oxides, it is shown that the choice of molybdenum as the cell material is detrimental. The use of an alumina Knudsen cell is proposed. GRA

N91-23578# Espace Studio, Turin (Italy).
TEST ON PARABOLIC FLIGHTS FOR STOWAGE IN WEIGHTLESSNESS
G. Musso, D. Pastrone, and Carlo Viberti (European Space Agency. European Space Research and Technology Center, ESTEC, Noordwijk, Netherlands) *In* ESA, Space and Sea Dec. 1990 p 103-106 (For primary document see N91-23563 15-42)
Copyright Avail: NTIS HC/MF A13

N91-23591# Computer Resources International A/S (Denmark).
A PROCEDURAL EXPERT SYSTEM FOR SPACECRAFT COMMAND AND CONTROL
Mogens Nielsen, J. M. Darroy, Francois Lecouat, Jean-Marc Brenot, and Joe Wheadon (European Space Agency. European Space Operations Center, Darmstadt, Germany, F.R.) *In* ESA, Space and Sea Dec. 1990 p 201-206 (For primary document see N91-23563 15-42)
(Contract ESA-7627/88/NL/DG)
Copyright Avail: NTIS HC/MF A13

19 SPACECRAFT INSTRUMENTATION

For related information see also *06 Aircraft Instrumentation* and *35 Instrumentation and Photography.*

N91-23229*# General Electric Co., Philadelphia, PA. Astro Space Div.
FEASIBILITY STUDY OF THE SUPERCONDUCTING GRAVITY GRADIOMETER (SGG) FLIGHT TEST ON THE EUROPEAN RETRIEVABLE CARRIER (EURECA) Final Report, Jun. 1990 - Jan. 1991
Jan. 1991 174 p Original contains color illustrations
(Contract NAS8-38138)
(NASA-CR-184157; NAS 1.26:184157) Avail: NTIS HC/MF A08; 3 functional color pages CSCL 14B

A study was performed to determine the feasibility of conducting a flight test of the Superconducting Gravity Gradiometer (SGG) Experiment Module on one of the reflights of the European Retrievable Carrier (EURECA). EURECA was developed expressly to accommodate space science experimentation, while providing a high quality microgravity environment. As a retrievable carrier, it offers the ability to recover science experiments after a nominal six months of operations in orbit. The study concluded that the SGG Experiment Module can be accommodated and operated in a EURECA reflight mission. It was determined that such a flight test would enable the verification of the SGG Instrument flight performance and validate the design and operation of the Experiment Module. It was also concluded that a limited amount of scientific data could be obtained on this mission. Author

N91-23230# European Space Agency, Paris (France).
QUALIFICATION OF CONCENTRATING MIRROR SYSTEMS WITH THE HERMES MEASUREMENT SYSTEM AND THE HELIOS SIMULATION PROGRAM
Juergen Kleih (Deutsche Forschungsanstalt fuer Luft- und Raumfahrt, Stuttgart, Germany, F.R.) Feb. 1991 71 p Transl. into ENGLISH of Beurteilung von Konzentri erenden Spiegelsystemen mit Hilfe des Nesssystems Hermes und des Simulationsprogramms Helios (Stuttgart, Fed. Republic of Germany, DLR), Aug. 1989 53 p Original language document was announced as N90-26394
(ESA-TT-1213; DLR-FB-89-51; ETN-91-99319) Avail: NTIS HC/MF A04

An overview of methods (direct and indirect) for measuring highly concentrated solar radiation, which were used for qualifying solar power plants (from the parabolic mirror up to the tower plant) is provided. In particular, it goes into the Hermes measuring system which was used to measure two membrane mirrors (of diameter 17 and 7.5 m respectively). Measurements were made of maximum radiant flux densities of more than 2 MW/sq m for the 17 m mirror and of more than 9 MW/sq m for the 7.5 m mirror. The HELIOS simulation program was used to check the measurement results. The agreement between measurement and calculation was satisfactory over all. ESA

20 SPACECRAFT PROPULSION AND POWER

Includes main propulsion systems and components, e.g., rocket engines; and spacecraft auxilliary power sources.

For related information see also *07 Aircraft Propulsion and Power, 28 Propellants and Fuels, 44 Energy Production and Conversion,* and *15 Launch Vehicles and Space Vehicles.*

N91-23231# Ben Gurion Univ. of the Negev, Beersheva (Israel). Center for MHD Studies.
LIQUID-METAL MHD POWER CONVERSION FOR SPACE ELECTRIC SYSTEMS
L. Blumenau, Herman Branover, A. El-Boher, E. Spero, Semion Sukoriansky, and E. Greenspan (Israel Atomic Energy Commission, Beersheba.) 1987 6 p Presented at the 4th Symposium on Space Nuclear Power Systems, Albuquerque, NM, 12-16 Jan. 1987 Sponsored by SOLMECS Corp. N.V. and Chief Scientists Office of the Israel Ministry of Industry and Trade
(Ser-S/27; ITN-88-85008) Avail: NTIS HC/MF A02

A number of LMMHD (Liquid Metal Magneto-Hydro-Dynamic) Power Conversion Systems (PCS) were conceived for SES (Space Electric Systems) applications. Variations of a single-stage PCS operating on the Wet Vapor Cycle can meet demands of most continuous mode applications. A two-stage version and an Ericsson Cycle PCS are also presented. ISA

N91-23232*# Wisconsin Univ., Madison.
MARS MANNED FUSION SPACESHIP
James Hedrick, Brent Buchholtz, Paul Ward, Jim Freuh, and Eric Jensen 1991 11 p
(Grant NAG3-1200)
(NASA-CR-188215; NAS 1.26:188215) Avail: NTIS HC/MF A03 CSCL 18A

Fusion Propulsion has an enormous potential for space exploration in the near future. In the twenty-first century, a usable and efficient fusion rocket will be developed and in use. Because of the great distance between other planets and Earth, efficient use of time, fuel, and payload is essential. A nuclear spaceship

would provide greater fuel efficiency, less travel time, and a larger payload. Extended missions would give more time for research, experiments, and data acquisition. With the extended mission time, a need for an artificial environment exists. The topics of magnetic fusion propulsion, living modules, artificial gravity, mass distribution, space connection, and orbital transfer to Mars are discussed. The propulsion system is a magnetic fusion reactor based on a tandem mirror design. This allows a faster, shorter trip time and a large thrust to weight ratio. The fuel proposed is a mixture of deuterium and helium-3. Helium-3 can be obtained from lunar mining. There will be minimal external radiation from the reactor resulting in a safe, efficient propulsion system. Author

N91-23233*# National Aeronautics and Space Administration. Lewis Research Center, Cleveland, OH.
DESTRUCTIVE PHYSICAL ANALYSIS RESULTS OF NI/H2 CELLS CYCLED IN LEO REGIME
Hong S. Lim, Gabriela R. Zelter, John J. Smithrick, and Stephen W. Hall (Naval Weapons Support Center, Crane, IN.) 1991 9 p Proposed for presentation at the 26th Intersociety Energy Conversion Engineering Conference, Boston, MA, 4-9 Aug. 1991; cosponsored by ANS, SAE, ACS, AIAA, ASME, IEEE, and AIChE
(Contract NAS3-22238)
(NASA-TM-104382; E-6191; NAS 1.15:104382) Avail: NTIS HC/MF A02 CSCL 21H

Six 48-Ah individual pressure vessel (IPV) Ni/H2 cells containing 26 and 31 percent KOH electrolyte were life cycle tested in low Earth orbit. All three cells containing 31 percent KOH failed (3729, 4165, and 11,355 cycles), while those with 26 percent KOH were cycled over 14,000 times in the continuing test. Destructive physical analysis (DPA) of the failed cells included visual inspections, measurements of electrode thickness, scanning electron microscopy, chemical analysis, and measurements of nickel electrode capacity in an electrolyte flooded cell. The cycling failure was due to a decrease of nickel electrode capacity. As possible causes of the capacity decrease, researchers observed electrode expansion, rupture, and corrosion of the nickel electrode substrate, active material redistribution, and accumulation of electrochemically undischargeable active material with cycling. Author

N91-23234*# National Aeronautics and Space Administration. Lewis Research Center, Cleveland, OH.
COMPONENT TECHNOLOGY FOR STIRLING POWER CONVERTERS
Lanny G. Thieme 1991 10 p Presented at the 26th Intersociety Energy Conversion Engineering Conference, Boston, MA, 4-9 Aug. 1991; sponsored by American Nuclear Society, SAE, American Chemical Society, AIAA, ASME, IEEE, and American Inst. of Chemical Engineers
(NASA-TM-104387; E-6175; NAS 1.15:104387) Avail: NTIS HC/MF A02 CSCL 10B

NASA Lewis Research Center has organized a component technology program as part of the efforts to develop Stirling converter technology for space power applications. The Stirling Space Power Program is part of the NASA High Capacity Power Project of the Civil Space Technology Initiative (CSTI). NASA Lewis is also providing technical management for the DOE/Sandia program to develop Stirling converters for solar terrestrial power producing electricity for the utility grid. The primary contractors for the space power and solar terrestrial programs develop component technologies directly related to their goals. This Lewis component technology effort, while coordinated with the main programs, aims at longer term issues, advanced technologies, and independent assessments. An overview of work on linear alternators, engine/alternator/load interactions and controls, heat exchangers, materials, life and reliability, and bearings is presented. Author

N91-23235# Arnold Engineering Development Center, Arnold Air Force Station, TN.
DIAGNOSTIC MEASUREMENTS ON AN ALUMINIZED PROPELLANT PLUME DURING SPIN AND NONSPIN TESTING Final Report, Apr. - Sep. 1990
K. S. Beale, W. K. McGregor, R. A. Frederick, R. A. Reed, and D. W. Roberds Feb. 1991 52 p
(Contract MIPR-133-90)
(AD-A232031; AEDC-TR-90-28; ARO-28121.1-EG-SDI) Avail: NTIS HC/MF A04 CSCL 21/8

Two identical aluminum-loaded solid-propellant rocket motors were tested at simulated altitudes of approximately 100,000 ft. One motor was fired under spin conditions, and the other was static-tested. Plume diagnostic measurements were made during the firings in the infrared to ultraviolet regions of the spectrum. Initial analysis of the data has been performed, and the results are summarized in this report. The data were analyzed with respect to radiant heating, searchlight emission, aluminum chloride absorption, spin effects, and particle mass distribution. GRA

N91-23236# Naval Postgraduate School, Monterey, CA. Dept. of Electrical and Computer Engineering.
AUTOMATIC PARTICLE SIZING FROM ROCKET MOTOR HOLOGRAMS Technical Report, Jan. 1986 - Dec. 1990
John P. Powers 1 Dec. 1990 87 p
(Contract MIPR-F04611-90-X-0057)
(AD-A232553; NPS-EC-91-003) Avail: NTIS HC/MF A05 CSCL 21/9

Microscopic particles within an optical hologram reconstruction have been successfully measured using an image digitizer and a PC/AT computer. The hologram was recorded during a test burn of some solid rocket fuel and captured a 2 in. x 2 in. volume of burning particles as they lift from the fuel surface during combustion. The computer processes the digitized images using feature identification algorithms and sizing in the feature's horizontal dimension, its vertical dimension and area. The operation of the algorithms have been validated against calibration objects. Statistical tests show that about 1,300 particles from several image frames are required to obtain a representative size distribution. Overlying speckle degrades the resolution of the image and can be reduced by a variety of techniques. The performance of these speckle-reduction techniques has been measured and compared in the areas of speckle reduction, loss of resolution, and processing time. Program sizes and processing times have been compared for both FORTRAN and C language versions of the processing program. GRA

N91-23171# Messerschmitt-Boelkow-Blohm G.m.b.H., Munich (Germany, F.R.).
HIGHLY INTEGRATED DUCTED ROCKET PROPULSION MODULES FOR FUTURE HYPERSONIC TACTICAL MISSILES
Hermann-L. Weinreich *In* AGARD, Hypersonic Combined Cycle Propulsion Dec. 1990 13 p (For primary document see N91-23147 15-07)
Copyright Avail: NTIS HC/MF A20; Non-NATO Nationals requests available only from AGARD/Scientific Publications Executive

23 CHEMISTRY AND MATERIALS (GENERAL)

N91-23237*# National Aeronautics and Space Administration. Langley Research Center, Hampton, VA.
POLY(1,3,4-OXADIAZOLES) VIA AROMATIC NUCLEOPHILIC DISPLACEMENT Patent Application
John W. Connell, inventor (to NASA), Paul M. Hergenrother, inventor (to NASA), and Peter Wolf, inventor (to NASA) (Badische Anilin- und Soda-Fabrik A.G., Mogendorf, Germany, F.R.) 22 Jan. 1991 20 p
(NASA-Case-LAR-14427-1; NAS 1.71:LAR-14427-1; US-Patent-Appl-SN-645089) Avail: NTIS HC/MF A03 CSCL 07A

Poly(1,3,4-oxadiazoles) (POX) are prepared by the aromatic nucleophilic displacement reaction of di(hydroxyphenyl) 1,3,4-oxadiazole monomers with activated aromatic dihalides or activated aromatic dinitro compounds. The polymerizations are carried out in polar aprotic solvents such as sulfolane or

diphenylsulfone using alkali metal bases such as potassium carbonate at elevated temperatures under nitrogen. The di(hydroxyphenyl) 1,3,4-oxadiazole monomers are synthesized by reacting 4-hydroxybenzoic hydrazide with phenyl 4-hydrobenzoate in the melt and also by reacting aromatic dihydrazides with two moles of phenyl 4-hydroxybenzoate in the melt. This synthetic route has provided high molecular weight POX of new chemical structure, is economically and synthetically more favorable than other routes, and allows for facile chemical structure variation due to the large variety of activated aromatic dihalides which are available. NASA

24 COMPOSITE MATERIALS

Includes physical, chemical, and mechanical properties of laminates and other composite materials.

For ceramic materials see *27 Nonmetallic Materials*.

N91-23238# Israel Aircraft Industries Ltd., Ben-Gurion Airport. Materials and Process Engineering.
IMPROVED QUALITY ACCEPTANCE PROCEDURE FOR INTERLAMINAR SHEAR STRENGTH
R. Feldman, D. Enkaoua, and H. Rosenthal May 1987 6 p
(IAITIC-87-1005; ITN-88-85004) Avail: NTIS HC/MF A02

An efficient and cost effective test method has been developed for the interlaminar shear strength determination of fiber reinforced plastics. The new technique is based on the use of a continuous beam specimen instead of the conventional small short beam configuration. Excellent correlation between the continuous and the short beam specimens has been obtained for various composite systems. ISA

N91-23239 Delaware Univ., Newark.
A SIMULATION OF THE DRAPING AND A MODEL OF THE CONSOLIDATION OF COMMINGLED FABRICS Ph.D. Thesis
Barry Paul VanWest 1990 351 p
Avail: Univ. Microfilms Order No. DA9101048

A preform material commonly used in the manufacture of fiber reinforced thermoplastic composites is commingled fabric composed of yarns containing both the reinforcement and the matrix in fiber form. A quality of commingled fabric is its drapeability, allowing it to conform to mold shapes prior to being consolidated into a rigid structure. The objective of this research is to develop a simulation of the draping process and a mathematical model of the subsequent consolidation process which will predict, for a given mold surface and processing parameters, the material characteristics necessary for determining the mechanical properties of the finished product. Combining the results of the draping simulation and consolidation analysis with a laminate analysis allows the prediction, for a given set of draping constraints and processing parameters, of the mechanical properties at any point in a composite structure formed from commingled fabric. Dissert. Abstr.

N91-23240 State Univ. of New York, Buffalo.
BROMINATION OF CARBON FIBERS AND CARBON-CARBON COMPOSITES Ph.D. Thesis
Chi-Ting Ho 1990 204 p
Avail: Univ. Microfilms Order No. DA9033704

Bulk chemical modification of carbon fibers and carbon-carbon composites was performed by bromination for the purposes of increasing the oxidation resistance and decreasing the electrical resistivity. Both purposes were achieved in Amoco Thornel P-100 pitch-based carbon fibers and in carbon-carbon composites that were heat treated up to 2000 C. For more graphitic carbons, namely Amoco P-X-7 pitch-based carbon fibers, du Pont E-130 pitch-based carbon fibers and carbon-carbon composites that were heat treated at 2700 C, the bromination also decreased electrical resistivity, but it decreased the oxidation resistance due to physical damage caused by the bromination. Two methods of bromination were used, namely exposure to Br2 and anodic oxidation in a KBr electrolyte. The first method caused substantial bromine uptake in all of the carbon fibers and carbon-carbon composites mentioned, whereas the second method failed to cause substantial bromine uptake in the carbon-carbon composites. For the more graphitic carbon fibers, both methods resulted in intercalated fibers that exhibited in-plane superlattice order at room temperature and up to 100 C, at which in-plane melting occurred. For the less graphite carbon fibers, the first method resulted in intercalated fibers that exhibited in-plane disorder at room temperature and down to -2 C, at which in-plane ordering occurred, whereas the second method resulted in intercalated fibers that exhibited in-plane order at room temperature and up to 100 C, at which in-plane melting occurred. Furthermore, Thornel P-100 fibers brominated by the second method exhibited more homogeneous intercalation, a more uniform chemical state of the intercalated bromine, a higher electron transfer, a lower bromine, and, most importantly, enhanced oxidation resistance, compared to those brominated by the first method. Dissert. Abstr.

N91-23241 Pennsylvania Univ., Philadelphia.
A STUDY OF THE MICROMECHANICS OF THE FIBER-MATRIX INTERPHASE IN MONOFILAMENT COMPOSITES, IN MONOTONIC LOADING, AND CYCLIC FATIGUE Ph.D. Thesis
Linda Sue Schadler 1990 314 p
Avail: Univ. Microfilms Order No. DA9101214

Macroscopic properties of continuous filament composites are dependent on the fiber-matrix interphase behavior: the ability of the interphase to transfer load from the matrix to the fiber, and the energy absorbed during interphase failure. A mono-filament composite system was employed to study the fiber-matrix interphase because fiber/fiber interaction and processing variability are eliminated. Several methods were used to observe the interphase behavior of carbon/thermoplastic matrix mono-filament composites including a fragmentation technique to measure the interphasial shear stress and a Raman spectroscopic technique. The first goal was to alter the interphase in a controlled manner by treating the fiber surface, and then correlating fiber surface morphology, fiber surface energy, fiber strength, and matrix properties with interphase micromechanics. The second goal was to study the role of the interphase in cyclic fatigue. The effects of cyclic loading direction, frequency, and amplitude were studied. Damage was characterized by fiber matrix debonding, a reduction of the average interphase shear stress, and changes in the locus of failure as determined by scanning electron microscopy fractography. Dissert. Abstr.

N91-23242*# Virginia Polytechnic Inst. and State Univ., Blacksburg. Dept. of Engineering Science and Mechanics.
THE DEVELOPMENT AND EVALUATION OF AN ALTERNATIVE POWDER PREPREGGING TECHNIQUE FOR USE WITH LaRC-TPI/GRAPHITE COMPOSITES Interim Report No. 85, Jun. 1988 - Dec. 1990
Andrea L. Ogden, Michael W. Hyer, Garth L. Wilkes, Alfred C. Loos, and Terry L. St.Clair (National Aeronautics and Space Administration. Langley Research Center, Hampton, VA.) Apr. 1991 174 p
(Grant NAG1-343)
(NASA-CR-188184; NAS 1.26:188184; CCMS-91-08; VPI-E-91-07)
Avail: NTIS HC/MF A08 CSCL 11D

An alternative powder prepregging method for use with LaRC-TPI (a thermoplastic polyimide)/graphite composites is investigated. The alternative method incorporates the idea of moistening the fiber prior to powder coating. Details of the processing parameters are given and discussed. The material was subsequently laminated into small coupons which were evaluated for processing defects using electron microscopy. After the initial evaluation of the material, no major processing defects were encountered but there appeared to be an interfacial adhesion problem. As a result, prepregging efforts were extended to include an additional fiber system, XAS, and a semicrystalline form of the matrix. The semicrystalline form of the matrix was the result of a complex heat treating cycle. Using scanning electron microscopy (SEM), the fiber/matrix adhesion was evaluated in these systems relative to the amorphous/XAS coupons. Based on these results,

amorphous and semicrystalline/AS-4 and XAS materials were prepregged and laminated for transverse tensile testing. The results of these tests are presented, and in an effort to obtain more information on the effect of the matrix, remaining semicrystalline transverse tensile coupons were transformed back to the amorphous state and tested. The mechanical properties of the transformed coupons returned to the values observed for the original amorphous coupons, and the interfacial adhesion, as observed by SEM, was better than in any previous sample.
Author

N91-23243 Washington Univ., Seattle.
THERMO-VISCOELASTIC BEHAVIOR OF COMPOSITE MATERIALS Ph.D. Thesis
In Hee Hwang 1990 240 p
Avail: Univ. Microfilms Order No. DA9104247

Time-dependent behavior of composite materials is described by an anisotropic thermo viscoelastic constitutive model. Based on the variational principle of linear viscoelasticity, a special finite element method was developed for the solution of thermo viscoelastic boundary value problems in anisotropic materials. Using the developed numerical procedure, the stress/strain distributions and histories around a circular hole in graphite/epoxy composites were obtained for both cases of mechanical and thermal loads. The results indicate that time-dependent effects are important in a composite with a matrix dominated layup. Such effects also strongly depend on the specific environmental condition and the applied load spectrum. Fracture mechanics of viscoelastic composites studied based on the first law of thermodynamics and a hereditary stress-strain equation. The viscoelastic energy release rate for predicting delamination growth in composite laminates was formulated as a crack closure integral which is solved by a finite element approach. Parametric studies were conducted to investigate the effect of ply orientation, delamination geometry, and loading condition on the time dependent interlaminar stress state along with the crack opening displacement and the energy release rate. The study shows that the interlaminar stresses and the energy release rate decrease with time under a constant load. To verify the theoretical solution, an experimental program was designed for creep test of IM7/8551-7 composites at an elevated temperature. Both in-plane transverse and shear relaxation moduli were determined experimentally. The deformation fields in several composites with circular holes were measured as a function of time using the moire interferometry technique. Dissert. Abstr.

N91-23244*# National Aeronautics and Space Administration. Langley Research Center, Hampton, VA.
RATE DEPENDENT STRESS-STRAIN BEHAVIOR OF ADVANCED POLYMER MATRIX COMPOSITES
Thomas S. Gates Apr. 1991 26 p
(NASA-TM-104070; NAS 1.15:104070) Avail: NTIS HC/MF A03 CSCL 11D

The formulation of an elastic/viscoplastic constitutive model which was used to predict the measured behavior of graphite/thermoplastic and graphite/bismaleimide composite materials at elevated temperature is described. The model incorporates the concepts of overstress and effective strain/strain to provide a simple formulation which was able to account for material behavior under monotonic tension or compression loads over a temperature range of 23 to 200 C. Observed behavior such as stress relaxation and steady state creep, in off-axis tension and compression tests, were predicted by the model. Material constants required by the model were extracted from simple off-axis test data.
Author

N91-23245# Sandia National Labs., Albuquerque, NM.
ION BEAM TESTING OF THE AEROLOR X-POINT DUMP PLATE FOR THE JOINT EUROPEAN TORUS
J. C. Salmonson, J. G. Watkins, R. D. Watson, and J. M. McDonald Jan. 1991 26 p
(Contract DE-AC04-76DP-00789)
(DE91-010719; SAND-89-1929) Avail: NTIS HC/MF A03

The durability of a carbon-carbon composite, Aerolor A05, X-point divertor dump plate to thermal fatigue was evaluated for the Joint European Torus (JET) at Sandia's Plasma Material Test Facility. Of primary interest was the effect of thermal cycling on the carbon-carbon threads of the bolted attachment scheme for the Aerolor X-point divertor. This report describes the testing performed at the Ion Beam Test System and the test and analysis results obtained in support of this effort. After completing 1000 thermal cycles, where the surface temperature of the 8 cm by 8 cm by 2.3 cm Aerolor tile reached 2200 C during a 10 s, 500 W/cm(sup 2) pulse, the tile survived without any noticeable damage. Post test inspection of the carbon-carbon threads showed only minor wear and no signs of significant damage. Thermal modeling of the test article using the ABAQUS finite element code agreed very well with experimental results. The thermal creep experienced by the M-12 stainless steel bolt during ion beam testing will not be expected to occur during normal operations in JET because of the longer cycle times between the thermal events. Finite element analysis indicates that the longer cycle times at the JET will reduce the peak temperatures in the vicinity of the bolt and bolt insert below the level at which thermal creep would occur. An additional margin of safety could be obtained by using Inconel or Nimonic fasteners.
DOE

N91-23246# Deutsche Forschungsanstalt fuer Luft- und Raumfahrt, Brunswick (Germany, F.R.). Abt. Verbundstrukuren.
CHARACTERIZATION OF COMPOSITE MATERIALS FOR AEROSPACE MATERIALS
Harald Twardy, Holger Hanselka, and Bernhard Beier Jul. 1990 25 p In GERMAN; ENGLISH summary Report will also be announced as translation (ESA-TT-1260)
(DLR-Mitt-90-15; ISSN-0939-298X; ETN-91-99061; ESA-TT-1260)
Avail: NTIS HC/MF A03; DLR, Wissenschaftliches Berichtswesen, VB-PL-DO, Postfach 90 60 58, 5000 Cologne, Fed. Republic of Germany, HC 11.50 DM

Fiber reinforced polymers are recommended construction materials for space and transatmospheric flight. A wide spectrum of ambient effects, such as temperature, moisture, radiation and their combination requires the variation of the mechanical and physical properties of polymers. Independently of the characterization of the reduced coefficients of elasticity, the thermal resistance to aging and the viscoelastic behavior under the influence of elevated temperatures are of prime interest.
ESA

N91-23247*# National Aeronautics and Space Administration. Lewis Research Center, Cleveland, OH.
COMBINED THERMAL AND BENDING FATIGUE OF HIGH-TEMPERATURE METAL-MATRIX COMPOSITES: COMPUTATIONAL SIMULATION
Pascal K. Gotsis Jun. 1991 24 p
(NASA-TM-104354; E-6140; NAS 1.15:104354) Avail: NTIS HC/MF A03 CSCL 11D

The nonlinear behavior of a high-temperature metal-matrix composite (HT-MMC) was simulated by using the metal matrix composite analyzer (METCAN) computer code. The simulation started with the fabrication process, proceeded to thermomechanical cyclic loading, and ended with the application of a monotonic load. Classical laminate theory and composite micromechanics and macromechanics are used in METCAN, along with a multifactor interaction model for the constituents behavior. The simulation of the stress-strain behavior from the macromechanical and the micromechanical points of view, as well as the initiation and final failure of the constituents and the plies in the composite, were examined in detail. It was shown that, when the fibers and the matrix were perfectly bonded, the fracture started in the matrix and then propagated with increasing load to the fibers. After the fibers fractured, the composite lost its capacity to carry additional load and fractured.
Author

N91-23248# Aerospatiale, Toulouse (France).
OBSERVATORY OF NEW MATERIALS. EVOLUTION PERSPECTIVES FOR THE MATERIALS USED IN CIVIL TRANSPORTATION AIRCRAFT [OBSERVATOIRE DES MATERIAUX NOUVEAUX. PERSPECTIVES D'EVOLUTION DES MATERIAUX UTILISES DANS LES AVIONS DE TRANSPORT CIVIL]
A. Ferran 31 Jan. 1991 48 p In FRENCH
(Rept-911-111-107; ETN-91-99271) Avail: NTIS HC/MF A03

It is shown that, in aeronautics, each material innovation is the cause of reactions in other competitive materials. The evolution of metallic and organic materials is considered. Aluminum alloys improvements were made with regard to fatigue strength, corrosion behavior, and damage tolerances. Newly developed aluminum lithium alloys showed a 9 pct. mass gain potential. New aluminum alloys, new titanium alloys, and new steels are presented. Titanium alloys are discussed. Titanium superplastic forming and diffusion bonding is illustrated. Landing gear steels and structural steel properties are given. Metallic Matrix Composite (MMC) evolution is presented. Aluminum matrix material characteristics are given. New materials for civil aircrafts are presented. A marked evolution towards composite material utilization is focused. ESA

N91-23249# Aerospatiale Aquitaine, Saint-Medard en Jalles (France). Strategic and Space Div.
CARBON-CARBON MATERIAL WITH OXIDATION PROTECTION
Jean-Luc Macret 1991 7 p
(Rept-911-430-103; ETN-91-99275) Avail: NTIS HC/MF A02

The development of an oxidation resistant carbon-carbon material family which meets requirements of reusability for space projects such as Hermes, asking for stuctural materials for high temperature applications up to 2000 C, is reported. Preform manufacturing and densification are described. Parts were successfully tested for the Hermes program including tests in a solar furnace. To decrease processing costs and to guarantee product quality automatic processes were implemented for each step of the fabrication: automatic looms for multidirectional weaving techniques and a centralized computer controlled densification workshop. The material was chosen for the nose cap and the wing leading edge sections of the Hermes Spaceplane. ESA

N91-23250# Aerospatiale Aquitaine, Saint-Medard en Jalles (France). Strategic and Space Div.
NEW DEVELOPMENTS IN COMPOSITES FOR SPACE APPLICATIONS
Jean F. Jamet and D. Cabanel 1991 8 p
(Rept-911-430-104; ETN-91-99276) Avail: NTIS HC/MF A02

Nonmetallic composites technology concerning organic composites, carbon-carbon and their protection, and ceramic composites is reviewed. Experience concerning wound structures (solid propulsion, space high pressure vessels, etc.) and related special technologies (resins formulation, low impregnation, high capacity winding machines, expert system for structural joining optimization, radio curing) are discussed. A large domain of temperature composites technology (from cryogenic to 4000 K reentry temperature) and dimensions (from 10 mm ceramic screws to 3000 mm organic matrix structures) are under study. Progression is achieved by scientific and innovative approaches and programs with a view to cost, performance and quality. ESA

N91-23251# Aerospatiale Aquitaine, Saint-Medard en Jalles (France). Strategic and Space Div.
OXIDATION RESISTANT CARBON/CARBON MATERIALS
O. Franc and Jean-Luc Macret 1991 5 p
(Rept-911-430-105; ETN-91-99277) Avail: NTIS HC/MF A01

A research and development program in Ceramic Matrix Composites (CMC) and oxidation resistant Carbon/Carbon (C/C Inox) is discussed. The proposal for C/C Inox to be used for the nose cap and wing leading edge of the Hermes Spaceplane is discussed. The fabrication of C/C material (weaving and densification) and C/C PAO (Protection Against Oxidation) including silicidation and PAO for leading edges and nose caps are described. C/C is concluded to have an excellent stability of properties in temperatures up to 3000 C but due to oxidation sensitivity a PAO is needed for application on space planes. ESA

N91-23252# Aerospatiale Aquitaine, Saint-Medard en Jalles (France). Strategic and Space Div.
NONDESTRUCTIVE INSPECTION FOR CARBON-CARBON WITH ADAPTED COATING FOR OXIDATION
P. Plotard and C. LeFloch 1991 10 p
(Rept-911-430-106; ETN-91-99278) Avail: NTIS HC/MF A02

During reentry in the atmosphere the Hermes Spaceplane will be exposed to very high temperature in oxidizing conditions (up to 1800 C and low pressure). The concerned parts are mainly the nose cap and the leading edges for which carbon/carbon material with adapted coating for oxidation was developed. The manned systems designed to withstand the whole conditions 30 times without damaging, need maximum reliability. Nondestructive testings to quantify functional characteristics of the material (coating thickness for example and critical defects for structural integrity such as delaminations or voids, decohesions, oxidation cavities) are described. The main features of the investigated and developed methods (eddy current, beta scattering, ultrasonics, thermography, Compton scattering) and the main results are presented. ESA

N91-23253# Aerospatiale Aquitaine, Saint-Medard en Jalles (France). Strategic and Space Div.
FIBER-REINFORCED GLASS-CERAMIC MATRIX COMPOSITES: NEW CLASS OF MATERIALS FOR SPACE APPLICATIONS
Jean F. Jamet 1991 6 p
(Rept-911-430-107; ETN-91-99279) Avail: NTIS HC/MF A02

A program aimed at developing a new family of reinforced glass and glass ceramic matrix and their associated technologies to realize large parts is discussed. The reinforcement by carbon fibers of three SiC Nicalon fibers is under development. The position of glass and glass ceramic composites in terms of thermostructural applications, including their advantages over metal matrix composites, is described. Glass synthesis methods and behaviors are discussed. The industrial technology of parts elaboration by hot directional and isostatic pressing facilities is discussed. The first SiC Nicalon reinforced basic composites are described. ESA

N91-23254# Aerospatiale Aquitaine, Saint-Medard en Jalles (France). Space and Strategic Systems Div.
THERMOSTRUCTURAL COMPOSITES: RECENT EVOLUTIONS AND IMPROVEMENTS
Jean F. Jamet 1991 11 p Presented at the French Aerospace 1990 Aeronautical and Space Conference, Washington, DC, 12-14 Jun. 1990
(Rept-911-430-109; ETN-91-99281) Avail: NTIS HC/MF A03

Recent evolutions and improvements in three material families are presented: glass ceramic matrix composites for uses up to 1000 C; ceramic matrix composites for uses up to 1500 C; oxidation resistant carbon/carbon composites for uses beyond 1500 up to 2000 C. The strengths of these thermostructural composites are summarized. Their usefulness in applications (temperature/time) in the fields of missiles and ramjets, hypersonic transportation systems, space planes, etc. is shown. ESA

N91-23255# Aerospatiale Aquitaine, Saint-Medard en Jalles (France).
NONDESTRUCTIVE MEASUREMENT OF THICKNESS AND DENSITY OF COMPOSITE MATERIALS BY COMPTON BACKSCATTERING [MESURE D'EPAISSEUR ET DE DENSITE DE MATERIAUX COMPOSITES PAR RETRODIFFUSION COMPTON]
D. Babot, G. Peix, P. Duvauchelle, G. Berodias (Institut National des Sciences Appliquees, Lyon, France), C. LeFloch, and P. Sarrazin 1991 8 p In FRENCH; ENGLISH summary
(Rept-911-430-112; ETN-91-99284) Avail: NTIS HC/MF A02

An experimental study was carried out to evaluate the capabilities of Compton backscattering for measuring the thickness

and the density in a non-invasive way of advanced materials, such as carbon-carbon for high temperature components of a gliding reentry vehicle. The principle of this method, which only requires access to one side of the object to be examined, is presented. The experimental results are given: the thickness measurement is obtained with an accuracy of 0.1 mm and a good reliability and the density is measured with an accuracy of plus or minus one percent. ESA

N91-23256# Aerospatiale Aquitaine, Saint-Medard en Jalles (France).
MECHANICAL CHARACTERiSATION OF FIBRE-MATRIX INTERFACE IN CERAMIC COMPOSITES BY AN INSTRUMENTED INDENTATION TEST
P. Peres and M. H. Ritti (Office National d'Etudes et de Recherches Aerospatiales, Paris, France) 1991 12 p In FRENCH; ENGLISH summary
(Rept-911-430-114; ETN-91-99286) Avail: NTIS HC/MF A03

The instrumental microindentation test gave a better understanding of rheological behavior of the interface in glass matrix composites and glass ceramic composites. The complete analysis of indentation curve is complicated. Good correlations with their macrostructural behaviors were obtained for these materials. Characterizations of other composite materials need analysis adapted to the push out mechanisms. Consequently results are not always strictly related to their fracture behaviors. ESA

N91-23257# Aerospatiale Aquitaine, Saint-Medard en Jalles (France).
CARBON/CARBON INOX THERMOSTRUCTURAL COMPOSITES: MECHANICAL AND TECTONIC BEHAVIOR OF ANTI-OXIDATION PROTECTION [LES COMPOSITES THERMOSTRUCTURAUX CARBONE/CARBONE INOX COMPORTEMENT: MECANIQUE ET TECTONIQUE DE LA PROTECTION ANTI-OXYDATION]
J. M. Lequertier 1991 16 p In FRENCH; ENGLISH summary
(Rept-911-430-115; ETN-91-99287) Avail: NTIS HC/MF A03

New materials are to be used for the nose cap and leading edges of Hermes vehicle during its reentry. Carbon/carbon composites protected against oxidation exhibit high specific thermomechanical properties and reusability in extreme conditions, such as atmospheric reentries. During high temperature processing, the thermal coefficient of expansion mismatch between the components involves, when cooling, the growth of microcracks in the carbon matrix and in the Oxidation Protection Coating (OPC). In the first OPC, a geometrical network of cracks is created, which constitutes an original arrangement of independent blocks of silicon carbide. The thermomechanical behavior of the carbon/carbon and its oxidation protection, e.g., tectonic behavior of the OPC, is explained considering a macroscopic or microscopic scale analysis. ESA

N91-23258# Aerospatiale Aquitaine, Saint-Medard en Jalles (France).
MATERIALS AND STRUCTURE FOR HERMES
O. Franc and Jean-Luc Macret 1991 14 p
(Rept-911-430-117; ETN-91-99289) Avail: NTIS HC/MF A03

The TPS (Thermal Protection System) for the Hermes Spaceplane, the manufacturing of oxidation resistant Carbon/Carbon (C/C Inox) to be used in the Spaceplane leading edges and nose cap, and nondestructive tests are described. The Hermes programs and configuration and elementary phases of a typical Hermes mission are outlined. The SIMOUN testing device for testing Hermes materials under conditions as close as possible to the reentry conditions by submission to a very hot air flux created by a plasma generator is outlined. The large parts feasibility is concluded to be demonstrated for the Hermes program, first thermomechanical characterization results measured on material and parts reaching the forecast performances. ESA

N91-23259# Aerospatiale Aquitaine, Saint-Medard en Jalles (France).
HIGH TEMPERATURE COMPOSITES IN SPACE PLANES AND MISSILES DEVELOPMENT
Jean F. Jamet 1991 12 p In FRENCH; ENGLISH summary
(Rept-911-430-119; ETN-91-99291) Avail: NTIS HC/MF A03

Carbon-carbon composites were developed to improve the thermomechanical and ablative properties of the first generation of ablative composites, such as silica phenolic composites. Carbon-carbon composites which were largely developed during the last ten years have the required thermomechanical properties for spaceplane reentry, corresponding to lower heat flux, 1800 C under low pressure, and light and large structures. But they must be protected against severe oxidation. New wearing densification and assembling technologies were also developed. The thermostructural composites can today give solutions to problems such as refractoriness, low density, toughness, and thermomechanical resistance. ESA

N91-23260# Aerospatiale Aquitaine, Saint-Medard en Jalles (France). Space and Strategic Systems Div.
CERAMICS IN AEROSPACE
Alain Hordonneau 1991 5 p
(Rept-911-430-127; ETN-91-99299) Avail: NTIS HC/MF A01

The development of ceramic parts for aerospace is discussed. The need for thermostructural material for the nozzle of launcher motors and the nose tip of reentry bodies is mentioned. Developments dedicated to atmosphere reentry of the Hermes Spaceplane are described. It is considered that Hermes will open the door to thermostructural applications on manned flights and that other applications including monolithic ceramics will consolidate the knowhow and lead raw material producers to manufacture fine powders, organometallic resins and fibers. ESA

N91-23261# Aerospatiale Aquitaine, Saint-Medard en Jalles (France). Strategic and Space Div.
STRUCTURAL MATERIALS FOR SPACE MIRRORS
C. Capitanio 1991 6 p
(Rept-911-430-128; ETN-91-99300) Avail: NTIS HC/MF A02

Results of evaluation of potential materials for the XMM telescope mirrors are presented. Tested substrates include SiC plane plates for XMM telescope and XMM reflection gratings and SiC shells for XMM telescope. Other materials described are carbon/resin, carbon/carbon, and glass matrix ceramics reinforced with fibers (SiC, carbon). The existence of new potentialities is shown but applications must be thoroughly studied before development decisions can be made. ESA

N91-23262# Aerospatiale Aquitaine, Saint-Medard en Jalles (France). Strategic and Space Div.
HOW TO KNOW CMC
F. Albugues and P. Peres 1991 13 p Previously announced as N91-11865
(Rept-911-430-130; ETN-91-99302) Avail: NTIS HC/MF A03

Thermostructural development of CMC (Ceramic Matrix Composites) is summarized. Nondestructive test methods, mechanical characterization and mathematical modeling are discussed. Production of structural composite materials for use in wing leading edges and nose caps of reusable space vehicles is addressed. Mechanical test validity of test sample, fracture behavior modeling and mechanical tests related to microstructure are described. The synergy of the different approaches presented is concluded to give much information and elements of behavior understanding for the 'young materials' that are CMC. ESA

N91-23263# Army Lab. Command, Watertown, MA. Material Technology Lab.
AN EXPERIMENTAL AND FINITE ELEMENT INVESTIGATION INTO THE NONLINEAR MATERIAL BEHAVIOR OF PIN-LOADED COMPOSITE LAMINATES Final Report
Steven M. Serabian Jan. 1991 278 p
(DA Proj. 1L1-62105-AH-84)

(AD-A232098; MTL-TR-91-2) Avail: NTIS HC/MF A13 CSCL 11/4

The effect of crossply linear intralaminar shear behavior on the modeling accuracy of pin-loaded ((0/9)n)s and (+45/-45)Ns composite laminates was quantitatively investigated. Both linear and nonlinear elastic three dimensional finite element approximations that included pin elasticity and contact angle formation were generated. These approximations were compared to both front surface in-plane and out-of plane experimental moire displacement contours generated from geometric and projection shadow moire techniques. A modified three point bend test was used to obtain values of laminate transverse shear moduli while through thickness contraction measurements on laminate tension tests were employed to obtain estimates of the Poisson ratio values. Nonlinear crossply intralaminar shear behavior was determined from the ASTM D3518-76 specification. GRA

N91-23264# Massachusetts Inst. of Tech., Cambridge. Corrosion Lab.

GALVANIC CORROSION OF ALUMINUM-MATRIX COMPOSITES Technical Report No. 2, 1 Mar. - 31 Dec. 1990

L. H. Hihara and R. M. Latanision Feb. 1991 33 p

(Contract N00014-89-J-1588)

(AD-A232138) Avail: NTIS HC/MF A03 CSCL 11/4

Galvanic-corrosion rates of Al-matrix composites were high in aerated chloride-containing solutions. Oxygen reduction was found to be the primary cathodic reaction. Aluminum corroded by pitting. The type of noble constituent (i.e., graphite, SiC, or TiB2) also affected galvanic-corrosion rates. For example, results indicated that the galvanic-corrosion rate of Al should be about 30 times greater when coupled to graphite than when coupled to SiC or TiB2. In dearated solutions, galvanic corrosion was negligible even if chlorides were present. The galvanic-corrosion rates were determined using the zero-resistance ammeter technique and from potentiodynamic polarization diagrams of ultrapure Al, 6061-T6 Al, graphite fiber, SiC, TiB2, and a commercial graphite fiber/6061-T6 Al metal-matrix composite. GRA

N91-23265# Lawrence Livermore National Lab., CA.

TENSOR TRANSFORMATIONS AND FAILURE CRITERIA FOR THE ANALYSIS OF FIBER COMPOSITE MATERIALS Final Report, Oct. 1986 - Mar. 1987

Richard M. Christensen Feb. 1991 41 p

(Contract W-7405-eng-48; DA Proj. 1L1-62618-AH-80)

(AD-A232238; BRL-CR-651) Avail: NTIS HC/MF A03 CSCL 11/4

Classical lamination theory for fiber composites is inherently limited to the two-dimensional conditions appropriate to thin shell configurations. A new derivation with appropriate tensor transformation is given which provides a fully three-dimensional lamination theory that is applicable to thick laminates involving out-of-plane stress teams. In connection with this work, a new failure criterion is derived for fiber composites, one which involves a minimum number of failure parameters and offers insight into the modes of failure. The key to both derivations is the restriction of five properties form of transversely isotropic media to a special form involving three independent properties. The reduced theoretical forms and the failure criterion are evaluated with respect to standard experimental data for fiber composites. GRA

N91-23266# Oxford Univ. (England). Dept. of Engineering Science.

MODELLING OF THE IMPACT RESPONSE OF FIBRE-REINFORCED COMPOSITES Final Report, 15 Nov. 1988 - 4 Nov. 1989

Y. L. Li, J. Harding, and C. Ruiz 30 Sep. 1990 248 p

(Grant AF-AFOSR-0129-87; AF Proj. 2302)

(AD-A232658; AFOSR-91-0152TR) Avail: NTIS HC/MF A11 CSCL 11/4

This Final Report on a three-year program with the above title summarizes the work that has been over this period in three different areas: (1) the development of experimental techniques for determining the impact mechanical properties of fiber reinforced epoxy laminates; (2) the experimental results obtained for the tensile, compressive and interlaminar shear properties of woven reinforced carbon/epoxy, glass/epoxy, Kevlar/epoxy, and hybrid carbon-glass/epoxy laminates; and (3) the attempts that have been made to model the experimentally observed behavior using (1) a simple laminate theory approach, and (2) the method of finite elements. The present position regarding the modelling of the response of composite materials to impact loading is then critically assessed and suggestions are made for future work required in this area. GRA

N91-23267# Stanford Univ., CA. Dept. of Materials Science and Engineering.

HIGH TEMPERATURE DEFORMATION PROCESSES AND STRENGTHENING MECHANISMS IN INTERMETALLIC PARTICULATE COMPOSITES Annual Technical Report, Nov. 1989 - Nov. 1990

William D. Nix 30 Jan. 1991 38 p

(Grant AF-AFOSR-0201-89; AF Proj. 2306)

(AD-A232737; AFOSR-91-0120TR) Avail: NTIS HC/MF A03 CSCL 11/4

Research on the high temperature deformation processes and strengthening mechanisms in Intermetallic Particulate Composites is described. Work during the second year of the grant includes high temperature compression tests of Ni3Al-Al2O3 composites; mechanical alloying of Ni3Al + Y2O3; transient deformation studies of the intermetallics Ni3Al, NiAl, and NiBe; and development of a model of dislocation structure control of plastic deformation. GRA

N91-23268# Wright Research Development Center, Wright-Patterson AFB, OH.

STRAIN RATE SENSITIVITY OF POLYMER-MATRIX COMPOSITES UNDER MODE I DELAMINATION Final Report, Jun. 1984 - Apr. 1987

M. D. Kistner Dec. 1990 37 p

(AD-A232761; WRDC-TR-90-4121) Avail: NTIS HC/MF A03 CSCL 07/6

This effort examines the combined effects of temperature and strain-rate upon the Mode I fracture toughness of advanced composites. The material systems used were As4/APC-2, a semi-crystalline thermoplastic matrix system; and AS4/3502, a thermosetting epoxy matrix system. The focus of this effort was to investigate whether the Mode I fracture toughness varies with temperature and strain-rate for these systems. The applied crack opening displacement rates utilized were from 0.02 to 20.0 inches per minute and a temperature range from ambient to 350 deg F. Post failure fractographic examinations were utilized to correlate significant variations in mechanical properties with fractographic features. Mechanical test results were summarized via data plots with error bars to show which effects were statistically significant. GRA

N91-23269# University of Southern Illinois, Carbondale.

INVESTIGATIONS OF OXIDATION PROTECTION SYSTEMS FOR CARBON-CARBON COMPOSITES FORMED BY CHEMICAL VAPOR DEPOSITION AND PLASMA-ASSISTED CHEMICAL VAPOR DEPOSITION TECHNIQUES Annual Interim Report, 1 Mar. 1989 - 28 Feb. 1991

J. Don, J. He, and M. A. Wright 21 Jan. 1991 73 p

(Grant AF-AFOSR-0130-88; AF Proj. 2306)

(AD-A232800; AFOSR-91-0122TR) Avail: NTIS HC/MF A04 CSCL 11/4

Conditions necessary for the preparation of pack cemented oxidation resistant reacted layers on carbon-carbon composites were developed. Reacted layers were produced containing SrC, ZrC, B4C. The oxidation resistance of such layers were listed in air at temperatures up to 1800 C and the results were compared. Additional surface layers deposited into the reacted layers consisted of SiC, ZrB2, SiC/ZrB2 and graded Sic/ZrC. These layers significantly improved the oxidation resistance of the layers generated by pack cementation. The oxidation resistance of the combined layer systems (pack cementation plus CVD) was

determined by subjecting each system to an air environmental in an isothermal and a cyclicly varying temperature environmental temperatures up to 1700 C. GRA

N91-24064*# National Aeronautics and Space Administration. Ames Research Center, Moffett Field, CA.
FLAME-RETARDANT COMPOSITE MATERIALS
Demetrius A. Kourtides *In* NASA, Washington, Technology 2000, Volume 2 1991 p 192-199 (For primary document see N91-24041 15-99)
Avail: NTIS HC/MF A16 CSCL 11D

25 INORGANIC AND PHYSICAL CHEMISTRY

Includes chemical analysis, e.g., chromatography; combustion theory; electrochemistry; and photochemistry.

For related information see also *77 Thermodynamics and Statistical Physics.*.

N91-23270 Stanford Univ., CA.
THE EFFECTS OF CONTROLLING VORTEX FORMATION ON THE PERFORMANCE OF A DUMP COMBUSTOR Ph.D. Thesis
Keith Robert McManus 1990 223 p
Avail: Univ. Microfilms Order No. DA9102314

The use of flow control methods to improve the performance of air breathing combustors, specifically with respect to controlling both volumetric energy release and combustion instability, is investigated. The flow control techniques were chosen for their ability to control vortex formation near the inlet of the combustor. Periodic spanwise forcing of the inlet boundary layer was used to control the spanwise vortex shedding process in the combustor. Delta wing vortex generators and vortex generator jets were used to introduce streamwise vorticity into the flow. These control strategies were applied separately and together to a laboratory-scale dump combustor, and the effects on combustor performance were determined. The effect of spanwise forcing on both nonreacting and reacting flowfields was to modulate the formation of spanwise coherent vortex structures just downstream of the flow separation. In the nonreacting flowfield, the shear layer spreading rate was increased when forcing was applied. In the reacting flow, forcing caused a modulation of the flame structure. Dissert. Abstr.

N91-23271*# National Aeronautics and Space Administration. Lyndon B. Johnson Space Center, Houston, TX.
STATIC FEED WATER ELECTROLYSIS SUBSYSTEM DEVELOPMENT Patent Application
Franz H. Schubert, inventor (to NASA) and David J. Grigger, inventor (to NASA) (Life Systems, Inc., Cleveland, OH.) 1 Feb. 1991 13 p
(NASA-Case-MSC-21577-1-SB; NAS 1.71:MSC-21577-1-SB; US-Patent-Appl-SN-748933) Avail: NTIS HC/MF A03 CSCL 07D

This disclosure is directed to an electrolysis cell forming hydrogen and oxygen at spaced terminals. The anode terminal is porous and able to form oxygen within the cell and permit escape of the gaseous oxygen through the anode and out through a flow line in the presence of backpressure. Hydrogen is liberated in the cell at the opposing solid metal cathode which is permeable to hydrogen but not oxygen so that the migratory hydrogen formed in the cell is able to escape from the cell. The cell is maintained at an elevated pressure so that oxygen liberated by the cell is delivered at elevated pressure without pumping to raise the pressure of the oxygen. NASA

N91-23272# Caterpillar Tractor Co., Peoria, IL.
DIRECT GAS INJECTION WITH GLOW PLUG IGNITION Annual Report, Aug. 1989 - Jul. 1990
B. G. Richards Aug. 1990 68 p
(Contract GRI-5086-293-1663)
(PB91-136390; GRI-90/0250) Avail: NTIS HC/MF A04 CSCL 21B

Design and procurement of prototype components such as gas injector, cylinder head, and piston for the single cylinder version of the 3500 Series (3501) Direct Injected (DI) natural gas engine were completed. Design calculations indicate that these components will meet the component functional specifications. Bench tests of the 3500 gas injector demonstrated that the gas injector will perform as designed. Testing plans for the coming year are outlined. Author

N91-23273 Cornell Univ., Ithaca, NY.
AN EXPERIMENTAL METHOD FOR STUDYING COMBUSTION OF AN UNSUPPORTED FUEL DROPLET AT REDUCED GRAVITY Ph.D. Thesis
Jiann Chyuan Yang 1990 267 p
Avail: Univ. Microfilms Order No. DA9106197

An experimental method to study combustion of free fuel droplets at reduced gravity was developed. Reduced gravity environment was achieved by performing the experiments in a drop tower. The experimental technique was based on the parabolic projectile motion of a fuel droplet. A test fuel droplet was propelled almost vertically upward from a droplet generator in a combustion chamber. As soon as the droplet reached the apex of its trajectory, the droplet was ignited, and simultaneously the camera which was positioned at the apex of the droplet trajectory and which was used to obtain photographic record of the burning droplet, the combustion chamber, and the associated instrumentation were released into free fall. In this way the burning droplet would experience reduced gravity, and at the same time the droplet was levitated with respect to the free falling package. Fuels studied were heptane (moderately sooting), toluene (highly sooting), methanol (non-sooting), and heptane-hexadecade mixtures. A soot shell was observed for heptane and toluene. No disruptive burning was observed. The flames front stand-off ratio was found to increase with time. Transmission electron micrographs of the collected soot samples showed that the size of the soot particles obtained under reduced gravity appear to be slightly larger than those obtained under the normal gravity of the Earth. Extinction of methanol droplets was consistently observed. Extinction diameters obtained from the present study ranged from 0.16 to 0.19 mm for a range of initial diameters from 0.04 to 0.43 mm. For heptane-hexadecane mixtures, micro-explosions were not observed. Mixture droplets appeared to burn to completion without extinction whereas the one hexadecane drop studied extinguished. Dissert. Abstr.

N91-23274# EG and G Mound Applied Technologies, Miamisburg, OH.
MEASUREMENT CONTROL FOR CALORIMETRIC ASSAY
D. A. Rakel 1991 8 p Presented at the Safeguards Workshop on Measurement Control, Albuquerque, 20-22 Feb. 1991
(Contract DE-AC04-88DP-43495)
(DE91-009445; MLM-3684; CONF-910299-1) Avail: NTIS HC/MF A02

An overview is presented of measurement control for calorimetric assay. The authors have gathered information from several ANSI and ASTM documents which address this topic and offer some additional information based on experience at EG and G Mound Applied Technologies. The scope is restricted to calorimetric assay for safeguarding tritium and plutonium-bearing materials. The physical models are discussed with respect to calorimetric assay and calorimetry; acceptable measurement criteria; reference bases; measurement uncertainty for both calorimetry and gamma ray spectrometry; controlling the measurement process for both calorimetry and gamma ray spectrometry; and assessment of the measurement processes. DOE

N91-23275# Georgia Inst. of Tech., Atlanta. School of Chemical Engineering.
HIGH TEMPERATURE MEMBRANES FOR H2S AND SO2 SEPARATIONS

J. Winnick 1990 13 p
(Contract DE-FG22-90PC-90293)
(DE91-008534; DOE/PC-90293/T1) Avail: NTIS HC/MF A03

Research during the period of 1 Sep. 1990 through 31 Dec. 1990 focused on developing a tape-casting method with several binder formulations. These formulae were based on methyl cellulose, polyvinyl butyral and acrylic as polymeric binders. Several plasticizers were used to provide a flexible tape product. Most of this work was applied towards the development of a membrane to be used in the SO2 separation process. The preparation of all three types is described. Several of the successful tapes were tested in the full cell apparatus with simulated flue gas flowing over both electrodes. Results of these tests are briefly discussed. Work in membrane development for the H2S separator process has been concentrated in two areas. These were utilization of Metoramics ceramic binder systems to produce flexible green tapes of MgO, as opposed to the borosilicate tapes made for the SO2 separation process, and work with full cell experiments using Zircar's woven zirconia cloths as a matrix material in the separator membranes. Results are discussed. DOE

N91-23276# Cornell Univ., Ithaca, NY. School of Applied and Engineering Physics.
MASS RESOLVED RESONANCE IONIZATION SPECTROSCOPY OF COMBUSTION RADICALS
1991 7 p
(Contract DE-FG02-86ER-13508)
(DE91-010603; DOE/ER-13508/5) Avail: NTIS HC/MF A02

Resonance-enhanced multiphoton ionization (REMPI) spectroscopy offers very low detection limits for nonperturbative, in situ, spatially resolved density measurements of combustion radicals. The REMPI approach is the only method currently available for ultrasensitive (sub part-per-million) monitoring of weakly fluorescing species. Even though REMPI spectroscopy has provided a remarkable body of new spectroscopic data on previously unobserved states of many molecules, the widespread application of REMPI for flame diagnostics is presently limited by the scarcity of spectroscopic data for Rydberg states of combustion radicals. The primary goal of this research is the discovery and characterization of such electronic states. DOE

N91-23277# Argonne National Lab., IL.
MICROBEAM TITANIUM ISOTOPIC ANALYSIS BY RESONANCE IONIZATION MASS SPECTROMETRY
D. R. Spiegel, A. M. Davis, R. N. Clayton (Chicago Univ., IL.), M. J. Pellin, W. F. Calaway, J. W. Burnett, S. R. Coon, C. E. Young, and D. M. Gruen 1991 3 p Presented at the Lunar and Planetary Science Conference, Houston, 18-22 Mar. 1991
(Contract W-31-109-eng-38)
(DE91-010799; ANL/CP-72318; CONF-9103134-2) Avail: NTIS HC/MF A01

The importance of isotopic anomalies in refractory inclusions in meteorites is well established. Measurements of the anomalies using conventional mass spectrometry are often rendered difficult, however, by isobarically interfering isotopes, for example, Ti-48 and Ca-48. Resonance ionization mass spectrometry (RIMS) can substantially reduce isobaric interferences in a number of systems. We have employed RIMS for the in situ detection of Ti atoms sputtered from pure Ti metal and from several terrestrial oxides containing both Ti and Ca. Tunable lasers were employed to resonantly ionize neutral Ti atoms. We have chosen Ti specifically because of the importance of Ti isotopic anomalies in cosmochemistry. DOE

N91-23278# European Space Agency, Paris (France).
GAS EVOLUTION AND BUBBLE FORMATION ON ELECTRODES
Michael Dinkelacker (Deutsche Forschungsanstalt fuer Luft- und Raumfahrt, Stuttgart, Germany, F.R.) Feb. 1991 177 p Transl. into ENGLISH of Zur Gasentwicklung und Blasenbildung an Elektroden (Stuttgart, Fed. Republic of Germany, DLR), May 1989 150 p Original language document was announced as N90-13629
(ESA-TT-1191; DLR-FB-89-35; ETN-91-99315) Avail: NTIS HC/MF A09

The influence of bubble formation on the electrode overvoltage in alkaline water eletrolysis is investigated using the example of the hydrogen electrode, as a function of current density, which is varied in a wide range. Fundamental phenomena of electrolytic gas evolution and bubble formation are examined in the current density range from 0.0001 to 0.00001 mA/sq cm, and similarities and differences to the thermal boiling are discussed. The experimental and theoretical results are discussed. ESA

N91-23279# York Univ., Downsview (Ontario). Dept. of Chemistry.
ELECTROCHEMICAL PARAMETERIZATION OF RHENIUM REDOX COUPLES
A. B. Lever 14 Feb. 1991 33 p
(Contract N00014-84-G-0201)
(AD-A232043; TR-37) Avail: NTIS HC/MF A03 CSCL 09/5

The observed rhenium potentials fo ReIV/III, ReIII/II, and ReII/I reversible couples for mononuclear species, are analyzed in terms of the electrochemical parameterization scheme based upon the RuIII/II couples. Two independent sets of ReII/I potentials are observed, which, if extended, would cross the ReIII/II correlation line. The possible significance of these sets is explored. The ReIV/II couple correlation is roughly parallel to one of the ReII/I correlation lines. The analysis leads to some interesting avenues for future synthetic studies. GRA

N91-23280# Army Cold Regions Research and Engineering Lab., Hanover, NH.
CRREL RESEARCH ON MATERIALS IN COLD ENVIRONMENTS
Piyush K. Dutta Dec. 1990 27 p
(DA Proj. 4A7-62730-AT-42)
(AD-A232133; CRREL-SR-90-42) Avail: NTIS HC/MF A03 CSCL 14/2

This report is a synopsis of the developments in the materials research program at CRREL. Focusing on studies of the low-temperature behavior materials, these developments are reviewed in three specific areas: creating a materials-property data base, researching composites and other materials and developing test facilities. Among materials, composites, being newer, were studied at depth. Temperature and strain rate were considered critical in influencing any material's durability; therefore, facilities were developed to provide precise control of these parameters. The program aims to meet the crucial need for designing structures and equipment using materials specifically adapted for cold regions and low-temperature applications. GRA

N91-23281# California Univ., Los Angeles.
SOLID-PHASE EQUILIBRIA FOR METAL-SILICON-OXYGEN TERNARY SYSTEMS. PART 2: Sc, Y, AND La Technical Report No. 9, Jun. 1990 - Feb. 1991
Haojie Yuan and R. S. Williams 28 Feb. 1991 18 p
(Contract N00014-90-J-1178)
(AD-A232150) Avail: NTIS HC/MF A03 CSCL 07/4

We have derived ternary phase diagrams of the type M-Si-O, where M=Sc, Y and La under the conditions of 298 K and 1 atm oxygen partial pressure. These phase diagrams provide a direct view of the thermodynamics that governs stabilities of phases containing these elements in contact with each other, and should be useful for integrating Y- and La-based oxide superconductors with Si. GRA

N91-23282# Cornell Univ., Ithaca, NY. School of Chemical Engineering.
CHARACTERIZATION OF THE GLASS TRANSITION USING A MICROINDENTER
Ferdinand Rodriguez and Treva Long 22 Feb. 1991 18 p Presented at the 199th National Meeting of the American Chemical Society, Boston, MA, 22-27 Apr. 1990

(Contract N00014-85-K-0474)
(AD-A232154; TR-19) Avail: NTIS HC/MF A03 CSCL 07/4

The microindenter described requires a very small sample (c. 10 mg), can be used with heating rates comparable to those in DSC (ie., 10 C/min), and gives a large, clearly defined change at the glass transition. The essential features are a needle probe and a linear variable differential transformer (LVDT). By suitably controlling the force on the needle, the rate of heating, and the sample thickness, reproducible results can be obtained. The small sample size permits a relatively fast heating rate. Most mechanical tests (often using oscillating stress and strain) require large samples with a corresponding long time for temperature equilibration to take place (ASTM D 4065). Another indentation test, the Vicat Softening Temperature (ASTM 1525) also uses a thick (3 mm) sample. Like the Vicat test, the present procedure is best suited to amorphous polymers. The application to plasticized samples of poly(methyl methacrylate) illustrates the utility of the method. GRA

N91-23283# Armed Forces Radiobiology Research Inst., Bethesda, MD.
AFRRI REPORTS, OCTOBER - DECEMBER 1990 Scientific Report
Jan. 1991 121 p
(AD-A232236; AFRRI-SR90-25; AFRRI-SR90-26; AFRRI-SR90-27; AFRRI-SR90-30; AFRRI-SR90-31; AFRRI-SR90-32; AFRRI-SR90-33; AFRRI-SR90-34; AFRRI-SR90-35) Avail: NTIS HC/MF A06 CSCL 06/5

This volume contains AFRRI Scientific Reports SR90-25 through SR90-36 for Oct. to Dec. 1990. Those include: (1) ESR study of electron transfer reactions between gamma-irradiated pyrimidines, adriamycin, and oxygen; (2) endothelial cells as a source of oxygen-free radicals; (3) yields of radiation-induced base products in DNA - effects of DNA conformation and gassing conditions; and (4) characteristics of noncovalent and covalent interactions of (+) and (-) anti benzoapyrene diol epoxide stereoisomers of different biological activities with DNA. GRA

N91-23284# Cornell Univ., Ithaca, NY.
AN EXPERIMENTAL STUDY OF FLAMELET SURFACES IN TURBULENT COMBUSTION
F. C. Gouldin 28 Dec. 1990 27 p
(Contract DAAL03-87-K-0039)
(AD-A232342; ARO-24693.2-EG) Avail: NTIS HC/MF A03 CSCL 21/2

The major objective of the research reported was to study the properties of constant scalar property surfaces in turbulent reacting flows. Two dimensional image measurements were made in premixed turbulent flames and in jets and jet flames. Point-in-space, time-series measurements were also made, and the data used to study the properties of surface crossing statistics in jets and premixed flames. In addition, the hypothesis that, for the purpose of estimating the mean surface area per unit volume, surfaces in turbulent flow can be represented by fractal surfaces was used to develop models for the mean chemical reaction rate in premixed flames and for the source term in the equation for intermittency in free jets. Also a new method for making conditional velocity measurements in premixed flames was developed and applied to obtain unique data for velocity in these flames and to study jumps, across flamelets, of certain velocity statistics. Major findings for the flows and conditions studied include: (1) for the premixed case flamelet surfaces are fractal as are constant mixture fraction surfaces in jets and constant temperature surfaces in jet flames; (2) in jets the surface fractal dimension is between 2.3 to 2.4; (3) level crossing sets from time-series data are not simple fractal sets; (4) the idea of fractal bursts is introduced to help interpret the crossing sets; and (5) unique fully-conditional velocity data give a measure of velocity jumps across flamelets in premixed combustion. GRA

N91-23285# Puerto Rico Univ., Rio Piedras. Dept. of Physics.
PHASE TRANSITIONS AT LIQUID SOLID INTERFACES: PADE APPROXIMANT FOR ADSORPTION ISOTHERMS AND VOLTAMMOGRAMS Summary Report
L. Blum and D. A. Huckaby 29 Jan. 1991 28 p Prepared in cooperation with Texas Christian University, Fort Worth, TX
(Contract N00014-90-J-1263)
(AD-A232623; TR-3) Avail: NTIS HC/MF A03 CSCL 20/13

A Pade approximant that is the natural extension of Langmuir's adsorption isotherm is used to study the adsorption in the liquid-solid interface. The coefficients of this approximant are generated by a recursion relation, and can be computed from the fugacity series in closed form. We apply this approximant to the underpotential deposition of metals on an electrode, and obtain voltammograms that show the sharp spikes seen in recent experiments. GRA

N91-23286# SRI International Corp., Menlo Park, CA. Molecular Physics Lab.
MULTIPHOTON DETECTION TECHNIQUES FOR F AND F2 Final Report, 1 Apr. 1988 - 31 Mar. 1990
Gregory W. Faris, Mark J. Dyer, William K. Bischel, and David L. Huestis 8 Nov. 1990 53 p
(Contract F49620-88-K-0003)
(AD-A232641; SRI-MP-90-141R; AFOSR-91-0054TR) Avail: NTIS HC/MF A04 CSCL 07/2

Research is described for the development of quantitative remote diagnostics for atomic and molecular fluorine, using ultraviolet multiphoton excitation followed by the detection of fluorescence or ionization. The first demonstration of resonant two-photon excitation of molecular fluorine is described, which allows sensitive detection of molecular fluorine. A high power UV-VUV laser source based on Raman-shifting a narrow band, tunable excimer laser in liquid-nitrogen-cooled isotopes of hydrogen has been developed and applied to two-photon detection of both molecular and atomic fluorine. GRA

N91-23287# Pennsylvania State Univ., University Park. Dept. of Materials Science and Engineering.
COMPUTER MODELING OF SOOT FORMATION COMPARING FREE RADICAL AND IONIC MECHANISMS Final Technical Report, 1 Dec. 1987 - 30 Nov. 1990
Michael Frenklach and Hai Wang 22 Jan. 1991 23 p
(Grant AF-AFOSR-0072-88; AF Proj. 2308)
(AD-A232820; AFOSR-91-0169TR) Avail: NTIS HC/MF A03 CSCL 21/2

This is a final report on collaborative study between AeroChem and Penn State, aimed at development of a quantitative physicochemical model of soot formation. The Penn State accomplishments during the past three-year period are: (1) the AeroChem ion-reaction mechanism was run with a flame code, and the computational results indicate that the formation of polycyclic aromatic hydrocarbons, the precursors to soot, via the ionic reaction pathway is slower than via the pathway involving neutral species; (2) a computer code for modeling large species and soot particle formation and growth was developed; (3) our neutral reaction mechanism was updated and tested; and (4) a detailed computer simulation of soot particle nucleation and growth in laminar premixed flames was successfully performed using our updated neutral reaction mechanism -- for the first time soot particle inception could be modeled from first principles, starting with fuel decomposition and going all the way to predicting, in quantitative agreement with experiment, soot particle properties. GRA

N91-23288# Battelle Memorial Inst., Columbus, OH.
THEORETICAL PREDICTION OF VIBRATIONAL INFRARED FREQUENCIES OF TERTIARY AMINES Final Report, Jun. - Aug. 1990
H. F. Hameka and G. R. Famini Feb. 1991 18 p Prepared in cooperation with Pennsylvania Univ., Philadelphia
(Contract DAAL03-86-D-0001; DA Proj. 1C1-62622-A-553)
(AD-A232880) Avail: NTIS HC/MF A03 CSCL 07/3

This report computes the vibrational frequencies of seven

amines. Experimental data are available for four of these molecules: trimethylamine, diethylmethylamine, bis(2-chloroethyl)methylamine, and triethylamine. The ratios are determined between the experimental and the computed frequencies of these molecules. The ratios are then used to derive a set of effective correction factors for the various vibrational modes. The vibrational frequencies are computed for three other tertiary amines: tris(chloromethyl) amine, tris(2-chloroethyl) amine (HN3), and bis(2-chloroethyl) ethylamine (HN1). The computed frequencies, the corresponding intensities, and the corrected frequencies are reported here. The authors emphasize that the correction factors are valid only for 3-21G computations. GRA

N91-23165# Technische Univ., Munich (Germany, F.R.).
EXPERIMENTAL INVESTIGATIONS ON THE TRANSITION FROM STABLE TO UNSTABLE COMBUSTION BY MEANS OF ACTIVE INSTABILITY CONTROL
S. Gleis, D. Vortmeyer, and W. Rau *In* AGARD, Hypersonic Combined Cycle Propulsion 7 p(SEE N91-23147 15-07) Dec. 1990 (For primary document see N91-23147 15-07)
Copyright Avail: NTIS HC/MF A20; Non-NATO Nationals requests available only from AGARD/Scientific Publications Executive

26 METALLIC MATERIALS

Includes physical, chemical, and mechanical properties of metals, e.g., corrosion; and metallurgy.

N91-23289# TiNi Alloy Co., Oakland, CA.
SHAPE-MEMORY ALLOY TACTICAL FEEDBACK ACTUATOR, PHASE 1 Final Report, 1 Feb. - 1 Aug. 1989
A. D. Johnson Aug. 1990 36 p
(Contract F33615-88-C-0541)
(AD-A231389; AAMRL-TR-90-039-Phase-1) Avail: NTIS HC/MF A03 CSCL 06/4

The hardware developed to realize a shape memory alloy (SMA) tactile stimulator is described. A 5x6 30 element array was developed to provide tactile stimulation to the human operator of a remotely controlled robotic system. It is verified that a tactile stimulator can be packaged in finger-pad size arrays and that computer control is feasible. Actuation profiles and design techniques are discussed. GRA

N91-23290 Wisconsin Univ., Madison.
PHASE EQUILIBRIA AND SOLIDIFICATION OF Al-Li AND Al-Li-Cu ALLOYS Ph.D. Thesis
Sinn-wen Chen 1990 188 p
Avail: Univ. Microfilms Order No. DA9100130

The phase equilibria of the Al-Li and Al-Li-Cu systems were studied using a combined experimental-computational method. The primary solidification phases, reaction sequences, and reaction temperatures during solidification of Al-rich Al-Li and Al-Li-Cu alloys were studied. Experimental techniques were developed to overcome the intrinsic difficulties encountered when working with the Al-Li and Al-Li-Cu alloys. Lithium loss, due to vaporization, oxidation, and interaction with the container materials, is the most common of these problems. Alloys with compositions in the region where the primary solidification phase was either alpha-Al, beta-AlLi, T(sub 2) Al6CuLi3, T(sub 1) Al2CuLi, T(sub B) Al7.5Cu4Li, or theta-(Al2Cu) were examined. All the invariant reactions in the Al-rich corner of Al-Li-Cu were determined. The temperatures and compositions of the binary eutectic, alpha + beta, and the ternary eutectic, alpha + T(sub 1) + T(sub B) were determined. The results along with thermodynamic and other phase equilibria data reported in the literature were assessed to obtain a set of internally consistent thermodynamic parameters for the Al-Li binary system. Based on experimental data and the thermodynamic models of Al-Li, Al-Cu, and Cu-Li, a thermodynamic description of the Al-Li-Cu ternary system for the Al-rich corner was developed. Isothermal sections at different temperatures and a liquidus projection were calculated and compared to experimental determinations. Combining the thermodynamic models and the Scheil equation or modified Scheil equation to include solid state back-diffusion, quantitative solidification paths were predicted. The calculated amount of the primary phase formed during solidification was compared to those observed from fast-cooling and slow-cooling experiments. Dissert. Abstr.

N91-23291# Lawrence Livermore National Lab., CA.
MODELING SECOND-PHASE FORMATION DURING RAPID RESOLIDIFICATION OF STAINLESS STEEL ALLOYS
J. W. Elmer, T. W. Eagar, and S. M. Allen (Massachusetts Inst. of Tech., Cambridge.) 28 Jan. 1991 10 p Presented at the Stainless Steels 1991, Chiba (Japan), 10-13 Jun. 1991
(Contract W-7405-eng-48)
(DE91-008567; UCRL-CR-106146; CONF-9106130-1) Avail: NTIS HC/MF A02

Many common stainless steel (SS) alloy microstructures consist of a mixture of ferrite and austenite phases, however, when these alloys are rapidly resolidified using laser beam (LB) or electron beam (EB) processes they solidify in the single-phase-austenite or single-phase-ferrite mode. This paper investigates the influence of solidification rate on the reduction, and eventual elimination, of second phases during the rapid solidification of SS alloys. The influence of solidification rate on the ferrite content of these alloys was studied by calculating the dendrite-tip undercooling and then incorporating these results into a solute-redistribution model to calculate the relative fractions of primary and secondary phase that solidify from the melt. Single-phase solidification was predicted at high cooling rates and was confirmed through STEM analysis, showing solidification microstructures void of any significant microchemical composition gradients. Results showed a rapid-solidification model was used to calculate the relative fractions of primary and secondary phases that form during the resolidification of stainless steel alloys. The rapid-solidification model shows that the ferrite content of primary-austenite solidified alloys decreases and the ferrite content of primary-ferrite solidified alloys increases with increasing cooling rate. Results of the model indicate that primary-austenite alloys will solidify in the single-phase mode at all interface velocities greater than about 20 mm/s. This value correlates well with experiments. Results of the model indicate that primary-ferrite alloys will solidify in the single-phase mode at all interface velocities greater than about 50 mm/s. The experimentally-observed interface velocity for single-phase-ferrite solidification is significantly less (10 mm/s). This discrepancy is proposed to be related to the relative difficulty of nucleating austenite from the eutectic liquid. DOE

N91-23292# Oak Ridge National Lab., TN.
ORDER AND DISORDER IN METALLIC ALLOYS
B. L. Gyorffy, G. M. Stocks, D. M. Nicholson, B. Ginatempo, and D. D. Johnson (Sandia National Labs., Albuquerque, NM.) 1990 26 p Presented at the Royal Society Conference in Honor of Prof. V. Heine, London (UK), 5-6 Sep. 1990
(Contract DE-AC05-84OR-21400)
(DE91-009120; CONF-9009353-1) Avail: NTIS HC/MF A03

The electronic structure of random crystalline metallic alloys is an important chapter in the quantum theory of solids. After atoms, molecules and ordered crystalline solids this is the next most tractable problem of positively charged nuclei and the electron glue between them. Moreover, it is the simplest non-trivial example where the theme of order-disorder is fully developed. In short the electronic states have new features and they drive novel phenomena such as phase separation and compositional ordering. In this talk the authors shall review the current state of the first principles understanding of the electronic structure and the way it determines the compositional short and long range order (de Fountain 1979; Kchaheturyan 1986). Central to the discussion below are two assumptions: one is that of a rigid lattice and the other is that specifying the occupancy variable xi(sub i), which takes on the value 1 if there is an A atom at the i-th site and 0 if the atom at bar R(sub i) is the B type, for all sites defines all compositional configurations. The first of these may be relaxed in favor of a symmetry statement, that on the average the system is invariant under a set of translations which define a lattice, without

seriously effecting the conceptual framework we are about to describe. Whilst the second, which is essentially the adiabatic theorem, can be relinquished only at the expense of an entirely new start involving diffusion. In short the authors shall consider configurations specified by the sets (xi(sub i)) and average over all such sets with appropriate weights. DOE

N91-23293# Michigan Technological Univ., Houghton. Dept. of Metallurgical Engineering.
BOUNDARY STABILITY UNDER NONEQUILIBRIUM CONDITIONS
S. A. Hackney, M. R. Plichta, and J. K. Lee 1991 13 p
(Contract DE-FG02-87ER-45315)
(DE91-009262; DOE/ER-45315/15) Avail: NTIS HC/MF A03

The past two decades have seen a tremendous advance in the basic understanding of interfacial structure at equilibrium. However, the contributions of interfaces to the overall behavior of a material in service (in a power plant or nuclear reactor) occurs under conditions far from equilibrium. This research program is focused on understanding the interaction of nonequilibrium conditions with the equilibrium microstructure of the interface, the net result being increased knowledge of design parameters for materials and materials interfaces to be exposed to the nonequilibrium conditions so prevalent in energy generation systems. To this end, the research program, Boundary Stability Under Nonequilibrium Conditions studies the microscopic behavior of interfaces under the experimentally and theoretically simulated conditions of stress and thermal fatigue, compositional inhomogeneities, and gradients in capillarity forces. DOE

N91-23294# Sandia National Labs., Albuquerque, NM.
THE SOLIDIFICATION BEHAVIOR OF AN ALLOY 625/718 VARIANT
M. J. Cieslak 1991 10 p Presented at the Special Emphasis Symposium on Superalloys 718, 625, and Various Derivatives, Pittsburgh, 23-26 Jun. 1991
(Contract DE-AC04-76DP-00789)
(DE91-009544; SAND-91-0499C; CONF-910614-2) Avail: NTIS HC/MF A02

The solidification behavior of Custom Age 625 PLUS(reg sign) is examined using an integrated analytical approach. Like its predecessors, Alloys 625 and 718, the solidification behavior of this new alloy is dominated by the presence and segregation of Nb, which gives rise to a (gamma)/Laves terminal solidification constituent. DOE

N91-23295# Oak Ridge National Lab., TN.
EVALUATION OF FILLER METALS FOR HIGH-STRENGTH STAINLESS STEELS
R. W. Swindeman, G. M. Goodwin, J. F. King, C. D. Lundin, and C. Y. P. Qiao (Tennessee Univ., Knoxville.) 1991 19 p Presented at the 3rd International Conference on Improved Coal-Fired Power Plants, San Francisco, 2-5 Apr. 1991
(Contract DE-AC05-84OR-21400)
(DE91-009931; CONF-910417-1) Avail: NTIS HC/MF A03

Weldments were produced in types 316, 17-14CuMo, and high strength 14Cr-16Ni-2Mo stainless steel base metals with four filler metals-alloy 82, 17-14CuMo stainless steel, controlled residual element CRE 16-8-2 stainless steel, and alloy 556. The welds were evaluated on the basis of microstructure, strength, and ductility. All of the base metals were prone to hot cracking, but steels high in phosphorus were the most likely to produce poor welds. The CRE 16-8-2 stainless steel filler metal produced the best combination of creep strength and ductility, while alloy 556 produced the best long-time creep strength. Tensile and creep failures usually occurred in the alloy 82, 17-14CuMo stainless steel, or CRE 16-8-2 stainless steel filler metal of weldments tested transverse to the weld. At low temperatures (600 to 700 C) and short times the alloy 556 filler metal usually failed, while at high temperature (700 to 800 C) and long times, the weldment usually failed in the base metal. In weldments creep tested parallel to the welding direction cracking initiated in the CRE 16-8-2 stainless steel filler, even though cracks were observed in the heat-affected zone of the base metal. The mechanical performance of weldments in 14Cr-16Ni-2Mo stainless steel tubing alloys was satisfactory in spite of the observed tendency for cracking. However, it was concluded that further development of the welding technology would be needed before the high-strength alloys would be commercially acceptable. DOE

N91-23296# Los Alamos National Lab., NM.
RE-ANALYSIS OF PHOTOEMISSION DATA FOR CuO: REVISION OF THE CONFIGURATION-ENERGY SCHEME FOR CUPRATE MATERIALS
B. H. Brandow 1991 8 p Presented at the Electronic Structure and Mechanisms for High Temperature Superconductivity, Coral Gables, 3-9 Jan. 1991
(Contract W-7405-eng-36)
(DE91-009952; LA-UR-91-892; CONF-910145-3) Avail: NTIS HC/MF A02

The author has recently carried out a very careful analysis of photoemission and inverse photoemission (BIS) data for CuO, probably the most refined and thorough analysis for any transition-metal compound to date. This has led to a configuration-energy scheme for cuprate materials which is quite different from a generally-accepted one, due largely to Sawatzky and co-workers. For example, it is commonly believed that the doping holes in La(2-x)Sr(x)CuO(4) are hosted almost entirely within oxygen 2p orbitals. He finds instead that these holes are shared roughly equally by 2p and 3d orbitals. In this report he shall sketch the motivations for this study the main results, and some of the lessons and surprises encountered along the way. DOE

N91-23297# Massachusetts Inst. of Tech., Cambridge. Dept. of Materials Science and Engineering.
DETERMINISTIC ANALYSIS OF PROCESSES AT CORRODING METAL SURFACES AND THE STUDY OF ELECTROCHEMICAL NOISE IN THESE SYSTEMS
R. M. Latanision 1 Dec. 1990 9 p
(Contract DE-FG02-89ER-45388)
(DE91-009997; DOE/ER-45388/1) Avail: NTIS HC/MF A02

Electrochemical corrosion is pervasive in virtually all engineering systems and in virtually all industrial circumstances. Although engineers now understand how to design systems to minimize corrosion in many instances, many fundamental questions remain poorly understood and, therefore, the development of corrosion control strategies is based more on empiricism than on a deep understanding of the processes by which metals corrode in electrolytes. Fluctuations in potential, or current, in electrochemical systems have been observed for many years. To date, all investigations of this phenomenon have utilized non-deterministic analyses. A proposal is made to study electrochemical noise from a deterministic viewpoint by comparison of experimental parameters, such as first and second order moments (non-deterministic), with computer simulation of corrosion at metal surfaces. In this way it is proposed to analyze the origins of these fluctuations and to elucidate the relationship between these fluctuations and kinetic parameters associated with metal dissolution and cathodic reduction reactions. This research program addresses in essence two areas of interest: computer modeling of corrosion processes in order to study the electrochemical processes on an atomistic scale; and experimental investigations of fluctuations in electrochemical systems and correlation of experimental results with computer modeling. In effect, the noise generated by mathematical modeling will be analyzed and compared to experimental noise in electrochemical systems. DOE

N91-23298# Oak Ridge National Lab., TN.
CREEP AND CREEP-RUPTURE BEHAVIOR OF ALLOY 718
C. R. Brinkman, M. K. Booker, and J. L. Ding 1991 23 p Presented at the Special Emphasis Symposium on Superalloys 718, 625, and Various Derivatives, Pittsburgh, 23-26 Jun. 1991
(Contract DE-AC05-84OR-21400)
(DE91-007706; CONF-910614-1) Avail: NTIS HC/MF A03

Data obtained from creep and creep-rupture tests conducted

on 18 heats of Alloy 718 were used to formulate models for predicting high temperature time dependent behavior of this alloy. Creep tests were conducted on specimens taken from a number of commercial product forms including plate, bar, and foregoing material that had been procured and heat treated in accordance with ASTM specifications B-670 or B-637. Data were obtained over the temperature range of 427 to 760 C at test times to about 87,000 h. Comparisons are given between experimental data and the analytical models. The analytical models for creep-rupture included one based on lot-centering regression analysis and two based on the Minimum Commitment Method. A master curve approach was used to develop and equation for estimating creep deformation up to the onset of tertiary creep. DOE

N91-23299# Arizona State Univ., Tempe. Dept. of Chemical, Bio, and Materials Science Engineering.
HIGH-TEMPERATURE ALLOYS FOR HIGH-POWER THERMIONIC SYSTEMS
Kwang S. Shin, D. L. Jacobson, L. Dcruz, Anhua Luo, and Bor-Ling Chen Aug. 1990 133 p
(Contract DE-AC03-87SF-17170)
(DE91-009292; DOE/SF-17170/T25) Avail: NTIS HC/MF A07

The need for structural materials with useful strength above 1600 K has stimulated interest in refractory-metal alloys. Tungsten possesses an extreme high modulus of elasticity as well as the highest melting temperature among metals, and hence is being considered as one of the most promising candidate materials for high temperature structural applications such as space nuclear power systems. This report is divided into three chapters covering the following: (1) the processing of tungsten base alloys; (2) the tensile properties of tungsten base alloys; and (3) creep behavior of tungsten base alloys. Separate abstracts were prepared for each chapter. DOE

N91-23300# California Univ., Berkeley. Lawrence Berkeley Lab.
THE STRENGTH AND TOUGHNESS OF STAINLESS STEELS AT CRYOGENIC TEMPERATURE
J. W. Morris, Jr. Jan. 1991 9 p Presented at the Stainless Steels 1991, Chiba (Japan), 10-13 Jun. 1991
(Contract DE-AC03-76SF-00098)
(DE91-009771; LBL-30254; CONF-9106130-2) Avail: NTIS HC/MF A02

The mechanical criterion that most often governs the use of stainless steels at cryogenic temperature is the combination of yield strength and fracture toughness. The strength-toughness combination depends on the fracture mode, which should be ductile. The toughness in the ductile mode is affected by the strength, the tensile properties, and the inclusion density. To maximize toughness, the alloy should have a high work hardening rate and a low inclusion count. The toughness of metastable austenitic steels is governed by a balance between stress relaxation by the strain-induced martensitic transformation and the brittleness of the fresh martensite. This balance also governs the response of metastable steels to a high magnetic field; the toughness of relatively stable steels increases when a field is imposed, while that of relatively unstable steels decreases. DOE

N91-23301# Deutsche Forschungsanstalt fuer Luft- und Raumfahrt, Cologne (Germany, F.R.). Inst. fuer Raumsimulation.
CONTAINERLESS UNDERCOOLING AND SOLIDIFICATION OF PURE METALS
Dieter M. Herlach Oct. 1990 35 p Submitted for publication
(DLR-FB-90-48; ISSN-0939-2963; ETN-91-99068) Avail: NTIS HC/MF A03; DLR, Wissenschaftliches Berichtswesen, VB-PL-DO, Postfach 90 60 58, 5000 Cologne, Fed. Republic of Germany, HC 15 DM

Drop tubes and electromagnetic levitation are described as techniques for containerless processing. The constraints of maximum undercoolability of metals are discussed with respect to thermodynamic considerations and the onset of homogeneous nucleation. Dendrite growth occurring in undercooled melts is described on the basis of experimental investigations and modern dendrite growth theories. The importance of the knowledge of thermophysical properties in the understanding of both nucleation and crystal growth in undercooled melts is pointed out. Experimental techniques which allow the measurement of the dependence of such properties on temperature, in particular by using electromagnetic positioning in future space missions, are presented. Investigations of the nucleation and growth behavior combined with undercooling and solidification studies give a comprehensive description of phase formation and the development of microstructures. ESA

N91-23302# Technische Univ., Brunswick (Germany, F.R.). Fakultaet fuer Maschinenbau und Elektrotechnik.
GAS CONTENTS AND WELDABILITY OF ALUMINUM DIE CASTINGS Ph.D. Thesis [GASGEHALT UND SCHWEISSEIGNUNG VON ALUMINIUM-DRUCKGUSS]
Peter Lutze 1989 180 p In GERMAN
(ETN-91-99188) Avail: NTIS HC/MF A09

The weldability of aluminum die casting is detoriated by its gas contents, which is conditioned by the casting practice. Die casting can contain hydrogen and great quantities of insoluble nitrogen. Hydrogen absorption can be avoided by using forced aeration, setting up a high enough transformation temperature, or by using release agents. Gas absorption by piston lubricants can be limited by careful dosage. Carbon monoxide and methane are also detected in the castings. They can form carbide slags in arc weldings, which limit the weldability. The melting bath in holding furnaces has to be degassed, in order to obtain low enough gas contents in castings during fusion welding. The inert gas welding process requires gas free castings, as fusion bath degassing is limited. The so called vaccum die casting fabricated with a forced degassing and no air trapping, but which still contains high quantities of hydrogen can, for example be used in electron beam welding. ESA

N91-23303# Puerto Rico Univ., Rio Piedras. Dept. of Physics.
STRUCTURE OF ELECTROCHEMICALLY DEPOSITED COPPER ON GOLD (III) ALLOY
Joseph G. Gordon, L. S. Kau, Mahesh G. Samant, and L. Blum 29 Jan. 1991 5 p LIMITED REPRODUCIBILITY: Availability: Document partially illegible
(Contract N00014-90-J-1263)
(AD-A232345) Avail: NTIS HC/MF A01 CSCL 07/4

We measured the X-ray absorption spectrum from a half monolayer (as determined from the deposition charge) of Cu deposited on Au(III) in a sulfuric acid solution. The measurements were performed in situ, with the gold electrode immersed in solution, and at controlled potential. The exciting X-rays were incident at grazing angle and the spectrum was detected by measuring the fluorescence from the monolayer with an energy dispersive IIPGe detector. Spectra were obtained with the electric vector of the X-rays both perpendicular and parallel to the sample surface. GRA

N91-23304# Virginia Univ., Charlottesville. Dept. of Physics.
RAPIDLY SOLIDIFIED METALLIC ALLOYS WITH UNUSUAL SEMMETRY PROPERTIES
S. J. Poon and G. J. Shiflet 17 Dec. 1990 7 p
(Contract DAAL03-87-K-0057)
(AD-A232384; ARO-24122.15-MS) Avail: NTIS HC/MF A02 CSCL 11/6

A new class of metallic glasses based on aluminum is synthesized. The unusual structural and formality of these glasses were investigated by x ray and neutron diffraction, and by high-resolution electron lattice imaging experiments. The glassy nature is confirmed and a dense-random-packing of rare-earth atoms is observed. This new class of aluminum-based metallic glasses has a low density, high tensile strength, and good corrosion-resistant properties which are important for technological applications. Extensive structural studied were performaed on icosahedral and decagonal crystals. Diffraction measurements were compared with atomic models proposed for quasicrystals. It is found that the decoration of Penrose tiling provides an adequate

description of experimental findings in icosahedral crystals. In the case of decagonal crystals, there is strong evidence for an entropy stabilization mechanism. Structural defects in complex crystals closely related to icosahedral crystals were studied. The defects were found to be of the planar type and their structure forms the basis of icosahedral phase formation. GRA

N91-23305# Naval Postgraduate School, Monterey, CA.
PHASE TRANSFORMATIONS AND MICROSTRUCTURAL EVOLUTION IN AGED Mn-Cu-BASED ALLOYS M.S. Thesis
Guy V. Holsten Jun. 1990 100 p
(AD-A232473) Avail: NTIS HC/MF A05 CSCL 11/6

The transformation behavior of aged Mn-Cu-based alloys was studied via transmission electron microscopy. The evolution of several unique forms of diffraction contrast, such as tweed and flickering, was characterized and correlated with the underlying transformation behavior. Convergent beam microbeam compositional analysis and high resolution lattice imaging techniques were employed to assist in the interpretations. It was determined that upon aging these alloys, a FCC solid solution decomposes into a fine dispersion of Mn-rich and Mn-poor regions which coarsen with further aging. This decomposition was modeled using finite difference techniques. The Mn-rich regions were determined to undergo a crystallographic transformation which involves a slight tetragonal distortion upon cooling. For short aging times, when the elastic strain fields around each of the finely dispersed FCT regions overlap sufficiently, tweed contrast is observed. GRA

N91-23306# Aeronautical Research Labs., Melbourne (Australia).
EXAMINATION OF THE MICROSTRUCTURE OF 7050 ALUMINUM ALLOY SAMPLES Aircraft Materials Technical Memo.
S. A. Barter, N. Athiniotis, and L. Lambrianidis Aug. 1990 32 p
(AD-A232544; ARL-MAT-TM-403; DODA-AR-006-113) Avail: NTIS HC/MF A03 CSCL 11/6

As part of the evaluation of the structural life of the F/A-18 fighter aircraft, samples of the Aluminum Alloy 7050 taken from several different fatigue specimens, including F/A-18 FS 488 Bulkhead fatigue test articles, several laboratory fatigue tests specimens, and elsewhere, were examined metallurgically. The microstructure of the bulkhead material was also examined using thin foils in a Transmission Electron Microscope. These examinations revealed marked variations in the grain size, orientation and morphology, which were found to depend to some extent on the thickness of the original rolled plate material, and may have a marked effect on the initiation of fatigue in F/A-18 major structural components. GRA

N91-23307# Dayton Univ., OH.
POST-OVERLOAD FATIGUE CRACK RECOVERY IN POWDER METAL ALUMINUM-LITHIUM AL-905XL FORGING Technical Report, Aug. 1989 - Sep. 1990
Russell R. Cervay Jan. 1991 35 p
(Contract F33615-88-C-5437)
(AD-A232550; UDR-TR-90-102; WL-TR-91-4008) Avail: NTIS HC/MF A03 CSCL 11/6

An overload fatigue investigation was conducted to determine whether variation in the relative humidity would effect the post-overload retardation recovery period of a dispersion hardened powder metal aluminum, alloy AL905XL forging. Constant amplitude and single spike overload tests were conducted in laboratory air, and in low and high humidity air environments. Post-overload crack opening load and crack propagation velocity were observed to determine the number of delay cycles required for the velocity and crack opening load to return to the values immediately preceding overload. Crack retardation increased in the high humidity environment and for shorter crack lengths attributable to increased crack closure. GRA

N91-23308# Materials Research Society, Pittsburg, PA.
HIGH TEMPERATURE ORDERED INTERMETALLIC ALLOYS Final Report
John B. Ballance, James O. Stiegler, and David P. Pope 2 Jan. 1991 14 p
(Grant AF-AFOSR-0367-90; AF Proj. 2305)
(AD-A232769; AFOSR-91-0142TR) Avail: NTIS HC/MF A03 CSCL 11/6

The subject continues to enjoy the attention of a large number of theorists interested in understanding the tendency for brittleness in intermetallics. Some intermetallics are brittle because of a lack of a sufficient number of slip systems while others have a more than adequate number. Materials of the former type are receiving more attention than the latter from theorists, most of whom are attempting to find ways to decrease specific fault energies and thereby encourage the formation of specific dislocations, dislocation pairs separated by APB in NiAl. To date these theoretical attempts have been unsuccessful, although there are increasing reasons for hope of future successes. The properties of TiAl-based alloys received a great deal of attention, both from a scientific and from an engineering point of view. The role of interstitials in controlling microstructure and subsequent mechanical properties is becoming recognized as very important, just as in disordered Ti-based and Ti3Al-based alloys. GRA

N91-24065*# National Aeronautics and Space Administration. Langley Research Center, Hampton, VA.
SUPERPLASTIC FORMING OF Al-Li ALLOYS FOR LIGHTWEIGHT, LOW-COST STRUCTURES
Stephen J. Hales and John A. Wagner *In* NASA, Washington, Technology 2000, Volume 2 1991 p 200-209 (For primary document see N91-24041 15-99)
Avail: NTIS HC/MF A16 CSCL 11F

N91-24066*# National Aeronautics and Space Administration. John F. Kennedy Space Center, Cocoa Beach, FL.
LOCALIZED CORROSION OF HIGH PERFORMANCE METAL ALLOYS IN AN ACID/SALT ENVIRONMENT
L. G. MacDowell and C. Ontiveros (California State Polytechnic Univ., Pomona.) *In* NASA, Washington, Technology 2000, Volume 2 1991 p 210-217 (For primary document see N91-24041 15-99)
Avail: NTIS HC/MF A16 CSCL 11F

27 NONMETALLIC MATERIALS

Includes physical, chemical, and mechanical properties of plastics, elastomers, lubricants, polymers, textiles, adhesives, and ceramic materials.

For composite materials see *24 Composite Materials.*

N91-23309 Georgia Inst. of Tech., Atlanta.
HIGH SHEAR STRESS RHEOLOGY OF LIQUID LUBRICANTS Ph.D. Thesis
Scott Bair 1990 209 p
Avail: Univ. Microfilms Order No. DA9105421

It is well known that non-Newtonian behavior may manifest when the liquid under study is a high molecular weight polymer, a mixture of a polymer and low viscosity liquid, or a suspension. However, it is shown that at sufficiently high shear stress even traditionally Newtonian liquids become highly nonlinear and that they display a yield stress analogous to that of solids and of roughly the same magnitude. This phenomena has implications for any engineering application for which a very large shear stress must be sustained by a liquid such as metalworking, bearing lubrication, liquid jet machining, and ballistic impacts. Included are measurements of the variation of viscosity with pressure and temperature and the determination of the glass transition temperature and dielectric relaxation time at elevated pressure. These studies motivated the search for solid-like response of liquid lubricants at high pressure and subsequently, measurements of elastic modulus and yield strength. The observed variation of yield

strength of these liquids with shear rate led to the conclusion that a rate independent limiting shear stress model is appropriate. Measurements on liquids above the glass transition temperature showed that the limiting stress concept governs the high shear stress rheology in the liquid state as well as for amorphous solids. A constitutive law is presented which includes viscous, elastic and plastic behavior, and appears to be consistent with all observed behavior in uniaxial shear. Many rheometers were developed. Shear stresses were generated in liquids essentially free of thermal effects to levels about one hundred times greater than were achieved before. Viscosities as high as 10(exp 12) Pa were measured and PVT data were generated on liquids at pressures to 1.7 GPa (250,000 psi). Dissert. Abstr.

N91-23310# Philips Display Components Co., Ann Arbor, MI.
CHEVRON-NOTCHED, FLEXURE TESTS FOR MEASURING THE ELEVATED TEMPERATURE FRACTURE RESISTANCE OF STRUCTURAL CERAMICS
M. G. Jenkins, M. K. Ferber, A. Ghosh, and J. T. Peussa (Federation of Finnish Metal, Engineering, and Electronic Technology Industries, Helsinki.) 1991 28 p Presented at the Chevron-Notch Fracture Test Experience Metals and Non-Metals Conference, Indianapolis, 6 May 1991
(Contract DE-AC05-84OR-21400)
(DE91-009117; CONF-9105138-1) Avail: NTIS HC/MF A03

Chevron notched, three point flexure specimens were used to study the quasi-static fracture behavior of a variety of structural ceramics at temperatures to 1400 C. Types of materials tested included monolithic ceramics (SiC, Si3N4, MgAl2O4), self-reinforced monoliths (acicular grained Si3N4), (acicular grained mullite), and ceramic matrix composites (SiC whisker/Al2O3 matrix, TiB2 particulate/SiC matrix, SiC fiber/CVI SiC matrix, Al2O3 fiber/CVI SiC matrix). Fracture resistance behavior of thee materials was quantified as three distinct regimes of the fracture histories. At crack initiation, the apparent fracture toughness was evaluated as the critical stress intensity factor, K sub IC. During stable crack propagation, the crack growth resistance was characterized by the instantaneous strain energy release rate, G sub R, using a compliance method assuming linear-elastic unloading to calculate the effective crack lengths. At final fracture, the complete fracture process was quantified using the work-of-fracture, (gamma sub WOF), which can be equated to the fracture surface energy for linear-elastic materials. Results indicate that the chevron-notched, three point flexure specimen facilitates the study of fracture behavior in a wide range of brittle and quasi-brittle materials at elevated temperatures. The unique features of the chevron geometry, which are automatic crack initiation and inherent stable crack growth are crucial to the successful evaluation of the fracture tests. DOE

N91-23311*# National Aeronautics and Space Administration. Lewis Research Center, Cleveland, OH.
MECHANICAL BEHAVIOR AND FAILURE PHENOMENON OF AN IN SITU-TOUGHENED SILICON NITRIDE
Jonathan A. Salem, Sung R. Choi, Marc R. Freedman, and Michael G. Jenkins (Oak Ridge National Lab., TN.) 1990 22 p Presented at the 43rd Annual Pacific Coast Meeting, Seattle, WA, 25-27 Oct. 1990; sponsored by the American Ceramic Society
(Contract DE-AI05-870R-21749)
(NASA-TM-103741; E-5983; NAS 1.15:103741) Avail: NTIS HC/MF A03 CSCL 11C

The Weibull modulus, fracture toughness and crack growth resistance of an in-situ toughened, silicon nitride material used to manufacture a turbine combustor were determined from room temperature to 1371 C. The material exhibited an elongated grain structure that resulted in improved fracture toughness, nonlinear crack growth resistance, and good elevated temperature strength. However, low temperature strength was limited by grains of excessive length (30 to 100 microns). These excessively long grains were surrounded by regions rich in sintering additives. Author

N91-23312# Argonne National Lab., IL.
APPLICATIONS OF ENERGETIC PARTICLES IN IMPROVING COATING ADHESION PROPERTIES
G. R. Fenske 1990 10 p Presented at the Potential Applications of Concentrated Solar Photons Workshop, Golden, 7-8 Nov. 1990
(Contract W-31-109-eng-38)
(DE91-008833; ANL/CP-72530; CONF-9011183-1) Avail: NTIS HC/MF A02

This paper addresses one approach (on-beam-assisted deposition, or IBAD) that utilizes energetic ion beams to enhance the adhesion of metallic films to metallic and ceramic substrates. In one application, IBAD is used to improve the adhesion of silver films to ceramic substrates that are subjected to sliding wear conditions at elevated temperatures. In another application, the IBAD process is used to improve the adhesion and modify the microstructure of chromium films deposited on low-Cr steel. Both applications suggest that adhesion can be increased by a number of mechanisms including (1) physical and chemical sputtering of surface contaminants (e.g., hydrocarbons and adsorbed water molecules); (2) preferential sputtering of a particular element of a compound, thus producing a surface enriched in a species that is chemically active with the depositing species; (3) activating chemical states; (4) mechanically roughening the surface, producing more surface area for bonding and sites to arrest surface cracks; and (5) recoil-mixing during the initial stage of film deposition. DOE

N91-23313# Pacific Northwest Lab., Richland, WA.
STRESS-DENSITY VARIATIONS IN ALUMINA SEDIMENTS: EFFECTS OF POLYMER CHEMISTRY
C. H. Schilling, J. J. Lanutti, W. H. Shih, and I. A. Aksay Jan. 1991 7 p Presented at the Materials Research Society Meeting, Boston, Dec. 1990
(Contract DE-AC06-76RL-01830)
(DE91-009055; PNL-SA-18573; CONF-901273-3) Avail: NTIS HC/MF A02

Achieving spatially uniform, high density microstructures during the shape-forming of colloidal ceramics is paramount for eliminating packing structure heterogeneities that impair physical properties of ceramics after sintering. The maximum density obtainable for a given sample depends largely on: (1) the magnitude of the effective stresses, and (2) plastic properties, which in turn are significantly altered by processing parameters affecting interparticle friction and adhesion. To quantify the effects of processing parameters on consolidation, the authors present a novel approach for analyzing sediments by gamma-ray densitometry and a fluid mechanics model. This method enables them to correlate processing parameters with spatial variations of the packing density and the local effective stress. Significant variations in plasticity can arise through modification of interparticle forces by changing the chemistry of surface-adsorbed polymers or ions. In the present study, they address the question of how to design surface-adsorbed polysiloxanes to enhance particle rearrangement into densely packed structures. Polysiloxanes are excellent lubricants (e.g., silicon oil) due to the low rotational energy of the Si-O-Si bonds comprising the polymer backbone. These inorganic polymers are also available with a broad range of chemical structures that can pyrolyze to various inorganic silicon-based compounds under appropriate conditions. They analyzed stress-density correlations of alumina sediments as a function of two major variations in additive chemistry: (1) the attachment of polar (carbonyl) pendants to the siloxane backbone, and (2) changes in the molecular weight of nonpolar (MeHSiO)(sub X) (hydrosiloxane). DOE

N91-23314# Sandia National Labs., Albuquerque, NM.
SHOCK CHARACTERIZATION OF EPOXY: FORTY-TWO VOLUME PERCENT GLASS MICROBALLOONS
L. J. Weirick Feb. 1991 20 p
(Contract DE-AC04-76DP-00789)
(DE91-009616; SAND-90-1018) Avail: NTIS HC/MF A03

In the late 1960's, a series of shock experiments were done on ceramic filled epoxies. The results from the shock characterization of these mixtures were compared to unfilled epoxy

with rho sub 0 = 1.185 g/cu cm. In that the volume percent fill was kept essentially constant, the shock Hugoniots formed a consistent family of curves relative to their initial densities. The present study examined the shock characteristics of an anhydride cured epoxy (Epon 828 base) filled with approx. 42 volume pct. glass microballoons (GMB) with a density of 0.94 g/cu cm. The Hugoniot relationship was determined between the shock pressures of 0.5 and 4.2 GPa. A light gas gun was used to impact samples of the epoxy-GMB material onto targets of known impedance and known Hugoniot equation. A Velocity Interferometer System for Any Reflector (VISAR) laser interferometer system was used to measure the particle velocity in the known target material. From the measured projectile velocity and the Hugoniot of the known material, the particle velocity, shock velocity and pressure in the epoxy-GMB was determined. The Hugoniot relationship of the epoxy-GMB material is compared to those of the previous mixtures. A comparison of the epoxy-GMB material to a porous epoxy is also made. Shock attenuation studies were also done on this material. It was found that the shock wave profile consisted of an elastic and a plastic wave due to the initial strength of the glass microballoons, 0.24 GPa; the crushing of the glass microballoons, and the final state of dense epoxy, containing a small amount of glass. This material fits the P-alpha model very well. DOE

N91-23315# Los Alamos National Lab., NM.
ELECTRODEPOSITED COATINGS FOR DIAMOND TURNING APPLICATIONS
A. Mayer, R. D. Bramlett, R. D. Day, C. J. Evans, and R. S. Polvani (National Inst. of Standards and Technology, Gaithersburg, MD.) 1991 7 p Presented at the American Society for Precision Engineering Conference, Tucson, 15-18 Apr. 1991
(Contract W-7405-eng-36)
(DE91-009950; LA-UR-91-884; CONF-9104206-1) Avail: NTIS HC/MF A02

Electrodeposited coatings are attractive for precision machining operations because thick coatings can be economically applied, with good adhesion, to a variety of substrates. Approximately 20 pure metals and a large number of alloys can be deposited from aqueous solutions. Fused salt and organic solvent electrolytes can be used to lengthen the list of metals that can be electrodeposited. However, both the choice of the metallic coating and the control of the plating process are critical for success in precision finishing of electrodeposited coatings. Some preliminary results at the National Institute of Standards and Technology and at the Lawrence Livermore National Laboratory suggest that electrodeposited nickel-phosphorus alloys are excellent coatings for single point diamond turning from the standpoint of material properties and low tool wear. Electrodeposited aluminum and aluminum alloy coatings also merit consideration for precision finishing where weight is an important factor. DOE

N91-23316# Oak Ridge National Lab., TN.
NDE (NONDESTRUCTIVE EXAMINATION) DEVELOPMENT FOR CERAMICS FOR ADVANCED HEAT ENGINES
R. W. McClung and D. R. Johnson 1991 10 p Presented at the 36th International Gas Turbine and Aeroengine Congress and Exposition: ASME Turbo Expo, Orlando, 3-6 Jun. 1991
(Contract DE-AC05-84OR-21400)
(DE91-005516; CONF-910601-2) Avail: NTIS HC/MF A02

The Department of Energy (DOE) Ceramic Technology for Advanced Heat Engines (CTAHE) project was initiated in 1983 to meet the ceramic technology needs of DOE's advanced heat engines programs (i.e., advanced gas turbines and low heat rejection diesels). The objective is to establish an industrial ceramic technology base for reliable and cost-effective high-temperature components. Reliability of ceramics was recognized as the major technology need. To increase the material reliability of current and new ceramics, advances were needed in component design methodology, materials processing technology, and data base/life prediction. Nondestructive examination (NDE) was identified as one of the key elements in the approach to high-reliability components. An assessment was made of the current status of NDE for structural ceramics, and a report was prepared containing the results and recommendations for needed development. Based on these recommendations, a long-range NDE development program has been established in the CTAHE project to address these needs. DOE

N91-23317# Edgerton, Germeshausen and Grier, Inc., Idaho Falls, ID.
MEASUREMENT OF PARTICLE SIZE, VELOCITY AND TEMPERATURE IN THE PLASMA SPRAY COATING PROCESS
J. R. Fincke and W. D. Swank 1991 13 p Presented at the 1st ASME/JSME Fluids Engineering Conference, Portland, 23-26 Jun. 1991
(Contract DE-AC07-76ID-01570)
(DE91-006208; EGG-M-90469; CONF-910684-3) Avail: NTIS HC/MF A03

The quality and uniformity of coatings fabricated by the plasma spray process is controlled by the condition of the particles on impact. In this work a measurement technique for simultaneously obtaining particle size, velocity, and temperature is used to characterize the particle spray field. Particle size and velocity are obtained from a combination laser particle sizing system and laser Doppler velocimeter (LDV). The particle temperature is determined by a two-color pyrometer technique and the relative particle number density is derived from the data rate. The fraction of unheated or unprocessed particles which result from temperature and velocity fluctuations is also obtained. This fraction can approach 10 percent by mass of the total particle flow. DOE

N91-23318# Oak Ridge National Lab., TN.
LOW HEAT REJECTION DIESEL CERAMIC COUPON TESTS
C. R. Brinkman, K. C. Liu, R. L. Graves, and B. H. West 1991 15 p Presented at the 4th International Symposium on Ceramic Materials and Components for Engines, Goeteborg, Sweden, 10-12 Jun. 1991
(Contract DE-AC05-84OR-21400)
(DE91-006274; CONF-910617-1) Avail: NTIS HC/MF A03

Results are reported from studies in which several monolithic ceramic materials in the form of modulus-of-rupture bars were exposed for 100 h to the combustion conditions found in either a small single- or two-cylinder diesel engine. Fuels included a standard Phillips D-2 diesel or synthetic mixture of the Phillips D-2 and an aromatic blend. The ceramics included two commercial grades of partially stabilized zirconia (PSZ-TS and PSZ-MS), silicon nitride (GTE WESGO SNW-1000 and Norton NT-154), and (Hexoloy SA) silicon carbide. Significant reductions in postexposure four-point bend fracture strength occurred in the PSZ-TS material irrespective of whether it was exposed in the single- or two-cylinder engine. Only a small decrease in fracture strength occurred in the PSZ-MS material, and essentially no decrease in fracture strength occurred in the silicon nitride (GTE WESGO SNW-1000) when tested at room temperature. The Norton NT-154 silicon nitride was tested at both room temperature and at 700 C over several strain rates ranging from 1 x 10(exp -4) to 1 x 10(exp -7)/per s. Room temperature tests indicated that the engine exposed bars actually showed a slight increase in average strength, 830 MPa, versus 771 MPa for the unexposed material. Elevated temperature strength comparisons showed no reduction in strength due to previous engine exposure. Hexoloy SA silicon carbide showed no reduction in fracture strength when tested at 700 C. DOE

N91-23319# European Space Agency, Paris (France).
HARDENING MECHANISMS AND ANALYSIS OF THE STRUCTURE OF THE TGDDM/DDS EPOXY RESIN SYSTEM
Andre-Jean Attias (Office National d'Etudes et de Recherches Aerospatiales, Paris, France) Feb. 1991 235 p Transl. into ENGLISH of Etude des Mecanismes de la Reticulation et Analyse de la Structure de la Resine Epoxy TGMDA/DDS (Paris, France, ONERA), 1988 212 p Original language document was announced as A90-12662
(ESA-TT-1202; ONERA-NT-1988-8; ETN-91-99317) Avail: NTIS HC/MF A11

A combination of chemical and spectroscopic methods are used in an attempt to describe as quantitatively as possible the

different kinds of a curved epoxy matrix, the tetraglycidyl 4,4'diamino diphenylmethane (TGDDM)/4,4'-diamino diphenylsulfone (DDS) system. The chemical approach involved the synthesis of model compounds typifying the hypothesis that can be made about reactions taking place during the curing. Model reactions between diepoxy and amino compounds are followed using chemical and chromatographic methods and spectroscopic analysis, in order to correlate the structure of the products formed with the relativity of the initial molecules, the temperature of cure and the proportions of reactants. The experimental conditions are reviewed and the recorded spectra containing poorly resolved peaks are interpreted in the aliphatic carbon region by decomposing it into elementary lines; structural assignments of these lines are made. On the basis of the anticipated mechanisms, the structural groups of the network, as well as their variations during curing processes, are quantified. A relatively detailed picture of the network is given. ESA

N91-23320 National Physical Lab., Teddington (England). Div. of Materials Metrology.
COMMITTEE DRAFT FOR AN ISO STANDARD ON THE ACQUISITION AND PRESENTATION OF MULTIPOINT DATA FOR PLASTICS
G. D. Dean Feb. 1991 27 p
(NPL-DMM(A)-24; ISSN-0959-2426; ETN-91-99329) Copyright Avail: National Physical Lab., Teddington, Middlesex TW11 OLW, England

A standard for the acquisition and presentation of multipoint data is presented. The standard was developed in stages by dividing the contents into mechanical properties, thermal and processing properties and environmental influences or properties. Test procedures are specified for the following mechanical properties of plastics: dynamic modulus, tensile properties at constant testing speed (ultimate stress and strain and tensile stress-strain curves), tensile creep and charpy impact strength. Test procedures are specified for the following thermal and processing properties of plastics: enthalpy/temperature curve, linear expansion/temperature curve and melt shear viscosity. ESA

N91-23321# Aeronautical Research Inst. of Sweden, Stockholm. Structures Dept.
DETERMINATION OF THE DEVIATORIC MATERIAL RESPONSE FUNCTIONS FOR PRESTRAINED RUBBERS
Adam Zdunek Feb. 1991 41 p
(Contract STU-79-6159)
(FFA-TN-1990-29; ETN-91-99341) Avail: NTIS HC/MF A03

The mechanical responses of two natural rubber compounds are examined in order to secure the material parameters for nonlinear finite element analysis. The materials are subjected to combined static torsion and extension, and to small, steady state torsional oscillations superposed on a large static simple extension. These materials are assumed to be incompressible and isotropic in their undeformed state, and a time strain separable relaxation modulus tensor is employed in order to characterize their steady state harmonic viscoelastic response. The combined static torsion and extension experiment is used to determine the basic delayed elastic response functions. A Rivlin type, third order accurate, strain energy expression is used for that purpose. The torsional storage and loss moduli are determined under quasistatic conditions as functions of frequency and axial static prestrain. The time strain separability seem to be a reasonable approximation in the relative limited range of deformations magnitudes considered for the investigated natural gum rubbers. The experimental methodology is discussed in some detail. ESA

N91-23322# Michigan Univ., Ann Arbor.
MECHANISTIC STUDIES OF PRESSURE-ASSISTED SUPERPLASTICITY OF STRUCTURAL CERAMICS Annual Report, Nov. 1989 - Nov. 1990
I-Wei Chen Dec. 1990 4 p
(Grant AF-AFOSR-0289-87; AF Proj. 2306)
(AD-A232034; AFOSR-91-0020TR) Avail: NTIS HC/MF A01 CSCL 11/2

Microstructural and deformation studies have been conducted for superplastic zirconia and sialon ceramics. A methodology based on space charge concept is established for grain size control of zirconia ceramics. A direct correlation between grain boundary mobility and stress-strain curve is demonstrated. For silicon nitride ceramics, both single phase alpha prime and beta prime sialons have been shown to be superplastic, and they exhibit a novel shear-thickening behavior which is interpreted by the breakdown of interparticle structural forces at high temperatures. Deformation experiments and numerical simulations of multiaxial superplastic forming are also reported. GRA

N91-23323# Cornell Univ., Ithaca, NY. School of Chemical Engineering.
DISSOLUTION OF POLY(P-HYDROXYSTYRENE): MOLECULAR WEIGHT EFFECTS
Treva Long and Ferdinand Rodriguez 22 Feb. 1991 14 p
(Contract N00014-85-K-0474)
(AD-A232155; TR-20) Avail: NTIS HC/MF A03 CSCL 07/3

Dissolution rates of PPHS films were measured in aqueous base solvents and in 4-methyl-2-pentanone (MIBK) using laser interferometry. Molecular weights from 6,000 to 100,000 were employed. The films were spun on silicon wafers from MIBK solutions and baked 1 hour at 160 C. The most striking feature of dissolution behavior is the peculiar way in which rate varies with molecular weight. Below a molecular weight of about 20,000, the rate decreases with molecular weight as one might expect. Above 30,000, the rate in aqueous base is much higher and seems to be almost independent of molecular weight. The behavior in MIBK, while more conventional, shows some of the same features. Another feature found with PPHS that is not usual with other polymers is a decrease in dissolution rate with increased thickness. Conventional wisdom would predict that retained solvents (after baking) in thick films would accelerate dissolution compared to think films. GRA

N91-23324# Florida Univ., Gainesville. Dept. of Chemistry.
CHAIN PROPAGATION/STEP PROPAGATION POLYMERIZATION. REGULAR THERMOPLASTIC ELASTOMERS Final Report, 15 Mar. 1986 - 15 Aug. 1989
K. B. Wagener 15 Jan. 1991 3 p
(Contract DAAL03-86-K-0050)
(AD-A232356; ARO-23396.16-CH) Avail: NTIS HC/MF A01 CSCL 07/6

This research has produced a new polymer synthesis technique for generating well defined segmented thermoplastic elastomers. Chain propagation using ring opening chemistry has been coupled with step propagation techniques to create solvent resistant segmented elastomers, wherein each segment possesses a narrow molecular weight distribution. GRA

N91-23325# Defence Research Establishment Atlantic, Dartmouth (Nova Scotia).
THE EFFECT OF POST-CURE AND ANTIMONY TRIOXIDE ADDITION ON THE GLASS TRANSITION OF POLYESTER AND VINYL ESTER RESIN SYSTEMS
R. M. Morchat, I. A. Keough, and J. G. Dwyer Dec. 1990 26 p
(AD-A232523; DREA-TM-90/208) Avail: NTIS HC/MF A03 CSCL 11/9

The effect of post-curing on the glass transition temperature (Tg) of a variety of styrene cross-linked polyester and vinyl ester resins was determined by monitoring the changes to Tg using a Differential Scanning Calorimeter. The effect of adding the inorganic fire-retardant, antimony trioxide, on the Tg of these resin systems was also investigated. Results indicated that the effect of post-curing was to increase the amount of cross-linking of the polyester and vinyl ester resins, as evident by the beneficial increase in the glass transition temperature and changes to the storage modulus. The addition of up to 10 parts per hundred resin (phr) of the fire-retardant, antimony trioxide, had a negligible effect on the onset of the glass transition point. GRA

N91-23326# Pennsylvania State Univ., University Park.
POINT DEFECT EFFECTS ON HOT CORROSION OF ZIRCONIA-BASED COATINGS Annual Report, Jan. 1990 - Jan. 1991
R. Reidy, D.-H. Kim, and G. Simkovich 23 Jan. 1991 26 p
(Contract N00014-86-K-0133)
(AD-A232662) Avail: NTIS HC/MF A03 CSCL 11/3

Thermal barrier coatings are vulnerable to certain types of hot corrosion: sulfidation and vanadic attack. Stabilized zirconia, an often used thermal barrier coating, is degraded by dissolution of the stabilizing components, mass transport in the coating must occur. The presence of point defects in a crystalline solid greatly affect the transport properties in that solid. The nature and concentration of these defects can be altered which, in turn, can impart large changes in the transport properties of a material (e.g., ionic conductivity and diffusion). In this study, we are determining the defect structures of yttria and ceria-stabilized zirconium oxides. Using electrical conductivity measurements, the activation energy of yttria-stabilized have been examined as a function of frequency, composition, and oxygen activity. Conductivity measurements on ceria-stabilized zirconia have shown anomalous results. At low oxygen activities, ZrO2-CeO2 samples did not reach equilibrium. The cause for this phenomenon has yet to be determined. Transport properties of molten Na2SO4 have been investigated to aid in understanding hot corrosion processes at 1173 K. An A.C. impedance technique for the total electrical conductivity, the potentiostatic polarization method for ionic transport number, and the steady state polarization method of Wagner and Hebb for the electronic conductivity were employed as a function of Na2O activity in the melt by controlling gas atmosphere. GRA

N91-23327# United Technologies Research Center, East Hartford, CT.
A STUDY OF THE CRITICAL FACTORS CONTROLLING THE SYNTHESIS OF CERAMIC MATRIX COMPOSITES FROM PRECERAMIC POLYMERS Final Report, 1 Oct. 1987 - 15 Nov. 1990
J. R. Strife, J. P. Wesson, and H. H. Streckert 15 Dec. 1990 53 p
(Contract F49620-87-C-0093)
(AD-A232686; UTRC/R90-917810-5; AFOSR-91-0055TR) Avail: NTIS HC/MF A04 CSCL 07/6

In this three year program, vinylmethylsilane copolymers which were processable at ambient pressure were studied as precursors for silicon carbide matrix composites. Using measurements of curing characteristics, rheological properties, and pyrolysis kinetics, fabrication cycles for processing carbon fabric reinforced composites were identified. Composites exhibiting a range of useful mechanical properties were demonstrated. The primary shortcomings of a commercially available vinylmethylsilane polymer used in composite fabrication were identified as extremely sensitive to oxygen contamination during processing and excess carbon in the pyrolyzed products. Analytical methods showed that 900 C pyrolysis products were amorphous ceramics consisting primarily of SiO-C complexes. The amorphous ceramic was unstable above 1200 C where CO and CO2 release initiated. Ceramic products converted at 1440 C showed increases in Beta-SiC and and SiO2 content at the expense of Si-O-C content. Polymer modifications were pursued to improve the converted ceramic thermal stability and stoichiometry. Novel methylvinylsilanes with reactive endgroups exhibited significantly reduced oxygen sensitivity and high ceramic convertibility. GRA

N91-23328# Northwestern Univ., Evanston, IL. Dept. of Materials Science and Engineering.
OXIDATION STUDIES OF FLUORINE CONTAINING DIAMOND FILMS
K. J. Grannen, D. V. Tsu, R. J. Meilunas, and R. P. Chang 26 Feb. 1991 18 p
(Contract N00014-89-J-1848)
(AD-A232696; TR-3) Avail: NTIS HC/MF A03 CSCL 07/2

The thermogravimetric method is used to study the oxidation properties of plasma grown diamond films both with and without fluorine. The oxidation experiments are carried out over a temperature range of 600 to 800 C and in pure oxygen at one atmospheric pressure. Our experiments show diamond films with fluorine are more resistant (by as much as a factor of 4 at 700 C) to oxidation. The activation energy for oxidation, on the other hand, is at least a factor of 2.3 lower for diamond films with fluorine. These results lead us to postulate that oxidation mechanisms for diamond films are quite different depending on whether there is fluorine or not. For diamond films without fluorine the oxidation seems to proceed as a rate limited reaction, while for films with fluorine the oxidation seems to be a diffusion limited reaction. There is also a weak dependence of oxidation rates on film density, crystal texture, and the phase composition of the diamond film. GRA

N91-23329# Virginia Polytechnic Inst. and State Univ., Blacksburg. Polymer Materials and Interfaces Lab.
THERMOFORMING OF IN-SITU REINFORCED THERMOPLASTIC COMPOSITES
T. Sun, A. Datta, J. P. DeSouza, and D. G. Baird Jan. 1991 20 p
(Contract DAAL03-88-K-0104)
(AD-A232816; ARO-25344.9-MS) Avail: NTIS HC/MF A03 CSCL 07/3

The conditions under which the LCP reinforced thermoplastic composites can be thermoformed have been investigated. Two liquid crystalline polymers (a copolyester of terephthalic acid, phenyl hydroquinone, and phenyl ethyl hydroquinon and a copolyester of p-hydroxy benzoic acid and 6-hydroxy 2-naphthoic acid) were used. An amorphous (polyetherimide) and a semi-crystalline (polypropylene) have been used as the matrix materials for making the composites. The thermoformability has been studied as a function of the sheet preheating temperature, and the mold temperature for various compositions of composites. Morphology and molecular orientation of the thermoformed parts before and after thermoforming have also been studied. GRA

N91-23330# Virginia Polytechnic Inst. and State Univ., Blacksburg. Dept. of Chemical Engineering.
GENERATION OF CONTINUOUS LIQUID CRYSTALLINE POLYMER REINFORCEMENTS IN THERMOPLASTICS BY A NOVEL BLENDING PROCESS
A. M. Sukhadia, A. Datta, and D. G. Baird Jan. 1991 19 p
(Contract DAAL03-88-K-0104)
(AD-A232824; ARO-25344.10-MS) Avail: NTIS HC/MF A03 CSCL 11/9

The focus of this work was to investigate the potential of enhancing the mechanical properties of thermoplastic resins, with an emphasis on those which are considered commodity resins, by blending with liquid crystalline polymers (LCPs). There is an inherent problem, however, in achieving this goal in that thermotropic LCPs often have higher melting (or processing) temperatures than most thermoplastic polymers such as poly(ethylene terephthalate) (PET) and polypropylene (PP). To overcome this limitation a novel blending technique was developed in our laboratory in which the LCP and matrix polymers were plasticated in two separate extruders, and the melts then were brought together in a mixing head. Blends of PET and PP with several LCPs were successfully generated by the above technique. Either rods or flat films were extruded by attaching an appropriate die to the exit of the mixing head. The morphology of the blends showed that the LCP phase formed continuous reinforcing fibrils in the respective matrix material. A high degree of molecular orientation was also observed by means of wide-angle x ray diffraction studies. Significant enhancements in the mechanical properties of rods, flat films and injection molded plaques of the blends correlated well with the morphology and orientation measurements. GRA

N91-23331# Iowa State Univ. of Science and Technology, Ames. Dept. of Chemistry.
ATRANE AND QUADROPED FRAMEWORKS IN EARLY TRANSITION METAL AND SILICON GRO STEREOCHEMISTRY: MONOMERS AND OLIGOMERS Final Report, 1 Nov. 1987 - 31 Oct. 1990
J. G. Verkade Jan. 1991 16 p
(Grant AF-AFOSR-0081-88)
(AD-A232837; AFOSR-91-0174TR) Avail: NTIS HC/MF A03 CSCL 07/2

An exploration of the chemistry of silatranes and azasilatranes has been carried out. The first isolation and structural characterization of silatrane adducts in which the exocyclic axial oxygen behaves as a Lewis base site was accomplished. Azasilatrane phosphine-nitrogen complexes were prepared with Lewis acid sites on the complex bonding to the axial oxygen. An axial silatranium cation was prepared. The range of axial-substituents for azalilatranes was explored and found to be limited to H, OR, OAr, R, and Ar. Attempts to obtain pentacoordination by nitrogen by replacing the axial hydrogen by azide using trimethylsilylazide resulted instead in trimethylsilyl/substitution of the equatorial nitrogens and an azide salt. Pyrolysis of the azide salt afforded the pentacoordinated azide. Nitrogen pentacoordination was also obtained from a thioisocyanide salt. A number of other equatorial nitrogen substituted azasilatranes were prepared. Attempts to couple azasilatrane to a Si-Si bonded dimer were unsuccessful. Azasilatrane-based polymers were prepared and characterized. The azasilatrane studies were extended to azastannatranes. GRA

N91-24062*# National Aeronautics and Space Administration. Lewis Research Center, Cleveland, OH.
FLEXIBLE FLUOROPOLYMER FILLED PROTECTIVE COATINGS
Bruce A. Banks, Michael J. Mirtich, James S. Sovey, Henry Nahra, and Sharon K. Rutledge *In* NASA, Washington, Technology 2000, Volume 2 1991 p 179-184 (For primary document see N91-24041 15-99)
Avail: NTIS HC/MF A16 CSCL 11C

N91-24063*# National Aeronautics and Space Administration. Ames Research Center, Moffett Field, CA.
A CONFORMAL OXIDATION-RESISTANT, PLASMA-POLYMERIZED COATING
Morton A. Golub, Theodore Wydeven, and Narcinda R. Lerner *In* NASA, Washington, Technology 2000, Volume 2 1991 p 185-191 (For primary document see N91-24041 15-99)
Avail: NTIS HC/MF A16 CSCL 11C

28 PROPELLANTS AND FUELS

Includes rocket propellants, igniters, and oxidizers; their storage and handling procedures; and aircraft fuels.

For related information see also *07 Aircraft Propulsion and Power, 20 Spacecraft Propulsion and Power,* and *44 Energy Production and Conversion.*

N91-23332# Onan Corp., Minneapolis, MN.
DEVELOPMENT OF A LOW COST PEAK SHAVING GENERATOR SET Final Report, Oct. 1987 - Jun. 1989
J. R. Iverson Dec. 1989 485 p
(Contract GRI-5087-298-1508)
(PB91-136374; GRI-90/0089) Avail: NTIS HC/MF A21 CSCL 07D

The findings of the research on the market potential and requirements for a low cost natural gas fueled peak shaving generator set, and tests on an automotive derived engine for durability and performance are summarized. Because some electric utilities assess their customers a significant demand charge to offset the capital investment needed to meet peak energy consumption, the use of on-site generator sets fueled by relatively inexpensive natural gas to reduce the customer's peak energy consumption may result in significant cost savings for the customer. A market research survey was used to ascertain the current market and equipment requirements, and to forecast the market potential for a low installed cost ($200/kW) peak shaving generator set. Testing was conducted on several configurations of a Ford automotive-derived engine to determine if appropriate performance and durability goals for the application could be met. GRA

N91-23333# Lawrence Livermore National Lab., CA.
RESPONSE OF SIMULATED PROPELLANTS AND EXPLOSIVES TO PROJECTILE IMPACT Ph.D. Thesis
W. Yuan Nov. 1990 338 p
(Contract W-7405-eng-48)
(DE91-009777; UCRL-CR-106704) Avail: NTIS HC/MF A15

This dissertation deals with experimental, analytical and numerical investigations into the response of two types of simulated propellants and explosives, known as Propergol, to projectile impact. The targets consisted of a polymeric mixture composed of potassium chloride, plaster of Paris and a polyurethane binder. Following the determination of the constitutive behavior of Propergol, experiments were conducted to study their penetration, perforation and fragmentation by projectiles. Both pneumatic and powder guns were employed in the tests, permitting impact velocities ranging from 40 to 1100 m/s, for flat- and conically-tipped as well as armor-piercing projectiles. The specimens include monolithic, composite and constrained Propergol circular disks and cylinders of 140 mm diameter with thicknesses ranging from 9 to 90 mm. Penetration tests were also conducted on model warheads loaded with the simulant material. Ballistic limit velocities for various target/projectile combinations were determined. Damage modes, such as cracking and fragmentation, were examined using experimental evidence including high-speed film data and microscopic photographs. Two types of fragments, Propergol clusters and crystalline particles, were recognized, and their size distributions were found to fit exponential functions. The dependent of fragment number and volume on initial projectile velocity was also studied. DOE

N91-23334# Pittsburgh Univ., PA. Dept. of Chemical and Petroleum Engineering.
A NOVEL PROCESS FOR METHANOL SYNTHESIS
J. W. Tierney and I. Wender 1990 23 p
(Contracts DE-FG22-89PC-89786; DE-FG22-84PC-71257)
(DE91-009808; DOE/PC-89786/T1) Avail: NTIS HC/MF A03

A bench-scale reactor is being used to conduct studies of the conversion of synthesis gas to methanol by a novel process. During the last quarter, the authors investigated the effect of various catalysts on the rate of MeOH synthesis. The success of salts such as alkali formates and carbonates as catalysts indicates the regeneration of the homogeneous catalyst in the presence of Cu-chromite. This could also explain the increased tolerance of the process to the presence of small amounts of H2O. Mathematical equations were written to explain the non-linearity of the rate (in gmoles/min) with catalyst concentration and the effect of feed flow rate. An on-line gas sampling valve was installed. Efforts are continuing to install an on-line liquid sampling valve. A major difficulty is due to the fact that liquid flow is not continuous. DOE

N91-23335# Ballistic Research Labs., Aberdeen Proving Ground, MD.
QUANTUM CHEMICAL STUDIES OF CANDIDATE HIGH ENERGY DENSITY MATERIAL COMPOUNDS Final Report, May 1987 - Aug. 1989
George F. Adams and Cary F. Chabalowski Jan. 1991 45 p
(Contracts MIPR-F04611-87-X-0059; MIPR-F04611-88-C-0067)
(AD-A232393; AL-TR-89-055) Avail: NTIS HC/MF A03 CSCL 20/8

This report describes the development and application of ab-initio quantum chemical methods that are especially relevant to the study of high-energy density materials species. Two major quantum chemical program systems, MESA and BROOKLYN, were developed during the tenure of this research effort. Each of these

development efforts was performed, in large part, at the Ballistic Research Laboratory (BRL) and The John Hopkins University. The results of quantum studies on molecular systems that are thought to be relevant to high-energy density material research are reported. Theses include detailed descriptions of the electronic excited states of He2, the energy loss mechanisms for the He-H2 systems, detailed structural studies data for a series of triborane species, and analysis of the stability of four-atom metal clusters with molecular formulae B2Li2 and B2Be2, and a preliminary theoretical study of the energy storage potential of hydrogen halide-doped rare gas solids. GRA

N91-23336# SRI International Corp., Menlo Park, CA. Molecular Physics Lab.
IONIC SOLID HYDROGEN FUEL: EXPERIMENTAL INVESTIGATION OF CLUSTER-IMPACT FUSION Final Report, 1 Jul. - 30 Sep. 1990
Young K. Bae, D. C. Lorents, S. Young, and K. R. Stalder 24 Jan. 1991 20 p
(Contract F49620-90-C-0048)
(AD-A232642; SRI-MP-91-005; AFOSR-91-0059TR) Avail: NTIS HC/MF A03 CSCL 18/1

The investigation of a new fusion method is discussed: the use of deuterium-containing clusters for igniting fusion (cluster-impact fusion, CIF). If CIF becomes practical, the energy density that can be achieved with the DT fuel is 3.4 x 10(exp 14) J/kg, which is eight orders of magnitude larger than the energy density of LOX/H2 (1,600,000 j/kg). For missions with specific impulse less than 100,000 s, the CIF rocket performance will be essentially identical to that of antimatter. Under the current project, a new cluster-impact fusion facility was successfully built and demonstrated by extending the existing hydrogen cluster facility. The new fusion method discovered at Brookhaven is very promising; thus, means of increasing the fusion yield to a practical level for rocket propulsion applications is being investigated. GRA

29 MATERIALS PROCESSING

Includes space-based development of products and processes for commercial applications.

For biological materials see *55 Space Biology*.

No abstracts in this category.

31 ENGINEERING (GENERAL)

Includes vacuum technology; control engineering; display engineering; cryogenics; and fire prevention.

N91-23337# Israel Aircraft Industries Ltd., Ben-Gurion Airport.
MIK-GUIDED BOMB SIMULATION
Yaron Sharf Apr. 1987 93 p In HEBREW; ENGLISH summary
(IAITIC-87-1003; ITN-88-85002) Avail: NTIS HC/MF A05

MIK is a 3 degrees of freedom (x,y,z) simulation of a guided bomb. It can be used as a synthesis and analysis tool in the early stages of the system design. There are 3 options of calculation: (1) single trajectory; (2) acquisition envelope; and (3) kill envelope. Though simple, the simulation is accurate enough to represent the bomb with good fidelity. The report includes user's instructions and a detailed example. ISA

N91-23338# Linnhoff March, Inc., San Mateo, CA.
RESEARCH AND DEVELOPMENT OPPORTUNITIES FOR NATURAL GAS FUELED REFRIGERATION IN INDUSTRIAL PROCESSES Final Report, Aug. 1988 - Mar. 1990
H. W. Klavers Jun. 1990 120 p
(Contract GRI-5087-233-1461)
(PB91-136432; GRI-90/0074) Avail: NTIS HC/MF A06 CSCL 13B

Currently, nearly all refrigeration systems in industrial processes are driven by electric motors. Natural gas has a negligible share of the industrial refrigeration market. The objective of the study was to identify opportunities for and potential barriers to the use of gas fueled refrigeration in industrial processes. A large number of industrial processes were surveyed to determine their potential for gas fueled refrigeration. Three processes were selected for further analysis using Pinch Technology. Cogeneration proved to be the most cost-effective way to incorporate gas fueled refrigeration in all three processes. Significant energy cost reductions can be achieved at paybacks of less than three years. It was concluded that the thermodynamically most efficient system to provide gas fueled refrigeration must include a heat engine. GRA

N91-23339# Cornell Univ., Ithaca, NY.
DEVELOPMENT AND UTILIZATION OF NEW DIAGNOSTICS FOR DENSE-PHASE PNEUMATIC TRANSPORT
M. Y. Louge and J. T. Jenkins 1990 10 p
(Contract DE-AC22-88PC-88947)
(DE91-008947; DOE/PC-88947/T9) Avail: NTIS HC/MF A02

Dense-phase pneumatic transport is an attractive means of conveying solids. Unfortunately, because of the high solid concentrations, this transport method is a difficult regime in which to carry out detailed measurements. Hence most details of the flow are unknown. In this context, the main objective is to develop probes for local measurements of solid velocity and holdup in dense gas-solid flows. In particular, capacitance probes were designed to measure local, time dependent particle concentrations, and a new optical fiber probe based on laser induced phosphorescence to measure particle velocities. The principles for the capacitance and optical diagnostics were given in the first and second quarterly reports. A final version of the optical fiber probe was designed in the previous reporting period. Because granular flows depends strongly on the nature of their interaction with a boundary, the authors have sought in the present reporting period to verify the boundary conditions recently calculated by Jenkins, using computer simulations. DOE

N91-23340*# National Aeronautics and Space Administration. Lewis Research Center, Cleveland, OH.
A SIMPLIFIED DYNAMIC MODEL OF THE SPACE SHUTTLE MAIN ENGINE
Ahmet Duyar, Vasfi Eldem (Florida Atlantic Univ., Boca Raton.), Walter Merrill, and Ten-Huei Guo 1991 12 p Presented at the American Control Conference, Boston, MA, 26-28 Jun. 1991; sponsored by the American Automatic Control Council
(NASA-TM-104421; E-6133; NAS 1.15:104421) Avail: NTIS HC/MF A03 CSCL 21H

A simplified model is presented of the space shuttle main engine (SSME) dynamics valid within the range of operation of the engine. This model is obtained by linking the linearized point models obtained at 25 different operating points of SSME. The simplified model was developed for use with a model-based diagnostic scheme for failure detection and diagnostics studies, as well as control design purposes. Author

N91-23341*# National Aeronautics and Space Administration. Ames Research Center, Moffett Field, CA.
COMPUTATIONAL NEEDS SURVEY OF NASA AUTOMATION AND ROBOTICS MISSIONS. VOLUME 1: SURVEY AND RESULTS
Gloria J. Davis May 1991 30 p
(NASA-TM-103860; A-91093-Vol-1; NAS 1.15:103860) Avail: NTIS HC/MF A03 CSCL 13B

NASA's operational use of advanced processor technology in space systems lags behind its commercial development by more than eight years. One of the factors contributing to this is that mission computing requirements are frequently unknown, unstated, misrepresented, or simply not available in a timely manner. NASA

must provide clear common requirements to make better use of available technology, to cut development lead time on deployable architectures, and to increase the utilization of new technology. A preliminary set of advanced mission computational processing requirements of automation and robotics (A&R) systems are provided for use by NASA, industry, and academic communities. These results were obtained in an assessment of the computational needs of current projects throughout NASA. The high percent of responses indicated a general need for enhanced computational capabilities beyond the currently available 80386 and 68020 processor technology. Because of the need for faster processors and more memory, 90 percent of the polled automation projects have reduced or will reduce the scope of their implementation capabilities. The requirements are presented with respect to their targeted environment, identifying the applications required, system performance levels necessary to support them, and the degree to which they are met with typical programmatic constraints. Volume one includes the survey and results. Volume two contains the appendixes. Author

N91-23342# Ballistic Research Labs., Aberdeen Proving Ground, MD.
POWER PACKS: A PASSIVE APPROACH TO EXTINGUISHING FIRE IN COMBAT VEHICLES Final Report, Aug. 1988 - Jun. 1989
Anthony E. Finnerty and Stanley Polyanski Jan. 1991 57 p
(DA Proj. 1L1-62601-AH-91)
(AD-A232020; BRL-TR-3191) Avail: NTIS HC/MF A04 CSCL 19/1

Thin (12.7 and 6.4 mm) panels of fire extinguishing powder in a honeycomb matrix were tested for their ability to extinguish fires in the FAASV ammunition resupply vehicle. These powder packs were applied to the exterior of hydraulic fluid reservoirs and fuel cells for protection from hydrocarbon fires caused by shaped charge jets penetrating the fluid containers. It was found that a surround of 12.7-mm-thick panels was required to achieve a sub 250-ms fire-out time with no second-degree burns expected to personnel with hot hydraulic fluid reservoirs. Power packs as thin as 6.4 mm provided the same protection in the case of hot diesel fuel. GRA

N91-23343# Army Engineer Waterways Experiment Station, Vicksburg, MS. Information Technology Lab.
REVIEW OF FINITE ELEMENT PROCEDURES FOR EARTH RETAINING STRUCTURES Final Report
Robert M. Ebeling Dec. 1990 42 p
(AD-A232230; WES/MP/ITL-90-5) Avail: NTIS HC/MF A03 CSCL 13/13

This miscellaneous paper presents a review of previous work in which the finite element method was used to analyze the soil structure interaction of earth retaining structures such as U-frame locks, gravity walls, and basement walls. This method of analysis results in the computation of stresses and displacement for both the structure and the soil backfill. Applications of the procedure have shown the importance of modeling the actual construction process as closely as possible and the use of a nonlinear stress-strain soil model. Additional requirements include modeling the interface between the soil backfills and the wall using interface elements. This paper also includes two recent applications of the finite element method for the analysis of earth retaining structures which are loaded so heavily that a gap develops along the interface between the base of the structure and its foundation. The results are compared to those computed using the conventional force equilibrium method of analysis. GRA

N91-23344# Naval Research Lab., Washington, DC.
TRIPOD OPERATORS FOR THE INTERPRETATION OF RANGE IMAGES
Frank Pipitone 19 Feb. 1991 31 p
(AD-A232631; NRL-MR-6780) Avail: NTIS HC/MF A03 CSCL 12/9

A new kind of feature extraction operator for range images is introduced that facilitates object recognition in several ways. It consists of three points in 3-space fixed at the vertices of an equilateral triangle and one or more curves, called test curves, fixed in the reference frame of the triangle. This mathematical structure is then moved as a rigid body until the vertices all lie on the surface of some range image or modeled object. The point(s) of intersection of the test curve(s) and the surface are used to define local shape features which are invariant under rigid motions. These features can be used to automatically find distinctive regions at which they begin recognition, to rapidly screen candidate modeled objects for a match, and to speed pruning in the generation of interpretation trees. Tripod operators are applicable to all three dimensional shapes, and reduce the need for specialized feature detectors. GRA

32 COMMUNICATIONS AND RADAR

Includes radar; land and global communications; communications theory; and optical communications.

For related information see also *04 Aircraft Communications and Navigation* and *17 Space Communications, Spacecraft Communications, Command and Tracking.* For search and rescue see *03 Air Transportation and Safety,* and *16 Space Transportation.*

N91-23345# Israel Aircraft Industries Ltd., Ben-Gurion Airport.
A METHOD OF CONSTRUCTING A PAIR OF PSEUDORANDOM SEQUENCES WITH A USEFUL CROSSCORRELATION FUNCTION
G. Sarafian and B. Z. Kaplan Jan. 1987 11 p
(IAITIC-87-1001; ITN-88-85000) Avail: NTIS HC/MF A03

The paper deals with synthesizing pseudorandom signals which possess an odd crosscorrelation function of useful characteristics. The characteristics are applicable for signal tracking systems such as those associated with ranging instrumentation and spreadspectrum communication. Another property of the signals developed in the paper is that they possess a zero dc component. This property may be applied for radiating useful carrierless signals. ISA

N91-23346*# Honeywell, Inc., Bloomington, MN. Sensors and Signal Processing Lab.
A 30 GHz MONOLITHIC RECEIVE MODULE Final Report, 1 Nov. 1982 - 31 Oct. 1990
J. Mondal, T. Contolatis, J. Geddes, P. Bauhahn, and V. Sokolov Nov. 1990 112 p
(Contract NAS3-23356)
(NASA-CR-187085; NAS 1.26:187085) Avail: NTIS HC/MF A06 CSCL 20N

The technical achievements and deliveries made during the duration of the program to develop a 30 GHz monolithic receive module for communication feed array applications and to deliver submodules and 30 GHz monolithic receive modules for experimental evaluation are discussed. Key requirements include an overall receive module noise figure of 5 dB, a 30 dB RF-to-RF gain with six levels of intermediate gain control, a five bit phase shifter, and a maximum power consumption of 250 mW. In addition, the monolithic receive module design addresses a cost goal of less than one thousand dollars (1980 dollars) per module in unit buys of 5,000 or more, and a mechanical configuration that is applicable to a spaceborne phase array system. An additional task for the development and delivery of 32 GHz phase shifter integrated circuit (IC) for deep space communication is also described. Author

N91-23347*# National Aeronautics and Space Administration. Lewis Research Center, Cleveland, OH.
AN ASSESSMENT OF TECHNOLOGY ALTERNATIVES FOR TELECOMMUNICATIONS AND INFORMATION MANAGEMENT FOR THE SPACE EXPLORATION INITIATIVE
Denise S. Ponchak and John E. Zuzek Apr. 1991 25 p
(NASA-TM-103783; E-6058; NAS 1.15:103783) Avail: NTIS HC/MF A03 CSCL 17B

On the 20th anniversary of the Apollo 11 lunar landing, President Bush set forth ambitious goals for expanding human presence in the solar system. The Space Exploration Initiative (SEI) addresses these goals beginning with Space Station Freedom, followed by a permanent return to the Moon, and a manned mission to Mars. A well designed, adaptive Telecommunications, Navigation, and Information Management (TNIM) infrastructure is vital to the success of these missions. Utilizing initial projections of user requirements, a team under the direction of NASA's Office of Space Operations developed overall architectures and point designs to implement the TNIM functions for the Lunar and Mars mission scenarios. Based on these designs, an assessment of technology alternatives for the telecommunications and information management functions was performed. This technology assessment identifies technology developments necessary to meet the telecommunications and information management system requirements for SEI. Technology requirements, technology needs and alternatives, the present level of technology readiness in each area, and a schedule for development are presented. Author

N91-23348# State Dept., Washington, DC. Task Force on Telecommunications and Broadcasting in Eastern Europe.
EASTERN EUROPE: PLEASE STAND BY Final Report, 1989 - 1990
D. L. Dougan, J. Hoagland, J. Koehler, T. Marshall, and E. Sekulow May 1990 163 p
(PB91-14336) Avail: NTIS HC/MF A08 CSCL 17B

The objectives of the Task Force on Telecommunications and Broadcasting in Eastern Europe are: (1) to assess and evaluate the current infrastructure, policies, and plans for telecommunications and broadcasting; (2) to make recommendations to the Department of State for short and long-term U.S. private sector involvement and initiatives; and (3) to share with key host country leaders perspective and expertise of senior U.S. corporate leaders on potential opportunities and obstacles of telecommunications and broadcasting in economic development. GRA

N91-23349# Sandia National Labs., Albuquerque, NM.
EFFECT OF ATMOSPHERIC VARIATIONS ON ELECTROMAGNETIC DISTANCE MEASUREMENTS
O. M. Solomon, Jr. Dec. 1990 36 p
(Contract DE-AC04-76DP-00789)
(DE91-009726; SAND-90-0945) Avail: NTIS HC/MF A03

Some field tests of the CUBIC CR-100 distance measuring equipment are described. The distance measurements depend on the refractivity of the atmospheric. The CR-100 uses 320 for the refractivity. For the Albuquerque area on a clear spring day, 220 is a more realistic value for refractivity. This difference of 100 between the actual and assumed refractivities causes the range error to accumulate at the rate of 1 meter per 10,000 meters of range. For example, a difference of 100 in refractivity forces the measured range to contain an error of 5 meters for a 50,000 meter baseline. DOE

N91-23350# Los Alamos National Lab., NM.
DISTRIBUTED RADAR SENSORS FOR AIRCRAFT DETECTION
G. H. Canavan Apr. 1991 20 p
(Contract W-7405-eng-36)
(DE91-009845; LA-11898-MS) Avail: NTIS HC/MF A03

Radars suitable for aircraft detection could be deployed on singlet space-based interceptor (SBI) platforms. They could operate at short ranges and still achieve useful search rates. Powers are modest and insensitive to frequency; the dominant costs are the pulsers and phased-array elements. A fundamental simplification results from mounting the radar on the life jacket rather than the SBI. Many satellites could be processed to derive aircraft trajectories sufficiently accurate for the commitment of fighters or defensive missiles. DOE

N91-23351# Los Alamos National Lab., NM.
THE STATISTICAL PROPERTIES OF ELECTROMAGNETIC FIELDS WITH APPLICATION TO RADIATION AND SCATTERING
T. H. Lehman (Lehman, T. H., Albuquerque, NM) and E. K. Miller 1991 5 p Presented at the 1991 Institute of Electrical and Electronics Engineers (IEEE) AP-S Symposium, Ontario, 24-28 Jun. 1991
(Contract W-7405-eng-36)
(DE91-007467; LA-UR-91-226; CONF-9106118-1) Avail: NTIS HC/MF A01

Determining the relationships between different average values is an important step in any physics-based statistical theory. If these relationships exist and exhibit certain properties, then probability densities or distributions can be assigned to the field variables and the transition from an average-value theory to a statistical theory is complete. For electromagnetics, no such average-value relationships have been demonstrated to exist. The derivation of these relationships and their range of validity are the subject of consideration here. For purposes of this discussion, attention is limited to the fields inside a complex cavity, but with the ultimate goal of deriving the statistics of the far radiated and scattered fields of complex envelopes. DOE

N91-23352# Sandia National Labs., Albuquerque, NM.
EXPERIMENTAL STUDY OF NARROW SLOT, CAVITY-BACKED APERTURES WITH FINITE WALL CONDUCTIVITY
R. P. Jedlicka, S. P. Castillo, and L. K. Warne 1991 4 p Presented at the 1991 Institute of Electrical and Electronics Engineers (IEEE) AP-S Symposium, Ontario (Canada), 24-28 Jun. 1991
(Contract DE-AC04-76DP-00789)
(DE91-009039; SAND-91-0445C; CONF-9106118-2) Avail: NTIS HC/MF A01

Electromagnetic coupling to electronic components or subsystems is a concern in modern system design. Undesired coupling can cause interference or, in the extreme, system upset. To be able to characterize the coupling is an important step to understanding the limitations on system performance. Often the approach is taken to shield the electronic equipment inside some kind of enclosure. However, there are usually inadvertent cracks or bowing at mechanical interfaces. These gaps are apparent slot apertures. An equivalent antenna/local transmission line model for narrow slot apertures with depth including losses has been developed. It may be applied tortuous paths and hence may be used to model practical situations. This model has been previously verified by measuring the coupling through narrow slot apertures with varying width and depth. These measurements were performed for brass slots radiating into a half-space. The results were in good agreement with the model of Warne and Chen. The models, as well as the measurements showed that for very narrow slots the wall loss becomesdominant -- it has been demonstrated that the inclusion of loss is important in making realistic coupling estimates in practical configurations. This paper presents results showing the effects of varying conductivity and surface preparations for half-space coupling as well as different loadings of the narrow slot apertures. The coupling through narrow slot apertures having depth was measured for a variety of resonant cavity loadings. The loadings were chosen such that the cavity resonant frequencies were above, near and below the resonant peak of the half-space coupling curve. Measurements were made in the 2 to 4 GHz band with vertical polarization. DOE

N91-23353# Oak Ridge National Lab., TN.
THE EFFECT OF REALISTIC ANTENNA GEOMETRIES ON PLASMA LOADING PREDICTIONS
P. M. Ryan, F. W. Baity, D. B. Batchelor, R. H. Goulding, D. J. Hoffman, and J. S. Tolliver 1991 5 p Presented at the 18th European Conference on Controlled Fusion and Plasma Physics, Berlin, Fed. Republic of Germany, 3-7 Jun. 1991
(Contract DE-AC05-84OR-21400)
(DE91-010782; CONF-910609-5) Avail: NTIS HC/MF A01

Plasma loading resistances for Ion Cyclotron Resonance Heating (ICRH) antennas are often calculated with sophisticated plasma models and only rudimentary antenna geometries. This paper presents techniques for modifying loading calculations for cavity antennas to account for such realities as return currents in the antenna sidewalls and backplane, the transmission and reflection properties of the Faraday shield, the end effects due to a finite length antenna, the reduction in phase velocity due to strap interaction with the Faraday shield, and the effect of slots in the cavity sidewalls and dividing septa. DOE

N91-23354*# National Aeronautics and Space Administration. Lewis Research Center, Cleveland, OH.
SYSTEM-LEVEL INTEGRATED CIRCUIT (SLIC) DEVELOPMENT FOR PHASED ARRAY ANTENNA APPLICATIONS
K. A. Shalkhauser and C. A. Raquet 1991 8 p Presented at the International Symposium on Optical Engineering and Photonics, Orlando, FL, 4-5 Apr. 1991; sponsored by Society of Photo-Optical Instrumentation Engineers
(NASA-TM-104392; E-6207; NAS 1.15:104392) Avail: NTIS HC/MF A02 CSCL 20N

A microwave/millimeter wave system-level integrated circuit (SLIC) being developed for use in phased array antenna applications is described. The program goal is to design, fabricate, test, and deliver an advanced integrated circuit that merges radio frequency (RF) monolithic microwave integrated circuit (MMIC) technologies with digital, photonic, and analog circuitry that provide control, support, and interface functions. As a whole, the SLIC will offer improvements in RF device performance, uniformity, and stability while enabling accurate, rapid, repeatable control of the RF signal. Furthermore, the SLIC program addresses issues relating to insertion of solid state devices into antenna systems, such as the reduction in number of bias, control, and signal lines. Program goals, approach, and status are discussed. Author

N91-23355# Deutsche Forschungsanstalt fuer Luft- und Raumfahrt, Cologne (Germany, F.R.). Abt. Lasertechnik.
SIMULATION OF A BACKSCATTER LIDAR SYSTEM
Juergen Streicher Oct. 1990 115 p In GERMAN; ENGLISH summary
(DLR-FB-90-50; ISSN-0939-2963; ETN-91-99070) Avail: NTIS HC/MF A06; DLR, Wissenschaftliches Berichtswesen, VB-PL-DO, Postfach 90 60 58, 5000 Cologne, Fed. Republic of Germany, HC 39 DM

A simulation program for a lidar system was developed to determine the visibility, so that the effects of the system and the atmosphere parameters could be easily presented. Different stability evaluation algorithms were examined, using the single scattering equation. Multiple scattering was included in the program with the calculation of double scattering lidar returns. The improvement of a commercial lidar and the draft for a new one was proposed, using the simulation program. ESA

N91-23356# Deutsche Forschungsanstalt fuer Luft- und Raumfahrt, Oberpfaffenhofen (Germany, F.R.). Abt. fuer Hochfrequenzphysik.
POLARIMETRIC RADAR OBSERVATIONS OF TIME-VARIANT RANDOM TARGETS Ph.D. Thesis - Kaiserlautern Univ.
Karl Tragl Oct. 1990 143 p In GERMAN; ENGLISH summary Original contains color illustrations
(DLR-FB-90-52; ISSN-0939-2963; ETN-91-99072) Avail: NTIS HC/MF A07; DLR, Wissenschaftliches Berichtswesen, VB-PL-DO, Postfach 90 60 58, 5000 Cologne, Fed. Republic of Germany, HC 68 DM

A new concept is presented which allows a statistical characterization of the time and polarization dependent backscattering features of random targets. The radar data observed can be related to the microphysical characteristics of the observed targets. The polarization dependence of the mean radar data is developed, using a covariance matrix approach for random targets. Optimal polarization is determined. This concept is used to analyze polarimetric time series data of rain and chaff, acquired with a weather radar. Particular polarimetric scattering features of rain and chaff can be derived. ESA

N91-23357# Deutsche Forschungsanstalt fuer Luft- und Raumfahrt, Oberpfaffenhofen (Germany, F.R.). Abt. fuer Hochfrequenzphysik.
EFFICIENT NUMERICAL TECHNIQUES FOR THE ANALYSIS OF COMPLEX MICROSTRIP-ANTENNAS AND MICROSTRIP ARRAYS Ph.D. Thesis - Wuppertal Univ.
Georg Splitt Aug. 1990 154 p In GERMAN; ENGLISH summary Report will also be announced as translation (ESA-TT-1259)
(DLR-FB-90-53; ISSN-0939-2963; ETN-91-99073; ESA-TT-1259) Avail: NTIS HC/MF A08; DLR, Wissenschaftliches Berichtswesen, VB-PL-DO, Postfach 90 60 58, 5000 Cologne, Fed. Republic of Germany, HC 49.50 DM

Several design parameters such as input impedance and bandwidth of microstrip structures with arbitrary shape embedded in multilayered dielectrics are obtained. More complex feed methods and the behavior of stacked microstrip antennas are examined. The accuracy of the numerical analyses presented is verified experimentally. ESA

N91-23358 Physics and Electronics Lab. TNO, The Hague (Netherlands).
TIME-DOMAIN ANALYSIS OF ONE-DIMENSIONAL ELECTROMAGNETIC SCATTERING BY LOSSY MEDIA Final Report
J. J. A. Klaasen Oct. 1990 53 p
(Contract A86/K/012)
(FEL-90-A211; TD-90-2479; ETN-91-99093) Copyright Avail: Physics and Electronics Lab. TNO, P.O. Box 96864, 2509 JG The Hague, Netherlands

A study was performed to investigate the electromagnetic scattering in the time domain by a plane interface between two half spaces. One half space is assumed to be vacuum, while the other half space is homogeneous and consists of lossy material. The incident field is assumed to be a uniform plane wave. Thus, the one dimensional scattering problem is addressed. Both horizontal and vertical polarization of the incident field are addressed. Starting with the equations for the reflected and transmitted waves in the s- or Laplace-domain, corresponding time domain expressions are obtained by applying the inverse Laplace transform analytically. These time domain results are in closed form, i.e., they are given in terms of elementary functions or integrals of elementary functions. Numerical results are presented for the scattering of a unit-step and a nuclear electromagnetic pulse (NEMP), using the derived time domain expressions. The numerical implementation uses a time marching procedure. ESA

N91-23359 Physics and Electronics Lab. TNO, The Hague (Netherlands).
SAR PROCESSOR FOR THE ERS-1 DATA PHASE 1, SIMPLE PROCESSOR Final Report
F. P. P. deVries Aug. 1990 57 p Sponsored by Netherlands Agency for Aerospace Programs
(FEL-90-B033; TD-90-1717; ETN-91-99094) Copyright Avail: Physics and Electronics Lab. TNO, P.O. Box 96864, 2509 JG The Hague, Netherlands

A description of a simple digital synthetic aperture radar (SAR) processor as the first phase in the development of an experimental digital processing facility for ERS-1 SAR data is presented. The processor consists of a software package, containing the principal processing functions. The constituent software modules were designed, implemented, and tested by simulated data and Seasat SAR data on a VAX 6310 computer. The numerically computer results were in agreement with the theoretical ones. Profiles and photographs from various points in the processing chain are shown. The additional processing functions are indicated for the next phase: the precison processor. These additions serve to enhance the image quality and to reduce the computation time. The precision processor will be able to process the future SAR data from the

ERS-1 satellite. Implementation of the precision processor's software package on a supercomputer enables processing of a very large amount of SAR data within reasonable time. ESA

N91-23360 Physics and Electronics Lab. TNO, The Hague (Netherlands).
CALCULATION OF NEAR-FIELD SCATTERING USING THE PLANE-WAVE FORMULATION AND THE PHYSICAL OPTICS METHOD Final Report
M. H. Vogel Jul. 1990 69 p
(FEL-90-B215; TD-90-2771; ETN-91-99095) Copyright Avail: Physics and Electronics Lab. TNO, P.O. Box 96864, 2509 JG The Hague, Netherlands

Taking Maxwell's equations as a starting point, the problem of scattering of electromagnetic fields by an object is solved. The derivation of equations for the scattered fields is based on the so called plane wave formulation, in which an arbitrary incident wave is described as a superposition of an infinite number of plane waves. Special attention is paid to the case where the scattering object is perfectly conducting and has linear dimensions that are much larger than the wavelength of the incident radiation. For this case, the method of physical optics is applied. The surface of the object is subsequently divided into many triangular panels, and the fields scattered by the object are found by vectorial addition of the contributions of the individual panels. An important advantage of this is the possibility to calculate the scattered fields in the so called near field region of the object, while otherwise satisfactory results would only be obtained at relatively large distances from the object (in the so called far field region). ESA

N91-23361 Physics and Electronics Lab. TNO, The Hague (Netherlands).
CALCULATION OF ELECTROMAGNETIC FIELDS IN THE NEAR-FIELD REGION OF A MOVING SCATTERING OBJECT Final Report
M. H. Vogel Jul. 1990 34 p
(FEL-90-B216; TD-90-2772; ETN-91-99096) Copyright Avail: Physics and Electronics Lab. TNO, P.O. Box 96864, 2509 JG The Hague, Netherlands

The problem of scattering of electromagnetic fields by perfectly conducting, moving objects is solved with the Lorentz transformation and the plane wave formulation. Apart from the physical optics approximation, the solution is exact. The result is subsequently applied to the special case of monostatic reflection by an object that moves slowly with respect to the velocity of light. The result can be used to predict the time dependent reflection from an aircraft that passes the antenna of a proximity fuze, and the optimum fuze algorithm can be selected. ESA

N91-23362# Grenoble-1 Univ. (France). Groupe Calcul Parallele.
OPTIMAL MULTINODE BROADCAST ON A MESH CONNECTED GRAPH WITH REDUCED BUFFERIZATION
Abderezak Touzene and Brigitte Plateau 25 Sep. 1990 11 p Sponsored by French Program Communication, Cooperation and Concurrency
(RR-825-I; ETN-91-99222) Avail: NTIS HC/MF A03

An optimal all to all communication procedure for a mesh connected graph with wraparound is described. The procedure is based on a spanning tree method and uses a reduced bufferization space. A communication step is defined as the simultaneous send/receive of a data unit on each node on its 4 links. For the all to all procedure, each node must receive p squared minus 1 data if p squared is the total number of nodes in the mesh. ESA

N91-23363# European Space Agency, Paris (France).
ANALYSIS OF THE VHF-UHF ELECTROMAGNETIC RADIATION OF LIGHTNING: APPLICATION TO A MODEL OF THE NEGATIVE STEPPED LEADER PROPAGATION
Isabelle Taudiere (Office National d'Etudes et de Recherches Aerospatiales, Paris, France) Mar. 1991 172 p Transl. into ENGLISH of Analyse du Rayonnement Electromagnetique VHF-UHF de l'Eclair: Application a un Modele d'Avance du Precurseur Negatif (Paris, France, ONERA), 1989 165 p Original language document was announced as N89-29000
(ESA-TT-1172; ONERA-NT-1989-1; ETN-91-99313) Avail: NTIS HC/MF A08

The space and time characteristics of the VHF-UHF radiation from lightning are analyzed on the bases of 300 MHz emission sources, localized in three dimensions by interferometric measurements. The main phases that contribute to the development of intracloud lightning are examined in detail, also using electric field measurements at the lower frequency. This research is complemented by an experimental and theoretical analysis of long discharge (8m) radio emissions generated with both polarities in the laboratory. These investigations revealed that the VHF radiation is associated with the channel reillumination phase accompanying each step in the negative spark. The outcome of this work is the creation of a simple model for the propagation of the negative leader. The current and the radiated field during this phase of the discharge are computed from an equivalent electric circuit using the physical laws governing the variation of resistance. The extrapolation of these results to the case of the stepped leader of natural lightning is discussed. ESA

N91-23364# Royal Signals and Radar Establishment, Malvern (England).
IMPLICATIONS OF ADAPTIVE CANCELLATION ARRAY PROCESSING FOR DESIGN OF A SPACE-BASED SURVEILLANCE RADAR
J. L. Mather, A. C. Fairhead, and M. P. Warden Jan. 1991 25 p
(RSRE-Memo-4410; BR116334; ETN-91-99321) Copyright Avail: NTIS HC/MF A03

The system design issues associated with the use of adaptive jammer rejection in the context of possible specifications for a space based surveillance radar are examined. The adaptive nulling requirements of the system cannot be considered in isolation. Adaptive processing has implications for the entire system, from design of the antenna array, through to the choice of DCs and the requirements of subsequent coherent integration and detection processing. Three different classes of adaptive processing architecture are considered: the sidelobe canceller, the fully adaptive array, and the generalized sidelobe canceller. These are shown to achieve different tradeoffs between inherent complexity, requirements upon the system specification, flexibility and performance. ESA

N91-23365# Kansas Univ. Center for Research, Inc., Lawrence. Radar Systems and Remote Sensing Lab.
SCATTERING FROM THIN APERTURES IN COATED CONDUCTORS USING FDTD Final Report
Kenneth D. Demarest and Panayiotis A. Tirkas Dec. 1990 95 p
(Contract F30602-88-D-0027)
(AD-A232125; RADC-TR-90-377) Avail: NTIS HC/MF A05 CSCL 09/1

The Finite-Difference Time-Domain (FDTD) technique is applied to scattering problems involving thin dielectric sheets, conductor-backed dielectric sheets and conductor-backed dielectric sheets containing cracks in the dielectric coating. The FDTD technique is first applied in a brute force method to solve the scattering problems. Then, coarse cells are used whereby the dimensions of the scatterer can be smaller than the dimensions of the FDTD unit cell. This approach, referred to as the thin equation approach, is computationally more efficient than the brute force method. Numerical results are shown in the frequency domain. Specifically, radar cross section (RCS) and near-field results obtained using a two-dimensional FDTD code are presented. GRA

N91-23366# Mitre Corp., Bedford, MA.
ANTENNA PERFORMANCE INFLUENCED BY THE FINITE EXTENT AND CONDUCTIVITY OF GROUND PLANES: A COLLECTION OF REPRINTS

J. R. Wait Sep. 1990 260 p
(AD-A232132; MTR-M90-79) Avail: NTIS HC/MF A12 CSCL 09/1

Project 91260 High-Frequency (HF) Antenna Element Modeling is a MITRE sponsored research project to develop computer programs and accurate models for predicting the element pattern, radiation efficiency, and input impedance of HF monopole elements on ground planes of various forms that rest on or are in close proximity to earth. A unique aspect of this project has been the use of a technical advisor group composed of outside interested investigators to assist MITRE personnel in the development and evaluation of analytical models. A collection of twenty-two reprints was assembled on antenna performance influenced by the finite extent and conductivity of ground planes primarily in the presence of earth. The objective of this collection is to provide a focus and filter of relevant papers. Also included discussions of U.S. Navy Electronics Laboratory reports related to reprint 1.11 (Wait and Walters, 1963) and an annotated listing of selected related publications. A biography of Wait and a complete listing of his referenced papers through April 1990 are given in the appendices. GRA

N91-23367# Defence Research Establishment, Ottawa (Ontario).
THE 2-D ACOUSTO-OPTIC SIGNAL PROCESSORS FOR SIMULTANEOUS SPECTRUM ANALYSIS AND DIRECTION FINDING
Jim P. Lee Nov. 1990 86 p In ENGLISH and FRENCH
(AD-A232148; DREO-1049) Avail: NTIS HC/MF A05 CSCL 17/4

Two dimensional (2-D) Fourier transforming acousto-optic signal processors, for simultaneous direction finding (DF) and spectrum analysis of radar signals over a wide instantaneous bandwidth, are shown to be useful for Radar Electronics Support Measures (ESM) applications. A comprehensive treatment on the analysis and design of two general 2-D acousto-optic architectures is provided. In one architecture, a linear antenna array is employed, and in the other a novel circular antenna array with a Butler matrix beamformer is used. Emphasis is placed on the DF characteristics of both architectures. The effects of scaling factor, acoustic transducer height, Gaussian laser illumination profile, RF input noise, amplitude, and phase tracking errors on the DOA pattern produced by each architecture are addressed. Design criteria and comparison between the two architectures are also provided. GRA

N91-23368# Michigan State Univ., East Lansing. Div. of Engineering Research.
RADAR TARGET DISCRIMINATION AND IDENTIFICATION USING EXTINCTION-PULSES AND SINGLE-MODE EXTRACTION PULSES Final Report, 1 Jun. 1987 - 31 Jan. 1991
Kun-Mu Chen, Dennis P. Nyquist, and Edward J. Rothwell 31 Jan. 1991 228 p
(Contract N00014-87-K-0336)
(AD-A232162) Avail: NTIS HC/MF A11 CSCL 17/9

The goal of this research program is to develop an efficient new radar target discrimination and identification scheme based on the natural frequencies of the target. It consists of synthesizing aspect independent discriminant signals including extinction pulse (E-pulses) and single mode extraction pulses (S-pulses) which, when convolved numerically with late-time transient response of an expected target, lead to zero or single-mode responses. When the synthesized discriminant signals for an expected target are convolved with the radar return from a different target, the resulting signals will be significantly different from the expected zero or single-mode responses; thus, the differing targets can be discriminated. Major achievements on various topics under this research program are described in this report. GRA

N91-23369# Carnegie-Mellon Univ., Pittsburgh, PA.
DECENTRALIZED COMPUTING TECHNOLOGY FOR FAULT-TOLERANT, SURVIVABLE C3I SYSTEMS, VOLUME 1 Final Report, Aug. 1985 - Dec. 1988
J. D. Northcutt, E. D. Jensen, Edward J. Burke, Raymond K. Clark, and James G. Hanko Jun. 1990 212 p
(Contract F30602-85-C-0274)
(AD-A232289; RADC-TR-90-101-Vol-1) Avail: NTIS HC/MF A10 CSCL 12/5

Alpha is an operating system for the mission-critical integration and operation of large, complex, distribution, real time systems. Such systems are becoming increasingly common in both military (e.g., BM/C3, combat platform management) and industrial factory and plant automation (e.g., automobile manufacturing) contexts. They differ substantially from the better-known timesharing systems, numerically-oriented supercomputers, and networks of personal workstations. More surprisingly, they also depart significantly from traditional real-time systems, which are predominantly for low level periodic sampled data monitoring and control. GRA

N91-23370# Carnegie-Mellon Univ., Pittsburgh, PA.
DECENTRALIZED COMPUTING TECHNOLOGY FOR FAULT-TOLERANT, SURVIVABLE C3I SYSTEMS, VOLUME 2 Final Report, Aug. 1985 - Dec. 1988
J. D. Northcutt, E. D. Jensen, Edward J. Burke, Raymond K. Clark, and James G. Hanko Jun. 1990 152 p
(Contract F30602-85-C-0274)
(AD-A232290; RADC-TR-90-101-Vol-1) Avail: NTIS HC/MF A08 CSCL 12/5

Alpha is an operating system for the mission-critical integration and operation of large, complex, distributed, real time systems. Such systems are becoming increasingly common in both military (e.g., BM/C3, combat platform management) and industrial factory and plant automation (e.g., automobile manufacturing) contexts. They differ substantially from the better-known timesharing systems, numerically-oriented supercomputers, and networks of personal workstations. More surprisingly, they also depart significantly from traditional real-time systems, which are predominantly for low-level periodic sampled data monitoring and control. GRA

N91-23371# Carnegie-Mellon Univ., Pittsburgh, PA.
DECENTRALIZED COMPUTING TECHNOLOGY FOR FAULT-TOLERANT, SURVIVABLE C3I SYSTEMS. VOLUME 3: SYSTEM/SUBSYSTEM SPECIFICATION Final Report, Aug. 1985 - Dec. 1988
J. D. Northcutt, E. D. Jensen, Edward J. Burke, Raymond K. Clark, and James G. Hanko Jun. 1990 196 p
(Contract F30602-85-C-0274)
(AD-A232291; RADC-TR-90-101-Vol-3) Avail: NTIS HC/MF A09 CSCL 12/5

Alpha is an operating system for the mission critical integration and operation of large, complex, distributed, real time systems. Such systems are becoming increasingly common in both military (e.g., BM/C3, combat platform management) and industrial factory and plant automation (e.g., automobile manufacturing) contexts. They differ substantially from the better-known timesharing systems, numerically-oriented supercomputers, and networks of personal workstations. More surprisingly, they also depart significantly from traditional real time systems, which are predominately for low-level periodic sampled data monitoring and control. GRA

N91-23372# Naval Research Lab., Washington, DC.
HIGH-QUALITY 800-b/s VOICE PROCESSING ALGORITHM Interim Report
G. S. Kang and L. J. Fransen 25 Feb. 1991 41 p
(AD-A232352; NRL-9301) Avail: NTIS HC/MF A03 CSCL 25/4

The 2400-b/s linear predictive coder (LPC) is currently being widely deployed to support tactical voice communication over narrowband channels. However, there is a need for lower-data-rate voice encoders for special applications: improved performance in high-bit-error conditions, low-probability-of-intercept (LPI) voice communications, and integrated voice/data systems. As a result

of continued research, the intelligibility of very-low-data-rate (600 to 800 b/s) voice processors has steadily improved, from the upper 70s about a decade ago to the middle 80s in recent years. This report presents a new 800-b/s voice-encoding method that produces an intelligibility score of 92 (measured by the Diagnostic Rhyme Test (DRT)). This high score compares favorably with that attained by the 2400-b/s LPC. GRA

N91-23373# Air Force Inst. of Tech., Wright-Patterson AFB, OH.
BACKSCATTERING BY NONSPHERICAL PARTICLES, USING THE COUPLED-DIPOLE METHOD: AN APPLICATION IN RADAR METEOROLOGY Ph.D. Thesis
Clifton E. Dungey Dec. 1990 153 p
(AD-A232371; AFIT/CI/CIA-90-039D) Avail: NTIS HC/MF A08 CSCL 04/2

In the coupled-dipole method, an arbitrary particle is modeled as an array of N polarizable subunits each of which gives rise to only electric dipole radiation. Of all scattering angles, backscattering is the most sensitive to small changes in particle size and shape. The coupled-dipole method's ability and limitations for calculating backscattering are demonstrated. For particles with size parameter less than that associated with the first backscattering minimum, the coupled-dipole method agrees favorably with Mie theory. For particles with larger size parameters, the agreement decreases, but accuracy generally improves by increasing the number of dipolar subunits in the array. Backscattering of 94 GHz Doppler radar by raindrops can be used to infer clear air velocity; backscattering by ice crystals may provide similar information. Backscattering at 94 GHz by randomly oriented ice plates or columns does not agree with backscattering by equal-volume ice spheres for size parameters greater than 0.8. Backscattering depends on zenith angle for ice crystals whose principle axes are confined to the horizontal plane. The relationship between first backscattering minimum and size parameter varies with particle shape and zenith angle. Backscattering of vertically polarized light is more sensitive to the presence of ice columns while horizontally polarized light is more sensitive to ice plates. GRA

N91-23374# Naval Postgraduate School, Monterey, CA.
ERROR CONTROL CODING FOR MULTI-FREQUENCY MODULATION M.S. Thesis
Robert W. Ives Jun. 1990 81 p
(AD-A232421) Avail: NTIS HC/MF A05 CSCL 25/5

Multi-frequency modulation (MFM) has been developed at NPS using both quadrature-phase-shift-keyed (QPSK) and quadrature-amplitude-modulated (QAM) signals with good bit error performance at reasonable signal-to-noise ratios. Improved performance can be achieved by the introduction of error control coding. This report documents a FORTRAN simulation of the implementation of error control coding into an MFM communication link with additive white Gaussian noise. Four Reed-Solomon codes were incorporated, two for 16-QAM and two for 32-QAM modulation schemes. The error control codes used were modified from the conventional Reed-Solomon codes in that one information symbol was sacrificed to parity in order to use a simplified decoding algorithm which requires no iteration and enhances error detection capability. Bit error rates as a function of SNR and E(sub b)/N(sub 0) were analyzed, and bit error performance was weighed against reduction in information rate to determine the value of the codes. GRA

N91-23375# Naval Postgraduate School, Monterey, CA.
A STUDY OF PC-BASED HF IONOSPHERIC PROPAGATION PREDICTIONS FOR USE IN NAVAL COMMUNICATIONS M.S. Thesis
Georgios H. Giakoumakis Jun. 1990 63 p
(AD-A232466) Avail: NTIS HC/MF A04 CSCL 20/14

High frequency (HF) ionospheric propagation predictions have been available on mainframe computers since the late 1960s. Since the advent of low cost, computationally powerful personnel computers, several propagation codes have been ported from mainframes to PC's. This study compares results from two versions of the IONCAP and PROPHET HF propagation prediction codes to a database of measured electric field strengths. IONCAP-PC 2.5 predictions were compared to IONCAP-VAX 85.04 predictions and to those from PROPHET 3.2 (PC-version). A database of measured signal strengths from the CCIR containing over 16,000 points or cases was used as a benchmark for comparing code results. For both IONCAP-PC 2.5 and PROPHET 3.2, field strength predictions were low in more than 50 percent of the cases examined. This was particularly true for PROPHET, which is considered to be a conservative model. PROPHET features quick solution, graphical outputs, and a user-friendly environment, in comparison to IONCAP. IONCAP-PC 2.5, which is an improved version of a previous mainframe IONCAP, produced slightly more accurate predictions than IONCAP 85.04, and substantially better results than those from PROPHET. GRA

N91-23376# Naval Postgraduate School, Monterey, CA.
ERROR PROBABILITIES OF FREQUENCY HOPPED MFSK WITH SELF-NORMALIZATION COMBINING IN A FADING CHANNEL WITH PARTIAL-BAND INTERFERENCE M.S. Thesis
Michael W. Briske Jun. 1990 123 p
(AD-A232467) Avail: NTIS HC/MF A06 CSCL 12/9

Research entails derivation of statistical description of output from an MFSK receiver which uses self-normalization of the output from quadratic detectors. The system uses fast frequency hopping to provide diversity and assumes independent channels for each hop when the signal is recombined. The effects of fading channels are investigated for both Rayleigh and Rician fading channel descriptions. Probability of bit error for the uncoded performance is plotted for various signal-to-noise ratios (SNR) and different levels of diversity versus worst-case partial-band jamming. Analysis for Forward Error Correction coding is included for rate 1/2 and 1/3 convolutional codes and (n,k) Reed-Solomon Block codes. Probability of bit error is plotted for each code with various signal-to-noise ratios and diversity levels 1 to 4 versus worst-case partial-band jamming. GRA

N91-23377# Naval Research Lab., Washington, DC.
DIGITAL BEAMFORMING AND PULSE COMPRESSION IN AN ADAPTIVE ARRAY RADAR SYSTEM Memorandum Report
Frederick W. Lee and M. Burroughs 25 Feb. 1991 36 p
(AD-A232713; NRL-MR-6788) Avail: NTIS HC/MF A03 CSCL 17/9

New digital techniques for forming antenna beam patterns and matched filtering of radar waveforms are investigated and compared to the traditional analog methods. The development at NRL of an integrated digital processor for performing both adaptive beamforming and pulse compression is presented along with performance data obtained from experiments performed in the Adaptive Processing Laboratory. GRA

N91-23378# Defence Research Establishment, Ottawa (Ontario).
AN INVESTIGATION OF CFAR TECHNIQUES FOR AIRBORNE RADARS
Gary E. Vrckovnik and Denis Faubert Dec. 1990 57 p
(AD-A232724; DREO-1056) Avail: NTIS HC/MF A04 CSCL 17/9

In this report, techniques for performing constant false alarm rate (CFAR) processing, with airborne pulse-Doppler radars are described. Cell-averaging, greatest-of, and smallest-of CFAR processors are implemented on interference environments of thermal noise, and thermal noise plus clutter. For the particular radar conditions considered, a 60 dB clutter peak appears across all of the range gates. While these three processors were successful in the thermal noise environment, they suffered large CFAR losses in the presence of the clutter peak. The smallest-of CFAR algorithm performed much worse than the other two, due to its tendency to underestimate the interference powers. Although enlarging the reference window improves the performance of all the processors, it is clear that for the complicated clutter situation examined, more sophisticated CFAR techniques are required. Author (GRA)

N91-23379# Naval Postgraduate School, Monterey, CA.
AN ANALYSIS OF MLAYER: A MULTILAYER TROPOSPHERIC PROPAGATION PROGRAM M.S. Thesis
Lean-Weng Yeoh Jun. 1990 158 p
(AD-A232733; NPS62-90-009) Avail: NTIS HC/MF A08 CSCL 12/5

MLAYER, a computer program, was developed by the Naval Ocean Systems Center (NOSC) for calculating the signal levels of electromagnetic waves propagating in a multilayer tropospheric waveguide environment over seawater. The program is an extension of the XWVG which is a trilinear ducting program. Modifications of the XWVG were carried out to handle multilayer tropospheric ducts. A number of modifications and improvements on the program made over the past several years were not documented. A detailed documentation of MLAYER was also not available. The object of this thesis is to develop a technical documentation for MLAYER using the program as baseline. The study aims to put together the theoretical formulations (specific to MLAYER) into a complete self-contained document. This is to facilitate potential users with better appreciation of the capabilities, limitations, approximations and assumptions used in the mathematical modelling techniques. As far as possible, the same terminologies and functional variables used by Baumgartner (in the XWVG development) and by Pappert (in the MLAYER development) are adopted to enable one to relate this document to the program. Step-by-step derivation of certain equations was carried out and checked for compatibility with the algorithm in the program. GRA

N91-24067*# National Aeronautics and Space Administration. Lewis Research Center, Cleveland, OH.
DIGITAL CODEC FOR REAL-TIME PROCESSING OF BROADCAST QUALITY VIDEO SIGNALS AT 1.8 BITS/PIXEL
Mary Jo Shalkhauser and Wayne A. Whyte *In* NASA, Washington, Technology 2000, Volume 2 1991 p 221-228 Previously announced in IAA as A90-51306 (For primary document see N91-24041 15-99)
Avail: NTIS HC/MF A16 CSCL 17B

N91-24068*# Jet Propulsion Lab., California Inst. of Tech., Pasadena.
RECENT ADVANCES IN CODING THEORY FOR NEAR ERROR-FREE COMMUNICATIONS
K.-M. Cheung, L. J. Deutsch, S. J. Dolinar, R. J. McEliece, F. Pollara, M. Shahshahani, and L. Swanson *In* NASA, Washington, Technology 2000, Volume 2 1991 p 229-241 (For primary document see N91-24041 15-99)
Avail: NTIS HC/MF A16 CSCL 17B

33 ELECTRONICS AND ELECTRICAL ENGINEERING

Includes test equipment and maintainability; components, e.g., tunnel diodes and transistors; microminiaturization; and integrated circuitry.

For related information see also *60 Computer Operations and Hardware* and *76 Solid-State Physics.*

N91-23380*# National Aeronautics and Space Administration. Goddard Space Flight Center, Greenbelt, MD.
MAGNETOSTRICTIVE ROLLER DRIVE MOTOR Patent Application
John M. Vranish, inventor (to NASA) 10 Jan. 1991 17 p
(NASA-Case-GSC-13369-1; NAS 1.71:GSC-13369-1; US-Patent-Appl-SN-645972) Avail: NTIS HC/MF A03 CSCL 09A

A magnetostrictive drive motor is disclosed which has a rotary drive shaft in the form of a drum which is encircled by a plurality of substantially equally spaced roller members in the form of two sets of cones which are in contact with the respective cam surfaces on the inside surface of an outer drive ring. The drive ring is attached to sets of opposing pairs of magnetostrictive rods. Each rod in a pair is mutually positioned end to end within respective energizing coils. When one of the coils in an opposing pair is energized, the energized rod expands while the other rod is caused to contract, causing the drive ring to rock, i.e., rotate slightly in either the clockwise or counterclockwise direction, depending upon which rod in a pair is energized. As the drive ring is activated in repetitive cycles in either direction, one set of drive cones attempts to roll up their respective cam surface but are pinned between the drive shaft drum and the drive ring. As the frictional force preventing sliding builds up, the cones become locked, setting up reaction forces including a tangential component which is imparted to the drive shaft drum to provide a source of motor torque. Simultaneously the other set of cones are disengaged from the drive shaft drum. Upon deactivation of the magnetostrictive rod coils, the force on the drive cones is released, causing the system to return to an initial rest position. By repetitively cycling the energization of the magnetostrictive rods, the drive shaft drum indexes in microradian rotational steps. NASA

N91-23381# Oak Ridge National Lab., TN.
RADIOLUMINESCENT (RL) LIGHTING SYSTEM DEVELOPMENT PROGRAM
K. W. Haff, D. J. Pruett, D. W. Ramey, F. J. Schultz, and J. A. Tompkins Mar. 1991 39 p
(Contract DE-AC05-84OR-21400)
(DE91-009743; ORNL/TM-11648) Avail: NTIS HC/MF A03

The Oak Ridge National Laboratory (ORNL) has been actively engaged in the development of radioluminescent (RL) lights for the past 10 years. Primary emphasis of the program at ORNL has been on the development and improvement of gas-tube technology lights that have been manufactured by private industry for over 30 years. The primary use of these lights until this time has been exit signs with some small numbers of applications in other areas. The goal of the ORNL program was to improve the light output and brightness of the lights to an acceptable level for use as airfield marker signs, runway lights, and taxiway lights. This goal was achieved in that a greater than 100 percent light output was obtained in commercial lights purchased for the U.S. Air Force and for the State of Florida. The results are presented of the radioluminescence tests for tritiated titanium. DOE

N91-23382# Sandia National Labs., Albuquerque, NM.
RECENT ADVANCES WITH QUIESCENT POWER SUPPLY CURRENT (I(SUB DDQ)) TESTING AT SANDIA USING THE HP82000
A. W. Righter, D. J. Leong, and L. B. Cox 1991 29 p Presented at the 1991 International HP 82000 User Group Meeting, Tampa, 4 Apr. 1991
(Contract DE-AC04-76DP-00789)
(DE91-009254; SAND-91-0560C; CONF-9104198-1) Avail: NTIS HC/MF A03

Last year at the HP82000 Users Group Meeting, Sandia National Laboratories gave a presentation on I(sub DDQ) testing. This year, some advances are presented on this testing including DUT board fixturing, external DC PMU measurement, and automatic IDD-All circuit calibration. Implementation is examined more than theory, with results presented from Sandia tests. After a brief summary I(sub DDQ) theory and testing concepts, how the break (hold state) vector and data formatting present a test vector generation concern for the HP82000 is described. Fixturing of the DUT board for both types of I(sub DDQ) measurement is then discussed, along with how the continuity test and test vector generation must be taken into account. Results of a test including continuity, IDD-All and I(sub DDQ) Value measurements is shown. Next, measurement of low current using an external PMU is discussed, including noise considerations, implementation and some test results showing nA-range measurements. A method is presented for automatic calibration of the IDD-All analog comparator circuit using RM BASIC on the HP82000, with implementation and measurement results. Finally, future directions for research in this area is explored. DOE

N91-23383# Beta Power, Inc., Salt Lake City, UT.
CONCEPTUAL DESIGN STUDY OF HIGH-PERFORMANCE SODIUM/METAL CHLORIDE BATTERIES FOR ELECTRIC VEHICLE APPLICATIONS
Jul. 1990 137 p
(Contract DE-AC02-89CH-10406)
(DE91-009618; DOE/CH-10406/T3) Avail: NTIS HC/MF A07

The U.S. DOE interest in Sodium/Metal Chloride batteries stems from three major potentialities which this system appears to offer. The first is enhanced battery reliability over its sister technology, Sodium/Sulfur. This is directly related to the short circuit failure characteristic of metal chloride cells, which, in turn, permits cell networks which take advantage of this failure mode. The second benefit is the inherent safety which stems from the low vapor pressure of the reactants and the tendency for the salt to seal-off small fracture sites in the electrolyte. The low vapor pressure allows rectangular cells to be utilized, which results in excellent packing density of cells within the battery. Finally, the specific energy of the metal chloride battery is comparable to a sodium/sulfur battery, and, as this study has concluded, cell designs are possible which offer substantial performance advantages, especially in volumetric energy density. The workplan that was established for this study was composed of four tasks: cell design, battery design, manufacturing cost and cell development plan. The cell modeling activity led the design efforts by providing design direction and associated performance figures. Three generic design concepts were explored based on different electrolyte geometries. These included multi-tube (common header), segmented flat plate and bipolar flat plate designs. The first two designs could be designated as either central cathode or outside cathode configurations. Each of these designs offered a large electrolyte surface area per unit cell volume and each brought their own advantages and disadvantages. DOE

N91-23384# SRI International Corp., Menlo Park, CA.
SOLID POLYMER ELECTROLYTES FOR RECHARGEABLE BATTERIES
S. C. Narang and D. D. Macdonald Nov. 1990 13 p
(Contract DE-AC03-76SF-00098)
(DE91-010231; LBL-29829) Avail: NTIS HC/MF A03

SRI International has synthesized novel solid polymer electrolytes for high energy density, rechargeable lithium batteries. We have systematically replaced the oxygens in polyethylene oxide (PEO) with sulfur to reduce the strong hard-acid hard-base interaction, while retaining the favorable helical conformation of the polymer backbone. The best polymer electrolyte produced so far is suitable for a medium power battery. In another effort, we have synthesized single ion conducting polymer electrolytes based on polyethyleneimine, polyphosphazene, and polysiloxane backbones. The single ion conducting polymer electrolytes will allow greater depth of charge and discharge by preventing dc polarization. The best conductivity so far with single ion conductors is 1.0 x 10(exp -3)/Scm at room temperature. Further optimization of electrical and mechanical properties will allow the use of these polymer electrolytes in the fabrication of rechargeable lithium batteries. DOE

N91-23385# Central Research Inst. of Electric Power Industry, Tokyo (Japan). Energy and Environment Lab.
EVALUATION OF CATHODE MATERIALS FOR HIGH ENERGY LITHIUM SECONDARY BATTERIES
N. Terada, K. Takei, T. Ikeya, and T. Iwahori May 1990 42 p
In JAPANESE; ENGLISH summary
(DE91-764240; CRIE-T-89074) Avail: NTIS HC/MF A03

Batteries of higher energy density are desired to realize a load conditioner of longer life and more compact geometry. Experimental researches were carried out by using test batteries using vanadium oxides and a manganese oxide which are expected to theoretically have higher energy density and higher voltage than those of molybdenum sulfide. Characteristic tests were carried out by manufacturing test batteries through the selection of vanadium oxides (three kinds) and a managanese oxide as the positive electrode material, indicating that all these materials had about two times larger energy density than that of molybdenum sulfide. Of all tested materials, lithium vanadium oxide, LiV3O8, had the maximum energy density (570Wh/kg). It seemed that the close relation existed between the inflection point of the voltage curve and the occupying rate of lithium inserting sites in the crystal composed of the positive electrode for the LiV3O8 material. DOE

N91-23386# Sandia National Labs., Albuquerque, NM.
SOLUTIONS TO CURRENT INDUCED AVALANCHE BURNOUT
T. F. Wrobel and L. M. Choate 1990 7 p Presented at the 8th Symposium on Space Nuclear Power System, Albuquerque., 6-9 Jun. 1991
(Contract DE-AC04-76DP-00789)
(DE90-013196; SAND-90-1712C; CONF-910627-1) Avail: NTIS HC/MF A02

Reviews of normal breakdown and current induced avalanche breakdown mechanisms in silicon power transistors are presented. We show the applicability of the current induced avalanche model to heavy ion induced burnouts. Finally, we present solutions to current induced avalanche in silicon power semiconductors. DOE

N91-23387# Oregon State Univ., Corvallis. Dept. of Electrical and Computer Engineering.
CONTROL ASPECTS OF THE BRUSHLESS DOUBLY-FED MACHINE
H. K. Lauw and S. Krishnan Sep. 1990 79 p
(Contract DE-BI79-85BP-24332)
(DE91-009707; DOE/BP-24332/1) Avail: NTIS HC/MF A05

This report covers the investigations into the control aspects of a variable-speed generation (VSG) system using a brushless double-fed generator excited by a series-resonant converter. The brushless double-fed machine comprises two sets of stator 3-phase systems which are designed with common windings. The rotor is a cage rotor resembling the low-cost and robust squirrel cage of a conventional induction machine. The system was actually designed and set up in the Energy Laboratory of the Department of Electrical and Computer Engineering at Oregon State University. The series-resonant converter designed to achieve effective control for variable-speed generation with the brushless doubly-fed generator was adequate in terms of required time response and regulation as well as in providing for adequate power quality. The three elements of the VSG controller, i.e., voltage or reactive power controller, the efficiency maximizer and the stabilizer, could be designed using conventional microprocessor elements with a processing time well within the time period required for sampling the variables involved with executing the control tasks. The report treats in detail the stability problem encountered in running the machine at certain speed regions, even if requirements for steady-state stability are satisfied. In this unstable region, shut down of the VSG system is necessary unless proper stabilization controls are provided for. The associated measures to be taken are presented. DOE

N91-23388# Sandia National Labs., Albuquerque, NM.
S-PARAMETER MEASUREMENTS AND APPLICATIONS OF SUPERCONDUCTING FLUX FLOW TRANSISTORS
J. S. Martens, V. M. Hietala, T. E. Zipperian, D. S. Ginley, C. P. Tigges, and J. M. Phillips (Bell Telephone Labs., Inc., Murray Hill, NJ.) 1991 25 p Presented at the International Microwave Symposium, Boston, 11-14 Jun. 1991
(Contract DE-AC04-76DP-00789)
(DE91-009763; SAND-91-0381C; CONF-910690-2) Avail: NTIS HC/MF A03

The authors have performed microwave two-port S-parameter measurements and modelling on Superconducting Flux Flow Transistors (SFFTSs). These transistors, based on the magnetic control of flux flow in an array of High Temperature Superconducting (HTS) weak links, can exhibit significant available power gain at microwave frequencies (over 20 dB at 7-10 GHz in some devices). The input impedance is largely inductive while the output impedance

is resistive and inductive. The characteristics are such that these devices are potentially useful in numerous applications including matched amplifiers. DOE

N91-23389# Sandia National Labs., Albuquerque, NM.
CONCEPTUAL DESIGN AND SYSTEM STUDIES FOR A 600 kW REPETITIVE PULSE TRANSFORMER
D. J. Hall, D. Pavlik, J. F. Roach (Westinghouse Electric Corp., Pittsburgh, PA.), and H. C. Harjes 1991 28 p Presented at the 8th IEEE Pulsed Power Conference, San Diego, 17-19 Jun. 1991
(Contract DE-AC04-76DP-00789)
(DE91-010585; SAND-90-2780C; CONF-910640-2) Avail: NTIS HC/MF A03

Pulse transformer conceptual design and system studies were conducted at the Westinghouse Science and Technology Center for the Sandia National Laboratories' Repetitive High Energy Pulsed Power (RHEPP) System. The RHEPP system relies on magnetic switches to achieve pulse compression from 120 Hz ac to microsecond pulses. A 600 kW, 120 Hz Westinghouse alternator supplies ac prime power at 10 kV (rms). Two magnetic switching stages will compress the pulses to 115 usec prior to the pulse transformer. The transformer steps the voltage up to 254 kV. The pulse transformer has an 18:1 turns ratio and is capable of continuous duty operation. System studies were conducted to minimize transformer loss and leakage inductance within transformer size constraints. The optimized design had a 3-step nickel iron core with 9 primary turns. DOE

N91-23390# Argonne National Lab., IL.
CHARACTERIZATION OF ACTIVE MATERIALS AND ELECTRODES FOR BATTERY R AND D
L. Redey 1991 10 p Presented at the 179th Meeting of the Electrochemical Society, Washington, 5-10 May 1991
(Contract W-31-109-eng-38)
(DE91-010758; ANL/CP-72112; CONF-910552-9) Avail: NTIS HC/MF A02

A powerful characterization system and procedure used to measure cell and electrode performance parameters are described. The characterization utilizes an interrupted-galvanostatic cycling technique. Cell voltage, electrode potential, voltage loss, and relaxation are measured under precisely controlled experimental conditions in test cells which are equipped with one or more reference electrodes and voltage taps. These measured quantities are used to evaluate the performance of the test cell or its electrodes. The electrodes and cell are built to mimic the design parameters of a full-size cell. An important quantity calculated from measured data is the area-specific impedance (ASI(sub t), in units of ohm x sq cm). The measured ASI(sub t) vs utilization plots are used to assess the specific power and specific energy characteristics of full-size battery cells. DOE

N91-23391# Superconducting Super Collider Lab., Dallas, TX.
A CONTROLLED MASTER FREQUENCY OSCILLATOR FOR THE SSC LOW ENERGY BOOSTER
L. K. Mestha Jan. 1991 21 p
(Contract DE-AC02-89ER-40486)
(DE91-011004; SSCL-343) Avail: NTIS HC/MF A03

A variable frequency oscillator is normally used to generate the master frequency for an accelerator. For the low energy booster (LEB) at the Superconducting Super Collider (SSC) the prospects of using a direct digital synthesizer (DDS) to vary the frequency from 47 MHz to 59 MHz are considered. A digital signal processor (DSP) which can be loaded with the desired frequency values is interfaced to the DDS. These values are launched on the DDS at known intervals to ramp the frequency smoothly. In this paper the observations made while ramping the frequency are discussed. The design principle of the digital synchronization of the LEB frequency source with the medium energy booster (MEB) frequency source is also briefly discussed. When developed, such a system can be used to synchronize the two machines. DOE

N91-23392 Physics and Electronics Lab. TNO, The Hague (Netherlands).
DESIGN OF INHERENTLY WIDE-BAND MICROWAVE FREQUENCY DOUBLER AND TRIPLER IN MICROSTRIP Final Report
J. C. Henkus Oct. 1990 40 p Original contains color illustrations
(FEL-90-B255; TD-90-3214; ETN-91-99097) Copyright Avail: Physics and Electronics Lab. TNO, P.O. Box 96864, 2509 JG The Hague, Netherlands

Two modern wide band frequency agile radar systems, currently under construction require the development of a wide band S band frequency doubler and a wide band X band frequency tripler. The wide band requirement, however, is hard to meet when using the classical approach. Wave form invariance as an alternative concept to achieve inherently wide band behavior is proposed. From this, a new design goal is derived and formulated: constant admittance at the terminals of the nonlinear device within each harmonic sub band. A frequency doubler was designed and built based on this concept; the conversion efficiency measures (1.0 +/- 0.7) dB in the 2.8 to 3.6 GHz design band. A frequency tripler was designed and built based on this concept; the conversion efficiency measures (-10.4 +/- 0.6) dB in the 8.5 to 10.5 GHz design band. Both examples prove the validity and practical suitability of the alternative concept. ESA

N91-23393# Grenoble-1 Univ. (France). Techniques de l'Informatique, des Mathematiques, de la Microelectronique et de la Microscopie Quanti
BASIC PROPERTIES OF STRONGLY CODE DISJOINT CHECKERS
M. Nicolaidis Sep. 1990 29 p
(RR-824-I; ETN-91-99221) Avail: NTIS HC/MF A03

In order to ensure total self checking, checkers have been introduced by Carter and defined by Anderson to be totally self checking: that is they are code disjoint, self testing, and fault secure. Checkers which are only code disjoint and self testing are also discussed. Strongly code disjoint checkers are not fault secure. Some researchers feel that the fault secure property is indeed necessary. This lack of agreement about the basic concepts of checkers is an important drawback in further research on self checking checkers. The various arguments used in the debate are presented. Aspects of the problem over which there is the most disagreement are highlighted. Some important points concerning strongly code disjoint checkers are discussed. ESA

N91-23394# Royal Signals and Radar Establishment, Malvern (England).
A TRANSMISSION LINE METHOD FOR THE MEASUREMENT OF MICROWAVE PERMITTIVITY AND PERMEABILITY
P. G. Lederer Dec. 1990 37 p
(RSRE-Memo-4450; BR116535; ETN-91-99323) Copyright Avail: NTIS HC/MF A03

A method for determining complex permittivity and permeability at microwave frequencies from two port S parameter measurements of lossy solids in coaxial or waveguide transmission lines is described. The use of the TRL (Through Reflect Line) calibration scheme allows the measuring system to be calibrated right up to the specimen faces thereby eliminating most of the sample cell from the measurement and allowing suitable materials to be molded directly into the specimen cell in order to eliminate air gaps between specimen and transmission line walls. Some illustrative measurements for dielectric and magnetic materials are presented. ESA

N91-23395# Royal Signals and Radar Establishment, Malvern (England).
SILICON AVALANCHE PHOTODIODE ACTIVE-QUENCHING CIRCUIT
M. Jonhson and R. Jones Dec. 1990 14 p Original contains color illustrations
(AD-A233633; RSRE-Memo-4454; BR116434; ETN-91-99326)

Copyright Avail: Defence Research Information Centre, Kentigern House, 65 Brown Street, Glasgow, G2 8EX, Scotland

Research shows that actively quenched silicon Avalanche Photo Diodes (APD) can be sucessfully operated throughout the visible region. Two patented circuits exist which were assembled as printed circuit board prototypes. A silicon hybrid of the most recent circuit, having two independent channels, is demonstrated to operate at a photon couting rate in excess of 40 MHz. If the APDs are cooled a dynamic range approaching that of the average photomultiplier tube is possible. Two problems with the hybrid circuit are identified and a way forward to eliminate the problems is proposed. ESA

N91-23396# European Space Agency. European Space Research and Technology Center, ESTEC, Noordwijk (Netherlands). Product Assurance and Safety Dept.
CHECKLIST FOR THICK-FILM HYBRID MICROCIRCUITS MANUFACTURER AND LINE SURVEY
Nov. 1990 56 p
(ESA-PSS-01-607-Issue-1; ISSN-0379-4059; ETN-91-99339)
Copyright Avail: NTIS HC/MF A04

A checklist intended for use in the capability survey of a thick film hybrid microcircuit manufacturer's management, production activities, tests facilities, and technical skills is presented. It provides the procuring activity with an evaluation of the manufacturer's ability to execute a contract successfully and of his capability to supply high reliability space hardware. ESA

N91-23397# European Space Agency. European Space Research and Technology Center, ESTEC, Noordwijk (Netherlands). Product Assurance and Safety Dept.
CHECKLIST FOR THIN-FILM HYBRID MICROCIRCUITS MANUFACTURER AND LINE SURVEY
Nov. 1990 61 p
(ESA-PSS-01-611-Issue-1; ISSN-0379-4059; ETN-91-99340)
Copyright Avail: NTIS HC/MF A04

A checklist intended for use in the capability survey of a thin film hybrid microcircuit manufacturer's management, production activities, test facilities and technical skills is presented. It provides the procuring activity with an evaluation of the manufacturer's ability to execute a contract successfully and of his capability to supply high reliability hardware. ESA

N91-23398# Naval Research Lab., Washington, DC.
OBSERVATION OF HARMONIC GYRO-BACKWARD-WAVE OSCILLATION IN A 100 GHz CARM OSCILLATOR EXPERIMENT
Robert B. McCowan, Carol A. Sullivan, Steven H. Gold, and Arne W. Fliflet 16 Feb. 1991 21 p
(AD-A232063; NRL-MR-6765) Avail: NTIS HC/MF A03 CSCL 09/3

A cyclotron autoresonance maser (CARM) oscillator experiment is reported, using a 600 keV, 200 A electron beam, and a whispering gallery-mode rippled-wall Bragg cavity. This device was designed to produce tens of megawatts of radiation at 100 GHz from a CARM interaction, but instead has produced only moderate powers (tens of kWs) in fundamental gyrotron modes near 35 GHz, in third-harmonic-gyro-BWO modes, and possible third-harmonic gyrotron modes at frequencies near the expected CARM frequency, with no discernable CARM radiation. The lack of observable CARM radiation is attributed to excessive ripple on the voltage waveform and to mode competition. Calculations of the spectrum and growth rate of the backward-wave oscillations are consistent with the experimental observation. GRA

N91-23399# Astropower, Inc., Newark, DE.
ELECTRONIC GaAs-ON-SILICON MATERIAL FOR ADVANCED HIGH-SPEED OPTOELECTRONIC DEVICES Final Report, 1 Aug. 1988 - 30 Jun. 1990
Michael G. Mauk and James B. McNeely Jan. 1991 91 p
(Contract DAAL03-88-C-0023)
(AD-A232088; ARO-26207.1-EL-SBI) Avail: NTIS HC/MF A05 CSCL 09/5

A new technology for the heteroepitaxial growth of GaAs films on silicon substrates is developed. The process utilizes a combined close-spaced vapor transport (CSVT) and liquid-phase epitaxy (LPE) technique. A thin film of GaAs is grown directly on silicon by a close-spaced vapor transport reaction using water vapor as the transport agent. This initial layer is used to seed the subsequent growth of additional layers of GaAs or AlGaAs by LPE. Selective modes of growth on oxide-masked silicon substrates were optimized. Stable light-emitting diodes were fabricated in GaAs-on-silicon material. The process is being scaled for 3-inch diameter substrates. GRA

N91-23400# Naval Ocean Systems Center, San Diego, CA.
PHOTORESPONSE STUDIES OF ION-DAMAGED GERMANIUM FOR OPTOELECTRONIC SWITCH APPLICATIONS Final Report, Jun. - Oct. 1986
S. D. Russell Dec. 1990 18 p
(AD-A232091; NOSC/TD-1963) Avail: NTIS HC/MF A03 CSCL 09/1

In light of the potential of germanium optoelectronic (OE) switches for OE/time division multiplexing (OE/TDM) applications, preliminary research into the effect of crystalline damage on its photoresponse was performed. This document reports the results of this proposed method to decrease the photocurrent decay time for high-speed OE switches. GRA

N91-23401# Massachusetts Inst. of Tech., Cambridge. Lab. for Computer Science.
DESIGN AND IMPLEMENTATION OF A PACKET SWITCHED ROUTING CHIP
Christopher F. Joerg Dec. 1990 121 p
(Contract N00014-84-K-0099)
(AD-A232286; MIT/LCS/TR-482) Avail: NTIS HC/MF A06 CSCL 25/5

Monsoon is a parallel processing dataflow computer that will require a high bandwidth interconnection network. A packet switched routing chip (PaRC) is described that will be used as the basis of this network. PaRC is a 4 by 4 routing switch which has been designed and fabricated as a CMOS gate array. PaRC will receive packets via one of its four input ports, store the packet in an on-chip buffer, and eventually transmit the packet via one of its four output ports. PaRC operates at 50 MHz, and each port has a bandwidth of 800 Mbits per second. Each input port operates asynchronously and has enough buffering to store four packets. The buffering and scheduling algorithms used in PaRC were designed to provide high utilization of the available bandwidth, while providing low latency for non-blocked packets. In addition, PaRC provides a mechanism whereby a processor can quickly receive acknowledgment when a message it sent has been received. Although the design of PaRC has been driven by the needs of Monsoon, PaRC has been designed to be suitable for a wide variety of communication networks. Author (GRA)

N91-23402# Ohio State Univ., Columbus. Electroscience Lab.
JOINT SERVICES ELECTRONICS PROGRAM Annual Report No. 13
Leon Peters, Jr. Nov. 1990 64 p
(Contract N00014-89-K-1007)
(AD-A232331; ESL-721563-2) Avail: NTIS HC/MF A04 CSCL 09/1

The transfer of the compact range and target identification technology initiated under JSEP support for time domain studies continues to make large advances. Using other sources of support, design for a mini-chamber has now been generated and has been constructed. This range is designed to study smaller targets at higher frequencies. The research has proven to be of intense interest to DoD and the aerospace industry and our compact range consortium represents a major cross section of the aerospace and electronic industries, including additional major support from several DoD agencies. In fact, the total support in these experimental studies substantially exceeds our JSEP support. This research is truly guiding a major portion of this technology in the

USA and has been extremely important for stealth technology advances. GRA

N91-23403# Cornell Univ., Ithaca, NY. Dept. of Materials Science and Engineering.
FUNDAMENTAL STUDIES OF ELECTRONIC PACKAGING MATERIALS AND STRUCTURES: SURFACE AND INTERFACES Final Report
C. B. Carter, D. L. Kohlstedt, E. J. Kramer, C-Y. Li, and A. L. Ruoff 12 Dec. 1990 27 p
(Contract DAAL03-87-K-0104)
(AD-A232336; ARO-24417.18-EL) Avail: NTIS HC/MF A03 CSCL 13/4

Layered structures consisting of metals, ceramics and polymers are used extensively for signal and power distribution both at the chip level and in electronic packages. The structural integrity of the interfaces between layers in such structures is an important consideration in the design and fabrication of a variety of devices and components. Various variables including surface composition and structure that control interfacial adhesion are investigated. Interfaces between metal/ceramic, metal/polymer and between polymer/polymer are studied in the research reported. GRA

N91-23404# Naval Postgraduate School, Monterey, CA.
PARAMETRIC MODELING AND ESTIMATION OF PULSE PROPAGATION ON MICROWAVE INTEGRATED CIRCUIT INTERCONNECTIONS Ph.D. Thesis
Edward M. Siomacco Jun. 1990 156 p
(AD-A232465) Avail: NTIS HC/MF A08 CSCL 09/1

The modeling of picosecond pulse propagation on microwave integrated circuit interconnections is considered. Autoregressive moving-average (ARMA) and autoregressive (AR) parametric models are derived for lossy dispersive microstrip transmission lines and cascaded microstrip step discontinuities. We formulated mathematical expressions to relate the model parameters to the physical microstrip properties. New lumped distributed equivalent circuit interconnections are modeled using frequency-dependent lumped parameters and lossy distributed transmission-line sections. We verified the equivalent circuit models through computer simulations and experimental measurements. Modern parameters estimation techniques are applied to system identification modeling. We develop several algorithms to estimate the model parameters from input and/or output measurements. The performance of the algorithms are evaluated using computer simulations and experimental results. GRA

N91-23405# Naval Research Lab., Washington, DC.
BACKGROUND SIMULATION AND FILTER DESIGN USING ITERATED FUNCTION SYSTEMS
Ira B. Schwartz and Laurie Reuter 19 Feb. 1991 51 p Prepared in cooperation with George Washington Univ., Washington, DC, and Bell Communications Research, Inc., Morristown, NJ
(AD-A232632; NRL-MR-6784) Avail: NTIS HC/MF A04 CSCL 20/3

Design of filters which detect known signals in unknown backgrounds are considered from a deterministic viewpoint. Backgrounds which appear in Nature rather than being smooth, may appear fractal within a given waveband of interest. In this paper, derivations are given for the design of filters for both smooth backgrounds, and fractal backgrounds. The main theoretical tool for the fractal design is the Iterated Function System (IFS). It is shown how the IFS models generalize the smooth models of the background and the corresponding filters. Derivations of the false alarm rate in terms of the filters are given. Numerical examples demonstrating background simulation as well as convolution of the filters with signals embedded in noise having fractal dimension are presented. GRA

N91-23406# California Univ., Santa Barbara.
HIGH QUALITY THREE DIMENSIONAL ELECTRON GASES IN SEMICONDUCTORS Final Report, 1 Jan. 1988 - 31 Dec. 1990
Arthur C. Gossard 8 Jan. 1991 26 p
(Grant AF-AFOSR-0099-88; AF Proj. 2305)
(AD-A232779; AFOSR-91-0161TR) Avail: NTIS HC/MF A03 CSCL 09/1

The construction of high quality three-dimensional electron gases by the growth of wide parabolic GaAs quantum wells with modulation doping was successfully pursued. The concept has worked -- by growth of wide, specially shaped wells with remote doping, high mobility electrons can be allowed to spread out over regions thousands of Angstroms thick and have three-dimensional behavior without the impurity scattering and carrier freezeout of conventional semiconductors. Electron mobilities of several hundred thousand sq cm/Vs were achieved. The wide parabolically shaped well system is fundamentally new, and the structures are showing a variety of new behavior. Electrical quantum conductivity phenomena due to occupancy of several subbands were observed. Cyclotron resonance, plasma resonance, and coupled cyclotron/plasma resonances have been found and all have characteristics of a three-dimensional gas in a parabolic potential. GRA

N91-24069*# National Aeronautics and Space Administration. Lewis Research Center, Cleveland, OH.
MICROWAVE INTEGRATED CIRCUITS FOR SPACE APPLICATIONS
Regis F. Leonard and Robert R. Romanofsky *In* NASA, Washington, Technology 2000, Volume 2 1991 p 242-248
(For primary document see N91-24041 15-99)
Avail: NTIS HC/MF A16 CSCL 09C

34 FLUID MECHANICS AND HEAT TRANSFER

Includes boundary layers; hydrodynamics; fluidics; mass transfer; and ablation cooling.

For related information see also *02 Aerodynamics* and *77 Thermodynamics and Statistical Physics.*

N91-23407# Ben Gurion Univ. of the Negev, Beersheva (Israel). Center for MHD Studies.
FLOWS WITH STRONGLY ANISOTROPIC TURBULENCE-DYNAMIC AND HEAT TRANSFER ASPECTS
Herman Branover and Semion Sukoriansky 1986 29 p Presented at the 10th Symposium on Turbulence, Rolla, MO, 22-24 Sep. 1986 Sponsored by SOLMECS (Israel) Ltd.
(Ser-20/P; ITN-88-85009) Avail: NTIS HC/MF A03

Turbulent flows with clearly expressed inverse energy cascades have been arranged and studied. The experiments have been performed with mercury flows submitted to the influence of external magnetic fields. Turbulence intensity data, and even more energy spectra, indicated the existence of an inverse energy cascade. Such small scale flows can possibly be used for simulation of some phenomena in atmospheric turbulence. The present work was undertaken with the goal of providing additional evidence for verification of hypotheses on turbulence structure and transfer mechanism changes developed in previous studies. For this purpose, provisions have been made which allowed intensity and spectrum measurements at different distances from flow entrance into the magnetic field so that time dependent expansion of magnetic field influence on different parts of spectra could be detected. Furthermore, different turbulizing grids have been introduced which permitted making comparisions between small and large scale forced turbulence with different directions of turbulizing elements in respect to the magnetic field (rods with axes perpendicular or parallel to magnetic field direction). Heat transfer processes in such flows have been assessed and strong enhancement of heat transfer have been predicted. This prediction has been confirmed also experimentally. These results are important for a number of technological applications, specifically for the design of nuclear fusion reactors. ISA

N91-23408*# TRW Space Technology Labs., Redondo Beach, CA.
IN-SPACE TECHNOLOGY EXPERIMENTS PROGRAM. A HIGH EFFICIENCY THERMAL INTERFACE (USING CONDENSATION HEAT TRANSFER) BETWEEN A 2-PHASE FLUID LOOP AND HEATPIPE RADIATOR: EXPERIMENT DEFINITION PHASE Final Report
John A. Pohner, Brian P. Dempsey, and LeRoy M. Herold Jul. 1990 52 p
(Contract NAS5-30357)
(NASA-CR-186869; NAS 1.26:186869; TRW-P331.LM1.90.185)
Avail: NTIS HC/MF A04 CSCL 20D

Space Station elements and advanced military spacecraft will require rejection of tens of kilowatts of waste heat. Large space radiators and two-phase heat transport loops will be required. To minimize radiator size and weight, it is critical to minimize the temperature drop between the heat source and sink. Under an Air Force contract, a unique, high-performance heat exchanger is developed for coupling the radiator to the transport loop. Since fluid flow through the heat exchanger is driven by capillary forces which are easily dominated by gravity forces in ground testing, it is necessary to perform microgravity thermal testing to verify the design. This contract consists of an experiment definition phase leading to a preliminary design and cost estimate for a shuttle-based flight experiment of this heat exchanger design. This program will utilize modified hardware from a ground test program for the heat exchanger. Author

N91-23409*# National Aeronautics and Space Administration. Lewis Research Center, Cleveland, OH.
SIMULATION OF BRUSH INSERT FOR LEADING-EDGE-PASSAGE CONVECTIVE HEAT TRANSFER
R. C. Hendricks, M. J. Braun, V. Canacci, and R. L. Mullen (Case Western Reserve Univ., Cleveland, OH.) 1991 12 p Presented at the 4th International Symposium on Transport Phenomena in Heat and Mass Transfer, Sydney, Australia, 14-18 Jul. 1991; sponsored by New South Wales Univ.
(NASA-TM-103801; E-6093; NAS 1.15:103801) Avail: NTIS HC/MF A03 CSCL 20D

Current and proposed high speed aircraft have high leading edge heat transfer (to 160 MW/sq m, 100 Btu/sq in/sec) and surface temperatures to 1370 K (2000 F). Without cooling, these surfaces could not survive. In one proposal the coolant hydrogen is circulated to the leading edge through a passage and returned to be consumed by the propulsion system. Simulated flow studies and visualizations have shown flow separation within the passage with a stagnation locus that isolates a zone of recirculation at the most critical portion of the passage, namely the leading edge itself. A novel method is described for mitigating the flow separation and the isolated recirculation zones by using a brush insert in the flow passage near the leading edge zone, thus providing a significant increase in heat transfer. Author

N91-23410*# National Aeronautics and Space Administration. Langley Research Center, Hampton, VA.
PASSIVE LAMINAR FLOW CONTROL OF CROSSFLOW VORTICITY Patent Application
Bruce J. Holmes, inventor (to NASA) 2 Nov. 1990 18 p
(NASA-Case-LAR-13563-1; NAS 1.71:LAR-13563-1; US-Patent-Appl-SN-608494) Avail: NTIS HC/MF A03 CSCL 20D

A passive laminar flow crossflow vorticity control system includes an aerodynamic or hydrodynamic surface having geometric perturbations. The perturbations include peaks and valleys having a predetermined spacing and aligned approximately in a streamline direction to force the formation of crossflow vortices. This minimizes amplification and growth of the vortices, thus delaying transition to turbulence and reducing overall drag. NASA

N91-23411 Pennsylvania State Univ., University Park.
A COMPUTATIONALLY EFFICIENT MODELLING OF LAMINAR SEPARATION BUBBLES Ph.D. Thesis
Paolo Dini 1990 169 p
Avail: Univ. Microfilms Order No. DA9104867

In predicting the aerodynamic characteristics of airfoils operating at low Reynolds numbers, it is often important to account for the effects of laminar (transitional) separation bubbles. Previous approaches to the modeling of this viscous phenomenon range from fast by sometimes unreliable empirical correlations for the length of the bubble and the associated increase in momentum thickness, to more accurate but significantly slower displacement thickness iteration methods employing inverse boundary layer formulations in the separated regions. Since the penalty in computational time associated with the more general methods is unacceptable for airfoil design applications, use of an accurate yet computationally efficient model is highly desirable. To this end, a semi-empirical bubble model was developed and incorporated into the Eppler and Somers airfoil design and analysis program. The generality and the efficiency were achieved by successfully approximating the local viscous/inviscid interaction, the transition location, and the turbulent reattachment process within the framework of an integral boundary-layer method. Comparisons of the predicted aerodynamic characteristics with experimental measurements for several airfoils show excellent and consistent agreement for Reynolds numbers from 2,000,000 down to 100,000. Dissert. Abstr.

N91-23412 Washington Univ., Seattle.
NUMERICAL SIMULATIONS OF INSTABILITIES IN COMPRESSIBLE MIXING LAYERS Ph.D. Thesis
Moeljo Soetrisno 1990 234 p
Avail: Univ. Microfilms Order No. DA9104297

Direct numerical simulations were performed to investigate several aspects of ideal gas, inviscid, two and three dimensional, temporally growing, confined, high speed mixing layers. The stability, dynamics, and mixing characteristics of individual modes of instabilities as well as their nonlinear interactions were investigated. Growth rates obtained from the numerical simulations were shown to be in excellent agreement with both linear stability theory and experimental results. Two different types of two dimensional instabilities were detailed: the Kelvin-Helmholtz and the acoustic mode instability, which consists of supersonic/supersonic and supersonic/subsonic types depending on the phase speed of the structure. Dissert. Abstr.

N91-23413 Cornell Univ., Ithaca, NY.
BLOCK IMPLICIT MULTIGRID SOLUTION OF THE EULER EQUATIONS Ph.D. Thesis
Yoram Yadlin 1990 177 p
Avail: Univ. Microfilms Order No. DA9106233

A diagonal implicit multigrid (BDIM) scheme was developed to solve the Euler equations of inviscid, compressible flows in three-dimensions, and was implemented within the framework of block structured grids. A multigrid alternating direction implicit (ADI) scheme was developed for a single-block grid in three dimensions, using a diagonalization procedure resulting in a computationally efficient code. The scheme was applied to compute transonic flow past a swept wing and found accurate and efficient. Ways to implement the multigrid ADI scheme on block-structured grids were investigated. Two modes of multigrid cycles were developed: one in which the multigrid cycle advances concurrently on all blocks (horizontal mode) and one in which the multigrid cycle advances independently in each block (vertical mode). The efficiency and accuracy of both modes were investigated by applying the schemes to compute transonic flow past the NACA-0012 airfoil. Both modes were implemented to run on a shared-memory parallel computer. Computations of transonic flow past a swept wing illustrate the accuracy and efficiency of the scheme. Speed-up results are presented to illustrate the ability of the scheme to calculate complex flows in the short turn around time required in any design application. Dissert. Abstr.

N91-23414# Argonne National Lab., IL.
TWO-PHASE FLOW PATTERNS AND FRICTIONAL PRESSURE GRADIENTS IN A SMALL RECTANGULAR CHANNEL

M. W. Wambsganss, J. A. Jendrzejczyk, D. M. France, and N. T. Obot Nov. 1990 46 p
(Contract W-31-109-eng-38)
(DE91-009652; ANL-90/46) Avail: NTIS HC/MF A03

In horizontal flow through a rectangular channel, the channel cross section can be oriented so that the long side is either vertical or horizontal. The effect of cross section orientation on the fluid dynamic characteristics of two phase flow is of interest in plate-fin heat exchanger design because a heat exchanger can be similarly oriented to operate in either of the two orientations. An earlier study of two phase flow patterns and frictional pressure gradients in a small rectangular channel with the channel cross section oriented with the long side vertical was performed and reported. The results are presented of a complementary study of the same channel, but with the channel cross section oriented so that the long side was horizontal. Flow patterns were studied and a flow pattern map, using superficial gas and liquid velocities as coordinates, was developed. Measured two phase frictional pressure drops were analyzed using the concept of two phase flow multipliers. Results from the two channel orientations were compared. While there are some notable differences in flow patterns at low mass qualities and low mass fluxes, in the practical range of interest for plate-fin heat exchanger design the effects on frictional pressure gradient are minimal and the modified correlation developed from the earlier study is shown to be also applicable for design purposes when the long side is horizontal.
DOE

N91-23415# Edgerton, Germeshausen and Grier, Inc., Idaho Falls, ID.
PARTICLE-FLUID TWO-PHASE FLOW MODELING
J. A. Trapp, G. A. Mortensen, and V. H. Ransom (Purdue Univ., West Lafayette, IN.) 1991 12 p Presented at the International Topical Meeting on Advances in Mathematics, Computation and Reactor Physics, Pittsburgh, 28 Apr. - 2 May 1991
(Contract DE-AC07-76ID-01570)
(DE91-010102; EGG-M-90413; CONF-910414-29) Avail: NTIS HC/MF A03

The present state-of-the-art models in two-phase flow (e.g., RELAP5, TRAC, etc.) are based on the fully-averaged two-fluid concept. A new particle-fluid model is described that is intermediate between the numerically intractable local instant description and the fully-averaged two-fluid model. This new model uses a Lagrangian description for the dispersed phases, bubbles and droplets, and an Eulerian description for the continuous phases, liquid and vapor. The model described in this paper is limited to dispersed bubbles in a continuous phase. Plans are to expand the model to include two dispersed phases and two continuous phases. Interaction between each dispersed phase and its surrounding continuous phase takes place through void fraction coupling as well as interface mass, momentum, and energy transfer. Fully-averaged two-fluid models use correlations for determining flow regime transitions. One motivation for this particle-fluid model is to be able to predict these flow regime transitions as well as being able to use more mechanistic models for dispersed phase coalescence, breakup, wakes, etc. Graphical results from a subcooled boiling stream-water simulation using the particle-fluid model are shown. Currently, this subcooled boiling simulation as well as air-water and liquid-vapor Freon simulations are being compared with experimental data.
DOE

N91-23416*# National Aeronautics and Space Administration. Lewis Research Center, Cleveland, OH.
LOW REYNOLDS NUMBER TWO-EQUATION MODELING OF TURBULENT FLOWS
V. Michelassi and T.-H. Shih May 1991 24 p Presented at the 43d Annual Pacific Coast Meeting, Seattle, WA, 25-27 Oct. 1990; sponsored by the American Ceramic Society
(NASA Order C-99066-G)
(NASA-TM-104368; ICOMP-91-06; E-6169; NAS 1.15:104368; CMOTT-91-01) Avail: NTIS HC/MF A03 CSCL 20D

A k-epsilon model that accounts for viscous and wall effects is presented. The proposed formulation does not contain the local wall distance thereby making very simple the application to complex geometries. The formulation is based on an existing k-epsilon model that proved to fit very well with the results of direct numerical simulation. The new form is compared with nine different two-equation models and with direct numerical simulation for a fully developed channel flow at Re = 3300. The simple flow configuration allows a comparison free from numerical inaccuracies. The computed results prove that few of the considered forms exhibit a satisfactory agreement with the channel flow data. The model shows an improvement with respect to the existing formulations.
Author

N91-23417 Pittsburgh Univ., PA.
FLOW BETWEEN ECCENTRIC ROTATING CYLINDERS Ph.D. Thesis
Qimin Dong 1990 196 p
Avail: Univ. Microfilms Crder No. DA9107769

The flow between eccentric rotating infinite cylinders is studied. The dependence of the critical Reynolds number on eccentricity is investigated for 3-D isothermal flow. The method of analysis is Fourier expansion of the Navier-Stokes and continuity equations in the axial direction, followed by projection onto B-spline polynomial subspace. The effects are examined of coupling the equations of motion to the equation of energy, by allowing variation of the fluid viscosity with temperature, for 2-D Non-isothermal flow. The coupling of motion to heat transfer plays a significant role in determining the streamline pattern, in the positioning of separation and reattachment points, in the magnitude of torque, and in determining the rate at which heat is transferred between the cylinders.
Dissert. Abstr.

N91-23418 Oxford Univ. (England).
ANALYSIS OF THE MULTIGRID METHOD PHh.D. Thesis
Tasneem Mohammad Shah 1989 203 p
Avail: Univ. Microfilms Order No. BRD-91529

The analysis of a multigrid method that uses the couple method for solving the incompressible Navier-Stokes equations for the driven cavity and the backward-facing step problems in two and three dimensions. An efficient line solver called symmetrical coupled Gauss-Seidel (SCGS/LS) based upon the SCGS scheme is developed, which acts as a smoother for the nonlinear multigrid method. The Fourier analysis of both SCGS/LS and SCGS are carried out for the two problems which yield lower and upper bounds on the theoretical smoothing factors. Comparing the smoothing capabilities of SCGS/LS and SCGS it is found that the SCGS is not as good in annihilating the high frequency modes at high Reynolds numbers. This is confirmed by numerical experiments using both schemes. The Fourier analysis of both schemes is extended to the three-dimensional lid-driven cavity. Theoretical smoothing factors are obtained by sweeping Fourier modes in the primary flow direction and compared with those obtained numerically. The two-dimensional backward-facing step problem is solved for Reynolds numbers up to 1250. At these values of Reynolds numbers, two secondary separation regions at the opposite sides of the wall are discovered which have not been reported previously. When the SCGS/LS scheme is applied to the three dimensional lid-driven cavity, the results are found to be less efficient than the two dimensional case. This may be due to mismatch in sweeping and flow directions.
Dissert. Abstr.

N91-23419 Michigan Univ., Ann Arbor.
AN EXPERIMENTAL INVESTIGATION OF VORTEX PAIR INTERACTION WITH A CLEAN OR CONTAMINATED FREE SURFACE Ph.D. Thesis
Amir Hossein Hirsa 1990 148 p
Avail: Univ. Microfilms Order No. DA9034438

The interaction between a pair of trailing vortices and a free surface was studied. The vortices were produced by a submerged delta wing and a negative angle of attack. In order to isolate and study the interaction, an apparatus was built to generate reproducible vortex pairs with the same Reynolds number and Froude number as the trailing vortices. The apparatus consisted of a pair of counter rotating flaps which were moved by a computer

controlled stepping motor. The vortex pairs generated with the flaps were laminar and remained laminar during the time that significant interaction with the free surface was observed. The Froude number for the vortices was low and the resulting surface deformations were small. Particle image velocimetry along with flow visualization were used to study the flow field. Striations were also observed during the interaction of the vortex pair with the free surface. The striations were found to be caused by cross-stream vortices which are stretched by the strain field between the trailing vortices and their images. Contaminants on the free surface were found to have a large influence on both the free surface deformations and the flow field of the vortices. Also, a Reynolds ridge on the free surface was observed on each side of the wake. The effect of surface contamination was studied by adding known amounts of an insoluble surfactant to the free surface. Surface depressions, termed scars, were observed above the primary vortices as well as the secondary vortices, although in the case on the secondary vortices the depression was much greater. Dissert. Abstr.

N91-23420 Clarkson Univ., Potsdam, NY.
THERMODYNAMICALLY CONSISTENT FORMULATIONS FOR RAPID GRANULAR AND TURBULENT MULTIPHASE FLOWS Ph.D. Thesis
Sameer A. Abu-Zaid 1990 160 p
Avail: Univ. Microfilms Order No. DA9107406

The development of thermodynamically consistent turbulence models for granular and two-phase solid-liquid flows is discussed. The rapid flow of nearly elastic granular materials is studied as well as turbulent flows of dispersed multiphase solid-liquid mixtures. Using the developed turbulence model, simple shear flows of dense solid-liquid mixtures were studied. The equations governing the transport of mass, momentum and fluctuation kinetic energy for different phases are considered. The resulting coupled equations for phasic fluctuation kinetic energies are solved by an iterative method, and variations of normal and shear stresses with shear rate and solid volume fraction are studied. It is shown that the model predictions agree reasonably well with the available experimental data. Variations of production, dissipation, and energy sources of the different phases with solid volume fraction are also discussed. Dissert. Abstr.

N91-23421 Stanford Univ., CA.
A NUMERICAL STUDY OF THE STRATIFIED TURBULENT EKMAN LAYER Ph.D. Thesis
Gary Neil Coleman 1990 264 p
Avail: Univ. Microfilms Order No. DA9102245

The three dimensional time-dependent turbulent flow in the stratified Ekman layer over a smooth surface is computed numerically by directly solving the Navier-Stokes equations. Neutrally-, unstably-, and stably-stratified conditions are considered, using the Boussinesq approximation to account for buoyancy effects. All relevant scales of motion are included in the simulation so that no turbulence model is needed. Interest is in the Ekman layer because it is an idealization of the earth's boundary layer and therefore, provides information concerning atmospheric turbulence models and allows study of basic questions regarding small-scale geophysical flows. Results of the neutrally-stratified simulations indicate that the horizontal component of the rotation vector has a significant influence on the turbulence; thus, the f-plane approximation is inaccurate. Asymptotic similarity theory and a higher order correction are first tested for the low Reynolds number simulated, and then used to predict the friction velocity and stress direction at the surface for unstratified flows at arbitrary Reynolds number. A correlation for the variation of these quantities with latitude and wind angle is also proposed which gives an acceptable fit to the simulation results. Numerous instances were found in which results of large eddy simulation (LES) studies are very similar for neutral, unstable, and stable flows to those produced here using direct simulation. The usefulness of direct simulation, which produces flow fields less dependent than LES upon modeling assumptions, as an atmospheric research tool is demonstrated.
Dissert. Abstr.

N91-23422 State Univ. of New York, Stony Brook.
TURBULENT MIXING IN NONREACTING AND REACTING FLOWS: A PDF APPROACH AT THE TWO-POINT LEVEL Ph.D. Thesis
Tai-Lun Jiang 1990 120 p
Avail: Univ. Microfilms Order No. DA9106814

The evolution of the two-point scalar probability density function (PDF) in a stationary isotropic turbulent velocity field is numerically studied using the FCT (Flux-Corrected-Transport) algorithm. The model employs the LMSE (least-mean-square minimization of an error function) closure for molecular diffusion and the EDQNM (eddy-damped quasi-normal Markovian) analogy for turbulent convection. Dissert. Abstr.

N91-23423 Texas A&M Univ., College Station.
FLOW FIELD STUDY OF A RECTANGULAR JET Ph.D. Thesis
David Herman Swan 1990 240 p
Avail: Univ. Microfilms Order No. DA9106999

A rectangular jet has a complex three dimensional flow field. The objective was to increase the understanding of the rectangular jet. To do this, two rectangular nozzles were constructed and the subsonic jet velocities were measured, analyzed, and interpreted. The study concentrated on the near field region where the three dimensional flow field develops. The analysis included the time averaged velocity field, the complete Reynolds stress tensor, vorticity, turbulent kinetic energy production, and other parameters. Comparisons were made with previous studies. Also, a method of determining the mean pressure change in the jet flow field based on velocity and Reynolds stress tensor gradients was presented and compared with experimental data and numerical predictions. The results, analysis and interpretation were frequently related to previous theoretical vortex system models. As a result of discrepancies, a new vortex system model is presented. This study contributes substantially to the current understanding of three dimensional jet flow fields. Dissert. Abstr.

N91-23424# University of Southern California, Los Angeles. Dept. of Mechanical Engineering.
MECHANICS/HEAT-TRANSFER RELATION FOR PARTICULATE MATERIALS
C. S. Campbell Jan. 1991 9 p
(Contract DE-FG22-88PC-88913)
(DE91-008356; DOE/PC-88913/T8) Avail: NTIS HC/MF A02

This quarter has seen the conclusion of the shear cell study. It was shown that the apparent thermal conductivity of a sheared granular materials increases linearly with the shear rate. Interestingly enough, the apparent viscosity also varies linearly with the shear rate and it may be argued that both vary as the square root of the granular temperature just as kinetic theory predicts that the viscosity and thermal conductivity of a monatonic hard sphere gas varies as the square root of the thermodynamic temperature. The apparent Prandtl number of the shared material is a function only of the solid fraction, (nu). As a closing summary, this quarterly report is devoted to the discussion of the conductivity measurements. DOE

N91-23425# Wisconsin Univ., Madison. Dept. of Chemical Engineering.
INTERPHASE TRANSPORT AND MULTISTAGE SEPARATIONS
W. E. Stewart 15 Sep. 1990 6 p
(Contract DE-FG02-84ER-13291)
(DE91-009627; DOE/ER-13291/6) Avail: NTIS HC/MF A02

New matrix formulas were developed for calculation of multicomponent simultaneous heat and mass transfer, thus generalizing the methods given in Paper 2 for isothermal systems. Formulas were given for two choices of state variables: mole fractions and temperature; and mole fractions and molar enthalpy. The latter choice usually leads to simpler calculations, and was used in our fractionation model. A two phase boundary layer model and collocation method was also developed for steady state simulation of crossflow sieve trays. The dimensionless coefficient a(sub 00) in the boundary layer model was studied as a function of various sets of dimensionless groups for a sieve tray in

quasi-steady operation. Various correlation forms were constructed for the two phase heat and mass transfer function a(sub 00), and fitted them to published sieve-tray fractionation data from three sources. The fitting was done by multiresponse parameter estimation with the subroutine GREG. The variances of the data from the three laboratories were taken into account directly by use of the appropriate multiresponse objective function, with a separate response function for observations from each laboratory. Equal variances were assigned to gas and liquid composition measurements, and mass-balance closure adjustments were optimized by estimating key values for each experiment simultaneously with the parameters of the model considered.
DOE

N91-23426# Lawrence Livermore National Lab., CA.
NUMERICAL MODELING OF TURBULENT DISPERSION AROUND STRUCTURES USING A PARTICLE-IN-CELL METHOD
R. L. Lee and J. M. Leone, Jr. 1991 18 p Presented at the 84th Annual Meeting and Exhibition of the Air and Waste Management Association (AWMA), Vancouver (Canada), 16-21 Jun. 1991
(Contract W-7405-eng-48)
(DE91-009757; UCRL-JC-105271; CONF-910659-5) Avail: NTIS HC/MF A03

A methodology is described wherein two numerical models are exercised in order to predict the turbulent transport and dispersion around a surface mounted rectangular block. This methodology can be expanded in the future to treat more irregularly shaped single buildings or clusters of buildings. The calculational procedure which is proposed consists of two separate steps, namely: (1) prediction of the turbulent wind field and (2) employment of the calculated wind field to drive a transport dispersion model. It is well known that external flow past nonstreamlined bodies is usually very complex, exhibiting separation and reattachment regions, high pressure gradients and turbulence levels, and unsteadiness. The approach employed is to solve the Reynolds-averaged Boussinesq equations with turbulence represented via a k-(epsilon) model. This particular turbulence model has been applied extensively to many classes of flows including those which are influenced by buoyancy, stratification and rotation effects. It has a good reputation for reliability and is also computationally economical compared to more complex models. Recently, a number of calculations of turbulent flows over surface mounted cubes which use a k-(epsilon) turbulence model in conjunction with finite difference techniques were presented. In contrast, the flow model developed uses a modified finite element method (FEM). A K-Theory version of this model was employed to simulate flows which describe the dispersion of heavier-than-air gases and the atmospheric boundary layer. The present model is algorithmically identical to the earlier model except two additional equations were required for the turbulence model and a building-block specification is used to represent structures for computational efficiency.
DOE

N91-23427# Wisconsin Univ., Milwaukee. Dept. of Mechanical Engineering.
INTERFACIAL CHARACTERISTIC MEASUREMENTS IN HORIZONTAL BUBBLY TWO-PHASE FLOW
Z. Wang, W. D. Huang, S. Srinivasmurthy, and G. Kocamustafaogullari Oct. 1990 181 p
(Contract DE-FG02-87ER-13764)
(DE91-009803; DOE/ER-13764/T2) Avail: NTIS HC/MF A09

Advances in the study of two-phase flow increasingly require detailed internal structure information upon which theoretical models can be formulated. The void fraction and interfacial area are two fundamental parameters characterizing the internal structure of two-phase flow. However, little information is currently available on these parameters, and it is mostly limited to vertical flow configurations. In view of the above, the internal phase distribution of concurrent, air-water bubbly flow in a 50.3 mm diameter transparent pipeline has been experimentally investigated by using a double-sensor resistivity probe. Liquid and gas volumetric superficial velocities ranged from 3.74 to 5.60 m/s and 0.25 to 1.59 m/s, respectively, and average void fractions ranged from 2.12 to 22.5 percent. The local values of void fractions, interfacial area concentration, mean bubble diameter, bubble interface velocity, bubble chord-length and bubble frequency distributions were measured. The experimental results indicate that the void fraction interfacial area concentration and bubble frequency have local maxima near the upper pipe wall, and the profiles tend to flatten with increasing void fraction. The observed peak void fraction can reach 0.65, the peak interfacial area can go up to 900 approximately 1000 sq m/cu m, and the bubble frequency can reach a value of 2200 per s. These ranges of values have never been reported for vertical bubbly flow. It is found that either decreasing the liquid flow rate or increasing the gas flow would increase the local void fraction, the interfacial area concentration and the bubble frequency.
DOE

N91-23428# Los Alamos National Lab., NM.
A THREE-DIMENSIONAL FREE-LAGRANGE CODE FOR MULTIMATERIAL FLOW SIMULATIONS
M. S. Sahota and H. E. Trease 1991 13 p Presented at the 4th ASME-JSME International Symposium on Liquid-Solid Flow, Portland, 23-26 Jun. 1991
(Contract W-7405-eng-36)
(DE91-002309; LA-UR-90-3383; CONF-910664-1) Avail: NTIS HC/MF A03

A time-dependent, three-dimensional, compressible, multi-component, free-Lagrange code is currently under development at the Los Alamos National Laboratory. The code uses fixed-mass particles (called mass points) surrounded by median Lagrangian cells. These mass points are free to change their nearest-neighbor connections as they follow the fluid motion, which ensures accuracy in the differencing of equations and allows simulation of flows with extreme distortions. All variables, including velocity, are mass-point centered and time-advancement is performed using the finite-volume technique. The code conserves mass, momentum, and energy exactly, except in some pathological situations. The Voronoi connections algorithm were utilized for Delaunay tetrahedralization of the median mesh during mesh generations and mesh reconnections. The code is highly vectorized and utilizes all eight processors on a Cray YMP. Also, the code was recently mapped to the massively parallel Connection Machine. Some of the applications for the free-Lagrange method include atomspheric and ocean-circulation models, oil-reservoir and high-velocity impact simulations. These applications are in addition to the standard model problems of high-explosive driven shock-wave problems that involve high degree of deformation, shear flow, and turbulent mixing.
DOE

N91-23429# Lawrence Livermore National Lab., CA.
NUMERICAL SIMULATION OF A VISCOUS VORTEX RING INTERACTION WITH A DENSITY INTERFACE
D. L. Marcus and J. B. Bell Oct. 1990 18 p Presented at the 10th AIAA Computational Fluid Dynamics Conference in Conjunction With the 22nd AIAA Fluid Dynamics, Plasma Dynamics and Lasers Conference and the 26th AIIA Thermophysics Conference, Honolulu, 24-26 Jun. 1991
(Contract W-7405-eng-48)
(DE91-002790; UCRL-JC-105183; CONF-910651-2) Avail: NTIS HC/MF A03

When a vortex-dominated flow interacts with a sharp density interface, the dynamics are characterized by the interaction of baroclinically generated vorticity with the already existing vorticity field. This can be seen in many natural and technology settings; examples are the interaction of a ship or submarine wake with a thermocline, the collision of a buoyant thermal with a temperature inversion, and the interaction of a vortex flow with a flame front. This problem also serves as a generic model for turbulent mixing and entrainment processes across sharp density interfaces. The interaction between vortices and a free surface, with corresponds to the case where the density jump is very large, has been studied fairly extensively, both experimentally and computationally. By comparison, the literature for the more general case of vortex

pairs and rings interacting with sharp density interfaces is relatively sparse. Experiments and numerical studies have been performed, but the numerical simulations were confined primarily to vortex pairs, restricted to the inviscid case, and the effect of density variation modeled under the Boussinesq approximation. The experiments were also confined to the Boussinesq regime. The motion of a vortex ring was studied in a sharply stratified, viscous fluid via a numerical solution of the full Navier-Stokes equations with finite-amplitude density variation. Both Boussinesq and non-Boussinesq flow regimes will be studied, the effect of viscosity on the interaction will be examined, and three-dimensional aspects of the motion will be addressed, such as Widnall instability of the vortex ring and vortex reconnection at the interface. DOE

N91-23430# Lawrence Livermore National Lab., CA.
HAIRPIN VORTICES, SINGULARITIES, AND TRANSITION TO TURBULENCE IN THREE-DIMENSIONAL SHEAR FLOWS
D. L. Marcus and J. B. Bell Oct. 1990 17 p Presented at the 10th AIAA Computational Fluid Dynamics Conference in Conjunction With the 22nd AIAA Fluid Dynamics, Plasma Dynamics and Lasers Conference and the 26th AIIA Thermophysics Conference, Honolulu, 24-26 Jun. 1991
(Contract W-7405-eng-48)
(DE91-002792; UCRL-JC-105182; CONF-910651-1) Avail: NTIS HC/MF A03

The evolution of a transversely perturbed co-flowing jet was studied in a triply periodic box by means of a second-order projection method for the three-dimensional Euler equations. Advection-diffusion equations are solved without enforcing the incompressibility constraint, and the resulting velocity field is projected onto a divergence-free subspace. The method is unique in its treatment of nonlinear advection; it incorporates a second-order, upstream-centered differencing procedure that provides a robust treatment of nonsmooth data without introducing spurious oscillations, even in the limit of vanishing viscosity. The flow is visualized by following the evolution of a tracer function initialized on the surface of the tube. A volume rendering of the vorticity field with an opacity profile and color map which shows that hairpin vortices abound and that vorticity intensifies greatly at their tips was performed. Strong numerical evidence was presented that the vorticity becomes unbounded, and that accompanying the onset of the singularity is a decay in the mean kinetic energy. Following the onset, a Kolmogorov (k exp -5/3) range emerges in the energy spectrum. DOE

N91-23431# Sandia National Labs., Albuquerque, NM.
DEVELOPING NATURAL CONVECTION IN A FLUID LAYER WITH LOCALIZED HEATING AND LARGE VISCOSITY VARIATION
C. E. Hickox and Tze Yao Chu 1991 25 p Presented at the 1st ASME/JSME Fluids Engineering Conference, Portland, 23-26 Jun. 1991
(Contract DE-AC04-76DP-00789)
(DE91-005240; SAND-90-1850C; CONF-910684-2) Avail: NTIS HC/MF A03

Numerical simulations and laboratory experiments are used to elucidate aspects of transient natural convection in a magma chamber. The magma chamber is modeled as a horizontal fluid layer confined within an enclosure of square planform and heated from below by a strip heater centered on the lower boundary of the enclosure. The width of the strip heater and the depth of the fluid layer are one-fourth of the layer width. Corn syrup is used as the working fluid in order to approximate the large viscosity variation with temperature and the large Prandtl number typical of magma. The quiescent, uniform, fluid layer is subjected to instantaneous heating from the strip heater producing a transient flow which is dominated by two counter-rotating convective cells. Experimentally determined characteristics of the developing flow are compared with numerical simulations carried out with a finite element computer program. The results of numerical simulations are in essential agreement with experimental data. Differences between the numerical simulations and experimental measurements are conjectured to result from non-ideal effects present in the experiment which are difficult to represent accurately in a numerical simulation. DOE

N91-23432# Sandia National Labs., Albuquerque, NM.
BENCHMARKING NUMERICAL PREDICTIONS WITH FORCE AND MOMENT MEASUREMENTS ON SLENDER, SUPERCAVITATING BODIES
C. E. Hailey, E. L. Clark, and J. K. Cole 1991 18 p Presented at the 1991 Cavitation and Multiphase Flow Conference, Portland, 23-26 Jun. 1991
(Contract DE-AC04-76DP-00789)
(DE91-007066; SAND-90-3227C; CONF-9106114-1) Avail: NTIS HC/MF A03

High-speed water-entry is a very complex, dynamic process. As a first attempt at modeling the process, a numerical solution was developed at Sandia National Laboratories for predicting the forces and moments acting on a body with a steady supercavity, that is, a cavity which extends beyond the base of the body. The solution is limited to supercavities on slender, axisymmetric bodies at small angles of attack. Limited data were available with which to benchmark the axial force predictions at zero angle of attack. Even less data were available with which to benchmark the pitching moment and normal force predictions at nonzero angles of attack. A water tunnel test was conducted to obtain force and moment data on a slender shape. This test produced limited data because of waterproofing problems with the balance. A new balance was designed and a second water tunnel test was conducted at Tracor Hydronautics, Inc. This paper describes the numerical solution, the experimental equipment and test procedures, and the results of the second test. DOE

N91-23433*# Institute for Computer Applications in Science and Engineering, Hampton, VA.
AN ANALYSIS OF RNG BASED TURBULENCE MODELS FOR HOMOGENEOUS SHEAR FLOW Final Report
Charles G. Speziale, Thomas B. Gatski, and Nessan Fitzmaurice (Case Western Reserve Univ., Cleveland, OH.) Apr. 1991 13 p Submitted for publication
(Contract NAS1-18605)
(NASA-CR-187552; NAS 1.26:187552; ICASE-91-37) Avail: NTIS HC/MF A03 CSCL 20D

In a recent paper, the authors compared the performance of a variety of turbulence models including the k-epsilon model and the second-order closure model based on Renormalization Group (RNG) Methods. The performance of these RNG models in homogeneous turbulent shear flow was found to be quite poor, apparently due to the value of the constant C(sub epsilon1) in the modeled dissipation rate equation which was substantially lower than its traditional value. However, recently a correction has been made in the RNG based calculation of C(sub epsilon1). It is shown that with the new value of C(sub epsilon1), the performance of the RNG k-epsilon model is substantially improved. On the other hand, while the predictions of the revised RNG second-order closure model are better, some lingering problems still remain which can be easily remedied by the addition of higher order terms. Author

N91-23434*# Institute for Computer Applications in Science and Engineering, Hampton, VA.
NON-LINEAR INTERACTION OF A DETONATION/VORTICITY WAVE Final Report
D. G. Lasseigne, T. L. Jackson (Old Dominion Univ., Norfolk, VA.), and M. Y. Hussaini Apr. 1991 28 p Submitted for publication
(Contract NAS1-18605)
(NASA-CR-187550; NAS 1.26:187550; ICASE-91-34) Avail: NTIS HC/MF A03 CSCL 20D

The interaction of an oblique, overdriven detonation wave with a vorticity disturbance is investigated by a direct two-dimensional numerical simulation using a multi-domain, finite-difference solution of the compressible Euler equations. The results are compared to those of linear theory, which predict that the effect of exothermicity on the interaction is relatively small except possibly near a critical

angle where linear theory no longer holds. It is found that the steady-state computational results agree with the results of linear theory. However, for cases with incident angle near the critical angle, moderate disturbance amplitudes, and/or sudden transient encounter with a disturbance, the effects of exothermicity are more pronounced than predicted by linear theory. Finally, it is found that linear theory correctly determines the critical angle. Author

N91-23435# Deutsche Forschungsanstalt fuer Luft- und Raumfahrt, Goettingen (Germany, F.R.). Abt. Instabilitaeten und Ableosung.

NUMERICAL SIMULATION AND TOPOLOGICAL ANALYSIS OF THE SEPARATED FLOW AROUND A SPHERE Ph.D. Thesis - Technische Univ.

Burkhard Schulte-Werning Jun. 1990 113 p In GERMAN; ENGLISH summary Original contains color illustrations
(DLR-FB-90-43; ISSN-0171-1342; ETN-91-99065) Avail: NTIS HC/MF A06; DLR, Wissenschaftliches Berichtswesen, VB-PL-DO, Postfach 90 60 58, 5000 Cologne, Fed. Republic of Germany, HC 42.50 DM

The bifurcation behavior of separated flows is investigated by the numerical simulation of the viscous flow around a sphere. The beam warming type algorithms are used to calculate the compressible Navier-Stokes equations in the low subsonic range for laminar flow. The properties of the numerical solution are analyzed in detail. The development of steady secondary separation induced by the ring vortex in the wake is investigated, assuming axisymmetric flow. In the spatial flow field, the onset of three dimensional effects is investigated and the separation structure is analyzed topologically in dependency on the Reynolds number. The visualization of the entire spatial wake structure is done by stream and vortex lines. ESA

N91-23436# Von Karman Inst. for Fluid Dynamics, Rhode-Saint-Genese (Belgium).

INVESTIGATION OF ROE'S 2D WAVE DECOMPOSITION MODELS FOR THE EULER EQUATIONS

P. DePalma, H. Deconinck, and R. Struijs Jul. 1990 70 p
(Contract AERO-0003-C)
(VKI-TN-172; ETN-91-99112) Avail: NTIS HC/MF A04

A new technique to solve the two dimensional (2D) Euler equations by modeling the solution with a discrete number of simple waves is implemented. The global solution is obtained by superposition of elementary solutions consisting of plane waves. The traveling directions of these waves are not fixed in advance but depend on the local flow gradient at each time step. Three different wave decomposition models were considered and implemented based on four acoustic waves: (1) one entropy wave and respective vorticity; (2) one shear wave propagating in the perpendicular direction to the streamlines; and (3) one shear wave propagating in the direction of the pressure gradient. Different first order upwind fluctuation splitting schemes were tested both for triangular and quadrilateral cells. Different test cases were solved with the new method: shear flow, oblique shock reflection, ramp flow, nozzle flow; a comparison among the results obtained with the different decomposition models and numerical schemes is presented. ESA

N91-23437# Von Karman Inst. for Fluid Dynamics, Rhode-Saint-Genese (Belgium).

AERO-THERMAL INVESTIGATION OF A HIGHLY LOADED TRANSONIC LINEAR TURBINE GUIDE VANE CASCADE. A TEST CASE FOR INVISCID AND VISCOUS FLOW COMPUTATIONS

T. Arts, M. LambertdeRouvroit, and A. W. Rutherford Sep. 1990 91 p
(VKI-TN-174; ETN-91-99114) Avail: NTIS HC/MF A05

An experimental aerothermal investigation of a highly loaded transonic turbine nozzle guide vane mounted in a linear cascade arrangement is presented. The measurements were performed in a short duration isentropic light piston compression tube facility, allowing a correct simulation of Mach and Reynolds numbers as well as of the gas to wall temperature ratio compared to the values currently observed in modern aeroengines. The experimental program consisted of the following: (1) flow periodicity checks by means of wall static pressure measurements and Schlieren flow visualizations; (2) blade velocity distribution measurements by means of static pressure tappings; (3) blade convective heat transfer measurements by means of static pressure tappings; (4) blade convective heat transfer measurements by means of platinium thin films; (5) downstream loss coefficient and exit flow angle determinations by using a new fast traversing mechanism; and (6) free stream turbulence intensity and spectrum measurements. These different measurements were performed for several combinations of the free stream flow parameters looking at the relative effects on the aerodynamic blade performance and blade convective heat transfer of Mach number, Reynolds number, and freestream turbulence intensity. ESA

N91-23438 National Physical Lab., Teddington (England).

THE SOLIDIFICATION OF A MOLTEN DROPLET ON AN INCLINED PLANE

D. H. Ferriss Jan. 1991 18 p
(NPL-DMM(A)-20; ISSN-0959-2423; ETN-91-99120) Copyright Avail: National Physical Laboratory, Teddington, TW11 0LW, England

Model equations which govern the heat and mass transfer within a molten droplet on an inclined plane which is losing heat to its surroundings by conduction and radiation effects are derived. Relevant parameter groups which characterize the problem are identified. Options for numerical solution of the problem and some solutions obtained for a reduced steady state form are discussed. ESA

N91-23439*# National Aeronautics and Space Administration. Lewis Research Center, Cleveland, OH.

A SYSTEM-APPROACH TO THE ELASTOHYDRODYNAMIC LUBRICATION POINT-CONTACT PROBLEM

Sang Gyu Lim and David E. Brewe (Case Western Reserve Univ., Cleveland, OH.) 1991 17 p Presented at the Annual Meeting of the Society of Tribologists and Lubrication Engineers, Montreal, Quebec, 29 Apr. - 2 May 1991
(DA Proj. 1L1-61101-AH-45)
(NASA-TM-104342; E-6116; NAS 1.15:104342; AVSCOM-TR-90-C-031) Avail: NTIS HC/MF A03 CSCL 20D

The classical EHL (elastohydrodynamic lubrication) point contact problem is solved using a new system-approach, similar to that introduced by Houpert and Hamrock for the line-contact problem. Introducing a body-fitted coordinate system, the troublesome free-boundary is transformed to a fixed domain. The Newton-Raphson method can then be used to determine the pressure distribution and the cavitation boundary subject to the Reynolds boundary condition. This method provides an efficient and rigorous way of solving the EHL point contact problem with the aid of a supercomputer and a promising method to deal with the transient EHL point contact problem. A typical pressure distribution and film thickness profile are presented and the minimum film thicknesses are compared with the solution of Hamrock and Dowson. The details of the cavitation boundaries for various operating parameters are discussed. Author

N91-23440*# Purdue Univ., West Lafayette, IN. School of Aeronautics and Astronautics.

FORMULATION OF BOUNDARY CONDITIONS FOR THE MULTIGRID ACCELERATION OF THE EULER AND NAVIER STOKES EQUATIONS Final Technical Report, 20 Feb. 1988 - 19 Mar. 1990

Thomas Neil Jentink and William J. Usab, Jr. 19 Mar. 1990 153 p
(Grant NAG3-875)
(NASA-CR-188234; NAS 1.26:188234) Avail: NTIS HC/MF A08 CSCL 20D

An explicit, Multigrid algorithm was written to solve the Euler and Navier-Stokes equations with special consideration given to the coarse mesh boundary conditions. These are formulated in a manner consistent with the interior solution, utilizing forcing terms

to prevent coarse-mesh truncation error from affecting the fine-mesh solution. A 4-Stage Hybrid Runge-Kutta Scheme is used to advance the solution in time, and Multigrid convergence is further enhanced by using local time-stepping and implicit residual smoothing. Details of the algorithm are presented along with a description of Jameson's standard Multigrid method and a new approach to formulating the Multigrid equations. Author

N91-23441# European Space Agency, Paris (France).
NUMERICAL SIMULATION OF INCOMPRESSIBLE INHOMOGENEOUS TURBULENCE IN A PLANE CHANNEL FLOW
Veronique Deschamps (Office National d'Etudes et de Recherches Aerospatiales, Paris, France) Feb. 1991 246 p Transl. into ENGLISH of Simulation Numerique de laTurbulence Inhomogene Incompressible dans un Ecoulement de Canal Plan (Paris, France, ONERA), 1988 236 p Original language document was announced as N90-18686
(ESA-TT-1199; ONERA-NT-1988-5; ETN-91-99316) Avail: NTIS HC/MF A11

The numerical simulation of an inhomogeneous incompressible turbulence in a plane channel flow is discussed. The physical problem is modeled by Navier-Stokes equations for an incompressible fluid with periodic boundary conditions in homogeneous directions and no slip conditions in the inhomogeneous direction. The flow rate and energy predictions obtained after integration of momentum and energy equations depend strongly on the imposed mean pressure gradient. In the numerical method, derivatives are discretized by a fourth order finite difference scheme in space and a second order one in time; the incompressibility condition is achieved by a global technique. Substantial gains in computing time are obtained by a numerical procedure which adjusts the mean pressure gradient at the appropriate level to maintain a constant flow rate during time integration. A detailed analysis of the simulations, first validated by experiments, is completed by energy balances for each Reynolds stress component. Use of direct simulation in statistical modeling, especially second order modeling, is discussed. Promising results obtained by large eddy simulation with subgrid models are shown. ESA

N91-23442# European Space Agency, Paris (France).
NUMERICAL SIMULATION OF TRANSITION IN THREE DIMENSIONAL BOUNDARY LAYERS
Friedrich Meyer (Deutsche Forschungsanstalt fuer Luft- und Raumfahrt, Goettingen, Germany, F.R.) Feb. 1991 136 p Transl. into ENGLISH of Numerische Simulation der Transition in Dreidimensionalen Grenzschichten (Goettingen, Fed. Republic of Germany, DLR), Jun. 1989 104 p Original language document was announced as N90-13728
(ESA-TT-1203; DLR-FB-89-12; ETN-91-99318) Avail: NTIS HC/MF A07; Original German version available from DLR, Wissenschaftliches Berichtswesen, VB-PL-DO, Postfach 90 60 58, 5000 Cologne, Fed. Republic of Germany, HC 40 Deutsche marks

Linear and nonlinear stages of laminar/turbulent transition in a three dimensional boundary layer, initiated by cross flow instability, are investigated using stability theory and numerical simulation of the incompressible Navier-Stokes equations. The conditions in the calculations are matched to those of a transition experiment for a swept, flat plate. Falkner-Skan-Cooke similarity profiles are used to describe the basic parallel flow. A quasi two dimensional treatment of the problem produces a nonlinear saturation of the stationary cross flow vortices. The nonlinear interaction between the stationary vortices and traveling waves is investigated in more detail. The development of the mean flow, fluctuations and instantaneous flow parameters is documented. The development of the flow depends strongly upon the initial perturbations that are chosen. In general, good agreement is observed between comparable stages of simulation and experiment. The nonlinear interactions produce a marked distortion of the streamwise and crossflow profiles and an increase in mean wall shear stress. ESA

N91-23443# Cranfield Inst. of Tech., Bedford (England). Dept. of Aerodynamics.
RIEMANN PROBLEMS AND THE WAF METHOD FOR THE TWO-DIMENSIONAL SHALLOW WATER EQUATIONS
E. F. Toro Apr. 1990 73 p
(Cranfield-Aero-9005; ISBN-1-871564-06-9; ETN-91-99334)
Avail: NTIS HC/MF A04

An exact Riemann solver for the shallow water equations and several approximate Riemann solvers are presented. These solutions are used locally to compute numerically the global solution of the general initial boundary value problem for the shallow water equations. The numerical method used is the Weighted Average Flux (WAF) method proposed previously. This is a conservative, shock capturing high resolution method. For shallow water flows where nonlinear effects are important or where abrupt changes (hydraulic jumps) are to be expected the present algorithms can be useful in practice. ESA

N91-23444# Cranfield Inst. of Tech., Bedford (England). Dept. of Aerodynamics.
THE DRAG OF SPHERES AT POROSITES RANGING FROM AN ISOLATED SPHERE TO A PACKED BED
J. Pike Jul. 1990 21 p
(Cranfield-Aero-9012; ISBN-1-871564-12-3; ETN-91-99335)
Avail: NTIS HC/MF A03; Cranfield Inst. of Tech., Coll. of Aeronautics, Cranfield, Bedford MK43 0AL, England, HC 8 Sterling pounds

A drag expression is suggested for spheres which have porosities or void fractions of from 0.4 to 1, which is applicable for Reynolds numbers (Re) of up to 0.00001. The expression matches reliable data correlations for the drop of isolated spheres, the drag of spheres in packed beds and the drag of spheres at Re less than 0.001. The lack of data at intermediate porosities and Re of about 0.00001 means that the estimate is not reliable in this region. More data is needed to improve the accuracy, but the estimate can be used for applications not requiring great acuracy. ESA

N91-23445# Arnold Engineering Development Center, Arnold Air Force Station, TN.
COMPUTATION OF INLET REFERENCE PLANE FLOW-FIELD FOR A SUBSCALE FREE-JET FOREBODY/INLET MODEL AND COMPARISON TO EXPERIMENTAL DATA Final Report, 1 Jan. 1989 - 31 Jul. 1990
M. D. McClure and J. R. Sirbaugh Feb. 1991 77 p Prepared in cooperation with Sverdrup Technology, Inc., Arnold AFS, TN
(AD-A232101; AEDC-TR-90-21) Avail: NTIS HC/MF A05 CSCL 20/4

The computational fluid dynamics (CFD) computer code PARC3D was used to predict the inlet reference plane (IRP) flow field for a side-mounted inlet and forebody simulator in a free jet for five different flow conditions. The calculations were performed for free-jet conditions, mass flow rates, and inlet configurations that matched the free-jet test conditions. In addition, viscous terms were included in the main flow so that the viscous free-jet shear layers emanating from the free-jet nozzle exit were modeled. A measure of the predicted accuracy was determined as a function of free-stream Mach number, angle-of-attack, and sideslip angle. GRA

N91-23446# Applied Research Lab., State College, PA.
A TWO-SCALE SOLUTION OF THE FORCED RAYLEIGH-PLESSET EQUATION GOVERNING THE DYNAMICS OF CAVITATION BUBBLE VAPOROUS GROWTH
B. W. Lathrop and B. R. Parkin Feb. 1991 157 p
(Contract N00014-88-K-0404)
(AD-A232129; PSU/ARL-TR-91-002) Avail: NTIS HC/MF A08 CSCL 20/4

A two-scale analysis of the forced Rayleigh Plesset equation of cavitation bubble dynamics is performed. The problem of cavitation inception as it relates to bubble dynamics involves vaporous cavitation nucleus growth as it is influenced by the pressure distribution on a submerged body. This brings into

prominence two widely varying time scales. The laboratory time is characterized by the bubble's travel over the body, while the bubble time is characterized by the very high natural frequency oscillations of the individual bubble. The laboratory time is expected to much longer than the bubble time; thus they can be related by a very small parameter, epsilon. Using these two time scales, a perturbation expansion is performed on the forced Rayleigh-Plesset equation and its initial conditions up to the third order in epsilon. The resulting zero and first order equations are solved, subject to these solutions being independent of the laboratory time. In this case the integrability condition for each step is thereby identically satisfied. GRA

N91-23447# Notre Dame Univ., IN. Dept. of Aerospace and Mechanical Engineering.
EFFECTS OF THREE-DIMENSIONAL IMPOSED DISTURBANCE ON BLUFF-BODY NEAR WAKE FLOWS Annual Report, 1 Oct. 1989 - 30 Sep. 1990
Albin A. Szewczyk and Peter Bearman 6 Dec. 1990 6 p
(Contract N00014-90-J-4083)
(AD-A232137) Avail: NTIS HC/MF A02 CSCL 20/4

The long term goals of the project are: (1) Mechanics of the development, modification and control of the near wake behind a nominally 2-D; (2) Understanding the effects of controlled 3-D disturbance on the region of absolute instability. Comparison of classical bluff body wake flow entrainment mechanisms by Gerrard with instability concepts; (3) Implication of the imposed disturbances for cut-off blunt trailing edge (BB) vis a vis a circular cylinder (CC); and (4) Mechanics of uniform and nonuniform flow past a circular cylinder with a free-end. GRA

N91-23448# Spectral Sciences, Inc., Burlington, MA.
STRATEGY COMBINING REGIONALLY ADAPTED PROCESSES (SCRAP) Final Report, 1 Jul. - 31 Dec. 1990
M. M. Pervaiz 30 Jan. 1991 62 p
(Contract DAAL03-90-C-0014)
(AD-A232158; SSI-TR-183; ARO-27961.1-EG-SBI) Avail: NTIS HC/MF A04 CSCL 20/4

A local Navier-Stokes (NS) algorithm to simulate a physically and geometrically complex flow is presented. The domain is subdivided into blocks which facilitate the generation of global mesh and splitting of schemes. Basic types are inviscid, viscous and interaction blocks. In the interaction block a local procedure is used to decide whether to use NS or Euler equations. Each block also employs subdomain adaptation to capture small scale features. The method concentrates resources by modeling complex physics in only important regions. Physics adaptation treats those cells for which local stress is more than 1 percent of the maximum value as viscous cells. Subdomain adaptation is carried out by monitoring the first differences of selected variables. The cells for which these differences are large are locally divided. The SCRAP technique is demonstrated via a two dimensional model problem. It significantly reduces computational requirements and is comparatively more accurate than conventional schemes. Up to two orders of magnitude savings in computer time have been achieved, compared to a globally fine solution of full NS equations. The agreement with previous full NS computations over fine grids is excellent. Future work will extend the approach to three dimensional configurations. Phase 2 will simulate flows for complex configurations at large attack angles. GRA

N91-23449# Georgia Inst. of Tech., Atlanta. School of Aerospace Engineering.
FRACTAL IMAGE COMPRESSION OF RAYLEIGH, RAMAN, LIF AND LDV DATA IN TURBULENT REACTING FLOWS Final Report, Oct. 1987 - Sep. 1990
Warren C. Strahle and Jechiel I. Jagoda Nov. 1990 9 p
(Grant AF-AFOSR-0001-88; AF Proj. 2308)
(AD-A232237; AFOSR-91-0033TR) Avail: NTIS HC/MF A02 CSCL 20/4

Fractal geometry analysis methods, analytical modeling, and several experimental diagnostics were applied to an experimental reacting flow in a two-dimensional subsonic wind tunnel with a backward facing step and provision for injection of inerts and combustibles through the porous floor behind the step. Experiments used laser velocimetry and Raman spectroscopy measurements for two components of the mean and fluctuating velocity and the local nitrogen concentration, which was found in this flow to be an accurate temperature sensor. The fuel used was hydrogen diluted with argon or nitrogen. Fractal geometry yielded a new nonlinear adaptive filter and an interpolation method for improving the statistics of sparsely separated data points. Analytical modeling was improved over from a prior program, and a two equation turbulent model now reproduces many of the observed features of the reacting flow. GRA

N91-23450# California Inst. of Tech., Pasadena. Graduate Aeronautical Labs.
CHEMICAL REACTIONS IN TURBULENT MIXING FLOWS Final Report, 16 Apr. 1989 - 30 Sep. 1990
Paul E. Dimotakis, James E. Broadwell, and Anthony Leonard 15 Nov. 1990 46 p
(Grant AF-AFOSR-0155-88; AF Proj. 2308)
(AD-A232610; AFOSR-91-0195TR) Avail: NTIS HC/MF A03 CSCL 20/4

This research conducted fundamental investigations of turbulent mixing, chemical reaction and combustion processes in turbulent, subsonic and supersonic flows. This program is comprised of an experimental effort, an analytical effort, a computational effort, a modeling effort, and a diagnostics development and data-acquisition effort; the latter as dictated by specific needs of the experimental part of the overall program. Our approach has been to carry out a series of detailed theoretical and experimental studies primarily in two, well-defined, fundamentally important flow fields: free shear layers and axisymmetric jets. To elucidate molecular transport effects, experiments and theory concern themselves with both liquids and gases, primarily in moderate to high Reynolds number flows. Modeling has been focused on both shear layers and turbulent jets, with an effort to include the physics of the molecular transport processes, as well as formulations of models that permit the full chemical kinetics of the combustion process to be incorporated. Our recent analytical efforts have concentrated on a hydrodynamic analysis of the stability of compressible shear layers. The computational studies are, at present, focussed at fundamental issues pertaining to the computational simulation of both compressible and incompressible flows. GRA

N91-23451# Pennsylvania State Univ., University Park. Applied Research Lab.
FUNDAMENTAL HYDRODYNAMICS RESEARCH Quarterly Report, 1 Oct. - 31 Dec. 1990
S. A. Abdallah, H. L. Petrie, and P. J. Morris 31 Dec. 1990 21 p
(Contract N00014-87-K-0196)
(AD-A232650) Avail: NTIS HC/MF A03 CSCL 20/4

This report discusses hydrodynamics research which falls into two basic thrust areas: (1) Turbomachinery -- to develop an improved understanding of the fluid mechanics and acoustics associated with low-speed turbomachines and marine propulsors and to employ this knowledge to the development of improved propulsor and turbomachine design methods; and (2) Drag reduction -- to develop fundamental understanding of the mechanisms that cause drag on bodies and surfaces and to explore novel methods to reduce drag. Under each thrust area, one or more projects are conducted under the direction of the principal investigator who initiated the given task. All tasks are designed to provide results that will improve the scientific understanding of various hydrodynamic phenomena associated with the operation of submerged bodies and surfaces. GRA

N91-23452# State Univ. of New York, Stony Brook. Dept. of Applied Mathematics and Statistics.
NONLINEAR WAVES IN REAL MATERIALS Final Report, 1 Dec. 1989 - 30 Nov. 1990
James Glimm 30 Nov. 1990 19 p

(Grant AF-AFOSR-0075-90; AF Proj. 2304)
(AD-A232654; AFOSR-90-0148TR) Avail: NTIS HC/MF A03 CSCL 20/4

Using the interface methods developed by the principal investigator and co-workers, significant progress has been made in the studies of fluid flow focused on chaotic mixing and shock interactions. The studies were carried out only in two dimensions on sequential machines. In most of the cases for realistic problems of physical interest, further progress requires development of three dimensional algorithms. These algorithms, used for scientific purposes, including multiple computation to explore the solution dependence on physical parameters, will require extensive computer resources, which cost-effective parallel computations will allow. Our collective research supported by this grant has been to develop parallel algorithms for three dimensional fluid computations based on the interface methods. GRA

N91-23453# McDonnell-Douglas Research Labs., Saint Louis, MO.
VORTEX SYSTEM EVOLUTION IN 2- AND 3-D SWEPT TRAILING EDGE FLOWS Final Report, 1 Sep. 1987 - 31 Aug. 1989
Frederick W. Roos, Jerome T. Kegelman, Richard W. Wlezien, David E. Parekh, and Valdis Kibens 24 Jul. 1990 31 p
(Contract F49620-86-C-0090)
(AD-A232692; MDC-QA056; AFOSR-91-0048TR) Avail: NTIS HC/MF A03 CSCL 20/4

Instability wavefront orientation and vortex system interaction were studied in a swept-trailing-edge mixing layer and in a slanted nozzle jet flowfield at low subsonic velocities. Flow visualization and image processing, and hot-wire data comprised the main body of experimental observations. The response of full-span wave systems of swept and unswept orientation were documented as a function of acoustic excitation introduced through a thin slot at the trailing edge. The lateral spreading of a wave system with only partial-span excitation was shown to be asymmetrical in a swept mixing layer. The jet flowfield was studied using a simultaneous axial and transverse laser sheet illumination. Excitation frequency dependence and amplitude dependence of instability wave system orientation was characterized. Digitized flow visualization images were decomposed to show the axial and helical shear layer modes. GRA

N91-23454# Wisconsin Univ., Madison. Center for Mathematical Sciences.
INTERDISCIPLINARY RESEARCH ON VISCOELASTICITY AND RHEOLOGY Final Technical Report, 23 May 1987 - 14 Oct. 1990
John A. Nohel 14 Dec. 1990 11 p
(Contract DAAL03-87-K-0036)
(AD-A232700; ARO-23932.16-MA) Avail: NTIS HC/MF A03 CSCL 20/4

Viscoelastic materials with fading memory, e.g., polymers, suspensions, emulsions, exhibit behavior that is intermediate between the nonlinear hyperbolic response of purely elastic materials and the strongly diffusive, parabolic response of viscous fluids. The following problems that are an outgrowth of earlier research were investigated during the reporting period: Provide numerical and analytic explanation of several striking phenomena observed in experiments in shear flows of highly elastic and very viscous non-Newtonian fluids in pressure-driven and piston-driven flows and in Couette flow. Such phenomena can lead to material instabilities deemed capable of severely disrupting advanced materials engineering and process design problems of polymer melts that include spinning of synthetic fibers and injection molding. GRA

N91-23455# New York Univ., New York. Inst. of Mathematical Sciences.
ADAPTIVE METHODS FOR COMPRESSIBLE FLUID DYNAMICS Final Report, 1 May - 31 Oct. 1990
Marsha J. Berger 1 May 1990 70 p LIMITED REPRODUCIBILITY: Availability: Document partially illegible
(Grant AF-AFOSR-0148-86; AF Proj. 2304)
(AD-A232786; AFOSR-91-0196TR) Avail: NTIS HC/MF A04 CSCL 20/4

Two major research efforts have been supported by this grant. The first is the development of an adaptive algorithm for hyperbolic conservation laws with simple physical geometry. This work is based on a combination of two approaches - an adaptive mesh refinement technique that concentrates computational effort where is most needed, and a high order Godunov method developed for high Mach number compressible flow. This approach has aided in the resolution of the weak von Neumann paradox in shock reflection. It was used to perform the first calculation of Kelvin Helmholtz instability along the slip line in ramp reflection off an oblique wedge. When combined with other algorithms, for example, multifluid tracking, it could categorize refraction patterns when a shock hits an oblique material interface. When combined with an elliptic grid generator, it was used to study the diffraction of a shock over an obstacle. In each of these cases, this approach to time-dependent fluid flow yielded factors of 10 to 100 improvement in efficiency over equivalent fine grid calculation with uniform resolution. GRA

N91-23456# Michigan Univ., Ann Arbor. Gas Dynamics Lab.
HIGH RESOLUTION MEASUREMENTS OF STRAINED DIFFUSION AND REACTION LAYER STRUCTURE AND EXTINCTION IN TURBULENT FLOWS Annual Report, period ending 31 Oct. 1990
Werner J. Dahm 31 Oct. 1990 49 p
(Grant AF-AFOSR-0541-89; AF Proj. 2308)
(AD-A232794; AFOSR-91-0111TR) Avail: NTIS HC/MF A03 CSCL 20/4

This research program represents a combined experimental and theoretical effort with the following three major objectives: (1) to develop high-resolution, multi-dimensional, quantitative, imaging diagnostic capabilities for obtaining direct experimental measurements of the fine scale structure associated with the molecular mixing and chemical reaction processes in turbulent flow; (2) to use this measurement technique to experimentally determine the physical characteristics of the fine structure associated with molecular mixing and chemical reactions in turbulent flows; and (3) to incorporate results from these measurements into an improved understanding of the molecular mixing, chemical reaction, and local extinction processes in reacting turbulent flows. GRA

N91-23457# Ballistic Research Labs., Aberdeen Proving Ground, MD.
DIFFUSIVE, ELECTROSTATIC CONCENTRATION OF DISINTEGRATION PRODUCTS OF INERT GASES IN VORTEX FLOW Final Report, 1-31 Oct. 1990
Thomas A. Korjack Feb. 1991 24 p
(AD-A232876; BRL-TR-3207) Avail: NTIS HC/MF A03 CSCL 20/3

The problem of steady-state mass transfer of decaying products resulting from the disintegration of an inert gas is considered for a vortex pipe flow configuration under variable electrostatic fields. The flow configuration consists of two smoothly joined sections: one stationary and the other rotating with constant angular velocity. The products of disintegration are filtered out far upstream, but are again generated by radioactive decay of flowing inert gas along the tube. Bulk concentrations result due to electrostatic force and diffusion. It was found that increasing the electrostatic charge caused a decrease in penetration; also, a decrease in charge profile was accompanied by an increase in potential since the particles become annihilated at the boundaries. GRA

35 INSTRUMENTATION AND PHOTOGRAPHY

Includes remote sensors; measuring instruments and gages; detectors; cameras and photographic supplies; and holography.

For aerial photography see *43 Earth Resources and Remote Sensing.* For related information see also *06 Aircraft Instrumentation,* and *19 Spacecraft Instrumentation.*

N91-23458*# Lockheed Missiles and Space Co., Palo Alto, CA.
INFRARED FOCAL PLANE PERFORMANCE IN THE SOUTH ATLANTIC ANOMALY Final Report
Frank A. Junga 30 Sep. 1989 65 p
(Contract NAS2-12898)
(NASA-CR-186197; NAS 1.26:186197; LMSC-F279280) Avail: NTIS HC/MF A04 CSCL 14B

Proton-induced pulse height distributions (PHD's) in Si:XX detectors were studied analytically and experimentally. In addition, a preliminary design for a flight experiment to characterize the response of Si:XX detectors to the trapped proton environment and verify PHD models was developed. PHD's were computed for two orbit altitudes for a variety of shielding configurations. Most of the proton-induced pulses have amplitudes less that about 3.5 x 10(exp 5) e-h pairs. Shielding has a small effect on the shape of the PHD's. The primary effect of shielding is to reduce the total number of pulses produced. Proton-induced PHD's in a Si:Sb focal plane array bombarded by a unidirectional 67-MeV beam were measured. The maximum pulse height recorded was 6 x 10(exp 5) pairs. The distribution had two peaks: the larger peak corresponded to 3.8 x 10(exp 5) pairs and the smaller peak to 1.2 x 10(exp 5) pairs. The maximum pulse height and the larger peak are within a factor of two of predicted values. The low-energy peak was not expected, but is believed to be an artifact of inefficient charge collection in the detector. The planned flight experiment will be conducted on a Space Shuttle flight. Lockheed's helium extended life dewar (HELD) will be used to provide the required cryogenic environment for the detector. Two bulk Si:Sb arrays and two Si:As impurity band conduction arrays will be tested. The tests will be conducted while the Space Shuttle passes through the South Atlantic Anomaly. PHD's will be recorded and responsivity changes tracked. This experiment will provide a new database on proton-induced PHD's, compare two infrared detector technologies in a space environment, and provide the data necessary to validate PHD modeling. Author

N91-23459# QuesTech, Inc., Falls Church, VA.
THERMAL CONTROL SYSTEM FOR THE INVESTIGATION OF SPECIFIC ABSORPTION RATES FOR SPECIMENS EXPOSED TO ELECTROMAGNETIC RADIATION Final Report, 1 Sep. 1989 - 31 Aug. 1990
D. M. Smolenski 31 Aug. 1990 16 p
(Contract F33615-87-D-0650)
(AD-A231329; C-6734-006; USAFSAM-JA-90-68) Avail: NTIS HC/MF A03 CSCL 18/6

A thermal control system was developed to automatically maintain biological and chemical specimens at a controlled thermal profile during exposure to electromagnetic radiation to aid in the investigation of specific absorption rates. Hot and cold air supplies are mixed using mass flow control valves to generate an air source of controlled temperature at a constant mass flow rate. This air source is used to cool or heat the specimen which is within a low thermal mass holder. By maintaining a constant mass flow rate for the air, the temperature difference between the input and exhaust air will directly indicate the heat energy removed/added to the specimen. A non-radiofrequency field perturbing temperature probe is inserted into the specimen to provide the temperature information to the controller. GRA

N91-23460*# National Aeronautics and Space Administration. Lewis Research Center, Cleveland, OH.
METHOD OF PRODUCING A PLUG TYPE HEAT FLUX GAUGE Patent Application
Curt H. Liebert, inventor (to NASA) 8 Apr. 1991 13 p
(NASA-Case-LEW-14967-2; NAS 1.71:LEW-14967-2; US-Patent-Appl-SN-685962) Avail: NTIS HC/MF A03 CSCL 14B

A method of making a plug-type heat flux gauge in a material specimen in which a thermoplug is integrally formed in the specimen is disclosed. The thermoplug and concentric annulus are formed in the material specimen by electrical discharge machining and trepanning procedures. The thermoplug is surrounded by a concentric annulus through which thermocouple wires are routed. The end of each thermocouple wire is welded to the thermoplug, with each thermocouple wire welded at a different location along the length of the thermoplug. NASA

N91-23461*# National Aeronautics and Space Administration. Langley Research Center, Hampton, VA.
A NON-CONTACTING VELOCITY MEASUREMENT SYSTEM Patent Application
Tom D. Finley, inventor (to NASA) 19 Nov. 1990 19 p
(NASA-Case-LAR-14466-1; NAS 1.71:LAR-14466-1; US-Patent-Appl-SN-615733) Avail: NTIS HC/MF A03 CSCL 14B

A method and system for measuring the velocity of an object following a known path include a plurality of magnets positioned along the path in preferably an equally spaced manner and at least one electronic switch such as a latching type Hall effect switch mounted on the object. Successive magnets are positioned such that alternating polarities face the path along which the object moves. The switch has two operative conditions such that as the switch passes over each magnet, the switch is triggered from its current condition to its other condition. A second electronic switch is used to sense the direction of motion of the object along the path. A data system calculates the average velocity of the movement of the object along the path in response to signals from the switches. NASA

N91-23462*# National Aeronautics and Space Administration. Lyndon B. Johnson Space Center, Houston, TX.
TWO DIMENSIONAL VERNIER Patent Application
Richard D. Juday, inventor (to NASA) 14 Jan. 1991 15 p
(NASA-Case-MSC-21700-1; NAS 1.71:MSC-21700-1; US-Patent-Appl-SN-640775) Avail: NTIS HC/MF A03 CSCL 14B

A two dimensional vernial scale is disclosed utilizing a cartesian grid on one plate member with a polar grid on an overlying transparent plate member. The polar grid has multiple concentric circles at a fractional spacing of the spacing of the cartesian grid lines. By locating the center of the polar grid on a location on the cartesian grid, interpolation can be made of both the X and Y fractional relationship to the cartesian grid by noting which circles coincide with a cartesian grid line for the X and Y direction. NASA

N91-23463# Lawrence Livermore National Lab., CA.
QUANTITATIVE FILM RADIOGRAPHY
G. Devine, D. Dobie, J. Fugina, J. Hernandez, C. Logan, P. Mohr, R. Moss, B. Schumacher, E. Updike, and D. Weirup 26 Feb. 1991 27 p
(Contract W-7405-eng-48)
(DE91-009718; UCRL-ID-106201) Avail: NTIS HC/MF A03

A system of quantitative radiography was developed in order to produce quantitative images displaying homogeneity of parts. The materials characterized are synthetic composites and may contain important subtle density variations not discernible by examining a raw film x radiograph. In order to quantitatively interpret film radiographs, it is necessary to digitize, interpret, and display the images. The integrated system of quantitative radiography displays accurate, high resolution pseudo-color images in units of density. Approximately 10,000 parts per year were characterized in hundreds of different configurations and compositions with this system. The following areas are discussed: the method; film processor monitoring and control; verifying film and processor performance; and correction of scatter effects. DOE

N91-23464# California Univ., Berkeley. Lawrence Berkeley Lab.
POSSIBILITIES FOR PROJECTION X RAY LITHOGRAPHY USING HOLOGRAPHIC OPTICAL ELEMENTS
M. R. Howells and C. Jacobsen Dec. 1990 4 p Presented at the Soft X Ray Projection Lithography Topical Meeting, Monterey, 10-12 Apr. 1991
(Contract DE-AC03-76SF-00098)
(DE91-009770; LBL-30057; CONF-9104203-1) Avail: NTIS HC/MF A01

Although there is a considerable literature on proximity x ray lithography, the interest in projection x ray techniques has arisen fairly recently, mainly due to the efforts of the AT and T group. The advantages of the projection approach seem to be the elimination of transmission masks and other problems of close proximity, the opportunity for demagnifying a mask of a coarser spatial scale, and, given a rigid, reflection mask, the possibility of cooling. The assumption behind the pursuit of these advantages is that the technical challenges of making the optical system that will perform the projection and the x ray source that will illuminate it are tractable on some timescale. The optical fabrication tolerances and other design issues involved in carrying out projection using a conventional reflection system have been investigated by Rogers and Jewell. These authors find that the needed tolerances are well beyond the present state of the art even for spherical surfaces and the required surfaces in these schemes are aspheric. An alternative approach is presented to the process of projection which, of course, has its own, different challenges. It is a matter of one's judgment and technological starting point to decide which one of these (or other) approaches will provide the easiest path to a working x ray projection lithography. DOE

N91-23465# Lawrence Livermore National Lab., CA.
A SUBMICRON RESOLUTION MONOLITHIC CAPACITIVE DISPLACEMENT SENSOR WITH DIGITAL OUTPUT
W. Current and Pak Shing Chau 31 Oct. 1990 40 p Prepared in cooperation with California Univ., Davis, CA
(Contract W-7405-eng-48)
(DE91-009765; UCRL-CR-105944) Avail: NTIS HC/MF A03

The goal of the project is to design, layout, fabricate, and test a monolithic capacitive displacement sensor prototype. This design is initially motivated for application in electronic tagging devices; however, the final design is general enough for other applications, such as monitoring movement of micro-machine parts. This new design utilizes a split grating electrodes configuration which makes the extraction of displacement information more convenient than other configurations. The measurement resolution is designed to be less than 1 micron. The overall design takes one master clock input, one reset input and requires 5V and (+ or -) 2.5V power supplies and several external resistors. The output is 9-bit digital encoding of the displacement measured. One of the advantages of a capacitive displacement sensor is that it works on a noncontacting measurement principle. It is non-invasive, compact, and its sensitivity to spurious rotation, tilt or transverse movement of the electrode planes is very small. Applications of this type of sensor are numerous. For instance, calipers, electronic tagging devices, and a displacement feedback block for micromachined structures. DOE

N91-23466# SRI International Corp., Menlo Park, CA. Molecular Physics Lab.
CHANNEL DIAGNOSTICS FOR THE MULTI-PULSE-PROPAGATION EXPERIMENTS AT ATA
K. R. Stalder, M. S. Williams, and D. J. Eckstrom Nov. 1990 62 p
(Contract W-7405-eng-48)
(DE91-009772; UCRL-CR-106596) Avail: NTIS HC/MF A04

Three different channel diagnostic instruments were prepared for the Fall and Winter 1989 to 1990 Advanced Test Accelerator (ATA) multi-pulse propagation experiments. The first diagnostic consisted of an eight beam laser deflection measurement of channel density profiles and time histories. Reduced density channels were observed under a variety of accelerator operating conditions. The magnitude, size, and position of these channels were measured and are explained on the basis of the prevailing beam conditions. The second diagnostic, consisting of optical emission measurements of beam currents and channel temperatures, confirmed previous observations of shorter optical Faraday cup pulses and, under some operating conditions, behavior uncorrelated with beam bug signals. The latter observations may be related to beam hose instabilities. Vibrational temperatures deduced from the optical fluorescence signals also show a trend of increasing during the later pulses in a burst. The third diagnostic, a CO2 interferometer designed to measure on-axis conductivity levels, was built but not deployed. DOE

N91-23467 National Physical Lab., Teddington (England).
SCATTERING IN ELECTRON SPECTROMETERS
M. P. Seah Jan. 1991 30 p
(NPL-DMM(A)-19; ISSN-0959-2423; ETN-91-99119) Copyright Avail: National Physical Laboratory, Teddington, TW11 0LW, England

The unwanted scattering of electrons in electron spectrometers leads to a loss of sensitivity, distortion of the spectral background, and problems in calibrating spectrometer intensity/energy transmission functions. Methods to analyze the extent of the contribution and how to reduce it to a significant level are developed. It appears that in the spectrometer, the major contribution arises from high energy electrons which strike the outer hemisphere giving rise to a spectrum of secondary electrons. These cause the scattered electron contribution to vary as Ep(exp -2.3), where Ep is the pass energy, to increase approximately in proportion to the spectrometer input slit area, to fall approximately inversely with an increase in the lens magnification from 1 to 3 and in the constant Delta E made, to increase with the analyzed electron energy. Thus, for each lens magnification, there exists a range of slits and pass energies for which the scattering may be maintained at less than 1 percent. ESA

N91-23468# Aerospatiale, Cannes (France).
ISOCAM: THE ISO'S SATELLITE INFRA-RED CAMERA
L. deSa and S. Taride 1991 7 p
(Rept-911-440-104; CA-5/90; ETN-91-99306) Avail: NTIS HC/MF A02

The main thermal analysis and definition problems and the cryogenic breadboard test difficulties of ISOCAM are reviewed. ISOCAM is an infrared camera experiment to be mounted aboard the ISO (Infrared Space Observatory) satellite. The misssion is to collect data on near infrared wavelength astronomy (2 to 200 microns). The telescope is cooled down through an open loop of superfluid helium. The cold source interface which cools down detectors, stepping motors, wheels, mechanisms, filters, lenses and mirror, is detailed. ESA

N91-23469# Ballistic Research Labs., Aberdeen Proving Ground, MD.
TIME RATES OF GENERALIZED STRAIN TENSORS. PART 1: COMPONENT FORMULAS Final Report, Jan. - Aug. 1990
Michael J. Scheidler Jan. 1991 27 p
(AD-A232497; BRL-TR-3195) Avail: NTIS HC/MF A03 CSCL 12/2

Hill derived a simple component formula for the material time derivative of a generalized Lagrangian strain tensor. We examine Hill's derivation in detail and explain why it is generally valid only when the principal stretches are distinct. We then give a proof of Hill's formula which is valid for any C2 motion and any C1 strain measure. Our proof is based on a component form of the chain rule for a tensor valued function of a time-dependent symmetric tensor. This result is also used to derive component formulas for the Jaumann rate of a generalized Eulerian strained tensor. Finally, we apply the general formulas to the logarithmic strain tensors. GRA

N91-23470# Case Western Reserve Univ., Cleveland, OH.
HIGH ENERGY DENSE RIBBON BEAMS AND HIGH HARMONIC GYROTRON AT MILLIMETER WAVELENGTHS Final Report, 1 Mar. 1986 - 30 Jun. 1990
Altan M. Ferendeci 10 Jan. 1991 105 p
(Grant AF-AFOSR-0114-86; AF Proj. 2301)
(AD-A232839; AFOSR-91-0160TR) Avail: NTIS HC/MF A06 CSCL 12/5

The progress made on the ribbon (sheet) beams and the rectangular harmonic gyrotron is presented. A relativistic three dimensional electron gun simulation program, called 3-D TRAJ is completed. A 3-D general numerical Poisson solvers is included in the program to take into account the nonuniform electrode boundaries that are common to ribbon beam guns or that may be required for any other gun structure. A novel computer technique is developed to generate the complicated 3-D general boundary data file of the MIG type guns by using a bot-map technique. At the same time, a theoretical approach to the design of MIG type guns is also undertaken. The location and the shape of the cathode is determined from the various conservation equations. Using the laminar flow equations and Harker synthesis technique, the required anode shapes are then determined. Finally, the resulting electrode shapes are used in the simulation of the MIG-gun using the 3-D TRAJ program. Experimental set-up to test the various MIG type electron guns and the axially grooved rectangular gyrotron is close to being completed. GRA

N91-23471# Woods Hole Oceanographic Inst., MA.
ARCTIC REMOTE AUTONOMOUS MEASUREMENT PLATFORM POST CEAREX ENGINEERING REPORT
K. R. Peal Nov. 1990 73 p
(Contract N00014-86-C-0126)
(AD-A232843; WHOI-90-46) Avail: NTIS HC/MF A04 CSCL 14/3

A series of instrumented Arctic buoys has been developed. The buoys are designed to be deployed in pack ice to measure and record data from meteorological and ocean sensors as well as from an accelerometer inside the buoy. Sophisticated in-situ data processing is performed reducing the data capacity required for the system's optical disk recorder. Engineering development is described which aimed to identify and solve performance problems related to hardware and software deficiencies. One of the major hardware problems was that the optical disk was unreliable when exposed to the Arctic environment. Redesign was performed to insulate parts of the system from the cold. The test and evaluation sequence is described as well as the present status of all portions of the system. Sample field data are presented including multiband acoustic spectra as well as time series environmental data. GRA

36 LASERS AND MASERS

Includes parametric amplifiers.
For related information see also *76 Solid-State Physics.*

N91-23472*# National Aeronautics and Space Administration. Langley Research Center, Hampton, VA.
BIREFRINGENT FILTER DESIGN Patent Application
Clayton H. Bair, inventor (to NASA) 8 Apr. 1991 19 p
(NASA-Case-LAR-13887-1; NAS 1.71:LAR-13887-1; US-Patent-Appl-SN-681288) Avail: NTIS HC/MF A03 CSCL 20E

A birefringent filter is provided for tuning the wavelength of a broad band emission laser. The filter comprises thin plates of a birefringent material having thicknesses which are non-unity, integral multiples of the difference between the thicknesses of the two thinnest plates. The resulting wavelength selectivity is substantially equivalent to the wavelength selectivity of a conventional filter which has a thinnest plate having a thickness equal to this thickness difference. The present invention obtains an acceptable tuning of the wavelength while avoiding a decrease in optical quality associated with conventional filters wherein the respective plate thicknesses are integral multiples of the thinnest plate. NASA

N91-23473 Saint Andrew's Univ. (Scotland).
OPTICAL PARAMETRIC OSCILLATORS PUMPED BY EXCIMER LASERS Ph.D. Thesis
Majid Ebrahimzadeh 1989 219 p
Avail: Univ. Microfilms Order No. BRDX91075

The development of a new generation of pulsed optical parametric oscillators (OPO's) is described. These oscillators are based on two nonlinear materials, urea and beta-BaB2O4 (BBO), and pumped by excimer lasers to provide broadly tunable coherent radiation in new regions of the electromagnetic spectrum, particularly in the ultraviolet and the visible. The constructed pump laser was used to investigate spontaneous parametric fluorescence in a home grown urea sample, in order to characterize the crystal and to compare the observed spectrum with the calculated OPO turning curves. The main thrust of the project was the development of an OPO based on urea as the nonlinear medium and pumped at 308 nm by the narrow band XeCl excimer laser. Such an OPO was successfully constructed using an 8-mm-long home grown crystal, and continuously tunable output from 572 to 667 nm was generated with a 2.5 percent energy conversion efficiency. The tuning range of the device was later extended to 537 to 720 nm by utilizing a 15-mm-long homegrown urea sample. Its conversion efficiency was improved to as high as 37 percent and 90 degree phase-matching, with a greater than or equal to 10 percent efficiency over a 100 nm range in the visible spectrum. Finally, in an effort to achieve even higher efficiencies, experiments in a 25-mm-long commercial urea crystal were performed, and exceptionally high external energy conversion efficiencies were demonstrated. The latter part of the project was concerned with the design and development of a similar device based on the nonlinear material, BBO, to provide continuously tunable radiation over a much broader tuning range, particularly in the blue and the near ultraviolet. Dissert. Abstr.

N91-23474 California Univ., Berkeley.
STUDY OF PHASE-LOCKED DIODE LASER ARRAY AND DFB/DBR SURFACE EMITTING LASER DIODE Ph.D. Thesis
Wei Hsin 1990 213 p
Avail: Univ. Microfilms Order No. DA9103725

New types of phased-array and surface-emitting lasers are designed. The importance and approaches (or structures) of different phased array and surface emitting laser diodes are reviewed. The following are described: (1) a large optical cavity channel substrate planar laser array with layer thickness chirping; (2) a vertical cavity surface emitter with distributed feedback (DFB) optical cavity and a transverse junction buried heterostructure; (3) a microcavity distributed Bragg reflector (DBR) surface emitter; and (4) two surface emitting laser structures which utilized lateral current injection schemes to overcome the problems occurring in the vertical injection scheme. Dissert. Abstr.

N91-23475 Georgia Inst. of Tech., Atlanta.
SIGNALS AND NOISE IN LASERS AND ATOM-FIELD INTERACTIONS Ph.D. Thesis
Gautam Vemuri 1990 406 p
Avail: Univ. Microfilms Order No. DA9105469

The interaction of signals and noise in tunable lasers and the interaction of two-level atoms with intense fluctuating laser fields were studied. Numerical methods were developed and used to study otherwise intractable problems. A fast, accurate numerical algorithm was developed to simulate exponentially correlated noise, and was used to study several different types of problems. The effect of injected signals on the transient dynamics of a dye laser, the counter intuitive phenomena of stochastic resonance, the pulse height statistics of synchronously pumped dye lasers, and the development of a Monte Carlo technique for the study of a two-level atom interacting simultaneously with a coherent and a chaotic field are studied. Dissert. Abstr.

N91-23476# Brookhaven National Lab., Upton, NY.
SPATIAL DYNAMICS OF PICOSECOND CO2 LASER PULSES PRODUCED BY OPTICAL SWITCHING IN Ge
I. Pogorelsky, A. S. Fisher, J. Veligdan, and P. Russell (Princeton Univ., NJ.) 1991 13 p Presented at the 4th Society of Photo-Optical Instrumentation Engineers (SPIE) International Symposium, Los Angeles, 20-25 Jan. 1991
(Contracts DE-AC02-76CH-00016; DE-AC06-83ER-40128)
(DE91-010368; BNL-45802; CONF-910123-22) Avail: NTIS HC/MF A03

The design, test and optimization of a picosecond CO2 pulse-forming system are presented. The system switches a semiconductor's optical characteristics at 10 microns under the control of a synchronized 1.06-micron Nd:YAG picosecond laser pulse. An energy-efficient version of such a system using collimated beams is described. A simple, semi-empirical approach is used to simulate the switching process, specifically including the spatial distributions of the laser energy and phase, which are relevant for experiments in laser-driven electron acceleration. DOE

N91-23477# Sandia National Labs., Albuquerque, NM.
STRAINED QUANTUM WELL LEAKY-MODE DIODE LASER ARRAYS
T. H. Shiau, S. Sun, C. F. Schaus, K. Zheng (New Mexico Univ., Albuquerque.), G. R. Hadley, and J. P. Hohimer 1991 7 p Presented at the OE/LASE 1991: 4th Society of Photo-Optical Instrumentation Engineers (SPIE) International Symposium, Los Angeles, 20-25 Jan. 1991
(Contract DE-AC04-76DP-00789)
(DE91-009982; SAND-90-1745C; CONF-910123-18) Avail: NTIS HC/MF A02

A new type of diode laser array (denoted leaky-mode or antiguided) has recently been reported. Despite their success, these devices are difficult to fabricate since they require a deep wet-chemical etch which must be accurately controlled. The authors report a new strained GaInAs quantum well device structure which is produced by etching a thin (0.12 microns), transparent GaAs waveguide layer. These devices have demonstrated fundamental mode operation up to 2 A (172 mW/per facet at 1 A) at 1 percent duty cycle pulsed condition and 700 mA (62.5 mW/per facet) for CW operation. DOE

N91-23478# Lawrence Livermore National Lab., CA.
HIGH-POWER PERFORMANCE OF A COPPER LASER PUMPED DYE MASTER-OSCILLATOR-POWER-AMPLIFIER CHAIN
I. L. Bass, E. S. Bliss, R. E. Bonanno, P. M. Castle, M. Feldman, R. P. Hackel, P. R. Hammond, S. A. Johnson, R. Kichinski, and K. P. Neeb et al 1991 7 p Presented at the CLEO 1991: Conference on Lasers and Electro-Optics, Baltimore, 12-17 May 1991
(Contract W-7405-eng-48)
(DE91-010460; UCRL-JC-105285; CONF-910595-8) Avail: NTIS HC/MF A02

A dye master-oscillator-power-amplifier chain pumped by copper lasers produced 1200 W output at 50 percent conversion efficiency and a greater than 10 kHz pulse repetition frequency. A description of the amplifier chain is presented. DOE

N91-23479# Lawrence Livermore National Lab., CA.
A 43 WATT CW TI:SAPPHIRE LASER
G. V. Erbert, I. L. Bass, R. P. Hackel, S. Jenkins, K. Kanz, and J. A. Paisner 1991 8 p Presented at the CLEO '91: Conference on Lasers and Electro-Optics, Baltimore, 12-17 May 1991
(Contract W-7405-eng-48)
(DE91-010468; UCRL-JC-105286; CONF-910595-7) Avail: NTIS HC/MF A02

Using four argon-ion lasers to pump a 2-rod Ti:Sapphire laser we have achieved 43 watts CW output power at high efficiency with a low order spatial mode. The laser was enclosed in a vacuum system and the rods were cooled with liquid nitrogen to minimize thermally induced aberrations in the rods. DOE

N91-23480# New York Univ., New York. Dept. of Physics.
THEORETICAL STUDIES RELATING TO THE INTERACTION OF RADIATION WITH MATTER Final Report, 1 Aug. 1987 - 31 Dec. 1990
P. R. Berman 15 Feb. 1991 12 p
(Contract N00014-87-K-0303)
(AD-A232107) Avail: NTIS HC/MF A03 CSCL 20/5

The following topics are discussed: (1) coherent transients; (2) laser spectroscopy, (3) pressure induced resonances; (4) laser assisted collisions; (5) quantum jumps; (6) interaction of atoms with broad band width radiation; (7) exchange collision kernel; (8) laser cooling of neutral atoms; (9) laser assisted collisions; (10) magnetic state polarization; and (11) broadband noise. GRA

N91-23481# Ortel Corp., Alhambra, CA.
VERTICAL EMITTING, RING GEOMETRY, ULTRA-LOW THRESHOLD AND ULTRA-HIGH SPEED QUANTUM WELL LASERS FOR OPTICAL INTERCONNECT Final Report, Jul. 1988 - Dec. 1990
Michael Mittelstein and Nadav Bar-Chaim Jan. 1991 131 p
(Contract N00014-88-C-0483; DARPA Order 6325)
(AD-A232122) Avail: NTIS HC/MF A07 CSCL 09/3

The main emphasis for this contract was placed on the efforts as highlighted in the chapter captions: (1) introduction to optical interconnects, (2) conventional laser; (3) design of laser structures; (4) achieving buried ring structures; (5) buried ring quantum well structure, (6) champion results and reproducibility of buried lasers; (7) ridge wave guide laser fabrication; (8) grating fabrication; (9) grating fabrication facility; (10) test station; and (11) material investigation. GRA

N91-23482# Air Force Inst. of Tech., Wright-Patterson AFB, OH.
A NUMERICAL MODEL OF LASER INDUCED FLUORESCENCE IN A HYDROGEN PLASMA Ph.D. Thesis
Marc R. Hallada 11 Sep. 1990 212 p
(AD-A232240; AFIT/CI/CIA-90-037D) Avail: NTIS HC/MF A10 CSCL 20/5

Discrepancies between observed and predicted level populations before and during laser induced fluorescence in a hydrogen plasma are partially resolved using improved numerical models. The plasma parameters investigated (.45 Torr is less than or = 1 eV) correspond to the z-pinch plasma produced in the LIF experiments. Using a rate equation model, it is found that the H-ion and the molecular species H2, H2(+), and H3(+) play important roles in such plasmas. The dissociative recombination of H2(+) and H3(+) preferentially populate the n = 3 and n = 2 atomic hydrogen levels, respectively. Vibrationally excited H2 produces H- via dissociative attachment, while the mutual neutralization of H- and H+ populates the n = 3 level. In addition, the initial z-pinch appears to cause electrons and ions to stream directly to the walls, where they remain attached for several hundred microseconds. This reduces the plasma density by over 50 percent and causes ambipolar diffusion to overshadow recombination in the electron density decay. With these additional species and processes, many of the experimental observables, both before and during laser illumination, are reproduced. The agreement with experiment is further improved by a kinetics equation model which confirms the importance of radiation trapping and its role in producing a hot, non-Maxwellian bump in the electron distribution in the vicinity of 10 eV. GRA

N91-23483# Illinois Univ., Urbana. Dept. of Electrical and Computer Engineering.
BROAD AREA DISTRIBUTED GAIN, DISTRIBUTED INDEX PROFILE GaAlAs SEMICONDUCTOR LASER DIODES Final Report, 15 Jan. 1988 - 14 Jan. 1991
James J. Coleman 14 Feb. 1991 96 p
(Contract N00014-88-K-2005)
(AD-A232332) Avail: NTIS HC/MF A05 CSCL 09/3

High-power operation of a simple non-planar index-guided quantum well heterostructure periodic laser array structure is described, in which lateral lasing is prevented in a manner that

still allows for uniform and continuous front facet light emission. The compositional disordering and compensation effects of MeV oxygen implantation have been applied to form stripe geometry graded barrier quantum well heterostructure lasers. A new broad area as well as narrow stripe window laser structure is described, in which a nonabsorbing window region is formed in the vicinity of the mirror facets by utilizing a selectively etched substrate and the advantageous properties of uniform MOCVD growth on nonplanar substrates. The growth and characterization of strained layer InGaAs-GaAs heterostructure lasers by MOCVD has been addressed. Ethyldimethylindium has been shown to be suitable as a precursor for the growth of indium compounds. The results of time-zero characterization of strained-layer In(x)Ga(1-x)As-GaAs quantum well heterostructure laser diodes with 70-A-thick wells and indium mole fractions between 0.08 and 0.42 are reported. High power, in-phase locked operation of a wide aperture array is reported in which the lateral lasing and amplified spontaneous emission, characteristic of wide aperture arrays, are suppressed by a nonplanar active region. The antiguiding behavior of InGaAs-GaAs strained layer lasers has been exploited for form multiple-element oxide-defined-stripe phase-locked high power long wavelength (lambda greater than 0.95 microns) strained layer quantum well heterostructure diode arrays operating in the in-phase fundamental array mode. GRA

N91-23484# New Orleans Univ., LA.
BIMANES AND RELATED HETEROCYCLES AS LASER DYES
J. H. Boyer 10 Jan. 1991 29 p
(Contract DAAL03-89-K-0161)
(AD-A232335; ARO-27529.1-CH) Avail: NTIS HC/MF A03 CSCL 09/3

The relative efficiencies (RE) for laser activity in the spectral region 500 to 530 nm were obtained for 37 syn-bimanes by reference to coumarin 30 (RE 100). The RE for laser activity in the spectral region 520 to 620 nm were obtained for over 20 pyrromethene-BF2 complexes (P-BF2) by reference to rhodamine 6G (RE 100). GRA

N91-23485# Dayton Univ., OH. Graduate School of Engineering and Research.
STUDIES OF NOISE IN SEMICONDUCTOR LASER ARRAYS Final Report, Feb. 1989 - Feb. 1990
Elsa Garmire, Ramadas Pillai, and Pedro Menendez-Valdes Dec. 1990 62 p Prepared in cooperation with University of Southern California, Los Angeles
(Contract F30602-88-D-0028)
(AD-A232411; RADC-TR-90-401; Rept-93928-12/RI-62240X)
Avail: NTIS HC/MF A04 CSCL 09/3

Measurements were made of noise in laser arrays, both commercial gain-guided and experimental 10 element index-guided. Relative Intensity Noise (RIN) was found to be comparable to single element gain guided arrays, with approximately 15 dB more noise than from a distributed feedback (DFB) laser. Comparable results for gain-guided and index-guided lasers, with supporting theoretical studies, indicate that mode competition is probably the source of the increased noise. Because the arrays produce more power, the increased noise does not necessarily degrade the signal-to-noise ratio. The results indicate that if the system is operating in the receiver-noise-limited regime (less than 0.1 milliwatts of detected optical power), use of an array will increase the overall signal-to-noise ratio. It was also shown that a reduction in laser noise can be achieved by low frequency modulation. For example, modulation at 10 MHz resulted in a decrease in noise by 5 to 10 dB at 100 MHz. GRA

N91-23486# Naval Research Lab., Washington, DC.
A NEW ASYMPTOTIC THEORY FOR THE PERIODICALLY FORCED LASER Interim Report
Thomas Erneux and Ira B. Schwartz 19 Feb. 1991 15 p Prepared in cooperation with Northwestern Univ., Evanston, IL
(AD-A232633; NRL-MR-6787) Avail: NTIS HC/MF A03 CSCL 09/3

Sustained relaxation oscillations and irregular spiking have been observed in many periodically modulated lasers. These observations have been substantiated numerically by recent studies of the laser rate equations. In this paper, we propose a new asymptotic analysis of the laser equations which assumes that the laser oscillations correspond to relaxation oscillations. We identify a large parameter and construct these periodic solutions using perturbation techniques. We obtain the equations for the Poincare map and determine the first period doubling bifurcation. GRA

N91-23487# Army Environmental Hygiene Agency, Aberdeen Proving Ground, MD.
LASER HAZARDS BIBLIOGRAPHY, JANUARY 1991
David H. Sliney, Anita Robinson, and Shawn Sparks 31 Jan. 1991 278 p
(AD-A232690) Avail: NTIS HC/MF A13 CSCL 09/3

The Laser Hazards Bibliography consists of 3414 references in the open literature broken into subject categories which relate to general biological effects, the eye, the skin, laser safety, laser propagation in the atmosphere, and laser measurements. GRA

N91-23833# Tel-Aviv Univ. (Israel). School of Physics and Astronomy.
TEMPERATURE DISTRIBUTION AND THERMAL DAMAGE DURING TISSUE ABLATION BY CO2 LASER IRRADIATION: MODEL AND EXPERIMENT Abstract Only
A. Avidor, A. Sagi, A. Katzir, and S. Akselrod *In its* Bulletin of the Israel Physical Society, Volume 33, 1987. Annual Meeting 1987: Program and Abstracts 1987 p 17 (For primary document see N91-23832 15-70)
Avail: NTIS HC/MF A08

N91-24077*# National Aeronautics and Space Administration. Langley Research Center, Hampton, VA.
FREQUENCY DOMAIN LASER VELOCIMETER SIGNAL PROCESSOR
James F. Meyers and R. Jay Murphy (Macrodyne, Inc., Clifton Park, NY.) *In* NASA, Washington, Technology 2000, Volume 2 1991 p 315-324 (For primary document see N91-24041 15-99)
Avail: NTIS HC/MF A16 CSCL 20E

N91-24079*# National Aeronautics and Space Administration. Goddard Space Flight Center, Greenbelt, MD.
LASER OPTICAL DISK POSITION ENCODER WITH ACTIVE HEADS
Eric P. Osborne *In* NASA, Washington, Technology 2000, Volume 2 1991 p 333-340 (For primary document see N91-24041 15-99)
Avail: NTIS HC/MF A16 CSCL 20E

37 MECHANICAL ENGINEERING

Includes auxiliary systems (nonpower); machine elements and processes; and mechanical equipment.

N91-23488 Minnesota Univ., Minneapolis.
A TRIBOLOGICAL STUDY OF SLIDING CONTACT INTERACTION Ph.D. Thesis
Ciuter Chang 1990 128 p
Avail: Univ. Microfilms Order No. DA9100930

In order to explore the role of a protective overcoat and to understand its mechanical response under sliding contact interaction, detailed stress analysis was performed. Various material properties such as elastic stiffness, thickness, plastic deformation, and residual stress were investigated. It was found that elastic stiffness affects the stress distribution significantly. The stiffer the coating layer is, the lower the stress state of the substrate. The interface between the coating layer and the substrate plays a critical role since the stress is highly concentrated around the interface region. It was found that the stress state would be improperly estimated for materials which behave elasto-plastically if only elastic analysis is performed. The residual stress state in

the coating layer has important effects on the tribological performance, e.g., a compressive residual stress in the coating layer would reduce the stress state while tensile residual stress would enhance the stress state in the coating layer.
Dissert. Abstr.

N91-23489# Ohio State Univ., Columbus. Dept. of Electrical Engineering.
AUTOMATED HANDLING AND ASSEMBLING OF NON-RIGID OBJECTS Semiannual Report No. 2, 15 Jul. 1990 - 14 Jan. 1991
Yuan F. Zheng 14 Jan. 1991 65 p
(Contract N00014-90-J-1516)
(AD-A231246) Avail: NTIS HC/MF A04 CSCL 23/3

Three topics were studied. The first topic addresses the strategies of automated handling and assembling of non-rigid objects by using multiple end effectors, the second topic studies the shape reconstruction of two dimensional objects, and the third topic is the construction of a laser range finder for identification of the third dimension of an object. The first topic investigated optimal tool structures for handling 1-D and 2-D objects. Previously, Vacuum pads were proposed to pick up large deformable sheet by the difference of the air pressure. By using two ordinary end effectors, just like the two hands of human beings, deformable objects can be manipulated without using a large tool. The study has developed an optimal mechanism for coordinating the end effectors so the machine consumes the minimum energy and no damage is made to the object. The second topic identifies the deformed shape of 1-D objects. For 2-D objects, there does not exist closed form solution to the governing equation of the deformation. Our goal is to sense a few data points on the deformed surface. Based on these points, a numerical model can be driven which can reconstruct the entire surface with a good approximation. This numerical model can also be modified to deformation behavior of the object. The third topic develops a laser range finder so all 3-D of an object can be identified. The laser range finder is a very important tool for the research, since a 2-D object becomes 3-D once it is deformed. For 3-D objects, the thrid dimension is important to completely identify the shape of an object ever before the deformation occurs. GRA

N91-23490*# National Aeronautics and Space Administration. Lyndon B. Johnson Space Center, Houston, TX.
ELECTROMAGNETIC ATTACHMENT MECHANISM Patent Application
Leo G. Monford, Jr., inventor (to NASA) 31 Dec. 1990 36 p
(NASA-Case-MSC-21463-1; NAS 1.71:MSC-21463-1;
US-Patent-Appl-SN-636531) Avail: NTIS HC/MF A03 CSCL 13I

An electromagnetic attachment mechanism is disclosed for use as an end effector of a remote manipulator system. A pair of electromagnets, each with a U-shaped magnetic core with a pull-in coil and two holding coils are mounted by a spring suspension system on a base plate of the mechanism housing with end pole pieces adapted to move through openings in the base plate when the attractive force of the electromagnets is exerted on a strike plate of a grapple fixture affixed to a target object. The pole pieces are spaced by an air gap from the strike plate when the mechanism first contacts the grapple fixture. An individual control circuit and power source is provided for the pull-in coil and one holding coil of each electromagnet. A back-up control circuit connected to the two power sources and a third power source is provided for the remaining holding coils. When energized, the pull-in coils overcome the suspension system and air gap and are automatically de-energized when the pole pieces move to grapple and impose a preload force across the grapple interface. A battery backup is a redundant power source for each electromagnet in each individual control circuit and is automatically connected upon failure of the primary source. A centerline mounted camera and video monitor are used in cooperation with a target pattern on the reflective surface of the strike plate to effect targeting and alignment. NASA

N91-23491*# National Aeronautics and Space Administration. Lyndon B. Johnson Space Center, Houston, TX.
METALLIC THREADED COMPOSITE FASTENER Patent Application
Thomas J. Dunn, inventor (to NASA) 31 Jan. 1991 14 p
(NASA-Case-MSC-21580-1; NAS 1.71:MSC-21580-1;
US-Patent-Appl-SN-648772) Avail: NTIS HC/MF A03 CSCL 13I

A metallic threaded composite fastener, particularly suited for high temperature applications, has a body member made of high temperature resistant composite material with a ceramic coating. The body member has a head portion configured to be installed in a countersunk hole and a shank portion which is noncircular and tapered. One part of the shank may be noncircular and the other part tapered, or the two types of surface could be combined into a frustum of a noncircular cone. A split collar member made of high strength, high temperature tolerant metal alloy is split into two halves and the interior of the halves are configured to engage the shank. The exterior of the collar has a circumferential groove which receives a lock ring to secure the collar halves to the shank. In the assembled condition torque may be transmitted from the body to the split collar by the engaged noncircular portions to install and remove the fastener assembly into or from a threaded aperture and shear loads in the collar threads are transferred to the shank tapered portion as a combination of radial compression and axial tension loads. Thus, tension loads may be applied to the fastener shank without damaging the ceramic coating. NASA

N91-23492*# National Aeronautics and Space Administration. Lyndon B. Johnson Space Center, Houston, TX.
ENERGY DISSIPATOR Patent Application
Horacio M. DeLaFuente, inventor (to NASA), Kornel Nagy, inventor (to NASA), and Clarence J. Wesselski, inventor (to NASA) 15 Feb. 1991 17 p
(NASA-Case-MSC-21555-1; NAS 1.71:MSC-21555-1;
US-Patent-Appl-SN-656925) Avail: NTIS HC/MF A03 CSCL 13I

An all metal energy dissipator construction is disclosed for dissipating kinetic energy force (F) by rolling balls which are forced by a tapered surface on an expandable sleeve to frictionally load a force rod. The balls are maintained in an initial position by a plate member which is biased by a spring member. A spring member returns the force rod to its initial position after a loading force is removed. NASA

N91-23493*# National Aeronautics and Space Administration. Lyndon B. Johnson Space Center, Houston, TX.
PRELOADED LATCHING DEVICE Patent Application
Clarence J. Wesselski, inventor (to NASA) and Kornel Nagy, inventor (to NASA) 25 Feb. 1991 20 p
(NASA-Case-MSC-21730-1; NAS 1.71:MSC-21730-1;
US-Patent-Appl-SN-660755) Avail: NTIS HC/MF A03 CSCL 13I

A latching device is disclosed which is lever operated sequentially to actuate a set of collet fingers to provide a radial expansion and to actuate a force mechanism to provide a compressive gripping force for attaching first and second devices to one another. The latching device includes a body member having elongated collet fingers which, in a deactuated condition, is insertable through bores on the first and second devices so that gripping terminal portions on the collet fingers are proximate to the end of the bore of the first device while a spring assembly on the body member is located proximate to the outer surface of a second device. A lever is rotatable through 90 deg to move a latching rod to sequentially actuate and expand collet fingers and to actuate the spring assembly by compressing it. During the first 30 deg of movement of the lever, the collet fingers are actuated by the latching rod to provide a radial expansion and during the last 60 deg of movement of the lever, the spring assembly acts as a force mechanism and is actuated to develop a compressive latching force on the devices. The latching rod and lever are connected by a camming mechanism. The amount of spring force in the spring assembly can be adjusted; the body member can be

permanently attached by a telescoping assembly to one of the devices; and the structure can be used as a pulling device for removing annular bearings or the like from blind bores. NASA

N91-23494 Iowa Univ., Iowa City.
COMPUTATIONAL LIFE PREDICTION METHODOLOGY FOR MECHANICAL SYSTEMS USING DYNAMIC SIMULATION, FINITE ELEMENT ANALYSIS, AND FATIGUE LIFE PREDICTION METHODS Ph.D. Thesis
Woon Kyung Baek 1990 178 p
Avail: Univ. Microfilms Order No. DA9103187

An integrated life prediction methodology using dynamic simulation, finite element analysis, the fatigue life prediction method, and experimental validation for the finite life evaluation of a mechanical system are presented. As a practical example, a multi-body dynamic model of an existing ground vehicle was developed, using kinematic joints and components. The vehicle model was hypothetically run over a measured road profile at constant speed. From this dynamic analysis, load histories were obtained for each component. A lower control arm, which is a critical suspension component, was selected for the component fatigue life prediction, and a finite element model of this component was developed. Several high stress regions were identified from the finite element stress analysis. Local notch stresses at each high stress region were then obtained at potential fatigue crack initiation points, which can be called potential fatigue critical locations (PFCL's). Dynamic stress histories at PFCL's were produced by the quasi-static approach. The local strain life method was used to predict fatigue lives of each PFCL. To validate this computerized procedure, the lower control arm was experimentally tested for stress and fatigue durability. The brittle coating method was used to identify high stress regions. Experimental stress analysis was performed using strain gages. The experimental results and predicted results based upon finite element analysis were very close. Also, fatigue durability tests were done for the component by repeatedly applying the same load history that was applied to the finite element model until a ¿ mm long fatigue crack formed. The breakthrough in this integration is that dynamic stress and fatigue life can be predicted in early design stages without experimental measurement of either loads or stresses.
Dissert. Abstr.

N91-23495 Iowa Univ., Iowa City.
H-INFINITY APPROACH TO MANIPULATOR CONTROL Ph.D. Thesis
Chang Ho Cho 1990 146 p
Avail: Univ. Microfilms Order No. DA9103198

Robust stability and performance in the presence of uncertainties have always been crucial issues in the synthesis of feedback control systems. The inherent difference between the real physical plant and its numerical design/analysis model yields plant uncertainty. In addition, external disturbances and changes in operating environment give rise to model uncertainty. Because the classical linear quadratic optimal control theory has no systematic way to deal with such uncertainties, H infinity optimal control theory has received great attention in recent years as a means to overcome them. However, a myriad of papers concerning the H infinity control theory published during the last decade have mainly focused on the qualitative points of view such as formulating general control problems in the H infinity framework and developing various solution techniques. A quantitative aspect of the theory is exploited. For this purpose, a highly nonlinear time-varying system, a robotic manipulator, is modeled as a linear time-invariant system. A robust tracking problem is then formulated as an H infinity optimization problem based on the linearized model. Using Yoular parameterization of all stabilizing controllers and Glover's algorithm for Hankel-norm approximation problems, the optimization problem is solved to yield a robust controller. Most real plants are strictly proper systems, so that an inner-outer factorization is not possible. Hence, the H infinity optimization problem can not be solved directly. To overcome that difficulty, a model reduction technique is introduced. Because the H infinity control theory yields a high order controller in general, the model reduction technique is again used to reduce the final order of the system. Dissert. Abstr.

N91-23496 Wisconsin Univ., Madison.
FINITE ELEMENT BASED DYNAMICAL MODELING OF FLEXIBLE OPEN-LOOP MANIPULATORS WITH EXPERIMENTAL RESULTS Ph.D. Thesis
Daniel W. Williams 1990 334 p
Avail: Univ. Microfilms Order No. DA9033802

The dynamic analysis of a two-link flexible open-loop manipulator is presented. Equations of motion based on a hybrid rigid body/finite element model are developed. The segregated finite element approach to modeling the separate links of the manipulator was developed. This leads to greater freedom in the selection of element types by eliminating inter-element compatibility requirements at the joints of the manipulator. In developing the equations of motion for this system, the Lagrange equation is separately applied to the rigid body and elastic displacement freedoms of each link. This leads to a coupled set of differential equations involving all the dynamic freedoms of the manipulator. The significance of this approach is that no assumptions about the rigid body motion are made. The resulting equations of motion include not only the standard linear finite element dynamic terms, but also several additional terms. These added terms represent important effects such as coupling between rigid body and elastic motion and nonlinear inertia loading phenomena. The presence of non-standard terms in the formulation precludes the use of standard finite element analysis solution procedures. Experimental results are presented for verification of the equations of motion developed in this work. Verification of the model is done through comparisons of experimental results with theoretical analysis in modal frequency predictions, forced time responses and free vibrational time responses. Two additional developments are included. In the first, an inverse kinematic analysis procedure is presented in which the effects of link deformations are included. The second development presented is that of a modified beam finite element which allows for regions of rigidity at either or both of the ends of the beam.
Dissert. Abstr.

N91-23497 Washington Univ., Saint Louis, MO.
AN ANALYTIC STUDY OF GENERAL DYNAMIC MODEL AND NONLINEAR FEEDBACK CONTROL OF FLEXIBLE ROBOT ARMS Ph.D. Thesis
Xuru Ding 1989 210 p
Avail: Univ. Microfilms Order No. DA9103984

Using Hamilton's principle, a complete dynamic model is derived for a large class of flexible robot arms under very general assumptions. The dynamic model is in the form of a set of integro partial differential equations and the dynamic boundary conditions associated with them. This complex dynamic model is reduced to its simpler version if a flexible robot arm consists of Euler Bernoulli beam links. The most important feature of the dynamic model is that it provides much more information than its finite dimensional counterparts for system analysis, error estimation, and control design. A two-joint flexible robot arm is used to illustrate the control scheme. State space expression of the dynamic model for this robot arm is derived which describes and infinite dimensional system in hybrid state variables (distributed and lumped). Nonlinear dynamic/static state feedback and diffeomorphic state transformations are utilized to achieve the input-output linearization and decoupling for two types of output functions reflecting end-effector position. Regulation and trajectory tracking schemes are discussed. The issue of stability of the closed-loop system is addressed in light of the concept of zero dynamics. By frequency domain analysis, the conclusion of local stability of the closed-loop system is reached. Finally, some suggestions on further research in this direction are given. Dissert. Abstr.

N91-23498# EG and G Mound Applied Technologies, Miamisburg, OH.
UNIPUNCH CAPABILITY STUDY
M. E. Sterrett and R. S. Ramachandran 25 Feb. 1991 13 p

(Contract DE-AC04-88DP-43495)
(DE91-008825; MLM-3679) Avail: NTIS HC/MF A03

A universal mechanical operating system (designated the Unipunch), which is a flexibly adjustable punching system used at Mound to punch clearance and tooling holes in flexible circuit materials, was studied to determine its capabilities. A designed experiment was done to investigate the possible effects of production variables on the parts produced. Results of the experiment showed that the consistency and reproducibility of the product is independent of such variables as sequence, operator, and removal and reinstallation of die stations, and that those variables which do affect product reproducibility can be easily controlled when the parts are punched for production. The study also showed that the parts punched by the Unipunch system would meet the requirements of Mound's tool certification program and eliminate many hours of inspection. DOE

N91-23499# Carnegie-Mellon Univ., Pittsburgh, PA. Dept. of Electrical and Computer Engineering.
ON KINEMATIC DESIGN OF SERIAL LINK MANIPULATORS
C. J. J. Paredis and P. K. Khosla 1991 15 p Presented at the International Symposium on Intelligent Robotics, Bangalore, India, Jan. 1991
(Contract DE-FG02-89ER-14042)
(DE91-009414; CONF-910188-1) Avail: NTIS HC/MF A03

The Reconfigurable Modular Manipulator System (RMMS) consists of modular links and joints which can be assembled into many manipulator configurations. This capability allows the RMMS to be rapidly reconfigured in order to custom tailor it to specific tasks. A important issue, related to the RMMS, is the determination of the optimal manipulator configuration for a specific task. The problem is addressed of mapping kinematic task specifications into a kinematic manipulator configuration. For the design of 2 degrees of freedom planar manipulators, an analytical solution is derived. Since, for problems with more than 2 design parameters, analytical solutions become impractical, a numerical approach was also developed for the design of 6 degrees of freedom manipulators. DOE

N91-23500*# National Aeronautics and Space Administration. Lewis Research Center, Cleveland, OH.
EFFECTS OF RIM THICKNESS ON SPUR GEAR BENDING STRESS
G. D. Bibel, S. K. Reddy, M. Savage, and R. F. Handschuh (Army Aviation Systems Command, Cleveland, OH.) 1991 14 p Presented at the 27th Joint Propulsion Conference, Sacramento, CA, 24-26 Jun. 1991; sponsored by AIAA, SAE, and ASME
(DA Proj. 1L1-62211-A-47-A)
(NASA-TM-104388; E-6197; NAS 1.15:104388; AVSCOM-TR-91-C-015) Avail: NTIS HC/MF A03 CSCL 13I

Thin rim gears find application in high-power, light-weight aircraft transmissions. Bending stresses in thin rim spur gear tooth fillets and root areas differ from the stresses in solid gears due to rim deformations. Rim thickness is a significant design parameter for these gears. To study this parameter, a finite element analysis was conducted on a segment of a thin rim gear. The rim thickness was varied and the location and magnitude of the maximum bending stresses reported. Design limits are discussed and compared with the results of other researchers. Author

N91-23501*# National Aeronautics and Space Administration. Lewis Research Center, Cleveland, OH.
GOVERNMENT/INDUSTRY RESPONSE TO QUESTIONNAIRE ON SPACE MECHANISMS/TRIBOLOGY TECHNOLOGY NEEDS
Robert L. Fusaro May 1991 76 p
(NASA-TM-104358; E-6148; NAS 1.15:104358) Avail: NTIS HC/MF A05 CSCL 13I

President Bush has proposed that the U.S. undertake an ambitious mission of manned and robotic exploration of the solar system. This mission will require advanced mechanical moving components, such as bearings, gears, seals, lubricants, etc. There has been concern in the NASA community that the current technology level in these mechanical component/tribology areas may not be adequate to meet the goals of such a mission. To attempt to answer this, NASA-Lewis has sent out a questionnaire to government and industry workers (who have been involved in space mechanism research, design, and implementation) to ask their opinion if the current space mechanisms technology (mechanical components/tribology) is adequate to meet future NASA Missions needs and goals. If they deemed that the technology base inadequate, they were asked to specify the areas of greatest need. The unedited remarks of those who responded to the survey are presented. Author

N91-23502*# National Aeronautics and Space Administration. Marshall Space Flight Center, Huntsville, AL.
PARAMETRIC STUDY IN WELD MISMATCH OF LONGITUDINALLY WELDED SSME HPFTP INLET
J. B. Min, K. L. Spanyer, and R. M. Brunair (Sverdrup Technology, Inc., Saint Louis, MO.) Apr. 1991 25 p
(NASA-TM-103534; NAS 1.15:103534) Avail: NTIS HC/MF A03 CSCL 13I

Welded joints are an essential part of pressure vessels such as the Space Shuttle Main Engine (SSME) Turbopumps. Defects produced in the welding process can be detrimental to weld performance. Recently, review of the SSME high pressure fuel turbopump (HPFTP) titanium inlet x rays revealed several weld discrepancies such as penetrameter density issues, film processing discrepancies, weld width discrepancies, porosity, lack of fusion, and weld offsets. Currently, the sensitivity of welded structures to defects is of concern. From a fatigue standpoint, weld offset may have a serious effect since local yielding, in general, aggravates cyclic stress effects. Therefore, the weld offset issue is considered. Using the finite element method and mathematical formulations, parametric studies were conducted to determine the influence of weld offsets and a variation of weld widths in longitudinally welded cylindrical structures with equal wall thickness on both sides of the joint. From the study, the finite element results and theoretical solutions are presented. Author

N91-23503 Illinois Univ., Chicago.
WAVE GAITS, FOLLOW-THE-LEADER GAITS AND GAIT TRANSITIONS OF LEGGED ROBOTS Ph.D. Thesis
Benjamin Byoung-Soo Choi 1990 197 p
Avail: Univ. Microfilms Order No. DA9107630

Gait study is essential to both design and control of a legged robot. Two major gaits of slow motion, gait transitions between these two gaits, and other higher-speed gaits such as follow the leader gait are studied. The wave gait is the most stable gait and is observed in insect walk. The previous studies of the wave gait have been extensive. The previous studies were extended in two ways: (1) an analytical method is applied to prove the optimum of stability of the wave gait and (2) the leg number was extended to 2n where n is an integer greater than 2. The follow the leader gait is observed in animal walk, and is a very effective gait especially on rough terrain since it greatly reduces the demand on foothold selections which eases the control. The formulation, stability, and special algorithms for tough terrain maneuvering of the follow the leader gait are extensively studied. Finally, gait transition is required whenever a legged robot needs to change its gait. The transitions between the two slow motion gaits, between walk and trot, and between trot and gallop are studied. Mathematical models of these transitions are derived and simulated using computer graphics.
Dissert. Abstr.

N91-23504 Florida Univ., Gainesville.
ARTICULATION OF SPATIAL ROBOTS Ph.D. Thesis
Yong Je Choi 1990 154 p
Avail: Univ. Microfilms Order No. DA9106400

The development of the theory for articulation of spatial robots with special geometry such as the PUMA and TRS robots is described. The theory for articulation consists of the analysis of geometrical capability of a robot and the geometry of interference. Application of the research results to a collision-free path planning problem is demonstrated for the PUMA robot. The geometric capability of a robot is analyzed by use of robot attributes such

as workspace and dexterity. The investigation of permissible orientations for the regional structure of a robot under given geometric constraints is also carried out. The geometry of interference was developed by investigating the representation of an object placed in Euclidean three-space. By using affine coordinates, a representation scheme of simplexes provided a simple, yet powerful, computational method for checking the intersection of objects. A general displacement of an object with respect to a reference object was investigated in order to develop a mapping of relative displacements into image points. The inverse mapping was also derived and used as a rapid decision-making tool for collision-free path planning. The idea of machine intelligence of robots via geometry was implemented by means of a blueprint algorithm in which the theory for robot articulation takes on the role of a basis for preprocessing a robot working environment and path planning among obstacles. Finally, an automatic planning software which demonstrates the application capability of the theory for articulation of a spatial robot was developed by fully utilizing computer graphics animation with realistic visualization of numerous simulations. Dissert. Abstr.

N91-23505# Oak Ridge National Lab., TN.
ROBOT SELF-LOCATION IN UNKNOWN ENVIRONMENTS
E. R. Stuck Feb. 1991 40 p
(Contract DE-AC05-84OR-21400)
(DE91-010450; ORNL/TM-11718; CESAR-91/03) Avail: NTIS HC/MF A03

It is often necessary for robots to navigate in environments which are not known in advance. In this context, self-location is the problem of determining how far and in what direction motion has occurred. Because of wheel slippage and other errors, odometry cannot be depended upon to provide precise or accurate positional information. Triangulating from visual features can help make position estimation more accurate. Work exploring the problem of robot self-location in unknown environments is described. A set of programs which present a partial solution to this self-location problem were developed and integrated. These programs use a sequence of images which are acquired as the camera moves between positions with a motion which is known approximately. Visual features are extracted from the images and matched through time. Triangulation using these features then provides a rough estimate of the range of these features from the camera. Kalman filtering (not implemented) can then be used to integrate the information from odometry and vision to provide a better estimate of the position of the robot. DOE

N91-23506# Central Research Inst. of Electric Power Industry, Tokyo (Japan). Energy and Environment Lab.
WATER-COOLING TECHNIQUE OF HIGH TEMPERATURE GAS TURBINE BLADE
T. Sakuma May 1990 26 p In JAPANESE; ENGLISH summary
(DE91-764238; CRIE-T-89059) Avail: NTIS HC/MF A03

A simulation code has been developed that can simulate the thermal stress and temperature distribution of water cooled blades with a concentric tube type open thermopsyphon. The code has proven that it is possible to keep the blade temperature under 600 C and the thermal stress under 20 kg/sq mm in a gas turbine with inlet gas temperature of 1500 C. Thus, the range of blade material selections is increased and the way is opened for the simplification of cooling structures which contributes to the reduction of manufacturing costs. Furthermore, a simulation code has also been developed that can simulate the thermal efficiency of the Brayton cycle of the water cooled gas turbine. The code has proven that higher thermal efficiency for blades and nozzles is obtained by a water cooling system than by the air or steam cooling systems that are currently under development. DOE

N91-23507# Sandia National Labs., Albuquerque, NM.
RAYBOT: A PRACTICAL IMPLEMENTATION OF A HIERARCHICAL CONTROL SYSTEM FOR TELEROBOTIC LAND VEHICLES
R. Byrne 1990 10 p Presented at the 1991 American Control Conference, Boston, 26 Jun. 1991
(Contract DE-AC04-76DP-00789)
(DE90-017029; SAND-90-2231C; CONF-910638-1) Avail: NTIS HC/MF A02

A hierarchical control architecture for telerobotic vehicles intended to yield a modular, flexible, and easily expanded control system is presented. This architecture is proposed for applications where simple teleoperation is required but where additional capabilities might be quickly added without major changes to the control system. Similarities to the NASREM architecture are noted. Results are given from hardware implementation of the control system on a telerobotic vehicle, Raybot, at Sandia National Laboratories. DOE

N91-23508# Oak Ridge National Lab., TN.
ON THE CONTROL OF TWO MANIPULATORS HOLDING A RIGID OBJECT IN THE PRESENCE OF UNCERTAINTY
D. Dawson (Clemson Univ., SC.) and M. A. Unseren 1991 23 p Presented at the 1991 American Control Conference, Boston, 26 Jun. 1991 Prepared in cooperation with Clemson Univ., SC
(Contract DE-AC05-84OR-21400)
(DE90-017742; CONF-910638-2) Avail: NTIS HC/MF A03

A dynamical model and a control architecture are developed for the closed chain motion of two six joint manipulators holding a rigid object in a three-dimensional workspace. Dynamic and kinematic constraints are determined and combined with the equations of motion of the manipulators to obtain a dynamical model of the entire system in the joint space. Reduced order dynamic equations are developed with regard to the position and force control variables. Control laws are then determined so as to decouple the force and position controlled degrees of freedom (DOF) during motion of the system. These control laws are a feedback linearization approach and an adaptive motion controller in conjunction with a robust force controller. A discussion of these control laws is presented. DOE

N91-23509# Oak Ridge National Lab., TN.
POTENTIAL IMPACT OF ENHANCED FRACTURE-TOUGHNESS DATA ON FRACTURE MECHANICS ASSESSMENT OF PWR VESSEL INTEGRITY FOR PRESSURIZED THERMAL SHOCK
T. L. Dickson and T. J. Theiss 1991 9 p Presented at the American Society of Mechanical Engineers (ASME) Pressure Vessels and Piping Conference, San Diego, 23-27 Jun. 1991
(Contract DE-AC05-84OR-21400)
(DE91-009554; CONF-910602-14) Avail: NTIS HC/MF A02

The Heavy Section Steel Technology (HSST) Program is involved with the generation of enhanced fracture-initiation toughness and fracture-arrest toughness data of prototypic nuclear reactor vessel steels. These two sets of data are enhanced because they have distinguishing characteristics that could potentially impact PWR pressure vessel integrity assessments for the pressurized-thermal shock (PTS) loading condition which is a major plant-life extension issue to be confronted in the 1990s. A series of large-scale fracture-mechanics experiments have produced crack-arrest (K sub Ia) data with the distinguishing characteristic that the values are considerably above 220 MPa times the square root of m. The implicit limit of the ASME Code and the limit used in the Integrated Pressurized Thermal Shock (IPTS) studies. Currently, the HSST Program is planning experiments to verify and quantify for A533B steel the distinguishing characteristic of elevated the distinguishing characteristic of elevated initiation-fracture toughness for shallow flaws which has been observed for other steels. The results of the analyses indicated that application of the enhanced K(sub Ia) data does reduce the conditional probability of failure P(F/E); however, it does not appear to have the potential to significantly impact the results of PTS analyses. The application of enhanced fracture-initiation-toughness data for shallow flaws also reduces P(F/E), and does appear to have a potential for significantly affecting the results of PTS analyses. DOE

N91-23510# Edgerton, Germeshausen and Grier, Inc., Idaho Falls, ID.
HEAT AND MASS TRANSFER IN THE GAS TUNGSTEN AND GAS METAL ARC WELDING PROCESSES
A. D Watkins, H. B. Smartt, C. J. Einerson, and J. A. Watkins 1990 15 p Presented at the 22nd ICHMT International Symposium on Manufacturing and Materials Processing, Dubrovnik (Yugoslavia), Aug. 1990
(Contract DE-AC07-76ID-01570)
(DE91-010089; EGG-M-90015; CONF-9008199-1) Avail: NTIS HC/MF A03

The heat transferred from an electrode negative, argon gas tungsten arc to an anode was measured for a wide range of conditions suitable for mechanized welding. The results are given as (1) the arc efficiency, and (2) the anode heat and current input distributions for various anode materials over a range of current and voltage. The nominal arc is Gaussian, (approx.) 4 mm in diameter, with (approx.) 75 (pct.) heat transfer efficiency. Variations from these values are discussed in terms of the electrical and thermal energy transport mechanisms. Heat transferred to the workpiece (cathode) during direct current, electrode positive gas metal arc welding (GMAW) was measured for various parameters applicable to machine welding. The results are presented as a function of electrode speed for changing voltages and contact tip to workpiece distances. The total heat transfer efficiency was nominally 85 (pct.) for a 0.89 mm diameter steel electrode using an argon-2 (pct.) oxygen shielding gas; the nominal heat transfer efficiency of the droplet component was 40 (pct.). The average droplet temperatures ranged from 2400 to 3100 K, depending on the process parameters. A new method of measuring the heat transferred from the arc to the workpiece, using a boiling liquid nitrogen calorimeter, was developed that gives rapid, accurate values. DOE

N91-23511# Oak Ridge National Lab., TN.
PERFORMANCE OF VISUAL AND ULTRASOUND SENSING BY AN AUTONOMOUS ROBOT
M. Beckerman and D. L. Barnett Jan. 1991 34 p
(Contract DE-AC05-84OR-21400)
(DE91-010452; ORNL/TM-11733; CESAR-90/54) Avail: NTIS HC/MF A03

This paper presents results of an experimental study of the reliability of an autonomous mobile robot operating in an unstructured environment. Examined in the study are the principal components of the visual and ultrasound sensor systems used to guide navigation and manipulation tasks of the robot. Performance criteria are established with respect to the requirements of the integrated robotic system. Repeated measurements are done of the geometric and spatial quantities used for docking the robot at a mock-up control panel, and for locating control panel devices to be manipulated. The systematic and random components of the errors in the measured quantities are exhibited, their origins are identified, and means for their reduction are developed. We focus on refinements of visual area data using ultrasound range data, and on extraction of yaw by visual and by ultrasound methods. Monte Carlo methods are used to study the sensor fusion, and angle-dependence considerations are used to characterize the precision of the yaw measurements. Issues relating to sensor models and sensor fusion, viewed as essential strategic components of intelligent systems, are then discussed. DOE

N91-23512*# National Aeronautics and Space Administration. Lewis Research Center, Cleveland, OH.
QUANTIFYING OIL FILTRATION EFFECTS ON BEARING LIFE
William M. Needelman (Pall Corp., Glen Cove, NY.) and Erwin V. Zaretsky Jun. 1991 14 p
(NASA-TM-104350; E-5862; NAS 1.15:104350) Avail: NTIS HC/MF A03 CSCL 13I

Rolling-element bearing life is influenced by the number, size, and material properties of particles entering the Hertzian contact of the rolling element and raceway. In general, rolling-element bearing life increases with increasing level of oil filtration. Based upon test results, two equations are presented which allow for the adjustment of bearing L(sub 10) or catalog life based upon oil filter rating. It is recommended that where no oil filtration is used catalog life be reduced by 50 percent. Author

N91-23513*# National Aeronautics and Space Administration. Lewis Research Center, Cleveland, OH.
MODAL ANALYSIS OF MULTISTAGE GEAR SYSTEMS COUPLED WITH GEARBOX VIBRATIONS
F. K. Choy, Y. F. Ruan, Y. K. Tu (Akron Univ., OH.), J. J. Zakrajsek, and D. P. Townsend 1991 34 p Prepared for presentation at the International Conference on Motion and Power Transmissions, Hiroshima, Japan, 24-26 Nov. 1991; sponsored in part by Japan Society of Mechanical Engineers, ASME, I.Mech.E., VDI, I.E.T., CSME
(DA Proj. 1L1-62211-A-47-A)
(NASA-TM-103797; E-6085; NAS 1.15:103797; AVSCOM-TR-90-C-033) Avail: NTIS HC/MF A03 CSCL 13I

An analytical procedure to simulate vibrations in gear transmission systems is presented. This procedure couples the dynamics of the rotor-bearing gear system with the vibration in the gear box structure. The model synthesis method is used in solving the overall dynamics of the system, and a variable time-stepping integration scheme is used in evaluating the global transient vibration of the system. Locally each gear stage is modeled as a multimass rotor-bearing system using a discrete model. The modal characteristics are calculated using the matrix-transfer technique. The gearbox structure is represented by a finite element models, and modal parameters are solved by using NASTRAN. The rotor-gear stages are coupled through nonlinear compliance in the gear mesh while the gearbox structure is coupled through the bearing supports of the rotor system. Transient and steady state vibrations of the coupled system are examined in both time and frequency domains. A typical three-geared system is used as an example for demonstration of the developed procedure. Author

N91-23514*# National Aeronautics and Space Administration. Lewis Research Center, Cleveland, OH.
MAXIMUM LIFE SPUR GEAR DESIGN
M. Savage, M. J. Mackulin (Akron Univ., OH.), H. H. Coe, and J. J. Coy 1991 14 p Presented at the 27th Joint Propulsion Conference, Sacramento, CA, 24-27 Jun. 1991; cosponsored by AIAA, SAE, ASME, and ASEE Prepared in cooperation with Army Aviation Systems Command, Cleveland, OH
(Grant NAG3-1047; DA Proj. 1L1-62211-37-A)
(NASA-TM-104361; E-6157; NAS 1.15:104361; AVSCOM-TR-90-C-024) Avail: NTIS HC/MF A03 CSCL 13I

Optimization procedures allow one to design a spur gear reduction for maximum life and other end use criteria. A modified feasible directions search algorithm permits a wide variety of inequality constraints and exact design requirements to be met with low sensitivity to initial guess values. The optimization algorithm is described, and the models for gear life and performance are presented. The algorithm is compact and has been programmed for execution on a desk top computer. Two examples are presented to illustrate the method and its application. Author

N91-23515*# National Aeronautics and Space Administration. Lewis Research Center, Cleveland, OH.
EVALUATION AND RANKING OF CANDIDATE CERAMIC WAFER ENGINE SEAL MATERIALS
Bruce M. Steinetz May 1991 26 p
(NASA-TM-103795; E-6082; NAS 1.15:103795) Avail: NTIS HC/MF A03 CSCL 11A

Modern engineered ceramics offer high temperature capabilities not found in even the best superalloy metals. The high temperature properties of several selected ceramics including aluminum oxide, silicon carbide, and silicon nitride are reviewed as they apply to hypersonic engine seal design. A ranking procedure is employed to objectively differentiate among four different monolithic ceramic materials considered, including: a cold-pressed and sintered aluminum oxide; a sintered alpha-phase silicon carbide; a hot-isostatically pressed silicon nitride; and a cold-pressed and

sintered silicon nitride. This procedure is used to narrow the wide range of potential ceramics considered to an acceptable number for future detailed and costly analyses and tests. The materials are numerically scored according to their high temperature flexural strength; high temperature thermal conductivity; resistance to crack growth; resistance to high heating rates; fracture toughness; Weibull modulus; and finally according to their resistance to leakage flow, where materials having coefficients of thermal expansion closely matching the engine panel material resist leakage flow best. The cold-pressed and sintered material (Kyocera SN-251) ranked the highest in the overall ranking especially when implemented in engine panels made of low expansion rate materials being considered for the engine, including Incoloy and titanium alloys.
Author

N91-23516# Laboratoire d'Automatique et d'Analyse des Systemes, Toulouse (France).
TIME-OPTIMAL MOTION OF ROBOTIC MANIPULATORS INCLUDING NONLINEAR DYNAMICS Ph.D. Thesis - Toulouse Univ.
Jean-Yves Fourquet 1990 144 p In FRENCH; ENGLISH summary
(LAAS-90403; ETN-91-99239) Avail: NTIS HC/MF A07

Time optimal motions for robotic manipulators both for imposed and free paths are described. In both cases, the complete dynamic model of the robotic manipulator are taken into account. The problem is viewed as a nonlinear systems optimization problem. This kind of problem has no standard solution and the approach proposed uses the necessary conditions furnished by the theory. The imposed path problem is solved. Using the extended maximum principle, it is shown that the control is always on the boundary of the region of admissible controls when the motion is not on the boundary of the region of admissible states. An algorithm based on non standard arguments and leading to the optimal solution while involving reduced complexity is presented. The necessary conditions for optimality are met by two candidate solutions: bang-bang and singular ones. The case of bang-bang controls is outlined. A simple parametric optimization method is then presented. Study is focused on singular controls. Some new results are obtained concerning the existence of the controls that are needed as well as their possible characterization and structure. Emphasis is placed on the importance of the characterizations presented in view of efficient numerical implementation. The case of two degrees of freedom structures is discussed. ESA

N91-23517# Naval Postgraduate School, Monterey, CA. Dept. of Computer Science.
RULE-BASED MOTION COORDINATION FOR THE ADAPTIVE SUSPENSION VEHICLE ON TERNARY-TYPE TERRAIN Final Report, Oct. 1988 - Dec. 1989
S. H. Kwak and R. B. McGhee Dec. 1990 177 p
(AD-A232224; NPS-CS-91-006) Avail: NTIS HC/MF A09 CSCL 17/7

This study investigates the utility of rule based coordination of motion for ternary-type terrain locomotion by a hexapod walking machine. The ternary-type terrain considered is composed of permitted areas, forbidden areas, and ditch areas. The logic for generating motion coordination is written in Prolog while the simulation of the terrain and of the vehicle kinematics, as well as low-level on-board computer functions, are written in extended Common Lisp and Flavors. It is found that this approach, which utilizes multiple programming paradigms for programming motion coordination logic and simulation objects, results in code that is much easier to understand and modify than previous motion coordination programs written in Pascal. Thus, the code development effort and time are greatly reduced. The authors believe that both the methodology and the motion coordination logic presented in this report possess sufficient merit to justify full-scale physical testing in the Adaptive Suspension Vehicle at the Ohio State University. GRA

N91-23518# Ballistic Research Labs., Aberdeen Proving Ground, MD.
ENERGY-EFFICIENT PENETRATION OF TARGETS Final Report, Oct. 1985 - Sep. 1989
Konrad Frank and John A. Zook Feb. 1991 42 p
(DA Proj. 1L1-62618-AH-80)
(AD-A232227; BRL-MR-3885) Avail: NTIS HC/MF A03 CSCL 19/10

In general, the performance of a kinetic energy (KE) penetrator against most armor targets increases with velocity regardless of the particular penetrator/target interaction mode. It is possible to show that there exists an optimum velocity which maximizes the performance of an impacting penetrator for a given expenditure of energy. Simple graphical methods are described that determine the optimum velocity from general performance/velocity plots. These graphic methods may also be applied to experimental data alone. In addition, simple analytic models which describe the velocity dependent penetration/perforation performance of KE penetrators are examined and extended. These models may be used to assess explicitly the influence of parameters such as target strength and density; and penetrator mass, strength, and density. For some models in this analysis, the explicit relations between the optimum striking velocity for a specified KE value and the penetrator/target parameters are described. GRA

N91-23519# Rensselaer Polytechnic Inst., Troy, NY. Dept. of Mechanical Engineering.
FUNDAMENTAL RESEARCH ON TRIBOLOGY Final Report, 1 Jul. 1986 - 31 Dec. 1990
James L. Lauer 14 Jan. 1991 12 p
(Contract DAAL03-86-K-0076)
(AD-A232446; ARO-23525.41-EG) Avail: NTIS HC/MF A03 CSCL 20/11

A multidisciplinary program of basic research was conducted with emphasis on potential ways of reducing friction and wear under conditions of boundary lubrication. A special aim was the development of lubricating systems for applications at temperatures above 300 C. Both experimental and theoretical (computer modeling) approaches were used in parallel. Among the most important results were: Stable carbonaceous gases or vapors (ethylene, benzene propane, propanol) form a lubricating carbon deposit on nickel-containing steels at temperatures above 350 C. Under water fresh metal surfaces are exposed providing continuous catalytic regeneration of the solid lubricant as long as the gas is supplied. The same concept also works on ceramic surfaces such as silicon nitride, Sialon, silicon carbide or zirconia. However, the nature of the carbon (possibly cracking-type coke) is spectroscopically different. Friction coefficients as low as 0.02 and negligible wear could be achieved. A parallel ultrahigh vacuum SEM study showed catalytic carbon deposition on nickel from ethylene in the same temperature range where the friction coefficient was low. New computer models of polymer friction in the temperature-controlled region and of EHD by fracture mechanics were devised. GRA

N91-23580# MATRA Espace, Toulouse (France).
SPACE AND TELESCIENCE ROBOTICS: DEVELOPMENT OF CONCEPTS AND REFERENCE TECHNOLOGIES FOR TELEDETECTION AND ROBOTICS IN EXTREME ENVIRONMENTS [ROBOTIQUE SPATIALE ET TELESCIENCE: ESSOR DE CONCEPTS ET TECHNOLOGIES DE REFERENCE POUR LA TELEDETECTION ET LA ROBOTIQUE EN MILIEUX EXTREMES]
G. Andre and J. Tailhades *In* ESA, Space and Sea Dec. 1990 p 117-129 In FRENCH (For primary document see N91-23563 15-42)
Copyright Avail: NTIS HC/MF A13

N91-23581# Tecnomare S.p.A. (Italy).
TELEROBOTICS: A KEY AREA FOR POSSIBLE TECHNOLOGY TRANSFER FROM UNDERWATER TO SPACE
Walter Prendin, Antonio Terribile, and Simonetta DiPippo (Italian

Space Agency, Rome.) *In* ESA, Space and Sea Dec. 1990 p 131-137 (For primary document see N91-23563 15-42)
Copyright Avail: NTIS HC/MF A13

N91-23582# National Space Development Agency, Ibaraki (Japan).
RESEARCH AND DEVELOPMENT OF FUTURE SPACE ROBOTICS IN NASDA
Tsutomu Iwata, Mitsushige Oda, and Taichi Nakamura *In* ESA, Space and Sea Dec. 1990 p 139-143 (For primary document see N91-23563 15-42)
Copyright Avail: NTIS HC/MF A13

N91-23585# Cybernetix, Marseille (France). Societe d'Ingenierie.
TELEMANIPULATION SYSTEM ASSISTED BY COMPUTER FOR UNDER WATER APPLICATIONS [SYSTEME DE TELEMANIPULATION ASSISTEE PAR ORDINATEUR POUR LES APPLICATIONS SOUS-MARINS]
D. Sangouard, C. Leveque, and G. Clement (Commissariat a l'Energie Atomique, Fontenay-aux-Roses, France) *In* ESA, Space and Sea Dec. 1990 p 163-169 In ENGLISH and FRENCH (For primary document see N91-23563 15-42)
Copyright Avail: NTIS HC/MF A13

N91-23590# Institut Francais de Recherche pour l'Exploitation de la Mer, La Seyne sur Mer.
EVALUATION OF MULTISENSOR FUSION SCHEME FOR THE LOCALIZATION OF UNDERWATER REMOTELY OPERATED VEHICLES
V. Rigaud and B. Duchene *In* ESA, Space and Sea Dec. 1990 p 195-200 (For primary document see N91-23563 15-42)
Copyright Avail: NTIS HC/MF A13

N91-24075*# National Aeronautics and Space Administration. John F. Kennedy Space Center, Cocoa Beach, FL.
ROBOTIC CONTROL AND INSPECTION VERIFICATION
Virgil Leon Davis *In* NASA, Washington, Technology 2000, Volume 2 1991 p 298-307 (For primary document see N91-24041 15-99)
Avail: NTIS HC/MF A16 CSCL 13H

38 QUALITY ASSURANCE AND RELIABILITY

Includes product sampling procedures and techniques; and quality control.

N91-23520# Argonne National Lab., IL.
A FIRST-PRINCIPLES GENERIC METHODOLOGY FOR REPRESENTING THE KNOWLEDGE BASE OF A PROCESS DIAGNOSTIC EXPERT SYSTEM
J. Reifman, L. L. Briggs, and T. Y. C. Wei 1990 19 p Presented at the 4th International Conference on Industrial and Engineering Applications of Artificial Intelligence and Expert Systems, Kauai, 2-5 Jun. 1991
(Contract W-31-109-eng-38)
(DE90-017693; CONF-910648-1) Avail: NTIS HC/MF A03

In this paper we present a methodology for identifying faulty component candidates of process malfunctions through basic physical principles of conservation, functional classification of components, and information from the process schematics. The basic principles of macroscopic balance of mass, momentum, and energy in thermal hydraulic control volumes are applied in a novel approach to incorporate deep knowledge into the knowledge base. Additional deep knowledge is incorporated through the functional classification of process components according to their influence in disturbing the macroscopic balance equations. Information from the process schematics is applied to identify the faulty component candidates after the type of imbalance in the control volumes is matched against the functional classification of the components. Except for the information from the process schematics, this approach is completely general and independent of the process under consideration. The use of basic first-principles, which are physically correct, and the process-independent architecture of the diagnosis procedure allow for the verification and validation of the system. A prototype process diagnosis expert system is developed and a test problem is presented to identify faulty component candidates in the presence of a single failure in a hypothetical balance of plant of a liquid metal nuclear reactor plant. DOE

N91-23521*# National Aeronautics and Space Administration. Lewis Research Center, Cleveland, OH.
A PRELIMINARY INVESTIGATION OF ACOUSTO-ULTRASONIC NDE OF METAL MATRIX COMPOSITE TEST SPECIMENS
Harold E. Kautz and Brad A. Lerch May 1991 13 p
(NASA-TM-104339; E-5651-1; NAS 1.15:104339) Avail: NTIS HC/MF A03 CSCL 09D

Acousto-ultrasonic (AU) measurements were performed on a series of tensile specimens composed of 8 laminated layers of continuous, SiC fiber reinforced Ti-15-3 matrix. The following subject areas are covered: AU signal analysis; tensile behavior; AU and interrupted tensile tests; AU and thermally cycled specimens; AU and stiffness; and AU and specimen geometry. Author

N91-24074*# National Aeronautics and Space Administration. Langley Research Center, Hampton, VA.
QUANTITATIVE NONDESTRUCTIVE EVALUATION: REQUIREMENTS FOR TOMORROW'S RELIABILITY
Joseph S. Heyman *In* NASA, Washington, Technology 2000, Volume 2 1991 p 287-297 (For primary document see N91-24041 15-99)
Avail: NTIS HC/MF A16 CSCL 14D

39 STRUCTURAL MECHANICS

Includes structural element design and weight analysis; fatigue; and thermal stress.

For applications see *05 Aircraft Design, Testing and Performance* and *18 Spacecraft Design, Testing and Performance.*

N91-23522# Israel Aircraft Industries Ltd., Ben-Gurion Airport. Ground Tests Engineering.
COMPUTERIZED SYSTEM FOR STATIC AND FATIGUE LARGE SCALE STRUCTURAL TESTS: A CASE STUDY
Uri BenShalom May 1987 11 p
(IAITIC-87-1007; ITN-88-85006) Avail: NTIS HC/MF A03

A computerized system was developed at IAI (Israel Aircraft Industries) for large scale static and fatigue tests. The evolution of the new software system, the base-design of old systems, divergence of the original design from previous concepts, and insight gained during system development are discussed. ISA

N91-23523# National Inst. of Standards and Technology, Boulder, CO. Materials Reliability Div.
DATA-REDUCTION AND ANALYSIS PROCEDURES USED IN NIST'S THERMOMECHANICAL PROCESSING RESEARCH
Yi-Wen Cheng and Christian L. Sargent Aug. 1990 68 p
(PB91-132282; NISTIR-3950) Avail: NTIS HC/MF A04 CSCL 20K

The data-reduction procedures and computer programs used to reduce and analyze the data obtained with a hot-deformation apparatus are described. The measured raw data with the apparatus include temperature vs. time, specimen's relative length (dilation) vs. time, actuator movement (stroke) vs. time, and load vs. time. Four computer programs were written for data reduction and analysis to determine the cooling rates, the true stress-true strain curves, the true strain rates, and the phase-transformation temperatures. Local averaging techniques were used to smooth the data of temperature, dilation, stroke, and load. Source codes

for the computer programs are included. Example results of the analyses are presented and an example of the program execution is given. GRA

N91-23524# National Inst. of Standards and Technology, Boulder, CO. Materials Reliability Div.
STUDY OF STATIC AND DYNAMIC FRACTURE USING STRAIN MEASUREMENTS
J. R. Berger and J. W. Dally Sep. 1990 188 p
(PB91-132217; NISTIR-3952) Avail: NTIS HC/MF A09 CSCL 20K

The analysis of strain fields surrounding both stationary and propagating cracks is presented. Series expansions of the static and dynamic strain fields are developed. Gage orientation angles are then studied to optimize the strain response. The orientation angles are found to be dependent on gage type and material. Algorithms are developed which use the temporal or spatial strain variations to extract fracture parameters. The accuracy of the parameter determinations is shown to be excellent, and limits are placed on the validity of the developed methods. The methods are then applied to the analysis of a large scale crack arrest test conducted in a pressure vessel steel. The behavior of the crack-tip position with time and the propagation toughness with time, temperature, and position are determined. From this information, details of the conditions at crack arrest are extracted. The relationship between the propagation toughness and crack velocity is then constructed. GRA

N91-23525 California Univ., Berkeley.
REDUCED VECTOR BASIS FOR DYNAMIC ANALYSIS OF LARGE DAMPED STRUCTURES Ph.D. Thesis
Yau-Cheung Yiu 1990 188 p
Avail: Univ. Microfilms Order No. DA9103938

The reduced vector basis approach is used to unify the classical and modern methods to solve the dynamic responses of large damped linear structures. The classical eigenvector basis is re-examined. The generalized Ritz method is used to provide a more direct and efficient solution to the forced vibration problem. The concept of load dependent and response dependent vector bases is developed. Physical interpretation, mathematical rigor and computational efficiency are emphasized in this reduced vector basis approach. The solution technique is extended to a class of structures with positive semi-definite stiffness matrices. A self-equilibrating elastic force approach is used to extract basis vectors for structures with zero strain energy modes. A new dynamic substructure solution technique is formulated in the reduced vector basis. Load dependent and boundary motion vector bases define the vector subspace for the dynamic response of substructures. This enables the reduced vector basis technique to be effectively implemented for large linear structures with damping.
Dissert. Abstr.

N91-23526# Sandia National Labs., Albuquerque, NM.
BOBBIN STRESSES GENERATED BY WIRE WINDING
K. Metzinger, S. Attaway, and F. Mello 1991 9 p Presented at the 1st International Conference on Web Handling, Stillwater, 19-21 May 1991
(Contract DE-AC04-76DP-00789)
(DE91-009545; SAND-90-3182; CONF-9105148-3) Avail: NTIS HC/MF A02

The prediction of bobbin stresses generated by wire winding is now possible by combining a finite element structural code and a rigid body motion code. In this combination of computer codes, the bobbin and the individual wire wraps are considered to be axisymmetric. Each wire wrap is modeled with a single one-node element that has stiffness, mass, and radius. The distributed radial load that a wire wrap exerts on the bobbin or other wires is calculated by using a relationship developed for a thin ring with a circular cross section. In this analysis, a layer of wire wraps with a specified tension is applied to a bobbin. The bobbin contracts radially until an equilibrium position is reached. When a second layer is added, the bobbin and each wire in the first layer reach a new equilibrium position. The tensions and the distributed radial loads associated with each displaced wire in the first layer change accordingly. As additional layers are added, the tensions and the distributed radial loads for all the previously applied wires are adjusted to reflect their new positions. The stresses in the bobbin can be determined for any number of wire layers. Bobbin fixturing during winding can be simulated by imposing suitable boundary conditions on the bobbin's finite element mesh. A simple test problem is presented, providing a comparison between the finite element results and a closed-form solution. Quantitative results for bobbin stresses and wire tensions and then presented for more realistic coils. The impact of bobbin fixturing and wire packing structure on the stresses in the bobbin are also discussed. DOE

N91-23527# Lawrence Livermore National Lab., CA.
FINITE ELEMENT ANALYSIS OF THE LATERAL BUCKLING OF A CANTILEVERED I BEAM
S. C. Lovejoy 30 Jan. 1991 25 p
(Contract W-7405-eng-48)
(DE91-010123; UCRL-ID-106827) Avail: NTIS HC/MF A03

This report summarizes the investigation of modeling lateral buckling of a cantilever beam subjected to a uniform shear load on the free end using NIKE3D. First an analytic solution is presented using the theory of elastic stability and elastic beam theory. Four finite element models are then investigated and compared to the analytic solution. The four finite element models can be put into groups of two. The first group uses shell elements to model the beam. One model uses the Hughes/Liu shell formulation and the other uses the YASE shell formulation. The second group uses brick elements to model the beam with the first using the standard B-bar element formulation and the other using the B-bar with incompatible modes formulation. The Hughes/Liu model did not converge at any load but the remaining three models gave interesting and meaningful results that appear to be in good agreement with the analytic model. DOE

N91-23528 Rhode Island Univ., Kingston.
THE TRANSIENT RESPONSE OF HEAVILY FLUID-LOADED ELASTIC PLATES AND CYLINDRICAL SHELLS Ph.D. Thesis
Duraisingh Diamond Ebenezer 1990 306 p
Avail: Univ. Microfilms Order No. DA9106511

A new method to determine the transient responses of heavily fluid-loaded planar vibrators and cylindrical shells to broad band time-dependent excitations is presented. When the vibrator is excited, the acoustic radiation loading on it introduces a feedback loop into the system making the fluid-loaded response more difficult to determine than the in-vacuo response. The transient acoustic radiation loading on the vibrator is obtained by two methods. In the case of planar vibrators, a wave vector time domain method is used in conjunction with the differential form of the boundary value problem. In the case of cylindrical shells, the radiation loading when the shell is in a fluid with uniform inviscid axial flow is obtained by the same method. It is also obtained by using the integral equation for the pressure. In both methods, the velocity of the vibrator is expressed as a sum of the products of the modal velocities and the modes which form a complete set of orthogonal functions. The acoustic modal forces are then expressed as a sum of the convolution of the radiation impulse responses and the modal velocities. In order to determine the transient response of the vibrator to a time-dependent excitation, the orthogonal property of the modes is used to develop a set of coupled convolution integral equations for the time dependent modal velocities. The equations are then rearranged to facilitate their numerical solution. Analytical expressions are obtained for the impulse responses of the pc fluid-loaded admittances. These impulse responses which are the modal velocities when the high frequency approximation is made for the effect of fluid loading are then used to compute the model velocities when the effect of coupling is included. The coupled equations are solved by marching forward in time. Several numerical results are presented to illustrate the methods. Dissert. Abstr.

N91-23529 California Univ., Los Angeles.
A STATISTICAL MODEL OF FRACTURES Ph.D. Thesis
Narbik Manukian 1990 208 p
Avail: Univ. Microfilms Order No. DA9105883

A dynamic, statistical lattice model is formulated of microscopic fractures based on the physics of 1-D fractures and Glauber's dynamic Ising model. Spatial heterogeneities, interactions between fractures and interaction of fractures with external forces are included. The stress-corrosion growth and healing of microfractures are described. This model is also adapted to describe macroscopic fracture propagation in 1-D along a fault lane. Asperities are modeled by a heterogeneous distribution of breaking strengths. Dissert. Abstr.

N91-23530# Florida Univ., Gainesville.
STRESS ANALYSIS OF A DOUBLE-DOUBLER JOINT IN COMPOSITE STRUCTURE Ph.D. Thesis
Myung-Kyun Park 1990 201 p
Avail: Univ. Microfilms Order No. DA9106461

A linear elastic stress analysis using the finite element method for a double-doubler adhesive joint is provided. The joint is modeled such that the variation of stresses and strains through the adhesive thickness can be determined. The linear elastic stress analysis is focused on three areas: (1) the interfacial stress distribution between the adherend and adhesive; (2) cohesive stress distribution in the adhesive; and (3) stress distribution across the thickness of the adhesive layer at the ends of the layer. A parametric study on the double-doubler joint is performed. Since the stress distribution in the adhesive layer depends on several parameters (geometrical and material), an understanding of the influence of these various parameters will lead to better joint design for specific requirements. Parameters that describe the singular behavior near the bonding edges between the adherend and the adhesive layer are devised by applying the existing elastic solution for stress singularities to the double-doubler joint problem. The specified boundary displacement method is then used to determine the values of parameters. These parameters can be used as a means of failure prediction by comparing the calculated parameters with known critical values of the parameters for the material and comparison of stresses very near the bonding corners where stress singularities occur. Dissert. Abstr.

N91-23531 Texas Univ., Austin.
SYSTEM MODELING AND IDENTIFICATION OF FLEXIBLE STRUCTURES Ph.D. Thesis
Young Jae Lee 1990 205 p
Avail: Univ. Microfilms Order No. DA9105597

The problem of both order and parameter estimation is addressed for large flexible structures. Lattice filters which have properties that make them attractive for both order and parameter identification of linear systems are extended to a flexible structure. The numerical difficulties with the technique of embedding an autoregressive moving average (ARMA) model within a vector autoregressive (AR) equation are avoided by using a periodic lattice filter. System order is estimated by applying Akaike's Information Criterion (AIC) to each channel of the periodic lattice filter. Several examples, including the nonstationary case, are simulated to demonstrate filter performance in estimating order and parameters. In addition, the nonrational transfer function of an important component of a flexible structure, the beam, is analyzed. The pattern of beam zeros is investigated as a function of sensor and actuator separation. Displacement sensors are used for two cases in which a force input and a moment input are separately applied at one end of the beam. The beam position at which the rigid body mode is unobservable is the center of percussion and is located for each case. Contrary to general opinion, zeros do not simply approach the origin along the real axis. When the displacement sensor is located at a center of percussion, the first pair of zeros appear on the imaginary axis and move away from the origin along the imaginary axis. Dissert. Abstr.

N91-23532 Clemson Univ., SC.
COMPUTERIZED SYMBOLIC CLOSED-FORM DYNAMICS AND CONTROL ANALYSIS OF HYBRID RIGID AND ELASTIC MULTIBODY SYSTEMS Ph.D. Thesis
Junghsen Lieh 1990 240 p
Avail: Univ. Microfilms Order No. DA9107674

A closed-form formalism for hybrid rigid and flexible systems is developed based on the principal of virtual work. Principal body coordinates and a moving (or an accelerating) reference frame are used in the formalism. The formalism is in matrix-vector form and can be applied to both holonomic and nonholonomic systems. Euler-Bernoulli beam theory and the assumed mode method are employed to represent elastic deformations. The formalism is implemented in the symbolic algebraic language MAPLE on SUN workstations. Matrix computations and integration of shape functions of elastic modes are performed symbolically. The output equations can be nonlinear or linear in FORTRAN code ready for simulation. Procedures that can symbolically simplify and linearize the equations of motion are provided. Optimal control theory is implemented, and the optimal feedback gains are computed numerically using the algebraic Riccati equation. Several existing models are used to validate the closed-form formalism. The symbolic equations of motion are also verified through manual derivation using the Newton-Euler and Lagrange methods. Simulation and control analyses for a wide range of rigid and elastic mechanical systems are presented. Dissert. Abstr.

N91-23533 Texas A&M Univ., College Station.
STOCHASTIC MICROMECHANICAL MODELING OF CLEAVAGE FRACTURE IN THE DUCTILE-BRITTLE TRANSITION REGION Ph.D. Thesis
David I. Auen Stienstra 1990 278 p
Avail: Univ. Microfilms Order No. DA9106998

The large scatter in cleavage fracture toughness values of steels in the ductile to brittle transition region have made characterization and design difficult. Current weakest link statistical models predict that cleavage toughness data will follow a two-parameter Weibull distribution with known shape parameter. The current models that inadequately describe the data are shown, followed by the revised model and its application to the problem of design. Because studies indicated that crack propagation may also be important, the model was revised to include modified weakest link behavior in which the effects of propagation were included. Through the vehicle of statistics, micromechanics were used to predict the macroscopic properties. The revised model successfully predicted the trend toward higher than expected Weibull shape parameters. A three parameter Weibull distribution was found to be an empirically effective approximation to the model and the data. The revised model was applied to the problems of nuclear pressure vessel design in the transition region, and to the problem of local brittle zones in weldments. Dissert. Abstr.

N91-23534# Argonne National Lab., IL.
APPROXIMATING THE DYNAMIC RESPONSE OF STRAIN-HARDENING STRUCTURES
C. K. Youngdahl 1991 25 p Presented at the American Society of Mechanical Engineers (ASME) Pressure Vessels and Piping Conference, San Diego, 23-27 Jun. 1991
(Contract W-31-109-eng-38)
(DE91-006392; CONF-910602-4) Avail: NTIS HC/MF A03

A mode approximation method is being developed to predict the dynamic plastic deformation of strain-hardening structures. A mode shape having time-dependent coefficients is based on quasi-static deformation profiles. Two stress fields are associated with the modal shape, one satisfying the dynamic relations and the other satisfying the constitutive equations. The application of suitable matching conditions results in a set of simultaneous differential and algebraic equations for the amplitude coefficients and plastic region size. Using the example of a simply supported beam, the effect of varying the number of matching conditions on the accuracy of the solution is presented. DOE

N91-23535# Oak Ridge National Lab., TN.
INTERLAMINAR STRAINS AT THE FREE-EDGE OF A HOLE FOR THICK COMPOSITES IN COMPRESSION
R. G. Boeman 1991 16 p Presented at the 1991 Society for Experimental Mechanics Spring Conference, Milwaukee, 9-13 Jun. 1991
(Contract DE-AC05-84OR-21400)
(DE91-008883; CONF-9106131-1) Avail: NTIS HC/MF A03

The experimental technique of moire interferometry was extended to take measurements of in-plane deformations on the cylindrical surface of a hole in thick laminated composites. A replication scheme was developed to produce high-frequency diffraction gratings on singly-curved surfaces. Techniques were developed to interrogate specimen gratings on 25.4 mm (1 in.) diameter holes in order to study free-edge effects on the hole surface. Interlaminar deformations were measured on a ply-by-ply basis for the first time on the cylindrical surface of a hole. Results are presented for a graphite/epoxy composite laminate with a (902/04)P(sub 4s) stacking sequence. Interlaminar normal and shear strains were determined and plotted versus the ply number at angular locations of 0, 45, and 90 degrees with respect to the loading axis. Strong variations of strains with angular position were revealed. Interlaminar shear strains along a 0/90 degree interface were measured and plotted as a function of the angular position. The shape of the curve compares favorably with analytical results found in the literature for a similar geometry. DOE

N91-23536# Sandia National Labs., Albuquerque, NM.
MECHANICAL STATES IN WOUND HETEROGENEOUS TAPES BY THE FINITE ELEMENT METHOD
R. K. Thomas 1991 7 p Presented at the 1st International Conference on Wed Handling, Stillwater, 19-21 May 1991
(Contract DE-AC04-76DP-00789)
(DE91-009255; SAND-90-3129C; CONF-9105148-2) Avail: NTIS HC/MF A02

The problem of predicting the mechanical stress and deformation states in wound tapes that result from the winding process is addressed by application of the finite element method. The generally heterogeneous tape construction is approximated by continuum finite elements each of which represents many tape plies. Material behavior within the finite element continuum is assumed to be orthotropic elastic. The actual winding process, in which stressed plies are added to an already stressed but partially wound tape, is simulated by sequentially activating layers of finite elements which have initial stress equal to the average winding stress. This model was implemented in the 3-D code JAC3D. Numerical results are presented for the case of a regular 2-D circular geometry, for which analytical solutions have been reported in the literature. The favorable comparison between finite element results and analytical results for this example problem validate the finite element approach. DOE

N91-23537# Sandia National Labs., Albuquerque, NM.
MECHANICAL STRESS STATES IN HETEROGENEOUS, WOUND ROLLS
R. C. Reuter, Jr. 1991 8 p Presented at the 1st International Conference on Wed Handling, Stillwater, 19-21 May 1991
(Contract DE-AC04-76DP-00789)
(DE91-009257; SAND-90-3049C; CONF-9105148-1) Avail: NTIS HC/MF A02

A method is presented of predicting the internal stress states in rolls wound with simultaneous supply spools of dissimilar material. The method is based on linear, orthotropic behavior of the mandrel and web materials, and is sufficiently general to allow completely arbitrary choices for the web materials and their respective winding tensions. The generality of the method also permits the introduction and termination of additional webs of arbitrary material at any time during the winding process. The method is analytical, and utilizes an elasticity solution with rigorous satisfaction of boundary conditions between each ply of the wound roll. A prototypical wound capacitor is used as an example to provide for numerical results of the internal stress states induced during the winding process. Differences in the winding tension loss of the two dissimilar web materials is discussed and explained, as are other mechanical threats to roll stability and performance. The influence of winding tension variations on internal, wound stress states is also discussed. DOE

N91-23538# Argonne National Lab., IL.
A THEORY FOR FLUIDELASTIC INSTABILITY OF TUBE-SUPPORT-PLATE INACTIVE MODES
Y. Cai, S. S. Chen, and S. Chandra (Northeast Utilities Service Co., Hartford, CT.) Sep. 1990 45 p
(Contract W-31-109-eng-38)
(DE91-009676; ANL-90/38) Avail: NTIS HC/MF A03

Fluidelastic instability of loosely supported tubes, vibrating in a tube-support-plate (TSP) inactive mode, is suspected to be one of the main causes of tube failure in some operating steam generators and heat exchangers. A mathematical model is presented for fluidelastic instability of loosely supported tubes exposed to nonuniform crossflow. The model incorporates all motion dependent fluid forces based on the unsteady flow theory. In the unstable region associated with a TSP-inactive mode, tube motion can be described by two linear models: TSP-inactive mode when tubes do not strike the TSP, and TSP-active mode when tubes do strike the TSP. A bilinear model (consisting of these linear models) presented simulates the characteristics of fluidelastic instability of loosely supported tubes in stable and unstable regions associated with TSP-inactive modes. Analytical results obtained with the model are compared with published experimental data; they agree reasonably well. The prediction procedure presented for fluidelastic instability response of loosely supported tubes is applicable to the stable and unstable regions of the TSP-inactive mode. DOE

N91-23539*# National Aeronautics and Space Administration. Langley Research Center, Hampton, VA.
APPLICATION OF ELASTIC AND ELASTIC-PLASTIC FRACTURE MECHANICS METHODS TO SURFACE FLAWS
D. E. McCabe, H. A. Ernst (Georgia Inst. of Tech., Atlanta.), and J. C. Newman, Jr. 1990 53 p Presented at the 22nd National Symposium on Fracture Mechanics, Atlanta, 26-28 Jun. 1990
(Contract DE-AC05-84OR-21400)
(NASA-TM-104964; NAS 1.15:104964; DE91-009936; CONF-900610-2) Avail: NTIS HC/MF A04 CSCL 20K

Fuel tanks that are part of the External Tank assembly for the Space Shuttle are made of relatively thin 2219-T87 aluminum plate. These tanks contain about 917 m of fusion weld seam, all of which is nondestructively inspected for flaws and all those found are repaired. The tanks are subsequently proof-tested to a pressure that is sufficiently severe to cause weld metal yielding in a few local regions of the weld seam. The work undertaken in the present project was to develop a capability to predict flaw growth from undetected surface flaws that are assumed to be located in the highly stressed regions. The technical challenge was to develop R-curve prediction capability for surface cracks in specimens that contain the flaws of unusual sizes and shapes deemed to be of interest. The test techniques developed and the elastic-plastic analysis concepts adopted are presented. The flaws of interest were quite small surface cracks that were narrow-deep ellipses that served to exacerbate the technical difficulties involved. DOE

N91-23540# Westinghouse Hanford Co., Richland, WA.
A COMPARISON BETWEEN CLASSICAL AND SUBSTRUCTURING FINITE-ELEMENT STRESS ANALYSIS OF A COMPLEX VACUUM VESSEL SHELL
M. A. Rezvani and H. H. Ziada Jan. 1991 6 p Presented at the American Society of Mechanical Engineers (ASME) Pressure Vessels and Piping Conference, San Diego, 23-27 Jun. 1991
(Contract DE-AC06-87RL-10930)
(DE91-010035; WHC-SA-1007; CONF-910602-18) Avail: NTIS HC/MF A02

In this study, the middle part of a vacuum vessel was considered for stress analysis. This section consisted of a cylindrical shell with flanges at the ends to be connected to the other parts of

the vessel. Because of the nature of the design, many penetrations to the shell result in a complex structure. The shell was modeled and analyzed using a commercially available finite-element package. The package had substructuring capability that allowed the structure to be modeled and analyzed in sections and assembled at the end. For stress analysis, the structure was modeled and analyzed both as a unit and as a substructure. This paper compares stress results, analysis effort, and time for the two methods (structure as a unit and the structure as a substructure). Substructuring becomes advantageous when a finite-element model is very large or very complicated. Also, during the design process when intermediate analysis steps are required, application of substructuring will reduce the modeling time as well as computer central processing unit (CPU) time for the analysis. DOE

N91-23541# Westinghouse Hanford Co., Richland, WA.
USE OF PERSONAL COMPUTERS IN PERFORMING A LINEAR MODAL ANALYSIS OF A LARGE FINITE-ELEMENT MODEL
G. R. Wagenblast and M. D. Northey Mar. 1991 8 p Presented at the American Society of Mechanical Engineers (ASME) Pressure Vessels and Piping Conference, San Diego, 23-27 Jun. 1991
(Contract DE-AC06-87RL-10930)
(DE91-010112; WHC-SA-1006; CONF-910602-23) Avail: NTIS HC/MF A02

This paper presents the use of personal computers in performing a dynamic frequency analysis of a large (2801 degrees of freedom) finite-element model. Large model linear time history dynamic evaluations of safety related structures were previously restricted to mainframe computers using direct integration analysis methods. This restriction was a result of the limited memory and speed of personal computers. With the advances in memory capacity and speed of the personal computers, large finite-element problems now can be solved in the office in a timely and cost effective manner. Presented in three sections, this paper describes the procedure used to perform the dynamic frequency analysis of the large (2801 degrees of freedom) finite-element model on a personal computer. Section 2.0 describes the structure and the finite-element model that was developed to represent the structure for use in the dynamic evaluation. Section 3.0 addresses the hardware and software used to perform the evaluation and the optimization of the hardware and software operating configuration to minimize the time required to perform the analysis. Section 4.0 explains the analysis techniques used to reduce the problem to a size compatible with the hardware and software memory capacity and configuration. DOE

N91-23542# Argonne National Lab., IL.
A THEORY FOR FLUIDELASTIC INSTABILITY OF TUBE-SUPPORT-PLATE INACTIVE MODES
Y. Cai, S. S. Chen, and S. Chandra (Northeast Utilities Service Co., Hartford, CT.) 1990 38 p Presented at the American Society of Mechanical Engineers (ASME) Pressure Vessels and Piping Conference, San Diego, 23-27 Jun. 1991
(Contract W-31-109-eng-38)
(DE91-006001; CONF-910602-2) Avail: NTIS HC/MF A03

Fluidelastic instability of loosely supported tubes, vibrating in a tube support plate (TSP)-inactive mode, is suspected to be one of the main causes of tube failures in some operating steam generators and heat exchangers. A mathematical model, which incorporates all motion-dependent fluid-forces based on the unsteady flow theory, is presented here for fluidelastic instability of loosely supported tubes exposed to nonuniform crossflow. In the unstable region associated with a TSP-inactive mode, the tube motion can be described by two linear models: TSP-inactive mode when tubes do not contact with the TSP and TSP-active mode when tubes contact the TSP. A bilinear model, consisting of these linear models, is presented in this paper to simulate the characteristics of fluidelastic instability of loosely supported tubes in the stable and unstable region associated with TSP-inactive modes. The analytical results are compared with published experimental data; they agree reasonably well. The prediction procedure presented for fluidelastic instability response of loosely supported tubes is applicable in the stable and unstable regions of TSP-inactive mode. DOE

N91-23543# Westinghouse Hanford Co., Richland, WA.
FATIGUE EVALUATION OF PIPING SYSTEMS WITH LIMITED VIBRATION TEST DATA
S. N. Huang Nov. 1990 25 p Presented at the American Society of Mechanical Engineers (ASME) Pressure Vessels and Piping Conference, San Diego, 23-27 Jun. 1991
(Contract DE-AC06-87RL-10930)
(DE91-007167; WHC-SA-0988; CONF-910602-6) Avail: NTIS HC/MF A03

The safety-related piping in a nuclear power plant may be subjected to pump- or fluid-induced vibrations that, in general, affect only local areas of the piping systems. Pump- or fluid-induced vibrations typically are characterized by low levels of amplitudes and a high number of cycles over the lifetime of plant operation. Thus, the resulting fatigue damage to the piping systems could be an important safety concern. In general, tests and/or analyses are used to evaluate and qualify the piping systems. Test data, however, may be limited because of lack of instrumentation in critical piping locations and/or because of difficulty in obtaining data in inaccessible areas. This paper describes and summarizes a method to use limited pipe vibration test data, along with analytical harmonic response results from finite-element analyses, to assess the fatigue damage of nuclear power plant safety-related piping systems. DOE

N91-23544# Oak Ridge National Lab., TN.
REDUCTION FACTORS FOR CREEP STRENGTH AND FATIGUE LIFE OF MODIFIED 9 Cr-1 Mo STEEL WELDMENTS
J. J. Blass, R. L. Battiste, and D. G. OConnor 1991 7 p Presented at the American Society of Mechanical Engineers (ASME) Pressure Vessels and Piping Conference, San Diego, 23-27 Jun. 1991
(Contract DE-AC05-84OR-21400)
(DE91-009919; CONF-910602-16) Avail: NTIS HC/MF A02

The provisions of ASME B and PV Code Case N-47 currently include reduction factors for creep strength and fatigue life of weldments. To provide experimental confirmation of such factors for modified 9 Cr-1 Mo steel, tests of tubular specimens were conducted at 538 C (1000 F). Three creep rupture specimens with longitudinal welds were tested in tension; and, of three with circumferential welds, two were tested in tension and one in torsion. In each specimen with a circumferential weld, a nonuniform axial distribution of strain was easily visible. The test results were compared to an existing empirical model of creep rupture life. For the torsion test, the comparison was based on a definition of equivalent normal stress recently adopted in Code Case N-47. Some 27 fatigue specimens, with longitudinal, circumferential, or no welds, were tested under axial or torsional strain control. In specimens with welds, fatigue cracking initiated at fusion lines. In axial tests cracks grew in the circumferential direction, and in torsional tests cracks grew along fusion lines. The test results were compared to empirical models of fatigue life based on two definition of equivalent normal strain range. The results have provided some needed confirmation of the reduction factors for creep strength and fatigue life of modified 9 Cr-1 Mo steel weldments currently under consideration by ASME Code committees. DOE

N91-23545# Oak Ridge National Lab., TN.
EXPERIENCE WITH CONVENTIONAL INELASTIC ANALYSIS PROCEDURES IN VERY HIGH TEMPERATURE APPLICATIONS
R. H. Mallet, J. M. Thompson (Mallett Software Technology, Inc., McMurray, PA.), and R. W. Swindeman 1991 8 p Presented at the American Society of Mechanical Engineers (ASME) Pressure Vessels and Piping Conference, San Diego, 23-27 Jun. 1991
(Contract DE-AC05-84OR-21400)
(DE91-009937; CONF-910602-15) Avail: NTIS HC/MF A02

Conventional incremental plasticity and creep analysis procedures for inelastic analysis are applied to hot flue gas cleanup

system components. These flue gas systems operate at temperatures where plasticity and creep are very much intertwined while the two phenomena are treated separately in the conventional inelastic analysis procedure. Data for RA333 material are represented in forms appropriate for the conventional inelastic analysis procedures. Behavior is predicted for typical operating cycles. Creep-fatigue damage is estimated based upon usage fractions. Excessive creep damage is predicted; the major contributions occur during high stress short term intervals caused by rapid temperature changes. These results are presented for discussion of the results and their interpretation in terms of creep-fatigue damage for very high temperature applications.
DOE

N91-23546# Westinghouse Hanford Co., Richland, WA.
BUCKLING ANALYSIS OF A COMPLEX VACUUM VESSEL USING THE FINITE-ELEMENT METHOD
M. S. Shurrab and H. H. Ziada Jan. 1991 8 p Presented at the ASME Pressure Vessels and Piping Conference, San Diego, 23-27 Jun. 1991
(Contract DE-AC06-87RL-10930)
(DE91-010032; WHC-SA-1009; CONF-910602-20) Avail: NTIS HC/MF A02

The vacuum vessel used for this study consists of four sections. These sections vary in thickness and geometry and are connected to each other by flanges. The vacuum vessel was modeled and analyzed using a commercially available finite element code that has the capability to solve buckling problems by using axisymmetric shell and 3-D models. The buckling analysis was performed for the whole vacuum vessel. Buckling pressure for each model was calculated using the code. A technique was developed to analyze the resulting data and mode shapes to determine the buckling pressure for each individual section of the vacuum vessel. Results obtained from each model were similar and they compared favorably with results obtained from the closed form solutions. The main advantage of the finite element method is that it allows the buckling pressure for each individual section of a complex structure to be determined from the overall buckling analysis.
DOE

N91-23547# Superconducting Super Collider Lab., Dallas, TX.
CONSTANT OF MOTION AND DYNAMIC EQUATIONS FOR ONE-DIMENSIONAL AUTONOMOUS SYSTEM AND RADIATION DAMPING
G. Lopez Sep. 1990 20 p
(Contract DE-AC02-89ER-40486)
(DE91-011002; SSCL-308) Avail: NTIS HC/MF A03

The dynamic equations for a one-dimensional autonomous system along with their dynamic transformations are expressed in terms of the constant of motion of the system. The relation between Liouville's theorem and Hamilton's equations with the constant of motion is studied. This approach is applied to the radiation damping suffered by a charged particle inside the beam circulating around a collider-ring accelerator.
DOE

N91-23548*# National Aeronautics and Space Administration. Lewis Research Center, Cleveland, OH.
COMPUTATIONAL SIMULATION OF ACOUSTIC FATIGUE FOR HOT COMPOSITE STRUCTURES
Surendra N. Singhal, Pappu L. N. Murthy, Christos C. Chamis, Vinod K. Nagpal, and Edhi Sutjahjo (Sverdrup Technology, Inc., Brook Park, OH.) 1991 18 p Presented at the 32nd Structures, Structural Dynamics, and Materials Conference, Baltimore, MD, 8-10 Apr. 1991; cosponsored by AIAA, ASME, ASCE, AHS, and ASC Previously announced in IAA as A91-32099
(Contract NAS3-25266)
(NASA-TM-104379; E-6184; NAS 1.15:104379) Avail: NTIS HC/MF A03 CSCL 20K

Predictive methods/computer codes for the computational simulation of acoustic fatigue resistance of hot composite structures subjected to acoustic excitation emanating from an adjacent vibrating component are discussed. Select codes developed over the past two decades at the NASA Lewis Research Center are used. The codes include computation of acoustic noise generated from a vibrating component, degradation in material properties of a composite laminate at use temperature, dynamic response of acoustically excited hot multilayered composite structure, degradation in the first ply strength of the excited structure due to acoustic loading, and acoustic fatigue resistance of the excited structure, including the propulsion environment. Effects of the laminate lay-up and environment on the acoustic fatigue life are evaluated. The results show that, by keeping the angled plies on the outer surface of the laminate, a substantial increase in the acoustic fatigue life is obtained. The effect of environment (temperature and moisture) is to relieve the residual stresses leading to an increase in the acoustic fatigue life of the excited panel.
Author

N91-23549*# National Aeronautics and Space Administration. Lewis Research Center, Cleveland, OH.
SIMULATION OF PROBABILISTIC WIND LOADS AND BUILDING ANALYSIS
Ashwin R. Shah (Sverdrup Technology, Inc., Brook Park, OH.) and Christos C. Chamis 1991 16 p Proposed for presentation at the 9th Biennial Conference on Reliability, Stress Analysis, and Failure Prevention, Miami, FL, 22-25 Sep. 1991; sponsored by ASME
(NASA-TM-103744; E-5987; NAS 1.15:103744) Avail: NTIS HC/MF A03 CSCL 20K

Probabilistic wind loads likely to occur on a structure during its design life are predicted. Described here is a suitable multifactor interactive equation (MFIE) model and its use in the Composite Load Spectra (CLS) computer program to simulate the wind pressure cumulative distribution functions on four sides of a building. The simulated probabilistic wind pressure load was applied to a building frame, and cumulative distribution functions of sway displacements and reliability against overturning were obtained using NESSUS (Numerical Evaluation of Stochastic Structure Under Stress), a stochastic finite element computer code. The geometry of the building and the properties of building members were also considered as random in the NESSUS analysis. The uncertainties of wind pressure, building geometry, and member section property were qualified in terms of their respective sensitivities on the structural response.
Author

N91-23550*# National Aeronautics and Space Administration. Lewis Research Center, Cleveland, OH.
INCORPORATING FINITE ELEMENT ANALYSIS INTO COMPONENT LIFE AND RELIABILITY
Richard August (Sverdrup Technology, Inc., Brook Park, OH.) and Erwin V. Zaretsky 1991 9 p Presented at the Ninth Biennial Conference on Reliability, Stress Analysis, and Failure Prevention, Miami, FL, 22-25 Sep. 1991; sponsored by ASME
(Contract NAS3-25266)
(NASA-TM-104400; E-6220; NAS 1.15:104400) Avail: NTIS HC/MF A02 CSCL 20K

A method for calculating a component's design survivability by incorporating finite element analysis and probabilistic material properties was developed. The method evaluates design parameters through direct comparisons of component survivability expressed in terms of Weibull parameters. The analysis was applied to a rotating disk with mounting bolt holes. The highest probability of failure occurred at, or near, the maximum shear stress region of the bolt holes. Distribution of failure as a function of Weibull slope affects the probability of survival. Where Weibull parameters are unknown for a rotating disk, it may be permissible to assume Weibull parameters, as well as the stress-life exponent, in order to determine the disk speed where the probability of survival is highest.
Author

N91-23551# Technical Research Centre of Finland, Espoo. Metals Lab.
EVALUATION OF CATASTROPHIC FAILURE RISK IN PRESSURE VESSELS. RESULTS OF PRESSURE VESSEL TEST WITH A LARGE VESSEL (HC2-TEST)
Heikki Keinanen, Rauno Rintamaa, Tero Oberg, Matti Sarkimo,

Heli Talja, and Arja Saarenheimo Sep. 1990 66 p Sponsored by Nordic Council of Ministers; Technology Development Center of Finland; Finnish Ministry of Trade and Industry; Neste Oy; Imattra Power Co.; Oy Hubber Ab; Finnish Center for Radiation and Nuclear Safety; Swedish Nuclear Power Inspectorate
(VTT-RR-708; ISBN-951-38-3790-4; ISSN-0358-5077; ETN-91-99049) Copyright Avail: NTIS HC/MF A04; Government Printing Center, P.O. Box 516, SF-00101 Helsinki, Finland, HC 62 Finnish marks

Within the Nordic countries a four year research program in the area of elastic plastic fracture mechanics was initiated in 1985. Seven laboratories from Denmark, Finland, Norway and Sweden are participating in the program. The main technical objective of the program is to clarify how catastrophic fracture can be prevented in pressure vessels and piping by using the leak before break concept. The major experimental effect of the program is destructive pressurization of a large size pressure vessel up to rupture. The vessel has dimensions similar to a nuclear reactor pressure vessel and has been in operation for 20 years in a Finnish oil refinery plant. The material characterization of the vessel was partially carried out within an extensive Nordic round robin program. Two pressure tests were carried out. In both tests an artificial sharp axial surface flaw was made on the inner wall of the vessel. The experimental details of the last test including repair welding of the vessel, flaw preparation, instrumentation and material are described. The fracture behavior and experimental results are reported. The failure pressure is compared to estimates of the analytical pretest calculations. Strain gages and COD (Crack Opening Displacement) sensors gave early data on ductile crack initiation and growth. Acoustic Emission (AE) monitoring located the flaw in early loading stages through crack tip plastification. AE testing for crack growth monitoring seems to require previous fracture mechanics consideration and engineering methods like Batelle's limit load and R6 load method give quite conservative rupture pressure estimates. ESA

N91-23552# Universitaet der Bundeswehr Muenchen, Neubiberg (Germany, F.R.). Inst. fuer Mechanik.
LINEAR BENDING OF CURVED TUBES WITHOUT BOUNDARY INFLUENCE [ROHRE 1: LINEARE BIEGUNG VON ROHRKRUEMMERN OHNE RANDEINFLUSS]
Werner Huebner Dec. 1989 90 p In GERMAN; ENGLISH summary
(Contract DFG-Em-29/2-2)
(ETN-91-99255) Avail: NTIS HC/MF A05

It is shown that a tube with initial curvature should not be treated by the beam theory, because even approximated calculations yield wrong results. The bending behavior of curved tubes without boundary influence is treated. This means that any displacements at the edges are allowed. The main three solution methods are presented: the displacement approach function, the stress approach function, and the linearized Reissuer Meissner equations. The results of these three methods are identical. All relationships are presented in a form which is also suitable for the treatment of tubes with flanges. The resultant stress distributions are presented as dependent on the geometric relationships. ESA

N91-23553# European Space Agency, Paris (France).
THRESHOLD FOR FATIGUE CRACK PROPAGATION AT SIMULATED OPERATING LOADS
Daniel E. Castro (Deutsche Forschungsanstalt fuer Luft- und Raumfahrt, Cologne, Germany, F.R.) Mar. 1991 134 p Transl. into ENGLISH of Schwellwert fuer die Ermuedungsrissausbreitung bei Betriebsaehnlichen Belastungen (Cologne, Fed. Republic of Germany, DLR), 1989 103 p Original language document was announced as N90-13815
(ESA-TT-1187; DLR-FB-89-33; ETN-91-99314) Avail: NTIS HC/MF A07

The influence of load history on the threshold for crack propagation is investigated. In the same context measurements of crack opening load intensity factor were conducted in order to ascertain the influence of this parameter on measurements of the fatigue threshold. It emerges that the existence of the fatigue threshold is always independent of load history. However, the fatigue threshold is low in proportion to the magnitude of oscillation amplitude and maximum load intensity factor relating to previous load. The test results are discussed on the basis of crack closure effects and microstructure modifications in the plastic zone. ESA

N91-23554# Army Lab. Command, Watertown, MA. Material Technology Lab.
MODEL SENSITIVITY IN STRESS-STRENGTH RELIABILITY COMPUTATIONS Final Report
Donald M. Neal, William T. Matthews, and Mark G. Vangel Jan. 1991 27 p Presented at the 36th ARD Conference on the Design Experiments in Army Research, Development and Testing
(AD-A232023; MTL-TR-91-3) Avail: NTIS HC/MF A03 CSCL 01/3

There has been a recent interest in determining high statistical reliability in risk assessment of aircraft components. This report identifies the potential consequences of incorrectly assuming a particular statistical distribution for stress or strength data used in obtaining the high reliability values. The computation of the reliability is defined as the probability of the strength being greater than the stress over the range of stress values. This method is often referred to as the stress strength model. A sensitivity analysis was performed involving a comparison of reliability results in order to evaluate the effects of assuming specific statistical distributions. Both known population distributions, and those that differed slightly from the known, were considered. Results showed substantial differences in reliability estimates even for almost nondetectable differences in the assumed distributions. These differences represent a potential problem in using the stress strength model for high reliability computations, since in practice it is impossible to ever know the exact (population) distribution. An alternative reliability computation procedure is examined involving determination of a lower bound on the reliability values using extreme value distributions. This procedure reduces the possibility of obtaining nonconservative reliability estimates. Results indicated the method can provide conservative bounds when computing high reliability. GRA

N91-23555# Air Force Inst. of Tech., Wright-Patterson AFB, OH.
ANALYSIS OF TRUSS FRAMES BY METHOD OF THE STIFFNESS MATRIX M.S. Thesis
Ronald L. Kruse Dec. 1990 98 p
(AD-A232053; AFIT/CI/CIA-90-127) Avail: NTIS HC/MF A05 CSCL 13/13

The development of the general stiffness coefficients and load constants are presented for the flat Pratt and gabled Pratt truss frames. The stiffness coefficients and load constants are derived through the application of the theorem of least work. The elemental stiffness matrices for the flat and gabled Pratt truss frames are assembled using the respective stiffness coefficients for each type of truss. Two examples illustrate the procedures for computing numerical solutions for each type of truss frame. GRA

N91-23556# Naval Research Lab., Washington, DC.
A COMPLEX SYSTEMS APPROACH TO METALLIC FRACTURE SURFACE CHARACTERIZATION
George C. Kirby, III and Peter Matic 6 Feb. 1991 54 p
(AD-A232546; NRL-MR-6429) Avail: NTIS HC/MF A04 CSCL 20/11

The physical scale of observation and the mathematical formation of description are important choices for the modeling of physical phenomena. The role of local interactions in relating complex features at different scales in inelastic material fracture is important since material damage has local origins while fracture is a large scale event. In this investigation, the relationship between large scale and small continuum scale fracture surface features are quantified in terms of local, small scale interactions. Experimental measurement of local fracture surface orientation were obtained from processing video images of the fracture surface under different illumination directions. The image processing

mapped pixel intensities into a set of three local fracture surface inclination classes defined with respect to the macroscopic surface normal and crack growth direction. GRA

N91-23557# Texas A&M Univ., College Station.
ELASTIC/PLASTIC FRACTURE MECHANICS. PART 2: MARINE STRUCTURAL APPLICATIONS Final Report
T. L. Anderson Apr. 1990 92 p
(Contract DTCG23-88-C-20037)
(AD-A232560; SSC-345-Pt-2) Avail: NTIS HC/MF A05 CSCL 20/11

This document contains the results of experimental and analytical studies of fracture in the ductile-brittle transition zone for two ship steels, EH36 and HSLA 80. Tensile, Charpy and fracture toughness test results using different strain rates are presented. Fracture toughness was quantified by the J integral and the crack tip opening displacement (CTOD). Elastic-plastic finite element analysis was combined with a local failure criterion to derive size limits for J and CTOD testing in the transition regions. Relationships between J and CTOD testing in the transition regions. Relationships between J and CTOD were explored both experimentally and analytically. A theoretical Charpy-fracture toughness relationship was used to predict CTOD transition curves for the steels. Charpy and CTOD transition temperatures were compared for a number of steels. GRA

N91-23558# California Inst. of Tech., Pasadena. Div. of Engineering and Applied Science.
ON THE CONSTRUCTION OF TWO-PHASE EQUILIBRIA IN A NON-ELLIPTIC HYPERELASTIC MATERIAL
Eliot Fried Sep. 1990 69 p
(Contract N00014-90-J-1871)
(AD-A232628; TR-2) Avail: NTIS HC/MF A04 CSCL 20/11

This work focuses on the construction of equilibrated two phase antiplane shear deformations of a non-elliptic isotropic and incompressible hyperelastic material. It is shown that this material can sustain metastable two phase equilibria which are neither piecewise homogeneous nor axisymmetric, but, rather, involve non-planar interfaces which completely segregate inhomogeneously deformed material in distinct elliptic phases. These results are obtained by studying a constrained boundary value problem involving an interface across which the deformation gradient jumps. The boundary value problem is recast as an integral equation and conditions on the interface sufficient to guarantee the existence of a solution to this equation are obtained. The constraints, which enforce the segregation of material in the two elliptic phases, are then studied. Sufficient conditions for their satisfaction are also secured. These involve additional restrictions on the interface across which the deformation gradient jumps-which, with all restrictions satisfied, constitutes a phase boundary. An unaccountably infinite number of such phase boundaries are shown to exist. It is demonstrated that, for each of these, there exists a solution-unique up to an additive constant-for the constrained boundary value problem. As an illustration, approximate solutions which correspond to a particular class of phase boundaries are then constructed. Finally, the kinetics and stability of an arbitrary element within this class of phase boundaries are analyzed in the context of a quasistatic motion. GRA

N91-23559# California Univ., Los Angeles. Dept. of Civil Engineering.
DEVELOPMENT OF A MICROMECHANIC THEORY OF CONSTITUTIVE RELATIONS OF POLYCRYSTALLINE SOLIDS Annual Progress Report, 1 Nov. 1989 - 31 Oct. 1990
Tung-Hua Lin, Xiao-Qiang Wu, and Wei Zhong 30 Nov. 1990 38 p
(Grant AF-AFOSR-0096-89; AF Proj. 2302)
(AD-A232697; AFOSR-91-0116TR) Avail: NTIS HC/MF A03 CSCL 20/11

To analyze structures loaded at elevated temperatures, the stress-strain-time relation of the material is required. This relation given by age hardening and strain hardening theories commonly used often have large discrepancies with experimental results and hence give large errors in the analysis. Lin et al., 1977, suggested calculating polycrystal creep properties from the creep data of single crystals. However, the plastic and creep property of crystals varies larger than those in a polycrystal. There will be significant error to use single crystal data in polycrystal calculations. A f.c.c. crystal has 12 slip system. Plastic and creep property of a crystal depends on the slip in all the 12 slip systems. Instead of waiting for more informative single crystal tests data, we attempt to use the available polycrystal tests. Presently the polycrystal creep property is derived from polycrystal test from its axial and combined tension and shear tests but the non-radial loading data were not used. The non-radial loading has a large effect on the polycrystal creep property. Hence this inclusion of non-radial loading data in the formulation of the polycrystal creep response will improve the calculated strain-time relations and will enhance the accuracy of creep analysis. GRA

N91-23560# Maryland Univ., College Park. Inst. for Physical Science and Technology.
HIERARCHIC MODELING OF PLATES Final Report
Ivo Babuska and L. Li Dec. 1990 36 p
(Contract N00014-90-J-1030)
(AD-A232754; BN-1118) Avail: NTIS HC/MF A03 CSCL 20/11

The problem of partial differential equations on a special domain omega typically the thin domain is usually simplified by various dimensional reduction techniques. The aim is to approximately solve the 3 dimensional problem by a two dimensional formulation. This approach is widely applied in the connections with plates and shells. Today many plates and shells theories (models) are used in practice. The principles of derivation of these models can be divided into 3 groups: (1) Physical derivation; (2) Asymptotic analysis; and (3) Numerical hierarchical approaches. GRA

N91-23561# Maryland Univ., College Park. Inst. for Physical Science and Technology.
ACCURACY OF THE REISSNER-MINDLIN AND THE (1,1,2) MODEL FOR THE CLAMPED-IN PLATE PROBLEM Final Report
L. Li and Ivo Babuska Dec. 1990 15 p
(Contract N00014-90-J-1030; NSF CCR-88-20279)
(AD-A232755; BN-1117) Avail: NTIS HC/MF A03 CSCL 20/4

It is shown that the Reissner Mindlin plate model for clamped in boundary condition does not capture the boundary layer behavior for the bending moments. This boundary layer is present in the 3 dimensional formulation. In contrast the (1,1,2) model shows this boundary layer. The strength of the boundary layer for the(1,1,2) model is analyzed. GRA

N91-23562# Maryland Univ., College Park. Inst. for Physical Science and Technology.
THE PROBLEM OF PLATE MODELING THEORETICAL AND COMPUTATIONAL RESULTS Final Report
Ivo Babuska and L. Li Dec. 1990 64 p
(Contract N00014-90-J-1030; NSF CCR-88-20279)
(AD-A232756; BN-1116) Avail: NTIS HC/MF A04 CSCL 20/11

The problem of various plate models, properties of their solution and the question of how well these models approximate the 3 dimensional formulation is analyzed in detail. The boundary layer and corner singularities of the solution are analyzed. A hierarchy of the models converging to the 3 dimensional solution is constructed. The detailed numerical computations show various basic aspects of plate modeling in a concrete setting. GRA

42 GEOSCIENCES (GENERAL)

N91-23563# European Space Agency, Paris (France).
SPACE AND SEA

Jocelyne Landeau, ed. Dec. 1990 296 p In ENGLISH and FRENCH Colloquium held in Paris, France, 24-26 Sep. 1990 (ESA-SP-312; ETN-91-99115) Copyright Avail: NTIS HC/MF A13

Programs, opinions, experimentation, and discussions covering subjects as wide as life and work in confined environments, the evolution of present assisting equipment and the application of satellite technology to the marine environment are presented. These include ways in which the sea/deep water can be used to train astronauts and evaluate space equipment. For individual titles, see N91-23564 through N91-23608.

N91-23564# Deutsche Forschungsanstalt fuer Luft- und Raumfahrt, Cologne (Germany, F.R.). Inst. for Aerospace Medicine.

THE DIVING LABORATORY AS A SIMULATION ENVIRONMENT FOR MANNED SPACEFLIGHT c53

J. Wenzel, L. Vogt, and R. D. Fischer *In* ESA, Space and Sea Dec. 1990 p 11-13 (For primary document see N91-23563 15-42)

Copyright Avail: NTIS HC/MF A13

The underwater environment presents an interesting laboratory condition for the simulation and validation of manned space operations. Similarities between sea and space include both internal and external strains for the person under consideration. Some of the arguments are illustrated by video sequences comparing astronauts' activities during underwater training, parabola flight, and space mission. It is concluded that both basic training and mission specific simulation underwater is a valuable tool for the preparation of actual manned space projects. ESA

N91-23565# Deutsche Forschungsanstalt fuer Luft- und Raumfahrt, Hamburg (Germany, F.R.). Dept. of Aviation and Space Psychology.

PSYCHOLOGICAL SELECTION OF ASTRONAUTS: RECENT DEVELOPMENTS AT THE DLR TESTING CENTRE IN HAMBURG (FED. REPUBLIC OF GERMANY) c53

C. Fassbender, K. M. Goeters, and D. Manzey *In* ESA, Space and Sea Dec. 1990 p 15-19 (For primary document see N91-23563 15-42)

Copyright Avail: NTIS HC/MF A13

Since 1977 the Department of Aviation and Space Psychology of the DLR has been regularly involved in astronaut (payload specialist) selection on a European as well as on a national level. For several of these selection campaigns the DLR has devised and applied its own test system consisting of a combination of paper pencil tests, apparatus tests, and personal interview. The DLR selection procedures incorporate diverse factors of performance (e.g., perception, memory, multiple task performance) as well as of personality (e.g., social capability, motivation, stress resistance). With the plan for a European participation in the Space Station Freedom new challenges are posed for the selection of all kinds of astronauts because of the specific demands of long duration space flights. These new challenges are discussed with regard to the problems of astronauts and recent developments at the DLR testing center concerning feasible psychological selection criteria and test methods for astronaut selection are presented. ESA

N91-23566# Norwegian Underwater Technology Center Ltd., Laksevaag.

EFFECTS OF WEIGHTLESSNESS (SEA WATER IMMERSION) ON BODY FLUID BALANCE AND CNS FUNCTIONS c52

A. Hope, R. Vaernes, T. Bergan, M. Warncke, H. Sundland, C. Jepsen, and B. Lorenz (Deutsche Forschungsanstalt fuer Luft- und Raumfahrt, Hamburg, Germany, F.R.) *In* ESA, Space and Sea Dec. 1990 p 21-24 Sponsored by Norwegian Space Center, Oslo (For primary document see N91-23563 15-42)

Copyright Avail: NTIS HC/MF A13

The effects of weightlessness on body fluid balance and Central Nervous System (CNS) functions are explored. A body fluid loss of more than 3 kg was previously observed during three half hours of pool diving with the traditional hot water suits used during offshore diving. It was argued that this fluid loss, equalling 4 to 5 percent of body weight (BW), was caused by sweating and/or by diffusional effects of hyperosmotic sea water. The present two hour immersion experiment in thermoneutral (34.5 C) and warm (38 C) sea water (SW) showed that: the BW reduction of 0.8 kg during immersion in thermoneutral SW was caused by the diuresis (3.2 ml/min) blood samples and insensible water loss. Sweating did not occur and no indication of osmotic water loss was observed; in warm water immersion diuresis was reduced to 0.75 ml/min whereas the BW reduction was 1.7 kg. On average 1.2 kg fluid was lost by sweating; auditive evoked potentials (P 300) were unchanged and mental performance was not impaired during or after immersion. ESA

N91-23567# JCLP Hyperbarie, Paris (France).

SUBSEA HABITATS AND SPACE SIMULATION c54

Jean Claude LePechon *In* ESA, Space and Sea Dec. 1990 p 25-30 Sponsored in part by Atelier d'Architecture Aquatique, France (For primary document see N91-23563 15-42)

Copyright Avail: NTIS HC/MF A13

Saturation diving was developed in the 1960's with subsea habitats and then used in the 1970's with deep diving systems and hyperbaric centers. Simulation of confinement can be carried out in saturation while simulation and training to extravehicular activity (EVA) must be performed in a pool. An integrated underwater safe center project which combines hyperbaric confinement and EVA sorties in a pool is presented. This center can also be used to train ground base team and payload specialists in communication techniques and procedures, during confinement and EVA exercices. ESA

N91-23568# Soviet-French Joint Venture, Moscow (USSR).

REAL TIME ANALYSIS SYSTEMS OF THE PHYSICAL PARAMETERS OF THE ENVIRONMENT AND THE STATE OF A HUMAN ORGANISM FOR A LONG TERM EXPOSURE AT DIFFERENT GAS MIXTURES AND PRESSURE UP TO 100 BAR c52

G. I. Kurenkov, A. LeLevier, B. O. Jachontov, and A. V. Rozhkov *In* ESA, Space and Sea Dec. 1990 p 31-35 (For primary document see N91-23563 15-42)

Copyright Avail: NTIS HC/MF A13

The changes of physical parameters of environment during diving cause the responsive reaction of the human organism, which depends on the value and the continuance of the influence. Taking into account the fact that in the conditions of the deep water diving the physical factors and organism state change constantly, the creation of the system of their real time (RT) analysis becomes actual. The RT system has necessary technical devices for automation of a system for divers' safety according to the parameters of pressure, humidity, constant CO2, O2, He, N2, and state of a human organism for a long term exposure at mixtures with different gases and pressure. The RT system was created and tested in the hyperbaric complex, USSR. ESA

N91-23569# OHB-System G.m.b.H., Bremen (Germany, F.R.). Space and Environmental Technology.

PAYLOAD RELATED CREW OPERATIONS: FROM PAST MISSIONS TO COLUMBUS c54

James R. Kass, Erich Schafhauser, and Carlo Viberti (European Space Agency. European Space Research and Technology Center, ESTEC, Noordwijk, Netherlands) *In* ESA, Space and Sea Dec. 1990 p 37-41 (For primary document see N91-23563 15-42)

Copyright Avail: NTIS HC/MF A13

Manned operations in an orbiting laboratory for extended periods of time have many characteristics in common with work in the deep sea, and are accompanied by a number of similar problems. The scenario of manned payload operations in space are addressed: some aspects with their parallel in deep sea work become evident. The analysis results from a study carried out with the ESA/ESTEC in preparation for the Columbus program, and uses as a baseline the lessons learned from past manned missions. Some highlights of these results are presented. ESA

N91-23570# Centre d'Etudes et de Recherches de Chronobiologie Humaine, Nice (France). Lab. Souterrain de Chronobiologie.
SOME PROBLEMS OF DESYNCHRONISATION OF SLEEP-WAKEFULNESS AND CIRCADIAN RHYTHMS FOR LONG DURATION SPACEFLIGHTS **c52**
Michel Siffre *In* ESA, Space and Sea Dec. 1990 p 43-59 (For primary document see N91-23563 15-42)
Copyright Avail: NTIS HC/MF A13

Operational requirements of a space mission often impose a diminution of sleep duration increasing the time of activity. This puts the body in state of internal and/or external desynchronization i.e., biological rhythms are in shift or phase opposition between one function and another and with local launch time. This creates desynchronisis which is known to impair performance. But changes in circadian periodicities are not tolerated in the same manner by all individuals. Crew selection guidelines must be developed based on chronobiological and neurobiological bases, so that circadian rhythms can be adapted to the repetitive work schedule shift and to repetitive partial sleep loss. The underground environment, where temperature is perfectly thermostated and atmosphere naturally renewed, makes a remarquable analog environment for spaceflights simulations, and for testing habitability and the effects of lack of external time synchronizers on humans. ESA

N91-23571# Compagnie Maritime d'Expertises, Marseille (France).
LONG DURATION HYPERBARIC CONFINEMENT: HYDRA 9 **c52**
B. Gardette, M. Comet, C. Gortan, M. Novara (European Space Agency. European Space Research and Technology Center, ESTEC, Noordwijk, Netherlands), and H. G. Delauze *In* ESA, Space and Sea Dec. 1990 p 63-68 (For primary document see N91-23563 15-42)
Copyright Avail: NTIS HC/MF A13

Hydra 9 cnshore saturation dive was designed to define three important parameters: the utilization range (minimum and maximum depths) on hydrox (H2-O2); the long term (49 days) effects of hydrogen on exposition of human beings; and the study of human reaction to a long duration confinement and isolation in a pressurized chamber (73 days), considered as a simulation of space long duration flight by the European Space Agency. Fundamental results of the acute and chronic hydrogen effects and the human reaction to long duration confinement and isolation, were obtained. These reults will allow the optimization of the PH2 used in hydreliox breathing mixtures for very deep industrial interventions (500 to 700 msw) and the increase of European knowhow in long duration manned space missions. ESA

N91-23572# Japan Marine Science and Technology Center, Tokyo. Diving Science and Technology Dept.
MANNED DIVING ACTIVITIES IN JAMSTEC **c52**
Nobuo Ito *In* ESA, Space and ESA Dec. 1990 p 69-73 (For primary document see N91-23563 15-42)
Copyright Avail: NTIS HC/MF A13

JAMSTEC (Japanese Marine Science and Technology Center) is engaged in research in diving technology, and also in training courses. Manned hyperbaric experiment series have been conducted since 1974 to ensure the safety of open sea operations and the medical fitness of divers. In July 1988, their diving record in the open sea reached 300 m. In the process of research and development on diving science and technology up to 300 m depth, experiences and results were stored. After being trained and educated, about 2500 commercial divers and managers have graduated from the courses and are currently engaged in various commercial activities during the past 17 years. ESA

N91-23573# Societe d'Architectures en Milieux Extremes, Paris (France).
EUROPEAN STAKES AND MEASURES PERMITTING THE MANAGEMENT OF GEOMETRIC DIMENSIONS [ENJEUX EUROPEENS ET MESURES PERMETTANT DE GERER LES DIMENSIONS GEOMETRIQUES] **c54**
M. Fabre *In* ESA, Space and Sea Dec. 1990 p 75-80 In FRENCH (For primary document see N91-23563 15-42)
Copyright Avail: NTIS HC/MF A13

Within the Columbus program, the studies defining and optimizing the pressurized spaces must be based on extremely rigorous and highly performant modular and repetitive geometric dimensions, in compliance with ergonomic data inherent to the indispensable presence of man. These studies must also satisfy the following demands: they must comply, at all levels, with the geometric dimensional concepts of the decimal metric system and the international norms inherent to this system; they must be compatible, as much for the Columbus Attached Laboratory and the Columbus autonomous laboratory or Free Flyer as for the Hermes hold and pressurized airlock and the dynamic envelope of the cylindrical portion of the Ariane cap, with the most highly performant industrial geometric dimension norms and rules of international level, whether or not they come from the U.S. or are in use in Japan, USSR, etc.; they must generate a unique base denominator of geometric measurement in compliance with the international metric system. ESA

N91-23574# Compagnie Maritime d'Expertises, Marseille (France). Diving and Safety Dept.
COMPARISONS BETWEEN UNDERWATER AND SPACE WORKING ENVIRONMENTS FOR ON BOARD ACTIVITIES OPTIMIZATION (COLUMBUS SPACE PROGRAMME) **c54**
Jean-Pierre Imbert and Carlo Viberti (European Space Agency. European Space Research and Technology Center, ESTEC, Noordwijk, Netherlands) *In* ESA, Space and Sea Dec. 1990 p 85-88 (For primary document see N91-23563 15-42)
Copyright Avail: NTIS HC/MF A13

The design of the standard racks for the Columbus laboratories, along with the rack transfer scenario, needs to be evaluated for the definition and optimization of crew on board tasks. In water tests seem to be the best way to conduct intravehicular activity (IVA) simulation and the problem of such tests definition is addressed. The method of intervention is reviewed under the light of the commercial diving experience: it seems that closed circuit breathing apparatus could be used which would make IVA simulation more realistic. The water physical properties are expected to induce differences but adequate arrangement of the rack mock up could minimize these biases. Obviously, underwater simulation is best to study operational problems, including supervision and monitoring. ESA

N91-23575# European Space Agency. European Space Research and Technology Center, ESTEC, Noordwijk (Netherlands).
EVA SERVICING: THE HERMES CAPABILITY **c54**
A. Accensi, I. Skoog, and J. Chevallier (Avions Marcel Dassault-Breguet Aviation, Saint-Cloud, France) *In its* Space and Sea Dec. 1990 p 89-94 (For primary document see N91-23563 15-42)
Copyright Avail: NTIS HC/MF A13

Experience demonstrates that external intervention capabilities are an integral part of an in orbit infrastructure; allied to the development of Hermes and Columbus, ESA has embarked upon the establishment of an Extra Vehicular Activity (EVA) capability. Following the establishment of EVA mission requirements, ESA initiated in 1987, preparatory studies for the evaluation of operational scenarii and alternative design concepts which resulted in the definition of the technical requirements for the Europen EVA system. The various design options for meeting these requirements were evaluated in detail within the on going Hermes phase C activities. The design tradeoff placed particular attention to the close man system integration of the EVA system; crew safety and human factors engineering were consequently used as key design drivers in the derivation of the EVA system design reference. ESA

N91-23576# Center for Industrial Research, Oslo (Norway).
MAN-MACHINE INTERACTIONS AND MULTIMEDIA APPLIED TO ROV OPERATIONS **c54**

Eivind Kjennerud *In* ESA, Space and Sea Dec. 1990 p 95-99 (For primary document see N91-23563 15-42)
Copyright Avail: NTIS HC/MF A13

To evaluate new technology for improving efficiency and safety in the man machine interface in Remotely Operated Vehicles (ROV) underwater interventions, a demo lab was built. By means of recent research in multimedia applications and artificial reality, an attempt to create a more intuitive and operator friendly control room environment is made. ESA

N91-23577# Companhia Espacial Portuguesa Ltd., Lisbon.
THE BERLENGA UNDERWATER SURVEY PROJECT **c54**
Dinis Afonso Ribeiro *In* ESA, Space and Sea Dec. 1990 p 101-102 (For primary document see N91-23563 15-42)
Copyright Avail: NTIS HC/MF A13

A very general overview of a planned underwater survey is given and some practical ways to establish better contacts in Portugal are suggested. Applying high technology to underwater archaeology may provide a symbolic way to link projects aimed at the future, with the study of past explorations, easing the future shock in the Portuguese society. ESA

N91-23578# Espace Studio, Turin (Italy).
TEST ON PARABOLIC FLIGHTS FOR STOWAGE IN WEIGHTLESSNESS **c18**
G. Musso, D. Pastrone, and Carlo Viberti (European Space Agency. European Space Research and Technology Center, ESTEC, Noordwijk, Netherlands) *In* ESA, Space and Sea Dec. 1990 p 103-106 (For primary document see N91-23563 15-42)
Copyright Avail: NTIS HC/MF A13

The small dimensions of the internal environment of the Attached Pressurized Module (APM) make it necessary to optimize the available space. A rational use of the space to store different items with different functions for the on orbit environments and to carry out the foreseen operations (e.g., racks handling by crew) is of permanent importance. In the first design phase the subunit rack subdivides the available space into five subunits which could be used as drawers. The whole internal volume of these subunit/drawers can be occupied by open cell polyurethane foam drawer shaped blocks, able to contain items to be stored inside convenient modular housing slots. Thanks also to the polyurethane foam elastic deformability, the blocks are capable of retaining different sizes and mass of objects both on orbit and during launch phases. The related necessity to analyze in real microgravity the overall concept for on board racks handling and transfer procedures is also shortly addressed and a proposal for parabolic flights tests is provided. ESA

N91-23579# Compagnie Maritime d'Expertises, Marseille (France).
NEUTRAL BUOYANCY AND MICROGRAVITY: EXTRAVEHICULAR ACTIVITIES WITH A HUMID WATER SUIT [SIMULATION DES ACTIVITES SPATIALES EXTRA VEHICULAIRES EN IMMERSION AVEC UN SCAPHANDRE HUMIDE] **c54**
C. Gortan, L. Decramer, and D. Hornet (Dassault Espace, Saint-Cloud, France) *In* ESA, Space and Sea Dec. 1990 p 107-112 In FRENCH (For primary document see N91-23563 15-42)
Copyright Avail: NTIS HC/MF A13

Within the framework of simulation of extravehicular activities in water, water immersion provides great interest with regard to the use of equipment, recreating axes near as possible the principle mobility constraints which astronauts confront in pressurized space suit. The humid water suit is considered. In immersion, the use of this equipment requires diving breathing apparatus to be carried and therefore astronauts need elementary diving training. The small constraint is well compensated by the possibilities offered by this equipment. In fact, in water it is possible to simulate almost all the phases of extravehicular sorties, including dressing and undressing, operations which are impossible with a pressurized clothing. Before a pressurized submergeable model of the European space suit is available, this humid water suit concept should be immediately usable in the development phase of the Hermes program for the evaluation of diverse interfaces linked to extravehicular activities both in the equipment planning and in procedures. ESA

N91-23580# MATRA Espace, Toulouse (France).
SPACE AND TELESCIENCE ROBOTICS: DEVELOPMENT OF CONCEPTS AND REFERENCE TECHNOLOGIES FOR TELEDETECTION AND ROBOTICS IN EXTREME ENVIRONMENTS [ROBOTIQUE SPATIALE ET TELESCIENCE: ESSOR DE CONCEPTS ET TECHNOLOGIES DE REFERENCE POUR LA TELEDETECTION ET LA ROBOTIQUE EN MILIEUX EXTREMES] **c37**
G. Andre and J. Tailhades *In* ESA, Space and Sea Dec. 1990 p 117-129 In FRENCH (For primary document see N91-23563 15-42)
Copyright Avail: NTIS HC/MF A13

Recent progress in the technology of teleoperation and spatial robotics within European projects are presented. The concepts of internal and external service robotics as well as telescience are recalled. The present developments in critical technologies and simulators which support the system studies are described. The common points with regard to the needs and technology transfer potential within the domain of robotic intervention in extreme environments are evoked. ESA

N91-23581# Tecnomare S.p.A. (Italy).
TELEROBOTICS: A KEY AREA FOR POSSIBLE TECHNOLOGY TRANSFER FROM UNDERWATER TO SPACE **c37**
Walter Prendin, Antonio Terribile, and Simonetta DiPippo (Italian Space Agency, Rome.) *In* ESA, Space and Sea Dec. 1990 p 131-137 (For primary document see N91-23563 15-42)
Copyright Avail: NTIS HC/MF A13

Underwater telerobotics have significantly developed in the last decades due to the increasing interest to substitute divers for inspection maintenance and repair of hydrocarbon production platforms. Technologies being developed by Tecnomare such as: supervisory control, man machine interface, visions systems, manipulation and manipulator vehicle control, which could find direct application to space robotics are discussed. Examples of possible expected applications of said technologies to the development of the Italian Space Agency (ASI) SPIDER program are specifically given with indication of the necessary adaptations. ESA

N91-23582# National Space Development Agency, Ibaraki (Japan).
RESEARCH AND DEVELOPMENT OF FUTURE SPACE ROBOTICS IN NASDA **c37**
Tsutomu Iwata, Mitsushige Oda, and Taichi Nakamura *In* ESA, Space and Sea Dec. 1990 p 139-143 (For primary document see N91-23563 15-42)
Copyright Avail: NTIS HC/MF A13

Space robotics is a key technology for future space activities. The space robotics will support and extend manned capability in orbit. NASDA, recognizing that the space automation and robotics are key issues for future space activities, is making every effort of research and development in this technology area. Japanese Experimental Module Remote Manipulator System (JEMRMS) which will be a part of Space Station Freedom is under development. Research on the space robotics is now concentrated on advanced space robotics. In the robotics mission of Engineering Test Satellite 7 (ETS-7) which is to be launched in 1996, fundamental robotics technologies such as dynamic cooperative control, teleoperation and exchange of Orbital Replacement Units (ORUs) will be demonstrated in orbit. ESA

N91-23583# McDonnell-Douglas Space Systems Co., Houston, TX. Space Station Div.
EVA/ROBOTICS INTEGRATION FOR SPACE STATION FREEDOM **c54**
R. M. Machell, L. V. Ramon, and D. E. Anderson *In* ESA,

Space and Sea Dec. 1990 p 145-149 (For primary document see N91-23563 15-42)
Copyright Avail: NTIS HC/MF A13

Space Station Freedom is being designed to be assembled and maintained on orbit by astronauts in space suits and by the use of telerobotic devices. Undersea experience in the cooperative use of divers and robots is being applied to the integration of astronauts in Extra Vehicular Activity (EVA) and telerobots for on orbit assembly and external maintenance tasks. Evaluation of on orbit assembly and external maintenance tasks and worksites will determine which tasks should be done by EVA and which by telerobots. Priority emphasis is being given to telerobotics wherever practical. Neutral buoyancy testing in underwater test tanks is being conducted to evaluate EVA worksites and tasks in simulated weightlessness. Common designs for EVA and telerobotics hardware interfaces are being developed. The extensive analysis and test activities provide substantial confidence in the ability to assemble and maintain the Space Station Freedom on orbit.
ESA

N91-23584# Deutsche Forschungsanstalt fuer Luft- und Raumfahrt, Oberpfaffenhofen (Germany, F.R.). Inst. for Flight Systems Dynamics.
MULTISENSORY TELEROBOTIC CONCEPTS FOR SPACE AND UNDERWATER APPLICATIONS c54
G. Hirzinger, J. Dietrich, and B. Brunner *In* ESA, Space and Sea Dec. 1990 p 151-161 (For primary document see N91-23563 15-42)
Copyright Avail: NTIS HC/MF A13

The telerobotic concepts as presently developed for a space Robot Technology Experiment (ROTEX) to fly with the next Spacelab mission D2 in 1992 are outlined; the robot is supposed to work in an autonomous mode, teleoperated by astronauts, and teleoperated from ground. One of its key features is a recently developed multi sensory gripper with highly integrated, miniaturized sensor technology including stiff and compliant six axis force torque sensing, nine laser range finders, tactile arrays, grasp force control using a new electrical gripper drive and a stereo camera pair. Sensory feedback schemes and man machine interface concepts using a six degrees of freedom control ball and stereo imaging is explained. Sensory simulation on ground using advanced stereo graphics is supposed to predict the sensor based path refinement on board, while real time fusion of stereo images and laserscan information helps to predict the motion of floating objects to be grasped. A lightweight robot concept with new intelligent joint drives and grid structure composite arms for the astronaut training on ground is discussed. The telerobotic concepts are structured thus that they are equally applicable to space and underwater situations.
ESA

N91-23585# Cybernetix, Marseille (France). Societe d'Ingenierie.
TELEMANIPULATION SYSTEM ASSISTED BY COMPUTER FOR UNDER WATER APPLICATIONS [SYSTEME DE TELEMANIPULATION ASSISTEE PAR ORDINATEUR POUR LES APPLICATIONS SOUS-MARINS] c37
D. Sangouard, C. Leveque, and G. Clement (Commissariat a l'Energie Atomique, Fontenay-aux-Roses, France) *In* ESA, Space and Sea Dec. 1990 p 163-169 In ENGLISH and FRENCH (For primary document see N91-23563 15-42)
Copyright Avail: NTIS HC/MF A13

The automation of underwater mannual tasks (particularly in the domain of inspection, maintenance and repair) through the use of a teleoperation system is far better then the performances of conventional systems presently on the market. The work performed to put a telemanipulation system, capable of resolving automation problems of underwater operations, on the market, is described.
ESA

N91-23586# European Space Agency. European Space Research and Technology Center, ESTEC, Noordwijk (Netherlands).
HOW TO DESIGN EFFICIENT MMI FOR SPACE c54
Muriel Didier *In its* Space and Sea Dec. 1990 p 173-177 (For primary document see N91-23563 15-42)
Copyright Avail: NTIS HC/MF A13

The difficulties met when trying to design an efficient Man Machine Interface (MMI) for space are addressed and a way that can be followed to turn the difficulties around is shown. The problems of designing MMI for space come mainly from the environment (microgravity environment) and not so much from the task and the operator that can be easily identified. The methodologies and tools usually used when designing for a 4 g environment have to be adapted to the 0 g environment. The experience gained on Columbus when designing restraints for the crew project gives an example of a way that can be followed.
ESA

N91-23587# Fokker Space and Systems, Amsterdam (Netherlands).
BUILDING REAL-TIME SIMULATORS FOR SPACE APPLICATIONS c14
J. A. Hoogstraten *In* ESA, Space and Sea Dec. 1990 p 179-186 (For primary document see N91-23563 15-42)
Copyright Avail: NTIS HC/MF A13

Simulation is used in nearly all fields of engineering to study situations that would be too hazardous, time consuming, costly or otherwise unable to be created in real life. Situations involving real world interfaces, such as the control exercised by a human operator, are extra demanding due to the real time behavior they require of the simulator. The role of real time simulation for space applications in the context of the development of a robotic arm, the Hermes Robot Arm (HERA) is described and illustrated. It is shown that the general approach is valid also for other applications in the space environment. Some considerations on commonality in the context of the design and development of a generally applicable simulation facility, the European Real Time Operations Simulator (EUROSIM), are listed.
ESA

N91-23588# Direction des Constructions et Armes Navales, Toulon (France).
A KO2 REBREATHER FOR EVA DENITROGENATION PROCEDURE c52
E. Radziszewski and Jean Claude LePechon (JCLP Hyperbarie, Paris, France) *In* ESA, Space and Sea Dec. 1990 p 187-190 (For primary document see N91-23563 15-42)
Copyright Avail: NTIS HC/MF A13

In order to test the use of a KO2 rebreather for space denitrogenation, the performances of a standard KO2 unit were evaluated and thermal comfort discussed. After pure O2 rinsing out of the lungs and of the counter lung nitrogen, the experimental protocol includes periods of rest and exercise. Nitrogen excretion is then evaluated, as well as oxygen contamination of the cabin atmosphere. The equipment tested proved to be acceptable for denitrogenation, some minor improvements are recommended and feasibility and advantages of the method for Extra Vehicular Activity (EVA) and emergency O2 breathing are reviewed.
ESA

N91-23589# Societe d'Etudes des Systemes d'Automation, Toulouse (France).
OBJECT ORIENTED PROGRAMMING IN MMI: A SOFTWARE TOOL FOR ANALYSIS AND PLANIFICATION OF A RADAR IMAGING MISSION c54
J. L. Wippler and J. P. Aguttes (Centre National d'Etudes Spatiales, Toulouse, France) *In* ESA, Space and Sea Dec. 1990 p 191-194 (For primary document see N91-23563 15-42)
Copyright Avail: NTIS HC/MF A13

The design of a system analysis computerized tool used to be focused mainly on the modelization of the phenomena in study. When in a prephase A study, since many options are still open and many technical teams are involved, this leads to a simulation package that can be difficult to use and to modify. Such a computerized tool, implemented on a personal computer compatible, in the MS Windows environment and using object oriented programming is described. This tool carries powerful modeling capabilities, yet features flexibility and evolution potential,

while presenting a friendly user interface for ease of use to cooperants in the 'Radar 2000' program. It is composed of several cooperative components: a worldwide radar mission data base; a system builder to create a scanario; and a simulator to evaluate overall mission performances. From several similar object oriented projects, a tentative conclusion on the usefulness of such object oriented approaches can be drawn. ESA

N91-23590# Institut Francais de Recherche pour l'Exploitation de la Mer, La Seyne sur Mer.
EVALUATION OF MULTISENSOR FUSION SCHEME FOR THE LOCALIZATION OF UNDERWATER REMOTELY OPERATED VEHICLES **c37**
V. Rigaud and B. Duchene *In* ESA, Space and Sea Dec. 1990 p 195-200 (For primary document see N91-23563 15-42)
Copyright Avail: NTIS HC/MF A13

A study of computer assistance for the manned guidance of the Subsea Remotely Operated Vehicle (ROV) is presented. It is shown that many problems are common in spatial and undersea mobile robotics. In this approach concerning vehicle localization, it is possible to estimate an optimal location by fusing data derived from log and gyroscope or a non optimal location by composition of compass, depthmeter, and log data. However, this relative reckoning is achieved by taking into account a hypothesis on the value of the undercurrent. Therefore, a second model of the reckoning module that improves the ROV location close to an offshore jacket is propounded that fuses data given by an echo sounders belt and takes into account an a priori CAD map of the surrondings. This new estimate is indenpendent of the undercurrent, and it is possible with the help of the operator to match this absolute model with the relative one in an asynchronous way. This matching gives a new hypothesis on the value of the undercurrent and resets the dead reckoning module. ESA

N91-23591# Computer Resources International A/S (Denmark).
A PROCEDURAL EXPERT SYSTEM FOR SPACECRAFT COMMAND AND CONTROL **c18**
Mogens Nielsen, J. M. Darroy, Francois Lecouat, Jean-Marc Brenot, and Joe Wheadon (European Space Agency. European Space Operations Center, Darmstadt, Germany, F.R.) *In* ESA, Space and Sea Dec. 1990 p 201-206 (For primary document see N91-23563 15-42)
(Contract ESA-7627/88/NL/DG)
Copyright Avail: NTIS HC/MF A13

A project within the European Space Agency's Advanced Systems and Technology Program to study the applicability of expert systems for day to day space operations is presented. A prototype of an expert system is developed, to operate together with an existing spacecraft control system at the European Space Operations Centre and eventually function as an operator's assistant in controlling satellites. The aim of the project is to examine the extent to which the reliability and effectiveness of operations can be enhanced by such means through the development of a prototype system. The developed operator's assistant is dedicated to controlling a process with severe safety and time constraints so major attention was dedicated to the man machine interaction. ESA

N91-23592# Paris VI Univ. (France). Lab. d'Oceanographie Dynamique et de Climatologie.
OCEAN MODELING FOR CLIMATE STUDY [MODELISATION OCEANIQUE POUR LES ETUDES DE CLIMAT] **c47**
P. Delecluse *In* ESA, Space and Sea Dec. 1990 p 209-214 In FRENCH (For primary document see N91-23563 15-42)
Copyright Avail: NTIS HC/MF A13

The ocean is a strong climate regulator and the study of climate variations needs to take into account its circulation. For many years, the numerical resolution used in the models of the general ocean circulation was dictated through the example of general atmospheric circulation models or through the capacity of available computers. This type of resolution is not completely capable of reproducing the strength of the oceans flows which have a strong intrinsic turbulence. The development of the strength of calculations has permitted the rapid expansion of high resolution regional models, notably in the lower latitudes, which have shown that the contribution of the resolution was fundamental; however, it was equally necessary to carry the efforts to other physical parameters such as vertical turbulence. The application of lower latitude ocean circulation models has conferred a growing confidence in the numerical tool and has initiated a fruitful synergism between observation and modelization. If technological developments continue to progress and if the data acquisition efforts started with the World Ocean Circulation Experiment (WOCE) program continue, the extension of these global climate circulation results and the development of climate simulations can be hoped for. ESA

N91-23593# Institut de Mecanique de Grenoble (France).
SATELLITE DATA UTILIZATION IN OCEAN CIRCULATION MODELS [UTILISATION DES DONNEES SPATIALES DANS LES MODELES DE CIRCULATION OCEANIQUE] **c48**
B. Barnier, M. Boukthir, and J. Verron *In* ESA, Space and Sea Dec. 1990 p 215-220 In FRENCH Sponsored by CNES; CNRS; and Direction des Recherches, Etudes et Techniques, France (For primary document see N91-23563 15-42)
Copyright Avail: NTIS HC/MF A13

Two examples are presented of the use of satellite data in a numerical model. The model is composed of simplified physics that simulate the ocean circulation forced by the wind on a pond-scale. It is shown that the assimilation of the surface data in the model, which is used to obtain the altimetry of the Topex/Poseidon satellite mission (i.e., the difference in level of free ocean surface), is potentially capable of calculating the deep circulation to a satisfactory precision. It is also shown that the simple technique of assimilation used in the ocean model correlates well with the information towards the depths. How the full force of the wind, which will provide the altimetry of the ERS-1 and NSCAT missions, can cause the ocean basin circulations is studied, given their time-spatial sampling linked to the satellite coverage and to the disposition of the sensors. From this point of view, the ERS-1 mission could present some partial insufficiencies while the NSCAT mission appears more appropriate. ESA

N91-23594# Technische Univ., Delft (Netherlands). Faculty of Aerospace Engineering.
EXTRACTION OF MESOSCALE OCEAN CURRENTS INFORMATION FROM GEOSAT ALTIMETER DATA **c48**
K. F. Wakker, M. C. Naeije, R. Scharroo, and B. A. C. Ambrosius *In* ESA, Space and Sea Dec. 1990 p 221-226 Sponsored by Space Research Organization Netherlands; Beleidscommissie Remote Sensing, Delft, Netherlands; and IBM Nederland NV (For primary document see N91-23563 15-42)
Copyright Avail: NTIS HC/MF A13

A satellite altimeter data processing technique optimized for the detection of mesoscale ocean currents is reported. The technique allows the computation of the relative dynamic sea surface topography and the relative ocean flow field at a specified epoch from altimeter measurements which are irregularly distributed in space and time. It has a multisatellite capability, which will be important for the near future when the ERS-1 and the Topex/Poseidon altimeters are operational in the same time frame. The technique was applied to extract from Geosat altimeter measurements mesoscale ocean currents information for the region of the Algulhas Current, the South Indian Ocean, the South East Atlantic and the North Atlantic. Various mesoscale eddies were identified and some charateristics of the eddies were determined. ESA

N91-23595# Institut de Mecanique de Grenoble (France).
SEA LEVEL AND SATELLITE TECHNIQUES [NIVEAU DE LA MER ET TECHNIQUES SATELLITAIRES] **c48**
C. LeProvost *In* ESA, Space and Sea Dec. 1990 p 227-232 In FRENCH; ENGLISH summary (For primary document see N91-23563 15-42)
Copyright Avail: NTIS HC/MF A13

The ocean topography is complex both spatially and temporally. Since the last century, sea level measurements have been carried out around the world, primarily for the needs of hydrography, with a high density in developed economic areas but very scarce elsewhere (the southern ocean and the high latitudes). Twenty years ago, observations of the sea surface were extended to the open sea for scientific purposes. The use of satellite technologies greatly contributes to this field. With satellite data transmission facilities, isolated automatic stations can operate on remote islands or in hostile areas. Operational sea level monitoring networks are becoming a reality. Synoptic observations of the sea level with satellite altimetry is also being investigated and will ultimately contribute to the monitoring of the global ocean circulation. The possibility offered by spatial techniques to link tide gauge stations to a world geodetic system is a major contribution to the problem of mean sea level changes. ESA

N91-23596# Paris VI Univ., Villefranche-sur-Mer (France). Lab. de Physique et Chimie Marines.
PRIMARY OCEAN PRODUCTION: CARBON AND PARTICLE FLUX [PRODUCTION PRIMAIRE OCEANIQUE: FLUX DE CARBONE ET DE PARTICULES] c48
Andre Morel *In* ESA, Space and Sea Dec. 1990 p 233-240 In FRENCH Submitted for publication (For primary document see N91-23563 15-42)
Copyright Avail: NTIS HC/MF A13

The role of the ocean and its vegetation with regard to the carbon and other cycles is discussed. Comprehension of the flux between the atmosphere and the ocean in stationary conditions at the interface and at the interior of the ocean is considered. Present incertitudes with regard to the marine biomass carbon content, the flux entering, the net carbon flux at the base of the superficial layer, and the flux in a column of water down to the sediment are presented. Possible progressions are given. ESA

N91-23597# Centre National d'Etudes des Telecommunications, Issy-les-Moulineaux (France).
ENERGY EXCHANGE STUDY AT THE OCEAN SURFACE BY SATELLITE OBSERVATION [ETUDE DES ECHANGES D'ENERGIE A LA SURFACE OCEANIQUE, A PARTIR D'OBSERVATIONS SPATIALES] c48
Laurence Eymard *In* ESA, Space and Sea Dec. 1990 p 241-245 In FRENCH (For primary document see N91-23563 15-42)
Copyright Avail: NTIS HC/MF A13

The flux at the ocean atmosphere interface is the object of growing interest on account of its importance for the understanding of the Earth climatic system. Since the traditional ways of measuring are not being adapted to climatic studies within international programs, more and more work is devoted to the development of satellite investigation techniques. The determination of the surface flux, showing what satellite observations can bring, the problems to resolved, and how the flux is treated in present or future large programs are considered. ESA

N91-23598# Direction de la Meteorologie Nationale, Paris (France).
SATELLITE DATA UTILIZATION FOR MODELING SEA STATES [UTILISATION DES DONNEES SATELLITAIRES POUR LA MODELISATION DE L'ETAT DE LA MER] c48
A. Guillaume *In* ESA, Space and Sea Dec. 1990 p 247-249 In FRENCH (For primary document see N91-23563 15-42)
Copyright Avail: NTIS HC/MF A13

The results of the LEWEX (Labrador Extreme Waves Experiment) campaign which took place in the Labrador Sea in March 1987 enable the data needed for the validation of models which forecast the sea state to be better understood. The possibilites offered by the altimeter satellites to respond to these needs are analyzed from the following two examples: a comparison of the winds of the model of central Europe with Geosat observations; and a wind wave validation of the western Mediterranean Sea from Geosat data. ESA

N91-23599# Institut Francais de Recherche pour l'Exploitation de la Mer, Brest (France).
WIND AND SEA STATE LOCAL CLIMATOLOGY BY MEANS OF SATELLITE RADAR ALTIMETER MEASUREMENTS c47
J. Tournadre and R. Ezraty *In* ESA, Space and Sea Dec. 1990 p 251-256 (For primary document see N91-23563 15-42)
Copyright Avail: NTIS HC/MF A13

A feasibility study of a new approach to determine the local Significant Wave Height (SWH) and wind speed climatology using a satellite borne radar altimeter is presented. Geosat altimetric data, from the Exact Repeat Mission (ERM) and in situ data from the Frigg and Palanca oil fields are used for this study. Because of the satellite sampling scheme, altimetric measurements are considered for an area surrounding the location where the climatology is to be estimated. This asks a question about the representativeness of the satellite climatology. Analysis of the spatial consistency scale of the wind and SWH statistics and comparison between in situ and altimetric data is possible. Due to a poor dynamic of the relation between the wind speed and the altimetric backscatter coefficient it is not possible to estimate the wind speed climatology with a good precision. ESA

N91-23600# Universite des Sciences et Techniques de Lille (France). Lab. d'Optique Atmospherique.
USING SATELLITE REMOTE SENSING IMAGERY FOR MARGINAL ICE ZONE RESEARCH IN THE ARCTEMIZ PROJECT c43
C. Kergomard, J. C. Gascard, and M. Fily (Grenoble-1 Univ., France) *In* ESA, Space and Sea Dec. 1990 p 257-262 Sponsored by Inst. Francais de Recherche pour l'Exploitation de la Mer, France; CNES; CNRS; and Direction des Recherches, Etudes et Techniques (For primary document see N91-23563 15-42)
Copyright Avail: NTIS HC/MF A13

Four main satellite remote sensing tools are available for sea ice monitoring at different scales and spatial resolution. All four were tested for use in the Arctic Eurasian Marginal Ice Zone project. Among them, visible and infrared imagery from the NOAA-AVHRR (Advanced Very High Resolution Radiometer) was primarily used in the course of in situ experiments in the Fram Strait area. In the near future, extensive use of the ERS-1 Synthetic Aperture Radar (SAR) data is planned for monitoring of mass and heat exchanges between the Arctic and Atlantic Ocean through the Fram strait. ESA

N91-23601# Rutherford Appleton Lab., Chilton (England). Space Science Dept.
ATSR: PRECISE SEA SURFACE TEMPERATURE FROM THE ERS-1 SATELLITE c48
D. Llewellyn-Jones, R. Bernard, and Laurence Eymard (Centre de Recherches en Physique de l'Environnement, Issy-les-Moulineaux, France) *In* ESA, Space and Sea Dec. 1990 p 265-266 (For primary document see N91-23563 15-42)
Copyright Avail: NTIS HC/MF A13

The Along Track Scanning Radiometer (ATSR) instrument is described. It is to fly as an 'announcement of opportunity' experimental package on ESA's ERS-1 satellite due for launch in April 1991. The ATSR's instrument's ability to meet its demanding performance objectives (of measuring sea surface temperature to better than 0.5 K accuracy) depends critically upon a number of novel design features. The way in which these features enable ATSR to achieve its measurement objectives are outlined. ESA

N91-23602# Centre National d'Etudes Spatiales, Toulouse (France).
VALIDATION REQUIREMENTS FOR THE TOPEX/POSEIDON ALTIMETER MISSION c48
Y. Menard, S. Arnault, J. M. Molines (SBS, Aix-en-Provence, France), P. Vincent, L. Gourdeau, and M. Dorrer *In* ESA, Space and Sea Dec. 1990 p 267-273 (For primary document see N91-23563 15-42)
Copyright Avail: NTIS HC/MF A13

The joint NASA/CNES Topex/Poseidon mission will be mainly

dedicated to the large scale oceanic circulation observation. The satellite payload will include two altimeters, one radiometer and two precise orbit determination systems, Doris and GPS (Glob Positioning System). Such a system will provide sea lev measurements with an absolute decimetric accuracy. In previous studies local differences were observed which can be due to real oceanographic effects or to imperfections in the altimetric data. In order to discern and to characterize the various error sources, a careful validation of altimetric data is required. For the Topex/Poseidon mission a complete verification plan has been proposed by CNES. First, a single point system verification will be achieved at a site located in the Mediterranean Sea, the Italian Lampedusa island, instrumented with tide gages, laser station and other adequate sensors. Additional verification activities will include regional verification experiments, meteorological model comparisons and statistical analysis. This verification effort will be specially intense during the first six months of the mission to ensure a permanent control of the system and cross calibrations with other satellite systems. ESA

N91-23603# CLS Argos, Toulouse (France). Groupe Oceanographique.
COLLECTION AND PROCESSING OF OCEANOGRAPHIC DATA AT CLS [COLLECTE ET TRAITEMENT DE DONNEES OCEANOGRAPHIQUES A CLS] **c48**
Pierre-Yves LeTraon *In* ESA, Space and Sea Dec. 1990 p 275-278 In FRENCH (For primary document see N91-23563 15-42)
Copyright Avail: NTIS HC/MF A13

The principal activity of CLS is to collect in situ or satellite oceanographic data. The data presently collected comes from the Argos satellite system localization and acquisition system. However CLS, being responsible for the future CTDP (French acronym for Doris Poseidon processing center), will receive altimetric data from the Franco-American Topex-Poseidon mission and will participate in their processing. An oceanographic group has been created at CLS to develop aspects concerning the processing of in situ and satellite oceanographic data. The objective of this group is to supply the user with valid data, which is rapidly accessible and interpretable. It therefore carries out systematic processing that the user does not wish to do himself or supplies him with studies and software which will permit him to carry and desire processing. ESA

N91-23604# Consiglio Nazionale delle Ricerche, Florence (Italy). Ist. di Ricerca sulle Onde Elettromagnetiche.
REMOTE SENSING OF THE SEA AT IROE/CNR **c48**
Bruno Radicati, Giovanna Cecchi, Luca Pantani, and Ivan Pippi *In* ESA, Space and Sea Dec. 1990 p 279-283 (For primary document see N91-23563 15-42)
Copyright Avail: NTIS HC/MF A13

The rapid growth of sea pollution, due to man made activities, has produced consequent damage to all kinds of marine life and sea connected activities. There is a growing interest in sea monitoring research. The main activity of the research group 'land and sea remote sensing' is the development of new sensors and techniques in the visible and infrared regions of the electromagnetic spectrum. The research and sea romote sensing was carried out along two main lines: lidar and passive sensors. ESA

N91-23605# European Space Agency. European Space Research and Technology Center, ESTEC, Noordwijk (Netherlands).
SIGNAL DETECTION OF MERIS IN OCEANOGRAPHIC APPLICATIONS **c43**
J.-L. Bezy, M. Morel, M. Rast, and P. Bardey (ACRI S.A., Sophia Antipolis, France) *In its* Space and Sea Dec. 1990 p 285-290 (For primary document see N91-23563 15-42)
Copyright Avail: NTIS HC/MF A13

An overview of the Medium Resolution Imaging Spectrometer (MERIS) signal detection over the ocean is given. As a first step, the coverage capabilities of the instrument are assessed taking the limitations imposed by illumination conditions and sensor parameters into account. In this context, an evaluation is made of the influence of Sun glint. As a second step, preliminary ocean calculations are carried out assuming standard atmospheric conditions and average marine constituents concentrations. ESA

N91-23606# Ifremer, Paris (France).
SATELLITE AND AERONAUTICAL TECHNOLOGIES SERVING THE MANAGEMENT OF LIVING MARINE RESOURCES [TECHNOLOGIES AERONAUTIQUES ET SATELLITAIRES AU SERVICE DE LA GESTION DES RESSOURCES VIVANTES MARINES] **c43**
J. Y. LeGall *In* ESA, Space and Sea Dec. 1990 p 291-294 In FRENCH (For primary document see N91-23563 15-42)
Copyright Avail: NTIS HC/MF A13

Four recent examples which gave rise to the original development technologies are chosen to illustrate the present or potential contribution of satellite and aeronautical remote sensing and telecommunications in the exploitation and management of living marine resources through fishing and agriculture. The four examples are successively: the use of the Argos system for the management of a coastal prawn farm; estimation of oyster stocks using aerial photographs and digital video images; detection of shoals of red tuna through airborne SAR (Synthetic Aperture Radar); and the contribution of satellite remote sensing of the surface temperature of the sea to the intertropical industrial tuna fishery. Space platforms and passive (video camera, radiometers) and active (hyperfrequency radars) captors on board carrier planes, helicopters and/or satellites are discussed. ESA

N91-23607# Alcatel Espace, Toulouse (France).
CHARACTERISTICS AND PERFORMANCE OF AN OPERATIONAL WINDSCATTEROMETER **c47**
D. Marquet and N. Lannelongue *In* ESA, Space and Sea Dec. 1990 p 297-301 (For primary document see N91-23563 15-42)
Copyright Avail: NTIS HC/MF A13

Meteorologists and oceanologists of the scientific community have demonstrated the need for such a powerful instrument for research, survey and forecast. Moreover such an instrument should ensure service continuity at a reasonable cost. A cost optimized wind scatterometer of very good performance and the way to attain an optimized instrument are described. The study covers C band and Ku band wind scatterometers. A summary of the basic principles of wind scatterometry is given, and the models employed are presented. The instrument design and optimization is described. In conclusion, a comparative table is presented and projected characteristics are given. ESA

N91-23608# Aerospatiale, Cannes (France).
MEDIUM RESOLUTION IMAGING SPECTROMETER (MERIS) **c74**
G. Baudin, R. Bessudo, M. A. Cutter, D. Lobb, and J. L. Bezy (European Space Agency. European Space Research and Technology Center, ESTEC, Noordwijk, Netherlands) *In* ESA, Space and Sea Dec. 1990 p 303-308 Sponsored in part by Dornier-Werke G.m.b.H. (For primary document see N91-23563 15-42)
Copyright Avail: NTIS HC/MF A13

The Medium Resolution Imaging Spectrometer (MERIS) is an optical instrument which is intended to be flown on the first European Polar Platform, scheduled for launch in 1997. The instrument has a spectral range of 400 nm to 1050 nm, a swath width of 1500 km, a spectral resolution of 1.25 nm and spatial resolution of 250 m. The instrument has applications in the fields of oceanographic, land and atmospheric research. ESA

43 EARTH RESOURCES AND REMOTE SENSING

Includes remote sensing of earth resources by aircraft and spacecraft; photogrammetry; and aerial photography.

For instrumentation see *35 Instrumentation and Photography.*

N91-23609# Instituto de Pesquisas Espaciais, Sao Jose dos Campos (Brazil).

DETECTION OF MINING ACTIVITIES IN THE YANOMANI INDIAN RESERVE THROUGH LANDSAT-TM IMAGERY Final Report [DETECCAO DE ATIVIDADES DE MINERACAO NA RESERVA INDIGENA DO GRUPO YANOMAMI ATRAVES DE IMAGENS DO LANDSAT-TM]

Chan Chiang Liu, Pedro Hernandez Filho, and Antonio Tebaldi Tardin Oct. 1990 17 p In PORTUGUESE; ENGLISH summary Original contains color illustrations

(INPE-5182-RPE/638) Avail: NTIS HC/MF A03; 3 functional color pages

Color composites of LANDSAT-TM images in the bands 3, 4, and 5, with blue, green, and red filters respectively, were visually interpreted in order to detect areas of altered mining activity in the Yamoni Indian Reserve, which covers the west side of Roraima State and a small part in the extreme north of the Amazonas State. Results are presented in thematic maps on the scale of 1:250,000 and 1:100,000 showing placer-mining activities and flight strips. River and streams with water soil sediments, due to mining activities, were also identified. Author

N91-23610# Army Engineer Topographic Labs., Fort Belvoir, VA.

HYPERSPECTRAL IMAGERY: WHAT IS IT, WHAT CAN IT DO Scientific Paper, 7-9 May 1990

Jack N. Rinker 4 Sep. 1990 26 p Presented at the 7th USACE Remote Sensing Symposium, Portland, OR, 7-9 May 1990

(AD-A231164; ETL-R-151) Avail: NTIS HC/MF A03 CSCL 17/8

Because all materials reflect, absorb, or emit photons in ways characteristic of their molecular makeup, a high resolution trace of the transmitted, reflected, emitted, or luminesced radiation versus wavelength forms a graphical record unique to a given material. The laboratory use of spectral measurements to identify minerals, pigments, and organic and inorganic compounds is an established and reliable technique; and, the reasoning goes, if such could be done from air or space, it would give remote sensing a similar capability. Unfortunately, the useful absorption bands are narrow, 10 nanometers (nm) or less, and cannot be recorded with broad band systems such as LANDSAT. With the advent of the Airborne Visible Infrared Imaging Spectrometer (AVIRIS) and similar systems, the narrow band capability entered the remote sensing domain. AVIRIS is a true spectrometer, collecting reflecting solar energy (0.4 to 2.5 micra) in about 220 channels, or images, each in a spectral bandwidth of about 9.6 nm. This type of narrow band information is called hyperspectral. GRA

N91-23611 Miami Univ., Coral Gables, FL.

INFRARED AND VISIBLE STUDIES OF PAKISTAN PORTION OF ARABIAN SEA USING INSAT GEOSTATIONARY SATELLITE Ph.D. Thesis

Labeed Iqbal Kazi 1990 179 p

Avail: Univ. Microfilms Order No. DA9104432

Data from the INSAT-IB geosynchronous satellite was used to make maps of albedo, solar energy, and temperature distribution over the Arabian Sea which includes Pakistan's fifth province in the ocean. Visible data in the range of 10.5 to 12.5 microns were used. Four months of data were processed to show the different kinds of variation in ocean temperatures and the albedo. The months chosen were July 1985, October 1985, January 1986, and April 1986. In July, a large number of clouds were over the Arabian Sea because of the monsoons, and it was difficult to find a cloud free day in order to calculate the ocean temperatures. First, the albedo maps were drawn for all four months and only three days for each month, which had no clouds or minimum number of clouds over the Arabian Sea, were chosen. The minimum albedo and solar energy maps for all four months were drawn. For each month, three albedo and sea surface temperature maps are discussed in detail. For cloud free areas, sea surface temperature measurements appear to be reasonable when compared with monthly mean values obtained from sources other than INSAT IB. However, values calculated by using INSAT IB infrared data were found to be, in general, slightly lower than the monthly mean surface temperature values. This difference may be improved by fine tuning the coefficients which are used in the correction for atmospheric attenuation and zenith angle.

Dissert. Abstr.

N91-23612# Deutsche Forschungsanstalt fuer Luft- und Raumfahrt, Oberpfaffenhofen (Germany, F.R.). Abt. Fernerkundung.

THE APPLICABILITY OF THEMATIC MAPPER DATA TO THE CLASSIFICATION OF TREE SPECIES AND NATURAL AGE CLASSES Ph.D. Thesis - Freiburg Univ.

Mathias Schardt Sep. 1990 203 p In GERMAN; ENGLISH summary Original contains color illustrations

(DLR-FB-90-44; ISSN-0171-1342; ETN-91-99066) Avail: NTIS HC/MF A10; DLR, Wissenschaftliches Berichtswesen, VB-PL-DO, Postfach 90 60 58, 5000 Cologne, Fed. Republic of Germany, HC 80 DM

The use of Thematic Mapper data for the classification of tree species and natural age classes is investigated. The development of methods for multitemporal classifications and for the inclusion of digital terrain models into the process of classification is emphasized. The applicability of Shuttle Imaging Radar (SIR) B data to detailed forest classifications is examined, and the data from three different test sites are evaluated. ESA

N91-23613# Deutsche Forschungsanstalt fuer Luft- und Raumfahrt, Oberpfaffenhofen (Germany, F.R.). Abt. fuer Fernerkundungsanwendungen.

CORRECTION OF RELIEF-INDUCED RADIOMETRIC DISTORTIONS IN SEASAT-A SAR IMAGES FOR THE EXAMPLE OF THE SUBSCENE OF BONN (FED. REPUBLIC OF GERMANY) AND VICINITIES Thesis - Technische Univ.

Thomas Bayer Oct. 1990 133 p In GERMAN; ENGLISH summary Original contains color illustrations

(DLR-FB-90-54; ISSN-0939-2963; ETN-91-99074) Avail: NTIS HC/MF A07; DLR, Wissenschaftliches Berichtswesen, VB-PL-DO, Postfach 90 60 58, 5000 Cologne, Fed. Republic of Germany, HC 69 DM

The scene is geocoded using a digital elevation model and a processor based algorithm. The influence of relief undulations on image grey value variations is investigated by setting up a model for the reconstruction of the imaging geometry and by the application of statistical methods. Thirteen different functions for the correction of the relief influence are derived by means of empirical backscatter models. These correction functions are applied to the SAR (Synthetic Aperture Radar) image data of forest and agriculture land use classes. The results of these corrections are evaluated and compared, using digital image processing methods and statistical measurements. ESA

N91-23614# Deutsche Forschungsanstalt fuer Luft- und Raumfahrt, Oberpfaffenhofen (Germany, F.R.). Abt. fuer Optische Fernerkundung.

ANALYSIS ON FOREST DECLINE CLASSIFICATION OF THE BEECH USING AIRBORNE MULTISPECTRAL SCANNER DATA Ph.D. Thesis - Freiburg Univ.

Ralf Baumgarten Nov. 1990 250 p In GERMAN; ENGLISH summary Original contains color illustrations

(DLR-FB-90-56; ISSN-0939-2963; ETN-91-99075) Avail: NTIS HC/MF A11; DLR, Wissenschaftliches Berichtswesen, VB-PL-DO, Postfach 90 60 58, 5000 Cologne, Fed. Republic of Germany, HC 75 DM

Methods for the recognition classification and mapping of forest

decline are developed. Three different systems are used to collect the data: the airborne Thematic Mapper Daedalus 1268, and the two satellite systems LANDSAT TM and SPOT. Airborne scanner data from three different altitudes were examined. Spectral signatures of individual trees were collected and analyzed. Procedures to optimize image interpretation and classification were introduced, and the results were checked with different methods. ESA

N91-23615# Aerospatiale, Cannes (France).
REMOTE SENSING PERFORMANCES
Charles Carton 1991 12 p Presented at Conference on Space Technology: Satellite Application Development, Manama, Bahrain, 6-7 Mar. 1990
(Rept-911-440-101; CA-3/90; ETN-91-99303) Avail: NTIS HC/MF A03

The optical payloads of meteorological geostationary satellites and low orbit observation systems are addressed. Current observation systems are outlined including the imaging, data dissemination and data collection missions of Meteosat. Imaging performances are summarized. Next generation systems including the U.S. GOES-Next three axis stabilized satellite and Europe's Meteosat Second Generation (MSG) are discussed. The main performances of candidate designs are compared to the existing Meteosat Operational Program (MOP). Applications and requirements of low orbit observation systems are described. Passive optical sensing payloads are described with illustrations of four approaches for multispectral imaging and optical layouts of two typical payloads. Active sensing payloads are outlined with a summary of main ranging and altimetry performances and an illustration of the GLRS (Geoscience Laser Ranging Sensor) overall mission. ESA

N91-23600# Universite des Sciences et Techniques de Lille (France). Lab. d'Optique Atmospherique.
USING SATELLITE REMOTE SENSING IMAGERY FOR MARGINAL ICE ZONE RESEARCH IN THE ARCTEMIZ PROJECT
C. Kergomard, J. C. Gascard, and M. Fily (Grenoble-1 Univ., France) *In* ESA, Space and Sea Dec. 1990 p 257-262 Sponsored by Inst. Francais de Recherche pour l'Exploitation de la Mer, France; CNES; CNRS; and Direction des Recherches, Etudes et Techniques (For primary document see N91-23563 15-42)

N91-23605# European Space Agency. European Space Research and Technology Center, ESTEC, Noordwijk (Netherlands).
SIGNAL DETECTION OF MERIS IN OCEANOGRAPHIC APPLICATIONS
J.-L. Bezy, M. Morel, M. Rast, and P. Bardey (ACRI S.A., Sophia Antipolis, France) *In its* Space and Sea Dec. 1990 p 285-290 (For primary document see N91-23563 15-42)
Copyright Avail: NTIS HC/MF A13

N91-23606# Ifremer, Paris (France).
SATELLITE AND AERONAUTICAL TECHNOLOGIES SERVING THE MANAGEMENT OF LIVING MARINE RESOURCES [TECHNOLOGIES AERONAUTIQUES ET SATELLITAIRES AU SERVICE DE LA GESTION DES RESSOURCES VIVANTES MARINES]
J. Y. LeGall *In* ESA, Space and Sea Dec. 1990 p 291-294 In FRENCH (For primary document see N91-23563 15-42)
Copyright Avail: NTIS HC/MF A13

N91-24054*# National Aeronautics and Space Administration. Goddard Space Flight Center, Greenbelt, MD.
THE LAND ANALYSIS SYSTEM (LAS)
Yun-Chi Lu and Fred M. Irani (ST Systems Corp., Lanham, MD.) *In* NASA, Washington, Technology 2000, Volume 2 1991 p 115-121 (For primary document see N91-24041 15-99)
Avail: NTIS HC/MF A16 CSCL 08B

N91-24055*# National Aeronautics and Space Administration. Goddard Space Flight Center, Greenbelt, MD.
POTENTIAL COMMERCIAL USES OF EOS REMOTE SENSING PRODUCTS
Leslie L. Thompson *In* NASA, Washington, Technology 2000, Volume 2 1991 p 122-129 (For primary document see N91-24041 15-99)
Avail: NTIS HC/MF A16 CSCL 08B

44 ENERGY PRODUCTION AND CONVERSION

Includes specific energy conversion systems, e.g., fuel cells; global sources of energy; geophysical conversion; and windpower.

For related information see also *07 Aircraft Propulsion and Power, 20 Spacecraft Propulsion and Power,* and *28 Propellants and Fuels.*

N91-23616*# National Aeronautics and Space Administration. Lewis Research Center, Cleveland, OH.
MATERIAL PROCESSING WITH HYDROGEN AND CARBON MONOXIDE ON MARS
Aloysius F. Hepp, Geoffrey A. Landis (Sverdrup Technology, Inc., Cleveland, OH.), and Diane L. Linne 1991 11 p Presented at the 10th Biennial Conference on Space Manufacturing, Princeton, NJ, 15-19 May 1991; sponsored by the Space Studies Inst.
(NASA-TM-104405; E-6230; NAS 1.15:104405) Avail: NTIS HC/MF A03 CSCL 10B

Several novel proposals are examined for propellant production from carbon dioxide and monoxide and hydrogen. Potential uses were also examined of CO as a fuel or as a reducing agent in metal oxide processing as obtained or further reduced to carbon. Hydrogen can be reacted with CO to produce a wide variety of hydrocarbons, alcohols, and other organic compounds. Methanol, produced by Fischer-Tropsch chemistry may be useful as a fuel; it is easy to store and handle because it is a liquid at Mars temperatures. The reduction of CO2 to hydrocarbons such as methane or acetylene can be accomplished with hydrogen. Carbon monoxide and hydrogen require cryogenic temperatures for storage as liquids. Noncryogenic storage of hydrogen may be accomplished using hydrocarbons, inorganic hydrides, or metal hydrides. Noncryogenic storage of CO may be accomplished in the form of iron carbonyl (FE(CO)5) or other metal carbonyls. Low hydrogen content fuels such as acetylene (C2H2) may be effective propellants with low requirements for earth derived resources. The impact on manned Mars missions of alternative propellant production and utilization is discussed. Author

N91-23617*# National Aeronautics and Space Administration. Lewis Research Center, Cleveland, OH.
SOLAR THERMAL ENERGY RECEIVER Patent Application
Karl W. Baker, inventor (to NASA) and Miles O. Dustin, inventor (to NASA) 27 Mar. 1991 14 p
(NASA-Case-LEW-14949-1; NAS 1.71:LEW-14949-1; US-Patent-Appl-SN-676910) Avail: NTIS HC/MF A03 CSCL 10A

A plurality of heat pipes in a shell receive concentrated solar energy and transfer the energy to a heat activated system. To provide for even distribution of the energy despite uneven impingement of solar energy on the heat pipes, absence of solar energy at times, or failure of one or more of the heat pipes, energy storage means are disposed on the heat pipes which extend through a heat pipe thermal coupling means into the heat activated device. To enhance energy transfer to the heat activated device, the heat pipe coupling cavity means may be provided with extensions into the device. For use with a Stirling engine having passages for working gas, heat transfer members may be positioned to contact the gas and the heat pipes. The shell may be divided into sections by transverse walls. To prevent cavity working fluid from collecting in the extensions, a porous body is positioned in the cavity. NASA

N91-23618# Midwest Research Inst., Golden, CO.
OPTIMIZATION OF TRANSPARENT AND REFLECTING ELECTRODES FOR AMORPHOUS SILICON SOLAR CELLS
R. G. Gordon, Jianhua Hu, J. Musher, and C. Giunta Feb. 1991 44 p Prepared in cooperation with Harvard Univ., Cambridge, MA
(Contract DE-AC02-83CH-10093)
(DE91-002132; SERI/TP-214-4141) Avail: NTIS HC/MF A03

The specific objectives of this research are to: (1) deposit and characterize textured zinc oxide with improved conductivities (less than 8 ohms/square sheet resistance) and optical transmission (greater than 85 percent for 450 to 700 nm), for use as front and back contacts in hydrogenated amorphous silicon p-i-n devices; (2) study the surface morphology of zinc oxide films deposited by chemical vapor deposition at atmospheric pressure (APCVD), their crystallite sizes, shapes and orientations, and their nucleation (early growth) as a function of chemical precursors and reaction conditions; (3) optimize the growth process to produce structures that provide good light trapping in an amorphous silicon film deposited on the zinc oxide film; (4) study the deposition rate of zinc oxide films as a function of temperature, and concentration and types of reactants; (5) maximize the growth rate, subject to the conditions of maintaining satisfactory film properties, including high transparency (85 percent), high conductivity (8 ohm/square sheet resistance), and good light trapping; (6) develop techniques for deposition of fluorinated zinc oxide films by APCVD on amorphous silicon films in the temperature range of 250 to 280 C for use as back contacts; (7) deposit titanium nitride films at a temperature of about 250 C by APCVD on amorphous silicon as diffusion barrier, and then deposit highly reflective metals such as aluminum or silver; (8) anneal samples and test for metal diffusion through the TiN into the silicon; (9) optimize the TiN film for minimum diffusion consistent with maintaining desirable TiN film properties; and (10) incorporate the front and back contacts including the TiN barrier layer developed under this research into amorphous silicon p-i-n devices and determine the film parameters that provide the greatest improvement in the device solar energy conversion efficiency. DOE

N91-23619# Sandia National Labs., Albuquerque, NM.
PV CONCENTRATORS TODAY AND TOMORROW
A. B. Maish and J. L. Chamberlin 1991 4 p Presented at the 10th European Photovoltaic Solar Energy Conference and Exhibition, Lisbon, Portugal, 8-12 Apr. 1991
(Contract DE-AC04-76DP-00789)
(DE91-010577; SAND-90-2164C; CONF-910425-1) Avail: NTIS HC/MF A01

The U.S. Department of Energy's photovoltaic concentrator cell and module development program has expanded with the commencement of a significant program jointly funded with four cell and four system manufacturers. This paper reviews the status of crystalline silicon, III-V cell and concentrator module research, with emphasis being given to activities by participants in the DOE program. Also covered is a summary of the fundamental reason for pursuing the concentrator option, namely the high probability of achieving efficiency and cost targets necessary to meet competitive energy cost goals. DOE

N91-23620*# National Aeronautics and Space Administration. Lewis Research Center, Cleveland, OH.
SEI ROVER SOLAR-ELECTROCHEMICAL POWER SYSTEM OPTIONS
Colleen A. Withrow, Lisa L. Kohout, David J. Bents, and Anthony J. Colozza (Sverdrup Technology, Inc., Brook Park, OH.) May 1991 19 p Presented at the 26th Intersociety Energy Conversion Engineering Conference, Boston, MA, 4-9 Aug. 1991; sponsored by American Nuclear Society, SAE, American Chemical Society, AIAA, ASME, IEEE, and American Inst. of Chemical Engineers
(Contract NAS3-25266)
(NASA-TM-104402; E-6224; NAS 1.15:104402) Avail: NTIS HC/MF A03 CSCL 10A

A trade study of power system technology for proposed lunar vehicles and servicers is presented. A variety of solar-based power systems were selected and analyzed for each. The analysis determined the power system mass, volume, and deployed area. A comparison was made between periodic refueling/recharging systems and onboard power systems to determine the most practical system. The trade study concluded that the power system significantly impacts the physical characteristics of the vehicle. The refueling/recharging systems were lighter and more compact, but dependent on availability of established lunar base infrastructure. Onboard power systems pay a mass penalty for being fully developed systems. Author

45 ENVIRONMENT POLLUTION

Includes atmospheric, noise, thermal, and water pollution.

N91-23621# Ministry of Defence, Haifa (Israel). Center for Military Analyses.
LATERAL DISPERSION OF RADIOACTIVE RELEASE. DRAFT FOR COMMENTS
Itzhak Ravid and Noomi Abigadol Jun. 1987 27 p Sponsored by the Israel Electric Corp. Ltd.
(CEMA-86/17; ITN-89-85014) Avail: NTIS HC/MF A03

The prevailing models of atmospheric dispersion, used for the probabilistic risk assessments (PRA) of nuclear power plants, underestimates systematically the lateral dispersion of radioactive release by not allowing for the considerable shift of wind-direction during the time of the release. The bias is mainly significant in case of a slow wind. The paper examines references to empirical data, on which the prevailing estimates are based, and suggests that the references have been widely misinterpreted. Empirical data suggest that the lateral dispersion in cases of slow wind is much larger than indicated by prevailing estimates. Respectively, maximum concentration levels are lower than anticipated. Due to the fact that acute fatalities depend on a threshold of radiation level, the consequence of the exaggerated estimates of concentration is that PRA models drastically overestimate the number of acute fatalities following a potential severe radioactive accident. On the other hand, the models underestimate the extent of the area inflicted by a lower level of radiation. ISA

N91-23622# Air Force Inst. of Tech., Wright-Patterson AFB, OH.
FORECASTING ATMOSPHERIC PARTICULATE SULFUR CONCENTRATIONS USING NATIONAL WEATHER SERVICE SYNOPTIC CHARTS M.S. Thesis
Stephen L. Brueske Aug. 1990 147 p
(AD-A231634; AFIT/CI/CIA-90-146) Avail: NTIS HC/MF A07 CSCL 13/2

The goal of this research is to increase the understanding meteorological and chemical mechanisms that control atmospheric particulate sulfur concentrations, using standard meteorological charts. Aerosol particles were collected at nine sampling sites and analyzed in steps corresponding to 2 hour time intervals. Atmospheric particulate sulfur concentration variations were found to vary in predictable ways, depending on the synoptic-scale weather system affecting the sampling sites. Insight into how synoptic-scale meteorological process affect atmospheric particulate sulfur concentrations are developed. GRA

N91-23623# Environmental Protection Agency, Seattle, WA. Policy Planning and Evaluation Branch.
REGION 10 ENVIRONMENTAL INDICATORS Report, FY 1989
Rick Albright, John Armstrong, Elaine Barrick, Joan Cabreza, Jayne Carlin, Rob Goldberg, Gil Haselberger, Dick Hetherington, Dru Keenan, and Laurie Kral et al Oct. 1990 182 p
(PB91-136580; EPA/910/9-90/018) Avail: NTIS HC/MF A09 CSCL 13B

This is EPA Region 10's third annual summary of environmental indicators for air, water, and land media. The region's programs in air, water, toxics, pesticides, and hazardous waste are attempting to characterize their progress in addressing environmental

degradation via the measures described in the report. The FY 89 report builds upon the FY 88 document with the addition of: (1) FY 89 data; (2) new measures and deletions; and (3) new programmatic areas where indicators were developed, including underground injection control (UIC), accidental release, and terrestrial environments. GRA

N91-23624# New Orleans Univ., LA. Environmental Inst.
THE CHANGING FACE OF THE ENVIRONMENTAL ISSUE
Susan E. Howell and Shirley Laska Jan. 1990 16 p
(Grant NA85AA-D-SG141)
(PB91-138081; LSU-T-90-004; WP-1) Avail: NTIS HC/MF A03
CSCL 13B

The environment may prove to be one of the most important public policy issues of the 1990's. It is already one of the most salient issues on the public agenda. Public opinion on this issue is changing rapidly, and in one direction. Whenever public opinion on an issue changes this much the next natural question concerns whether there are also changes in the demographic bases of opinion. The answer has clear policy implications. Decision makers will have to rely on a base of public support to formulate and implement environmental regulatory policy. These questions are addressed. Examining these changes empirically requires longitudinal data throughout the 1980's using a similar measure of opinion on the environment. The National Election Studies from the ICPSR provide such data since one of the environmental questions was asked in the 1980, 1984, and 1988 presidential election surveys. Author

N91-23625# Corvallis Environmental Research Lab., OR. Office of Research and Development.
NATIONAL STREAM SURVEY DATABASE GUIDE
Mark E. Mitch, Philip R. Kaufmann, Alan T. Herlihy, W. Scott Overton, and Michael J. Sale Jul. 1990 104 p Sponsored in part by Utah State Univ. and Oregon State Univ.
(Contracts EPA-68-03-3249; EPA-68-02-3889; EPA-68-02-3994; EPA-68-03-3246; EPA-68-C8-0006; DE-AC05-84OR-21400)
(PB91-141804; EPA/600/8-90/005) Avail: NTIS HC/MF A06
CSCL 13B

The National Stream Survey (NSS), conducted in the spring of 1985 and 1986, is one component of the U.S. Environmental Protection Agency's National Acid Precipitation Assessment Program. The NSS was a synoptic, spring survey of 500 streams in regions of the Southeastern and Mid-Atlantic United States expected to contain large numbers of low alkalinity streams. The NSS is based on a probability sample from an explicitly defined population of surface waters. In the NSS, 500 streams were sampled, representing a regional population of 64,700 stream reaches. The NSS database includes stream and watershed physical characteristics, in situ measurements, and water chemistry data. Accompanying the database is a comprehensive user's guide that provides an overview of the NSS design, database structure, and transfer media. GRA

N91-23626# Brookhaven National Lab., Upton, NY.
TROPOSPHERIC SAMPLING WITH AIRCRAFT
P. H. Daum and S. R. Springston Mar. 1991 50 p Presented at the 199th National Meeting of the American Chemical Society (ACS), Boston, 22-27 Apr. 1990
(Contract DE-AC02-76CH-00016)
(DE91-009472; BNL-45879; CONF-900402-13) Avail: NTIS HC/MF A03

As the atmospheric chemical community focuses more intensely on issues of global concern, requiring survey of the chemical composition of the remote atmosphere and study of chemical processes occurring well above the surface, a larger number of programs will use aircraft as either the principal sampling platform, or to augment measurements made by other means. Because aircraft measurements impose different, and frequently more stringent sets of requirements on techniques used to measure trace atmospheric species than surface measurements, there is a need to review these requirements and to show how various measurement methods have been designed or altered to meet the needs of aircraft use. We will focus our attention here on measurement of trace chemical species, that definition including trace gases as well as aerosol particles and cloud droplets. DOE

N91-23627# Atlantic Council of the United States, Washington, DC.
ENERGY-RELATED ENVIRONMENTAL ISSUES IN A GLOBAL CONTEXT
R. W. Fri (Resources for the Future, Inc., Washington, DC.) 1990 7 p Presented at the US/Japan Energy Policy Dialogue, Washington, DC, 8 Nov. 1990
(Contract DE-FG01-89IE-10763)
(DE91-009538; CONF-9011186-1) Avail: NTIS HC/MF A02

Few subjects have received more attention in the past few years than the tension between energy and the environment. The fundamental issue behind this tension is how to provide required energy series in a sustainable way. This issue stretches beyond a global agenda to an intergenerational one. An agenda this expansive cannot be addressed by business-as-usual means, but requires more fundamental thinking about the conditions that must exist in the future to deal successfully with this agenda, and how these conditions can be brought about. First, it's self-evident that heavy investments should be made in research and development. The New Earth 21 proposal from Japan is a good example of this sort of program, as is Energy Technology R and D: What Could Make A Difference, by Oak Ridge National Laboratory. Next, heavy investments must be made in science as well as technology. In particular, science should focus on reducing uncertainty about risks, for uncertainty can make unnecessary risk averse. Only greater scientific understanding can tell if this risk aversion is misplaced. The final two conditions are institutional in nature. One is that a way must be found to build demand for both energy services and environmental protection. This is a special challenge in developing countries, because most of the energy growth and environmental problems of the future will be there. Lastly, global interdependence means sharing scare resources. The developed and developing worlds depend on one another, both economically and environmentally. We must face the issue of transferring financial and technology resources from the wealthy to the poor, even at some expense to the former. Technology, science, demand creation and resource transfers are large and general ideas. But if these large issues are not attended to, the future tensions between basic needs for energy and the environment will become unbearable. DOE

N91-23628# Lawrence Livermore National Lab., CA.
GRAVITY SPREADING IN THE DISPERSION OF DENSE GAS PLUMES
D. L. Ermak Mar. 1991 6 p Presented at the International Conference and Workshop on Modeling and Mitigating the Consequences of Accidental Releases of Hazardous Materials, New Orleans, 6-10 May 1991
(Contract W-7405-eng-48)
(DE91-010155; UCRL-JC-105011; CONF-910530-1) Avail: NTIS HC/MF A02

The atmospheric dispersion of a denser-than-air release is affected by several physical phenomena that either do not occur or are unimportant in a trace gas release. The main phenomena are directly related to the density structure of the dense gas cloud. They are damping of the turbulence level due to stable density stratification within the cloud and alteration of the ambient velocity field due to gravity flow resulting from horizontal gradients in the cloud density. The phenomena of gravity spreading of a denser-than-air cloud dispersing over flat terrain is addressed. Specifically, an attempt was made to interpret the gravity spreading results observed in wind-tunnel studies conducted by CPP Inc. DOE

N91-23629 Ohio State Univ., Columbus.
ATMOSPHERIC CIRCULATION AND POLEWARD SENSIBLE HEAT FLUX VARIATIONS ASSOCIATED WITH THE RECENT

NORTHERN HEMISPHERE WARMING Ph.D. Thesis
Marilyn Noreen Raphael 1990 307 p
Avail: Univ. Microfilms Order No. DA9105196

The premise that the Northern Hemisphere has been warming since about 1975 was discussed. The following subject areas were covered: (1) identifying the nature and extent of the warming at the surface and 700 mb constant pressure level; and (2) the relationship between temperature changes and those of the atmospheric circulation and the meridional flux of kinematic sensible heat at the 700 mb constant pressure level. The data used are grid-averaged 700 mb geopotential heights and temperatures and land-based surface station temperatures. Regression analysis of the long-term seasonal averages of temperature was used to give an estimate of the overall trend of the 700 mb temperatures. The results are presented and discussed. Dissert. Abstr.

N91-23630# Los Alamos National Lab., NM.
AN EXPANDING GRID PHOTOCHEMICAL MODEL FOR VISIBILITY APPLICATIONS
M. D. Williams and G. Streit 1 Mar. 1991 30 p Presented at the 84th Annual Meeting and Exhibition of the Air and Waste Management Association (AWMA), Vancouver, British Columbia, 16-21 Jun. 1991
(Contract W-7405-eng-36)
(DE91-009947; LA-UR-91-847; CONF-910659-10) Avail: NTIS HC/MF A03

Photochemical models for visibility applications normally suffer from several limitations which impair their application to point-source plumes. Lagrangian type models suffer from an inability to handle wind shear and reversing winds Eulerian based systems smear the plume unrealistically during the early part of its travel. To avoid these problems a new model has been developed and compared to measurements near a southwestern power plant. The new system is quasi-Lagrangian in that the grid at any point in time covers the volume occupied by contaminants at that time. Consequently, the modeled volume is small during the early portion of the plume and expands with time. The model is driven by winds, temperatures, and turbulences provided by a three-dimensional, prognostic, higher order turbulence, atmospheric circulation model (HOTMAC). In comparison with plume measurements in the southwest, the model produced reasonable predictions of dispersion and ozone, but underestimated sulfate formation. Nitrate predictions were much too low. DOE

N91-23631# Lawrence Livermore National Lab., CA.
SENSITIVITY OF NUMERICAL DISPERSION MODELING TO EXPLOSIVE SOURCE PARAMETERS
R. L. Baskett (EG and G Energy Measurements, Inc., Pleasanton, CA.) and R. T. Cederwall 13 Feb. 1991 18 p Presented at the 84th Annual Meeting and Exhibition of the Air and Waste Management Association (AWMA), Vancouver (Canada), 16-21 Jun. 1991
(Contracts W-7405-eng-48; DE-AC08-88NV-10617)
(DE91-009476; UCRL-JC-105277; CONF-910659-3; EGG-10617-411) Avail: NTIS HC/MF A03

The calculation of downwind concentrations from non-traditional sources, such as explosions, provides unique challenges to dispersion models. The U.S. Department of Energy has assigned the Atmospheric Release Advisory Capability (ARAC) at the Lawrence Livermore National Laboratory (LLNL) the task of estimating the impact of accidental radiological releases to the atmosphere anywhere in the world. The experience includes responses to over 25 incidents in the past 16 years, and about 150 exercises a year. Examples of responses to explosive accidents include the 1980 Titan 2 missile fuel explosion near Damascus, Arkansas and the hydrogen gas explosion in the 1986 Chernobyl nuclear power plant accident. Based on judgment and experience, the source geometry and the amount of toxic material aerosolized as well as its particle size distribution were frequently estimated. To expedite the real-time response, some automated algorithms and default assumptions about several potential sources were developed. It is useful to know how well these algorithms perform against real-world measurements and how sensitive the dispersion model is to the potential range of input values. The algorithms used to simulate explosive events are presented, these methods were compared with limited field data measurements, and their sensitivity to input parameters was analyzed. DOE

N91-23632# Lawrence Livermore National Lab., CA.
TREATMENT OF DENSER-THAN-AIR RELEASES IN AN ADVECTION-DIFFUSION MODEL: THERMODYNAMIC EFFECTS
D. L. Ermak and R. Lange Mar. 1991 19 p Presented at the 84th Annual Meeting and Exhibition of the Air and Waste Management Association (AWMA), Vancouver (Canada), 16-21 Jun. 1991
(Contract W-7405-eng-48)
(DE91-010152; UCRL-JC-106798; CONF-910659-12) Avail: NTIS HC/MF A03

The manufacture, transportation, and use of hazardous chemicals is increasing world-wide, and with this increase has come an increase in the frequency of serious chemical accidents. This situation emphasizes the need for realistic simulations of toxic and dense gas releases for both emergency response and planning purposes. To meet this need, we are modifying an existing advection-diffusion, particle-in-cell type model to include the dispersion effects associated with denser-than-air releases. In this paper, we present the mathematical description of this approach to treating the thermal transport within a cold, heavy gas cloud. A section briefly describes the overall dense-gas, advection-diffusion, particle-in-cell model. This is followed by a more detailed description of the thermodynamics. First the case of adiabatic mixing is treated, and then the more complex situation with ground heating is considered. Two example problems are also presented to demonstrate the validity of the method. DOE

N91-23633# Carnegie-Mellon Univ., Pittsburgh, PA. Robotics Inst.
STEPS TOWARD ENVIRONMENTALLY COMPATIBLE PRODUCT AND PROCESS DESIGN: A CASE FOR GREEN ENGINEERING
D. Navinchandra 23 Dec. 1990 8 p
(AD-A232888; CMU-RI-TR-90-34) Avail: NTIS HC/MF A02 CSCL 24/3

Green Engineering is the study of product and process design for environmental friendliness without compromising product quality and commercial viability. The aim is to identify, develop, and exploit new technologies that can bolster productivity without costing the environment. This is one of the challenges engineers will face in the coming century. Over the past decade, a lot of research and effort has been put into understanding issues such as waste management, materials recovery, and HazMin (Minimization of Hazardous materials and practices) as they relate to products after they enter the waste stream. Attention should also be focused on the product design itself. The idea is to inject concerns about environmental friendliness into the design process; where, the assessment of environmental friendliness is based on a life cycle view of the product. This includes the product's manufacturing process, distribution, use, and final disposal. GRA

46 GEOPHYSICS

Includes aeronomy; upper and lower atmosphere studies; ionospheric and magnetospheric physics; and geomagnetism.

For space radiation see *93 Space Radiation.*

N91-23634# National Park Service, Anchorage, AK.
PROCEEDINGS OF THE SECOND GLACIER BAY SCIENCE SYMPOSIUM
A. M. Milner, ed. and J. D. Wood, Jr., ed. 29 Oct. 1990 183 p Symposium held in Gustavus, AK, 19-22 Sep. 1988 Sponsored in part by Glacier Bay Science Board
(PB91-110163; ISBN-0-943475-03-1) Avail: NTIS HC/MF A09 CSCL 08G

The proceedings of the Second Glacier Bay Science

Symposium, held at the Glacier Bay Lodge in Glacier Bay National Park and Preserve, Alaska, on September 19 to 22, 1988 are presented. Thirty one scientific papers on the ecology, biotic communities, geology, geomorphology, and the influence of man on nature in the Glacier Bay National Park and Preserve and adjacent areas in southeastern Alaska are presented. Author

N91-23635# Southern Methodist Univ., Dallas, TX. Dept. of Statistical Science.
SOME REMARKS ON COMPLIANCE TESTING
H. L. Gray and Wayne A. Woodward Sep. 1990 57 p
(Contract F19628-88-K-0042)
(AD-A231936; GL-TR-90-0282; SR-3) Avail: NTIS HC/MF A04
CSCL 17/10

Several issues are discussed concerning compliance testing. First, the F-number is discussed and an alternative definition is provided which is identical to the common definition when sigma sub w is known but which is applicable to a broader range of testing situations. Compliance of a single new event given is discussed along with a collection of events for which both CORRTEX and seismic readings are available. These tests are considered in the case which sigma sub sei is assumed to be known and in the case in which sigma sub sei is unknown but the ratio sigma cub sei/sigma sub cor is known. The robustness is examined of these tests under situations for which perfect knowledge of sigma sub sei or the ratio is unknown and it is shown that the test based on the ratio is more robust to errors in specification of the variances. The estimation is also discussed of sigma sub sei based on the events for which both CORRTEX and seismic data are known. A brief discussion of the use of the mixture-of-normals model for purposes of estimating the seismic variance is also given. GRA

N91-23636 Pennsylvania State Univ., University Park.
ATMOSPHERIC TELECONNECTIONS: EMPHASIS ON THE EL NINO/SOUTHERN OSCILLATION AND MONSOONS Ph.D. Thesis
Song Yang 1990 270 p
Avail: Univ. Microfilms Order No. DA9104998

Teleconnections usually refer to the dynamic link between the tropics and higher latitudes associated with the El Nino Southern Oscillation (ENSO) cycle. However, there is a considerable amount of evidence which suggests that there are many geographically remote cause-effect relationships existing around the globe that may also be called teleconnections. This study examines some of these relationships. In particular, the following topics are addressed: (1) the relationship between the Asian summer monsoon and the longitudinal heating gradient between the Asian and the African desert; (2) the control of the tropical heating in the summer hemisphere on the location and intensity of the extratropical westerly jets in the winter hemisphere; (3) the relationship between the monsoons and ENSO in the winter and summer; (4) the relationships between zonal wind and perturbative kinetic energy (PKE) and the mechanisms for the generation of PKE in the mid-latitudes and tropics; and (5) the significance of ENSO-related interannual atmospheric energy variations and their transmission. Dissert. Abstr.

N91-23637 California Univ., Berkeley.
HIGH-PRECISION FOURIER TRANSFORM SPECTROSCOPY OF ATMOSPHERIC MOLECULES Ph.D. Thesis
Mark Abrams 1990 361 p
Avail: Univ. Microfilms Order No. DA9103622

Precise measurements of the spectra of atmospheric molecules are critical for the characterization of physical and chemical processes in the atmosphere. In particular, laboratory determinations of line and band oscillator strengths of the hydroxyl radical are necessary for understanding the dynamics of the ozone layer and ozone chemistry. The distribution of ozone in the atmosphere is mediated by a diffusion reaction between ozone and atomic hydrogen which produces vibrationally excited OH and the infrared night glow of the atmosphere. Broadband high resolution measurements of the OH spectrum require the use of Fourier transform spectrometers; however, even the largest instruments do not offer sufficient resolution to resolve the narrow emission lines observed in low temperature diffusion reactions. The minimum line width that can be observed, without significant line-shape distortion, is three to five times greater than the resolution width of the instrument. When a spectral line is under-resolved, the observed line shape is dominated by the instrumental line shape, and the amount of information that can be obtained is restricted. In addition to the degradation of the intensity, information about the line width, shape, and asymmetry is lost. A technique for resolution enhancing under-resolved Fourier transform spectra using bandwidth limited Voigt fitting was developed and utilized to obtain accurate line positions and line shapes in the spectrum of the diffusion reaction. Methods of resolution enhancement, signal detection, and the quality of spectral data are used to examine the limits of high resolution Fourier transform spectroscopy. The data obtained from the analysis of the OH spectrum emphasize the need for accurate spectroscopy and photometry. Dissert. Abstr.

N91-23638 Minnesota Univ., Minneapolis.
HYDROMAGNETIC WAVE COUPLING IN THE MAGNETOSPHERE Ph.D. Thesis
Dong-Hun Lee 1990 107 p
Avail: Univ. Microfilms Order No. DA9103317

The hydromagnetic wave phenomena in the magnetosphere has been an area of space physics and plasma physics where theory has been successful in explaining many features in satellite experiments and ground-based observations. Magnetohydrodynamic (MHD) waves, which are composed of transverse Alven waves and compressional waves, are usually coupled in space due to an inhomogeneous plasma density and curved magnetic field lines. In addition to these effects, hot temperature plasmas invoke various ultra low frequency (ULF) wave phenomena via macroscopic wave instabilities or wave particle resonant interactions. These properties of the coupling between the two different MHD waves were analytically and numerically studied in a simplified model such as the box model with straight field lines. However, the real magnetosphere is rather close to a dipole field, even though the night side of the magnetosphere is significantly distorted from dipole geometry. The curvature of field lines plays an important role in understanding hydromagnetic wave coupling in the magnetosphere since the MHD wave propagation depends strongly on the curved magnetic fields. The study of the hydromagnetic wave properties on an inhomogeneous and curved magnetic field system by considering realistic geometry is emphasized. Most of the current theories are reviewed and a number of observations are introduced according to the wave excitation mechanism. Studies are also performed with the development of numerical models such as the two and three dimensional MHD dipole models. An attempt is made to understand and classify the hydromagnetic wave behavior in inhomogeneous and hot plasmas with respect to the energy sources and their frequency band in the magnetosphere. Therefore, various excitation mechanisms for hydromagnetic waves are examined to compare analytical and numerical results with the observations.
Dissert. Abstr.

N91-23639 Princeton Univ., NJ.
MODELS OF PLANETARY WAVE PROPAGATION IN THE MIDDLE ATMOSPHERE Ph.D. Thesis
Chung-Chun Ma 1990 127 p
Avail: Univ. Microfilms Order No. DA9104355

Linear steady-state models were used to study the propagation of quasi-stationary planetary waves through zonally symmetric basic states with both meridional and vertical wind shears. Simulations from a comprehensive general circulation model were analyzed to provide realistic basic state and forcing. A quasi-geostrophic and a primitive-equation model were constructed. The models were found to give very different results when the Rossby number of the mean flow is large (around 0.4). The quasi-geostrophic model tends to give larger amplitude and longer vertical wavelength than the primitive-equation model. The wind shear and curvature of the

basic state were found to play dominant roles in determining the refractive properties for wave propagation and wave structures in the upper stratosphere and mesosphere. The polar-night jet acts like a waveguide which allows waves to propagate to high altitudes. The forcing at the lower boundary has a smaller effect on the response away from the lower boundary. The linear response to tropospheric forcing was also found to be sensitive to the method of parameterization of Rayleigh friction near the critical lines. It is less sensitive to the background dissipation and the static stability parameters. When the linear solutions were compared to the planetary waves simulated by the general circulation model, certain discrepancies were found. The linear model can generally reproduce the location of maximum amplitude response and phase structure successfully, but tends to underestimate the wave amplitude. Diagnostic tools such as refractive indices, Eliassen-Palm fluxes and ray tracing techniques were used to study the relationship between the linear response and the basic state. They were found to be complementary in providing a better knowledge of wave propagation. Dissert. Abstr.

N91-23640 Cornell Univ., Ithaca, NY.
INCOHERENT SCATTER MEASUREMENTS AND INFERRED ENERGY FLUXES IN THE EQUATORIAL F-REGION IONOSPHERE Ph.D. Thesis
Joseph Ellsworth Pingree 1990 374 p
Avail: Univ. Microfilms Order No. DA9106193

Faraday rotation and incoherent scatter correlation function measurements made using the Jicamarca Radio Observatory are used to infer the electron density and the electron and ion temperature of the equatorial F-region ionosphere over an altitude range of 150 to 1035 km. The electron density profiles obtained from the Faraday rotation and the total backscattered power appear self-consistent and the peak density agrees with simultaneous ionosonde readings. Temperature measurements made using two different antenna pointing positions (3 and 6 degrees) are not consistent. The electron temperature obtained at 3 deg is less than the corresponding ion temperature during the night and during the day at altitudes where one would expect the two species to be in thermal equilibrium. Electron and ion temperatures obtained at 6 deg do appear equal at time when they are expected to be equal. Data taken at Jicamarca using an older version of this experimental technique using the 3 deg antenna position appear to show the same problem. An exhaustive study of potential systematic experimental errors fails to provide an explanation for the inconsistency. A new technique is used to obtain the neutral temperature profile, the electron-ion energy flux, and more accurate electron and ion temperatures from the incoherent scatter autocorrelation function by using the equality of the electron-ion and ion-neutral energy flux as an additional constraint during the least squares fitting process. The electron, ion, and neutral temperature profiles obtained from the constrained least squares process are used to compute the electron-neutral energy flux and using a measured solar EUV spectrum, the energy flux form the photoelectrons to thermal electrons is computed. The sum of the electron-ion and electron-neutral energy fluxes is shown to be consistent with the photoelectron to thermal electron energy flux calculated using a solar spectrum obtained on a day with similar solar activity as the day when the incoherent scatter data were obtained. Dissert. Abstr.

N91-23641 Sheffield Univ. (England).
THEORETICAL STUDIES OF LARGE-SCALE FEATURES OF THE EARTH'S MID- TO HIGH-LATITUDE IONOSPHERE Ph.D. Thesis
Shaun Quegan 1982 309 p
Avail: Univ. Microfilms Order No. BRDX91352

Recent results on the plasmapause, mid-latitude trough, light-ion trough, and high-latitude troughs are reviewed. Their relations to each other and to convection reversal boundaries and particle precipitation zones are discussed. The transformations between the geographic and geomagnetic coordinate systems are derived for an offset dipolar magnetic field. Numerical methods for calculation of plasma motions along equipotential streamlines are described, and applied to calculations of convection paths both with and without allowance for universal time effects. The continuity and momentum equations are derived in a form suitable for calculation of the behavior of a multi-component plasma moving under electric field drifts, and numerical methods for their solution are described. These methods are then applied to a study of ionospheric behavior at high latitudes and in the transplasmaspause region. Included are the effect of the high latitude convection electric field and its penetration of the plasmasphere, polar wind flows, particle precipitation, and neutral air winds. On the dayside, the light-ion trough is shown to arise naturally as a result of light-ion flows increasing with latitude. On the nightside, chemical links with the mid-latitude trough produce more complicated behavior. The mid-latitude trough is predicted to occur on different field lines at different times during the evening and night. Light-ion fluxes are shown to have a significant effect on the mid-latitude trough, particularly in the post-midnight sector. Diffusion coefficients for three major ions are derived and discussed for a mixture of O(+), H(+), and He(+) ions. The basic model is extended to include He(+), and the morphology of He(+) at mid- to high latitudes is studied. Anomalous dominance of He(+) in the topside ionosphere is shown to results from slow convection of depleted plasma through regions where the upper atmosphere is sunlit, while the lower atmosphere is in darkness. Dissert. Abstr.

N91-23642 Princeton Univ., NJ.
MECHANISMS OF EQUATORIAL SUPERROTATION: STUDIES WITH TWO-LEVEL MODELS Ph.D. Thesis
R. Saravanan 1990 189 p
Avail: Univ. Microfilms Order No. DA9105733

The presence of strong equatorial winds in the same direction as planetary rotation, often referred to as superrotation, is a conspicuous feature of the atmospheres of planets such as Venus and Jupiter. But this kind of superrotation is not observed in the Earth's troposphere, which is characterized by weak easterlies near the equator. Superrotating climatologies have been encountered in numerical experiments with two-level global primitive equation models, even for Earth-like parameter ranges. An attempt is made to explain the existence of these anomalous superrotating climatologies, in the hope that this may help to understand why some planets have superrotating atmospheres, while others do not. The response of an idealized dry two-level primitive equation model to stationary heating in the tropics is studied. Following the work of other investigators, it is shown that sufficiently strong tropical eddy heating produces a sudden transition to a superrotating climatology. The development of strong westerly flow in the tropics is accompanied by a dramatic reversal in the direction of horizontal eddy momentum flux transport. It is noted that the presence of strong equatorial westerlies can cause the equator to become a turning point for eddies of large zonal wavenumbers. The response to tropical eddy heating is then compared to the response to an imposed westerly torque. The similarities between these two kinds of responses indicated that the torque due to mid-latitude transient eddies breaking in the tropics plays a crucial role in this transition to superrotation. It is argued that although weak equatorial westerlies would allow mid-latitude transients to penetrate deeper into the tropics, stronger westerlies would tend to reflect these transients away from the deep tropics. This argument is preceded by a discussion of axisymmetric motions in the two-level model and their interaction with barotropic eddies. Also discussed is the sensitivity of this superrotating transition to some of the important model parameters, such as static stability and rotation rate. Dissert. Abstr.

N91-23643 Cornell Univ., Ithaca, NY.
LARGE SCALE TURBULENCE IN THE EQUATORIAL ELECTROJET Ph.D. Thesis
Corrado Ronchi 1990 262 p
Avail: Univ. Microfilms Order No. DA9106317

The turbulent dynamics of kilometer-scale irregularities of the daytime equatorial electrojet are studied analytically and numerically, within the framework of a two-fluid nonlocal theory of the gradient drift instability. The emphasis is on the effects of

including the altitude variations of the relevant physical parameters, such as mobilities and diffusion coefficients, on the nonlinear evolution of the instability. In the linear regime, researchers investigated how the nonlocal modes differ from the local ones by applying eikonal analysis to the motion of wave packets propagating in a inhomogeneous medium. The mechanism by which velocity shear can stabilize part of the linearly unstable spectrum is discussed and described in detail. Dissert. Abstr.

N91-23644 Minnesota Univ., Minneapolis.
ECHO 7: MAGNETOSPHERIC PROPERTIES DETERMINED BY ARTIFICIAL ELECTRON BEAMS Ph.D. Thesis
Robert James Nemzek 1990 337 p
Avail: Univ. Microfilms Order No. DA9107452

The sounding rocket Echo 7 was launched from the Poker Flat Research Range. An on-board accelerator injected high-power electron beams into the magnetospheric tail near L = 6.5. After mirroring at the southern conjugate point, about 20 percent of the initial beam electrons returned to the North as Conjugate Echoes, where detectors (scintillators and spectrometers) on four subpayloads measured their energy and bounce time. The other 80 percent of the beam was pitch angle diffused by wave near the equatorial plane either into the conjugate atmosphere or up to mirror points above the payload. Comparison of measured values to calculations showed that the actual magnetosphere during the flight was well-described by the Tsyganenko-Usmanov model magnetosphere with a Kp value of 2- or 2+. Analysis of echo energies yielded values for the highly variable magnetospheric convection electric field. Dissert. Abstr.

N91-23645 California Univ., Los Angeles.
THE POLAR WIND AND IONOSPHERIC OUTFLOW Ph.D. Thesis
Margaret Wein-Mei Chen 1990 286 p
Avail: Univ. Microfilms Order No. DA9105840

The dynamic outflow of ions from the Earth's polar ionosphere and its consequences in the polar and equatorial regions of the magnetosphere are studied. In the polar region, a physical explanation of how the escape of O(+) in the polar wind can become significantly enhanced by O(+) heating. A time-dependent hydrodynamic code is developed to model the dynamic polar wind outflow. It was found that the enhance O(+) temperatures increase the ion pressure gradient force helping to accelerate O(+) scale height. Kinetic processes are examined which could lead to polar wind heating. Results from the observational study reveal that upflowing field-aligned O(+) and H(+) beams of approximately 10 to 100 eV are a free energy source in the polar cap. The electrostatic stability of the polar wind in the presence of these ion beams is then studied. Depending on the parameters, slow ion acoustic and/or cyclotron modes can be driven unstable. When the O(+) beam density is dominant over the H(+) by large-amplitude ion cyclotron waves (ICW). First, the ICW decays into daughter electromagnetic and acoustic waves. Second, the acoustic waves heat the H(+) in the parallel direction by Landau trapping. Finally, the increase of the parallel velocity enlarges the ICW resonance region resulting in perpendicular heating.
Dissert. Abstr.

N91-23646 Royal Netherlands Meteorological Inst., De Bilt.
TECHNICAL DESCRIPTION OF THE HIGH-RESOLUTION AIR MASS TRANSFORMATION MODEL AT KNMI
E. I. F. deBruijn and A. A. M. Holtslag 1990 33 p
(KNMI-TR-125; ISSN-0169-1708; ETN-91-99101) Copyright
Avail: Royal Netherlands Meteorological Institute, P.O. Box 201, 3730 AE De Bilt, Wilhelminalaan 10, Netherlands

A technical description of the high resolution Air Mass Transformation (AMT) model is presented. The AMT model is intended for short range weather forecasts of the temperature and humidity profile, the structure of the boundary layer, the boundary layer height, and the amount of boundary layer clouds. As such the model consists of a one dimensional multilayer boundary layer model, which is advected from a source region to a receptor point by trajectories. The trajectories are calculated within a limited area model. The initial profiles for temperature and humidity are obtained from observed radiosondes. The several parts and subprograms of the model are described and documented. The implementation of the model on computer systems is discussed. ESA

N91-23647 Institut d'Aeronomie Spatiale de Belgique, Brussels.
TEMPERATURE DEPENDENCE OF ULTRAVIOLET ABSORPTION CROSS-SECTIONS OF ALTERNATIVE CHLOROFLUOROETHANES
D. Gillotay and Paul C. Simon 1991 31 p Submitted for publication
(Aeronomica-Acta-A-358-1991; ISSN-0065-3713; ETN-91-99110)
Avail: Institut d'Aeronomie Spatiale de Belgique, 3 Avenue Circulaire, B-1180 Brussels, Belgium

The absorption cross sections of HCFC-123 (CF3-CHCl2), HCFC-141b (CH3-CFCl2) and HCFC-142b (CH3-CF2Cl) are measured between 170 and 250 nm for temperatures ranging from 295 to 210 K with uncertainties between 2 and 4 percent. They are compared with other available determinations. Temperature effects are discussed and parametrical formulae are proposed to compute the absorption cross section for wavelengths and temperatures useful in atmospheric modeling calculations. Photodissociation coefficients are presented and their temperature dependence is discussed. ESA

N91-23648# Cologne Univ. (Germany, F.R.). Inst. fuer Geophysik und Meteorologie.
ENERGY PARTITION OF FREE ROSSBY WAVES IN GLOBAL ATMOSPHERIC OSCILLATIONS [ENERGIEANTEIL FREIER ROSSBYWELLEN AN GLOBALEN ATMOSPHAERISCHEN SCHWINGUNGEN]
Hendrik Elbern 1990 125 p In GERMAN; ENGLISH summary
(Contract BMFT-07KF2112-1)
(Mitt-74; ISSN-0069-5882; ETN-91-99124) Avail: NTIS HC/MF A06

A dataset of four years of daily European Center Midterm Weather Forecast (ECMWF) global operational analyses was projected onto normal modes constructed by the solution of the Laplace tidal equations. A time series analysis was set up to identify free Rossly waves and to quantify the energy distributions of free propagating, forced propagating, standing and quasistationary waves. Eighteen modes could be identified. The energy partition of free propagating waves varies from 43 pct. in the case of the 16 day wave down to about 5 pct. in the case of higher indexed modes. ESA

N91-23649# Observatorio del Ebro, Roquetas (Spain).
IONOSPHERE 1984, VOLUME 72 [IONOSPHERA 1984, VOL. 72]
1989 146 p In SPANISH
(ISSN-0211-5166; ETN-91-98908) Avail: NTIS HC/MF A07

The ionospheric data collected by the Ebro observatory in 1984 are presented. The measured parameters include height and frequencies of the E1, Es, F and F2 layers. Frequencies are measured with an error of less than 0.1 mHz. ESA

N91-23650# Observatorio del Ebro, Roquetas (Spain).
IONOSPHERE 1985, VOLUME 73 [IONOSFERA 1984, VOL. 73]
1989 191 p In SPANISH
(ISSN-0211-5166; ETN-91-98909) Avail: NTIS HC/MF A09

The ionospheric data collected by the Ebro observatory in 1985 are presented. The measured parameters include height and frequencies of the E1, Es, F and F2 layers. Frequencies are measured with an error of less than 0.1 MHz. ESA

N91-23651 Politecnico di Milano (Italy). Dipt. di Elettronica.
PROPAGATION OF SEISMIC WAVES IN NONELASTIC MEDIA [PROPAGAZIONE DI ONDE SISMICHE IN MEZZI NON ELASTICI]
Giancarlo Bernasconi and Giuseppe Drufuca 1990 22 p In ITALIAN; ENGLISH summary

(Rept-90-065; ETN-91-99091) Avail: Politecnico di Milano, Piazza Leonardo di Vinci 32, 20133 Milan, Italy

A decay of energy and a phase velocity dispersion due to the absorption of the medium is observed in the propagation of seismic waves in real media. The analysis of absorption effects is developed starting from the relations between stress and strain, which leads to an extension of the theory of linear elastic media to non elastic ones. A first order theory of wave propagation in nonelastic media is presented and a version of the reflectivity method for the calculation of synthetic seismograms with the inclusion of absorption is developed. Absorption implies not only decrease of energy, but also more subtle propagation effects. The spectral behavior is discussed and examples are shown of reflections arising from discontinuities of pure absorption properties of the medium. The reflectivity method thus developed is a powerful tool for fast and accurate modeling of the propagation of waves in layered media. ESA

N91-23652# Cologne Univ. (Germany, F.R.).
REMOTE SENSING OF ATMOSPHERIC TEMPERATURE FIELDS AND THE LONG WAVE RADIATION BUDGET IN THE ANTARCTIC [FERNERKUNDUNG ATMOSPHAERISCHER TEMPERATURRFELDER UND DER LANGWELLIGEN STRAHLUNGSBILANZ IN DER ANTARKTIS]
Hans-Joachim Lutz 1990 88 p In GERMAN; ENGLISH summary
(ISSN-0069-5882; ETN-91-99187) Avail: NTIS HC/MF A05

A modified version of the International Tiros operational vertical sounder Processing Package (ITPP) was developed to retrieve temperature profiles in the Antarctic. Significant improvements of the simultaneous retrieval results were achieved, using a new climatological first guess and selected channels of High resolution Infrared Sounder (HIRS). Discrepancies of the measured brightness temperatures of several HIRS channels were detected at low temperatures. The retrieval results for several orbits were compared with radiosonde data. The analyses of the geopotential heights were compared with the analyses of the European Center for Medium range Weather Forecast (ECMWF). The comparison of the measured and calculation radiation budget at the surface yields a standard deviation of 9.6 W/sq m for cloudfree cases and 49 W/sq m over all. ESA

N91-23653# Max-Planck-Inst. fuer Meteorologie, Hamburg (Germany, F.R.).
DETERMINATION OF THE TEMPERATURE PROFILE OF THE TROPOSPHERE WITH A TWO FREQUENCY LIDAR Ph.D. Thesis - Hamburg Univ. [BESTIMMUNG DES TEMPERATURPROFILS DER TROPOSPHAERE MIT ZWEI-FREQUENZ-LIDAR]
Felix A. Theopold Dec. 1990 98 p In GERMAN
(Examenarbeit-8; ISSN-0938-5177; ETN-91-99189) Avail: NTIS HC/MF A05

The determination of the vertical profile of the tropospheric temperature with a Differential Absorption Lidar (DIAL) is based on the temperature dependent absorption of spectral narrow band pulsed laser light by oxygen in the atmosphere. The error analysis shows the high requirements to be fulfilled by the laser/system. The neglect of the Rayleigh Brillouin scattering for realistic atmospheric situation can lead to an error of up to 10 K in temperature determination. The insufficient properties of a laser system for a DIAL measurement based on a continuous wave colored ring laser with pulse amplifier are demonstrated. The measurements carried out with a DIAL system composed of two colored lasers pumped by excimer laser confirm the results of the theoretical analysis. ESA

N91-23654# Bonn Univ. (Germany, F.R.). Physikalisches Inst.
IRON DENSITY MEASUREMENTS IN POLAR ATMOSPHERE Thesis [MESSUNGEN VON EISENDICHTEN IN DER POLAREN HOCHATMOSPHAERE]
Josef Hoeffner Oct. 1990 110 p In GERMAN; ENGLISH summary
(Bonn-IR-90-53; ISSN-0172-8741; ETN-91-99192) Avail: NTIS HC/MF A06

A new iron lidar is described. The first neutral iron density measurements, are presented. The applicability of different iron resonance lines is discussed. The construction of the instrument based on the former sodium lidar is reported. Adjustment problems concerning the new wave length meter are investigated, and possible solutions are proposed. A program for data acquisition and real time pre-analysis is presented, which was developed especially for the new instrument. ESA

N91-23655# Atmospheric and Environmental Research, Inc., Cambridge, MA.
DESIGN OF AN ENHANCED GLOBAL SPECTRAL MODEL
T. Nehrkorn, R. N. Hoffman, and J.-F. Louis 26 Oct. 1990 58 p
(Contract F19628-89-C-0112)
(AD-A232123; GL-TR-90-0309; SR-1) Avail: NTIS HC/MF A04 CSCL 04/2

The objective of this study is the development of a vectorized, multiprocessing global spectral model (GSM) with enhanced physical parameterizations. The starting point for this work is the current Geophysics Laboratory (GL) GSM. The multitasking and vectorization design for the GSM are described. One proposes to implement the latitude tasking scheme for multiprocessing the loop over latitude in the calculation of spectral tendencies and adjusted model variables. The general truncation version of the hydrodynamics code will be used. Wavenumber calculations will be multiprocessed and vectorized over wavenumber. All gridpoint calculations will be vectorized over longitude. The physics packages will be modified to bring them into close compliance with the plug compatibility rules. GRA

N91-23656# Naval Postgraduate School, Monterey, CA. Dept. of Physics.
ATMOSPHERIC OPTICAL TURBULENCE MEASUREMENTS TAKEN AT ANDERSON MESA, FLAGSTAFF, ARIZONA BETWEEN 13-19 NOVEMBER 1989
Gail T. Vaucher, Christopher A. Vaucher, and Donald L. Walters 11 Jan. 1991 77 p
(AD-A232222; NPS-PH-91-004) Avail: NTIS HC/MF A05 CSCL 03/1

From 13 to 19 November 1989, the Naval Postgraduate School Atmospheric Optics Group acquired atmospheric optical turbulence measurements at the 31-inch Lowell Observatory telescope dome facility on Anderson Mesa, 16 km southeast of Flagstaff, Arizona. The parameters measured, the transverse coherence length and the isoplanatic angle, were part of an ongoing site survey for a large-scale, ground-based, synthetic aperture system (100 to 300 m baseline stellar interferometer). This report compiles, analyses and summarizes the acquired optical data. Also discussed are the synoptic meteorological events present during the data acquisition period. GRA

N91-23657# Air Force Inst. of Tech., Wright-Patterson AFB, OH.
THERMAL ION UPWELLING IN THE HIGH-ALTITUDE IONOSPHERE Ph.D. Thesis
Richard W. Cannata 1990 241 p
(AD-A232372; AFIT/CI/CIA-90-035D) Avail: NTIS HC/MF A11 CSCL 04/1

High latitude observations of thermal ion outflows, traditionally known as the polar wind, and heavy ion upwellings, consisting chiefly of heated O(+), suggest that the terrestrial ionosphere acts as an important, and at times, dominant source of ions for the magnetosphere. The topside ionospheric processes responsible for modulating both types of polar ion flows were examined to quantify the magnitudes and compositional variability of steady-state polar wind flows and to identify the role of low-altitude frictional heating in transient heavy (0+) upwellings. Theoretical and experimental approaches were used to elucidate the high-latitude processes that influence ionospheric source strength and transient behavior. A time-dependent hydrodynamic model was

used to examine solar cycle and seasonal dependencies under steady-state assumptions. Seasonal influences were found with large wintertime flux variations for both ions caused by ionization source strengths. A marked shift towards O(+) enriched upwellings occurred at solar maximum and for wintertime, at certain noontime locations. The role of low-altitude ion frictional heating was examined by coupling the National Center for Atmospheric Research's Thermosphere/Ionosphere General Circulation Model (NCAR-TIGCM) to the polar wind model to specify time-dependent frictional heating during a period of observed high-altitude O(+) outflow. Preferential O(+) heating resulted in a factor of four increase in modeled O(+) fluxes, which coincides in both space and time with the observed heavy ion outflows. Finally, the role of frictional heating and global heating morphology was related to observations of high-altitude ion outflows using Dynamics Explorer-2 satellite data and incoherent scatter radar observations. GRA

N91-23658# Air Force Inst. of Tech., Wright-Patterson AFB, OH.
A SEARCH FOR STRANGE ATTRACTORS IN THE SATURATION OF MIDDLE ATMOSPHERE GRAVITY WAVES Ph.D. Thesis
Jason P. Tuell Sep. 1990 264 p
(AD-A232468) Avail: NTIS HC/MF A12 CSCL 04/1

Evidence is sought for the strange attractor associated with the saturation of middle atmosphere gravity waves in the echo data from a partial reflection radar located in Saskatoon, Canada. Theiler's extension of the Grassberger-Procaccia correlation integral algorithm was used to estimate the fractal dimension of the attractor. Breaking gravity waves are thought to decay to turbulence, transporting momentum from the lower to upper atmosphere. By extending laboratory study results to middle atmosphere gravity waves, it seems reasonable to expect to find a strange attractor in gravity wave saturation. Echo data was analyzed because it offered a high sampling rate. The Grassberger-Procaccia algorithm places stringent requirements upon the amount of data necessary to obtain an accurate estimate of the system dimension; a large number of points is required. The strange attractor was not detected with dimension less than 3 in the data from the Saskatoon partial reflection radar for the time scales (6 min 39 s) which were studied. This study can not assert that a strange attractors is absent in gravity wave absorption. Data requirements to implement the Grassberger Procaccia algorithm make it unlikely that such an attractor, if it exists, will be detected. GRA

N91-23659# Arcon Corp., Waltham, MA.
HIGH-ALTITUDE NON-EQUILIBRIUM INFRARED EMISSION MODELS Final Report, 11 Jun. 1986 - 30 Nov. 1990
Peter P. Wintersteiner, Robert A. Joseph, and Armand J. Paboojian 30 Nov. 1990 129 p
(Contract F19628-86-C-0118)
(AD-A232503; GL-TR-90-0311) Avail: NTIS HC/MF A07 CSCL 04/1

This report describes the development and implementation of models for predicting infrared emission in non-LTE regions of the Earth's atmosphere. Such models are used to stimulate particular atmospheric conditions, both quiescent and aurorally-distributed, in order to extract information from infrared radiance data sets and study the roles of different basic physical processes affecting the upper atmosphere. The first line-by-line radiative excitation model for the upper atmosphere, RAD, was developed. The model was applied to the calculation of populations of infrared-active states of CO2 and CO, and the conditions of the SPIRE experiments were simulated. The role of atomic oxygen in exciting the CO2 bending modes was elucidated. Auroral emissions were modeled, and the field widened interferometer data set was analyzed using a method of spectral decomposition. The NO band heads were identified in the lower-thermosphere emissions. The mathematical procedures underlying the model, especially the RAD model, and the physical process incorporated in them are described. Results are presented from running the models. GRA

N91-23660# Air Force Geophysics Lab., Hanscom AFB, MA.
AURORAL BOUNDARY INDEX FROM 1983 TO 1990 Environmental Research Papers
D. Madden and M. S. Gussenhoven 21 Dec. 1990 41 p
(AF Proj. 7601)
(AD-A232845; GL-TR-90-0358; GL-ERP-1075) Avail: NTIS HC/MF A03 CSCL 04/1

Since the release of the auroral boundary index for the Defense Meteorological Satellite Program (DMSP)/F2 satellite, equivalent midnight auroral equatorward boundaries have been routinely processed for the DMSP/F6,/F7,/F8 and /F9 satellites at the AFGL. The auroral equatorward boundary selection algorithm was modified from that for the SSJ/3 particle detector on the/F2 satellite to work for the next generation SSJ/4 instrument that flies on the later satellites. The final product presented here is comprised of a series of solar rotation plots, stacked five per page for the period 1 January 1983 to 15 May 1990. The equivalent midnight boundaries that are plotted are a subset of the complete data base. Only those boundaries occurring in the evening sector are used since there is little ambiguity in their selection. In addition, we apply other criteria that are somewhat satellite dependent. The original set of criteria used on the boundaries from the /F6 and /F7 satellites were modified when boundaries from /F8 and /F9 satellites became available. Since all plots of boundaries that made their way to the public before 1988 used the original criteria, both original and modified criteria are explained. GRA

N91-23661# Air Force Environmental Technical Applications Center, Scott AFB, IL.
A SMOOTHING ALGORITHM FOR UPPER-AIR SOUNDINGS
Gregory J. Reding Feb. 1991 24 p
(AD-A232853; USAFETAC/PR-91/004) Avail: NTIS HC/MF A03 CSCL 04/1

This report describes the development of a filtering algorithm for smoothing vertical traces of temperature, pressure, and density through the atmosphere. An overlapping mean method employing an exponential weighting function was applied over several adjacent levels to calculate a smoothed value for the required point. The exponential function was chosen because it decreases symmetrically from a central value and easily incorporates a variable bandwidth; this lets users smooth profiles to the desired resolution. Upper air data needs to be interpolated to evenly-spaced intervals in the vertical prior to program execution; if it is not, resulting profiles will not be hydrostatically consistent. Based on spectral analysis of samples from two test sites, no noise was introduced into the smoothed profiles. GRA

47 METEOROLOGY AND CLIMATOLOGY

Includes weather forecasting and modification.

N91-23662*# National Aeronautics and Space Administration. Pasadena Office, CA.
MICROWAVE TEMPERATURE PROFILER FOR CLEAR AIR TURBULENCE PREDICTION Patent Application
Bruce L. Gary, inventor (to NASA) (Jet Propulsion Lab., California Inst. of Tech., Pasadena.) 27 Nov. 1990 33 p
(Contract NAS7-918)
(NASA-Case-NPO-18115-1-CU; NAS 1.71:NPO-18115-1-CU; US-Patent-Appl-SN-618790) Avail: NTIS HC/MF A03 CSCL 04B

A method is disclosed for determining Richardson Number, Ri, or its reciprocal, RRi, for clear air prediction using measured potential temperature and determining the vertical gradient of potential temperature, d(theta)/dz. Wind vector from the aircraft instrumentation versus potential temperature, dW/D(theta), is determined and multiplies by d(theta)/dz to obtain dW/dz. Richardson number or its reciprocal is then determined from the relationship Ri = K(d(theta)/dz divided (dW/dz)squared) for use in detecting a trend toward a threshold value for the purpose of predicting clear air turbulence. Other equations for this basic

relationship are disclosed together with the combination of other atmospheric observables using multiple regression techniques.
NASA

N91-23663 Wisconsin Univ., Madison.
ASSIMILATION OF ERBE DATA WITH NONLINEAR PROGRAMMING TECHNIQUE TO IMPROVE CLOUD COVER DIAGNOSIS Ph.D. Thesis
Xiangqian Wu 1990 113 p
Avail: Univ. Microfilms Order No. DA9034859

A method is developed to assimilate satellite radiation data for the purpose of improving fractional cloud cover diagnosis within a numerical weather prediction (NWP) model. The method employs a nonlinear programming technique to find a set of feasible parameters for the diagnosis such that the difference between the observed and model produced outgoing longwave radiation (OLR) is minimized. The theoretical basis and methodology of the method are provided. The method was applied in two forecast experiments using a NWP model. The results from the winter case demonstrated that the root-mean-square (RMS) difference between the observed and the forecast OLR can be reduced by 50 percent when the radiatively optimized cloud diagnosis is used, and the remaining RMS error is within the background noise. The optimized diagnosis also reduced the RMS error in the summer experiment, but the reduction is inadequate, possibly because of the inability of the current cloud diagnosis in handling convective activity. The optimization procedure is both stable and sensitive. The largest impact of the optimized cloud diagnosis is that on the forecast of surface temperature, while the impact on the forecast of other model variables is insignificant, partly due to the model's simplified cloud process, and partly due to the limited model integration time compared to the time scale of radiative forcing. Several ways in which the method can be used are discussed.
Dissert. Abstr.

N91-23664 Pennsylvania State Univ., University Park.
SURFACE LAYER TRANSFER PROCESSES OVER VEGETATION: A MICROMETEOROLOGICAL FIELD EXPERIMENT OF LONG DURATION Ph.D. Thesis
Elsalem Rabadi and Jaser Khelaif 1990 169 p
Avail: Univ. Microfilms Order No. DA9104871

A measurement program conducted over a variety of agricultural crops during the years 1986 to 1989 is described. The program aimed at defining, measuring, and describing the parameters which control the transfer of heat, water vapor, momentum, and other scalar qualities over various crop types. The measurements included standard micrometeorological and subsoil variables. Eddy correlation techniques, using a sonic anemometer and infrared Ophir hygrometer, were employed to estimate the fluxes of sensible and latent heat and momentum in the surface layer. Sensible heat flux was also estimated from the Delta-T (profile) method. The subsoil measurements included ground surface heat flux, soil temperature, and moisture profiles. Other measuring techniques and results are discussed.
Dissert. Abstr.

N91-23665 Purdue Univ., West Lafayette, IN.
MAINTENANCE OF SHORT-TERM SUBTROPICAL WIND MAXIMA IN THE SOUTHERN HEMISPHERE: OBSERVATIONAL AND MODELING STUDY Ph.D. Thesis
James Wilson Hurrell 1990 175 p
Avail: Univ. Microfilms Order No. DA9104650

Observational and general circulation model (GCM) data were used to investigate the short-term relationship between tropical heating and subtropical westerly maxima in the Southern Hemisphere during SOP-1, FGGE (5 January to 4 March, 1979). Enhancements of the subtropical westerlies were found to be highly correlated to episodes of maximum poleward moving divergent outflow from the tropics, and the response of the subtropical zonal flow to the tropical divergence appears to be almost instantaneous (i.e., less than 12 hours). Moreover, the divergent meridional wind accounts for much of the total ageostropic meridional wind in the subtropics and, consequently, results in strong Coriolis accelerations in the entrance regions of the westerly maxima.
Dissert. Abstr.

N91-23666 Pennsylvania State Univ., University Park.
OBSERVATIONAL STUDY OF THE ABOVE-INVERSION STRUCTURE AND MARINE STRATOCUMULUS CLOUD CLEARING EPISODES DURING FIRE Ph.D. Thesis
Kevin Arlyn Kloesel 1990 136 p
Avail: Univ. Microfilms Order No. DA9104908

Data from the First International Satellite Cloud Climatology Project Regional Experiment (FIRE) were combined with NOAA synoptic products, a trajectory analysis scheme, and satellite imagery to document the existence and causes of layers of air characterized by high ozone concentrations and low specific humidity values, and layers of air characterized by high specific humidity values and low ozone concentrations above the marine stratocumulus cloud regime off the coast of California. The ozone concentrations and specific humidity values observed were larger than those expected in the region just above the subsidence inversion off the California coast. In addition, the data mentioned above were used to study the periodic clearing of a large region of marine stratocumulus observed during FIRE. The large clear regions observed in the marine stratocumulus cloud regime that periodically develop off the coast of California appear to be caused by the subtropical anticyclone. These large-scale clearing episodes are directly correlated with the ridging of the subtropical anticyclone into the U.S. Pacific Northwest, resulting in offshore flow effects. The subsidence associated with the subtropical anticyclone may also help cause the clearing episodes, or prevent the redevelopment of these clouds in the clear regions. The clearing of large regions of marine stratocumulus clouds may impact climate because of the contribution of these clouds to the global albedo.
Dissert. Abstr.

N91-23667 Washington Univ., Seattle.
THE ANNUAL MARCH OF CONVECTION, SEA SURFACE TEMPERATURE, AND SURFACE WINDS IN THE TROPICS Ph.D. Thesis
Todd Porter Mitchell 1990 239 p
Avail: Univ. Microfilms Order No. DA9026012

The annual march of convective rainfall and sea surface temperature (SST) in the tropics is described, using satellite measurements and surface observations from ships-of-opportunity. The annual march of the rainfall and SST on the equator is found to be characterized by a strong annual cycle, with the warmest temperatures and heaviest precipitation occurring in Mar.-Apr. These features of the zonal mean climatology are dominated by the annual march in the 180 deg belt of longitude spanning the eastern Pacific and Africa. The peculiar annual cycle in equatorial convection and SST in this hemisphere appears to be due to the equatorial asymmetry in the coasts of Africa and South America, which results in pools of relatively warm water along 10 deg N, which persist throughout the year. The onset of the oceanic convection following the March equinox is seen as a westward extension of the Northern Hemisphere summer continental monsoons of west Africa and Central America over the preexisting warm pools. The invigorated oceanic convection gives rise to strong southerly winds on and to the north of the equator, with the associated wind stresses acting to produce equatorial cold tongues on the eastern side of both basins through ocean dynamical processes. Following the September equinox the continental monsoon convection drifts southward into the Southern Hemisphere, while the oceanic ITCZs (Intertropical Convergence Zones) remain strong near 10 deg N over both oceans. The cold equatorial SSTs during these months prevent the oceanic ITZCs from drifting southward. The competition for moisture and equatorial subsidence associated with the oceanic convection may contribute to the absence of strong equatorial zonal mean convection during these months.
Dissert. Abstr.

N91-23668 Washington Univ., Seattle.
OBSERVED CHANGES IN THE ACTIVITY OF BAROCLINIC WAVES AND THEIR FEEDBACKS DURING THE LIFE CYCLES OF LOW-FREQUENCY CIRCULATION ANOMALIES IN THE NORTHERN HEMISPHERE WINTER Ph.D. Thesis
Hisashi Nakamura 1990 265 p
Avail: Univ. Microfilms Order No. DA9104279

Variations in the baroclinic wave activity and their feedback were investigated, using a long data set of the tropospheric circulation in the Northern Hemisphere winter. Composite analysis based upon a large number of anomaly events was performed relative to the onset and decay times of five anomaly patterns in the low-frequency circulation. The two polarities of these patterns correspond to the blocking and zonally-extended westerlies. A slowly-varying envelope function is defined locally to represent the amplitude modulation of baroclinic waves associated with the evolving low-frequency circulation anomalies. The most striking feature observed during the blocking onset is the anomalously high values of the envelope function upstream which, in most cases, correspond to the development of a deep surface low. In the composite maps that were adjusted to minimize the cancellation between the individual eddy components, one or two strong anticyclonic baroclinic eddies appear to advect the low potential vorticity air systematically from the subtropics into the midlatitude where the blocking anticyclone is developing. These interactions tend to be nonlinear if the block is developing far north of the mean storm tracks. The vorticity flux feedback of baroclinic eddies appears to account for less than 30 percent of the observed growth of the low-frequency circulation anomalies during their onset, and to be even smaller during the decay stage. Anomalous vorticity advection by the low-frequency circulation can explain most of the observed evolution of these anomalies during their onset and decay stages. In contrast, the eddy feedback tends to be relatively important in maintaining those anomalies in their fully developed stage. Dissert. Abstr.

N91-23669 Yale Univ., New Haven, CT.
THE APPLICATION OF EQUILIBRIUM CLIMATE MODELS TO QUESTIONS OF GLACIATION AT HIGH LATITUDES Ph.D. Thesis
Robert James Oglesby 1990 243 p
Avail: Univ. Microfilms Order No. DA9034229

One of the outstanding features of the Earth's paleoclimatic record is the presence or absence of wide-spread continental glaciation. A potentially valuable tool to use as an aid in such a pursuit is the equilibrium climate model (ECM), which can be solved for the fast response variables of climate as a function of slow response climatic variables or external forcing. The capabilities of the ECM to provide useful results when applied to paleoclimatic questions concerning glaciation are evaluated. In the first case study the statistical dynamical model (SDM) was used to examine the implications of a warmer deep ocean for maintenance of ice-free conditions during the Cretaceous (approximately 65 to 130 Ma). When deep ocean temperatures are prescribed to values indicated for the Cretaceous, the model yielded warm mid-to-high latitude surface conditions in agreement with the geologic record. In the second case study the CCM1 was used to examine mechanisms potentially important for the initiation of Antarctic glaciation, which occurred no later than 38 to 40 Ma. The most fundamental result of this study is the difficulty of establishing an ice-free Antartic in CCM1 even under extreme imposed conditions. In the third and final case study, CCM1 was used to examine the initiation of Northern Hemisphere glaciation, such as occurred around 2.4 Ma. Emphasized was the role of snow cover as an initial condition. In the study concerned with model error, uncertainties were investigated in the formulations of the CCM1 computation of snowfall and snow melt. It was determined the CCM1: may be capable of being used to qualitatively evaluate mechanisms potentially important in determining glacial versus nonglacial conditions; may in some cases be used to provide a quantitative computation of the net snow accumulation that in turn is used to support a qualitative conclusion regarding the sign of the net accumulation; and cannot be used to provide a determination of the magnitude of the net snow accumulation reliable enough to permit either implicit or explicit long-term integration.
Dissert. Abstr.

N91-23670*# Alabama Univ., Huntsville. Atmospheric Science and Remote Sensing Lab.
ANALYSIS AND MODELING OF SUMMERTIME CONVECTIVE CLOUD AND PRECIPITATION STRUCTURE OVER THE SOUTHEASTERN UNITED STATES Final Report, 15 Sep. 1987 - 31 Dec. 1990
Kevin R. Knupp 28 May 1991 128 p
(Grant NAG8-654)
(NASA-CR-188119; NAS 1.26:188119) Avail: NTIS HC/MF A07 CSCL 04B

A summary of an investigation of deep convective cloud systems that typify the summertime subtropical environment of northern Alabama is presented. The major portion of the research effort included analysis of data acquired during the 1986 Cooperative Huntsville Meteorological Experiment (COHMEX), which consisted of the joint programs Satellite Precipitation and Cloud Experiment (SPACE) under NASA direction, the Microburst and Service Thunderstorm (MIST) Program under NSF sponsorship, and the FAA-Lincoln Laboratory Weather Study (FLOWS). This work relates closely to the SPACE component of COHMEX, one of the general goals of which was to further the understanding of kinematic and precipitation structure of convective cloud systems. The special observational plateforms that were available under the SPACE/COHMEX Program are shown. The original objectives included studies of both isolated deep convection and of (small) mesoscale convection systems that are observed in the Southeast environment. In addition, it was proposed to include both observational and comparative numerical modeling studies of these characteristic cloud systems. Changes in scope were made during the course of this investigation to better accommodate both the manpower available and the data that was acquired. A greater emphasis was placed on determination of the internal structure of small mesoscale convective systems, and the relationship of internal dynamical and microphysical processes to the observed cloud top behavior as inferred from GOES IR (30 min) data. The major accomplishments of this investigation are presented.
Author

N91-23671 Liverpool Univ. (England).
SURFACE CLOUD OBSERVATIONS FOR RADIATION, CLIMATOLOGY AND INCORPORATION INTO SATELLITE-BASED NEPHANALYSES Ph.D. Thesis
Alan Howard Goodman 1989 423 p
Avail: Univ. Microfilms Order No. BRDX91518

An investigation of the potential value of surface cloud observations was undertaken with special regard to their role in surface radiation modeling, global cloud climatologies, and as an aid in satellite cloud retrieval. Surface cloud observations were evaluated on a variety of spatial scales in order to highlight specific applications. The range of methods for obtaining cloud parameters from satellite radiances and from the ground is discussed. Intercomparison of satellite and surface retrievals shows that close agreement is often reached in terms of large scale cloud amounts, but that surface observations can provide valuable small scale information in situations where the satellite algorithm may fail. All-sky camera images were used to illustrate the difficulties of reporting low optical cloud depth accurately from the surface and also to demonstrate how total and layered amounts can be observed with greater precision. The parameterization of surface radiation fluxes is shown to be highly dependent on conventional cloud data and an analysis of high temporal resolution all-sky imagery revealed how rapid changes in cloudiness may affect the performance of radiation models over different time scales. The use of climatological cloud type contingency probabilities in improving the three dimensional nature of satellite cloud retrievals were examined. The main theme of this work, exploiting conventional cloud data to improve the results of satellite algorithms, is extended to include climatological examples of the U.S.A.F. three dimensional Nephanalysis. Comparisons of these

against preliminary results from the International Satellite Cloud Climatology Project (ISCCP) show good agreement, while unexpected discrepancies were identified when comparing the ISCCP and surface climatologies. Dissert. Abstr.

N91-23672 Reading Univ. (England).
LOCALISED SYMMETRIC INSTABILITY: AN INITIAL VALUE PROBLEM Ph.D. Thesis
M. W. Holt 1990 276 p
Avail: Univ. Microfilms Order No. BRDX91571

Conditional symmetric instability is a possible mechanism for the formation of rainbands at a cold front, though recent observations suggest that the atmosphere at a cold front may be neutral to the instability. Previous studies of the motion of the dry analog (symmetric instability) are extended by considering a localized finite amplitude perturbation in a slantwise unstable atmosphere. Classical normal mode theory of symmetric instability is reviewed, and an expression for the inviscid normal mode within a confined region is obtained. Previously this was not thought possible. The maximum kinetic energy predicted by parcel theory for the flow is several times larger than arises in a numerical model, and this shows that parcel energy is lost to generate buoyancy as the parcel displaces the surrounding air, even though the parcel ascends at close to neutral buoyancy. For a weakly viscous atmosphere, a finite amount of background instability is required for the flow to be unstable. The steady state response to localized diabatic or frictional forcing in a slantwise stable baroclinic atmosphere is found using a lagrangian geometric model that consists of a mesoscale lens of zero potential vorticity. Such localized forcing may arise as a result of line convection at an active cold front, and it is suggested that the steady state provides an explanation for the condition of slantwise neutrality which has recently been observed at certain cold fronts. Dissert. Abstr.

N91-23673 Michigan Univ., Ann Arbor.
NEUTRAL WIND VORTICES IN THE HIGH-LATITUDE THERMOSPHERE Ph.D. Thesis
Jeffrey Paul Thayer 1990 297 p
Avail: Univ. Microfilms Order No. DA9034528

The neutral dynamics of the high-latitude thermosphere were investigated using measurements obtained from the Dynamics Explorer-2 spacecraft and ground-based Fabry-Perot interferometers located in Greenland, and numerical simulations from the National Center for Atmospheric Research's Thermosphere/Ionosphere General Circulation Model (NCAR-TIGCM). Large-scale mean neutral wind patterns under various geophysical conditions were determined through extensive analysis of the neutral wind observations made by the DE-2 spacecraft. The mean neutral wind observations demonstrate the existence of coherent, large-scale neutral wind vortices in the high-latitude thermosphere and show that these vortices are persistent features in the mean neutral wind circulation. The mean neutral wind vortices in the high-latitude thermosphere are shown to vary spatially depending on the orientation of the interplanetary magnetic field (IMF) and the level of geomagnetic activity. The NCAR-TIGM was used to provide numerical simulations of the high-latitude neutral circulation corresponding to the geophysical conditions under which the average neutral wind patterns from DE-2 observations were organized. The high-latitude neutral wind vortices determined from the DE-2 observations and simulated by the NCAR-TIGCM were analyzed by determining the kinematic properties of the wind fields. This analysis showed that the dynamics of the high-latitude neutral thermosphere is dominated by rotational motion, imparted primarily through the ion-drag force, rather than by divergent motion, imparted primarily through the pressure gradient force set up by Joule and solar heating. The numerical simulations of the NCAR-TIGCM provide information on the forces which generate the neutral wind forces in the high-latitude thermosphere. The force analysis illustrates that the ion-drag force contributes significantly to the local time rate of change of the nondivergent component of the neutral wind, while the pressure gradient, Coriolis, and momentum advection forces, as well as the ion-drag force contribute to the local time rate of change of the irrotational component of the neutral wind. Dissert. Abstr.

N91-23674# Edgerton, Germeshausen and Grier, Inc., Idaho Falls, ID.
IMPLEMENTATION OF THE FAA RESEARCH AND DEVELOPMENT ELECTROMAGNETIC DATABASE
R. L. McDowall, D. J. Grush, D. M. Cook, and M. S. Glynn (Federal Aviation Administration, Atlantic City, NJ.) 1991 13 p Presented at the 1991 International Conference on Lightning and Static Electricity, Cocoa Beach, 16-19 Apr. 1991
(Contract DE-AC07-76ID-01570)
(DE91-010063; EGG-M-90364; CONF-9104163-3) Avail: NTIS HC/MF A03

The Idaho National Engineering Laboratory (INEL) has been assisting the Federal Aviation Administration (FAA) in developing a database of information about lightning. The FAA Research and Development Electromagnetic Database (FRED) will ultimately contain data from a variety of airborne and groundbased lightning research projects. An outline is presented of the data currently available in FRED. The data sources which the FAA intends to incorporate into FRED are also listed. In addition, how the researcher may access and use the FRED menu system is described. DOE

N91-23675# National Severe Storms Lab., Norman, OK.
THE TERMINAL DOPPLER WEATHER RADAR TORNADIC VORTEX SIGNATURE DETECTION ALGORITHM Interim Report
Steven V. Vasiloff and Arthur Witt Dec. 1990 21 p Original contains color illustrations
(Contract DTFA01-80-Y-10524)
(DOT-FAA-NR-91-5) Avail: NTIS HC/MF A03

An algorithm for real-time detection of tornadoes, using single-Doppler radar, is described. This algorithm searches for tornadic vortex signatures (TVSs) which are characterized by strong azimuthal shear in Doppler velocity fields. A TVS usually indicates that a tornado is occurring. The algorithm searches for azimuthal radial velocity differences, above a certain threshold, between adjacent gates at constant range. It then builds these 'pattern vectors' into features for each scan in elevation, and finally determines the vertical correlation among features. When at least three features are vertically correlated and the lowest one is below a prescribed minimum-height threshold, a TVS is declared, indicating that a tornado is occurring. If the lowest feature is not below the height threshold, a 'potential TVS (PTVS)' is declared, indicating that a tornado may soon occur. The TVS algorithm was tested on five tornadoes that occurred in Colorado and Missouri. Each tornado had an associated TVS, which was detected by the algorithm. In all cases, either a PTVS or TVS preceded each tornado, resulting in a 4 minute average lead time. Evaluated on a scan-by-scan basis, the Probability of Detection (POD) is 78 percent. No TVS false alarms and only a 3 PTVS false alarms occurred for these 5 cases. The algorithm was also tested on two rotating microbursts with no detections occurring. Author

N91-23676# Deutsche Forschungsanstalt fuer Luft- und Raumfahrt, Oberpfaffenhofen (Germany, F.R.). Inst. fuer Physik der Atmosphaere.
ON THE AIRFLOW OVER THE ALPS DURING SOUTH FOEHN Thesis - Ludwig-Maximilians-Univ.
Klaus-Peter Hoinka Jul. 1990 197 p In GERMAN; ENGLISH summary
(DLR-FB-90-30; ISSN-0939-2963; ETN-91-99062) Avail: NTIS HC/MF A09; DLR, Wissenschaftliches Berichtswesen, VB-PL-DO, Postfach 90 60 58, 5000 Cologne, Fed. Republic of Germany, HC 52.50 DM

Conventional meteorological data is presented, and analyzed. Numerical simulations are performed. The characteristic structures of the tropospheric flow over and around the Alps and the associated wind and leeward side circulations are examined. The momentum exchange due to gravity waves generated by the Alps

is determined by discussing its magnitude derived from measurements and from data simulated by a numerical model. ESA

N91-23677# Deutsche Forschungsanstalt fuer Luft- und Raumfahrt, Oberpfaffenhofen (Germany, F.R.). Abt. Wolkenphysik.
INVESTIGATION OF MICRO- AND MACROPHYSICAL STRUCTURES AND PROCESSES IN HAIL CLOUDS WITH RESPECT TO THEIR MODIFICATION
Hartmut Hoeller and Peter Meischner Aug. 1990 55 p In GERMAN; ENGLISH summary Original contains color illustrations
(DLR-FB-90-38; ISSN-0171-1342; ETN-91-99064) Avail: NTIS HC/MF A04; DLR, Wissenschaftliches Berichtswesen, VB-PL-DO, Postfach 90 60 58, 5000 Cologne, Fed. Republic of Germany, HC 75 DM

The results of radar observations of hailstorms performed from May 1987 to July 1989 are summarized. The measurments were obtained by the Doppler polarization radar and the Falcon research aircraft. The general conditions of hail formation in thunderstorms and the feasibility of hail suppression by artificial impacts is discussed. Some case studies showing the dispersal of the seeding material and the typical radar structures connected with hail formation in many thunderstorms are presented. Their significance for hail suppression is demonstrated. ESA

N91-23678 Royal Netherlands Meteorological Inst., De Bilt. Physical Meteorology Dept.
QUANTITATIVE PROCESSING OF METEOSAT DATA: IMPLEMENTATION AT KNMI: APPLICATIONS
Sara H. Muller 1990 48 p
(KNMI-TR-127; ISSN-0169-1708; ETN-91-99103) Copyright Avail: Royal Netherlands Meteorological Institute, P.O. Box 201, 3730 AE De Bilt, Wilhelminalaan 10, Netherlands

A general description of Meteosat (European Meteorological Satellite) primary data is given. Meteosat data can be received both in digital form (primary data) and analog form (secondary data). These data types are called PDUS/SDUS (Primary/Secondry Data User Station). The reception and processing of PDUS data is described. Calibration and localization procedures are discussed. The need for and use of atmospheric corrections are summarized. An overview of different methods for the retrieval of quantitative information about clouds, surface and atmosphere is given. Software utilities are described. ESA

N91-23679# Stockholm Univ. (Sweden). Dept. of Meteorology.
GROUPING OF CLOUDS AND INTERNAL GRAVITY WAVES IN A NON-HYDROSTATIC MODEL OF MOIST CONVECTION
Xiang-Yu Huang Feb. 1991 48 p
(Contract NFR-G-GU-1705-311)
(DM-55; ISSN-0349-0467; ETN-91-99337) Avail: NTIS HC/MF A03

A nonhydrostatic model for moist convection is formulated to study some fundamental aspects of cumulus dynamics, in particular, cloud grouping through gravity wave interactions. The Boussinesq approximated equations of motion are used and the convective cells are assumed to extend vertically through the entire model domain. A hydrological cycle is included where condensed water is advected with the motion field and removed through precipitation. The three dimensionality of the model does not alter the qualitative conclusions from an earlier two dimensional study, but gives a more realistic spatial distribution of clouds. The inclusion of the cloud water favors the generation of internal gravity waves and thus, the grouping of clouds. The model sensitivity to parameters is systematically studied. The stratification of the atmosphere, the dissipation of the model, and the autoconversion rate of cloud water are the most important parameters in determining the model clouds and the development of moist convection. Results also point out some aspects of moist convection, which should be taken into account when parameterizing moist convection in mesoscale numerical models. ESA

N91-23680# Stockholm Univ. (Sweden). Dept. of Meteorology.
A ONE DIMENSIONAL WIND PROFILE MODEL WITH STABILITY AND EDDY VISCOSITY ESTIMATIONS FROM SODAR DATA
Hans Dahlquist (Swedish Military Weather Service, Stockholm.) Feb. 1991 49 p
(DM-56; ISSN-0349-0467; ETN-91-99338) Avail: NTIS HC/MF A03

In a one dimensional wind profile, model methods for eddy viscosity and stability estimations from sodar data are evaluated with soundings. For eddy viscosity parameterization, the ageostrophic method and mixing length theory are investigated. Three methods for estimating the static stability are evaluated: a wind profile adjustment method, gravity wave analysis of sodar backscatter and flux profile functions for windspeed, and standard deviation of vertical windspeed. For the wind profile model, the strong influence of homogeneous terrain in different wind directions is demonstrated. The new model with variable momentum flux (VF) with height shows better results than an earlier constant flux model. The VF model can be used for extending the sodar profile up to 1500 m. ESA

N91-23681# Naval Postgraduate School, Monterey, CA.
EFFECTS OF THE NORTHEAST MONSOON ON THE EQUATORIAL WESTERLIES OVER INDONESIA M.S. Thesis
Chih-Lyeu Chen Jun. 1990 64 p
(AD-A232106) Avail: NTIS HC/MF A04 CSCL 04/2

The possible cross equatorial influences of the Northern Hemisphere on the zonal wind along 10 deg S in the Indonesia-Arafura Sea region are studied by using a 14-year data set. Composites of time series of individual circulation parameters and surface flow charts reveal a correlation between the northeastern monsoon of the Northern Hemisphere and the Southern Hemisphere summer monsoon. The correlation is significantly stronger during the middle season compared to late season. During the late season distinct patterns of changes are found in the Australian monsoon trough and upper tropospheric flow. This reflects a stronger connection between summer monsoon and midlatitude baroclinic systems within the Southern Hemisphere. Thus the mid-season events of the southern monsoon wind strengthening are more influenced by surges in the northeast monsoon in the Northern Hemisphere; while the late-season events may be due to midlatitude baroclinic effects in the Southern Hemisphere rather than the northern cold surges. GRA

N91-23682# Air Force Inst. of Tech., Wright-Patterson AFB, OH.
INITIALIZATION OF CLOUD AND RADIATION IN THE FLORIDA STATE UNIVERSITY GLOBAL SPECTRAL MODEL Ph.D. Thesis
Allan M. Weiner 1990 262 p
(AD-A232425; AFIT/CI/CIA-90-038D) Avail: NTIS HC/MF A12 CSCL 04/2

Satellite observed Outgoing Longwave Radiation (OLR) is used to initialize the clouds and radiation of the Florida State University Global Spectral Model. A one-parameter method and two different six-parameter methods of initialization are formulated. The one-parameter method is shown to be the most efficient and produce the best results. The effects of the cloud and radiation initialization on a five day forecast are presented. The initialization procedure produces a better forecast of OLR than the control experiment by such a large extent that the five day forecast of the initialization experiment has approximately the same verification score as the initial data of the control experiment. The cloud forecasts (high, middle, and low) of the initialization experiment prominently show the cloud signatures of the monsoon, the Pacific and Atlantic Ocean intertropical convergent zones (ITCZs), and the African rainbelt, but the cloud signatures of the control experiment are weak or nonexistent. The moist static stability budgets show that the initialization procedure had a large impact on the forecast after five days of integration by producing a monsoon and typhoon that were stronger and better defined. Additionally, radiative destabilization forcing budgets of the

initialization experiment were an order of magnitude greater than the control experiment for the Atlantic Ocean ITCZ. The effect of initialization on precipitation forecasts was also investigated. It was found that the model precipitation decreased after initialization. This is attributed to the model formulation of precipitation, and a new formulation is suggested for further investigation. GRA

N91-23683# Naval Postgraduate School, Monterey, CA.
EVALUATION OF GENERALIZED THRESHOLDS IN AN OBJECTIVE MULTISPECTRAL SATELLITE CLOUD ANALYSIS M.S. Thesis
Thomas J. Neu Jun. 1990 61 p
(AD-A232716) Avail: NTIS HC/MF A04 CSCL 04/2

An objective algorithm is developed and evaluated for classifying 11 cloud types. The multispectral technique uses daytime images of AVHRR channel 1 (0.68 microns), channel 4 (10.8 microns), and channel 5 (12.0 microns). Visual reflectance is scaled by the solar zenith angle in order to prepare standardized albedos. Infrared brightness temperatures provide cloud height information through comparison with a representative temperature sounding. Channel 4-5 temperature differences (split-window) distinguish between ice clouds with variable emissivities and thick precipitating clouds. A statistical texture analysis on the standardized albedos separates stratiform from cumuliform clouds. Generalized thresholds were set for each of these parameters to discriminate between cloud types. The evaluation judges model performance based on four case studies located at different latitudes with varying solar zenith angles. Overall results compiled between the cases show a 67 percent agreement for manual and model classifications. General results compiled for clear, low clouds, middle clouds, high clouds, and precipitation cloud types were even more successful with 94, 90, 50, 87, and 95 percent agreement, respectively. The color enhanced automated product provides a legible, quick and accurate tool for cloud type analysis. GRA

N91-23684# Air Force Environmental Technical Applications Center, Scott AFB, IL.
SWANEA (SOUTHWEST ASIA-NORTHEAST AFRICA): A CLIMATOLOGICAL STUDY. VOLUME 2: THE MIDDLE EAST PENINSULA
Michael J. Vojtesak, Kevin P. Martin, Gregory Myles, and Michael T. Gilford Feb. 1991 246 p
(AD-A232776; USAFETAC/TN-91/002-Vol-2) Avail: NTIS HC/MF A11 CSCL 04/2

This volume is a climatological study of the Middle East Peninsula; an area that includes the Red Sea Coastal Plains, Arabian Desert, Fertile Crescent, and Persian Gulf Coastal Plains. After describing the general geography of land areas in the Middle East Peninsula, it discusses major meteorological features of the entire study area. Each major subregion (based on (climatic commonality) is then broken into its own geography and general weather sections. Finally, the four so-called seasons in each of these subregions are discussed in detail. Topics include wind direction/velocity, ocean surface temperature, atmospheric temperature, cloud cover, jet streams, and monsoons. GRA

N91-23685# Air Force Environmental Technical Applications Center, Scott AFB, IL.
RANGE REFERENCE ATMOSPHERE, SHEMYA
Jan. 1991 168 p
(AD-A232813; USAFETAC/PR-91/003) Avail: NTIS HC/MF A08 CSCL 04/2

This range reference atmosphere (RRA) is a statistical model (derived from upper-air observations) of the atmosphere from 0 to 70 km over the Shemya range complex. The RRA provides tabulations of monthly and annual means, standard deviations, and skewness coefficients for wind speed, pressure, temperature, density, water vapor pressure, virtual temperature, and dew point temperature. It also gives means and standard deviation for the zonal and meridional wind components and hydrostatic model atmosphere. Methodology is included, along with graphic displays of wind statistics that can be derived from the wind data. GRA

N91-23686# Air Force Environmental Technical Applications Center, Scott AFB, IL.
RANGE REFERENCE ATMOSPHERE, THULE
Feb. 1991 180 p
(AD-A232831; USAFETAC/PR-91/006) Avail: NTIS HC/MF A09 CSCL 04/2

This range reference atmosphere (RRA) is a statistical model (derived from upper-air observations) of the atmosphere from 0 to 70 km over the Thule range complex. The RRA provides tabulations of monthly and annual means, standard deviations, and skewness coefficients for wind speed, pressure, temperature, density, water vapor pressure, virtual temperature, and dew point temperature. It also gives means and standard deviation for the zonal and meridional wind components and hydrostatic model atmosphere. Methodology is included, along with graphic displays of wind statistics that can be derived from the wind data. GRA

N91-23592# Paris VI Univ. (France). Lab. d'Oceanographie Dynamique et de Climatologie.
OCEAN MODELING FOR CLIMATE STUDY [MODELISATION OCEANIQUE POUR LES ETUDES DE CLIMAT]
P. Delecluse *In* ESA, Space and Sea Dec. 1990 p 209-214 In FRENCH (For primary document see N91-23563 15-42)
Copyright Avail: NTIS HC/MF A13

N91-23599# Institut Francais de Recherche pour l'Exploitation de la Mer, Brest (France).
WIND AND SEA STATE LOCAL CLIMATOLOGY BY MEANS OF SATELLITE RADAR ALTIMETER MEASUREMENTS
J. Tournadre and R. Ezraty *In* ESA, Space and Sea Dec. 1990 p 251-256 (For primary document see N91-23563 15-42)
Copyright Avail: NTIS HC/MF A13

N91-23607# Alcatel Espace, Toulouse (France).
CHARACTERISTICS AND PERFORMANCE OF AN OPERATIONAL WINDSCATTEROMETER
D. Marquet and N. Lannelongue *In* ESA, Space and Sea Dec. 1990 p 297-301 (For primary document see N91-23563 15-42)
Copyright Avail: NTIS HC/MF A13

48 OCEANOGRAPHY

Includes biological, dynamic, and physical oceanography; and marine resources.

For related information see also *43 Earth Resources and Remote Sensing.*

N91-23687# Deutsche Forschungsanstalt fuer Luft- und Raumfahrt, Cologne (Germany, F.R.). Abt. Satellitendatenakquisition.
SEA ICE MONITORING IN THE EAST GREENLAND SEA IN MAY 1988 BY MEANS OF REMOTE SENSING, WITH SPECIAL EMPHASIS ON THE COMPUTER-AIDED AVHRR-BASED EXTRACTION OF SEA ICE MOTIONS Ph.D. Thesis - Ludwig-Maximilians-Univ.
Stefan Werner Dech Aug. 1990 284 p In GERMAN; ENGLISH summary Submitted for publication Original contains color illustrations
(DLR-FB-90-36; ISSN-0939-2963; ETN-91-99078) Avail: NTIS HC/MF A13; DLR, Wissenschaftliches Berichtswesen, VB-PL-DO, Postfach 90 60 58, 5000 Cologne, Fed. Republic of Germany, HC 78 DM

NOAA 9/NOAA 10 Advanced Very High Resolution Radiometer (AVHRR) recorded 256 passes using the transportable High Resolution Picture Transmission (HRPT) receiving station of the German air and space organization from May 4 to 26, 1988. Selected data were used for an interactive extraction of the sea ice motions by means of vector description and digital image processing techniques. The drift characteristics information obtained was quantified and its dynamics analyzed. The influence

of parameters such as ice concentration, ice thickness and surface roughness on the ice drift was investigated, using optimized AVHRR data and two LANDSAT 5 Thematic Mapper scenes close to the the fast ice border, and 173 vertical aerial photographs along the ice edge. ESA

N91-23688 Royal Netherlands Meteorological Inst., De Bilt. Div. of Oceanographic Research.
A GUIDE TO THE NEDWAM WAVE MODEL
Gerrit Burgers 1990 88 p
(KNMI-WR-90-04; ISSN-0169-1651; ETN-91-99105) Copyright Avail: Royal Netherlands Meteorological Institute, P.O. Box 201, 3730 AE De Bilt, Wilhelminalaan 10, Netherlands

Nedwam is a numerical model for making North Sea wave forecasts. The model physics of Nedwam is the same as that of the global wave model WAM. Nedwam models the evolution of the two dimensional wave variance spectrum at each point of a stereographic grid which covers the North Sea and a large part of the Norwegian sea. The geographic grid contions 612 grid points. The grid spacing is approximately 75 km. The wave variance spectrum is defined on a wave vector grid of 25 frequencies by 12 directions. The various terms in the central equation of wave physics have direct counterparts in the Nedwam model. Therefore, it will be relatively easy to change Nedwam if better representations for the various terms in this equation become available of if one wants to include data assimilation. As the total number of model variables is rather large , 612 x 25 x 12 = 183600, the Nedwam model requires much more computer time and memory than previous wave models. On the other hand, it produces more detailed information, as in principle the full two dimensional wave spectrum is available for all times and places. One can ask for example the significant wave heights, the peak periods, the wave directions and the spectra at any grid point. ESA

N91-23689# Naval Postgraduate School, Monterey, CA.
SEA ICE CLASSIFICATION USING SYNTHETIC APERTURE RADAR M.S. Thesis
Frank W. Garcia, Jr. Jun. 1990 116 p
(AD-A232248; NPS68-90-004) Avail: NTIS HC/MF A06 CSCL 08/12

This study employs Synthetic Aperture Radar (SAR) imagery from the Marginal Ice Zone Experiment (MIZEX) 1987 to identify an optimal set of statistical descriptors that accurately classify three types of ice (first-year, multiyear, odden) and open water. Two groups of statistics, univariate and texture, are compared and contrasted with respect to their skill in classifying the ice types and open water. Individual statistical descriptors are subjected to principal component analysis and discriminant analysis. Principal component analysis was of little use in understanding features of each ice and open water group. Discriminant analysis was valuable in identifying which statistics held the most power. When combined, univariate and texture statistics classified the groups with 89.5 percent accuracy, univariate alone with 86.8 percent accuracy and texture alone with 75.4 percent accuracy. Range and inertia were the strongest univariate and texture discriminators with 74.6 and 50.8 percent accuracy, respectively. Despite the use of a non-calibrated SAR, univariate statistics were able to classify the images with greater accuracy than texture statistics. GRA

N91-23690# Naval Postgraduate School, Monterey, CA.
PARALLEL-PROCESSOR-BASED GAUSSIAN BEAM TRACER FOR USE IN OCEAN ACOUSTIC TOMOGRAPHY M.S. Thesis
Roderick S. Scott Jun. 1990 137 p
(AD-A232420) Avail: NTIS HC/MF A07 CSCL 17/1

A parallel processor band acoustic ray tracing algorithm is presented for use in predicting multipath arrival times and amplitudes, for use in ocean acoustic tomography experiments. The Runge-Kutta-Fehlberg numerical integration method was chosen, out of three other methods, to numerically solve the ray equations. Cubic splines were used to interpolate the sound speed profile and bottom bathymetry data. The method of Gaussian beam tracing was used to compute the multipath amplitudes at a given receiver location. The ray tracing algorithm is written in C, and is designed to run using a Macintosh II-based host application and a transputer based, parallel processing workfarm. GRA

N91-23691# Woods Hole Oceanographic Inst., MA.
NEAR-EQUATORIAL DEEP CIRCULATION IN THE INDIAN AND PACIFIC OCEANS M.S. Thesis
Gregory C. Johnson Sep. 1990 161 p
(Contracts N00014-87-K-0001; N00014-89-J-1076)
(AD-A232635; WHOI-90-50) Avail: NTIS HC/MF A08 CSCL 08/3

Flow of deep and bottom water in the near-equatorial Indian Ocean, Atlantic Ocean, and Pacific Ocean is described through analysis of CTD data. Zero velocity surfaces are chosen using water-mass properties in conjunction with the thermal-wind field and used to obtain transport estimates. In the Somali Basin a deep western boundary current with an estimated transport of 4,000,000 cu m/s moves north on the continental rise of Africa at 3 deg S. Equatorial observations suggest that this current turns eastward at the equator. In the Pacific Ocean at 10 deg N two deep western boundary currents with estimated mass transport of 5,000,000 cu m/s and 8,100,000 cu m/s move north off the Caroline and Marshall Islands respectively. A current with an estimated transport of 4,700,000 cu m/s moves south over the western flank of the East Pacific Rise. This current feeds a westward jet at the equator and brings the net northward transport of bottom water at 10 deg N to 8,400,000 cu m/s. Effects of ocean basin geometry, bottom bathymetry and vertical diffusivity as well as a model meridional inertial current on a sloping bottom near the equator are discussed in conjunction with the observational results. GRA

N91-23593# Institut de Mecanique de Grenoble (France).
SATELLITE DATA UTILIZATION IN OCEAN CIRCULATION MODELS [UTILISATION DES DONNEES SPATIALES DANS LES MODELES DE CIRCULATION OCEANIQUE]
B. Barnier, M. Boukthir, and J. Verron *In* ESA, Space and Sea Dec. 1990 p 215-220 In FRENCH Sponsored by CNES; CNRS; and Direction des Recherches, Etudes et Techniques, France (For primary document see N91-23563 15-42)
Copyright Avail: NTIS HC/MF A13

N91-23594# Technische Univ., Delft (Netherlands). Faculty of Aerospace Engineering.
EXTRACTION OF MESOSCALE OCEAN CURRENTS INFORMATION FROM GEOSAT ALTIMETER DATA
K. F. Wakker, M. C. Naeije, R. Scharroo, and B. A. C. Ambrosius *In* ESA, Space and Sea Dec. 1990 p 221-226 Sponsored by Space Research Organization Netherlands; Beleidscommissie Remote Sensing, Delft, Netherlands; and IBM Nederland NV (For primary document see N91-23563 15-42)
Copyright Avail: NTIS HC/MF A13

N91-23595# Institut de Mecanique de Grenoble (France).
SEA LEVEL AND SATELLITE TECHNIQUES [NIVEAU DE LA MER ET TECHNIQUES SATELLITAIRES]
C. LeProvost *In* ESA, Space and Sea Dec. 1990 p 227-232 In FRENCH; ENGLISH summary (For primary document see N91-23563 15-42)
Copyright Avail: NTIS HC/MF A13

N91-23596# Paris VI Univ., Villefranche-sur-Mer (France). Lab. de Physique et Chimie Marines.
PRIMARY OCEAN PRODUCTION: CARBON AND PARTICLE FLUX [PRODUCTION PRIMAIRE OCEANIQUE: FLUX DE CARBONE ET DE PARTICULES]
Andre Morel *In* ESA, Space and Sea Dec. 1990 p 233-240 In FRENCH Submitted for publication (For primary document see N91-23563 15-42)
Copyright Avail: NTIS HC/MF A13

N91-23597# Centre National d'Etudes des Telecommunications, Issy-les-Moulineaux (France).
ENERGY EXCHANGE STUDY AT THE OCEAN SURFACE BY SATELLITE OBSERVATION [ETUDE DES ECHANGES D'ENERGIE A LA SURFACE OCEANIQUE, A PARTIR D'OBSERVATIONS SPATIALES]
Laurence Eymard *In* ESA, Space and Sea Dec. 1990 p 241-245 In FRENCH (For primary document see N91-23563 15-42)
Copyright Avail: NTIS HC/MF A13

N91-23598# Direction de la Meteorologie Nationale, Paris (France).
SATELLITE DATA UTILIZATION FOR MODELING SEA STATES [UTILISATION DES DONNEES SATELLITAIRES POUR LA MODELISATION DE L'ETAT DE LA MER]
A. Guillaume *In* ESA, Space and Sea Dec. 1990 p 247-249 In FRENCH (For primary document see N91-23563 15-42)
Copyright Avail: NTIS HC/MF A13

N91-23601# Rutherford Appleton Lab., Chilton (England). Space Science Dept.
ATSR: PRECISE SEA SURFACE TEMPERATURE FROM THE ERS-1 SATELLITE
D. Llewellyn-Jones, R. Bernard, and Laurence Eymard (Centre de Recherches en Physique de l'Environnement, Issy-les-Moulineaux, France) *In* ESA, Space and Sea Dec. 1990 p 265-266 (For primary document see N91-23563 15-42)
Copyright Avail: NTIS HC/MF A13

N91-23602# Centre National d'Etudes Spatiales, Toulouse (France).
VALIDATION REQUIREMENTS FOR THE TOPEX/POSEIDON ALTIMETER MISSION
Y. Menard, S. Arnault, J. M. Molines (SBS, Aix-en-Provence, France), P. Vincent, L. Gourdeau, and M. Dorrer *In* ESA, Space and Sea Dec. 1990 p 267-273 (For primary document see N91-23563 15-42)
Copyright Avail: NTIS HC/MF A13

N91-23603# CLS Argos, Toulouse (France). Groupe Oceanographique.
COLLECTION AND PROCESSING OF OCEANOGRAPHIC DATA AT CLS [COLLECTE ET TRAITEMENT DE DONNEES OCEANOGRAPHIQUES A CLS]
Pierre-Yves LeTraon *In* ESA, Space and Sea Dec. 1990 p 275-278 In FRENCH (For primary document see N91-23563 15-42)
Copyright Avail: NTIS HC/MF A13

N91-23604# Consiglio Nazionale delle Ricerche, Florence (Italy). Ist. di Ricerca sulle Onde Elettromagnetiche.
REMOTE SENSING OF THE SEA AT IROE/CNR
Bruno Radicati, Giovanna Cecchi, Luca Pantani, and Ivan Pippi *In* ESA, Space and Sea Dec. 1990 p 279-283 (For primary document see N91-23563 15-42)
Copyright Avail: NTIS HC/MF A13

51 LIFE SCIENCES (GENERAL)

N91-23692# Lawrence Livermore National Lab., CA.
ABSOLUTE CALIBRATION IN VIVO MEASUREMENT SYSTEMS
D. A. Kruchten and D. P. Hickman Feb. 1991 8 p
(Contract W-7405-eng-48)
(DE91-009719; UCRL-ID-106311) Avail: NTIS HC/MF A02

Lawrence Livermore National Laboratory (LLNL) is currently investigating a new method for obtaining absolute calibration factors for radiation measurement systems used to measure internally deposited radionuclides in vivo. Absolute calibration of in vivo measurement systems will eliminate the need to generate a series of human surrogate structures (i.e., phantoms) for calibrating in vivo measurement systems. The absolute calibration of in vivo measurement systems utilizes magnetic resonance imaging (MRI) to define physiological structure, size, and composition. The MRI image provides a digitized representation of the physiological structure, which allows for any mathematical distribution of radionuclides within the body. Using Monte Carlo transport codes, the emission spectrum from the body is predicted. The in vivo measurement equipment is calibrated using the Monte Carlo code and adjusting for the intrinsic properties of the detection system. The calibration factors are verified using measurements of existing phantoms and previously obtained measurements of human volunteers. DOE

N91-23693# Ames Lab., IA.
EXCITED STATE STRUCTURE, ENERGY AND ELECTRON TRANSFER DYNAMICS OF PHOTOSYNTHETIC REACTION CENTERS: A HOLE BURNING STUDY Ph.D. Thesis
De-Ming Tang 22 Mar. 1991 254 p
(Contract W-7405-eng-82)
(DE91-010181; IS-T-1490) Avail: NTIS HC/MF A12

The excited state structure, early time energy, and electron transfer dynamics for the bacterial photosynthetic reaction center of Rhodoseudomonas viridis, Rhodobacter sphaeroides, and the green plant photosynthetic reaction center of Photosystem 2 (PS 2) have been determined by hole burning spectroscopy. Transient hole burned spectra of the bacterial reaction centers reveal a special pair Franck-Condon marker mode progression with a superimposed zero phonon hole. Such progression is found to be absent in the green plant Photosystem 2 which raises the question of structural similarities between the PS 2 and bacterial reaction centers. The excited state decay times are obtained for all systems and found to be consistent with time domain experiments. Similar temperature dependence of the decay kinetics have been observed for both bacterial and PS 2 reaction centers. Study of different preparations of reaction center of Photosystem 2 utilizing hole burning spectroscopy indicates that Triton X-100 detergent significantly affect the absorption and persistent hole burned spectra and disrupts the energy transfer from the accessory chlorophyll to the active pheophytin. The comparison between the bacterial reaction centers and Photosystem 2 has been presented and discussed in order to understand the difference in their early time dynamics and the excited state structure. A theoretical model has been developed based on the principle of linear electron-phonon coupling and imhomogeneous broadening. Our experimental results are found to be in good agreement with the theoretical calculations. DOE

N91-23694*# National Aeronautics and Space Administration, Washington, DC.
SPACE LIFE SCIENCES: A STATUS REPORT
Feb. 1990 60 p Original contains color illustrations
(NASA-NP-120; NAS 1.83:120) Avail: NTIS HC/MF A04; 41 functional color pages CSCL 06B

The scientific research and supporting technology development conducted in the Space Life Sciences Program is described. Accomplishments of the past year are highlighted. Plans for future activities are outlined. Some specific areas of study include the following: Crew health and safety; What happens to humans in space; Gravity, life, and space; Sustenance in space; Life and planet Earth; Life in the Universe; Promoting good science and good will; Building a future for the space life sciences; and Benefits of space life sciences research. E.R.

N91-23695# Lawrence Livermore National Lab., CA.
PROBLEMS IN UNDERSTANDING THE ORGANIZATION, STRUCTURE AND FUNCTION OF CHROMOSOMES
E. M. Bradbury 1990 17 p Presented at the NATO Symposium, Scilly, Italy, May 1990
(Contracts W-7405-eng-36; DE-FG03-88ER-60673)
(DE91-009939; LA-UR-91-732; CONF-9005329-1) Avail: NTIS HC/MF A03

Despite intensive investigation of mammalian chromosomes,

the basic rules that govern their organization, structure, and functions are largely unknown. This situation results from the current limitations in available technologies to elucidate the structures of such complex biological systems. Whereas the powerful techniques of molecular biology have successfully addressed at high resolution functional problems at the level of nucleic acid sequences, many lower resolution questions concerning the architecture of the cell nucleus, long range order in chromosomes, and higher order chromatin structures remain largely unanswered. Techniques are now emerging that should help to remedy this situation. The use of confocal microscopy with molecular probes will tell us at the level of the light microscope a great deal about the organization of the nucleus and how it changes in different cell types; advanced light sources have the potential to image hydrated biological systems down to 10 nm, and scanning electron tunneling and atomic force microscopies have demonstrated their ability to image molecules though their ability to usefully image biomolecules such as DNA remains to be shown. DOE

N91-23696# California Inst. of Biological Research, La Jolla.
NEW HOSTS AND VECTORS FOR GENOME CLONING
28 Feb. 1991 3 p Submitted for publication
(Contract DE-FG03-90ER-60997)
(DE91-009996; DOE/ER-60997/T1) Avail: NTIS HC/MF A01

The main goal was to develop new bacterial hosts and vectors for cloning human DNA in the bacterium E. coli. Because human DNA is both A+T-rich and highly repetitive, many human sequences are unstable as inserts in vectors that are propagated in bacteria. During the past eight months, what fraction of human DNA inserts in cosmid vectors is unstable was assessed, new host strains were developed that help stabilize unstable sequence features of human DNA, and the development was begun of a new generation of cloning vectors that should permit the more stable maintenance and more facile analysis of large human DNA inserts. DOE

N91-23697# Los Alamos National Lab., NM.
ROBOTICS FOR RECOMBINANT DNA AND HUMAN GENETICS RESEARCH
T. J. Beugelsdijk 1990 29 p Presented at the 5th International Conference on Advanced Robotics, Pisa (Italy), 20-22 Jun. 1991
(Contract W-7405-eng-36)
(DE90-016440; LA-UR-90-2884; CONF-910637-1) Avail: NTIS HC/MF A03

In October of 1989, molecular biologists throughout the world formally embarked on ultimately determining the set of genetic instructions for a human being. Called the Manhattan Project by some, a molecular biological pursuit of this goal is projected to require approximately 3000 man years of effort over a 15-year period. The Humane Genome Initiative is a worldwide research effort that has the goal of analyzing the structure of human deoxyribonucleic acid (DNA) and determining the location of all human genes. The Department of Energy (DOE) has designated three of its national laboratories as centers for the Human Genome Project. These are Los Alamos National Laboratory (LANL), Lawrence Livermore National Laboratory (LLNL), and Lawrence Berkeley Laboratory (LBL). These laboratories are currently working on different, but complementary technology development areas in support of the Human Genome Project. The robotics group at LANL is currently working on developing the technologies that address the problems associated with physical mapping. This article describes some of these problems and discusses some of the robotics approaches and engineering tolls applicable to their solution. DOE

N91-23698# California Univ., Berkeley. Lawrence Berkeley Lab.
STRUCTURAL STUDIES OF MANGANESE AND HALIDE IN THE PHOTOSYNTHETIC OXYGEN EVOLVING COMPLEX Ph.D. Thesis
V. J. DeRose Oct. 1990 214 p
(Contract DE-AC03-76SF-00098)
(DE91-009071; LBL-30077) Avail: NTIS HC/MF A10

Electron paramagnetic resonance (EPR) and x ray absorption spectroscopy (XAS) were used as probes of the manganese atoms of the oxygen evolving complex (OEC). XAS studies at liquid helium temperatures allowed the observation of a scatterer at greater then 3 A from the absorbing manganese. Extended x ray absorption fine structure (EXAFS) data taken on preparations from both spinach and the thermophilic cyanobacterium Synechococcus sp. fit to nearly identical parameters. By comparison with model compounds the scatterer at greater than 3 A fits well to a single manganese-manganese distance per the four manganese in the OEC cluster. The correlation between fluoride inhibition of oxygen evolution activity and enhancement of the g = 4 EPR signal which arises from the OEC in the S(sub 2) state was ascertained. The narrowing of the EPR signal is interpreted as being due to fluoride binding to the manganese. A damping of the scattering due to manganese at 2.7 A was observed in data from the fluoride-treated preparations poised in the S2 state. EXAFS of bromide-substituted PSII preparations from Synechococcus showed no change relative to EXAFS of chloride-containing samples. The substructure observed by high resolution EPR of the S2-state multiline signal also shows no change in the presence of bromide. These results argue strongly against the presence of a halide ligand bridging the manganese in the OEC, but do not exclude a single terminal halide ligand. Electron spin echo spectroscopy of (sup 15)N-containing preparations from Synechococcus identify nuclear envelope modulation due to nitrogen near the manganese of the OEC. The modulation frequency is consistent with its arising from an amino acid ligand such as a histidine. DOE

N91-23699# Technical Research Associates, Salt Lake City, UT.
ISOLATION, CLONING AND EXPRESSION OF THE GENES FOR MICROBIAL POLYURETHANE DEGRADATION Technical Report, 15 Nov. 1990 - 15 Feb. 1991
Gail L. Bowers-Irons, Robert Pryor, Usha Charyulu, and Ramesh K. Prakash 20 Feb. 1991 9 p
(Contract N00014-90-C-0182)
(AD-A232108) Avail: NTIS HC/MF A02 CSCL 06/5

New degradation tests are in progress to determine if polyurethane (Impranil-R) and/or urethane (Sigma) can be used as a sole carbon source. Fifteen different cultures have been inoculated into 10 ml polyurethane- and urethane-minimal salts solutions. The DNA vector and fungal host, received from the Fungal Genetics Stock Center, Department of Microbiology, University of Kansas Medical Center are cosmid pSV50 in an E. coli host, LM83, and Neurospora crassa wild type strain (74-OR23-1VA), FGSC 2489. The genomic library will be constructed in E. coli HB101. The fungal vector host will be used for expression of the genes from HAFB-2F-Br. While the DNA isolation procedure is being optimized, concurrent experiments will be done to optimize the transformation frequency of both the E. coli competent cells and the Neurospora crassa host using previously published procedures. GRA

52 AEROSPACE MEDICINE

Includes physiological factors; biological effects of radiation; and effects of weightlessness on man and animals.

N91-23700* National Aeronautics and Space Administration, Washington, DC.
AEROSPACE MEDICINE AND BIOLOGY: A CONTINUING BIBLIOGRAPHY WITH INDEXES (SUPPLEMENT 346)
Feb. 1989 50 p
(NASA SP-7011(346); NAS 1.21:7011(346)) Avail: NTIS HC A03; NTIS standing order as PB89-912300, $15.00 domestic, $30.00 foreign CSCL 06E

This bibliography lists 134 reports, articles and other documents introduced into the NASA Scientific and Technical Information System during Jan. 1991. Subject coverage includes: aerospace

medicine and psychology, life support systems and controlled environments, safety equipment, exobiology and extraterrestrial life, and flight crew behavior and performance. Author

N91-23701* National Aeronautics and Space Administration, Washington, DC.
AEROSPACE MEDICINE AND BIOLOGY: A CONTINUING BIBLIOGRAPHY WITH INDEXES (SUPPLEMENT 347)
Feb. 1989 64 p
(NASA-SP-7011(347); NAS 1.21:7011(347)) Avail: NTIS HC A04; NTIS standing order as PB89-912300, $17.00 domestic, $34.00 foreign CSCL 06E

This bibliography lists 166 reports, articles and other documents introduced into the NASA Scientific and Technical Information System during Feb. 1991. Subject coverage includes: aerospace medicine and psychology, life support systems and controlled environments, safety equipment, exobiology and extraterrestrial life, and flight crew behavior and performance. Author

N91-23702* National Aeronautics and Space Administration, Washington, DC.
AEROSPACE MEDICINE AND BIOLOGY: A CONTINUING BIBLIOGRAPHY WITH INDEXES (SUPPLEMENT 348)
Apr. 1991 60 p
(NASA-SP-7011(348); NAS 1.21:7011(348)) Avail: NTIS HC A04; NTIS standing order as PB91-912300, $15.00 domestic, $30.00 foreign CSCL 06E

This bibliography lists 154 reports, articles and other documents introduced into the NASA Scientific and Technical Information System during Mar. 1991. Subject coverage includes: aerospace medicine and psychology, life support systems and controlled environments, safety equipment, exobiology and extraterrestrial life, and flight crew behavior and performance. Author

N91-23703 Institute for Perception RVO-TNO, Soesterberg (Netherlands).
OTOLITH RESPONSES IN MAN DURING PARABOLIC FLIGHT Final Report
J. T. Marcus 5 Oct. 1990 28 p Sponsored by Space Research Organization Netherlands
(Contract A88/M/318)
(IZF-1990-A-32; TD-90-3407; ETN-91-99098) Copyright Avail: Institute for Perception RVO-TNO, P.O. Box 23, 3769 ZG Soesterberg, Netherlands

The influence of the varying gravito inertial (Gz) force during parabolic flight on the human otolith function is investigated. It is hypothesized that the Gz force initiates an otolith ocular response, that manifests itself primarily in modulation of optokinetic nystagmus slow phase eye velocity. Six subjects were seated in the ESA Caravelle, facing perpendicular to the aircraft's longitudinal axis. The Gz profile was subsequently: 1.8 Gz pull up, 0 G microgravity and 1.8 Gz recover, each phase lasting about 20 s. Vertical eye movements were recorded by electronystagmography throughout the parabolic maneuver. Conditions were: visual fixation, darkness, and optokinetic stimulation of 50 deg/s in an upward or downward direction, projected on a cylindrical screen at 0.6 m viewing distance. No consistent nystagmus or gaze shift was measured in darkness. An ANOVA revealed, however, a Gz modulation of OKN-SPV with downward enhancement of 5 deg/s in the 1.8 Gz hypergravity, as compared to the 0 G condition as well as to the 1 Gz condition. The otolith ocular pathway is modulating optokinetic eye movements in parabolic flight. The significant modulation in the transitions between 1 Gz and 1.8 Gz has relevance to the pilot, who experiences these transitions commonly. ESA

N91-23704*# National Aeronautics and Space Administration. Ames Research Center, Moffett Field, CA.
TRANSCAPILLARY FLUID SHIFTS IN HEAD AND NECK TISSUES DURING AND AFTER SIMULATED MICROGRAVITY
S. E. Parazynski (Denver General Hospital, CO.), Alan R. Hargens, B. Tucker, M. Aratow, J. Styf, and A. Crenshaw Apr. 1991 19 p
(NASA-TM-103847; A-91096; NAS 1.15:103847) Avail: NTIS HC/MF A03 CSCL 06S

To understand the mechanism, magnitude, and time course of facial puffiness that occurs in microgravity, seven male subjects were tilted 6 degrees head down for 8 hr, and all four Starling transcapillary pressures were directly measured before, during, and after tilt. Head-down tilt (HDT) caused facial edema and a significant elevation of microvascular pressures measured in the lower lip: capillary pressures increased from 27.2 +/- 5 mm Hg pre-HDT to 33.9 +/- 1.7 mm Hg by the end of tilt. Subcutaneous and intramuscular interstitial fluid pressures in the neck also increased as a result of HDT, while interstitial fluid colloid osmotic pressures remained unchanged. Plasma colloid osmotic pressures dropped significantly after 4 hr of HDT, suggesting a transition from fluid filtration to absorption in capillary beds between the heart and feet during HDT. After 4 hr of seated recovery from HDT, microvascular pressures remained significantly elevated by 5 to 8 mm Hg above baseline values, despite a significant HDT diuresis and the orthostatic challenge of an upright, seated posture. During the control (baseline) period, urine output was 46.7 ml/hr; during HDT, it was 126.5 ml/hr. These results indicate that facial edema resulting from HDT is primarily caused by elevated capillary pressures and decreased plasma colloid osmotic pressures. Elevation of cephalic capillary pressures sustained for 4 hr after HDT suggests that there is a compensatory vasodilation to maintain microvascular perfusion. The negativity of interstitial fluid pressures above heart level also has implications for the maintenance of tissue fluid balance in upright posture. Author

N91-23705# Laboratoire d'Automatique et d'Analyse des Systemes, Toulouse (France).
RESEARCH AND DEVELOPMENT INVOLVED IN CREATING A QUANTITATIVE EEG CARTOGRAPHY WIDE BAND ANALYSIS SYSTEM Ph.D. Thesis - Toulouse Univ. [ETUDE ET REALISATION D'UN SYSTEME RAPIDE DE CARTOGRAPHIE D'EEG QUANTIFIE A LARGE BANDE D'ANALYSE]
Mohamed Bouamar 1991 162 p In FRENCH; ENGLISH summary Sponsored by Vivre Debout Association
(LAAS-91002; ETN-91-99240) Avail: NTIS HC/MF A08

Ways of improving the analysis band and the speed of processing systems in quantitative electroencephalography are described. The study and the realization of a fast system allowing for the acquisition and spectral analysis of a great number of electroencephalographic signals is presented. It is a multichannel acquisition system with large band and low noise differential inputs, linked to a master slave processing system built around a PC/AT and Digital Signal Processor (DSP). The system offers the user many possibilities of analysis leading to greatly varied study over a large frequency range. The evaluation of system performances is achieved by a simulation study of errors in processor calculations. In order to validate the system, a set of measurements on real electroencephalographic signals is achieved to highlight its analysis capacities and correlate the corresponding results with the clinical results. ESA

N91-23706# Wright State Univ., Dayton, OH.
HEPATIC METABOLISM OF PERFLUORINATED CARBOXYLIC ACIDS: A NUCLEAR MAGNETIC RESONANCE INVESTIGATION Annual Report, 15 Feb. - 14 Dec. 1990
Nicholas V. Reo 14 Dec. 1990 11 p
(Grant AF-AFOSR-0148-90; AF Proj. 2312)
(AD-A232033; AFOSR-91-0021TR) Avail: NTIS HC/MF A03 CSCL 06/1

This research project employs nuclear magnetic resonance (NMR) spectroscopy to investigate the metabolic aspects of the toxicity associated perfluorinated carboxylic acids. Fluorine-19 NMR has been used to monitor the metabolic fate of perfluoro-n-octanoic acid (PFOA) and perfluoro-n-decanoic acid (PFDA) in a rat. Spectra obtained at various times following the administration of PFOA and PFDA depict the presence of the parent compounds in samples of bile, serum, urine, and liver in vivo. Urine spectra also indicate the presence of a possible metabolite which has not been identified at this time. Carbon-13 NMR is providing information regarding

the effects of PFOA and PFDA on hepatic carbohydrate metabolism. Preliminary data indicate that hepatic glycogenesis is severely inhibited in rats at 3 days post treatment with PFDA. Plasma glucose and hepatic glucose appear to behave similar to control animals during the first three days post treatment with PFDA, but data obtained at days 6 and 7 indicate that hepatic glucose utilization may be slowed. These data are preliminary and experiments are currently in progress to further characterize the perfluorocarbon-induced dysfunctions of liver metabolism. GRA

N91-23707# Uniformed Services Univ. of the Health Sciences, Bethesda, MD.
MOLECULAR STUDIES OF CYTOKINE INDUCTION Final Report, 1 Jun. - 15 Nov. 1989
Carl W. Dieffenbach 31 May 1990 32 p
(Contract MDA905-89-C-0014)
(AD-A232221) Avail: NTIS HC/MF A03 CSCL 06/5

While many of the molecular events in viral replication are well studied, the mechanisms by which viral infections trigger such constitutional symptoms as fever and malaise are unknown. We investigate the hypothesis that these viral constitutional symptoms can be triggered by the accumplation and release of dsRNA arising from viral replication. Total lung RNA from mice acutely infected with influenza virus but not from sham-infected mice was shown to induce fever, excess slow-wave sleep and enhanced amplitudes of electroencephalographic slow waves when injected into the rabbit brain. Influenza viral dsRNA was demonstrated in the active lung RNA preparations by reverse transcriptase-polymerase chain reaction techniques and was shown to be responsible for the rabbit responses by differential nuclease digestion. GRA

N91-23708# Washington Univ., Saint Louis, MO.
CONTROL OF BIOSONAR BEHAVIOR BY THE AUDITORY CORTEX Final Report, Jul. 1987 - Oct. 1990
Nobuo Suga and Stephen Gaioni 21 Dec. 1990 15 p
(Grant AF-AFOSR-0250-87; AF Proj. 2313)
(AD-A232699; AFOSR-91-0145TR) Avail: NTIS HC/MF A03 CSCL 06/4

The major aim of this project was to examine, by means of critical lesion experiments, whether the functional organization of the mustached bat's, Pteronotus parnellii, auditory cortex is related to biosonar behavior in the manner inferred from pervious neurophysiological experiments. First, we quantitatively analyzed the behavioral adjustments the bat makes in the frequency, intensity, duration, and rate of emission of its biosonar pulses during target-directed flight. Next, we examined changes in these behavioral adjustments following bilateral ablation of either the entire auditory cortex, or more localized cortical regions. We then focused on the role of the auditory cortex in the perception of biosonar signals. This was accomplished by conditioning the bats to discriminate between biosonar signals that varied along some stimulus parameter (e.g., echo delay) using a leg flexion shock avoidance procedure. We then created of the auditory cortex. Major results of each of these lines of research are described in this report. GRA

N91-23709# Naval Biodynamics Lab., New Orleans, LA.
HUMAN SHORT-LATENCY SOMATOSENSORY EVOKED POTENTIALS IN IMPACT ACCELERATION RESEARCH: EQUIPMENT, PROCEDURES, AND TECHNIQUES Final Report, 1984 - 1990
David Matson 1 Oct. 1990 23 p Sponsored by Naval Medical Research and Development Command, Bethesda, MD
(AD-A232732; NBDL-89R001) Avail: NTIS HC/MF A03 CSCL 05/8

The Naval Biodynamics Laboratory has been investigating the neurophysiological effects of impact acceleration on humans. The goal of this research program is to establish impact injury thresholds for properly restrained personnel. The techniques and equipment configurations developed for neuro-physiological impact research and offers suggestions for future research are summarized. The efforts have focused on the use of somatosensory evoked potentials to assess the integrity of the central nervous system of humans undergoing impact accelerations. In the experiments human research volunteers were exposed to impact acceleration ranging from three to fifteen times the force of gravity (3 to 15 g's) in various directions. These experiments provide data to help determine thresholds of injury to cervico-cortical neural pathways during impact events and indicate that the potential for injury may be reduced if these injury thresholds are taken into consideration in the designs of cockpits and emergency aircraft egress and recovery systems. GRA

N91-23566# Norwegian Underwater Technology Center Ltd., Laksevaag.
EFFECTS OF WEIGHTLESSNESS (SEA WATER IMMERSION) ON BODY FLUID BALANCE AND CNS FUNCTIONS
A. Hope, R. Vaernes, T. Bergan, M. Warncke, H. Sundland, C. Jepsen, and B. Lorenz (Deutsche Forschungsanstalt fuer Luft- und Raumfahrt, Hamburg, Germany, F.R.) *In* ESA, Space and Sea Dec. 1990 p 21-24 Sponsored by Norwegian Space Center, Oslo (For primary document see N91-23563 15-42)
Copyright Avail: NTIS HC/MF A13

N91-23568# Soviet-French Joint Venture, Moscow (USSR).
REAL TIME ANALYSIS SYSTEMS OF THE PHYSICAL PARAMETERS OF THE ENVIRONMENT AND THE STATE OF A HUMAN ORGANISM FOR A LONG TERM EXPOSURE AT DIFFERENT GAS MIXTURES AND PRESSURE UP TO 100 BAR
G. I. Kurenkov, A. LeLevier, B. O. Jachontov, and A. V. Rozhkov *In* ESA, Space and Sea Dec. 1990 p 31-35 (For primary document see N91-23563 15-42)
Copyright Avail: NTIS HC/MF A13

N91-23570# Centre d'Etudes et de Recherches de Chronobiologie Humaine, Nice (France). Lab. Souterrain de Chronobiologie.
SOME PROBLEMS OF DESYNCHRONISATION OF SLEEP-WAKEFULNESS AND CIRCADIAN RHYTHMS FOR LONG DURATION SPACEFLIGHTS
Michel Siffre *In* ESA, Space and Sea Dec. 1990 p 43-59 (For primary document see N91-23563 15-42)
Copyright Avail: NTIS HC/MF A13

N91-23571# Compagnie Maritime d'Expertises, Marseille (France).
LONG DURATION HYPERBARIC CONFINEMENT: HYDRA 9
B. Gardette, M. Comet, C. Gortan, M. Novara (European Space Agency. European Space Research and Technology Center, ESTEC, Noordwijk, Netherlands), and H. G. Delauze *In* ESA, Space and Sea Dec. 1990 p 63-68 (For primary document see N91-23563 15-42)
Copyright Avail: NTIS HC/MF A13

N91-23572# Japan Marine Science and Technology Center, Tokyo. Diving Science and Technology Dept.
MANNED DIVING ACTIVITIES IN JAMSTEC
Nobuo Ito *In* ESA, Space and ESA Dec. 1990 p 69-73 (For primary document see N91-23563 15-42)
Copyright Avail: NTIS HC/MF A13

N91-23588# Direction des Constructions et Armes Navales, Toulon (France).
A KO2 REBREATHER FOR EVA DENITROGENATION PROCEDURE
E. Radziszewski and Jean Claude LePechon (JCLP Hyperbarie, Paris, France) *In* ESA, Space and Sea Dec. 1990 p 187-190 (For primary document see N91-23563 15-42)
Copyright Avail: NTIS HC/MF A13

N91-24056*# National Aeronautics and Space Administration. Ames Research Center, Moffett Field, CA.
SIMULATION OF BLOOD FLOW THROUGH AN ARTIFICIAL HEART
Cetin Kiris, I-Dee Chang (Stanford Univ., CA.), Stuart E. Rogers, and Dochan Kwak *In* NASA, Washington, Technology 2000,

Volume 2 1991 p 133-145 (For primary document see N91-24041 15-99)
Avail: NTIS HC/MF A16 CSCL 06P

N91-24057*# National Aeronautics and Space Administration. Marshall Space Flight Center, Huntsville, AL.
THREE-DIMENSIONAL STRUCTURE OF HUMAN SERUM ALBUMIN
Daniel C. Carter, Xiao-min He, Pamela D. Twigg, and Elena Casale *In* NASA, Washington, Technology 2000, Volume 2 1991 p 146-150 (For primary document see N91-24041 15-99)
Avail: NTIS HC/MF A16 CSCL 06P

N91-24058*# National Aeronautics and Space Administration. Ames Research Center, Moffett Field, CA.
A NON-INVASIVE MEASURE OF MINERALS AND ELECTROLYTES IN TISSUE
Sara B. Arnaud and Burton Silver (IntraCellular Diagnostics, Inc., San Jose, CA.) *In* NASA, Washington, Technology 2000, Volume 2 1991 p 151-154 (For primary document see N91-24041 15-99)
Avail: NTIS HC/MF A16 CSCL 06P

N91-24076*# National Aeronautics and Space Administration. Langley Research Center, Hampton, VA.
THE TRANSFER OF TECHNOLOGY TO MEASURE SKIN BURN DEPTH IN HUMANS
William T. Yost and John H. Cantrell *In* NASA, Washington, Technology 2000, Volume 2 1991 p 308-314 (For primary document see N91-24041 15-99)
Avail: NTIS HC/MF A16 CSCL 06P

53 BEHAVIORAL SCIENCES

Includes psychological factors; individual and group behavior; crew training and evaluation; and psychiatric research.

N91-23710# Federal Aviation Administration, Washington, DC. Research and Development Service.
INDIVIDUAL DIFFERENCES UNDERLYING PILOT COCKPIT ERROR Ph.D. Thesis - George Mason Univ.
Eleana S. Edens Apr. 1991 231 p
(DOT/FAA/RD-91/13) Avail: NTIS HC/MF A11

This research attempted to isolate personality, attitude, and cognitive factors that may influence pilot cockpit error. The mediating influence of situational awareness, psychological stress level, and pilot hazardous thought styles was also investigated. Within the literature addressing individual differences and performance, the focus was on individual differences and cockpit behavior and individual differences as predictors of aircraft accident involvement. Only a brief summary of the general literature of individual differences and performance is presented, as that body of studies is so vast. The study found that pilot situational awareness and pilot psychological stress levels do predict the frequency of attention/perception and judgement/decision pilot cockpit error. It was not established that individual difference variables (personality, individual attitudes, or cognitive ability) affected either the development of situational awareness or the display of psychological stress. Nor did the individual difference variables contribute substantially to hazardous cognitive styles. Hazardous cognitive styles were not related to pilot error in this study. Author

N91-23711# Advisory Group for Aerospace Research and Development, Neuilly-Sur-Seine (France). Aerospace Medical Panel.
HUMAN PERFORMANCE ASSESSMENT METHODS. ADDENDUM
Eric Farmer, ed. Mar. 1991 78 p Lecture series held in Downsview, Ontario, 5-6 Jun. 1989; in Soesterberg, Netherlands, 12-13 Jun. 1989; and in Rome, Italy, 15-16 Jun. 1989
(AGARD-AG-308-Add; ISBN-92-835-0600-6) Copyright Avail: NTIS HC/MF A05; Non-NATO Nationals requests available only from AGARD/Scientific Publications Executive

The results are presented of the second phase of AGARD Aerospace Medical Panel Working Group 12 on Human Performance Assessment Methods. The major goal of WG 12 was to develop the Standardized Tests for Research on Environmental Stressors or STRES Battery, satisfying conventional psychometric criteria such as reliability, validity and sensitivity for which an extensive data base may now be compiled among the NATO nations. The protocol for the 7 selected tests is presented. AGARDograph 308 also serves as the Lecture Series Notes for AGARD Aerospace Medical Panel Lecture Series 163, Human Performance Assessment Methods. Author

N91-23712# Syracuse Univ., NY. Dept. of Physics.
MECHANISMS OF HIGHER BRAIN FUNCTIONS: A STUDY OF MODELS OF PERCEPTION Final Report, 1 Apr. 1987 - 30 Sep. 1990
Erich Harth 10 Dec. 1990 7 p
(Contract DAAL03-87-K-0034)
(AD-A232389; ARO-24111.10-LS) Avail: NTIS HC/MF A02 CSCL 06/5

A model of visual perception, in which the influence of feedback pathways to the lateral geniculate nucleus was considered, was studied in extensive computer simulations. It was assumed that optimization algorithms were implemented by neutral circuitry and that a scalar feedback composed of central responses acts as objective function in the process. It is shown that under very simple assumptions a number of cognitive functions are performed by the model. The mathematical properties of the Alopex algorithms were studied and the method was applied successfully to a variety of optimization problems. GRA

N91-23713# Morehouse Coll., Atlanta, GA. Dept. of Psychology.
CULTURAL PARAMETERS OF STRESS Final Report, May - Aug. 1990
Vernessa R. Clark Feb. 1991 14 p
(Contract DAAL03-86-D-0001)
(AD-A232526; ARI-RN-91-29) Avail: NTIS HC/MF A03 CSCL 05/8

This paper discusses the role of culture diversity in the mediation of stress appraisal. First a discussion of mediators, such as ratings of life events and perceived control, is presented. This discussion is followed by a brief discussion of ways in which people of different cultures contend with stress. GRA

N91-23714# Massachusetts Inst. of Tech., Cambridge. Dept. of Brain and Cognitive Sciences.
STRATEGIES TO SUSTAIN AND ENHANCE PERFORMANCE IN STRESSFUL ENVIRONMENTS Annual Technical Report, 15 Dec. 1989 - 14 Dec. 1990
Richard J. Wurtman, Andrew B. Dollins, and Harry J. Lynch 31 Jan. 1991 7 p
(Grant AF-AFOSR-0125-90; AF Proj. 2312)
(AD-A232698; AFOSR-91-0110TR) Avail: NTIS HC/MF A02 CSCL 06/10

This grant involves three studies. The first study is designed to determine the efficacy of the catecholamine precursor L-Tyrosine in reducing pilot performance deficits caused by a night of sleep deprivation. Preparations for this study and underway and testing should begin in mid-1991. The remaining studies are designed to examine the dose-response relationships between human plasma melatonin levels and various performance and behavioral indices. Towards this end, we will manipulate nocturnal melatonin levels by exposing people to varying intensities of light (Study 2), daytime levels by administering exogenous melatonin (Study 3). Testing for Study 2 should be complete and testing for Study 2 begun by April 1991. GRA

N91-23715# SRI International Corp., Menlo Park, CA.
SPATIOTEMPORAL CHARACTERISTICS OF VISUAL LOCALIZATION Final Report, Aug. 1988 - Oct. 1990
Christina A. Burbeck Nov. 1990 157 p
(Contract F49620-88-K-0008)
(AD-A232734; AFOSR-91-0053TR) Avail: NTIS HC/MF A08 CSCL 06/4

Psychophysical experiments were conducted to investigate how the human visual system determines the spatial structure of a visual scene. The theoretical basis of the research centers on three ideas: that local spatial filters constitute an initial stage of contrast-encoding; that the properties of these initial filters can affect accuracy of the judgements of the perceived separation; and that the actual encoding of interobject separation occurs at a higher level of processing with its own properties. The properties of the higher levels of processing can be determined by controlling the input from the local spatial filters. Unlike thresholds that are determined primarily at lower levels of processing, thresholds for spatial relationships were found to be highly sensitive to the context in which the stimuli are presented and highly insensitive to those spatial and temporal characteristics that are known to play major roles in the determination of contrast detection thresholds. Context was found to affect both the threshold and the perceived value of interobject separations. Furthermore, the effects of context vary over time, being profound at short durations (100 ms) and small or negligible at long durations (500 ms). The effects of context on the accuracy of judgements of spatial relationships at brief durations were found to depend on the spatial proximity and spatial similarity of the targets and the background context. GRA

N91-23716# Vision Sciences Research Corp., San Ramon, CA.
QUANTIFYING IMPROVED VISUAL PERFORMANCE THROUGH VISION TRAINING Final Report, 1 Jul. - 31 Dec. 1990
Arthur P. Ginsburg 22 Feb. 1991 57 p LIMITED REPRODUCIBILITY: Availability: Document partially illegible
(Contract F49620-90-C-0063)
(AD-A232799; AFOSR-91-0188TR) Avail: NTIS HC/MF A04 CSCL 06/4

This project developed a criterion-free vision training test to improve contrast sensitivity in normal and abnormal vision. The scientific development, evaluation and refinement of noninvasive techniques for improving contrast sensitivity is important since contrast sensitivity is predictive of much everyday visual performance. Two novel techniques of contrast sensitivity training were tested. Static contrast sensitivity at low and high spatial frequencies was first measured and then trained on a CRT display. Additional measures were obtained before and after training on a contrast sensitivity chart and on detection and discrimination of complex targets. Large increases in contrast sensitivity due to vision training were found in some normal and amblyopic observers. There were large individual differences in the amount of improvement on contrast sensitivity and performance tasks. Increased contrast sensitivity ranged from 11.5 to 69.2 percent in normals and from 1.5 to 69.5 percent in amblyopes. Improvement in detection and discrimination of real-world targets ranged from 0 to 81.2 percent in normals and from 0 to 96.2 percent in amblyopes. These results suggest that two-alternative forced-choice methods are effective training procedures in many normal and amblyopic observers. GRA

N91-23564# Deutsche Forschungsanstalt fuer Luft- und Raumfahrt, Cologne (Germany, F.R.). Inst. for Aerospace Medicine.
THE DIVING LABORATORY AS A SIMULATION ENVIRONMENT FOR MANNED SPACEFLIGHT
J. Wenzel, L. Vogt, and R. D. Fischer *In* ESA, Space and Sea Dec. 1990 p 11-13 (For primary document see N91-23563 15-42)
Copyright Avail: NTIS HC/MF A13

N91-23565# Deutsche Forschungsanstalt fuer Luft- und Raumfahrt, Hamburg (Germany, F.R.). Dept. of Aviation and Space Psychology.
PSYCHOLOGICAL SELECTION OF ASTRONAUTS: RECENT DEVELOPMENTS AT THE DLR TESTING CENTRE IN HAMBURG (FED. REPUBLIC OF GERMANY)
C. Fassbender, K. M. Goeters, and D. Manzey *In* ESA, Space and Sea Dec. 1990 p 15-19 (For primary document see N91-23563 15-42)
Copyright Avail: NTIS HC/MF A13

54 MAN/SYSTEM TECHNOLOGY AND LIFE SUPPORT

Includes human engineering; biotechnology; and space suits and protective clothing.

For related information see also *16 Space Transportation.*

N91-23717# Navy Clothing and Textile Research Facility, Natick, MA.
EFFECTIVENESS OF A PROTOTYPE MICROCLIMATE COOLING SYSTEM FOR USE WITH CHEMICAL PROTECTIVE CLOTHING Final Report, Jul. 1989 - May 1990
Nancy A. Pimental, Walter B. Teal, and Barbara A. Avellini Dec. 1990 26 p
(AD-A231572; NCTRF-180) Avail: NTIS HC/MF A03 CSCL 06/9

Facility conducted laboratory evaluations of a prototype, portable microclimate cooling system (MCS) designed for use with chemical protective clothing. The MCS circulates chilled liquid through a torso vest. A backpack unit contains an ice pack; a pump and motor assembly and a rechargeable battery are mounted on a chest or waist strap. Total weight of the MCS is 9.3 kg (20.4 lbs). To examine the effectiveness of the system in reducing heat strain, seven male test subjects participated in a laboratory heat stress evaluation. To determine the cooling power and efficiency of the MCS, thermal manikin testing was conducted. GRA

N91-23718*# National Aeronautics and Space Administration. John F. Kennedy Space Center, Cocoa Beach, FL.
ATMOSPHERIC LEAKAGE AND CONDENSATE PRODUCTION IN NASA'S BIOMASS PRODUCTION CHAMBER. EFFECT OF DIURNAL TEMPERATURE CYCLES
Raymond M. Wheeler, John H. Drese (Bionetics Corp., Cocoa Beach, FL.), and John C. Sager Feb. 1991 15 p
(Contract NAS10-11624)
(NASA-TM-103819; NAS 1.15:103819) Avail: NTIS HC/MF A03 CSCL 06K

A series of tests were conducted to monitor atmospheric leakage rate and condensate production in NASA's Biomass Production Chamber (BPC). Water was circulated through the 64 plant culture trays inside the chamber during the tests but no plants were present. Environmental conditions were set to a 12-hr photoperiod with either a matching 26 C (light)/20 C (dark) thermoperiod, or a constant 23 C temperature. Leakage, as determined by carbon dioxide decay rates, averaged about 9.8 percent for the 26 C/20 C regime and 7.3 percent for the constant 23 C regime. Increasing the temperature from 20 C to 26 C caused a temporary increase in pressure (up to 0.5 kPa) relative to ambient, while decreasing the temperature caused a temporary decrease in pressure of similar magnitude. Little pressure change was observed during transition between 23 C (light) and 23 C (dark). The lack of large pressure events under isothermal conditions may explain the lower leakage rate observed. When only the plant support inserts were placed in the culture trays, condensate production averaged about 37 liters per day. Placing acrylic germination covers over the tops of culture trays reduced condensate production to about 7 liters per day. During both tests, condensate production from the lower air handling system was 60 to 70 percent greater than from the upper system, suggesting imbalances exist in chilled and hot water flows for the two air

handling systems. Results indicate that atmospheric leakage rates are sufficiently low to measure CO2 exchange rates by plants and the accumulation of certain volatile contaminants (e.g., ethylene). Control system changes are recommended in order to balance operational differences (e.g., humidity and temperature) between the two halves of the chamber. Author

N91-23719 Institute for Perception RVO-TNO, Soesterberg (Netherlands).
THE DEVELOPMENT OF HIGHLY PRACTICED SKILLS: A STARTING POINT FOR DRIVER MODELLING Final Report
W. B. Verwey Oct. 1990 32 p
(IZF-1990-B-16; TD-90-3409; ETN-91-99099) Copyright Avail: Institute for Perception RVO-TNO, P.O. Box 23, 3769 ZG Soesterberg, Netherlands

In order to develop reliable intelligent interfaces in motor cars, a driver model should be developed which reflects human information processing mechanisms and, more specifically, mechanisms of skill acquisition, namely involuntary priming and voluntary preparation. On this basis three alternative models of skill acquisition are proposed that differ with respect to the effects of voluntary control at the perceptual and response level of information processing. Subjects carried out two-choice reactions in rapid succession. The most important experimental manipulations were whether the first choice reaction predicted the second and the degree of transfer of training to conditions where predictivity changed. Stimulus presentation was for some subjects always visual whereas for other subjects only the first stimulus was visual and the second was auditory. The results support a model asserting that involuntary effects of priming evolve only at the perceptual level but not at the response level. They support earlier findings that preparation for the second reaction occurs, in part, before execution of the first one. Correlational analyses of individual differences indicate that an overlapping strategy during training yields involuntary priming whereas a sequential strategy without overlapping preparation does not. The results are in close agreement with a connectionist control model of human information processing which consists of separate processing modules each of which can be described as a neural network. Implication for the Generic Intelligent Driver Support (GIDS) system are presented. ESA

N91-23720# Defence and Civil Inst. of Environmental Medicine, Downsview (Ontario).
HEAT STRAIN AND WORK TOLERANCE TIMES WITH VARYING LEVELS OF CANADIAN FORCES NBC PROTECTIVE CLOTHING, AMBIENT TEMPERATURE, PHYSICAL WORK INTENSITY, AND WORK/REST SCHEDULES Final Report
T. McLellan, I. Jacobs, and B. Bain Nov. 1990 96 p
(AD-A232653; DCIEM-90-51) Avail: NTIS HC/MF A05 CSCL 06/5

Canadian Forces personnel must be able to sustain operations in an environment contaminated with nuclear, biological and/or chemical (NBC) agents. Clothing has been designed that protects the individual from a hostile NBC environment. This clothing, however, impairs body heat loss. The degree of impairment is magnified if metabolic heat production is increased and/or environmental temperature increases. The purpose of the present study, therefore, was to examine the effects of environmental temperature and metabolic rate on soldiers' physical work tolerance times (WTT) while wearing various levels of NBC clothing. Twenty-three male soldiers were allocated to exercise at either a light or heavy metabolic rate in an environmental chamber that controlled ambient conditions at either a cool 18 C or hot 30 C temperature. Subjects were tested wearing three levels of protective clothing: their regular combat fatigues (Low); fatigues and the NBC overgarment (Med); fatigues, NBC overgarment, rubber gloves and boots, and protective respirator (High). WTT was defined as the time until body temperature increased to 39.3 C (normal being 37 C), heart rate reached 95 percent of an individual's maximum, dizziness or nausea precluded further exercise or 5 hours had elapsed. GRA

N91-23721# Naval Biodynamics Lab., New Orleans, LA.
SHIP ROLL STABILIZATION AND HUMAN PERFORMANCE Final Report
T. R. Morrison, T. G. Dobie, G. C. Willems, and J. L. Endler Jan. 1991 27 p Sponsored by Naval Medical Research and Development Command, Bethesda, MD
(AD-A232721; NBDL-90R007) Avail: NTIS HC/MF A03 CSCL 06/10

The purpose of this study was to assess possible performance enhancements due to roll stabilization. Psychomotor performance was assessed under no motion, roll stabilized, and non-roll stabilized motion conditions in the Naval Biodynamics Laboratory Ship Motion Simulator. Twelve human research volunteers participated as subjects in the study. The motion conditions were measured and recorded at sea abroad an FFG-7 class frigate outfitted with five roll stabilizers. The following performance tests were used: four-choice reaction time; memory and search task; critical instability tracking. Three questionnaires were used, namely motion sickness symptomatology, magnitude estimate of motion sickness, and magnitude estimate of motion. It was found that subject performance was not affected by roll stabilized motion compared to non-roll stabilized motion in these experimental conditions. Subjects accurately judged the non-roll stabilized motion condition to be greater than the roll stabilized condition, but reported no differences in motion sickness in the two conditions. GRA

N91-23722# University of Northern Arizona, Flagstaff.
EFFECTS OF BRIGHT ILLUMINATION ON ORAL TEMPERATURE AND COGNITIVE PERFORMANCE IN HUMANS DURING NIGHTTIME HOURS Technical Report, May - Dec. 1990
Patrick Hannon, George Brainard, William Gibson, Jonathan French, and David Arnall 15 Jan. 1991 2 p
(Grant AF-AFOSR-0305-90; AF Proj. 2312)
(AD-A232787; AFOSR-91-0064TR) Avail: NTIS HC/MF A01 CSCL 05/8

The objective of this study was to compare the effects of bright and dim illumination on sublingual temperature and behavioral measures to determine if illumination treatment can reduce fatigue and enhance human work performance during specific evening and nighttime periods. Lighting levels for work are typically task specified for actual optimal visual stimulation without considering potential biological and behavioral effects of the light stimuli. This research effort investigated the possibility that human performance may be less than optimal under the 50 to 500 lux light environment that is typical of many work station settings and that performance may be improved under bright wide spectrum illumination. The document presents this information in a one page presentation. GRA

N91-23723# Aerospace Medical Research Labs., Wright-Patterson AFB, OH.
QUANTIFYING PERFORMANCE DEGRADATION DUE TO THE HUMAN-MACHINE INTERFACE OF TELEMANIPULATORS Interim Report, Jan. - Dec. 1990
Steven J. Remis and Daniel W. Repperger Dec. 1990 101 p
(AF Proj. 7231)
(AD-A232814; AAMRL-SR-90-510) Avail: NTIS HC/MF A06 CSCL 23/2

As a first step in evaluating operator interfaces to telerobots, task performance data were collected from humans hands-on, with and without the subjects wearing a unilateral exoskeletal device. These baseline studies show the degradation in task performance caused solely by the exoskeleton, exclusive of any slave robotic system. This subsystems-level approach to performance measurement is motivated by the increasing modularity among robotic designs, and the need to quantify the performance degradation caused by each subsystem. The experiments described in this paper show that the unilateral exoskeleton decreases the human's available information capacity by approximately 36 percent, depending on the subject and the difficulty of the task. This decrease in available information capacity is similar when

viewing the peg-into-hole task using the one dimension of Fitts' Law or when breaking this task into the two tasks of ballistic motion and accurate positioning. Future work involves evaluating the teleoperated performance of these tasks, plus similar hands-on and teleoperated experiments with the operator wearing a bilateral exoskeleton. This matrix of experiments can be repeated for other telerobotic interfaces to understand the benefits and limitations of the variety of available human machine interfaces. GRA

N91-23567# JCLP Hyperbarie, Paris (France).
SUBSEA HABITATS AND SPACE SIMULATION
Jean Claude LePechon *In* ESA, Space and Sea Dec. 1990 p 25-30 Sponsored in part by Atelier d'Architecture Aquatique, France (For primary document see N91-23563 15-42)
Copyright Avail: NTIS HC/MF A13

N91-23569# OHB-System G.m.b.H., Bremen (Germany, F.R.). Space and Environmental Technology.
PAYLOAD RELATED CREW OPERATIONS: FROM PAST MISSIONS TO COLUMBUS
James R. Kass, Erich Schafhauser, and Carlo Viberti (European Space Agency. European Space Research and Technology Center, ESTEC, Noordwijk, Netherlands) *In* ESA, Space and Sea Dec. 1990 p 37-41 (For primary document see N91-23563 15-42)
Copyright Avail: NTIS HC/MF A13

N91-23573# Societe d'Architectures en Milieux Extremes, Paris (France).
EUROPEAN STAKES AND MEASURES PERMITTING THE MANAGEMENT OF GEOMETRIC DIMENSIONS [ENJEUX EUROPEENS ET MESURES PERMETTANT DE GERER LES DIMENSIONS GEOMETRIQUES]
M. Fabre *In* ESA, Space and Sea Dec. 1990 p 75-80 In FRENCH (For primary document see N91-23563 15-42)
Copyright Avail: NTIS HC/MF A13

N91-23574# Compagnie Maritime d'Expertises, Marseille (France). Diving and Safety Dept.
COMPARISONS BETWEEN UNDERWATER AND SPACE WORKING ENVIRONMENTS FOR ON BOARD ACTIVITIES OPTIMIZATION (COLUMBUS SPACE PROGRAMME)
Jean-Pierre Imbert and Carlo Viberti (European Space Agency. European Space Research and Technology Center, ESTEC, Noordwijk, Netherlands) *In* ESA, Space and Sea Dec. 1990 p 85-88 (For primary document see N91-23563 15-42)
Copyright Avail: NTIS HC/MF A13

N91-23575# European Space Agency. European Space Research and Technology Center, ESTEC, Noordwijk (Netherlands).
EVA SERVICING: THE HERMES CAPABILITY
A. Accensi, I. Skoog, and J. Chevallier (Avions Marcel Dassault-Breguet Aviation, Saint-Cloud, France) *In its* Space and Sea Dec. 1990 p 89-94 (For primary document see N91-23563 15-42)
Copyright Avail: NTIS HC/MF A13

N91-23576# Center for Industrial Research, Oslo (Norway).
MAN-MACHINE INTERACTIONS AND MULTIMEDIA APPLIED TO ROV OPERATIONS
Eivind Kjennerud *In* ESA, Space and Sea Dec. 1990 p 95-99 (For primary document see N91-23563 15-42)
Copyright Avail: NTIS HC/MF A13

N91-23577# Companhia Espacial Portuguesa Ltd., Lisbon.
THE BERLENGA UNDERWATER SURVEY PROJECT
Dinis Afonso Ribeiro *In* ESA, Space and Sea Dec. 1990 p 101-102 (For primary document see N91-23563 15-42)
Copyright Avail: NTIS HC/MF A13

N91-23579# Compagnie Maritime d'Expertises, Marseille (France).
NEUTRAL BUOYANCY AND MICROGRAVITY: EXTRAVEHICULAR ACTIVITIES WITH A HUMID WATER SUIT [SIMULATION DES ACTIVITES SPATIALES EXTRA VEHICULAIRES EN IMMERSION AVEC UN SCAPHANDRE HUMIDE]
C. Gortan, L. Decramer, and D. Hornet (Dassault Espace, Saint-Cloud, France) *In* ESA, Space and Sea Dec. 1990 p 107-112 In FRENCH (For primary document see N91-23563 15-42)
Copyright Avail: NTIS HC/MF A13

N91-23583# McDonnell-Douglas Space Systems Co., Houston, TX. Space Station Div.
EVA/ROBOTICS INTEGRATION FOR SPACE STATION FREEDOM
R. M. Machell, L. V. Ramon, and D. E. Anderson *In* ESA, Space and Sea Dec. 1990 p 145-149 (For primary document see N91-23563 15-42)
Copyright Avail: NTIS HC/MF A13

N91-23584# Deutsche Forschungsanstalt fuer Luft- und Raumfahrt, Oberpfaffenhofen (Germany, F.R.). Inst. for Flight Systems Dynamics.
MULTISENSORY TELEROBOTIC CONCEPTS FOR SPACE AND UNDERWATER APPLICATIONS
G. Hirzinger, J. Dietrich, and B. Brunner *In* ESA, Space and Sea Dec. 1990 p 151-161 (For primary document see N91-23563 15-42)
Copyright Avail: NTIS HC/MF A13

N91-23586# European Space Agency. European Space Research and Technology Center, ESTEC, Noordwijk (Netherlands).
HOW TO DESIGN EFFICIENT MMI FOR SPACE
Muriel Didier *In its* Space and Sea Dec. 1990 p 173-177 (For primary document see N91-23563 15-42)
Copyright Avail: NTIS HC/MF A13

N91-23589# Societe d'Etudes des Systemes d'Automation, Toulouse (France).
OBJECT ORIENTED PROGRAMMING IN MMI: A SOFTWARE TOOL FOR ANALYSIS AND PLANIFICATION OF A RADAR IMAGING MISSION
J. L. Wippler and J. P. Aguttes (Centre National d'Etudes Spatiales, Toulouse, France) *In* ESA, Space and Sea Dec. 1990 p 191-194 (For primary document see N91-23563 15-42)
Copyright Avail: NTIS HC/MF A13

N91-24052*# National Aeronautics and Space Administration. Ames Research Center, Moffett Field, CA.
PHYSICAL/CHEMICAL CLOSED-LOOP WATER-RECYCLING
Cal C. Herrmann (Bionetics Corp., Moffett Field, CA.) and Theodore Wydeven *In* NASA, Washington, Technology 2000, Volume 2 1991 p 95-105 (For primary document see N91-24041 15-99)
Avail: NTIS HC/MF A16 CSCL 06K

N91-24053*# National Aeronautics and Space Administration. John C. Stennis Space Center, Bay Saint Louis, MS.
NEW RESEARCH ON BIOREGENERATIVE AIR/WATER PURIFICATION SYSTEMS
Anne H. Johnson, R. D. Ellender, and Paul J. Watkins (University of Southern Mississippi, Hattiesburg.) *In* NASA, Washington, Technology 2000, Volume 2 1991 p 107-113 (For primary document see N91-24041 15-99)
Avail: NTIS HC/MF A16 CSCL 06K

N91-24059*# Jet Propulsion Lab., California Inst. of Tech., Pasadena.
OXYGEN PRODUCTION USING SOLID-STATE ZIRCONIA ELECTROLYTE TECHNOLOGY
Jerry W. Suitor and Douglas J. Clark *In* NASA, Washington,

Technology 2000, Volume 2 1991 p 155-160 (For primary document see N91-24041 15-99)
Avail: NTIS HC/MF A16 CSCL 06K

N91-24060*# National Aeronautics and Space Administration. John F. Kennedy Space Center, Cocoa Beach, FL.
MONITORING AND CONTROL TECHNOLOGIES FOR BIOREGENERATIVE LIFE SUPPORT SYSTEMS/CELSS
William M. Knott and John C. Sager *In* NASA, Washington, Technology 2000, Volume 2 1991 p 161-167 (For primary document see N91-24041 15-99)
Avail: NTIS HC/MF A16 CSCL 06K

55 SPACE BIOLOGY

Includes exobiology; planetary biology; and extraterrestrial life.

No abstracts in this category.

59 MATHEMATICAL AND COMPUTER SCIENCES (GENERAL)

No abstracts in this category.

60 COMPUTER OPERATIONS AND HARDWARE

Includes hardware for computer graphics, firmware, and data processing.

For components see *33 Electronics and Electrical Engineering.*

N91-23724*# National Aeronautics and Space Administration. Lyndon B. Johnson Space Center, Houston, TX.
PROGRAMMABLE REMAPPER FOR IMAGE PROCESSING Patent Application
Tim E. Fisher, inventor (to NASA), Richard D. Juday, inventor (to NASA), and Jeffrey B. Sampsell, inventor (to NASA) (Texas Instruments, Inc., Dallas.) 30 Mar. 1989 45 p
(NASA-Case-MSC-21350-1; NAS 1.71:MSC-21350-1; US-Patent-Appl-SN-331551) Avail: NTIS HC/MF A03 CSCL 09B

A video-rate coordinate remapper includes a memory for storing a plurality of transformations on look-up tables for remapping input images from one coordinate system to another. Such transformations are operator selectable. The remapper includes a collective processor by which certain input pixels of an input image are transformed to a portion of the output image in a many-to-one relationship. The remapper includes an interpolative processor by which the remaining input pixels of the input image are transformed to another portion of the output image in a one-to-many relationship. The invention includes certain specific transforms for creating output images useful for certain defects of visually impaired people. The invention also includes means for shifting input pixels and means for scrolling the output matrix. NASA

N91-23725# Deutsche Forschungsanstalt fuer Luft- und Raumfahrt, Brunswick (Germany, F.R.). Abt. Flugversuchstechnik.
THREE-DIMENSIONAL GRAPHICAL REPRESENTATION OF OBJECTS ACCORDING TO MOVEMENT DATA IN REALTIME
Klaus Alvermann 30 Oct. 1990 37 p In GERMAN; ENGLISH summary
(DLR-FB-90-51; ISSN-0939-2963; ETN-91-99071) Avail: NTIS HC/MF A03; DLR, Wissenschaftliches Berichtswesen, VB-PL-DO, Postfach 90 60 58, 5000 Cologne, Fed. Republic of Germany, HC 15.50 DM

A system capable of showing three dimensional images of flying objects is described. The flight data are received by real time simulation or by telemetry. The system is implemented on a personal computer and a transputer network, which allows real time representation, e.g., there are enough images per second to have a smooth movement. The basic concepts of three dimensional images are defined, the mathematical background is prepared, and both implementations are described. ESA

N91-23726# Grenoble-1 Univ. (France). Lab. Artemis.
AUTOMATIC FORMAL VERIFICATION OF VHDL DESCRIPTIONS: A FIRST PROTOTYPE
Ashraf Salem and Dominique Borrione Jun. 1990 15 p
(RR-823-I; ETN-91-99220) Avail: NTIS HC/MF A03

The principles of the formal verification of very large scale integration (VLSI) designs described in very high speed integrated circuit hardware description language (VHDL), in terms of a functional model, are presented. Structural, data flow and behavioral descriptions of circuits at the boolean level are translated into a functional form, which is then fed to the TACHE specialized prover. The proof system takes two VHDL architectures as input for the same entity (after syntactic analysis by commercially available software) with one considered as the specification and the other as the implementation, and automatically produces an equivalence proof between them. The method applies to combinational as well as sequential circuits. This prototype proof system, written in LeLisp, is the first fully automatic system available for a significant subset of VHDL. It is predicted to contribute to the acceptance of formal verification as valuable design verification tool. ESA

N91-23727# Laboratoire d'Automatique et d'Analyse des Systemes, Toulouse (France).
SATURATION AND VOTE FOR THE FAULT TOLERANCE IN DISTRIBUTED SYSTEMS Ph.D. Thesis - Toulouse Univ.
Mourad Allia 1990 158 p In FRENCH; ENGLISH summary
(LAAS-90390; ETN-91-99238) Avail: NTIS HC/MF A08

Saturation, a technique used to improve dependability of distributed systems is described. Saturation is a technique that enables improved tolerance of hardware faults in the context of a Local Area Network (LAN). It is based on increasing the redundancy of tasks by means of the use of the idle stations in order to increase both the number of tolerated faults and the efficiency by which dormant faults are revealed. Fault tolerance is obtained through majority voting on all messages issued from the different task copies. The design of a distributed scheduling and majority voting algorithm that enables the saturation technique to be implemented is described. The algorithm was formally specified using Estelle as formal description technique and validated by simulation using the Veda simulator. By evaluating the reliability of this technique through Markov modeling, it is shown that this technique provides an improvement in system dependability. The saturation principle, the functional definition of the distributed algorithm, the formal specification in Estelle, the validation with and without fault injection and the evaluation of dependability are discussed. ESA

N91-23728# Naval Postgraduate School, Monterey, CA.
EVALUATION OF FERROELECTRIC MATERIALS FOR MEMORY APPLICATIONS M.S. Thesis
Carl E. Josefson Jun. 1990 98 p
(AD-A232112) Avail: NTIS HC/MF A05 CSCL 12/6

Ferroelectric materials have wide application in areas such as piezoelectric transducers, pyroelectric detectors, and electro-optics. Now thin-film ferroelectric materials are being integrated with conventional semiconductor processes to produce memory devices. Memories based on this technology potentially offer nonvolatile data storage and extended read-write endurance in comparison with EEPROMs, without speed or power penalties.

These memories are also radiation hard. Considerable interest in ferroelectric memory exists in the Department of Defense (DOD) because of these characteristics. However, several problems remain unsolved and no memory devices have been produced as yet. The physical mechanisms (as they are understood) are discussed, the claims made for the technology are examined, and the potential roadblocks, such as cycle dependent fatigue, time dependent degradation of memory retention, and fabrication problems, are evaluated. GRA

N91-23729# Air Force Inst. of Tech., Wright-Patterson AFB, OH.
DATA TYPE COHERENCY IN HETEROGENEOUS SHARED MEMORY MULTIPROCESSORS M.S. Thesis
Michael W. Strevell Dec. 1990 141 p
(AD-A232114; AFIT/CI/CIA-90-032D) Avail: NTIS HC/MF A07 CSCL 12/6

A heterogeneous shared memory multiprocessor, which contains different types of specialized processors, may execute a complex problem faster than either a homogeneous multiprocessor or a heterogeneous network. However, since dissimilar processors often use different representations for primitive data types, the shared data must be transformed. Analytical performance models and queueing models predict the performance advantages are provided by hardware transformation units, caching of unshared data, and local memory. Conversely, caching of shared data and the location of the transformation units have a less significant effect on performance. The primary applications for these type of designs are in special purpose applications which require maximum performance and tight coupling between heterogeneous processors. The linking that must be done at compile time makes these designs less suited for general purpose applications and development work. GRA

N91-23730# Naval Postgraduate School, Monterey, CA.
DESIGNING A VIRTUAL-MEMORY IMPLEMENTATION USING THE MOTOROLA MC68010 16-BIT MICROPROCESSOR WITH MULTI-PROCESSOR CAPABILITY INTERFACED TO THE VMEbus M.S. Thesis
David M. Sendek Jun. 1990 74 p
(AD-A232554) Avail: NTIS HC/MF A04 CSCL 25/5

The primary purpose of this thesis is to explore and discuss the hardware design of a bus-oriented microprocessor system. A bus-oriented microprocessor system permits it to be expanded to a multi-processor system. Through the use of a bus controller and bus arbiter, as discussed in this thesis, the necessary logic is in place to control bus access by system users. Bus access may be initiated to share another sub-system's resource, such as memory. To accommodate memory sharing between two systems, a dual-port memory controller can be used to resolve memory access between the two systems. This thesis discusses the design of a MC68010 microprocessor system integrated on the VMEbus with dual-ported memory capability. Additional features of the MC68010 microprocessor system include memory-management and interrupt control. The memory-management features permit protected memory and virtual-memory to be implemented on the system, while an interrupt handler is used to assist the MC68010 microprocessor in exception processing. GRA

N91-24051*# Jet Propulsion Lab., California Inst. of Tech., Pasadena.
INTEGRATED VERTICAL BLOCH LINE (VBL) MEMORY
R. R. Katti, J. C. Wu, and H. L. Stadler *In* NASA, Washington, Technology 2000, Volume 2 1991 p 86-92 (For primary document see N91-24041 15-99)
Avail: NTIS HC/MF A16 CSCL 09B

61 COMPUTER PROGRAMMING AND SOFTWARE

Includes computer programs, routines, alogorithms, and specific applications, e.g., CAD/CAM.

N91-23731*# Houston Univ., Clear Lake, TX. Software Engineering Professional Education Center.
HYPERMEDIA 1990 STRUCTURED HYPERTEXT TUTORIAL
J. Scott Johnson (NTERGAID, Inc., Fairfield, CT.) 3 Dec. 1990 77 p
(Contract NCC9-16)
(NASA-CR-187921; NAS 1.26:187921) Copyright Avail: NTIS HC/MF A05 CSCL 09B

Hypermedia 1990 structured Hypertext tutorial is presented in the form of view-graphs. The following subject areas are covered: structured hypertext; analyzing hypertext documents for structure; designing structured hypertext documents; creating structured hypertext applications; structuring service and repair documents; maintaining structured hypertext documents; and structured hypertext conclusion. Author

N91-23732# Massachusetts Inst. of Tech., Cambridge. Artificial Intelligence Lab.
TRANSITION SPACE
Gary C. Borchardt Nov. 1990 42 p
(Contract N00014-85-K-0124)
(AD-A231404; AI-M-1238) Avail: NTIS HC/MF A03 CSCL 12/5

Informal causal descriptions of physical systems abound in sources such as encyclopedias, reports and user manuals. Yet these descriptions remain largely opaque to computer processing. A representational framework is proposed in which such descriptions are viewed as providing partial specifications of paths in a space of possible transitions, or transition space. In the framework, the task of comprehending informal causal descriptions emerges as one of completing the specifications of paths in transition space - filling causal gaps and relating accounts of activity varied by analogy and abstraction. Drawing on results from perceptual psychology, a specific representation for events is outlined, along with a set of operations for use in comprehending and answering questions regarding informal causal descriptions. The use of the representation and its operations is illustrated in the context of a simple description concerning rocket propulsion. GRA

N91-23733 Wisconsin Univ., Madison.
THE INTEGRATION OF REMOTE SENSING, GEOGRAPHIC INFORMATION SYSTEM, AND EXPERT SYSTEM TECHNOLOGIES FOR LANDCOVER CLASSIFICATION Ph.D. Thesis
Paul Victor Bolstad 1990 338 p
Avail: Univ. Microfilms Order No. DA9030781

Approaches to supervised, computer-aided landcover mapping were developed which incorporate satellite imagery and spatial data with remote sensing, geographic information system, and artificial intelligence techniques. These approaches were developed in response to observed deficiencies in current standard computer-aided classification methodologies, both in the time and level of expertise requirements for human image-analysts, and in classification accuracies. These approaches were directed at both the training and classification stages of supervised landcover mapping. The first approach facilitates the maintenance and application of general and specific knowledge in training set selection and refinement. The second approach involved the integration of thematic spatial and image data in landcover classification. Spatial data operators, image and thematic spatial data, and knowledge of the relationships between cover types and thematic data are combined using expert system techniques. Results from comparative tests of classification accuracies based on two study sites, two different operators, and two image dates indicate that the new approaches provide significantly higher

classification accuracies with less analyst input when compared to traditional techniques over a range of conditions.
Dissert. Abstr.

N91-23734 Georgia Inst. of Tech., Atlanta.
DATA TRANSFER OVER MULTIPLEXED LOGICAL DATA LINKS SHARING A SINGLE PHYSICAL CIRCUIT Ph.D. Thesis
Koo-Don Chung 1990 154 p
Avail: Univ. Microfilms Order No. DA9105428

The performance and the characteristics were examined of the data transfer over a single physical circuit which is shared by multiple, logical data links. In the sharing of the communication medium, a proper transmission control (or multiplexing) scheme must be utilized. In particular, cyclic transmission control schemes are considered in which, at most, one data unit (or frame) for each logical data link user can be transmitted in each transmission cycle. This type of transmission control was extensively studied during the last two decades. However, an exact analysis has not been derived except for some special cases. Dissert. Abstr.

N91-23735# Oak Ridge National Lab., TN.
MODELING SPEEDUP IN PARALLEL SPARSE MATRIX FACTORIZATION
L. S. Ostrouchov (Tennessee Univ., Knoxville.), M. T. Heath, and C. H. Romine Dec. 1990 28 p
(Contract DE-AC05-84OR-21400)
(DE91-010215; ORNL/TM-11786) Avail: NTIS HC/MF A03

This paper is an attempt to explain the observed performance of sparse matrix factorization algorithms on parallel computers. In particular, we examine whether the disappointing performance of these algorithms is due to insufficient parallelism in the problem or to the architectural characteristics of existing parallel computers. Through a series of theoretical models of increasing realism, we first determine upper and lower bounds on the speedup that can be expected in practice for this problem, and end with a parameterized model that is capable of reproducing the full range of behavior within these bounds, including the speedups actually observed in practice. This model suggests that the current limits on speedup in sparse factorization are due to poor communication performance of the present generation of parallel computer architectures rather than to a lack of parallelism in the problem.
DOE

N91-23736# Edgerton, Germeshausen and Grier, Inc., Idaho Falls, ID.
THE CERBERUS VER. 02 CODE: A PARALLEL SIX-EQUATION THERMAL-HYDRAULIC-SYSTEM SIMULATION CODE
H. Makowitz Jan. 1991 17 p Presented at the International Topical Meeting on Advances in Mathematics, Computation and Reactor Physics, Pittsburgh, 28 Apr. - 2 May 1991
(Contract DE-AC07-76ID-01570)
(DE91-010079; EGG-M-90365; CONF-910414-28) Avail: NTIS HC/MF A03

CERBERUS, a six-equation parallel thermal-hydraulic system simulation code, has been developed at the Idaho National Engineering Laboratory (INEL). The starting point of CERBERUS is the RELAP5/MOD2.5 system simulation code that has been developed for single, central processing unit (cpu), shared memory, Single Instruction Multiple Data (SIMD), computer architectures. The near-term development targets for CERBERUS are shared memory, Multiple Instruction Multiple Data (MIMD), four- to sixteen-cpu machines such as the CRAY X-MP/48 and Y-MP/832, which are respectively, four- and eight-cpu computers. The major features of the CERBERUS Ver. 02 code and the experiences with it on a CRAY Y-MP8/8-128 are summarized. DOE

N91-23737# California Univ., Berkeley. Lawrence Berkeley Lab.
CANONICAL VS. MICRO-CANONICAL SAMPLING METHODS IN A 2D ISING MODEL
J. Kepner Dec. 1990 38 p
(Contract DE-AC03-76SF-00098)
(DE91-010204; LBL-30056) Avail: NTIS HC/MF A03

Canonical and micro-canonical Monte Carlo algorithms were implemented on a 2D Ising model. Expressions for the internal energy, U, inverse temperature, Z, and specific heat, C, are given. These quantities were calculated over a range of temperature, lattice sizes, and time steps. Both algorithms accurately simulate the Ising model. To obtain greater than three decimal accuracy from the micro-canonical method requires that the more complicated expression for Z be used. The overall difference between the algorithms is small. The physics of the problem under study should be the deciding factor in determining which algorithm to use. DOE

N91-23738*# Illinois Univ., Urbana-Champaign. Coordinated Science Lab.
PERFORMANCE ANALYSIS OF GARBAGE COLLECTION AND DYNAMIC REORDERING IN A LISP SYSTEM Ph.D. Thesis
Rene Lim Llames May 1991 93 p
(Grants NAG1-613; NSF MIP-86-04893)
(NASA-CR-188205; NAS 1.26:188205; UILU-ENG-91-2230; CRHC-91-20) Avail: NTIS HC/MF A05 CSCL 09B

Generation based garbage collection and dynamic reordering of objects are two techniques for improving the efficiency of memory management in Lisp and similar dynamic language systems. An analysis of the effect of generation configuration is presented, focusing on the effect of a number of generations and generation capabilities. Analytic timing and survival models are used to represent garbage collection runtime and to derive structural results on its behavior. The survival model provides bounds on the age of objects surviving a garbage collection at a particular level. Empirical results show that execution time is most sensitive to the capacity of the youngest generation. A technique called scanning for transport statistics, for evaluating the effectiveness of reordering independent of main memory size, is presented. Author

N91-23739*# Illinois Univ., Urbana-Champaign. Coordinated Science Lab.
A USER-ORIENTED SYNTHETIC WORKLOAD GENERATOR
Wei-Lun Kao May 1991 49 p
(Grant NAG1-613)
(NASA-CR-188197; NAS 1.26:188197; UILU-ENG-91-2229; CRHC-91-19) Avail: NTIS HC/MF A03 CSCL 09B

A user oriented synthetic workload generator that simulates users' file access behavior based on real workload characterization is described. The model for this workload generator is user oriented and job specific, represents file I/O operations at the system call level, allows general distributions for the usage measures, and assumes independence in the file I/O operation stream. The workload generator consists of three parts which handle specification of distributions, creation of an initial file system, and selection and execution of file I/O operations. Experiments on SUN NFS are shown to demonstrate the usage of the workload generator. Author

N91-23740# Los Alamos National Lab., NM.
INFORMATION DYNAMICS OF SELF-PROGRAMMABLE MATTER
C. Knudsen, R. Feldberg, and S. Rasmussen 1990 24 p Presented at the Complex Dynamics and Biological Evolution Conference, Middlefart, Denmark, 6-10 Aug. 1990
(Contract W-7405-eng-36)
(DE91-009954; LA-UR-91-896; CONF-9008198-1) Avail: NTIS HC/MF A03

Using the simple observation that programs are identical to data, programs alter data, and thus, programs alter programs, the authors have constructed a self-programming system based on a parallel von Neumann architecture. This system has the same fundamental property as living systems have: the ability to evolve new properties. They demonstrate how this constructive dynamical system is able to develop complex cooperative structures with adaptive responses to external perturbations. The experiments with this system are discussed with special emphasis on the relation between information theoretical measures (entropy and mutual

information functions) and on the emergence of complex functional properties. Decay and scaling of long-range correlations are studied by calculation of mutual information functions. DOE

N91-23741# California Univ., Berkeley. Lawrence Berkeley Lab.
COMPUTER PROGRAMS FOR SIMULATION OF ELECTRODEPOSITION
K. G. Jordon and C. W. Tobias Dec. 1990 359 p
(Contract DE-AC03-76SF-00098)
(DE91-010203; LBL-29925) Avail: NTIS HC/MF A16

In this report, FORTRAN programs and subroutines useful for modelling moving boundaries in electrochemical systems are listed. These programs were used by Kenneth Guy Jordan to simulate moving boundaries during electrodeposition in presence of transport limited additives that acted either by blocking the electrode to electrodeposition, or dissolving the electrode instantaneously upon their arrival, lowering the current efficiency. The programs were also used to analyze the behavior of evolving surface profiles during periodic current reversal. DOE

N91-23742# Los Alamos National Lab., NM.
USE OF A GENETIC ALGORITHM TO ANALYZE ROBUST STABILITY PROBLEMS
T. M. Murdock, W. E. Schmitendorf, and S. Forrest 1990 17 p Presented at the 1991 American Control Conference, Boston, 26 Jun. 1991
(Contract W-7405-eng-36)
(DE91-005895; LA-UR-90-4168; CONF-910638-3) Avail: NTIS HC/MF A03

This note presents a genetic algorithm technique for testing the stability of a characteristic polynomial whose coefficients are functions of unknown but bounded parameters. This technique is fast and can handle a large number of parametric uncertainties. We also use this method to determine robust stability margins for uncertain polynomials. Several benchmark examples are included to illustrate the two uses of the algorithm. DOE

N91-23743# Argonne National Lab., IL.
TABLE-LOOKUP ALGORITHMS FOR ELEMENTARY FUNCTIONS AND THEIR ERROR ANALYSIS
Ping Tak Peter Tang 1991 7 p Presented at the 10th Institute of Electrical and Electronics Engineers (IEEE) Symposium on Computer Arithmetic, Grenoble, France, 26-28 Jun. 1991
(Contract W-31-109-eng-38)
(DE91-006047; CONF-9106103-1) Avail: NTIS HC/MF A02

Table-lookup algorithms for calculating elementary functions offer superior speed and accuracy when compared with more traditional algorithms. With careful design, we show that it is feasible to implement table-lookup algorithms in hardware. Furthermore, we present a uniform approach to carry out tight error analysis for such implementations. DOE

N91-23744# Lawrence Livermore National Lab., CA.
SCIENTIFIC VISUALIZATION SOFTWARE FOR YOUR PC: FREE AND AVAILABLE NOW
G. D. Greenly, Jr. Mar. 1991 19 p Presented at the 84th Annual Meeting and Exhibition of the Air and Waste Management Association (AWMA), Vancouver (Canada), 16-21 Jun. 1991
(Contract W-7405-eng-48)
(DE91-010156; UCRL-JC-106647; CONF-910659-11) Avail: NTIS HC/MF A03

Super computers provide todays scientist the compute power to easily handle very large numerical models. The National Center for Supercomputing Applications (NCSA), at the University of Illinois at Urbana-Champaign, has developed a suite of new public domain software for the visualization of scientific data on personal computers (PC). Hierarchical Data Format (HDF), a flexible file format, designed at NCSA for sharing 2-D graphical and floating point data arrays among different programs and machines, is the core capability of this free software. HDF allows the researcher to store raster images, their dimensions, color tables, annotations, and units of measure all in the same file. HDF output files can be viewed on a PC using this suite of software applications. This paper discusses the NCSA software, how it can be used with the Macintosh II family of computers, with their superior color graphics capability, and how the software can be obtained free of charge. Information regarding use of the software with other PCs and workstations is also presented. DOE

N91-23745# Argonne National Lab., IL.
VISUAL PRESENTATION AND COMPUTER ANIMATION
Hua Wang 1991 9 p Presented at the 7th International Conference on Advanced Science and Technology, Argonne, 30 Mar. 1991
(Contract W-31-109-eng-38)
(DE91-010599; ANL/CP-72651; CONF-9103133-2) Avail: NTIS HC/MF A02

This paper presents an assessment of the current computer graphics and video technologies as they applied to the fields of visual presentation and computer animation, including a discussion of inherent incompatibilities between computer graphics and video systems. The near-term technology trend is directed towards the integration of sound, video and computer graphics into a multimedia, desktop presentation system. With the forthcoming High-Definition Television (HDTV) standard, it can be predicted that computer graphics and video will eventually be integrated to a desktop video system. Recent advances in technology development to achieve these goals are described. DOE

N91-23746# Deutsche Forschungsanstalt fuer Luft- und Raumfahrt, Oberpfaffenhofen (Germany, F.R.). Abt. Prozessortechnik.
IMAGE DATA COMPRESSION IN JPEG STANDARD
Pavel Filip and Gerald Schlotzhauer Nov. 1990 35 p In GERMAN; ENGLISH summary
(DLR-FB-90-59; ISSN-0939-2963; ETN-91-99076) Avail: NTIS HC/MF A03; DLR, Wissenschaftliches Berichtswesen, VB-PL-DO, Postfach 90 60 58, 5000 Cologne, Fed. Republic of Germany, HC 15 DM

The influence of different parameters on the performance of the Joint Photographic Experts Group (JPEG) standard algorithm and its modifications are investigated. The rate distortion theory is evaluated for the JPEG standard process. The results are presented and discussed. ESA

N91-23747 Politecnico di Milano (Italy). Dipt. di Elettronica.
DESIGNING LOGIC CONTROLLERS WITH PETRI NETS
Luca Ferrarini and C. Maffezzoni 1990 20 p
(Rept-90-029; ETN-91-99083) Avail: Politecnico di Milano, Piazza Leonardo da Vinci 32, 20133 Milan, Italy

A conceptual and practical environment to design logic controllers which is based on a special version of Petri nets tailored to this aim is presented. One purpose is to provide control engineers not only with powerful graphic tools to manipulate designs quickly and simulation tools to check system performance in particular operative conditions but also with analytic tools to formally verify controller correctness. Most of the theoretical analysis carried out links algebraic theory of Petri nets with the fundamental concepts of net invariants and dead locks. An example from an electrical power plant field is thoroughly examined through all design stages. ESA

N91-23748 Politecnico di Milano (Italy). Dipt. di Elettronica.
AN INCREMENTAL APPROACH TO LOGIC CONTROLLERS DESIGN WITH PETRI NETS
Luca Ferrarini 1990 24 p
(Rept-90-030; ETN-91-99084) Avail: Politecnico di Milano, Piazza Leonardo da Vinci 32, 20133 Milan, Italy

A conceptual and practical methodology to design logic control systems with Petri nets is proposed. In particular, a special version of Petri nets, tailored to represent logic controllers and used to develop a prototype computer aided design/computer aided engineering environment is considered. This methodology is based on a number of theorems stated and proved, and consists of an incremental approach to the design. This means that the designer

can concentrate on simple control problems that can be solved using a few basic net structures. Then he is provided with particular types of connection to aggregate separate designs into a more complex structure. This one, in its turn, can be used as a component in other aggregations. Simple rules are provided that guarantee the preservation, after the merging of previous designs, of extremely important net properties, like boundedness, cyclicness and lifeness. To do so, it is sufficient to analyze an opportune graph based on the flow of information exchanged among tasks. ESA

N91-23749 Politecnico di Milano (Italy). Dipt. di Elettronica.
ON THE INITIALIZATION PROBLEM IN THE DESIGN OF STRUCTURALLY CONSTRAINED DIGITAL REGULATORS
Nicola Schiavoni and Arturo Locatelli 1990 19 p Sponsored in part by MURST and CNR
(Rept-90-039; ETN-91-99085) Avail: Politecnico di Milano, Piazza Leonardo da Vinci 32, 20133 Milan, Italy

It is well known that the design of regulators under stucture and/or complexity constraints cannot in general be performed by resorting to classical techniques, such as standard linear quadratic Gaussian optimal control or pole placement: as a rule, the result of the application of such techniques is in fact constituted by a centralized and high order regulator. On the contrary, parameter optimization methods are well suited to comply with a number of requirements concerning the information structure of the regulator and its implementation by means of low order and commercially available components. However, most of the numerical algorithms commonly utilized within the framework of the parameter optimization approach to the solution of the control problems, require the knowledge of a stabilizing regulator as a starting point. This is not a trivial question whenever robust zero error asymptotic regulation is called for in presence of nonvanishing exogeneous signals, as then the open loop control system cannot be asymptotically stable. Some solutions are presented to the problem of determining a least order stabilizing regulator subject to structural constraints such that robust zero error regulation is achieved in the presence of ramp type exogeneous signals. ESA

N91-23750 Politecnico di Milano (Italy). Dipt. di Elettronica.
TIMED HIGH-LEVEL NETS
Marco Trubian 1990 29 p
(Rept-90-050; ETN-91-99088) Avail: Politecnico di Milano, Piazza Leonardo da Vinci 32, 20133 Milan, Italy

The relationships between high level nets and timed Petri nets are investigated, extending previous results where a unifying Petri net based model for time representation was proposed. The representation of time in a Petri net extension called Environment/Relationship (ER) nets is recalled and its generality is assessed. The relationships of ER nets with the best known high level nets is investigated. In paticular, the overall equivalence of ER nets, colored Petri nets, and predicate/transition nets is shown, and the mechanism for time representation introduced in ER nets to both colored Petri nets and predicate/transition nets is extended. It is shown that these models cannot be simplified without significantly constraining the timing aspects that can be modeled. ESA

N91-23751 Politecnico di Milano (Italy). Dipt. di Elettronica.
REALIZATION OF A RANDOMIZED ALGORITHM FOR THE EXACT PERFECT MATCHING PROBLEM, WITH A NEW CONSTRUCTIVE PROCEDURE
Vincenzo Caglioti Nov. 1990 17 p
(Rept-90-056; ETN-91-99089) Avail: Politecnico di Milano, Piazza Leonardo da Vinci 32, 20133 Milan, Italy

Exact value matroid problems are introduced and the general aspect of a randomized algorithm for their solutions is presented. The perfect matching is recalled, and its relationship with the parity based problem is illustrated. A finite field algorithm for the determination of the existence of a perfect matching of a given value is examined. A fast constructive procedure for a perfect matching of a given value, given the knowledge of its existence, is illustrated. Both procedures are implemented. Some concluding remarks, in which some directions for further research are suggested are presented. ESA

N91-23752 Politecnico di Milano (Italy). Dipt. di Elettronica.
ON THE USE OF GENETIC ALGORITHMS TO SOLVE THE TIME-TABLE PROBLEM
Alberto Colorni, Marco Dorigo, and Vittorio Maniezzo Dec. 1990 25 p
(Rept-90-060; ETN-91-99090) Avail: Politecnico di Milano, Piazza Leonardo da Vinci 32, 20133 Milan, Italy

The results of research relative to the ascertainment of the possibilities offered by genetic algorithms (GA's) to solve the timetable problems are presented. This problem was chosen since it is very representative of a class (that of hard constrained problems, with reference to real world applications) which has not yet been extensively tackled using GA's and for which there are, therefore, no ultimate results regarding the effectiveness of GA's. The model and the outcomes of the utilization of the implemented system to the case of the generation of a school timetable are presented. ESA

N91-23753# Royal Signals and Radar Establishment, Malvern (England).
NODEN USER'S GUIDE AND INSTALLATION MANUAL
C. H. Pygott Nov. 1990 33 p
(RSRE-Memo-4438; BR115906; ETN-91-99118) Copyright Avail: NTIS HC/MF A03

This document is intended to provide the NODEN user with a guide to the facilities of the tools and an explanation of some of the error messages that may generated. The aim of the NODEN tool set is to show that an implementation meets its specification under all circumstances. The basic operation of the NODEN tool set and the detailed operation of the compiler, analyzer and comparison programs are described. The annexes of this memo provide a guide to the installation of the NODEN tools on Digital Equipment Corporation VAX machines (under VMS) and SUN 3 workstations. ESA

N91-23754# Norwegian Defence Research Establishment, Kjeller.
CESAR OPERATING SYSTEM
Svein-Erik Soegaard 17 Jan. 1991 93 p
(FFI-91/7002; ISSN-0802-2437; ETN-91-99122) Avail: NTIS HC/MF A05

The design and implementation of the CESAR Operating System (COS) is described. It can be divided into the following functional units: VRTX, which is a software component providing real time, multitasking operating system functions for embedded microprocessor functions; VEXT (VRTX Extensions) which adds a number of functions to a plain VRTX system; the Compute Control System (CCS) which keeps track of the MALU and TRAP programs and controls the computation of MALU; Data Control System (DCS), to manage the space in the different memories and to control transfers between them. An independent module called the CP monitor is also described. Data structures are detailed as well as more complex parts of the routines. Functional models are described using data flow diagrams with real time extensions. The layout of the data structures are shown using the C programming language. ESA

N91-23755# Grenoble-1 Univ. (France). Geometrie Algorithmique.
SEARCHING ALGORITHMS FOR THE REAL ROOTS OF A BEZIER FUNCTION [ALGORITHMES DE RECHERCHES DE ZEROS D'UNE FONCTION DE BEZIER]
Denis Marchepoil and Patrick Chenin Nov. 1990 81 p In FRENCH; ENGLISH summary
(RR-834-I-and-M; ETN-91-99234) Avail: NTIS HC/MF A05

Numerical analysis used to search for the real roots of polynomials in an interval is discussed. Finding efficiency and stable methods are particularly useful in Computer Aided Design (CAD) problems, image processing and image synthesis. An ordered set of roots is obtained in order to carry out ray tracing operations.

Algorithms which give roots included in the interval in ordered sets without hypothesis on the polynomial are proposed and compared. Bernstein basis and subdivision techniques as well as Newton iterations allow isolating intervals to be derived and provide good accuracy on the roots. ESA

N91-23756# Grenoble-1 Univ. (France). Lab. d'Informatique Fondamentale et d'Intelligence Artificielle.
SPECIFICATIONS FOR REUSABLE SOFTWARE COMPONENTS [SPECIFICATION DE COMPOSANTS LOGICIELS REUTILISABLES]
Didier Bert Oct. 1990 25 p In FRENCH; ENGLISH summary (RR-828-I-IMAG-116-LIFIA; ETN-91-99235) Avail: NTIS HC/MF A03

The specifications of Ada software components of sequential programs are considered in terms of their reusability potential. Such reusability will reduce software costs as well as making program writing and maintenance easier. Ways in which specifications can be connected to Ada component interfaces are shown. Several well defined relationships can exist between one specification and some interfaces. Application of such a mechanism in establishing a library of software components is discussed. ESA

N91-23757# Aerospatiale Aquitaine, Saint-Medard en Jalles (France).
ACLICO: A COMPUTER AIDED DESIGN SYSTEM FOR BONDED JOINTS [ACLICO: UN SYSTEME D'AIDE A LA CONCEPTION DES LIAISONS COLLEES]
Laborie 1991 16 p In FRENCH; ENGLISH summay (Rept-911-430-101; ETN-91-99273) Avail: NTIS HC/MF A03

The system is an expert system designed for the selection of adhesive bonding configurations of composites or other materials in space structures. It is shown that the increasing use of composite materials in space structures makes it necessary to acquire a perfect knowledge of adhesive bonding technique. Computer aided selection is required for the five thousand adhesives which are currently used. The joint type is to be classified, stress distribution is to be optimized, polymerization and the thermomechanical behavior of the joint are to be examined. The fabrication technology is investigated. The program architecture is described. A data base for adhesives was created. ESA

N91-23758# Aerospatiale Aquitaine, Saint-Medard en Jalles (France).
PRESENTATION OF A COMPUTER PROGRAM FOR ANALYSING RESULTS OF ONE SHOT DEVICE SENSITIVITY TESTS: APPLICATION TO THE CASE OF A ONE SHOT DEGENERATED SEQUENCE
C. Saubade 1991 7 p In FRENCH; ENGLISH summary (Rept-911-430-126; ETN-91-99298) Avail: NTIS HC/MF A02

The principle of the determination, using likelihood function, of the mean, standard deviation, and safety, and reliability thresholds confidence intervals is presented. A computer program using this principle is given, in which the integration of the likelihood function in the mu, sigma area is done using the Monte Carlo method. An example of application, analyzing a degenerated one shot sequence with a study of the influence of the number of devices tested on the confidence intervals, is reported. The proposed method can be used when the number of components tested is small. This avoids having a test sequence with impossible application when the number of tested components was previously limited. It also avoids doing complementary testing when the thresholds determined with the initial test sequence are consistent with the specifications of the tested component. ESA

N91-23759# Aeronautical Research Inst. of Sweden, Stockholm. Structures Dept.
A MOVING BOUNDARY ALGORITHM FOR THE SOLUTION OF CONTACT PROBLEMS IN LINEAR ELASTICITY. PART 1: BASIC THEORY AND MODEL EXAMPLES
Ulf Ringertz and Boerje Andersson Feb. 1991 35 p Sponsored by Defence Material Administration, Stockholm, Sweden (FFA-TN-1991-08-Pt-1; ETN-91-99342) Avail: NTIS HC/MF A03

A numerical method for the solution of contact problems in linear elasticity is presented. Three dimensional bodies in frictionless contact are studied. The general case where the contact surfaces are not known a priori is treated in detail. A moving boundary algorithm for solving this class of problems is proposed. The primary unknowns in the algorithm are the parameters describing the shape of the contact surfaces. Stress intensity functions K(i)(y) of different orders are defined. It is shown that the first intensity function satisfies K(i)(y) = 0 along the contact lines not a priori known. The solution to the contact problem is posed as a nonlinear least squares problem. Given an initial shape of the contact surface, the algorithm generates a sequence of strictly improving approximations in the sense that the integral K upper bound(2) lower bound(1)(y)dy is reduced in each iteration. The h-p version of the finite element method is used to extract the intensity functions K(1) with an error that decreases exponentially with respect to the number of degrees of freedom used. The basic theory is reviewed and an algorithm for the solution of the contact problem is defined. Model problems, for which analytical solutions exist, are solved to illustrate the accuracy and reliability of the proposed strategy. ESA

N91-23760# Naval Postgraduate School, Monterey, CA.
A METHOD FOR MACHINERY CONDITION MONITORING OF TRANSIENT PHENOMENA USING THE PSEUDO WIGNER-VILLE DISTRIBUTION M.S. Thesis
Graham W. Rossano Jun. 1990 171 p
(AD-A232014) Avail: NTIS HC/MF A08 CSCL 12/5

The Pseudo Wigner-Ville Distribution is a time frequency representation of an input time signal and is ideally suited for portraying nonstationary signals. A working computer program is presented and the effect of preprocessing and postprocessing data manipulations is shown. The program has been developed for analyzing data for use in machinery condition monitoring diagnostics and will be a valuable asset for analyzing transient machinery. A practical example showing pump speed variations with time is also presented. Due to the fact that the Pseudo Wigner-Ville Distribution can be used to analyze both steady state and transient operations, along with the fact that it can be calculated on virtually any computer, this method could revolutionize machinery condition monitoring and diagnostics. GRA

N91-23761# Naval Postgraduate School, Monterey, CA.
INTEGRATION OF THE EXECUTION SUPPORT SYSTEM FOR THE COMPUTER-AIDED PROTOTYPING SYSTEM (CAPS) M.S. Thesis
Frank V. Palazzo Sep. 1990 138 p
(AD-A232015) Avail: NTIS HC/MF A07 CSCL 12/5

With the rapidly falling cost of computer hardware continuing to drive software expenses up, attention has turned to ways to effect savings. One approach that shows particular promise is rapid prototyping. Rapid prototyping is the use of executable models of a software system to firm up the requirements before a significant amount of time and effort has been invested in implementation. The computer aided prototyping system (CAPS) is a rapid prototyping system that automates many of the manual processes of prototyping, allowing for quicker prototype construction and even further cost savings. Within CAPS, there exists an execution support system. The purpose of the execution support system is to take the description of a prototype written in the prototyping language PSDL and to convert this into an executable prototype which can then be shown to the user. Previous research resulted in separate implementations for the components of the execution support system, but these components were never integrated into a functioning system. It is the development of this tool which is the subject of this thesis. GRA

N91-23762# Army Construction Engineering Research Lab., Champaign, IL.
MAINTENANCE RESOURCE PREDICTION MODEL (MRPM) USER'S MANUAL Final Report

Edgar S. Neely, Robert D. Neathammer, and James R. Stirn Jan. 1991 280 p
(AD-A232019; CERL-ADP-P-91/12) Avail: NTIS HC/MF A13 CSCL 12/7

The Maintenance Resource Prediction Model (MRPM) is a computer system designed to assist in planning and programming maintenance resources, based on the anticipated resource requirements of actual installation facilities, for prediction periods of 1 to 10 years. This User's Manual provide improved maintenance resource data for use in facility planning, design, and maintenance activities. This manual explains this application of the MRPM computer system to installation facility data base information, to help Army planners in preparing DD Form 1391 documentation, designers in life cycle cost component selection, and maintainers in resource planning. This data base and computer system is presently used by U.S. Army Corps of Engineers (USACE) designers at district and installation levels, and by resource programmers at the USACE Headquarters, Army Major Command, and installation levels. These products may also prove useful to other Government agencies and to the private sector. GRA

N91-23763# Carnegie-Mellon Univ., Pittsburgh, PA. Dept. of Computer Science.
TOWARDS REAL-TIME GOMS Technical Report, 1989 - 1991
Bonnie E. John, Alonso H. Vera, and Allen Newell 28 Dec. 1990 91 p
(Contract N00014-89-J-1975)
(AD-A232028; CMU-CS-90-195) Avail: NTIS HC/MF A05 CSCL 23/2

We present an analysis of an expert performing a highly interactive computer task. The analysis uses GOMS (goals-operators-methods-selection rules) models are implemented within an unified theory of cognition called Soar. Two models are presented, one with function-level operators which perform high level functions in the domain, and one with keystroke level operators which describe hand movements. For a segment of behavior in which the expert accomplished about 30 functions in about 30 seconds, the function level model predicted the observed behavior well, while the keystroke level model predicted only about half of the observed hand movements. These results, including the discrepancy between the models, are discussed. GRA

N91-23764# Naval Underwater Systems Center, New London, CT.
MAPPING AN ADAPTABLE EIGENSTRUCTURE TECHNIQUE ONTO THE TOPOLOGIX HYPERCUBE Final Report, Oct. 1989 - Oct. 1990
M. H. Leonhardt 30 Dec. 1990 50 p
(AD-A232032; NUSC-TR-8807) Avail: NTIS HC/MF A03 CSCL 17/1

Eigenstructure methods provide accuracy and stability to signal processing applications, such as the enhanced minimum variance distortionless response (EMVDR) algorithm. Eigenstructure methods, however, require the high throughput that is only available in parallel computer systems. One such system is the hypercube multiprocessor, which, along with high throughput, also provides distributed memory and efficient networking. This report describes the implementation of an eigenstructure method on the Topologix hypercube architecture that will produce the eigenstructure required in the EMVDR beamformer. GRA

N91-23765# Maryland Univ., College Park. Inst. for Advanced Computer Studies.
GENERALIZED DISJUNCTIVE WELL-FOUNDED SEMANTICS FOR LOGIC PROGRAMS
Chitta Baral, Jorge Lobo, and Jack Minker Mar. 1990 51 p
(Contract DAAG29-85-K-0177)
(AD-A232064; UMIACS-TR-90-39; CS-TR-2436; ARO-22648.19-EL) Avail: NTIS HC/MF A04 CSCL 12/5

Generalized disjunction well-founded semantics (GDWFS) are extensions of the generalized well-founded semantics (GWFS) of Baral, Lobo, and Minker to disjunctive logic programs. We describe fixpoint, model theoretic and procedural semantics and show their equivalence. The fixpoint semantics are similar to the fixpoint semantics of GWFS, except that they iterate over states (a pair of sets; one a set of disjunctions of atoms and the other a pair of conjunctions of atoms), rather than partial interpretations. The model theoretic semantics are based on a dynamic stratification of the program. The procedural semantics are based on SLIS refutations, +trees, and SLISNF trees. We compare the GDWFS with the strong well-founded semantics of Ross and the stationary model semantics of Przymusinski. GRA

N91-23766# Texas Univ., Austin. Computer and Vision Research Center.
SYNERGETIC MULTISENSOR FUSION Final Report, 1 Jul. 1987 - 30 Sep. 1990
J. K. Aggarwal 30 Nov. 1990 60 p
(Contract DAAL03-87-K-0089)
(AD-A232089; ARO-25021.5-PH) Avail: NTIS HC/MF A04 CSCL 12/6

Synergetic multisensor fusion is the process of integrating information obtained from different sensing modalities in order to extract additional information that cannot be obtained by separately processing the signals from the different sensors. The development of a computer vision system using synergetic multisensor fusion is a complex task which encompasses: sensor modeling; environment modeling; determining the analytic models used to interrelate the different sensing mechanisms; determining the models used to interrelate the sensed parameters of imaged objects (such as thermal emissivity, visual reflectance, and radar reflectance); and devising algorithms to exploit the derived models. We have developed powerful and robust algorithms for computer vision tasks based upon synergetic multisensor fusion. Our approach is suitable for applications such as object recognition, tracking, surveillance, and autonomous guidance. GRA

N91-23767# Naval Ocean Systems Center, San Diego, CA.
MATHEMATICAL TECHNIQUES FOR THE PERFORMANCE ORIENTED DESIGN (POD) TOOL Final Report
A. Sterrett Aug. 1990 18 p
(AD-A232092; NOSC/TD-1936) Avail: NTIS HC/MF A03 CSCL 12/7

Mathematical techniques for the NOSC Performance Oriented Design (POD) tool are described using Response Time, Throughput, and Utilization techniques for computer systems. Queueing Networks that represent computer systems are analyzed using Mean Value Analysis (MVA) with performance measures such as Response Time, Throughput, Queue Length, and Device Utilization. Simple algorithms for solving basic queueing systems are included such as the POD algorithms for a Mixed Model System. Modeling Synchronization in ADA based systems is explained using the Rendezvous Analysis technique. The document concludes with an explanation of the basic Distributed Mean Value Analysis (DMVA) algorithm. GRA

N91-23768# Naval Ocean Systems Center, San Diego, CA.
AN EVENT-ACTIVATION RECORD APPROACH TO SIMULATION MODELING IN Ada: USER'S GUIDE Final Report, Nov. 1989 - Jul. 1990
H. Mumm and R. Ollerton Dec. 1990 76 p
(AD-A232093; NOSC/TD-1944) Avail: NTIS HC/MF A05 CSCL 12/5

This document explains how to install and use the Event-Activation Record Approach to Simulation Modeling in Ada (EARS) simulation libraries, Version 1.0, that were developed by the Naval Ocean Systems Center, Code 854. This software was designed to compile and execute using the Vax Ada compiler. EARS is a discrete-event simulation system that uses an event-activation record approach. It has capabilities similar to those provided by SIMSCRIPT. All simulations that can be modeled in SIMSCRIPT can be modeled using EARS. From a set of use-defined event types, EARS automatically generates much of the source code for many Ada packages and subprograms that are needed for simulation development. This allows a user to quickly start writing an EARS simulation. The user tailors the simulation to a

particular application by adding Ada source code to the generated program units and by writing additional ones. This document contains an actual simulation example using EARS. The document also includes the Ada source code for linked list packages, statistical packages, and hash table packages, as well as examples of how they are used. GRA

N91-23769# Army Construction Engineering Research Lab., Champaign, IL.
LIFE CYCLE MANAGEMENT AUTOMATION PROGRAMMER'S MANUAL Final Report
Don Kermath, Yung Pan, Jui-tine Lee, and Gonzalo Perez Jan. 1991 107 p
(AD-A232247; CERL-ADP-P-91/05) Avail: NTIS HC/MF A06
CSCL 12/5

Life Cycle Management Automation is a microcomputer system to manage the Army Reserve Inventory of Facilities through their entire life cycle, from acquisition to disposal. The system is made up of several computer programs, all of which access a common database. The programs included in the LCM are: UNIT, FACILITY, AMSA, BACKLOG, ProjDoc, MINOR, and REAL ESTATE. The programs UNIT, FACILITY, and AMSA collect the basic data used by BACKLOG ProjDoc, MINOR, and REAL ESTATE. BACKLOG generates the 5-year plan. ProjDoc produces Military Construction, Army Reserve (MCAR) project documentation in minutes. MINOR manages the Minor Construction Program. REAL ESTATE manages the Real Estate Program. LCM requires no special computer training. It runs on IBM-compatible computers with at least 420 K memory, PC DOS 3.1 or higher, 1 floppy disk drive, 8 to 15 megabytes of free hard disk space for the program, and a printer with a 12-character per inch capability. GRA

N91-23770# Massachusetts Inst. of Tech., Cambridge. Lab. for Computer Science.
AN IN-DEPTH ANALYSIS OF CONCURRENT B-TREE ALGORITHMS
Paul Wang Feb. 1991 133 p
(Contract N00014-89-J-1988)
(AD-A232287; MIT/LCS/TR-496) Avail: NTIS HC/MF A07
CSCL 12/6

The B tree is a data structure designed to efficiently support dictionary operations for a variety of applications. In order to increases throughput, many algorithms have been proposed to maintain concurrent operations on B-tree. Replicating objects in memory can play a large role in concurrent B-tree performance, especially for large distributed and parallel systems. Because most replication schemes are coherent, readers generally cannot operate concurrently with a writer. This thesis presents two new concurrent B-trees algorithms. The first is an link algorithm that uses coherent replication; it is based on the Lehman-Yao algorithm which performs better than any other proposed concurrent B-tree algorithm. The second is a similar algorithm that uses multi-version memory, a new semantics for replicated memory. Multi-version memory weakens the semantics of coherent replication by allowing readers to read old versions of data. As a result, readers can perform in parallel with a writer. Also, implementations of multi-version memory require less communication and synchronization. Simulation experiments comparing a variety of concurrent B-tree algorithms show that the first algorithm has better performance than previously proposed algorithms and that the second algorithm has significantly better performance and scaling properties than any algorithms using coherent replicated memory. GRA

N91-23771# Naval Postgraduate School, Monterey, CA.
SOFTWARE TESTING FOR EVOLUTIONARY ITERATIVE RAPID PROTOTYPING M.S. Thesis
Edward V. Davis, Jr. Dec. 1990 294 p
(AD-A232555) Avail: NTIS HC/MF A13 CSCL 12/5

Rapid prototyping is emerging as a promising software development paradigm. It provides a systematic and automatable means of developing a software system under circumstances where initial requirements are not well known or where requirements change frequently during development. To provide high software quality assurance requires sufficient software testing. The unique nature of evolutionary iterative prototyping is not well-suited for classical testing methodologies, therefore the need exists for a testing methodology tailored for this prototyping paradigm. This thesis surveys current prototyping and testing practices to provide a foundation for developing a software testing methodology for prototyping. The thesis then describes a testing methodology for rapid prototyping, Spiral Testing, and the Test Goal Tracking System (TGTS), a requirements-based testing tool developed for use with the Computer Aided Prototyping System (CAPS). TGTS provides the first in an anticipated family of testing tools to support the CAPS environment. This thesis shows key prototyping characteristics impinging on testing, the value of Spiral Testing and the feasibility and qualities of complementary testing tools to support evolutionary iterative rapid prototyping. GRA

N91-23772# Maryland Univ. Baltimore County, Catonsville. Dept. of Mathematics and Statistics.
DUALITY METHODS FOR INFINITE DIMENSIONAL OPTIMIZATION PROBLEMS Final Technical Report, 15 Jun. 1988 - 14 Nov. 1990
Marc Teboulle 14 Nov. 1990 9 p
(Grant AF-AFOSR-0218-88; AF Proj. 2304)
(AD-A232605; AFOSR-91-0147TR) Avail: NTIS HC/MF A02
CSCL 12/4

This report includes a description of the progress and accomplishments achieved on our research program for the period June 15, 1988 to November 14, 1990. Preliminary reports and publications of the research results are listed in section 6. Papers presented at conferences and seminars are listed in Section 7. Our proposal is in the general area of Nonlinear Optimization and the research issues focus on duality methods for infinite dimensional optimization problems and applications. The proposal covered the following areas: (1) duality methods in convex optimization; (2) applications of generalized entropy; (3) semi-infinite programming; (4) nonsmooth optimization; and (5) stochastic programming. GRA

N91-23773# Pennsylvania Univ., Philadelphia. School of Engineering and Applied Science.
SOFTWARE REVERSE ENGINEERING Final Report, 1 Mar. 1988 - 30 Apr. 1990
Noah S. Prywes 11 Jan. 1991 5 p
(Grant AF-AFOSR-0116-88; AF Proj. 2304)
(AD-A232644; AFOSR-91-0149TR) Avail: NTIS HC/MF A01
CSCL 12/5

The goal of this research was to develop algorithms to translate procedural languages (such as FORTRAN and PASCAL) to non procedural languages. Such algorithms are desirable for a number of reasons. Their semantics are easier to understand since they resemble a set of specification for action rather than the traditional flow of control. They are easier to modify since statements are not dependent on one another. It is easier to verify their correctness since standard theorem provers used for program verifications require programs to be in non procedural form. Lately, with the increase need in DoD of translating old programs to new languages such as Ada (reverse software engineering). It is advantageous to reduce old program to a common non-procedural form before translation from that form to the target language. This will permit the recapture of the program's semantics, make desired modification, check its correctness, etc. Accomplishments are (1) algorithms to translate FORTRAN programs to MODEL (FORTRAN represents a procedural language and MODEL represents a non-procedural declarative language); and (2) an algorithm to translate concurrent FORTRAN programs to MODEL. GRA

N91-23774# Massachusetts Inst. of Tech., Cambridge. Lab. for Computer Science.
ARE WAIT-FREE ALGORITHMS FAST
Hagit Attiya, Nancy Lynch, and Nir Shavit Mar. 1991 43 p
(Contract N00014-89-J-1988)
(AD-A232829; MIT/LCS/TM-442) Avail: NTIS HC/MF A03
CSCL 12/6

The time complexity of wait-free algorithms in normal executions, where no failures occur and processes operate at approximately the same speed, is considered. A lower bound of log n on the time complexity of any wait-free algorithm that achieves approximate agreement among n processes is proved. In contrast, there exists a non-wait-free algorithm that solves this problem in constant time. This implies an omega (log n) time separation between the wait-free and non-wait-free computation models. On the positive side, an O(log n) time wait-free approximate agreement algorithm is presented; the complexity of this algorithm is within a small constant of the lower bound. GRA

N91-23775# Yale Univ., New Haven, CT. Dept. of Computer Science.
A FAST ALGORITHM FOR THE EVALUATION OF TRIGONOMETRIC SERIES
A. Dutt Jan. 1991 26 p
(Grant NSF DMS-90-12751)
(AD-A232848; YALEU/DCS/RR-841) Avail: NTIS HC/MF A03 CSCL 12/1

Fourier techniques have been a popular analytical tool in the study of physics and engineering for more than two centuries. A reason for the usefulness of such techniques is that certain trigonometric functions are eigenfunctions of the differentiation operator and can be effectively used to model solutions of differential equations which arise in the fields mentioned above. With the arrival of digital computers, it became theoretically possible to calculate the Fourier series and Fourier transform of a function numerically. This was unrealistic in practice however owing to the prohibitive complexity of even modesty sized problems. A major break-through in overcoming this difficulty was the development of the Fast Fourier Transform (FFT) algorithm in the 1960s which established Fourier analysis as a useful and practical numerical tool. This paper presents an algorithm for the rapid evaluation of expressions of a certain form. GRA

N91-23834# Tel-Aviv Univ. (Israel). School of Physics and Astronomy.
AN ON-LINE COMPUTERIZED SYSTEM FOR BLOOD-FLOW MEASUREMENTS Abstract Only
D. Eylon, V. Benary, S. Akselrod, T. Kaspi, and Y. Heilbronn (Belinson Medical Center, Petah Tiqva, Israel) *In its* Bulletin of the Israel Physical Society, Volume 33, 1987. Annual Meeting 1987: Program and Abstracts 1987 p 20 (For primary document see N91-23832 15-70)
Avail: NTIS HC/MF A08

N91-24043*# National Aeronautics and Space Administration. Lyndon B. Johnson Space Center, Houston, TX.
CLIPS: A TOOL FOR THE DEVELOPMENT AND DELIVERY OF EXPERT SYSTEMS
Gary Riley *In* NASA, Washington, Technology 2000, Volume 2 1991 p 11-15 (For primary document see N91-24041 15-99)
Avail: NTIS HC/MF A16 CSCL 09B

N91-24045*# Jet Propulsion Lab., California Inst. of Tech., Pasadena.
ELECTRONIC NEUROPROCESSORS
Anil Thakoor *In* NASA, Washington, Technology 2000, Volume 2 1991 p 26-33 (For primary document see N91-24041 15-99)
Avail: NTIS HC/MF A16 CSCL 09B

N91-24048*# National Aeronautics and Space Administration. Goddard Space Flight Center, Greenbelt, MD.
TRANSPORTABLE APPLICATIONS ENVIRONMENT (TAE) PLUS: A NASA USER INTERFACE DEVELOPMENT AND MANAGEMENT SYSTEM
Martha R. Szczur *In* NASA, Washington, Technology 2000, Volume 2 1991 p 56-66 (For primary document see N91-24041 15-99)
Avail: NTIS HC/MF A16 CSCL 09B

N91-24049*# National Aeronautics and Space Administration. Lyndon B. Johnson Space Center, Houston, TX.
APPLICATIONS OF FUZZY LOGIC TO CONTROL AND DECISION MAKING
Robert N. Lea and Yashvant Jani (LinCom Corp., Houston, TX.) *In* NASA, Washington, Technology 2000, Volume 2 1991 p 67-75 (For primary document see N91-24041 15-99)
Avail: NTIS HC/MF A16 CSCL 09B

N91-24050*# National Aeronautics and Space Administration. Lyndon B. Johnson Space Center, Houston, TX.
GENETIC ALGORITHMS
Lui Wang and Steven E. Bayer (Mitre Corp., Houston, TX.) *In* NASA, Washington, Technology 2000, Volume 2 1991 p 76-85 (For primary document see N91-24041 15-99)
Avail: NTIS HC/MF A16 CSCL 09B

62 COMPUTER SYSTEMS

Includes computer networks and special application computer systems.

N91-23776*# Santa Clara Univ., CA. Dept. of Computer Engineering.
THE TURBOLAN PROJECT. PHASE 1: PROTOCOL CHOICES FOR HIGH SPEED LOCAL AREA NETWORKS. PHASE 2: TURBOLAN INTELLIGENT NETWORK ADAPTER CARD, (TINAC) ARCHITECTURE Final Report
Hasan S. AlKhatib 10 May 1991 137 p Sponsored in cooperation with Furukawa Electric Co.
(Contract NCC2-621)
(NASA-CR-188175; NAS 1.26:188175) Avail: NTIS HC/MF A07 CSCL 09B

The hardware and the software architecture of the TurboLAN Intelligent Network Adapter Card (TINAC) are described. A high level as well as detailed treatment of the workings of various components of the TINAC are presented. The TINAC is divided into the following four major functional units: (1) the network access unit (NAU); (2) the buffer management unit; (3) the host interface unit; and (4) the node processor unit. Author

N91-23777 Cornell Univ., Ithaca, NY.
DYNAMIC LOAD BALANCING ON HIGHLY PARALLEL MULTICOMPUTER SYSTEMS Ph.D. Thesis
Marc Hubert Willebeek-LeMair 1990 174 p
Avail: Univ. Microfilms Order No. DA9106210

Multiprocessor systems were shown to be very efficient at solving problems that can be partitioned into tasks with uniform computation and communication patterns. However, there exists a large class of non-uniform problems with uneven and unpredictable computation and communication requirements. Several non-uniform problems are investigated in order to characterize the nature of such problems. Dynamic load balancing (DLB) schemes can significantly improve the performance of multicomputer systems when solving non-uniform problems. A general DLB model is developed. This model is organized as a four phase process: (1) processor load evaluation; (2) load balancing profitability determination; (3) task migration strategy; and (4) task selection strategy. The focus herein is on distributed DLB approaches which can be scaled to support highly parallel systems. Dissert. Abstr.

N91-23778# Grenoble-1 Univ. (France). Groupe Calcul Parallele.
A METHOD FOR HANDLING COMPLEX MARKOV MODELS OF PARALLEL SYSTEMS
Brigitte Plateau and Karim Atif 25 Sep. 1990 31 p Sponsored by French Program Communication, Cooperation and Concurrency
(RR-826-I; ETN-91-99223) Avail: NTIS HC/MF A03

The performance of parallel systems is studied. The performance models of such systems are often complex to describe

and hard to solve. The method presented uses a modular representation of the system as a network of state transition graphs. The state space explosion is handled by a decomposition technique. The dynamic behavior of the algorithm is analyzed under Markovian assumptions. The rate transition matrix of the chain is automatically derived using tensor algebra operators, under a format which involves very limited storage cost. ESA

N91-23779# Grenoble-1 Univ. (France). Lab. de Genie Informatique.
STATISTICAL PROCESS ALLOCATION IN A PARALLEL PROCESSING ARCHITECTURE
E.-G. Talbi and Traian Muntean Nov. 1990 27 p In FRENCH Sponsored by EEC
(RR-833-I; ETN-91-99224) Avail: NTIS HC/MF A03

A comparative analysis of various research projects in the area of process allocation in parallel processing architectures is presented. A classification scheme for statistical allocation algorithms is presented. The scheme is based on the models used in problem formulation and the strategies used to solve them. The limitations of process allocation techniques are outlined taking into consideration that the performance of a program run on a parallel processing architecture depends for a large part on task allocation effectiveness. ESA

N91-23780# Grenoble-1 Univ. (France). Lab. d'Informatique Fondamentale et d'Intelligence Artificielle.
GENERALIZATION OF THE FP2 PARALLEL LANGUAGE BY MEANS OF NET THEORY [UNE GENERALISATION DES PRESENTATIONS FP2 A L'AIDE DE LA THEORIE DES RESEAUX]
Z. Belmesk (Universite des Sciences et de la Technologie Houari Boumediene, Algiers, Algeria) and P. Schnoebelen Nov. 1990 42 p In FRENCH; ENGLISH summary
(RR-832-I-IMAG-99-LIFIA; ETN-91-99237) Avail: NTIS HC/MF A03

Ways in which a net theoretical implementation of the FP2 parallel language is used to overcome problems with combinatorial explosions in the implementation of parallelism are described. FP2 programs are implemented via special interpreted Petri nets (called RFP2 nets). Formal results on correctness and efficiency are given. General motions of net theory are reviewed. The basic concepts underlying FP2 language are outlined. The RFP2 networks are defined. The main properties of these networks are defined along with the transformation corrections necessary. A practical evaluation of the networks is carried out by means of a complexity analysis. ESA

N91-23781# David Taylor Research Center, Bethesda, MD. Computer and Information Services Dept.
COMPUTER CENTER REFERENCE MANUAL, VOLUME 2 Final Report
David V. Sommer and Sharon E. Good 30 Sep. 1990 487 p
(AD-A232370; DTRC/CISD-90/02) Avail: NTIS HC/MF A21 CSCL 12/7

The Computer Center in the Computer and Information Services Department of the David Taylor Research Center has installed an integrated supercomputer network. This manual provides an introduction to the network. Some information has been distilled from many individual documents and augmented to reflect usage at DTRC. Control statement examples and descriptions of hardware and software are included, as is information on moving files among the CDC CYBER 860 (with the Mass Storage System), the DEC VAXcluster, the secure DEC VAX, and the CRAY X-MP, creating and executing batch jobs, and using the interactive systems. Volume 1 describes the CRAY X-MP, the Mass Storage System, and the DEC VAXes. Volume 2 describes the CDC CYBER 860. GRA

63 CYBERNETICS

Includes feedback and control theory, artificial intelligence, robotics and expert systems.

For related information see also *54 Man/System Technology and Life Support.*

N91-23782# Naval Ocean Research and Development Activity, Bay Saint Louis, MS.
PORTABLE INTELLIGENT DIAGNOSTIC AIDS
C. R. Holland Mar. 1990 8 p
(AD-A230883; NORDA-PR-90-020-252) Avail: NTIS HC/MF A02 CSCL 23/2

Effective troubleshooting of complex equipment typically requires large amounts of equipment, documentation, and training. The considerable burden this imposes on military resources must be reduced. Computer technology offers the possibility of untiring intelligent machines which compute and advise. As Diagnostic Tutors and Expert Aids, such machines should be effective force multipliers with minimal logistics impact. What constitutes a good diagnostic aid; the state of present achievability; the avoidance of development failure; and some future potentials are explored. Key characteristics of successful Expert Systems developments are beginning to come into focus. While the ideal diagnostic aid may rarely be achieved; practical, supportable aids are beginning to emerge from various laboratories. While intelligent machines are still infants, even kids can do amazing things. GRA

N91-23783*# National Aeronautics and Space Administration. Pasadena Office, CA.
OBSTACLE AVOIDANCE FOR REDUNDANT ROBOTS USING CONFIGURATION CONTROL Patent Application
Homayoun Seraji, inventor (to NASA) (Jet Propulsion Lab., California Inst. of Tech., Pasadena.) et al 11 Sep. 1990 26 p (Contract NAS7-918)
(NASA-Case-NPO-17852-1-CU; NAS 1.71:NPO-17852-1-CU; US-Patent-Appl-SN-615668) Avail: NTIS HC/MF A03 CSCL 09B

A redundant robot control scheme is provided for avoiding obstacles in a workspace during the motion of an end effector along a preselected trajectory by stopping motion of the critical point on the robot closest to the obstacle when the distance between is reduced to a predetermined sphere of influence surrounding the obstacle. Algorithms are provided for conveniently determining the critical point and critical distance. NASA

N91-23784# Los Alamos National Lab., NM.
APPLICATIONS OF NEURAL NETWORKS TO PROCESS CONTROL AND MODELING
C. W. Barnes, S. K. Brown, G. W. Flake, R. D. Jones, M. K. ORourke, and Y. C. Lee 1991 7 p Presented at the International Conference on Artificial Neural Networks, Helsinki (Finland), 24-28 Jun. 1991
(Contract W-7405-eng-36)
(DE91-007389; LA-UR-91-126; CONF-9106117-1) Avail: NTIS HC/MF A02

Modeling and control of physical processes are universal parts of modern life, from control of chemical plants to riding a bicycle. Often, an effective model of the process is not known so that traditional control theory is of little use. If a process can be represented by a set of a data which captures it behavior over a range of parameter settings, a neural net can inductively model the process and form the basis of an optimization procedure. A neural network architecture is presented which is particularly effective in process modeling and control. Its effectiveness is discussed in several application areas as well as some of the non-ideal characteristics present in real control problems which effect the form and style of the network architecture and learning algorithm. DOE

N91-23785# Oak Ridge National Lab., TN.
ANALYSIS OF NEUTRON NOISE SPECTRA USING NEURAL NETWORKS
K. Korsah and R. E. Uhrig 1991 7 p Presented at the

Annual Meeting of the American Nuclear Society (ANS), Orlando, 2-6 Jun. 1991
(Contract DE-AC05-84OR-21400)
(DE91-007676; CONF-910603-7) Avail: NTIS HC/MF A02

Neural network architectures based on the back-propagation paradigm have been developed to recognize the features, and detect resonance shifts in, power spectral density (PSD) data. The goal is to advance the state of the art in the application of noise analysis techniques to monitor nuclear reactor internals. The initial objectives have been to use PSD data, acquired over a period of about 2 years by PSDREC (power spectral density recognition system), to develop neural networks that are able to differentiate between normal neutron power spectral density data and anomalous spectral data, and detect significant shifts in the positions of spectral resonances while reducing the effect of small shifts. Neural network systems referred to in this paper as spectral feature detectors (SFDs) and integral network filters have been developed to meet these objectives. The performance of the SFDs is the subject of this paper. DOE

N91-23786*# Purdue Univ., West Lafayette, IN. Lab. for Applications of Remote Sensing.
STATISTICAL METHODS AND NEURAL NETWORK APPROACHES FOR CLASSIFICATION OF DATA FROM MULTIPLE SOURCES
Jon Atli Benediktsson and Philip H. Swain Dec. 1990 254 p
(Grant NAGw-925)
(NASA-CR-188207; NAS 1.26:188207; TR-EE-90-64) Avail: NTIS HC/MF A12 CSCL 09B

Statistical methods for classification of data from multiple data sources are investigated and compared to neural network models. A problem with using conventional multivariate statistical approaches for classification of data of multiple types is in general that a multivariate distribution cannot be assumed for the classes in the data sources. Another common problem with statistical classification methods is that the data sources are not equally reliable. This means that the data sources need to be weighted according to their reliability but most statistical classification methods do not have a mechanism for this. This research focuses on statistical methods which can overcome these problems: a method of statistical multisource analysis and consensus theory. Reliability measures for weighting the data sources in these methods are suggested and investigated. Secondly, this research focuses on neural network models. The neural networks are distribution free since no prior knowledge of the statistical distribution of the data is needed. This is an obvious advantage over most statistical classification methods. The neural networks also automatically take care of the problem involving how much weight each data source should have. On the other hand, their training process is iterative and can take a very long time. Methods to speed up the training procedure are introduced and investigated. Experimental results of classification using both neural network models and statistical methods are given, and the approaches are compared based on these results. Author

N91-23787*# Pennsylvania Univ., Philadelphia. Dept. of Computer and Information Science.
IMAGE WAVELET DECOMPOSITION AND APPLICATIONS
N. Treil, S. Mallat, and R. Bajcsy Apr. 1989 43 p Sponsored in part by DEC Corp., IBM Corp., and LORD Corp.
(Contracts NAG5-1045; F49620-85-K-0018; DAAG29-84-K-0061; DAAG29-84-9-0027; N00014-85-K-0807; NSF MCS-81-19196; NSF IRI-84-10413; NSF INT-85-14199; NSF DMC-85-17315; NIH-NS-10939-11)
(NASA-CR-188217; NAS 1.26:188217; MS-CIS-89-22; Grasp-Lab-177) Avail: NTIS HC/MF A03 CSCL 09B

The general problem of computer vision has been investigated for more that 20 years and is still one of the most challenging fields in artificial intelligence. Indeed, taking a look at the human visual system can give us an idea of the complexity of any solution to the problem of visual recognition. This general task can be decomposed into a whole hierarchy of problems ranging from pixel processing to high level segmentation and complex objects recognition. Contrasting an image at different representations provides useful information such as edges. An example of low level signal and image processing using the theory of wavelets is introduced which provides the basis for multiresolution representation. Like the human brain, we use a multiorientation process which detects features independently in different orientation sectors. So, images of the same orientation but of different resolutions are contrasted to gather information about an image. An interesting image representation using energy zero crossings is developed. This representation is shown to be experimentally complete and leads to some higher level applications such as edge and corner finding, which in turn provides two basic steps to image segmentation. The possibilities of feedback between different levels of processing are also discussed. Author

N91-23788# Technical Research Centre of Finland, Espoo. Electronics Lab.
A MODEL-BASED APPROACH TO HIGH-LEVEL ROBOT CONTROL WITH VISUAL GUIDANCE Ph.D. Thesis - Oulu Univ.
Tapio Heikkila Nov. 1990 136 p Sponsored by Academy of Finland; Tauno Toenning Foundation; Walter Ahlstroem Foundation; and Finnish Technology Foundation
(VTT-Publ-71; ISBN-951-38-3942-7; ISSN-0358-5069; ETN-91-99123) Copyright Avail: NTIS HC/MF A07, Government Printing Office, P.O. Box 516, SF-00101 Helsinki, Finland, HC 98 Finnish marks

The intelligent robot control problem is approached by viewing the computational elements and their relations in the higher levels of control hierarchy. A conceptual model with a four level hierarchical framework is proposed, consisting of three generic activities: planning, executing, and monitoring. The time dependency aspects are considered by including time constraints in plans and by describing the time relations between planning, executing, and monitoring with a specific metacontrol mechanism. Further examination is made in three case studies: a human operator support; a knowledge based task and action planner; and visual guidance for a general approach motion. For individual titles, see N91-23789 through N91-23796.

N91-23789# Technical Research Centre of Finland, Oulu.
A SOLUTION FOR THE MAN/MACHINE-INTERFACE IN ROBOTICS: A HIGH LEVEL CONTROL LANGUAGE WITH ENHANCED INTERACTION EQUIPMENT
Tapio Heikkila, Timo Torvikoski, and Arne Halme (Helsinki Univ. of Technology, Espoo, Finland) *In its* A Model-Based Approach to High-Level Robot Control with Visual Guidance Nov. 1990 5 p Repr. from Analysis, Design and Evaluation of Man-Machine Systems (Oxford, England, Pergamon Press), 1988 p 221-225 Presented at 3d IFAC/IFIP/IEA/IFORS Conference, Oulu, Finland, 14-16 Jun. 1988 (For primary document see N91-23788 15-63) Copyright Avail: NTIS HC/MF A07, Government Printing Office, P.O. Box 516, SF-00101 Helsinki, Finland, HC 98 Finnish marks

Man machine interface which allows an ultraflexible programming and control of a robotic cell is introduced. The interface consists of a high level task oriented control language and a set of interaction equipment. The system is designed for use in applications where the robot has to be taught or reprogrammed frequently because of individual jobs, small series or a radically changing working environment. When needed, the system allows the operator to work interactively on line with the robot work cell so that tasks can be processed immediately after communicating them through the interfacing system. The main principles used in task allocation between the human and the robot and in language structuring are explained and the man machine communication facility is described. Alternatives to represent the world model information are discussed. An example is given to illustrate the main principles. ESA

N91-23790# Helsinki Univ. of Technology, Espoo (Finland). Lab. of Automation Technology.
AN INTERACTIVE ROBOT CONTROL SYSTEM
Arne Halme, Tapio Heikkila, and Timo Torvikoski (Oulu Univ.,

Finland) *In* Technical Research Centre of Finland, A Model-Based Approach to High-Level Robot Control with Visual Guidance Nov. 1990 8 p Repr. from International Journal of Robotics and Automation, v. 2, no. 3, 1987 p 155-162 (For primary document see N91-23788 15-63)
Copyright Avail: NTIS HC/MF A07, Government Printing Office, P.O. Box 516, SF-00101 Helsinki, Finland, HC 98 Finnish marks

The concept of interactive control was addressed. An interactive robot control scheme, based on environment modeling and task oriented programming, was developed. A human operator makes a model of the robot's working environment using his own visual understanding by analyzing necessary features of the real environment. Tasks defined by the operator and executed by the robot are commanded by using very high level task oriented commands which utilize data in the environment model. Programming is done at the real working environment online and the operator can supervize the robot immediately during task execution if necessary. A microcomputer based control system and microrobot based workcell is described with some programming examples. ESA

N91-23791# Technical Research Centre of Finland, Oulu. Electronics Lab.
MONITORING AN ASSEMBLY TASK BY PERCEPTION REQUESTS
Tapio Heikkila, Paavo Karkkainen, and Sakari Pieska *In its* A Model-Based Approach to High-Level Robot Control with Visual Guidance Nov. 1990 9 p Repr. from Proceedings of the 1987 Workshop (Los Altos, CA, Morgan Kaufmann Publishers, Inc.), 1987 p 381-389 Presented at 1987 Workshop, Saint Charles, IL, 5-7 Oct. 1987 (For primary document see N91-23788 15-63)
Copyright Avail: NTIS HC/MF A07, Government Printing Office, P.O. Box 516, SF-00101 Helsinki, Finland, HC 98 Finnish marks

Reliability and flexibility are general requirements demanded from modern robotic asembly systems. As demands for accuracy are increasing within new application areas, needs for sensory feedback to adapt to arising uncertain and erroneous situations are clear. Problems on providing an assembly robot with a real time control system and sensory enhancements are addressed and solutions relying on knowledge based techniques are presented with experimental examples from a pilot assembly system. The system is for electronic assembly tasks. ESA

N91-23792# Technical Research Centre of Finland, Oulu. Electronics Lab.
INTELLIGENT PLANNING IN CONTROLLING ELECTRONICS ASSEMBLY
Tapio Heikkila, Sakari Pieska, and Paavo Karkkainen *In its* A Model-Based Approach to High-Level Robot Control with Visual Guidance Nov. 1990 4 p Repr. from International Workshop on Artificial Intelligence for Industrial Applications (IEEE Computer Society Press), 1988 p 347-350 Presented at International Workshop on Artificial Intelligence for Industrial Applications, Hitachi, Japan, 25-27 May 1988 (For primary document see N91-23788 15-63)
Copyright Avail: NTIS HC/MF A07, Government Printing Office, P.O. Box 516, SF-00101 Helsinki, Finland, HC 98 Finnish marks

As the application areas of modern robotic systems become wider, requirements related to both robotic equipment and control methodology issues are getting harder. Demands for reliability and flexibility together with high accuracies imply use of proper planning and programming methods for the system to be able to use effectively versatile facilities. The need for sensory feedback in assembly tasks to cope with several uncertain and erroneous situations is clear because of the accumulation of the errors. A control system assisting the effective usage of assembly equipment including a sensory subsystem in a precision assembly unit is described. With knowledge based solutions the information for controlling and monitoring the assembly tasks is generated in advance as an assembly plan, in which the use of sensor modules and other assembly equipment is included. Some experimental results are discussed. The system is for electronics assembly tasks. ESA

N91-23793# Technical Research Centre of Finland, Oulu.
PLANNING OF VISUAL FEEDBACK WITH ROBOT-SENSOR CO-OPERATION
Tapio Heikkila, Toshio Matsushita, and Tomomasa Sato (Tsukuba Univ., Japan) *In its* A Model-Based Approach to High-Level Robot Control With Visual Guidance Nov. 1990 6 p Repr. from International Workshop on Intelligent Robots and Systems (IEEE), 1988 p 763-768 Presented at International Workshop on Intelligent Robots and Systems, Tokyo, Japan, 31 Oct. - 2 Nov. 1988 Sponsored by Technology Development Centre of Finland (For primary document see N91-23788 15-63)
Copyright Avail: NTIS HC/MF A07, Government Printing Office, P.O. Box 516, SF-00101 Helsinki, Finland, HC 98 Finnish marks

The properties of manipulation tasks and varying environments demand careful planning of the sensor feedbacked task execution. Alternatives for visual feedback strategies are worked out. A planning method, where attention is paid on analyzing the assembly states of the target objects by the information maintained in a geometric model, is presented. As a result, vision feedback scheme with proper sensing conditions and assisting motions for the sensing, is produced. This method is for the insertion phase of assembly type tasks. ESA

N91-23794# Technical Research Centre of Finland, Oulu.
ROBOT-SENSOR CO-OPERATION PLANNING FOR VISUAL GUIDANCE
Tapio Heikkila, Toshio Matsushita, and Tomomasa Sato (Tsukuba Univ., Japan) *In its* A Model-Based Approach to High-Level Robot Control with Visual Guidance Nov. 1990 8 p Repr. from Proceedings of the 6th Scandinavian Conference on Image Analysis (Oulu, Finland), 1989 p 860-867 Presented at 6th Scandinavian Conference on Image Analysis, Oulu, Finland, 19-22 Jun. 1989 Sponsored by Technology Development Centre of Finland (For primary document see N91-23788 15-63)
Copyright Avail: NTIS HC/MF A07, Government Printing Office, P.O. Box 516, SF-00101 Helsinki, Finland, HC 98 Finnish marks

A planning method for visually guided manipulation tasks is described. The planning is based on geometric modeling of the manipulated objects and the robot system. The main planning functions are feature selection for the vision sensor and definition of assisting motions for the robot. The system is for the insertion phase of assembly type tasks. ESA

N91-23795# Technical Research Centre of Finland, Oulu. Electronics Lab.
A LINE BASED OBJECT LOCALIZING METHOD FOR ROBOT VISION
Tapio Heikkila, Toshio Matsushita, and Tomomasa Sato (Tsukuba Univ., Japan) *In its* A Model-Based Approach to High-level Robot Control with Visual Guidance Nov. 1990 10 p Repr. from SICE Robotics Meeting (Tokyo, Japan), RS-88-9-11, 1988 p 21-30 Presented at SICE Robotics Meeting, Tokyo, Japan, 5 Dec. 1988 (For primary document see N91-23788 15-63)
Copyright Avail: NTIS HC/MF A07, Government Printing Office, P.O. Box 516, SF-00101 Helsinki, Finland, HC 98 Finnish marks

An object localizing method, in which three dimensional lines are utilized as basic comparable features is presented. As measured data, points from three dimensional lines, acquired by a vision sensor are used, and this data is compared to the corresponding geometric edge model of the localized object. As preliminary fitting criteria the distance of the measured points to the three dimensional line of the edge is used. To avoid nonlinearities, this is divided into distances to two perpendicular planes intersecting with the line. The solution, i.e., the object location with the six degrees of freedom translation and rotation parameters, is derived by applying Newton's iterative method. ESA

N91-23796# Technical Research Centre of Finland, Oulu. Electronics Lab.
OBJECT POSE ESTIMATION BASED ON ONE-DEGREE-OF-FREEDOM SENSOR
Tapio Heikkila *In its* A Model-Based Approach to High-Level

Robot Control with Visual Guidance Nov. 1990 8 p Repr. from International Workshop on Intelligent Robots and Systems 1990 (IEEE), v. 2, 1990 p 903-910 Presented at International Workshop on Intelligent Robots and Systems '90, Tsuchiura, Japan, 3-6 Jul. 1990 Sponsored by Academy of Finland (For primary document see N91-23788 15-63)
Copyright Avail: NTIS HC/MF A07, Government Printing Office, P.O. Box 516, SF-00101 Helsinki, Finland, HC 98 Finnish marks

An object localizing method for visual motion guidance which determines the six degrees of freedom geometric relation between two objects is described. It is based on utilizing a combination of a simple fiber optic proximiy sensor and robot motions. The basic principle is to estimate the six translational and orientational parameters between two objects with Newton's method. Experimental tests show, that the method is well applicable for correcting robot motions from gripping errors. ESA

N91-23797# Naval Air Development Center, Warminster, PA. Air Vehicle and Crew Systems Technology Dept.
WORST-CASE DESIGN OF OPTIMAL CONTROLLERS OVER A FINITE HORIZON Final Report, Sep. - Dec. 1990
M. B. Subrahmanyam Jan. 1991 36 p
(AD-A232353; NADC-91005-60) Avail: NTIS HC/MF A03
CSCL 12/4

A worst-case optimal control problem is posed and solved making use of a minimax formulation. The emphasis is on the synthesis of optimal controllers whereas the usual H(infinity) methods give conditions for the synthesis of suboptimal ones. The solution for the nonzero initial condition case is expressed as a state feedback controller. Two dynamic Riccati equations need to be solved to synthesize the optimal controller in this case. Also formulas giving the variation in performance in terms of parameter variations are derived. GRA

N91-23798# International Business Machines Corp., San Jose, CA.
CONFERENCE ON THEORETICAL ASPECTS OF REASONING ABOUT KNOWLEDGE Final Report, 4 Mar. - 3 Dec. 1990
Moshe Y. Vardi 3 Dec. 1990 4 p Conference held in Pacific Grove, CA, 4-7 Mar. 1990
(Contract F49620-90-C-0020)
(AD-A232657; AFOSR-91-0125TR) Avail: NTIS HC/MF A01
CSCL 12/9

The Third Conference on Theoretical Aspects of Reasoning about Knowledge was held at the Asilomar Conference Center in Pacific Grove. Seventy-nine papers, covering aspects of reasoning about knowledge in artificial intelligence, computer science, economics, and philosophy, were submitted in response to a call for papers. The program committee considered all the papers carefully; at least three and usually four committee members read each paper. In the end, nineteen papers were selected based on their contribution, novelty, interest to an interdisciplinary audience, and relevance to the scope of the conference. In addition to the contributed papers, the program included tutorial sessions and an invited talk, intended to provide an overview of several tropics. The proceedings of the conference were published by Morgan Kaufmann Publishers. GRA

N91-23799# Naval Postgraduate School, Monterey, CA.
USER INTERFACE TO AN ICAI SYSTEM THAT TEACHES DISCRETE MATH M.S. Thesis
Roy K. Calcote and Richard A. Howard Jun. 1990 367 p
(AD-A232693) Avail: NTIS HC/MF A16 CSCL 12/5

The main thrust of this thesis is the design of a usable Intelligent Computer Aided Instruction (ICAI) user interface that does not use a natural language processor and runs on a personal computer. Discrete mathematics is the knowledge domain for this project and the Discrete Math Tutor (DMT) is the name of the tutoring system. The DMT will allow the average student to benefit from a tutoring system now and not have to wait until the artificial intelligence researchers solve the natural language interface problem. GRA

N91-23800# California Univ., Los Angeles.
PROCESSING PROBLEMS IN THE IRUS QUERIES: AN EMPIRICAL VERIFICATION OF PROBLEM COVERAGE IN THE NATURAL LANGUAGE SOURCEBOOK Research Report, 1 Feb. - 30 Aug. 1990
Patricia Mutch Aug. 1990 28 p
(Contract N00014-86-K-0395; NR Proj. RR0-4206)
(AD-A232780) Avail: NTIS HC/MF A03 CSCL 05/7

The Natural Language Sourcebook (Read, Dyer, Baker, Mutch, Butler, Quilici, and Reeves, 1990), a database of processing problems an intelligent computer system might have with natural language, was developed as part of the Artificial Intelligence Measurement System (AIMS). One important use of the Sourcebook is as a means for evaluating intelligent computer systems with regard to their ability to handle specific processing problems. An empirical verification is provided for the problem coverage in the Natural Language Sourcebook by referencing output from one intelligent computer system, IRUS (Bates, Stallard, and Moser, 1985), to the Sourcebook exemplars. GRA

N91-23801# University of Southern California, Los Angeles. Dept. of Mathematics.
APPROXIMATION METHODS FOR THE IDENTIFICATION AND CONTROL OF DISTRIBUTED PARAMETER SYSTEMS WITH APPLICATIONS TO FLEXIBLE STRUCTURES Final Report, 1 Oct. 1987 - 31 Oct. 1990
I. G. Rosen 15 Jan. 1991 14 p
(Grant AF-AFOSR-0356-87; AF Proj. 2304)
(AD-A232805; AFOSR-91-0155TR) Avail: NTIS HC/MF A03
CSCL 12/4

A brief overview and summary of results obtained in the development, analysis, and testing of approximation theory and techniques for the identification and control of distributed parameter systems is provided. The research carried out under this grant can be classified into seven sub-headings. These include: (1) the identification of nonlinear distributed parameter systems, (2) the identification and control of thermoelastic systems, (3) the identification and control of degenerate distributed parameter systems, (4) discrete-time linear quadratic control of distributed parameter systems, (5) optimal LQG control of discrete time parabolic systems, (6) optimal fixed finite order compensators for infinite dimensional systems, and (7) convergence of Galerkin approximations to operator Riccati equations. Our results in each of these areas is described separately and in turn. GRA

N91-23802# Carnegie-Mellon Univ., Pittsburgh, PA. Robotics Inst.
CLASSIFICATION USING MULTI-LAYERED PERCEPTRONS
Selwyn Piramuthu, Michael J. Shaw, and James A. Gentry Dec. 1990 48 p
(AD-A232810; CMU-RI-TR-90-29) Avail: NTIS HC/MF A03
CSCL 12/3

There has been an increasing interest in the applicability of neural networks in disparate domains. The use of multi-layered perceptrons, a type of neural network topology, for financial classification problems, with promising results is described. Back-propagation, which is the learning algorithm most often used in multi-layered perceptrons, however, is inherently an inefficient search procedure. Improved procedures are presented which have much better convergence properties. Using several financial classification applications as examples, the efficacy of using multi-layered perceptrons with improved learning algorithms is shown. The modified learning algorithms have better performance, in terms of classification/prediction accuracies, than the methods previously used in the literature, such as probit analysis and similarity-based learning techniques. GRA

N91-23803# Carnegie-Mellon Univ., Pittsburgh, PA. Robotics Inst.
A DISTRIBUTED PROBLEM-SOLVING APPROACH TO RULE INDUCTION: LEARNING IN DISTRIBUTED ARTIFICIAL INTELLIGENCE SYSTEMS

Michael J. Shaw and Riyaz Sikora Nov. 1990 34 p
(AD-A232822; CMU-RI-TR-90-28) Avail: NTIS HC/MF A03
CSCL 12/9

One of the interesting characteristics of multi-agent problem solving in distributed artificial intelligence (DAI) systems is that the agents are able to learn from each other, thereby, facilitating the problem solving process and enhancing the quality of the solution generated. This paper aims at studying the multi-agent learning mechanism involved in a specific group learning situation: the induction of concepts from training examples. Based on the mechanism, a distributed problem solving approach to inductive learning, referred to as DLS, is developed and analyzed. This approach not only provides a method for solving the inductive learning problem in a distributed fashion, it also helps shed light on the essential elements contributing to multi-agent learning in DAI systems. An empirical study is used to evaluate the efficacy of DLS for rule induction as well as its performance patterns in relation to various group parameters. The ensuing analysis helps form a model for characterizing multi-agent learning. GRA

N91-24042*# National Aeronautics and Space Administration. Lyndon B. Johnson Space Center, Houston, TX.
INTELLIGENT COMPUTER-AIDED TRAINING AND TUTORING
R. Bowen Loftin (Houston Univ., TX.) and Robert T. Savely *In* NASA, Washington, Technology 2000, Volume 2 1991 p 3-10 (For primary document see N91-24041 15-99)
Avail: NTIS HC/MF A16 CSCL 09B

N91-24046*# Jet Propulsion Lab., California Inst. of Tech., Pasadena.
INTELLIGENT VISION SYSTEM FOR AUTONOMOUS VEHICLE OPERATIONS
Marija S. Scholl *In* NASA, Washington, Technology 2000, Volume 2 1991 p 34-43 (For primary document see N91-24041 15-99)
Avail: NTIS HC/MF A16 CSCL 09B

N91-24047*# National Aeronautics and Space Administration. Lyndon B. Johnson Space Center, Houston, TX.
SOFTWARE REENGINEERING
Ernest M. Fridge, III *In* NASA, Washington, Technology 2000, Volume 2 1991 p 47-55 (For primary document see N91-24041 15-99)
Avail: NTIS HC/MF A16 CSCL 09B

64 NUMERICAL ANALYSIS

Includes iteration, difference equations, and numerical approximation.

N91-23804# Israel Aircraft Industries Ltd., Ben-Gurion Airport.
A SIMPLE SOLUTION TO THE SINGULAR LINEAR MINIMUM-VARIANCE ESTIMATION PROBLEM
U. Shaked and E. Soroka (Tel-Aviv Univ., Israel) Apr. 1987 12 p Revised
(IAITIC-87-1002-Rev; ITN-88-85001) Avail: NTIS HC/MF A03

A simple expression is obtained for the transfer function matrix of the minimum-variance estimator for the states of a linear stationary continuous-time right invertible system whose output is measured perfectly. Using the s-domain approach it is shown that the optimal estimator first finds the driving noise input that achieves, when applied on the minimum-phase image model of the system, an output spectrum which is identical to the measurement spectrum. This input is then applied on a state-space representation of the minimum-phase image to produce the optimal estimate. ISA

N91-23805# Oak Ridge National Lab., TN.
PARALLELIZING THE SPECTRAL TRANSFORM METHOD, PART 1
P. H. Worley and J. B. Drake Mar. 1991 29 p
(Contract DE-AC05-84OR-21400)
(DE91-010453; ORNL/TM-11747-Pt-1) Avail: NTIS HC/MF A03

The spectral transform method is a standard numerical technique used to solve partial differential equations on the sphere in global climate modeling. In particular, it is used in CCM1 and CCM2, the Community Climate Models developed at the National Center for Atmospheric Research. Initial experiences are described in parallelizing a program that uses the spectral transform method to solve the nonlinear shallow water equations on the sphere, showing that an efficient implementation is possible on the Intel iPSC/860. The use of PICL, a portable instrumented communication library, and ParaGraph, a performance visualization tool, in tuning the implementation is also described. The Legendre transform and the Fourier transform comprise the computational kernel of the spectral transform method. A case study is made of parallelizing the Legendre transform. For many problem sizes and numbers of processors, the spectral transform method can be parallelized efficiently by parallelizing only the Legendre transform. A subsequent paper will discuss parallelizing the Fourier transform as well. DOE

N91-23806# Purdue Univ., West Lafayette, IN. School of Electrical Engineering.
A SURVEY OF DECISION TREE CLASSIFIER METHODOLOGY
S. Rasoul Safavian and David Landgrebe Sep. 1990 46 p
(Grant NSF ECS-85-07405)
(NASA-CR-188208; NAS 1.26:188208; TR-EE-90-54) Avail: NTIS HC/MF A03

Decision Tree Classifiers (DTC's) are used successfully in many diverse areas such as radar signal classification, character recognition, remote sensing, medical diagnosis, expert systems, and speech recognition. Perhaps, the most important feature of DTC's is their capability to break down a complex decision-making process into a collection of simpler decisions, thus providing a solution which is often easier to interpret. A survey of current methods is presented for DTC designs and the various existing issue. After considering potential advantages of DTC's over single stage classifiers, subjects of tree structure design, feature selection at each internal node, and decision and search strategies are discussed. Author

N91-23807# Von Karman Inst. for Fluid Dynamics, Rhode-Saint-Genese (Belgium).
TWO DIMENSIONAL OPTIMIZATION OF SMOOTHING PROPERTIES OF MULTISTAGE SCHEMES APPLIED TO HYPERBOLIC EQUATIONS
L. A. Catalano and H. Deconinck Jul. 1990 77 p
(Contract AERO-0003-C)
(VKI-TN-173; ETN-91-99113) Avail: NTIS HC/MF A05

A numerical technique for optimizing the smoothing properties of multistage explicit time integration schemes for a general spatial discretization of the two dimensional advection equation is presented. The optimized schemes were implemented as smoothers in a multigrid code and their efficiency is compared with the classical Runge-Kutta schemes and, when possible, with the forward Euler scheme. They are applied as many times as the number of stages of the optimized one. The multigrid code was tested for different first and second order (MUSCL) upwind finite volume space discretization operators, using a FAS or a saw tooth cycle. ESA

N91-23808# Grenoble-1 Univ. (France). Lab. de Modelisation et Calcul.
Q-SPLINES
Rekha Kulkarni (Indian Inst. of Tech., Bombay.) and Pierre-Jean Laurent Oct. 1990 32 p Presented at the Seminar of Computational Geometry, Grenoble, France, 16 Mar. 1990
(RR-830-M; ETN-91-99231) Avail: NTIS HC/MF A03

The minimization of an integral (limits a and b) (x''(t))(exp 2)(q(t))(exp -1) dt where q is a piecewise polynomial function is considered. The case in which q is a continuous and piecewise linear on the subdivision is studied. The values q sub i = q(t sub i) act as shape parameters. The solution is a C(exp 2) quartic spline which suprisingly has all the advantages of a cubic spline. ESA

N91-23809# Grenoble-1 Univ. (France). Lab. de Modelisation et Calcul.
NILPOTENT NORMAL FORM VIA CARLEMAN LINEARIZATION (FOR SYSTEMS OF ORDINARY DIFFERENTIAL EQUATIONS)
Jean Della-Dora and Guoting Chen (Strasbourg Univ., France) Feb. 1991 25 p
(RR-838-M; ETN-91-99232) Avail: NTIS HC/MF A03

The normal form problem for a nonlinear derivation whose linear part is nilpotent is studied. Systems of nonlinear differential equations are studied in conjuction. Infinite dimensional matrix formalism (the Carleman linearization procedure) is used to approach the problem. The formalism seems to fit well with the algorithmic point of view. The algorithm is treated in a slightly different way to obtain examples for the computation of the normal form of systems of nonlinear differential equations. The previous problem is then treated as a Jordan normal form problem. ESA

N91-23810# Grenoble-1 Univ. (France). Lab. d'Informatique Fondamentale et d'Intelligence Artificielle.
CONGRUENCE PROPERTIES OF THE PROCESS EQUIVALENCE INDUCED BY TEMPORAL LOGIC
P. Schnoebelen Oct. 1990 18 p
(RR-831-I-IMAG-118-LIFIA; ETN-91-99236) Avail: NTIS HC/MF A03

Process equivalence generated by branching time temporal logic in the framework of deterministic programs without branching restriction is studied. It is shown that this equivalent congruence works for most usual process combining operators, but does not work for several versions of parallel composition. Investigations are extended by clarifying the relationships between indistiguishability equivalences generated by temporal logics and the bisimulation congruence. ESA

N91-23811# Royal Signals and Radar Establishment, Malvern (England).
FUNCTIONAL APPROXIMATION BY FEED-FORWARD NETWORKS: A LEAST SQUARES APPROACH TO GENERALISATION
Andrew R. Webb 11 Jan. 1991 37 p
(RSRE-Memo-4453; BR116507; ETN-91-99324) Copyright Avail: Defence Research Information Centre, Kentigern House, 65 Brown Street, Glasgow, G2 8EX, Scotland

A least squares approach to function approximation and generalization is considered. The particular problem addressed is one in which the training data is noiseless (perhaps specified by an assumed model or obtained during some calibration procedure) and the requirement is to define a mapping which approximates the data and which generalizes to situations in which data samples are corrupted by noise. The least squares approach produces a generalizer which is the vector of posterior probabilities and has the form of a radial basis function network for a finite number of training samples. The finite sample approximation is valid provided that the noise on the expected operating conditions is large compared to the sample spacing in the data space. In the other extreme of small noise perturbations, it is shown that better generalization will occur if the training error criterion (the sum square error on the training set) is modified by the addition of a specific regularization term. This is illustrated by an approximator which has a feed forward architecture and applied to the problem of point source location using the outputs of an array of receivers in the focal plane of a lens. ESA

N91-23812# Loughborough Univ. of Technology (England). Dept. of Mathematical Sciences.
ON THE STRUCTURE OF POLYNOMIAL MODELS OF 2-D SYSTEMS
D. S. Johnson, A. C. Pugh, and G. E. Hayton (Hull Univ., England) Feb. 1991 18 p
(Maths-Rept-A-139; ETN-91-99327) Avail: NTIS HC/MF A03

The structure of two Dimensional (2-D) systems is investigated by using the polynomials of a Matrix Fraction Description (MFD) and the more general model of a Rosenbrock System Matrix (RSM). It is shown that although there are two types of MFD, the type is unique to the given transfer function matrix. The basic structure theorem governing all MFDs of the given two dimensional transfer function matrix is derived. In the case of two dimensional RSM models, the question of minimality is considered and the relationship between different RSM realizations of a given transfer function matrix is discussed. ESA

N91-23813# Loughborough Univ. of Technology (England). Dept. of Mathematical Sciences.
ON 2+1-DIMENSIONAL NONLINEAR INTEGRABLE SYSTEMS OF LOEWNER-TYPE
B. G. Konopelchenko (Academy of Sciences, USSR, Novosibirsk) and C. Rogers Mar. 1991 16 p Sponsored by United Kingdom Science and Engineering Research Council, and Canadian Natural Sciences and Engineering Research Council
(Maths-Rept-A-140; ETN-91-99328) Avail: NTIS HC/MF A03

A wide class of (2+1)-dimensional nonlinear systems integrable by the inverse spectral transform method is presented. These are matrix generalizations on a nonlinear system originally introduced in a gas dynamic context by Loewner in 1952. The class of system investigated includes (2+1)-dimensional integrable generalizations of the chiral fields model equation, the non abelian sine Gordon equation, the Toda lattice equation as well as (2+1)-dimensional integrable systems on Grassmannian manifolds, including equations on CP(exp n) and RP(exp n). Certain (2+1)-dimensional integrable generalizations of the sine Gordon equation, invariant under rotation in the plane, are among the system considered. ESA

N91-23814# SRI International Corp., Menlo Park, CA.
ADVANCED METHODS OF APPROXIMATE REASONING Final Report, Sep. 1989 - Sep. 1990
Enrique H. Ruspini 30 Nov. 1990 120 p
(Contract DAAL03-89-K-0156)
(AD-A232140; SRI-ECU-8139; ARO-26364.2-EL) Avail: NTIS HC/MF A06 CSCL 12/9

This research was directed toward establishing basic conceptual foundations for approximate reasoning concepts and toward the development of frameworks that facilitate the development and comparison of applicable techniques. Approximate reasoning is the common name utilized to describe automated techniques for the representation and manipulation of imprecise, uncertain, unreliable, and vague information. Our attention was focused primarily on the development of conceptual bases for possibilities or fuzzy logic. Using a conceptual framework, previously employed to explain the meaning of the Dempster-Shafer calculus of evidence (i.e., possible-world semantics), we developed a semantic model for possibilistic logics that clearly shows them to be substantially different from their probabilistic counterparts both in meaning and in formal structure. GRA

N91-23815# Maryland Univ., College Park. Inst. for Physical Science and Technology.
ON LOCKING AND ROBUSTNESS IN THE FINITE ELEMENT METHOD Final Report
Ivo Babuska and Manil Suri May 1990 62 p Also avail: as Report No. MD-90-14-IB
(Contract N00014-89-J-1030; AF-AFOSR-0252-89)
(AD-A232245; BN-1112; TR90-14; MD-90-14-IB) Avail: NTIS HC/MF A04 CSCL 12/1

A numerical scheme for the approximation of a parameter dependent problem is said to exhibit locking if the accuracy of the approximations deteriorates as the parameter tends to a limiting value. A robust numerical scheme for the problem is one that is essentially uniformly convergent for all values of the parameter. Precose mathematical definitions were developed for these terms, their quantitative characterization given, and some general theorems proved involving locking and robustness. A model problem involving heat transfer is analyzed in detail using this mathematical framework and various related computational results are described. Applications of the theory to some different problems involving locking are presented. GRA

N91-23816# Maryland Univ., College Park. Inst. for Physical Science and Technology.
THE H-P VERSION OF THE FINITE ELEMENT METHOD IN THE PLATE MODELLING PROBLEM Final Report
Ivo Babuska and L. Li Nov. 1990 18 p
(Contract N00014-90-J-1030; NSF CCR-88-20279)
(AD-A232246; BN-1115; TR90-40) Avail: NTIS HC/MF A03
CSCL 12/1

The paper addresses the problem of plate modeling within the framework of the h-p version of the finite element method. A natural hierarchy of models is constructed. The lowest member of the hierarchy is the well known Reissner-Mindlin model. It is shown that higher degree elements do not show any locking effects for the models under consideration. GRA

N91-23817# Old Dominion Univ., Norfolk, VA. Dept. of Mathematical Sciences.
LARGE AND MODERATE DEVIATION LIMIT THEOREMS FOR ARBITRARY SEQUENCES OF RANDOM VARIABLES WITH APPLICATIONS Final Report, 15 May 1988 - 15 Nov. 1990
Narasinga R. Chaganty 3 Jan. 1991 11 p
(Contract DAAL03-88-K-0076)
(AD-A232334; ARO-24834.4-MA) Avail: NTIS HC/MF A03
CSCL 12/3

In this research project we have obtained several limit theorems for arbitrary and dependent sequences of random variables. The limit theorems considered in this project fall into three categories: large deviation local limit theorems; strong large deviation theorems; and strong moderate deviation theorems. These three categories are dependent in the sense they all are subcategories of large deviation theory. The theory of large deviations and its many users are well described in the book by Ellis (1985) and the monograph by Varadhan (1984). This work generalized several classical limit theorems that were obtained in the literature for independent and identically distributed random variables. The technical details of the work done under this contract are briefly outlined. GRA

N91-23818# Wisconsin Univ., Madison. Center for Mathematical Sciences.
PRINCIPAL COMPONENTS OF MINUS M-MATRICES Technical Summary Report
Michael Neumann and Hans Schneider Feb. 1991 24 p
(Grants AF-AFOSR-0047-88; NSF DMS-80-07030; NSF DMS-89-01445; NSF DMS-87-01971)
(AD-A232354; CMS-TSR-91-5) Avail: NTIS HC/MF A03 CSCL 12/1

This paper determines the nonnegativity of the principal components of an n x n nonnegative matrix P in terms of the marked reduced graph R(A) of A = P - rho(P)I, the minus M matrix which can be associated with P. This result is then applied to consider various types of nonnegative bases for the Perron eigenspace of P which can be extracted from a certain nonnegative matrix which is a polynomial in P. A characterization was also obtained for the eigenprojection on the Perron eigenspace of P to be, itself, a nonnegative matrix. The results provide new proofs and extensions of results of Friedland and Schneider and of Hartwig, Neumann, and Rose. GRA

N91-23819# Houston Univ., TX. Dept. of Electrical Engineering.
COMPUTATIONS, PROPERTIES, AND APPLICATIONS OF MATRIX-VALUED FUNCTIONS TO MATHEMATICAL SCIENCE AND CONTROL SYSTEMS Final Report, 1 Jan. 1987 - 31 Dec. 1990
Leang S. Shieh 1 Jan. 1991 13 p
(Contract DAAL03-87-K-0001)
(AD-A232448; ARO-23669.29-MA) Avail: NTIS HC/MF A03
CSCL 12/1

A complete study of the principal nth root of a complex matrix and associated matrix-valued functions is presented in this research report. The principal nth root of a matrix is shown to be useful for the following: constructing the matrix-sign function and the (generalized) matrix-sector function; solving the matrix Lyapunov and Riccati equations; separating matrix eigenvalues relative to a circle, sector and a sector of a circle in the lambda-plane; block-diagonalization (parallel decomposition) and block-triangularization (cascaded decomposition) of a general system matrix; generalizing the block-partial-fraction expansion of a rational matrix; and modeling a continuous-time system from the identified discrete-time model. Also, in this research report, new definitions and computational algorithms have been presented to determine the rectangular and polar representations of a complex matrix. Furthermore, their applications to control systems have been discussed. Finally, utilizing the developed algorithms, a multi-stage design procedure has been established to design discrete-time controllers to achieve pole-assignment in a specified region for a large-scale discrete-time multivariable system. GRA

N91-23820# Wisconsin Univ., Madison.
SOME PROBLEMS IN NONLINEAR ANALYSIS Final Report, 23 May 1987 - 22 May 1990
Michael G. Crandall and Paul H. Rabinowitz 17 Dec. 1990 7 p
(Contract DAAL03-87-K-0043)
(AD-A232701; ARO-24092.15-MA) Avail: NTIS HC/MF A02
CSCL 12/2

Crandall has worked on several questions including applications of nonlinear semigroup theory to nonlinear diffusion problems, the abstract theory of evolution equations, the theoretical basis for Hamilton Jacobi equations in infinite dimensions and its application to dynamic programming in infinite dimensional control and differential games, and the theory of viscosity solutions of fully nonlinear second order partial differential equations. Rabinowitz has worked on a variety of problems which have the common feature that they all involve the development of methods in the calculus of variations and their application to differential equations. In particular he treated the existence of periodic solutions of smooth Hamiltonian systems and systems involving singular potentials, the existence of various types of connecting orbits of Hamiltonian systems such as homoclinic and heteroclinic solutions, and the existence of multiple solutions of semilinear elliptic equations.
GRA

65 STATISTICS AND PROBABILITY

Includes data sampling and smoothing; Monte Carlo method; and stochastic processes.

N91-23821*# Purdue Univ., West Lafayette, IN. School of Electrical Engineering.
TOPICS IN INFERENCE AND DECISION-MAKING WITH PARTIAL KNOWLEDGE
S. Rasoul Safavian and David Landgrebe Sep. 1990 49 p
(Grants NAGw-925; NSF ECS-85-07405)
(NASA-CR-188209; NAS 1.26:188209; TR-EE-90-53) Avail: NTIS HC/MF A03 CSCL 12A

Two essential elements needed in the process of inference and decision-making are prior probabilities and likelihood functions. When both of these components are known accurately and precisely, the Bayesian approach provides a consistent and coherent solution to the problems of inference and decision-making. In many situations, however, either one or both of the above components may not be known, or at least may not be known precisely. This problem of partial knowledge about prior probabilities and likelihood functions is addressed. There are at least two ways to cope with this lack of precise knowledge: robust methods, and interval-valued methods. First, ways of modeling imprecision and indeterminacies in prior probabilities and likelihood functions are examined; then how imprecision in the above components carries over to the posterior probabilities is examined. Finally, the problem of decision making with imprecise posterior probabilities and the consequences of such actions are addressed. Application areas where the above problems may occur are in statistical pattern recognition problems, for example, the problem of classification of high-dimensional multispectral remote sensing image data.
Author

N91-23822# Grenoble-1 Univ. (France). Lab. de Genie Informatique.
OPTIMAL SYSTOLIC NETWORK FOR GAUSSIAN ELIMINATION
Ibrahima Sakho and Traian Muntean Jan. 1991 19 p
(RR-837-I; ETN-91-99226) Avail: NTIS HC/MF A03

Several techniques for synthesizing systolic algorithms are described. The algorithms are generally executed in an optimal number of computation steps but rarely on networks with optimized size. It is shown that one of these algorithms, the Gaussian elimination for an nx(n+1) matrix can be executed with best results, that is in 3n-1 steps on (n+1)(exp 2)/4 processors. The method consists of considering the execution scheme of the algorithm as a sequence of bipartite graphs and constructing a regular maximum matching for any of them. ESA

N91-23823# Grenoble-1 Univ. (France). Lab. de Modelisation et Calcul.
DETECTION OF OUTLIERS AND ROBUST ESTIMATION USING FUZZY CLUSTERING
Bernard VanCutsem and Isak Gath Jul. 1990 19 p Submitted for publication
(RR-822-M; ETN-91-99228) Avail: NTIS HC/MF A03

A method for the identification of one or several outliers, and of robust estimation of the underlying parameters, based on fuzzy partition, is described. Performance measures (fuzzy hypervolume and average partition density) aimed at estimating the quality of a partition into two clusters are calculated, after performing a jackknife procedure on the original data sample. Traditional tests of significance for detection of outliers are applied to the sequences of fuzzy hypervolume and average partition density. It is shown through simulation experiments on both univariate and multivariate data, and on real data, that by applying this technique the sensitivity of the tests for identification of outlying observations increases. Robust estimation of the mean and standard deviation is carried out successfully on the contaminated data, using as a weight parameter the degree of membership of the data points in the cluster in which the outlying observations had a low degree of membership. ESA

N91-23824# Grenoble-1 Univ. (France). Lab. de Modelisation et Calcul.
A PARTICULAR LINEAR MODEL OF VARIANCE COMPONENTS [UN MODELE LINEAIRE PARTICULIER A COMPOSANTES DE LA VARIANCE]
Christian Lavergne Oct. 1990 12 p In FRENCH
(RR-827-M; ETN-91-99229) Avail: NTIS HC/MF A03

A model of particular variance components is presented. Estimates of the unknown parameter involved in the matrix of variances and covariances of the model are proposed. An estimation method is introduced using a classic average quadratic error method. An example of a model of this type in which the matrices of the model are specified gives a simple expression to the estimator obtained by the least squares method. The ease of calculations possible with this estimator is further improved by an asymptotic law under simple hypothesis. This law allows a test to control the asymptotic level to be developed. ESA

N91-23825# Grenoble-1 Univ. (France). Lab. de Modelisation et Calcul.
NONPARAMETRIC ESTIMATION IN CHANGE-POINT HAZARD RATE MODELS FOR CENSORED DATA: A COUNTING PROCESS APPROACH
A. Antoniadis and G. Gregoire Jan. 1991 25 p
(RR-836-I-and-M; ETN-91-99233) Avail: NTIS HC/MF A03

A nonparametric method for estimating the amplitude of a changepoint in changepoint hazard models under random censorship is described. Within the general framework of counting processes, using the kernel method of estimation in partial linear models, a consistent estimator for the rate of change at the breakpoint is obtained. The resulting hazard rate function estimate is shown to be consistent. The performance of the estimators are checked via simulations. A kernel type semiparametric estimator is derived for the intensity of a semiparametric counting process model. ESA

N91-23826# North Carolina Univ., Chapel Hill. Center for Stochastic Processes.
CONVERGENCE OF ONE-DIMENSIONAL DIFFUSION PROCESSES TO A JUMP PROCESS RELATED TO POPULATION GENETICS
Masaru Iizuka and Yukio Ogura Jun. 1990 34 p
(Contract F49620-85-C-0144)
(AD-A232121; TR-300; AFOSR-90-0855TR) Avail: NTIS HC/MF A03 CSCL 06/3

A conjecture on the convergence of diffusion models in population genetics to a simple Markov chain model is proved. The notion of bi-generalized diffusion processes and their limit theorems are used systematically to prove the conjecture. Three limits; strong selection-weak mutation limit, moderate selection-weak mutation limit, weak selection-weak mutation limit are considered for typical diffusion models in population genetics. GRA

N91-23827# South Carolina Univ., Columbia. Dept. of Statistics.
STATISTICAL MODELS AND INFERENCE PROCEDURES FOR STRUCTURAL AND MATERIALS RELIABILITY Final Report, 1 Jul. 1987 - 30 Nov. 1990
James D. Lynch, William J. Padgett, and Stephen D. Durham Dec. 1990 10 p
(Contract DAAL03-87-K-0101)
(AD-A232634; ARO-24653.20-MA) Avail: NTIS HC/MF A02 CSCL 12/3

The objectives of this project were to develop and understand probability and statistical models which adequately describe the reliability of composite materials. Prerequisite to the study of fibrous composites was the study of the failure characteristics of brittle fibers (e.g., carbon fibers) that are used in such composites. Thus, new approaches to the reliability of structures with respect to their strength to withstand an environmental stress were considered. More specifically, it was shown that the probability distribution for the tensile strength of brittle fibers had the IFR property and that is carried over to composite containing such fibers. A new probability distribution for the strength of brittle materials was developed and its characteristics were studied. Some general stress-strength models were also developed and applied to the failure of systems subject to cyclic loading. Involved in the failure of composite materials was the development of new graphical and inferential statistical methods for estimating mixtures of failure distributions or mixtures of hazard functions. The related program of competing risks models was also investigated. GRA

66 SYSTEMS ANALYSIS

Includes mathematical modeling; network analysis; and operations research.

N91-23828# Ministry of Defence, Haifa (Israel). Center for Military Analyses.
ON THE MANY-ON-ONE STOCHASTIC DUEL
Moshe Kress May 1986 20 p
(CEMA-86/11; ITN-89-85013) Avail: NTIS HC/MF A03

The general many-to-one stochastic duel conditioned on the order in which targets are attacked is investigated and the state probabilities are derived for the first time. The results are illustrated by an example of a three-on-one stochastic duel with negative exponential interfiring times. Some aspects of the tradeoff between individual firepower and the nominal size of a force are investigated. ISA

N91-23829 Virginia Univ., Charlottesville.
SUFFICIENT COMPARISON AND MODELING OF FORECASTS Ph.D. Thesis
Dou Long 1990 241 p
Avail: Univ. Microfilms Order No. DA9029903

A Bayesian decision-theoretic approach is taken to modeling and comparing forecasts (information sources). The focus is on the binary relation of sufficiency, which was originally introduced for comparing statistical experiments. The premise of the sufficient comparison of forecasts is that the order induced by the sufficiency relation implies the order in terms of the Bayes risks, regardless of the loss function and the prior distribution of the decision maker. A comprehensive survey of the conditions for the existence of the sufficiency relation is provided. Modeling of forecasts in terms of likelihood functions plays an important part in this research, which is studied when the state variables are binary, multiple, or continuous in nature, while the forecasts can be categorical, probabilistic, or combined. The conditions that lead to the sufficiency relation are explored under the models developed, by solving integral equations, by formulating numerical algorithms, by studying transformations of forecasts, or by the use of characteristic functions. Dissert. Abstr.

N91-23830 Washington Univ., Saint Louis, MO.
DEGENERATION OF LINEAR MULTIVARIABLE SYSTEMS UNDER HIGH GAIN AND DYNAMIC COMPENSATION Ph.D. Thesis
Patrice Edoete Mensah 1989 95 p
Avail: Univ. Microfilms Order No. DA9103985

The degeneration phenomenon of linear multivariable time invariant systems under output feedback high gain and dynamic compensation is discussed. Consider m-input, p-output linear time invariant strictly proper plants of McMillan degree n together with compensators of degree q greater than or equal to 0. It is shown that for a generic set of plants and for a suitable parameterization of the set of compensators, n greater than or equal to max(m,p) is a necessary and sufficient condition for the closed loop system to be continuous as a function of the compensator parameters. Next, it is shown that for q greater than 0, the pole placement map always has points of discontinuity. Recall an earlier result of Byrnes: if $q = 0$, then, for a generic plant, mp less than or equal to n is a necessary and sufficient condition for the continuity of the pole placement map. For the case of min(m,p), a different parameterization is used to show that $n + q$ greater than or equal to $\max(m,p)(q+1)$ is a necessary and sufficient condition for the closed loop system to be continuous with respect to the compensator parameters. The case of proper plants for this parameterization are also analyzed. Finally, a necessary and sufficient condition for the zero input response (assuming non-zero initial conditions) of a special class of parameter dependent systems is given. Dissert. Abstr.

N91-23831 Texas Univ., Austin.
CONTROL SYNTHESIS BASED UPON A GAME THEORETIC APPROACH Ph.D. Thesis
Ihnseok Rhee 1990 166 p
Avail: Univ. Microfilms Order No. DA9105644

The relationship between the linear exponential Gaussian problem and the linear quadratic game is elaborated. A disturbance attenuation problem for finite-time is considered by a game theoretic approach where the control, restricted to the function of the measurement history, plays against adversaries composed of the process and measurement disturbances, and the initial conditions. A zero-sum game, formulated as a quadratic performance criterion subject to linear, time-varying dynamics and measurements, is solved by a calculus of variation technique. Necessary and sufficient conditions for the saddle point to be strictly concave with respect to all disturbances and initial conditions, and sufficient conditions for various process disturbance strategies to satisfy the saddle point condition are given. A disturbance attenuation problem is solved based on the results of the game problem. For time-invariant systems, it is shown that, under certain conditions, the time-varying controller becomes time-invariant on the infinite time interval. The resulting controller satisfies an H(infinity) norm bound. A game theoretic approach is easily accommodated to designing a controller for a linear time invariant system with parameter uncertainties. The uncertain system is represented as an internal feedback loop where the parameter uncertainties are embedded in the system as fictitious disturbances. The consideration of the fictitious disturbances as players against the control leads to the construction of a finite time linear quadratic game. It is shown that the resulting time invariant controller stabilizes the uncertain system for a prescribed parameter uncertainty bound. The game theoretic controller is applied to the momentum management/attitude control of the space station whose moments of inertia are subject to variations. Dissert. Abstr.

67 THEORETICAL MATHEMATICS

Includes topology and number theory.

No abstracts in this category.

70 PHYSICS (GENERAL)

For precision time and time interval (PTTI) see *35 Instrumentation and Photography;* for geophysics, astrophysics or solar physics see *46 Geophysics, 90 Astrophysics,* or *92 Solar Physics.*

N91-23832# Tel-Aviv Univ. (Israel). School of Physics and Astronomy.
BULLETIN OF THE ISRAEL PHYSICAL SOCIETY, VOLUME 33, 1987. ANNUAL MEETING 1987: PROGRAM AND ABSTRACTS Abstracts Only
1987 162 p Meeting held in Tel-Aviv, Israel, 22-23 Nov. 1987; sponsored by Tel-Aviv Univ. and IBM-Israel
(ITN-89-85012) Avail: NTIS HC/MF A08

The 1987 meeting of the IPS (Israel Physical Society) produced papers on: laser irradiation, blood circulation measurements, cosmic voids, crystal structures of 4d transition metals, supersymmetry, high temperature superconductors, quantum theory, neutrinos in galactic formation, x ray emission lines, accretion disks, chemical lasers, optical and mechanical properties of silver halides, and photoconductivity. Symposia on synchrotron radiation and the Strategic Defense Initiative were also held. For individual titles, see N91-23833 through N91-23843.

N91-23833# Tel-Aviv Univ. (Israel). School of Physics and Astronomy.
TEMPERATURE DISTRIBUTION AND THERMAL DAMAGE DURING TISSUE ABLATION BY CO2 LASER IRRADIATION: MODEL AND EXPERIMENT Abstract Only **c36**
A. Avidor, A. Sagi, A. Katzir, and S. Akselrod *In its* Bulletin of the Israel Physical Society, Volume 33, 1987. Annual Meeting 1987: Program and Abstracts 1987 p 17 (For primary document see N91-23832 15-70)
Avail: NTIS HC/MF A08

The work is based on a previous numerical model which was developed for calculating the temperature distribution in material exposed to CO2 laser beam. The model also evaluates the thermal damage caused to the tissue. The original model was found to be accurate in describing the behavior of soft tissue exposed to low power irradiation, but not for higher powers causing tissue removal. This original model was extended so as to include absorption of radiation in depth, boiling and evaporation of water content, ablation, and material removal at high temperatures, as a result of high irradiation power. The temperature field as a function of time was measured with accurately located thermocouples in biological tissue exposed to high power pulses of CO2 laser causing ablation. Good agreement was obtained between the experimental results and the predicted theoretical dependence of temperature

as a function of time at different locations in the tissue. This model may be applied for determining temperature distribution during laser cutting and designing the conditions of laser irradiation in order to minimize the resulting thermal damage during laser surgery. ISA

N91-23834# Tel-Aviv Univ. (Israel). School of Physics and Astronomy.

AN ON-LINE COMPUTERIZED SYSTEM FOR BLOOD-FLOW MEASUREMENTS Abstract Only **c61**

D. Eylon, V. Benary, S. Akselrod, T. Kaspi, and Y. Heilbronn (Belinson Medical Center, Petah Tiqva, Israel) *In its* Bulletin of the Israel Physical Society, Volume 33, 1987. Annual Meeting 1987: Program and Abstracts 1987 p 20 (For primary document see N91-23832 15-70)

Avail: NTIS HC/MF A08

A complete system for measurement of blood flow in biological tissue during the hydrogen clearance method was developed. The method enables measurement of blood flow in regions where only capillary blood vessels exist (microcirculation), so the flow cannot be measured directly. Current readings from microelectrodes implanted in tissue are amplified and filtered using a dedicated electronic module. This module is connected to a microcomputer, which performs data acquisition at accurate time-intervals. A best fit method, exspecially devised for fitting the type of curves predicted by the physical model for inert gas clearance from tissue, i.e., multi-exponential decay curves, is then used to fit the data and obtain the flows and relative weights of up to two separate components. Results can be obtained with high reliability within a relatively short time, enabling a reduction of the time during which the subject has to be held in a steady state, an essential requirement of the method. ISA

N91-23835# Technion - Israel Inst. of Tech., Haifa. Dept. of Physics.

FIRST PRINCIPLES CALCULATION OF THE CRYSTAL STRUCTURES IN THE 4d TRANSITION METALS Abstract Only **c76**

N. Davidson, G. Barak, and J. Ashkenazi *In* Tel-Aviv Univ., Bulletin of the Israel Physical Society, Volume 33, 1987. Annual Meeting 1987: Annual Meeting 1987: Program and Abstracts 1987 p 26 (For primary document see N91-23832 15-70)

Avail: NTIS HC/MF A08

The energy differences between the fcc, bcc, and hcp structures of the 4d transition metals at zero temperature are calculated from first principles using the linear muffin-tin orbital (LMTO) and the linear augmented plane waves (LAPW) band-structure methods within the density functional theory. For zero pressure the calculations predict the correct structure of all the 4d transition metals within the numerical error. For non-zero pressures, the calculations predict a hcp yields fcc structural phase transition in Yttrium at 175 Kbar, a hcp yields fcc transition in Zirconium at 140 Kbar, and no transition in Palladium up to 1 Mbar, in qualitative agreement with experiments. ISA

N91-23836# Hebrew Univ., Jerusalem (Israel). Racah Inst. of Physics.

SUPERSYMMETRIC MATTER AT FINITE TEMPERATURE Abstract Only **c77**

G. Horwitz and G. Kalbermann *In* Tel-Aviv Univ., Bulletin of the Israel Physical Society, Volume 33, 1987. Annual Meeting 1987: Program and Abstracts 1987 p 37 (For primary document see N91-23832 15-70)

Avail: NTIS HC/MF A08

In recent years supersymmetry has gained acceptance as a way to solve longstanding problems in field theory, such as zero point vacuum energy which in turn may explain the smallness of the cosmological constant at the present time. Its applicability to the early universe needs its treatment at finite temperature. Girardello, Grisaru, and Salmonson found that thermal effects necessarily break the symmetry contrary to usual restoration of symmetries at high temperature. They used a partition function unconstrained by the charge operator. Later Alvarez and Gavela included a term in the partition function involving the supersymmetry charge. The approximate expressions were found for the partition function and the specific heat. Kapusta, Pratt, and Visnijac extended the investigation by finding the eigenstates of the charge and energy operators and developed the partition function and the chemical potential as a function of temperture. The above mentioned concepts have been generalized and applied to one fermion, one boson degree of freedom. The partition function is built as Z = Tr(exp - beta(H) + (Xi)Q(sub 1)) where the supersymmetric charge is Q(sub 1) = ab(+) + a(+)b. Using this expression, a steepest descent method was applied to calculate the thermodynamic properties of the ensemble at finite temperature. Alternatively, Clifford numbers were used in building the conserved supersymmetric charge operator mean Q = gamma(Q) + Q(sub 1)gamma, gamma squared = 1. Bosonic and fermionic eigenstates were discovered, the Hilbert space of states is consequently doubled. A hidden U(1) symmetry arises by attaching a phase to the supersymmetry charge. ISA

N91-23837# Tel-Aviv Univ. (Israel). School of Physics and Astronomy.

OPTICAL AND MECHANICAL PROPERTIES OF MIXED SILVER HALIDE CRYSTALS Abstract Only **c76**

N. Barkay, F. Moser, A. Saar, and A. Katzir *In its* Bulletin of the Israel Physical Society, Volume 33, 1987. Annual Meeting 1987: Program and Abstracts 1987 p 39 (For primary document see N91-23832 15-70)

Avail: NTIS HC/MF A08

Mixed silver halide crystals of varied compositions were grown from the melt. Spectral measurements of disc-shaped samples a few mm thick were taken by a Cary 17 spectrometer in the visible range, and by a Perkin-Elmer 283 spectrometer in the infrared range. The absorption edges in the visible and infrared regions were measured. Plots of the wavelength vs. composition at a constant absorption coefficient reveal the same trend at both edges. As the composition varies from pure AgCl to pure AgBr, the wavelength increased monotonically. The Br-rich crystals show a stronger variation at the infrared edge. The behavior of the infrared edge, caused by the multiphonon absorption, fits the 'one-mode' type ionic mixed crystal, in which frequency varies continously with concentration between the modes of the pure crystals, although the bonding in the samples has a partially covalent nature. The behavior of the visible edge, corresponds to the continuous variation of the energy gap with concentration. The microhardness of the mixed crystals, as measured by the standard Vickers indentor method on randomly oriented samples, was higher than that of the single crystals compromising them. The results fit a model, with an additional internal stress field in the mixed crystals. The random distribution of different sized anions results in curved dislocations and produces a fluctuating stress field on the slip plane which increases the work required to move a dislocation. ISA

N91-23838# Wise Observatory, Tel Aviv (Israel).

MATTER IN COSMIC VOIDS Abstract Only **c90**

N. Brosch *In* Tel-Aviv Univ., Bulletin of the Israel Physical Society, Volume 33, 1987. Annual Meeting 1987: Program and Abstracts 1987 p 52 (For primary document see N91-23832 15-70)

Avail: NTIS HC/MF A08

An attempt was made to observe baryonic matter in nearby cosmic voids. This includes absorption line spectroscopy in the UV and in the radio, as well as emission line observations. In some cases, absorption lines from Lyman alpha and ionized metals were detected at void redshifts. One void and its nearby superdusters were surveyed in 21 cm and no small H I clouds were found. ISA

N91-23839# Weizmann Inst. of Science, Rehovoth (Israel).

BIASED GALAXY FORMATION IN THE NEUTRINO SCENARIO Abstract Only **c90**

Erez Braun, Avishai Dekel, and Paul R. Shapiro (Texas Univ., Austin.) *In* Tel-Aviv Univ., Bulletin of the Israel Physical Society,

Volume 33, 1987. Annual Meeting 1987: Program and Abstracts 1987 p 53 (For primary document see N91-23832 15-70)
Avail: NTIS HC/MF A08

The timing problem of the neutrino-dominated cosmogonic scenario, i.e., the apparent conflict between the inferred young age for the large-scale structure and the observationally indicated older ages of galaxies and quasars, is considered. It can be reduced by 'anti-biasing' of galactic formation. By applying a variety of alternative prescriptions for galactic formation to the N-body simulations of the neutrino scenario, it was found that the clustering of galaxies could be suppressed relative to the neutrinos to an extent that solves the timing problem. It requires the galaxies to form preferentially in the flat 'pancake' relative to the denser 'filaments' and compact clusters. This could result either from differences in the efficiency of the galactic formation itself, or due to feedback influence from a first generation of objects (e.g., quasars) which suppress the formation of incipient galaxies locally. Various illustrative examples are presented in order to quantify the requirements from such anti-bias mechanisms, and their physical plausibility is discussed. Other aspects of the neutrino cosmogony are discussed in view of the proposed anti-biasing, concluding that no fatal flaw is seen in the picture. ISA

N91-23840# Tel-Aviv Univ. (Israel). School of Physics and Astronomy.
THE SPECTRUM OF MASSIVE ACCRETION DISKS Abstract Only **c90**
Ari Laor *In its* Bulletin of the Israel Physical Society, Volume 33, 1987. Annual Meeting 1987: Program and Abstracts 1987 p 54 (For primary document see N91-23832 15-70)
Avail: NTIS HC/MF A08

A likely process for energy production of quasars is the release of gravitational energy from matter accretion onto a compact and massive object. One of the possible configurations is a thin accretion disk around a massive black hole (10(exp 8) to 10(exp 10) solar mass). The blue bump which appears in most quasar spectra might originate from such a disk. Thin accretion disk models are characterized by three basic parameters: the mass of the central black hole; the accretion rate; and the viscosity parameter. There is a certain range of parameters which allows the existence of a self-consistent model. The structure of the disk was calculated for this range solving, at each radius, the vertical structure and assuming radiative energy transfer. The local spectrum was calculated taking into account the opacity from free-free, bound-free (hydrogen and helium) and electron scattering, including Comptonization. The final result if the integrated disk spectrum as a function of the disk inclination angle. The effects of gravitational redshift, Doppler shift, and beaming were also included. Several theoretical spectra are presented and the comparisons with the observations are discussed. ISA

N91-23841# Bar-Ilan Univ., Ramat-Gan (Israel). Dept. of Physics.
A HIGH RESOLUTION STUDY OF THE Cu K ALPHA(SUB 1,2) X-RAY EMISSION LINES Abstract Only **c76**
Nissan Maskil and Moshe Deutsch *In* Tel-Aviv Univ., Bulletin of the Israel Physical Society, Volume 33, 1987. Annual Meeting 1987: Program and Abstracts 1987 p 57 (For primary document see N91-23832 15-70)
Avail: NTIS HC/MF A08

The deviation of the x ray emission line of the 3d transition elements from the expected Lorenzian shape was attributed to intra-atomic correlation of the core electron with the unpaired 3d electron, or alternatively to shake-up type many-electron effects. As conclusions of previous studies of the Cu K alpha(sub 1,2) lines are contradictory, the remeasurement of these lines was undertaken with an energy resolution of 10(exp -4), using the monolithic double crystal x ray spectrometer. No fine structure was detected in any of the lines except a small and rather broad shoulder on the low-energy side of each peak. The absolute wavelength of the Cu K alpha(sub 2) line was determined to be wavelength = (1.544413 + or - .000002) A. This represents a factor of 2 improvement in accuracy over the existing value. The lineshape and shoulder are analyzed by computer fitting within the framework of the many-body theory of Doniach and Sunjic, yielding satisfactory agreement. ISA

N91-23842# Technion - Israel Inst. of Tech., Haifa. Dept. of Physics.
THEORY OF THE NEW HIGH-TEMPERATURE SUPERCONDUCTORS Abstract Only **c76**
J. Ashkenazi, C. G. Kuper, and R. Tyk *In* Tel-Aviv Univ., Bulletin of the Israel Physical Society, Volume 33, 1987. Annual Meeting 1987: Program and Abstracts 1987 p 60 (For primary document see N91-23832 15-70)
Avail: NTIS HC/MF A08

The newly-discovered high-temperature superconductors have a highly anisotropic electronic band structure. The electrons can be regarded as 'heavy' along one axis and 'light' at right angles to it; to a good approximation the electronic motion in the 'light' plane can be decoupled from that in the 'heavy' direction. Plasma oscillations along the heavy axis have therefore a rather low frequency, but still much higher than the Debye-cutoff phonon frequency. These plasmons interact strongly with the conduction electrons, whose motion is essentially in the light plane. The strength of this interaction arises primarily from the sensitivity to charge fluctuations of the copper-3d and barium (or lanthanum) 4f orbitals (which appear as components in the wave functions of the Bloch electrons near the Fermi surface). The electron-electron attraction induced by plasmon exchange can lead to formation of cooper pairs. The Debye-energy prefactor in the BCS expression for the transition temperature is replaced by the much larger plasmon energy. Furthermore, the strength of the interaction will ensure that the exponential factor is not too small. ISA

N91-23843# Tel-Aviv Univ. (Israel). School of Physics and Astronomy.
EXPLORING THE MESOSCOPIC DOMAIN WHERE CLASSICAL AND QUANTUM PHENOMENA MEET Abstract Only **c77**
Eshel Ben-Jacob *In its* Bulletin of the Israel Physical Society, Volume 33, 1987. Annual Meeting 1987: Program and Abstracts 1987 p 61 (For primary document see N91-23832 15-70)
(Grant NSF DMR-86-08305)
Avail: NTIS HC/MF A08

Today man-made elements can be fabricated and monitored to a size comparable to that of macromolecules, which is on the threshold of the mesoscopic domain between the microworld and the macroworld. It is already evident that effects are to be encountered in this domain and new understanding of the physical reality is required. For example, the response of an ultra-small electronic system is not solely a characteristic of the system itself but depends crucially on the way it is connected to the external world, in direct relation to the questions of quantum measurements. Dissipation and response can be separated in space and time. This requires a new definition of response and leads to the response exhibiting quantum effects with no classical analogs. Specifically, current oscillation in small normal rings and charge oscillations in small capacitance tunnel junctions (Josephson and normal), resulting from the Aharonov-Bohm effect (rings) and charge discreteness (junctions) are discussed. The existence is shown of a new type of fluctuation in these systems and their study via master equation approach. While aimes at the construction of smaller and faster logical elements, the new mesoscopic concepts should also provide a better understanding of biological activity, which takes place mostly in this domain (e.g., protein synthesis in the cell, active transport, and cell differentiation). The application of the new understanding is briefly discussed to construct a possible description of the dynamics of the nerve gates. ISA

N91-23844# Institut National des Sciences Appliquees, Lyon (France). Lab. de Mecanique des Structures.
DYNAMIC STUDY OF CYCLICALLY SYMMETRIC STRUCTURES: APPLICATION TO ROTATING A WHEEL OF A CENTRIFUGAL COMPRESSOR Ph.D. Thesis [ETUDE DYNAMIQUE DES STRUCTURES A SYMETRIE CYCLIQUE EN ROTATION: APPLICATION A UNE ROUE DE COMPRESSEUR CENTRIFUGE]
Alain Berlioz 1991 164 p In FRENCH Sponsored by Ministere de la Recherche et de l'Enseignement Superieur
(ISAL-91-0004; ETN-91-99241) Avail: NTIS HC/MF A08

An effective method of calculating the dimensions of rotating structures, such as pump or centrifugal compressor wheels, is presented. The general equations used in the analysis of any rotating solid are reviewed. A theoretical model destined for use on bodies of cyclical symmetry submitted to centrifugal forces is presented. The model is validated using simple representative examples. It is then applied to a real centrifugal compressor wheel. Modes and frequencies of the wheel are established experimentally at rest by shock and harmonic excitation tests and while rotating using shock tests. The experimental results are compared to the theoretical results. Perfect agreement is found between the two. ESA

N91-23845# Royal Signals and Radar Establishment, Malvern (England).
THE UNITED KINGDOM WAVEGUIDE POWER STANDARDS ABOVE 40 GHz
P. J. Ide Dec. 1990 78 p
(RSRE-90023; BR116237; ETN-91-99320) Copyright Avail: NTIS HC/MF A05

The United Kingdom national standards for power in waveguide consist of commercial thermistor mounts whose effective efficiencies were measured at discrete frequencies. The effective efficiencies are determined using microcalorimeters, and an analysis of the uncertainties involved and a description of microcalorimeters are given. The multistate reflectometers which are used to compare the standards and calibrate power meters are described. ESA

N91-23846# Royal Signals and Radar Establishment, Malvern (England).
THE COORDINATE-FREE REPRESENTATION OF ROTATIONAL MOTIONS
R. J. A. Tough Feb. 1991 12 p
(RSRE-Memo-4445; BR116612; ETN-91-99322) Copyright Avail: NTIS HC/MF A03

The rotation of a rigid body may be represented by a unit axis and the angle of rotation about that axis. The representation in this form of the rotation equivalent to the two successive rotations is investigated and equations of motion of the body in terms of its angular velocity are derived. The relationship of the results to those of the quantum theory of angular momentum is discussed with particular reference to the Baker Campbell Hansdorff expansion. ESA

N91-23847# Naval Postgraduate School, Monterey, CA. Dept. of Physics.
SUMMARY OF BASIC RESEARCH IN THERMOACOUSTIC HEAT TRANSPORT: 1990 Annual Report, 1 Oct. 1989 - 30 Sep. 1990
Anthony A. Atchley and Thomas J. Hofler Oct. 1990 30 p
(AD-A232223; NPS-PH-91-002PR) Avail: NTIS HC/MF A03 CSCL 20/13

This annual report details progress in basic research in thermoacoustic heat transport made during the period October 1, 1989 through September 30, 1990. Four projects are discussed. The first project involves measurements of thermoacoustic phenomena using thermoacoustic couples (TACs). The purpose of the second project is to examine means of visualizing thermoacoustic processes. The third project is an investigation of heat driven prime movers. The fourth project considers the performance of thermoacoustic heat engines that operate with an acoustic sound field that is not a perfect standing wave. A publications, patents, presentations, and honors report is also included. GRA

71 ACOUSTICS

Includes sound generation, transmission and attenuation. For noise pollution see *45 Environmental Pollution.*

N91-23848# Science Applications International Corp., McLean, VA. Foreign Applied Sciences Assessment Center.
SOVIET ATMOSPHERIC ACOUSTICS RESEARCH
H. E. Bass, R. T. Lacoss, T. E. Landers, A. Powell, R. Raspet, and J. D. Revell Aug. 1990 229 p
Avail: NTIS HC/MF A11

The development of low observable air vehicles by the U.S. coupled with the historic propensity of the Soviet Union toward the defense of its border raises the possibility of Soviet development of acoustic systems for detection and tracking of air vehicles as part of such defenses. Soviet research in atmospheric acoustics are reviewed and assessed. Topics considered relevant were aircraft noise, background acoustic noise, propagation, meteorological remote sensing, microphone technology, processing of acoustic signals, and acoustic-gravity waves and ionospheric detection. An indication is provided of the maturity of the Soviet technology base required for the development of potential acoustic detection and tracking systems. Author

N91-23849*# United Technologies Research Center, East Hartford, CT.
UNIFIED AEROACOUSTICS ANALYSIS FOR HIGH SPEED TURBOPROP AERODYNAMICS AND NOISE. VOLUME 2: DEVELOPMENT OF THEORY FOR WING SHIELDING Final Report
R. K. Amiet May 1991 41 p
(Contract NAS3-23720)
(NASA-CR-185192; NAS 1.26:185192) Avail: NTIS HC/MF A03 CSCL 20A

A unified theory for aerodynamics and noise of advanced turboprops is presented. The theory and a computer code developed for evaluation at the shielding benefits that might be expected by an aircraft wing in a wing-mounted propeller installation are presented. Several computed directivity patterns are presented to demonstrate the theory. Recently with the advent of the concept of using the wing of an aircraft for noise shielding, the case of diffraction by a surface in a flow has been given attention. The present analysis is based on the case of diffraction of no flow. By combining a Galilean and a Lorentz transform, the wave equation with a mean flow can be reduced to the ordinary equation. Allowance is also made in the analysis for the case of a swept wing. The same combination of Galilean and Lorentz transforms lead to a problem with no flow but a different sweep. The solution procedures for the cases of leading and trailing edges are basically the same. Two normalizations of the solution are given by the computer program. FORTRAN computer programs are presented with detailed documentation. The output from these programs compares favorably with the results of other investigators. B.G.

N91-23850*# Hamilton Standard, Windsor Locks, CT.
UNIFIED AEROACOUSTICS ANALYSIS FOR HIGH SPEED TURBOPROP AERODYNAMICS AND NOISE. VOLUME 3: APPLICATION OF THEORY FOR BLADE LOADING, WAKES, NOISE, AND WING SHIELDING Final Report
D. B. Hanson, C. J. McColgan, R. M. Ladden, and R. J. Klatte May 1991 128 p
(Contract NAS3-23720)
(NASA-CR-185193; NAS 1.26:185193) Avail: NTIS HC/MF A07 CSCL 20A

Results of the program for the generation of a computer prediction code for noise of advanced single rotation, turboprops (prop-fans) such as the SR3 model are presented. The code is based on a linearized theory developed at Hamilton Standard in

which aerodynamics and acoustics are treated as a unified process. Both steady and unsteady blade loading are treated. Capabilities include prediction of steady airload distributions and associated aerodynamic performance, unsteady blade pressure response to gust interaction or blade vibration, noise fields associated with thickness and steady and unsteady loading, and wake velocity fields associated with steady loading. The code was developed on the Hamilton Standard IBM computer and has now been installed on the Cray XMP at NASA-Lewis. The work had its genesis in the frequency domain acoustic theory developed at Hamilton Standard in the late 1970s. It was found that the method used for near field noise predictions could be adapted as a lifting surface theory for aerodynamic work via the pressure potential technique that was used for both wings and ducted turbomachinery. In the first realization of the theory for propellers, the blade loading was represented in a quasi-vortex lattice form. This was upgraded to true lifting surface loading. Originally, it was believed that a purely linear approach for both aerodynamics and noise would be adequate. However, two sources of nonlinearity in the steady aerodynamics became apparent and were found to be a significant factor at takeoff conditions. The first is related to the fact that the steady axial induced velocity may be of the same order of magnitude as the flight speed and the second is the formation of leading edge vortices which increases lift and redistribute loading. Discovery and properties of prop-fan leading edge vortices were reported in two papers. The Unified AeroAcoustic Program (UAAP) capabilites are demonstrated and the theory verified by comparison with the predictions with data from tests at NASA-Lewis. Steady aerodyanmic performance, unsteady blade loading, wakes, noise, and wing and boundary layer shielding are examined. Author

N91-23851*# Hamilton Standard, Windsor Locks, CT.
UNIFIED AEROACOUSTICS ANALYSIS FOR HIGH SPEED TURBOPROP AERODYNAMICS AND NOISE. VOLUME 4: COMPUTER USER'S MANUAL FOR UAAP TURBOPROP AEROACOUSTIC CODE Final Report
R. W. Menthe, C. J. McColgan, and R. M. Ladden May 1991 123 p
(Contract NAS3-23720)
(NASA-CR-185194; NAS 1.26:185194) Avail: NTIS HC/MF A06 CSCL 20A

The Unified AeroAcoustic Program (UAAP) code calculates the airloads on a single rotation prop-fan, or propeller, and couples these airloads with an acoustic radiation theory, to provide estimates of near-field or far-field noise levels. The steady airloads can also be used to calculate the nonuniform velocity components in the propeller wake. The airloads are calculated using a three dimensional compressible panel method which considers the effects of thin, cambered, multiple blades which may be highly swept. These airloads may be either steady or unsteady. The acoustic model uses the blade thickness distribution and the steady or unsteady aerodynamic loads to calculate the acoustic radiation. The users manual for the UAAP code is divided into five sections: general code description; input description; output description; system description; and error codes. The user must have access to IMSL10 libraries (MATH and SFUN) for numerous calls made for Bessel functions and matrix inversion. For plotted output users must modify the dummy calls to plotting routines included in the code to system-specific calls appropriate to the user's installation. Author

N91-23852*# Hamilton Standard, Windsor Locks, CT.
UNIFIED AEROACOUSTICS ANALYSIS FOR HIGH SPEED TURBOPROP AERODYNAMICS AND NOISE. VOLUME 5: PROPAGATION OF PROPELLER TONE NOISE THROUGH A FUSELAGE BOUNDARY LAYER Final Report
B. Magliozzi and D. B. Hanson May 1991 71 p
(Contract NAS3-23720)
(NASA-CR-185195; NAS 1.26:185195) Avail: NTIS HC/MF A04 CSCL 20A

An analysis of tone noise propagation through a boundary layer and fuselage scattering effects was derived. This analysis is a three dimensional and the complete wave field is solved by matching analytical expressions for the incident and scattered waves in the outer flow to a numerical solution in the boundary layer flow. The outer wave field is constructed analytically from an incident wave appropriate to the source and a scattered wave in the standard Hankel function form. For the incident wave, an existing function - domain propeller noise radiation theory is used. In the boundary layer region, the wave equation is solved by numerical methods. The theoretical analysis is embodied in a computer program which allows the calculation of correction factors for the fuselage scattering and boundary layer refraction effects. The effects are dependent on boundary layer profile, flight speed, and frequency. Corrections can be derived for any point on the fuselage, including those on the opposite side from the source. The theory was verified using limited cases and by comparing calculations with available measurements from JetStar tests of model prop-fans. For the JetStar model scale, the boundary layer refraction effects produce moderate fuselage pressure reinforcements aft of and near the plane of rotation and significant attenuation forward of the plane of rotation at high flight speeds. At lower flight speeds, the calculated boundary layer effects result in moderate amplification over the fuselage area of interest. Apparent amplification forward of the plane of rotation is a result of effective changes in the source directivity due to boundary layer refraction effects. Full scale effects are calculated to be moderate, providing fuselage pressure amplification of about 5 dB at the peak noise location. Evaluation using available noise measurements was made under high-speed, high-altitude flight conditions. Comparisons of calculations made of free field noise, using a current frequency-domain propeller noise prediction method, and fuselage effects using this new procedure show good agreement with fuselage measurements over a wide range of flight speeds and frequencies. Correction factors for the JetStar measurements made on the fuselage are provided in an Appendix. Author

N91-23853# Aerospatiale, Toulouse (France).
NOISE INSIDE AIRCRAFT FUSELAGES SUBJECTED TO AIRBORNE EXCITATIONS
M. Goulain 1991 26 p Presented at Internoise 90, 13-15 Aug. 1990
(Rept-911-111-104; ETN-91-99268) Avail: NTIS HC/MF A03

Noises inside a cockpit and a cabin and airborne and structureborne noise are summarized with the use of graphics. The necessity of having a model of acoustic and vibration transmission is outlined. The history and complexity of models, fuselage test in laboratory and a comparison of theory and experiment are discussed. The modal method is concluded to give a good understanding of the transmission phenomena through an aircraft fuselage in a 0.15 to 2.3 frequency range. The ease of use of these methods allow parametrical studies for preliminary design for noise reduction purpose. ESA

N91-23854# European Space Agency, Paris (France).
THE PROPAGATION OF ACOUSTIC DISTURBANCES IN THE TRANSONIC FLOW FIELDS OF WINGS
Ralph Voss (Deutsche Forschungsanstalt fuer Luft- und Raumfahrt, Goettingen, Germany, F.R.) Feb. 1991 199 p Transl. into ENGLISH of Ueber die Ausbreitung Akustischer Stroerungen in Transsonischen Stroemungsfelden von Tragfluegeln (Goettingen, Fed. Republic of Germany, DLR), 1988 146 p
(ESA-TT-1126; DLR-FB-88-13; ETN-91-99312) Avail: NTIS HC/MF A09; Original German version available from DLR, Wissenschaftliches Berichtswesen, VB-PL-DO, Postfach 90 60 58, 5000 Cologne, Fed. Republic of Germany, HC 53.50 Deutschs marks

The propagation of small disturbances in the vicinity of transonic wings with a mixture of subsonic and supersonic regions is theoretically investigated on the basis of the geometrical acoustics approximation. Waves, beams, and the spatial density distribution of the dissipated disturbance energy are numerically calculated using a system of eighteen differential equations. The effects of various two dimensional and three dimensional fields, of the location of the source and of reflections on the wing surface are

investigated. The results of the acoustic theory are used to derive a general influence function for sources of disturbance in arbitrary transonic fields. This function represents a first step towards a new surface panel method for calculating unsteady transonic flows. The acoustic results are compared with measured unsteady pressure distributions on oscillating transonic wings and with the results of a numerical field panel method. ESA

N91-24078*# National Aeronautics and Space Administration. Langley Research Center, Hampton, VA.
A FIELD-DEPLOYABLE DIGITAL ACOUSTIC MEASUREMENT SYSTEM
David L. Gray, Kenneth D. Wright, II, and Wayne D. Rowland *In* NASA, Washington, Technology 2000, Volume 2 1991 p 325-332 (For primary document see N91-24041 15-99)
Avail: NTIS HC/MF A16 CSCL 20A

72 ATOMIC AND MOLECULAR PHYSICS

Includes atomic structure, electron properties, and molecular spectra.

N91-23855# Los Alamos National Lab., NM.
LOS ALAMOS SCIENCE, NUMBER 19, 1990
N. G. Cooper, ed. 1990 214 p
(Contract W-7405-eng-36)
(DE91-009371; LA-UR-90-3000) Avail: NTIS HC/MF A10

The physics of various neutron scattering processes are explored, the experimental techniques and instruments that make neutron scattering so versatile are introduced, and the single equation that unifies the interpretation of neutron scattering data is discussed. The history of the field, its successes around the world, its present problems in the United States, and the plans for opening it to a wide spectrum of users from academia and industry is also discussed. This article traces neutrons from their birth in the spallation target through beam-tailoring devices and scattering samples to their death in neutron detectors. Small-angle neutron scattering experiments provide evidence that calmodulin, a protein that mediates calcium regulation of biological processes, is flexible in solution. Neutron scattering can detect subtle structures beneath the disorder that give advanced materials their extraordinary combinations of strength, elasticity, and low density. Recent neutron scattering experiments on model systems are revealing how metal atoms loosen the bonds of hydrogen molecules, and essential first step in hydrogenation reactions. Combining data from neutron and x ray diffraction is the only way to resolve ambiguities in the crystal structure of various materials, including high temperature superconductors. Although the Bose condensate cannot be observed directly, an interpretation of neutron scattering data according to a new first-principles theory of final-state effects has at last confirmed its existence in superfluid helium. The maximum entropy method was applied successfully to neutron scattering data and could even influence the design of neutron scattering instruments. DOE

N91-23856# California Univ., Berkeley. Lawrence Berkeley Lab.
A GUIDE TO EXPERIMENTAL ELEMENTARY PARTICLE PHYSICS LITERATURE, 1985-1989
S. I. Alekhin, V. V. Bazeeva, V. V. Ezhela, B. B. Filimonov, S. B. Lugovsky, A. S. Nikolaev, N. L. Petrova, S. R. Slabospitsky, S. I. Striganov, and Y. G. Stroganov et al Nov. 1990 400 p
(Contract DE-AC03-76SF-00098)
(DE91-010209; LBL-90-Rev-11/90) Avail: NTIS HC/MF A17

We present an indexed guide to experimental high energy physics literature for the years 1985 to 1989. No actual data are given, but approximately 3500 papers are indexed by Beam/Target/Momentum, Reaction/Momentum (including the final state), Final State Particle, and Accelerator/Experiment/ Detector. DOE

N91-23857# Oak Ridge National Lab., TN.
FEW-BODY PROBLEMS, ELECTRON-CORRELATION EFFECTS, AND BEYOND
R. A. Phaneuf 1 Apr. 1991 11 p
(Contract DE-AC05-84OR-21400)
(DE91-010030; ORNL/FTR-3875) Avail: NTIS HC/MF A03

The Third US-Mexico Cooperative Joint Symposium on Atomic and Molecular Physics drew 50 participants from Mexico, the United States, and Europe. The theme of the symposium/workshop was Few-body problems, electron-correlation effects, and beyond. Among the 42 invited speakers were many distinguished atomic physicists who presented recent research results and perspectives in a workshop atmosphere. A well-balanced program covered most aspects of atomic and molecular collision physics. Particular excitement was generated by new experimental results reported for laser-stimulated radiative recombination of electrons with protons, and by theoretical results on the role of scarred wavefunctions as manifestations of classical chaos in photoionization. DOE

N91-23858# Lawrence Livermore National Lab., CA.
MAGNETIC SUBSTATES POPULATED BY DOUBLE ELECTRON CAPTURE IN SLOW ION ATOM COLLISIONS
K. L. Randall 13 Dec. 1990 75 p
(Contract W-7405-eng-48)
(DE91-010122; UCRL-ID-106591) Avail: NTIS HC/MF A04

The work presented is the first measurement of the angular distribution of Auger electrons following double electron capture by a beam of slow highly charged ions. From this, relative cross sections for the population of individual M(sub L) substates were determined. DOE

N91-23859# Oak Ridge National Lab., TN.
MONTE CARLO SIMULATION OF SUPERCRITICAL SOLUTIONS IN THE GRAND CANONICAL ENSEMBLE
V. M. Shah, P. R. Bienkowski, and H. D. Cochran (Tennessee Univ., Knoxville.) 1991 8 p Presented at the 2nd International Conference on Supercritical Fluids, Boston, 20-22 May 1991
(Contract DE-AC05-84OR-21400)
(DE91-009152; CONF-9105137-2) Avail: NTIS HC/MF A02

Molecular simulations have been undertaken of pure, repulsive, and attractive supercritical Lennard-Jones solutions using the Monte Carlo technique in the grand canonical ensemble for the same systems and states used in a previous study by the molecular dynamics technique in the canonical ensemble. The pure supercritical fluid exhibited structure which differed somewhat between the canonical and grand canonical simulations at distances of three or four diameters from a central particle. The grand canonical simulation was shown to have chemical potential in agreement with the calculations from the equation of state and to be thermodynamically consistent. Simulations of the repulsive mixture in the grand canonical ensemble were characterized by substantial statistical scatter so that the special capabilities of the grand canonical simulation -- fluctuation analysis and thermodynamic consistency testing -- could not be employed. The attractive supercritical mixture studied previously was found to be within the two-phase region when studied in the grand canonical ensemble. The only previous simulation of mixtures in the grand canonical ensemble did not attempt to apply the fluctuation analysis or the thermodynamic consistency test; so, the negative results of this work are new. DOE

N91-23860# California Univ., Berkeley. Lawrence Berkeley Lab.
INVESTIGATION OF NEUTRAL ATOM AND ION EMISSION DURING LASER CONDITIONING OF MULTILAYER HfO2-SiO2 COATINGS
M. Schildbach, L. L. Chase, and A. V. Hamza 1990 9 p Presented at the 22nd Boulder Damage Symposium, Boulder, 25-26 Oct. 1990
(Contract W-7405-eng-48)
(DE91-009749; UCRL-JC-105106; CONF-9010287-7) Avail: NTIS HC/MF A02

It has been recently shown that the optical damage thresholds of multilayer coatings can be increased by up to a factor of two by conditioning the coating at laser fluences below the optical damage threshold. The laser conditioning mechanism of HfO2-SiO2 coatings was studied by observing the laser induced emission of neutral constituents of the coatings during laser conditioning. They observe the ejection of Hf, Si and oxygen (O or O2, or both) neutrals starting at fluences of about 10 J/sq cm, considerably below our measured unconditioned damaged threshold of about 16 to 18 J/sq cm. A threshold pulse fluence was observed for laser conditioning, which is also about 10 J/sq cm. This identical threshold for neutral emission and laser conditioning suggests that the neutral emission is caused by the laser conditioning process. The emitted neutrals have extremely high kinetic energies, on the order of several tens of eV. On the basis of this information, they propose that the laser conditioning process is caused by microscopic damage that involves cracking of the coating layers, resulting in the ejection of the high energy particles via a fractoemission process. This microscopic damage apparently raises the damage threshold by either reducing the absorption of coating defects or by relieving the thermal stresses that cause cracking, particle emission, and possible plasma formation by laser ionization of the neutrals. DOE

N91-23861# Argonne National Lab., IL.
COMMENT ON: ANALYTIC SOLUTION OF THE STOCHASTIC-LIOUVILLE MODEL OF SPIN-EXCHANGE
D. M. Bartels and R. G. Lawler 1991 5 p
(Contract W-31-109-eng-38)
(DE91-010570; ANL/PP-67244) Avail: NTIS HC/MF A01

In the title article, an analytical expression was derived for the rate constant for Heisenberg exchange between free radicals in solution based on a realistic model of the exchange interaction and the stochastic Liouville description of radical pair dynamics. The resulting rate constant was then evaluated relative to the recombination rate constant for the reactive radical CH2OO(-) using data reported some time ago by Syage, et. al. It was concluded that the exchange includes a substantial long-range component mediated by the solvent. In repeating this calculation, however, we find that an important statistical factor was omitted, and it is in fact necessary to postulate long-range exchange in this system. DOE

N91-23862# Argonne National Lab., IL.
RECENT RESULTS AND FUTURE PROSPECTS FOR THE POLARIZED BEAM AT FERMILAB
A. Yokosawa 1990 10 p Presented at the Polarized Collider Workshop, University Park, 15-17 Nov. 1990
(Contract W-31-109-eng-38)
(DE91-010590; ANL-HEP-CP-91-03; CONF-9011177-7) Avail: NTIS HC/MF A02

We summarize activities concerning the Fermilab polarized beams. Included are a brief description of the polarized-beam facility, measurements of beam polarization by polarimeters, asymmetry measurements in the pi(sup o) production at high p(sub perpendicular) and in the lambda(sigma(sup o)), pi(sup +/-), pi(sup o) production at large x(sub F), and delta(sigma(sub L)) (pp, (anti p)p) measurements (Fermilab E-704). In the future we plan to investigate the proton-spin crisis by determining the gluon spin distribution in inclusive production of direct gamma, chi(sup 2), and and J/psi. DOE

N91-23863# Pennsylvania Univ., Philadelphia. Dept. of Physics.
THE SUDBURY NEUTRINO OBSERVATORY PROJECT AND THE KAMIOKANDE 2 PROJECT
E. W. Beier Mar. 1991 10 p
(Contract DE-FG02-88ER-40479)
(DE91-010641; DOE/ER-40479/3) Avail: NTIS HC/MF A02

This document is a technical progress report on work performed at the University of Pennsylvania during the current year on the Sudbury Neutrino Observatory project and on the Kamiokande II project. The motivation for both experiments is the measurement of neutrinos emitted by the sun. The Kamiokande II experiment was an adaptation of an existing nucleon decay detector located in Japan to search for neutrinos emitted by the sun. It has been operational since 1986. Data taking was concluded in 1990 and work will terminate at the end of this grant year. The topics discussed in this report are: the Sudbury Neutrino Observatory project; photomultiplier tube measurements; photomultiplier bases; signal processing electronics; electronics system issues; software management and development; and Kamiokande II. DOE

N91-23864# Oak Ridge National Lab., TN.
COMPUTED SECONDARY-PARTICLE ENERGY SPECTRA FOLLOWING NONELASTIC NEUTRON INTERACTIONS WITH C-12 FOR E(n) BETWEEN 15 AND 60 MeV: COMPARISONS OF RESULTS FROM TWO CALCULATIONAL METHODS
J. K. Dickens Apr. 1991 71 p
(Contract DE-AC05-84OR-21400)
(DE91-010454; ORNL/TM-11812) Avail: NTIS HC/MF A04

The organic scintillation detector response code SCINFUL has been used to compute secondary-particle energy spectra, d(sigma)/dE, following nonelastic neutron interactions with C-12 for incident neutron energies between 15 and 60 MeV. The resulting spectra are compared with published similar spectra computed by Brenner and Prael who used an intranuclear cascade code, including alpha clustering, a particle pickup mechanism, and a theoretical approach to sequential decay via intermediate particle-unstable states. The similarities of and the differences between the results of the two approaches are discussed. DOE

N91-23865# Lawrence Livermore National Lab., CA.
SURFACE ELECTRON EMISSION INDUCED BY SLOW MULTICHARGED IONS
J. N. Bardsley and B. M. Penetrante 1 Feb. 1991 8 p Presented at the Symposium on Surface Science, Obertraun, Austria, 10-16 Feb. 1991
(Contract W-7405-eng-48)
(DE91-010469; UCRL-JC-106476; CONF-9102102-1) Avail: NTIS HC/MF A02

At the recent workshop on highly charged ions at Giessen, Hanspeter Winter presented a fascinating paper entitled, What ions experience on their way into a metal surface. The discussion follows the traditional approach which we will term the adiabatic quantum model (AQM). The electrons are drawn from the metal to the ion when the attractive potentials binding electrons to the solid and ionic nucleus overlap and the intervening barrier disappears. For highly charged ions this process, called resonance neutralization, transfers the electrons into orbits with very large principle quantum numbers. These weakly bound electrons then exchange energy through their Coulomb interactions, some rising into continuum states and others falling into more deeply bound levels. The rate at which this process occurs is estimated from Auger rates assuming between stationary quantum states. This is not simple, since there is little information on this process for such high quantum numbers, and very many states are involved. In this talk we will present an alternative picture (CDM) based upon elementary field emission theory and a classical description of the dynamics of the plasma formed by the emitted electrons. Since the quantum level spacings are so low and very little time is spent by each electron in a specific quantum state, we believe that the use of classical dynamics will lead to a more accurate description than could be obtained using quantum theory with current computers. Furthermore, the treatment of the simultaneous interactions between many charged particles is much simpler in classical mechanics. DOE

N91-23866# Argonne National Lab., IL.
COLD MODERATORS FOR PULSED NEUTRON SOURCES
J. M. Carpenter 1990 25 p Presented at the International Workshop on Cold Neutron Sources, Los Alamos, 5-8 Mar. 1990
(Contract W-31-109-eng-38)
(DE91-010594; ANL/CP-72633; CONF-9003100-5) Avail: NTIS HC/MF A03

This paper reviews cold moderators in pulsed neutron sources and provides details of the performance of different cold moderator

materials and configurations. Analytical forms are presented which describe wavelength spectra and emission time distributions. Several types of cooling arrangements used in pulsed source moderators are described. Choices of materials are surveyed. The author examines some of the radiation damage effects in cold moderators, including the phenomenon of burping in irradiated cold solid methane. DOE

N91-23867# General Electric Co., Schenectady, NY. Knolls Atomic Power Lab.
BENCHMARK MEASUREMENTS AND CALCULATIONS OF A 3-DIMENSIONAL NEUTRON STREAMING EXPERIMENT
D. A. Barnett, Jr. Feb. 1991 37 p Presented at the International Topical Meeting on Advances in Mathematics, Computation and Reactor Physics, Pittsburgh, 28 Apr. - 2 May 1991
(Contract DE-AC12-76SN-00052)
(DE91-010692; KAPL-4721; CONF-910414-33) Avail: NTIS HC/MF A03

An experimental assembly known as the Dog-Legged Void assembly was constructed to measure the effect of neutron streaming in iron and void regions. The primary purpose of the measurements was to provide benchmark data against which various neutron transport calculation tools could be compared. The measurements included neutron flux spectra at four places and integral measurements at two places in the iron streaming path as well as integral measurements along several axial traverses. These data have been used in the verification of Oak Ridge National Laboratory's three-dimensional discrete ordinates code, TORT. For a base case calculation using one-half inch mesh spacing, finite difference spatial differencing, an S(sub 16) quadrature and P(sub 1) cross sections in the MUFT multigroup structure, the calculated solution agreed to within 18 percent with the spectral measurements and to within 24 percent of the integral measurements. Variations on the base case using a fewgroup energy structure and P(sub 1) and P(sub 3) cross sections showed similar agreement. Calculations using a linear nodal spatial differencing scheme and fewgroup cross sections also showed similar agreement. For the same mesh size, the nodal method was seen to require 2.2 times as much CPU time as the finite difference method. A nodal calculation using a typical mesh spacing of 2 inches, which had approximately 32 times fewer mesh cells than the base case, agreed with the measurements to within 34 percent and yet required on 8 percent of the CPU time. DOE

N91-23868# Iowa State Univ. of Science and Technology, Ames.
INTERMEDIATE/HIGH ENERGY NUCLEAR PHYSICS
1991 14 p
(Contract DE-FG02-87ER-40371)
(DE91-010702; DOE/ER-40371/4) Avail: NTIS HC/MF A03

This progress report discusses: the quark cluster model; solving quantum field theories in non-perturbative regime; relativistic wave equations, quarkonia and e(sup +)e(sup (minus)) resonances; thermal properties of nuclei; and relativistic heavy ions and other projects. DOE

N91-23869# Vanderbilt Univ., Nashville, TN. Dept. of Physics and Astronomy.
MICROSCOPIC HEAVY-ION THEORY
V. E. Oberacker and A. S. Umar 1991 9 p
(Contract DE-FG05-87ER-40376)
(DE91-010739; DOE/ER-40376/4) Avail: NTIS HC/MF A02

This report discusses the following topics: EM lepton pair production in relativistic heavy ion collisions; string-parton model for relativistic heavy ion collisions; study of fission dynamics via muon-induced fission; mean-field studies with B-splines; the Basis-Spline collocation method; and relativistic generalization of the collective model. DOE

N91-23870# Texas A&M Univ., College Station. Cyclotron Inst.
EXCITATION OF ATOMS AND MOLECULES IN COLLISIONS WITH HIGHLY CHARGED IONS
R. L. Watson 1 Mar. 1991 5 p
(Contract DE-FG05-84ER-13262)
(DE91-010740; DOE/ER-13262/7) Avail: NTIS HC/MF A01

Much of the work this year has been directed toward studies of charge exchange and ionization in single collisions of heavy ions with gaseous atoms and molecules. A study of the double ionization of He by high energy N(sup 7+) ions, which began last year, was extended up in energy to 40 MeV/amu. These measurements verified the deviations from the predictions of theory observed in our previous work and indicated that the energy required to reach the limiting value of the ratio of double-to-single ionization cross sections may be as high as 70 MeV/amu. DOE

N91-23871# Georgia State Univ., Atlanta. Dept. of Physics and Astronomy.
LIGHT PARTICLE EMISSIONS IN HEAVY ION REACTIONS
G. A. Petitt, Xin-Tao Liu, J. Smathers, and Ziang Zhang Mar. 1991 16 p
(Contract DE-FG05-84ER-40162)
(DE91-010746; DOE/ER-40162/T5) Avail: NTIS HC/MF A03

We are completing another successful year of experimental work at the Holifield Heavy Ion Research Facility (HHIRF), the Los Alamos white neutron source facility, Brookhaven National Laboratory (BNL) and Georgia State University (GSU). A paper on energy division between the two heavy fragments in deep inelastic reactions between (sup 58)Ni + (sup 165)Ho was published in Physical Review C during the year. We have partially completed analysis of the data on the (sup 32)S + (sup 93)Nb system taken with the HILI detector system at the HHIRF. This paper discusses work on these topics and discusses the setup of a neutron detector for a neutron reaction experiment. DOE

N91-23872# Cincinnati Univ., OH.
RESEARCH IN PARTICLE THEORY
F. Mansouri, P. Suranyi, L. C. R. Wijewardhana, and L. Witten Oct. 1990 15 p
(Contract DE-FG02-84ER-40153)
(DE91-010749; DOE/ER-40153/7) Avail: NTIS HC/MF A03

A 2+1 dimensional deSitter Chern-Simons theory has been constructed and shown to be consistent. Wilson loop variables have been computed and shown to close under Poisson bracket operation for N = 2 Poincare supergravity. It has also been shown that there are two equivalent pictures of describing two particle scattering in 2+1 dimensional gravity theory, which are related by multivaiued gauge transformations. We have generalized the Jackiw-Johnson sumrule, relating Goldstone boson decay constants to the dynamical masses of fermions, to an arbitrary symmetry group. We have analyzed dynamical parity breaking in 2+1 dimensional 4-fermi theories. Finally, we have found the partition function for a system of free parabosons and parafermions of order two. DOE

N91-23873# Oak Ridge National Lab., TN.
LOW-ENERGY COLLISIONS OF MULTIPLY CHARGED IONS WITH ELECTRONS, ATOMS AND SURFACES
R. A. Phaneuf, F. W. Meyer, D. C. Gregory, C. C. Havener, P. A. ZeijlmansvanEmmichoven, S. H. Overbury, D. M. Zehner, G. H. Dunn, J. S. Thompson, and E. K. Waahlin 1991 15 p Presented at the 3rd US/Mexico Atomic and Molecular Physics Workshop, Mexico City, Mexico, 13-16 Mar. 1991
(Contract DE-AC05-84OR-21400)
(DE91-010779; CONF-9103146-2) Avail: NTIS HC/MF A03

Results are presented from recent experiments at the Oak Ridge National Laboratory electron cyclotron resonance Multicharged Ion Research Facility which have addressed low-energy interactions of multiply charged ions with electrons, hydrogen atoms and metal surfaces. The specific processes for which results are reported are electron-impact excitation, electron capture and ion neutralization. The objective of these studies is a more detailed understanding of the mechanisms which govern the interactions of multicharged ions at low (or near-threshold) collision energies. DOE

N91-23874# Rome Univ. (Italy). Dipt. di Fisica.
STUDY OF THE RESPONSE OF A CRYSTAL BALL MADE OF NaI(Tl) FOR HEAVY IONS EXPERIMENTS [STUDIO DELLA RISPOSTA DI UNA CRISTAL BALL DI NAI(TI) PER ESPERIMENTI CON IONI PESANTI]
R. Marcovaldi (Istituto Nazionale di Fisica Nucleare, Rome, Italy) 6 Sep. 1990 14 p In ITALIAN
(Nota-Interna-957; ETN-91-98878) Avail: NTIS HC/MF A03

Angular correlation measurements and gamma decay multiplicity observations allow information on the angular momentum of the excited nucleii to be obtained. The characteristics of an experimental detector sphere built with 112 NaI(Tl) crystals in a spherical configuration with 30 cm radius are analyzed. This detector allows work up to 40 to 50 MeV in a total solid angle of 4pi/112. A Monte Carlo program was used to verify the algorithm used to calculate the angular distribution and multiplicity. ESA

N91-23875# Rome Univ. (Italy). Dipt. di Fisica.
THE BIRTH OF THE 'STRANGE' PARTICLE PHYSICS [LA NASCITA DELLA FISICA DELLE PARTICELLE 'STRANE']
M. Grilli and F. Sabastiani 18 Sep. 1990 62 p In ENGLISH and ITALIAN
(Nota-Interna-958; ETN-91-98879) Avail: NTIS HC/MF A04

The history of fundamental particles is discussed, from the discovery of the mu meson in 1944 to the quark theory in 1964. Letter fragments from Anderson, Blackett and Butler are included. ESA

N91-23876# Rome Univ. (Italy). Dipt. di Fisica.
EXPERIMENTS ON FRANK-HERTZ SETUP [ESPERIMENTI ALLA FRANCK-HERTZ]
V. Bouche 6 Nov. 1990 68 p In ITALIAN
(Nota-Interna-961; ETN-91-98882) Avail: NTIS HC/MF A04

Theoretical atomic physics subjects and experimental setups discussed in university teaching are presented. The subjects include: inelastic scattering; monochromatic electrons; particle collisions; cross sections; ionizing transitions; the original Frank-Hertz experiment; and sodium and mercury calculations. ESA

N91-23877# Rutherford High Energy Lab., Chilton (England). Particle Physics Experiments Selection Panel.
PARTICLE PHYSICS EXPERIMENTS, 1990
B. A. Roberts, comp. 1991 167 p
(RAL-91-001; ETN-91-99330) Avail: NTIS HC/MF A08

Work carried out on experiments relating to particle physics is described including: neutrino and antineutrino interactions with protons using a bubble chamber; A Two Arm Spectrometer Solenoid (TASSO); OPAL (Omni Purpose Apparatus for LEP (Large Electron Positron storage ring)); DELPHI (Detector with Lepton, Photon and Hadron Identification); H1 and ZEUS (detectors for HERA). Unedited contributions from 149 experiments are presented. ESA

N91-23878# Naval Research Lab., Washington, DC.
QUANTUM EXTENSION OF CHILD-LANGMUIR LAW
Y. Y. Lau, D. Chernin, D. G. Colombant, and P. T. Ho 18 Feb. 1991 13 p
(ARPA Order 4395)
(AD-A232407; NRL-MR-6782) Avail: NTIS HC/MF A03 CSCL 20/10

Using a simple mean field model of the electron-electron interaction, the effect was studied of space charge in a planar diode. The results show, in particular, that the classical value for the limiting current in such a diode can be exceeded by a large factor due to the effect of tunneling. The smooth transition of the solutions from the quantum to the classical (non-quantum) regime is demonstrated. GRA

N91-23879# Puerto Rico Univ., Rio Piedras. Dept. of Physics.
THE DIRECT CORRELATION FUNCTION OF A MIXTURE OF HARD IONS IN THE MEAN SPHERICAL APPROXIMATION Summary Report
L. Blum and Yaakov Rosenfeld (Israel Atomic Energy Commission, Beersheba.) 29 Jan. 1991 10 p Submitted for publication
(Contract N00014-90-J-1263)
(AD-A232452; TR-1) Avail: NTIS HC/MF A02 CSCL 20/3

It is shown that the direct correlation function of a mixture or hard ions in the mean spherical approximation of Hiroike, (MSA) can be expressed in terms of overlap functions of charged spherical spherical shells. In particular, if the system has a mixture of pairs of ions of equal size and opposite charge, then the MSA direct correlation function is given by the electrostatic energy of a pair of charged function is given by the electrostatic energy of a pair of charged shells, of radius equal to the radius of the hard ion plus 1/21. As in the theory of Rosenfeld this direct correlation function can be derived from a free energy functional, and a simple extension to non-uniform systems is given. GRA

N91-23880# Puerto Rico Univ., Rio Piedras. Dept. of Physics.
IN-SITU SURFACE X RAY SCATTERING MEASUREMENTS OF ELECTROCHEMICALLY DEPOSITED BISMUTH ON SILVER (III): STRUCTURE, COMPRESSIBILITY, AND COMPARISON WITH EX-SITU LEED MEASUREMENTS Summary Report
Michael F. Toney, Joseph G. Gordon, Mahesh G. Samant, Gary L. Borges, and David G. Wiesler 29 Jan. 1991 32 p Prepared in cooperation with IBM Research Lab., San Jose, CA, and Washington Univ., Seattle
(Contract N00014-90-J-1263)
(AD-A232624; TR-4) Avail: NTIS HC/MF A03 CSCL 20/8

We report in-situ surface x ray scattering measurements of the structure and compressibility of electrochemically deposited Bi monolayers on Ag(111) and compare the in-situ structure with results from previous ex-situ experiments on emersed electrodes, where the structure was studied with low-energy diffraction (LEED). We find that the Bi monolayer forms an unusual structure: a two-dimensional rectangular lattice is uniaxially commensurate with the hexagonal Ag (111) surface along the Ag zone axes (2'11) direction. There are two Bi adatoms per rectangular unit cell and one adatom is displaced from the centered-rectangular position by approximately or equal to 0.25 A along the commensurate direction. The displacement shortens two of the Bi-Bi near-neighbor bond distances but lengthens two others and may reflect the tendency toward covalent bonding in Bi. With increasing coverage (Decreasing applied potential), the Bi monolayer compresses uniaxially along the incommensurate direction Ag zone axes (011'), which preserves the uniaxially commensurate structure. GRA

N91-23881# Princeton Univ., NJ. Dept. of Chemistry.
MOLECULAR DYNAMICS SIMULATOR FOR OPTIMAL CONTROL OF MOLECULAR MOTION Final Report, 20 Sep. 1989 - 19 Sep. 1990
Herschel Rabitz 12 Dec. 1990 27 p
(Contract DAAL03-89-K-0173)
(AD-A232801; ARO-27577.1-CH) Avail: NTIS HC/MF A03 CSCL 20/5

In recognition of recent interest in developing optimal control techniques for manipulating molecular motion, this paper introduces a computer-driven electro-mechanical analog of this process. The resultant Molecular Dynamic Simulator (MDS) is centered around a linear air track for which the atoms of the controlled molecule are simulated as nearly frictionless carts on the track. Bonds in the simulated molecule are described by precision springs, and the interaction with an external optical field is simulated through a computer-based linear driver. When the MDS is operated in the harmonic regime, it can be used as an exact analog of molecular scale quantum systems through Ehrenfest's Theorem, or equivalently as a classical set of coupled oscillators. The tools of optimal control theory currently being applied at the molecular scale are used to design the forcing function for the MDS. Optical encoders are used to measure bond distances for graphic representation of the MDS behavior. Bond breaking can also be simulated by bond-length sensitive trigger-release mechanisms. The MDS is especially useful as a modelling tool to bridge theoretical studies and eventual laboratory experiments at the true molecular scale. GRA

73 NUCLEAR AND HIGH-ENERGY PHYSICS

Includes elementary and nuclear particles; and reactor theory.

For space radiation see *93 Space Radiation.*

N91-23882# California Univ., Berkeley. Lawrence Berkeley Lab.

CALCULATION OF CROSS SECTIONS FOR BINARY REACTIONS BETWEEN HEAVY ION PROJECTILES AND HEAVY ACTINIDE TARGETS

D. C. Hoffman and M. M. Hoffman Nov. 1990 42 p
(Contract DE-AC03-76SF-00098)
(DE91-010222; LBL-29502) Avail: NTIS HC/MF A03

The computer program, described in this report, is identified as PWAVED5. It was developed to calculate cross sections for nucleon transfer reactions in low energy heavy ion bombardments. The objective was to calculate cross sections that agree with experimental results for ions of different charge and mass and to develop a predictive capability. It was undertaken because previous heavy ion calculations, for which programs were readily available, appeared to focus primarily on reactions resulting in compound nucleus formation and were not particularly applicable to calculations of binary reaction cross sections at low interaction energies. There are to principal areas in which this computation differs from several other partial wave calculations of heavy-ion reaction cross sections. First, this program is designed specifically to calculate cross sections for nucleon exchange interactions and to exclude interactions that are expected to result in fusion of the two nuclei. A second major difference in this calculation is the use of a statistical distribution to assign the total interaction cross section to individual final mass states. DOE

N91-23883# Oak Ridge National Lab., TN.

PRESSURE DYNAMICS MODELING FOR THE DESIGN OF THE ADVANCED NEUTRON SOURCE REACTOR

M. I. Khayat, H. L. Dodds (Tennessee Univ., Knoxville.), and J. March-Leuba 1991 6 p Presented at the Annual Meeting of the American Nuclear Society (ANS), Orlando, 2-6 Jun. 1991
(Contract DE-AC05-84OR-21400)
(DE91-007860; CONF-910603-8) Avail: NTIS HC/MF A02

This paper summarizes the development of a computer model to study the pressure and flow dynamics of the Advanced Neutron Source (ANS) reactor. Included in this paper are some applications of this model to aid in the conceptual design of the reactor cooling systems. The ANS will be primarily a neutron scattering facility, but it is also being designed for isotope production and irradiation experiments. To accomplish these goal, the ANS design is based on a high power (362 MW(sub fis)) compact core (67 L) surrounded by a large (1.75 m radius) D2O reflector where most of the neutrons generated in the core by fission are moderated and available for scattering experiments. DOE

N91-23884# Edgerton, Germeshausen and Grier, Inc., Idaho Falls, ID.

GAS CORE REACTORS FOR DIRECT NUCLEAR PROPULSION

B. G. Schnitzler Jun. 1990 120 p
(Contract DE-AC07-76ID-01570)
(DE91-010050; EGG-NE-9087) Avail: NTIS HC/MF A06

Gas core nuclear reactors offer the potential for achieving very high specific impulse in a space propulsion engine. The absence of any solid material in the core allows operation with propellant exhaust temperatures in excess of 10,000 K. Specific impulses above 19,600 m/s (2000 seconds) can be achieved with hydrogen at these conditions. An EG and G Exploratory Research and Development Program (ERDP) was initiated at Idaho National Engineering Laboratory with the objectives of developing gas core reactor analysis capability and performing a preliminary performance characterization of the gas core direct nuclear propulsion engines. This report summarizes the analytical methods development and the results of the preliminary gas core characterization efforts. DOE

N91-23885# Sandia National Labs., Albuquerque, NM.

PULSED POWER PERFORMANCE OF THE NEW RLA (RECIRCULATING LINEAR ACCELERATOR)

D. L. Smith, M. G. Mazarakis, L. F. Bennett, and W. R. Olson 1991 2 p Presented at the 8th IEEE Pulsed Power Conference, San Diego, 17-19 Jun. 1991
(Contract DE-AC04-76DP-00789)
(DE91-004723; SAND-90-2883C; CONF-910640-1) Avail: NTIS HC/MF A01

The Recirculating Linear Accelerator (RLA) is returning to operation with a new electron beam injector and a modified accelerating cavity. Upon completion of our experimental program the RLA will capture the injected beam on an IFR guiding plasma channel in either a spiral or a closed racetrack drift tube. The relativistic beam will be efficiently recirculated for up to four passes through two or more accelerating cavities, in phase with the ringing cavity voltage waveforms, and thereby increased in energy to 10 MeV before being extracted. The inductively isolated four-stage injector was designed to produce beam parameters of 4 MeV, 10 to 20 kA, and 40 to 55 ns FWHM. The three-line radial cavity is being modified to improve the 1 MV accelerating voltage pulse shape while an advanced cavity design study is in progress. The actual versus predicted pulsed-power performance of the RLA injector and cavity and the associated driving hardware is discussed. DOE

N91-23886# Brookhaven National Lab., Upton, NY.

LECTURES ON ACCELERATOR PHYSICS

A. Luccio 11 Mar. 1991 90 p Presented at the School on Electromagnetic Interactions With Intermediate Energy Hadrons, Folgaria (Italy), 27 Jan. - 3 Feb. 1991
(Contract DE-AC02-76CH-00016)
(DE91-010376; BNL-45935; AGS/AD-91-1; CONF-910195-1-Exc)
Avail: NTIS HC/MF A05

This report contains lecture notes on beam dynamics and acceleration concepts in particle accelerators. The following subject areas are covered: electromagnetic probes; electron beams; electron storage ring; electron linac; and classical microtron. DOE

N91-23887*# California Univ., Berkeley.

SCIENCE REQUIREMENTS FOR HEAVY NUCLEI COLLECTION (HNC) EXPERIMENT ON NASA LONG DURATION EXPOSURE FACILITY (LDEF) MISSION 2 Final Report

P. Buford Price Jun. 1991 77 p
(Contract NAS1-17806)
(NASA-CR-187527; NAS 1.26:187527) Avail: NTIS HC/MF A05 CSCL 20H

The Heavy Nuclei Collection (HNC) is a passive array of stacks of a special glass, 14 sheets thick, that record tracks of ultraheavy cosmic rays for later readout by automated systems on Earth. The primary goal is to determine the relative abundances of both the odd- and even-Z cosmic rays with Z equal to or greater than 50 with statistics a factor at least 60 greater than obtained in HEAO-3 and to obtain charge resolution at least as good as 0.25 charge unit. The secondary goal is to search for hypothetical particles such as superheavy elements. The HNC detector array will have a cumulative collection power equivalent to flying 32 sq m of detectors in space for 4 years. The array will be flown as a free-flight spacecraft and/or attached to Space Station Freedom. Author

N91-23888# Naval Research Lab., Washington, DC.

DENSITY CHANNEL TRACKING STUDIES ON PULSERAD Memorandum Report

D. P. Murphy, R. E. Pechacek, D. P. Taggart, and R. A. Meger 2 Mar. 1991 34 p
(AD-A232649; NRL-MR-6770) Avail: NTIS HC/MF A03 CSCL 20/7

High current charged particle beams can be guided by reduced density channels. This tracking occurs when the distribution of plasma currents in the density channel causes a net attractive force to be exerted on the electron beam. A relativistic electron

beam injected parallel to a spatially offset reduced density channel is pulled toward the channel. The force exerted on the beam is predicted to increase as the beam current increases and as the offset between the beam and the channel increases out to offsets equal to the beam radius. An experiment with a 1-MV, 10 kA beam was performed which demonstrates this effect. GRA

74 OPTICS

Includes light phenomena; and optical devices.
For lasers see *36 Lasers and Masers.*

N91-23889*# National Aeronautics and Space Administration. Langley Research Center, Hampton, VA.
NON-MECHANICAL OPTICAL PATH SWITCHING AND ITS APPLICATION TO DUAL BEAM SPECTROSCOPY INCLUDING GAS FILTER CORRELATION RADIOMETRY Patent Application
Glen W. Sachse, inventor (to NASA) and Liang-Guo Wang, inventor (to NASA) (College of William and Mary, Hampton, VA.) 11 Feb. 1991 19 p
(NASA-Case-LAR-14588-1-CU; NAS 1.71:LAR-14588-1-CU; US-Patent-Appl-SN-653605) Avail: NTIS HC/MF A03 CSCL 20F

A non-mechanical optical switch is provided for alternately switching a monochromatic or quasi-monochromatic light beam along two optical paths. A polarizer polarizes light into a single, e.g., vertical component which is then rapidly modulated into vertical and horizontal components by a polarization modulator. A polarization beam splitter then reflects one of these components along one path and transmits the other along the second path. In the specific application of gas filter correlation radiometry, one path is directed through a vacuum cell and one path is directed through a gas correlation cell containing a desired gas. Reflecting mirrors cause these two paths to intersect at a second polarization beam splitter which reflects one component and transmits the other to recombine them into a polarization modulated beam which can be detected by an appropriate single sensor. NASA

N91-23890*# National Aeronautics and Space Administration. Pasadena Office, CA.
REAL TIME PRE-DETECTION DYNAMIC RANGE COMPRESSION Patent Application
Hua-Kuang Liu, inventor (to NASA) (Jet Propulsion Lab., California Inst. of Tech., Pasadena.) 5 Dec. 1990 15 p
(Contract NAS7-918)
(NASA-Case-NPO-18098-1-CU; NAS 1.71:NPO-18098-1-CU; US-Patent-Appl-SN-633746) Avail: NTIS HC/MF A03 CSCL 20F

A real time, pre-detection optical dynamic range compression system uses a photorefractive crystal, such as BaTiO3 or LiNbO3, in which light induced scattering from crystal inhomogeneities of the optical input occurs as a nonlinear function of the input intensity. The greater the intensity, the faster random interference gratings are created to scatter the incident light. The unscattered portion of the optical signal is therefore reduced in dynamic range over time. The amount or range of dynamic range compression may be controlled by adjusting the time of application of the unscattered crystal output to the photodetector with regard to the time of application of the optical input to the crystal. NASA

N91-23891*# Polatomic, Inc., Richardson, TX.
METAL THIN-FILM OPTICAL POLARIZERS FOR SPACE APPLICATIONS, PHASE 2 Final Report
Robert E. Slocum 28 May 1991 124 p
(Contract NAS7-1037)
(NASA-CR-188202; NAS 1.26:188202) Avail: NTIS HC/MF A06 CSCL 20F

A light polarizing material was developed for wavelengths in the visible and near infrared spectral band (400 to 3,000 nm). The material is comprised of ellipsoidal silver particles uniformly distributed and aligned on the surface of an optical material. A method is set forth for making polarizing material by evaporatively coating a smooth glass surface with ellipsoidal silver particles. The wavelength of peak absorption is chosen by selecting the aspect ratio of the ellipsoidal metal particles and the refractive index of the material surrounding the metal particles. The wavelength of peak absorption can be selected to fall at a desired wavelength in the range from 400 to 3,000 nm by control of the deposition process. This method is demonstrated by evaporative deposition of silver particles directly on to a smooth optical surface. By applying a multilayer silver coating of a glass disc, a contrast of greater than 40,000 was achieved at 590 nm. A polarizing filter was designed, fabricated, and assembled which achieved contrast of 100,00 at 59 nm and can serve as a replacement for crystal polarizers. Author

N91-23892# Sandia National Labs., Albuquerque, NM.
MEASUREMENTS OF PASSIVE-SCALAR SPECTRA FOR GRID TURBULENCE USING A NONLINEAR OPTICAL TECHNIQUE
T. J. OHern, J. R. Torczynski, D. R. Neal, R. N. Shagam, and H. F. Robey (Lawrence Livermore National Lab., CA.) 1991 18 p Presented at the 1st ASME/JSME Fluids Engineering Conference, Portland, 23-26 Jun. 1991
(Contract DE-AC04-76DP-00789)
(DE91-005310; SAND-90-2541C; CONF-910684-1) Avail: NTIS HC/MF A03

A nonlinear optical technique has been applied to grid turbulence measurements. A laser beam passing through a turbulent region acquires phase perturbations related to the density perturbations it encounters. If the laser beam is then passed through a crystal of barium titanate (BaTiO3), a photorefractive nonlinear optical material, the small-amplitude perturbations to the beam are passed but the large-amplitude unperturbed portion of the beam is deflected away from the beam path. An optical Fourier transform of the perturbations performed by a lens yields the two-dimensional density-perturbation (passive-scalar) spectrum at the lens focal plane or, alternatively, a photorefractive schlieren photograph at the lens image plane. As a test application for this technique, a system was assembled to study the downstream evolution of the density-perturbation spectrum in grid turbulence produced by an electrically heated screen spanning the test section of a wind tunnel. Near the screen, the spectrum is found to consist primarily of large-amplitude peaks at the fundamental and the first few harmonics of the screen-wake spatial frequency. As expected, these amplitudes are observed to decay rapidly in the downstream direction. DOE

N91-23893# Oak Ridge National Lab., TN.
TWO-CHANNEL SPECTROSCOPIC POLARIZATION MODULATION ELLIPSOMETRY
G. E. Jellison, Jr. Mar. 1991 22 p Presented at the International Conference on Metallurgical Coatings and Thin Films, San Diego, 22-26 Apr. 1991
(Contract DE-AC05-84OR-21400)
(DE91-010131; CONF-9104187-1) Avail: NTIS HC/MF A03

A new spectroscopic ellipsometer is described, where the incoming light is dynamically polarized using a photoelastic modulator, and the reflected light is separated into orthogonally polarized beams using a Wollaston prism. Both beams are detected using photomultiplier tubes whose bias voltage is dynamically controlled for constant dc. All three of the associated ellipsometry parameters (N = cos2 psi, S = sin2 psi sin Delta, C = sin2 psi cos Delta) can be determined simultaneously in a single scan (240 to 840 nm or 5.16 to 1.47 eV). This instrument was used to study the optical properties of thin SiO2 films from 3 to 325 nm in thickness. Using a biased estimator fitting technique, the raw ellipsometric data can be fit to an air-SiO2 interface-Si model, where the optical functions of the SiO2 layer and the interface region are approximated using a one-term Sellmeier approximation, and a 50 pct. voids, 50 pct. SiO2 Bruggeman effective medium approximation, respectively. The refractive index of the SiO2 layer is dependent on film thickness, increasing with decreasing film thickness, but always being greater than fused quartz. The thickness of the interfacial region increases with increasing film

thickness, being less than 0.2 nm for film thicknesses less than 20 nm. DOE

N91-23894# Edgerton, Germeshausen and Grier, Inc., Los Alamos, NM.
DESIGN OF A TWENTY-ELEMENT LONG FOCAL LENGTH ZOOM LENS
R. M. Malone, B. C. Frogget, D. A. Grafton, and F. R. Mitchell 1990 7 p Presented at the 34th SPIE Annual International Technical Symposium on Optical and Optoelectronic Applied Science and Engineering, San Diego, 8-13 Jul. 1990
(Contract DE-AC08-88NV-10617)
(DE91-010770; EGG-10617-5039; CONF-900756-60) Avail: NTIS HC/MF A02

An optical lens system with varying magnification has been designed for a 70-mm image format. Twenty optical elements were needed to provide for the 345- to 1050-mm focal length zoom range as well as the proper color correction over the visible spectrum. A 4-in diameter port window limits the f/(number sign) of the optical lens system. Operation of the lens system is done by actuating stepping motors through a MacPlus computer. This lens system was designed for Los Alamos National Laboratory Group M-8, because no commercial zoom lens existed that would change its reduction from 1/15 to 1/4 at a focusing range of 5 meters. Additionally, we required a larger, non-standard image size that could be recorded by a rotating mirror streak camera. A Nikkor lens sales manual does offer a long focal length, 35-mm lens only upon special order. The closest focusing range of this Nikkor lens is 6 meters. DOE

N91-23895# Rome Univ. (Italy). Dipt. di Fisica.
DEVELOPMENT OF A DIGITAL CORRELATOR TO MEASURE THE SEMI-ELASTIC SCATTERING OF LIGHT [SVILUPPO DI UN CORRELATORE DIGITALE PER MISURE DI SCATTERING QUASI ELASTICO DELLA LUCE]
G. Bolle and P. Codastefano 30 Jul. 1990 23 p In ITALIAN
(Nota-Interna-955; ETN-91-98876) Avail: NTIS HC/MF A03

Light scattering is discussed. The time autocorrelation concept is introduced to study the possibility of clipping a signal, considering a limited sequence of events only. In this way a linearity is obtained between the pulses autocorrelation and the scattered light intensity. The implementation of a digital correlator for very fast counts (10(exp -8) intervals) is described. ESA

N91-23896# Cornell Univ., Ithaca, NY. School of Applied and Engineering Physics.
WAVELENGTH INDEPENDENT OPTICAL LITHOGRAPHY AND MICROSCOPY Final Report, 1 Sep. 1987 - 31 Aug. 1990
Michael Isaacson 30 Oct. 1990 48 p
(Grant AF-AFOSR-0381-87; AF Proj. 2306)
(AD-A232036; AFOSR-91-0022TR) Avail: NTIS HC/MF A03 CSCL 20/6

During the past contract period we have successfully established the field or near-field optics and subwavelength light beam technology. We have experimentally verified some of the physical parameters upon which the collimation of light in the near-field depends and have demonstrated that collimation better than one tenth the wavelength can be achieved in both transmission imaging and reflection imaging. We have also verified that lithographic replication at one fifth the wavelength is attainable. In addition, we have also demonstrated that darkline defects in GRIN-SCH-SQW diode lasers can be directly observed at high spatial resolution using methods of lenseless near-field imaging. GRA

N91-23897# Arizona State Univ., Tempe.
MAGNETO-OPTICAL PROPERTIES OF QUANTUM WELLS WITH ARBITRARY POTENTIAL PROFILES Final Report, 15 Sep. 1989 - 15 Aug. 1990
Krishan K. Bajaj 15 Aug. 1990 23 p
(Grant AF-AFOSR-0534-89; AF Proj. 2306)
(AD-A232037; AFOSR-91-0023TR) Avail: NTIS HC/MF A03 CSCL 20/3

Calculations were performed on the following problem areas: (1) binding energies and oscillator strengths of excitons in quantum wells in a magnetic field, (2) excitonic luminescence line shape due to interfacial quality in quantum wells in a magnetic field, (3) effect of magnetic field on the excitonic luminescence linewidth in semiconductor alloys, (4) binding energies and oscillator strengths of excitions in quantum wells of different potential profiles in the presence of a magnetic field, and (5) magneto-optics of coupled double quantum wells. GRA

N91-23898# Army Armament Research and Development Command, Dover, NJ. Fire Support Armament Center.
FIBER OPTIC SENSORS FOR THE MILITARY
Nanette M. Shoenfelt Feb. 1991 22 p
(AD-A232100; ARFSD-TR-90024) Avail: NTIS HC/MF A03 CSCL 20/6

Fiber optics have traditionally been used for communication systems. These fibers are convenient to use because they are not susceptible to electromagnetic interference. Now, fibers are being used in more fields. Sensors are a new application for fiber optics. They can be used to sense temperature, chemicals, and position. What makes optical fibers attractive for sensing is that different wavelengths of light can be used for different sensing applications. The military is now starting to use fiber optic sensors for the guidance and control of munitions. Author (GRA)

N91-23899# Army Missile Command, Redstone Arsenal, AL.
EVALUATION OF A FERROELECTRIC LIQUID CRYSTAL SPATIAL LIGHT MODULATOR Final Report
Tracy D. Hudson, R. K. Worcester, and Don A. Gregory 9 Jan. 1991 31 p
(AD-A232117; AD-E951609; AMSMI/TR-RD-RE-90-6) Avail: NTIS HC/MF A03 CSCL 20/6

Key performance characteristics of an optically-addressed ferroelectric liquid crystal spatial light modulator have been measured and compare favorably with other commercially available SLMs. Several characteristics which are important for optical pattern recognition, including imaging resolution, visibility, and response time, are discussed in this communication. The maximum resolution was measured to be 40 lp/mm with an imaging response time of 60 Hz. This differs substantially from previously published results. This is primarily due to operating the device so as to maintain good resolution with moderate illumination. Furthermore, experimental results to determine the modulated response of the read beam as a function of the write light intensity will also be presented. Author (GRA)

N91-23900# California Univ., Los Angeles.
LUMINESCENCE AND ABSORPTION SPECTRA OF C60 FILMS Technical Report No. 12, Jun. 1990 - Feb. 1991
Christian Reber, Lawrence Yee, John McKiernan, Jeffrey I. Zink, and R. S. Williams Feb. 1991 13 p
(Contract N00014-90-J-1178)
(AD-A232153) Avail: NTIS HC/MF A03 CSCL 20/6

Solid films of C-60 deposited on CaF2 under ultrahigh vacuum show luminescence in the 700 to 1100nm spectral range at 20 K. A 1400/cm progression in the a sub g soccerball inflation mode is observed. The low temperature absorption spectrum exhibits similar fine structure. The characterization of vibronic splittings in the ground and emitting state and the transition intensity mechanism are discussed. GRA

N91-23901# Calspan-Buffalo Univ. Research Center, NY.
PULSE COMPRESSION OF 100 PICOSECOND PULSES AT 1.319 MICRONS Final Report, May 1989 - May 1990
Jason P. Sokoloff, Steven T. Johns, Mark F. Krol, and John L. Stacy Dec. 1990 22 p Prepared in cooperation with Arizona Univ., Tucson
(Contract F30602-88-D-0026)
(AD-A232552; RADC-TR-90-389) Avail: NTIS HC/MF A03 CSCL 20/6

A facility providing temporally short pulses is extremely useful for investigating the limitations of optical detectors, or signal

processing networks. For instance, two picosecond (ps) pulses have a 500 GHz bandwidth and can therefore be used in experimental systems designed for operation one to two orders of magnitude faster than those presently in use. This report describes the fiber-grating pair optical pulse compression set-up which compresses 110 to 120 picosecond pulses, with a 1.319 micron wavelength, down to 1 to 2 ps. The exact temporal width of these pulses is measured by an autocorrelator. It is easy to compress pulses with a wavelength less than 1.32 micron if they have the following qualities: (1) their spectral bandwidth is larger than the inverse of their temporal pulse width, and (2) the instantaneous frequency varies linearly across the pulse (i.e., it has a linear chirp). In a fiber-grating pair compression stage the light pulse is first coupled into a fiber. GRA

N91-23902# Stanford Univ., CA. High Temperature Gasdynamics Lab.
ADVANCED DIAGNOSTICS FOR REACTING FLOWS Annual Report, 1 Oct. 1989 - 30 Sep. 1990
R. K. Hanson 29 Oct. 1990 36 p
(Grant AF-AFOSR-0067-89; AF Proj. 2308)
(AD-A232609) Avail: NTIS HC/MF A03 CSCL 14/2

The program aimed at establishing advanced optical diagnostic techniques applicable to combustion gases and plasmas, with some emphasis on high speed flows. The primary flowfields parameters of interest are species concentrations (including electrons), temperature, mass density, pressure, and velocity, and quantities derivable from these parameter such as mass flow rate (from the product of density and velocity). The techniques under study are based on laser spectroscopy, particularly laser absorption and laser induced fluorescence, with the latter capable of providing both single-point and multi-point (2-D and 3-D) measurements. Laser sources include tunable CW lasers (ring dye and semiconductor diode lasers) and tunable pulsed lasers (excimer-pumped dye and narrow-line width excimer). The CW laser are spectrally narrow, allowing study of a new class of techniques based on spectral lineshapes and shifts, while the pulsed lasers provide intense bursts of photons needed for techniques based on light-scattering phenomena. Accomplishments of note include: the first simultaneous measurements of temperature, pressure and velocity in high speed flows; the first application of tunable semiconductor diode lasers to absorption and fluorescence measurements in high temperature plasmas and supersonic flows; the first application of the planar laser-induced fluorescence (PLIF) technique to nonequilibrium shock tube flows; and further advances in the development of a laser-photolysis shock tube for rate constant measurements of elementary combustion reactions. GRA

N91-23903# Hughes Research Labs., Malibu, CA.
THEORY OF NOVEL NONLINEAR OPTICS Final Report, 1 Feb. 1988 - 31 Oct. 1990
Juan F. Lam Oct. 1990 119 p
(Contract F49620-88-C-0042)
(AD-A232659; HAC-REF-G3658) Avail: NTIS HC/MF A06 CSCL 20/6

A study of novel nonlinear optical processes is presented, along with comparison with available experimental data. Five key areas were investigated using novel theoretical approaches. Analysis of phase conjugate optics of rare earth doped solids predicts inhomogeneous saturation behavior, pair quenching effects and concentration dependent filtering property, in agreement with experiments. Theory of millimeter wave phase conjugation and novel modulation techniques for communication purposes in semiconductor superlattices are described. The physics of self-pumped phase conjugation in resonant systems are quantified, and the demonstration of a self-pumped phase conjugate mirror at diode laser wavelengths is achieved. A theoretical model, based on the Davydov Hamiltonian, gives absorption lineshapes in agreement with experiments, and predicts the onset of bistability and energy transfer in two-beam coupling. An analysis of the role of multiple longitudinal phonon coupling to Wannier excitions yields Fano-like profiles in four-wave mixing spectroscopy. GRA

N91-23904# Massachusetts Inst. of Tech., Cambridge. Research Lab. of Electronics.
ANALOG PROCESSING OF OPTICAL WAVEFRONTS USING INTEGRATED GUIDED-WAVE OPTICS Final Report, 15 Mar. 1987 - 31 Jul. 1990
Robert H. Rediker 30 Nov. 1990 40 p
(Contract F49620-87-C-0043)
(AD-A232703; AFOSR-91-0049TR) Avail: NTIS HC/MF A03 CSCL 20/6

Integrated Guided-Wave Optics has many advantages for the analog processing of optical wavefronts. These include small-size, high-speed, simplicity, reliability and reproducibility. The fabrication technique is similar to that of integrated circuits. The thrust of this program was to develop an integrated guided-wave optic system, in GaAs and GaAlAs for use at GaAs laser wavelength, to remove abberations from a laser beam and to steer the beam. The system would in addition have the capability to appropriately phase the outputs from a multiplicity of power amplifiers or injection-locked lasers. It was also the intent of the program to design and build the optical circuits so they are compatible with on-chip electronic circuits in order to minimize the required number of off-chip leads. The research program was proposed by MIT Research Laboratory of Electronics with part of the work being performed at MIT Lincoln Laboratory. In general, guided-wave component evaluation, analysis and understanding of optimization was performed at MIT Research Laboratory of Electronics, while the fabrication and actual optimization was performed at MIT Lincoln Laboratory. GRA

N91-23905# Sparta, Inc., Lexington, MA.
ULTRA-DENSE OPTICAL MASS STORAGE Final Report, 1 Sep. 1990 - 28 Feb. 1991
Steven A. Lis and Philip D. Henshaw 11 Feb. 1991 100 p
(Contract F49620-90-C-0056)
(AD-A232767; LTR91-005) Avail: NTIS HC/MF A05 CSCL 20/6

This Final Report describes the results of a Phase 1 SBIR project to investigate the feasibility and practicality of utilizing Spectral Hole Burning (SHB) media as the basis of a high capacity optical memory system. Our concept has the potential for providing enormous storage capacities (on the order of 10th to the 12th power bits and larger) in commercially viable systems. This report summarizes our analyses and shows that the necessary system components as well as material properties presently exist (or are under rapid development) which can make such a memory system a practical reality and not simply a theoretical possibility. The ultimate system design is expected to be a high capacity unit of modest physical size which has low power requirements, high data rate, and an access time suitable to be useful to a broadbased user community. GRA

N91-23906# Alabama Univ., Huntsville. Dept. of Physics.
ANALYSIS OF POLARIZING OPTICAL SYSTEMS FOR DIGITAL OPTICAL COMPUTING WITH SYMMETRIC SELF ELECTROOPTIC DEVICES Annual Report, 30 Sep. 1989 - 30 Mar. 1991
Russell A. Chipman, J. L. Pezzaniti, and David B. Chenault 31 Mar. 1991 28 p
(Grant AF-AFOSR-0542-89; AF Proj. 2305)
(AD-A232768; AFOSR-91-0121TR) Avail: NTIS HC/MF A03 CSCL 09/5

Two architectural approaches have dominated the field of optical computing. The first approach uses integrated optics to connect logic gates in arbitrary configurations similar to a conventional computer. An optical computer built with this approach competes directly with a conventional computer. The approach is successful when it results in a computer which is more powerful and can be made more cheaply. The second approach makes use of two dimensional arrays of logic devices interconnected in free space. This approach cannot provide arbitrary connections as do integrated optics but the density and the bandwidth of free space interconnects can be much larger than what is offered by conventional interconnects. A more fundamental advantage of

optical interconnects is that lower energy communications appear to be possible than with electronic interconnects. GRA

N91-23907# University of Southern California, Los Angeles. Optical Materials and Devices Lab.
PHOTONIC MATERIALS AND DEVICES FOR OPTICAL INFORMATION PROCESSING AND COMPUTING APPLICATIONS Annual Report, 15 May 1987 - 14 May 1990
Armand R. Tanguay, Jr. Feb. 1991 340 p LIMITED REPRODUCIBILITY: Availability: Document partially illegible
(Contract F49620-87-C-0056)
(AD-A232771; USC-OMDL-2001; AFOSR-91-0046TR) Avail: NTIS HC/MF A15 CSCL 09/5

The research program is focused on a critical evaluation of advanced photonic materials and device concepts for the implementation of optical information processing and computing systems. The effort ranges from a detailed investigation of the fundamental physical and technological limitations that impact the potential computational gain (e.g., increases in throughput, decreases in decision time subsequent to processing, or minimization of the energy expended during computation) of optical information processing and computing systems, through the invention and characterization of key enabling devices such as two dimensional spatial light modulators and volume holographic optical elements, to the development of advanced techniques for materials growth, deposition, and processing that have a critical impact on potential device performance. This multifaceted evaluation of novel materials, device, and system concepts has been directly responsible for the invention and characterization of a number of photonic devices and materials processing techniques that exhibit both high performance and capacity for practical manufacturing. The primary program thrusts can be organized into three principal categories: (1) fundamental and technological limitations of optical information processing and computing; (2) electrically and optically addressed spatial light modulators; and (3) volume holographic optical elements. GRA

N91-23908# Arnold Engineering Development Center, Arnold Air Force Station, TN.
AERO-OPTICS MEASUREMENT SYSTEM FOR THE AEDC AERO-OPTICS TEST FACILITY Final Report, Oct. 1986 - Dec. 1990
F. L. Crosswy and A. G. Havener Feb. 1991 87 p Prepared in cooperation with Calspan Corp., Arnold AFS, TN
(AD-A232852; AEDC-TR-90-20) Avail: NTIS HC/MF A05 CSCL 20/6

A fundamental problem associated with hypersonic, endoatmospheric, optically guided vehicles for interception of ballistic reentry vehicles is target image degradation caused by the complex flow field of the intercept vehicle. The image degradation mechanisms are collectively referred to as aero-optics (AO) effects. The AEDC aero-optics measurement system provides the hardware, software, techniques, and expertise for measurement of the fundamental AO effects parameters in a ground test facility. The AO measurement system is presently configured for use in AEDC Tunnel C, a continuous flow hypersonic wind tunnel. AO effects measurements are based upon image analysis, image jitter, and holographic interferometry techniques. The primary purpose of this report is to provide hardware descriptions for the imaging and holography systems and their associated data acquisition and data reduction systems. Information is also provided in the appendixes, which describe several AO measurements technology advances in various stages of development. GRA

N91-23909# University of Southern California, Los Angeles. Signal and Image Processing Inst.
NONLINEAR REAL-TIME OPTICAL SIGNAL PROCESSING Final Technical Report, 1 Jul. 1984 - 31 Jan. 1990
A. A. Sawchuk 1 Sep. 1990 128 p
(Grant AF-AFOSR-0181-84; AF Proj. 2305)
(AD-A232889; AFOSR-91-0168TR) Avail: NTIS HC/MF A07 CSCL 20/6

During the period 1 Jul. 1984 to 31 Jan. 1990, the research under Grant AFOSR-84-0181 has been concerned with binary parallel optical computing architectures with particular attention to cellular logic and symbolic substitution for pattern recognition and numerical operations. The approach has been to experimentally implement binary optical cellular logic processors and interconnection arrays; define an instruction set and software suited to optical computing systems; and to study generalizations of optical cellular logic processors such as the cellular hypercube. The results include the experimental implementation of a 54-gate binary optical cellular logic processor with instruction decoders, input/output, memory and test/branch functions; the completion of a binary image algebra (BIA) description of cellular logic, image analysis and symbolic operations; and the development of binary image algebra algorithms for scale and shift invariant patterns recognition. Additional work concerns the relationship of parallel computation paradigms to optical computing and halftone screen techniques for implementing general nonlinear functions. GRA

N91-23608# Aerospatiale, Cannes (France).
MEDIUM RESOLUTION IMAGING SPECTROMETER (MERIS)
G. Baudin, R. Bessudo, M. A. Cutter, D. Lobb, and J. L. Bezy (European Space Agency. European Space Research and Technology Center, ESTEC, Noordwijk, Netherlands) *In* ESA, Space and Sea Dec. 1990 p 303-308 Sponsored in part by Dornier-Werke G.m.b.H. (For primary document see N91-23563 15-42)
Copyright Avail: NTIS HC/MF A13

N91-24070*# National Aeronautics and Space Administration. Goddard Space Flight Center, Greenbelt, MD.
OPTICAL COMMUNICATION FOR SPACE MISSIONS
M. Firtmaurice *In* NASA, Washington, Technology 2000, Volume 2 1991 p 249-258 (For primary document see N91-24041 15-99)
Avail: NTIS HC/MF A16 CSCL 20F

N91-24071*# National Aeronautics and Space Administration. John F. Kennedy Space Center, Cocoa Beach, FL.
OPTICAL SHUTTER SWITCHING MATRIX
Charles H. Grove *In* NASA, Washington, Technology 2000, Volume 2 1991 p 259-267 (For primary document see N91-24041 15-99)
Avail: NTIS HC/MF A16 CSCL 20F

N91-24072*# Jet Propulsion Lab., California Inst. of Tech., Pasadena.
FIBER OPTIC TACTICAL LOCAL NETWORK (FOTLAN)
L. A. Bergman, R. Hartmayer, W. H. Wu, P. Cassell, G. Edgar, J. Lambert, R. Mancini, J. Jeng, and C. Pardo *In* NASA, Washington, Technology 2000, Volume 2 1991 p 268-275 (For primary document see N91-24041 15-99)
Avail: NTIS HC/MF A16 CSCL 20F

75 PLASMA PHYSICS

Includes magnetohydrodynamics and plasma fusion.

For ionospheric plasmas see *46 Geophysics*. For space plasmas see *90 Astrophysics*.

N91-23910# Ben Gurion Univ. of the Negev, Beersheva (Israel). Center for MHD Studies.
TURBULENCE AND THE FEASIBILITY OF SELF-COOLED LIQUID-METAL BLANKETS FOR FUSION REACTORS
Herman Branover, Semion Sukoriansky, G. Talmage, and E. Greenspan (Israel Atomic Energy Commission, Beersheba.) 1986 9 p Presented at the 1986 American Nuclear Society Meeting, Reno, NV, 15-19 Jun. 1986 Revised Submitted for publication
(Ser-10/P-Rev; ITN-88-85007) Avail: NTIS HC/MF A02

Effects of anisotropic turbulence, which can develop in the flow of liquid metal in a transverse magnetic field, on the heat transfer-rate and on self-cooled blanket design and performance are investigated using recent experimental evidence and an

approximate analytical model. It is found that the anisotropic turbulence might enhance the heat transfer rate by an order of magnitude without affecting the magnetohydrodynamics pressure drop. The enhanced heat transfer rate opens new interesting possibilities for the design of self-cooled liquid metal blankets, including the possibility of: (1) designing simple yet efficient poloidal-flow blankets; (2) reducing the pressure drop; and (3) increasing the exit coolant temperature and, hence thermal-to-electrical energy conversion efficiency of conventional blanket concepts. A thorough investigation of the anisotropic turbulent flow phenomena is essential for enabling a realistic assessment of their implications. This investigation ought to include large-scale experiments that enable simulation of realistic fusion reactor conditions. ISA

N91-23911# Avco-Everett Research Lab., MA.
MHD CHANNEL GAS-SIDE ELEMENT EROSION-CORROSION STUDIES
R. J. Pollina, W. Simpsom, and L. C. Farrar (Montec Associates, Inc., Butte, MT.) 1990 7 p Presented at the 28th Symposium on Engineering Aspects of Magnetohydrodynamics; University Coal Research and Historically Black Colleges and Universities Contractors Review, Chicago, 26-28 Jun. 1990; 16-19 Jul. 1990
(Contracts DE-FG22-88PC-88928; DE-AC22-87PC-90274)
(DE91-008561; CONF-9006105-14; CONF-900749-1) Avail: NTIS HC/MF A02

The problems connected with gas side corrosion for the design of the 1A4 channel hardware are explored and the results to date are presented of gas side wear rate tests in the Mark 7 facility. They show that the proposed designs meet a 2000 hour lifetime criterion based upon materials test results. They also show the improvement in cathode lifetime obtained with lower voltage intercathode gaps. The corrosion is discussed of these materials and how lifetimes are dependent upon gap voltage and average metal temperature is shown. The final choice of materials is determined primarily by the outcome of these tests and also by the question of the manufacturability of the prospective designs. DOE

N91-23912# Texas Univ., Austin. Fusion Research Center.
ON STANDARD FORMS FOR TRANSPORT EQUATIONS AND FLUXES, PART 2
D. W. Ross Mar. 1990 13 p
(Contract DE-FG05-88ER-53266)
(DE91-010421; DOE/ER-53266/30; FRCR-357-Pt-2) Avail: NTIS HC/MF A03

Quasilinear expressions for anomalous particle and energy fluxes arising from electrostatic plasma turbulence in a tokamak are reviewed yet again. Further clarifications are made, and the position taken in a previous report is modified. There, the total energy flux, Q(sub j), and the conductive heat flux, q(sub j), were correctly defined, and the anomalous Q(sub j) was correctly calculated. It was shown that the anomalous energy transport can be correctly described by nabla Q*(sub j), where Q*(sub j) = 3/5 Q(sub j), with ali remaining source terms such as (Hermitian conjugate of p(sub j)nabla times the Hermitian conjugate of V(sub j)) cancelling. Here, a revised discussion is given of the identification of the anomalous conductive flux, q(sub j), in which the distinction between Q(sub j) and Q*(sub j) is reconsidered. It is shown that there is more than one consistent way to define q(sub j). Transport calculations involving only theoretical electrostatic turbulent fluxes are unaffected by these distinctions since Q(sub j) or Q*(sub j), rather than q(sub j), is the quantity naturally calculated in the theory. However, an ambiguity remains in experimental transport analysis if the measured particle flux Gamma(sub j) = n(sub j)V(sub j) is to be used in the energy equation. This is because we cannot be sure how properly to treat the source terms p(sub j)nabla times V(sub j) or (Hermitian conjugate of p(sub j)nabla times the Hermitian conjugate of V(sub j)). DOE

N91-23913# Oak Ridge National Lab., TN.
ICRF HEATING ON THE BURNING PLASMA EXPERIMENT (BPX)
D. B. Batchelor, M. D. Carter, R. H. Goulding, D. J. Hoffman, E. F. Jaeger, P. M. Ryan, D. W. Swain, J. S. Tolliver, J. J. Yugo, and R. J. Goldston (Princeton Univ., NJ.) et al 1991 5 p Presented at the 18th European Conference on Controlled Fusion and Plasma Physics, Berlin, Fed. Republic of Germany, 3-7 Jun. 1991
(Contract DE-AC05-84OR-21400)
(DE91-010390; CONF-910609-4) Avail: NTIS HC/MF A01

Radio frequency (RF) power in the ion cyclotron range of frequencies (ICRF) has been chosen as the primary heating technique for BPX. This decision is based on the wide success of ICRF heating in existing experiments (JET, TFTR, JT-60), the capability of ion cyclotron waves to penetrate the high-density plasmas of BPX, the ability to concentrate ICRF power deposition near the plasma center, and the ready availability of high-power sources at the appropriate frequency. The primary task of the ICRF system is to heat the plasma to ignition. However, other important roles are envisaged; these include the stabilization of sawteeth, preheating of the plasma during current ramp-up, and possible control of the plasma current profile by means of fast-wave current drive. We give a brief overview of the RF system, describe the operating scenarios planned for BPX, and discuss some of the antenna design issues for BPX. DOE

N91-23914# Oak Ridge National Lab., TN.
TRANSPORT ANALYSIS OF STELLARATOR REACTORS
S. L. Painter (Tennessee Univ., Knoxville.) and J. F. Lyon Feb. 1991 47 p
(Contract DE-AC05-84OR-21400)
(DE91-010489; ORNL/TM-11756) Avail: NTIS HC/MF A03

The performance of deuterium-tritium stellarator reactors is studied with a new, fast one-dimensional (1-D) transport survey code that is based on the spectral collocation method. Two operating modes with different signs of the assumed radial electric field are identified. The operating mode with a positive electric field is characterized by high temperatures and moderate densities, whereas the other mode has lower temperatures and higher densities. Both modes lead to possible reactors that could tolerate a large alpha-particle energy loss. The sensitivity to device parameters and to profile assumptions is examined. Scaling expressions useful for parametric studies are obtained for different quantities of interest, and the 1-D code results are compared with results derived from an empirical scaling relation. Deuterium-helium-3 operation is also feasible but is more demanding. The implications for stellarator reactor design optimization are discussed. DOE

N91-23915# Oak Ridge National Lab., TN.
INVERSION OF CHORDAL DATA FROM THE ATF TORSATRON
L. R. Baylor, C. H. Ma, and S. Hiroe Feb. 1991 21 p
(Contract DE-AC05-84OR-21400)
(DE91-010490; ORNL/TM-11758) Avail: NTIS HC/MF A03

A method to obtain electron density profiles from chordal interferometric measurements of a tokamak plasma has been extended to the non-axisymmetric stellarator geometry of the Advanced Toroidal Facility (ATF) torsatron. The method requires a known magnetic flux surface geometry expressed in spectral form. The method has been applied to both interferometer density data and bolometer irradiance data from ATF, and results are presented. The resulting inverted density profiles are integrated along a horizontal path and compare favorably with line integral measurements of the density. Sensitivities of the resulting profiles to variations in the flux surface geometry and errors in the measurements are discussed. DOE

N91-23916# Oak Ridge National Lab., TN.
ION CONFINEMENT AND RADIATION LOSSES IN THE ADVANCED TOROIDAL FACILITY
R. C. Isler, R. J. Colchin, M. R. Wade, J. F. Lyon, R. H. Fowler, J. A. Rome, S. Hiroe, L. R. Baylor, A. England, and C. H. Ma et al 1991 5 p Presented at the 18th European Conference on Controlled Fusion and Plasma Physics, Berlin, Fed. Republic of

Germany, 3-7 Jun. 1991
(Contract DE-AC05-84OR-21400)
(DE91-010382; CONF-910609-2) Avail: NTIS HC/MF A01

Collapses of stored energy are typically observed in low-density (bar-n(sub e) approximately 10(exp 13) per cu cm) extensively gettered ATF plasmas when the electron density rises to the ECH cutoff point, and the central heating is supplied only by neutral-beam-injection (NBI). However, the decline of stored energy can be avoided if the density is raised rapidly to about 5 x 10(exp 13) per cu cm. Three mechanisms have been proposed to explain the collapses: (1) impurity radiation, (2) excitation of an electron instability driven by the neutral beams, or (3) poor coupling of the beam ions to the thermal plasmas. Detailed spectroscopic studies of plasma cleanliness as a function of the gettering procedure have shown that radiation is an unlikely candidate for initiating collapses, although it may become an important loss mechanism once the electron temperature has fallen to a low level. No specific electron instability has yet been identified with injection, but recent experimental and computational work indicates that losses by shinethrough and charge exchange strongly influence the evolution of low-density plasmas. This report discusses the beam particle losses, thermal ions, and the evolution of radiation profiles. DOE

N91-23917# Oak Ridge National Lab., TN.
HEAVY ION BEAM PROBE MEASUREMENTS OF ECH METHOD PLASMA IN THE ADVANCED TOROIDAL FACILITY
S. C. Aceto, J. G. Schwelberger, J. J. Zielinski, K. A. Connor, T. P. Crowley, J. W. Heard, R. L. Hickok, P. E. McLaren, A. Ouroua, and V. J. Simcic (Rensselaer Polytechnic Inst., Troy, NY.) et al 1991 5 p Presented at the 18th European Conference on Controlled Fusion and Plasma Physics, Berlin, Fed. Republic of Germany, 3-7 Jun. 1991
(Contract DE-AC05-84OR-21400)
(DE91-010391; CONF-910609-3) Avail: NTIS HC/MF A01

A Heavy Ion Beam Probe (HIBP) has been installed on the Advanced Toroidal Facility (ATF) and used to measure the plasma potential and also make density fluctuation measurements during ECH plasmas. The initial results of the potential profile measurements are presented and related to spectroscopic rotation measurements using simple momentum balance equations. Also, a summary of the density fluctuation measurements made to date is given along with a brief comparison with similar HIBP measurements made on the TEXT tokamak. DOE

N91-23918# Texas Univ., Austin. Fusion Research Center.
COMPARISON OF DRIFT WAVE MODELS WITH FLUCTUATION DATA FROM THE INTERIOR OF THE TEXT TOKAMAK
D. W. Ross, R. V. Bravenec, C. P. Ritz, M. L. Sloan, J. R. Thompson, A. J. Wootton, P. M. Schoch, J. W. Heard, T. P. Crowley, and R. L. Hickok (Rensselaer Polytechnic Inst., Troy, NY.) et al Dec. 1990 30 p
(Contracts DE-FG05-88ER-53266; DE-FG05-88ER-53267; DE-FG03-86ER-53225)
(DE91-010424; DOE/ER-53266/36; FRCR-381) Avail: NTIS HC/MF A03

Experimental evidence for and against drift waves as the origin of the observed fluctuations and anomalous transport in the plasma interior is reviewed. Fluctuation spectra observed by far-infrared scattering and a heavy ion beam probe (HIBP) are compared. The FIR system observes broad S(k,(omega)), which are spatially resolved at large k and readily identified with electron drift waves. At higher densities, a clear feature, which may be associated with ion temperature gradient modes, appears as well. A quasi-coherent feature in the drift wave range of phase velocities is also found at the inner mid-plane. But interior HIBP measurements using a thallium beam have, by a two-point correlation method, measured wave numbers far too small to be those of drift waves of either variety. Some recent measurements with a cesium beam have produced phase velocities more closely in accord with drift waves at low frequencies. It is suggested that a new mode may be present, which is not drift wave-like. However, the phase velocity and coherence of the HIBP data exhibit qualitative features that suggest possible instrumental effects. Several of these are investigated, which individually do not appear to reconcile the data with a pure drift wave model. They are sample volume size, common mode effects such as cross talk or path integrals of beam attenuation, and two-stream instabilities. Reconciliation of these measurements is important to transport studies: calculated particle and energy fluxes depend sensitively on the frequency and wave number spectrum employed. The theoretical considerations about two-point correlations and possible instrumental effects are also relevant to other diagnostics using this technique. DOE

N91-23919# Sandia National Labs., Albuquerque, NM.
INTENSE LIGHT-ION BEAMS PROVIDE A ROBUST, COMMON-DRIVER PATH TOWARDS IGNITION, GAIN AND COMMERCIAL FUSION ENERGY
J. J. Ramirez, D. L. Cook, J. K. Rice, M. K. Matzen, D. L. Johnson, J. D. Boyes, C. L. Olson, K. R. Prestwich, M. J. Clauser, and T. A. Mehlhorn et al 1991 11 p Presented at the International Atomic Energy Agency (IAEA) Technical Committee Meeting on Drivers for Inertial Confinement Fusion (ICF), Osaka, Japan, 15-19 Apr. 1991
(Contract DE-AC04-76DP-00789)
(DE91-010584; SAND-91-0043C; CONF-9104210-1) Avail: NTIS HC/MF A03

Intense light-ion beams are being developed for investigations of Inertial Confinement Fusion (ICF). This effort has concentrated on developing the Particle Beam Fusion Accelerator II (PBFA-II) at Sandia as a driver for ICF target experiments, on design concepts for a high-yield, high-gain Laboratory Microfusion Facility (LMF), and on a comprehensive system study of a light-ion beam driven commercial fusion reactor (LIBRA). This paper reports on the status of design concepts and research in these areas. DOE

N91-23920# Massachusetts Inst. of Tech., Cambridge. Plasma Fusion Center.
EXPERIMENTAL AND THEORETICAL RESEARCH IN APPLIED PLASMA PHYSICS
M. Porkolab 1991 126 p
(Contract DE-FG02-91ER-54109)
(DE91-010657; DOE/ER-54109/T1) Avail: NTIS HC/MF A07

This report contains papers on the following topics: fusion theory and computations; theory of thermonuclear plasmas; user service center; high poloidal beta studies on PBX-M; fast electron cyclotron emission (ECE) fluctuation diagnostic for ballooning mode studies; x-ray imaging diagnostic; millimeter/submillimeter-wave fusion ion diagnostics; small scale turbulence and nonlinear dynamics in plasmas -- continuation proposal; plasma turbulence and transport; and phase contrast interferometer diagnostic for long wavelength fluctuations in DIII-D. DOE

N91-23921# Department of Energy, Washington, DC. Office of Fusion Energy.
COMPUTING FOR MAGNETIC FUSION ENERGY RESEARCH: THE NEXT FIVE YEARS
L. Mann, ed., A. Glasser, ed. (Los Alamos National Lab., NM.), and N. Sauthoff, ed. Feb. 1991 44 p
(DE91-010686; DOE/ER-0493T) Avail: NTIS HC/MF A03

This report considers computing needs in magnetic fusion for the next five years. It is the result of two and a half years of effort by representatives of all aspects of the magnetic fusion community. The report also factors in the results of a survey that was distributed to the laboratories and universities that support fusion. There are four areas of computing support discussed: theory, experiment, engineering, and systems. DOE

N91-23922# General Atomic Co., San Diego, CA.
APPLIED PLASMA PHYSICS
Mar. 1991 55 p
(Contract DE-AC03-89ER-53277)
(DE91-010696; GA-A-20362) Avail: NTIS HC/MF A04

This report discusses research in the following areas: applied plasma physics overview; fusion plasma theory; fusion user service center; and diagnostics. DOE

N91-23923# General Atomic Co., San Diego, CA.
FUSION TECHNOLOGY DEVELOPMENT
Mar. 1991 30 p
(Contract DE-AC03-89ER-52153)
(DE91-010697; GA-A-20363) Avail: NTIS HC/MF A03

This report discusses the development and technology overview of plasma technologies and fusion technologies. In particular, this report discusses research on RF technologies, plasma facing components, reactor design studies, and fusion nuclear technology. DOE

N91-23924# New York Univ., New York. Courant Inst. of Mathematical Sciences.
HALL EFFECTS ON ANOMALOUS HEAT, PARTICLE AND HELICITY TRANSPORTS THROUGH TEARING-MODE TURBULENCE
Z. Yoshida, H. R. Strauss, and E. Hameiri Jan. 1991 17 p
(Contract DE-FG02-86ER-53223)
(DE91-010730; DOE/ER-53223/158; MF-122) Avail: NTIS HC/MF A03

The helicity transport in a current-carrying plasma results in heat and particle transports in the direction opposite to the helicity flux. Tearing-mode turbulence produces helicity flux that is proportional to the gradient of equilibrium parallel current. The helicity flux is a consequence of a fluctuating electric field with a circularly polarized component, which also causes a nonlinear parallel current (primarily an electron flux) and a nonlinear polarization current (primarily an ion flux). Such anomalous heat and particle fluxes are driven by the free-energy associated with the perturbed magnetic field in the tearing-mode turbulence, and are typically directed inward to the plasma. Both fluxes becomes large when the gradient of the equilibrium current is large. DOE

N91-23925 Institut d'Aeronomie Spatiale de Belgique, Brussels.
A METHOD FOR SOLVING POISSON'S EQUATION IN GEOPHYSICAL AND ASTROPHYSICAL PLASMA
J. Lemaire, A. Barakat, J. M. Lesceux, and B. Shizgal (British Columbia Univ., Vancouver.) 1990 18 p Presented at 17th International Symposium on Rarefied Gas Dynamics, Aachen, Fed. Republic of Germany, 8-14 Jul. 1990 Submitted for publication
(Aeronomica-Acta-A-357-1990; ISSN-0065-3713; ETN-91-99109)
Avail: Institut d'Aeronomie Spatiale de Belgique, 3 Avenue Circulaire, B-1180 Brussels, Belgium

The Quasi Neutrality (QN) equation is usually solved by an iterative procedure to obtain the electrostatic potential distribution in plasmas. A new numerical method to obtain the same result more efficiently, based on the numerical integration of the differential form of the QN equation, is presented. In the case when the QN approximation fails to be a valid approximation of Poisson's Equation (PE), the latter equation needs to be solved. A robust numerical method to solve PE, with boundary conditions at two different altitudes, is proposed. The method consists of integrating numerically by the Quadrature Discretization Method (QDM) a differential form of PE. For boundary conditions corresponding to the QN solution the result coincides with the QN solution. ESA

N91-23926# Aerospatiale Aquitaine, Saint-Medard en Jalles (France).
PLASMA TORCHES DIMENSIONING AND OPTIMIZATION
S. Muller 1991 8 p
(Rept-911-430-111; ETN-91-99283) Avail: NTIS HC/MF A02

A set of codes which enable dimensioning and optimization of non transferred plasma torches made up of two coaxial cylindrical electrodes cooled up in the 100 kW power range is described. These torches are used in ballistic, space and industrial fields. The sharp model of exchanges between the electric arc and the plasma producing gas requires a thorough knowledge of the physical properties of this plasma producing gas so a specific study was carried out on the air. Equations taken into account include mass conservation, Navier-Stokes and energy conservation equations. An experimental data bank gathers the plasma torches performances described. The modular structure of the package and its continuous feedback between theoretical and experimental data bank improves constantly with new experimentation. ESA

N91-23927# Aerospatiale Aquitaine, Saint-Medard en Jalles (France).
AEROSPATIALE INDUSTRIAL THERMAL PLASMAS
Maxime Labrot 1991 10 p
(Rept-911-430-113; ETN-91-99285) Avail: NTIS HC/MF A02

Work carried out on nontransferred plasma torches of 2, 4, and 0.8 MW to be used in metallurgic, iron making, casting foundry, and environment industrial plants is described. The plants operation, the plasma system behavior, and the main process' results are described. Research and development programs on transferred and nontransferred arc torches are reported. ESA

N91-23928# Aerospatiale Aquitaine, Saint-Medard en Jalles (France).
AEROSPATIALE INDUSTRIAL THERMAL PLASMA ACTIVITIES
Maxime Labrot 1991 16 p Presented at EPRI/CMP Plasma Symposium, Palo Alto, CA, Mar. 1990
(Rept-911-430-122; ETN-91-99294) Avail: NTIS HC/MF A03

Details of nontransferred arc torches, plasma systems in industrial use and operational plasma applications are listed. A plasma application on a foundry cupola is detailed. The setting up of a plasma system is described. Research and development activities are summarized. ESA

N91-23929# Aerospatiale Aquitaine, Saint-Medard en Jalles (France).
PLASMA ON A FOUNDRY CUPOLA
Didier Pineau 1991 20 p Presented at EPRI/CMP Plasma Symposium, Palo Alto, CA, Mar. 1990
(Rept-911-430-125; ETN-91-99297) Avail: NTIS HC/MF A03

An experiment of a plasma torch on a production foundry cupola is reported. The test runs were conducted on a hot blast cupola, the blast temperature in the absence of plasma being 400 C. With the torch, the temperature of the blast was increased to 1000 C. The experiment was conducted for the manufacture of car engines with a 2.5 MW transportable plasma system. The cupola was boosted with a 4 MW torch and results included an increase in production of 45 percent, a decrease in coke rate and no more new iron in the loads. The plasma torch and hot air cupola furnace are described. ESA

N91-23930# Ballistic Research Labs., Aberdeen Proving Ground, MD.
TEMPERATURE MEASUREMENTS OF ET PLASMAS USING ATOMIC EMISSION SPECTROSCOPY Final Report, 1 Nov. 1988 - 24 May 1989
Steven W. Bunte. Richard A. Beyer, and Alexander E. Zielinski Feb. 1991 23 p
(DA Proj. 1L1-62618-AH-80)
(AD-A232498; BRL-TR-3196) Avail: NTIS HC/MF A03 CSCL 20/3

The electrothermal accelerator (ET gun) is an advanced propulsion technique in which an electrically generated high temperature, high pressure plasma interacts with a working fluid to produce the gases necessary to accelerate a projectile. In the development of ET technology, the characterization of the temperature and pressures generated by this plasma is critical for modeling of the ET process and ultimately, complete understanding of a fielded weapon system. The results are reported here of an experimental effort aimed at determining the temperature of ET plasmas using atomic emission spectroscopy. The ultimate goal of this work is to develop a technique at the benchtop level that will be directly transferable to measuring the temperature in a large scale ET gun. GRA

N91-23931# Texas Technological Univ., Lubbock. Dept. of Electrical Engineering.
THEORETICAL AND NUMERICAL STUDY OF ANOMALOUS TURBULENT TRANSPORT IN PLASMAS Final Report, 15 Jun. 1986 - 14 Dec. 1990
Osamu Ishihara 5 Feb. 1991 38 p LIMITED REPRODUCIBILITY: Availability: Document partially illegible
(Grant AF-AFOSR-0156-86; AF Proj. 2301)
(AD-A232688; AFOSR-91-0123TR) Avail: NTIS HC/MF A03 CSCL 20/9

Theoretical and computational analysis of particle transport in a plasma turbulence was carried out. Particle behavior was investigated by test particle simulations in different types of plasma turbulence, including drift wave turbulence, ion acoustic turbulence, and Langmuir turbulence. Resonance broadening in real space around the mode rational surface was confirmed in drift wave turbulence. Nonresonant interaction of waves and particles were studied in ion acoustic turbulence. Resonance broadening in velocity space was found as a result of the non-Markovian process in Langmuir turbulence. A semiclassical quantum plasma approach was also applied to plasma turbulence. Some instabilities in toroidal geometry were studied as eigen value problems. GRA

76 SOLID-STATE PHYSICS

Includes superconductivity.

For related information, see also *33 Electronics and Electrical Engineering* and *36 Lasers and Masers.*

N91-23932 Oregon Graduate Inst. of Science and Technology, Beaverton.
LOW-TEMPERATURE LASER-INDUCED SELECTIVE AREA GROWTH OF COMPOUND SEMICONDUCTOR Ph.D. Thesis
Sudarsan Uppili 1990 177 p
Avail: Univ. Microfilms Order No. DA9101238

Laser induced epitaxial growth of gallium phosphide was investigated as a low temperature, spatially selective process using both pyrolytic and photolytic reaction. A focussed beam from an argon ion laser operating at 514.5 nm was used to direct-write epitaxial microstructures of homoepitaxial GaP using a pyrolytic process. The precursors were trimethyl gallium (TMG) and tertiary butylphosphine (TBP). Dependence of the epitaxial growth on several deposition parameters was examined. An ArF excimer laser was also used to achieve homoepitaxy and heteroepitaxy of gallium phosphide on gallium arsenide at 500 C using TMG and TBP as the precusor gases. Dependence of homoepitaxial growth of GaP on several parameters is examined. The crystalline properties of the film were determined using transmission electron microscopy (TEM). Electrical properties of p-n diodes fabricated via Zn doping were also examined. Defect structures in excimer laser-assisted epitaxial GaP on (100) GaP and (100) GaAs were examined using TEM. Periodic structures were obtained using nominally unpolarized excimer laser radiation, during heteroepitaxial growth of GaP on GaAs. Both crystalline properties and chemical composition of these structures were examined. Microanalysis showed modulation in composition in the ripple structure resulting from the thermal variation caused by the optical interference during growth. Electrical conductivity measurements of GaP during pulsed lasers irradiation indicated that in the absence of gases, there was appreciable heating of the semiconductor. However, a very small quantity of hydrogen or helium cooled the substrate appreciably. This suggested that the average temperature rise of the substrate was not an important factor in the temperature calculations used in the present investigation. Dissert. Abstr.

N91-23933*# National Aeronautics and Space Administration. Marshall Space Flight Center, Huntsville, AL.
PROTEIN CRYSTAL GROWTH TRAY ASSEMBLY Patent Application
Daniel C. Carter, inventor (to NASA) and Teresa Y. Miller, inventor (to NASA) 23 Oct. 1990 17 p
(NASA-Case-MFS-28507-1; NAS 1.71:MFS-28507-1; US-Patent-Appl-SN-601954) Avail: NTIS HC/MF A03 CSCL 20B

A protein crystal growth tray assembly includes a tray that has a plurality of individual crystal growth chambers. Each chamber has a movable pedestal which carries a protein crystal growth compartment at an upper end. The several pedestals for each tray assembly are ganged together for concurrent movement so that the solutions in the various pedestal growth compartments can be separated from the solutions in the tray's growth chambers until the experiment is to be activated. NASA

N91-23934# Quaid-i-Azam Univ., Islamabad (Pakistan). Dept. of Physics.
EFFECT OF TRANSITION METAL DOPANTS ON HIGH T(SUB c) SUPERCONDUCTIVITY M.S. Thesis
Maobool Ahmad 1990 110 p
(PB91-130138) Avail: NTIS HC/MF A06 CSCL 20L

The magnetic transport properties of chromium doped high temperature semiconductors, YBa2Cu3(1-x)Cr(x)O(7-delta), were studied. The samples were studied for x = 0.000, 0.020, 0.033. The samples were found to retain the orthorhombic phase in all three materials and the characteristic temperature T(c) decreases strongly with chromium concentration. The magnetic properties also show weakening as chromium is added. The magnetization m(H), the lower critical field H(c1), and the critical current obtained from the m(H) loops show strong decrease as chromium is added. The transport properties in the presence of magnetic field 0 less than H less than 20 KOe, however, do not show a strong sensitivity to the chromium dopants. The data is consistent with the view that CR dopants replace Cu atoms primarily in the Cu-O chains and hence, transport properties in the Cu-O(2) planes are not drastically affected. GRA

N91-23935# California Univ., Berkeley. Lawrence Berkeley Lab.
MAGNET CABLE MANUFACTURING
J. Royet Oct. 1990 64 p
(Contract DE-AC03-76SF-00098)
(DE91-010210; LBL-29345) Avail: NTIS HC/MF A04

The cable is the heart of a superconducting accelerator magnet. Since the initial development of the Rutherford Cable more than twenty years ago, many improvements in manufacturing techniques have increased the current carrying capacity. When the Tevatron cable was specified fifteen years ago the current carrying capacity was 1800 A/sq mm at a field of 5.3T. During the intervening years it has been increased to 3000 A/sq mm. These improvements were due to refinements in the fabrication of the strands and the formation of the cable from the strands. The metallurgists were able to impart significant gains in performance by improving the homogeneity of the conductor. The engineers and technicians who designed and built the modern cabling machines made an enormous contribution by significantly reducing the degradation of wire performance that occurs when the wire was cabled. The fact that these gains were made while increasing the speed of cabling is one of the technological advances that made accelerators like the superconducting super collider (SSC) possible. This article describes the cabling machines that were built to manufacture the cable for the full scale SSC prototype magnets and the low beta quadrupoles for the Fermilab Tevatron. This article also presents a compendium of the knowledge that was gained in the struggle to make high performance cable to exacting dimensional standards and at the throughput needed for the SSC. The material is an important part of the technology transfer from the Department of Energy Laboratories to industry. DOE

N91-23936 Notre Dame Univ., IN.
STRUCTURAL AND ELECTRONIC PROPERTIES OF THE ORDERED TERNARY 3-5 SEMICONDUCTORS Ph.D. Thesis
Dan Teng 1990 172 p
Avail: Univ. Microfilms Order No. DA9106650

Modern-growth techniques have allowed control of deposition down to the monolayer level. Under certain experimental conditions,

some materials spontaneously form ordered structures. These new ordered ternary compounds have recently attracted widespread attention. Five forms of ordered ternary III-V semiconductors are investigated. Three aspects of these semiconductors are investigated: (1) the determination of the locations of atoms in the crystal; (2) the electric band structure; and (3) the behaviors of the interband optical transition. To focus on trends and characteristic features of these new materials, phenomenological models are used. A Keating-type model is employed to calculate the structural properties. In this model, strain energy comes from the changes of the bond lengths and the bond angles from their equilibrium positions and follows Hooke's Law. For band-structure calculations, two empirical theories are employed: a simple tight-binding theory and a valence-force field model. Strain-included tetragonal and internal distortions as well as the spin-orbit interaction cause a splitting of the top of valence band. Trends in this splitting and the band gap variation are studied for the 18 combinations of III-V elements. The Hopfield quasicubic crystal-field model is found to accurately describe this splitting for all chalcopyrite compounds. But Hopfield's model is found to fail for several (0,0,1) and (1,1,1) superlattice compounds containing large strain distortions. It is also confirmed that band-gap narrowing is the result of noncubic crystal-field splitting, strain effects, and the chemical difference between different anions or cations of a ternary compound. As an application of these studies, the imaginary part of the dielectric constant of a realistic material, the GaP(sub 1)/InP(sub 1) (1,1,1) superlattice are calculated. Dissert. Abstr.

N91-23937 Stevens Inst. of Tech., Hoboken, NJ.
NONEQUILIBRIUM GREEN'S FUNCTIONS AND QUANTUM TRANSPORT THEORY FOR SEMICONDUCTOR MICROSTRUCTURES Ph.D. Thesis
Hum Chi Tso 1990 233 p
Avail: Univ. Microfilms Order No. DA9103501

Nonlinear quantum transport theory and its linear limit are examined for semiconductor microstructures, including quantum wells and superlattices. The problem of linear cyclotron resonance is treated using a memory function approach for a type I semiconductor superlattice with interacting quantum wells subject to impurity and phonon scatterings. Furthermore, a fully microscopic quantum field theoretical description of transport is developed in terms of nonequilibrium generating Green's functions, culminating in the analysis of the transient time development of negative absolute minority electron mobility at low temperature in an electron-hole plasma in a quantum well. In this connection, the microscopic dynamics for a coupled electron-hole-phonon system with electron-electron and hole-hole interactions are set fourth, as well as the electron-hole attraction responsible for drag phenomena. The coupled fields equations for the one-electron and one-hole Green's functions, and for the electron-hole Green's functions, and for the two-electron and two-hole Green's functions, which involve the mixed Green's functions for the one electron or one hole and phonon state variable are derived. The effective interactions are also derived on this basis as well as the dressed phonon propagator. A generalized shielded potential approximation is propounded and an exact variational differential counterpart of the GKB ansatz is developed after separating of the gauge dependence of the physical Green's function in the presence of interactions. Linearized time-dependent coupled electron and hole Wigner function transport equations are analyzed numerically to study the transient time development of negative electron mobility, including both electron and hole overshoot phenomena, and the approach to steady state subject to dynamic nonlocal electron and hole screening effects. Dissert. Abstr.

N91-23938 Ohio State Univ., Columbus.
MEAN-FIELD THEORIES OF THE HUBBARD MODEL AND PERIODIC ORBITS IN CHAOTIC MAPS Ph.D. Thesis
Wolfgang Wenzel 1990 254 p
Avail: Univ. Microfilms Order No. DA9105237

A Hartree-Fock mean field treatment is presented for the Hubbard model in two dimensions at zero temperature, including incommensurate spin and charge density waves on the square and triangular lattice. For the square lattice, the mean field phase diagram for small deviations from half filling and all U are calculated. For the triangular lattice the Mott-Hubbard Metal-Insulation transition at half filling is completely described. A new methodology is developed to calculate periodic orbits for a certain class of chaotic maps. The method permits the calculation of all periodic orbits of a given order to machine accuracy. Author

N91-23939# Sandia National Labs., Albuquerque, NM.
HIGH POWER LIGHT ACTIVATED SEMICONDUCTOR SWITCHES WITH SUB-NANOSECOND RISE TIME
F. J. Zutavern, G. M. Loubriel, M. T. Buttram, M. W. OMalley, W. D. Helgeson, and D. L. McLaughlin 1991 4 p Presented at the International Microwave Symposium, Boston, 11-14 Jun. 1991
(Contract DE-AC04-76DP-00789)
(DE91-009250; SAND-90-3189C; CONF-910690-1) Avail: NTIS HC/MF A01

This paper presents a summary of results from experiments with large GaAs, InP, and silicon photoconductive semiconductor switches (PCSS). Linear and high gain (lock-on) switching modes will be described. We have used individual PCSS to switch voltages as high as 120 kV and currents as high as 4.2 kA and have produced rise times as fast as 200 ps in the linear mode and 600 ps in the initiation of lock-on. The high gain switching mode is important to applications which must be compact or operate at high repetition rates. The highest power which we have switched to date with a pulsed semiconductor laser diode array (100 W) is 40 MW. The potential development of these switches for future applications will also be discussed. DOE

N91-23940# Brookhaven National Lab., Upton, NY.
THEORY OF THE CRITICAL CURRENT DENSITY IN YBa2Cu3O7 CERAMICS
Zhi-Xiong Cai and D. O. Welch 1991 5 p Presented at the 4th Annual Workshop on the Recent Development of Computer Simulation Studies in Condensed Matter Physics, Athens, 18-22 Feb. 1991
(Contract DE-AC02-76CH-00016)
(DE91-009443; BNL-45806; CONF-910298-1) Avail: NTIS HC/MF A01

One of the stumbling blocks in the practical application of the high (Tc) ceramic materials is their low critical current densities as compared to typical values for single crystals and epitaxial thin films. It is generally believed that the predominate factor limiting the critical current is the weak link behavior of the superconducting current at grain boundaries. Grain alignment has been used to obtain favorable orientations of the grains and/or obtain favorable grain boundaries. The case is studied where the c-axes of the grains are aligned, in a common direction. This type of alignment is obtained by a variety of techniques, such as the application of a uniaxial pressure during processing or magnetic alignment of powder particles. In these samples the relative orientation of the two grains at grain boundaries involves a rotation about the c-axis. Conduction across these boundaries would be within the ab-plane, which has a larger coherence length than that in c-axis. DOE

N91-23941# Sandia National Labs., Albuquerque, NM.
ELECTRONIC PROPERTIES OF Si-DOPED n-DOPING-INTRINSIC-p-DOPING-INTRINSIC (nipi) STRUCTURES IN GaAs
C. Y. Fong, R. F. Gallup (California Univ., Davis.), and J. S. Nelson 1990 10 p Presented at the SPIE International Conference on Physical Concepts of Materials for Novel Optoelectronic Devices Applications, Aachen, Fed. Republic of Germany, 27 Oct. - 2 Nov. 1990
(Contract DE-AC04-76DP-00789)
(DE91-009474; SAND-91-0586C; CONF-901047-2) Avail: NTIS HC/MF A02

The electronic properties of heavily and orderly Si-doped nipi structures in GaAs are studied theoretically using the ab-initio self-consistent pseudopotential method within the local density approximation. Two nipi (n-doping Intrinsic p-doping Intrinsic) configurations are considered. Besides investigating the nature of

the impurity-related band edge states, the xy-planar-averaged local ionic and self-consistent potentials are also analyzed. The screening effect of the host crystal on the doping induced potential is found to be small. The effects of the doping induced electric field and the strain due to dopings are also examined. DOE

N91-23942# Los Alamos National Lab., NM.
MICROSTRUCTURE OF EPITAXIAL YBa2Cu3O7 THIN FILMS
T. E. Mitchell 1990 18 p Presented at the 2nd International Ceramic Science and Technology Congress, Orlando, 12-15 Nov. 1990
(Contract W-7405-eng-36)
(DE91-009951; LA-UR-91-887; CONF-901125-11) Avail: NTIS HC/MF A03

Thin epitaxial films of YBa2Cu3O7 on single crystal substrates have been prepared in situ by laser ablation and by post situ annealing of evaporated films of Cu, Y and BaF2. Substrates include (001) SrTiO3, LaGaO3, and LaAlO3. For both in situ and post situ annealed films, epitaxial (001) grains of YBa2Cu3O7 form near the substrate but (100) and (010) grains tend to nucleate for thicknesses greater than approximately 0.5 microns. 90 deg grain boundaries are therefore common, as well as other defects such as small angle boundaries dislocations and stacking faults. High resolution electron microscopy of the substrate/superconductor interface shows regions of perfect epitaxy, distorted areas, amorphous regions and areas of interdiffusion. The relationship of observed microstructure to critical current density is discussed. DOE

N91-23943# Los Alamos National Lab., NM.
FERMI SURFACE OF YBCO BY DHVA
J. L. Smith, C. M. Fowler, B. L. Freeman, W. L. Hults, J. C. King, and F. M. Mueller Jan. 1991 7 p Presented at the Workshop on Electronic Structures and Mechanisms for High Temperature Superconductivity, Miami, 3-9 Jan. 1991
(Contract W-7405-eng-36)
(DE91-009963; LA-UR-91-964; CONF-910190-2) Avail: NTIS HC/MF A02

These proceedings demonstrate how far scientist have come in the last four years of high temperature superconductivity. Knowledge of the energy bands and Fermi surfaces from experiment has come rather late. Photoemission, first showed proof of the validity of the energy band calculations. Positron annihilation, presented by West, after a rough start, is now giving evidence of the Fermi surface. Both of these techniques involve electronic excitations and hence, although they show the Fermi surface, do not put as severe a constraint on various models for superconductivity as does the de Haas-van Alphen (dHvA) effect. This is a true measurement of the electronic ground state in an applied magnetic field where the frequency of oscillatory magnetization yields extremal cross-sectional areas of the Fermi surface. The authors have already reported some of their Fermi surface work at two conferences but present here discussion of several more important aspects of the work. DOE

N91-23944# Los Alamos National Lab., NM.
STRAIN RELEASE IN GaAs/Ga(1-x)/In(x)As STRAINED LAYER SUPERLATTICES GROWN ON (112) SUBSTRATES
T. E. Mitchell and O. Unal 1991 7 p Presented at the 7th Oxford Conference on Microscopy of Semiconducting Materials, London, England, 25-28 Mar. 1991
(Contract W-7405-eng-36)
(DE91-009972; LA-UR-91-1043; CONF-910322-1) Avail: NTIS HC/MF A02

GaAs/Ga(1-x)In(x)As strained layer superlattices with well-widths of 7 nm, barrier widths of 14 nm and periods of 10 to 30 have been examined by TEM for (112) substrates. Individual layers are below the critical thickness while the overall SLS is above its critical thickness. Two sets of primary 79 deg dislocations are observed lying along group of zone axes (1'3'2) directions, while for larger periods two additional sets of secondary 60 deg dislocations are observed lying along zone axes (11'0). This is discussed in terms of the resolved shear stresses resulting from coherency strains. DOE

N91-23945# Argonne National Lab., IL.
SINTERING AND HOT ISOSTATIC PRESSING OF Bi2Sr2CaCu2O(x)
A. S. Nash, P. Nash (Illinois Inst. of Tech., Chicago.), R. B. Poeppel, and K. C. Goretta Jan. 1991 10 p Presented at the High-Temperature Superconductors: Processing and Microstructure Property Relationships, New Orleans, 17-21 Feb. 1991
(Contract W-31-109-eng-38)
(DE91-010797; ANL/CP-71063; CONF-910212-4) Avail: NTIS HC/MF A02

The Bi2Sr2CaCu2O(x) phase was synthesized by solid-state reaction of oxides and carbonates. Initial compositions of Bi:Sr:Ca:Cu were 4:3:3:6 and 2:1.7:1:2. Pellets of the pure powder and powder containing 2.5, 5, or 15 wt percent Ag were cold-pressed and either sintered or hot isostatically pressed (HIPped). For HIPping, the pellets were encased in thin Ag sheets, canned in steel, and pressed at 105 MPa in argon at 800 or 850 C. HIPping produced dense specimens, but sintering did not. HIPping induced very little decomposition of the Bi2Sr2CaCu2O(x), but a post-HIP anneal was needed to raise the transition temperature above 80 K. The Ag additions appeared to minimize microcracking during HIPping at 800 C. Little microcracking was evident in any of the specimens HIPped at 850 C. DOE

N91-23946*# National Aeronautics and Space Administration. Lewis Research Center, Cleveland, OH.
ADVANCES IN SILICON CARBIDE CHEMICAL VAPOR DEPOSITION (CVD) FOR SEMICONDUCTOR DEVICE FABRICATION
J. Anthony Powell, Jeremy B. Petit (Sverdrup Technology, Inc., Brook Park, OH.), and Lawrence G. Matus 1991 8 p Presented at the First International High Temperature Electronics Conference, Albuquerque, NM, 16-20 Jun. 1991; sponsored by Sandia National Labs., AF Wright Research and Development Center, and New Mexico Univ.
(NASA-TM-104410; E-6237; NAS 1.15:104410) Avail: NTIS HC/MF A02 CSCL 20L

Improved SiC chemical vapor deposition films of both 3C and 6H polytypes were grown on vicinal (0001) 6H-SiC wafers cut from single-crystal boules. These films were produced from silane and propane in hydrogen at one atmosphere at a temperature of 1725 K. Among the more important factors which affected the structure and morphology of the grown films were the tilt angle of the substrate, the polarity of the growth surface, and the pregrowth surface treatment of the substrate. With proper pregrowth surface treatment, 6H films were grown on 6H substrates with tilt angles as small as 0.1 degrees. In addition, 3C could be induced to grow within selected regions on a 6H substrate. The polarity of the substrate was a large factor in the incorporation of dopants during epitaxial growth. A new growth model is discussed which explains the control of SiC polytype in epitaxial growth on vicinal (0001) SiC substrates. Author

N91-23947# Aerospatiale Aquitaine, Saint-Medard en Jalles (France).
EURECA 1 AMF 117 EXPERIMENT: AN ANALYSIS OF THERMAL AND SOLUTAL TRANSFER DURING THE CRYSTAL GROWTH OF CdTe BY THE THM PROCESS
Joel Boucherie, Jean-Claude Launay, and Eric Arquis (Bordeaux 1 Univ., Talence, France) 1991 11 p In FRENCH; ENGLISH summary
(Rept-911-430-118; ETN-91-99290) Avail: NTIS HC/MF A03

Fluid phase motions and their interactions with single crystal growth processes are described. Within the context of the growth experiment of CaTe by THM (Traveling Heater Method), the concentration driven convection is integrated with the thermal convection. A numerical method previously tested for thermal natural convection is extended to the thermosolutal convection case. The problem is described by the Navier-Stokes and continuity equations coupled with two convection diffusion equations. Two

kinds of boundary conditions are being introduced: active walls, e.g., solid fluid interfaces, and non active walls e.g., enclosure walls. Results of the determination of characteristic dimensionless parameters are presented in different configurations. ESA

N91-23948# Aerospatiale Aquitaine, Saint-Medard en Jalles (France).
EURECA 1 AMF 117 EXPERIENCE: THERMAL AND SOLUTAL TRANSFER ANALYSIS FOR CdTe IN TELLURIUM DURING CRYSTAL GROWTH BY THE THM METHOD [EURECA 1 EXPERIENCE AMF 117: ANALYSE DES TRANSFERTS (THERMIQUE ET SOLUTAL) DE CDTE DANS TE LORS DE LA CROISSANCE PAR LA METHODE THM]
Joel Boucherie, Jean-Claude Launay, and Eric Arquis (Bordeaux 1 Univ., Talence, France) 1991 19 p In FRENCH Presented at 33rd ISTN Colloque de Metallurgie: Cinquieme COMET
(Rept-911-430-120; ETN-91-99292) Avail: NTIS HC/MF A03

Within the context of the growth experiment of CdTe by THM (Traveling Heater Method), the solutal convective aspect was integrated in thermal convection. The Rayleigh numbers comparison showed that the solutal aspect would be more active. In the numerical modelization, equations of motion are coupled to equations of conservation through the solution source term in quasi stationary conditions. In boundary conditions, active and inactive boundaries and radiation are integrated. The equation system is solved by the control volume method. Results based on the determination of non dimensional characteristic values are presented in graphical format. ESA

N91-23949# Royal Signals and Radar Establishment, Malvern (England).
LIQUID-CRYSTAL CHARACTERIZATION USING THE Z-SCAN TECHNIQUE
K. J. McEwan and S. Young Jan. 1991 16 p
(RSRE-Memo-4451; BR116433; ETN-91-99325) Copyright
Avail: NTIS HC/MF A03

The laser technique known as Z-Scan to examine the nonlinear optical behavior of a typical liquid crystal (5CB) in the isotropic phase is used. By matching the laser pulse length with the molecular reorientational relaxation time, the transient regime is examined and successfully modeled. For 5BC, which has a nematic to isotropic phase transition at 35.5 C, it is shown that the effective optical nonlinearity decreases rapidly with temperature above 55 C, which suggests an operational temperature range of 20 C. The largest effect is observed where the relaxation time matches the pulse length of the laser. ESA

N91-23950# Colorado State Univ., Fort Collins. Dept. of Electrical Engineering.
OPTOELECTRONIC III-V HETEROSTRUCTURES ON SI SUBSTRATES Annual Report, 15 Sep. 1989 - 14 Sep. 1990
Gary Y. Robinson 14 Sep. 1990 42 p
(Grant AF-AFOSR-0513-89; AF Proj. 2306)
(AD-A232035; AFOSR-91-0019TR) Avail: NTIS HC/MF A03 CSCL 09/5

The objectives of this research program is to investigate the epitaxial growth and properties of heterostructures of the III-V semiconductors, particularly the InGaAsP/InP system, on Si substrates. The heterostructures are being grown by gas-source molecular beam epitaxy (GSMBE), a technique which have previously used to produce high performance optoelectronic devices using lattice-matched InGaAs/InP and InGaAsP/InP heterostructures and to grow high quality InP layers on Si wafers. The research is focused on exploring methods to reduce misfit dislocations and thus, achieve InGaAsP/InP heteroepitaxial materials suitable for high quality optoelectronic devices on Si substrates. InP and lattice-matched InGaAsP alloys are the primary material for high speed optoelectronic telecommunication systems, and an InP-on-Si materials technology would enable VLSI photonics to become a reality. GRA

N91-23951# CPS Superconducors, Inc., Milford, MA.
COMPOSITE CERAMIC SUPERCONDUCTING WIRES FOR ELECTRIC MOTOR APPLICATIONS Technical Report, 1 Oct. - 31 Dec. 1990
Mark V. Parish 31 Dec. 1990 58 p
(Contract N00014-88-C-0512)
(AD-A232074; CPSS-1290-01) Avail: NTIS HC/MF A04 CSCL 09/1

A process for producing technologically useful HTSC wire for application in a prototype HTSC electric motor is proceeding. These fibers are produced continuously and lengths of up to 1.0 meter have been successfully textured. Work this past quarter has advanced our understanding of the relationship between processing conditions, microstructure, electrical characteristics, and improvements in fiber uniformity. BiSCCO ribbon wire was further developed. The development of a robust process for producing a reproducible BiSCCO powder for use as process feedstock have been defined this quarter. Emerson Electric has designed, constructed, and tested the brushless trapped magnetic flux permanent magnet motor. GRA

N91-23952# Litton Systems, Inc., Charlotte, NC. Airtron Div.
CONTRACT CRYSTAL GROWTH AND FABRICATION SERVICES Quarterly Report No. 7, Nov. 1990 - Jan. 1991
M. H. Randles 19 Feb. 1991 2 p
(Contract N00014-89-C-2222)
(AD-A232120) Avail: NTIS HC/MF A01 CSCL 20/2

This program is intended to give the scientists at the Naval Research Laboratory the ability to evaluate new solid state laser crystals. The crystal requested and grown was Erbium Scandium Gallium Garnet (ESGG). The melt composition is listed in Table 1. It was assumed that the distribution coefficients are unity and that the crystal composition will be the same as the melt. The crystal grew well. Some strain and surface cracking exists. The best material is in the center of the boule. No fluorescence was observed with a bright fiber optic inspection light or long wave UV source. GRA

N91-23953# Case Western Reserve Univ., Cleveland, OH.
TRANSPORT AND NUCLEATION PROCESSES IN THE VAPOR GROWTH OF DIAMOND Progress Report, 1 Jul. 1989 - 31 Dec. 1990
John C. Angus, J. A. Mann, Jr., Yaxin Wang, Mahendra Sunkara, and Paul A. Washlock 31 Jan. 1991 34 p
(Contract N00014-89-J-3167)
(AD-A232135) Avail: NTIS HC/MF A03 CSCL 07/4

Rule-based computer modeling was used to study the initial stages of diamond nucleation from the vapor and the relationship of observed crystalline morphology to the nucleation and growth mechanisms. The enhanced growth rates of nuclei with multiple twins were confirmed and plausible mechanisms for the formation of five- and twenty-fold twinned crystals found. Two-dimensional simulations of a hot-filament reactor are being made. The flow field, temperature field and species concentrations for reactors of arbitrary geometry are obtained. At present the chemical reaction is restricted to ten simultaneous reactions. The program is being further modified to handle more complex chemistry. Experimental work on the seeding of diamond nucleation with specific compounds has proceeded in parallel with the modeling studies. The compound 3, 4, 9, 10-perylene tetracarboxylic acid dianhydride was found to be a strong nucleation promoter, while adamantane and its derivatives were not. GRA

N91-23954# California Univ., Los Angeles.
X RAY DIFFRACTION AND ELECTRON SPECTROSCOPY OF EPITAXIAL MOLECULAR C60 FILMS Technical Report No. 11, Jun. 1990 - Feb. 1991
William M. Tong, Douglas A. Ohlberg, Hong K. You, R. S. Williams, and Samir J. Anz 28 Feb. 1991 21 p
(Contract N00014-90-J-1178)
(AD-A232152) Avail: NTIS HC/MF A03 CSCL 09/1

Films of the new carbon allotrope, molecular C60, also known as Buckminsterfullerence, have been grown on Si(111) substrates

by molecular beam epitaxy. The films have been characterized with x-ray two-theta diffraction, x-ray photoelectron spectroscopy, Auger electron spectroscopy, and electron energy loss spectroscopy. The diffraction data from oriented films show that close-packed planes of C60 molecules are stacked parallel to the substrate surface, but that the correlation length for x-ray scattering is less than 200 angstroms. The electron spectroscopic data shows that the C atoms of C60 are essentially sp2-bonded, but there are significant differences with respect to graphite. GRA

N91-23955# North Carolina State Univ., Raleigh.
RESEARCH AND DEVELOPMENT ON ADVANCED SILICON CARBIDE THIN FILM GROWTH TECHNIQUES AND FABRICATION OF HIGH POWER AND MICROWAVE FREQUENCY SILICON CARBIDE-BASED DEVICE STRUCTURES Annual Letter Report, FY-90
Robert F. Davis Dec. 1990 50 p
(Contract N00014-88-K-0341)
(AD-A232160) Avail: NTIS HC/MF A03 CSCL 07/2

The RF operation of MESFETs and bipolar transistors fabricated from both alpha- and beta-SiC have been modeled. The results show that SiC has considerable promise for producing microwave power MESFETs with RF output power capability greater (approx. 4 times) than can be obtained with any of the commonly used semiconductors (e.g., GaAs), this due to the high breakdown field of SiC that allows high bias voltage to be applied. These device modeling efforts have been used as a guide to design a new MESFET mask set with a aS micron gate length and reduced gate pad area. For the first time, positive gain was observed for a SiC transistor at microwave frequencies. The highest values for Ft and Fmax were 2.9 GHz and 1.9 GHz, respectively. The highest current and power gains observed at 1.0 GHz were 8.5 dB and 7 db, respectively. Avalanche characteristics for a 6H-SiC IMPATT were observed for the first time. Heteroepitaxial growth of Ti on (0001) 6H-SiC has been achieved at room and elevated temperatures. Current voltage measurements display shifts toward ohmic behavior after annealing at 400 C. Molecular beam epitaxy equipment has been designed and commissioned. GRA

N91-23956# Duke Univ., Durham, NC. Dept. of Chemistry.
SYNTHESIS AND CHARACTERIZATION OF INDIUM-ARSENIC COMPOUNDS CONTAINING A FOUR-MEMBERED In-Ad-In-As OR In-As-In-Cl RING: CRYSTAL STRUCTURES OF ((Me3SiCH2)2 InAs(SiMe3)2)2 AND (Me3SiCH2)2 InAs(SiMe3)2 In(CH2SiMe3)2Cl
R. L. Wells, L. J. Jones, A. T. McPhail, and A. Alvanipour 25 Feb. 1991 24 p
(Contract N00014-89-J-1545)
(AD-A232368; DU/DC/TR-18) Avail: NTIS HC/MF A03 CSCL 20/2

Recently, organogallium-arsenic compounds containing four-membered rings consisting of mixed-bridging of the gallium atoms by one arsenic atom and one halogen atom have been synthesized via dehalosilyation between an organogallium halide and a silylarsine. Until now, our studies regarding the formation of mixed bridge systems involving the heavier elements of Groups III and V have focused only on gallium and arsenic. In order to investigate the generality of this behavior, analogous reactions utilizing an organoindium halide were carried out. GRA

N91-23957# Howard Univ., Washington, DC.
LASER ASSISTED CVD GROWTH OF AlN AND GaN Annual Report No. 1, 1 Aug. 1989 - 31 Aug. 1990
Joshua B. Halpern, Joan M. Frye, Gary Harris, and M. Aluko 31 Aug. 1990 27 p
(Contract F49620-89-C-0108)
(AD-A232379; AFOSR-91-0005TR) Avail: NTIS HC/MF A03 CSCL 09/3

This is the first annual report of a project for investigating laser assisted CVD growth of AlN and GaN. In the first year, three experimental systems have been built. The first is a small, mobile CVD test system for evaluating growth schemes and detection methods for gas and heterogeneous phases. The second is a tunable diode laser spectrometer for monitoring gas phase components in a CVD reactor. The third is a dye laser system for monitoring atoms and small free radicals in the CVD system. First experiments have been done with all three systems. In particular we are investigating the use of 248 nm photolysis of trimethylaluminum near a slightly heated substrate in a mixture of TMA1 and hydrazine for growth of AlN. GRA

N91-23958# Minnesota Univ., Minneapolis.
EPITAXIAL IRON FILMS Annual Report, 15 Dec. 1989 - 14 Dec. 1990
E. D. Dahlberg and P. I. Cohen 15 Jan. 1991 58 p
(Contract AF-AFOSR-0248-89; AF Proj. 2306)
(AD-A232419; AFOSR-91-0113TR) Avail: NTIS HC/MF A04 CSCL 09/1

This research involves studies of the magnetic properties of high quality thin and multilayered magnetic films. Both ultra high vacuum sputtering and molecular beam epitaxy techniques are utilized to prepare the films. Electrical transport is the primary probe to measure the magnetic properties of the films. Of special interest has been the determination of the temperature dependence of the magnetic anisotropy energies of epitaxial iron films and the transport properties of multilayers. In the anisotropy energy work the effects of interfacial strain and morphology have been the focus. GRA

N91-23959# Puerto Rico Univ., Rio Piedras. Dept. of Physics.
SURFACE X RAY SCATTERING MEASUREMENTS OF THE SUBSTRATE INDUCED SPATIAL MODULATION OF AN INCOMMENSURATE ADSORBED MONOLAYER
Michael F. Toney, Joseph G. Cordon, Mahesh G. Samant, Gary L. Borges, and Larry B. Sorensen 29 Jan. 1991 36 p Prepared in cooperation with IBM Research Lab., San Jose, CA, and Washington Univ., Seattle
(Contract N00014-90-J-1263)
(AD-A232625; TR-5) Avail: NTIS HC/MF A03 CSCL 20/2

We report in-situ surface x ray scattering measurements of electrochemically deposited Tl monolayers on Ag(111). We find that the Tl adlayer forms an incommensurate, two dimensional solid and we determine the spatial modulation in the Tl monolayer that is induced by the periodic potential of the substrate. The modulation of the Tl monolayer changes the intensity of the x ray scattering from the Ag substrate (the Ag crystal truncation rods), since the modulation wavevectors are commensurate with the substrate periodicity. By measuring the intensity changes along the Ag truncation rods, we determined the first Fourier component of the longitudinal part of the substrate induced modulation to be 0.03 A, and the spacing of the Tl monolayer above the Ag surface to be 3.05 A. GRA

N91-23960# California Inst. of Tech., Pasadena.
IN BASED III-V MICROSTRUCTURES WITH NOVEL ELECTRONIC PROPERTIES Final Report, 15 Sep. 1986 - 14 Feb. 1990
T. C. McGill, Jr. 30 Oct. 1990 98 p
(Grant AF-AFOSR-0306-86; AF Proj. 2306)
(AD-A232695; AFOSR-91-0151TR) Avail: NTIS HC/MF A05 CSCL 09/1

This program addresses the development of microstructures for high density and high speed electronics. The molecular beam epitaxy technology for InAs and GaSb were developed for growth in GaAs substrates. Three new single barrier negative resistance devices were demonstrated. Double barrier negative resistance devices based on InAs/AlSb/InAs/AlSb/InAs heterostructures were fabricated. These currently hold all the power and frequency records. GRA

N91-23961# Hughes Research Labs., Malibu, CA.
DEVELOPMENT OF Si/SiGe HETEROSTRUCTURES Final Report, Sep. 1987 - Aug. 1990
R. J. Hauenstein, J. L. Veteran, and M. H. Young Jan. 1991 35 p

(Contract F49620-87-C-0104; DARPA Order 6140)
(AD-A232747; AFOSR-91-0050TR) Avail: NTIS HC/MF A03 CSCL 20/2

New molecular beam epitaxy (MBE) materials growth and doping processes were developed for the fabrication of Si/SiGe heterostructure devices. These new materials processes are applied to the demonstration of cryogenic n-p-n Si/Si 1-x Gex/Si heterojunction bipolar transistors (HBT). This application has special significance as an enabling DoD technology for fast low noise, high performance readout and signal processing circuits for IR focal systems. Reliable, versatile methods were developed to grow very high quality Si/SiGe strained layer heterostructures and multilayers. In connection with this program methods were developed to dope the Si and SiGe with B, Sb and Ga. B and Sb were found to be the preferred dopants for p and n regions respectively, of the HBT devices. The test devices clearly displayed gain enhancement due to the heterojunction and provided useful gains from room temperature down to 10 K. GRA

N91-23962# Air Force Inst. of Tech., Wright-Patterson AFB, OH. Foreign Technology Div.
SZ SERIES GaAs SUPER HIGH-SPEED LOGIC GATE: OPTIMUM CHOICE. HIGH TECH; HIGH SPEED; HIGH QUALITY
11 Jan. 1991 5 p Transl. into ENGLISH from JSIO, Semiconductor Technology (China), no. 3, 1989
(AD-A232819; FTD-ID(RS)T-1365-90) Avail: NTIS HC/MF A01 CSCL 09/1

The modernized, maximum speed SZ series GaAs gate products are recommended: single-gate minimum transmission delay can be lower than 150ps; single-gate minimum rise time and fall time can be lower than 150 ps. The inputs and outputs can all be connected to ECL circuits. Used together with FETs, they can drive 50 ohm load lines. Wide application in the development of advanced and large-size, super high-speed computers in high-speed information processing systems, such as optical fiber communications and digital microwave communications. The oscillation frequency of the ring oscillator can reach 500 MHz; the extracted clock frequency of the clock extraction circuit can reach 2000 MHz. GRA

N91-23963# Waterloo Univ. (Ontario). Dept. of Chemistry.
A RAMAN SPECTROSCOPIC AND ELECTROCHEMICAL STUDY OF THE PHOTOINDUCED CRYSTALLIZATION OF TRIETHYLENEDIAMINE TRIIODIDE UPON A SILVER ELECTRODE Technical Report No. 18, Aug. - Dec. 1990
Toru Ozek and Donald E. Irish 15 Feb. 1991 28 p
(Contract N00014-87-J-1118)
(AD-A232828) Avail: NTIS HC/MF A03 CSCL 20/2

When a silver electrode, electrochemically coated with AgI, is immersed in an electrolyte containing NaI and the diprotonated form of 1,4-diazabicyclo 2.2.2 octane (abbreviated DABCO-H22+), and is bathed in 514.5 nm radiation from an argon ion laser through the objective of the microscope attachment of the DILOR Omars-89 Raman spectrophotometer, crystals form from the focal point. These are attributed to DABCO-h22+ 213-. Both spectroscopic and electrochemical experiments are described and interrelated. A mechanism for this photoinduced electrochemical crystal growth is presented. GRA

N91-23835# Technion - Israel Inst. of Tech., Haifa. Dept. of Physics.
FIRST PRINCIPLES CALCULATION OF THE CRYSTAL STRUCTURES IN THE 4d TRANSITION METALS Abstract Only
N. Davidson, G. Barak, and J. Ashkenazi *In* Tel-Aviv Univ., Bulletin of the Israel Physical Society, Volume 33, 1987. Annual Meeting 1987: Annual Meeting 1987: Program and Abstracts 1987 p 26 (For primary document see N91-23832 15-70)
Avail: NTIS HC/MF A08

N91-23837# Tel-Aviv Univ. (israel). School of Physics and Astronomy.
OPTICAL AND MECHANICAL PROPERTIES OF MIXED SILVER HALIDE CRYSTALS Abstract Only
N. Barkay, F. Moser, A. Saar, and A. Katzir *In its* Bulletin of the Israel Physical Society, Volume 33, 1987. Annual Meeting 1987: Program and Abstracts 1987 p 39 (For primary document see N91-23832 15-70)
Avail: NTIS HC/MF A08

N91-23841# Bar-Ilan Univ., Ramat-Gan (Israel). Dept. of Physics.
A HIGH RESOLUTION STUDY OF THE Cu K ALPHA(SUB 1,2) X-RAY EMISSION LINES Abstract Only
Nissan Maskil and Moshe Deutsch *In* Tel-Aviv Univ., Bulletin of the Israel Physical Society, Volume 33, 1987. Annual Meeting 1987: Program and Abstracts 1987 p 57 (For primary document see N91-23832 15-70)
Avail: NTIS HC/MF A08

N91-23842# Technion - Israel Inst. of Tech., Haifa. Dept. of Physics.
THEORY OF THE NEW HIGH-TEMPERATURE SUPERCONDUCTORS Abstract Only
J. Ashkenazi, C. G. Kuper, and R. Tyk *In* Tel-Aviv Univ., Bulletin of the Israel Physical Society, Volume 33, 1987. Annual Meeting 1987: Program and Abstracts 1987 p 60 (For primary document see N91-23832 15-70)
Avail: NTIS HC/MF A08

N91-24061*# National Aeronautics and Space Administration. Lewis Research Center, Cleveland, OH.
SILICON CARBIDE, AN EMERGING HIGH TEMPERATURE SEMICONDUCTOR
Lawrence G. Matus and J. Anthony Powell *In* NASA, Washington, Technology 2000, Volume 2 1991 p 171-178 (For primary document see N91-24041 15-99)
Avail: NTIS HC/MF A16 CSCL 20L

N91-24080*# National Aeronautics and Space Administration. Lewis Research Center, Cleveland, OH.
AEROSPACE APPLICATIONS OF HIGH TEMPERATURE SUPERCONDUCTIVITY
V. O. Heinen and D. J. Connolly *In* NASA, Washington, Technology 2000, Volume 2 1991 p 343-345 (For primary document see N91-24041 15-99)
Avail: NTIS HC/MF A16 CSCL 20L

N91-24081*# National Aeronautics and Space Administration. Lewis Research Center, Cleveland, OH.
SUPERCONDUCTING MICROWAVE ELECTRONICS AT LEWIS RESEARCH CENTER
Joseph D. Warner, Kul B. Bhasin, and Regis F. Leonard *In* NASA, Washington, Technology 2000, Volume 2 1991 p 346-354 (For primary document see N91-24041 15-99)
Avail: NTIS HC/MF A16 CSCL 20L

N91-24082*# National Aeronautics and Space Administration. Goddard Space Flight Center, Greenbelt, MD.
MELT-PROCESSED BULK SUPERCONDUCTORS: FABRICATION AND CHARACTERIZATION FOR POWER AND SPACE APPLICATIONS
Hamid Hojaji, Aaron Barkatt, Shouxiang Hu, Arthur N. Thorpe, Matthew F. Ware, David Davis (Howard Univ., Washington, DC.), and Sidney Alterescu *In* NASA, Washington, Technology 2000, Volume 2 1991 p 356-364 (For primary document see N91-24041 15-99)
(Grant NAG5-1017)
Avail: NTIS HC/MF A16 CSCL 20L

N91-24083*# National Aeronautics and Space Administration. Langley Research Center, Hampton, VA.
DESCRIPTION OF THE LARGE GAP MAGNETIC SUSPENSION SYSTEM (LGMSS) GROUND-BASED EXPERIMENT

Nelson J. Groom *In* NASA, Washington, Technology 2000, Volume 2 1991 p 365-377 (For primary document see N91-24041 15-99)
Avail: NTIS HC/MF A16 CSCL 20L

77 THERMODYNAMICS AND STATISTICAL PHYSICS

Includes quantum mechanics; theoretical physics; and Bose and Fermi statistics.

For related information see also *25 Inorganic and Physical Chemistry* and *34 Fluid Mechanics and Heat Transfer.*

N91-23964# Oklahoma Univ., Norman. School of Chemical Engineering and Materials Science.
ADVANCED WORKING FLUIDS: THERMODYNAMIC PROPERTIES Final Report, 1 Dec. 1987 - 30 Nov. 1989
Lloyd L. Lee and Kevin L. Gering Oct. 1990 188 p
(Contract GRI-5087-233-1616)
(PB91-136465; GRI-90/0102) Avail: NTIS HC/MF A09 CSCL 20M

Electrolytes are used as working fluids in gas fired heat pump chiller engine cycles. To find out which molecular parameters of the electrolytes impact on cycle performance, a molecular theory is developed for calculating solution properties, enthalpies, vapor-liquid equilibria, and engine cycle performance. Aqueous and ammoniac single and mixed salt solutions in single and multisolvent systems are investigated. An accurate correlation is developed to evaluate properties for concentrated electrolyte solutions. Sensitivity analysis is used to determine the impact of molecular parameters on the thermodynamic properties and cycle performance. The preferred electrolytes are of 1-1 valence type, small ion size, high molecular weight, and in strongly colligative cosolvent. The operating windows are determined for a number of absorption fluids of industrial importance. Author

N91-23965 North Carolina Univ., Chapel Hill.
INITIAL DATA FOR THE TWO-BODY PROBLEM OF GENERAL RELATIVITY Ph.D. Thesis
Gregory Brown Cook 1990 233 p
Avail: Univ. Microfilms Order No. DA9106088

A formalism for constructing initial-data sets which represent two black holes in some initial configuration (including non-vanishing linear and angular momenta for each hole) is reviewed. Based on this formalism, computational techniques are developed which allow for the complete specification of initial data describing both one and two black holes with individually specifiable linear and angular momenta. Bispherical coordinates are used to construct very accurate initial-data sets. Dissert. Abstr.

N91-23966 Aberdeen Univ. (Scotland).
SYMMETRIES IN GENERAL RELATIVITY Ph.D. Thesis
John D. Steele 1989 142 p
Avail: Univ. Microfilms Order No. BRDX91626

The purpose is to study those non-flat space-times in General Relativity that admit high dimensional Lie groups of symmetries, in particular motions, homotheties, conformals and affines, and to improve a theorem on the relationship between the first three of these, first proved by Bilyalov and also by Defrise-Carter. The basic mathematical theory and notations are set, covering manifolds, tensors, Lie groups, metrics, connections, and groups of transformations. The concepts of General Relativity are introduced. A study is presented of a particular class of solutions to Einstein equations, called generalized p.p. waves, characterized in various equivalent waves but here defined as space-times admitting a covariantly constant null bivector. Motions, homotheties, and affines are considered. The proof of the Bilyalov-Defrise-Carter theorem is also presented. Author

N91-23836# Hebrew Univ., Jerusalem (Israel). Racah Inst. of Physics.
SUPERSYMMETRIC MATTER AT FINITE TEMPERATURE Abstract Only
G. Horwitz and G. Kalbermann *In* Tel-Aviv Univ., Bulletin of the Israel Physical Society, Volume 33, 1987. Annual Meeting 1987: Program and Abstracts 1987 p 37 (For primary document see N91-23832 15-70)
Avail: NTIS HC/MF A08

N91-23843# Tel-Aviv Univ. (Israel). School of Physics and Astronomy.
EXPLORING THE MESOSCOPIC DOMAIN WHERE CLASSICAL AND QUANTUM PHENOMENA MEET Abstract Only
Eshel Ben-Jacob *In its* Bulletin of the Israel Physical Society, Volume 33, 1987. Annual Meeting 1987: Program and Abstracts 1987 p 61 (For primary document see N91-23832 15-70)
(Grant NSF DMR-86-08305)
Avail: NTIS HC/MF A08

80 SOCIAL SCIENCES (GENERAL)

Includes educational matters.

No abstracts in this category.

81 ADMINISTRATION AND MANAGEMENT

Includes management planning and research.

N91-23967# Technion - Israel Inst. of Tech., Haifa. Inst. for Advanced Studies in Science and Technology.
SURVEY: POTENTIAL OF THE ISRAELI INDUSTRY FOR SPACE TECHNOLOGY Progress Report, Apr. - May 1987 [MISHAL: POTENTSIAL HATAASIA HAISRAELIT BETCHUM HACHALAL]
A. Golod and D. Weiss Jun. 1987 63 p In HEBREW Sponsored in part by the Adler Fund for Space Research
(CEMA-86-17; ITN-89-85015) Avail: NTIS HC/MF A04

This research takes place within the framework of a broader survey on civilian uses of space. In order to estimate the potential contribution of the Israeli industry to space technologies and to discern industrial leaders' opinion - a written survey was undertaken among a representative sample of industrial plants belonging to the broad array of technologies related to the subject. The response rate to the questionnaire was 50 percent. It included general questions as well as questions specific to the plant of the responsee. The analysis of the answers points out an insufficient awareness as well as the impossibility of coping with marketing problems without help. The responsees prefer the establishment of a central authority (not necessarily governmental) which would coordinate all activities and instigate cooperation between the different industries. From a technological aspect the responsees consider the Israeli industry as being able to compete successfully with the rest of the world in view of the fact that its main advantages are sophistication and adaptability. ISA

N91-23968# Army Construction Engineering Research Lab., Champaign, IL.
LIFE CYCLE MANAGEMENT AUTOMATION USER'S MANUAL, VERSION 1.1 Final Report
Gonzalo Perez, Don Kermath, Yung Pan, and Donald Murnock Jan. 1991 172 p
(AD-A232096; CERL-ADP-P-91/14) Avail: NTIS HC/MF A08 CSCL 12/5

Life Cycle Management Automation (LCMA) is a microcomputer system to help manage the Army Reserve Inventory of Facilities

through their entire life cycle, from acquisition to disposal. The system is made up of several computer programs, all of which access a common database. The programs included in the LCM are: UNIT, FACILITY, AMSA, BACKLOG, ProjDoc, and MINOR. BACKLOG generates the 5-year plan. ProDoc produces Military Construction, Army Reserve (MCAR) project documentation in minutes. MINOR manages the Minor Construction Program. LCMA requires no special computer training. It runs on IBM-compatible computers with at least 420 K memory, MD DOS 3.1 or higher, 1 floppy disk drive, 8 to 15 megabytes of free hard disk space for the program, and a printer with a 12 character per inch capability. LCMA software was developed and fielded by the Facility System Division (FS) of the U.S. Army Construction Engineering Research Laboratory (USACERL). Subsequent versions and program documentation for LCMA will be available from the U.S. Army Corps of Engineers, Huntsville, Division (CEHND). GRA

82 DOCUMENTATION AND INFORMATION SCIENCE

Includes information management; information storage and retrieval technology; technical writing; graphic arts; and micrography.

For computer documentation see *61 Computer Programming and Software.*

N91-23969# American Association for the Advancement of Science, Washington, DC.

PROCEEDINGS OF THE 1991 AMERICAN ASSOCIATION FOR THE ADVANCEMENT OF SCIENCE ANNUAL MEETING PROGRAM

Arthur Herschman, ed. and Susan M. OConnell, ed. Feb. 1991 163 p Proceedings of the 157th National Meeting, Washington, DC, 14-19 Feb. 1991

Avail: NTIS HC/MF A08

The schedule of meetings for the 1991 American Association for the Advancement of Science Annual Meeting in Washington, DC, February 14 to 19 is given. Summaries are given of the topics and issues to be discussed in such areas as energy technology, computers, astronomy, physics, climate, medical science, health care, agriculture, economics, sociology, and science education.

Author

N91-23970*# Old Dominion Univ., Norfolk, VA. Dept. of Computer Science.

BUILDING A GENERALIZED DISTRIBUTED SYSTEM MODEL

Progress Report, period ended 31 Jul. 1991

Ravi Mukkamala May 1991 70 p

(Grant NAG1-1114)

(NASA-CR-188181; NAS 1.26:188181) Avail: NTIS HC/MF A04 CSCL 05B

A number of topics related to building a generalized distributed system model are discussed. The effects of distributed database modeling on evaluation of transaction rollbacks, the measurement of effects of distributed database models on transaction availability measures, and a performance analysis of static locking in replicated distributed database systems are covered. For individual titles, see N91-23971 through N91-23975.

N91-23971*# Old Dominion Univ., Norfolk, VA. Dept. of Computer Science.

BUILDING A GENERALIZED DISTRIBUTED SYSTEM MODEL

Annual Report

Ravi Mukkamala and E. C. Foudriat *In its* Building a Generalized Distributed System Model May 1991 9 p (For primary document see N91-23970 15-82)

Avail: NTIS HC/MF A04 CSCL 05B

A modeling tool for both analysis and design of distributed systems is discussed. Since many research institutions have access to networks of workstations, the researchers decided to build a tool running on top of the workstations to function as a prototype as well as a distributed simulator for a computing system. The effects of system modeling on performance prediction in distributed systems and the effect of static locking and deadlocks on the performance predictions of distributed transactions are also discussed. While the probability of deadlock is considerably small, its effects on performance could be significant. Author

N91-23972*# Old Dominion Univ., Norfolk, VA. Dept. of Computer Science.

EFFECTS OF DISTRIBUTED DATABASE MODELING ON EVALUATION OF TRANSACTION ROLLBACKS

Ravi Mukkamala *In its* Building a Generalized Distributed System Model May 1991 7 p Proceedings of the Winter Simulation Conference, 1990 (For primary document see N91-23970 15-82)

Avail: NTIS HC/MF A04 CSCL 05B

Data distribution, degree of data replication, and transaction access patterns are key factors in determining the performance of distributed database systems. In order to simplify the evaluation of performance measures, database designers and researchers tend to make simplistic assumptions about the system. Here, researchers investigate the effect of modeling assumptions on the evaluation of one such measure, the number of transaction rollbacks in a partitioned distributed database system. The researchers developed six probabilistic models and expressions for the number of rollbacks under each of these models. Essentially, the models differ in terms of the available system information. The analytical results obtained are compared to results from simulation. It was concluded that most of the probabilistic models yield overly conservative estimates of the number of rollbacks. The effect of transaction commutativity on system throughput is also grossly undermined when such models are employed.

Author

N91-23973*# Old Dominion Univ., Norfolk, VA. Dept. of Computer Science.

MEASURING THE EFFECTS OF DISTRIBUTED DATABASE MODELS ON TRANSACTION AVAILABILITY MEASURES

Ravi Mukkamala *In its* Building a Generalized Distributed System Model May 1991 41 p (For primary document see N91-23970 15-82)

Avail: NTIS HC/MF A04 CSCL 05B

Data distribution, data replication, and system reliability are key factors in determining the availability measures for transactions in distributed database systems. In order to simplify the evaluation of these measures, database designers and researchers tend to make unrealistic assumptions about these factors. Here, the effect of such assumptions on the computational complexity and accuracy of such evaluations is investigated. A database system is represented with five parameters related to the above factors. Probabilistic analysis is employed to evaluate the availability of read-one and read-write transactions. Both the read-one/write-all and the majority-read/majority-write replication control policies are considered. It is concluded that transaction availability is more sensitive to variations in degrees of replication, less sensitive to data distribution, and insensitive to reliability variations in a heterogeneous system. The computational complexity of the evaluations is found to be mainly determined by the chosen distributed database model, while the accuracy of the results are not so much dependent on the models. Author

N91-23974*# Old Dominion Univ., Norfolk, VA. Dept. of Computer Science.

PERFORMANCE ANALYSIS OF STATIC LOCKING IN REPLICATED DISTRIBUTED DATABASE SYSTEMS

Yinghong Kuang and Ravi Mukkamala *In its* Building a Generalized Distributed System Model May 1991 4 p (For primary document see N91-23970 15-82)

(Grants NAG1-1114; NAG1-1154)

Avail: NTIS HC/MF A04 CSCL 05B

Data replications and transaction deadlocks can severely affect the performance of distributed database systems. Many current evaluation techniques ignore these aspects, because it is difficult to evaluate through analysis and time consuming to evaluate

through simulation. Here, a technique is discussed that combines simulation and analysis to closely illustrate the impact of deadlock and evaluate performance of replicated distributed databases with both shared and exclusive locks. Author

N91-23975*# Old Dominion Univ., Norfolk, VA. Dept. of Computer Science.
A NOTE ON THE PERFORMANCE ANALYSIS OF STATIC LOCKING IN DISTRIBUTED DATABASE SYSTEMS
Yinghong Kuang and Ravi Mukkamala *In its* Building a Generalized Distributed System Model May 1991 9 p (For primary document see N91-23970 15-82)
Avail: NTIS HC/MF A04 CSCL 05B

Even though transaction deadlocks can severely affect the performance of distributed database systems, many current evaluation techniques ignore this aspect. Shyu and Li proposed an evaluation method which takes deadlocks into consideration. However, their technique is limited to exclusive locking. Using this technique, researchers illustrate the impact of deadlocks in the presence of shared locking on distributed database performance. Author

N91-23976*# National Aeronautics and Space Administration. John C. Stennis Space Center, Bay Saint Louis, MS.
DIGITAL DATA REGISTRATION AND DIFFERENCING COMPRESSION SYSTEM Patent Application
Gary A. Ransford, inventor (to NASA) and Vivien J. Cambridge, inventor (to NASA) (Sverdrup Technology, Inc., Bay Saint Louis, MS.) 1 Oct. 1990 38 p
(NASA-Case-SSC-00010-1; NAS 1.71:SSC-00010-1; US-Patent-Appl-SN-591643) Avail: NTIS HC/MF A03 CSCL 05B

A process is disclosed for x ray registration and differencing which results in more efficient compression. Differencing of registered modeled subject image with a modeled reference image forms a differenced image for compression with conventional compression algorithms. Obtention of a modeled reference image includes modeling a relatively unrelated standard reference image upon a three-dimensional model, which three-dimensional model is also used to model the subject image for obtaining the modeled subject image. The registration process of the modeled subject image and modeled reference image translationally correlates such modeled images for resulting correlation thereof in spatial and spectral dimensions. Prior to compression, a portion of the image falling outside a designated area of interest may be eliminated, for subsequent replenishment with a standard reference image. The compressed differenced image may be subsequently transmitted and/or stored, for subsequent decompression and addition to a standard reference image so as to form a reconstituted or approximated subject image at either a remote location and/or at a later moment in time. Overall effective compression ratios of 100:1 are possible for thoracic x ray digital images. NASA

N91-23977 Washington Univ., Seattle.
ACCESS AND EFFICIENCY IN REAGAN-ERA INFORMATION POLICY: A CASE STUDY OF THE ATTEMPT TO PRIVATIZE THE NATIONAL TECHNICAL INFORMATION SERVICE Ph.D. Thesis
Robert Keith Stewart 1990 310 p
Avail: Univ. Microfilms Order No. DA9104302

This case study of public policy debate was undertaken to learn more about how information policy is made in the United States. The question of how guiding philosophies of government shape Federal information resources management policy (FIRMP) is addressed. By the mid-1980's, there was an apparent shift in the direction of FIRMP away from ideas of access and toward the idea of efficiency. The attempted privatization of the National Technical Information Service (NTIS) case study was used to try to learn how important the ideas of efficiency and access were to the policy makers as they determined whether to model Federal information policy according to a library or warehouse metaphor. After several attempts on the part of the Reagan Administration to privatize NTIS, the Office of Management and Budget in early 1987 instructed the Department of Commerce to formulate a process whereby NTIS would be privatized. DoD assembled a task-force comprised of Commerce, NTIS, and Office of Management and Budget personnel. The role that policy makers see the Federal Government playing in matters of acquiring and disseminating information in the late 1980's is addressed. In addition, the process of policy-making at the Federal level, and the impact that the process can have on policy decisions are examined. Of particular interest is the ability or inability of policy makers to engage in discourse relative to the central issues in the policy debate. It is demonstrated that a view in progress approach can reveal: (1) much about the policy-making process that might otherwise be hidden from historians or researchers who rely on printed documents; (2) that guiding philosophies about government and information do not solely determine the outcome of such policy debates; and (3) that policy can be shaped by staff-level government workers in the legislative and executive branches of government. Dissert. Abstr.

N91-23978 California Univ., Berkeley.
KNOWLEDGE-BASED RETRIEVAL OF INFORMATION AS A PROCESS OF EVIDENTIAL REASONING Ph.D. Thesis
Lung Albert Chen 1990 156 p
Avail: Univ. Microfilms Order No. DA9103653

Knowledge-based retrieval of information was proved to enhance the performance of conventional retrieval systems. Systems like RUBRIC (RUle-Based Retrieval of Information by Computer) and KADR (Knowledge-Assisted Document Retrieval) have successfully incorporated the techniques developed in the research of knowledge-based systems to solve the retrieval problem. Current knowledge-based retrieval systems, however, share several common problems. They are designed either for special users or their reasoning mechanism is not general enough. When developed for specific users, they reflect user preference instead of expert knowledge; when the reasoning mechanism is not sufficiently general, an inadequate model could lead to counterexamples. The focus is to design a theoretically sound knowledge-based retrieval system for general users. In this system, expert knowledge serves as a basis for automatic query information and query evaluation; furthermore, the entire retrieval of information is considered to be a process of evidential reasoning. The foundation of the reasoning methodology is Dempster-Shafer theory and its extension. The new approach subsumes the conventional Boolean system and has advantages over the other retrieval systems. REDER (REtrieval of Documents on Evidential Reasoning) is a prototype of such a system and demonstrates a complete process of knowledge-based retrieval of information. The results of a retrieval experiment verifies the performance of this system. Dissert. Abstr.

N91-23979 University of Southwestern Louisiana, Lafayette.
QUERY PROCESSING FOR DEDUCTIVE DATABASES WITH NULL VALUES Ph.D. Thesis
Ding-An Chiang 1990 175 p
Avail: Univ. Microfilms Order No. DA9104582

With the introduction of null values into a database, the database becomes incomplete. Most research on null values were considered on the efficiency issue, and did not provide a sound and complete query evaluation algorithm for an arbitrary query. However, from the point of view of establishing a good theoretical foundation, a sound and complete query evaluation algorithm for databases with null values is essential. A sound and complete query evaluation algorithm to an arbitrary query for databases will null values is proposed. In the real world, query languages are domain independent. Since there is no algorithm to test whether or not a given query is domain independent, a sound and complete query evaluation algorithm to a class of safe queries for databases with null values is proposed. It is also proven that the problem of finding all definite answers to the simplest class of positive queries with arbitrary selective conditions is NP-hard. To consolidate and advance the state of research in query processing for databases with indexed null values, the logical foundation is provided for

reasoning with null values. Deductive programs can be used to answer an arbitrary query for a database with null values.
Dissert. Abstr.

N91-23980# Louisiana State Univ., Baton Rouge.
DATABASE CONSTRAINT ENFORCEMENT: A DECOMPOSITIONAL APPROACH Ph.D. Thesis
Yuejian Sheng 1990 151 p
Avail: Univ. Microfilms Order No. DA9104171

An efficient and integrated approach is presented to integrity constraint checking for advanced data base systems. The proposed approach essentially consists of three phases: constraint decomposition, global enforcement strategy, and local enforcement tuning. The fundamental assumption underlying this approach is that most data base updates satisfy integrity constraints. A second assumption is that transactions are localized and data base updates are nonuniform in their distribution. Based on these assumptions, the proposed approach will achieve a significant performance increase over previous approaches. Dissert. Abstr.

N91-23981 Rutgers - The State Univ., Newark, NJ.
ROBUSTNESS IN REPLICATED DATABASES Ph.D. Thesis
Rajiv Tewari 1990 236 p
Avail: Univ. Microfilms Order No. DA9103997

Replicated distributed databases store copies of database items at multiple sites to increase availability and response time of transactions. However, replication places a concomitant responsibility on the database system to maintain consistency and serializability of replicated data. Site and communication failures can disrupt the database processing, decreasing the availability of the database. Robustness is the resistance of the database to site and communication link features, and network partitioning; and is a highly desirable property in systems requiring near real time response. The general file allocation problem for allocation of file copies to sites in a distributed computing system with nodes and links that have a given probability of failure are considered. This problem is formulated as a nonlinear integer programming problem with availability and reliability constraints that model several consistency control protocols. A modified drop-add heuristic solution procedure is proposed and its performance evaluated. Using the file allocation provided by this solution and an input parameter, two robust protocols that provide improved availability while maintaining reliability and consistency of the replicated database are developed. The first protocol assumes serializability as the correctness criteria. The correctness of this protocol is demonstrated using serializability theory for replicated data, both for site failures and communication link failures. The second protocol relaxes the assumption of serializability as the correctness criteria for replicated databases, and utilizes a property known as eventual serializability. This protocol is proven to be correct using formal techniques, and the performance of the merge protocol is analyzed by simulation techniques, showing that the merge protocol performs better than previously proposed protocols.
Dissert. Abstr.

N91-23982# Office of Management and Budget, Washington, DC. Office of Information and Regulatory Affairs.
FIVE-YEAR PLAN FOR MEETING THE AUTOMATIC DATA PROCESSING AND TELECOMMUNICATIONS NEEDS OF THE FEDERAL GOVERNMENT
Nov. 1990 150 p
(PB91-103549) Avail: NTIS HC/MF A07; also available SOD HC $10.00 as 041-001-00355-0 CSCL 05B

Information is provided on the information systems and technology activities of the Federal government and fulfillment of the requirements of the Paperwork Reduction Act of 1980. The plan covers fiscal years 1991 through 1992. Three parts are included: (1) a summary of resource estimates; (2) a discussion of themes and directions; and (3) strategic overviews. Author

N91-23983 North Carolina Univ., Chapel Hill.
AN EXPERT SYSTEM FOR SEARCHING IN FULL-TEXT Ph.D. Thesis
Susan Evalyn Gauch 1990 406 p
Avail: Univ. Microfilms Order No. DA9106105

Techniques to improve full-text information retrieval by experienced computer users who are novice users of retrieval systems are explored. An expert system which automatically reformulates Boolean user queries to improve search results is presented. The expert system differs from other intelligent database functions in two ways: it works with semantically and syntactically unprocessed text; and the expert system contains a knowledge base of domain independent search strategies. The passages retrieved are presented to the user in decreasing order of estimated relevancy. This combination of user interface features provides powerful, yet simple, access to full-text documents. Experimental results demonstrate that the expert system can improve the search efficiency of novice searchers without decreasing their search effectiveness. Furthermore, an evaluation of the ranking algorithm confirms that, in general, the system presents potentially relevant passages to the user before irrelevant passages. Dissert. Abstr.

N91-23984# Department of Energy, Washington, DC. Office of Information Resources Management Policy, Plans, and Oversight.
INFORMATION RESOURCES MANAGEMENT LONG-RANGE PLAN
Dec. 1990 269 p
(DE91-009745; DOE/AD-0005) Avail: NTIS HC/MF A12

The Information Resources Management (IRM) activities which support the diverse programmatic missions in the Department of Energy are complex. IRM requirements are continually changing to reflect changes in technology, policy, and program mission. Long-range planning for IRM has been developed to assure that adequate support is available for cost-effective accomplishment of mission objectives. IRM is vital to the successful accomplishment of the programmatic missions in the Department. This is evidenced by the fact that the estimated information technology resources (ITR) cost for FY 1991, approximately $1.58 billion, is about 9 percent of the total Departmental FY 1991 budget request, while the total estimated ITR cost for the entire Federal Government is less than 1.7 percent of the total Federal budget request for the same time period. Recognizing the ever-increasing importance of IRM to the Department, activities in this area were reorganized this year. This reorganization centralized IRM within DOE and created a clear division of responsibility between policy and operations. Management of the information technology resources within IRM (e.g., information systems, computing resources, and telecommunications) were consolidated with printing and publishing activities, records management, IRM standards, and telecommunications and unclassified computer security. The Office of Scientific and Technical Information continues to have the responsibility for information management support and direction for DOE's scientific and technical information. This Plan reflects this transition and, therefore, incorporates information on other areas of IRM, where information is available. The management plan and status of Information Systems, Computing Resources and Telecommunication Systems is provided with charts and graphs. DOE

N91-23985# Oak Ridge K-25 Site, TN.
ACTIVE DESIGN DATABASE (ADDB) USER'S MANUAL
R. L. Schwarz, ed. and J. A. Nations, ed. Feb. 1991 27 p
(Contract DE-AC05-84OT-21400)
(DE91-010431; K/CSD/TM-97) Avail: NTIS HC/MF A03

This manual is a guide to the Active Design Database (ADDB) on the Martin Marietta Energy Systems, Inc., IBM 3084 unclassified computer. The ADDB is an index to all CADAM models in the unclassified CADAM database and provides query and report capabilities. Section 2.0 of this manual presents an overview of the ADDB, describing the system's purpose; the functions it performs; hardware, software, and security requirements; and help and error functions. Section 3.0 describes how to access the system and how to operate the system functions using Database 2 (DB2), Time Sharing Option (TSO), and Interactive System Productivity Facility (ISPF) features employed by this system. Appendix A

contains a dictionary of data elements maintained by the system. The data values are collected from the unclassified CADAM database. Appendix B provides a printout of the system help and error screens. DOE

N91-23986# Lawrence Livermore National Lab., CA.
THE INTELLIGENT DATABASE: USING INGRES TO MANAGE THE EXTERNAL ANALYSIS OF YOUR DATA
A. D. Dougan, E. H. Willes, Jr., W. M. Buckley, A. Delucchi, and D. R. Manatt Mar. 1991 12 p Presented at the North America INGRES Users Association Annual (NAIUA) Meeting, San Jose, 19-23 May 1991
(Contract W-7405-eng-48)
(DE91-010465; UCRL-JC-105865; CONF-9105160-1) Avail: NTIS HC/MF A03

We have developed an application that uses a database to store the methods and rules for our analysis. Our rules are in the form of equations that are generated by a user and subject to frequent editing. We send the equations to a spreadsheet for calculation. When the results are defined as best, the answers are sent back to the database for storage. Our ad hoc methodology is thus stored with the input data and results for better quality assurance and documentation. DOE

N91-23987# Oak Ridge K-25 Site, TN.
SECURITY ASPECTS OF DATABASE MANAGEMENT SYSTEMS
S. E. Hicks and K. C. Evans Mar. 1991 122 p
(Contract DE-AC05-84OT-21400)
(DE91-010677; K/DSRD-461) Avail: NTIS HC/MF A06

Research and development in the area of database management technology began in the 1960s. From this work, the first commercially available data base management system (DBMS) were introduced. These initial DBMSs used the hierarchical and networked data models discussed in section 1.1.1.5.2 and 1.1.1.5.3. of this report. During the 1970s, research focused on the relational data model. Section 1.1.1.5.1 describes this model. Relational database management systems became commercially available in the early 1980s and remain the most widely used type of DBMS today. Emerging research is taking advantage of advances in artificial intelligence and programming languages. One result has been the advent of the object-oriented data model, discussed in section 1.1.1.5.4. Due to the extensive dependence on database management systems by the majority of society, data security has become a growing concern. The purpose of this report is to provide an information baseline for the Department of Energy (DOE) on the current DBMS security technology. The document begins with an overview of DBMS use and architectures, followed by a summary of security concepts. The remaining sections discuss DBMS security issues, research and vendor efforts, standards activities, and DOE DBMS security needs. Because the vast majority of database security research in focused on relational DBMSs, the discussions in this report focus on the relational database model. DOE

N91-23988# Technische Univ., Eindhoven (Netherlands).
INFORMATION PLAN STUDY: A STRATEGY MODEL Ph.D. Thesis [INFORMATIEPLANSTUDIE: MODEL VOOR STRATEGIE]
Norbert Johannes Wie Greveling 1990 310 p In DUTCH; ENGLISH summary
(ISBN-90-6233-638-8; ETN-91-99217) Copyright Avail: NTIS HC/MF A14

A number of aspects of the development of information services are addressed. The concept of the Information Plan Study (IPS), a decision making process by which management gives direction to the development of information services, is introduced. This concerns the formulation of an information strategy and/or information plan allowing placement of centrally different missions as well as different design alternatives. Several reference information models in IPS are presented, with a distinction between survey, design, and decision models. The main stages of an IPS, the survey, the formulation of an information strategy, and the information planning are explained. The possibilities for the use of reference models besides IPS are illustrated. One of the main conclusions is that there are several types of IPS and hence that explicit survey stage is necessary. ESA

N91-23989# Grenoble-1 Univ. (France). Groupe d'Etude pour la Traduction Automatique.
ON A PHONETIC AND STRUCTURAL ENCODING OF CHINESE CHARACTERS IN CHINESE TEXTS
C. Boitet and F. X. Tcheou Dec. 1990 10 p
(RR-835-I; ETN-91-99225) Avail: NTIS HC/MF A02

Phonic and Structural (PS) encoding of Chinese characters is proposed for representing Chinese texts on any computer, using universally available characters (all contained in the PL/I character set), in a readable, yet unambiguous way. More than 80 percent of the 14,872 characters of the CIHAI dictionary are unambiguously represented with simple PS encoding. Iterated PS encoding is designed to help make clear the complete collection of Chinese characters since ancient times. PS encoding is geared more toward exchange and processing than storage. Easy to construct with a standard dictionary and a table of keys, this scheme might also be used by non experts to input Chinese texts while learning Chinese characters. It may be adapted to the encoding of Chinese characters in Japanese and Korean texts. ESA

N91-23990# Gesellschaft fuer Strahlen- und Umweltforschung m.b.H., Munich (Germany, F.R.). Projektgruppe Umweltgefaehrdungspotentiale von Chemikalien.
INFORMATION SYSTEM FOR ENVIRONMENTAL CHEMICALS Final Report [INFORMATIONSSYSTEM UMWELTCHEMIKALIEN]
Kristina Voigt, Joachim Benz, and Andreas Eder Jun. 1990 97 p In GERMAN
(GSF-Ber-21/90; ISSN-0721-1694; ETN-91-99257) Copyright Avail: NTIS HC/MF A05

An electronic data processing aided system was created, in order to allow and optimize the information access on chemicals. Data banks were developed, which include the contents of data sources. As data sources are allotted in printed documents, online data, and reprints, three data banks were created. The efficiency of this information system was examined with regard to the occurrence parameter in the environment, e.g., in water, ground, air, drinkable water and eatables, using 68 environment concerned substances. A hierarchical thesaurus was developed. The number of pieces of information per substance was between zero and several hundred. The results were stored in the PUC 68 data bank. For the access to online data bank, a communication software was developed, tested and applied. The user surface of this software corresponds approximately to TELNET. ESA

N91-23991# Stockholm Univ. (Sweden). Dept. of Meteorology.
THE REDUCED VERSION OF THE DERF 2 DATA SET ON A WORM OPTICAL DISK
Brian Reinhold and Aake Johansson 18 Feb. 1991 17 p
(DM-54; ISSN-0349-0467; ETN-91-99336) Avail: NTIS HC/MF A03

The organization of the reduced DERF (Dynamic Extended Range Forecasting) data set placed on the WORM (Write Once Read Many) optical disk cartridge so that a user may access the data through a high level language (such as FORTRAN) is described. Some compiled programs that are also provided with the disk to read and examine the data are described. The programs can be used only on Personal Computers (PCs) based on the Intel 80xxx chips often referred to as IBM compatible PCs. ESA

N91-23992# Maryland Univ., College Park. Inst. for Advanced Computer Studies.
NULL VALUES IN DEFINITE PROGRAMS
Yuan Liu and Jack Minker Apr. 1990 27 p
(Contract DAAL03-88-K-0087)
(AD-A232065; UMIACS-TR-90-48; CS-TR-2447;
ARO-25870.29-MA) Avail: NTIS HC/MF A03 CSCL 12/5

Null values are a special kind of incomplete information that appear in relational database applications. There are several kinds

of null values. The ones modeled in this paper are those that represent entitles that are known to exist but whose exact values are only known to be in a finite subset of constants in a given domain. For example, if we know that Paul is the grandfather of John, then we know that there is someone who is the father of John and a child of Paul. If we futher assume that there are only finitely many individuals, then this someone can be represented by the kind of null value mentioned here. In this paper, we incorporate these null values into definite programs by using a new kind of symbols called S-constants. We present model theoretic, proof theoretic, and fixpoint semantics for such programs. In the above example, given the additional knowledge that Mike is the father of Joe, these semantics allow us to answer the question of whether or not John and Joe are brothers. If the (unknown) father of John is Mike then they are brothers. The proposed semantics reduce to the usual semantics for definite programs when there are no null values present. GRA

N91-23993# Maryland Univ., College Park. Inst. for Advanced Computer Studies.
COMBINING KNOWLEDGE BASES CONSISTING OF FIRST ORDER THEORIES
Chitta Baral, Sarit Kraus, Jack Minker, and V. S. Subrahmanian Sep. 1990 28 p
(Contract DAAG29-85-K-0177; NSF IRI-89-07122)
(AD-A232090; UMIACS-TR-90-117; CS-TR-2531;
ARO-22648.20-EL) Avail: NTIS HC/MF A03 CSCL 12/5

This document discusses the construction of an expert system by encoding the knowledge of different experts. Suppose the knowledge provided by each expert is encoded into a knowledge base. Then the process of combining the knowledge of these different experts is an important and non-trivial problem. We study this problem here when the expert systems are considered to be first order theories. We present techniques for resolving inconsistencies in such knowledge bases. We also provide algorithms for implementing these techniques. GRA

N91-23994# Naval Postgraduate School, Monterey, CA.
A METHODOLOGY FOR HANDLING DATA ERRORS AND INCONSISTENCIES IN DATABASE CONVERSIONS M.S. Thesis
Mark R. Hendrickson Jun. 1990 128 p
(AD-A232113) Avail: NTIS HC/MF A07 CSCL 12/7

A database management system (DBMS) can have numerous errors and inconsistencies in its data. Examples of errors and inconsistencies that may be contained in a DBMS are: referential integrity violations, logical inconsistencies, redundancies, and out-of-range values. During a conversion of database management systems, the errors and inconsistencies in the source system must be corrected so the data entered into the new target DBMS will be accurate. The goal of this thesis is to examine: (1) a source database management system to determine what errors and inconsistencies are possible; (2) to propose a methodology to detect them; and (3) to correct such errors and inconsistencies prior to entering the data into the target DBMS. In applying my proposals, the thesis will examine the specific systems utilized by the United States Military Academy (USMA) at West Point, New York. The Academy uses a UNISYS 1100/72 mainframe computer in support of its existing network model DBMS. West Point proposes to convert the network model to a relational model system. The thesis will also address the general applicability of this methodology to other database management system conversions. GRA

N91-23995# Assistant Secretary of the Air Force, Washington, DC. Deputy Director for Scientific and Technical Information.
ABRIDGED USAF STINFO PROGRAM MANAGER'S OVERVIEW MANUAL
Walter R. Blados and Charlie Maiorana (INFO/tek, Washington, DC.) Aug. 1990 114 p
(AD-A232483; USAF-STINFO-MANAGEMENT-90/9;
SAF/AQT-SR-90-016) Avail: NTIS HC/MF A06 CSCL 05/2

This manual is an abridgement of document SAF/AQT-SR-90-001, The USAF STINFO Program Overview. It also includes updated STINFO management information, and can be used in conjunction with the earlier document. This Abridgement gives guidance to the local STINFO Program Manager concerning responsibilities for managing the flow of STINFO out of and into the local organization. The overall objective of the USAF STINFO Program Manager is to support the DoD Scientific and Technical Information (STI) Program, in order to increase the effectiveness of the scientific and technical efforts of the DoD community. GRA

N91-23996# Assistant Secretary of the Air Force, Washington, DC. Deputy Director for Scientific and Technical Information.
THE VALUE OF STINFO
Walter R. Blados and Charlie Maiorana Jul. 1990 17 p Prepared in cooperation with INFO/tek, Washington, DC
(AD-A232484; USAF-STINFO-MANAGEMENT-90/7;
SAF/AQT-SR-90-014) Avail: NTIS HC/MF A03 CSCL 05/2

This document, prepared for video production, has as its goal to inspire the reader (or viewer of the video) to examine one's attitudes towards Scientific and Technical Information (STINFO). It discusses the value of STINFO and the role it plays in the technical world, briefly mentions some of the past attempts to place a quantitative value on STINFO, and tries to have the reader realize how important STINFO is. The reader should become a supporter and more complete user of STINFO products and services. This document may be used in conjunction with the video, or separately. GRA

N91-23997# Assistant Secretary of the Air Force, Washington, DC. Deputy Director for Scientific and Technical Information.
INTERACTING WITH DTIC
Walter R. Blados and Charlie Maiorana Jul. 1990 23 p Prepared in cooperation with INFO/tek, Washington, DC
(AD-A232485; USAF-STINFO-MANAGEMENT-90/6;
SAF/AQT-SR-90-013) Avail: NTIS HC/MF A03 CSCL 05/2

This document, prepared for video production, is an overview of how the USAF STINFO Program Manager interacts with the Defense Technical Information Center (DTIC). It is additionally informational for the USAF endusers of DoD scientific and technical information (STI), the managers, scientists, and engineers. The role of the STINFO Program Manager is to contribute to DTIC's collections and databases, act as facilitator of its use, and promote DTIC services in the local organization. This document may be used in conjunction with the video, or separately. GRA

N91-24044*# National Aeronautics and Space Administration. Goddard Space Flight Center, Greenbelt, MD.
DISTRIBUTED, COOPERATING KNOWLEDGE-BASED SYSTEMS
Walt Truszkowski *In* NASA, Washington, Technology 2000, Volume 2 1991 p 16-25 (For primary document see N91-24041 15-99)
Avail: NTIS HC/MF A16 CSCL 05B

83 ECONOMICS AND COST ANALYSIS

Includes cost effectiveness studies.

No abstracts in this category.

84 LAW, POLITICAL SCIENCE AND SPACE POLICY

Includes NASA appropriation hearings; aviation law; space law and policy; international law; international cooperation; and patent policy.

N91-23998# Office of Technology Assessment, Washington, DC.
FEDERALLY FUNDED RESEARCH: DECISIONS FOR A DECADE
GPO May 1991 297 p
(OTA-SET-490) Avail: NTIS HC/MF A13; also available SOD HC $12.00 as 052-003-01241-3

Given the exceptional history, strength, and character of U.S. research, there will always be more opportunities than can be funded, more deserving researchers competing than can be sustained, and more institutions seeking to expand than the prime sponsor (the Federal Government) can fund. The objective for government, then, is to ensure continued funding for a full portfolio of first-rate research and a high caliber research work force to assure long term scientific progress. Analyzed herein is what the Office of Technology Assessment identifies as four pressing challenges for the research system in the 1990s: setting priorities in funding, understanding trends in research expenditures; preparing human resources for the future research work force; and supplying appropriate data fpr ongoing research decision making. Managing the Federal research system requires more than funding; it means devising ways to retain the diversity and creativity that have distinguished U.S. contribution to scientific knowledge. Author

85 URBAN TECHNOLOGY AND TRANSPORTATION

Includes applications of space technology to urban problems; technology transfer; technology assessment; and surface and mass transportation.

For related information see also *03 Air Transportation and Safety, 16 Space Transportation,* and *44 Energy Production and Conversion.*

N91-23999# Oregon Inst. of Tech., Klamath Falls. Geo-Heat Center.
DIRECT USE R/D ASSISTANCE
P. J. Lienau, G. Culver, and K. Rafferty 1990 71 p
(Contract DE-FG07-87ID-12693)
(DE91-009976; DOE/ID-12693/1) Avail: NTIS HC/MF A04

Progress in technology transfer and R and D of geothermal direct uses in three areas, by the Geo-Heat Center, are reviewed in this report. First, technical assistance was provided to 81 projects covering the entire development process from resource information to troubleshooting problems after a project has been completed. Second, applied research was conducted on: the performance of materials and equipment used in 13 geothermal district heating systems, wellbore/aquifer interaction and worldwide utilization of downhole heat exchangers, development of a U.S. direct-use site data base, and development of information on transmission/distribution piping and analysis of uninsulated pipe for geothermal district heating systems. Third, an overview is presented on a technology transfer program which included: publishing a Guidebook, topical papers, and quarterly Bulletin, advising and referrals on projects, presentation and tours, geothermal library, and reporting activities to the Geothermal Progress Monitor. Papers on applied research projects have been processed separately for inclusion on the data base. DOE

N91-24000# Institute for Defense Analyses, Alexandria, VA.
TECHNOLOGY TRANSFER IN A CHANGING NATIONAL SECURITY ENVIRONMENT Final Report, May - Nov. 1990
Ronald A. Finkler, Gordon L. Boezer, Erling J. Foss, Norman D. Jorstad, and A. J. Ramsbotham Dec. 1990 58 p
(AD-A232458; AD-E501354; IDA-P-2409; IDA/HQ-90-35599)
Avail: NTIS HC/MF A04 CSCL 05/2

This paper examines U.S. export control, with particular emphasis on technology transfer as it affects our relationship with Japan. It describes the evolution of export control in the United States, including the Bucy Report, the impact of Afghanistan, and policy changes regarding the People's Republic of China. U.S. control mechanisms for critical technology currently in place are described; these include the Export Administration Regulations, the International Traffic in Arms Regulations (ITAR), and the Militarily Critical Technologies List (MCTL). The evolution of Japan's technology base and export control mechanisms are discussed, as well as its military capabilities. Japan and the United States have had different philosophies regarding export control with the United States more likely to use controls as part of its foreign policy. However, U.S. export control policy is increasingly seen as having an important economic security aspect in addition to its national security objectives. Changes in Eastern Europe and the Soviet Union have placed the issue of export control in a new perspective. Therefore, the paper also examines in some detail the major developments in the European community which will affect the future technology environment and its relationship to national security. A primary purpose of the paper was to enhance mutual understanding between the U.S. and Japan and to facilitate the resolution of differences in the technology security arena.
GRA

88 SPACE SCIENCES (GENERAL)

No abstracts in this category.

89 ASTRONOMY

Includes radio, gamma-ray, and infrared astronomy, and astrometry.

N91-24001 Georgia State Univ., Atlanta.
APPLICATIONS OF SPECKLE INTERFEROMETRY AND SPECKLE PHOTOMETRY TO THE HYADES CLUSTER Ph.D. Thesis
Edmund Gerard Dombrowski 1990 270 p
Avail: Univ. Microfilms Order No. DA9101933

Applications of speckle interferometry and speckle photometry were used to study seven Hyades binaries. They are ADS 3135, 3210, 3248, 3475, and 3483, Finsen 342 and 51 Tauri. Analysis of these systems resulted in newly defined orbital parameters and differential magnitudes. This information was used to determine the Hyades distance modulus, in which a well-defined eclipsing spectroscopic binary, HD 27130, served as an anchor to the solution. This resulted in a new distance modulus, m minus M equals 3.42 plus or minus 0.04 magnitudes, which corresponds to a cluster distance of 48.4 plus or minus 0.9 parsecs.
Dissert. Abstr.

N91-24002 Southampton Univ. (England).
THE SUPERNOVA REMNANT G109.1-1.0 AND THE X-RAY PULSAR 1E2259+586 Ph.D. Thesis
Simon Robert Davies 1989 202 p
Avail: Univ. Microfilms Order No. BRDX91248

The supernova remnant (SNR) G109.1-1.0 has three features of particular interest: a central X-ray pulsar, 1E2259+586; jet-like emission curving out from the pulsar across the SNR; and a possible interaction with a nearby molecular cloud associated with the H 2 regions S147-S153. Work on all three of these aspects is presented using data from a wide range of wavelengths. The discovery and early observations of G109.1-1.0 and 1E2259+586 are reviewed, as well as the theoretical interpretations of these

results. The relationship between G109.1-1.0 and the molecular could is investigated using archive far-IR, and CO emission provides convincing evidence of a physical interaction. The jet-like feature also appears to be part of this general correlation, and the possible significance for different interpretations of this emission are discussed. X-ray results are presented from the study of archive data from two satellites, HEAO-1 and EXOSAT. These reveal 1E2259+f86 to be a unique object in terms of its spindown, and x-ray properties in general. A search to detect the optical/IR counterpart of 1E2259+586 does not provide any firm conclusions, although it does reveal that an earlier identification is probably incorrect. An attempt is made to develop a low mass x-ray binary (LMXRB) model for 1E2259+586 that is consistent with these observational results, relating 1E2259+586 to G109.1-1.0. Other possible models for 1E2259+586 are also discussed in the light of the observational data presented. It is concluded that the LMXRB model is the most convincing to date, but that conformation will probably have to wait until results from new x-ray satellites become available. Dissert. Abstr.

N91-24003 California Univ., Berkeley.
STUDIES OF THE DIFFUSE BACKGROUND AND INTERSTELLAR DUST AT FAR ULTRAVIOLET WAVELENGTHS Ph.D. Thesis
Mark Viglino Hurwitz 1990 107 p
Avail: Univ. Microfilms Order No. DA9103732

The diffuse background at wavelengths between 1000 and 2000 A, the far ultraviolet band, contains information about the nature of dust in the interstellar medium. Unfortunately, a survey of current literature on this topic reveals widely discrepant observations of the background, and equally varied reports as to the parameters that describe the scattering properties of interstellar dust grains. The data analyzed have two enormous advantages over those used by previous researchers: the instrument design provided for elimination of virtually all sources of contamination (including point sources, out-of-band and out-of-field scattering, and detection dark current), and the data are spectroscopic, allowing the various astrophysical processes which contribute to the background to be identified and treated independently. The model used to extract the scattering properties of the dust from the observations is also superior to those previously employed, for the following reasons: the source function for the scattered light is allowed to vary along the line of sight, the stellar radiation field which illuminates the grains is based on a realistic distribution of stars and dust in the Galaxy, and the radiative transfer is valid for large optical depths. These advantages permit the analysis of low-altitude, high-column density targets, which are shown to be crucial in determining the scattering properties of the grains.
Dissert. Abstr.

N91-24004 Washington Univ., Seattle.
H II REGIONS AND YOUNG STAR CLUSTERS IN THE MAGELLANIC CLOUDS Ph.D. Thesis
Myung Gyoon Lee 1990 656 p
Avail: Univ. Microfilms Order No. DA9104260

The stellar content in H II regions and young star clusters of the Magellanic Clouds (MC) was studied by using UBV CCD photometry. The purposes of this study are threefold: to investigate the evolution of massive stars in the H II regions and young star cluster; to derive stellar luminosity functions and to determine the stellar initial mass functions; and to study the structural properties of young star clusters in the Magellanic Clouds. A summary of results are (1) The reddening was determined from the color-color diagram, showing E(B-V) = 0.03-0.04 for the LMC and 0.03-0.22 for the SMC. Then the Zero Age Main Sequence fitting method was used to measure the distances of these clusters. The distances thus derived are (m - M)(sub 0) = 18.4 + or - 0.2 for NGC 2004 and (m - M)(sub 0) = 18.8 + or - 0.3 for NGC 371. Finally, ages were measured by using the convective overshoot models with mass loss, given by Maeder and Meynet (1988). Ages of star clusters in H II regions range from 0 to 8 Myr, and ages of the young clusters studied vary from 8 to 80 Myr. Most of the clusters show an age spread up to 50 Myr, sometimes indicating multiple star formation (NGC 1850, NGC 2004, NGC 2100). (2) The initial mass function of stars in H II regions and young star clusters were determined from the main sequence luminosity functions in U, B, and V. The results show that the IMFs of stars in MC H II regions and young clusters are similar in slope to those for various objects in the Galaxy and the Magellanic Clouds. This leads to the conclusion that the slope of the stellar IMFs for m is greater than or equal to 3 solar mass does not depend on the metallicities, on the masses, nor on the morphological types of galaxies. (3) UBV CCD surface photometry of 7 LMC clusters and 2 SMC clusters is presented. The radial surface brightness profiles of most of these clusters are well fitted by the single-mass isotropic King models. The surface photometry, supplemented by star counts from the literature, was used to determine the structural parameters of the clusters. Dissert. Abstr.

N91-24005 Southampton Univ. (England).
IMAGING AND BACKGROUND IN LOW-ENERGY GAMMA RAY ASTRONOMY Ph.D. Thesis
Fan Lei 1989 226 p
Avail: Univ. Microfilms Order No. BRDX91262

The current status of low energy gamma ray astronomy is reviewed and the conclusion drawn that the next generation of low energy gamma ray telescopes will require high sensitivity, good timing, and spectral resolution. High angular resolution imaging capability is also considered essential. The imaging of low energy gamma rays is hampered by the difficulties encountered in developing high resolution position sensitive detectors. To this end, an improved Rotation Modulation Collimator (RMC) imaging technique, the phoswich multi-pitch RMC, is discussed. This imaging method employs currently available detector and pulse-shape discrimination techniques and is capable of producing images with an angular resolution which is comparable with that of the Coded Aperture Mask (CAM) imaging techniques. The imaging property of this new technique is studied. A comparison of three of the main imaging techniques used in low energy gamma ray astronomy, CAM, Fourier Transform Collimator, and RMC, is performed in terms of both theoretical performances and simulated imaging of the Galactic Center region. A realistic assessment of the possible applications of these three techniques to different types of astronomical Observations is also given. The atmospheric gamma ray radiation was measured by a number of balloon and satellite-borne instruments. A model of this radiation is developed based on the data as measured by a Compton telescope designed by the Max-Planck group. Emission spectra, as predicted by the model, are compared with various observed data, both inside and outside the atmosphere. The sources of background noise in low energy gamma ray telescopes are discussed. A comprehensive model of the background sources is developed and a generalized simulation program is presented which uses a combination of Monte Carlo methods and empirical calculations. Photon, proton, and neutron induced backgrounds are all considered as well as the effects of spacecraft and orbit. The model is applied to some existing telescopes and good agreements are obtained, and interpreted as a demonstration of the model validity. Prediction of background level is made for several future missions. A proposed satellite gamma ray telescope, GRASP, is briefly described.
Dissert. Abstr.

N91-24006 Stanford Univ., CA.
SOFT X RAY/EXTREME ULTRAVIOLET IMAGES OF THE SOLAR ATMOSPHERE WITH NORMAL INCIDENCE MULTILAYER OPTICS Ph.D. Thesis
Joakim Fredrik Lindblom 1990 250 p
Avail: Univ. Microfilms Order No. DA9102302

The first high resolution Soft X-Ray/Extreme Ultraviolet (XUV) images of the Sun with normal incidence multilayer optics were obtained by the Standford/MSFC Rocket X-Ray Spectroheliograph on 23 Oct. 1987. Numerous images at selected wavelengths from 8 to 256 A were obtained simultaneously by the diverse array of telescopes flown on-board the experiment. These telescopes included single reflection normal incidence multilayer systems (Herschelian), double reflection multilayer systems (Cassegrain), a

grazing incidence mirror system (Wolter-Schwarzschild), and hybrid systems using normal incidence multilayer optics in conjunction with the grazing incidence primary (Wolter-Cassegrain). Filters comprised of approximately 1700 A thick aluminum supported on a nickel mesh were used to transmit the soft x ray/EUV radiation while preventing the intense visible light emission of the Sun from fogging the sensitive experimental T-grain photographic emulsions. These systems yielded high resolution soft x ray/EUV images of the solar corona and transition region, which reveal magnetically confined loops of hot solar plasma, coronal plumes, polar coronal holes, supergranulation, and features associated with overlying cool prominences. The development, testing, and operation of the experiments, and the results from the flight are described. The development of a second generation experiment, the Multi-Spectral Solar Telescope Array, which is scheduled to fly in the summer of 1990, and a recently approved Space Station experiment, the Ultra-High Resolution XUV Spectroheliograph, which is scheduled to fly in 1996 are also described. Dissert. Abstr.

N91-24007 Cornell Univ., Ithaca, NY.
AN OBSERVATIONAL STUDY OF ARM STRUCTURE IN NORMAL SPIRAL GALAXIES Ph.D. Thesis
Christopher Magri 1990 650 p
Avail: Univ. Microfilms Order No. DA9106258

Multivariate data were obtained and analyzed in an effort to develop a new classification system for spiral galaxies, one which is not necessarily based on morphological properties. By comparing morphological measures with the intrinsic parameters on which the new system is based, it can be seen just how fundamentally important a galactic property arm structure truly is. A sample of 492 moderately bright northern Sa, SBa, Sc, and SBc spirals was chosen for statistical analysis. The literature was searched for redshifts, optical and near-infrared photometric data, 20 cm fluxes, and H I 21 cm line parameters. New observations were made at 20 and 21 cm; in addition, IRAS fluxes were obtained from archival data. These data were subjected to principal component analysis, modified in that non-detections were explicitly acknowledged. Spiral galaxies have two fundamental properties, confirming previous work done with fewer data. While scale (bulk) is most important, galaxies of given scale can vary in form (color, bulge/disk ratio, H I surface density). Arm strength is unrelated to other properties. Forty-five spatially isolated spirals were chosen for two-color optical CCD imaging, for 20 cm continuum imaging, and for CO 2.6 mm spectroscopy. Isolated Sa's are often found to be misclassified; they are either armless SO's or else peculiar victims of collisions. Isolated Sc's are surprising in that all but the most isolated examples have symmetric arms over at least part of the disk, contrary to the predictions of stochastic models for arm formation. Given the extreme isolation of all highly chaotic disks, the presence of tidal companions (or at least candidates) for the other normal isolated spirals, the apparent prevalence of violent processes in isolated Sa's, and recent N-body simulations of tidal encounters, it is likely that arm structure in most spirals is produced by tidal encounters with small companions. Arm structure is not an intrinsic property of a given galaxy. All of these results can be explained by supposing that protogalactic environments is the determining influence for spirals. Dissert. Abstr.

N91-24008 Wisconsin Univ., Madison.
THE ENVELOPES OF RV TAURI VARIABLES Ph.D. Thesis
Mark Allen Nook 1990 296 p
Avail: Univ. Microfilms Order No. DA9101551

The envelopes of RV Tauri stars are studied with optical spectropolarimetry and infrared photometry. Infrared photometry measures the amount and absorption optical depth of dust in the circumstellar envelope of these objects. The polarimetry can probe the geometric distributions of the envelope and photospheres of the RV Tauri variables. The IR photometry shows that the RV Tauri stars have large circumstellar shells. The data show that a strong difference exists between the RV Tauri stars that do and do not vary in mean brightness: the stars that vary in mean brightness have dust envelopes with larger optical depths. Comparison of broadband polarimetry and the IR colors suggests that a correlation exists between the two. This implies that relatively warm circumstellar dust is important in the formation of the observed polarization. The spectropolarimetry suggests that relatively warm circumstellar dust is important in the formation of the observed polarization. The spectropolarimetry suggests that the mechanisms that produce the polarization are different for the objects that do and do not show TiO absorption near minimum. The type B objects do not show TiO absorption and show wavelength and temporal variations in the polarization described by sporadic scattering of homogeneous photospheric radiation by localized regions containing small particles, presumably newly formed dust. In the case of AC Her, the localized region is confined to a specific plane. The spectropolarimetry of the type A stars which do develop TiO bands near minima show variation across the TiO absorption bands reminiscent of late-type variables.
Author

N91-24009 Louisiana State Univ., Baton Rouge.
SENSITIVE CRYOGENIC TRANSDUCER DEVELOPMENT AND ANALYSIS FOR USE ON GRAVITY WAVE DETECTORS Ph.D. Thesis
Norbert Daniel Solomonson 1990 151 p
Avail: Univ. Microfilms Order No. DA9104173

The design and development of an improved superconducting inductively modulated transducer are discussed. The transducer is designed to optimize the performance of a 2-mode, resonant bar, gravitational wave antenna. A detailed theoretical analysis which includes are relevant noise sources is described. Conditions for optimizing 2-mode detector performance are derived, and design curves are presented. Based on the results of this analysis, an optimal transducer has been designed for use on the Louisiana State University gravitational wave detector. The fabrication and testing of several optimal mass 400gm transducer resonators are described. The effects of low temperature annealing on the mechanical Qs of the Nb resonators are discussed.
Dissert. Abstr.

N91-24010 Southampton Univ. (England).
INSTRUMENTATION AND DATA ANALYSIS FOR HARD X RAY ASTRONOMY Ph.D. Thesis
Shuang Nan Zhang 1989 319 p
Avail: Univ. Microfilms Order No. BRDX91272

The current status of hard x ray astronomy is reviewed. The applicability of various hard x ray detectors in such new telescopes are discussed and the current status of hard x ray telescope design is reviewed. Background production mechanisms in hard x ray telescopes are discussed and some techniques for background reduction are also discussed. A simple method for estimating the optimum detector thickness is presented and the use of some detector materials which should minimize the neutron background is proposed. Three imaging techniques are briefly described. A simple discussion about their relative merits has suggested that the rotating modulation collimator (RMC) technique based on an improved detector technique provides the best imaging system. The pulse shape discrimination (PSD) technique is essential for the realization of such new detectors. The basic principles of various PSD methods are made for hard x ray phoswich detector applications. A new fast-veto technique is proposed and may be used in a quadruple phoswich detector system to provide good energy resolution and efficient background rejection. A proposed satellite-borne hard x ray telescope (CHIXSAT), which would use such detectors as its main detection elements, is described. A range of statistical data analysis methods for hard x ray and gamma ray astronomy are studied. Fisher's fact test is found to give the most reliable significance test. Methods for parameter estimation, including upper limit calculations, are described. The sensitivity of a telescope is defined with clear statistical meaning and a method for estimating the sensitivity is derived. A new method, called the chi(exp 3)-test is proposed to be unbiased and have a very high power for multiple on-off observations, especially in searching for transient sources. Dissert. Abstr.

N91-24011 Hawaii Univ., Honolulu.
A NEAR-INFRARED SEARCH FOR BROWN DWARFS IN THE PLEIADES Ph.D. Thesis
Douglas Anthony Simons 1990 190 p
Avail: Univ. Microfilms Order No. DA9107050

Deep mosaic imaging of the Pleiades was conducted at wavelengths of 0.9 microns (I-band) and 2.2. microns (K-band) in an effort to find free-floating low mass cluster members. Fields outside of the cluster were also imaged as part of a control data set to check the overall significance of the results, leading to a total of 575 arcmin squared of data. Photometry of all detected point sources led to the detection of 29 plus or minus objects that lie near the Pleiades main sequence when compared to the control data set. These objects have theoretical masses of approximately 0.1 to 0.04 solar masses and are described well by a power law distribution with a slope of minus 2.8. The vast majority of the sources detected were background field stars. The derived number-magnitude counts for these field stars agree well with established Galaxy models with a measured lower limit on the local space density of stars of 0.06 pc sup minus 3.

Dissert. Abstr.

N91-24012 Council for National Academic Awards (England).
A STUDY OF THE END POINT PATH GEOMETRY IN METEOR BURST SYSTEMS USING A MICROCOMPUTER SIGNAL LOGGER Ph.D. Thesis
John C. Worsnop 1990 179 p
Avail: Univ. Microfilms Order No. BRDX91545

Radio propagation experiments generally need large amounts of data to be gathered over extended periods. The design of a signal logger for unattended gathering of signal statistics from a meteor burst radio path, using two receiving antennas is described. Using a VHF broadcast radio station as a signal source, the data logger was used to investigate the properties of signals received with one antenna directed at the path midpoint and a second at the receiving station zenith (end point). Calculations of path loss at 70 and 50 MHz showed that the midpoint path loss should be lower than the end point path loss by up to 3 dB for ranges up to about 900 km but higher above this range. Calculations for the 70 MHz 1173 km experimental path showed that the path loss for end point illumination should be in the order of 1 dB less than that for midpoint. Results suggested a larger percentage of large amplitude signals on the end point antenna, but the mean end point path loss in the order of 1 dB greater than midpoint. Burst durations were found to be lower on end point but not to the extent predicted by theory. The sampling rate of the data logger was initially thought to be the main contributory factor to this effect, but further experiments showed this was not the case. Duty cycle of the two path geometries was also compared, and a computer model written, predicting a 4:1 advantage for midpoint. Results confirmed the model, showing the advantage varying from 1.14 to 6.36 with a mean value of 4.0. This ratio shows a small reduction during periods of high shower activity. In conclusion, the data logger was proven, its limitation discussed, and the limitations and advantages of end point illumination investigated.

Dissert. Abstr.

N91-24013# Lawrence Livermore National Lab., CA.
HARD X RAY IMAGING TELESCOPE
P. Lubin (California Univ., Santa Barbara.) 1 Mar. 1990 10 p
(Contract W-7405-eng-48)
(DE90-015815; UCRL-CR-103554) Avail: NTIS HC/MF A02

This final report covers the work carried out under the LLNL Contract Number B063682, Subcontractor Regents University of California at Santa Barbara. The research carried out under this contract involves the construction of a telemetry, target acquisition and guidance system, and of a light-weight gondola to house an x ray spectrometer. This work is part of the design and construction of the balloon experiment, GRATIS, which will perform the first arcminute imaging of cosmic sources in the 30 to 200 keV energy band. Observations conducted with GRATIS are expected to provide data relevant to several key problems in high energy astrophysics including the physical processes responsible for the high energy tail observed in the soft gamma-ray spectra of clusters of galaxies and the origin of both the diffuse and point source components of the gamma-ray emission from the Galactic Center. This report discusses the scientific motivations for this experiment, presents several aspects of the design and construction of the hardware components, gives an overview of the stabilized platform, and demonstrates the expected performance and sensitivity.

DOE

90 ASTROPHYSICS

Includes cosmology; celestial mechanics; space plasmas; and interstellar and interplanetary gases and dust.

For related information see also *75 Plasma Physics*.

N91-24014 Washington Univ., Seattle.
PHENOMENOLOGICAL ASPECTS OF SCALAR FIELDS IN ASTROPHYSICS, COSMOLOGY AND PARTICLE PHYSICS Ph.D. Thesis
Helmut Walter Zaglauer 1990 138 p
Avail: Univ. Microfilms Order No. DA9103178

Specific phenomenological consequences of scalar fields in the standard model of elementary particle physics and in the Brans-Dicke scalar-tension theory of gravity are investigated. Calculation of the effective potential of the Higgs scalar in the standard model shows that for a top quark mass above 86 GeV, a stringent lower bound on the mass of the Higgs boson arises from the requirement of vacuum stability. With the help of a simplified model of cosmic ray collisions, it is argued that even very long-lived false vacuum states would have decayed through quantum tunneling induced by those collisions. The rate of change of the orbital period of very close binary systems such as the Binary Pulsar or the 11 minute binary 4U1820-30 due to the emission of gravitational radiation is analyzed. Observations of orbital period changes in such systems may give constraints on the strength of the coupling of the scalar field to the metric in Brans-Dicke theory that could be comparable to or even exceed results from solar-system based experiments. These bounds can be extended to massive Brans-Dicke type scalar fields, as long as their range is larger than the wave-zone of the binary system.

Dissert. Abstr.

N91-24015*# Fermi National Accelerator Lab., Batavia, IL.
A PROPOSED SEARCH FOR DARK-MATTER AXIONS IN THE 0.6-16 MICRO-eV RANGE
Karl vanBibber, P. Sikivie, N. S. Sullivan, D. B. Tanner, Michael S. Turner, and D. M. Moltz (California Univ., Berkeley. Lawrence Berkeley Lab.) Mar. 1991 13 p Presented at conference
(Contracts NAGw-1340; W-7405-eng-48; DE-FG05-86ER-40272; DE-FG02-90ER-40560)
(NASA-CR-188173; NAS 1.26:188173; FERMILAB-Conf-91/81-A)
Avail: NTIS HC/MF A03 CSCL 03B

A proposed experiment is described to search for dark matter axions in the mass range 0.6 to 16 micro-eV. The method is based on the Primakoff conversion of axions into monochromatic microwave photons inside a tunable microwave cavity in a large volume high field magnet, as described by Sikivie. This proposal capitalizes on the availability of two Axicell magnets from the decommissioned Mirror Fusion Test Facility (MFTF-B) fusion machine at LLNL. Assuming a local dark matter density in axions of rho = 0.3 GeV/cu cm, the axion would be found or ruled out at the 97 pct. c.l. in the above mass range in 48 months. Author

N91-24016*# Fermi National Accelerator Lab., Batavia, IL.
A COSMIC SUPERFLUID PHASE
Ben-Ami Gradwohl Feb. 1991 15 p Sponsored in part by DOE
(Grant NAGw-1340)
(NASA-CR-188171; NAS 1.26:188171; FERMILAB-Pub-91/55-A)
Avail: NTIS HC/MF A03 CSCL 03B

The universe may have undergone a superfluid-like phase during its evolution, resulting from the injection of nontopological charge

into the spontaneously broken vacuum. In the presence of vortices this charge is identified with angular momentum. This leads to turbulent domains on the scale of the correlation length. By restoring the symmetry at low temperatures, the vortices dissociate and push the charges to the boundaries of these domains. The model can be scaled (phenomenologically) to very low energies, it can be incorporated in a late time phase transition and form large scale structure in the boundary layers of the correlation volumes. The novel feature of the model lies in the fact that the dark matter is endowed with coherent motion. The possibilities of identifying this flow around superfluid vortices with the observed large scale bulk motion is discussed. If this identification is possible, then the definite prediction can be made that a more extended map of peculiar velocities would have to reveal large scale circulations in the flow pattern. Author

N91-24017 Cornell Univ., Ithaca, NY.
OBSERVATION AND THEORY OF THE RADAR AURORA Ph.D. Thesis
John David Sahr 1990 284 p
Avail: Univ. Microfilms Order No. DA9106227

Plasma density irregularities occurring near the Aurora Borealis cause scattering of HF, VHF, and UHF radio waves. The scattering is so strong that a small radar, such as the Cornell University Portable Radar Interferometer (CUPRI), can easily detect this radar aurora. Analysis of the resulting radar signal provides great detail about the spatial and temporal characteristics of these auroral E region irregularities. Observations are presented of the radar aurora from recent campaigns in northern Sweden. After reviewing the basic theory and observations of auroral electrojet irregularities, a simple nonlinear fluid theory of electrojet ion-acoustic waves is introduced, and reduced to a form of the three-wave interaction equations. This theory provides a simple mechanism for excitation of linearly stable waves at large aspect and flow angles, as well as a prediction of the power spectra that a coherent scatter radar should observe. In addition, this theory may be able to account for type 3 waves without resorting to ion gyro modes, such as the electrostatic ion-cyclotron wave. During the course of the research a simple new radar transmitting mode and signal processing algorithm was generated which very simply solves a frequency aliasing problem that often occurs in CUPRI auroral radar studies when a single-pulse spectral mode is used. Several new radar data analysis routines were developed, including the principally cross-beam image and scatter plots of the second versus first moments of the power spectrum of the irregularities. Analysis of vertical interferometer data shows that type 3 waves originate at ordinary electrojet altitudes, not in the upper E region, from which it is concluded that the electrostatic ion-cyclotron mode does not generate type 3 waves. The measured height of type 3 waves and other spectral analyses provide support for the pure ion-acoustic theory of type 3 waves. Suggestions are offered for hardware improvements to the CUPRI radar, new experiments to test new and existing theories, as well as specific paths for further theoretical exploration. Dissert. Abstr.

N91-24018 Washington Univ., Seattle.
ULTRAVIOLET GAS ABSORPTION AND DUST EXTINCTION TOWARD M8 AND THE OUTER GALACTIC DISK Ph.D. Thesis
Donald Reese Boggs 1990 196 p
Avail: Univ. Microfilms Order No. DA9104201

Two investigations of variations of the UV extinction law are presented. First, extinction differences are compared to environmental differences within the young cluster NGC 6530. Highly ionized gas appears in two distinct regions with the cluster, as the radial velocities of C IV and Si IV toward B-stars in the cluster center are reduced relative to velocities toward stars on the opposite side of a dark lane. Photoionization models reproduce the column densities and C IV/Si IV ratios to the hotter stars well, but cannot account for the high ions near the central B-stars. When only the central stars are considered, a strong correlation between high ion column densities with distance from cluster member W93 may be ionizing the gas in the cluster center. The strength and width of the 2175 A bump extinction toward stars within the central region decreases rapidly with distance from W93 in a manner similar to the decrease in high ion column density. The bump extinction may be enhanced near W93 by irradiated graphitic grains. Second, differences in the gas-to-dust ratio and UV extinction law between the outer galaxy and the local Milky Way are searched for with IUE spectra. All targets are at least 4 kpc beyond the solar circle, where a metallicity comparable to that of the Large Magellanic Cloud (LMC) is expected. If the empirical trend of decreasing bump strength and increasing far-UV extinction with decreasing metallicity seen for the galaxy, LMC, and Small Magellanic Cloud (SMC) is truly an abundance effect, the extinction law toward the program stars should approximate the law of the LMC. The 2175 A bump of the outer stars is as strong as that of the average galactic extinction curve. The far-UV extinction rise, however, is significantly steeper toward the distant stars. After extinction due to local dust is subtracted, the average far-UV extinction law is comparable to the average LMC law.
Dissert. Abstr.

N91-24019 Arizona Univ., Tucson.
CRYOMAGMATISM IN THE OUTER SOLAR SYSTEM Ph.D. Thesis
Jeffrey Stuart Kargel 1990 308 p
Avail: Univ. Microfilms Order No. DA9103039

Cryovolcanism has played an important role in the geological histories of many icy satellites. Cryovolcanism, like the more familiar silicate volcanism on Earth and the other terrestrial planets, takes many forms. Many individual cryovolcanic landforms are morphologically similar to terrestrial volcanic landforms and can be explained with similar mechanisms. However, assemblages of cryovolcanic, tectonic, and impact structures form varied landscapes quite alien in their collective expression. Many variables can affect the cryovolcanic style of a satellite but none more so than cryolava composition. The compositional variable is examined in considerable detail. Existing knowledge of phase equilibria and physical properties of cosmochemically relevant unary, binary, and multi-component chemical systems are summarized. Where published knowledge was found lacking, measurements of the physical chemistry of volatile mixtures are presented. Cryovolcanic landscapes are briefly toured, and knowledge of the physical chemistry of volatile mixtures is applied to problems of cryovolcanological interest. Aqueous cryolavas may range in composition from salt-water brines to cryogenic ammonia-water-rich multi-components solutions possibly involving methanol, ammonium sulfide, alkali chlorides, and many other potential components. Cryomagmatic distillation can greatly accentuate the importance of trace and minor constituents of icy satellites. The viscosities, densities, and other physical properties of these liquids vary considerably and depend sensitively on their exact compositions. These properties affect everything from cryovolcanic eruptive styles and landforms, to the way cryovolcanic crusts respond to tectonic stress. It is believed that the compositional variable is directly or indirectly implicated in a wide varity of geomorphic aspects of contrast among the icy satellites. Thus, even though as yet any specific morphology can be attributed to a specific composition, there appears to be a powerful link between composition of the ices originally accreted by a satellite and its subsequent interior evolution and exterior geomorphic appearance. Dissert. Abstr.

N91-24020 Pennsylvania State Univ., University Park.
BOUNDARY CONDITIONS IN QUANTUM COSMOLOGY Ph.D. Thesis
Paschalis George Paschali 1990 100 p
Avail: Univ. Microfilms Order No. DA9104947

The Hartle-Hawking and the Vilenkin boundary conditions were applied, and their results were compared for a minisuperspace model. This is a spacially totally symmetric universe filled with a homogeneous scalar field of finite range (0, phi(sub 0)) and with bounded self-interacting potential. The W.K.B. wavefunctions for both boundary proposals were found and analyzed. They pick identical classical trajectories which all inflate. By calculating how the period of inflation changes with the classical trajectory, it was found that the inflation increases as the maximum of the potential,

phi(sub 0)/2, is approached. The probability distribution predicted by the two proposals were checked among the above classical trajectories. It was found that Vilenkin-Hawking boundary conditions favor evolutions with long inflation but Hartle-Hawking boundary conditions favor evolutions of short inflation. Using a naive interpretation of the wavefunction, an attempt to predict the size of the universe was made. It was found that Vilenkin boundary conditions can provide an explanation for the size of the universe if a large enough phi(sub 0) is chosen. The above considerations are in terms of absolute probabilities which may not be very meaningful for the case of the universe. The probability distribution for the flatness parameter, omega, at constant energy density for both boundary proposals was found. The Hartle-Hawking boundary conditions, for reasonable values of the parameters predict an omega far away from one which conflicts with observations. The Vilenkin boundary conditions predict an omega close to one, in agreement with observations. Dissert. Abstr.

N91-24021 Wisconsin Univ., Madison.
RECENT STAR FORMATION AND THE GALAXY COLLISIONS IN NGC 520 Ph.D. Thesis
Spencer Adam Stanford 1990 208 p
Avail: Univ. Microfilms Order No. DA9034850

Multiwavelength data on the peculiar galaxy system NGC 520 are presented. Stellar velocity dispersions and infrared imaging conclusively show that the system consists of two colliding disk galaxies. H I and 21 cm mapping show that an H I tidal tail lies in nearly the same location as a southern optical tail, and connects the main body with UGC 957, a dwarf galaxy approximately 6 minutes to the north. Dynamical simulations of the system indicate that three galaxies have interacted: UGC 957 probably produced the diffuse northern extension of the southern tail during the collision, and two disks collided approximately 3 x 10(exp 8) years ago to form the main body of NGC 520. Equivalent width measurements of optical absorption lines indicate that much of the extranuclear regions of both disk galaxies experienced a short period of enhanced star formation approximately 3 x 10(exp 8) years ago. The star formation rate (SFR) at the secondary nucleus probably remained elevated until only approximately 10(exp 8) years ago. The starburst at the primary nucleus continues to produce massive stars, and its SFR is currently many times higher than that of the nucleus of an isolated disk galaxy. The relative stellar population mix appears to change from the outer towards the inner regions of each galaxy in a way that suggests that either a starburst propagated inwards or the strength of the burst increased inwards. The close similarity of the time since first contact between the two galaxies to the turnoff age of the extranuclear burst population strongly suggests a causal connection between the collision and the initiation of the starburst. Uncertainties of about a factor of two in both the burst age and the collision age prevent a strong statement of this conclusion. Dissert. Abstr.

N91-24022 North Carolina Univ., Chapel Hill.
THE THERMODYNAMIC STABILITY OF SYSTEMS CONTAINING BLACK HOLES Ph.D. Thesis
Gregory Lee Comer 1990 109 p
Avail: Univ. Microfilms Order No. DA9106087

The thermodynamic properties of systems containing gravitational fields with the topology of black holes are presented. The described system is composed of pure black holes whereas the other contains black holes in thermal equilibrium with their own radiation (modeled by a renormalized radiation stress-energy tensor). The partition functions required are obtained from Euclidean path integrals. The different partition functions are generated using the fact that the boundary conditions for a well-posed problem in general relativity are precisely those of an associated well-posed problem in statistical mechanics. The form of the partition functions is such that a straightforward method for determining thermodynamic stability can be established. Dissert. Abstr.

N91-24023 Kent Univ., Canterbury (England).
STUDIES OF MOLECULAR EXCITATION IN STAR FORMATION REGIONS Ph.D. Thesis
Ivan Stuart Bishop 1989 210 p
Avail: Univ. Microfilms Order No. BRDX91292

The physical properties associated with two distinct types of molecular cloud structure are investigated. Observations are presented of hot, dense core regions typified by the IRC2 region of OMC1, and much cooler, more rarefied bipolar outflow sources such as L379. Emphasis is placed on the analysis of optically thin (non-LTE) transitions of two symmetric top molecular species, methyl cyanide and propyne. A statistical equilibrium model (SEM) code was developed that exploited the quantum mechanical properties of these species. Possible pitfalls in modeling are identified and benefits of using symmetric tops in preference to linear molecules are highlighted. Kinetic temperature and H2 density estimates are derived using the SEM for IRC2 and the ultracompact H II regions G34.3 + 0.15 and W28A2. Both IRC2 and G34.3 possess hot, dense material traced by methyl cyanide. Propyne, however, is excited in regions of lower excitation and greater spatial extend than methyl cyanide in G34.3 and W28. The 12-CO observations of S140 and a new bipolar outflow associated with L370 are presented. The morphology of S140 is discussed in detail. The importance of making optically thin observations using low noise receivers at interferometric spatial resolutions is discussed as one means of circumventing optical depth and beam filling difficulties. Dissert. Abstr.

N91-24024 Yale Univ., New Haven, CT.
PRIMORDIAL LITHIUM, STELLAR EVOLUTION, AND COSMOLOGY: LITHIUM IN HALO STARS FROM STANDARD, DIFFUSIVE, AND ROTATIONAL STELLAR EVOLUTION AND IMPLICATIONS FOR COSMOLOGY Ph.D. Thesis
Constantine Plato Deliyannis 1990 339 p
Avail: Univ. Microfilms Order No. DA9035334

A grid of theoretical evolutionary sequences of models for old, low metallicity stars was constructed from the fully convective pre-main sequence phase to the giant branch. These continuous tracks are especially designed to analyze the history of surface Li abundance (both Li-6 and Li-7) during their evolution. Several mechanisms were examined that could alter the surface Li abundance of stars at different phases of evolution. In particular, nuclear burning at the base of the convection zone (occurring primarily during the pre-main sequence and early main sequence), diffusion by gravitational settling (main sequence and turnoff), convective dredge-up (early post-main sequence), and dilution (post-main sequence) were considered. The relative importance of each process is very sensitive to stellar mass, chemical composition, and ratio of mixing length to pressure scale height, alpha. To apply these models to a detailed analysis of the available data on Li abundances measured in halo stars, Li insochrones were constructed for different ages, alpha, and compositions. It was shown that when peculiar care is taken to preserve numerical accuracy, the standard theory of stellar evolution agrees closely with the observations of extreme halo stars that satisfy simultaneously the criteria of low metallicity and high space velocity. These stars are among the oldest stars known, and they broadly sample the protogalaxy. Among other results, it was also found that taking into account the effect of internal stellar rotation on stellar structure and evolution does not affect estimates for the ages of globular clusters; however, helium diffusion in the outer layers of stars might reduce age estimates for globular clusters by approximately 10 to 25 percent, bringing them close to cosmological age estimates derived from measurements of the Hubble constant. Dissert. Abstr.

N91-24025 Ohio State Univ., Columbus.
THEORETICAL STUDIES OF QSO ABSORPTION LINES AND THE INTERGALACTIC MEDIUM Ph.D. Thesis
Michael Lynn Fisher 1990 215 p
Avail: Univ. Microfilms Order No. DA9105105

A new numerical approximation is offered for the effective recombination coefficient. The approximation is accurate for all

sizes of nebulae and all temperatures. The new effective recombination coefficient is used to model instability in Lyman alpha forest clouds because of radiation pressure. Clouds are modeled at the epoch of initial ionization, z(sub on) = 5, 10, and 20, and at the epoch z = 2.5. The neutral hydrogen column density of the Lyman alpha clouds at z = 2.5 is limited to N(sub H I) is less than or equal to 10(exp 16.5)/sq cm because of this instability. The distribution function for the Lyman alpha clouds is then integrated over the allowed column densities to determine the fractional amount of baryons contained in the clouds. It is found that the fractional mass of the clouds is omega(sub clouds) = 0.6 H(sub 100) omega(sub b). With the assumption of pressure equilibrium between the Lyman alpha clouds and the intergalactic medium, IGM, and the previous results, a lower limit can be set upon the temperature of the IGM at the epoch z = 2.5, T(sub e) is greater than or equal to 1.5 x 10(exp 7) K, for H(sub 0) = 75 km/s/Mpc. With this boundary condition, the thermal history of the IGM, and its effect upon the cosmic microwave background, CMBR, is calculated. It is shown that this model of a hot ionized IGM remains constant with the preliminary results of the Cosmic Background Explorer, COBE. Dissert. Abstr.

N91-24026 California Univ., Los Angeles.
RADIO AND INFRARED STUDIES OF MASS-LOSING EVOLVED STARS Ph.D. Thesis
Joel Harvey Kastner 1990 319 p
Avail: Univ. Microfilms Order No. DA9105844

Mass-losing red giant stars represent links between the late stages of stellar evolution and the chemical evolution of the galaxy. The mechanisms which lead to profuse mass loss are addressed, and the global rate of mass return to the interstellar medium (ISM) by red giants is estimated. Mass loss rates in gas, M(sub g), for 150 red giants in the solar neighborhood are estimated from a model of the circumstellar envelope and by employing a self-consistant treatment of the kinetic temperature of the gas and revised estimates of CO photodissociation radii. Analysis of the mass loss rates indicates that between 0.3 and 0.7 solar mass per year is returned to the ISM by evolved stars in the Galaxy. This is similar to an estimate of the global mass loss rate based on the white dwarf birthrate. In the solar neighborhood, roughly equal amounts are contributed by carbon-rich and oxygen-rich red giants. Comparison of M(sub g) with mass loss rates in dust shows that the dust constitutes typically approximately 1/200 of the envelope by mass. Trends in the results for mass loss rate, outflow velocity, and dust-to-gas ratio are discussed. In related studies, the results of a search for massive carbon stars in the galaxy and near-IR imaging polarimetry of the reflection nebulosity around four preplanetary nebulae are presented. In the former program, CO emission was detected for the first time from 46 evolved stars. Preliminary analysis suggests that some of the carbon stars among them are luminous, with masses of approximately 4 solar mass. In the latter study, polarization maps of CRL 2688, CRL 618, OH231.8 + 4.2, and IRC + 10216 indicate that the imaged near-IR flux is scattered emission from embedded central sources. From a simple model, dust density gradients and total dust masses for each object are estimated. Dissert. Abstr.

N91-24027# Lawrence Livermore National Lab., CA. Inst. of Geophysics and Planetary Physics.
RELATIVISTIC SHOCK WAVES AND THE EXCITATION OF PLERIONS
J. Arons, Y. A. Gallant (California Univ., Berkeley.), Masahiro Hoshino, C. E. Max, and A. Bruce Langdon Jan. 1991 15 p Presented at the IAU Colloquium 128: The Magnetospheric Structure and Emission Mechanisms of Radio Pulsars', Logow (Poland), 18 Jun. 1991
(Contract W-7405-eng-48)
(DE91-007623; UCRL-JC-105642; CONF-9106119-1) Avail: NTIS HC/MF A03

The shock termination of a relativistic magnetohydrodynamic wind from a pulsar is the most interesting and viable model for the excitation of the synchrotron sources observed in plerionic supernova remnants. The structure of relativistic magnetosonic shock waves in plasmas composed purely of electrons and positrons, was studied as well as those whose composition includes heavy ions as a minority constituent by number. Relativistic shocks in symmetric pair plasmas create fully thermalized distributions of particles and fields downstream. Therefore, such shocks are not good candidates for the mechanism which converts rotational energy lost from a pulsar into the nonthermal synchrotron emission observed in plerions. However, when the upstream wind contains heavy ions which are minority constituent by number density, but carry the bulk of the energy density, much of the energy of the shock goes into a downstream, nonthermal power law distribution of positrons with energy distribution N(E)dE is proportional to E(exp -s). In a specific model presented in some detail, s = 3. These characteristics are close to those assumed for the pairs in macroscopic MHD wind models of plerion excitation. The essential mechanism is collective synchrotron emission of left-handed extraordinary modes by the ions in the shock front at high harmonics of the ion cyclotron frequency, with the downstream positrons preferentially absorbing almost all of this radiation, mostly at their fundamental (relativistic) cyclotron frequencies. Possible applications to models of plerions and to constraints on theories of energy loss from pulsars are briefly outlines. DOE

N91-24028# Lawrence Livermore National Lab., CA.
MAGNETOSPHERIC STRUCTURE OF ROTATION POWERED PULSARS
J. Arons (California Univ., Berkeley.) Jan. 1991 42 p Presented at the IAU Colloquium 128: The Magnetospheric Structure and Emission Mechanisms of Radio Pulsars', Logow, Poland, 18 Jun. 1991
(Contract W-7405-eng-48)
(DE91-007622; UCRL-JC-105643; CONF-9106119-2) Avail: NTIS HC/MF A03

Theoretical work is surveyed on the structure of the magnetospheres of rotation powered pulsars, within the observational constraints set by their observed spindown, their ability to power synchrotron nebulae and their ability to produce beamed collective radio emission, while putting only a small fraction of their energy into incoherent X- and gamma radiation. No single theory was found that has yet given a consistent description of the magnetosphere, but it is concluded that models based on a dense outflow of pairs from the polar caps, permeated by a lower density flow of heavy ions, are the most promising for future research. DOE

N91-24029 Max-Planck-Inst. fuer Physik und Astrophysik, Garching (Germany, F.R.). Inst. fuer Extraterrestrische Physik.
THE MOLECULAR INTERSTELLAR MEDIUM AND THE NEAR-INFRARED CONTINUUM OF THE BARRED LINER NGC 6764
A. Eckart, M. Cameron, J. M. Jackson, R. Genzel, A. I. Harris, W. Wild, and H. Zinnecker (Wuerzburg Univ., Germany, F.R.) Oct. 1990 40 p Submitted for publication
(MPE-Preprint-193; ETN-91-99081) Copyright Avail: Fachinformationszentrum Karlsruhe, 7514
Leopoldshafen-Eggenstein 2, Fed. Republic of Germany

Measurements of isotopic CO line emission and J, H, K near infrared continuum emission of the barred spiral 6764 are reported. The optical, near infrared, and millimeter data are in excellent agreement with a brief and intense starburst at the nucleus. This finding is supported by the Wolf-Rayet emission line features seen in the nucleus of the galaxy which is direct evidence for recent massive star formation. By comparing NGC 6764 to a starburst galaxy, elliptical radio galaxy, Seyfert galaxy, and a quasar it is concluded that, judged from the two lowest rotational levels of CO, these sources show common beam averaged properties of the molecular gas. The bulk of the nuclear molecular line emission arises in warm, dense, optically thick gas. The CO line emission in the disks and arms of the galaxies arises from cold and probably subthermally excited gas. ESA

N91-23838# Wise Observatory, Tel Aviv (Israel).
MATTER IN COSMIC VOIDS Abstract Only

N. Brosch *In* Tel-Aviv Univ., Bulletin of the Israel Physical Society, Volume 33, 1987. Annual Meeting 1987: Program and Abstracts 1987 p 52 (For primary document see N91-23832 15-70)
Avail: NTIS HC/MF A08

N91-23839# Weizmann Inst. of Science, Rehovoth (Israel).
BIASED GALAXY FORMATION IN THE NEUTRINO SCENARIO Abstract Only
Erez Braun, Avishai Dekel, and Paul R. Shapiro (Texas Univ., Austin.) *In* Tel-Aviv Univ., Bulletin of the Israel Physical Society, Volume 33, 1987. Annual Meeting 1987: Program and Abstracts 1987 p 53 (For primary document see N91-23832 15-70)
Avail: NTIS HC/MF A08

N91-23840# Tel-Aviv Univ. (Israel). School of Physics and Astronomy.
THE SPECTRUM OF MASSIVE ACCRETION DISKS Abstract Only
Ari Laor *In its* Bulletin of the Israel Physical Society, Volume 33, 1987. Annual Meeting 1987: Program and Abstracts 1987 p 54 (For primary document see N91-23832 15-70)
Avail: NTIS HC/MF A08

91 LUNAR AND PLANETARY EXPLORATION

Includes planetology; and manned and unmanned flights. For spacecraft design or space stations see *18 Spacecraft Design, Testing and Performance.*

N91-24030*# Space Systems/Loral, Palo Alto, CA.
UNATTENDED NETWORK OPERATIONS TECHNOLOGY ASSESSMENT STUDY. TECHNICAL SUPPORT FOR DEFINING ADVANCED SATELLITE SYSTEMS CONCEPTS Final Report
Kent M. Price, Mark Holdridge, Jide Odubiyi, Allan Jaworski, and Herbert K. Morgan (Loral AeroSys, Seabrook, MD.) Apr. 1991 60 p
(Contract NAS3-25092)
(NASA-CR-187080; NAS 1.26:187080; SSL-TR00729) Avail: NTIS HC/MF A04 CSCL 03B

The results are summarized of an unattended network operations technology assessment study for the Space Exploration Initiative (SEI). The scope of the work included: (1) identified possible enhancements due to the proposed Mars communications network; (2) identified network operations on Mars; (3) performed a technology assessment of possible supporting technologies based on current and future approaches to network operations; and (4) developed a plan for the testing and development of these technologies. The most important results obtained are as follows: (1) addition of a third Mars Relay Satellite (MRS) and MRS cross link capabilities will enhance the network's fault tolerance capabilities through improved connectivity; (2) network functions can be divided into the six basic ISO network functional groups; (3) distributed artificial intelligence technologies will augment more traditional network management technologies to form the technological infrastructure of a virtually unattended network; and (4) a great effort is required to bring the current network technology levels for manned space communications up to the level needed for an automated fault tolerance Mars communications network. Author

N91-24031 York Univ. (England).
LUNAR VOLCANISM AND THE THERMAL EVOLUTION OF THE MOON Ph.D. Thesis
Andrew Martin Mullis 1989 370 p
Avail: Univ. Microfilms Order No. BRDX91198

The constraints on lunar evolution are reviewed. A thermal model of lunar evolution is constructed, and it is shown that, the present thermal state of the Moon is principally determined by, the rate of heat generation in the lunar interior, and the rate of heat loss through the lithosphere. It is shown that, if there has been no global lunar expansion since 3.9 AE, a lower limit to the initial lunar temperature profile may be obtained by requiring that, some melt must exist at depth within the Moon, during the period of extensive surface volcanism, between 3.9-3.2 AE. A simple model of differentiation under gravity is developed, which is able to account for the large negative p-wave velocity gradient in the upper mantle. It is proposed that the extensive outpouring of basaltic lava between 3.9-3.2 AE, may have been driven by differential thermoelastic stress in the lithosphere. In order to estimate the total volume of basaltic lava extruded on to the lunar surface, a model for the formation of the mascon gravity anomalies is constructed. It is suggested that even the very largest basins (Imbrium and Orientale) may have excavated only to the base of the crust. A lower limit of 5 x 10(exp 6) cu km is derived for the volume of basaltic lava extruded onto the lunar surface. It is shown that the volume of lava produced is consistent with an initially uniformly warm state for the lunar interior. This is consistent with the view that the Moon formed from a reservoir of material ejected from the earth, following core mantle segregation, by the impact of a single large body. Dissert. Abstr.

N91-24032 Cornell Univ., Ithaca, NY.
SATURN'S F RING: IMAGING AND SIMULATION Ph.D. Thesis
Robert Andrew Kolvoord 1990 274 p
Avail: Univ. Microfilms Order No. DA9106187

The narrow width of Saturn's F ring belies its dynamical complexity. The kinks, clumps, and braids discovered by the Voyager spacecraft give the ring an ever-changing appearance when viewed at different times or from different orientations. In an attempt to quantify the longitudinal variations of the F ring in detail, a suite of Voyager 1 and 2 images of the F ring were examined in detail, using a fast Fourier transformation (FFT) to identify the periodicities present as a function of azimuthal extent. The results show a small and well-defined set of periodic signals that can be interpreted as implying the presence of a few previously unseen small moonlets abutting the ring, in addition to Prometheus and Pandora, the F ring shepherds. Complementary to the imaging results, the perturbations of a prototypical narrow planetary ring by nearby satellites is modeled using Gauss' equations for both two and three dimensions in hope of understanding the evolutionary mechanisms needed to create the variety of features observed in the ring. The dynamical simulation includes small satellites inside, amidst, and outside the ring proper, orbiting for many synodic periods. These simulations are animated to provide better insight into the temporally varying nature of the induced phenomena. Nonplanar trajectories for both the ring particles and the local perturbers are also examined. While no evidence for braiding is apparent in any of these models, the importance of the relative positions of the various perturbers is demonstrated. Collisions are also included in a probabilistic sense, demonstrating the efficiency with which they can damp out periodic structure in the ring and hence, the limited longevity of imposed features in the system. The simulations, when examined using an FFT, show periodicities similar to those exhibited in the imaging study, when satellites with similar orbits to those around the actual F ring are used as perturbers. Dissert. Abstr.

N91-24033 Hawaii Univ., Honolulu.
COMPOSITION AND DISTRIBUTION OF CARBONATES, SULFATES, AND HYDRATES ON THE MARTIAN SURFACE FROM EARTH-BASED SPECTROSCOPY BETWEEN 3-5 MICRONS Ph.D. Thesis
Diana Lee Blaney 1990 174 p
Avail: Univ. Microfilms Order No. DA9107019

Earth-based telescopic data provides information on the mineralogy of the Martian surface. Data was collected during the 1986 and 1988 Earth-Mars oppositions between 3 to 5 microns to study carbonates, sulfates, and hydrates. The 1986 and 1988 data are presented and discussed. Dissert. Abstr.

N91-24034 State Univ. of New York, Stony Brook.
NEAR-INFRARED MILLIARCSECOND OBSERVATIONS BY

THE LUNAR OCCULTATION TECHNIQUE Ph.D. Thesis
Wenping Chen 1990 121 p
Avail: Univ. Microfilms Order No. DA9106822

The application of the lunar occultation technique in the near-infrared was summarized to obtain structural information of celestial objects at milliarcsecond resolution. The technique was applied to search for binary systems among pre-main-sequence (PMS) objects. Of the 31 stellar systems surveyed in the Taurus and Ophiuchus star forming regions, 9 binaries were found. The projected separations between the components range from 0.01 to 0.7, or 1 to 100 AU at the distances to these regions. Results indicate that at least 30 percent of the PMS population are binaries with separation of approximately 1 to 150 AU. This frequency is consistent with that of the solar-type main-sequence stars, implying that binaries have formed at very early stages of stellar evolution. Among the systems discovered at infrared K band, there appears no tendency towards equal brightness between components. The 1986-1989 series of lunar occultations of the Galactic center provided an opportunity to study the infrared sources at very high angular resolution. Four observations, all at K, three by array imaging and one by single-detection photometry were obtained. These observations have enabled reliable measurement of the flux and the size limits to be estimated at sub- and milliarcsecond resolution of the discrete sources around the central square pc of the compact, nonthermal radio source Sgr A*. All the discrete sources brighter than K is approximately 10 mag are smaller than a few hundred AUs, and thus cannot be large stellar clusters; they are probably not very luminous stars. Dissert. Abstr.

N91-24035 California Inst. of Tech., Pasadena.
MICROWAVE IMAGING OF SATURN'S DEEP ATMOSPHERE AND RINGS Ph.D. Thesis
Arie William Grossman 1990 204 p
Avail: Univ. Microfilms Order No. DA9107383

An analysis of microwave images of Saturn's atmosphere and rings is presented. Interferometer observations at wavelengths of 0.27, 2.01, 6.17, and 20.13 cm, and precise application of synthesis imaging techniques yielded brightness and polarization maps of unsurpassed resolution and sensitivity. Linear polarization is detected from the ring ansea, and brightness variations in the deep atmosphere and the rings are revealed. The disk-integrated spectrum of Saturn is interpreted within the context of a radiative transfer model that requires the NH3 mixing ratio to take on a value of 0.9 to 1.1 x 10(exp -4) directly below the ammonia ice cloud at a pressure of 1.4 bar. The NH3 mixing ratio increases with depth to a value of 5.0 to 6.5 x 10(exp -4) at a pressure of 6 bar. The variation of NH3 with depth can be entirely accounted for by the presence of 11 to 14 times solar abundance of H2S, which reacts with NH3 to produce a substantial NH4SH cloud. Latitudinal variations in brightness temperature indicate that the saturated vapor abundance of ammonia decreases by 50 percent from equator to pole within the cloud deck. At greater depths, the latitudinal variations of ammonia are consistent with alternating zones of concentration and depletion caused by vertical motions. An apparent depletion in northern mid-lattitudes is well-correlated with a decrease in infrared opacity and depressed cloud top levels, indicating deep-seated downwelling. The size, composition, and shape of particles comprising the rings of Saturn are constrained by modeling the emission, scattering, and extinction of radiation by the rings. Azimuthal variations in brightness and linear polarization favor a model in which the particles are irregularly shaped. Dissert. Abstr.

92 SOLAR PHYSICS

Includes solar activity, solar flares, solar radiation and sunspots.

For related information see *93 Space Radiation.*

N91-24036# Oak Ridge National Lab., TN.
GEOMAGNETIC STORMS: POTENTIAL ECONOMIC IMPACTS ON ELECTRIC UTILITIES
P. R. Barnes and J. W. VanDyke 20 Mar. 1991 9 p Presented at the 4th Annual Electric Utility Business Environment Conference and Exhibition, Denver, 20-22 Mar. 1991
(Contract DE-AC05-84OR-21400)
(DE91-009523; CONF-910378-1) Avail: NTIS HC/MF A02

Geomagnetic storms associated with sunspot and solar flare activity can disturb communications and disrupt electric power. A very severe geomagnetic storm could cause a major blackout with an economic impact of several billion dollars. The vulnerability of electric power systems in the northeast United States will likely increase during the 1990s because of the trend of transmitting large amounts of power over long distance to meet the electricity demands of this region. A comprehensive research program and a warning satellite to monitor the solar wind are needed to enhance the reliability of electric power systems under the influence of geomagnetic storms. DOE

93 SPACE RADIATION

Includes cosmic radiation; and inner and outer earth's radiation belts.

For biological effects of radiation see *52 Aerospace Medicine.* For theory see *73 Nuclear and High-Energy Physics.*

N91-24037 Nottingham Univ. (England).
INVESTIGATION OF THE MUON COMPONENT OF EAS INITIATED BY PRIMARY RADIATION FROM HERCULES X-1 Ph.D. Thesis
Steven Keith Barley 1990 317 p
Avail: Univ. Microfilms Order No. BRD-91040

The detection and analysis of the muon component of extensive air showers (EAS) from the binary star Hercules X-1 are presented. The data used in the analysis was recorded during the period July 1986 to September 1988 by the Nottingham muon detector, working in conjunction with the University of Leeds' GREX array, located at the Haverah Park experimental station. A full description of the operation of the Nottingham muon detector is provided, with details of the installation of a diagnostic shower simulation system, implementation of software and hardware to facilitate a reduction in EAS event processing time, and results from a recalibration of the recording electronics. The obtained EAS muon density measurements are used to develop a mean muon lateral distribution from which prediction can be made to compare the muon content of signal and background showers in point source analyses. A comprehensive review of the observational evidence and theoretical predictions for the nature of the Hercules X-1/HZ Herculis binary system is performed, with a brief summary of experimental observations from other point sources. A description of the technique employed in the investigation of possible gamma ray emission from the direction of Hercules X-1 is made, and the results reported. The examined data set showed no evidence for a significant long term signal from Hercules X-1 even on the bases of muon content selection criteria. A discussion of these results in relation to observations made by other groups is given along with suggestions for future work. Dissert. Abstr.

N91-24038 Wisconsin Univ., Madison.
THE BLACK WIDOW PULSAR PSR 1957+20: A POTENTIAL VHE GAMMA-RAY SOURCE Ph.D. Thesis
John Patrick Finley 1990 135 p
Avail: Univ. Microfilms Order No. DA9100135

The eclipsing millisecond binary pulsar PSR 1957 plus 20 was observed for 49.35 hours with the Air Gerenkov Telescope of the Haleakala Gamma Ray Observatory during the summer of 1989. Initial data analysis indicates that the null hypothesis of no signal present from the source direction has a 2 percent chance probability of being the correct hypothesis. Reanalysis of the data after selections intended to enhance the signal-to-noise reduces the chance probability of the background fluctuations causing the observed effects to 0.3 percent. The data from each of the two independent telescopes are consistent with the entire data sample.

Comparison of the absolute phase of the effect with observations at radio wavelengths indicate that the emission, if real, is in phase agreement with the radio signal. Data from the summer 1990 observing season will be necessary to establish PSR 1957 plus 20 as a source of very high energy gamma rays. Dissert. Abstr.

N91-24039 Hawaii Univ., Honolulu.
A SEARCH FOR VERY HIGH-ENERGY GAMMA RAYS FROM CYGNUS X-3 Ph.D. Thesis
Constantine Sinnis 1990 267 p
Avail: Univ. Microfilms Order No. DA9107051

Cygnus X-3 is an x ray binary system approximately 10 kpc away from earth, lying in the plane of the galactic disc. Since the observation of intense radio jets emanating from the system, it has continued to confound experimentalists and theorists alike. In certain models of gamma ray production, Cygnus X-3 could supply the power necessary to sustain the high energy (E greater that 10(exp 17) eV) galactic cosmic ray population against leakage. By any model, the experimental results indicate that it is the most intense source of high energy cosmic rays observed. An attempt is made to verify the previous observations and elucidate the nature of the gamma ray emission. Taking a conservative viewpoint, an upper limit is set to the time averaged flux from Cygnus X-3 of 5.8 x 10(exp -11) gamma prime scm(exp -2)s(exp -1) above 300 GeV. However, there is evidence, of low statistical significance (2 sigma), that Cygnus X-3 is a sporadic emitter of gamma rays, with a measured flux of 3.3 +/- 0.7 x 10(exp -10) gamma prime scm(exp -2)s(exp -1), and a duty cycle of 6 percent; though it appears that this emission is not correlated with the 4.8 hr x ray period. Dissert. Abstr.

N91-24040 Max-Planck-Inst. fuer Physik und Astrophysik, Garching (Germany, F.R.). Inst. fuer Extraterrestrische Physik.
THE HIGH ENERGY SPECTRUM OF THE 1983, AUGUST 1b GAMMA-RAY BURST
M. Boer, K. Hurley, M. Niel, G. Vedrenne, A. V. Kuznetsov, R. A. Sunyaev, O. V. Terekhov, E. E. Fenimore, R. W. Klebesadel, and J. G. Laros, 7AA541 (Los Alamos National Lab., NM.) Oct. 1990 10 p Presented at Los Alamos Workshop on Gamma-Ray Bursts, Taos, NM, 29 Jul. - 3 Aug. 1990 Submitted for publication
(MPE-Preprint-194; ETN-91-99082) Copyright Avail: Fachinformationszentrum Karlsruhe, 7514
Leopoldshafen-Eggenstein 2, Fed. Republic of Germany

The 1983 August 1b gamma ray burst was observed by the Prognoz 9, ICE, Vela 5a and 5b GRB (Gamma Ray Burst) detectors. It was one of the most intense bursts to date and presents a very peculiar spectrum, variable over time intervals less than one second at high energy. Preliminary photon spectra of this burst and some considerations on the size of the high energy emission region and the source distance are presented. The observation of GRB830801b demonstrates the need for GRB observations over an extended energy range (at least from below a keV to over 100 MeV) and with a good temporal resolution. ESA

99 GENERAL

N91-24041*# National Aeronautics and Space Administration, Washington, DC.
TECHNOLOGY 2000, VOLUME 2
1991 369 p Conference held in Washington, DC, 27-28 Nov. 1990
(NASA-CP-3109-Vol-2; NAS 1.55:3109-Vol-2) Avail: NTIS HC/MF A16 CSCL 05A

Technology 2000 was the first major industrial conference and exposition spotlighting NASA technology and technology transfer. It's purpose was, and continues to be, to increase awareness of existing NASA-developed technologies that are available for immediate use in the development of new products and processes, and to lay the groundwork for the effective utilization of emerging technologies. Included are sessions on: computer technology and software engineering; human factors engineering and life sciences; materials science; sensors and measurement technology; artificial intelligence; environmental technology; optics and communications; and superconductivity. For individual titles, see N91-24042 through N91-24083.

N91-24042*# National Aeronautics and Space Administration. Lyndon B. Johnson Space Center, Houston, TX.
INTELLIGENT COMPUTER-AIDED TRAINING AND TUTORING **c63**
R. Bowen Loftin (Houston Univ., TX.) and Robert T. Savely *In* NASA, Washington, Technology 2000, Volume 2 1991 p 3-10 (For primary document see N91-24041 15-99)
Avail: NTIS HC/MF A16 CSCL 09B

Specific autonomous training systems based on artificial intelligence technology for use by NASA astronauts, flight controllers, and ground-based support personnel that demonstrate an alternative to current training systems are described. In addition to these specific systems, the evolution of a general architecture for autonomous intelligent training systems that integrates many of the features of traditional training programs with artificial intelligence techniques is presented. These Intelligent Computer-Aided Training (ICAT) systems would provide, for the trainee, much of the same experience that could be gained from the best on-the-job training. By integrating domain expertise with a knowledge of appropriate training methods, an ICAT session should duplicate, as closely as possible, the trainee undergoing on-the-job training in the task environment, benefitting from the full attention of a task expert who is also an expert trainer. Thus, the philosophy of the ICAT system is to emulate the behavior of an experienced individual devoting his full time and attention to the training of a novice - proposing challenging training scenarios, monitoring and evaluating the actions of the trainee, providing meaningful comments in response to trainee errors, responding to trainee requests for information, giving hints (if appropriate), and remembering the strengths and weaknesses displayed by the trainee so that appropriate future exercises can be designed. Author

N91-24043*# National Aeronautics and Space Administration. Lyndon B. Johnson Space Center, Houston, TX.
CLIPS: A TOOL FOR THE DEVELOPMENT AND DELIVERY OF EXPERT SYSTEMS **c61**
Gary Riley *In* NASA, Washington, Technology 2000, Volume 2 1991 p 11-15 (For primary document see N91-24041 15-99)
Avail: NTIS HC/MF A16 CSCL 09B

The C Language Integrated Production System (CLIPS) is a forward chaining rule-based language developed by the Software Technology Branch at the Johnson Space Center. CLIPS provides a complete environment for the construction of rule-based expert systems. CLIPS was designed specifically to provide high probability, low cost, and easy integration with external systems. Other key features of CLIPS include a powerful rule syntax, an interactive development environment, high performance, extensibility, a verification/validation tool, extensive documentation, and source code availability. The current release of CLIPS, version 4.3, is being used by over 2,500 users throughout the public and private community including: all NASA sites and branches of the military, numerous Federal bureaus, government contractors, 140 universities, and many companies. Author

N91-24044*# National Aeronautics and Space Administration. Goddard Space Flight Center, Greenbelt, MD.
DISTRIBUTED, COOPERATING KNOWLEDGE-BASED SYSTEMS **c82**
Walt Truszkowski *In* NASA, Washington, Technology 2000, Volume 2 1991 p 16-25 (For primary document see N91-24041 15-99)
Avail: NTIS HC/MF A16 CSCL 05B

Some current research in the development and application of distributed, cooperating knowledge-based systems technology is addressed. The focus of the current research is the spacecraft

ground operations environment. The underlying hypothesis is that, because of the increasing size, complexity, and cost of planned systems, conventional procedural approaches to the architecture of automated systems will give way to a more comprehensive knowledge-based approach. A hallmark of these future systems will be the integration of multiple knowledge-based agents which understand the operational goals of the system and cooperate with each other and the humans in the loop to attain the goals. The current work includes the development of a reference model for knowledge-base management, the development of a formal model of cooperating knowledge-based agents, the use of testbed for prototyping and evaluating various knowledge-based concepts, and beginning work on the establishment of an object-oriented model of an intelligent end-to-end (spacecraft to user) system. An introductory discussion of these activities is presented, the major concepts and principles being investigated are highlighted, and their potential use in other application domains is indicated. Author

N91-24045*# Jet Propulsion Lab., California Inst. of Tech., Pasadena.
ELECTRONIC NEUROPROCESSORS **c61**
Anil Thakoor *In* NASA, Washington, Technology 2000, Volume 2 1991 p 26-33 (For primary document see N91-24041 15-99)
Avail: NTIS HC/MF A16 CSCL 09B

The JPL Center for Space Microelectronics Technology (CSMT) is actively pursuing research in the neural network theory, algorithms, and electronics as well as optoelectronic neural net hardware implementations, to explore the strengths and application potential for a variety of NASA, DoD, as well as commercial application problems, where conventional computing techniques are extremely time-consuming, cumbersome, or simply non-existent. An overview of the JPL electronic neural network hardware development activities and some of the striking applications of the JPL electronic neuroprocessors are presented. Author

N91-24046*# Jet Propulsion Lab., California Inst. of Tech., Pasadena.
INTELLIGENT VISION SYSTEM FOR AUTONOMOUS VEHICLE OPERATIONS **c63**
Marija S. Scholl *In* NASA, Washington, Technology 2000, Volume 2 1991 p 34-43 (For primary document see N91-24041 15-99)
Avail: NTIS HC/MF A16 CSCL 09B

A complex optical system consisting of a 4f optical correlator with programmatic filters under the control of a digital on-board computer that operates at video rates for filter generation, storage, and management is described. Author

N91-24047*# National Aeronautics and Space Administration. Lyndon B. Johnson Space Center, Houston, TX.
SOFTWARE REENGINEERING **c63**
Ernest M. Fridge, III *In* NASA, Washington, Technology 2000, Volume 2 1991 p 47-55 (For primary document see N91-24041 15-99)
Avail: NTIS HC/MF A16 CSCL 09B

Programs in use today generally have all of the function and information processing capabilities required to do their specified job. However, older programs usually use obsolete technology, are not integrated properly with other programs, and are difficult to maintain. Reengineering is becoming a prominent discipline as organizations try to move their systems to more modern and maintainable technologies. The Johnson Space Center (JSC) Software Technology Branch (STB) is researching and developing a system to support reengineering older FORTRAN programs into more maintainable forms that can also be more readily translated to a modern languages such as FORTRAN 8x, Ada, or C. This activity has led to the development of maintenance strategies for design recovery and reengineering. These strategies include a set of standards, methodologies, and the concepts for a software environment to support design recovery and reengineering. A brief description of the problem being addressed and the approach that is being taken by the STB toward providing an economic solution to the problem is provided. A statement of the maintenance problems, the benefits and drawbacks of three alternative solutions, and a brief history of the STB experience in software reengineering are followed by the STB new FORTRAN standards, methodology, and the concepts for a software environment. Author

N91-24048*# National Aeronautics and Space Administration. Goddard Space Flight Center, Greenbelt, MD.
TRANSPORTABLE APPLICATIONS ENVIRONMENT (TAE) PLUS: A NASA USER INTERFACE DEVELOPMENT AND MANAGEMENT SYSTEM **c61**
Martha R. Szczur *In* NASA, Washington, Technology 2000, Volume 2 1991 p 56-66 (For primary document see N91-24041 15-99)
Avail: NTIS HC/MF A16 CSCL 09B

The transportable Applications Environment Plus (TAE Plus), developed at the NASA Goddard Space FLight Center, is a portable, What you see is what you get (WYSIWYG) user interface development and management system. Its primary objective is to provide an integrated software environment that allows interactive prototyping and development of graphical user interfaces, as well as management of the user interface within the operational domain. TAE Plus is being applied to many types of applications, and what TAE Plus provides, how the implementation has utilizes state-of-the-art technologies within graphic workstations, and how it has been used both within and without NASA are discussed. Author

N91-24049*# National Aeronautics and Space Administration. Lyndon B. Johnson Space Center, Houston, TX.
APPLICATIONS OF FUZZY LOGIC TO CONTROL AND DECISION MAKING **c61**
Robert N. Lea and Yashvant Jani (LinCom Corp., Houston, TX.) *In* NASA, Washington, Technology 2000, Volume 2 1991 p 67-75 (For primary document see N91-24041 15-99)
Avail: NTIS HC/MF A16 CSCL 09B

Long range space missions will require high operational efficiency as well as autonomy to enhance the effectivity of performance. Fuzzy logic technology has been shown to be powerful and robust in interpreting imprecise measurements and generating appropriate control decisions for many space operations. Several applications are underway, studying the fuzzy logic approach to solving control and decision making problems. Fuzzy logic aigorithms for relative motion and attitude control have been developed and demonstrated for proximity operations. Based on this experience, motion control algorithms that include obstacle avoidance were developed for a Mars Rover prototype for maneuvering during the sample collection process. A concept of an intelligent sensor system that can identify objects and track them continuously and learn from its environment is under development to support traffic management and proximity operations around the Space Station Freedom. For safe and reliable operation of Lunar/Mars based crew quarters, high speed controllers with ability to combine imprecise measurements from several sensors is required. A fuzzy logic approach that uses high speed fuzzy hardware chips is being studied. Author

N91-24050*# National Aeronautics and Space Administration. Lyndon B. Johnson Space Center, Houston, TX.
GENETIC ALGORITHMS **c61**
Lui Wang and Steven E. Bayer (Mitre Corp., Houston, TX.) *In* NASA, Washington, Technology 2000, Volume 2 1991 p 76-85 (For primary document see N91-24041 15-99)
Avail: NTIS HC/MF A16 CSCL 09B

Genetic algorithms are mathematical, highly parallel, adaptive search procedures (i.e., problem solving methods) based loosely on the processes of natural genetics and Darwinian survival of the fittest. Basic genetic algorithms concepts are introduced, genetic algorithm applications are introduced, and results are presented from a project to develop a software tool that will enable the widespread use of genetic algorithm technology. Author

N91-24051*# Jet Propulsion Lab., California Inst. of Tech., Pasadena.
INTEGRATED VERTICAL BLOCH LINE (VBL) MEMORY c60
R. R. Katti, J. C. Wu, and H. L. Stadler *In* NASA, Washington, Technology 2000, Volume 2 1991 p 86-92 (For primary document see N91-24041 15-99)
Avail: NTIS HC/MF A16 CSCL 09B

Vertical Bloch Line (VBL) Memory is a recently conceived, integrated, solid state, block access, VLSI memory which offers the potential of 1 Gbit/sq cm areal storage density, data rates of hundreds of megabits/sec, and submillisecond average access time simultaneously at relatively low mass, volume, and power values when compared to alternative technologies. VBLs are micromagnetic structures within magnetic domain walls which can be manipulated using magnetic fields from integrated conductors. The presence or absence of BVL pairs are used to store binary information. At present, efforts are being directed at developing a single chip memory using 25 Mbit/sq cm technology in magnetic garnet material which integrates, at a single operating point, the writing, storage, reading, and amplification functions needed in a memory. The current design architecture, functional elements, and supercomputer simulation results are described which are used to assist the design process. Author

N91-24052*# National Aeronautics and Space Administration. Ames Research Center, Moffett Field, CA.
PHYSICAL/CHEMICAL CLOSED-LOOP WATER-RECYCLING c54
Cal C. Herrmann (Bionetics Corp., Moffett Field, CA.) and Theodore Wydeven *In* NASA, Washington, Technology 2000, Volume 2 1991 p 95-105 (For primary document see N91-24041 15-99)
Avail: NTIS HC/MF A16 CSCL 06K

Water needs, water sources, and means for recycling water are examined in terms appropriate to the water quality requirements of a small crew and spacecraft intended for long duration exploration missions. Inorganic, organic, and biological hazards are estimated for waste water sources. Sensitivities to these hazards for human uses are estimated. The water recycling processes considered are humidity condensation, carbon dioxide reduction, waste oxidation, distillation, reverse osmosis, pervaporation, electrodialysis, ion exchange, carbon sorption, and electrochemical oxidation. Limitations and applications of these processes are evaluated in terms of water quality objectives. Computerized simulation of some of these chemical processes is examined. Recommendations are made for development of new water recycling technology and improvement of existing technology for near term application to life support systems for humans in space. The technological developments are equally applicable to water needs on Earth, in regions where extensive water recycling is needed or where advanced water treatment is essential to meet EPA health standards. Author

N91-24053*# National Aeronautics and Space Administration. John C. Stennis Space Center, Bay Saint Louis, MS.
NEW RESEARCH ON BIOREGENERATIVE AIR/WATER PURIFICATION SYSTEMS c54
Anne H. Johnson, R. D. Ellender, and Paul J. Watkins (University of Southern Mississippi, Hattiesburg.) *In* NASA, Washington, Technology 2000, Volume 2 1991 p 107-113 (For primary document see N91-24041 15-99)
Avail: NTIS HC/MF A16 CSCL 06K

For the past several years, air and water purification systems have been developed and used. This technology is based on the combined activities of plants and microorganisms as they function in a natural environment. More recently, researchers have begun to address the problems associated with indoor air pollution. Various common houseplants are currently being evaluated for their abilities to reduce concentrations of volatile organic compounds (VOCS) such as formaldehyde and benzene. With development of the Space Exploration Initiative, missions will increase in duration, and problems with resupply necessitates implementation of regenerative technology. Aspects of bioregenerative technology have been included in a habitat known as the BioHome. The ultimate goal is to use this technology in conjunction with physicochemical systems for air and water purification within closed systems. This study continued the risk assessment of bioregenerative technology with emphasis on biological hazards. In an effort to evaluate the risk for human infection, analyses were directed at enumeration of fecal streptococci and enteric viruses with the BioHome waste water treatment system. Author

N91-24054*# National Aeronautics and Space Administration. Goddard Space Flight Center, Greenbelt, MD.
THE LAND ANALYSIS SYSTEM (LAS) c43
Yun-Chi Lu and Fred M. Irani (ST Systems Corp., Lanham, MD.) *In* NASA, Washington, Technology 2000, Volume 2 1991 p 115-121 (For primary document see N91-24041 15-99)
Avail: NTIS HC/MF A16 CSCL 08B

The Land Analysis System (LAS) is an interactive software system, available in the public domain, for the analysis, display, and management of multispectral and other digital image data. The system was developed to support earth sciences research and development activities. LAS provides over 240 applications functions and utilities, a flexible user interface, complete on-line and hardcopy documentation, extensive image data file management, reformatting, and conversion utilities, and high level device independent access to image display hardware. The capabilities are summarized of the latest release of the system (version 5). Emphasis is given to the system portability and the isolation of hardware and software dependencies in this release. Author

N91-24055*# National Aeronautics and Space Administration. Goddard Space Flight Center, Greenbelt, MD.
POTENTIAL COMMERCIAL USES OF EOS REMOTE SENSING PRODUCTS c43
Leslie L. Thompson *In* NASA, Washington, Technology 2000, Volume 2 1991 p 122-129 (For primary document see N91-24041 15-99)
Avail: NTIS HC/MF A16 CSCL 08B

The instrument complement of the Earth Observing System (EOS) satellite system will generate data sets with potential interest to a variety of users who are now just beginning to develop geographic information systems tailored to their special applications and/or jurisdictions. Other users may be looking for a unique product that enhances competitive position. The generally distributed products from EOS will require additional value added processing to derive the unique products desired by specific users. Entrepreneurs have an opportunity to create these proprietary level 4 products from the EOS data sets. Specific instruments or collections of instruments could provide information for crop futures trading, mineral exploration, television and printed medium news products, regional and local government land management and planning, digital map directories, products for third world users, ocean fishing fleet probability of harvest forecasts, and other areas not even imagined at this time. The projected level 3 product are examined that will be available at launch from EOS instruments and commercial uses of the data after value added processing is estimated. Author

N91-24056*# National Aeronautics and Space Administration. Ames Research Center, Moffett Field, CA.
SIMULATION OF BLOOD FLOW THROUGH AN ARTIFICIAL HEART c52
Cetin Kiris, I-Dee Chang (Stanford Univ., CA.), Stuart E. Rogers, and Dochan Kwak *In* NASA, Washington, Technology 2000, Volume 2 1991 p 133-145 (For primary document see N91-24041 15-99)
Avail: NTIS HC/MF A16 CSCL 06P

A numerical simulation of the incompressible viscous flow through a prosthetic tilting disk heart valve is presented in order to demonstrate the current capability to model unsteady flows with moving boundaries. Both steady state and unsteady flow calculations are done by solving the incompressible Navier-Stokes equations in 3-D generalized curvilinear coordinates. In order to handle the moving boundary problems, the chimera grid embedding

scheme which decomposes a complex computational domain into several simple subdomains is used. An algebraic turbulence model for internal flows is incorporated to reach the physiological values of Reynolds number. Good agreement is obtained between the numerical results and experimental measurements. It is found that the tilting disk valve causes large regions of separated flow, and regions of high shear. Author

N91-24057*# National Aeronautics and Space Administration. Marshall Space Flight Center, Huntsville, AL.
THREE-DIMENSIONAL STRUCTURE OF HUMAN SERUM ALBUMIN **c52**
Daniel C. Carter, Xiao-min He, Pamela D. Twigg, and Elena Casale *In* NASA, Washington, Technology 2000, Volume 2 1991 p 146-150 (For primary document see N91-24041 15-99)
Avail: NTIS HC/MF A16 CSCL 06P

The binding locations to human serum albumin (HSA) of several drug molecules were determined at low resolution using crystallographic methods. The principal binding sites are located within subdomains IIA and IIIA. Preliminary studies suggest that an approach to increasing the in vivo efficacy of drugs which are rendered less effective or ineffective by virtue of their interaction with HSA, would be the use of competitive displacement in drug therapies and/or the development of a general inhibitor to the site within subdomain IIIA. These findings also suggest that the facilitated transfer of various ligands across organ/circulatory interfaces such as liver, kidney, and brain may be associated with binding to the IIIA subdomain. Author

N91-24058*# National Aeronautics and Space Administration. Ames Research Center, Moffett Field, CA.
A NON-INVASIVE MEASURE OF MINERALS AND ELECTROLYTES IN TISSUE **c52**
Sara B. Arnaud and Burton Silver (IntraCellular Diagnostics, Inc., San Jose, CA.) *In* NASA, Washington, Technology 2000, Volume 2 1991 p 151-154 (For primary document see N91-24041 15-99)
Avail: NTIS HC/MF A16 CSCL 06P

A system for collecting epithelial cells from the oral mucosa for the determination of ion concentration is discussed with application to the study of man's adaptation to microgravity. A number of characteristics of these cells influenced the choice for clinical testing. They are non-cornified epithelial cells located on the inferior aspect of the tongue; therefore, they are well protected from trauma. They have the capability of reflecting relatively recent physiologic changes since they are renewed every three days and have aerobic metabolism. Most importantly, they are easily accessible and can be removed by a wooden applicator stick with minimum discomfort. Smears of cells removed in this manner show predominantly individual cells rather than sheets of contiuous cells. This facilitates the visual isolation of single cells with the electron microscope for analysis. NASA's principle effort in the development of a test to measure the ion concentration in sublingual cells has been research by the biomedical program carried out by scientists with expertise in skeletal metabolism. These efforts were directed toward determining the biological meaning and deviations in interacellular ions in nonhuman primates and in male volunteers for experiments in a model for weightlessness. A brief one page summary of the experiments and results are presented. K.S.

N91-24059*# Jet Propulsion Lab., California Inst. of Tech., Pasadena.
OXYGEN PRODUCTION USING SOLID-STATE ZIRCONIA ELECTROLYTE TECHNOLOGY **c54**
Jerry W. Suitor and Douglas J. Clark *In* NASA, Washington, Technology 2000, Volume 2 1991 p 155-160 (For primary document see N91-24041 15-99)
Avail: NTIS HC/MF A16 CSCL 06K

High purity oxygen is required for a number of scientific, medical, and industrial applications. Traditionally, these needs have been met by cryogenic distillation or pressure swing adsorption systems designed to separate oxygen from air. Oxygen separation from air via solid-state zirconia electrolyte technology offers an alternative to these methods. The technology has several advantages over the traditional methods, including reliability, compactness, quiet operation, high purity output, and low power consumption. Author

N91-24060*# National Aeronautics and Space Administration. John F. Kennedy Space Center, Cocoa Beach, FL.
MONITORING AND CONTROL TECHNOLOGIES FOR BIOREGENERATIVE LIFE SUPPORT SYSTEMS/CELSS **c54**
William M. Knott and John C. Sager *In* NASA, Washington, Technology 2000, Volume 2 1991 p 161-167 (For primary document see N91-24041 15-99)
Avail: NTIS HC/MF A16 CSCL 06K

The development of a controlled Ecological Life Support System (CELSS) will require NASA to develop innovative monitoring and control technologies to operate the different components of the system. Primary effort over the past three to four years has been directed toward the development of technologies to operate a biomass production module. Computer hardware and software required to operate, collect, and summarize environmental data for a large plant growth chamber facility were developed and refined. Sensors and controls required to collect information on such physical parameters as relative humidity, temperature, irradiance, pressure, and gases in the atmosphere; and PH, dissolved oxygen, fluid flow rates, and electrical conductivity in the nutrient solutions are being developed and tested. Technologies required to produce high artificial irradiance for plant growth and those required to collect and transport natural light into a plant growth chamber are also being evaluated. Significant effort was directed towards the development and testing of a membrane nutrient delivery system required to manipulate, seed, and harvest crops, and to determine plant health prior to stress impacting plant productivity are also being researched. Tissue culture technologies are being developed for use in management and propagation of crop plants. Though previous efforts have focussed on development of technologies required to operate a biomass production module for a CELSS, current efforts are expanding to include technologies required to operate modules such as food preparation, biomass processing, and resource (waste) recovery which are integral parts of the CELSS. Author

N91-24061*# National Aeronautics and Space Administration. Lewis Research Center, Cleveland, OH.
SILICON CARBIDE, AN EMERGING HIGH TEMPERATURE SEMICONDUCTOR **c76**
Lawrence G. Matus and J. Anthony Powell *In* NASA, Washington, Technology 2000, Volume 2 1991 p 171-178 (For primary document see N91-24041 15-99)
Avail: NTIS HC/MF A16 CSCL 20L

In recent years, the aerospace propulsion and space power communities have expressed a growing need for electronic devices that are capable of sustained high temperature operation. Applications for high temperature electronic devices include development instrumentation within engines, engine control, and condition monitoring systems, and power conditioning and control systems for space platforms and satellites. Other earth-based applications include deep-well drilling instrumentation, nuclear reactor instrumentation and control, and automotive sensors. To meet the needs of these applications, the High Temperature Electronics Program at the Lewis Research Center is developing silicon carbide (SiC) as a high temperature semiconductor material. Research is focussed on developing the crystal growth, characterization, and device fabrication technologies necessary to produce a family of silicon carbide electronic devices and integrated sensors. The progress made in developing silicon carbide is presented, and the challenges that lie ahead are discussed. Author

N91-24062*# National Aeronautics and Space Administration. Lewis Research Center, Cleveland, OH.
FLEXIBLE FLUOROPOLYMER FILLED PROTECTIVE COATINGS **c27**
Bruce A. Banks, Michael J. Mirtich, James S. Sovey, Henry Nahra, and Sharon K. Rutledge *In* NASA, Washington, Technology 2000, Volume 2 1991 p 179-184 (For primary document see N91-24041 15-99)
Avail: NTIS HC/MF A16 CSCL 11C

Metal oxide films such as SiO2 are known to provide an effective barrier to the transport of moisture as well as gaseous species through polymeric films. Such thin film coatings have a tendency to crack upon flexure of the polymeric substrate. Sputter co-deposition of SiO2 with 4 to 15 percent fluoropolymers was demonstrated to produce thin films with glass-like barrier properties that have significant increases in strain to failure over pure glass films which improves their tolerance to flexure on polymeric substrates. Deposition techniques capable of producing these films on polymeric substrates are suitable for durable food packaging and oxidation/corrosion protection applications. Author

N91-24063*# National Aeronautics and Space Administration. Ames Research Center, Moffett Field, CA.
A CONFORMAL OXIDATION-RESISTANT, PLASMA-POLYMERIZED COATING **c27**
Morton A. Golub, Theodore Wydeven, and Narcinda R. Lerner *In* NASA, Washington, Technology 2000, Volume 2 1991 p 185-191 (For primary document see N91-24041 15-99)
Avail: NTIS HC/MF A16 CSCL 11C

A comparative study was made of the surface recession (etching) of thin films of plasma polymerized tetrafluoro ethylene (PPTFE), polytetrafluoro ethylene (PTFE), and ion-beam sputter deposited polytetrafluoro ethylene (SPTFE) exposed to ground-state atomic oxygen downstream from a nonequilibrium radio-frequency O2 plasma. At 22 C, the etch rates for PTFE, SPTFE, and PPTFE were in the ratio of 8.7:1.8:1.0. A thin, conformal coating of PPTFE (etch rate of 0.3 nm/h at 22 C) was found to protect an underlying cast film of a reactive polymer, cis-1,4 polybutadiene, against ground-state atomic oxygen attack for the time required to fully etch away the PPTFE coating. From ESCA analysis, PTFE exhibited only minor surface oxidation (uptake of 0.5 atom percent O) upon etching, its F/C ratio decreasing slightly from 2.00 to 1.97; PPTFE exhibited considerable surface oxidation (uptake of 5.9 atom percent O) intermediate between those of PTFE and PPTFE, with a decrease in F/C ratio from 1.73 to 1.67. A plasma-polymerized fluorocarbon coating such as PPTFE might be useful for space applications to protect polymers that are vulnerable to oxidation or degradation by oxygen atoms. Author

N91-24064*# National Aeronautics and Space Administration. Ames Research Center, Moffett Field, CA.
FLAME-RETARDANT COMPOSITE MATERIALS **c24**
Demetrius A. Kourtides *In* NASA, Washington, Technology 2000, Volume 2 1991 p 192-199 (For primary document see N91-24041 15-99)
Avail: NTIS HC/MF A16 CSCL 11D

The properties of eight different graphite composite panels fabricated using four different resin matrices and two types of graphite reinforcement are described. The resin matrices included: VPSP/BMI, a blend of vinylpolystyryl pyridine and bismaleimide; BMI, a bismaleimide; and phenolic and PSP, a polystyryl pyridine. The graphite fiber used was AS-4 in the form of either tape or fabric. The properties of these composites were compared with epoxy composites. It was determined that VPSP/BMI with the graphite tape was the optimum design giving the lowest heat release rate. Author

N91-24065*# National Aeronautics and Space Administration. Langley Research Center, Hampton, VA.
SUPERPLASTIC FORMING OF Al-Li ALLOYS FOR LIGHTWEIGHT, LOW-COST STRUCTURES **c26**
Stephen J. Hales and John A. Wagner *In* NASA, Washington, Technology 2000, Volume 2 1991 p 200-209 (For primary document see N91-24041 15-99)
Avail: NTIS HC/MF A16 CSCL 11F

Superplastic forming of advanced aluminum alloys is being evaluated as an approach for fabricating low-cost, light-weight, cryogenic propellant tanks. Built-up structure concepts (with inherent reduced scrap rate) are under investigation to offset the additional raw material expenses incurred by using aluminum lithium alloys. This approach to fabrication offers the potential for significant improvements in both structural efficiency and overall manufacturing costs. Superplasticity is the ability of specially processed material to sustain very large forming strains without failure at elevated temperatures under controlled deformation conditions. It was demonstrated that superplastic forming technology can be used to fabricate complex structural components in a single operation and increase structural efficiency by as much as 60 percent compared to conventional configurations in skin-stiffened structures. Details involved in the application of this technology to commercial grade superplastic aluminum lithium material are presented. Included are identification of optimum forming parameters, development of forming procedures, and assessment of final part quality in terms of cavitation volume and thickness variation. Author

N91-24066*# National Aeronautics and Space Administration. John F. Kennedy Space Center, Cocoa Beach, FL.
LOCALIZED CORROSION OF HIGH PERFORMANCE METAL ALLOYS IN AN ACID/SALT ENVIRONMENT **c26**
L. G. MacDowell and C. Ontiveros (California State Polytechnic Univ., Pomona.) *In* NASA, Washington, Technology 2000, Volume 2 1991 p 210-217 (For primary document see N91-24041 15-99)
Avail: NTIS HC/MF A16 CSCL 11F

Various vacuum jacketed cryogenic supply lines at the Space Shuttle launch site at Kennedy Space Center use convoluted flexible expansion joints. The atmosphere at the launch site has a very high salt content, and during a launch, fuel combustion products include hydrochloric acid. This extremely corrosive environment has caused pitting corrosion failure in the thin walled 304L stainless steel flex hoses. A search was done to find a more corrosion resistant replacement material. The study focussed on 19 metal alloys. Tests which were performed include electrochemical corrosion testing, accelerated corrosion testing in a salt fog chamber, and long term exposure at a beach corrosion testing site. Based on the results of these tests, several nickel based alloys were found to have very high resistance to this corrosive environment. Also, there was excellent agreement between the electrochemical tests and the actual beach exposure tests. This suggests that electrochemical testing may be useful for narrowing the field of potential candidate alloys before subjecting samples to long term beach exposure. Author

N91-24067*# National Aeronautics and Space Administration. Lewis Research Center, Cleveland, OH.
DIGITAL CODEC FOR REAL-TIME PROCESSING OF BROADCAST QUALITY VIDEO SIGNALS AT 1.8 BITS/PIXEL **c32**
Mary Jo Shalkhauser and Wayne A. Whyte *In* NASA, Washington, Technology 2000, Volume 2 1991 p 221-228 Previously announced in IAA as A90-51306 (For primary document see N91-24041 15-99)
Avail: NTIS HC/MF A16 CSCL 17B

Advances in very large scale integration and recent work in the field of bandwidth efficient digital modulation techniques have combined to make digital video processing technically feasible an potentially cost competitive for broadcast quality television transmission. A hardware implementation was developed for DPCM (differential pulse code midulation)-based digital television bandwidth compression algorithm which processes standard NTSC composite color television signals and produces broadcast quality video in real time at an average of 1.8 bits/pixel. The data compression algorithm and the hardware implementation of the

codec are described, and performance results are provided.
Author

N91-24068*# Jet Propulsion Lab., California Inst. of Tech., Pasadena.
RECENT ADVANCES IN CODING THEORY FOR NEAR ERROR-FREE COMMUNICATIONS **c32**
K.-M. Cheung, L. J. Deutsch, S. J. Dolinar, R. J. McEliece, F. Pollara, M. Shahshahani, and L. Swanson *In* NASA, Washington, Technology 2000, Volume 2 1991 p 229-241 (For primary document see N91-24041 15-99)
Avail: NTIS HC/MF A16 CSCL 17B

Channel and source coding theories are discussed. The following subject areas are covered: large constraint length convolutional codes (the Galileo code); decoder design (the big Viterbi decoder); Voyager's and Galileo's data compression scheme; current research in data compression for images; neural networks for soft decoding; neural networks for source decoding; finite-state codes; and fractals for data compression. Author

N91-24069*# National Aeronautics and Space Administration. Lewis Research Center, Cleveland, OH.
MICROWAVE INTEGRATED CIRCUITS FOR SPACE APPLICATIONS **c33**
Regis F. Leonard and Robert R. Romanofsky *In* NASA, Washington, Technology 2000, Volume 2 1991 p 242-248 (For primary document see N91-24041 15-99)
Avail: NTIS HC/MF A16 CSCL 09C

Monolithic microwave integrated circuits (MMIC), which incorporate all the elements of a microwave circuit on a single semiconductor substrate, offer the potential for drastic reductions in circuit weight and volume and increased reliability, all of which make many new concepts in electronic circuitry for space applications feasible, including phased array antennas. NASA has undertaken an extensive program aimed at development of MMICs for space applications. The first such circuits targeted for development were an extension of work in hybrid (discrete component) technology in support of the Advanced Communication Technology Satellite (ACTS). It focused on power amplifiers, receivers, and switches at ACTS frequencies. More recent work, however, focused on frequencies appropriate for other NASA programs and emphasizes advanced materials in an effort to enhance efficiency, power handling capability, and frequency of operation or noise figure to meet the requirements of space systems. Author

N91-24070*# National Aeronautics and Space Administration. Goddard Space Flight Center, Greenbelt, MD.
OPTICAL COMMUNICATION FOR SPACE MISSIONS **c74**
M. Firtmaurice *In* NASA, Washington, Technology 2000, Volume 2 1991 p 249-258 (For primary document see N91-24041 15-99)
Avail: NTIS HC/MF A16 CSCL 20F

Activities performed at NASA/GSFC (Goddard Space Flight Center) related to direct detection optical communications for space applications are discussed. The following subject areas are covered: (1) requirements for optical communication systems (data rates and channel quality; spatial acquisition; fine tracking and pointing; and transmit point-ahead correction); (2) component testing and development (laser diodes performance characterization and life testing; and laser diode power combining); (3) system development and simulations (The GSFC pointing, acquisition and tracking system; hardware description; preliminary performance analysis; and high data rate transmitter/receiver systems); and (4) proposed flight demonstration of optical communications. Author

N91-24071*# National Aeronautics and Space Administration. John F. Kennedy Space Center, Cocoa Beach, FL.
OPTICAL SHUTTER SWITCHING MATRIX **c74**
Charles H. Grove *In* NASA, Washington, Technology 2000, Volume 2 1991 p 259-267 (For primary document see N91-24041 15-99)
Avail: NTIS HC/MF A16 CSCL 20F

The interface switching systems are discussed which are related to those used in the Space Shuttle ground control system, transmission systems, communications systems, and airborne radar electronic countermeasure systems. The main goal is to identify a need that exists throughout the comprehensive information processing and communications disciplines supporting the Space Shuttle and Space Station programs, and introduce one viable approach to satisfy that need. The proposed device, described in NASA patent entitled 'Optical Shutter Switch Matrix', is discussed.
Author

N91-24072*# Jet Propulsion Lab., California Inst. of Tech., Pasadena.
FIBER OPTIC TACTICAL LOCAL NETWORK (FOTLAN) **c74**
L. A. Bergman, R. Hartmayer, W. H. Wu, P. Cassell, G. Edgar, J. Lambert, R. Mancini, J. Jeng, and C. Pardo *In* NASA, Washington, Technology 2000, Volume 2 1991 p 268-275 (For primary document see N91-24041 15-99)
Avail: NTIS HC/MF A16 CSCL 20F

A 100 Mbit/s FDDI (fiber distributed data interface) network interface unit is described that supports real-time data, voice and video. Its high-speed interrupt-driven hardware architecture efficiently manages stream and packet data transfer to the FDDI network. Other enhancements include modular single-mode laser-diode fiber optic links to maximize node spacing, optic bypass switches for increased fault tolerance, and a hardware performance monitor to gather real-time network diagnostics. Author

N91-24073*# Jet Propulsion Lab., California Inst. of Tech., Pasadena.
HIGH PRECISION APPLICATIONS OF THE GLOBAL POSITIONING SYSTEM **c04**
Stephen M. Lichten *In* NASA, Washington, Technology 2000, Volume 2 1991 p 276-284 (For primary document see N91-24041 15-99)
Avail: NTIS HC/MF A16 CSCL 17G

The Global Positioning System (GPS) is a constellation of U.S. defense navigation satellites which can be used for military and civilian positioning applications. A wide variety of GPS scientific applications were identified and precise positioning capabilities with GPS were already demonstrated with data available from the present partial satellite constellation. Expected applications include: measurements of Earth crustal motion, particularly in seismically active regions; measurements of the Earth's rotation rate and pole orientation; high-precision Earth orbiter tracking; surveying; measurements of media propagation delays for calibration of deep space radiometric data in support of NASA planetary missions; determination of precise ground station coordinates; and precise time transfer worldwide. Author

N91-24074*# National Aeronautics and Space Administration. Langley Research Center, Hampton, VA.
QUANTITATIVE NONDESTRUCTIVE EVALUATION: REQUIREMENTS FOR TOMORROW'S RELIABILITY **c38**
Joseph S. Heyman *In* NASA, Washington, Technology 2000, Volume 2 1991 p 287-297 (For primary document see N91-24041 15-99)
Avail: NTIS HC/MF A16 CSCL 14D

Quantitative Nondestructive Evaluation (QNDE) is the technology of measurement, analysis, and prediction of the state of material/structural systems for safety, reliability, and mission assurance. QNDE has impact on everyday life from the cars we drive, the planes we fly, the buildings we work or live in, literally to the infrastructure of our world. Here, researchers highlight some of the new sciences and technologies that are part of a safer, cost effective tomorrow. Specific technologies that are discussed are thermal QNDE of aircraft structural integrity, ultrasonic QNDE for materials characterization, and technology spinoffs from aerospace to the medical sector. In each case, examples are given of how new requirements result in enabling measurement

technologies, which in turn change the boundaries of design/practice. Author

N91-24075*# National Aeronautics and Space Administration. John F. Kennedy Space Center, Cocoa Beach, FL.
ROBOTIC CONTROL AND INSPECTION VERIFICATION c37
Virgil Leon Davis *In* NASA, Washington, Technology 2000, Volume 2 1991 p 298-307 (For primary document see N91-24041 15-99)
Avail: NTIS HC/MF A16 CSCL 13H

Three areas of possible commercialization involving robots at the Kennedy Space Center (KSC) are discussed: a six degree-of-freedom target tracking system for remote umbilical operations; an intelligent torque sensing end effector for operating hand valves in hazardous locations; and an automatic radiator inspection device, a 13 by 65 foot robotic mechanism involving completely redundant motors, drives, and controls. Aspects concerning the first two innovations can be integrated to enable robots or teleoperators to perform tasks involving orientation and panal actuation operations that can be done with existing technology rather than waiting for telerobots to incorporate artificial intelligence (AI) to perform 'smart' autonomous operations. The third robot involves the application of complete control hardware redundancy to enable performance of work over and near expensive Space Shuttle hardware. The consumer marketplace may wish to explore commercialization of similiar component redundancy techniques for applications when a robot would not normally be used because of reliability concerns. Author

N91-24076*# National Aeronautics and Space Administration. Langley Research Center, Hampton, VA.
THE TRANSFER OF TECHNOLOGY TO MEASURE SKIN BURN DEPTH IN HUMANS c52
William T. Yost and John H. Cantrell *In* NASA, Washington, Technology 2000, Volume 2 1991 p 308-314 (For primary document see N91-24041 15-99)
Avail: NTIS HC/MF A16 CSCL 06P

Discussed here is the use of ultrasonic techniques originally used to locate cracks in metal structues to measure burn wound depth in humans. Acoustic impedance, performance tests, and the theoretical model are discussed. Measurements of skin burns on anesthetized pigs made with the the ultrasonic instrumentation were in agreement with diagnoses made by a physician, and subsequently confirmed by the healing process. Researchers felt that the concept proved useful in a clinical setting and that the instrument and concept were ready to extend to the manufacturer. Author

N91-24077*# National Aeronautics and Space Administration. Langley Research Center, Hampton, VA.
FREQUENCY DOMAIN LASER VELOCIMETER SIGNAL PROCESSOR c36
James F. Meyers and R. Jay Murphy (Macrodyne, Inc., Clifton Park, NY.) *In* NASA, Washington, Technology 2000, Volume 2 1991 p 315-324 (For primary document see N91-24041 15-99)
Avail: NTIS HC/MF A16 CSCL 20E

A new scheme for processing signals from laser velocimeter systems is described. The technique utilizes the capabilities of advanced digital electronics to yield a signal processor capable of operating in the frequency domain maximizing the information obtainable from each signal burst. This allows a sophisticated approach to signal detection and processing, with a more accurate measurement of the chirp frequency resulting in an eight-fold increase in measurable signals over the present high-speed burst counter technology. Further, the required signal-to-noise ratio is reduced by a factor of 32, allowing measurements within boundary layers of wind tunnel models. Measurement accuracy is also increased up to a factor of five. Author

N91-24078*# National Aeronautics and Space Administration. Langley Research Center, Hampton, VA.
A FIELD-DEPLOYABLE DIGITAL ACOUSTIC MEASUREMENT SYSTEM c71
David L. Gray, Kenneth D. Wright, II, and Wayne D. Rowland *In* NASA, Washington, Technology 2000, Volume 2 1991 p 325-332 (For primary document see N91-24041 15-99)
Avail: NTIS HC/MF A16 CSCL 20A

A field deployable digital acoustic measurement system was developed to support acoustic research programs at the Langley Research Center. The system digitizes the acoustic inputs at the microphone, which can be located up to 1000 feet from the van which houses the acquisition, storage, and analysis equipment. Digitized data from up to 12 microphones is recorded on high density 8mm tape and is analyzed post-test by a microcomputer system. Synchronous and nonsynchronous sampling is available with maximum sample rates of 12,500 and 40,000 samples per second respectively. The high density tape storage system is capable of storing 5 gigabytes of data at transfer rates up to 1 megabyte per second. System overall dynamic range exceeds 83 dB. Author

N91-24079*# National Aeronautics and Space Administration. Goddard Space Flight Center, Greenbelt, MD.
LASER OPTICAL DISK POSITION ENCODER WITH ACTIVE HEADS c36
Eric P. Osborne *In* NASA, Washington, Technology 2000, Volume 2 1991 p 333-340 (For primary document see N91-24041 15-99)
Avail: NTIS HC/MF A16 CSCL 20E

An angular position encoder that minimizes the effects of eccentricity and other misalignments between the disk and the read stations by employing heads with beam steering optics that actively track the disk in directions along the disk radius and normal to its surface is discussed. The device adapts features prevalent in optical disk technology to the application of angular position sensing. Author

N91-24080*# National Aeronautics and Space Administration. Lewis Research Center, Cleveland, OH.
AEROSPACE APPLICATIONS OF HIGH TEMPERATURE SUPERCONDUCTIVITY c76
V. O. Heinen and D. J. Connolly *In* NASA, Washington, Technology 2000, Volume 2 1991 p 343-345 (For primary document see N91-24041 15-99)
Avail: NTIS HC/MF A16 CSCL 20L

Space application of high temperature superconducting (HTS) materials may occur before most terrestrial applications because of the passive cooling possibilities in space and because of the economic feasibility of introducing an expensive new technology which has a significant system benefit in space. NASA Lewis Research Center has an ongoing program to develop space technology capitalizing on the potential benefit of HTS materials. The applications being pursued include space communications, power and propulsion systems, and magnetic bearings. In addition, NASA Lewis is pursuing materials research to improve the performance of HTS materials for space applications. Author

N91-24081*# National Aeronautics and Space Administration. Lewis Research Center, Cleveland, OH.
SUPERCONDUCTING MICROWAVE ELECTRONICS AT LEWIS RESEARCH CENTER c76
Joseph D. Warner, Kul B. Bhasin, and Regis F. Leonard *In* NASA, Washington, Technology 2000, Volume 2 1991 p 346-354 (For primary document see N91-24041 15-99)
Avail: NTIS HC/MF A16 CSCL 20L

Over the last three years, NASA Lewis Research Center has investigated the application of newly discovered high temperature superconductors to microwave electronics. Using thin films of YBa2Cu3O7-delta and Tl2Ca2Ba2Cu3Ox deposited on a variety of substrates, including strontium titanate, lanthanum gallate, lanthanum aluminate and magnesium oxide, a number of microwave circuits have been fabricated and evaluated. These include a cavity

resonator at 60 GHz, microstrip resonators at 35 GHz, a superconducting antenna array at 35 GHz, a dielectric resonator at 9 GHz, and a microstrip filter at 5 GHz. Performance of some of these circuits as well as suggestions for other applications are reported. Author

N91-24082*# National Aeronautics and Space Administration. Goddard Space Flight Center, Greenbelt, MD.
MELT-PROCESSED BULK SUPERCONDUCTORS: FABRICATION AND CHARACTERIZATION FOR POWER AND SPACE APPLICATIONS c76
Hamid Hojaji, Aaron Barkatt, Shouxiang Hu, Arthur N. Thorpe, Matthew F. Ware, David Davis (Howard Univ., Washington, DC.), and Sidney Alterescu *In* NASA, Washington, Technology 2000, Volume 2 1991 p 356-364 (For primary document see N91-24041 15-99)
(Grant NAG5-1017)
Avail: NTIS HC/MF A16 CSCL 20L

Melt-process- bulk superconducting materials based on variations on the base YBa2Cu3O(x) were produced in a variety of shapes and forms. Very high values of both zero-field and high-field magnetization were observed. These are useful for levitation and power applications. Magnetic measurements show that the effects of field direction and intensity, temperature and time are consistent with an aligned grain structure with multiple pinning sites and with models of thermally activated flux motion. Author

N91-24083*# National Aeronautics and Space Administration. Langley Research Center, Hampton, VA.
DESCRIPTION OF THE LARGE GAP MAGNETIC SUSPENSION SYSTEM (LGMSS) GROUND-BASED EXPERIMENT c76
Nelson J. Groom *In* NASA, Washington, Technology 2000, Volume 2 1991 p 365-377 (For primary document see N91-24041 15-99)
Avail: NTIS HC/MF A16 CSCL 20L

A description of the Large Gap Magnetic Suspension System (LGMSS) ground-based experiment is presented. The LGMSS provides five degrees of freedom control of a cylindrical suspended element which is levitated above a floor-mounted array of air core electromagnets. The uncontrolled degree of freedom is rotation about the long axis of the cylinder (roll). Levitation and control forces are produced on a permanent magnet core which is embedded in the cylinder. The cylinder also contains light emitting diodes (LEDs), assorted electrons, and a power supply. The LEDs provide active targets for an optical position measurement system which is being developed in-house at the Langley Research Center. The optical position measurement system will provide six degrees of freedom position information for the LGMSS control system. Author

N91-24084# Advisory Group for Aerospace Research and Development, Neuilly-Sur-Seine (France).
AGARD HIGHLIGHTS 91/1, MARCH 1991
Mar. 1991 62 p
(AGARD-Highlights-91/1) Copyright Avail: NTIS HC/MF A04; Non-NATO Nationals requests available only from AGARD/Scientific Publications Executive

The accomplishments of AGARD are examined. Biographies are provided on the new AGARD chairman and the new director. An overview is given on the 'Danish National Day.' An article on 'Helicopters and V/STOL Aircraft - Post Development and Future Prospects' is presented. B.G.

N91-24085*# National Aeronautics and Space Administration, Washington, DC.
AERONAUTICS AND SPACE REPORT OF THE PRESIDENT Activities Report, 1989-1990
1991 177 p
Avail: NTIS HC/MF A09 CSCL 05A

The years 1989 to 1990 activities are reported including human space flight, unmanned expendable launch vehicles, space science and applications, space communications operations, space research and technology, and aeronautics research and technology. Contributions made by the 14 participating government organizations are outline. Each organization's aeronautics and/or space activities for the year are presented. The organizations involved include: (1) NASA; (2) Dept. of Defense; (3) Dept. of Commerce; (4) Dept. of Energy; (5) Dept. of the Interior; (6) Dept. of Agriculture; (7) Federal Communications Commission; (8) Dept. of Transportation; (9) Environmental Protection Agency; (10) National Science Foundation; (11) Smithsonian Institution; (12) Dept. of State; (13) Arms Control and Disarmament; and (14) United States Information Agency. Author

N91-24086# Deutsche Forschungsanstalt fuer Luft- und Raumfahrt, Cologne (Germany, F.R.).
[ACTIVITIES REPORT OF THE DLR] Annual Report 1989/90 [JAHRESBERICHT 1989/90]
Thomas H. Weyer Sep. 1990 87 p In GERMAN
(ISSN-0938-2194; ETN-91-99252) Copyright Avail: NTIS HC/MF A05

The activities of the five research centers of the German research organization for air and space transportation during the year 1989/90 are described. Air flight, spaceceflight, and energy techniques are discussed. With regard to air flight the following research work was carried out: aerodynamic efficiency improvement, flight dynamical simulation, new helicopter technology, new propulsion unit development, air traffic, and personnel selection. Under the topic of space flight the follwing areas of research were addressed: space vehicles, rocket launchers, operating tasks for space missions, and research in space. Weightlessness research in the field of materials and bioscience, multi-axis vibration simulator development for satellites, and ozone measuring aircraft is presented. Energy techniques in the field of fossil fuel combustion, solar and hydrogen energy, and high energy lasers are discussed. ESA

Typical Subject Index Listing

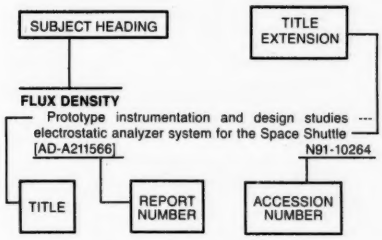

The subject heading is a key to the subject content of the document. Titles, report numbers, and accession numbers of pertinent documents are provided under each subject heading. When the title is insufficiently descriptive of the document content, a title extension has been added, separated from the title by three hyphens. The report number helps to indicate the type of document cited (e.g., NASA report, NASA translation, NASA contractor report). The accession number is the number by which the document abstracts are arranged in this journal and by which the document is sold or requested. The titles, with title extensions if present, are arranged under each subject heading in ascending accession number order. The subject headings have been selected from the latest revision of the *NASA Thesaurus* (NASA SP-7064).

A

A-320 AIRCRAFT
The electrical flight control system of A320 Airbus: A fault tolerant system
[REPT-911-111-103] N91-23192

ABLATION
Temperature distribution and thermal damage during tissue ablation by CO2 laser irradiation: Model and experiment N91-23833

ABLATIVE MATERIALS
High temperature composites in space planes and missiles development
[REPT-911-430-119] N91-23259

ABNORMALITIES
Quantifying improved visual performance through vision training
[AD-A232799] N91-23716

ABSORPTION COOLING
Thermal control system for the investigation of specific absorption rates for specimens exposed to electromagnetic radiation
[AD-A231329] N91-23459

ABSORPTION CROSS SECTIONS
Temperature dependence of ultraviolet absorption cross-sections of alternative chlorofluoroethanes
[AERONOMICA-ACTA-A-358-1991] N91-23647

ABSORPTION SPECTRA
Hyperspectral imagery: What is it, what can it do
[AD-A231164] N91-23610
Propagation of seismic waves in nonelastic media
[REPT-90-065] N91-23651
Determination of the temperature profile of the troposphere with a two frequency lidar
[EXAMENARBEIT-8] N91-23653
Luminescence and absorption spectra of C60 films
[AD-A232153] N91-23900
The envelopes of RV Tauri variables N91-24008
Ultraviolet gas absorption and dust extinction toward M8 and the outer galactic disk N91-24018
Theoretical studies of QSO absorption lines and the intergalactic medium N91-24025

ABSTRACTS
Bulletin of the Israel Physical Society, volume 33, 1987. Annual Meeting 1987: Program and Abstracts
[ITN-89-85012] N91-23832

ABUNDANCE
Composition and distribution of carbonates, sulfates, and hydrates on the Martian surface from earth-based spectroscopy between 3-5 microns N91-24033

AC GENERATORS
Component technology for stirling power converters
[NASA-TM-104387] N91-23234

ACCELERATION TOLERANCE
Human short-latency somatosensory evoked potentials in impact acceleration research: Equipment, procedures, and techniques
[AD-A232732] N91-23709

ACCIDENT PREVENTION
Treatment of denser-than-air releases in an advection-diffusion model: Thermodynamic effects
[DE91-010152] N91-23632

ACCRETION DISKS
Bulletin of the Israel Physical Society, volume 33, 1987. Annual Meeting 1987: Program and Abstracts
[ITN-89-85012] N91-23832
The spectrum of massive accretion disks N91-23840

ACCURACY
Higher accuracy requirements for the satisfactory position calculation of an artificial satellite
[GKSS-90/E/25] N91-23203

ACETATES
Comment on: Analytic solution of the Stochastic-Liouville model of spin-exchange
[DE91-010570] N91-23861

ACID RAIN
National stream survey database guide
[PB91-141804] N91-23625

ACOUSTIC EMISSION
Evaluation of catastrophic failure risk in pressure vessels. Results of pressure vessel test with a large vessel (HC2-test)
[VTT-RR-708] N91-23551

ACOUSTIC EXCITATION
Computational simulation of acoustic fatigue for hot composite structures
[NASA-TM-104379] N91-23548

ACOUSTIC FATIGUE
Computational simulation of acoustic fatigue for hot composite structures
[NASA-TM-104379] N91-23548

ACOUSTIC IMPEDANCE
The transfer of technology to measure skin burn depth in humans N91-24076

ACOUSTIC INSTABILITY
Numerical simulations of instabilities in compressible mixing layers N91-23412

ACOUSTIC MEASUREMENT
A preliminary investigation of acousto-ultrasonic NDE of metal matrix composite test specimens
[NASA-TM-104339] N91-23521
Soviet atmospheric acoustics research N91-23848
A field-deployable digital acoustic measurement system N91-24078

ACOUSTIC PROPAGATION
Soviet atmospheric acoustics research N91-23848

ACOUSTIC PROPERTIES
Experimental investigations on the transition from stable to unstable combustion by means of active instability control N91-23165
Summary of basic research in thermoacoustic heat transport: 1990
[AD-A232223] N91-23847

ACOUSTICS
Fundamental hydrodynamics research
[AD-A232650] N91-23451

ACOUSTO-OPTICS
The 2-D acousto-optic signal processors for simultaneous spectrum analysis and direction finding
[AD-A232148] N91-23367

ACTINIDE SERIES COMPOUNDS
Calculation of cross sections for binary reactions between heavy ion projectiles and heavy actinide targets
[DE91-010222] N91-23882

ACTIVE CONTROL
Unsteady flow structure from swept edges subjected to controlled motion
[AD-A232714] N91-23094
Experimental investigations on the transition from stable to unstable combustion by means of active instability control N91-23165
Integrated multidisciplinary optimization of actively controlled fiber composite wings N91-23190

ACTIVITY (BIOLOGY)
Exploring the mesoscopic domain where classical and quantum phenomena meet N91-23843

ACTUATORS
Shape-memory alloy tactical feedback actuator, phase 1
[AD-A231389] N91-23289
Preloaded latching device
[NASA-CASE-MSC-21730-1] N91-23493
Molecular studies of cytokine induction
[AD-A232221] N91-23707

ADA (PROGRAMMING LANGUAGE)
Specifications for reusable software components
[RR-828-I-IMAG-116-LIFIA] N91-23756
An event-activation record approach to simulation modeling in Ada: User's guide
[AD-A232093] N91-23768

ADAPTIVE CONTROL
Joint services electronics program
[AD-A232331] N91-23402
On the control of two manipulators holding a rigid object in the presence of uncertainty
[DE90-017742] N91-23508
Rule-based motion coordination for the adaptive suspension vehicle on ternary-type terrain
[AD-A232224] N91-23517
On the use of genetic algorithms to solve the time-table problem
[REPT-90-060] N91-23752

ADAPTIVE FILTERS
Implications of adaptive cancellation array processing for design of a space-based surveillance radar
[RSRE-MEMO-4410] N91-23364
Fractal image compression of Rayleigh, Raman, LIF and LDV data in turbulent reacting flows
[AD-A232237] N91-23449
System modeling and identification of flexible structures N91-23531

ADHESION
Applications of energetic particles in improving coating adhesion properties
[DE91-008833] N91-23312

ADHESIVE BONDING
Stress analysis of a double-doubler joint in composite structure N91-23530
ACLICO: A computer aided design system for bonded joints
[REPT-911-430-101] N91-23757

ADIABATIC CONDITIONS
Order and disorder in metallic alloys
[DE91-009120] N91-23292

ADSORPTION
Phase transitions at liquid solid interfaces: Pade approximant for adsorption isotherms and voltammograms
[AD-A232623] N91-23285
Surface x ray scattering measurements of the substrate induced spatial modulation of an incommensurate adsorbed monolayer
[AD-A232625] N91-23959

ADVANCED VERY HIGH RESOLUTION RADIOMETER
Evaluation of generalized thresholds in an objective multispectral satellite cloud analysis
[AD-A232716] N91-23683

ADVECTION
Treatment of denser-than-air releases in an advection-diffusion model: Thermodynamic effects
[DE91-010152] N91-23632

Observed changes in the activity of baroclinic waves and their feedbacks during the life cycles of low-frequency circulation anomalies in the Northern Hemisphere winter N91-23668

AEROACOUSTICS
Unified aeroacoustics analysis for high speed turboprop aerodynamics and noise. Volume 2: Development of theory for wing shielding [NASA-CR-185192] N91-23849
Unified aeroacoustics analysis for high speed turboprop aerodynamics and noise. Volume 3: Application of theory for blade loading, wakes, noise, and wing shielding [NASA-CR-185193] N91-23850
Unified aeroacoustics analysis for high speed turboprop aerodynamics and noise. Volume 4: Computer user's manual for UAAP turboprop aeroacoustic code [NASA-CR-185194] N91-23851
Unified aeroacoustics analysis for high speed turboprop aerodynamics and noise. Volume 5: Propagation of propeller tone noise through a fuselage boundary layer [NASA-CR-185195] N91-23852

AEROASSIST
Technologies for aerobraking [NASA-TM-102854] N91-23207
Simulation and analyses of the aeroassist flight experiment attitude update method [NASA-TM-102174] N91-23210

AEROBRAKING
Technologies for aerobraking [NASA-TM-102854] N91-23207

AEROCAPTURE
Technologies for aerobraking [NASA-TM-102854] N91-23207

AERODYNAMIC BALANCE
Model rotor icing tests in the NASA Lewis icing research tunnel [NASA-TM-104351] N91-23184

AERODYNAMIC CHARACTERISTICS
Aerodynamic preliminary analysis system 2. Part 1: Theory [NASA-CR-182076] N91-23080
Aerodynamic preliminary analysis system 2. Part 2: User's manual [NASA-CR-182077] N91-23081
IAI hypersonic wind tunnel [IAITIC-87-1006] N91-23194
A computationally efficient modelling of laminar separation bubbles N91-23411
AGARD highlights 91/1, March 1991 [AGARD-HIGHLIGHTS-91/1] N91-24084

AERODYNAMIC COEFFICIENTS
Atmospheric turbulence review of space shuttle launches [NASA-TM-4289] N91-23215

AERODYNAMIC CONFIGURATIONS
Aerodynamic preliminary analysis system 2. Part 1: Theory [NASA-CR-182076] N91-23080
Flying qualities of the X-29 forward swept wing aircraft N91-23127
Integrated multidisciplinary optimization of actively controlled fiber composite wings N91-23190

AERODYNAMIC DRAG
Atmospheric turbulence review of space shuttle launches [NASA-TM-4289] N91-23215

AERODYNAMIC HEAT TRANSFER
Simulation of brush insert for leading-edge-passage convective heat transfer [NASA-TM-103801] N91-23409

AERODYNAMIC INTERFERENCE
Procedure for determination of three-dimensional wind tunnel wall interferences and wall adaptation in compressible subsonic flow using measured wall pressures [DLR-FB-90-46] N91-23088

AERODYNAMIC LOADS
Simulation of iced wing aerodynamics [NASA-TM-104362] N91-23086

AERODYNAMIC NOISE
A study of the noise mechanisms of transonic blade-vortex interactions [NASA-CR-188199] N91-23084
Unified aeroacoustics analysis for high speed turboprop aerodynamics and noise. Volume 3: Application of theory for blade loading, wakes, noise, and wing shielding [NASA-CR-185193] N91-23850
Unified aeroacoustics analysis for high speed turboprop aerodynamics and noise. Volume 4: Computer user's manual for UAAP turboprop aeroacoustic code [NASA-CR-185194] N91-23851
Unified aeroacoustics analysis for high speed turboprop aerodynamics and noise. Volume 5: Propagation of propeller tone noise through a fuselage boundary layer [NASA-CR-185195] N91-23852

AERODYNAMIC STALLING
Flying qualities experience on the AMX aircraft N91-23112

AERODYNAMICS
Aeronautical engineering: A cumulative index to a continuing bibliography (supplement 261) [NASA-SP-7037(261)] N91-23073
Aeronautical engineering: A continuing bibliography with indexes (supplement 262) [NASA-SP-7037(262)] N91-23074
Simulation of iced wing aerodynamics [NASA-TM-104362] N91-23086
Icing simulation: A survey of computer models and experimental facilities [NASA-TM-104366] N91-23087
Agility: A rational development of fundamental metrics and their relationship to flying qualities N91-23129
A computer aided multivariable control systems design technique with application to aircraft flying qualities [AD-A232549] N91-23144
Aerodynamics and stabilization of combustion of hydrogen jets injected into subsonic airflow N91-23164
Passive laminar flow control of crossflow vorticity [NASA-CASE-LAR-13563-1] N91-23410

AEROELASTICITY
Buffet induced structural/flight-control system interaction of the X-29A aircraft [NASA-TM-101735] N91-23133

AERONAUTICAL ENGINEERING
Aeronautical engineering: A cumulative index to a continuing bibliography (supplement 261) [NASA-SP-7037(261)] N91-23073
Aeronautical engineering: A continuing bibliography with indexes (supplement 262) [NASA-SP-7037(262)] N91-23074
Satellite and aeronautical technologies serving the management of living marine resources N91-23606

AERONAUTICAL SATELLITES
Characteristics of a future aeronautical satellite communications system [NASA-TM-104389] N91-23102
Satellite and aeronautical technologies serving the management of living marine resources N91-23606

AEROSPACE ENGINEERING
Government/industry response to questionnaire on space mechanisms/tribology technology needs [NASA-TM-104358] N91-23501
Electronic neuroprocessors N91-24045
Aerospace applications of high temperature superconductivity N91-24080

AEROSPACE ENVIRONMENTS
The Combined Release and Radiation Effects Satellite program (CRRES): A unique series of scientific experiments [NASA-TM-104957] N91-23213
Satellite utilization by civil aviation [REPT-911-111-105] N91-23216
Payload related crew operations: From past missions to Columbus N91-23569
Comparisons between underwater and space working environments for on board activities optimization (Columbus space programme) N91-23574
Space life sciences: A status report [NASA-NP-120] N91-23694

AEROSPACE INDUSTRY
Experimentation facilities for thermomechanical static tests with analytic test specimens at Aerospatiale [REPT-911-430-108] N91-23197
Survey: Potential of the Israeli industry for space technology [CEMA-86-17] N91-23967

AEROSPACE MEDICINE
A test of the American Safety Flight Systems, Inc. prebreather/portable oxygen system [AD-A232723] N91-23100
Flight mechanics/air navigation research field. A 1990 Scientific report of the German Air and Space Research Organization [ISSN-0720-7808] N91-23103
Space life sciences: A status report [NASA-NP-120] N91-23694
Aerospace medicine and biology: A continuing bibliography with indexes (supplement 346) [NASA-SP-7011(346)] N91-23700
Aerospace medicine and biology: A continuing bibliography with indexes (supplement 347) [NASA-SP-7011(347)] N91-23701
Aerospace medicine and biology: A continuing bibliography with indexes (supplement 348) [NASA-SP-7011(348)] N91-23702

AEROSPACE PLANES
Hypersonic propulsion: Past and present N91-23148
Hypersonic propulsion: Status and challenge N91-23153
Supersonic-hypersonic inlet studies for aerospaceplane N91-23160
Materials for hypersonic engines N91-23177

AEROSPACE SCIENCES
Aeronautics and space report of the President N91-24085

AEROSPACE SYSTEMS
Large space structures fielding plan [AD-A232097] N91-23227

AEROSPACE VEHICLES
Characterization of composite materials for aerospace materials [DLR-MITT-90-15] N91-23246

AEROTHERMODYNAMICS
Problems of hypersonic aerothermodynamics [MBB-FE202/5/PUB/436] N91-23090
Technologies for aerobraking [NASA-TM-102854] N91-23207
Aero-thermal investigation of a highly loaded transonic linear turbine guide vane cascade. A test case for inviscid and viscous flow computations [VKI-TN-174] N91-23437

AFRICA
Atmospheric teleconnections: Emphasis on the El Nino/Southern Oscillation and monsoons N91-23636

AFTERBURNING
Turbojet potential for hypersonic flight N91-23155

AGING (METALLURGY)
Phase transformations and microstructural evolution in aged Mn-Cu-based alloys [AD-A232473] N91-23305

AGREEMENTS
Are wait-free algorithms fast [AD-A232829] N91-23774

AIR BREATHING ENGINES
NASA aeropropulsion research in support of propulsion systems of the 21st century [NASA-TM-104403] N91-23083
Airbreathing propulsion for space transport: New concepts, special problems and attempts at solutions N91-23154
Airbreathing propulsion for transatmospheric flight N91-23156
Design considerations for combined air breathing-rocket propulsion systems [AIAA-90-0098] N91-23158
Cryogenic hydrogen-induced air-liquefaction technologies N91-23159
Supersonic-hypersonic inlet studies for aerospaceplane N91-23160

AIR CONDITIONING EQUIPMENT
Effectiveness of a prototype microclimate cooling system for use with chemical protective clothing [AD-A231572] N91-23717

AIR COOLING
Research on aerodynamic control of blade tip clearance flow in air-cooled turbine [DE91-764223] N91-23182

AIR FLOW
Aerodynamics and stabilization of combustion of hydrogen jets injected into subsonic airflow N91-23164
Interfacial characteristic measurements in horizontal bubbly two-phase flow [DE91-009803] N91-23427
On the airflow over the Alps during south Foehn [DLR-FB-90-30] N91-23676

AIR INTAKES
Hypersonic Combined Cycle Propulsion [AGARD-CP-479] N91-23147

AIR MASSES
Technical description of the high-resolution air mass transformation model at KNMI [KNMI-TR-125] N91-23646

AIR NAVIGATION
Flight mechanics/air navigation research field. A 1990 Scientific report of the German Air and Space Research Organization [ISSN-0720-7808] N91-23103
Navigation, guidance, and trajectory optimization for hypersonic vehicles N91-23150

AIR POLLUTION
Lateral dispersion of radioactive release. Draft for comments [CEMA-86/17] N91-23621
Forecasting atmospheric particulate sulfur concentrations using national weather service synoptic charts [AD-A231634] N91-23622

AIR QUALITY
New research on bioregenerative air/water purification systems N91-24053

AIR SAMPLING
Tropospheric sampling with aircraft [DE91-009472] N91-23626

AIR TRAFFIC
Flight mechanics/air navigation research field. A 1990 Scientific report of the German Air and Space Research Organization
[ISSN-0720-7808] N91-23103
AIR TRAFFIC CONTROL
Near midair collisions as an indicator of general aviation collision risk N91-23096
Microwave landing system modeling with application to air traffic control
[NASA-TM-102832] N91-23099
Flight mechanics/air navigation research field. A 1990 Scientific report of the German Air and Space Research Organization
[ISSN-0720-7808] N91-23103
Airborne Collision Avoidance System (ACAS) in controlled air traffic. Aspects of reciprocal influence in Secondary Surveillance Radar (SSR) radio loads
[ETN-91-99253] N91-23105
Differential GPS terminal area test results
[AD-A232668] N91-23106
The limits of the landing process of aircraft
[DLR-FB-90-49] N91-23137
Precision runway monitor demonstration report
[AD-A232671] N91-23198
AIR TRANSPORTATION
Engine technology challenges for a 21st century high speed civil transport
[NASA-TM-104363] N91-23098
Activities report of the DLR
[ISSN-0938-2194] N91-24086
AIR WATER INTERACTIONS
Primary ocean production: Carbon and particle flux N91-23596
Energy exchange study at the ocean surface by satellite observation N91-23597
AIRBORNE EQUIPMENT
Airborne Collision Avoidance System (ACAS) in controlled air traffic. Aspects of reciprocal influence in Secondary Surveillance Radar (SSR) radio loads
[ETN-91-99253] N91-23105
An investigation of CFAR techniques for airborne radars
[AD-A232724] N91-23378
Satellite and aeronautical technologies serving the management of living marine resources N91-23606
AIRBORNE/SPACEBORNE COMPUTERS
The electrical flight control system of A320 Airbus: A fault tolerant system
[REPT-911-111-103] N91-23192
AIRCRAFT ACCIDENTS
Near midair collisions as an indicator of general aviation collision risk N91-23096
Individual differences underlying pilot cockpit error
[DOT/FAA/RD-91/13] N91-23710
AIRCRAFT CONFIGURATIONS
Integration of handling quality aspects into the aerodynamic design of modern unstable fighters N91-23125
A review of high angle of attack requirements for combat aircraft N91-23130
X-31A at first flight N91-23131
Navigation, guidance, and trajectory optimization for hypersonic vehicles N91-23150
AIRCRAFT CONSTRUCTION MATERIALS
Characterization of composite materials for aerospace materials
[DLR-MITT-90-15] N91-23246
Observatory of new materials. Evolution perspectives for the materials used in civil transportation aircraft
[REPT-911-111-107] N91-23248
AIRCRAFT CONTROL
Real time estimation of aircraft angular attitude
[IAITIC-87-1004] N91-23107
Flying Qualities
[AGARD-CP-508] N91-23108
MIL-STD-1797 is not a cookbook N91-23111
Handling qualities guidelines for the design of fly-by-wire flight control systems for transport aircraft N91-23119
Determination of decision-height windows for decelerating IMC approaches in helicopters N91-23124
The electrical flight control system of A320 Airbus: A fault tolerant system
[REPT-911-111-103] N91-23192
AIRCRAFT DESIGN
The art of flying qualities testing N91-23109
Integration of handling quality aspects into the aerodynamic design of modern unstable fighters N91-23125
Agility: A rational development of fundamental metrics and their relationship to flying qualities N91-23129
A review of high angle of attack requirements for combat aircraft N91-23130
X-31A at first flight N91-23131
A new architecture and expert system for aircraft design synthesis N91-23132
Application of multidisciplinary optimization methods to the design of a supersonic transport
[NASA-TM-104073] N91-23135
Design and construction of a composite airframe for UAV research
[AD-A232422] N91-23143
A computer aided multivariable control systems design technique with application to aircraft flying qualities
[AD-A232549] N91-23144
IAI hypersonic wind tunnel
[IAITIC-87-1006] N91-23194
AIRCRAFT DETECTION
Distributed radar sensors for aircraft detection
[DE91-009845] N91-23350
AIRCRAFT ENGINES
NASA aeropropulsion research in support of propulsion systems of the 21st century
[NASA-TM-104403] N91-23083
Engine technology challenges for a 21st century high speed civil transport
[NASA-TM-104363] N91-23098
AIRCRAFT GUIDANCE
Navigation, guidance, and trajectory optimization for hypersonic vehicles N91-23150
AIRCRAFT HAZARDS
Icing simulation: A survey of computer models and experimental facilities
[NASA-TM-104366] N91-23087
Near midair collisions as an indicator of general aviation collision risk N91-23096
AIRCRAFT INDUSTRY
Estimating fixed and variable costs of airframe manufacturers
[AD-A232661] N91-23077
Integration of propulsive systems: Selection and compromise
[REPT-911-111-101] N91-23187
AIRCRAFT INSTRUMENTS
Aircraft Command in Emergency Situations (ACES). Phase 1: Concept development
[DOT/FAA/CT-90/21] N91-23097
An engineering study of altitude determination deficiencies of the Service Aircraft Instrumentation Package (SAIP)
[AD-A232055] N91-23145
Tropospheric sampling with aircraft
[DE91-009472] N91-23626
Microwave temperature profiler for clear air turbulence prediction
[NASA-CASE-NPO-18115-1-CU] N91-23662
AIRCRAFT LANDING
The limits of the landing process of aircraft
[DLR-FB-90-49] N91-23137
AIRCRAFT MANEUVERS
Agility: A rational development of fundamental metrics and their relationship to flying qualities N91-23129
AIRCRAFT MODELS
The costs and benefits of aircraft availability
[AD-A232660] N91-23076
Navigation, guidance, and trajectory optimization for hypersonic vehicles N91-23150
Model rotor icing tests in the NASA Lewis icing research tunnel
[NASA-TM-104351] N91-23184
AIRCRAFT NOISE
A study of the noise mechanisms of transonic blade-vortex interactions
[NASA-CR-188199] N91-23084
Soviet atmospheric acoustics research N91-23848
Unified aeroacoustics analysis for high speed turboprop aerodynamics and noise. Volume 2: Development of theory for wing shielding
[NASA-CR-185192] N91-23849
Unified aeroacoustics analysis for high speed turboprop aerodynamics and noise. Volume 3: Application of theory for blade loading, wakes, noise, and wing shielding
[NASA-CR-185193] N91-23850
Unified aeroacoustics analysis for high speed turboprop aerodynamics and noise. Volume 4: Computer user's manual for UAAP turboprop aeroacoustic code
[NASA-CR-185194] N91-23851
Unified aeroacoustics analysis for high speed turboprop aerodynamics and noise. Volume 5: Propagation of propeller tone noise through a fuselage boundary layer
[NASA-CR-185195] N91-23852
Noise inside aircraft fuselages subjected to airborne excitations
[REPT-911-111-104] N91-23853
A field-deployable digital acoustic measurement system N91-24078
AIRCRAFT PERFORMANCE
Flying Qualities
[AGARD-CP-508] N91-23108
MIL-STD-1797 is not a cookbook N91-23111
Development of MIL-8785C into a handling qualities specification for a new European fighter aircraft N91-23114
Do civil flying qualities requirements address military missions for off-the-shelf procurement N91-23115
AIRCRAFT PILOTS
Estimation of pilot ratings via pilot modeling N91-23121
AIRCRAFT RELIABILITY
The certification of the aircraft integrated propulsive system
[REPT-911-111-102] N91-23188
AIRCRAFT SAFETY
Near midair collisions as an indicator of general aviation collision risk N91-23096
Aircraft Command in Emergency Situations (ACES). Phase 1: Concept development
[DOT/FAA/CT-90/21] N91-23097
The art of flying qualities testing N91-23109
AIRCRAFT SPECIFICATIONS
Flying Qualities
[AGARD-CP-508] N91-23108
MIL-STD-1797 is not a cookbook N91-23111
Flying qualities experience on the AMX aircraft N91-23112
The development of alternate criteria for FBW handling qualities N91-23113
Development of MIL-8785C into a handling qualities specification for a new European fighter aircraft N91-23114
Do civil flying qualities requirements address military missions for off-the-shelf procurement N91-23115
AIRCRAFT STABILITY
The art of flying qualities testing N91-23109
The development of alternate criteria for FBW handling qualities N91-23113
Integration of handling quality aspects into the aerodynamic design of modern unstable fighters N91-23125
B-1B high AOA testing in the evaluation of a stall inhibitor system N91-23126
Evaluation techniques for highly augmented aircraft
[DLR-FB-90-35] N91-23191
AIRCRAFT STRUCTURES
Computerized system for static and fatigue large scale structural tests: A case study
[IAITIC-87-1007] N91-23522
Quantitative nondestructive evaluation: Requirements for tomorrow's reliability N91-24074
AIRCRAFT WAKES
An experimental study of an axisymmetric turbulent boundary layer disturbed by a periodic freestream N91-23078
Aircraft wake vortices: An assessment of the current situation
[AD-A231658] N91-23079
A vortex panel method for calculating aircraft downwash on parachute trajectories
[DE91-009764] N91-23085
AIRFOILS
Icing simulation: A survey of computer models and experimental facilities
[NASA-TM-104366] N91-23087
Advanced ice protection systems test in the NASA Lewis icing research tunnel
[NASA-TM-103757] N91-23183
A computationally efficient modelling of laminar separation bubbles N91-23411
AIRFRAMES
Estimating fixed and variable costs of airframe manufacturers
[AD-A232661] N91-23077
Application of multidisciplinary optimization methods to the design of a supersonic transport
[NASA-TM-104073] N91-23135
Design and construction of a composite airframe for UAV research
[AD-A232422] N91-23143
AIRPORTS
Literature review on geotextiles to improve pavements for general aviation airports
[AD-A232871] N91-23199
ALABAMA
Analysis and modeling of summertime convective cloud and precipitation structure over the Southeastern United States
[NASA-CR-188119] N91-23670
ALASKA
Proceedings of the Second Glacier Bay Science Symposium
[PB91-110163] N91-23634
ALBEDO
Infrared and visible studies of Pakistan portion of Arabian Sea using INSAT geostationary satellite N91-23611

ALBUMINS
Three-dimensional structure of human serum albumin N91-24057

ALGORITHMS
Computation of viscous shock/shock hypersonic interactions with an implicit flux split scheme [AD-A232405] N91-23093
The application of neural networks to the SSME startup transient [NASA-CR-187138] N91-23205
High-quality 800-b/s voice processing algorithm [AD-A232352] N91-23372
An investigation of CFAR techniques for airborne radars [AD-A232724] N91-23378
An analysis of MLAYER: A multilayer tropospheric propagation program [AD-A232733] N91-23379
Design and implementation of a packet switched routing chip [AD-A232286] N91-23401
Turbulent mixing in nonreacting and reacting flows: A PDF approach at the two-point level N91-23422
Formulation of boundary conditions for the multigrid acceleration of the Euler and Navier Stokes equations [NASA-CR-188234] N91-23440
Riemann problems and the WAF method for the two-dimensional shallow water equations [CRANFIELD-AERO-9005] N91-23443
Strategy Combining Regionally Adapted Processes (SCRAP) [AD-A232158] N91-23448
Nonlinear waves in real materials [AD-A232654] N91-23452
Adaptive methods for compressible fluid dynamics [AD-A232786] N91-23455
Articulation of spatial robots N91-23504
Robot self-location in unknown environments [DE91-010450] N91-23505
Study of static and dynamic fracture using strain measurements [PB91-132217] N91-23524
Auroral boundary index from 1983 to 1990 [AD-A232845] N91-23660
A smoothing algorithm for upper-air soundings [AD-A232853] N91-23661
Surface cloud observations for radiation, climatology and incorporation into satellite-based nephanalyses N91-23671
The terminal Doppler weather radar tornadic vortex signature detection algorithm [DOT-FAA-NR-91-5] N91-23675
Evaluation of generalized thresholds in an objective multispectral satellite cloud analysis [AD-A232716] N91-23683
Parallel-processor-based Gaussian beam tracer for use in ocean acoustic tomography [AD-A232420] N91-23690
Mechanisms of higher brain functions: A study of models of perception [AD-A232389] N91-23712
Saturation and vote for the fault tolerance in distributed systems [LAAS-90390] N91-23727
Modeling speedup in parallel sparse matrix factorization [DE91-010215] N91-23735
Canonical vs. micro-canonical sampling methods in a 2D Ising model [DE91-010204] N91-23737
Use of a genetic algorithm to analyze robust stability problems [DE91-005895] N91-23742
Table-lookup algorithms for elementary functions and their error analysis [DE91-006047] N91-23743
Image data compression in JPEG standard [DLR-FB-90-59] N91-23746
Realization of a randomized algorithm for the exact perfect matching problem, with a new constructive procedure [REPT-90-056] N91-23751
On the use of genetic algorithms to solve the time-table problem [REPT-90-060] N91-23752
Searching algorithms for the real roots of a Bezier function [RR-834-I-AND-M] N91-23755
Mapping an adaptable Eigenstructure technique onto the topologix hypercube [AD-A232032] N91-23764
Synergetic multisensor fusion [AD-A232089] N91-23766
An in-depth analysis of concurrent B-tree algorithms [AD-A232287] N91-23770
Software reverse engineering [AD-A232644] N91-23773
Are wait-free algorithms fast [AD-A232829] N91-23774
A fast algorithm for the evaluation of trigonometric series [AD-A232848] N91-23775
A method for handling complex Markov models of parallel systems [RR-826-I] N91-23778
Obstacle avoidance for redundant robots using configuration control [NASA-CASE-NPO-17852-1-CU] N91-23783
Classification using multi-layered perceptrons [AD-A232810] N91-23802
Computations, properties, and applications of matrix-valued functions to mathematical science and control systems [AD-A232448] N91-23819
Optimal systolic network for Gaussian elimination [RR-837-I] N91-23822
Query processing for deductive databases with null values N91-23979
Applications of fuzzy logic to control and decision making N91-24049
Genetic algorithms N91-24050
Recent advances in coding theory for near error-free communications N91-24068

ALLOTROPY
X ray diffraction and electron spectroscopy of epitaxial molecular C60 films [AD-A232152] N91-23954

ALLOYS
Localized corrosion of high performance metal alloys in an acid/salt environment N91-24066

ALPHA PARTICLES
Applied plasma physics [DE91-010696] N91-23922

ALPINE METEOROLOGY
On the airflow over the Alps during south Foehn [DLR-FB-90-30] N91-23676

ALPS MOUNTAINS (EUROPE)
On the airflow over the Alps during south Foehn [DLR-FB-90-30] N91-23676

ALTITUDE
An engineering study of altitude determination deficiencies of the Service Aircraft Instrumentation Package (SAIP) [AD-A232055] N91-23145

ALTITUDE CONTROL
Real time estimation of aircraft angular attitude [IAITIC-87-1004] N91-23107

ALTITUDE SIMULATION
Diagnostic measurements on an aluminized propellant plume during spin and nonspin testing [AD-A232031] N91-23235

ALUMINUM
Galvanic corrosion of aluminum-matrix composites [AD-A232138] N91-23264
Gas contents and weldability of aluminum die castings [ETN-91-99188] N91-23302
Application of elastic and elastic-plastic fracture mechanics methods to surface flaws [NASA-TM-104964] N91-23539

ALUMINUM ALLOYS
Galvanic corrosion of aluminum-matrix composites [AD-A232138] N91-23264
Phase equilibria and solidification of Al-Li and Al-Li-Cu alloys N91-23290
Examination of the microstructure of 7050 aluminum alloy samples [AD-A232544] N91-23306
Post-overload fatigue crack recovery in powder metal aluminum-lithium AL-905XL forging [AD-A232550] N91-23307
High temperature ordered intermetallic alloys [AD-A232769] N91-23308
Superplastic forming of Al-Li alloys for lightweight, low-cost structures N91-24065

ALUMINUM CHLORIDES
Diagnostic measurements on an aluminized propellant plume during spin and nonspin testing [AD-A232031] N91-23235

ALUMINUM GALLIUM ARSENIDES
Electronic GaAs-on-silicon material for advanced high-speed optoelectronic devices [AD-A232088] N91-23399
Vertical emitting, ring geometry, ultra-low threshold and ultra-high speed quantum well lasers for optical interconnect [AD-A232122] N91-23481

ALUMINUM NITRIDES
Laser assisted CVD growth of AlN and GaN [AD-A232379] N91-23957

ALUMINUM OXIDES
Stress-density variations in alumina sediments: Effects of polymer chemistry [DE91-009055] N91-23313

AMBULANCES
Air ambulance helicopter operational analysis [DOT/FAA/RD-91/7] N91-23134

AMINES
Theoretical prediction of vibrational infrared frequencies of tertiary amines [AD-A232880] N91-23288

AMINO ACIDS
Structural studies of manganese and halide in the photosynthetic oxygen evolving complex [DE91-009071] N91-23698

AMORPHOUS SILICON
Optimization of transparent and reflecting electrodes for amorphous silicon solar cells [DE91-002132] N91-23618

AMPLIFICATION
Research and development on advanced silicon carbide thin film growth techniques and fabrication of high power and microwave frequency silicon carbide-based device structures [AD-A232160] N91-23955

AMPLIFIERS
A 30 GHz monolithic receive module [NASA-CR-187085] N91-23346

AMPLITUDE DISTRIBUTION ANALYSIS
Infrared focal plane performance in the South Atlantic anomaly [NASA-CR-186197] N91-23458

AMPLITUDE MODULATION
Error control coding for multi-frequency modulation [AD-A232421] N91-23374

ANALOG CIRCUITS
Analog processing of optical wavefronts using integrated guided-wave optics [AD-A232703] N91-23904

ANGLE OF ATTACK
B-1B high AOA testing in the evaluation of a stall inhibitor system N91-23126
A review of high angle of attack requirements for combat aircraft N91-23130
Buffet inc[illegible]:ced structural/flight-control system interaction of the X-29A aircraft [NASA-TM-101735] N91-23133

ANGULAR DISTRIBUTION
Magnetic substates populated by double electron capture in slow ion atom collisions [DE91-010122] N91-23858

ANGULAR MOMENTUM
The coordinate-free representation of rotational motions [RSRE-MEMO-4445] N91-23846
Study of the response of a crystal ball made of NaI(Tl) for heavy ions experiments [NOTA-INTERNA-957] N91-23874

ANGULAR VELOCITY
The coordinate-free representation of rotational motions [RSRE-MEMO-4445] N91-23846

ANISOTROPIC FLUIDS
Flows with strongly anisotropic turbulence-dynamic and heat transfer aspects [SER-20/P] N91-23407
Turbulence and the feasibility of self-cooled liquid-metal blankets for fusion reactors [SER-10/P-REV] N91-23910

ANISOTROPY
Thermo-viscoelastic behavior of composite materials N91-23243
Theory of the new high-temperature superconductors N91-23842

ANTARCTIC REGIONS
Remote sensing of atmospheric temperature fields and the long wave radiation budget in the Antarctic [ISSN-0069-5882] N91-23652
The application of equilibrium climate models to questions of glaciation at high latitudes N91-23669

ANTENNA ARRAYS
System-Level Integrated Circuit (SLIC) development for phased array antenna applications [NASA-TM-104392] N91-23354
Implications of adaptive cancellation array processing for design of a space-based surveillance radar [RSRE-MEMO-4410] N91-23364
Digital beamforming and pulse compression in an adaptive array radar system [AD-A232713] N91-23377
Joint services electronics program [AD-A232331] N91-23402

ANTENNA COMPONENTS
Antenna performance influenced by the finite extent and conductivity of ground planes: A collection of reprints [AD-A232132] N91-23366

ANTENNA DESIGN
Characteristics of a future aeronautical satellite communications system
[NASA-TM-104389] N91-23102
Implications of adaptive cancellation array processing for design of a space-based surveillance radar
[RSRE-MEMO-4410] N91-23364
Antenna performance influenced by the finite extent and conductivity of ground planes: A collection of reprints
[AD-A232132] N91-23366
ANTENNA FEEDS
A 30 GHz monolithic receive module
[NASA-CR-187085] N91-23346
ANTENNA RADIATION PATTERNS
Antenna performance influenced by the finite extent and conductivity of ground planes: A collection of reprints
[AD-A232132] N91-23366
Digital beamforming and pulse compression in an adaptive array radar system
[AD-A232713] N91-23377
ANTENNAS
The effect of realistic antenna geometries on plasma loading predictions
[DE91-010782] N91-23353
ANTIBIOTICS
AFRRI reports, October - December 1990
[AD-A232236] N91-23283
ANTIMATTER
Ionic solid hydrogen fuel: Experimental investigation of cluster-impact fusion
[AD-A232642] N91-23336
ANTIMISSILE DEFENSE
Distributed radar sensors for aircraft detection
[DE91-009845] N91-23350
ANTIMONY COMPOUNDS
The effect of post-cure and antimony trioxide addition on the glass transition of polyester and vinyl ester resin systems
[AD-A232523] N91-23325
ANTIOXIDANTS
Carbon/carbon inox thermostructural composites: Mechanical and tectonic behavior of anti-oxidation protection
[REPT-911-430-115] N91-23257
APERTURES
Experimental study of narrow slot, cavity-backed apertures with finite wall conductivity
[DE91-009039] N91-23352
Scattering from thin apertures in coated conductors using FDTD
[AD-A232125] N91-23365
APPLICATIONS PROGRAMS (COMPUTERS)
Simulation of a backscatter lidar system
[DLR-FB-90-50] N91-23355
Water-cooling technique of high temperature gas turbine blade
[DE91-764238] N91-23506
Bobbin stresses generated by wire winding
[DE91-009545] N91-23526
Use of personal computers in performing a linear modal analysis of a large finite-element model
[DE91-010112] N91-23541
Computer programs for simulation of electrodeposition
[DE91-010203] N91-23741
Presentation of a computer program for analysing results of one shot device sensitivity tests: Application to the case of a one shot degenerated sequence
[REPT-911-430-126] N91-23758
Software reverse engineering
[AD-A232644] N91-23773
Calculation of cross sections for binary reactions between heavy ion projectiles and heavy actinide targets
[DE91-010222] N91-23882
Transportable Applications Environment (TAE) Plus: A NASA user interface development and management system N91-24048
APPROACH
Microwave landing system modeling with application to air traffic control
[NASA-TM-102832] N91-23099
Determination of decision-height windows for decelerating IMC approaches in helicopters N91-23124
APPROACH CONTROL
Differential GPS terminal area test results
[AD-A232668] N91-23106
APPROXIMATION
Approximation methods for the identification and control of distributed parameter systems with applications to flexible structures
[AD-A232805] N91-23801
Functional approximation by feed-forward networks: A least squares approach to generalisation
[RSRE-MEMO-4453] N91-23811
On locking and robustness in the finite element method
[AD-A232245] N91-23815
ARABIAN SEA
Infrared and visible studies of Pakistan portion of Arabian Sea using INSAT geostationary satellite N91-23611
ARABSAT
Predictions and verification of ESD tests made with sphere injections on a flight representative telecommunication satellite: ARABSAT STM
[REPT-911-440-109] N91-23224
ARC SPRAYING
Measurement of particle size, velocity and temperature in the plasma spray coating process
[DE91-006208] N91-23317
ARCHAEOLOGY
The Berlenga underwater survey project N91-23577
ARCHITECTURE (COMPUTERS)
A new architecture and expert system for aircraft design synthesis N91-23132
Raybot: A practical implementation of a hierarchical control system for telerobotic land vehicles
[DE90-017029] N91-23507
Implementation of the FAA research and development electromagnetic database
[DE91-010063] N91-23674
Modeling speedup in parallel sparse matrix factorization
[DE91-010215] N91-23735
Canonical vs. micro-canonical sampling methods in a 2D Ising model
[DE91-010204] N91-23737
Scientific visualization software for your PC: Free and available now
[DE91-010156] N91-23744
Mapping an adaptable Eigenstructure technique onto the topologix hypercube
[AD-A232032] N91-23764
The TurboLAN project. Phase 1: Protocol choices for high speed local area networks. Phase 2: TurboLAN Intelligent Network Adapter Card, (TINAC) architecture
[NASA-CR-188175] N91-23776
Dynamic load balancing on highly parallel multicomputer systems N91-23777
Statistical process allocation in a parallel processing architecture
[RR-833-I] N91-23779
Applications of neural networks to process control and modeling
[DE91-007389] N91-23784
Analysis of polarizing optical systems for digital optical computing with symmetric self electrooptic devices
[AD-A232768] N91-23906
Building a generalized distributed system model N91-23971
The intelligent database: Using INGRES to manage the external analysis of your data
[DE91-010465] N91-23986
Security aspects of database management systems
[DE91-010677] N91-23987
Distributed, cooperating knowledge-based systems N91-24044
Electronic neuroprocessors N91-24045
Integrated Vertical Bloch Line (VBL) memory N91-24051
Fiber Optic Tactical Local Network (FOTLAN) N91-24072
ARCTIC REGIONS
Arctic remote autonomous measurement platform post CEAREX engineering report
[AD-A232843] N91-23471
ARGON LASERS
A Raman spectroscopic and electrochemical study of the photoinduced crystallization of triethylenediamine triiodide upon a silver electrode
[AD-A232828] N91-23963
ARMED FORCES (FOREIGN)
Heat strain and work tolerance times with varying levels of Canadian Forces NBC protective clothing, ambient temperature, physical work intensity, and work/rest schedules
[AD-A232653] N91-23720
ARMED FORCES (UNITED STATES)
A test of the American Safety Flight Systems, Inc. prebreather/portable oxygen system
[AD-A232723] N91-23100
Life cycle management automation programmer's manual
[AD-A232247] N91-23769
Interacting with DTIC
[AD-A232485] N91-23997
ARRAYS
Efficient numerical techniques for the analysis of complex microstrip-antennas and microstrip arrays
[DLR-FB-90-53] N91-23357
ARTIFICIAL INTELLIGENCE
The development of highly practiced skills: A starting point for driver modelling
[IZF-1990-B-16] N91-23719
Transition space
[AD-A231404] N91-23732
A Model-Based Approach to High-Level Robot Control with Visual Guidance
[VTT-PUBL-71] N91-23788
Conference on Theoretical Aspects of Reasoning About Knowledge
[AD-A232657] N91-23798
Processing problems in the IRUS queries: An empirical verification of problem coverage in the natural language sourcebook
[AD-A232780] N91-23800
A distributed problem-solving approach to rule induction: Learning in distributed artificial intelligence systems
[AD-A232822] N91-23803
Advanced methods of approximate reasoning
[AD-A232140] N91-23814
Knowledge-based retrieval of information as a process of evidential reasoning N91-23978
Intelligent computer-aided training and tutoring N91-24042
CLIPS: A tool for the development and delivery of expert systems N91-24043
Distributed, cooperating knowledge-based systems N91-24044
Intelligent vision system for autonomous vehicle operations N91-24046
Genetic algorithms N91-24050
Robotic control and inspection verification N91-24075
ARTIFICIAL SATELLITES
Higher accuracy requirements for the satisfactory position calculation of an artificial satellite
[GKSS-90/E/25] N91-23203
The Combined Release and Radiation Effects Satellite program (CRRES): A unique series of scientific experiments
[NASA-TM-104957] N91-23213
Satellite utilization by civil aviation
[REPT-911-111-105] N91-23216
Conference on Space Technology: Satellite Application Development
[REPT-911-440-103] N91-23219
Satellite maneuver evaluation tool
[AD-A232016] N91-23226
ASIA
Atmospheric teleconnections: Emphasis on the El Nino/Southern Oscillation and monsoons N91-23636
ASSEMBLING
Monitoring an assembly task by perception requests N91-23791
Intelligent planning in controlling electronics assembly N91-23792
ASSIMILATION
Assimilation of ERBE data with nonlinear programming technique to improve cloud cover diagnosis N91-23663
ASTRONAUT PERFORMANCE
Payload related crew operations: From past missions to Columbus N91-23569
ASTRONAUT TRAINING
Space and Sea
[ESA-SP-312] N91-23563
The diving laboratory as a simulation environment for manned spaceflight N91-23564
Subsea habitats and space simulation N91-23567
ASTRONAUTS
Psychological selection of astronauts: Recent developments at the DLR testing centre in Hamburg (Fed. Republic of Germany) N91-23565
ASTRONOMICAL MODELS
Biased galaxy formation in the neutrino scenario N91-23839
The spectrum of massive accretion disks N91-23840
Boundary conditions in quantum cosmology N91-24020
Saturn's F ring: Imaging and simulation N91-24032
ASTRONOMICAL OBSERVATORIES
ROSAT: An international mission exploring the high energy universe
[NASA-TM-104958] N91-23214
ASTROPHYSICS
Initial data for the two-body problem of general relativity N91-23965
Studies of the diffuse background and interstellar dust at far ultraviolet wavelengths N91-24003
Phenomenological aspects of scalar fields in astrophysics, cosmology and particle physics N91-24014
ASYMPTOTIC SERIES
A new asymptotic theory for the periodically forced laser
[AD-A232633] N91-23486
Large and moderate deviation limit theorems for arbitrary sequences of random variables with applications
[AD-A232334] N91-23817

ATLANTIC OCEAN
Infrared focal plane performance in the South Atlantic anomaly
[NASA-CR-186197] N91-23458
Near-equatorial deep circulation in the Indian and Pacific oceans
[AD-A232635] N91-23691
ATMOSPHERIC ATTENUATION
A search for strange attractors in the saturation of middle atmosphere gravity waves
[AD-A232468] N91-23658
ATMOSPHERIC BOUNDARY LAYER
Numerical modeling of turbulent dispersion around structures using a particle-in-cell method
[DE91-009757] N91-23426
Technical description of the high-resolution air mass transformation model at KNMI
[KNMI-TR-125] N91-23646
Observational study of the above-inversion structure and marine stratocumulus cloud clearing episodes during FIRE N91-23666
ATMOSPHERIC CHEMISTRY
Tropospheric sampling with aircraft
[DE91-009472] N91-23626
An expanding grid photochemical model for visibility applications
[DE91-009947] N91-23630
High-precision Fourier transform spectroscopy of atmospheric molecules N91-23637
Studies of molecular excitation in star formation regions N91-24023
ATMOSPHERIC CIRCULATION
Atmospheric circulation and poleward sensible heat flux variations associated with the recent Northern Hemisphere warming N91-23629
Atmospheric teleconnections: Emphasis on the El Nino/Southern Oscillation and monsoons N91-23636
Energy partition of free Rossby waves in global atmospheric oscillations
[MITT-74] N91-23648
Atmospheric optical turbulence measurements taken at Anderson Mesa, Flagstaff, Arizona between 13-19 November 1989
[AD-A232222] N91-23656
Observed changes in the activity of baroclinic waves and their feedbacks during the life cycles of low-frequency circulation anomalies in the Northern Hemisphere winter N91-23668
Localised symmetric instability: An initial value problem N91-23672
Neutral wind vortices in the high-latitude thermosphere N91-23673
ATMOSPHERIC COMPOSITION
Tropospheric sampling with aircraft
[DE91-009472] N91-23626
Iron density measurements in polar atmosphere
[BONN-IR-90-53] N91-23654
ATMOSPHERIC EFFECTS
The polar wind and ionospheric outflow N91-23645
ATMOSPHERIC GENERAL CIRCULATION MODELS
Models of planetary wave propagation in the middle atmosphere N91-23639
ATMOSPHERIC HEATING
The polar wind and ionospheric outflow N91-23645
ATMOSPHERIC MODELS
Atmospheric circulation and poleward sensible heat flux variations associated with the recent Northern Hemisphere warming N91-23629
Echo 7: Magnetospheric properties determined by artificial electron beams N91-23644
Technical description of the high-resolution air mass transformation model at KNMI
[KNMI-TR-125] N91-23646
Design of an enhanced global spectral model
[AD-A232123] N91-23655
High-altitude non-equilibrium infrared emission models
[AD-A232503] N91-23659
The application of equilibrium climate models to questions of glaciation at high latitudes N91-23669
Localised symmetric instability: An initial value problem N91-23672
Initialization of cloud and radiation in the Florida State University global spectral model
[AD-A232425] N91-23682
Range reference atmosphere, Shemya
[AD-A232813] N91-23685
Range reference atmosphere, Thule
[AD-A232831] N91-23686
Parallelizing the spectral transform method, part 1
[DE91-010453] N91-23805
Microwave imaging of Saturn's deep atmosphere and rings N91-24035
ATMOSPHERIC MOISTURE
Grouping of clouds and internal gravity waves in a non-hydrostatic model of moist convection
[DM-55] N91-23679
ATMOSPHERIC OPTICS
Atmospheric optical turbulence measurements taken at Anderson Mesa, Flagstaff, Arizona between 13-19 November 1989
[AD-A232222] N91-23656
ATMOSPHERIC PHYSICS
Hydromagnetic wave coupling in the magnetosphere N91-23638
ATMOSPHERIC RADIATION
High-altitude non-equilibrium infrared emission models
[AD-A232503] N91-23659
Imaging and background in low-energy gamma ray astronomy N91-24005
ATMOSPHERIC REFRACTION
Effect of atmospheric variations on electromagnetic distance measurements
[DE91-009726] N91-23349
ATMOSPHERIC SCATTERING
Simulation of a backscatter lidar system
[DLR-FB-90-50] N91-23355
ATMOSPHERIC SOUNDING
A smoothing algorithm for upper-air soundings
[AD-A232853] N91-23661
Evaluation of generalized thresholds in an objective multispectral satellite cloud analysis
[AD-A232716] N91-23683
ATMOSPHERIC TEMPERATURE
Atmospheric circulation and poleward sensible heat flux variations associated with the recent Northern Hemisphere warming N91-23629
Remote sensing of atmospheric temperature fields and the long wave radiation budget in the Antarctic
[ISSN-0069-5882] N91-23652
Evaluation of generalized thresholds in an objective multispectral satellite cloud analysis
[AD-A232716] N91-23683
ATMOSPHERIC TURBULENCE
Atmospheric turbulence review of space shuttle launches
[NASA-TM-4289] N91-23215
A numerical study of the stratified turbulent Ekman layer N91-23421
Atmospheric optical turbulence measurements taken at Anderson Mesa, Flagstaff, Arizona between 13-19 November 1989
[AD-A232222] N91-23656
ATOMIC COLLISIONS
Theoretical studies relating to the interaction of radiation with matter
[AD-A232107] N91-23480
Few-body problems, electron-correlation effects, and beyond
[DE91-010030] N91-23857
ATOMIC INTERACTIONS
Signals and noise in lasers and atom-field interactions N91-23475
ATOMIC PHYSICS
Few-body problems, electron-correlation effects, and beyond
[DE91-010030] N91-23957
Experiments on Frank-Hertz setup
[NOTA-INTERNA-961] N91-23876
ATOMIC SPECTRA
Temperature measurements of ET plasmas using atomic emission spectroscopy
[AD-A232498] N91-23930
ATOMIC STRUCTURE
Order and disorder in metallic alloys
[DE91-009120] N91-23292
Re-analysis of photoemission data for CuO: Revision of the configuration-energy scheme for cuprate materials
[DE91-009952] N91-23296
Theoretical studies relating to the interaction of radiation with matter
[AD-A232107] N91-23480
Theory of the new high-temperature superconductors N91-23842
Mean-field theories of the Hubbard model and periodic orbits in chaotic maps N91-23938
Electronic properties of Si-doped n-doping-intrinsic-p-doping-intrinsic (nipi) structures in GaAs
[DE91-009474] N91-23941
ATOMIC THEORY
Electronic properties of Si-doped n-doping-intrinsic-p-doping-intrinsic (nipi) structures in GaAs
[DE91-009474] N91-23941
ATOMS
Signals and noise in lasers and atom-field interactions N91-23475
ATTACK AIRCRAFT
Flying qualities experience on the AMX aircraft N91-23112
ATTITUDE CONTROL
An artificial neural network control system for spacecraft attitude stabilization
[AD-A232013] N91-23225
ATTITUDE STABILITY
An artificial neural network control system for spacecraft attitude stabilization
[AD-A232013] N91-23225
AUGER EFFECT
Magnetic substates populated by double electron capture in slow ion atom collisions
[DE91-010122] N91-23858
AURORAL ELECTROJETS
Observation and theory of the radar aurora N91-24017
AURORAS
Echo 7: Magnetospheric properties determined by artificial electron beams N91-23644
High-altitude non-equilibrium infrared emission models
[AD-A232503] N91-23659
Auroral boundary index from 1983 to 1990
[AD-A232845] N91-23660
AUSTENITE
Modeling second-phase formation during rapid resolidification of stainless steel alloys
[DE91-008567] N91-23291
AUTOCORRELATION
Development of a digital correlator to measure the semi-elastic scattering of light
[NOTA-INTERNA-955] N91-23895
AUTOMATIC CONTROL
Reactive procedure based decision making for satellite control
[REPT-911-440-106] N91-23221
Computational needs survey of NASA automation and robotics missions. Volume 1: Survey and results
[NASA-TM-103860] N91-23341
Thermal control system for the investigation of specific absorption rates for specimens exposed to electromagnetic radiation
[AD-A231329] N91-23459
Raybot: A practical implementation of a hierarchical control system for telerobotic land vehicles
[DE90-017029] N91-23507
Performance of visual and ultrasound sensing by an autonomous robot
[DE91-010452] N91-23511
Research and development of future space robotics in NASDA N91-23582
Telemanipulation system assisted by computer for under water applications N91-23585
Life cycle management automation programmer's manual
[AD-A232247] N91-23769
A Model-Based Approach to High-Level Robot Control with Visual Guidance
[VTT-PUBL-71] N91-23788
A solution for the man/machine-interface in robotics: A high level control language with enhanced interaction equipment N91-23789
Intelligent planning in controlling electronics assembly N91-23792
AUTONOMOUS NAVIGATION
Performance of visual and ultrasound sensing by an autonomous robot
[DE91-010452] N91-23511
AUTONOMY
Arctic remote autonomous measurement platform post CEAREX engineering report
[AD-A232843] N91-23471
Intelligent vision system for autonomous vehicle operations N91-24046
AUTOREGRESSIVE PROCESSES
Parametric modeling and estimation of pulse propagation on microwave integrated circuit interconnections
[AD-A232465] N91-23404
System modeling and identification of flexible structures N91-23531
AVAILABILITY
The costs and benefits of aircraft availability
[AD-A232660] N91-23076
AVALANCHE DIODES
Silicon avalanche photodiode active-quenching circuit
[AD-A233633] N91-23395
AXIAL LOADS
Metallic threaded composite fastener
[NASA-CASE-MSC-21580-1] N91-23491
AXISYMMETRIC BODIES
Benchmarking numerical predictions with force and moment measurements on slender, supercavitating bodies
[DE91-007066] N91-23432

AZOLES
Poly(1,3,4-oxadiazoles) via aromatic nucleophilic displacement
[NASA-CASE-LAR-14427-1] N91-23237

B

B STARS
Ultraviolet gas absorption and dust extinction toward M8 and the outer galactic disk N91-24018
B-1 AIRCRAFT
B-1B high AOA testing in the evaluation of a stall inhibitor system N91-23126
BACKGROUND NOISE
Imaging and background in low-energy gamma ray astronomy N91-24005
BACKSCATTERING
Nondestructive measurement of thickness and density of composite materials by Compton backscattering
[REPT-911-430-112] N91-23255
Simulation of a backscatter lidar system
[DLR-FB-90-50] N91-23355
Backscattering by nonspherical particles, using the coupled-dipole method: An application in radar meteorology
[AD-A232371] N91-23373
Incoherent scatter measurements and inferred energy fluxes in the equatorial F-region ionosphere N91-23640
BACKUPS
Electromagnetic attachment mechanism
[NASA-CASE-MSC-21463-1] N91-23490
BACKWARD FACING STEPS
Analysis of the multigrid method N91-23418
BACKWARD WAVES
Observation of harmonic gyro-backward-wave oscillation in a 100 GHz CARM oscillator experiment
[AD-A232063] N91-23398
BACTERIA
Excited state structure, energy and electron transfer dynamics of photosynthetic reaction centers: A hole burning study
[DE91-010181] N91-23693
New hosts and vectors for genome cloning
[DE91-009996] N91-23696
BALANCING
Dynamic load balancing on highly parallel multicomputer systems N91-23777
BALL BEARINGS
Quantifying oil filtration effects on bearing life
[NASA-TM-104350] N91-23512
BALLISTIC TRAJECTORIES
Aero-optics measurement system for the AEDC aero-optics test facility
[AD-A232852] N91-23908
BAND STRUCTURE OF SOLIDS
Theory of the new high-temperature superconductors N91-23842
Structural and electronic properties of the ordered ternary 3-5 semiconductors N91-23936
Fermi surface of YBCO by DHVA
[DE91-009963] N91-23943
BANDWIDTH
Efficient numerical techniques for the analysis of complex microstrip-antennas and microstrip arrays
[DLR-FB-90-53] N91-23357
Digital CODEC for real-time processing of broadcast quality video signals at 1.8 bits/pixel N91-24067
BARIUM COMPOUNDS
Measurements of passive-scalar spectra for grid turbulence using a nonlinear optical technique
[DE91-005310] N91-23892
BARIUM OXIDES
S-parameter measurements and applications of superconducting flux flow transistors
[DE91-009763] N91-23388
Microstructure of epitaxial YBa2Cu3O7 thin films
[DE91-009951] N91-23942
Fermi surface of YBCO by DHVA
[DE91-009963] N91-23943
BAROCLINIC INSTABILITY
Localised symmetric instability: An initial value problem N91-23672
BAROCLINIC WAVES
Observed changes in the activity of baroclinic waves and their feedbacks during the life cycles of low-frequency circulation anomalies in the Northern Hemisphere winter N91-23668
BAROCLINITY
Effects of the northeast monsoon on the equatorial westerlies over Indonesia
[AD-A232106] N91-23681
BARRED GALAXIES
The molecular interstellar medium and the near-infrared continuum of the barred liner NGC 6764
[MPE-PREPRINT-193] N91-24029
BARYONS
Matter in cosmic voids N91-23838
BASALT
Lunar volcanism and the thermal evolution of the moon N91-24031
BATS
Control of biosonar behavior by the auditory cortex
[AD-A232699] N91-23708
BAYES THEOREM
Topics in inference and decision-making with partial knowledge
[NASA-CR-188209] N91-23821
Sufficient comparison and modeling of forecasts N91-23829
BEAM CURRENTS
Channel diagnostics for the multi-pulse-propagation experiments at ATA
[DE91-009772] N91-23466
BEAM INJECTION
Pulsed power performance of the new RLA (Recirculating Linear Accelerator)
[DE91-004723] N91-23885
Ion confinement and radiation losses in the advanced toroidal facility
[DE91-010382] N91-23916
BEAMS (RADIATION)
High energy dense ribbon beams and high harmonic gyrotron at millimeter wavelengths
[AD-A232839] N91-23470
Parallel-processor-based Gaussian beam tracer for use in ocean acoustic tomography
[AD-A232420] N91-23690
Laser optical disk position encoder with active heads N91-24079
BEAMS (SUPPORTS)
Computerized symbolic closed-form dynamics and control analysis of hybrid rigid and elastic multibody systems N91-23532
BEDS
The drag of spheres at porosites ranging from an isolated sphere to a packed bed
[CRANFIELD-AERO-9012] N91-23444
BEND TESTS
Chevron-notched, flexure tests for measuring the elevated temperature fracture resistance of structural ceramics
[DE91-009117] N91-23310
BENDING FATIGUE
Combined thermal and bending fatigue of high-temperature metal-matrix composites: Computational simulation
[NASA-TM-104354] N91-23247
Effects of rim thickness on spur gear bending stress
[NASA-TM-104388] N91-23500
BENDING MOMENTS
Accuracy of the Reissner-Mindlin and the (1,1,2) model for the clamped-in plate problem
[AD-A232755] N91-23561
BENDING THEORY
Finite element analysis of the lateral buckling of a cantilevered I Beam
[DE91-010123] N91-23527
Linear bending of curved tubes without boundary influence
[ETN-91-99255] N91-23552
BIAS
Biased galaxy formation in the neutrino scenario N91-23839
BIBLIOGRAPHIES
Aeronautical engineering: A cumulative index to a continuing bibliography (supplement 261)
[NASA-SP-7037(261)] N91-23073
Aeronautical engineering: A continuing bibliography with indexes (supplement 262)
[NASA-SP-7037(262)] N91-23074
Laser hazards bibliography, January 1991
[AD-A232690] N91-23487
Aerospace medicine and biology: A continuing bibliography with indexes (supplement 346)
[NASA-SP-7011(346)] N91-23700
Aerospace medicine and biology: A continuing bibliography with indexes (supplement 347)
[NASA-SP-7011(347)] N91-23701
Aerospace medicine and biology: A continuing bibliography with indexes (supplement 348)
[NASA-SP-7011(348)] N91-23702
BINARY ALLOYS
Order and disorder in metallic alloys
[DE91-009120] N91-23292
BINARY DATA
Phenomenological aspects of scalar fields in astrophysics, cosmology and particle physics N91-24014
BINARY STARS
The supernova remnant G109.1-1.0 and the x-ray pulsar 1E2259+586 N91-24002
Investigation of the muon component of EAS initiated by primary radiation from Hercules X-1 N91-24037
BINDERS (MATERIALS)
High temperature membranes for H2S and SO2 separations
[DE91-008534] N91-23275
BIOASTRONAUTICS
A KO2 rebreather for EVA denitrogenation procedure N91-23588
Aerospace medicine and biology: A continuing bibliography with indexes (supplement 346)
[NASA-SP-7011(346)] N91-23700
Aerospace medicine and biology: A continuing bibliography with indexes (supplement 347)
[NASA-SP-7011(347)] N91-23701
Aerospace medicine and biology: A continuing bibliography with indexes (supplement 348)
[NASA-SP-7011(348)] N91-23702
BIODEGRADATION
Isolation, cloning and expression of the genes for microbial polyurethane degradation
[AD-A232108] N91-23699
BIODYNAMICS
Human short-latency somatosensory evoked potentials in impact acceleration research: Equipment, procedures, and techniques
[AD-A232732] N91-23709
BIOELECTRIC POTENTIAL
Human short-latency somatosensory evoked potentials in impact acceleration research: Equipment, procedures, and techniques
[AD-A232732] N91-23709
BIOGRAPHY
AGARD highlights 91/1, March 1991
[AGARD-HIGHLIGHTS-91/1] N91-24084
BIOLOGICAL EFFECTS
Laser hazards bibliography, January 1991
[AD-A232690] N91-23487
Space life sciences: A status report
[NASA-NP-120] N91-23694
Aerospace medicine and biology: A continuing bibliography with indexes (supplement 346)
[NASA-SP-7011(346)] N91-23700
Aerospace medicine and biology: A continuing bibliography with indexes (supplement 347)
[NASA-SP-7011(347)] N91-23701
Aerospace medicine and biology: A continuing bibliography with indexes (supplement 348)
[NASA-SP-7011(348)] N91-23702
Effects of bright illumination on oral temperature and cognitive performance in humans during nighttime hours
[AD-A232787] N91-23722
BIOLOGICAL MODELS (MATHEMATICS)
Convergence of one-dimensional diffusion processes to a jump process related to population genetics
[AD-A232121] N91-23826
BIOMASS
Monitoring and control technologies for bioregenerative life support systems/CELSS N91-24060
BIPOLAR TRANSISTORS
Solutions to current induced avalanche burnout
[DE90-013196] N91-23386
Development of Si/SiGe heterostructures
[AD-A232747] N91-23961
BIREFRINGENCE
Birefringent filter design
[NASA-CASE-LAR-13887-1] N91-23472
BIREFRINGENT FILTERS
Birefringent filter design
[NASA-CASE-LAR-13887-1] N91-23472
BISMUTH
In-situ surface x ray scattering measurements of electrochemically deposited bismuth on silver (III): Structure, compressibility, and comparison with ex-situ leed measurements
[AD-A232624] N91-23680
BISMUTH COMPOUNDS
Sintering and hot isostatic pressing of Bi2Sr2CaCu2O(x)
[DE91-010797] N91-23945
BLACK HOLES (ASTRONOMY)
The spectrum of massive accretion disks N91-23840
Initial data for the two-body problem of general relativity N91-23965
The thermodynamic stability of systems containing black holes N91-24022
BLADE TIPS
Research on aerodynamic control of blade tip clearance flow in air-cooled turbine
[DE91-764223] N91-23182
BLADE-VORTEX INTERACTION
A study of the noise mechanisms of transonic blade-vortex interactions
[NASA-CR-188199] N91-23084

BLANKETS (FUSION REACTORS)
Turbulence and the feasibility of self-cooled liquid-metal blankets for fusion reactors
[SER-10/P-REV] N91-23910
BLOCH BAND
Integrated Vertical Bloch Line (VBL) memory N91-24051
BLOOD CIRCULATION
Bulletin of the Israel Physical Society, volume 33, 1987. Annual Meeting 1987: Program and Abstracts
[ITN-89-85012] N91-23832
An on-line computerized system for blood-flow measurements N91-23834
BLOOD FLOW
Simulation of blood flow through an artificial heart N91-24056
BLUFF BODIES
Effects of three-dimensional imposed disturbance on bluff-body near wake flows
[AD-A232137] N91-23447
BODY CENTERED CUBIC LATTICES
First principles calculation of the crystal structures in the 4d transition metals N91-23835
BODY FLUIDS
Effects of weightlessness (sea water immersion) on body fluid balance and CNS functions N91-23566
BODY TEMPERATURE
Effects of bright illumination on oral temperature and cognitive performance in humans during nighttime hours
[AD-A232787] N91-23722
BOMBS (ORDNANCE)
MIK-guided bomb simulation
[IAITIC-87-1003] N91-23337
BOOLEAN ALGEBRA
Knowledge-based retrieval of information as a process of evidential reasoning N91-23978
BOROSILICATE GLASS
Mechanical characterisation of fibre-matrix interface in ceramic composites by an instrumented indentation test
[REPT-911-430-114] N91-23256
High temperature membranes for H2S and SO2 separations
[DE91-008534] N91-23275
BOUNDARIES
On the construction of two-phase equilibria in a non-elliptic hyperelastic material
[AD-A232628] N91-23558
BOUNDARY CONDITIONS
Boundary stability under nonequilibrium conditions
[DE91-009262] N91-23293
A system-approach to the elastohydrodynamic lubrication point-contact problem
[NASA-TM-104342] N91-23439
Formulation of boundary conditions for the multigrid acceleration of the Euler and Navier Stokes equations
[NASA-CR-188234] N91-23440
Accuracy of the Reissner-Mindlin and the (1,1,2) model for the clamped-in plate problem
[AD-A232755] N91-23561
Auroral boundary index from 1983 to 1990
[AD-A232845] N91-23660
Boundary conditions in quantum cosmology N91-24020
Theoretical studies of QSO absorption lines and the intergalactic medium N91-24025
BOUNDARY ELEMENT METHOD
Computer programs for simulation of electrodeposition
[DE91-010203] N91-23741
BOUNDARY LAYER CONTROL
A study of three dimensional turbulent boundary layer separation and vortex flow control using the reduced Navier Stokes equations
[NASA-TM-104407] N91-23089
Passive laminar flow control of crossflow vorticity
[NASA-CASE-LAR-13563-1] N91-23410
BOUNDARY LAYER FLOW
An experimental study of an axisymmetric turbulent boundary layer disturbed by a periodic freestream N91-23078
BOUNDARY LAYER SEPARATION
A study of three dimensional turbulent boundary layer separation and vortex flow control using the reduced Navier Stokes equations
[NASA-TM-104407] N91-23089
Some aspects of shock-wave boundary layer interaction relevant to intake flows N91-23161
BOUNDARY LAYER TRANSITION
Numerical simulation of transition in three dimensional boundary layers
[ESA-TT-1203] N91-23442
BOUNDARY LAYERS
Computation of viscous shock/shock hypersonic interactions with an implicit flux split scheme
[AD-A232405] N91-23093
BOUNDARY LUBRICATION
A system-approach to the elastohydrodynamic lubrication point-contact problem
[NASA-TM-104342] N91-23439
Fundamental research on tribology
[AD-A232446] N91-23519
BOUNDARY VALUE PROBLEMS
Thermo-viscoelastic behavior of composite materials N91-23243
Riemann problems and the WAF method for the two-dimensional shallow water equations
[CRANFIELD-AERO-9005] N91-23443
The transient response of heavily fluid-loaded elastic plates and cylindrical shells N91-23528
On the construction of two-phase equilibria in a non-elliptic hyperelastic material
[AD-A232628] N91-23558
Localised symmetric instability: An initial value problem N91-23672
Simulation of blood flow through an artificial heart N91-24056
BOUSSINESQ APPROXIMATION
Grouping of clouds and internal gravity waves in a non-hydrostatic model of moist convection
[DM-55] N91-23679
BRAIN
Mechanisms of higher brain functions: A study of models of perception
[AD-A232389] N91-23712
BRANCHING (MATHEMATICS)
Congruence properties of the process equivalence induced by temporal logic
[RR-831-I-IMAG-118-LIFIA] N91-23810
BRAYTON CYCLE
Water-cooling technique of high temperature gas turbine blade
[DE91-764238] N91-23506
BRIDGES (STRUCTURES)
Synthesis and characterization of indium-arsenic compounds containing a four-membered In-Ad-In-As or In-As-In-Cl ring: Crystal structures of ((Me3SiCH2)2 InAs(SiMe3)2)2 and (Me3SiCH2)2 InAs(SiMe3)2 In(CH2SiMe3)2Cl
[AD-A232368] N91-23956
BRIGHTNESS
Radioluminescent (RL) lighting system development program
[DE91-009743] N91-23381
Near-infrared milliarcsecond observations by the lunar occultation technique N91-24034
BRITTLE MATERIALS
Statistical models and inference procedures for structural and materials reliability
[AD-A232634] N91-23827
BROADCASTING
Communication and broadcasting satellites payload reconfiguration technologies
[REPT-911-440-102] N91-23218
Eastern Europe: Please stand by
[PB91-14336] N91-23348
Optimal multinode broadcast on a mesh connected graph with reduced bufferization
[RR-825-I] N91-23362
BROKEN SYMMETRY
Research in particle theory
[DE91-010749] N91-23872
BROMINATION
Bromination of carbon fibers and carbon-carbon composites N91-23240
BROWN DWARF STARS
A near-infrared search for brown dwarfs in the Pleiades N91-24011
BRUSHES
Simulation of brush insert for leading-edge-passage convective heat transfer
[NASA-TM-103801] N91-23409
BUBBLES
Gas evolution and bubble formation on electrodes
[ESA-TT-1191] N91-23278
A computationally efficient modelling of laminar separation bubbles N91-23411
Interfacial characteristic measurements in horizontal bubbly two-phase flow
[DE91-009803] N91-23427
A two-scale solution of the forced Rayleigh-Plesset equation governing the dynamics of cavitation bubble vaporous growth
[AD-A232129] N91-23446
BUCKLING
Buckling analysis of a complex vacuum vessel using the finite-element method
[DE91-010032] N91-23546
BUFFETING
Buffet induced structural/flight-control system interaction of the X-29A aircraft
[NASA-TM-101735] N91-23133
BUILDINGS
Use of personal computers in performing a linear modal analysis of a large finite-element model
[DE91-010112] N91-23541
Simulation of probabilistic wind loads and building analysis
[NASA-TM-103744] N91-23549
BUOYS
Arctic remote autonomous measurement platform post CEAREX engineering report
[AD-A232843] N91-23471
BURNS (INJURIES)
The transfer of technology to measure skin burn depth in humans N91-24076
BUS CONDUCTORS
Designing a virtual-memory implementation using the Motorola MC68010 16-bit microprocessor with multi-processor capability interfaced to the VMEbus
[AD-A232554] N91-23730

C

C (PROGRAMMING LANGUAGE)
CLIPS: A tool for the development and delivery of expert systems N91-24043
CADMIUM TELLURIDES
Eureca 1 AMF 117 experiment: An analysis of thermal and solutal transfer during the crystal growth of CdTe by the THM process
[REPT-911-430-118] N91-23947
Eureca 1 AMF 117 experience: Thermal and solutal transfer analysis for CdTe in tellurium during crystal growth by the THM method
[REPT-911-430-120] N91-23948
CALCIUM COMPOUNDS
Sintering and hot isostatic pressing of Bi2Sr2CaCu2O(x)
[DE91-010797] N91-23945
CALCULUS OF VARIATIONS
Control synthesis based upon a game theoretic approach N91-23831
CALIBRATING
Absolute calibration in vivo measurement systems
[DE91-009719] N91-23692
CALORIMETERS
Measurement control for calorimetric assay
[DE91-009445] N91-23274
The United Kingdom waveguide power standards above 40 GHz
[RSRE-90023] N91-23845
CAMERAS
Design of a twenty-element long focal length zoom lens
[DE91-010770] N91-23894
CANADA
Heat strain and work tolerance times with varying levels of Canadian Forces NBC protective clothing, ambient temperature, physical work intensity, and work/rest schedules
[AD-A232653] N91-23720
CANCELLATION CIRCUITS
Implications of adaptive cancellation array processing for design of a space-based surveillance radar
[RSRE-MEMO-4410] N91-23364
CANONICAL FORMS
Canonical vs. micro-canonical sampling methods in a 2D Ising model
[DE91-010204] N91-23737
Monte Carlo simulation of supercritical solutions in the grand canonical ensemble
[DE91-009152] N91-23859
CANTILEVER BEAMS
Finite element analysis of the lateral buckling of a cantilevered I Beam
[DE91-010123] N91-23527
CAPACITANCE
Development and utilization of new diagnostics for dense-phase pneumatic transport
[DE91-008947] N91-23339
A submicron resolution monolithic capacitive displacement sensor with digital output
[DE91-009765] N91-23465
CARBON
Primary ocean production: Carbon and particle flux N91-23596
X ray diffraction and electron spectroscopy of epitaxial molecular C60 films
[AD-A232152] N91-23954
CARBON CYCLE
Primary ocean production: Carbon and particle flux N91-23596
CARBON DIOXIDE
Material processing with hydrogen and carbon monoxide on Mars
[NASA-TM-104405] N91-23616

Atmospheric leakage and condensate production in NASA's biomass production chamber. Effect of diurnal temperature cycles
[NASA-TM-103819] N91-23718

CARBON DIOXIDE LASERS
Spatial dynamics of picosecond CO2 laser pulses produced by optical switching in Ge
[DE91-010368] N91-23476
Temperature distribution and thermal damage during tissue ablation by CO2 laser irradiation: Model and experiment N91-23833

CARBON FIBER REINFORCED PLASTICS
The development and evaluation of an alternative powder prepregging technique for use with LaRC-TPI/graphite composites
[NASA-CR-188184] N91-23242

CARBON FIBERS
Bromination of carbon fibers and carbon-carbon composites N91-23240
Nondestructive inspection for carbon-carbon with adapted coating for oxidation
[REPT-911-430-106] N91-23252
Materials and structure for Hermes
[REPT-911-430-117] N91-23258
Statistical models and inference procedures for structural and materials reliability
[AD-A232634] N91-23827
Flame-retardant composite materials N91-24064

CARBON MONOXIDE
Material processing with hydrogen and carbon monoxide on Mars
[NASA-TM-104405] N91-23616

CARBON STARS
Radio and infrared studies of mass-losing evolved stars N91-24026

CARBON 12
Computed secondary-particle energy spectra following nonelastic neutron interactions with C-12 for E(n) between 15 and 60 MeV: Comparisons of results from two calculational methods
[DE91-010454] N91-23864

CARBON-CARBON COMPOSITES
Bromination of carbon fibers and carbon-carbon composites N91-23240
Carbon-carbon material with oxidation protection
[REPT-911-430-103] N91-23249
New developments in composites for space applications
[REPT-911-430-104] N91-23250
Carbon/carbon inox thermostructural composites: Mechanical and tectonic behavior of anti-oxidation protection
[REPT-911-430-115] N91-23257
High temperature composites in space planes and missiles development
[REPT-911-430-119] N91-23259
Investigations of oxidation protection systems for carbon-carbon composites formed by chemical vapor deposition and plasma-assisted chemical vapor deposition techniques
[AD-A232800] N91-23269

CARBONATES
Composition and distribution of carbonates, sulfates, and hydrates on the Martian surface from earth-based spectroscopy between 3-5 microns N91-24033

CARBOXYLIC ACIDS
Hepatic metabolism of perfluorinated carboxylic acids: A nuclear magnetic resonance investigation
[AD-A232033] N91-23706

CARTESIAN COORDINATES
Two dimensional vernier
[NASA-CASE-MSC-21700-1] N91-23462

CASCADE FLOW
Aero-thermal investigation of a highly loaded transonic linear turbine guide vane cascade. A test case for inviscid and viscous flow computations
[VKI-TN-174] N91-23437

CASSEGRAIN OPTICS
Soft x ray/extreme ultraviolet images of the solar atmosphere with normal incidence multilayer optics N91-24006

CASTING
Gas contents and weldability of aluminum die castings
[ETN-91-99188] N91-23302
Aerospatiale industrial thermal plasmas
[REPT-911-430-113] N91-23927

CATALYSIS
Fundamental research on tribology
[AD-A232446] N91-23519

CATALYSTS
A novel process for methanol synthesis
[DE91-009808] N91-23334

CATECHOLAMINE
Strategies to sustain and enhance performance in stressful environments
[AD-A232698] N91-23714

CATHODES
Evaluation of cathode materials for high energy lithium secondary batteries
[DE91-764240] N91-23385

CATHODIC COATINGS
Evaluation of cathode materials for high energy lithium secondary batteries
[DE91-764240] N91-23385

CAUCHY PROBLEM
Riemann problems and the WAF method for the two-dimensional shallow water equations
[CRANFIELD-AERO-9005] N91-23443

CAUCHY-RIEMANN EQUATIONS
Riemann problems and the WAF method for the two-dimensional shallow water equations
[CRANFIELD-AERO-9005] N91-23443

CAUSES
Transition space
[AD-A231404] N91-23732

CAVITATION FLOW
Analysis of the multigrid method N91-23418
A two-scale solution of the forced Rayleigh-Plesset equation governing the dynamics of cavitation bubble vaporous growth
[AD-A232129] N91-23446

CAVITIES
Experimental study of narrow slot, cavity-backed apertures with finite wall conductivity
[DE91-009039] N91-23352

CAVITY RESONATORS
Superconducting microwave electronics at Lewis Research Center N91-24081

CELESTIAL BODIES
Near-infrared milliarcsecond observations by the lunar occultation technique N91-24034

CELLS (BIOLOGY)
AFRRI reports, October - December 1990
[AD-A232236] N91-23283
Molecular studies of cytokine induction
[AD-A232221] N91-23707

CEMENTATION
Investigations of oxidation protection systems for carbon-carbon composites formed by chemical vapor deposition and plasma-assisted chemical vapor deposition techniques
[AD-A232800] N91-23269

CENSORED DATA (MATHEMATICS)
Nonparametric estimation in change-point hazard rate models for censored data: A counting process approach
[RR-836-I-AND-M] N91-21825

CENTRAL NERVOUS SYSTEM
Effects of weightlessness (sea water immersion) on body fluid balance and CNS functions N91-23566

CENTRIFUGAL COMPRESSORS
Dynamic study of cyclically symmetric structures: Application to rotating a wheel of a centrifugal compressor
[ISAL-91-0004] N91-23844

CENTRIFUGAL FORCE
Dynamic study of cyclically symmetric structures: Application to rotating a wheel of a centrifugal compressor
[ISAL-91-0004] N91-23844

CERAMIC COATINGS
Metallic threaded composite fastener
[NASA-CASE-MSC-21580-1] N91-23491

CERAMIC FIBERS
A preliminary investigation of acousto-ultrasonic NDE of metal matrix composite test specimens
[NASA-TM-104339] N91-23521

CERAMIC MATRIX COMPOSITES
Oxidation resistant carbon/carbon materials
[REPT-911-430-105] N91-23251
Fiber-reinforced glass-ceramic matrix composites: New class of materials for space applications
[REPT-911-430-107] N91-23253
Thermostructural composites: Recent evolutions and improvements
[REPT-911-430-109] N91-23254
How to know CMC
[REPT-911-430-130] N91-23262
A study of the critical factors controlling the synthesis of ceramic matrix composites from preceramic polymers
[AD-A232686] N91-23327

CERAMICS
New developments in composites for space applications
[REPT-911-430-104] N91-23250
Mechanical characterisation of fibre-matrix interface in ceramic composites by an instrumented indentation test
[REPT-911-430-114] N91-23256
Ceramics in aerospace
[REPT-911-430-127] N91-23260
Chevron-notched, flexure tests for measuring the elevated temperature fracture resistance of structural ceramics
[DE91-009117] N91-23310
NDE (Nondestructive Examination) development for ceramics for advanced heat engines
[DE91-005516] N91-23316
Low heat rejection diesel ceramic coupon tests
[DE91-006274] N91-23318
Mechanistic studies of pressure-assisted superplasticity of structural ceramics
[AD-A232034] N91-23322
Fundamental studies of electronic packaging materials and structures: Surface and interfaces
[AD-A232336] N91-23403
Evaluation and ranking of candidate ceramic wafer engine seal materials
[NASA-TM-103795] N91-23515
Fundamental research on tribology
[AD-A232446] N91-23519
Theory of the critical current density in YBa2Cu3O7 ceramics
[DE91-009443] N91-23940
Composite ceramic superconducting wires for electric motor applications
[AD-A232074] N91-23951

CERTIFICATION
The certification of the aircraft integrated propulsive system
[REPT-911-111-102] N91-23188

CHANNEL FLOW
Two-phase flow patterns and frictional pressure gradients in a small rectangular channel
[DE91-009652] N91-23414
Low Reynolds number two-equation modeling of turbulent flows
[NASA-TM-104368] N91-23416
Numerical simulation of incompressible inhomogeneous turbulence in a plane channel flow
[ESA-TT-1199] N91-23441

CHAOS
Few-body problems, electron-correlation effects, and beyond
[DE91-010030] N91-23857
Mean-field theories of the Hubbard model and periodic orbits in chaotic maps N91-23938

CHARACTERIZATION
Characterization of composite materials for aerospace materials
[DLR-MITT-90-15] N91-23246
Principal components of minus M-matrices
[AD-A232354] N91-23818

CHARGE EXCHANGE
Excitation of atoms and molecules in collisions with highly charged ions
[DE91-010740] N91-23870

CHARGED PARTICLES
Constant of motion and dynamic equations for one-dimensional autonomous system and radiation damping
[DE91-011002] N91-23547
Hall effects on anomalous heat, particle and helicity transports through tearing-mode turbulence
[DE91-010730] N91-23924

CHARPY IMPACT TEST
Elastic/plastic fracture mechanics. Part 2: Marine structural applications
[AD-A232560] N91-23557

CHEMICAL ANALYSIS
Hardening mechanisms and analysis of the structure of the TGDDM/DDS epoxy resin system
[ESA-TT-1202] N91-23319

CHEMICAL BONDS
Chain propagation/step propagation polymerization. Regular thermoplastic elastomers
[AD-A232356] N91-23324
Synthesis and characterization of indium-arsenic compounds containing a four-membered In-Ad-In-As or In-As-In-Cl ring: Crystal structures of ((Me3SiCH2)2 InAs(SiMe3)2)2 and (Me3SiCH2)2 InAs(SiMe3)2 In(CH2SiMe3)2Cl
[AD-A232368] N91-23956
Three-dimensional structure of human serum albumin N91-24057

CHEMICAL COMPOSITION
Poly(1,3,4-oxadiazoles) via aromatic nucleophilic displacement
[NASA-CASE-LAR-14427-1] N91-23237
Fractal image compression of Rayleigh, Raman, LIF and LDV data in turbulent reacting flows
[AD-A232237] N91-23449
Tropospheric sampling with aircraft
[DE91-009472] N91-23626
Cryomagmatism in the outer solar system N91-24019

CHEMICAL EFFECTS
Effectiveness of a prototype microclimate cooling system for use with chemical protective clothing
[AD-A231572] N91-23717
CHEMICAL REACTIONS
Experimental investigations on the transition from stable to unstable combustion by means of active instability control N91-23165
Mixing and non-equilibrium chemical reaction in a compressible mixing layer
[NASA-CR-187084] N91-23181
Deterministic analysis of processes at corroding metal surfaces and the study of electrochemical noise in these systems
[DE91-009997] N91-23297
Hardening mechanisms and analysis of the structure of the TGDDM/DDS epoxy resin system
[ESA-TT-1202] N91-23319
Chemical reactions in turbulent mixing flows
[AD-A232610] N91-23450
High resolution measurements of strained diffusion and reaction layer structure and extinction in turbulent flows
[AD-A232794] N91-23456
Transport and nucleation processes in the vapor growth of diamond
[AD-A232135] N91-23953
Synthesis and characterization of indium-arsenic compounds containing a four-membered In-Ad-In-As or In-As-In-Cl ring: Crystal structures of ((Me3SiCH2)2 InAs(SiMe3)2)2 and (Me3SiCH2)2 InAs(SiMe3)2 In(CH2SiMe3)2Cl
[AD-A232368] N91-23956
CHEMICALS
Treatment of denser-than-air releases in an advection-diffusion model: Thermodynamic effects
[DE91-010152] N91-23632
CHILD-LANGMUIR LAW
Quantum extension of Child-Langmuir law
[AD-A232407] N91-23878
CHINA
On a phonetic and structural encoding of Chinese characters in Chinese texts
[RR-835-I] N91-23989
CHIPS (ELECTRONICS)
Analog processing of optical wavefronts using integrated guided-wave optics
[AD-A232703] N91-23904
CHIPS (MEMORY DEVICES)
Integrated Vertical Bloch Line (VBL) memory N91-24051
CHLORIDES
Conceptual design study of high-performance sodium/metal chloride batteries for electric vehicle applications
[DE91-009618] N91-23383
CHROMIUM
Effect of transition metal dopants on high T(sub c) superconductivity
[PB91-130138] N91-23934
CHROMIUM STEELS
Reduction factors for creep strength and fatigue life of modified 9 Cr-1 Mo steel weldments
[DE91-009919] N91-23544
CHROMOSOMES
Problems in understanding the organization, structure and function of chromosomes
[DE91-009939] N91-23695
New hosts and vectors for genome cloning
[DE91-009996] N91-23696
Robotics for recombinant DNA and human genetics research
[DE90-016440] N91-23697
CHRONOLOGY
The applicability of thematic mapper data to the classification of tree species and natural age classes
[DLR-FB-90-44] N91-23612
CINEMATOGRAPHY
Experimental investigations on the transition from stable to unstable combustion by means of active instability control N91-23165
CIRCADIAN RHYTHMS
Some problems of desynchronisation of sleep-wakefulness and circadian rhythms for long duration spaceflights N91-23570
CIRCLES (GEOMETRY)
Two dimensional vernier
[NASA-CASE-MSC-21700-1] N91-23462
CIRCUIT RELIABILITY
Basic properties of strongly code disjoint checkers
[RR-824-I] N91-23393
Automatic formal verification of VHDL descriptions: A first prototype
[RR-823-I] N91-23726
CIRCUITS
Electromagnetic attachment mechanism
[NASA-CASE-MSC-21463-1] N91-23490
CIRCULATION
Pulsed power performance of the new RLA (Recirculating Linear Accelerator)
[DE91-004723] N91-23885
CIVIL AVIATION
Engine technology challenges for a 21st century high speed civil transport
[NASA-TM-104363] N91-23098
Do civil flying qualities requirements address military missions for off-the-shelf procurement N91-23115
An investigation into the use of side-arm control for civil rotorcraft applications N91-23123
Integration of propulsive systems: Selection and compromise
[REPT-911-111-101] N91-23187
Satellite utilization by civil aviation
[REPT-911-111-105] N91-23216
Observatory of new materials. Evolution perspectives for the materials used in civil transportation aircraft
[REPT-911-111-107] N91-23248
CLASSIFICATIONS
Analysis on forest decline classification of the beech using airborne multispectral scanner data
[DLR-FB-90-56] N91-23614
Sea ice classification using synthetic aperture radar
[AD-A232248] N91-23689
Classification using multi-layered perceptrons
[AD-A232810] N91-23802
An observational study of arm structure in normal spiral galaxies N91-24007
CLASSIFIERS
A survey of decision tree classifier methodology
[NASA-CR-188208] N91-23806
CLEANING
Applications of energetic particles in improving coating adhesion properties
[DE91-008833] N91-23312
CLEAR AIR TURBULENCE
Microwave temperature profiler for clear air turbulence prediction
[NASA-CASE-NPO-18115-1-CU] N91-23662
CLEARANCES
Research on aerodynamic control of blade tip clearance flow in air-cooled turbine
[DE91-764223] N91-23182
CLEAVAGE
Stochastic micromechanical modeling of cleavage fracture in the ductile-brittle transition region N91-23533
Structural studies of manganese and halide in the photosynthetic oxygen evolving complex
[DE91-009071] N91-23698
CLIMATE
Ocean modeling for climate study N91-23592
Energy exchange study at the ocean surface by satellite observation N91-23597
The application of equilibrium climate models to questions of glaciation at high latitudes N91-23669
Parallelizing the spectral transform method, part 1
[DE91-010453] N91-23805
Proceedings of the 1991 American Association for the Advancement of Science Annual Meeting Program N91-23969
CLIMATOLOGY
Space and Sea
[ESA-SP-312] N91-23563
Ocean modeling for climate study N91-23592
Wind and sea state local climatology by means of satellite radar altimeter measurements N91-23599
Mechanisms of equatorial superrotation: Studies with two-level models N91-23642
The annual march of convection, sea surface temperature, and surface winds in the tropics N91-23667
Surface cloud observations for radiation, climatology and incorporation into satellite-based nephanalyses N91-23671
SWANEA (Southwest Asia-Northeast Africa): A climatological study. Volume 2: The Middle East Peninsula
[AD-A232776] N91-23684
CLIPS
Airborne rescue system
[NASA-CASE-ARC-11909-1] N91-23095
CLOSED ECOLOGICAL SYSTEMS
Atmospheric leakage and condensate production in NASA's biomass production chamber. Effect of diurnal temperature cycles
[NASA-TM-103819] N91-23718
New research on bioregenerative air/water purification systems N91-24053
Monitoring and control technologies for bioregenerative life support systems/CELSS N91-24060
CLOSURE LAW
Turbulent mixing in nonreacting and reacting flows: A PDF approach at the two-point level N91-23422
CLOTHING
Heat strain and work tolerance times with varying levels of Canadian Forces NBC protective clothing, ambient temperature, physical work intensity, and work/rest schedules
[AD-A232653] N91-23720
CLOUD COVER
Assimilation of ERBE data with nonlinear programming technique to improve cloud cover diagnosis N91-23663
Observational study of the above-inversion structure and marine stratocumulus cloud clearing episodes during FIRE N91-23666
Surface cloud observations for radiation, climatology and incorporation into satellite-based nephanalyses N91-23671
Initialization of cloud and radiation in the Florida State University global spectral model
[AD-A232425] N91-23682
SWANEA (Southwest Asia-Northeast Africa): A climatological study. Volume 2: The Middle East Peninsula
[AD-A232776] N91-23684
CLOUD HEIGHT INDICATORS
Evaluation of generalized thresholds in an objective multispectral satellite cloud analysis
[AD-A232716] N91-23683
CLOUD PHYSICS
Analysis and modeling of summertime convective cloud and precipitation structure over the Southeastern United States
[NASA-CR-188119] N91-23670
Grouping of clouds and internal gravity waves in a non-hydrostatic model of moist convection
[DM-55] N91-23679
Studies of molecular excitation in star formation regions N91-24023
CLOUD SEEDING
Investigation of micro- and macrophysical structures and processes in hail clouds with respect to their modification
[DLR-FB-90-38] N91-23677
CLOUDS (METEOROLOGY)
Surface cloud observations for radiation, climatology and incorporation into satellite-based nephanalyses N91-23671
COAL GASIFICATION
MHD channel gas-side element erosion-corrosion studies
[DE91-008561] N91-23911
COATING
Applications of energetic particles in improving coating adhesion properties
[DE91-008833] N91-23312
Measurement of particle size, velocity and temperature in the plasma spray coating process
[DE91-006208] N91-23317
COATINGS
Scattering from thin apertures in coated conductors using FDTD
[AD-A232125] N91-23365
Investigation of neutral atom and ion emission during laser conditioning of multilayer HfO2-SiO2 coatings
[DE91-009749] N91-23860
COCKPITS
Human short-latency somatosensory evoked potentials in impact acceleration research: Equipment, procedures, and techniques
[AD-A232732] N91-23709
CODERS
High-quality 800-b/s voice processing algorithm
[AD-A232352] N91-23372
Laser optical disk position encoder with active heads N91-24079
CODING
On a phonetic and structural encoding of Chinese characters in Chinese texts
[RR-835-I] N91-23989
COGENERATION
Research and development opportunities for natural gas fueled refrigeration in industrial processes
[PB91-136432] N91-23338
COGNITION
Individual differences underlying pilot cockpit error
[DOT/FAA/RD-91/13] N91-23710
Mechanisms of higher brain functions: A study of models of perception
[AD-A232389] N91-23712
COLD FRONTS
Localised symmetric instability: An initial value problem N91-23672
COLD NEUTRONS
Cold moderators for pulsed neutron sources
[DE91-010594] N91-23866

COLLIMATION
Wavelength independent optical lithography and microscopy
[AD-A232036] N91-23896
COLLISION AVOIDANCE
Airborne Collision Avoidance System (ACAS) in controlled air traffic. Aspects of reciprocal influence in Secondary Surveillance Radar (SSR) radio loads
[ETN-91-99253] N91-23105
Articulation of spatial robots N91-23504
COLLISION PARAMETERS
Experiments on Frank-Hertz setup
[NOTA-INTERNA-961] N91-23876
COLOR
An observational study of arm structure in normal spiral galaxies N91-24007
COLOR PHOTOGRAPHY
Quantitative film radiography
[DE91-009718] N91-23463
COLOR TELEVISION
Digital CODEC for real-time processing of broadcast quality video signals at 1.8 bits/pixel N91-24067
COLOR-COLOR DIAGRAM
H II regions and young star clusters in the magellanic clouds N91-24004
COLUMBUS SPACE STATION
Comparisons between underwater and space working environments for on board activities optimization (Columbus space programme) N91-23574
COMBAT
On the many-on-one stochastic duel
[CEMA-86/11] N91-23828
COMBINATORIAL ANALYSIS
On the use of genetic algorithms to solve the time-table problem
[REPT-90-060] N91-23752
COMBUSTIBLE FLOW
An experimental study of flamelet surfaces in turbulent combustion
[AD-A232342] N91-23284
High resolution measurements of strained diffusion and reaction layer structure and extinction in turbulent flows
[AD-A232794] N91-23456
Advanced diagnostics for reacting flows
[AD-A232609] N91-23902
COMBUSTION
Aerodynamics and stabilization of combustion of hydrogen jets injected into subsonic airflow N91-23164
Mass resolved resonance ionization spectroscopy of combustion radicals
[DE91-010603] N91-23276
Advanced diagnostics for reacting flows
[AD-A232609] N91-23902
COMBUSTION CHAMBERS
Design techniques for dual mode ram-scramjet combustors N91-23166
Use of secondary flows for rapid mixing in scramjet combustors N91-23167
Analytical and experimental investigations of the oblique detonation wave engine concept N91-23169
The effect of combustor flow nonuniformity on the performance of hypersonic nozzles N91-23173
A CFD study of jet mixing in reduced flow areas for lower combustor emissions
[NASA-TM-104411] N91-23185
The effects of controlling vortex formation on the performance of a dump combustor N91-23270
An experimental method for studying combustion of an unsupported fuel droplet at reduced gravity N91-23273
Mechanical behavior and failure phenomenon of an in situ-toughened silicon nitride
[NASA-TM-103741] N91-23311
A simplified dynamic model of the Space Shuttle main engine
[NASA-TM-104421] N91-23340
COMBUSTION CHEMISTRY
Chemical reactions in turbulent mixing flows
[AD-A232610] N91-23450
COMBUSTION EFFICIENCY
A CFD study of jet mixing in reduced flow areas for lower combustor emissions
[NASA-TM-104411] N91-23185
COMBUSTION PHYSICS
An experimental study of flamelet surfaces in turbulent combustion
[AD-A232342] N91-23284
Chemical reactions in turbulent mixing flows
[AD-A232610] N91-23450
COMBUSTION PRODUCTS
Automatic particle sizing from rocket motor holograms
[AD-A232553] N91-23236
Advanced diagnostics for reacting flows
[AD-A232609] N91-23902
COMBUSTION STABILITY
Experimental investigations on the transition from stable to unstable combustion by means of active instability control N91-23165
Highly integrated ducted rocket propulsion modules for future hypersonic tactical missiles N91-23171
The effects of controlling vortex formation on the performance of a dump combustor N91-23270
COMMAND AND CONTROL
A procedural expert system for spacecraft command and control N91-23591
COMMERCE
Steps toward environmentally compatible product and process design: A case for green engineering
[AD-A232688] N91-23633
Robotic control and inspection verification N91-24075
COMMERCIAL AIRCRAFT
Engine technology challenges for a 21st century high speed civil transport
[NASA-TM-104363] N91-23098
COMMUNICATION NETWORKS
Pulse compression of 100 picosecond pulses at 1.319 microns
[AD-A232552] N91-23901
Unattended network operations technology assessment study. Technical support for defining advanced satellite systems concepts
[NASA-CR-187080] N91-24030
COMMUNICATION SATELLITES
Communication and broadcasting satellites payload reconfiguration technologies
[REPT-911-440-102] N91-23218
Microwave integrated circuits for space applications N91-24069
Optical communication for space missions N91-24070
COMPARATOR CIRCUITS
Recent advances with quiescent power supply current ((sub DDQ)) testing at Sandia using the HP82000
[DE91-009254] N91-23382
COMPARTMENTS
Protein crystal growth tray assembly
[NASA-CASE-MFS-28507-1] N91-23933
COMPATIBILITY
European stakes and measures permitting the management of geometric dimensions N91-23573
COMPENSATORS
Degeneration of linear multivariable systems under high gain and dynamic compensation N91-23830
COMPLEX COMPOUNDS
Structural studies of manganese and halide in the photosynthetic oxygen evolving complex
[DE91-009071] N91-23698
COMPLEX SYSTEMS
Decentralized computing technology for fault-tolerant, survivable C3I systems, volume 1
[AD-A232289] N91-23369
Decentralized computing technology for fault-tolerant, survivable C3I systems, volume 2
[AD-A232290] N91-23370
Decentralized computing technology for fault-tolerant, survivable C3I systems. Volume 3: System/subsystem specification
[AD-A232291] N91-23371
A complex systems approach to metallic fracture surface characterization
[AD-A232546] N91-23556
COMPONENT RELIABILITY
NDE (Nondestructive Examination) development for ceramics for advanced heat engines
[DE91-005516] N91-23316
Checklist for thin-film hybrid microcircuits manufacturer and line survey
[ESA-PSS-01-611-ISSUE-1] N91-23397
Incorporating finite element analysis into component life and reliability
[NASA-TM-104400] N91-23550
Presentation of a computer program for analysing results of one shot device sensitivity tests: Application to the case of a one shot degenerated sequence
[REPT-911-430-126] N91-23758
COMPOSITE MATERIALS
Design and construction of a composite airframe for UAV research
[AD-A232422] N91-23143
Materials and material systems for combined cycle engines N91-23178
Integration of propulsive systems: Selection and compromise
[REPT-911-111-101] N91-23187
Rate dependent stress-strain behavior of advanced polymer matrix composites
[NASA-TM-104070] N91-23244
Observatory of new materials. Evolution perspectives for the materials used in civil transportation aircraft
[REPT-911-111-107] N91-23248
Nondestructive inspection for carbon-carbon with adapted coating for oxidation
[REPT-911-430-106] N91-23252
Nondestructive measurement of thickness and density of composite materials by Compton backscattering
[REPT-911-430-112] N91-23255
Materials and structure for Hermes
[REPT-911-430-117] N91-23258
An experimental and finite element investigation into the nonlinear material behavior of pin-loaded composite laminates
[AD-A232098] N91-23263
Metallic threaded composite fastener
[NASA-CASE-MSC-21580-1] N91-23491
Interlaminar strains at the free-edge of a hole for thick composites in compression
[DE91-008883] N91-23535
Statistical models and inference procedures for structural and materials reliability
[AD-A232634] N91-23827
Composite ceramic superconducting wires for electric motor applications
[AD-A232074] N91-23951
COMPOSITE STRUCTURES
Design and construction of a composite airframe for UAV research
[AD-A232422] N91-23143
Materials and material systems for combined cycle engines N91-23178
Carbon-carbon material with oxidation protection
[REPT-911-430-103] N91-23249
New developments in composites for space applications
[REPT 91-430-104] N91-23250
Structural materials for space mirrors
[REPT-911-430-128] N91-23261
Stress analysis of a double-doubler joint in composite structure N91-23530
Computational simulation of acoustic fatigue for hot composite structures
[NASA-TM-104379] N91-23548
Flame-retardant composite materials N91-24064
COMPRESSIBILITY
Mixing and non-equilibrium chemical reaction in a compressible mixing layer
[NASA-CR-187084] N91-23181
Preloaded latching device
[NASA-CASE-MSC-21730-1] N91-23493
In-situ surface x ray scattering measurements of electrochemically deposited bismuth on silver (III): Structure, compressibility, and comparison with ex-situ leed measurements
[AD-A232624] N91-23880
COMPRESSIBLE FLOW
Procedure for determination of three-dimensional wind tunnel wall interferences and wall adaptation in compressible subsonic flow using measured wall pressures
[DLR-FB-90-46] N91-23088
Mixing and non-equilibrium chemical reaction in a compressible mixing layer
[NASA-CR-187084] N91-23181
Block implicit multigrid solution of the Euler equations N91-23413
COMPRESSIBLE FLUIDS
Adaptive methods for compressible fluid dynamics
[AD-A232786] N91-23455
COMPRESSING
Preloaded latching device
[NASA-CASE-MSC-21730-1] N91-23493
COMPRESSION LOADS
Metallic threaded composite fastener
[NASA-CASE-MSC-21580-1] N91-23491
Interlaminar strains at the free-edge of a hole for thick composites in compression
[DE91-008883] N91-23535
COMPRESSION WAVES
Hydromagnetic wave coupling in the magnetosphere N91-23638
COMPRESSOR ROTORS
Effects of inlet distortion on the development of secondary flows in a subsonic axial inlet compressor rotor
[NASA-TM-104356] N91-23179
COMPTON EFFECT
Nondestructive measurement of thickness and density of composite materials by Compton backscattering
[REPT-911-430-112] N91-23255
COMPUTATION
Photonic materials and devices for optical information processing and computing applications
[AD-A232771] N91-23907

COMPUTATIONAL FLUID DYNAMICS
Hypersonic Combined Cycle Propulsion
[AGARD-CP-479] N91-23147
Hypersonic propulsion: Status and challenge N91-23153
Computational modeling and validation for hypersonic inlets N91-23162
Analytical and experimental investigations of the oblique detonation wave engine concept N91-23169
Pitot surveys of two moderately under-expanded jets N91-23172
The effect of combustor flow nonuniformity on the performance of hypersonic nozzles N91-23173
Viscous three-dimensional analyses for nozzles for hypersonic propulsion N91-23175
A three-dimensional Navier-Stokes stage analysis of the flow through a compact radial turbine
[NASA-TM-104420] N91-23186
Analysis of the multigrid method N91-23418
Computation of inlet reference plane flow-field for a subscale free-jet forebody/inlet model and comparison to experimental data
[AD-A232101] N91-23445
Adaptive methods for compressible fluid dynamics
[AD-A232786] N91-23455

COMPUTATIONAL GRIDS
Computation of viscous shock/shock hypersonic interactions with an implicit flux split scheme
[AD-A232405] N91-23093
Reacting shock waves in hypersonic propulsion applications N91-23174
Optimal multinode broadcast on a mesh connected graph with reduced bufferization
[RR-825-I] N91-23362
Block implicit multigrid solution of the Euler equations N91-23413
Analysis of the multigrid method N91-23418
A three-dimensional free-Lagrange code for multimaterial flow simulations
[DE91-002309] N91-23428
Strategy Combining Regionally Adapted Processes (SCRAP)
[AD-A232158] N91-23448
Adaptive methods for compressible fluid dynamics
[AD-A232786] N91-23455
Two dimensional vernier
[NASA-CASE-MSC-21700-1] N91-23462
Bobbin stresses generated by wire winding
[DE91-009545] N91-23526
A guide to the Nedwam wave model
[KNMI-WR-90-04] N91-23688

COMPUTER AIDED DESIGN
A computer aided multivariable control systems design technique with application to aircraft flying qualities
[AD-A232549] N91-23144
Integration of propulsive systems: Selection and compromise
[REPT-911-111-101] N91-23187
Maximum life spur gear design
[NASA-TM-104361] N91-23514
Automatic formal verification of VHDL descriptions: A first prototype
[RR-823-I] N91-23726
Searching algorithms for the real roots of a Bezier function
[RR-834-I-AND-M] N91-23755
ACLICO: A computer aided design system for bonded joints
[REPT-911-430-101] N91-23757
Active Design Database (ADDB) user's manual
[DE91-010431] N91-23985

COMPUTER AIDED MANUFACTURING
Active Design Database (ADDB) user's manual
[DE91-010431] N91-23985

COMPUTER AIDED MAPPING
The integration of remote sensing, geographic information system, and expert system technologies for landcover classification N91-23733

COMPUTER ANIMATION
Visual presentation and computer animation
[DE91-010599] N91-23745

COMPUTER ASSISTED INSTRUCTION
Satellite maneuver evaluation tool
[AD-A232016] N91-23226
User interface to an ICAI system that teaches discrete math
[AD-A232693] N91-23799
Intelligent computer-aided training and tutoring N91-24042

COMPUTER GRAPHICS
Satellite maneuver evaluation tool
[AD-A232016] N91-23226
Quantifying improved visual performance through vision training
[AD-A232799] N91-23716
Three-dimensional graphical representation of objects according to movement data in realtime
[DLR-FB-90-51] N91-23725
Scientific visualization software for your PC: Free and available now
[DE91-010156] N91-23744
Visual presentation and computer animation
[DE91-010599] N91-23745
Transportable Applications Environment (TAE) Plus: A NASA user interface development and management system N91-24048

COMPUTER NETWORKS
Mathematical techniques for the Performance Oriented Design (POD) tool
[AD-A232092] N91-23767
Computer center reference manual, volume 2
[AD-A232370] N91-23781
Computing for magnetic fusion energy research: The next five years
[DE91-010686] N91-23921
Building a generalized distributed system model
[NASA-CR-188181] N91-23970
Building a generalized distributed system model N91-23971
Effects of distributed database modeling on evaluation of transaction rollbacks N91-23972
Measuring the effects of distributed database models on transaction availability measures N91-23973
Performance analysis of static locking in replicated distributed database systems N91-23974
A note on the performance analysis of static locking in distributed database systems N91-23975

COMPUTER PROGRAM INTEGRITY
Software testing for evolutionary iterative rapid prototyping
[AD-A232555] N91-23771
Database constraint enforcement: A decompositional approach N91-23980

COMPUTER PROGRAMMING
Telemanipulation system assisted by computer for under water applications N91-23585
Integration of the execution support system for the Computer-Aided Prototyping System (CAPS)
[AD-A232015] N91-23761
Life cycle management automation programmer's manual
[AD-A232247] N91-23769
Software reverse engineering
[AD-A232644] N91-23773

COMPUTER PROGRAMS
NAS operational test and evaluation/integration of the Maintenance Management System (MMS) test plan
[DOT/FAA/CT-TN90/41] N91-23075
Aerodynamic preliminary analysis system 2. Part 1: Theory
[NASA-CR-182076] N91-23080
Theoretical and experimental performance of a solid fuel ramjet combustion cycle for hypersonic flight conditions N91-23170
Viscous three-dimensional analyses for nozzles for hypersonic propulsion N91-23175
Higher accuracy requirements for the satisfactory position calculation of an artificial satellite
[GKSS-90/E/25] N91-23203
Large space structures fielding plan
[AD-A232097] N91-23227
Computer modeling of soot formation comparing free radical and ionic mechanisms
[AD-A232820] N91-23287
SAR processor for the ERS-1 data phase 1, simple processor
[FEL-90-B033] N91-23359
Antenna performance influenced by the finite extent and conductivity of ground planes: A collection of reprints
[AD-A232132] N91-23366
An analysis of MLAYER: A multilayer tropospheric propagation program
[AD-A232733] N91-23379
Computation of inlet reference plane flow-field for a subscale free-jet forebody/inlet model and comparison to experimental data
[AD-A232101] N91-23445
Data-reduction and analysis procedures used in NIST's thermomechanical processing research
[PB91-132282] N91-23523
Technical description of the high-resolution air mass transformation model at KNMI
[KNMI-TR-125] N91-23646
A guide to the Nedwam wave model
[KNMI-WR-90-04] N91-23688
Programmable remapper for image processing
[NASA-CASE-MSC-21350-1] N91-23724
Transition space
[AD-A231404] N91-23732
The CERBERUS Ver. 02 code: A parallel six-equation thermal-hydraulic-system simulation code
[DE91-010079] N91-23736
Canonical vs. micro-canonical sampling methods in a 2D Ising model
[DE91-010204] N91-23737
Scientific visualization software for your PC: Free and available now
[DE91-010156] N91-23744
NODEN user's guide and installation manual
[RSRE-MEMO-4438] N91-23753
Specifications for reusable software components
[RR-828-I-IMAG-116-LIFIA] N91-23756
A method for machinery condition monitoring of transient phenomena using the pseudo Wigner-Ville distribution
[AD-A232014] N91-23760
Generalized disjunctive well-founded semantics for logic programs
[AD-A232064] N91-23765
Life cycle management automation programmer's manual
[AD-A232247] N91-23769
The TurboLAN project. Phase 1: Protocol choices for high speed local area networks. Phase 2: TurboLAN Intelligent Network Adapter Card, (TINAC) architecture
[NASA-CR-188175] N91-23776
Generalization of the FP2 parallel language by means of net theory
[RR-832-I-IMAG-99-LIFIA] N91-23780
Unified aeroacoustics analysis for high speed turboprop aerodynamics and noise. Volume 3: Application of theory for blade loading, wakes, noise, and wing shielding
[NASA-CR-185193] N91-23850
Unified aeroacoustics analysis for high speed turboprop aerodynamics and noise. Volume 5: Propagation of propeller tone noise through a fuselage boundary layer
[NASA-CR-185195] N91-23852
Nonlinear real-time optical signal processing
[AD-A232889] N91-23909
Life cycle management automation user's manual, version 1.1
[AD-A232096] N91-23968
The reduced version of the DERF 2 data set on a WORM optical disk
[DM-54] N91-23991
Software reengineering N91-24047
The Land Analysis System (LAS) N91-24054

COMPUTER STORAGE DEVICES
Evaluation of ferroelectric materials for memory applications
[AD-A232112] N91-23728
Designing a virtual-memory implementation using the Motorola MC68010 16-bit microprocessor with multi-processor capability interfaced to the VMEbus
[AD-A232554] N91-23730
Computer center reference manual, volume 2
[AD-A232370] N91-23781
Ultra-dense optical mass storage
[AD-A232767] N91-23905

COMPUTER SYSTEMS DESIGN
Maintenance Resource Prediction Model (MRPM) user's manual
[AD-A232019] N91-23762
Mathematical techniques for the Performance Oriented Design (POD) tool
[AD-A232092] N91-23767

COMPUTER SYSTEMS PERFORMANCE
Computational needs survey of NASA automation and robotics missions. Volume 1: Survey and results
[NASA-TM-103860] N91-23341
Recent advances with quiescent power supply current (I(sub DDQ)) testing at Sandia using the HP82000
[DE91-009254] N91-23382
Research and development involved in creating a quantitative EEG cartography wide band analysis system
[LAAS-91002] N91-23705
Automatic formal verification of VHDL descriptions: A first prototype
[RR-823-I] N91-23726
Saturation and vote for the fault tolerance in distributed systems
[LAAS-90390] N91-23727
A user-oriented synthetic workload generator
[NASA-CR-188197] N91-23739

COMPUTER TECHNIQUES
Automatic particle sizing from rocket motor holograms
[AD-A232553] N91-23236
Decentralized computing technology for fault-tolerant, survivable C3I systems, volume 1
[AD-A232289] N91-23369
Decentralized computing technology for fault-tolerant, survivable C3I systems, volume 2
[AD-A232290] N91-23370
Hypermedia 1990 structured Hypertext tutorial
[NASA-CR-187921] N91-23731

Performance analysis of garbage collection and dynamic reordering in a Lisp system
[NASA-CR-188205] N91-23738
Integration of the execution support system for the Computer-Aided Prototyping System (CAPS)
[AD-A232015] N91-23761
Molecular dynamics simulator for optimal control of molecular motion
[AD-A232801] N91-23881
Effects of distributed database modeling on evaluation of transaction rollbacks N91-23972
Performance analysis of static locking in replicated distributed database systems N91-23974
A note on the performance analysis of static locking in distributed database systems N91-23975
Intelligent computer-aided training and tutoring N91-24042

COMPUTER VISION
Performance of visual and ultrasound sensing by an autonomous robot
[DE91-010452] N91-23511
Telerobotics: A key area for possible technology transfer from underwater to space N91-23581
Synergetic multisensor fusion
[AD-A232089] N91-23766
Image wavelet decomposition and applications
[NASA-CR-188217] N91-23787
Intelligent vision system for autonomous vehicle operations N91-24046

COMPUTERIZED SIMULATION
Icing simulation: A survey of computer models and experimental facilities
[NASA-TM-104366] N91-23087
Hypersonic numerical simulation: Problems and perspectives. Hypersonic vehicles and numerical simulation in structural analysis
[REPT-911-111-106] N91-23091
Target maneuver models for improved homing guidance N91-23101
A CFD study of jet mixing in reduced flow areas for lower combustor emissions
[NASA-TM-104411] N91-23185
A three-dimensional Navier-Stokes stage analysis of the flow through a compact radial turbine
[NASA-TM-104420] N91-23186
Real-time simulation of constrained dynamic systems N91-23189
Simulation and analyses of the aeroassist flight experiment attitude update method
[NASA-TM-102174] N91-23210
Qualification of concentrating mirror systems with the Hermes measurement system and the Helios simulation program
[ESA-TT-1213] N91-23230
Response of simulated propellants and explosives to projectile impact
[DE91-009777] N91-23333
MIK-guided bomb simulation
[IAITIC-87-1003] N91-23337
Development and utilization of new diagnostics for dense-phase pneumatic transport
[DE91-008947] N91-23339
A simplified dynamic model of the Space Shuttle main engine
[NASA-TM-104421] N91-23340
Background simulation and filter design using iterated function systems
[AD-A232632] N91-23405
Numerical simulations of instabilities in compressible mixing layers N91-23412
Turbulent mixing in nonreacting and reacting flows: A PDF approach at the two-point level N91-23422
A three-dimensional free-Lagrange code for multimaterial flow simulations
[DE91-002309] N91-23428
Numerical simulation of a viscous vortex ring interaction with a density interface
[DE91-002790] N91-23429
Hairpin vortices, singularities, and transition to turbulence in three-dimensional shear flows
[DE91-002792] N91-23430
Developing natural convection in a fluid layer with localized heating and large viscosity variation
[DE91-005240] N91-23431
Numerical simulation and topological analysis of the separated flow around a sphere
[DLR-FB-90-43] N91-23435
Formulation of boundary conditions for the multigrid acceleration of the Euler and Navier Stokes equations
[NASA-CR-188234] N91-23440
Numerical simulation of transition in three dimensional boundary layers
[ESA-TT-1203] N91-23442
High energy dense ribbon beams and high harmonic gyrotron at millimeter wavelengths
[AD-A232839] N91-23470
Fundamental research on tribology
[AD-A232446] N91-23519
Computerized system for static and fatigue large scale structural tests: A case study
[IAITIC-87-1007] N91-23522
A comparison between classical and substructuring finite-element stress analysis of a complex vacuum vessel shell
[DE91-010035] N91-23540
Computational simulation of acoustic fatigue for hot composite structures
[NASA-TM-104379] N91-23548
Simulation of probabilistic wind loads and building analysis
[NASA-TM-103744] N91-23549
Satellite data utilization in ocean circulation models N91-23593
Sensitivity of numerical dispersion modeling to explosive source parameters
[DE91-009476] N91-23631
Data transfer over multiplexed logical data links sharing a single physical circuit N91-23734
The CERBERUS Ver. 02 code: A parallel six-equation thermal-hydraulic-system simulation code
[DE91-010079] N91-23736
A user-oriented synthetic workload generator
[NASA-CR-188197] N91-23739
Computer programs for simulation of electrodeposition
[DE91-010203] N91-23741
Ion confinement and radiation losses in the advanced toroidal facility
[DE91-010382] N91-23916
Physical/chemical closed-loop water-recycling N91-24052
Simulation of blood flow through an artificial heart N91-24056

COMPUTERS
Portable intelligent diagnostic aids
[AD-A230883] N91-23782
Proceedings of the 1991 American Association for the Advancement of Science Annual Meeting Program N91-23969

CONCENTRATORS
PV concentrators today and tomorrow
[DE91-010577] N91-23619

CONDENSATES
Atmospheric leakage and condensate production in NASA's biomass production chamber. Effect of diurnal temperature cycles
[NASA-TM-103819] N91-23718

CONDENSATION
In-Space technology experiments program. A high efficiency thermal interface (using condensation heat transfer) between a 2-phase fluid loop and heatpipe radiator: Experiment definition phase
[NASA-CR-186869] N91-23408

CONDUCTING POLYMERS
Solid polymer electrolytes for rechargeable batteries
[DE91-010231] N91-23384

CONDUCTORS
Scattering from thin apertures in coated conductors using FDTD
[AD-A232125] N91-23365

CONFERENCES
Flying Qualities
[AGARD-CP-508] N91-23108
Proceedings of the Second Glacier Bay Science Symposium
[PB91-110163] N91-23634
Few-body problems, electron-correlation effects, and beyond
[DE91-010030] N91-23857
Proceedings of the 1991 American Association for the Advancement of Science Annual Meeting Program N91-23969
Technology 2000, volume 2
[NASA-CP-3109-VOL-2] N91-24041

CONFIDENCE LIMITS
Presentation of a computer program for analysing results of one shot device sensitivity tests: Application to the case of a one shot degenerated sequence
[REPT-911-430-126] N91-23758

CONFIGURATION MANAGEMENT
Obstacle avoidance for redundant robots using configuration control
[NASA-CASE-NPO-17852-1-CU] N91-23783

CONFINEMENT
Space and Sea
[ESA-SP-312] N91-23563
The diving laboratory as a simulation environment for manned spaceflight N91-23564
Subsea habitats and space simulation N91-23567
Some problems of desynchronisation of sleep-wakefulness and circadian rhythms for long duration spaceflights N91-23570
Long duration hyperbaric confinement: Hydra 9 N91-23571

CONGRESSIONAL REPORTS
Strategic missiles: Uncertainties persist in the Advanced Cruise Missile (ACM) program
[AD-A232058] N91-23142

CONGRUENCES
Congruence properties of the process equivalence induced by temporal logic
[RR-831-I-IMAG-118-LIFIA] N91-23810

CONICAL NOZZLES
Pitot surveys of two moderately under-expanded jets N91-23172

CONSERVATION EQUATIONS
High energy dense ribbon beams and high harmonic gyrotron at millimeter wavelengths
[AD-A232839] N91-23470

CONSOLIDATION
A simulation of the draping and a model of the consolidation of commingled fabrics N91-23239

CONSTRAINTS
The limits of the landing process of aircraft
[DLR-FB-90-49] N91-23137
Real-time simulation of constrained dynamic systems N91-23189
Are wait-free algorithms fast
[AD-A232829] N91-23774
Database constraint enforcement: A decompositional approach N91-23980

CONSTRUCTION
Design and construction of a composite airframe for UAV research
[AD-A232422] N91-23143

CONSTRUCTION MATERIALS
Literature review on geotextiles to improve pavements for general aviation airports
[AD-A232871] N91-23199

CONTACT LOADS
A system-approach to the elastohydrodynamic lubrication point-contact problem
[NASA-TM-104342] N91-23439
A moving boundary algorithm for the solution of contact problems in linear elasticity. Part 1: Basic theory and model examples
[FFA-TN-1991-08-PT-1] N91-23759

CONTAINERLESS MELTS
Containerless undercooling and solidification of pure metals
[DLR-FB-90-48] N91-23301

CONTAMINATION
An experimental investigation of vortex pair interaction with a clean or contaminated free surface N91-23419

CONTINUITY EQUATION
Flow between eccentric rotating cylinders N91-23417

CONTINUOUS WAVE LASERS
A 43 watt CW Ti:Sapphire laser
[DE91-010468] N91-23479

CONTOURS
Experimental investigations on the transition from stable to unstable combustion by means of active instability control N91-23165

CONTRAST
Spatiotemporal characteristics of visual localization
[AD-A232734] N91-23715

CONTROL EQUIPMENT
Control aspects of the brushless doubly-fed machine
[DE91-009707] N91-23387

CONTROL SIMULATION
The development of highly practiced skills: A starting point for driver modelling
[IZF-1990-B-16] N91-23719

CONTROL STABILITY
Effects of three-dimensional imposed disturbance on bluff-body near wake flows
[AD-A232137] N91-23447
H-infinity approach to manipulator control N91-23495
Use of a genetic algorithm to analyze robust stability problems
[DE91-005895] N91-23742

CONTROL STICKS
An initial study into the influence of control stick characteristics on the handling qualities of a fly-by-wire helicopter N91-23122

CONTROL SURFACES
Research on aerodynamic control of blade tip clearance flow in air-cooled turbine
[DE91-764223] N91-23182
Analysis of the flutter characteristics of the advanced kinetic energy missile (ADKEM) control surface
[AD-A232377] N91-23193

CONTROL SYSTEMS DESIGN
Unsteady flow structure from swept edges subjected to controlled motion
[AD-A232714] N91-23094
B-1B high AOA testing in the evaluation of a stall inhibitor system N91-23126

Flying qualities of the X-29 forward swept wing aircraft N91-23127
A computer aided multivariable control systems design technique with application to aircraft flying qualities [AD-A232549] N91-23144
Integrated multidisciplinary optimization of actively controlled fiber composite wings N91-23190
Reactive procedure based decision making for satellite control [REPT-911-440-106] N91-23221
The effects of controlling vortex formation on the performance of a dump combustor N91-23270
Raybot: A practical implementation of a hierarchical control system for telerobotic land vehicles [DE90-017029] N91-23507
On the control of two manipulators holding a rigid object in the presence of uncertainty [DE90-017742] N91-23508
An interactive robot control system N91-23790
Planning of visual feedback with robot-sensor co-operation N91-23793
Robot-sensor co-operation planning for visual guidance N91-23794
Worst-case design of optimal controllers over a finite horizon [AD-A232353] N91-23797
Control synthesis based upon a game theoretic approach N91-23831
Applications of fuzzy logic to control and decision making N91-24049
Monitoring and control technologies for bioregenerative life support systems/CELSS N91-24060

CONTROL THEORY
Computerized symbolic closed-form dynamics and control analysis of hybrid rigid and elastic multibody systems N91-23532
Data transfer over multiplexed logical data links sharing a single physical circuit N91-23734
Use of a genetic algorithm to analyze robust stability problems [DE91-005895] N91-23742
Some problems in nonlinear analysis [AD-A232701] N91-23820

CONTROLLABILITY
Handling qualities of highly augmented unstable aircraft summary of an AGARD-FMP working group effort N91-23116
The handling qualities of the STOL and maneuver technology demonstrator from specification to flight test N91-23117
Metrics for roll response flying qualities N91-23118
Handling qualities guidelines for the design of fly-by-wire flight control systems for transport aircraft N91-23119
An initial study into the influence of control stick characteristics on the handling qualities of a fly-by-wire helicopter N91-23122
An investigation into the use of side-arm control for civil rotorcraft applications N91-23123
Determination of decision-height windows for decelerating IMC approaches in helicopters N91-23124
Integration of handling quality aspects into the aerodynamic design of modern unstable fighters N91-23125
Handling qualities evaluation for highly augmented helicopters N91-23128
A review of high angle of attack requirements for combat aircraft N91-23130
X-31A at first flight N91-23131
Evaluation techniques for highly augmented aircraft [DLR-FB-90-35] N91-23191

CONTROLLERS
An initial study into the influence of control stick characteristics on the handling qualities of a fly-by-wire helicopter N91-23122
Thermal control system for the investigation of specific absorption rates for specimens exposed to electromagnetic radiation [AD-A231329] N91-23459
An incremental approach to logic controllers design with Petri nets [REPT-90-030] N91-23748
Worst-case design of optimal controllers over a finite horizon [AD-A232353] N91-23797
Control synthesis based upon a game theoretic approach N91-23831
Applications of fuzzy logic to control and decision making N91-24049

CONVECTION
Theoretical studies of large-scale features of the Earth's mid- to high-latitude ionosphere N91-23641
Assimilation of ERBE data with nonlinear programming technique to improve cloud cover diagnosis N91-23663
The annual march of convection, sea surface temperature, and surface winds in the tropics N91-23667

CONVECTION CLOUDS
Analysis and modeling of summertime convective cloud and precipitation structure over the Southeastern United States [NASA-CR-188119] N91-23670
Grouping of clouds and internal gravity waves in a non-hydrostatic model of moist convection [DM-55] N91-23679

CONVECTIVE HEAT TRANSFER
Simulation of brush insert for leading-edge-passage convective heat transfer [NASA-TM-103801] N91-23409
Developing natural convection in a fluid layer with localized heating and large viscosity variation [DE91-005240] N91-23431
Aero-thermal investigation of a highly loaded transonic linear turbine guide vane cascade. A test case for inviscid and viscous flow computations [VKI-TN-174] N91-23437

CONVERGENCE
Classification using multi-layered perceptrons [AD-A232810] N91-23802

CONVOLUTION INTEGRALS
The transient response of heavily fluid-loaded elastic plates and cylindrical shells N91-23528

COOLING
Modeling second-phase formation during rapid resolidification of stainless steel alloys [DE91-008567] N91-23291
A 43 watt CW Ti:Sapphire laser [DE91-010468] N91-23479

COOLING SYSTEMS
Research on aerodynamic control of blade tip clearance flow in air-cooled turbine [DE91-764223] N91-23182
Fatigue evaluation of piping systems with limited vibration test data [DE91-007167] N91-23543
Cold moderators for pulsed neutron sources [DE91-010594] N91-23866

COPPER ALLOYS
Phase equilibria and solidification of Al-Li and Al-Li-Cu alloys N91-23290
Structure of electrochemically deposited copper on gold (III) alloy [AD-A232345] N91-23303
Phase transformations and microstructural evolution in aged Mn-Cu-based alloys [AD-A232473] N91-23305

COPPER OXIDES
Re-analysis of photoemission data for CuO: Revision of the configuration-energy scheme for cuprate materials [DE91-009952] N91-23296
S-parameter measurements and applications of superconducting flux flow transistors [DE91-009763] N91-23388
Microstructure of epitaxial YBa2Cu3O7 thin films [DE91-009951] N91-23942
Fermi surface of YBCO by DHVA [DE91-009963] N91-23943
Sintering and hot isostatic pressing of Bi2Sr2CaCu2O(x) [DE91-010797] N91-23945

CORIOLIS EFFECT
Maintenance of short-term subtropical wind maxima in the Southern Hemisphere: Observational and modeling study N91-23665

CORRELATION
Estimation of pilot ratings via pilot modeling N91-23121
The direct correlation function of a mixture of hard ions in the mean spherical approximation [AD-A232452] N91-23879

CORRELATORS
Development of a digital correlator to measure the semi-elastic scattering of light [NOTA-INTERNA-955] N91-23895

CORROSION
MHD channel gas-side element erosion-corrosion studies [DE91-008561] N91-23911

CORROSION PREVENTION
Galvanic corrosion of aluminum-matrix composites [AD-A232138] N91-23264

CORROSION RESISTANCE
Deterministic analysis of processes at corroding metal surfaces and the study of electrochemical noise in these systems [DE91-009997] N91-23297
Rapidly solidified metallic alloys with unusual semmetry properties [AD-A232384] N91-23304

CORROSION TESTS
Galvanic corrosion of aluminum-matrix composites [AD-A232138] N91-23264
A conformal oxidation-resistant, plasma-polymerized coating N91-24063
Localized corrosion of high performance metal alloys in an acid/salt environment N91-24066

COSMIC DUST
Studies of the diffuse background and interstellar dust at far ultraviolet wavelengths N91-24003
Ultraviolet gas absorption and dust extinction toward M8 and the outer galactic disk N91-24018

COSMIC RAY SHOWERS
Investigation of the muon component of EAS initiated by primary radiation from Hercules X-1 N91-24037

COSMIC RAYS
Science requirements for Heavy Nuclei Collection (HNC) experiment on NASA Long Duration Exposure Facility (LDEF) Mission 2 [NASA-CR-187527] N91-23887
Hard x ray imaging telescope [DE90-015815] N91-24013
A search for very high-energy gamma rays from Cygnus X-3 N91-24039

COSMOLOGY
Supersymmetric matter at finite temperature N91-23836
Phenomenological aspects of scalar fields in astrophysics, cosmology and particle physics N91-24014
A cosmic superfluid phase [NASA-CR-188171] N91-24016
Boundary conditions in quantum cosmology N91-24020
Primordial lithium, stellar evolution, and cosmology: Lithium in halo stars from standard, diffusive, and rotational stellar evolution and implications for cosmology N91-24024

COST EFFECTIVENESS
The costs and benefits of aircraft availability [AD-A232660] N91-23076
NDE (Nondestructive Examination) development for ceramics for advanced heat engines [DE91-005516] N91-23316
Research and development opportunities for natural gas fueled refrigeration in industrial processes [PB91-136432] N91-23338

COST ESTIMATES
Estimating fixed and variable costs of airframe manufacturers [AD-A232661] N91-23077
Information resources management long-range plan [DE91-009745] N91-23984

COST REDUCTION
Development of a low cost peak shaving generator set [PB91-136374] N91-23332
Specifications for reusable software components [RR-828-I-IMAG-116-LIFIA] N91-23756
Integration of the execution support system for the Computer-Aided Prototyping System (CAPS) [AD-A232015] N91-23761

COSTS
PV concentrators today and tomorrow [DE91-010577] N91-23619

COUETTE FLOW
Mechanics/heat-transfer relation for particulate materials [DE91-008356] N91-23424
Interdisciplinary research on viscoelasticity and rheology [AD-A232700] N91-23454

COUPLED MODES
Backscattering by nonspherical particles, using the coupled-dipole method: An application in radar meteorology [AD-A232371] N91-23373

COUPLES
Modal analysis of multistage gear systems coupled with gearbox vibrations [NASA-TM-103797] N91-23513

COUPLING
Electrochemical parameterization of rhenium redox couples [AD-A232043] N91-23279

CRACK ARREST
Study of static and dynamic fracture using strain measurements [PB91-132217] N91-23524

CRACK OPENING DISPLACEMENT
Evaluation of catastrophic failure risk in pressure vessels. Results of pressure vessel test with a large vessel (HC2-test) [VTT-RR-708] N91-23551

CRACK PROPAGATION
Chevron-notched, flexure tests for measuring the elevated temperature fracture resistance of structural ceramics [DE91-009117] N91-23310

Mechanical behavior and failure phenomenon of an in situ-toughened silicon nitride
[NASA-TM-103741] N91-23311
Potential impact of enhanced fracture-toughness data on fracture mechanics assessment of PWR vessel integrity for pressurized thermal shock
[DE91-009554] N91-23509
Study of static and dynamic fracture using strain measurements
[PB91-132217] N91-23524
A statistical model of fractures N91-23529
Stochastic micromechanical modeling of cleavage fracture in the ductile-brittle transition region N91-23533
Application of elastic and elastic-plastic fracture mechanics methods to surface flaws
[NASA-TM-104964] N91-23539
Threshold for fatigue crack propagation at simulated operating loads
[ESA-TT-1187] N91-23553

CRAY COMPUTERS
The CERBERUS Ver. 02 code: A parallel six-equation thermal-hydraulic-system simulation code
[DE91-010079] N91-23736

CREEP ANALYSIS
Experience with conventional inelastic analysis procedures in very high temperature applications
[DE91-009937] N91-23545
Development of a micromechanic theory of constitutive relations of polycrystalline solids
[AD-A232697] N91-23559

CREEP PROPERTIES
Creep and creep-rupture behavior of Alloy 718
[DE91-007706] N91-23298

CREEP RUPTURE STRENGTH
Creep and creep-rupture behavior of Alloy 718
[DE91-007706] N91-23298

CREEP STRENGTH
Reduction factors for creep strength and fatigue life of modified 9 Cr-1 Mo steel weldments
[DE91-009919] N91-23544

CREEP TESTS
Creep and creep-rupture behavior of Alloy 718
[DE91-007706] N91-23298

CREWS
A test of the American Safety Flight Systems, Inc. prebreather/portable oxygen system
[AD-A232723] N91-23100

CRITERIA
Control synthesis based upon a game theoretic approach N91-23831

CRITICAL EXPERIMENTS
Control of biosonar behavior by the auditory cortex
[AD-A232699] N91-23708

CROP GROWTH
Monitoring and control technologies for bioregenerative life support systems/CELSS N91-24060

CROSS CORRELATION
A method of constructing a pair of pseudorandom sequences with a useful crosscorrelation function
[IAITIC-87-1001] N91-23345

CROSS FLOW
Passive laminar flow control of crossflow vorticity
[NASA-CASE-LAR-13563-1] N91-23410
A theory for fluidelastic instability of tube-support-plate inactive modes
[DE91-009676] N91-23538

CROSS SECTIONS
Calculation of cross sections for binary reactions between heavy ion projectiles and heavy actinide targets
[DE91-010222] N91-23882

CRUISE MISSILES
Strategic missiles: Uncertainties persist in the Advanced Cruise Missile (ACM) program
[AD-A232058] N91-23142

CRYOGENIC FLUID STORAGE
Superplastic forming of Al-Li alloys for lightweight, low-cost structures N91-24065

CRYOGENIC ROCKET PROPELLANTS
Cryogenic hydrogen-induced air-liquefaction technologies N91-23159

CRYOGENIC TEMPERATURE
The strength and toughness of stainless steels at cryogenic temperature
[DE91-009771] N91-23300

CRYOGENICS
Development of a quiet supersonic wind tunnel with a cryogenic adaptive nozzle
[NASA-CR-186769] N91-23195
ISOCAM: The ISO's satellite infra-red camera
[REPT-911-440-104] N91-23468
Sensitive cryogenic transducer development and analysis for use on gravity wave detectors N91-24009
Cryomagmatism in the outer solar system N91-24019

CRYSTAL DEFECTS
Photoresponse studies of ion-damaged germanium for optoelectronic switch applications
[AD-A232091] N91-23400
Strain release in GaAs/Ga(1-x)/In(x)As strained layer superlattices grown on (112) substrates
[DE91-009972] N91-23944

CRYSTAL GROWTH
Rapidly solidified metallic alloys with unusual semmetry properties
[AD-A232384] N91-23304
Oxidation studies of fluorine containing diamond films
[AD-A232696] N91-23328
Protein crystal growth tray assembly
[NASA-CASE-MFS-28507-1] N91-23933
Eureca 1 AMF 117 experiment: An analysis of thermal and solutal transfer during the crystal growth of CdTe by the THM process
[REPT-911-430-118] N91-23947
Eureca 1 AMF 117 experience: Thermal and solutal transfer analysis for CdTe in tellurium during crystal growth by the THM method
[REPT-911-430-120] N91-23948
Contract crystal growth and fabrication services
[AD-A232120] N91-23952
Transport and nucleation processes in the vapor growth of diamond
[AD-A232135] N91-23953
Research and development on advanced silicon carbide thin film growth techniques and fabrication of high power and microwave frequency silicon carbide-based device structures
[AD-A232160] N91-23955
Laser assisted CVD growth of AlN and GaN
[AD-A232379] N91-23957
Development of Si/SiGe heterostructures
[AD-A232747] N91-23961

CRYSTAL LATTICES
Order and disorder in metallic alloys
[DE91-009120] N91-23292
Mean-field theories of the Hubbard model and periodic orbits in chaotic maps N91-23938

CRYSTAL OPTICS
Liquid-crystal characterization using the Z-scan technique
[RSRE-MEMO-4451] N91-23949

CRYSTAL STRUCTURE
First principles calculation of the crystal structures in the 4d transition metals N91-23835
Study of the response of a crystal ball made of NaI(Tl) for heavy ions experiments
[NOTA-INTERNA-957] N91-23874
In-situ surface x ray scattering measurements of electrochemically deposited bismuth on silver (III): Structure, compressibility, and comparison with ex-situ leed measurements
[AD-A232624] N91-23880
Structural and electronic properties of the ordered ternary 3-5 semiconductors N91-23936
Strain release in GaAs/Ga(1-x)/In(x)As strained layer superlattices grown on (112) substrates
[DE91-009972] N91-23944
Synthesis and characterization of indium-arsenic compounds containing a four-membered In-Ad-In-As or In-As-In-Cl ring: Crystal structures of ((Me3SiCH2)2 InAs(SiMe3)2)2 and (Me3SiCH2)2 InAs(SiMe3)2 In(CH2SiMe3)2Cl
[AD-A232368] N91-23956
Surface x ray scattering measurements of the substrate induced spatial modulation of an incommensurate adsorbed monolayer
[AD-A232625] N91-23959

CRYSTAL SURFACES
Surface x ray scattering measurements of the substrate induced spatial modulation of an incommensurate adsorbed monolayer
[AD-A232625] N91-23959

CRYSTALLINITY
Generation of continuous liquid crystalline polymer reinforcements in thermoplastics by a novel blending process
[AD-A232824] N91-23330

CRYSTALLIZATION
A Raman spectroscopic and electrochemical study of the photoinduced crystallization of triethylenediamine triiodide upon a silver electrode
[AD-A232828] N91-23963

CRYSTALLOGRAPHY
Los Alamos Science, Number 19, 1990
[DE91-009371] N91-23855

CRYSTALS
A high resolution study of the Cu K alpha(sub 1,2) x-ray emission lines N91-23841
Contract crystal growth and fabrication services
[AD-A232120] N91-23952

CUES
The flying qualities influence of delay in the fighter pilot's cuing environment N91-23120

CULTURE (SOCIAL SCIENCES)
Cultural parameters of stress
[AD-A232526] N91-23713

CURRENT DENSITY
Channel diagnostics for the multi-pulse-propagation experiments at ATA
[DE91-009772] N91-23466
Theory of the critical current density in YBa2Cu3O7 ceramics
[DE91-009443] N91-23940

CURRENT DISTRIBUTION
Density channel tracking studies on Pulserad
[AD-A232649] N91-23888

CURVATURE
Linear bending of curved tubes without boundary influence
[ETN-91-99255] N91-23552

CYCLOTRON FREQUENCY
ICRF heating on the Burning Plasma Experiment (BPX)
[DE91-010390] N91-23913

CYCLOTRON RESONANCE
High quality three dimensional electron gases in semiconductors
[AD-A232779] N91-23406

CYCLOTRON RESONANCE DEVICES
Observation of harmonic gyro-backward-wave oscillation in a 100 GHz CARM oscillator experiment
[AD-A232063] N91-23398
High energy dense ribbon beams and high harmonic gyrotron at millimeter wavelengths
[AD-A232839] N91-23470

CYGNUS CONSTELLATION
A search for very high-energy gamma rays from Cygnus X-3 N91-24039

CYLINDRICAL SHELLS
The transient response of heavily fluid-loaded elastic plates and cylindrical shells N91-23528

CYTOLOGY
Molecular studies of cytokine induction
[AD-A232221] N91-23707

D

DAMPING
Constant of motion and dynamic equations for one-dimensional autonomous system and radiation damping
[DE91-011002] N91-23547

DARK MATTER
A proposed search for dark-matter axions in the 0.6-16 micro-eV range
[NASA-CR-188173] N91-24015
A cosmic superfluid phase
[NASA-CR-188171] N91-24016

DATA ACQUISITION
Small Explorer project: Submillimeter Wave Astronomy Satellite (SWAS). Mission operations and data analysis plan
[NASA-CR-186954] N91-23212
Collection and processing of oceanographic data at CLS N91-23603

DATA BASE MANAGEMENT SYSTEMS
Implementation of the FAA research and development electromagnetic database
[DE91-010063] N91-23674
Robustness in replicated databases N91-23981
The intelligent database: Using INGRES to manage the external analysis of your data
[DE91-010465] N91-23986
Security aspects of database management systems
[DE91-010677] N91-23987
A methodology for handling data errors and inconsistencies in database conversions
[AD-A232113] N91-23994

DATA BASES
Differential GPS terminal area test results
[AD-A232668] N91-23106
CRREL research on materials in cold environments
[AD-A232133] N91-23280
The Berlenga underwater survey project N91-23577
National stream survey database guide
[PB91-141804] N91-23625
Auroral boundary index from 1983 to 1990
[AD-A232845] N91-23660
Life cycle management automation programmer's manual
[AD-A232247] N91-23769
An in-depth analysis of concurrent B-tree algorithms
[AD-A232287] N91-23770

Processing problems in the IRUS queries: An empirical verification of problem coverage in the natural language sourcebook
[AD-A232780] N91-23800
Life cycle management automation user's manual, version 1.1
[AD-A232096] N91-23968
Building a generalized distributed system model
[NASA-CR-188181] N91-23970
Effects of distributed database modeling on evaluation of transaction rollbacks N91-23972
Measuring the effects of distributed database models on transaction availability measures N91-23973
Performance analysis of static locking in replicated distributed database systems N91-23974
A note on the performance analysis of static locking in distributed database systems N91-23975
Query processing for deductive databases with null values N91-23979
Database constraint enforcement: A decompositional approach N91-23980
Robustness in replicated databases N91-23981
An expert system for searching in full-text N91-23983
Active Design Database (ADDB) user's manual
[DE91-010431] N91-23985
The intelligent database: Using INGRES to manage the external analysis of your data
[DE91-010465] N91-23986
Null values in definite programs
[AD-A232065] N91-23992

DATA COMPRESSION
Fractal image compression of Rayleigh, Raman, LIF and LDV data in turbulent reacting flows
[AD-A232237] N91-23449
Image data compression in JPEG standard
[DLR-FB-90-59] N91-23746
Digital data registration and differencing compression system
[NASA-CASE-SSC-00010-1] N91-23976
Digital CODEC for real-time processing of broadcast quality video signals at 1.8 bits/pixel N91-24067
Recent advances in coding theory for near error-free communications N91-24068

DATA LINKS
Data transfer over multiplexed logical data links sharing a single physical circuit N91-23734

DATA MANAGEMENT
Astromag data system concept
[NASA-CR-186341] N91-23211
Building a generalized distributed system model
[NASA-CR-188181] N91-23970
Effects of distributed database modeling on evaluation of transaction rollbacks N91-23972
Measuring the effects of distributed database models on transaction availability measures N91-23973
The Land Analysis System (LAS) N91-24054

DATA PROCESSING
Small Explorer project: Submillimeter Wave Astronomy Satellite (SWAS). Mission operations and data analysis plan
[NASA-CR-186954] N91-23212
Laboratory study of the thermochemical properties of materials used in spacecraft
[AD-A232124] N91-23228
High-quality 800-b/s voice processing algorithm
[AD-A232352] N91-23372
Arctic remote autonomous measurement platform post CEAREX engineering report
[AD-A232843] N91-23471
Extraction of mesoscale ocean currents information from Geosat altimeter data N91-23594
Collection and processing of oceanographic data at CLS N91-23603
Performance analysis of garbage collection and dynamic reordering in a Lisp system
[NASA-CR-188205] N91-23738
Information dynamics of self-programmable matter
[DE91-009954] N91-23740
Analysis of neutron noise spectra using neural networks
[DE91-007676] N91-23785
Statistical methods and neural network approaches for classification of data from multiple sources
[NASA-CR-188207] N91-23786
Five-year plan for meeting the automatic data processing and telecommunications needs of the Federal Government
[PB91-103549] N91-23982
Information system for environmental chemicals
[GSF-BER-21/90] N91-23990
Software reengineering N91-24047

DATA PROCESSING EQUIPMENT
Information system for environmental chemicals
[GSF-BER-21/90] N91-23990

DATA REDUCTION
Data-reduction and analysis procedures used in NIST's thermomechanical processing research
[PB91-132282] N91-23523
Analysis of neutron noise spectra using neural networks
[DE91-007676] N91-23785

DATA SMOOTHING
A smoothing algorithm for upper-air soundings
[AD-A232853] N91-23661

DATA STORAGE
Evaluation of ferroelectric materials for memory applications
[AD-A232112] N91-23728
Data type coherency in heterogeneous shared memory multiprocessors
[AD-A232114] N91-23729
The reduced version of the DERF 2 data set on a WORM optical disk
[DM-54] N91-23991

DATA STRUCTURES
Hypermedia 1990 structured Hypertext tutorial
[NASA-CR-187921] N91-23731
Data transfer over multiplexed logical data links sharing a single physical circuit N91-23734
An in-depth analysis of concurrent B-tree algorithms
[AD-A232287] N91-23770

DATA SYSTEMS
Astromag data system concept
[NASA-CR-186341] N91-23211
Measuring the effects of distributed database models on transaction availability measures N91-23973

DATA TRANSFER (COMPUTERS)
Data transfer over multiplexed logical data links sharing a single physical circuit N91-23734

DATA TRANSMISSION
Error control coding for multi-frequency modulation
[AD-A232421] N91-23374
Data transfer over multiplexed logical data links sharing a single physical circuit N91-23734
Fiber Optic Tactical Local Network (FOTLAN) N91-24072

DEACTIVATION
Magnetostrictive roller drive motor
[NASA-CASE-GSC-13369-1] N91-23380

DECISION MAKING
Reactive procedure based decision making for satellite control
[REPT-911-440-106] N91-23221
A survey of decision tree classifier methodology
[NASA-CR-188208] N91-23806
Topics in inference and decision-making with partial knowledge
[NASA-CR-188209] N91-23821
Photonic materials and devices for optical information processing and computing applications
[AD-A232771] N91-23907
Information plan study: A strategy model
[ISBN-90-6233-638-8] N91-23988
Applications of fuzzy logic to control and decision making N91-24049

DECISION THEORY
A survey of decision tree classifier methodology
[NASA-CR-188208] N91-23806
Sufficient comparison and modeling of forecasts N91-23829

DECODING
Error control coding for multi-frequency modulation
[AD-A232421] N91-23374
Recent advances in coding theory for near error-free communications N91-24068

DECOMPOSITION
Phase transformations and microstructural evolution in aged Mn-Cu-based alloys
[AD-A232473] N91-23305

DECOMPRESSION SICKNESS
A KO2 rebreather for EVA denitrogenation procedure N91-23588

DEEP SPACE
A 30 GHz monolithic receive module
[NASA-CR-187085] N91-23346
Multisensory telerobotic concepts for space and underwater applications N91-23584

DEEP WATER
Multisensory telerobotic concepts for space and underwater applications N91-23584

DEFECTS
Parametric study in weld mismatch of longitudinally welded SSME HPFTP inlet
[NASA-TM-103534] N91-23502
Programmable remapper for image processing
[NASA-CASE-MSC-21350-1] N91-23724

DEFENSE PROGRAM
Large space structures fielding plan
[AD-A232097] N91-23227
High precision applications of the global positioning system N91-24073

DEFOLIATION
Analysis on forest decline classification of the beech using airborne multispectral scanner data
[DLR-FB-90-56] N91-23614

DEFORMATION
Automated handling and assembling of non-rigid objects
[AD-A231246] N91-23489
Effects of rim thickness on spur gear bending stress
[NASA-TM-104388] N91-23500
Interlaminar strains at the free-edge of a hole for thick composites in compression
[DE91-008883] N91-23535
Mechanical states in wound heterogeneous tapes by the finite element method
[DE91-009255] N91-23536

DEGRADATION
Quantifying performance degradation due to the human-machine interface of telemanipulators
[AD-A232814] N91-23723

DEGREES OF FREEDOM
On kinematic design of serial link manipulators
[DE91-009414] N91-23499

DEICERS
Advanced ice protection systems test in the NASA Lewis icing research tunnel
[NASA-TM-103757] N91-23183

DEICING
Icing simulation: A survey of computer models and experimental facilities
[NASA-TM-104366] N91-23087
Advanced ice protection systems test in the NASA Lewis icing research tunnel
[NASA-TM-103757] N91-23183

DELAMINATING
Strain rate sensitivity of polymer-matrix composites under mode I delamination
[AD-A232761] N91-23268

DELTA WINGS
The performance of 60 deg delta wings: The effects of leading edge radius on vortex flaps and the wing
[CRANFIELD-AERO-9004] N91-23092
Unsteady flow structure from swept edges subjected to controlled motion
[AD-A232714] N91-23094
The performance of 60 deg delta wings: The effects of leading edge radius and vortex flaps
[CRANFIELD-AERO-9002] N91-23140
An experimental investigation of vortex pair interaction with a clean or contaminated free surface N91-23419

DEMAND (ECONOMICS)
Geomagnetic storms: Potential economic impacts on electric utilities
[DE91-009523] N91-24036

DENDRITIC CRYSTALS
Containerless undercooling and solidification of pure metals
[DLR-FB-90-48] N91-23301

DENITROGENATION
A KO2 rebreather for EVA denitrogenation procedure N91-23588

DENSITY (MASS/VOLUME)
Mechanics/heat-transfer relation for particulate materials
[DE91-008356] N91-23424

DENSITY DISTRIBUTION
Channel diagnostics for the multi-pulse-propagation experiments at ATA
[DE91-009772] N91-23466
A numerical model of laser induced fluorescence in a hydrogen plasma
[AD-A232240] N91-23482
Density channel tracking studies on Pulserad
[AD-A232649] N91-23888
Investigation of the muon component of EAS initiated by primary radiation from Hercules X-1 N91-24037

DENSITY MEASUREMENT
Nondestructive measurement of thickness and density of composite materials by Compton backscattering
[REPT-911-430-112] N91-23255
Iron density measurements in polar atmosphere
[BONN-IR-90-53] N91-23654
Heavy ion beam probe measurements of ECH method plasma in the advanced toroidal facility
[DE91-010391] N91-23917
Investigation of the muon component of EAS initiated by primary radiation from Hercules X-1 N91-24037

DEOXYRIBONUCLEIC ACID
AFRRI reports, October - December 1990
[AD-A232236] N91-23283
Problems in understanding the organization, structure and function of chromosomes
[DE91-009939] N91-23695

New hosts and vectors for genome cloning
[DE91-009996] N91-23696
Robotics for recombinant DNA and human genetics research
[DE90-016440] N91-23697
Isolation, cloning and expression of the genes for microbial polyurethane degradation
[AD-A232108] N91-23699

DEPTH MEASUREMENT
The transfer of technology to measure skin burn depth in humans N91-24076

DESIGN ANALYSIS
Aerodynamic preliminary analysis system 2. Part 2: User's manual
[NASA-CR-182077] N91-23081
MIL-STD-1797 is not a cookbook N91-23111
A new architecture and expert system for aircraft design synthesis N91-23132
Application of multidisciplinary optimization methods to the design of a supersonic transport
[NASA-TM-104073] N91-23135
Design techniques for dual mode ram-scramjet combustors N91-23166
Performance characteristics of hypersonic detonation wave ramjets N91-23168
The 2-D supersonic nozzle design N91-23176
Integrated multidisciplinary optimization of actively controlled fiber composite wings N91-23190
Development of a quiet supersonic wind tunnel with a cryogenic adaptive nozzle
[NASA-CR-186769] N91-23195
Conceptual design and system studies for a 600 kW repetitive pulse transformer
[DE91-010585] N91-23389
Design and implementation of a packet switched routing chip
[AD-A232286] N91-23401
A computationally efficient modelling of laminar separation bubbles N91-23411
Effects of rim thickness on spur gear bending stress
[NASA-TM-104388] N91-23500
Maximum life spur gear design
[NASA-TM-104361] N91-23514
Incorporating finite element analysis into component life and reliability
[NASA-TM-104400] N91-23550
How to design efficient MMI for space N91-23586
Automatic formal verification of VHDL descriptions: A first prototype
[RR-823-I] N91-23726
Gas core reactors for direct nuclear propulsion
[DE91-010050] N91-23884
Transport analysis of stellarator reactors
[DE91-010489] N91-23914

DESTRUCTION
Destructive physical analysis results of Ni/H2 cells cycled in LEO regime
[NASA-TM-104382] N91-23233

DESYNCHRONIZATION (BIOLOGY)
Some problems of desynchronisation of sleep-wakefulness and circadian rhythms for long duration spaceflights N91-23570

DETECTION
Multiphoton detection techniques for F and F2
[AD-A232641] N91-23286
Spatiotemporal characteristics of visual localization
[AD-A232734] N91-23715

DETONATION WAVES
Performance characteristics of hypersonic detonation wave ramjets N91-23168
Analytical and experimental investigations of the oblique detonation wave engine concept N91-23169
Non-linear interaction of a detonation/vorticity wave
[NASA-CR-187550] N91-23434

DEUTERIUM
Transport analysis of stellarator reactors
[DE91-010489] N91-23914

DIAGNOSIS
Development and utilization of new diagnostics for dense-phase pneumatic transport
[DE91-008947] N91-23339
Assimilation of ERBE data with nonlinear programming technique to improve cloud cover diagnosis N91-23663
A method for machinery condition monitoring of transient phenomena using the pseudo Wigner-Ville distribution
[AD-A232014] N91-23760
Portable intelligent diagnostic aids
[AD-A230883] N91-23782

DIAMONDS
Oxidation studies of fluorine containing diamond films
[AD-A232696] N91-23328
Transport and nucleation processes in the vapor growth of diamond
[AD-A232135] N91-23953

DIELECTRIC PERMEABILITY
A transmission line method for the measurement of microwave permittivity and permeability
[RSRE-MEMO-4450] N91-23394

DIELECTRICS
Design rules and system testing methods
[REPT-911-440-107] N91-23222

DIES
Gas contents and weldability of aluminum die castings
[ETN-91-99188] N91-23302
Unipunch capability study
[DE91-008825] N91-23498

DIESEL ENGINES
Low heat rejection diesel ceramic coupon tests
[DE91-006274] N91-23318

DIFFERENCE EQUATIONS
Digital data registration and differencing compression system
[NASA-CASE-SSC-00010-1] N91-23976

DIFFERENTIAL EQUATIONS
Strategy Combining Regionally Adapted Processes (SCRAP)
[AD-A232158] N91-23448
Nilpotent normal form via Carleman linearization (for systems of ordinary differential equations)
[RR-838-M] N91-23809

DIFFRACTION
Interlaminar strains at the free-edge of a hole for thick composites in compression
[DE91-008883] N91-23535
Unified aeroacoustics analysis for high speed turboprop aerodynamics and noise. Volume 2: Development of theory for wing shielding
[NASA-CR-185192] N91-23849

DIFFUSION THEORY
Some problems in nonlinear analysis
[AD-A232701] N91-23820

DIFFUSIVITY
Primordial lithium, stellar evolution, and cosmology: Lithium in halo stars from standard, diffusive, and rotational stellar evolution and implications for cosmology N91-24024

DIGESTING
Molecular studies of cytokine induction
[AD-A232221] N91-23707

DIGITAL COMPUTERS
Intelligent vision system for autonomous vehicle operations N91-24046

DIGITAL DATA
Development of a digital correlator to measure the semi-elastic scattering of light
[NOTA-INTERNA-955] N91-23895
Digital data registration and differencing compression system
[NASA-CASE-SSC-00010-1] N91-23976

DIGITAL ELECTRONICS
A submicron resolution monolithic capacitive displacement sensor with digital output
[DE91-009765] N91-23465

DIGITAL RADAR SYSTEMS
Digital beamforming and pulse compression in an adaptive array radar system
[AD-A232713] N91-23377

DIGITAL SYSTEMS
ADFCS and NOTAR (trademark): Two ways to fix flying qualities N91-23110
SAR processor for the ERS-1 data phase 1, simple processor
[FEL-90-B033] N91-23359
A controlled master frequency oscillator for the SSC low energy booster
[DE91-011004] N91-23391
A submicron resolution monolithic capacitive displacement sensor with digital output
[DE91-009765] N91-23465
On the initialization problem in the design of structurally constrained digital regulators
[REPT-90-039] N91-23749
A field-deployable digital acoustic measurement system N91-24078

DIGITAL TECHNIQUES
Automatic particle sizing from rocket motor holograms
[AD-A232553] N91-23236
Research and development involved in creating a quantitative EEG cartography wide band analysis system
[LAAS-91002] N91-23705
Digital CODEC for real-time processing of broadcast quality video signals at 1.8 bits/pixel N91-24067

DIMENSIONAL ANALYSIS
Dynamic study of cyclically symmetric structures: Application to rotating a wheel of a centrifugal compressor
[ISAL-91-0004] N91-23844

DIODES
Strained quantum well leaky-mode diode laser arrays
[DE91-009982] N91-23477

DIRECTION FINDING
The 2-D acousto-optic signal processors for simultaneous spectrum analysis and direction finding
[AD-A232148] N91-23367

DIRECTIONAL CONTROL
ADFCS and NOTAR (trademark): Two ways to fix flying qualities N91-23110

DISCRETE FUNCTIONS
Benchmark measurements and calculations of a 3-dimensional neutron streaming experiment
[DE91-010692] N91-23867

DISK GALAXIES
Recent star formation and the galaxy collisions in NGC 520 N91-24021

DISPERSING
Sensitivity of numerical dispersion modeling to explosive source parameters
[DE91-009476] N91-23631

DISPLACEMENT
Poly(1,3,4-oxadiazoles) via aromatic nucleophilic displacement
[NASA-CASE-LAR-14427-1] N91-23237
Linear bending of curved tubes without boundary influence
[ETN-91-99255] N91-23552

DISPLACEMENT MEASUREMENT
A submicron resolution monolithic capacitive displacement sensor with digital output
[DE91-009765] N91-23465

DISPLAY DEVICES
Precision runway monitor demonstration report
[AD-A232671] N91-23198
Development of Si/SiGe heterostructures
[AD-A232747] N91-23961

DISSOCIATION
A numerical model of laser induced fluorescence in a hydrogen plasma
[AD-A232240] N91-23482

DISTANCE MEASURING EQUIPMENT
Effect of atmospheric variations on electromagnetic distance measurements
[DE91-009726] N91-23349

DISTORTION
The effect of combustor flow nonuniformity on the performance of hypersonic nozzles N91-23173
Phase transformations and microstructural evolution in aged Mn-Cu-based alloys
[AD-A232473] N91-23305

DISTRIBUTED PARAMETER SYSTEMS
Approximation methods for the identification and control of distributed parameter systems with applications to flexible structures
[AD-A232805] N91-23801

DISTRIBUTED PROCESSING
Decentralized computing technology for fault-tolerant, survivable C3I systems. Volume 3: System/subsystem specification
[AD-A232291] N91-23371
Saturation and vote for the fault tolerance in distributed systems
[LAAS-90390] N91-23727
Dynamic load balancing on highly parallel multicomputer systems N91-23777
A distributed problem-solving approach to rule induction: Learning in distributed artificial intelligence systems
[AD-A232822] N91-23803
Building a generalized distributed system model N91-23971
Distributed, cooperating knowledge-based systems N91-24044
Fiber Optic Tactical Local Network (FOTLAN) N91-24072

DISTRIBUTION FUNCTIONS
Simulation of probabilistic wind loads and building analysis
[NASA-TM-103744] N91-23549
Theoretical studies of QSO absorption lines and the intergalactic medium N91-24025

DIURNAL VARIATIONS
Atmospheric leakage and condensate production in NASA's biomass production chamber. Effect of diurnal temperature cycles
[NASA-TM-103819] N91-23718

DIVING (UNDERWATER)
Space and Sea
[ESA-SP-312] N91-23563
The diving laboratory as a simulation environment for manned spaceflight N91-23564
Subsea habitats and space simulation N91-23567
Real time analysis systems of the physical parameters of the environment and the state of a human organism for a long term exposure at different gas mixtures and pressure up to 100 bar N91-23568
Manned diving activities in JAMSTEC N91-23572

Comparisons between underwater and space working environments for on board activities optimization (Columbus space programme) N91-23574

DOCUMENT STORAGE
Computer center reference manual, volume 2 [AD-A232370] N91-23781

DOCUMENTS
Antenna performance influenced by the finite extent and conductivity of ground planes: A collection of reprints [AD-A232132] N91-23366
Hypermedia 1990 structured Hypertext tutorial [NASA-CR-187921] N91-23731
A guide to experimental elementary particle physics literature, 1985-1989 [DE91-010209] N91-23856
An expert system for searching in full-text N91-23983

DOPED CRYSTALS
Oxidation studies of fluorine containing diamond films [AD-A232696] N91-23328
Effect of transition metal dopants on high T(sub c) superconductivity [PB91-130138] N91-23934
Advances in silicon carbide Chemical Vapor Deposition (CVD) for semiconductor device fabrication [NASA-TM-104410] N91-23946

DOPPLER RADAR
Backscattering by nonspherical particles, using the coupled-dipole method: An application in radar meteorology [AD-A232371] N91-23373
The terminal Doppler weather radar tornadic vortex signature detection algorithm [DOT-FAA-NR-91-5] N91-23675
Investigation of micro- and macrophysical structures and processes in hail clouds with respect to their modification [DLR-FB-90-38] N91-23677

DOWNWASH
A vortex panel method for calculating aircraft downwash on parachute trajectories [DE91-009764] N91-23085
Airborne rescue system [NASA-CASE-ARC-11909-1] N91-23095

DRAG
The drag of spheres at porosites ranging from an isolated sphere to a packed bed [CRANFIELD-AERO-9012] N91-23444

DRAG REDUCTION
Passive laminar flow control of crossflow vorticity [NASA-CASE-LAR-13563-1] N91-23410
Fundamental hydrodynamics research [AD-A232650] N91-23451

DROPS (LIQUIDS)
An experimental method for studying combustion of an unsupported fuel droplet at reduced gravity N91-23273
The solidification of a molten droplet on an inclined plane [NPL-DMM(A)-20] N91-23438

DUCTED ROCKET ENGINES
Highly integrated ducted rocket propulsion modules for future hypersonic tactical missiles N91-23171

DUMP COMBUSTORS
The effects of controlling vortex formation on the performance of a dump combustor N91-23270

DURABILITY
Development of a low cost peak shaving generator set [PB91-136374] N91-23332

DUST
Studies of the diffuse background and interstellar dust at far ultraviolet wavelengths N91-24003

DWARF GALAXIES
Recent star formation and the galaxy collisions in NGC 520 N91-24021

DYE LASERS
Signals and noise in lasers and atom-field interactions N91-23475
High-power performance of a copper laser pumped dye master-oscillator-power-amplifier chain [DE91-010460] N91-23478
Bimanes and related heterocycles as laser dyes [AD-A232335] N91-23484

DYES
Bimanes and related heterocycles as laser dyes [AD-A232335] N91-23484

DYNAMIC CHARACTERISTICS
An initial study into the influence of control stick characteristics on the handling qualities of a fly-by-wire helicopter N91-23122
Real-time simulation of constrained dynamic systems N91-23189
Determination of the deviatoric material response functions for prestrained rubbers [FFA-TN-1990-29] N91-23321
A two-scale solution of the forced Rayleigh-Plesset equation governing the dynamics of cavitation bubble vaporous growth [AD-A232129] N91-23446

DYNAMIC CONTROL
Worst-case design of optimal controllers over a finite horizon [AD-A232353] N91-23797
Degeneration of linear multivariable systems under high gain and dynamic compensation N91-23830

DYNAMIC LOADS
Dynamic load balancing on highly parallel multicomputer systems N91-23777

DYNAMIC MODELS
Target maneuver models for improved homing guidance N91-23101
Estimation of pilot ratings via pilot modeling N91-23121
Reacting shock waves in hypersonic propulsion applications N91-23174
Computational life prediction methodology for mechanical systems using dynamic simulation, finite element analysis, and fatigue life prediction methods N91-23494
An analytic study of general dynamic model and nonlinear feedback control of flexible robot arms N91-23497
On the control of two manipulators holding a rigid object in the presence of uncertainty [DE90-017742] N91-23508
Time-optimal motion of robotic manipulators including nonlinear dynamics [LAAS-90403] N91-23516
A statistical model of fractures N91-23529
Computerized symbolic closed-form dynamics and control analysis of hybrid rigid and elastic multibody systems N91-23532
Dynamic study of cyclically symmetric structures: Application to rotating a wheel of a centrifugal compressor [ISAL-91-0004] N91-23844
Pressure dynamics modeling for the design of the advanced neutron source reactor [DE91-007860] N91-23883

DYNAMIC RESPONSE
Integrated multidisciplinary optimization of actively controlled fiber composite wings N91-23190
Determination of the deviatoric material response functions for prestrained rubbers [FFA-TN-1990-29] N91-23321
Control aspects of the brushless doubly-fed machine [DE91-009707] N91-23387
Reduced vector basis for dynamic analysis of large damped structures N91-23525
Approximating the dynamic response of strain-hardening structures [DE91-006392] N91-23534
Computational simulation of acoustic fatigue for hot composite structures [NASA-TM-104379] N91-23548

DYNAMIC STRUCTURAL ANALYSIS
Use of personal computers in performing a linear modal analysis of a large finite-element model [DE91-010112] N91-23541

E

EARTH ATMOSPHERE
Energy-related environmental issues in a global context [DE91-009538] N91-23627

EARTH IONOSPHERE
Theoretical studies of large-scale features of the Earth's mid- to high-latitude ionosphere N91-23641
The polar wind and ionospheric outflow N91-23645
Ionosphere 1984, volume 72 [ISSN-0211-5166] N91-23649
Thermal ion upwelling in the high-altitude ionosphere [AD-A232372] N91-23657
A method for solving Poisson's equation in geophysical and astrophysical plasma [AERONOMICA-ACTA-A-357-1990] N91-23925

EARTH MAGNETOSPHERE
Echo 7: Magnetospheric properties determined by artificial electron beams N91-23644
The polar wind and ionospheric outflow N91-23645
A method for solving Poisson's equation in geophysical and astrophysical plasma [AERONOMICA-ACTA-A-357-1990] N91-23925

EARTH OBSERVATIONS (FROM SPACE)
Conference on Space Technology: Satellite Application Development [REPT-911-440-103] N91-23219

EARTH OBSERVING SYSTEM (EOS)
Potential commercial uses of EOS remote sensing products N91-24055

EARTH ORBITS
Destructive physical analysis results of Ni/H2 cells cycled in LEO regime [NASA-TM-104382] N91-23233

EARTH RADIATION BUDGET EXPERIMENT
Assimilation of ERBE data with nonlinear programming technique to improve cloud cover diagnosis N91-23663

EARTH RESOURCES
The Land Analysis System (LAS) N91-24054

ECCENTRICITY
Flow between eccentric rotating cylinders N91-23417

ECHOES
Control of biosonar behavior by the auditory cortex [AD-A232699] N91-23708

ECLIPSING BINARY STARS
Applications of speckle interferometry and speckle photometry to the Hyades cluster N91-24001
The Black Widow pulsar PSR 1957+20: A potential VHE gamma-ray source N91-24038

ECOLOGY
Proceedings of the Second Glacier Bay Science Symposium [PB91-110163] N91-23634

ECONOMIC DEVELOPMENT
Eastern Europe: Please stand by [PB91-14336] N91-23348

ECONOMICS
Software reengineering N91-24047

ECOSYSTEMS
Proceedings of the Second Glacier Bay Science Symposium [PB91-110163] N91-23634

EDDY VISCOSITY
A one dimensional wind profile model with stability and eddy viscosity estimations from sodar data [DM-56] N91-23680

EDEMA
Transcapillary fluid shifts in head and neck tissues during and after simulated microgravity [NASA-TM-103847] N91-23704

EDGE DETECTION
Image wavelet decomposition and applications [NASA-CR-188217] N91-23787

EDUCATION
Quantifying improved visual performance through vision training [AD-A232799] N91-23716
Intelligent computer-aided training and tutoring N91-24042

EIGENVALUES
Mapping an adaptable Eigenstructure technique onto the topologix hypercube [AD-A232032] N91-23764

EIGENVECTORS
Mapping an adaptable Eigenstructure technique onto the topologix hypercube [AD-A232032] N91-23764

EINSTEIN EQUATIONS
Symmetries in general relativity N91-23966

EKMAN LAYER
A numerical study of the stratified turbulent Ekman layer N91-23421

EL NINO
Atmospheric teleconnections: Emphasis on the El Nino/Southern Oscillation and monsoons N91-23636

ELASTIC BUCKLING
Finite element analysis of the lateral buckling of a cantilevered I Beam [DE91-010123] N91-23527

ELASTIC DEFORMATION
Computerized symbolic closed-form dynamics and control analysis of hybrid rigid and elastic multibody systems N91-23532
On the construction of two-phase equilibria in a non-elliptic hyperelastic material [AD-A232628] N91-23558

ELASTIC PLATES
The transient response of heavily fluid-loaded elastic plates and cylindrical shells N91-23528

ELASTIC PROPERTIES
Stress analysis of a double-doubler joint in composite structure N91-23530
Mechanical stress states in heterogeneous, wound rolls [DE91-009257] N91-23537
Application of elastic and elastic-plastic fracture mechanics methods to surface flaws [NASA-TM-104964] N91-23539
A moving boundary algorithm for the solution of contact problems in linear elasticity. Part 1: Basic theory and model examples [FFA-TN-1991-08-PT-1] N91-23759

ELASTIC SCATTERING
Los Alamos Science, Number 19, 1990
[DE91-009371] N91-23855
Development of a digital correlator to measure the semi-elastic scattering of light
[NOTA-INTERNA-955] N91-23895
ELASTOHYDRODYNAMICS
A system-approach to the elastohydrodynamic lubrication point-contact problem
[NASA-TM-104342] N91-23439
ELASTOMERS
Chain propagation/step propagation polymerization. Regular thermoplastic elastomers
[AD-A232356] N91-23324
ELECTRIC BATTERIES
Conceptual design study of high-performance sodium/metal chloride batteries for electric vehicle applications
[DE91-009618] N91-23383
Solid polymer electrolytes for rechargeable batteries
[DE91-010231] N91-23384
Characterization of active materials and electrodes for battery R and D
[DE91-010758] N91-23390
ELECTRIC CONDUCTORS
Calculation of electromagnetic fields in the near-field region of a moving scattering object
[FEL-90-B216] N91-23361
ELECTRIC CONNECTORS
Parametric modeling and estimation of pulse propagation on microwave integrated circuit interconnections
[AD-A232465] N91-23404
ELECTRIC CONTACTS
A system-approach to the elastohydrodynamic lubrication point-contact problem
[NASA-TM-104342] N91-23439
ELECTRIC CONTROL
The electrical flight control system of A320 Airbus: A fault tolerant system
[REPT-911-111-103] N91-23192
ELECTRIC CURRENT
Recent advances with quiescent power supply current (I(sub DDQ)) testing at Sandia using the HP82000
[DE91-009254] N91-23382
Theory of the critical current density in YBa2Cu3O7 ceramics
[DE91-009443] N91-23940
ELECTRIC DIPOLES
Backscattering by nonspherical particles, using the coupled-dipole method: An application in radar meteorology
[AD-A232371] N91-23373
ELECTRIC DISCHARGES
Analysis of the VHF-UHF electromagnetic radiation of lightning: Application to a model of the negative stepped leader propagation
[ESA-TT-1172] N91-23363
ELECTRIC FIELD STRENGTH
A study of PC-Based HF ionospheric propagation predictions for use in naval communications
[AD-A232466] N91-23375
ELECTRIC FIELDS
Re-analysis of photoemission data for CuO: Revision of the configuration-energy scheme for cuprate materials
[DE91-009952] N91-23296
Analysis of the VHF-UHF electromagnetic radiation of lightning: Application to a model of the negative stepped leader propagation
[ESA-TT-1172] N91-23363
Transport analysis of stellarator reactors
[DE91-010489] N91-23914
ELECTRIC GENERATORS
Control aspects of the brushless doubly-fed machine
[DE91-009707] N91-23387
ELECTRIC MOTOR VEHICLES
Conceptual design study of high-performance sodium/metal chloride batteries for electric vehicle applications
[DE91-009618] N91-23383
ELECTRIC MOTORS
Composite ceramic superconducting wires for electric motor applications
[AD-A232074] N91-23951
ELECTRIC POTENTIAL
Characterization of active materials and electrodes for battery R and D
[DE91-010758] N91-23390
Pulsed power performance of the new RLA (Recirculating Linear Accelerator)
[DE91-004723] N91-23885
ELECTRIC POWER PLANTS
Geomagnetic storms: Potential economic impacts on electric utilities
[DE91-009523] N91-24036
ELECTRIC WIRE
Composite ceramic superconducting wires for electric motor applications
[AD-A232074] N91-23951
ELECTRICAL FAULTS
Recent advances with quiescent power supply current (I(sub DDQ)) testing at Sandia using the HP82000
[DE91-009254] N91-23382
Solutions to current induced avalanche burnout
[DE90-013196] N91-23386
ELECTRICAL IMPEDANCE
The transient response of heavily fluid-loaded elastic plates and cylindrical shells N91-23528
ELECTRICAL PROPERTIES
High quality three dimensional electron gases in semiconductors
[AD-A232779] N91-23406
Structural and electronic properties of the ordered ternary 3-5 semiconductors N91-23936
Electronic properties of Si-doped n-doping-intrinsic-p-doping-intrinsic (nipi) structures in GaAs
[DE91-009474] N91-23941
Composite ceramic superconducting wires for electric motor applications
[AD-A232074] N91-23951
ELECTRICAL RESISTIVITY
Bromination of carbon fibers and carbon-carbon composites N91-23240
Channel diagnostics for the multi-pulse-propagation experiments at ATA
[DE91-009772] N91-23466
ELECTRICITY
Liquid-metal MHD power conversion for space electric systems
[SER-S/27] N91-23231
ELECTRO-OPTICS
Optoelectronic III-V heterostructures on SI substrates
[AD-A232035] N91-23950
Optical shutter switching matrix N91-24071
ELECTROCHEMICAL CORROSION
Galvanic corrosion of aluminum-matrix composites
[AD-A232138] N91-23264
Deterministic analysis of processes at corroding metal surfaces and the study of electrochemical noise in these systems
[DE91-009997] N91-23297
ELECTROCHEMISTRY
Electrochemical parameterization of rhenium redox couples
[AD-A232043] N91-23279
A Raman spectroscopic and electrochemical study of the photoinduced crystallization of triethylenediamine triiodide upon a silver electrode
[AD-A232828] N91-23963
ELECTRODEPOSITION
Structure of electrochemically deposited copper on gold (III) alloy
[AD-A232345] N91-23303
Electrodeposited coatings for diamond turning applications
[DE91-009950] N91-23315
Computer programs for simulation of electrodeposition
[DE91-010203] N91-23741
In-situ surface x ray scattering measurements of electrochemically deposited bismuth on silver (III): Structure, compressibility, and comparison with ex-situ leed measurements
[AD-A232624] N91-23880
Surface x ray scattering measurements of the substrate induced spatial modulation of an incommensurate adsorbed monolayer
[AD-A232625] N91-23959
ELECTRODES
Destructive physical analysis results of Ni/H2 cells cycled in LEO regime
[NASA-TM-104382] N91-23233
Gas evolution and bubble formation on electrodes
[ESA-TT-1191] N91-23278
Characterization of active materials and electrodes for battery R and D
[DE91-010758] N91-23390
Optimization of transparent and reflecting electrodes for amorphous silicon solar cells
[DE91-002132] N91-23618
A Raman spectroscopic and electrochemical study of the photoinduced crystallization of triethylenediamine triiodide upon a silver electrode
[AD-A232828] N91-23963
ELECTROENCEPHALOGRAPHY
Research and development involved in creating a quantitative EEG cartography wide band analysis system
[LAAS-91002] N91-23705
ELECTROLYSIS
Static feed water electrolysis subsystem development
[NASA-CASE-MSC-21577-1-SB] N91-23271
Gas evolution and bubble formation on electrodes
[ESA-TT-1191] N91-23278
ELECTROLYTE METABOLISM
A non-invasive measure of minerals and electrolytes in tissue N91-24058
ELECTROLYTES
Destructive physical analysis results of Ni/H2 cells cycled in LEO regime
[NASA-TM-104382] N91-23233
High temperature membranes for H2S and SO2 separations
[DE91-008534] N91-23275
Deterministic analysis of processes at corroding metal surfaces and the study of electrochemical noise in these systems
[DE91-009997] N91-23297
Electrodeposited coatings for diamond turning applications
[DE91-009950] N91-23315
Advanced working fluids: Thermodynamic properties
[PB91-136465] N91-23964
ELECTROLYTIC CELLS
Oxygen production using solid-state zirconia electrolyte technology N91-24059
ELECTROMAGNETIC ABSORPTION
Determination of the temperature profile of the troposphere with a two frequency lidar
[EXAMENARBEIT-8] N91-23653
ELECTROMAGNETIC ACCELERATION
On the efficiency of rail accelerators
[PML-1990-64] N91-23204
Temperature measurements of ET plasmas using atomic emission spectroscopy
[AD-A232498] N91-23930
ELECTROMAGNETIC FIELDS
The statistical properties of electromagnetic fields with application to radiation and scattering
[DE91-007467] N91-23351
Implementation of the FAA research and development electromagnetic database
[DE91-010063] N91-23674
ELECTROMAGNETIC INTERFERENCE
Error probabilities of frequency hopped MFSK with self-normalization combining in a fading channel with partial-band interference
[AD-A232467] N91-23376
ELECTROMAGNETIC MEASUREMENT
Effect of atmospheric variations on electromagnetic distance measurements
[DE91-009726] N91-23349
ELECTROMAGNETIC PULSES
Pulse compression of 100 picosecond pulses at 1.319 microns
[AD-A232552] N91-23901
ELECTROMAGNETIC RADIATION
Analysis of the VHF-UHF electromagnetic radiation of lightning: Application to a model of the negative stepped leader propagation
[ESA-TT-1172] N91-23363
Error probabilities of frequency hopped MFSK with self-normalization combining in a fading channel with partial-band interference
[AD-A232467] N91-23376
Thermal control system for the investigation of specific absorption rates for specimens exposed to electromagnetic radiation
[AD-A231329] N91-23459
Constant of motion and dynamic equations for one-dimensional autonomous system and radiation damping
[DE91-011002] N91-23547
ELECTROMAGNETIC SCATTERING
Time-domain analysis of one-dimensional electromagnetic scattering by Lossy media
[FEL-90-A211] N91-23358
Calculation of near-field scattering using the plane-wave formulation and the physical optics method
[FEL-90-B215] N91-23360
Calculation of electromagnetic fields in the near-field region of a moving scattering object
[FEL-90-B216] N91-23361
Joint services electronics program
[AD-A232331] N91-23402
ELECTROMAGNETIC WAVE TRANSMISSION
Time-domain analysis of one-dimensional electromagnetic scattering by Lossy media
[FEL-90-A211] N91-23358
An analysis of MLAYER: A multilayer tropospheric propagation program
[AD-A232733] N91-23379
ELECTROMAGNETS
Electromagnetic attachment mechanism
[NASA-CASE-MSC-21463-1] N91-23490
Description of the Large Gap Magnetic Suspension System (LGMSS) ground-based experiment N91-24083

ELECTRON ACCELERATORS
Lectures on accelerator physics
[DE91-010376] N91-23886
ELECTRON AVALANCHE
Solutions to current induced avalanche burnout
[DE90-013196] N91-23386
ELECTRON BEAMS
Channel diagnostics for the multi-pulse-propagation experiments at ATA
[DE91-009772] N91-23466
Echo 7: Magnetospheric properties determined by artificial electron beams N91-23644
ELECTRON CAPTURE
Magnetic substates populated by double electron capture in slow ion atom collisions
[DE91-010122] N91-23858
Low-energy collisions of multiply charged ions with electrons, atoms and surfaces
[DE91-010779] N91-23873
ELECTRON CYCLOTRON HEATING
Heavy ion beam probe measurements of ECH method plasma in the advanced toroidal facility
[DE91-010391] N91-23917
ELECTRON DECAY RATE
A numerical model of laser induced fluorescence in a hydrogen plasma
[AD-A232240] N91-23482
ELECTRON DENSITY (CONCENTRATION)
Incoherent scatter measurements and inferred energy fluxes in the equatorial F-region ionosphere N91-23640
ELECTRON DENSITY PROFILES
Incoherent scatter measurements and inferred energy fluxes in the equatorial F-region ionosphere N91-23640
Inversion of chordal data from the ATF torsatron
[DE91-010490] N91-23915
ELECTRON DISTRIBUTION
A numerical model of laser induced fluorescence in a hydrogen plasma
[AD-A232240] N91-23482
ELECTRON EMISSION
Surface electron emission induced by slow multicharged ions
[DE91-010469] N91-23865
ELECTRON ENERGY
Incoherent scatter measurements and inferred energy fluxes in the equatorial F-region ionosphere N91-23640
ELECTRON MOBILITY
High quality three dimensional electron gases in semiconductors
[AD-A232779] N91-23406
ELECTRON PARAMAGNETIC RESONANCE
Structural studies of manganese and halide in the photosynthetic oxygen evolving complex
[DE91-009071] N91-23698
ELECTRON PLASMA
Comparison of drift wave models with fluctuation data from the interior of the TEXT tokamak
[DE91-010424] N91-23918
ELECTRON SCATTERING
Scattering in electron spectrometers
[NPL-DMM(A)-19] N91-23467
ELECTRON SPECTROSCOPY
X ray diffraction and electron spectroscopy of epitaxial molecular C60 films
[AD-A232152] N91-23954
ELECTRON STATES
Quantum chemical studies of candidate high energy density material compounds
[AD-A232393] N91-23335
ELECTRON TRANSFER
AFRRI reports, October - December 1990
[AD-A232236] N91-23283
Excited state structure, energy and electron transfer dynamics of photosynthetic reaction centers: A hole burning study
[DE91-010181] N91-23693
ELECTRON TUNNELING
Quantum extension of Child-Langmuir law
[AD-A232407] N91-23878
ELECTRONIC PACKAGING
Fundamental studies of electronic packaging materials and structures: Surface and interfaces
[AD-A232336] N91-23403
ELECTRONS
Re-analysis of photoemission data for CuO: Revision of the configuration-energy scheme for cuprate materials
[DE91-009952] N91-23296
High quality three dimensional electron gases in semiconductors
[AD-A232779] N91-23406
Few-body problems, electron-correlation effects, and beyond
[DE91-010030] N91-23857
Low-energy collisions of multiply charged ions with electrons, atoms and surfaces
[DE91-010779] N91-23873
ELECTROSTATIC CHARGE
Design rules and system testing methods
[REPT-911-440-107] N91-23222
Predictions and verification of ESD tests made with sphere injections on a flight representative telecommunication satellite: ARABSAT STM
[REPT-911-440-109] N91-23224
Diffusive, electrostatic concentration of disintegration products of inert gases in vortex flow
[AD-A232876] N91-23457
ELECTROSTATIC PROBES
Heavy ion beam probe measurements of ECH method plasma in the advanced toroidal facility
[DE91-010391] N91-23917
ELECTROSTATICS
The direct correlation function of a mixture of hard ions in the mean spherical approximation
[AD-A232452] N91-23879
On standard forms for transport equations and fluxes, part 2
[DE91-010421] N91-23912
ELEMENTARY PARTICLE INTERACTIONS
A guide to experimental elementary particle physics literature, 1985-1989
[DE91-010209] N91-23856
ELEMENTARY PARTICLES
A guide to experimental elementary particle physics literature, 1985-1989
[DE91-010209] N91-23856
Research in particle theory
[DE91-010749] N91-23872
Particle physics experiments, 1990
[RAL-91-001] N91-23877
A proposed search for dark-matter axions in the 0.6-16 micro-eV range
[NASA-CR-188173] N91-24015
ELLIPSOMETERS
Two-channel spectroscopic polarization modulation ellipsometry
[DE91-010131] N91-23893
EMISSION SPECTRA
High resolution imaging for Brackett gamma and H2 1-0 S(1) emission in the Seyfert galaxy NGC 1068
[MPE-PREPRINT-192] N91-23104
High-altitude non-equilibrium infrared emission models
[AD-A232503] N91-23659
Bulletin of the Israel Physical Society, volume 33, 1987. Annual Meeting 1987: Program and Abstracts
[ITN-89-85012] N91-23832
A high resolution study of the Cu K alpha(sub 1,2) x-ray emission lines N91-23841
Imaging and background in low-energy gamma ray astronomy N91-24005
The molecular interstellar medium and the near-infrared continuum of the barred liner NGC 6764
[MPE-PREPRINT-193] N91-24029
EMULSIONS
Interdisciplinary research on viscoelasticity and rheology
[AD-A232700] N91-23454
END EFFECTORS
Automated handling and assembling of non-rigid objects
[AD-A231246] N91-23489
Electromagnetic attachment mechanism
[NASA-CASE-MSC-21463-1] N91-23490
Multisensory telerobotic concepts for space and underwater applications N91-23584
Obstacle avoidance for redundant robots using configuration control
[NASA-CASE-NPO-17852-1-CU] N91-23783
Robotic control and inspection verification N91-24075
END-TO-END DATA SYSTEMS
Distributed, cooperating knowledge-based systems N91-24044
ENDOTHERMIC REACTIONS
Aerocoat thermal protections
[REPT-911-430-102] N91-23217
ENERGETIC PARTICLES
Applications of energetic particles in improving coating adhesion properties
[DE91-008833] N91-23312
ENERGY CONSUMPTION
Development of a low cost peak shaving generator set
[PB91-136374] N91-23332
ENERGY CONVERSION EFFICIENCY
Optical parametric oscillators pumped by excimer lasers N91-23473
ENERGY DISSIPATION
Mechanics/heat-transfer relation for particulate materials
[DE91-008356] N91-23424
Energy dissipator
[NASA-CASE-MSC-21555-1] N91-23492
Relativistic shock waves and the excitation of plerions
[DE91-007623] N91-24027
ENERGY DISTRIBUTION
Energy partition of free Rossby waves in global atmospheric oscillations
[MITT-74] N91-23648
ENERGY GAPS (SOLID STATE)
Electronic properties of Si-doped n-doping-intrinsic-p-doping-intrinsic (nipi) structures in GaAs
[DE91-009474] N91-23941
ENERGY LEVELS
Fermi surface of YBCO by DHVA
[DE91-009963] N91-23943
ENERGY POLICY
Energy-related environmental issues in a global context
[DE91-009538] N91-23627
ENERGY SPECTRA
The spectrum of massive accretion disks N91-23840
Computed secondary-particle energy spectra following nonelastic neutron interactions with C-12 for E(n) between 15 and 60 MeV: Comparisons of results from two calculational methods
[DE91-010454] N91-23864
The high energy spectrum of the 1983, August 1b gamma-ray burst
[MPE-PREPRINT-194] N91-24040
ENERGY STORAGE
Solar thermal energy receiver
[NASA-CASE-LEW-14949-1] N91-23617
SEI rover solar-electrochemical power system options
[NASA-TM-104402] N91-23620
ENERGY TECHNOLOGY
Computing for magnetic fusion energy research: The next five years
[DE91-010686] N91-23921
Proceedings of the 1991 American Association for the Advancement of Science Annual Meeting Program N91-23969
Activities report of the DLR
[ISSN-0938-2194] N91-24086
ENERGY TRANSFER
An experimental study of an axisymmetric turbulent boundary layer disturbed by a periodic freestream N91-23078
Multi-heat addition turbine engine
[NASA-CASE-LEW-15094-1] N91-23180
Energy exchange study at the ocean surface by satellite observation N91-23597
Solar thermal energy receiver
[NASA-CASE-LEW-14949-1] N91-23617
Excited state structure, energy and electron transfer dynamics of photosynthetic reaction centers: A hole burning study
[DE91-010181] N91-23693
On standard forms for transport equations and fluxes, part 2
[DE91-010421] N91-23912
ENGINE CONTROL
A simplified dynamic model of the Space Shuttle main engine
[NASA-TM-104421] N91-23340
ENGINE DESIGN
NASA aeropropulsion research in support of propulsion systems of the 21st century
[NASA-TM-104403] N91-23083
A study of supersonic and hypersonic ramjet engines in France from 1950 to 1974 (application on combined cycle aircraft engines) N91-23149
Trajectory optimization considerations for ramjet engines N91-23151
Airbreathing propulsion for space transport: New concepts, special problems and attempts at solutions N91-23154
Analytical and experimental investigations of the oblique detonation wave engine concept N91-23169
Materials and material systems for combined cycle engines N91-23178
Integration of propulsive systems: Selection and compromise
[REPT-911-111-101] N91-23187
The certification of the aircraft integrated propulsive system
[REPT-911-111-102] N91-23188
NDE (Nondestructive Examination) development for ceramics for advanced heat engines
[DE91-005516] N91-23316
Evaluation and ranking of candidate ceramic wafer engine seal materials
[NASA-TM-103795] N91-23515
ENGINE INLETS
A study of three dimensional turbulent boundary layer separation and vortex flow control using the reduced Navier Stokes equations
[NASA-TM-104407] N91-23089

Parametric study in weld mismatch of longitudinally welded SSME HPFTP inlet
[NASA-TM-103534] N91-23502

ENGINE PARTS
Evaluation and ranking of candidate ceramic wafer engine seal materials
[NASA-TM-103795] N91-23515

ENGINE TESTS
Low heat rejection diesel ceramic coupon tests
[DE91-006274] N91-23318

ENVIRONMENT EFFECTS
Steps toward environmentally compatible product and process design: A case for green engineering
[AD-A232888] N91-23633

ENVIRONMENT MANAGEMENT
The changing face of the environmental issue
[PB91-138081] N91-23624

ENVIRONMENT PROTECTION
Region 10 environmental indicators
[PB91-136580] N91-23623
The changing face of the environmental issue
[PB91-138081] N91-23624
National stream survey database guide
[PB91-141804] N91-23625
Energy-related environmental issues in a global context
[DE91-009538] N91-23627

ENVIRONMENT SIMULATION
A solution for the man/machine-interface in robotics: A high level control language with enhanced interaction equipment N91-23789
An interactive robot control system N91-23790

ENVIRONMENTAL CHEMISTRY
Information system for environmental chemicals
[GSF-BER-21/90] N91-23990

ENVIRONMENTAL TESTS
Ion beam testing of the Aerolor X-point dump plate for the Joint European Torus
[DE91-010719] N91-23245

EPITAXY
Low-temperature laser-induced selective area growth of compound semiconductor N91-23932
Microstructure of epitaxial YBa2Cu3O7 thin films
[DE91-009951] N91-23942
Advances in silicon carbide Chemical Vapor Deposition (CVD) for semiconductor device fabrication
[NASA-TM-104410] N91-23946
Silicon carbide, an emerging high temperature semiconductor N91-24061

EPOXY MATRIX COMPOSITES
Modelling of the impact response of fibre-reinforced composites
[AD-A232658] N91-23266
Strain rate sensitivity of polymer-matrix composites under mode I delamination
[AD-A232761] N91-23268
Hardening mechanisms and analysis of the structure of the TGDDM/DDS epoxy resin system
[ESA-TT-1202] N91-23319

EPOXY RESINS
Shock characterization of epoxy: Forty-two volume percent glass microballoons
[DE91-009616] N91-23314

EQUATIONS OF MOTION
Higher accuracy requirements for the satisfactory position calculation of an artificial satellite
[GKSS-90/E/25] N91-23203
Flow between eccentric rotating cylinders N91-23417
Finite element based dynamical modeling of flexible open-loop manipulators with experimental results N91-23496
On kinematic design of serial link manipulators
[DE91-009414] N91-23499
A theory for fluidelastic instability of tube-support-plate inactive modes
[DE91-009676] N91-23538
Constant of motion and dynamic equations for one-dimensional autonomous system and radiation damping
[DE91-011002] N91-23547
The coordinate-free representation of rotational motions
[RSRE-MEMO-4445] N91-23846

EQUATIONS OF STATE
Monte Carlo simulation of supercritical solutions in the grand canonical ensemble
[DE91-009152] N91-23859

EQUATORIAL ELECTROJET
Large scale turbulence in the equatorial electrojet N91-23643

EQUATORIAL REGIONS
The polar wind and ionospheric outflow N91-23645
Near-equatorial deep circulation in the Indian and Pacific oceans
[AD-A232635] N91-23691

EQUATORS
The annual march of convection, sea surface temperature, and surface winds in the tropics N91-23667

EQUILIBRIUM EQUATIONS
On the construction of two-phase equilibria in a non-elliptic hyperelastic material
[AD-A232628] N91-23558

EQUIPMENT SPECIFICATIONS
Development of a low cost peak shaving generator set
[PB91-136374] N91-23332
Computational needs survey of NASA automation and robotics missions. Volume 1: Survey and results
[NASA-TM-103860] N91-23341

EQUIVALENCE
Congruence properties of the process equivalence induced by temporal logic
[RR-831-I-IMAG-118-LIFIA] N91-23810

ERROR ANALYSIS
An engineering study of altitude determination deficiencies of the Service Aircraft Instrumentation Package (SAIP)
[AD-A232055] N91-23145
Error control coding for multi-frequency modulation
[AD-A232421] N91-23374
Error probabilities of frequency hopped MFSK with self-normalization combining in a fading channel with partial-band interference
[AD-A232467] N91-23376
Table-lookup algorithms for elementary functions and their error analysis
[DE91-006047] N91-23743
A methodology for handling data errors and inconsistencies in database conversions
[AD-A232113] N91-23994

ERROR CORRECTING CODES
Error control coding for multi-frequency modulation
[AD-A232421] N91-23374
Error probabilities of frequency hopped MFSK with self-normalization combining in a fading channel with partial-band interference
[AD-A232467] N91-23376

ERROR CORRECTING DEVICES
A methodology for handling data errors and inconsistencies in database conversions
[AD-A232113] N91-23994

ERRORS
Error probabilities of frequency hopped MFSK with self-normalization combining in a fading channel with partial-band interference
[AD-A232467] N91-23376
Incoherent scatter measurements and inferred energy fluxes in the equatorial F-region ionosphere N91-23640
The application of equilibrium climate models to questions of glaciation at high latitudes N91-23669
Intelligent computer-aided training and tutoring N91-24042

ESCHERICHIA
Isolation, cloning and expression of the genes for microbial polyurethane degradation
[AD-A232108] N91-23699

ESTIMATING
The drag of spheres at porosites ranging from an isolated sphere to a packed bed
[CRANFIELD-AERO-9012] N91-23444
A one dimensional wind profile model with stability and eddy viscosity estimations from sodar data
[DM-56] N91-23680

ESTIMATORS
A simple solution to the singular linear minimum-variance estimation problem
[IAITIC-87-1002-REV] N91-23804

ETCHING
Flexible fluoropolymer filled protective coatings N91-24062
A conformal oxidation-resistant, plasma-polymerized coating N91-24063

EUCLIDEAN GEOMETRY
Tripod operators for the interpretation of range images
[AD-A232631] N91-23344
Articulation of spatial robots N91-23504

EULER EQUATIONS OF MOTION
The effect of combustor flow nonuniformity on the performance of hypersonic nozzles N91-23173
Block implicit multigrid solution of the Euler equations N91-23413
Investigation of Roe's 2D wave decomposition models for the Euler equations
[VKI-TN-172] N91-23436
Aero-thermal investigation of a highly loaded transonic linear turbine guide vane cascade. A test case for inviscid and viscous flow computations
[VKI-TN-174] N91-23437
Formulation of boundary conditions for the multigrid acceleration of the Euler and Navier Stokes equations
[NASA-CR-188234] N91-23440

EURECA (ESA)
Feasibility study of the Superconducting Gravity Gradiometer (SGG) flight test on the European Retrievable Carrier (EURECA)
[NASA-CR-184157] N91-23229
Eureca 1 AMF 117 experiment: An analysis of thermal and solutal transfer during the crystal growth of CdTe by the THM process
[REPT-911-430-118] N91-23947
Eureca 1 AMF 117 experience: Thermal and solutal transfer analysis for CdTe in tellurium during crystal growth by the THM method
[REPT-911-430-120] N91-23948

EUROPE
Eastern Europe: Please stand by
[PB91-14336] N91-23348

EUROPEAN AIRBUS
The certification of the aircraft integrated propulsive system
[REPT-911-111-102] N91-23188

EUROPEAN SPACE PROGRAMS
The Eutelsat 2 programme
[REPT-911-440-108] N91-23223

EVALUATION
Strategic missiles: Uncertainties persist in the Advanced Cruise Missile (ACM) program
[AD-A232058] N91-23142
Measuring the effects of distributed database models on transaction availability measures N91-23973

EVOKED RESPONSE (PSYCHOPHYSIOLOGY)
Human short-latency somatosensory evoked potentials in impact acceleration research: Equipment, procedures, and techniques
[AD-A232732] N91-23709

EXCIMER LASERS
Optical parametric oscillators pumped by excimer lasers N91-23473
Low-temperature laser-induced selective area growth of compound semiconductor N91-23932

EXCIMERS
Multiphoton detection techniques for F and F2
[AD-A232641] N91-23286

EXCITATION
Magnetic substates populated by double electron capture in slow ion atom collisions
[DE91-010122] N91-23858
Relativistic shock waves and the excitation of plerions
[DE91-007623] N91-24027

EXCITONS
Magneto-optical properties of quantum wells with arbitrary potential profiles
[AD-A232037] N91-23897

EXHAUST EMISSION
A CFD study of jet mixing in reduced flow areas for lower combustor emissions
[NASA-TM-104411] N91-23185

EXOBIOLOGY
Aerospace medicine and biology: A continuing bibliography with indexes (supplement 346)
[NASA-SP-7011(346)] N91-23700
Aerospace medicine and biology: A continuing bibliography with indexes (supplement 347)
[NASA-SP-7011(347)] N91-23701
Aerospace medicine and biology: A continuing bibliography with indexes (supplement 348)
[NASA-SP-7011(348)] N91-23702
A non-invasive measure of minerals and electrolytes in tissue N91-24058
Monitoring and control technologies for bioregenerative life support systems/CELSS N91-24060

EXPERIMENTATION
A guide to experimental elementary particle physics literature, 1985-1989
[DE91-010209] N91-23856
Eureca 1 AMF 117 experiment: An analysis of thermal and solutal transfer during the crystal growth of CdTe by the THM process
[REPT-911-430-118] N91-23947
Eureca 1 AMF 117 experience: Thermal and solutal transfer analysis for CdTe in tellurium during crystal growth by the THM method
[REPT-911-430-120] N91-23948

EXPERT SYSTEMS
A new architecture and expert system for aircraft design synthesis N91-23132
Reactive procedure based decision making for satellite control
[REPT-911-440-106] N91-23221
A first-principles generic methodology for representing the knowledge base of a process diagnostic expert system
[DE90-017693] N91-23520

A procedural expert system for spacecraft command and control N91-23591
Hypermedia 1990 structured Hypertext tutorial [NASA-CR-187921] N91-23731
The integration of remote sensing, geographic information system, and expert system technologies for landcover classification N91-23733
ACLICO: A computer aided design system for bonded joints [REPT-911-430-101] N91-23757
Portable intelligent diagnostic aids [AD-A230883] N91-23782
Conference on Theoretical Aspects of Reasoning About Knowledge [AD-A232657] N91-23798
A distributed problem-solving approach to rule induction: Learning in distributed artificial intelligence systems [AD-A232822] N91-23803
Advanced methods of approximate reasoning [AD-A232140] N91-23814
Knowledge-based retrieval of information as a process of evidential reasoning N91-23978
An expert system for searching in full-text N91-23983
Combining knowledge bases consisting of first order theories [AD-A232090] N91-23993
CLIPS: A tool for the development and delivery of expert systems N91-24043
Distributed, cooperating knowledge-based systems N91-24044
Electronic neuroprocessors N91-24045

EXPLORER SATELLITES
Small Explorer project: Submillimeter Wave Astronomy Satellite (SWAS). Mission operations and data analysis plan [NASA-CR-186954] N91-23212

EXPLOSIONS
Sensitivity of numerical dispersion modeling to explosive source parameters [DE91-009476] N91-23631

EXPLOSIVES
Response of simulated propellants and explosives to projectile impact [DE91-009777] N91-23333

EXPONENTIAL FUNCTIONS
A smoothing algorithm for upper-air soundings [AD-A232853] N91-23661

EXTINGUISHING
Power packs: A passive approach to extinguishing fire in combat vehicles [AD-A232020] N91-23342

EXTRATERRESTRIAL RADIATION
The Combined Release and Radiation Effects Satellite program (CRRES): A unique series of scientific experiments [NASA-TM-104957] N91-23213

EXTRATERRESTRIAL RESOURCES
Material processing with hydrogen and carbon monoxide on Mars [NASA-TM-104405] N91-23616

EXTRAVEHICULAR ACTIVITY
The diving laboratory as a simulation environment for manned spaceflight N91-23564
EVA servicing: The Hermes capability N91-23575
Neutral buoyancy and microgravity: Extravehicular activities with a humid water suit N91-23579
EVA/robotics integration for Space Station Freedom N91-23583
A KO2 rebreather for EVA denitrogenation procedure N91-23588

EXTREME ULTRAVIOLET RADIATION
Soft x ray/extreme ultraviolet images of the solar atmosphere with normal incidence multilayer optics N91-24006

EXTREMELY HIGH FREQUENCIES
Characteristics of a future aeronautical satellite communications system [NASA-TM-104389] N91-23102

EYE (ANATOMY)
Laser hazards bibliography, January 1991 [AD-A232690] N91-23487

F

F REGION
Incoherent scatter measurements and inferred energy fluxes in the equatorial F-region ionosphere N91-23640

F-18 AIRCRAFT
Examination of the microstructure of 7050 aluminum alloy samples [AD-A232544] N91-23306

FABRICATION
High temperature membranes for H2S and SO2 separations [DE91-008534] N91-23275
High-temperature alloys for high-power thermionic systems [DE91-009292] N91-23299
System-Level Integrated Circuit (SLIC) development for phased array antenna applications [NASA-TM-104392] N91-23354
Magnet cable manufacturing [DE91-010210] N91-23935
Contract crystal growth and fabrication services [AD-A232120] N91-23952
Research and development on advanced silicon carbide thin film growth techniques and fabrication of high power and microwave frequency silicon carbide-based device structures [AD-A232160] N91-23955
Superplastic forming of Al-Li alloys for lightweight, low-cost structures N91-24065

FABRICS
A simulation of the draping and a model of the consolidation of commingled fabrics N91-23239

FACTOR ANALYSIS
Classification using multi-layered perceptrons [AD-A232810] N91-23802
A particular linear model of variance components [RR-827-M] N91-23824

FACTORIZATION
Modeling speedup in parallel sparse matrix factorization [DE91-010215] N91-23735

FAILURE
Destructive physical analysis results of Ni/H2 cells cycled in LEO regime [NASA-TM-104382] N91-23233
Mechanical behavior and failure phenomenon of an in situ-toughened silicon nitride [NASA-TM-103741] N91-23311

FAILURE ANALYSIS
A study of the micromechanics of the fiber-matrix interphase in monofilament composites, in monotonic loading, and cyclic fatigue N91-23241
Combined thermal and bending fatigue of high-temperature metal-matrix composites: Computational simulation [NASA-TM-104354] N91-23247
Tensor transformations and failure criteria for the analysis of fiber composite materials [AD-A232238] N91-23265
Evaluation of filler metals for high-strength stainless steels [DE91-009931] N91-23295
A simplified dynamic model of the Space Shuttle main engine [NASA-TM-104421] N91-23340
Solutions to current induced avalanche burnout [DE90-013196] N91-23386
Electromagnetic attachment mechanism [NASA-CASE-MSC-21463-1] N91-23490
A first-principles generic methodology for representing the knowledge base of a process diagnostic expert system [DE90-017693] N91-23520
A theory for fluidelastic instability of tube-support-plate inactive modes [DE91-006001] N91-23542
Incorporating finite element analysis into component life and reliability [NASA-TM-104400] N91-23550
Evaluation of catastrophic failure risk in pressure vessels. Results of pressure vessel test with a large vessel (HC2-test) [VTT-RR-708] N91-23551
Statistical models and inference procedures for structural and materials reliability [AD-A232634] N91-23827
Robustness in replicated databases N91-23981

FALSE ALARMS
An investigation of CFAR techniques for airborne radars [AD-A232724] N91-23378
Background simulation and filter design using iterated function systems [AD-A232632] N91-23405

FAR FIELDS
Study of phase-locked diode laser array and DFB/DBR surface emitting laser diode N91-23474

FAR ULTRAVIOLET RADIATION
Studies of the diffuse background and interstellar dust at far ultraviolet wavelengths N91-24003

FARADAY EFFECT
Incoherent scatter measurements and inferred energy fluxes in the equatorial F-region ionosphere N91-23640

FARM CROPS
Surface layer transfer processes over vegetation: A micrometeorological field experiment of long duration N91-23664

FAST FOURIER TRANSFORMATIONS
A fast algorithm for the evaluation of trigonometric series [AD-A232848] N91-23775

FASTENERS
Metallic threaded composite fastener [NASA-CASE-MSC-21580-1] N91-23491

FATIGUE (MATERIALS)
Examination of the microstructure of 7050 aluminum alloy samples [AD-A232544] N91-23306
Post-overload fatigue crack recovery in powder metal aluminum-lithium AL-905XL forging [AD-A232550] N91-23307
Experience with conventional inelastic analysis procedures in very high temperature applications [DE91-009937] N91-23545
Threshold for fatigue crack propagation at simulated operating loads [ESA-TT-1187] N91-23553

FATIGUE LIFE
Examination of the microstructure of 7050 aluminum alloy samples [AD-A232544] N91-23306
Computational life prediction methodology for mechanical systems using dynamic simulation, finite element analysis, and fatigue life prediction methods N91-23494
Reduction factors for creep strength and fatigue life of modified 9 Cr-1 Mo steel weldments [DE91-009919] N91-23544
Computational simulation of acoustic fatigue for hot composite structures [NASA-TM-104379] N91-23548
Threshold for fatigue crack propagation at simulated operating loads [ESA-TT-1187] N91-23553

FATIGUE TESTS
A study of the micromechanics of the fiber-matrix interphase in monofilament composites, in monotonic loading, and cyclic fatigue N91-23241
Post-overload fatigue crack recovery in powder metal aluminum-lithium AL-905XL forging [AD-A232550] N91-23307
Computerized system for static and fatigue large scale structural tests: A case study [IAITIC-87-1007] N91-23522
Fatigue evaluation of piping systems with limited vibration test data [DE91-007167] N91-23543
Threshold for fatigue crack propagation at simulated operating loads [ESA-TT-1187] N91-23553
Development of a micromechanic theory of constitutive relations of polycrystalline solids [AD-A232697] N91-23559

FAULT TOLERANCE
The electrical flight control system of A320 Airbus: A fault tolerant system [REPT-911-111-103] N91-23192
Decentralized computing technology for fault-tolerant, survivable C3I systems, volume 1 [AD-A232289] N91-23369
Decentralized computing technology for fault-tolerant, survivable C3I systems, volume 2 [AD-A232290] N91-23370
Decentralized computing technology for fault-tolerant, survivable C3I systems. Volume 3: System/subsystem specification [AD-A232291] N91-23371
Basic properties of strongly code disjoint checkers [RR-824-I] N91-23393
Saturation and vote for the fault tolerance in distributed systems [LAAS-90390] N91-23727

FEASIBILITY ANALYSIS
Wind and sea state local climatology by means of satellite radar altimeter measurements N91-23599

FEDERAL BUDGETS
Information resources management long-range plan [DE91-009745] N91-23984
Federally funded research: Decisions for a decade [OTA-SET-490] N91-23998

FEEDBACK
Observed changes in the activity of baroclinic waves and their feedbacks during the life cycles of low-frequency circulation anomalies in the Northern Hemisphere winter N91-23668

FEEDBACK CIRCUITS
Mechanisms of higher brain functions: A study of models of perception [AD-A232389] N91-23712

FEEDBACK CONTROL
H-infinity approach to manipulator control N91-23495
An analytic study of general dynamic model and nonlinear feedback control of flexible robot arms N91-23497
On the control of two manipulators holding a rigid object in the presence of uncertainty
[DE90-017742] N91-23508
On the initialization problem in the design of structurally constrained digital regulators
[REPT-90-039] N91-23749
Monitoring an assembly task by perception requests N91-23791
Intelligent planning in controlling electronics assembly N91-23792
Planning of visual feedback with robot-sensor co-operation N91-23793
Robot-sensor co-operation planning for visual guidance N91-23794
Degeneration of linear multivariable systems under high gain and dynamic compensation N91-23830
FEEDERS
Static feed water electrolysis subsystem development
[NASA-CASE-MSC-21577-1-SB] N91-23271
FEEDFORWARD CONTROL
The application of neural networks to the SSME startup transient
[NASA-CR-187138] N91-23205
An artificial neural network control system for spacecraft attitude stabilization
[AD-A232013] N91-23225
FERMI SURFACES
Theory of the new high-temperature superconductors N91-23842
Fermi surface of YBCO by DHVA
[DE91-009963] N91-23943
FERROELECTRICITY
Evaluation of ferroelectric materials for memory applications
[AD-A232112] N91-23728
Evaluation of a ferroelectric liquid crystal spatial light modulator
[AD-A232117] N91-23899
FIBER COMPOSITES
Integrated multidisciplinary optimization of actively controlled fiber composite wings N91-23190
Improved quality acceptance procedure for interlaminar shear strength
[IAITIC-87-1005] N91-23238
A study of the micromechanics of the fiber-matrix interphase in monofilament composites, in monotonic loading, and cyclic fatigue N91-23241
Rate dependent stress-strain behavior of advanced polymer matrix composites
[NASA-TM-104070] N91-23244
Characterization of composite materials for aerospace materials
[DLR-MITT-90-15] N91-23246
Fiber-reinforced glass-ceramic matrix composites: New class of materials for space applications
[REPT-911-430-107] N91-23253
Thermostructural composites: Recent evolutions and improvements
[REPT-911-430-109] N91-23254
Mechanical characterisation of fibre-matrix interface in ceramic composites by an instrumented indentation test
[REPT-911-430-114] N91-23256
Structural materials for space mirrors
[REPT-911-430-128] N91-23261
Tensor transformations and failure criteria for the analysis of fiber composite materials
[AD-A232238] N91-23265
Modelling of the impact response of fibre-reinforced composites
[AD-A232658] N91-23266
A study of the critical factors controlling the synthesis of ceramic matrix composites from preceramic polymers
[AD-A232686] N91-23327
A preliminary investigation of acousto-ultrasonic NDE of metal matrix composite test specimens
[NASA-TM-104339] N91-23521
Flame-retardant composite materials N91-24064
FIBER OPTICS
Fiber optic sensors for the military
[AD-A232100] N91-23898
Fiber Optic Tactical Local Network (FOTLAN) N91-24072
FIBER STRENGTH
A study of the micromechanics of the fiber-matrix interphase in monofilament composites, in monotonic loading, and cyclic fatigue N91-23241
FIELD EFFECT TRANSISTORS
Solutions to current induced avalanche burnout
[DE90-013196] N91-23386
Microwave integrated circuits for space applications N91-24069
FIELD THEORY (PHYSICS)
Supersymmetric matter at finite temperature N91-23836
Intermediate/high energy nuclear physics
[DE91-010702] N91-23868
Research in particle theory
[DE91-010749] N91-23872
Mean-field theories of the Hubbard model and periodic orbits in chaotic maps N91-23938
FIGHTER AIRCRAFT
Development of MIL-8785C into a handling qualities specification for a new European fighter aircraft N91-23114
The flying qualities influence of delay in the fighter pilot's cuing environment N91-23120
Agility: A rational development of fundamental metrics and their relationship to flying qualities N91-23129
X-31A at first flight N91-23131
Buffet induced structural/flight-control system interaction of the X-29A aircraft
[NASA-TM-101735] N91-23133
FILLERS
Evaluation of filler metals for high-strength stainless steels
[DE91-009931] N91-23295
FILTRATION
Quantifying oil filtration effects on bearing life
[NASA-TM-104350] N91-23512
New research on bioregenerative air/water purification systems N91-24053
FINE STRUCTURE
Luminescence and absorption spectra of C60 films
[AD-A232153] N91-23900
FINGERS
Preloaded latching device
[NASA-CASE-MSC-21730-1] N91-23493
FINITE DIFFERENCE THEORY
Mixing and non-equilibrium chemical reaction in a compressible mixing layer
[NASA-CR-187084] N91-23181
Phase transformations and microstructural evolution in aged Mn-Cu-based alloys
[AD-A232473] N91-23305
Scattering from thin apertures in coated conductors using FDTD
[AD-A232125] N91-23365
Non-linear interaction of a detonation/vorticity wave
[NASA-CR-187550] N91-23434
Numerical simulation of incompressible inhomogeneous turbulence in a plane channel flow
[ESA-TT-1199] N91-23441
FINITE ELEMENT METHOD
Thermo-viscoelastic behavior of composite materials N91-23243
An experimental and finite element investigation into the nonlinear material behavior of pin-loaded composite laminates
[AD-A232098] N91-23263
Determination of the deviatoric material response functions for prestrained rubbers
[FFA-TN-1990-29] N91-23321
Review of finite element procedures for earth retaining structures
[AD-A232230] N91-23343
Developing natural convection in a fluid layer with localized heating and large viscosity variation
[DE91-005240] N91-23431
The solidification of a molten droplet on an inclined plane
[NPL-DMM(A)-20] N91-23438
Computational life prediction methodology for mechanical systems using dynamic simulation, finite element analysis, and fatigue life prediction methods N91-23494
Finite element based dynamical modeling of flexible open-loop manipulators with experimental results N91-23496
Effects of rim thickness on spur gear bending stress
[NASA-TM-104388] N91-23500
Parametric study in weld mismatch of longitudinally welded SSME HPFTP inlet
[NASA-TM-103534] N91-23502
Modal analysis of multistage gear systems coupled with gearbox vibrations
[NASA-TM-103797] N91-23513
Bobbin stresses generated by wire winding
[DE91-009545] N91-23526
Finite element analysis of the lateral buckling of a cantilevered I Beam
[DE91-010123] N91-23527
Stress analysis of a double-doubler joint in composite structure N91-23530
Mechanical states in wound heterogeneous tapes by the finite element method
[DE91-009255] N91-23536
A comparison between classical and substructuring finite-element stress analysis of a complex vacuum vessel shell
[DE91-010035] N91-23540
Use of personal computers in performing a linear modal analysis of a large finite-element model
[DE91-010112] N91-23541
Buckling analysis of a complex vacuum vessel using the finite-element method
[DE91-010032] N91-23546
Incorporating finite element analysis into component life and reliability
[NASA-TM-104400] N91-23550
Computer programs for simulation of electrodeposition
[DE91-010203] N91-23741
A moving boundary algorithm for the solution of contact problems in linear elasticity. Part 1: Basic theory and model examples
[FFA-TN-1991-08-PT-1] N91-23759
On locking and robustness in the finite element method
[AD-A232245] N91-23815
The H-P version of the finite element method in the plate modelling problem
[AD-A232246] N91-23816
FINS
Analysis of the flutter characteristics of the advanced kinetic energy missile (ADKEM) control surface
[AD-A232377] N91-23193
FIRE EXTINGUISHERS
Power packs: A passive approach to extinguishing fire in combat vehicles
[AD-A232020] N91-23342
FIRE PREVENTION
Aircraft Command in Emergency Situations (ACES). Phase 1: Concept development
[DOT/FAA/CT-90/21] N91-23097
Power packs: A passive approach to extinguishing fire in combat vehicles
[AD-A232020] N91-23342
FIRES
Aircraft Command in Emergency Situations (ACES). Phase 1: Concept development
[DOT/FAA/CT-90/21] N91-23097
FISSION
Microscopic heavy-ion theory
[DE91-010739] N91-23869
Light particle emissions in heavy ion reactions
[DE91-010746] N91-23871
FLAME PROPAGATION
An experimental study of flamelet surfaces in turbulent combustion
[AD-A232342] N91-23284
FLAME RETARDANTS
The effect of post-cure and antimony trioxide addition on the glass transition of polyester and vinyl ester resin systems
[AD-A232523] N91-23325
Flame-retardant composite materials N91-24064
FLAME TEMPERATURE
A CFD study of jet mixing in reduced flow areas for lower combustor emissions
[NASA-TM-104411] N91-23185
FLAMES
Aerodynamics and stabilization of combustion of hydrogen jets injected into subsonic airflow N91-23164
Experimental investigations on the transition from stable to unstable combustion by means of active instability control N91-23165
Computer modeling of soot formation comparing free radical and ionic mechanisms
[AD-A232820] N91-23287
FLAMMABILITY
Fractal image compression of Rayleigh, Raman, LIF and LDV data in turbulent reacting flows
[AD-A232237] N91-23449
FLEXIBILITY
Microwave landing system modeling with application to air traffic control
[NASA-TM-102832] N91-23099
Flexible fluoropolymer filled protective coatings N91-24062
FLEXIBLE BODIES
An analytic study of general dynamic model and nonlinear feedback control of flexible robot arms N91-23497
System modeling and identification of flexible structures N91-23531
FLIGHT ALTITUDE
A test of the American Safety Flight Systems, Inc. prebreather/portable oxygen system
[AD-A232723] N91-23100
FLIGHT CHARACTERISTICS
Flying Qualities
[AGARD-CP-508] N91-23108
The art of flying qualities testing N91-23109

ADFCS and NOTAR (trademark): Two ways to fix flying qualities N91-23110
MIL-STD-1797 is not a cookbook N91-23111
Flying qualities experience on the AMX aircraft N91-23112
The development of alternate criteria for FBW handling qualities N91-23113
Development of MIL-8785C into a handling qualities specification for a new European fighter aircraft N91-23114
Do civil flying qualities requirements address military missions for off-the-shelf procurement N91-23115
Handling qualities of highly augmented unstable aircraft summary of an AGARD-FMP working group effort N91-23116
The handling qualities of the STOL and maneuver technology demonstrator from specification to flight test N91-23117
Metrics for roll response flying qualities N91-23118
The flying qualities influence of delay in the fighter pilot's cuing environment N91-23120
Estimation of pilot ratings via pilot modeling N91-23121
An initial study into the influence of control stick characteristics on the handling qualities of a fly-by-wire helicopter N91-23122
Flying qualities of the X-29 forward swept wing aircraft N91-23127
Agility: A rational development of fundamental metrics and their relationship to flying qualities N91-23129
Evaluation techniques for highly augmented aircraft [DLR-FB-90-35] N91-23191

FLIGHT CONDITIONS
Theoretical and experimental performance of a solid fuel ramjet combustion cycle for hypersonic flight conditions N91-23170

FLIGHT CONTROL
Flying Qualities [AGARD-CP-508] N91-23108
The art of flying qualities testing N91-23109
ADFCS and NOTAR (trademark): Two ways to fix flying qualities N91-23110
MIL-STD-1797 is not a cookbook N91-23111
Development of MIL-8785C into a handling qualities specification for a new European fighter aircraft N91-23114
Handling qualities of highly augmented unstable aircraft summary of an AGARD-FMP working group effort N91-23116
The flying qualities influence of delay in the fighter pilot's cuing environment N91-23120
Determination of decision-height windows for decelerating IMC approaches in helicopters N91-23124
Flying qualities of the X-29 forward swept wing aircraft N91-23127
Handling qualities evaluation for highly augmented helicopters N91-23128
Buffet induced structural/flight-control system interaction of the X-29A aircraft [NASA-TM-101735] N91-23133
Evaluation techniques for highly augmented aircraft [DLR-FB-90-35] N91-23191
The electrical flight control system of A320 Airbus: A fault tolerant system [REPT-911-111-103] N91-23192

FLIGHT MECHANICS
Flight mechanics/air navigation research field. A 1990 Scientific report of the German Air and Space Research Organization [ISSN-0720-7808] N91-23103
Handling qualities guidelines for the design of fly-by-wire flight control systems for transport aircraft N91-23119
Integration of handling quality aspects into the aerodynamic design of modern unstable fighters N91-23125

FLIGHT PATHS
Microwave landing system modeling with application to air traffic control [NASA-TM-102832] N91-23099

FLIGHT SAFETY
Near midair collisions as an indicator of general aviation collision risk N91-23096
Flight mechanics/air navigation research field. A 1990 Scientific report of the German Air and Space Research Organization [ISSN-0720-7808] N91-23103

FLIGHT SIMULATION
Handling qualities evaluation for highly augmented helicopters N91-23128
Analytical study of the effects of weight on Light Helicopter (LH) exposure to ground-based weapons [AD-A232024] N91-23141
Evaluation techniques for highly augmented aircraft [DLR-FB-90-35] N91-23191

FLIGHT SIMULATORS
An investigation into the use of side-arm control for civil rotorcraft applications N91-23123
Handling qualities evaluation for highly augmented helicopters N91-23128

FLIGHT TESTS
Flight mechanics/air navigation research field. A 1990 Scientific report of the German Air and Space Research Organization [ISSN-0720-7808] N91-23103
Differential GPS terminal area test results [AD-A232668] N91-23106
The art of flying qualities testing N91-23109
ADFCS and NOTAR (trademark): Two ways to fix flying qualities N91-23110
An investigation into the use of side-arm control for civil rotorcraft applications N91-23123
B-1B high AOA testing in the evaluation of a stall inhibitor system N91-23126
Handling qualities evaluation for highly augmented helicopters N91-23128
X-31A at first flight N91-23131
Long time measurements of landing gear loads on SAAB SF-340 commuter aircraft [FFA-TN-1990-53] N91-23138
Feasibility study of the Superconducting Gravity Gradiometer (SGG) flight test on the European Retrievable Carrier (EURECA) [NASA-CR-184157] N91-23229

FLOW DISTORTION
Effects of inlet distortion on the development of secondary flows in a subsonic axial inlet compressor rotor [NASA-TM-104356] N91-23179

FLOW DISTRIBUTION
An experimental study of an axisymmetric turbulent boundary layer disturbed by a periodic freestream N91-23078
Interferometric investigation of supersonic flow fields with shock-shock interactions N91-23082
Supersonic-hypersonic inlet studies for aerospaceplane N91-23160
Use of secondary flows for rapid mixing in scramjet combustors N91-23167
Pitot surveys of two moderately under-expanded jets N91-23172
Reacting shock waves in hypersonic propulsion applications N91-23174
Viscous three-dimensional analyses for nozzles for hypersonic propulsion N91-23175
Effects of inlet distortion on the development of secondary flows in a subsonic axial inlet compressor rotor [NASA-TM-104356] N91-23179
Mixing and non-equilibrium chemical reaction in a compressible mixing layer [NASA-CR-187084] N91-23181
A three-dimensional Navier-Stokes stage analysis of the flow through a compact radial turbine [NASA-TM-104420] N91-23186
IAI hypersonic wind tunnel [IAITIC-87-1006] N91-23194
The effects of controlling vortex formation on the performance of a dump combustor N91-23270
Two-phase flow patterns and frictional pressure gradients in a small rectangular channel [DE91-009652] N91-23414
An experimental investigation of vortex pair interaction with a clean or contaminated free surface N91-23419
Flow field study of a rectangular jet N91-23423
Numerical modeling of turbulent dispersion around structures using a particle-in-cell method [DE91-009757] N91-23426
Numerical simulation and topological analysis of the separated flow around a sphere [DLR-FB-90-43] N91-23435
Aero-thermal investigation of a highly loaded transonic linear turbine guide vane cascade. A test case for inviscid and viscous flow computations [VKI-TN-174] N91-23437
Riemann problems and the WAF method for the two-dimensional shallow water equations [CRANFIELD-AERO-9005] N91-23443
Computation of inlet reference plane flow-field for a subscale free-jet forebody/inlet model and comparison to experimental data [AD-A232101] N91-23445
Effects of three-dimensional imposed disturbance on bluff-body near wake flows [AD-A232137] N91-23447
Chemical reactions in turbulent mixing flows [AD-A232610] N91-23450
Vortex system evolution in 2- and 3-D swept trailing edge flows [AD-A232692] N91-23453
The propagation of acoustic disturbances in the transonic flow fields of wings [ESA-TT-1126] N91-23854
Aero-optics measurement system for the AEDC aero-optics test facility [AD-A232852] N91-23908

FLOW EQUATIONS
Investigation of Roe's 2D wave decomposition models for the Euler equations [VKI-TN-172] N91-23436
Strategy Combining Regionally Adapted Processes (SCRAP) [AD-A232158] N91-23448

FLOW MEASUREMENT
Effects of inlet distortion on the development of secondary flows in a subsonic axial inlet compressor rotor [NASA-TM-104356] N91-23179
The VKI hypersonic wind tunnels and associated measurement techniques [VKI-TM-46] N91-23196
High resolution measurements of strained diffusion and reaction layer structure and extinction in turbulent flows [AD-A232794] N91-23456
An on-line computerized system for blood-flow measurements N91-23834
Advanced diagnostics for reacting flows [AD-A232609] N91-23902

FLOW STABILITY
Vortex system evolution in 2- and 3-D swept trailing edge flows [AD-A232692] N91-23453
Interdisciplinary research on viscoelasticity and rheology [AD-A232700] N91-23454
A one dimensional wind profile model with stability and eddy viscosity estimations from sodar data [DM-56] N91-23680

FLOW THEORY
A theory for fluidelastic instability of tube-support-plate inactive modes [DE91-006001] N91-23542

FLOW VELOCITY
Effects of inlet distortion on the development of secondary flows in a subsonic axial inlet compressor rotor [NASA-TM-104356] N91-23179
Development and utilization of new diagnostics for dense-phase pneumatic transport [DE91-008947] N91-23339

FLOW VISUALIZATION
Aero-thermal investigation of a highly loaded transonic linear turbine guide vane cascade. A test case for inviscid and viscous flow computations [VKI-TN-174] N91-23437

FLUE GASES
High temperature membranes for H2S and SO2 separations [DE91-008534] N91-23275
Experience with conventional inelastic analysis procedures in very high temperature applications [DE91-009937] N91-23545

FLUENCE
Investigation of neutral atom and ion emission during laser conditioning of multilayer HfO2-SiO2 coatings [DE91-009749] N91-23860

FLUID DYNAMICS
Numerical simulations of instabilities in compressible mixing layers N91-23412

FLUID FILMS
A system-approach to the elastohydrodynamic lubrication point-contact problem [NASA-TM-104342] N91-23439

FLUID FLOW
Hairpin vortices, singularities, and transition to turbulence in three-dimensional shear flows [DE91-002792] N91-23430
Developing natural convection in a fluid layer with localized heating and large viscosity variation [DE91-005240] N91-23431
Nonlinear waves in real materials [AD-A232654] N91-23452
Adaptive methods for compressible fluid dynamics [AD-A232786] N91-23455
A theory for fluidelastic instability of tube-support-plate inactive modes [DE91-006001] N91-23542

FLUID MECHANICS
Development of a quiet supersonic wind tunnel with a cryogenic adaptive nozzle [NASA-CR-186769] N91-23195
Stress-density variations in alumina sediments: Effects of polymer chemistry [DE91-009055] N91-23313
Fundamental hydrodynamics research [AD-A232650] N91-23451

FLUORINATION
Oxidation studies of fluorine containing diamond films
[AD-A232696] N91-23328
FLUORINE COMPOUNDS
Hepatic metabolism of perfluorinated carboxylic acids: A nuclear magnetic resonance investigation
[AD-A232033] N91-23706
FLUOROHYDROCARBONS
Temperature dependence of ultraviolet absorption cross-sections of alternative chlorofluoroethanes
[AERONOMICA-ACTA-A-358-1991] N91-23647
FLUOROPOLYMERS
Flexible fluoropolymer filled protective coatings
N91-24062
FLUTTER ANALYSIS
Analysis of the flutter characteristics of the advanced kinetic energy missile (ADKEM) control surface
[AD-A232377] N91-23193
FLUX (RATE)
Energy exchange study at the ocean surface by satellite observation N91-23597
FLUX DENSITY
Quantum chemical studies of candidate high energy density material compounds
[AD-A232393] N91-23335
Evaluation of cathode materials for high energy lithium secondary batteries
[DE91-764240] N91-23385
Incoherent scatter measurements and inferred energy fluxes in the equatorial F-region ionosphere N91-23640
FLUX VECTOR SPLITTING
Computation of viscous shock/shock hypersonic interactions with an implicit flux split scheme
[AD-A232405] N91-23093
FLY BY WIRE CONTROL
Flying qualities experience on the AMX aircraft
N91-23112
The development of alternate criteria for FBW handling qualities N91-23113
Handling qualities guidelines for the design of fly-by-wire flight control systems for transport aircraft N91-23119
An initial study into the influence of control stick characteristics on the handling qualities of a fly-by-wire helicopter N91-23122
An investigation into the use of side-arm control for civil rotorcraft applications N91-23123
FOCAL PLANE DEVICES
Infrared focal plane performance in the South Atlantic anomaly
[NASA-CR-186197] N91-23458
FOOD PRODUCTION (IN SPACE)
Monitoring and control technologies for bioregenerative life support systems/CELSS N91-24060
FORCED VIBRATION
Reduced vector basis for dynamic analysis of large damped structures N91-23525
FORECASTING
Development of a low cost peak shaving generator set
[PB91-136374] N91-23332
Sufficient comparison and modeling of forecasts
N91-23829
FOREIGN POLICY
Technology transfer in a changing national security environment
[AD-A232458] N91-24000
FORESTS
Analysis on forest decline classification of the beech using airborne multispectral scanner data
[DLR-FB-90-56] N91-23614
FORGING
Post-overload fatigue crack recovery in powder metal aluminum-lithium AL-905XL forging
[AD-A232550] N91-23307
FORMALISM
Computerized symbolic closed-form dynamics and control analysis of hybrid rigid and elastic multibody systems N91-23532
Designing logic controllers with Petri nets
[REPT-90-029] N91-23747
Nilpotent normal form via Carleman linearization (for systems of ordinary differential equations)
[RR-838-M] N91-23809
Initial data for the two-body problem of general relativity N91-23965
FORMULATIONS
Formulation of boundary conditions for the multigrid acceleration of the Euler and Navier Stokes equations
[NASA-CR-188234] N91-23440
Hierarchic modeling of plates
[AD-A232754] N91-23560
FORTRAN
The reduced version of the DERF 2 data set on a WORM optical disk
[DM-54] N91-23991
FOUNDRIES
Aerospatiale industrial thermal plasmas
[REPT-911-430-113] N91-23927
Plasma on a foundry cupola
[REPT-911-430-125] N91-23929
FOURIER ANALYSIS
Analysis of the multigrid method N91-23418
A fast algorithm for the evaluation of trigonometric series
[AD-A232848] N91-23775
Surface x ray scattering measurements of the substrate induced spatial modulation of an incommensurate adsorbed monolayer
[AD-A232625] N91-23959
FOURIER SERIES
A fast algorithm for the evaluation of trigonometric series
[AD-A232848] N91-23775
FOURIER TRANSFORMATION
The 2-D acousto-optic signal processors for simultaneous spectrum analysis and direction finding
[AD-A232148] N91-23367
High-precision Fourier transform spectroscopy of atmospheric molecules N91-23637
A fast algorithm for the evaluation of trigonometric series
[AD-A232848] N91-23775
Parallelizing the spectral transform method, part 1
[DE91-010453] N91-23805
Measurements of passive-scalar spectra for grid turbulence using a nonlinear optical technique
[DE91-005310] N91-23892
FRACTALS
Background simulation and filter design using iterated function systems
[AD-A232632] N91-23405
Fractal image compression of Rayleigh, Raman, LIF and LDV data in turbulent reacting flows
[AD-A232237] N91-23449
FRACTIONATION
Interphase transport and multistage separations
[DE91-009627] N91-23425
FRACTURE MECHANICS
Thermo-viscoelastic behavior of composite materials
N91-23243
Mechanical characterisation of fibre-matrix interface in ceramic composites by an instrumented indentation test
[REPT-911-430-114] N91-23256
Potential impact of enhanced fracture-toughness data on fracture mechanics assessment of PWR vessel integrity for pressurized thermal shock
[DE91-009554] N91-23509
Fundamental research on tribology
[AD-A232446] N91-23519
Study of static and dynamic fracture using strain measurements
[PB91-132217] N91-23524
A statistical model of fractures N91-23529
Application of elastic and elastic-plastic fracture mechanics methods to surface flaws
[NASA-TM-104964] N91-23539
Evaluation of catastrophic failure risk in pressure vessels. Results of pressure vessel test with a large vessel (HC2-test)
[VTT-RR-708] N91-23551
Elastic/plastic fracture mechanics. Part 2: Marine structural applications
[AD-A232560] N91-23557
FRACTURE STRENGTH
Strain rate sensitivity of polymer-matrix composites under mode I delamination
[AD-A232761] N91-23268
Chevron-notched, flexure tests for measuring the elevated temperature fracture resistance of structural ceramics
[DE91-009117] N91-23310
Mechanical behavior and failure phenomenon of an in situ-toughened silicon nitride
[NASA-TM-103741] N91-23311
Potential impact of enhanced fracture-toughness data on fracture mechanics assessment of PWR vessel integrity for pressurized thermal shock
[DE91-009554] N91-23509
Evaluation and ranking of candidate ceramic wafer engine seal materials
[NASA-TM-103795] N91-23515
Stochastic micromechanical modeling of cleavage fracture in the ductile-brittle transition region
N91-23533
Computational simulation of acoustic fatigue for hot composite structures
[NASA-TM-104379] N91-23548
FRACTURES (MATERIALS)
How to know CMC
[REPT-911-430-130] N91-23262
A complex systems approach to metallic fracture surface characterization
[AD-A232546] N91-23556
FRACTURING
Stochastic micromechanical modeling of cleavage fracture in the ductile-brittle transition region
N91-23533
A complex systems approach to metallic fracture surface characterization
[AD-A232546] N91-23556
FRAMES
Analysis of truss frames by method of the stiffness matrix
[AD-A232053] N91-23555
FREE BOUNDARIES
A system-approach to the elastohydrodynamic lubrication point-contact problem
[NASA-TM-104342] N91-23439
FREE ENERGY
Order and disorder in metallic alloys
[DE91-009120] N91-23292
FREE FALL
An experimental method for studying combustion of an unsupported fuel droplet at reduced gravity N91-23273
FREE FLOW
An experimental study of an axisymmetric turbulent boundary layer disturbed by a periodic freestream
N91-23078
Computation of inlet reference plane flow-field for a subscale free-jet forebody/inlet model and comparison to experimental data
[AD-A232101] N91-23445
FREE JETS
Computation of inlet reference plane flow-field for a subscale free-jet forebody/inlet model and comparison to experimental data
[AD-A232101] N91-23445
FREE RADICALS
Computer modeling of soot formation comparing free radical and ionic mechanisms
[AD-A232820] N91-23287
Comment on: Analytic solution of the Stochastic-Liouville model of spin-exchange
[DE91-010570] N91-23861
FREQUENCIES
Frequency domain laser velocimeter signal processor
N91-24077
FREQUENCY ANALYZERS
A method for machinery condition monitoring of transient phenomena using the pseudo Wigner-Ville distribution
[AD-A232014] N91-23760
FREQUENCY CONTROL
A controlled master frequency oscillator for the SSC low energy booster
[DE91-011004] N91-23391
FREQUENCY MEASUREMENT
Ionosphere 1985, volume 73
[ISSN-0211-5166] N91-23650
Frequency domain laser velocimeter signal processor
N91-24077
FREQUENCY MODULATION
Error control coding for multi-frequency modulation
[AD-A232421] N91-23374
FRICTION
Energy dissipator
[NASA-CASE-MSC-21555-1] N91-23492
FRICTION FACTOR
Magnetostrictive roller drive motor
[NASA-CASE-GSC-13369-1] N91-23380
Two-phase flow patterns and frictional pressure gradients in a small rectangular channel
[DE91-009652] N91-23414
FRUSTUMS
Metallic threaded composite fastener
[NASA-CASE-MSC-21580-1] N91-23491
FUEL COMBUSTION
Theoretical and experimental performance of a solid fuel ramjet combustion cycle for hypersonic flight conditions
N91-23170
Automatic particle sizing from rocket motor holograms
[AD-A232553] N91-23236
The effects of controlling vortex formation on the performance of a dump combustor N91-23270
An experimental method for studying combustion of an unsupported fuel droplet at reduced gravity N91-23273
Low heat rejection diesel ceramic coupon tests
[DE91-006274] N91-23318
FUEL CONSUMPTION
Trajectory optimization considerations for ramjet engines N91-23151
FUEL INJECTION
Use of secondary flows for rapid mixing in scramjet combustors N91-23167
Analytical and experimental investigations of the oblique detonation wave engine concept N91-23169

FUNCTIONAL DESIGN SPECIFICATIONS
Characteristics of a future aeronautical satellite communications system [NASA-TM-104389] N91-23102
FUNCTIONS (MATHEMATICS)
Table-lookup algorithms for elementary functions and their error analysis [DE91-006047] N91-23743
Functional approximation by feed-forward networks: A least squares approach to generalisation [RSRE-MEMO-4453] N91-23811
Nonlinear real-time optical signal processing [AD-A232889] N91-23909
FUNGI
Isolation, cloning and expression of the genes for microbial polyurethane degradation [AD-A232108] N91-23699
FURNACES
Plasma on a foundry cupola [REPT-911-430-125] N91-23929
FUSELAGES
Unified aeroacoustics analysis for high speed turboprop aerodynamics and noise. Volume 5: Propagation of propeller tone noise through a fuselage boundary layer [NASA-CR-185195] N91-23852
Noise inside aircraft fuselages subjected to airborne excitations [REPT-911-111-104] N91-23853
FUSION REACTORS
Mars manned fusion spaceship [NASA-CR-188215] N91-23232
Turbulence and the feasibility of self-cooled liquid-metal blankets for fusion reactors [SER-10/P-REV] N91-23910
FUZZY SETS
Advanced methods of approximate reasoning [AD-A232140] N91-23814
Detection of outliers and robust estimation using fuzzy clustering [RR-822-M] N91-23823
FUZZY SYSTEMS
Detection of outliers and robust estimation using fuzzy clustering [RR-822-M] N91-23823
Applications of fuzzy logic to control and decision making N91-24049

G

G STARS
Near-infrared milliarcsecond observations by the lunar occultation technique N91-24034
GALACTIC CLUSTERS
Biased galaxy formation in the neutrino scenario N91-23839
Hard x ray imaging telescope [DE90-015815] N91-24013
Ultraviolet gas absorption and dust extinction toward M8 and the outer galactic disk N91-24018
GALACTIC EVOLUTION
Biased galaxy formation in the neutrino scenario N91-23839
A cosmic superfluid phase [NASA-CR-188171] N91-24016
Recent star formation and the galaxy collisions in NGC 520 N91-24021
GALACTIC NUCLEI
High resolution imaging for Brackett gamma and H2 1-0 S(1) emission in the Seyfert galaxy NGC 1068 [MPE-PREPRINT-192] N91-23104
GALACTIC STRUCTURE
An observational study of arm structure in normal spiral galaxies N91-24007
GALLIUM ARSENIDE LASERS
Vertical emitting, ring geometry, ultra-low threshold and ultra-high speed quantum well lasers for optical interconnect [AD-A232122] N91-23481
GALLIUM ARSENIDES
Electronic GaAs-on-silicon material for advanced high-speed optoelectronic devices [AD-A232088] N91-23399
Low-temperature laser-induced selective area growth of compound semiconductor N91-23932
Electronic properties of Si-doped n-doping-intrinsic-p-doping-intrinsic (nipi) structures in GaAs [DE91-009474] N91-23941
Strain release in GaAs/Ga(1-x)/In(x)As strained layer superlattices grown on (112) substrates [DE91-009972] N91-23944
Optoelectronic III-V heterostructures on SI substrates [AD-A232035] N91-23950
SZ series GaAs super high-speed logic gate: Optimum choice. High tech; high speed; high quality [AD-A232819] N91-23962
Microwave integrated circuits for space applications N91-24069
GALLIUM NITRIDES
Laser assisted CVD growth of AlN and GaN [AD-A232379] N91-23957
GALLIUM PHOSPHIDES
Low-temperature laser-induced selective area growth of compound semiconductor N91-23932
GAME THEORY
Some problems in nonlinear analysis [AD-A232701] N91-23820
GAMMA RAY ASTRONOMY
Imaging and background in low-energy gamma ray astronomy N91-24005
A search for very high-energy gamma rays from Cygnus X-3 N91-24039
The high energy spectrum of the 1983, August 1b gamma-ray burst [MPE-PREPRINT-194] N91-24040
GAMMA RAY BURSTS
The high energy spectrum of the 1983, August 1b gamma-ray burst [MPE-PREPRINT-194] N91-24040
GAMMA RAY SPECTROMETERS
Measurement control for calorimetric assay [DE91-009445] N91-23274
GAMMA RAY TELESCOPES
Imaging and background in low-energy gamma ray astronomy N91-24005
GAMMA RAYS
Study of the response of a crystal ball made of NaI(Tl) for heavy ions experiments [NOTA-INTERNA-957] N91-23874
Imaging and background in low-energy gamma ray astronomy N91-24005
Hard x ray imaging telescope [DE90-015815] N91-24013
The Black Widow pulsar PSR 1957+20: A potential VHE gamma-ray source N91-24038
GARNETS
Contract crystal growth and fabrication services [AD-A232120] N91-23952
GAS DENSITY
Gravity spreading in the dispersion of dense gas plumes [DE91-010155] N91-23628
GAS DISCHARGE TUBES
Radioluminescent (RL) lighting system development program [DE91-009743] N91-23381
GAS DYNAMICS
On 2+1-dimensional nonlinear integrable systems of Loewner-type [MATHS-REPT-A-140] N91-23813
GAS EVOLUTION
Gas evolution and bubble formation on electrodes [ESA-TT-1191] N91-23278
GAS EXCHANGE
Atmospheric leakage and condensate production in NASA's biomass production chamber. Effect of diurnal temperature cycles [NASA-TM-103819] N91-23718
GAS EXPANSION
Pitot surveys of two moderately under-expanded jets N91-23172
GAS FLOW
Diffusive, electrostatic concentration of disintegration products of inert gases in vortex flow [AD-A232876] N91-23457
GAS GENERATORS
Development of a low cost peak shaving generator set [PB91-136374] N91-23332
GAS GIANT PLANETS
Cryomagmatism in the outer solar system N91-24019
GAS INJECTION
Direct gas injection with glow plug ignition [PB91-136390] N91-23272
GAS JETS
Aerodynamics and stabilization of combustion of hydrogen jets injected into subsonic airflow N91-23164
Pitot surveys of two moderately under-expanded jets N91-23172
Flow field study of a rectangular jet N91-23423
GAS MIXTURES
Real time analysis systems of the physical parameters of the environment and the state of a human organism for a long term exposure at different gas mixtures and pressure up to 100 bar N91-23568
GAS STREAMS
Use of secondary flows for rapid mixing in scramjet combustors N91-23167
GAS TUNGSTEN ARC WELDING
Heat and mass transfer in the gas tungsten and gas metal arc welding processes [DE91-010089] N91-23510
GAS TURBINE ENGINES
Research on aerodynamic control of blade tip clearance flow in air-cooled turbine [DE91-764223] N91-23182
Water-cooling technique of high temperature gas turbine blade [DE91-764238] N91-23506
GAS TURBINES
Multi-heat addition turbine engine [NASA-CASE-LEW-15094-1] N91-23180
GASEOUS DIFFUSION
Diffusive, electrostatic concentration of disintegration products of inert gases in vortex flow [AD-A232876] N91-23457
Treatment of denser-than-air releases in an advection-diffusion model: Thermodynamic effects [DE91-010152] N91-23632
GASEOUS FISSION REACTORS
Gas core reactors for direct nuclear propulsion [DE91-010050] N91-23884
GASES
Gas contents and weldability of aluminum die castings [ETN-91-99188] N91-23302
Gravity spreading in the dispersion of dense gas plumes [DE91-010155] N91-23628
GASIFICATION
Theoretical and experimental performance of a solid fuel ramjet combustion cycle for hypersonic flight conditions N91-23170
GATES (CIRCUITS)
SZ series GaAs super high-speed logic gate: Optimum choice. High tech; high speed; high quality [AD-A232819] N91-23962
GAUSSIAN ELIMINATION
Optimal systolic network for Gaussian elimination [RR-837-I] N91-23822
GEARS
Effects of rim thickness on spur gear bending stress [NASA-TM-104388] N91-23500
Modal analysis of multistage gear systems coupled with gearbox vibrations [NASA-TM-103797] N91-23513
Maximum life spur gear design [NASA-TM-104361] N91-23514
GENE EXPRESSION
Robotics for recombinant DNA and human genetics research [DE90-016440] N91-23697
Isolation, cloning and expression of the genes for microbial polyurethane degradation [AD-A232108] N91-23699
GENES
Robotics for recombinant DNA and human genetics research [DE90-016440] N91-23697
GENETIC CODE
Robotics for recombinant DNA and human genetics research [DE90-016440] N91-23697
GENETIC ENGINEERING
New hosts and vectors for genome cloning [DE91-009996] N91-23696
Isolation, cloning and expression of the genes for microbial polyurethane degradation [AD-A232108] N91-23699
GENETICS
Robotics for recombinant DNA and human genetics research [DE90-016440] N91-23697
Convergence of one-dimensional diffusion processes to a jump process related to population genetics [AD-A232121] N91-23826
Genetic algorithms N91-24050
GEODESY
Precision orbit determination of global positioning system satellites N91-23202
GEODETIC ACCURACY
Precision orbit determination of global positioning system satellites N91-23202
GEODETIC COORDINATES
Sea level and satellite techniques N91-23595
GEODETIC SURVEYS
High precision applications of the global positioning system N91-24073
GEOGRAPHIC INFORMATION SYSTEMS
The integration of remote sensing, geographic information system, and expert system technologies for landcover classification N91-23733
Potential commercial uses of EOS remote sensing products N91-24055

GEOGRAPHY
SWANEA (Southwest Asia-Northeast Africa): A climatological study. Volume 2: The Middle East Peninsula
[AD-A232776] N91-23684
GEOLOGY
Cryomagmatism in the outer solar system N91-24019
GEOMAGNETIC TAIL
Echo 7: Magnetospheric properties determined by artificial electron beams N91-23644
GEOMAGNETISM
Neutral wind vortices in the high-latitude thermosphere N91-23673
Geomagnetic storms: Potential economic impacts on electric utilities
[DE91-009523] N91-24036
GEOMETRIC ACCURACY
European stakes and measures permitting the management of geometric dimensions N91-23573
GEOMETRICAL ACOUSTICS
The propagation of acoustic disturbances in the transonic flow fields of wings
[ESA-TT-1126] N91-23854
GEOMETRY
The effect of realistic antenna geometries on plasma loading predictions
[DE91-010782] N91-23353
Adaptive methods for compressible fluid dynamics
[AD-A232786] N91-23455
Near-equatorial deep circulation in the Indian and Pacific oceans
[AD-A232635] N91-23691
GEOMORPHOLOGY
Proceedings of the Second Glacier Bay Science Symposium
[PB91-110163] N91-23634
GEOPOTENTIAL HEIGHT
Atmospheric circulation and poleward sensible heat flux variations associated with the recent Northern Hemisphere warming N91-23629
GEOSAT SATELLITES
Extraction of mesoscale ocean currents information from Geosat altimeter data N91-23594
Wind and sea state local climatology by means of satellite radar altimeter measurements N91-23599
GEOTECHNICAL ENGINEERING
Review of finite element procedures for earth retaining structures
[AD-A232230] N91-23343
GEOTECHNICAL FABRICS
Literature review on geotextiles to improve pavements for general aviation airports
[AD-A232871] N91-23199
GEOTHERMAL ENERGY UTILIZATION
Direct use R/D assistance
[DE91-009976] N91-23999
GEOTHERMAL RESOURCES
Direct use R/D assistance
[DE91-009976] N91-23999
GERMANIUM
Photoresponse studies of ion-damaged germanium for optoelectronic switch applications
[AD-A232091] N91-23400
GLACIERS
The application of equilibrium climate models to questions of glaciation at high latitudes N91-23669
GLACIOLOGY
The application of equilibrium climate models to questions of glaciation at high latitudes N91-23669
GLASS
Shock characterization of epoxy: Forty-two volume percent glass microballoons
[DE91-009616] N91-23314
GLASS FIBER REINFORCED PLASTICS
Modelling of the impact response of fibre-reinforced composites
[AD-A232658] N91-23266
GLASS FIBERS
Fiber-reinforced glass-ceramic matrix composites: New class of materials for space applications
[REPT-911-430-107] N91-23253
Mechanical characterisation of fibre-matrix interface in ceramic composites by an instrumented indentation test
[REPT-911-430-114] N91-23256
GLASS TRANSITION TEMPERATURE
Characterization of the glass transition using a microindenter
[AD-A232154] N91-23282
The effect of post-cure and antimony trioxide addition on the glass transition of polyester and vinyl ester resin systems
[AD-A232523] N91-23325
GLAUBER THEORY
A statistical model of fractures N91-23529
GLOBAL ATMOSPHERIC RESEARCH PROGRAM
Maintenance of short-term subtropical wind maxima in the Southern Hemisphere: Observational and modeling study N91-23665
GLOBAL POSITIONING SYSTEM
Differential GPS terminal area test results
[AD-A232668] N91-23106
Precision orbit determination of global positioning system satellites N91-23202
High precision applications of the global positioning system N91-24073
GOLD ALLOYS
Structure of electrochemically deposited copper on gold (III) alloy
[AD-A232345] N91-23303
GOVERNMENT/INDUSTRY RELATIONS
Government/industry response to questionnaire on space mechanisms/tribology technology needs
[NASA-TM-104358] N91-23501
GOVERNMENTS
The changing face of the environmental issue
[PB91-138081] N91-23624
Access and efficiency in Reagan-era information policy: A case study of the attempt to privatize the National Technical Information Service N91-23977
Five-year plan for meeting the automatic data processing and telecommunications needs of the Federal Government
[PB91-103549] N91-23982
Information resources management long-range plan
[DE91-009745] N91-23984
Aeronautics and space report of the President N91-24085
GRAIN BOUNDARIES
Boundary stability under nonequilibrium conditions
[DE91-009262] N91-23293
Theory of the critical current density in YBa2Cu3O7 ceramics
[DE91-009443] N91-23940
GRANULAR MATERIALS
Thermodynamically consistent formulations for rapid granular and turbulent multiphase flows N91-23420
Mechanics/heat-transfer relation for particulate materials
[DE91-008356] N91-23424
GRAPH THEORY
Optimal systolic network for Gaussian elimination
[RR-837-I] N91-23822
GRAPHITE
Flame-retardant composite materials N91-24064
GRAPHITE-EPOXY COMPOSITES
Thermo-viscoelastic behavior of composite materials N91-23243
GRAPHS (CHARTS)
Energy-efficient penetration of targets
[AD-A232227] N91-23518
Designing logic controllers with Petri nets
[REPT-90-029] N91-23747
GRAVITATION
Gravity spreading in the dispersion of dense gas plumes
[DE91-010155] N91-23628
GRAVITATIONAL EFFECTS
An experimental method for studying combustion of an unsupported fuel droplet at reduced gravity N91-23273
Phenomenological aspects of scalar fields in astrophysics, cosmology and particle physics N91-24014
GRAVITATIONAL FIELDS
The thermodynamic stability of systems containing black holes N91-24022
GRAVITATIONAL PHYSIOLOGY
A non-invasive measure of minerals and electrolytes in tissue N91-24058
GRAVITATIONAL WAVES
Sensitive cryogenic transducer development and analysis for use on gravity wave detectors N91-24009
GRAVITY GRADIOMETERS
Feasibility study of the Superconducting Gravity Gradiometer (SGG) flight test on the European Retrievable Carrier (EURECA)
[NASA-CR-184157] N91-23229
GRAVITY WAVES
A search for strange attractors in the saturation of middle atmosphere gravity waves
[AD-A232468] N91-23658
Grouping of clouds and internal gravity waves in a non-hydrostatic model of moist convection
[DM-55] N91-23679
Sensitive cryogenic transducer development and analysis for use on gravity wave detectors N91-24009
GRAY SCALE
Correction of relief-induced radiometric distortions in Seasat-A SAR images for the example of the subscene of Bonn (Fed. Republic of Germany) and vicinities
[DLR-FB-90-54] N91-23613
GRAZING INCIDENCE
Soft x ray/extreme ultraviolet images of the solar atmosphere with normal incidence multilayer optics N91-24006
GREEN'S FUNCTIONS
Procedure for determination of three-dimensional wind tunnel wall interferences and wall adaptation in compressible subsonic flow using measured wall pressures
[DLR-FB-90-46] N91-23088
Nonequilibrium Green's functions and quantum transport theory for semiconductor microstructures N91-23937
GREENLAND
Range reference atmosphere, Thule
[AD-A232831] N91-23686
Sea ice monitoring in the east Greenland sea in May 1988 by means of remote sensing, with special emphasis on the computer-aided AVHRR-based extraction of sea ice motions
[DLR-FB-90-36] N91-23687
GRID GENERATION (MATHEMATICS)
A three-dimensional free-Lagrange code for multimaterial flow simulations
[DE91-002309] N91-23428
Formulation of boundary conditions for the multigrid acceleration of the Euler and Navier Stokes equations
[NASA-CR-188234] N91-23440
GROUND OPERATIONAL SUPPORT SYSTEM
Distributed, cooperating knowledge-based systems N91-24044
GROUND SUPPORT EQUIPMENT
Localized corrosion of high performance metal alloys in an acid/salt environment N91-24066
GROUP THEORY
Some problems in nonlinear analysis
[AD-A232701] N91-23820
GUIDANCE (MOTION)
A Model-Based Approach to High-Level Robot Control with Visual Guidance
[VTT-PUBL-71] N91-23788
GUIDANCE SENSORS
Robot-sensor co-operation planning for visual guidance N91-23794
A line based object localizing method for robot vision N91-23795
Object pose estimation based on one-degree-of-freedom sensor N91-23796
GUIDE VANES
Aero-thermal investigation of a highly loaded transonic linear turbine guide vane cascade. A test case for inviscid and viscous flow computations
[VKI-TN-174] N91-23437
GUMS (SUBSTANCES)
Determination of the deviatoric material response functions for prestrained rubbers
[FFA-TN-1990-29] N91-23321
GUSTS
Integrated multidisciplinary optimization of actively controlled fiber composite wings N91-23190
GYRATION
Observation of harmonic gyro-backward-wave oscillation in a 100 GHz CARM oscillator experiment
[AD-A232063] N91-23398

H

H II REGIONS
High resolution imaging for Brackett gamma and H2 1-0 S(1) emission in the Seyfert galaxy NGC 1068
[MPE-PREPRINT-192] N91-23104
H II regions and young star clusters in the magellanic clouds N91-24004
Studies of molecular excitation in star formation regions N91-24023
H LINES
High resolution imaging for Brackett gamma and H2 1-0 S(1) emission in the Seyfert galaxy NGC 1068
[MPE-PREPRINT-192] N91-23104
HABITATS
Subsea habitats and space simulation N91-23567
HAFNIUM OXIDES
Investigation of neutral atom and ion emission during laser conditioning of multilayer HfO2-SiO2 coatings
[DE91-009749] N91-23860
HAILSTORMS
Investigation of micro- and macrophysical structures and processes in hail clouds with respect to their modification
[DLR-FB-90-38] N91-23677
HALL EFFECT
A non-contacting velocity measurement system
[NASA-CASE-LAR-14466-1] N91-23461
Hall effects on anomalous heat, particle and helicity transports through tearing-mode turbulence
[DE91-010730] N91-23924

HALOS
Primordial lithium, stellar evolution, and cosmology: Lithium in halo stars from standard, diffusive, and rotational stellar evolution and implications for cosmology N91-24024

HAMILTONIAN FUNCTIONS
Constant of motion and dynamic equations for one-dimensional autonomous system and radiation damping
[DE91-011002] N91-23547

HARDENING (MATERIALS)
Hardening mechanisms and analysis of the structure of the TGDDM/DDS epoxy resin system
[ESA-TT-1202] N91-23319

HARDNESS TESTS
Characterization of the glass transition using a microindenter
[AD-A232154] N91-23282

HARDWARE
Electronic neuroprocessors N91-24045

HARMONIC OSCILLATION
Observation of harmonic gyro-backward-wave oscillation in a 100 GHz CARM oscillator experiment
[AD-A232063] N91-23398

HARMONICS
High energy dense ribbon beams and high harmonic gyrotron at millimeter wavelengths
[AD-A232839] N91-23470

HARTREE APPROXIMATION
Mean-field theories of the Hubbard model and periodic orbits in chaotic maps N91-23938

HAZARDS
Statistical models and inference procedures for structural and materials reliability
[AD-A232634] N91-23827

HEAD DOWN TILT
Transcapillary fluid shifts in head and neck tissues during and after simulated microgravity
[NASA-TM-103847] N91-23704

HEART RATE
Heat strain and work tolerance times with varying levels of Canadian Forces NBC protective clothing, ambient temperature, physical work intensity, and work/rest schedules
[AD-A232653] N91-23720

HEART VALVES
Simulation of blood flow through an artificial heart N91-24056

HEAT EXCHANGERS
Compact heat exchanger for an inverse components engine N91-23157
A new generation of radiators
[REPT-911-440-105] N91-23220
In-Space technology experiments program. A high efficiency thermal interface (using condensation heat transfer) between a 2-phase fluid loop and heatpipe radiator: Experiment definition phase
[NASA-CR-186869] N91-23408

HEAT FLUX
Method of producing a plug type heat flux gauge
[NASA-CASE-LEW-14967-2] N91-23460
Atmospheric circulation and poleward sensible heat flux variations associated with the recent Northern Hemisphere warming N91-23629
Surface layer transfer processes over vegetation: A micrometeorological field experiment of long duration N91-23664

HEAT GENERATION
Lunar volcanism and the thermal evolution of the moon N91-24031

HEAT PIPES
Solar thermal energy receiver
[NASA-CASE-LEW-14949-1] N91-23617

HEAT PUMPS
Advanced working fluids: Thermodynamic properties
[PB91-136465] N91-23964

HEAT RESISTANT ALLOYS
Creep and creep-rupture behavior of Alloy 718
[DE91-007706] N91-23298
High-temperature alloys for high-power thermionic systems
[DE91-009292] N91-23299
High temperature ordered intermetallic alloys
[AD-A232769] N91-23308
Metallic threaded composite fastener
[NASA-CASE-MSC-21580-1] N91-23491
Evaluation and ranking of candidate ceramic wafer engine seal materials
[NASA-TM-103795] N91-23515

HEAT SINKS
In-Space technology experiments program. A high efficiency thermal interface (using condensation heat transfer) between a 2-phase fluid loop and heatpipe radiator: Experiment definition phase
[NASA-CR-186869] N91-23408

HEAT TOLERANCE
Heat strain and work tolerance times with varying levels of Canadian Forces NBC protective clothing, ambient temperature, physical work intensity, and work/rest schedules
[AD-A232653] N91-23720

HEAT TRANSFER
Computation of viscous shock/shock hypersonic interactions with an implicit flux split scheme
[AD-A232405] N91-23093
Viscous three-dimensional analyses for nozzles for hypersonic propulsion N91-23175
Multi-heat addition turbine engine
[NASA-CASE-LEW-15094-1] N91-23180
Measurement control for calorimetric assay
[DE91-009445] N91-23274
Flows with strongly anisotropic turbulence-dynamic and heat transfer aspects
[SER-20/P] N91-23407
In-Space technology experiments program. A high efficiency thermal interface (using condensation heat transfer) between a 2-phase fluid loop and heatpipe radiator: Experiment definition phase
[NASA-CR-186869] N91-23408
Mechanics/heat-transfer relation for particulate materials
[DE91-008356] N91-23424
Interphase transport and multistage separations
[DE91-009627] N91-23425
The solidification of a molten droplet on an inclined plane
[NPL-DMM(A)-20] N91-23438
Heat and mass transfer in the gas tungsten and gas metal arc welding processes
[DE91-010089] N91-23510
Solar thermal energy receiver
[NASA-CASE-LEW-14949-1] N91-23617
Surface layer transfer processes over vegetation: A micrometeorological field experiment of long duration N91-23664
On locking and robustness in the finite element method
[AD-A232245] N91-23815
Summary of basic research in thermoacoustic heat transport: 1990
[AD-A232223] N91-23847
Eureca 1 AMF 117 experiment: An analysis of thermal and solutal transfer during the crystal growth of CdTe by the THM process
[REPT-911-430-118] N91-23947
Eureca 1 AMF 117 experience: Thermal and solutal transfer analysis for CdTe in tellurium during crystal growth by the THM method
[REPT-911-430-120] N91-23948

HEATING
Maintenance of short-term subtropical wind maxima in the Southern Hemisphere: Observational and modeling study N91-23665

HEAVY IONS
Light particle emissions in heavy ion reactions
[DE91-010746] N91-23871
Study of the response of a crystal ball made of NaI(Tl) for heavy ions experiments
[NOTA-INTERNA-957] N91-23874
Calculation of cross sections for binary reactions between heavy ion projectiles and heavy actinide targets
[DE91-010222] N91-23882
Heavy ion beam probe measurements of ECH method plasma in the advanced toroidal facility
[DE91-010391] N91-23917

HEAVY NUCLEI
Science requirements for Heavy Nuclei Collection (HNC) experiment on NASA Long Duration Exposure Facility (LDEF) Mission 2
[NASA-CR-187527] N91-23887

HELICOPTER CONTROL
ADFCS and NOTAR (trademark): Two ways to fix flying qualities N91-23110
Handling qualities evaluation for highly augmented helicopters N91-23128

HELICOPTERS
A study of the noise mechanisms of transonic blade-vortex interactions
[NASA-CR-188199] N91-23084
Airborne rescue system
[NASA-CASE-ARC-11909-1] N91-23095
An initial study into the influence of control stick characteristics on the handling qualities of a fly-by-wire helicopter N91-23122
Determination of decision-height windows for decelerating IMC approaches in helicopters N91-23124
Air ambulance helicopter operational analysis
[DOT/FAA/RD-91/7] N91-23134
AGARD highlights 91/1, March 1991
[AGARD-HIGHLIGHTS-91/1] N91-24084

HELIOSTATS
Qualification of concentrating mirror systems with the Hermes measurement system and the Helios simulation program
[ESA-TT-1213] N91-23230

HERMES MANNED SPACEPLANE
SIMOUN: A high temperature and low pressure testing facility for material characterization
[REPT-911-430-121] N91-23208
SIMOUN: A new test appliance for the development of Hermes thermal protections
[REPT-911-430-129] N91-23209
Materials and structure for Hermes
[REPT-911-430-117] N91-23258
Ceramics in aerospace
[REPT-911-430-127] N91-23260
EVA servicing: The Hermes capability N91-23575
Building real-time simulators for space applications N91-23587

HETEROGENEITY
Data type coherency in heterogeneous shared memory multiprocessors
[AD-A232114] N91-23729

HETEROJUNCTION DEVICES
Vertical emitting, ring geometry, ultra-low threshold and ultra-high speed quantum well lasers for optical interconnect
[AD-A232122] N91-23481
Broad area distributed gain, distributed index profile GaAlAs semiconductor laser diodes
[AD-A232332] N91-23483

HETEROJUNCTIONS
Optoelectronic III-V heterostructures on Si substrates
[AD-A232035] N91-23950
In based III-V microstructures with novel electronic properties
[AD-A232695] N91-23960
Development of Si/SiGe heterostructures
[AD-A232747] N91-23961

HEURISTIC METHODS
Statistical process allocation in a parallel processing architecture
[RR-833-I] N91-23779

HIERARCHIES
Hierarchic modeling of plates
[AD-A232754] N91-23560

HIGH ENERGY INTERACTIONS
A guide to experimental elementary particle physics literature, 1985-1989
[DE91-010209] N91-23856

HIGH FREQUENCIES
A study of PC-Based HF ionospheric propagation predictions for use in naval communications
[AD-A232466] N91-23375

HIGH GAIN
Degeneration of linear multivariable systems under high gain and dynamic compensation N91-23830

HIGH IMPULSE
Gas core reactors for direct nuclear propulsion
[DE91-010050] N91-23884

HIGH POLYMERS
High shear stress rheology of liquid lubricants N91-23309

HIGH RESOLUTION
Technical description of the high-resolution air mass transformation model at KNMI
[KNMI-TR-125] N91-23646
A high resolution study of the Cu K alpha(sub 1,2) x-ray emission lines N91-23841
Soft x ray/extreme ultraviolet images of the solar atmosphere with normal incidence multilayer optics N91-24006

HIGH SPEED
Technology needs for high-speed rotorcraft
[NASA-CR-177578] N91-23136
Electronic GaAs-on-silicon material for advanced high-speed optoelectronic devices
[AD-A232088] N91-23399
The TurboLAN project. Phase 1: Protocol choices for high speed local area networks. Phase 2: TurboLAN Intelligent Network Adapter Card, (TINAC) architecture
[NASA-CR-188175] N91-23776
Unified aeroacoustics analysis for high speed turboprop aerodynamics and noise. Volume 2: Development of theory for wing shielding
[NASA-CR-185192] N91-23849
Unified aeroacoustics analysis for high speed turboprop aerodynamics and noise. Volume 3: Application of theory for blade loading, wakes, noise, and wing shielding
[NASA-CR-185193] N91-23850
Unified aeroacoustics analysis for high speed turboprop aerodynamics and noise. Volume 4: Computer user's manual for UAAP turboprop aeroacoustic code
[NASA-CR-185194] N91-23851

Unified aeroacoustics analysis for high speed turboprop aerodynamics and noise. Volume 5: Propagation of propeller tone noise through a fuselage boundary layer [NASA-CR-185195] N91-23852

SZ series GaAs super high-speed logic gate: Optimum choice. High tech; high speed; high quality [AD-A232819] N91-23962

HIGH STRENGTH ALLOYS

Evaluation of filler metals for high-strength stainless steels [DE91-009931] N91-23295

HIGH STRENGTH STEELS

Evaluation of filler metals for high-strength stainless steels [DE91-009931] N91-23295

HIGH TEMPERATURE

High temperature deformation processes and strengthening mechanisms in intermetallic particulate composites [AD-A232737] N91-23267

High temperature membranes for H2S and SO2 separations [DE91-008534] N91-23275

High-temperature alloys for high-power thermionic systems [DE91-009292] N91-23299

Experience with conventional inelastic analysis procedures in very high temperature applications [DE91-009937] N91-23545

Development of a micromechanic theory of constitutive relations of polycrystalline solids [AD-A232697] N91-23559

Aerospace applications of high temperature superconductivity N91-24080

HIGH TEMPERATURE ENVIRONMENTS

Silicon carbide, an emerging high temperature semiconductor N91-24061

HIGH TEMPERATURE PLASMAS

Hydromagnetic wave coupling in the magnetosphere N91-23638

Advanced diagnostics for reacting flows [AD-A232609] N91-23902

Temperature measurements of ET plasmas using atomic emission spectroscopy [AD-A232498] N91-23930

Soft x ray/extreme ultraviolet images of the solar atmosphere with normal incidence multilayer optics N91-24006

HIGH TEMPERATURE RESEARCH

Silicon carbide, an emerging high temperature semiconductor N91-24061

HIGH TEMPERATURE SUPERCONDUCTORS

S-parameter measurements and applications of superconducting flux flow transistors [DE91-009763] N91-23388

Bulletin of the Israel Physical Society, volume 33, 1987. Annual Meeting 1987: Program and Abstracts [ITN-89-85012] N91-23832

Theory of the new high-temperature superconductors N91-23842

Effect of transition metal dopants on high T(sub c) superconductivity [PB91-130138] N91-23934

Theory of the critical current density in YBa2Cu3O7 ceramics [DE91-009443] N91-23940

Microstructure of epitaxial YBa2Cu3O7 thin films [DE91-009951] N91-23942

Fermi surface of YBCO by DHVA [DE91-009963] N91-23943

Composite ceramic superconducting wires for electric motor applications [AD-A232074] N91-23951

Aerospace applications of high temperature superconductivity N91-24080

Superconducting microwave electronics at Lewis Research Center N91-24081

HIGH TEMPERATURE TESTS

SIMOUN: A high temperature and low pressure testing facility for material characterization [REPT-911-430-121] N91-23208

SIMOUN: A new test appliance for the development of Hermes thermal protections [REPT-911-430-129] N91-23209

Carbon-carbon material with oxidation protection [REPT-911-430-103] N91-23249

Creep and creep-rupture behavior of Alloy 718 [DE91-007706] N91-23298

Chevron-notched, flexure tests for measuring the elevated temperature fracture resistance of structural ceramics [DE91-009117] N91-23310

Low heat rejection diesel ceramic coupon tests [DE91-006274] N91-23318

HISTORIES

The birth of the 'strange' particle physics [NOTA-INTERNA-958] N91-23875

AGARD highlights 91/1, March 1991 [AGARD-HIGHLIGHTS-91/1] N91-24084

HOLE BURNING

Excited state structure, energy and electron transfer dynamics of photosynthetic reaction centers: A hole burning study [DE91-010181] N91-23693

Ultra-dense optical mass storage [AD-A232767] N91-23905

HOLES (ELECTRON DEFICIENCIES)

Re-analysis of photoemission data for CuO: Revision of the configuration-energy scheme for cuprate materials [DE91-009952] N91-23296

HOLES (MECHANICS)

Incorporating finite element analysis into component life and reliability [NASA-TM-104400] N91-23550

HOLMIUM ISOTOPES

Light particle emissions in heavy ion reactions [DE91-010746] N91-23871

HOLOGRAPHIC INTERFEROMETRY

Interferometric investigation of supersonic flow fields with shock-shock interactions N91-23082

HOLOGRAPHY

Automatic particle sizing from rocket motor holograms [AD-A232553] N91-23236

Possibilities for projection x ray lithography using holographic optical elements [DE91-009770] N91-23464

HOMING

Target maneuver models for improved homing guidance N91-23101

Aero-optics measurement system for the AEDC aero-optics test facility [AD-A232852] N91-23908

HONEYCOMB STRUCTURES

Power packs: A passive approach to extinguishing fire in combat vehicles [AD-A232020] N91-23342

HORIZON

Worst-case design of optimal controllers over a finite horizon [AD-A232353] N91-23797

HORSESHOE VORTICES

Hairpin vortices, singularities, and transition to turbulence in three-dimensional shear flows [DE91-002792] N91-23430

HOSES

Localized corrosion of high performance metal alloys in an acid/salt environment N91-24066

HOT CORROSION

Point defect effects on hot corrosion of zirconia-based coatings [AD-A232662] N91-23326

HOT ISOSTATIC PRESSING

Sintering and hot isostatic pressing of Bi2Sr2CaCu2O(x) [DE91-010797] N91-23945

HOUSINGS

Electromagnetic attachment mechanism [NASA-CASE-MSC-21463-1] N91-23490

HOVERING

Technology needs for high-speed rotorcraft [NASA-CR-177578] N91-23136

HUMAN BEINGS

Robotics for recombinant DNA and human genetics research [DE90-016440] N91-23697

The transfer of technology to measure skin burn depth in humans N91-24076

HUMAN FACTORS ENGINEERING

Long duration hyperbaric confinement: Hydra 9 N91-23571

HUMAN PERFORMANCE

A test of the American Safety Flight Systems, Inc. prebreather/portable oxygen system [AD-A232723] N91-23100

Human Performance Assessment Methods. Addendum [AGARD-AG-308-ADD] N91-23711

Effects of bright illumination on oral temperature and cognitive performance in humans during nighttime hours [AD-A232787] N91-23722

Towards real-time GOMS [AD-A232028] N91-23763

HUMAN REACTIONS

The development of highly practiced skills: A starting point for driver modelling [IZF-1990-B-16] N91-23719

HUMAN RESOURCES

Federally funded research: Decisions for a decade [OTA-SET-490] N91-23998

HUMIDITY

Atmospheric leakage and condensate production in NASA's biomass production chamber. Effect of diurnal temperature cycles [NASA-TM-103819] N91-23718

HYBRID CIRCUITS

Silicon avalanche photodiode active-quenching circuit [AD-A233633] N91-23395

Checklist for thick-film hybrid microcircuits manufacturer and line survey [ESA-PSS-01-607-ISSUE-1] N91-23396

Checklist for thin-film hybrid microcircuits manufacturer and line survey [ESA-PSS-01-611-ISSUE-1] N91-23397

HYDRATES

Composition and distribution of carbonates, sulfates, and hydrates on the Martian surface from earth-based spectroscopy between 3-5 microns N91-24033

HYDRATION

Effects of weightlessness (sea water immersion) on body fluid balance and CNS functions N91-23566

HYDRAULIC CONTROL

A first-principles generic methodology for representing the knowledge base of a process diagnostic expert system [DE90-017693] N91-23520

HYDRAULIC EQUIPMENT

Control aspects of the brushless doubly-fed machine [DE91-009707] N91-23387

HYDRAZIDES

Poly(1,3,4-oxadiazoles) via aromatic nucleophilic displacement [NASA-CASE-LAR-14427-1] N91-23237

HYDROCARBON FUELS

Power packs: A passive approach to extinguishing fire in combat vehicles [AD-A232020] N91-23342

HYDROCARBONS

Mass resolved resonance ionization spectroscopy of combustion radicals [DE91-010603] N91-23276

HYDRODYNAMICS

Passive laminar flow control of crossflow vorticity [NASA-CASE-LAR-13563-1] N91-23410

A three-dimensional free-Lagrange code for multimaterial flow simulations [DE91-002309] N91-23428

Fundamental hydrodynamics research [AD-A232650] N91-23451

HYDROGEN

Design considerations of a high expansion ratio hydrogen turbine N91-23163

Aerodynamics and stabilization of combustion of hydrogen jets injected into subsonic airflow N91-23164

Static feed water electrolysis subsystem development [NASA-CASE-MSC-21577-1-SB] N91-23271

Material processing with hydrogen and carbon monoxide on Mars [NASA-TM-104405] N91-23616

HYDROGEN ENGINES

Compact heat exchanger for an inverse components engine N91-23157

HYDROGEN FUELS

Ionic solid hydrogen fuel: Experimental investigation of cluster-impact fusion [AD-A232642] N91-23336

Material processing with hydrogen and carbon monoxide on Mars [NASA-TM-104405] N91-23616

HYDROGEN OXYGEN FUEL CELLS

SEI rover solar-electrochemical power system options [NASA-TM-104402] N91-23620

HYDROGEN PLASMA

A numerical model of laser induced fluorescence in a hydrogen plasma [AD-A232240] N91-23482

HYDROGEN SULFIDE

High temperature membranes for H2S and SO2 separations [DE91-008534] N91-23275

HYDROSTATICS

Gravity spreading in the dispersion of dense gas plumes [DE91-010155] N91-23628

Range reference atmosphere, Shemya [AD-A232813] N91-23685

Range reference atmosphere, Thule [AD-A232831] N91-23686

HYDROXYL RADICALS

High-precision Fourier transform spectroscopy of atmospheric molecules N91-23637

HYGROMETERS

Surface layer transfer processes over vegetation: A micrometeorological field experiment of long duration N91-23664

HYPERBARIC CHAMBERS
Long duration hyperbaric confinement: Hydra 9 N91-23571
HYPERBOLIC DIFFERENTIAL EQUATIONS
The solidification of a molten droplet on an inclined plane
[NPL-DMM(A)-20] N91-23438
Two dimensional optimization of smoothing properties of multistage schemes applied to hyperbolic equations
[VKI-TN-173] N91-23807
HYPERCUBE MULTIPROCESSORS
Mapping an adaptable Eigenstructure technique onto the topologix hypercube
[AD-A232032] N91-23764
HYPERSONIC AIRCRAFT
Navigation, guidance, and trajectory optimization for hypersonic vehicles N91-23150
HYPERSONIC FLIGHT
Problems of hypersonic aerothermodynamics
[MBB-FE202/5/PUB/436] N91-23090
Hypersonic Combined Cycle Propulsion
[AGARD-CP-479] N91-23147
Hypersonic propulsion: Past and present N91-23148
A study of supersonic and hypersonic ramjet engines in France from 1950 to 1974 (application on combined cycle aircraft engines) N91-23149
Trajectory optimization considerations for ramjet engines N91-23151
Hypersonic propulsion: Status and challenge N91-23153
Airbreathing propulsion for space transport: New concepts, special problems and attempts at solutions N91-23154
Turbojet potential for hypersonic flight N91-23155
Compact heat exchanger for an inverse components engine N91-23157
Design considerations for combined air breathing-rocket propulsion systems
[AIAA-90-0098] N91-23158
Some aspects of shock-wave boundary layer interaction relevant to intake flows N91-23161
Analytical and experimental investigations of the oblique detonation wave engine concept N91-23169
Theoretical and experimental performance of a solid fuel ramjet combustion cycle for hypersonic flight conditions N91-23170
Reacting shock waves in hypersonic propulsion applications N91-23174
Viscous three-dimensional analyses for nozzles for hypersonic propulsion N91-23175
IAI hypersonic wind tunnel
[IAITIC-87-1006] N91-23194
HYPERSONIC FLOW
Reacting shock waves in hypersonic propulsion applications N91-23174
HYPERSONIC INLETS
Supersonic-hypersonic inlet studies for aerospaceplane N91-23160
Computational modeling and validation for hypersonic inlets N91-23162
HYPERSONIC SPEED
Hypersonic Combined Cycle Propulsion
[AGARD-CP-479] N91-23147
Hypersonic propulsion: Past and present N91-23148
Highly integrated ducted rocket propulsion modules for future hypersonic tactical missiles N91-23171
HYPERSONIC VEHICLES
Hypersonic numerical simulation: Problems and perspectives. Hypersonic vehicles and numerical simulation in structural analysis
[REPT-911-111-106] N91-23091
Performance characteristics of hypersonic detonation wave ramjets N91-23168
The effect of combustor flow nonuniformity on the performance of hypersonic nozzles N91-23173
HYPERSONIC WIND TUNNELS
IAI hypersonic wind tunnel
[IAITIC-87-1006] N91-23194
The VKI hypersonic wind tunnels and associated measurement techniques
[VKI-TM-46] N91-23196
HYPERSONICS
Aerodynamic preliminary analysis system 2. Part 1: Theory
[NASA-CR-182076] N91-23080
Aerodynamic preliminary analysis system 2. Part 2: User's manual
[NASA-CR-182077] N91-23081
Problems of hypersonic aerothermodynamics
[MBB-FE202/5/PUB/436] N91-23090
Hypersonic numerical simulation: Problems and perspectives. Hypersonic vehicles and numerical simulation in structural analysis
[REPT-911-111-106] N91-23091
Computation of viscous shock/shock hypersonic interactions with an implicit flux split scheme
[AD-A232405] N91-23093
Performance characteristics of hypersonic detonation wave ramjets N91-23168
Highly integrated ducted rocket propulsion modules for future hypersonic tactical missiles N91-23171
Materials for hypersonic engines N91-23177
Evaluation and ranking of candidate ceramic wafer engine seal materials
[NASA-TM-103795] N91-23515
HYPERVELOCITY IMPACT
Response of simulated propellants and explosives to projectile impact
[DE91-009777] N91-23333
HYPOBARIC ATMOSPHERES
A test of the American Safety Flight Systems, Inc. prebreather/portable oxygen system
[AD-A232723] N91-23100

I

I BEAMS
Finite element analysis of the lateral buckling of a cantilevered I Beam
[DE91-010123] N91-23527
ICE
Simulation of iced wing aerodynamics
[NASA-TM-104362] N91-23086
Icing simulation: A survey of computer models and experimental facilities
[NASA-TM-104366] N91-23087
Advanced ice protection systems test in the NASA Lewis icing research tunnel
[NASA-TM-103757] N91-23183
Model rotor icing tests in the NASA Lewis icing research tunnel
[NASA-TM-104351] N91-23184
ICE ENVIRONMENTS
Arctic remote autonomous measurement platform post CEAREX engineering report
[AD-A232843] N91-23471
Using satellite remote sensing imagery for marginal ice zone research in the ARCTEMIZ project N91-23600
Sea ice classification using synthetic aperture radar
[AD-A232248] N91-23689
ICE FLOES
Sea ice monitoring in the east Greenland sea in May 1988 by means of remote sensing, with special emphasis on the computer-aided AVHRR-based extraction of sea ice motions
[DLR-FB-90-36] N91-23687
ICE FORMATION
Simulation of iced wing aerodynamics
[NASA-TM-104362] N91-23086
Icing simulation: A survey of computer models and experimental facilities
[NASA-TM-104366] N91-23087
Advanced ice protection systems test in the NASA Lewis icing research tunnel
[NASA-TM-103757] N91-23183
Model rotor icing tests in the NASA Lewis icing research tunnel
[NASA-TM-104351] N91-23184
ICE MAPPING
Sea ice monitoring in the east Greenland sea in May 1988 by means of remote sensing, with special emphasis on the computer-aided AVHRR-based extraction of sea ice motions
[DLR-FB-90-36] N91-23687
ICE PREVENTION
Icing simulation: A survey of computer models and experimental facilities
[NASA-TM-104366] N91-23087
Advanced ice protection systems test in the NASA Lewis icing research tunnel
[NASA-TM-103757] N91-23183
ICE REPORTING
Sea ice monitoring in the east Greenland sea in May 1988 by means of remote sensing, with special emphasis on the computer-aided AVHRR-based extraction of sea ice motions
[DLR-FB-90-36] N91-23687
ICY SATELLITES
Cryomagmatism in the outer solar system N91-24019
IDEAL GAS
Numerical simulations of instabilities in compressible mixing layers N91-23412
IGNITION
Direct gas injection with glow plug ignition
[PB91-136390] N91-23272
An experimental method for studying combustion of an unsupported fuel droplet at reduced gravity N91-23273
ILLUMINANCE
Radioluminescent (RL) lighting system development program
[DE91-009743] N91-23381
ILLUMINATION
Effects of bright illumination on oral temperature and cognitive performance in humans during nighttime hours
[AD-A232787] N91-23722
IMAGE ANALYSIS
The integration of remote sensing, geographic information system, and expert system technologies for landcover classification N91-23733
Saturn's F ring: Imaging and simulation N91-24032
The Land Analysis System (LAS) N91-24054
IMAGE PROCESSING
SAR processor for the ERS-1 data phase 1, simple processor
[FEL-90-B033] N91-23359
Detection of mining activities in the Yanomani Indian Reserve through LANDSAT-TM imagery
[INPE-5182-RPE/638] N91-23609
Quantitative processing of Meteosat data: implementation at KNMI: Applications
[KNMI-TR-127] N91-23678
Sea ice classification using synthetic aperture radar
[AD-A232248] N91-23689
Absolute calibration in vivo measurement systems
[DE91-009719] N91-23692
Programmable remapper for image processing
[NASA-CASE-MSC-21350-1] N91-23724
Three-dimensional graphical representation of objects according to movement data in realtime
[DLR-FB-90-51] N91-23725
Image data compression in JPEG standard
[DLR-FB-90-59] N91-23746
Searching algorithms for the real roots of a Bezier function
[RR-834-I-AND-M] N91-23755
Synergetic multisensor fusion
[AD-A232089] N91-23766
Image wavelet decomposition and applications
[NASA-CR-188217] N91-23787
Aero-optics measurement system for the AEDC aero-optics test facility
[AD-A232852] N91-23908
Nonlinear real-time optical signal processing
[AD-A232889] N91-23909
Recent advances in coding theory for near error-free communications N91-24068
IMAGE RECONSTRUCTION
Correction of relief-induced radiometric distortions in Seasat-A SAR images for the example of the subscene of Bonn (Fed. Republic of Germany) and vicinities
[DLR-FB-90-54] N91-23613
Programmable remapper for image processing
[NASA-CASE-MSC-21350-1] N91-23724
Image wavelet decomposition and applications
[NASA-CR-188217] N91-23787
Digital data registration and differencing compression system
[NASA-CASE-SSC-00010-1] N91-23976
IMAGE RESOLUTION
Image wavelet decomposition and applications
[NASA-CR-188217] N91-23787
Imaging and background in low-energy gamma ray astronomy N91-24005
IMAGING SPECTROMETERS
Signal detection of MERIS in oceanographic applications N91-23605
Medium Resolution Imaging Spectrometer (MERIS) N91-23608
Hyperspectral imagery: What is it, what can it do
[AD-A231164] N91-23610
IMAGING TECHNIQUES
Tripod operators for the interpretation of range images
[AD-A232631] N91-23344
High resolution measurements of strained diffusion and reaction layer structure and extinction in turbulent flows
[AD-A232794] N91-23456
Absolute calibration in vivo measurement systems
[DE91-009719] N91-23692
Programmable remapper for image processing
[NASA-CASE-MSC-21350-1] N91-23724
Image wavelet decomposition and applications
[NASA-CR-188217] N91-23787
Wavelength independent optical lithography and microscopy
[AD-A232036] N91-23896
Evaluation of a ferroelectric liquid crystal spatial light modulator
[AD-A232117] N91-23899
Imaging and background in low-energy gamma ray astronomy N91-24005
An observational study of arm structure in normal spiral galaxies N91-24007

Instrumentation and data analysis for hard x ray astronomy N91-24010
A near-infrared search for brown dwarfs in the Pleiades N91-24011
Near-infrared milliarcsecond observations by the lunar occultation technique N91-24034

IMPACT ACCELERATION
Human short-latency somatosensory evoked potentials in impact acceleration research: Equipment, procedures, and techniques
[AD-A232732] N91-23709

IMPACT DAMAGE
Response of simulated propellants and explosives to projectile impact
[DE91-009777] N91-23333

IMPACT RESISTANCE
Modelling of the impact response of fibre-reinforced composites
[AD-A232658] N91-23266

IMPACT TESTS
Pyrotechnical safety of Aerospatiale tactical missiles: Application to conventional warhead
[REPT-911-320-101] N91-23139
Modelling of the impact response of fibre-reinforced composites
[AD-A232658] N91-23266

IMPEDANCE
Efficient numerical techniques for the analysis of complex microstrip-antennas and microstrip arrays
[DLR-FB-90-53] N91-23357

IMPINGEMENT
Interferometric investigation of supersonic flow fields with shock-shock interactions N91-23082

IMPULSES
The transient response of heavily fluid-loaded elastic plates and cylindrical shells N91-23528

IN-FLIGHT MONITORING
Aircraft Command in Emergency Situations (ACES). Phase 1: Concept development
[DOT/FAA/CT-90/21] N91-23097
Mechanical component diagnostic system
[AD-A232126] N91-23146
The electrical flight control system of A320 Airbus: A fault tolerant system
[REPT-911-111-103] N91-23192

INCOMPRESSIBLE FLOW
Analysis of the multigrid method N91-23418
Numerical simulation of incompressible inhomogeneous turbulence in a plane channel flow
[ESA-TT-1199] N91-23441

INCONEL (TRADEMARK)
The solidification behavior of an alloy 625/718 variant
[DE91-009544] N91-23294

INDEXES (DOCUMENTATION)
Aeronautical engineering: A cumulative index to a continuing bibliography (supplement 261)
[NASA-SP-7037(261)] N91-23073
Aeronautical engineering: A continuing bibliography with indexes (supplement 262)
[NASA-SP-7037(262)] N91-23074
Aerospace medicine and biology: A continuing bibliography with indexes (supplement 346)
[NASA-SP-7011(346)] N91-23700
Aerospace medicine and biology: A continuing bibliography with indexes (supplement 347)
[NASA-SP-7011(347)] N91-23701
Aerospace medicine and biology: A continuing bibliography with indexes (supplement 348)
[NASA-SP-7011(348)] N91-23702
A guide to experimental elementary particle physics literature, 1985-1989
[DE91-010209] N91-23856

INDIAN OCEAN
Near-equatorial deep circulation in the Indian and Pacific oceans
[AD-A232635] N91-23691

INDICATORS
Region 10 environmental indicators
[PB91-136580] N91-23623

INDIUM ARSENIDES
Strain release in GaAs/Ga(1-x)/In(x)As strained layer superlattices grown on (112) substrates
[DE91-009972] N91-23944
Optoelectronic III-V heterostructures on SI substrates
[AD-A232035] N91-23950

INDIUM PHOSPHIDES
Optoelectronic III-V heterostructures on SI substrates
[AD-A232035] N91-23950

INDOOR AIR POLLUTION
New research on bioregenerative air/water purification systems N91-24053

INDUCTION (MATHEMATICS)
A distributed problem-solving approach to rule induction: Learning in distributed artificial intelligence systems
[AD-A232822] N91-23803

INDUSTRIAL PLANTS
Research and development opportunities for natural gas fueled refrigeration in industrial processes
[PB91-136432] N91-23338
Aerospatiale industrial thermal plasmas
[REPT-911-430-113] N91-23927
Aerospatiale industrial thermal plasma activities
[REPT-911-430-122] N91-23928
Survey: Potential of the Israeli industry for space technology
[CEMA-86-17] N91-23967

INELASTIC COLLISIONS
Computed secondary-particle energy spectra following nonelastic neutron interactions with C-12 for E(n) between 15 and 60 MeV: Comparisons of results from two calculational methods
[DE91-010454] N91-23864

INELASTIC SCATTERING
Los Alamos Science, Number 19, 1990
[DE91-009371] N91-23855
Light particle emissions in heavy ion reactions
[DE91-010746] N91-23871
Experiments on Frank-Hertz setup
[NOTA-INTERNA-961] N91-23876

INERTIAL FUSION (REACTOR)
Intense light-ion beams provide a robust, common-driver path towards ignition, gain and commercial fusion energy
[DE91-010584] N91-23919

INERTIAL NAVIGATION
Simulation and analyses of the aeroassist flight experiment attitude update method
[NASA-TM-102174] N91-23210

INFERENCE
Topics in inference and decision-making with partial knowledge
[NASA-CR-188209] N91-23821
Statistical models and inference procedures for structural and materials reliability
[AD-A232634] N91-23827

INFORMATION DISSEMINATION
A guide to experimental elementary particle physics literature, 1985-1989
[DE91-010209] N91-23856
Access and efficiency in Reagan-era information policy: A case study of the attempt to privatize the National Technical Information Service N91-23977
Technology 2000, volume 2
[NASA-CP-3109-VOL-2] N91-24041

INFORMATION MANAGEMENT
An assessment of technology alternatives for telecommunications and information management for the space exploration initiative
[NASA-TM-103783] N91-23347
Access and efficiency in Reagan-era information policy: A case study of the attempt to privatize the National Technical Information Service N91-23977
Information resources management long-range plan
[DE91-009745] N91-23984
Information plan study: A strategy model
[ISBN-90-6233-638-8] N91-23988
Information system for environmental chemicals
[GSF-BER-21/90] N91-23990

INFORMATION PROCESSING (BIOLOGY)
Information dynamics of self-programmable matter
[DE91-009954] N91-23740

INFORMATION RETRIEVAL
A user-oriented synthetic workload generator
[NASA-CR-188197] N91-23739
Knowledge-based retrieval of information as a process of evidential reasoning N91-23978
An expert system for searching in full-text N91-23983
The intelligent database: Using INGRES to manage the external analysis of your data
[DE91-010465] N91-23986
The value of STINFO
[AD-A232484] N91-23996
Interacting with DTIC
[AD-A232485] N91-23997

INFORMATION SYSTEMS
Five-year plan for meeting the automatic data processing and telecommunications needs of the Federal Government
[PB91-103549] N91-23982
Information resources management long-range plan
[DE91-009745] N91-23984
Information plan study: A strategy model
[ISBN-90-6233-638-8] N91-23988
Information system for environmental chemicals
[GSF-BER-21/90] N91-23990
Interacting with DTIC
[AD-A232485] N91-23997

INFORMATION THEORY
Information dynamics of self-programmable matter
[DE91-009954] N91-23740

INFORMATION TRANSFER
The value of STINFO
[AD-A232484] N91-23996

INFRARED ASTRONOMY
The supernova remnant G109.1-1.0 and the x-ray pulsar 1E2259+586 N91-24002
A near-infrared search for brown dwarfs in the Pleiades N91-24011
Radio and infrared studies of mass-losing evolved stars N91-24026

INFRARED DETECTORS
Infrared focal plane performance in the South Atlantic anomaly
[NASA-CR-186197] N91-23458

INFRARED IMAGERY
Using satellite remote sensing imagery for marginal ice zone research in the ARCTEMIZ project N91-23600

INFRARED INSTRUMENTS
ISOCAM: The ISO's satellite infra-red camera
[REPT-911-440-104] N91-23468

INFRARED RADIATION
Infrared and visible studies of Pakistan portion of Arabian Sea using INSAT geostationary satellite N91-23611
High-altitude non-equilibrium infrared emission models
[AD-A232503] N91-23659
Evaluation of generalized thresholds in an objective multispectral satellite cloud analysis
[AD-A232716] N91-23683
The molecular interstellar medium and the near-infrared continuum of the barred liner NGC 6764
[MPE-PREPRINT-193] N91-24029

INFRARED RADIOMETERS
ATSR: Precise sea surface temperature from the ERS-1 satellite N91-23601

INFRARED SCANNERS
ATSR: Precise sea surface temperature from the ERS-1 satellite N91-23601

INFRARED SPACE OBSERVATORY (ISO)
ISOCAM: The ISO's satellite infra-red camera
[REPT-911-440-104] N91-23468

INFRARED SPECTRA
Theoretical prediction of vibrational infrared frequencies of tertiary amines
[AD-A232880] N91-23288

INJECTORS
Predictions and verification of ESD tests made with sphere injections on a flight representative telecommunication satellite: ARABSAT STM
[REPT-911-440-109] N91-23224
Direct gas injection with glow plug ignition
[PB91-136390] N91-23272

INLET FLOW
A study of three dimensional turbulent boundary layer separation and vortex flow control using the reduced Navier Stokes equations
[NASA-TM-104407] N91-23089
Some aspects of shock-wave boundary layer interaction relevant to intake flows N91-23161
Computational modeling and validation for hypersonic inlets N91-23162
Effects of inlet distortion on the development of secondary flows in a subsonic axial inlet compressor rotor
[NASA-TM-104356] N91-23179
Computation of inlet reference plane flow-field for a subscale free-jet forebody/inlet model and comparison to experimental data
[AD-A232101] N91-23445

INPUT/OUTPUT ROUTINES
Nonlinear real-time optical signal processing
[AD-A232889] N91-23909

INSPECTION
Robotic control and inspection verification N91-24075

INSTALLATION MANUALS
NODEN user's guide and installation manual
[RSRE-MEMO-4438] N91-23753

INSTRUMENT LANDING SYSTEMS
Microwave landing system modeling with application to air traffic control
[NASA-TM-102832] N91-23099

INSTRUMENT PACKAGES
An engineering study of altitude determination deficiencies of the Service Aircraft Instrumentation Package (SAIP)
[AD-A232055] N91-23145

INTEGRAL EQUATIONS
The transient response of heavily fluid-loaded elastic plates and cylindrical shells N91-23528

INTEGRATED CIRCUITS
A 30 GHz monolithic receive module
[NASA-CR-187085] N91-23346
System-Level Integrated Circuit (SLIC) development for phased array antenna applications
[NASA-TM-104392] N91-23354

Parametric modeling and estimation of pulse propagation on microwave integrated circuit interconnections
[AD-A232465] N91-23404
Analog processing of optical wavefronts using integrated guided-wave optics
[AD-A232703] N91-23904
Microwave integrated circuits for space applications N91-24069

INTEGRATED OPTICS
Analog processing of optical wavefronts using integrated guided-wave optics
[AD-A232703] N91-23904

INTERACTING GALAXIES
Recent star formation and the galaxy collisions in NGC 520 N91-24021

INTERACTIONAL AERODYNAMICS
Buffet induced structural/flight-control system interaction of the X-29A aircraft
[NASA-TM-101735] N91-23133
Some aspects of shock-wave boundary layer interaction relevant to intake flows N91-23161

INTERACTIVE CONTROL
A procedural expert system for spacecraft command and control N91-23591
A solution for the man/machine-interface in robotics: A high level control language with enhanced interaction equipment N91-23789
An interactive robot control system N91-23790

INTERFACES
Modeling second-phase formation during rapid resolidification of stainless steel alloys
[DE91-008567] N91-23291
Boundary stability under nonequilibrium conditions
[DE91-009262] N91-23293
Numerical simulation of a viscous vortex ring interaction with a density interface
[DE91-002790] N91-23429
Adaptive methods for compressible fluid dynamics
[AD-A232786] N91-23455
Quantifying performance degradation due to the human-machine interface of telemanipulators
[AD-A232814] N91-23723
Fiber Optic Tactical Local Network (FOTLAN) N91-24072

INTERFACIAL TENSION
Interfacial characteristic measurements in horizontal bubbly two-phase flow
[DE91-009803] N91-23427

INTERFERENCE GRATING
Vertical emitting, ring geometry, ultra-low threshold and ultra-high speed quantum well lasers for optical interconnect
[AD-A232122] N91-23481

INTERFEROMETERS
Interferometric investigation of supersonic flow fields with shock-shock interactions N91-23082
Experimental and theoretical research in applied plasma physics
[DE91-010657] N91-23920

INTERFEROMETRY
Inversion of chordal data from the ATF torsatron
[DE91-010490] N91-23915
Microwave imaging of Saturn's deep atmosphere and rings N91-24035

INTERGALACTIC MEDIA
Theoretical studies of QSO absorption lines and the intergalactic medium N91-24025

INTERMETALLICS
High temperature deformation processes and strengthening mechanisms in intermetallic particulate composites
[AD-A232737] N91-23267
High temperature ordered intermetallic alloys
[AD-A232769] N91-23308

INTERNAL COMBUSTION ENGINES
Direct gas injection with glow plug ignition
[PB91-136390] N91-23272

INTERNAL WAVES
Grouping of clouds and internal gravity waves in a non-hydrostatic model of moist convection
[DM-55] N91-23679

INTERNATIONAL COOPERATION
Satellite utilization by civil aviation
[REPT-911-111-105] N91-23216
Energy-related environmental issues in a global context
[DE91-009538] N91-23627

INTERNATIONAL RELATIONS
Technology transfer in a changing national security environment
[AD-A232458] N91-24000

INTERNATIONAL SYSTEM OF UNITS
European stakes and measures permitting the management of geometric dimensions N91-23573

INTERPLANETARY MAGNETIC FIELDS
Neutral wind vortices in the high-latitude thermosphere N91-23673

INTERPOLATION
Two dimensional vernier
[NASA-CASE-MSC-21700-1] N91-23462

INTERSTELLAR EXTINCTION
Ultraviolet gas absorption and dust extinction toward M8 and the outer galactic disk N91-24018

INTERSTELLAR GAS
Ultraviolet gas absorption and dust extinction toward M8 and the outer galactic disk N91-24018

INTERSTELLAR MATTER
High resolution imaging for Brackett gamma and H2 1-0 S(1) emission in the Seyfert galaxy NGC 1068
[MPE-PREPRINT-192] N91-23104
Studies of the diffuse background and interstellar dust at far ultraviolet wavelengths N91-24003
Radio and infrared studies of mass-losing evolved stars N91-24026
The molecular interstellar medium and the near-infrared continuum of the barred liner NGC 6764
[MPE-PREPRINT-193] N91-24029

INTERTROPICAL CONVERGENT ZONES
Initialization of cloud and radiation in the Florida State University global spectral model
[AD-A232425] N91-23682

INTRAVEHICULAR ACTIVITY
Comparisons between underwater and space working environments for on board activities optimization (Columbus space programme) N91-23574

INVARIANCE
Control synthesis based upon a game theoretic approach N91-23831

INVENTORIES
Life cycle management automation programmer's manual
[AD-A232247] N91-23769

INVISCID FLOW
Numerical simulations of instabilities in compressible mixing layers N91-23412
Block implicit multigrid solution of the Euler equations N91-23413
The transient response of heavily fluid-loaded elastic plates and cylindrical shells N91-23528

IODINE COMPOUNDS
Study of the response of a crystal ball made of NaI(Tl) for heavy ions experiments
[NOTA-INTERNA-957] N91-23874

ION ACOUSTIC WAVES
Theoretical and numerical study of anomalous turbulent transport in plasmas
[AD-A232688] N91-23931
Observation and theory of the radar aurora N91-24017

ION ATOM INTERACTIONS
Magnetic substates populated by double electron capture in slow ion atom collisions
[DE91-010122] N91-23858
Excitation of atoms and molecules in collisions with highly charged ions
[DE91-010740] N91-23870
Low-energy collisions of multiply charged ions with electrons, atoms and surfaces
[DE91-010779] N91-23873
Calculation of cross sections for binary reactions between heavy ion projectiles and heavy actinide targets
[DE91-010222] N91-23882

ION BEAMS
Ion beam testing of the Aerolor X-point dump plate for the Joint European Torus
[DE91-010719] N91-23245
Ion confinement and radiation losses in the advanced toroidal facility
[DE91-010382] N91-23916
Heavy ion beam probe measurements of ECH method plasma in the advanced toroidal facility
[DE91-010391] N91-23917

ION CONCENTRATION
A non-invasive measure of minerals and electrolytes in tissue N91-24058

ION CYCLOTRON RADIATION
ICRF heating on the Burning Plasma Experiment (BPX)
[DE91-010390] N91-23913

ION EMISSION
Investigation of neutral atom and ion emission during laser conditioning of multilayer HfO2-SiO2 coatings
[DE91-009749] N91-23860
Surface electron emission induced by slow multicharged ions
[DE91-010469] N91-23865

ION IRRADIATION
Calculation of cross sections for binary reactions between heavy ion projectiles and heavy actinide targets
[DE91-010222] N91-23882

ION MOTION
Thermal ion upwelling in the high-altitude ionosphere
[AD-A232372] N91-23657

ION TEMPERATURE
Incoherent scatter measurements and inferred energy fluxes in the equatorial F-region ionosphere N91-23640
Ion confinement and radiation losses in the advanced toroidal facility
[DE91-010382] N91-23916

IONIC COLLISIONS
Magnetic substates populated by double electron capture in slow ion atom collisions
[DE91-010122] N91-23858
Excitation of atoms and molecules in collisions with highly charged ions
[DE91-010740] N91-23870
Low-energy collisions of multiply charged ions with electrons, atoms and surfaces
[DE91-010779] N91-23873

IONIC REACTIONS
Computer modeling of soot formation comparing free radical and ionic mechanisms
[AD-A232820] N91-23287

IONIZATION
Excitation of atoms and molecules in collisions with highly charged ions
[DE91-010740] N91-23870
Theoretical studies of QSO absorption lines and the intergalactic medium N91-24025

IONOSPHERES
Ionosphere 1985, volume 73
[ISSN-0211-5166] N91-23650

IONOSPHERIC HEATING
Thermal ion upwelling in the high-altitude ionosphere
[AD-A232372] N91-23657

IONOSPHERIC PROPAGATION
A study of PC-Based HF ionospheric propagation predictions for use in naval communications
[AD-A232466] N91-23375
Ionosphere 1984, volume 72
[ISSN-0211-5166] N91-23649
Ionosphere 1985, volume 73
[ISSN-0211-5166] N91-23650

IONOSPHERIC SOUNDING
Ionosphere 1984, volume 72
[ISSN-0211-5166] N91-23649
Ionosphere 1985, volume 73
[ISSN-0211-5166] N91-23650

IONS
Surface electron emission induced by slow multicharged ions
[DE91-010469] N91-23865
Excitation of atoms and molecules in collisions with highly charged ions
[DE91-010740] N91-23870
The direct correlation function of a mixture of hard ions in the mean spherical approximation
[AD-A232452] N91-23879

IRON
Iron density measurements in polar atmosphere
[BONN-IR-90-53] N91-23654
Benchmark measurements and calculations of a 3-dimensional neutron streaming experiment
[DE91-010692] N91-23867
Aerospatiale industrial thermal plasmas
[REPT-911-430-113] N91-23927
Epitaxial iron films
[AD-A232419] N91-23958

IRRADIATION
Temperature distribution and thermal damage during tissue ablation by CO2 laser irradiation: Model and experiment N91-23833

IRREGULARITIES
Large scale turbulence in the equatorial electrojet N91-23643
Observation and theory of the radar aurora N91-24017

ISENTROPIC PROCESSES
Order and disorder in metallic alloys
[DE91-009120] N91-23292

ISING MODEL
A statistical model of fractures N91-23529
Canonical vs. micro-canonical sampling methods in a 2D Ising model
[DE91-010204] N91-23737

ISOMERS
AFRRI reports, October - December 1990
[AD-A232236] N91-23283

ISOTHERMAL FLOW
Flow between eccentric rotating cylinders N91-23417

ISOTHERMAL PROCESSES
Interphase transport and multistage separations
[DE91-009627] N91-23425

ISOTHERMS
Phase transitions at liquid solid interfaces: Pade approximant for adsorption isotherms and voltammograms
[AD-A232623] N91-23285
ISOTROPY
On the construction of two-phase equilibria in a non-elliptic hyperelastic material
[AD-A232628] N91-23558
Liquid-crystal characterization using the Z-scan technique
[RSRE-MEMO-4451] N91-23949
ITERATIVE SOLUTION
Navigation, guidance, and trajectory optimization for hypersonic vehicles N91-23150

J

J INTEGRAL
Elastic/plastic fracture mechanics. Part 2: Marine structural applications
[AD-A232560] N91-23557
JAMMING
Implications of adaptive cancellation array processing for design of a space-based surveillance radar
[RSRE-MEMO-4410] N91-23364
JAPAN
Technology transfer in a changing national security environment
[AD-A232458] N91-24000
JET AIRCRAFT
Handling qualities of highly augmented unstable aircraft summary of an AGARD-FMP working group effort N91-23116
Metrics for roll response flying qualities N91-23118
JET FLOW
An experimental study of flamelet surfaces in turbulent combustion
[AD-A232342] N91-23284
Flow field study of a rectangular jet N91-23423
Vortex system evolution in 2- and 3-D swept trailing edge flows
[AD-A232692] N91-23453
JET MIXING FLOW
A CFD study of jet mixing in reduced flow areas for lower combustor emissions
[NASA-TM-104411] N91-23185
JIMSPHERE BALLOONS
Atmospheric turbulence review of space shuttle launches
[NASA-TM-4289] N91-23215
JOINT EUROPEAN TORUS
Ion beam testing of the Aerolor X-point dump plate for the Joint European Torus
[DE91-010719] N91-23245
JOINTS (JUNCTIONS)
On kinematic design of serial link manipulators
[DE91-009414] N91-23499
Stress analysis of a double-doubler joint in composite structure N91-23530
ACLICO: A computer aided design system for bonded joints
[REPT-911-430-101] N91-23757
JORDAN FORM
Nilpotent normal form via Carleman linearization (for systems of ordinary differential equations)
[RR-838-M] N91-23809
JUDGMENTS
Spatiotemporal characteristics of visual localization
[AD-A232734] N91-23715

K

K LINES
A high resolution study of the Cu K alpha(sub 1,2) x-ray emission lines N91-23841
K-EPSILON TURBULENCE MODEL
Low Reynolds number two-equation modeling of turbulent flows
[NASA-TM-104368] N91-23416
Numerical modeling of turbulent dispersion around structures using a particle-in-cell method
[DE91-009757] N91-23426
An analysis of RNG based turbulence models for homogeneous shear flow
[NASA-CR-187552] N91-23433
KALMAN FILTERS
Simulation and analyses of the aeroassist flight experiment attitude update method
[NASA-TM-102174] N91-23210
KELVIN-HELMHOLTZ INSTABILITY
Numerical simulations of instabilities in compressible mixing layers N91-23412
KERNEL FUNCTIONS
Nonparametric estimation in change-point hazard rate models for censored data: A counting process approach
[RR-836-I-AND-M] N91-23825
KINEMATICS
A non-contacting velocity measurement system
[NASA-CASE-LAR-14466-1] N91-23461
Finite element based dynamical modeling of flexible open-loop manipulators with experimental results N91-23496
On kinematic design of serial link manipulators
[DE91-009414] N91-23499
KINETIC ENERGY
Analysis of the flutter characteristics of the advanced kinetic energy missile (ADKEM) control surface
[AD-A232377] N91-23193
Energy dissipator
[NASA-CASE-MSC-21555-1] N91-23492
Energy-efficient penetration of targets
[AD-A232227] N91-23518
KINETIC EQUATIONS
A numerical model of laser induced fluorescence in a hydrogen plasma
[AD-A232240] N91-23482
KNOWLEDGE
Conference on Theoretical Aspects of Reasoning About Knowledge
[AD-A232657] N91-23798
Combining knowledge bases consisting of first order theories
[AD-A232090] N91-23993
KNOWLEDGE BASES (ARTIFICIAL INTELLIGENCE)
A first-principles generic methodology for representing the knowledge base of a process diagnostic expert system
[DE90-017693] N91-23520
Conference on Theoretical Aspects of Reasoning About Knowledge
[AD-A232657] N91-23798
Combining knowledge bases consisting of first order theories
[AD-A232090] N91-23993
KNOWLEDGE REPRESENTATION
Hypermedia 1990 structured Hypertext tutorial
[NASA-CR-187921] N91-23731
KNUDSEN GAGES
Laboratory study of the thermochemical properties of materials used in spacecraft
[AD-A232124] N91-23228

L

LAMINAR BOUNDARY LAYER
Passive laminar flow control of crossflow vorticity
[NASA-CASE-LAR-13563-1] N91-23410
LAMINAR FLOW
A computationally efficient modelling of laminar separation bubbles N91-23411
LAMINATES
Improved quality acceptance procedure for interlaminar shear strength
[IAITIC-87-1005] N91-23238
A simulation of the draping and a model of the consolidation of commingled fabrics N91-23239
The development and evaluation of an alternative powder prepregging technique for use with LaRC-TPI/graphite composites
[NASA-CR-188184] N91-23242
An experimental and finite element investigation into the nonlinear material behavior of pin-loaded composite laminates
[AD-A232098] N91-23263
Fundamental studies of electronic packaging materials and structures: Surface and interfaces
[AD-A232336] N91-23403
LAND MANAGEMENT
Potential commercial uses of EOS remote sensing products N91-24055
LAND USE
Correction of relief-induced radiometric distortions in Seasat-A SAR images for the example of the subscene of Bonn (Fed. Republic of Germany) and vicinities
[DLR-FB-90-54] N91-23613
The Land Analysis System (LAS) N91-24054
LANDFORMS
Cryomagmatism in the outer solar system N91-24019
LANDING GEAR
Long time measurements of landing gear loads on SAAB SF-340 commuter aircraft
[FFA-TN-1990-53] N91-23138
LANDING LOADS
Long time measurements of landing gear loads on SAAB SF-340 commuter aircraft
[FFA-TN-1990-53] N91-23138
LANGUAGES
On a phonetic and structural encoding of Chinese characters in Chinese texts
[RR-835-I] N91-23989
LARGE SPACE STRUCTURES
Large space structures fielding plan
[AD-A232097] N91-23227
LASER APPLICATIONS
Theoretical studies relating to the interaction of radiation with matter
[AD-A232107] N91-23480
Automated handling and assembling of non-rigid objects
[AD-A231246] N91-23489
Advanced diagnostics for reacting flows
[AD-A232609] N91-23902
Low-temperature laser-induced selective area growth of compound semiconductor N91-23932
Liquid-crystal characterization using the Z-scan technique
[RSRE-MEMO-4451] N91-23949
Laser assisted CVD growth of AlN and GaN
[AD-A232379] N91-23957
Optical communication for space missions N91-24070
LASER ARRAYS
Study of phase-locked diode laser array and DFB/DBR surface emitting laser diode N91-23474
Strained quantum well leaky-mode diode laser arrays
[DE91-009982] N91-23477
Studies of noise in semiconductor laser arrays
[AD-A232411] N91-23485
LASER DAMAGE
Laser hazards bibliography, January 1991
[AD-A232690] N91-23487
Temperature distribution and thermal damage during tissue ablation by CO2 laser irradiation: Model and experiment N91-23833
Investigation of neutral atom and ion emission during laser conditioning of multilayer HfO2-SiO2 coatings
[DE91-009749] N91-23860
LASER DOPPLER VELOCIMETERS
Frequency domain laser velocimeter signal processor N91-24077
LASER INDUCED FLUORESCENCE
A numerical model of laser induced fluorescence in a hydrogen plasma
[AD-A232240] N91-23482
LASER MATERIALS
Bimanes and related heterocycles as laser dyes
[AD-A232335] N91-23484
LASER MODES
Strained quantum well leaky-mode diode laser arrays
[DE91-009982] N91-23477
LASER OUTPUTS
Signals and noise in lasers and atom-field interactions N91-23475
Temperature distribution and thermal damage during tissue ablation by CO2 laser irradiation: Model and experiment N91-23833
LASER PUMPING
Optical parametric oscillators pumped by excimer lasers N91-23473
High-power performance of a copper laser pumped dye master-oscillator-power-amplifier chain
[DE91-010460] N91-23478
LASER SPECTROSCOPY
Theoretical studies relating to the interaction of radiation with matter
[AD-A232107] N91-23480
LASER WELDING
Modeling second-phase formation during rapid resolidification of stainless steel alloys
[DE91-008567] N91-23291
LASERS
Signals and noise in lasers and atom-field interactions N91-23475
A new asymptotic theory for the periodically forced laser
[AD-A232633] N91-23486
Advanced diagnostics for reacting flows
[AD-A232609] N91-23902
Laser optical disk position encoder with active heads N91-24079
LATCHES
Preloaded latching device
[NASA-CASE-MSC-21730-1] N91-23493
LATENT HEAT
Surface layer transfer processes over vegetation: A micrometeorological field experiment of long duration N91-23664
LATERAL CONTROL
Metrics for roll response flying qualities N91-23118
LATTICES (MATHEMATICS)
System modeling and identification of flexible structures N91-23531

LAUNCH VEHICLE CONFIGURATIONS
Airbreathing propulsion for transatmospheric flight N91-23156
LAUNCHERS
Ceramics in aerospace
[REPT-911-430-127] N91-23260
LAUNCHING
On the efficiency of rail accelerators
[PML-1990-64] N91-23204
LAVA
Lunar volcanism and the thermal evolution of the moon N91-24031
LEADING EDGE SWEEP
The performance of 60 deg delta wings: The effects of leading edge radius on vortex flaps and the wing
[CRANFIELD-AERO-9004] N91-23092
The performance of 60 deg delta wings: The effects of leading edge radius and vortex flaps
[CRANFIELD-AERO-9002] N91-23140
LEADING EDGES
Simulation of iced wing aerodynamics
[NASA-TM-104362] N91-23086
Unsteady flow structure from swept edges subjected to controlled motion
[AD-A232714] N91-23094
Oxidation resistant carbon/carbon materials
[REPT-911-430-105] N91-23251
Simulation of brush insert for leading-edge-passage convective heat transfer
[NASA-TM-103801] N91-23409
LEAST SQUARES METHOD
A moving boundary algorithm for the solution of contact problems in linear elasticity. Part 1: Basic theory and model examples
[FFA-TN-1991-08-PT-1] N91-23759
Functional approximation by feed-forward networks: A least squares approach to generalisation
[RSRE-MEMO-4453] N91-23811
LENSES
Design of a twenty-element long focal length zoom lens
[DE91-010770] N91-23894
LEPTONS
Microscopic heavy-ion theory
[DE91-010739] N91-23869
LESIONS
Control of biosonar behavior by the auditory cortex
[AD-A232699] N91-23708
LEVERS
Preloaded latching device
[NASA-CASE-MSC-21730-1] N91-23493
LEVITATION
Melt-processed bulk superconductors: Fabrication and characterization for power and space applications N91-24082
Description of the Large Gap Magnetic Suspension System (LGMSS) ground-based experiment N91-24083
LEVITATION MELTING
Containerless undercooling and solidification of pure metals
[DLR-FB-90-48] N91-23301
LIFE (DURABILITY)
Destructive physical analysis results of Ni/H2 cells cycled in LEO regime
[NASA-TM-104382] N91-23233
Computational life prediction methodology for mechanical systems using dynamic simulation, finite element analysis, and fatigue life prediction methods N91-23494
Quantifying oil filtration effects on bearing life
[NASA-TM-104350] N91-23512
Maximum life spur gear design
[NASA-TM-104361] N91-23514
Incorporating finite element analysis into component life and reliability
[NASA-TM-104400] N91-23550
Life cycle management automation user's manual, version 1.1
[AD-A232096] N91-23968
LIFE SCIENCES
Space life sciences: A status report
[NASA-NP-120] N91-23694
LIFE SUPPORT SYSTEMS
Real time analysis systems of the physical parameters of the environment and the state of a human organism for a long term exposure at different gas mixtures and pressure up to 100 bar N91-23568
LIFT DRAG RATIO
The performance of 60 deg delta wings: The effects of leading edge radius on vortex flaps and the wing
[CRANFIELD-AERO-9004] N91-23092
The performance of 60 deg delta wings: The effects of leading edge radius and vortex flaps
[CRANFIELD-AERO-9002] N91-23140
LIGANDS
Electrochemical parameterization of rhenium redox couples
[AD-A232043] N91-23279
Structural studies of manganese and halide in the photosynthetic oxygen evolving complex
[DE91-009071] N91-23698
Three-dimensional structure of human serum albumin N91-24057
LIGHT AMPLIFIERS
High-power performance of a copper laser pumped dye master-oscillator-power-amplifier chain
[DE91-010460] N91-23478
LIGHT BEAMS
Wavelength independent optical lithography and microscopy
[AD-A232036] N91-23896
LIGHT EMITTING DIODES
Electronic GaAs-on-silicon material for advanced high-speed optoelectronic devices
[AD-A232088] N91-23399
LIGHT HELICOPTERS
Analytical study of the effects of weight on Light Helicopter (LH) exposure to ground-based weapons
[AD-A232024] N91-23141
LIGHT IONS
Theoretical studies of large-scale features of the Earth's mid- to high-latitude ionosphere N91-23641
Light particle emissions in heavy ion reactions
[DE91-010746] N91-23871
Intense light-ion beams provide a robust, common-driver path towards ignition, gain and commercial fusion energy
[DE91-010584] N91-23919
LIGHT MODULATION
Evaluation of a ferroelectric liquid crystal spatial light modulator
[AD-A232117] N91-23899
Photonic materials and devices for optical information processing and computing applications
[AD-A232771] N91-23907
LIGHT SCATTERING
Simulation of a backscatter lidar system
[DLR-FB-90-50] N91-23355
Real time pre-detection dynamic range compression
[NASA-CASE-NPO-18098-1-CU] N91-23890
Development of a digital correlator to measure the semi-elastic scattering of light
[NOTA-INTERNA-955] N91-23895
LIGHTING EQUIPMENT
Radioluminescent (RL) lighting system development program
[DE91-009743] N91-23381
LIGHTNING
Analysis of the VHF-UHF electromagnetic radiation of lightning: Application to a model of the negative stepped leader propagation
[ESA-TT-1172] N91-23363
LIMITS (MATHEMATICS)
Large and moderate deviation limit theorems for arbitrary sequences of random variables with applications
[AD-A232334] N91-23817
LINE SPECTRA
High-precision Fourier transform spectroscopy of atmospheric molecules N91-23637
The molecular interstellar medium and the near-infrared continuum of the barred liner NGC 6764
[MPE-PREPRINT-193] N91-24029
LINEAR ACCELERATORS
Pulsed power performance of the new RLA (Recirculating Linear Accelerator)
[DE91-004723] N91-23885
Lectures on accelerator physics
[DE91-010376] N91-23886
LINEAR FILTERS
A simple solution to the singular linear minimum-variance estimation problem
[IAITIC-87-1002-REV] N91-23804
LINEAR PREDICTION
High-quality 800-b/s voice processing algorithm
[AD-A232352] N91-23372
LINEAR SYSTEMS
On the initialization problem in the design of structurally constrained digital regulators
[REPT-90-039] N91-23749
A simple solution to the singular linear minimum-variance estimation problem
[IAITIC-87-1002-REV] N91-23804
A particular linear model of variance components
[RR-827-M] N91-23824
Degeneration of linear multivariable systems under high gain and dynamic compensation N91-23830
Control synthesis based upon a game theoretic approach N91-23831
LINEAR TRANSFORMATIONS
Nilpotent normal form via Carleman linearization (for systems of ordinary differential equations)
[RR-838-M] N91-23809
LINEARITY
Numerical simulation of transition in three dimensional boundary layers
[ESA-TT-1203] N91-23442
Linear bending of curved tubes without boundary influence
[ETN-91-99255] N91-23552
LINEARIZATION
Nilpotent normal form via Carleman linearization (for systems of ordinary differential equations)
[RR-838-M] N91-23809
LIOUVILLE EQUATIONS
Constant of motion and dynamic equations for one-dimensional autonomous system and radiation damping
[DE91-011002] N91-23547
LIQUEFACTION
Cryogenic hydrogen-induced air-liquefaction technologies N91-23159
LIQUID AIR
Cryogenic hydrogen-induced air-liquefaction technologies N91-23159
LIQUID AIR CYCLE ENGINES
Comparative study of different systems of combined cycle propulsion N91-23152
LIQUID COOLING
Water-cooling technique of high temperature gas turbine blade
[DE91-764238] N91-23506
LIQUID CRYSTALS
Generation of continuous liquid crystalline polymer reinforcements in thermoplastics by a novel blending process
[AD-A232824] N91-23330
Evaluation of a ferroelectric liquid crystal spatial light modulator
[AD-A232117] N91-23899
Liquid-crystal characterization using the Z-scan technique
[RSRE-MEMO-4451] N91-23949
LIQUID HYDROGEN
Cryogenic hydrogen-induced air-liquefaction technologies N91-23159
Simulation of brush insert for leading-edge-passage convective heat transfer
[NASA-TM-103801] N91-23409
LIQUID METALS
Liquid-metal MHD power conversion for space electric systems
[SER-S/27] N91-23231
Turbulence and the feasibility of self-cooled liquid-metal blankets for fusion reactors
[SER-10/P-REV] N91-23910
LIQUID NITROGEN
A 43 watt CW Ti:Sapphire laser
[DE91-010468] N91-23479
LIQUID PHASE EPITAXY
Electronic GaAs-on-silicon material for advanced high-speed optoelectronic devices
[AD-A232088] N91-23399
LIQUID-SOLID INTERFACES
Phase transitions at liquid solid interfaces: Pade approximant for adsorption isotherms and voltammograms
[AD-A232623] N91-23285
Particle-fluid two-phase flow modeling
[DE91-010102] N91-23415
LIQUIDS
High shear stress rheology of liquid lubricants N91-23309
LISP (PROGRAMMING LANGUAGE)
Performance analysis of garbage collection and dynamic reordering in a Lisp system
[NASA-CR-188205] N91-23738
LITHIUM
Solid polymer electrolytes for rechargeable batteries
[DE91-010231] N91-23384
LITHIUM ALLOYS
Phase equilibria and solidification of Al-Li and Al-Li-Cu alloys N91-23290
Post-overload fatigue crack recovery in powder metal aluminum-lithium AL-905XL forging
[AD-A232550] N91-23307
Superplastic forming of Al-Li alloys for lightweight, low-cost structures N91-24065
LITHIUM ISOTOPES
Primordial lithium, stellar evolution, and cosmology: Lithium in halo stars from standard, diffusive, and rotational stellar evolution and implications for cosmology N91-24024

LITHIUM OXIDES
Evaluation of cathode materials for high energy lithium secondary batteries
[DE91-764240] N91-23385
LITHOGRAPHY
Possibilities for projection x ray lithography using holographic optical elements
[DE91-009770] N91-23464
LITHOSPHERE
Lunar volcanism and the thermal evolution of the moon N91-24031
LIVER
Hepatic metabolism of perfluorinated carboxylic acids: A nuclear magnetic resonance investigation
[AD-A232033] N91-23706
LOAD TESTS
Improved quality acceptance procedure for interlaminar shear strength
[IAITIC-87-1005] N91-23238
A study of the micromechanics of the fiber-matrix interphase in monofilament composites, in monotonic loading, and cyclic fatigue N91-23241
Potential impact of enhanced fracture-toughness data on fracture mechanics assessment of PWR vessel integrity for pressurized thermal shock
[DE91-009554] N91-23509
Computerized system for static and fatigue large scale structural tests: A case study
[IAITIC-87-1007] N91-23522
LOADS (FORCES)
Energy dissipator
[NASA-CASE-MSC-21555-1] N91-23492
Simulation of probabilistic wind loads and building analysis
[NASA-TM-103744] N91-23549
LOCAL AREA NETWORKS
Saturation and vote for the fault tolerance in distributed systems
[LAAS-90390] N91-23727
The TurboLAN project. Phase 1: Protocol choices for high speed local area networks. Phase 2: TurboLAN Intelligent Network Adapter Card, (TINAC) architecture
[NASA-CR-188175] N91-23776
Fiber Optic Tactical Local Network (FOTLAN) N91-24072
LOCKING
On locking and robustness in the finite element method
[AD-A232245] N91-23815
Building a generalized distributed system model
[NASA-CR-188181] N91-23970
Performance analysis of static locking in replicated distributed database systems N91-23974
A note on the performance analysis of static locking in distributed database systems N91-23975
LOGIC CIRCUITS
Basic properties of strongly code disjoint checkers
[RR-824-I] N91-23393
SZ series GaAs super high-speed logic gate: Optimum choice. High tech; high speed; high quality
[AD-A232819] N91-23962
LOGIC DESIGN
Designing logic controllers with Petri nets
[REPT-90-029] N91-23747
An incremental approach to logic controllers design with Petri nets
[REPT-90-030] N91-23748
LOGIC PROGRAMMING
Rule-based motion coordination for the adaptive suspension vehicle on ternary-type terrain
[AD-A232224] N91-23517
An incremental approach to logic controllers design with Petri nets
[REPT-90-030] N91-23748
Generalized disjunctive well-founded semantics for logic programs
[AD-A232064] N91-23765
Null values in definite programs
[AD-A232065] N91-23992
Applications of fuzzy logic to control and decision making N91-24049
LONG DURATION EXPOSURE FACILITY
Science requirements for Heavy Nuclei Collection (HNC) experiment on NASA Long Duration Exposure Facility (LDEF) Mission 2
[NASA-CR-187527] N91-23887
LONG DURATION SPACE FLIGHT
Psychological selection of astronauts: Recent developments at the DLR testing centre in Hamburg (Fed. Republic of Germany) N91-23565
Some problems of desynchronisation of sleep-wakefulness and circadian rhythms for long duration spaceflights N91-23570
Long duration hyperbaric confinement: Hydra 9 N91-23571
Space life sciences: A status report
[NASA-NP-120] N91-23694
LONG WAVE RADIATION
Remote sensing of atmospheric temperature fields and the long wave radiation budget in the Antarctic
[ISSN-0069-5882] N91-23652
Initialization of cloud and radiation in the Florida State University global spectral model
[AD-A232425] N91-23682
LONGITUDINAL CONTROL
Handling qualities guidelines for the design of fly-by-wire flight control systems for transport aircraft N91-23119
LORENTZ TRANSFORMATIONS
Calculation of electromagnetic fields in the near-field region of a moving scattering object
[FEL-90-B216] N91-23361
LOSSY MEDIA
Time-domain analysis of one-dimensional electromagnetic scattering by Lossy media
[FEL-90-A211] N91-23358
A transmission line method for the measurement of microwave permittivity and permeability
[RSRE-MEMO-4450] N91-23394
LOW ALTITUDE
Air ambulance helicopter operational analysis
[DOT/FAA/RD-91/7] N91-23134
LOW COST
Development of a low cost peak shaving generator set
[PB91-136374] N91-23332
LOW PRESSURE
SIMOUN: A high temperature and low pressure testing facility for material characterization
[REPT-911-430-121] N91-23208
SIMOUN: A new test appliance for the development of Hermes thermal protections
[REPT-911-430-129] N91-23209
LOW REYNOLDS NUMBER
Low Reynolds number two-equation modeling of turbulent flows
[NASA-TM-104368] N91-23416
LOW SPEED WIND TUNNELS
The performance of 60 deg delta wings: The effects of leading edge radius on vortex flaps and the wing
[CRANFIELD-AERO-9004] N91-23092
The performance of 60 deg delta wings: The effects of leading edge radius and vortex flaps
[CRANFIELD-AERO-9002] N91-23140
LOW TEMPERATURE
CRREL research on materials in cold environments
[AD-A232133] N91-23280
LOW TEMPERATURE ENVIRONMENTS
CRREL research on materials in cold environments
[AD-A232133] N91-23280
LOW THRUST PROPULSION
Turbojet potential for hypersonic flight N91-23155
LOWER ATMOSPHERE
A search for strange attractors in the saturation of middle atmosphere gravity waves
[AD-A232468] N91-23658
LUBRICANTS
High shear stress rheology of liquid lubricants N91-23309
LUBRICATION
High shear stress rheology of liquid lubricants N91-23309
LUMINESCENCE
Radioluminescent (RL) lighting system development program
[DE91-009743] N91-23381
Magneto-optical properties of quantum wells with arbitrary potential profiles
[AD-A232037] N91-23897
Luminescence and absorption spectra of C60 films
[AD-A232153] N91-23900
LUMINOUS INTENSITY
Effects of bright illumination on oral temperature and cognitive performance in humans during nighttime hours
[AD-A232787] N91-23722
Luminescence and absorption spectra of C60 films
[AD-A232153] N91-23900
LUNAR BASES
Piloted rover technology study
[NASA-CR-186989] N91-23200
Component technology for stirling power converters
[NASA-TM-104387] N91-23234
LUNAR EVOLUTION
Lunar volcanism and the thermal evolution of the moon N91-24031
LUNAR EXPLORATION
Piloted rover technology study
[NASA-CR-186989] N91-23200
LUNAR OCCULTATION
Near-infrared milliarcsecond observations by the lunar occultation technique N91-24034
LUNAR ROVING VEHICLES
Piloted rover technology study
[NASA-CR-186989] N91-23200
SEI rover solar-electrochemical power system options
[NASA-TM-104402] N91-23620
LYMAN ALPHA RADIATION
Matter in cosmic voids N91-23838
Theoretical studies of QSO absorption lines and the intergalactic medium N91-24025

M

MACHINE LEARNING
An artificial neural network control system for spacecraft attitude stabilization
[AD-A232013] N91-23225
A distributed problem-solving approach to rule induction: Learning in distributed artificial intelligence systems
[AD-A232822] N91-23803
MACHINE TOOLS
Unipunch capability study
[DE91-008825] N91-23498
MACHINERY
A method for machinery condition monitoring of transient phenomena using the pseudo Wigner-Ville distribution
[AD-A232014] N91-23760
MAGELLANIC CLOUDS
H II regions and young star clusters in the magellanic clouds N91-24004
MAGMA
Developing natural convection in a fluid layer with localized heating and large viscosity variation
[DE91-005240] N91-23431
MAGNETIC ANOMALIES
Infrared focal plane performance in the South Atlantic anomaly
[NASA-CR-186197] N91-23458
MAGNETIC CONTROL
S-parameter measurements and applications of superconducting flux flow transistors
[DE91-009763] N91-23388
MAGNETIC CORES
Electromagnetic attachment mechanism
[NASA-CASE-MSC-21463-1] N91-23490
MAGNETIC FIELDS
Magneto-optical properties of quantum wells with arbitrary potential profiles
[AD-A232037] N91-23897
Applied plasma physics
[DE91-010696] N91-23922
Relativistic shock waves and the excitation of plerions
[DE91-007623] N91-24027
Integrated Vertical Bloch Line (VBL) memory N91-24051
MAGNETIC FLUX
Inversion of chordal data from the ATF torsatron
[DE91-010490] N91-23915
MAGNETIC MEASUREMENT
Melt-processed bulk superconductors: Fabrication and characterization for power and space applications N91-24082
MAGNETIC PROPERTIES
Epitaxial iron films
[AD-A232419] N91-23958
MAGNETIC STORMS
Geomagnetic storms: Potential economic impacts on electric utilities
[DE91-009523] N91-24036
MAGNETIC SUSPENSION
Description of the Large Gap Magnetic Suspension System (LGMSS) ground-based experiment N91-24083
MAGNETIC TAPES
Mechanical states in wound heterogeneous tapes by the finite element method
[DE91-009255] N91-23536
Mechanical stress states in heterogeneous, wound rolls
[DE91-009257] N91-23537
MAGNETIZATION
Sintering and hot isostatic pressing of Bi2Sr2CaCu2O(x)
[DE91-010797] N91-23945
Melt-processed bulk superconductors: Fabrication and characterization for power and space applications N91-24082
MAGNETO-OPTICS
Magneto-optical properties of quantum wells with arbitrary potential profiles
[AD-A232037] N91-23897
MAGNETOHYDRODYNAMIC FLOW
Flows with strongly anisotropic turbulence-dynamic and heat transfer aspects
[SER-20/P] N91-23407
The polar wind and ionospheric outflow N91-23645

Thermal ion upwelling in the high-altitude ionosphere
[AD-A232372] N91-23657
MAGNETOHYDRODYNAMIC GENERATORS
Liquid-metal MHD power conversion for space electric systems
[SER-S/27] N91-23231
MHD channel gas-side element erosion-corrosion studies
[DE91-008561] N91-23911
MAGNETOHYDRODYNAMIC STABILITY
Large scale turbulence in the equatorial electrojet N91-23643
Experimental and theoretical research in applied plasma physics
[DE91-010657] N91-23920
Hall effects on anomalous heat, particle and helicity transports through tearing-mode turbulence
[DE91-010730] N91-23924
Theoretical and numerical study of anomalous turbulent transport in plasmas
[AD-A232688] N91-23931
MAGNETOHYDRODYNAMIC TURBULENCE
Flows with strongly anisotropic turbulence-dynamic and heat transfer aspects
[SER-20/P] N91-23407
Turbulence and the feasibility of self-cooled liquid-metal blankets for fusion reactors
[SER-10/P-REV] N91-23910
MAGNETOHYDRODYNAMIC WAVES
Hydromagnetic wave coupling in the magnetosphere N91-23638
MAGNETOHYDRODYNAMICS
Relativistic shock waves and the excitation of plerions
[DE91-007623] N91-24027
MAGNETOMETERS
Feasibility study of the Superconducting Gravity Gradiometer (SGG) flight test on the European Retrievable Carrier (EURECA)
[NASA-CR-184157] N91-23229
MAGNETOSTRICTION
Magnetostrictive roller drive motor
[NASA-CASE-GSC-13369-1] N91-23380
MAGNETS
A non-contacting velocity measurement system
[NASA-CASE-LAR-14466-1] N91-23461
MAGNONS
Mean-field theories of the Hubbard model and periodic orbits in chaotic maps N91-23938
MAIN SEQUENCE STARS
H II regions and young star clusters in the magellanic clouds N91-24004
Near-infrared milliarcsecond observations by the lunar occultation technique N91-24034
MAINTENANCE
NAS operational test and evaluation/integration of the Maintenance Management System (MMS) test plan
[DOT/FAA/CT-TN90/41] N91-23075
Maintenance Resource Prediction Model (MRPM) user's manual
[AD-A232019] N91-23762
Software reengineering N91-24047
MALES
Transcapillary fluid shifts in head and neck tissues during and after simulated microgravity
[NASA-TM-103847] N91-23704
MAN MACHINE SYSTEMS
Man-machine interactions and multimedia applied to ROV operations N91-23576
How to design efficient MMI for space N91-23586
Object oriented programming in MMI: A software tool for analysis and planification of a radar imaging mission N91-23589
The development of highly practiced skills: A starting point for driver modelling
[IZF-1990-B-16] N91-23719
Quantifying performance degradation due to the human-machine interface of telemanipulators
[AD-A232814] N91-23723
A solution for the man/machine-interface in robotics: A high level control language with enhanced interaction equipment N91-23789
An interactive robot control system N91-23790
MAN-COMPUTER INTERFACE
Hypermedia 1990 structured Hypertext tutorial
[NASA-CR-187921] N91-23731
Scientific visualization software for your PC: Free and available now
[DE91-010156] N91-23744
Towards real-time GOMS
[AD-A232028] N91-23763
User interface to an ICAI system that teaches discrete math
[AD-A232693] N91-23799
Building a generalized distributed system model N91-23971
Transportable Applications Environment (TAE) Plus: A NASA user interface development and management system N91-24048
MANAGEMENT
European stakes and measures permitting the management of geometric dimensions N91-23573
MANAGEMENT ANALYSIS
Access and efficiency in Reagan-era information policy: A case study of the attempt to privatize the National Technical Information Service N91-23977
MANAGEMENT INFORMATION SYSTEMS
Abridged USAF STINFO program manager's overview manual
[AD-A232483] N91-23995
MANAGEMENT METHODS
Steps toward environmentally compatible product and process design: A case for green engineering
[AD-A232888] N91-23633
Life cycle management automation programmer's manual
[AD-A232247] N91-23769
Abridged USAF STINFO program manager's overview manual
[AD-A232483] N91-23995
MANAGEMENT PLANNING
Information resources management long-range plan
[DE91-009745] N91-23984
MANAGEMENT SYSTEMS
NAS operational test and evaluation/integration of the Maintenance Management System (MMS) test plan
[DOT/FAA/CT-TN90/41] N91-23075
An assessment of technology alternatives for telecommunications and information management for the space exploration initiative
[NASA-TM-103783] N91-23347
Decentralized computing technology for fault-tolerant, survivable C3I systems. Volume 3: System/subsystem specification
[AD-A232291] N91-23371
Transportable Applications Environment (TAE) Plus: A NASA user interface development and management system N91-24048
MANEUVERABILITY
Target maneuver models for improved homing guidance N91-23101
Agility: A rational development of fundamental metrics and their relationship to flying qualities N91-23129
A review of high angle of attack requirements for combat aircraft N91-23130
X-31A at first flight N91-23131
MANGANESE ALLOYS
Phase transformations and microstructural evolution in aged Mn-Cu-based alloys
[AD-A232473] N91-23305
MANGANESE COMPOUNDS
Structural studies of manganese and halide in the photosynthetic oxygen evolving complex
[DE91-009071] N91-23698
MANGANESE OXIDES
Evaluation of cathode materials for high energy lithium secondary batteries
[DE91-764240] N91-23385
MANIPULATORS
H-infinity approach to manipulator control N91-23495
Finite element based dynamical modeling of flexible open-loop manipulators with experimental results N91-23496
On kinematic design of serial link manipulators
[DE91-009414] N91-23499
On the control of two manipulators holding a rigid object in the presence of uncertainty
[DE90-017742] N91-23508
Time-optimal motion of robotic manipulators including nonlinear dynamics
[LAAS-90403] N91-23516
Telerobotics: A key area for possible technology transfer from underwater to space N91-23581
Telemanipulation system assisted by computer for under water applications N91-23585
MANNED LUNAR SURFACE VEHICLES
Piloted rover technology study
[NASA-CR-186989] N91-23200
MANNED MARS MISSIONS
Mars manned fusion spaceship
[NASA-CR-188215] N91-23232
An assessment of technology alternatives for telecommunications and information management for the space exploration initiative
[NASA-TM-103783] N91-23347
MANNED ORBITAL LABORATORIES
Payload related crew operations: From past missions to Columbus N91-23569
MANNED SPACE FLIGHT
The diving laboratory as a simulation environment for manned spaceflight N91-23564
MANNED SPACECRAFT
Payload related crew operations: From past missions to Columbus N91-23569
MANUALS
National stream survey database guide
[PB91-141804] N91-23625
Computer center reference manual, volume 2
[AD-A232370] N91-23781
Abridged USAF STINFO program manager's overview manual
[AD-A232483] N91-23995
MANUFACTURING
Estimating fixed and variable costs of airframe manufacturers
[AD-A232661] N91-23077
How to know CMC
[REPT-911-430-130] N91-23262
Checklist for thick-film hybrid microcircuits manufacturer and line survey
[ESA-PSS-01-607-ISSUE-1] N91-23396
Checklist for thin-film hybrid microcircuits manufacturer and line survey
[ESA-PSS-01-611-ISSUE-1] N91-23397
Steps toward environmentally compatible product and process design: A case for green engineering
[AD-A232888] N91-23633
Magnet cable manufacturing
[DE91-010210] N91-23935
MANY BODY PROBLEM
Order and disorder in metallic alloys
[DE91-009120] N91-23292
Biased galaxy formation in the neutrino scenario N91-23839
A high resolution study of the Cu K alpha(sub 1,2) x-ray emission lines N91-23841
Few-body problems, electron-correlation effects, and beyond
[DE91-010030] N91-23857
An observational study of arm structure in normal spiral galaxies N91-24007
MANY ELECTRON EFFECTS
A high resolution study of the Cu K alpha(sub 1,2) x-ray emission lines N91-23841
MAPPING
Programmable remapper for image processing
[NASA-CASE-MSC-21350-1] N91-23724
MARINE ENVIRONMENTS
Subsea habitats and space simulation N91-23567
MARINE METEOROLOGY
Observational study of the above-inversion structure and marine stratocumulus cloud clearing episodes during FIRE N91-23666
MARINE RESOURCES
Satellite and aeronautical technologies serving the management of living marine resources N91-23606
MARINE TECHNOLOGY
Elastic/plastic fracture mechanics. Part 2: Marine structural applications
[AD-A232560] N91-23557
MARKET RESEARCH
Development of a low cost peak shaving generator set
[PB91-136374] N91-23332
MARKOV CHAINS
Convergence of one-dimensional diffusion processes to a jump process related to population genetics
[AD-A232121] N91-23826
MARKOV PROCESSES
A method for handling complex Markov models of parallel systems
[RR-826-I] N91-23778
MARS (PLANET)
America at the threshold N91-23201
Material processing with hydrogen and carbon monoxide on Mars
[NASA-TM-104405] N91-23616
MARS SURFACE
Composition and distribution of carbonates, sulfates, and hydrates on the Martian surface from earth-based spectroscopy between 3-5 microns N91-24033
MARTENSITE
The strength and toughness of stainless steels at cryogenic temperature
[DE91-009771] N91-23300
MARTENSITIC TRANSFORMATION
The strength and toughness of stainless steels at cryogenic temperature
[DE91-009771] N91-23300
MASERS
Observation of harmonic gyro-backward-wave oscillation in a 100 GHz CARM oscillator experiment
[AD-A232063] N91-23398
MASS SPECTRA
Microbeam titanium isotopic analysis by resonance ionization mass spectrometry
[DE91-010799] N91-23277

MASS SPECTROMETERS
Laboratory study of the thermochemical properties of materials used in spacecraft
[AD-A232124] N91-23228
Microbeam titanium isotopic analysis by resonance ionization mass spectrometry
[DE91-010799] N91-23277
MASS SPECTROSCOPY
Mass resolved resonance ionization spectroscopy of combustion radicals
[DE91-010603] N91-23276
Microbeam titanium isotopic analysis by resonance ionization mass spectrometry
[DE91-010799] N91-23277
MASS TRANSFER
Point defect effects on hot corrosion of zirconia-based coatings
[AD-A232662] N91-23326
Particle-fluid two-phase flow modeling
[DE91-010102] N91-23415
Interphase transport and multistage separations
[DE91-009627] N91-23425
The solidification of a molten droplet on an inclined plane
[NPL-DMM(A)-20] N91-23438
Diffusive, eleçtrostatic concentration of disintegration products of inert gases in vortex flow
[AD-A232876] N91-23457
Heat and mass transfer in the gas tungsten and gas metal arc welding processes
[DE91-010089] N91-23510
Near-equatorial deep circulation in the Indian and Pacific oceans
[AD-A232635] N91-23691
MASSIVELY PARALLEL PROCESSORS
Electronic neuroprocessors N91-24045
MATCHED FILTERS
Digital beamforming and pulse compression in an adaptive array radar system
[AD-A232713] N91-23377
Characteristics and performance of an operational windscatterometer N91-23607
MATCHING
Realization of a randomized algorithm for the exact perfect matching problem, with a new constructive procedure
[REPT-90-056] N91-23751
MATERIALS RECOVERY
Steps toward environmentally compatible product and process design: A case for green engineering
[AD-A232888] N91-23633
MATERIALS TESTS
Laboratory study of the thermochemical properties of materials used in spacecraft
[AD-A232124] N91-23228
MATHEMATICAL LOGIC
Congruence properties of the process equivalence induced by temporal logic
[RR-831-I-IMAG-118-LIFIA] N91-23810
MATHEMATICAL MODELS
Near midair collisions as an indicator of general aviation collision risk N91-23096
Application of multidisciplinary optimization methods to the design of a supersonic transport
[NASA-TM-104073] N91-23135
The limits of the landing process of aircraft
[DLR-FB-90-49] N91-23137
Design techniques for dual mode ram-scramjet combustors N91-23166
Pitot surveys of two moderately under-expanded jets N91-23172
Evaluation techniques for highly augmented aircraft
[DLR-FB-90-35] N91-23191
Simulation and analyses of the aeroassist flight experiment attitude update method
[NASA-TM-102174] N91-23210
A simulation of the draping and a model of the consolidation of commingled fabrics N91-23239
Rate dependent stress-strain behavior of advanced polymer matrix composites
[NASA-TM-104070] N91-23244
An experimental and finite element investigation into the nonlinear material behavior of pin-loaded composite laminates
[AD-A232098] N91-23263
Phase transitions at liquid solid interfaces: Pade approximant for adsorption isotherms and voltammograms
[AD-A232623] N91-23285
Computer modeling of soot formation comparing free radical and ionic mechanisms
[AD-A232820] N91-23287
Deterministic analysis of processes at corroding metal surfaces and the study of electrochemical noise in these systems
[DE91-009997] N91-23297
Creep and creep-rupture behavior of Alloy 718
[DE91-007706] N91-23298
High-temperature alloys for high-power thermionic systems
[DE91-009292] N91-23299
Response of simulated propellants and explosives to projectile impact
[DE91-009777] N91-23333
A novel process for methanol synthesis
[DE91-009808] N91-23334
A simplified dynamic model of the Space Shuttle main engine
[NASA-TM-104421] N91-23340
The statistical properties of electromagnetic fields with application to radiation and scattering
[DE91-007467] N91-23351
Calculation of electromagnetic fields in the near-field region of a moving scattering object
[FEL-90-B216] N91-23361
Optimal multinode broadcast on a mesh connected graph with reduced bufferization
[RR-825-I] N91-23362
Antenna performance influenced by the finite extent and conductivity of ground planes: A collection of reprints
[AD-A232132] N91-23366
An analysis of MLAYER: A multilayer tropospheric propagation program
[AD-A232733] N91-23379
Control aspects of the brushless doubly-fed machine
[DE91-009707] N91-23387
Parametric modeling and estimation of pulse propagation on microwave integrated circuit interconnections
[AD-A232465] N91-23404
Background simulation and filter design using iterated function systems
[AD-A232632] N91-23405
A computationally efficient modelling of laminar separation bubbles N91-23411
Interphase transport and multistage separations
[DE91-009627] N91-23425
Interfacial characteristic measurements in horizontal bubbly two-phase flow
[DE91-009803] N91-23427
Numerical simulation of a viscous vortex ring interaction with a density interface
[DE91-002790] N91-23429
Benchmarking numerical predictions with force and moment measurements on slender, supercavitating bodies
[DE91-007066] N91-23432
Investigation of Roe's 2D wave decomposition models for the Euler equations
[VKI-TN-172] N91-23436
The solidification of a molten droplet on an inclined plane
[NPL-DMM(A)-20] N91-23438
Strategy Combining Regionally Adapted Processes (SCRAP)
[AD-A232158] N91-23448
Fractal image compression of Rayleigh, Raman, LIF and LDV data in turbulent reacting flows
[AD-A232237] N91-23449
Nonlinear waves in real materials
[AD-A232654] N91-23452
A numerical model of laser induced fluorescence in a hydrogen plasma
[AD-A232240] N91-23482
Automated handling and assembling of non-rigid objects
[AD-A231246] N91-23489
Finite element based dynamical modeling of flexible open-loop manipulators with experimental results N91-23496
Wave gaits, follow-the-leader gaits and gait transitions of legged robots N91-23503
Modal analysis of multistage gear systems coupled with gearbox vibrations
[NASA-TM-103797] N91-23513
Energy-efficient penetration of targets
[AD-A232227] N91-23518
System modeling and identification of flexible structures N91-23531
Computerized symbolic closed-form dynamics and control analysis of hybrid rigid and elastic multibody systems N91-23532
Approximating the dynamic response of strain-hardening structures
[DE91-006392] N91-23534
A theory for fluidelastic instability of tube-support-plate inactive modes
[DE91-009676] N91-23538
A theory for fluidelastic instability of tube-support-plate inactive modes
[DE91-006001] N91-23542
Buckling analysis of a complex vacuum vessel using the finite-element method
[DE91-010032] N91-23546
Model sensitivity in stress-strength reliability computations
[AD-A232023] N91-23554
A complex systems approach to metallic fracture surface characterization
[AD-A232546] N91-23556
On the construction of two-phase equilibria in a non-elliptic hyperelastic material
[AD-A232628] N91-23558
Accuracy of the Reissner-Mindlin and the (1,1,2) model for the clamped-in plate problem
[AD-A232755] N91-23561
The problem of plate modeling theoretical and computational results
[AD-A232756] N91-23562
An expanding grid photochemical model for visibility applications
[DE91-009947] N91-23630
Sensitivity of numerical dispersion modeling to explosive source parameters
[DE91-009476] N91-23631
Treatment of denser-than-air releases in an advection-diffusion model: Thermodynamic effects
[DE91-010152] N91-23632
Theoretical studies of large-scale features of the Earth's mid- to high-latitude ionosphere N91-23641
Mechanisms of equatorial superrotation: Studies with two-level models N91-23642
Propagation of seismic waves in nonelastic media
[REPT-90-065] N91-23651
Design of an enhanced global spectral model
[AD-A232123] N91-23655
High-altitude non-equilibrium infrared emission models
[AD-A232503] N91-23659
Assimilation of ERBE data with nonlinear programming technique to improve cloud cover diagnosis N91-23663
Grouping of clouds and internal gravity waves in a non-hydrostatic model of moist convection
[DM-55] N91-23679
A one dimensional wind profile model with stability and eddy viscosity estimations from sodar data
[DM-56] N91-23680
Range reference atmosphere, Shemya
[AD-A232813] N91-23685
Range reference atmosphere, Thule
[AD-A232831] N91-23686
A guide to the Nedwam wave model
[KNMI-WR-90-04] N91-23688
Modeling speedup in parallel sparse matrix factorization
[DE91-010215] N91-23735
Scientific visualization software for your PC: Free and available now
[DE91-010156] N91-23744
Maintenance Resource Prediction Model (MRPM) user's manual
[AD-A232019] N91-23762
Towards real-time GOMS
[AD-A232028] N91-23763
Synergetic multisensor fusion
[AD-A232089] N91-23766
A fast algorithm for the evaluation of trigonometric series
[AD-A232848] N91-23775
A method for handling complex Markov models of parallel systems
[RR-826-I] N91-23778
Applications of neural networks to process control and modeling
[DE91-007389] N91-23784
Statistical methods and neural network approaches for classification of data from multiple sources
[NASA-CR-188207] N91-23786
On the structure of polynomial models of 2-D systems
[MATHS-REPT-A-139] N91-23812
The H-P version of the finite element method in the plate modelling problem
[AD-A232246] N91-23816
Computations, properties, and applications of matrix-valued functions to mathematical science and control systems
[AD-A232448] N91-23819
A particular linear model of variance components
[RR-827-M] N91-23824
Statistical models and inference procedures for structural and materials reliability
[AD-A232634] N91-23827
On the many-on-one stochastic duel
[CEMA-86/11] N91-23828
Sufficient comparison and modeling of forecasts N91-23829
Biased galaxy formation in the neutrino scenario N91-23839

Dynamic study of cyclically symmetric structures: Application to rotating a wheel of a centrifugal compressor
[ISAL-91-0004] N91-23844
Comment on: Analytic solution of the Stochastic-Liouville model of spin-exchange
[DE91-010570] N91-23861
Theory of novel nonlinear optics
[AD-A232659] N91-23903
Nonlinear real-time optical signal processing
[AD-A232889] N91-23909
Plasma torches dimensioning and optimization
[REPT-911-430-111] N91-23926
Mean-field theories of the Hubbard model and periodic orbits in chaotic maps N91-23938
Electronic properties of Si-doped n-doping-intrinsic-p-doping-intrinsic (nipi) structures in GaAs
[DE91-009474] N91-23941
Effects of distributed database modeling on evaluation of transaction rollbacks N91-23972
Measuring the effects of distributed database models on transaction availability measures N91-23973
Primordial lithium, stellar evolution, and cosmology: Lithium in halo stars from standard, diffusive, and rotational stellar evolution and implications for cosmology N91-24024

MATHEMATICAL PROGRAMMING
Statistical process allocation in a parallel processing architecture
[RR-833-I] N91-23779

MATHEMATICAL TABLES
Table-lookup algorithms for elementary functions and their error analysis
[DE91-006047] N91-23743

MATRICES (CIRCUITS)
Optical shutter switching matrix N91-24071

MATRICES (MATHEMATICS)
Interphase transport and multistage separations
[DE91-009627] N91-23425
Computerized symbolic closed-form dynamics and control analysis of hybrid rigid and elastic multibody systems N91-23532
Modeling speedup in parallel sparse matrix factorization
[DE91-010215] N91-23735
Realization of a randomized algorithm for the exact perfect matching problem, with a new constructive procedure
[REPT-90-056] N91-23751
Principal components of minus M-matrices
[AD-A232354] N91-23818
Computations, properties, and applications of matrix-valued functions to mathematical science and control systems
[AD-A232448] N91-23819

MATRIX MATERIALS
New developments in composites for space applications
[REPT-911-430-104] N91-23250
Structural materials for space mirrors
[REPT-911-430-128] N91-23261
Generation of continuous liquid crystalline polymer reinforcements in thermoplastics by a novel blending process
[AD-A232824] N91-23330

MAXIMUM LIKELIHOOD ESTIMATES
Presentation of a computer program for analysing results of one shot device sensitivity tests: Application to the case of a one shot degenerated sequence
[REPT-911-430-126] N91-23758
Topics in inference and decision-making with partial knowledge
[NASA-CR-188209] N91-23821
Sufficient comparison and modeling of forecasts N91-23829

MAXWELL EQUATION
Calculation of near-field scattering using the plane-wave formulation and the physical optics method
[FEL-90-B215] N91-23360

MEASURING INSTRUMENTS
Qualification of concentrating mirror systems with the Hermes measurement system and the Helios simulation program
[ESA-TT-1213] N91-23230
High resolution measurements of strained diffusion and reaction layer structure and extinction in turbulent flows
[AD-A232794] N91-23456
Method of producing a plug type heat flux gauge
[NASA-CASE-LEW-14967-2] N91-23460
Tropospheric sampling with aircraft
[DE91-009472] N91-23626

MECHANICAL DRIVES
Magnetostrictive roller drive motor
[NASA-CASE-GSC-13369-1] N91-23380

MECHANICAL PROPERTIES
The development and evaluation of an alternative powder prepregging technique for use with LaRC-TPI/graphite composites
[NASA-CR-188184] N91-23242
CRREL research on materials in cold environments
[AD-A232133] N91-23280
High-temperature alloys for high-power thermionic systems
[DE91-009292] N91-23299
Rapidly solidified metallic alloys with unusual semmetry properties
[AD-A232384] N91-23304
NDE (Nondestructive Examination) development for ceramics for advanced heat engines
[DE91-005516] N91-23316
Committee draft for an ISO standard on the acquisition and presentation of multipoint data for plastics
[NPL-DMM(A)-24] N91-23320
Generation of continuous liquid crystalline polymer reinforcements in thermoplastics by a novel blending process
[AD-A232824] N91-23330
Quantum chemical studies of candidate high energy density material compounds
[AD-A232393] N91-23335
A study of PC-Based HF ionospheric propagation predictions for use in naval communications
[AD-A232466] N91-23375
Evaluation of catastrophic failure risk in pressure vessels. Results of pressure vessel test with a large vessel (HC2-test)
[VTT-RR-708] N91-23551
Elastic/plastic fracture mechanics. Part 2: Marine structural applications
[AD-A232560] N91-23557
Statistical models and inference procedures for structural and materials reliability
[AD-A232634] N91-23827
Optical and mechanical properties of mixed silver halide crystals N91-23837
Studies of molecular excitation in star formation regions N91-24023

MEDICAL ELECTRONICS
Research and development involved in creating a quantitative EEG cartography wide band analysis system
[LAAS-91002] N91-23705

MEDICAL SCIENCE
A test of the American Safety Flight Systems, Inc. prebreather/portable oxygen system
[AD-A232723] N91-23100
Proceedings of the 1991 American Association for the Advancement of Science Annual Meeting Program N91-23969

MEDITERRANEAN SEA
Satellite data utilization for modeling sea states N91-23598

MELTS (CRYSTAL GROWTH)
Contract crystal growth and fabrication services
[AD-A232120] N91-23952

MEMBRANES
High temperature membranes for H2S and SO2 separations
[DE91-008534] N91-23275

MEMORY (COMPUTERS)
Evaluation of ferroelectric materials for memory applications
[AD-A232112] N91-23728
Data type coherency in heterogeneous shared memory multiprocessors
[AD-A232114] N91-23729
Performance analysis of garbage collection and dynamic reordering in a Lisp system
[NASA-CR-188205] N91-23738
Integrated Vertical Bloch Line (VBL) memory N91-24051

MENTAL PERFORMANCE
Individual differences underlying pilot cockpit error
[DOT/FAA/RD-91/13] N91-23710
Human Performance Assessment Methods. Addendum
[AGARD-AG-308-ADD] N91-23711
Effects of bright illumination on oral temperature and cognitive performance in humans during nighttime hours
[AD-A232787] N91-23722

MERIDIONAL FLOW
Maintenance of short-term subtropical wind maxima in the Southern Hemisphere: Observational and modeling study N91-23665

MESONS
The birth of the 'strange' particle physics
[NOTA-INTERNA-958] N91-23875

MESOSCALE PHENOMENA
Extraction of mesoscale ocean currents information from Geosat altimeter data N91-23594
Analysis and modeling of summertime convective cloud and precipitation structure over the Southeastern United States
[NASA-CR-188119] N91-23670

MESOSPHERE
A search for strange attractors in the saturation of middle atmosphere gravity waves
[AD-A232468] N91-23658

METABOLISM
Hepatic metabolism of perfluorinated carboxylic acids: A nuclear magnetic resonance investigation
[AD-A232033] N91-23706
Heat strain and work tolerance times with varying levels of Canadian Forces NBC protective clothing, ambient temperature, physical work intensity, and work/rest schedules
[AD-A232653] N91-23720

METAL COATINGS
Electrodeposited coatings for diamond turning applications
[DE91-009950] N91-23315

METAL FILMS
Metal thin-film optical polarizers for space applications, phase 2
[NASA-CR-188202] N91-23891
Epitaxial iron films
[AD-A232419] N91-23958

METAL HALIDES
Conceptual design study of high-performance sodium/metal chloride batteries for electric vehicle applications
[DE91-009618] N91-23383

METAL MATRIX COMPOSITES
Combined thermal and bending fatigue of high-temperature metal-matrix composites: Computational simulation
[NASA-TM-104354] N91-23247
Galvanic corrosion of aluminum-matrix composites
[AD-A232138] N91-23264
Modelling of the impact response of fibre-reinforced composites
[AD-A232658] N91-23266
A preliminary investigation of acousto-ultrasonic NDE of metal matrix composite test specimens
[NASA-TM-104339] N91-23521

METAL OXIDE SEMICONDUCTORS
Recent advances with quiescent power supply current (I(sub DDQ)) testing at Sandia using the HP82000
[DE91-009254] N91-23382

METAL OXIDES
Re-analysis of photoemission data for CuO: Revision of the configuration-energy scheme for cuprate materials
[DE91-009952] N91-23296

METAL POWDER
Post-overload fatigue crack recovery in powder metal aluminum-lithium AL-905XL forging
[AD-A232550] N91-23307

METAL PROPELLANTS
Diagnostic measurements on an aluminized propellant plume during spin and nonspin testing
[AD-A232031] N91-23235

METAL SURFACES
Deterministic analysis of processes at corroding metal surfaces and the study of electrochemical noise in these systems
[DE91-009997] N91-23297
Fundamental research on tribology
[AD-A232446] N91-23519
A complex systems approach to metallic fracture surface characterization
[AD-A232546] N91-23556
In-situ surface x ray scattering measurements of electrochemically deposited bismuth on silver (III): Structure, compressibility, and comparison with ex-situ leed measurements
[AD-A232624] N91-23880

METALLIC GLASSES
Rapidly solidified metallic alloys with unusual semmetry properties
[AD-A232384] N91-23304

METALLIC STARS
Primordial lithium, stellar evolution, and cosmology: Lithium in halo stars from standard, diffusive, and rotational stellar evolution and implications for cosmology N91-24024

METALLICITY
Primordial lithium, stellar evolution, and cosmology: Lithium in halo stars from standard, diffusive, and rotational stellar evolution and implications for cosmology N91-24024

METALORGANIC CHEMICAL VAPOR DEPOSITION
Broad area distributed gain, distributed index profile GaAlAs semiconductor laser diodes
[AD-A232332] N91-23483

METALS
Fundamental studies of electronic packaging materials and structures: Surface and interfaces
[AD-A232336] N91-23403
Energy dissipator
[NASA-CASE-MSC-21555-1] N91-23492
Surface electron emission induced by slow multicharged ions
[DE91-010469] N91-23865
METASTABLE STATE
On the construction of two-phase equilibria in a non-elliptic hyperelastic material
[AD-A232628] N91-23558
METEORITES
Microbeam titanium isotopic analysis by resonance ionization mass spectrometry
[DE91-010799] N91-23277
METEOROLOGICAL PARAMETERS
Air ambulance helicopter operational analysis
[DOT/FAA/RD-91/7] N91-23134
Atmospheric turbulence review of space shuttle launches
[NASA-TM-4289] N91-23215
METEOROLOGICAL RADAR
Backscattering by nonspherical particles, using the coupled-dipole method: An application in radar meteorology
[AD-A232371] N91-23373
The terminal Doppler weather radar tornadic vortex signature detection algorithm
[DOT-FAA-NR-91-5] N91-23675
METEOROLOGICAL SATELLITES
Remote sensing performances
[REPT-911-440-101] N91-23615
METEOSAT SATELLITE
Remote sensing performances
[REPT-911-440-101] N91-23615
Quantitative processing of Meteosat data: Implementation at KNMI: Applications
[KNMI-TR-127] N91-23678
METHOD OF CHARACTERISTICS
The 2-D supersonic nozzle design N91-23176
METHYL ALCOHOL
A novel process for methanol synthesis
[DE91-009808] N91-23334
METHYL COMPOUNDS
Dissolution of Poly(p-hydroxystyrene): Molecular weight effects
[AD-A232155] N91-23323
MICROANALYSIS
Microbeam titanium isotopic analysis by resonance ionization mass spectrometry
[DE91-010799] N91-23277
MICROBEAMS
Microbeam titanium isotopic analysis by resonance ionization mass spectrometry
[DE91-010799] N91-23277
MICROCLIMATOLOGY
Effectiveness of a prototype microclimate cooling system for use with chemical protective clothing
[AD-A231572] N91-23717
MICROCOMPUTERS
Life cycle management automation user's manual, version 1.1
[AD-A232096] N91-23968
A study of the end point path geometry in meteor burst systems using a microcomputer signal logger N91-24012
MICROCRACKS
A statistical model of fractures N91-23529
MICROELECTRONICS
Checklist for thick-film hybrid microcircuits manufacturer and line survey
[ESA-PSS-01-607-ISSUE-1] N91-23396
Checklist for thin-film hybrid microcircuits manufacturer and line survey
[ESA-PSS-01-611-ISSUE-1] N91-23397
Electronic neuroprocessors N91-24045
MICROGRAVITY APPLICATIONS
Containerless undercooling and solidification of pure metals
[DLR-FB-90-48] N91-23301
Protein crystal growth tray assembly
[NASA-CASE-MFS-28507-1] N91-23933
MICROHARDNESS
Mechanical characterisation of fibre-matrix interface in ceramic composites by an instrumented indentation test
[REPT-911-430-114] N91-23256
Characterization of the glass transition using a microindenter
[AD-A232154] N91-23282
MICROMECHANICS
A study of the micromechanics of the fiber-matrix interphase in monofilament composites, in monotonic loading, and cyclic fatigue N91-23241
Combined thermal and bending fatigue of high-temperature metal-matrix composites: Computational simulation
[NASA-TM-104354] N91-23247
Stochastic micromechanical modeling of cleavage fracture in the ductile-brittle transition region N91-23533
Development of a micromechanic theory of constitutive relations of polycrystalline solids
[AD-A232697] N91-23559
MICROMETEOROLOGY
Surface layer transfer processes over vegetation: A micrometeorological field experiment of long duration N91-23664
MICROPARTICLES
Automatic particle sizing from rocket motor holograms
[AD-A232553] N91-23236
MICROPROCESSORS
Designing a virtual-memory implementation using the Motorola MC88010 16-bit microprocessor with multi-processor capability interfaced to the VMEbus
[AD-A232554] N91-23730
MICROSCOPY
Wavelength independent optical lithography and microscopy
[AD-A232036] N91-23896
MICROSTRIP ANTENNAS
Efficient numerical techniques for the analysis of complex microstrip-antennas and microstrip arrays
[DLR-FB-90-53] N91-23357
MICROSTRIP DEVICES
Design of inherently wide-band microwave frequency doubler and tripler in microstrip
[FEL-90-B255] N91-23392
MICROSTRIP TRANSMISSION LINES
Parametric modeling and estimation of pulse propagation on microwave integrated circuit interconnections
[AD-A232465] N91-23404
MICROSTRUCTURE
Boundary stability under nonequilibrium conditions
[DE91-009262] N91-23293
Phase transformations and microstructural evolution in aged Mn-Cu-based alloys
[AD-A232473] N91-23305
Examination of the microstructure of 7050 aluminum alloy samples
[AD-A232544] N91-23306
High temperature ordered intermetallic alloys
[AD-A232769] N91-23308
Mechanistic studies of pressure-assisted superplasticity of structural ceramics
[AD-A232034] N91-23322
Investigation of micro- and macrophysical structures and processes in hail clouds with respect to their modification
[DLR-FB-90-38] N91-23677
Nonequilibrium Green's functions and quantum transport theory for semiconductor microstructures N91-23937
Microstructure of epitaxial YBa2Cu3O7 thin films
[DE91-009951] N91-23942
Composite ceramic superconducting wires for electric motor applications
[AD-A232074] N91-23951
In based III-V microstructures with novel electronic properties
[AD-A232695] N91-23960
MICROTRONS
Lectures on accelerator physics
[DE91-010376] N91-23886
MICROWAVE ANTENNAS
Superconducting microwave electronics at Lewis Research Center N91-24081
MICROWAVE CIRCUITS
A 30 GHz monolithic receive module
[NASA-CR-187085] N91-23346
System-Level Integrated Circuit (SLIC) development for phased array antenna applications
[NASA-TM-104392] N91-23354
S-parameter measurements and applications of superconducting flux flow transistors
[DE91-009763] N91-23388
Parametric modeling and estimation of pulse propagation on microwave integrated circuit interconnections
[AD-A232465] N91-23404
Microwave integrated circuits for space applications N91-24069
Superconducting microwave electronics at Lewis Research Center N91-24081
MICROWAVE FREQUENCIES
Research and development on advanced silicon carbide thin film growth techniques and fabrication of high power and microwave frequency silicon carbide-based device structures
[AD-A232160] N91-23955
MICROWAVE IMAGERY
Microwave imaging of Saturn's deep atmosphere and rings N91-24035
MICROWAVE LANDING SYSTEMS
Microwave landing system modeling with application to air traffic control
[NASA-TM-102832] N91-23099
MICROWAVE OSCILLATORS
Observation of harmonic gyro-backward-wave oscillation in a 100 GHz CARM oscillator experiment
[AD-A232063] N91-23398
MICROWAVE RADIOMETERS
ATSR: Precise sea surface temperature from the ERS-1 satellite N91-23601
Microwave temperature profiler for clear air turbulence prediction
[NASA-CASE-NPO-18115-1-CU] N91-23662
MICROWAVE TRANSMISSION
A transmission line method for the measurement of microwave permittivity and permeability
[RSRE-MEMO-4450] N91-23394
MIDAIR COLLISIONS
Near midair collisions as an indicator of general aviation collision risk N91-23096
MIDDLE ATMOSPHERE
Models of planetary wave propagation in the middle atmosphere N91-23639
A search for strange attractors in the saturation of middle atmosphere gravity waves
[AD-A232468] N91-23658
MILITARY AIRCRAFT
The costs and benefits of aircraft availability
[AD-A232660] N91-23076
Flying Qualities
[AGARD-CP-508] N91-23108
MIL-STD-1797 is not a cookbook N91-23111
Flying qualities experience on the AMX aircraft N91-23112
The development of alternate criteria for FBW handling qualities N91-23113
Do civil flying qualities requirements address military missions for off-the-shelf procurement N91-23115
Analytical study of the effects of weight on Light Helicopter (LH) exposure to ground-based weapons
[AD-A232024] N91-23141
An engineering study of altitude determination deficiencies of the Service Aircraft Instrumentation Package (SAIP)
[AD-A232055] N91-23145
MILITARY HELICOPTERS
ADFCS and NOTAR (trademark): Two ways to fix flying qualities N91-23110
MILITARY OPERATIONS
Fiber optic sensors for the military
[AD-A232100] N91-23698
MILITARY TECHNOLOGY
Life cycle management automation programmer's manual
[AD-A232247] N91-23769
MILITARY VEHICLES
Power packs: A passive approach to extinguishing fire in combat vehicles
[AD-A232020] N91-23342
MILLIMETER WAVES
High energy dense ribbon beams and high harmonic gyrotron at millimeter wavelengths
[AD-A232839] N91-23470
MINERAL METABOLISM
A non-invasive measure of minerals and electrolytes in tissue N91-24058
MINIMAX TECHNIQUE
Worst-case design of optimal controllers over a finite horizon
[AD-A232353] N91-23797
MINING
Detection of mining activities in the Yanomani Indian Reserve through LANDSAT-TM imagery
[INPE-5182-RPE/638] N91-23609
MIRROR FUSION
A proposed search for dark-matter axions in the 0.6-16 micro-eV range
[NASA-CR-188173] N91-24015
MIRRORS
Structural materials for space mirrors
[REPT-911-430-128] N91-23261
MISSILE CONTROL
Target maneuver models for improved homing guidance N91-23101
Analysis of the flutter characteristics of the advanced kinetic energy missile (ADKEM) control surface
[AD-A232377] N91-23193
MISSILE TESTS
Pyrotechnical safety of Aerospatiale tactical missiles: Application to conventional warhead
[REPT-911-320-101] N91-23139

MISSILES
Highly integrated ducted rocket propulsion modules for future hypersonic tactical missiles N91-23171
Analysis of the flutter characteristics of the advanced kinetic energy missile (ADKEM) control surface [AD-A232377] N91-23193
High temperature composites in space planes and missiles development [REPT-911-430-119] N91-23259

MISSION PLANNING
Piloted rover technology study [NASA-CR-186989] N91-23200
Small Explorer project: Submillimeter Wave Astronomy Satellite (SWAS). Mission operations and data analysis plan [NASA-CR-186954] N91-23212
The Eutelsat 2 programme [REPT-911-440-108] N91-23223

MIXED CRYSTALS
Optical and mechanical properties of mixed silver halide crystals N91-23837

MIXED OXIDES
Effect of transition metal dopants on high T(sub c) superconductivity [PB91-130138] N91-23934

MIXING
Use of secondary flows for rapid mixing in scramjet combustors N91-23167
Mixing and non-equilibrium chemical reaction in a compressible mixing layer [NASA-CR-187084] N91-23181
Numerical simulations of instabilities in compressible mixing layers N91-23412

MIXING LAYERS (FLUIDS)
Use of secondary flows for rapid mixing in scramjet combustors N91-23167
Mixing and non-equilibrium chemical reaction in a compressible mixing layer [NASA-CR-187084] N91-23181
High resolution measurements of strained diffusion and reaction layer structure and extinction in turbulent flows [AD-A232794] N91-23456

MIXTURES
Monte Carlo simulation of supercritical solutions in the grand canonical ensemble [DE91-009152] N91-23859

MODAL RESPONSE
Use of personal computers in performing a linear modal analysis of a large finite-element model [DE91-010112] N91-23541

MODELS
Mechanisms of higher brain functions: A study of models of perception [AD-A232389] N91-23712
A Model-Based Approach to High-Level Robot Control with Visual Guidance [VTT-PUBL-71] N91-23788
Distributed, cooperating knowledge-based systems N91-24044

MODERATORS
Cold moderators for pulsed neutron sources [DE91-010594] N91-23866

MODULATORS
Non-mechanical optical path switching and its application to dual beam spectroscopy including gas filter correlation radiometry [NASA-CASE-LAR-14588-1-CU] N91-23889

MODULES
Highly integrated ducted rocket propulsion modules for future hypersonic tactical missiles N91-23171
A 30 GHz monolithic receive module [NASA-CR-187085] N91-23346

MOLDS
Thermoforming of in-situ reinforced thermoplastic composites [AD-A232816] N91-23329

MOLECULAR BEAM EPITAXY
Optoelectronic III-V heterostructures on SI substrates [AD-A232035] N91-23950
X ray diffraction and electron spectroscopy of epitaxial molecular C60 films [AD-A232152] N91-23954
Research and development on advanced silicon carbide thin film growth techniques and fabrication of high power and microwave frequency silicon carbide-based device structures [AD-A232160] N91-23955
Epitaxial iron films [AD-A232419] N91-23958
In based III-V microstructures with novel electronic properties [AD-A232695] N91-23960
Development of Si/SiGe heterostructures [AD-A232747] N91-23961

MOLECULAR CLOUDS
The supernova remnant G109.1-1.0 and the x-ray pulsar 1E2259+586 N91-24002
Studies of molecular excitation in star formation regions N91-24023

MOLECULAR COLLISIONS
Excitation of atoms and molecules in collisions with highly charged ions [DE91-010740] N91-23870

MOLECULAR DIFFUSION
Turbulent mixing in nonreacting and reacting flows: A PDF approach at the two-point level N91-23422
High resolution measurements of strained diffusion and reaction layer structure and extinction in turbulent flows [AD-A232794] N91-23456

MOLECULAR EXCITATION
Multiphoton detection techniques for F and F2 [AD-A232641] N91-23286
Excited state structure, energy and electron transfer dynamics of photosynthetic reaction centers: A hole burning study [DE91-010181] N91-23693
Excitation of atoms and molecules in collisions with highly charged ions [DE91-010740] N91-23870
Studies of molecular excitation in star formation regions N91-24023

MOLECULAR OSCILLATORS
Molecular dynamics simulator for optimal control of molecular motion [AD-A232801] N91-23881

MOLECULAR STRUCTURE
Stress-density variations in alumina sediments: Effects of polymer chemistry [DE91-009055] N91-23313
Quantum chemical studies of candidate high energy density material compounds [AD-A232393] N91-23335
Problems in understanding the organization, structure and function of chromosomes [DE91-009939] N91-23695
Molecular dynamics simulator for optimal control of molecular motion [AD-A232801] N91-23881
X ray diffraction and electron spectroscopy of epitaxial molecular C60 films [AD-A232152] N91-23954
Synthesis and characterization of indium-arsenic compounds containing a four-membered In-Ad-In-As or In-As-In-Cl ring: Crystal structures of ((Me3SiCH2)2 InAs(SiMe3)2)2 and (Me3SiCH2)2 InAs(SiMe3)2 In(CH2SiMe3)2Cl [AD-A232368] N91-23956

MOLECULAR THEORY
Advanced working fluids: Thermodynamic properties [PB91-136465] N91-23964

MOLECULAR WEIGHT
Poly(1,3,4-oxadiazoles) via aromatic nucleophilic displacement [NASA-CASE-LAR-14427-1] N91-23237
High shear stress rheology of liquid lubricants N91-23309
Stress-density variations in alumina sediments: Effects of polymer chemistry [DE91-009055] N91-23313
Dissolution of Poly(p-hydroxystyrene): Molecular weight effects [AD-A232155] N91-23323

MOLECULES
Thermoforming of in-situ reinforced thermoplastic composites [AD-A232816] N91-23329

MOLTEN SALTS
Electrodeposited coatings for diamond turning applications [DE91-009950] N91-23315

MOLYBDENUM ALLOYS
Reduction factors for creep strength and fatigue life of modified 9 Cr-1 Mo steel weldments [DE91-009919] N91-23544

MOLYBDENUM COMPOUNDS
Conceptual design study of high-performance sodium/metal chloride batteries for electric vehicle applications [DE91-009618] N91-23383

MOMENTS OF INERTIA
Control synthesis based upon a game theoretic approach N91-23831

MOMENTUM TRANSFER
Particle-fluid two-phase flow modeling [DE91-010102] N91-23415
Mechanisms of equatorial superrotation: Studies with two-level models N91-23642

MONITORS
Precision runway monitor demonstration report [AD-A232671] N91-23198
A submicron resolution monolithic capacitive displacement sensor with digital output [DE91-009765] N91-23465
Monitoring and control technologies for bioregenerative life support systems/CELSS N91-24060

MONOMERS
Atrane and quadroped frameworks in early transition metal and silicon GRO stereochemistry: Monomers and oligomers [AD-A232837] N91-23331

MONOMOLECULAR FILMS
X ray diffraction and electron spectroscopy of epitaxial molecular C60 films [AD-A232152] N91-23954

MONOPOLE ANTENNAS
Antenna performance influenced by the finite extent and conductivity of ground planes: A collection of reprints [AD-A232132] N91-23366

MONSOONS
Atmospheric teleconnections: Emphasis on the El Nino/Southern Oscillation and monsoons N91-23636
Effects of the northeast monsoon on the equatorial westerlies over Indonesia [AD-A232106] N91-23681

MONTE CARLO METHOD
The limits of the landing process of aircraft [DLR-FB-90-49] N91-23137
Signals and noise in lasers and atom-field interactions N91-23475
Canonical vs. micro-canonical sampling methods in a 2D Ising model [DE91-010204] N91-23737
Presentation of a computer program for analysing results of one shot device sensitivity tests: Application to the case of a one shot degenerated sequence [REPT-911-430-126] N91-23758
Monte Carlo simulation of supercritical solutions in the grand canonical ensemble [DE91-009152] N91-23859
Computed secondary-particle energy spectra following nonelastic neutron interactions with C-12 for E(n) between 15 and 60 MeV: Comparisons of results from two calculational methods [DE91-010454] N91-23864
Imaging and background in low-energy gamma ray astronomy N91-24005

MOON
America at the threshold N91-23201
Lunar volcanism and the thermal evolution of the moon N91-24031

MOONLETS
Saturn's F ring: Imaging and simulation N91-24032

MORPHOLOGY
Thermoforming of in-situ reinforced thermoplastic composites [AD-A232816] N91-23329
Transport and nucleation processes in the vapor growth of diamond [AD-A232135] N91-23953
An observational study of arm structure in normal spiral galaxies N91-24007

MOTION SICKNESS
Ship roll stabilization and human performance [AD-A232721] N91-23721

MOTION SIMULATION
Rule-based motion coordination for the adaptive suspension vehicle on ternary-type terrain [AD-A232224] N91-23517
Three-dimensional graphical representation of objects according to movement data in realtime [DLR-FB-90-51] N91-23725
Molecular dynamics simulator for optimal control of molecular motion [AD-A232801] N91-23881

MOTION SIMULATORS
Ship roll stabilization and human performance [AD-A232721] N91-23721

MOTION STABILITY
Wave gaits, follow-the-leader gaits and gait transitions of legged robots N91-23503
Rule-based motion coordination for the adaptive suspension vehicle on ternary-type terrain [AD-A232224] N91-23517
Ship roll stabilization and human performance [AD-A232721] N91-23721

MOTOR VEHICLES
The development of highly practiced skills: A starting point for driver modelling [IZF-1990-B-16] N91-23719

MULTICHANNEL COMMUNICATION
Optical shutter switching matrix N91-24071

MULTIGRID METHODS
Two dimensional optimization of smoothing properties of multistage schemes applied to hyperbolic equations [VKI-TN-173] N91-23807

MULTIPATH TRANSMISSION
Microwave landing system modeling with application to air traffic control
[NASA-TM-102832] N91-23099
Parallel-processor-based Gaussian beam tracer for use in ocean acoustic tomography
[AD-A232420] N91-23690
MULTIPHASE FLOW
Thermodynamically consistent formulations for rapid granular and turbulent multiphase flows N91-23420
MULTIPHOTON ABSORPTION
Mass resolved resonance ionization spectroscopy of combustion radicals
[DE91-010603] N91-23276
MULTIPROCESSING (COMPUTERS)
Design of an enhanced global spectral model
[AD-A232123] N91-23655
Data type coherency in heterogeneous shared memory multiprocessors
[AD-A232114] N91-23729
Designing a virtual-memory implementation using the Motorola MC68010 16-bit microprocessor with multi-processor capability interfaced to the VMEbus
[AD-A232554] N91-23730
Dynamic load balancing on highly parallel multicomputer systems N91-23777
MULTIPROGRAMMING
CESAR operating system
[FFI-91/7002] N91-23754
MULTISENSOR APPLICATIONS
Evaluation of multisensor fusion scheme for the localization of underwater remotely operated vehicles N91-23590
Synergetic multisensor fusion
[AD-A232089] N91-23766
MULTISPECTRAL BAND SCANNERS
Analysis on forest decline classification of the beech using airborne multispectral scanner data
[DLR-FB-90-56] N91-23614
MULTIVARIATE STATISTICAL ANALYSIS
Statistical methods and neural network approaches for classification of data from multiple sources
[NASA-CR-188207] N91-23786
Computations, properties, and applications of matrix-valued functions to mathematical science and control systems
[AD-A232448] N91-23819
MUONS
Investigation of the muon component of EAS initiated by primary radiation from Hercules X-1 N91-24037
MUTATIONS
Convergence of one-dimensional diffusion processes to a jump process related to population genetics
[AD-A232121] N91-23826

N

NARROWBAND
Hyperspectral imagery: What is it, what can it do
[AD-A231164] N91-23610
NASA PROGRAMS
America at the threshold N91-23201
Computational needs survey of NASA automation and robotics missions. Volume 1: Survey and results
[NASA-TM-103860] N91-23341
Technology 2000, volume 2
[NASA-CP-3109-VOL-2] N91-24041
Microwave integrated circuits for space applications N91-24069
NASTRAN
Modal analysis of multistage gear systems coupled with gearbox vibrations
[NASA-TM-103797] N91-23513
NATIONAL AEROSPACE PLANE PROGRAM
Hypersonic propulsion: Status and challenge N91-23153
Materials for hypersonic engines N91-23177
NATIONAL AIRSPACE SYSTEM
NAS operational test and evaluation/integration of the Maintenance Management System (MMS) test plan
[DOT/FAA/CT-TN90/41] N91-23075
NATURAL GAS
Direct gas injection with glow plug ignition
[PB91-136390] N91-23272
Research and development opportunities for natural gas fueled refrigeration in industrial processes
[PB91-136432] N91-23338
NATURAL LANGUAGE (COMPUTERS)
User interface to an ICAI system that teaches discrete math
[AD-A232693] N91-23799
Processing problems in the IRUS queries: An empirical verification of problem coverage in the natural language sourcebook
[AD-A232780] N91-23800
NAVIER-STOKES EQUATION
A study of three dimensional turbulent boundary layer separation and vortex flow control using the reduced Navier Stokes equations
[NASA-TM-104407] N91-23089
Computational modeling and validation for hypersonic inlets N91-23162
Viscous three-dimensional analyses for nozzles for hypersonic propulsion N91-23175
A three-dimensional Navier-Stokes stage analysis of the flow through a compact radial turbine
[NASA-TM-104420] N91-23186
Particle-fluid two-phase flow modeling
[DE91-010102] N91-23415
Flow between eccentric rotating cylinders N91-23417
Analysis of the multigrid method N91-23418
A numerical study of the stratified turbulent Ekman layer N91-23421
Numerical simulation of a viscous vortex ring interaction with a density interface
[DE91-002790] N91-23429
Developing natural convection in a fluid layer with localized heating and large viscosity variation
[DE91-005240] N91-23431
Aero-thermal investigation of a highly loaded transonic linear turbine guide vane cascade. A test case for inviscid and viscous flow computations
[VKI-TN-174] N91-23437
Formulation of boundary conditions for the multigrid acceleration of the Euler and Navier Stokes equations
[NASA-CR-188234] N91-23440
Numerical simulation of incompressible inhomogeneous turbulence in a plane channel flow
[ESA-TT-1199] N91-23441
Strategy Combining Regionally Adapted Processes (SCRAP)
[AD-A232158] N91-23448
NAVIGATION SATELLITES
High precision applications of the global positioning system N91-24073
NEAR FIELDS
Calculation of near-field scattering using the plane-wave formulation and the physical optics method
[FEL-90-B215] N91-23360
Wavelength independent optical lithography and microscopy
[AD-A232036] N91-23896
NEAR INFRARED RADIATION
A near-infrared search for brown dwarfs in the Pleiades N91-24011
NEAR WAKES
Effects of three-dimensional imposed disturbance on bluff-body near wake flows
[AD-A232137] N91-23447
NEBULAE
Theoretical studies of QSO absorption lines and the intergalactic medium N91-24025
Magnetospheric structure of rotation powered pulsars
[DE91-007622] N91-24028
NEGATIVE RESISTANCE DEVICES
In based III-V microstructures with novel electronic properties
[AD-A232695] N91-23960
NEPHANALYSIS
Surface cloud observations for radiation, climatology and incorporation into satellite-based nephanalyses N91-23671
NETWORK CONTROL
An artificial neural network control system for spacecraft attitude stabilization
[AD-A232013] N91-23225
Computer center reference manual, volume 2
[AD-A232370] N91-23781
Unattended network operations technology assessment study. Technical support for defining advanced satellite systems concepts
[NASA-CR-187080] N91-24030
NEURAL NETS
The application of neural networks to the SSME startup transient
[NASA-CR-187138] N91-23205
An artificial neural network control system for spacecraft attitude stabilization
[AD-A232013] N91-23225
Applications of neural networks to process control and modeling
[DE91-007389] N91-23784
Analysis of neutron noise spectra using neural networks
[DE91-007676] N91-23785
Statistical methods and neural network approaches for classification of data from multiple sources
[NASA-CR-188207] N91-23786
Classification using multi-layered perceptrons
[AD-A232810] N91-23802
Electronic neuroprocessors N91-24045
NEUROPHYSIOLOGY
Human short-latency somatosensory evoked potentials in impact acceleration research: Equipment, procedures, and techniques
[AD-A232732] N91-23709
NEUROSPORA
Isolation, cloning and expression of the genes for microbial polyurethane degradation
[AD-A232108] N91-23699
NEUTRAL ATMOSPHERES
Neutral wind vortices in the high-latitude thermosphere N91-23673
NEUTRAL ATOMS
Investigation of neutral atom and ion emission during laser conditioning of multilayer HfO2-SiO2 coatings
[DE91-009749] N91-23860
NEUTRAL BUOYANCY SIMULATION
The diving laboratory as a simulation environment for manned spaceflight N91-23564
Neutral buoyancy and microgravity: Extravehicular activities with a humid water suit N91-23579
EVA/robotics integration for Space Station Freedom N91-23583
NEUTRINOS
Biased galaxy formation in the neutrino scenario N91-23839
NEUTRON SCATTERING
Los Alamos Science, Number 19, 1990
[DE91-009371] N91-23855
NEUTRON SOURCES
Los Alamos Science, Number 19, 1990
[DE91-009371] N91-23855
Cold moderators for pulsed neutron sources
[DE91-010594] N91-23866
Pressure dynamics modeling for the design of the advanced neutron source reactor
[DE91-007860] N91-23883
NEUTRON SPECTRA
Analysis of neutron noise spectra using neural networks
[DE91-007676] N91-23785
Benchmark measurements and calculations of a 3-dimensional neutron streaming experiment
[DE91-010692] N91-23867
NEUTRONS
Computed secondary-particle energy spectra following nonelastic neutron interactions with C-12 for E(n) between 15 and 60 MeV: Comparisons of results from two calculational methods
[DE91-010454] N91-23864
Benchmark measurements and calculations of a 3-dimensional neutron streaming experiment
[DE91-010692] N91-23867
Light particle emissions in heavy ion reactions
[DE91-010746] N91-23871
NICKEL
Conceptual design study of high-performance sodium/metal chloride batteries for electric vehicle applications
[DE91-009618] N91-23383
NICKEL ALLOYS
Localized corrosion of high performance metal alloys in an acid/salt environment N91-24066
NICKEL HYDROGEN BATTERIES
Destructive physical analysis results of Ni/H2 cells cycled in LEO regime
[NASA-TM-104382] N91-23233
NIGHT
Effects of bright illumination on oral temperature and cognitive performance in humans during nighttime hours
[AD-A232787] N91-23722
NIOBIUM
The solidification behavior of an alloy 625/718 variant
[DE91-009544] N91-23294
NITROGENATION
Poly(1,3,4-oxadiazoles) via aromatic nucleophilic displacement
[NASA-CASE-LAR-14427-1] N91-23237
NITROUS OXIDES
A CFD study of jet mixing in reduced flow areas for lower combustor emissions
[NASA-TM-104411] N91-23185
NOISE (SOUND)
Computational simulation of acoustic fatigue for hot composite structures
[NASA-TM-104379] N91-23548
NOISE INTENSITY
Studies of noise in semiconductor laser arrays
[AD-A232411] N91-23485
NOISE PREDICTION (AIRCRAFT)
Noise inside aircraft fuselages subjected to airborne excitations
[REPT-911-111-104] N91-23853
NOISE PROPAGATION
Soviet atmospheric acoustics research N91-23848

Unified aeroacoustics analysis for high speed turboprop aerodynamics and noise. Volume 5: Propagation of propeller tone noise through a fuselage boundary layer
[NASA-CR-185195] N91-23852

NOISE REDUCTION
Noise inside aircraft fuselages subjected to airborne excitations
[REPT-911-111-104] N91-23853

NOISE SPECTRA
Analysis of neutron noise spectra using neural networks
[DE91-007676] N91-23785

NONDESTRUCTIVE TESTS
Nondestructive inspection for carbon-carbon with adapted coating for oxidation
[REPT-911-430-106] N91-23252
Nondestructive measurement of thickness and density of composite materials by Compton backscattering
[REPT-911-430-112] N91-23255
Materials and structure for Hermes
[REPT-911-430-117] N91-23258
How to know CMC
[REPT-911-430-130] N91-23262
NDE (Nondestructive Examination) development for ceramics for advanced heat engines
[DE91-005516] N91-23316
Quantitative nondestructive evaluation: Requirements for tomorrow's reliability N91-24074

NONEQUILIBRIUM CONDITIONS
Boundary stability under nonequilibrium conditions
[DE91-009262] N91-23293

NONLINEAR EQUATIONS
Non-linear interaction of a detonation/vorticity wave
[NASA-CR-187550] N91-23434
Interdisciplinary research on viscoelasticity and rheology
[AD-A232700] N91-23454

NONLINEAR FEEDBACK
An analytic study of general dynamic model and nonlinear feedback control of flexible robot arms N91-23497

NONLINEAR FILTERS
Background simulation and filter design using iterated function systems
[AD-A232632] N91-23405

NONLINEAR OPTICS
Optical parametric oscillators pumped by excimer lasers N91-23473
Measurements of passive-scalar spectra for grid turbulence using a nonlinear optical technique
[DE91-005310] N91-23892
Theory of novel nonlinear optics
[AD-A232659] N91-23903

NONLINEAR PROGRAMMING
Assimilation of ERBE data with nonlinear programming technique to improve cloud cover diagnosis N91-23663
Robustness in replicated databases N91-23981

NONLINEAR SYSTEMS
An experimental and finite element investigation into the nonlinear material behavior of pin-loaded composite laminates
[AD-A232098] N91-23263
Fractal image compression of Rayleigh, Raman, LIF and LDV data in turbulent reacting flows
[AD-A232237] N91-23449
Nonlinear waves in real materials
[AD-A232654] N91-23452
Time-optimal motion of robotic manipulators including nonlinear dynamics
[LAAS-90403] N91-23516
Duality methods for infinite dimensional optimization problems
[AD-A232605] N91-23772
Applications of neural networks to process control and modeling
[DE91-007389] N91-23784
Approximation methods for the identification and control of distributed parameter systems with applications to flexible structures
[AD-A232605] N91-23801
On 2+1-dimensional nonlinear integrable systems of Loewner-type
[MATHS-REPT-A-140] N91-23813
Some problems in nonlinear analysis
[AD-A232701] N91-23820

NONLINEARITY
Finite element based dynamical modeling of flexible open-loop manipulators with experimental results N91-23496
Nonlinear real-time optical signal processing
[AD-A232889] N91-23909
Liquid-crystal characterization using the Z-scan technique
[RSRE-MEMO-4451] N91-23949

NONPARAMETRIC STATISTICS
Nonparametric estimation in change-point hazard rate models for censored data: A counting process approach
[RR-836-I-AND-M] N91-23825

NONUNIFORMITY
The effect of combustor flow nonuniformity on the performance of hypersonic nozzles N91-23173
Dynamic load balancing on highly parallel multicomputer systems N91-23777

NORTH SEA
A guide to the Nedwam wave model
[KNMI-WR-90-04] N91-23688

NORTHERN HEMISPHERE
Atmospheric circulation and poleward sensible heat flux variations associated with the recent Northern Hemisphere warming N91-23629
The annual march of convection, sea surface temperature, and surface winds in the tropics N91-23667
Observed changes in the activity of baroclinic waves and their feedbacks during the life cycles of low-frequency circulation anomalies in the Northern Hemisphere winter N91-23668

NOSE CONES
Oxidation resistant carbon/carbon materials
[REPT-911-430-105] N91-23251

NOSE WHEELS
Long time measurements of landing gear loads on SAAB SF-340 commuter aircraft
[FFA-TN-1990-53] N91-23138

NOTCH TESTS
Chevron-notched, flexure tests for measuring the elevated temperature fracture resistance of structural ceramics
[DE91-009117] N91-23310

NOZZLE DESIGN
The effect of combustor flow nonuniformity on the performance of hypersonic nozzles N91-23173
The 2-D supersonic nozzle design N91-23176
Development of a quiet supersonic wind tunnel with a cryogenic adaptive nozzle
[NASA-CR-186769] N91-23195

NOZZLE FLOW
Hypersonic Combined Cycle Propulsion
[AGARD-CP-479] N91-23147
Viscous three-dimensional analyses for nozzles for hypersonic propulsion N91-23175
Vortex system evolution in 2- and 3-D swept trailing edge flows
[AD-A232692] N91-23453

NOZZLE GEOMETRY
The 2-D supersonic nozzle design N91-23176

NUCLEAR BINDING ENERGY
Magneto-optical properties of quantum wells with arbitrary potential profiles
[AD-A232037] N91-23897

NUCLEAR FUELS
Mars manned fusion spaceship
[NASA-CR-188215] N91-23232
Measurement control for calorimetric assay
[DE91-009445] N91-23274

NUCLEAR FUSION
Mars manned fusion spaceship
[NASA-CR-188215] N91-23232
Computing for magnetic fusion energy research: The next five years
[DE91-010686] N91-23921
Fusion technology development
[DE91-010697] N91-23923

NUCLEAR MAGNETIC RESONANCE
Absolute calibration in vivo measurement systems
[DE91-009719] N91-23692
Hepatic metabolism of perfluorinated carboxylic acids: A nuclear magnetic resonance investigation
[AD-A232033] N91-23706

NUCLEAR MODELS
Microscopic heavy-ion theory
[DE91-010739] N91-23869

NUCLEAR PHYSICS
A guide to experimental elementary particle physics literature, 1985-1989
[DE91-010209] N91-23856
Intermediate/high energy nuclear physics
[DE91-010702] N91-23868
The birth of the 'strange' particle physics
[NOTA-INTERNA-958] N91-23875

NUCLEAR POWER PLANTS
A first-principles generic methodology for representing the knowledge base of a process diagnostic expert system
[DE90-017693] N91-23520
Fatigue evaluation of piping systems with limited vibration test data
[DE91-007167] N91-23543
Lateral dispersion of radioactive release. Draft for comments
[CEMA-86/17] N91-23621

NUCLEAR PROPULSION
Mars manned fusion spaceship
[NASA-CR-188215] N91-23232
Gas core reactors for direct nuclear propulsion
[DE91-010050] N91-23884

NUCLEAR REACTIONS
Light particle emissions in heavy ion reactions
[DE91-010746] N91-23871

NUCLEAR REACTORS
Ion beam testing of the Aerolor X-point dump plate for the Joint European Torus
[DE91-010719] N91-23245
Pressure dynamics modeling for the design of the advanced neutron source reactor
[DE91-007860] N91-23883
Intense light-ion beams provide a robust, common-driver path towards ignition, gain and commercial fusion energy
[DE91-010584] N91-23919
Fusion technology development
[DE91-010697] N91-23923

NUCLEASE
Molecular studies of cytokine induction
[AD-A232221] N91-23707

NUCLEATION
Transport and nucleation processes in the vapor growth of diamond
[AD-A232135] N91-23953

NUCLEI (NUCLEAR PHYSICS)
Intermediate/high energy nuclear physics
[DE91-010702] N91-23868

NUCLEON-NUCLEON INTERACTIONS
Calculation of cross sections for binary reactions between heavy ion projectiles and heavy actinide targets
[DE91-010222] N91-23882

NUCLEONS
The Sudbury Neutrino Observatory project and the Kamiokande 2 project
[DE91-010641] N91-23863

NULL HYPOTHESIS
The Black Widow pulsar PSR 1957+20: A potential VHE gamma-ray source N91-24038

NUMERICAL ANALYSIS
Hypersonic numerical simulation: Problems and perspectives. Hypersonic vehicles and numerical simulation in structural analysis
[REPT-911-111-106] N91-23091
Efficient numerical techniques for the analysis of complex microstrip-antennas and microstrip arrays
[DLR-FB-90-53] N91-23357
Time-domain analysis of one-dimensional electromagnetic scattering by Lossy media
[FEL-90-A211] N91-23358
Benchmarking numerical predictions with force and moment measurements on slender, supercavitating bodies
[DE91-007066] N91-23432
Hierarchic modeling of plates
[AD-A232754] N91-23560
The problem of plate modeling theoretical and computational results
[AD-A232756] N91-23562

NUMERICAL CONTROL
Unsteady flow structure from swept edges subjected to controlled motion
[AD-A232714] N91-23094
An on-line computerized system for blood-flow measurements N91-23834

NUMERICAL FLOW VISUALIZATION
Numerical simulation of transition in three dimensional boundary layers
[ESA-TT-1203] N91-23442

NUMERICAL INTEGRATION
On 2+1-dimensional nonlinear integrable systems of Loewner-type
[MATHS-REPT-A-140] N91-23813
A method for solving Poisson's equation in geophysical and astrophysical plasma
[AERONOMICA-ACTA-A-357-1990] N91-23925

NUMERICAL STABILITY
Real-time simulation of constrained dynamic systems N91-23189

NUMERICAL WEATHER FORECASTING
Design of an enhanced global spectral model
[AD-A232123] N91-23655
Assimilation of ERBE data with nonlinear programming technique to improve cloud cover diagnosis N91-23663
Initialization of cloud and radiation in the Florida State University global spectral model
[AD-A232425] N91-23682

NYSTAGMUS
Otolith responses in man during parabolic flight
[IZF-1990-A-32] N91-23703

O

OBJECT PROGRAMS
Object oriented programming in MMI: A software tool for analysis and planification of a radar imaging mission N91-23589

OBLIQUE SHOCK WAVES
Interferometric investigation of supersonic flow fields with shock-shock interactions N91-23082
Analytical and experimental investigations of the oblique detonation wave engine concept N91-23169
Non-linear interaction of a detonation/vorticity wave [NASA-CR-187550] N91-23434

OBSERVATORIES
Ionosphere 1984, volume 72 [ISSN-0211-5166] N91-23649
Ionosphere 1985, volume 73 [ISSN-0211-5166] N91-23650

OBSTACLE AVOIDANCE
Articulation of spatial robots N91-23504
Obstacle avoidance for redundant robots using configuration control [NASA-CASE-NPO-17852-1-CU] N91-23783

OCEAN BOTTOM
Near-equatorial deep circulation in the Indian and Pacific oceans [AD-A232635] N91-23691

OCEAN CURRENTS
Extraction of mesoscale ocean currents information from Geosat altimeter data N91-23594
Validation requirements for the Topex/Poseidon altimeter mission N91-23602
Near-equatorial deep circulation in the Indian and Pacific oceans [AD-A232635] N91-23691

OCEAN DYNAMICS
Ocean modeling for climate study N91-23592
Extraction of mesoscale ocean currents information from Geosat altimeter data N91-23594

OCEAN MODELS
Ocean modeling for climate study N91-23592
Satellite data utilization in ocean circulation models N91-23593
Satellite data utilization for modeling sea states N91-23598

OCEAN SURFACE
Extraction of mesoscale ocean currents information from Geosat altimeter data N91-23594
Primary ocean production: Carbon and particle flux N91-23596
Energy exchange study at the ocean surface by satellite observation N91-23597

OCEAN TEMPERATURE
Infrared and visible studies of Pakistan portion of Arabian Sea using INSAT geostationary satellite N91-23611
The application of equilibrium climate models to questions of glaciation at high latitudes N91-23669

OCEANOGRAPHY
Space and Sea [ESA-SP-312] N91-23563
Ocean modeling for climate study N91-23592
Sea level and satellite techniques N91-23595
Primary ocean production: Carbon and particle flux N91-23596
Using satellite remote sensing imagery for marginal ice zone research in the ARCTEMIZ project N91-23600
Collection and processing of oceanographic data at CLS N91-23603
Signal detection of MERIS in oceanographic applications N91-23605

OCEANS
Arctic remote autonomous measurement platform post CEAREX engineering report [AD-A232843] N91-23471
The annual march of convection, sea surface temperature, and surface winds in the tropics N91-23667
Parallel-processor-based Gaussian beam tracer for use in ocean acoustic tomography [AD-A232420] N91-23690

OILS
Quantifying oil filtration effects on bearing life [NASA-TM-104350] N91-23512

OLIGOMERS
Atrane and quadroped frameworks in early transition metal and silicon GRO stereochemistry: Monomers and oligomers [AD-A232837] N91-23331

ON-LINE SYSTEMS
An on-line computerized system for blood-flow measurements N91-23834

ONBOARD DATA PROCESSING
Mechanical component diagnostic system [AD-A232126] N91-23146

ONE DIMENSIONAL FLOW
A one dimensional wind profile model with stability and eddy viscosity estimations from sodar data [DM-56] N91-23680

OPERATING SYSTEMS (COMPUTERS)
Decentralized computing technology for fault-tolerant, survivable C3I systems. Volume 3: System/subsystem specification [AD-A232291] N91-23371
CESAR operating system [FFI-91/7002] N91-23754
Transportable Applications Environment (TAE) Plus: A NASA user interface development and management system N91-24048

OPERATOR PERFORMANCE
Shape-memory alloy tactical feedback actuator, phase 1 [AD-A231389] N91-23289
Quantifying performance degradation due to the human-machine interface of telemanipulators [AD-A232814] N91-23723

OPERATORS (MATHEMATICS)
Tripod operators for the interpretation of range images [AD-A232631] N91-23344

OPERATORS (PERSONNEL)
Towards real-time GOMS [AD-A232028] N91-23763

OPTICAL COMMUNICATION
The TurboLAN project. Phase 1: Protocol choices for high speed local area networks. Phase 2: TurboLAN Intelligent Network Adapter Card, (TINAC) architecture [NASA-CR-188175] N91-23776
SZ series GaAs super high-speed logic gate: Optimum choice. High tech; high speed; high quality [AD-A232819] N91-23962
Optical communication for space missions N91-24070
Optical shutter switching matrix N91-24071

OPTICAL COMPUTERS
Analysis of polarizing optical systems for digital optical computing with symmetric self electrooptic devices [AD-A232768] N91-23906

OPTICAL CORRELATORS
Intelligent vision system for autonomous vehicle operations N91-24046

OPTICAL DATA PROCESSING
Pulse compression of 100 picosecond pulses at 1.319 microns [AD-A232552] N91-23901
Analysis of polarizing optical systems for digital optical computing with symmetric self electrooptic devices [AD-A232768] N91-23906

OPTICAL DATA STORAGE MATERIALS
Ultra-dense optical mass storage [AD-A232767] N91-23905

OPTICAL DISKS
The reduced version of the DERF 2 data set on a WORM optical disk [DM-54] N91-23991
Laser optical disk position encoder with active heads N91-24079

OPTICAL EQUIPMENT
Metal thin-film optical polarizers for space applications, phase 2 [NASA-CR-188202] N91-23891
Photonic materials and devices for optical information processing and computing applications [AD-A232771] N91-23907
Optical communication for space missions N91-24070

OPTICAL FIBERS
Development and utilization of new diagnostics for dense-phase pneumatic transport [DE91-008947] N91-23339
Fiber optic sensors for the military [AD-A232100] N91-23898

OPTICAL MATERIALS
Metal thin-film optical polarizers for space applications, phase 2 [NASA-CR-188202] N91-23891

OPTICAL MEASUREMENT
Atmospheric optical turbulence measurements taken at Anderson Mesa, Flagstaff, Arizona between 13-19 November 1989 [AD-A232222] N91-23656

OPTICAL MEASURING INSTRUMENTS
Design of a twenty-element long focal length zoom lens [DE91-010770] N91-23894

OPTICAL MEMORY (DATA STORAGE)
Ultra-dense optical mass storage [AD-A232767] N91-23905

OPTICAL PATHS
Non-mechanical optical path switching and its application to dual beam spectroscopy including gas filter correlation radiometry [NASA-CASE-LAR-14588-1-CU] N91-23889

OPTICAL POLARIZATION
Metal thin-film optical polarizers for space applications, phase 2 [NASA-CR-188202] N91-23891

OPTICAL PROPERTIES
Optical and mechanical properties of mixed silver halide crystals N91-23837
Real time pre-detection dynamic range compression [NASA-CASE-NPO-18098-1-CU] N91-23890
Liquid-crystal characterization using the Z-scan technique [RSRE-MEMO-4451] N91-23949

OPTICAL RADAR
Simulation of a backscatter lidar system [DLR-FB-90-50] N91-23355
Determination of the temperature profile of the troposphere with a two frequency lidar [EXAMENARBEIT-8] N91-23653
Iron density measurements in polar atmosphere [BONN-IR-90-53] N91-23654

OPTICAL SCANNERS
Remote sensing performances [REPT-911-440-101] N91-23615

OPTICAL SWITCHING
Spatial dynamics of picosecond CO2 laser pulses produced by optical switching in Ge [DE91-010368] N91-23476
Non-mechanical optical path switching and its application to dual beam spectroscopy including gas filter correlation radiometry [NASA-CASE-LAR-14588-1-CU] N91-23889
Optical shutter switching matrix N91-24071

OPTICAL TRACKING
Aero-optics measurement system for the AEDC aero-optics test facility [AD-A232852] N91-23908

OPTICAL TRANSITION
Structural and electronic properties of the ordered ternary 3-5 semiconductors N91-23936

OPTICAL WAVEGUIDES
Strained quantum well leaky-mode diode laser arrays [DE91-009982] N91-23477

OPTIMAL CONTROL
H-infinity approach to manipulator control N91-23495
Worst-case design of optimal controllers over a finite horizon [AD-A232353] N91-23797
Approximation methods for the identification and control of distributed parameter systems with applications to flexible structures [AD-A232805] N91-23801
A simple solution to the singular linear minimum-variance estimation problem [IAITIC-87-1002-REV] N91-23804
Molecular dynamics simulator for optimal control of molecular motion [AD-A232801] N91-23881

OPTIMIZATION
Integrated multidisciplinary optimization of actively controlled fiber composite wings N91-23190
Spatial dynamics of picosecond CO2 laser pulses produced by optical switching in Ge [DE91-010368] N91-23476
Maximum life spur gear design [NASA-TM-104361] N91-23514
Characteristics and performance of an operational windscatterometer N91-23607
Assimilation of ERBE data with nonlinear programming technique to improve cloud cover diagnosis N91-23663
Duality methods for infinite dimensional optimization problems [AD-A232605] N91-23772
Applications of neural networks to process control and modeling [DE91-007389] N91-23784
Two dimensional optimization of smoothing properties of multistage schemes applied to hyperbolic equations [VKI-TN-173] N91-23807
Plasma torches dimensioning and optimization [REPT-911-430-111] N91-23926

OPTOELECTRONIC DEVICES
Electronic GaAs-on-silicon material for advanced high-speed optoelectronic devices [AD-A232088] N91-23399
Photoresponse studies of ion-damaged germanium for optoelectronic switch applications [AD-A232091] N91-23400
Analysis of polarizing optical systems for digital optical computing with symmetric self electrooptic devices [AD-A232768] N91-23906

ORBIT CALCULATION
Precision orbit determination of global positioning system satellites N91-23202
ORBITAL ASSEMBLY
Astromag phase A assembly and servicing operations report
[NASA-CR-186262] N91-23206
EVA/robotics integration for Space Station Freedom N91-23583
ORBITAL MECHANICS
Satellite maneuver evaluation tool
[AD-A232016] N91-23226
ORBITAL SERVICING
Astromag phase A assembly and servicing operations report
[NASA-CR-186262] N91-23206
Space and telescience robotics: Development of concepts and reference technologies for teledetection and robotics in extreme environments N91-23580
ORDER-DISORDER TRANSFORMATIONS
Order and disorder in metallic alloys
[DE91-009120] N91-23292
ORGANOMETALLIC COMPOUNDS
Synthesis and characterization of indium-arsenic compounds containing a four-membered In-Ad-In-As or In-As-In-Cl ring: Crystal structures of ((Me3SiCH2)2 InAs(SiMe3)2)2 and (Me3SiCH2)2 InAs(SiMe3)2 In(CH2SiMe3)2Cl
[AD-A232368] N91-23956
ORTHOGONAL FUNCTIONS
The transient response of heavily fluid-loaded elastic plates and cylindrical shells N91-23528
OSCILLATIONS
A new asymptotic theory for the periodically forced laser
[AD-A232633] N91-23486
Energy partition of free Rossby waves in global atmospheric oscillations
[MITT-74] N91-23648
OSCILLATOR STRENGTHS
Magneto-optical properties of quantum wells with arbitrary potential profiles
[AD-A232037] N91-23897
OSCILLATORS
A controlled master frequency oscillator for the SSC low energy booster
[DE91-011004] N91-23391
High-power performance of a copper laser pumped dye master-oscillator-power-amplifier chain
[DE91-010460] N91-23478
OTOLITH ORGANS
Otolith responses in man during parabolic flight
[IZF-1990-A-32] N91-23703
OUTLIERS (STATISTICS)
Detection of outliers and robust estimation using fuzzy clustering
[RR-822-M] N91-23823
OXIDATION
Bromination of carbon fibers and carbon-carbon composites N91-23240
Carbon/carbon inox thermostructural composites: Mechanical and tectonic behavior of anti-oxidation protection
[REPT-911-430-115] N91-23257
MHD channel gas-side element erosion-corrosion studies
[DE91-008561] N91-23911
OXIDATION RESISTANCE
Bromination of carbon fibers and carbon-carbon composites N91-23240
Carbon-carbon material with oxidation protection
[REPT-911-430-103] N91-23249
Oxidation resistant carbon/carbon materials
[REPT-911-430-105] N91-23251
Nondestructive inspection for carbon-carbon with adapted coating for oxidation
[REPT-911-430-106] N91-23252
Investigations of oxidation protection systems for carbon-carbon composites formed by chemical vapor deposition and plasma-assisted chemical vapor deposition techniques
[AD-A232800] N91-23269
Oxidation studies of fluorine containing diamond films
[AD-A232696] N91-23328
A conformal oxidation-resistant, plasma-polymerized coating N91-24063
OXIDATION-REDUCTION REACTIONS
Electrochemical parameterization of rhenium redox couples
[AD-A232043] N91-23279
OXIDE FILMS
Optimization of transparent and reflecting electrodes for amorphous silicon solar cells
[DE91-002132] N91-23618
OXIDES
The effect of post-cure and antimony trioxide addition on the glass transition of polyester and vinyl ester resin systems
[AD-A232523] N91-23325
OXYGEN
Static feed water electrolysis subsystem development
[NASA-CASE-MSC-21577-1-SB] N91-23271
AFRRI reports, October - December 1990
[AD-A232236] N91-23283
Structural studies of manganese and halide in the photosynthetic oxygen evolving complex
[DE91-009071] N91-23698
OXYGEN ATOMS
A conformal oxidation-resistant, plasma-polymerized coating N91-24063
OXYGEN BREATHING
A KO2 rebreather for EVA denitrogenation procedure N91-23588
OXYGEN IONS
Point defect effects on hot corrosion of zirconia-based coatings
[AD-A232662] N91-23326
Thermal ion upwelling in the high-altitude ionosphere
[AD-A232372] N91-23657
OXYGEN PRODUCTION
Oxygen production using solid-state zirconia electrolyte technology N91-24059
OXYGEN SUPPLY EQUIPMENT
A test of the American Safety Flight Systems, Inc. prebreather/portable oxygen system
[AD-A232723] N91-23100
OZONE
High-precision Fourier transform spectroscopy of atmospheric molecules N91-23637
Observational study of the above-inversion structure and marine stratocumulus cloud clearing episodes during FIRE N91-23666
OZONOSPHERE
High-precision Fourier transform spectroscopy of atmospheric molecules N91-23637

P

PACIFIC OCEAN
Near-equatorial deep circulation in the Indian and Pacific oceans
[AD-A232635] N91-23691
PACKET SWITCHING
Design and implementation of a packet switched routing chip
[AD-A232286] N91-23401
PACKET TRANSMISSION
A study of the end point path geometry in meteor burst systems using a microcomputer signal logger N91-24012
PACKETS (COMMUNICATION)
Design and implementation of a packet switched routing chip
[AD-A232286] N91-23401
A study of the end point path geometry in meteor burst systems using a microcomputer signal logger N91-24012
Fiber Optic Tactical Local Network (FOTLAN) N91-24072
PAIR PRODUCTION
Microscopic heavy-ion theory
[DE91-010739] N91-23869
PANEL METHOD (FLUID DYNAMICS)
A vortex panel method for calculating aircraft downwash on parachute trajectories
[DE91-009764] N91-23085
The propagation of acoustic disturbances in the transonic flow fields of wings
[ESA-TT-1126] N91-23854
PANELS
Flame-retardant composite materials N91-24064
PARABOLIC FLIGHT
Test on parabolic flights for stowage in weightlessness N91-23578
Otolith responses in man during parabolic flight
[IZF-1990-A-32] N91-23703
PARACHUTES
A vortex panel method for calculating aircraft downwash on parachute trajectories
[DE91-009764] N91-23085
PARALLEL COMPUTERS
Modeling speedup in parallel sparse matrix factorization
[DE91-010215] N91-23735
Mapping an adaptable Eigenstructure technique onto the topologix hypercube
[AD-A232032] N91-23764
PARALLEL PROCESSING (COMPUTERS)
Design and implementation of a packet switched routing chip
[AD-A232286] N91-23401
Nonlinear waves in real materials
[AD-A232654] N91-23452
Modeling speedup in parallel sparse matrix factorization
[DE91-010215] N91-23735
The CERBERUS Ver. 02 code: A parallel six-equation thermal-hydraulic-system simulation code
[DE91-010079] N91-23736
Information dynamics of self-programmable matter
[DE91-009954] N91-23740
On the use of genetic algorithms to solve the time-table problem
[REPT-90-060] N91-23752
A method for handling complex Markov models of parallel systems
[RR-826-I] N91-23778
Statistical process allocation in a parallel processing architecture
[RR-833-I] N91-23779
Generalization of the FP2 parallel language by means of net theory
[RR-832-I-IMAG-99-LIFIA] N91-23780
PARALLEL PROGRAMMING
Generalization of the FP2 parallel language by means of net theory
[RR-832-I-IMAG-99-LIFIA] N91-23780
PARAMETER IDENTIFICATION
System modeling and identification of flexible structures N91-23531
A particular linear model of variance components
[RR-827-M] N91-23824
Nonparametric estimation in change-point hazard rate models for censored data: A counting process approach
[RR-836-I-AND-M] N91-23825
PARAMETERIZATION
Parametric modeling and estimation of pulse propagation on microwave integrated circuit interconnections
[AD-A232465] N91-23404
Real time analysis systems of the physical parameters of the environment and the state of a human organism for a long term exposure at different gas mixtures and pressure up to 100 bar N91-23568
PARAMETRIC AMPLIFIERS
Optical parametric oscillators pumped by excimer lasers N91-23473
PARTIAL DIFFERENTIAL EQUATIONS
Hierarchic modeling of plates
[AD-A232754] N91-23560
Parallelizing the spectral transform method, part 1
[DE91-010453] N91-23805
PARTICLE ACCELERATOR TARGETS
Shock characterization of epoxy: Forty-two volume percent glass microballoons
[DE91-009616] N91-23314
Light particle emissions in heavy ion reactions
[DE91-010746] N91-23871
PARTICLE ACCELERATORS
Intense light-ion beams provide a robust, common-driver path towards ignition, gain and commercial fusion energy
[DE91-010584] N91-23919
PARTICLE BEAMS
Intense light-ion beams provide a robust, common-driver path towards ignition, gain and commercial fusion energy
[DE91-010584] N91-23919
PARTICLE COLLISIONS
Experiments on Frank-Hertz setup
[NOTA-INTERNA-961] N91-23876
PARTICLE EMISSION
Light particle emissions in heavy ion reactions
[DE91-010746] N91-23871
PARTICLE IN CELL TECHNIQUE
Numerical modeling of turbulent dispersion around structures using a particle-in-cell method
[DE91-009757] N91-23426
PARTICLE INTERACTIONS
Computed secondary-particle energy spectra following nonelastic neutron interactions with C-12 for E(n) between 15 and 60 MeV: Comparisons of results from two calculational methods
[DE91-010454] N91-23864
The birth of the 'strange' particle physics
[NOTA-INTERNA-958] N91-23875
Particle physics experiments, 1990
[RAL-91-001] N91-23877
Quantum extension of Child-Langmuir law
[AD-A232407] N91-23878

PARTICLE MASS
A proposed search for dark-matter axions in the 0.6-16 micro-eV range
[NASA-CR-188173] N91-24015
PARTICLE MOTION
Approximating the dynamic response of strain-hardening structures
[DE91-006392] N91-23534
Theoretical and numerical study of anomalous turbulent transport in plasmas
[AD-A232688] N91-23931
PARTICLE PRODUCTION
Recent results and future prospects for the polarized beam at Fermilab
[DE91-010590] N91-23862
PARTICLE SIZE DISTRIBUTION
Automatic particle sizing from rocket motor holograms
[AD-A232553] N91-23236
Sensitivity of numerical dispersion modeling to explosive source parameters
[DE91-009476] N91-23631
PARTICLE THEORY
Microscopic heavy-ion theory
[DE91-010739] N91-23869
Research in particle theory
[DE91-010749] N91-23872
Particle physics experiments, 1990
[RAL-91-001] N91-23877
PARTICLE TRACKS
Density channel tracking studies on Pulserad
[AD-A232649] N91-23888
PARTICLE TRAJECTORIES
An experimental method for studying combustion of an unsupported fuel droplet at reduced gravity N91-23273
PARTICLES
Particle-fluid two-phase flow modeling
[DE91-010102] N91-23415
PARTICULATES
Mechanics/heat-transfer relation for particulate materials
[DE91-008356] N91-23424
Forecasting atmospheric particulate sulfur concentrations using national weather service synoptic charts
[AD-A231634] N91-23622
PARTONS
Microscopic heavy-ion theory
[DE91-010739] N91-23869
PATENT APPLICATIONS
Energy dissipator
[NASA-CASE-MSC-21555-1] N91-23492
PATTERN RECOGNITION
Tripod operators for the interpretation of range images
[AD-A232631] N91-23344
Robot self-location in unknown environments
[DE91-010450] N91-23505
A survey of decision tree classifier methodology
[NASA-CR-188208] N91-23806
Evaluation of a ferroelectric liquid crystal spatial light modulator
[AD-A232117] N91-23899
Nonlinear real-time optical signal processing
[AD-A232689] N91-23909
PATTERN REGISTRATION
Digital data registration and differencing compression system
[NASA-CASE-SSC-00010-1] N91-23976
PAVEMENTS
Literature review on geotextiles to improve pavements for general aviation airports
[AD-A232871] N91-23199
PAYLOAD STATIONS
Astromag phase A assembly and servicing operations report
[NASA-CR-186262] N91-23206
PAYLOADS
Communication and broadcasting satellites payload reconfiguration technologies
[REPT-911-440-102] N91-23218
The Eutelsat 2 programme
[REPT-911-440-108] N91-23223
Payload related crew operations: From past missions to Columbus N91-23569
Remote sensing performances
[REPT-911-440-101] N91-23615
PECULIAR GALAXIES
Recent star formation and the galaxy collisions in NGC 520 N91-24021
PENETRATION
Energy-efficient penetration of targets
[AD-A232227] N91-23518
PENINSULAS
SWANEA (Southwest Asia-Northeast Africa): A climatological study. Volume 2: The Middle East Peninsula
[AD-A232776] N91-23684
PENTANONE
Dissolution of Poly(p-hydroxystyrene): Molecular weight effects
[AD-A232155] N91-23323
PERCEPTION
Transition space
[AD-A231404] N91-23732
PERFORMANCE
Strategic missiles: Uncertainties persist in the Advanced Cruise Missile (ACM) program
[AD-A232058] N91-23142
PERFORMANCE PREDICTION
Building a generalized distributed system model N91-23971
PERFORMANCE TESTS
Materials and structure for Hermes
[REPT-911-430-117] N91-23258
High temperature deformation processes and strengthening mechanisms in intermetallic particulate composites
[AD-A232737] N91-23267
High temperature membranes for H2S and SO2 separations
[DE91-008534] N91-23275
Characterization of active materials and electrodes for battery R and D
[DE91-010758] N91-23390
Ship roll stabilization and human performance
[AD-A232721] N91-23721
Photonic materials and devices for optical information processing and computing applications
[AD-A232771] N91-23907
Aero-optics measurement system for the AEDC aero-optics test facility
[AD-A232852] N91-23908
Plasma on a foundry cupola
[REPT-911-430-125] N91-23929
Optical communication for space missions N91-24070
PERIODIC VARIATIONS
Saturn's F ring: Imaging and simulation N91-24032
PERMITTIVITY
A transmission line method for the measurement of microwave permittivity and permeability
[RSRE-MEMO-4450] N91-23394
PERSONAL COMPUTERS
Use of personal computers in performing a linear modal analysis of a large finite-element model
[DE91-010112] N91-23541
Scientific visualization software for your PC: Free and available now
[DE91-010156] N91-23744
User interface to an ICAI system that teaches discrete math
[AD-A232693] N91-23799
The reduced version of the DERF 2 data set on a WORM optical disk
[DM-54] N91-23991
PERSONALITY
Individual differences underlying pilot cockpit error
[DOT/FAA/RD-91/13] N91-23710
PERSONNEL DEVELOPMENT
Intelligent computer-aided training and tutoring N91-24042
PERSONNEL SELECTION
Subsea habitats and space simulation N91-23567
PERTURBATION
Passive laminar flow control of crossflow vorticity
[NASA-CASE-LAR-13563-1] N91-23410
PERTURBATION THEORY
On standard forms for transport equations and fluxes, part 2
[DE91-010421] N91-23912
PETRI NETS
Designing logic controllers with Petri nets
[REPT-90-029] N91-23747
An incremental approach to logic controllers design with Petri nets
[REPT-90-030] N91-23748
Timed high-level nets
[REPT-90-050] N91-23750
Generalization of the FP2 parallel language by means of net theory
[RR-832-I-IMAG-99-LIFIA] N91-23780
PHASE CONJUGATION
Theory of novel nonlinear optics
[AD-A232659] N91-23903
PHASE DIAGRAMS
Solid-phase equilibria for Metal-Silicon-Oxygen ternary systems. Part 2: Sc, Y, and La
[AD-A232150] N91-23281
PHASE LOCKED SYSTEMS
Study of phase-locked diode laser array and DFB/DBR surface emitting laser diode N91-23474
Broad area distributed gain, distributed index profile GaAlAs semiconductor laser diodes
[AD-A232332] N91-23483
Building a generalized distributed system model N91-23971
PHASE SHIFT
A 30 GHz monolithic receive module
[NASA-CR-187085] N91-23346
Spatial dynamics of picosecond CO2 laser pulses produced by optical switching in Ge
[DE91-010368] N91-23476
PHASE SHIFT CIRCUITS
A 30 GHz monolithic receive module
[NASA-CR-187085] N91-23346
PHASE SHIFT KEYING
Error control coding for multi-frequency modulation
[AD-A232421] N91-23374
PHASE TRANSFORMATIONS
Phase transitions at liquid solid interfaces: Pade approximant for adsorption isotherms and voltammograms
[AD-A232623] N91-23285
Phase equilibria and solidification of Al-Li and Al-Li-Cu alloys N91-23290
Modeling second-phase formation during rapid resolidification of stainless steel alloys
[DE91-008567] N91-23291
Phase transformations and microstructural evolution in aged Mn-Cu-based alloys
[AD-A232473] N91-23305
First principles calculation of the crystal structures in the 4d transition metals N91-23835
Monte Carlo simulation of supercritical solutions in the grand canonical ensemble
[DE91-009152] N91-23859
A cosmic superfluid phase
[NASA-CR-188171] N91-24016
PHASE VELOCITY
Modeling second-phase formation during rapid resolidification of stainless steel alloys
[DE91-008567] N91-23291
PHASED ARRAYS
System-Level Integrated Circuit (SLIC) development for phased array antenna applications
[NASA-TM-104392] N91-23354
Study of phase-locked diode laser array and DFB/DBR surface emitting laser diode N91-23474
PHENOMENOLOGY
Phenomenological aspects of scalar fields in astrophysics, cosmology and particle physics N91-24014
PHENYLS
Poly(1,3,4-oxadiazoles) via aromatic nucleophilic displacement
[NASA-CASE-LAR-14427-1] N91-23237
Hardening mechanisms and analysis of the structure of the TGDDM/DDS epoxy resin system
[ESA-TT-1202] N91-23319
PHONETICS
On a phonetic and structural encoding of Chinese characters in Chinese texts
[RR-835-I] N91-23989
PHOTOCHEMICAL REACTIONS
An expanding grid photochemical model for visibility applications
[DE91-009947] N91-23630
PHOTOCONDUCTIVITY
Bulletin of the Israel Physical Society, volume 33, 1987 Annual Meeting 1987: Program and Abstracts
[ITN-89-85012] N91-23832
High power light activated semiconductor switches with sub-nanosecond rise time
[DE91-009250] N91-23939
PHOTOELASTICITY
Two-channel spectroscopic polarization modulation ellipsometry
[DE91-010131] N91-23893
PHOTOELECTRIC EMISSION
Re-analysis of photoemission data for CuO: Revision of the configuration-energy scheme for cuprate materials
[DE91-009952] N91-23296
PHOTOELECTROCHEMISTRY
Material processing with hydrogen and carbon monoxide on Mars
[NASA-TM-104405] N91-23616
PHOTOGRAPHIC FILM
Quantitative film radiography
[DE91-009718] N91-23463
PHOTOIONIZATION
Mass resolved resonance ionization spectroscopy of combustion radicals
[DE91-010603] N91-23276
Few-body problems, electron-correlation effects, and beyond
[DE91-010030] N91-23857

A method for solving Poisson's equation in geophysical and astrophysical plasma
[AERONOMICA-ACTA-A-357-1990] N91-23925
PHOTOLITHOGRAPHY
Wavelength independent optical lithography and microscopy
[AD-A232036] N91-23896
PHOTOLYSIS
Low-temperature laser-induced selective area growth of compound semiconductor N91-23932
PHOTOMETRY
Applications of speckle interferometry and speckle photometry to the Hyades cluster N91-24001
A near-infrared search for brown dwarfs in the Pleiades N91-24011
PHOTOMULTIPLIER TUBES
The Sudbury Neutrino Observatory project and the Kamiokande 2 project
[DE91-010641] N91-23863
PHOTONS
Multiphoton detection techniques for F and F2
[AD-A232641] N91-23286
Hyperspectral imagery: What is it, what can it do
[AD-A231164] N91-23610
Photonic materials and devices for optical information processing and computing applications
[AD-A232771] N91-23907
PHOTOSENSITIVITY
Photoresponse studies of ion-damaged germanium for optoelectronic switch applications
[AD-A232091] N91-23400
PHOTOSYNTHESIS
Excited state structure, energy and electron transfer dynamics of photosynthetic reaction centers: A hole burning study
[DE91-010181] N91-23693
PHOTOVOLTAIC CONVERSION
PV concentrators today and tomorrow
[DE91-010577] N91-23619
PHYSICAL CHEMISTRY
Computer modeling of soot formation comparing free radical and ionic mechanisms
[AD-A232820] N91-23287
Cryomagmatism in the outer solar system N91-24019
PHYSICAL FACTORS
A complex systems approach to metallic fracture surface characterization
[AD-A232546] N91-23556
Real time analysis systems of the physical parameters of the environment and the state of a human organism for a long term exposure at different gas mixtures and pressure up to 100 bar N91-23568
PHYSICAL OPTICS
Calculation of near-field scattering using the plane-wave formulation and the physical optics method
[FEL-90-B215] N91-23360
Calculation of electromagnetic fields in the near-field region of a moving scattering object
[FEL-90-B216] N91-23361
PHYSICAL WORK
Heat strain and work tolerance times with varying levels of Canadian Forces NBC protective clothing, ambient temperature, physical work intensity, and work/rest schedules
[AD-A232653] N91-23720
PHYSIOLOGICAL RESPONSES
Otolith responses in man during parabolic flight
[IZF-1990-A-32] N91-23703
Transcapillary fluid shifts in head and neck tissues during and after simulated microgravity
[NASA-TM-103847] N91-23704
Strategies to sustain and enhance performance in stressful environments
[AD-A232698] N91-23714
PHYSIOLOGY
Absolute calibration in vivo measurement systems
[DE91-009719] N91-23692
PHYTOTRONS
Protein crystal growth tray assembly
[NASA-CASE-MFS-28507-1] N91-23933
PICOSECOND PULSES
Parametric modeling and estimation of pulse propagation on microwave integrated circuit interconnections
[AD-A232465] N91-23404
Spatial dynamics of picosecond CO2 laser pulses produced by optical switching in Ge
[DE91-010368] N91-23476
Pulse compression of 100 picosecond pulses at 1.319 microns
[AD-A232552] N91-23901
PILOT ERROR
Individual differences underlying pilot cockpit error
[DOT/FAA/RD-91/13] N91-23710
PILOT INDUCED OSCILLATION
The development of alternate criteria for FBW handling qualities N91-23113
Metrics for roll response flying qualities N91-23118
PILOT PERFORMANCE
Estimation of pilot ratings via pilot modeling N91-23121
Evaluation techniques for highly augmented aircraft
[DLR-FB-90-35] N91-23191
Strategies to sustain and enhance performance in stressful environments
[AD-A232698] N91-23714
PILOTLESS AIRCRAFT
Design and construction of a composite airframe for UAV research
[AD-A232422] N91-23143
PINS
An experimental and finite element investigation into the nonlinear material behavior of pin-loaded composite laminates
[AD-A232098] N91-23263
PIPE FLOW
Diffusive, electrostatic concentration of disintegration products of inert gases in vortex flow
[AD-A232876] N91-23457
PIPELINES
Interfacial characteristic measurements in horizontal bubbly two-phase flow
[DE91-009803] N91-23427
PIPES (TUBES)
A theory for fluidelastic instability of tube-support-plate inactive modes
[DE91-009676] N91-23538
Fatigue evaluation of piping systems with limited vibration test data
[DE91-007167] N91-23543
Linear bending of curved tubes without boundary influence
[ETN-91-99255] N91-23552
PITTING
Localized corrosion of high performance metal alloys in an acid/salt environment N91-24066
PIXELS
Programmable remapper for image processing
[NASA-CASE-MSC-21350-1] N91-23724
PLANAR STRUCTURES
Rapidly solidified metallic alloys with unusual semmetry properties
[AD-A232384] N91-23304
PLANE WAVES
Calculation of near-field scattering using the plane-wave formulation and the physical optics method
[FEL-90-B215] N91-23360
First principles calculation of the crystal structures in the 4d transition metals N91-23835
PLANETARY ATMOSPHERES
Mechanisms of equatorial superrotation: Studies with two-level models N91-23642
PLANETARY COMPOSITION
Composition and distribution of carbonates, sulfates, and hydrates on the Martian surface from earth-based spectroscopy between 3-5 microns N91-24033
PLANETARY EVOLUTION
Saturn's F ring: Imaging and simulation N91-24032
PLANETARY ROTATION
Mechanisms of equatorial superrotation: Studies with two-level models N91-23642
PLANETARY WAVES
Models of planetary wave propagation in the middle atmosphere N91-23639
Energy partition of free Rossby waves in global atmospheric oscillations
[MITT-74] N91-23648
PLANTS (BOTANY)
Excited state structure, energy and electron transfer dynamics of photosynthetic reaction centers: A hole burning study
[DE91-010181] N91-23693
PLASMA ACCELERATORS
Echo 7: Magnetospheric properties determined by artificial electron beams N91-23644
PLASMA CONDUCTIVITY
High quality three dimensional electron gases in semiconductors
[AD-A232779] N91-23406
PLASMA CONTROL
ICRF heating on the Burning Plasma Experiment (BPX)
[DE91-010390] N91-23913
Ion confinement and radiation losses in the advanced toroidal facility
[DE91-010382] N91-23916
PLASMA CURRENTS
ICRF heating on the Burning Plasma Experiment (BPX)
[DE91-010390] N91-23913
PLASMA DENSITY
Hydromagnetic wave coupling in the magnetosphere N91-23638
Inversion of chordal data from the ATF torsatron
[DE91-010490] N91-23915
Ion confinement and radiation losses in the advanced toroidal facility
[DE91-010382] N91-23916
Observation and theory of the radar aurora N91-24017
PLASMA DIAGNOSTICS
Comparison of drift wave models with fluctuation data from the interior of the TEXT tokamak
[DE91-010424] N91-23918
Experimental and theoretical research in applied plasma physics
[DE91-010657] N91-23920
Applied plasma physics
[DE91-010696] N91-23922
PLASMA DRIFT
Comparison of drift wave models with fluctuation data from the interior of the TEXT tokamak
[DE91-010424] N91-23918
Theoretical and numerical study of anomalous turbulent transport in plasmas
[AD-A232688] N91-23931
PLASMA ELECTRODES
Plasma torches dimensioning and optimization
[REPT-911-430-111] N91-23926
PLASMA GENERATORS
Materials and structure for Hermes
[REPT-911-430-117] N91-23258
PLASMA HEATING
ICRF heating on the Burning Plasma Experiment (BPX)
[DE91-010390] N91-23913
Fusion technology development
[DE91-010697] N91-23923
PLASMA INTERACTIONS
Theoretical and numerical study of anomalous turbulent transport in plasmas
[AD-A232688] N91-23931
PLASMA OSCILLATIONS
Theory of the new high-temperature superconductors N91-23842
Comparison of drift wave models with fluctuation data from the interior of the TEXT tokamak
[DE91-010424] N91-23918
PLASMA PHYSICS
Experimental and theoretical research in applied plasma physics
[DE91-010657] N91-23920
Applied plasma physics
[DE91-010696] N91-23922
PLASMA POTENTIALS
Heavy ion beam probe measurements of ECH method plasma in the advanced toroidal facility
[DE91-010391] N91-23917
PLASMA PROBES
Comparison of drift wave models with fluctuation data from the interior of the TEXT tokamak
[DE91-010424] N91-23918
PLASMA SPECTRA
Comparison of drift wave models with fluctuation data from the interior of the TEXT tokamak
[DE91-010424] N91-23918
PLASMA SPRAYING
Measurement of particle size, velocity and temperature in the plasma spray coating process
[DE91-006208] N91-23317
Oxidation studies of fluorine containing diamond films
[AD-A232696] N91-23328
PLASMA TEMPERATURE
Temperature measurements of ET plasmas using atomic emission spectroscopy
[AD-A232498] N91-23930
PLASMA TORCHES
Plasma torches dimensioning and optimization
[REPT-911-430-111] N91-23926
Aerospatiale industrial thermal plasmas
[REPT-911-430-113] N91-23927
Aerospatiale industrial thermal plasma activities
[REPT-911-430-122] N91-23928
Plasma on a foundry cupola
[REPT-911-430-125] N91-23929
PLASMA TURBULENCE
Hall effects on anomalous heat, particle and helicity transports through tearing-mode turbulence
[DE91-010730] N91-23924
Theoretical and numerical study of anomalous turbulent transport in plasmas
[AD-A232688] N91-23931
PLASMA WAVES
Echo 7: Magnetospheric properties determined by artificial electron beams N91-23644

PLASMAPAUSE
Theoretical studies of large-scale features of the Earth's mid- to high-latitude ionosphere N91-23641
PLASMAS (PHYSICS)
The effect of realistic antenna geometries on plasma loading predictions
[DE91-010782] N91-23353
Theoretical studies of large-scale features of the Earth's mid- to high-latitude ionosphere N91-23641
Surface electron emission induced by slow multicharged ions
[DE91-010469] N91-23865
Pulsed power performance of the new RLA (Recirculating Linear Accelerator)
[DE91-004723] N91-23885
Density channel tracking studies on Pulserad
[AD-A232649] N91-23888
On standard forms for transport equations and fluxes, part 2
[DE91-010421] N91-23912
Intense light-ion beams provide a robust, common-driver path towards ignition, gain and commercial fusion energy
[DE91-010584] N91-23919
PLASTIC DEFORMATION
High temperature deformation processes and strengthening mechanisms in intermetallic particulate composites
[AD-A232737] N91-23267
PLASTIC PROPERTIES
Stress-density variations in alumina sediments: Effects of polymer chemistry
[DE91-009055] N91-23313
Approximating the dynamic response of strain-hardening structures
[DE91-006392] N91-23534
Application of elastic and elastic-plastic fracture mechanics methods to surface flaws
[NASA-TM-104964] N91-23539
Experience with conventional inelastic analysis procedures in very high temperature applications
[DE91-009937] N91-23545
PLASTICS
Committee draft for an ISO standard on the acquisition and presentation of multipoint data for plastics
[NPL-DMM(A)-24] N91-23320
PLATES (STRUCTURAL MEMBERS)
Hierarchic modeling of plates
[AD-A232754] N91-23560
Accuracy of the Reissner-Mindlin and the (1,1,2) model for the clamped-in plate problem
[AD-A232755] N91-23561
The problem of plate modeling theoretical and computational results
[AD-A232756] N91-23562
The H-P version of the finite element method in the plate modelling problem
[AD-A232246] N91-23816
PLEIADES CLUSTER
A near-infrared search for brown dwarfs in the Pleiades N91-24011
PLOTTING
Auroral boundary index from 1983 to 1990
[AD-A232845] N91-23660
PLUGS
Direct gas injection with glow plug ignition
[PB91-136390] N91-23272
Method of producing a plug type heat flux gauge
[NASA-CASE-LEW-14967-2] N91-23480
PLUMES
Diagnostic measurements on an aluminized propellant plume during spin and nonspin testing
[AD-A232031] N91-23235
Gravity spreading in the dispersion of dense gas plumes
[DE91-010155] N91-23628
An expanding grid photochemical model for visibility applications
[DE91-009947] N91-23630
PLUTONIUM
Measurement control for calorimetric assay
[DE91-009445] N91-23274
PNEUMATIC CONTROL
Unipunch capability study
[DE91-008825] N91-23498
PNEUMATICS
Advanced ice protection systems test in the NASA Lewis icing research tunnel
[NASA-TM-103757] N91-23183
Development and utilization of new diagnostics for dense-phase pneumatic transport
[DE91-008947] N91-23339
PODS (EXTERNAL STORES)
Mathematical techniques for the Performance Oriented Design (POD) tool
[AD-A232092] N91-23767
POINCARE PROBLEM
A new asymptotic theory for the periodically forced laser
[AD-A232633] N91-23486
POINT DEFECTS
Point defect effects on hot corrosion of zirconia-based coatings
[AD-A232662] N91-23326
POISSON DENSITY FUNCTIONS
The limits of the landing process of aircraft
[DLR-FB-90-49] N91-23137
POISSON EQUATION
A method for solving Poisson's equation in geophysical and astrophysical plasma
[AERONOMICA-ACTA-A-357-1990] N91-23925
POLAR REGIONS
Theoretical studies of large-scale features of the Earth's mid- to high-latitude ionosphere N91-23641
The polar wind and ionospheric outflow N91-23645
Iron density measurements in polar atmosphere
[BONN-IR-90-53] N91-23654
Thermal ion upwelling in the high-altitude ionosphere
[AD-A232372] N91-23657
POLARIMETERS
Recent results and future prospects for the polarized beam at Fermilab
[DE91-010590] N91-23862
POLARIMETRY
Polarimetric radar observations of time-variant random targets
[DLR-FB-90-52] N91-23356
The envelopes of RV Tauri variables N91-24008
POLARITY
A non-contacting velocity measurement system
[NASA-CASE-LAR-14466-1] N91-23461
POLARIZED LIGHT
Two-channel spectroscopic polarization modulation ellipsometry
[DE91-010131] N91-23893
POLARIZED RADIATION
Recent results and future prospects for the polarized beam at Fermilab
[DE91-010590] N91-23862
POLARIZERS
Non-mechanical optical path switching and its application to dual beam spectroscopy including gas filter correlation radiometry
[NASA-CASE-LAR-14588-1-CU] N91-23889
Metal thin-film optical polarizers for space applications, phase 2
[NASA-CR-188202] N91-23891
POLARONS
Re-analysis of photoemission data for CuO: Revision of the configuration-energy scheme for cuprate materials
[DE91-009952] N91-23296
POLICIES
Eastern Europe: Please stand by
[PB91-14336] N91-23348
The changing face of the environmental issue
[PB91-138081] N91-23624
Access and efficiency in Reagan-era information policy: A case study of the attempt to privatize the National Technical Information Service N91-23977
POLITICS
The changing face of the environmental issue
[PB91-138081] N91-23624
POLLUTION
Region 10 environmental indicators
[PB91-136580] N91-23623
An expanding grid photochemical model for visibility applications
[DE91-009947] N91-23630
Steps toward environmentally compatible product and process design: A case for green engineering
[AD-A232888] N91-23633
POLLUTION CONTROL
Region 10 environmental indicators
[PB91-136580] N91-23623
POLLUTION MONITORING
Remote sensing of the sea at IROE/CNR N91-23604
Region 10 environmental indicators
[PB91-136580] N91-23623
POLLUTION TRANSPORT
Numerical modeling of turbulent dispersion around structures using a particle-in-cell method
[DE91-009757] N91-23426
POLYCRYSTALS
Development of a micromechanic theory of constitutive relations of polycrystalline solids
[AD-A232697] N91-23559
POLYESTER RESINS
The effect of post-cure and antimony trioxide addition on the glass transition of polyester and vinyl ester resin systems
[AD-A232523] N91-23325
POLYMER CHEMISTRY
Stress-density variations in alumina sediments: Effects of polymer chemistry
[DE91-009055] N91-23313
POLYMER MATRIX COMPOSITES
Rate dependent stress-strain behavior of advanced polymer matrix composites
[NASA-TM-104070] N91-23244
Mechanical characterisation of fibre-matrix interface in ceramic composites by an instrumented indentation test
[REPT-911-430-114] N91-23256
POLYMERIZATION
Poly(1,3,4-oxadiazoles) via aromatic nucleophilic displacement
[NASA-CASE-LAR-14427-1] N91-23237
Chain propagation/step propagation polymerization. Regular thermoplastic elastomers
[AD-A232356] N91-23324
POLYMERS
Solid polymer electrolytes for rechargeable batteries
[DE91-010231] N91-23384
Fundamental studies of electronic packaging materials and structures: Surface and interfaces
[AD-A232336] N91-23403
POLYMETHYL METHACRYLATE
Characterization of the glass transition using a microindenter
[AD-A232154] N91-23282
POLYNOMIALS
Q-splines
[RR-830-M] N91-23808
On the structure of polynomial models of 2-D systems
[MATHS-REPT-A-139] N91-23812
Principal components of minus M-matrices
[AD-A232354] N91-23818
POLYTETRAFLUOROETHYLENE
A conformal oxidation-resistant, plasma-polymerized coating N91-24063
POLYURETHANE FOAM
Test on parabolic flights for stowage in weightlessness N91-23578
POPULATION THEORY
Convergence of one-dimensional diffusion processes to a jump process related to population genetics
[AD-A232121] N91-23826
POROSITY
The drag of spheres at porosites ranging from an isolated sphere to a packed bed
[CRANFIELD-AERO-9012] N91-23444
POROUS MATERIALS
Shock characterization of epoxy: Forty-two volume percent glass microballoons
[DE91-009616] N91-23314
PORTABLE EQUIPMENT
Portable intelligent diagnostic aids
[AD-A230883] N91-23782
A field-deployable digital acoustic measurement system N91-24078
POSEIDON SATELLITE
Validation requirements for the Topex/Poseidon altimeter mission N91-23602
POSITION (LOCATION)
Higher accuracy requirements for the satisfactory position calculation of an artificial satellite
[GKSS-90/E/25] N91-23203
Two dimensional vernier
[NASA-CASE-MSC-21700-1] N91-23462
POSITION SENSING
Laser optical disk position encoder with active heads N91-24079
POSITRON ANNIHILATION
Fermi surface of YBCO by DHVA
[DE91-009963] N91-23943
POTABLE WATER
Physical/chemical closed-loop water-recycling N91-24052
POTASSIUM HYDROXIDES
Destructive physical analysis results of Ni/H2 cells cycled in LEO regime
[NASA-TM-104382] N91-23233
POTASSIUM OXIDES
A KO2 rebreather for EVA denitrogenation procedure N91-23588
POTENTIAL THEORY
Aerodynamic preliminary analysis system 2. Part 1: Theory
[NASA-CR-182076] N91-23080
Aerodynamic preliminary analysis system 2. Part 2: User's manual
[NASA-CR-182077] N91-23081
POWDER (PARTICLES)
The development and evaluation of an alternative powder prepregging technique for use with LaRC-TPI/graphite composites
[NASA-CR-188184] N91-23242

Measurement of particle size, velocity and temperature in the plasma spray coating process
[DE91-006208] N91-23317
Power packs: A passive approach to extinguishing fire in combat vehicles
[AD-A232020] N91-23342

POWDERED ALUMINUM
Diagnostic measurements on an aluminized propellant plume during spin and nonspin testing
[AD-A232031] N91-23235

POWER AMPLIFIERS
High-power performance of a copper laser pumped dye master-oscillator-power-amplifier chain
[DE91-010460] N91-23478
Analog processing of optical wavefronts using integrated guided-wave optics
[AD-A232703] N91-23904

POWER CONVERTERS
Component technology for stirling power converters
[NASA-TM-104387] N91-23234

POWER EFFICIENCY
Bimanes and related heterocycles as laser dyes
[AD-A232335] N91-23484
The United Kingdom waveguide power standards above 40 GHz
[RSRE-90023] N91-23845

POWER LINES
Magnet cable manufacturing
[DE91-010210] N91-23935

PRANDTL-MEYER EXPANSION
The 2-D supersonic nozzle design N91-23176

PRE-MAIN SEQUENCE STARS
Near-infrared milliarcsecond observations by the lunar occultation technique N91-24034

PRECIPITATION (METEOROLOGY)
Analysis and modeling of summertime convective cloud and precipitation structure over the Southeastern United States
[NASA-CR-188119] N91-23670

PRECISION GUIDED PROJECTILES
MIK-guided bomb simulation
[IAITIC-87-1003] N91-23337

PREDICTION ANALYSIS TECHNIQUES
Analytical and experimental investigations of the oblique detonation wave engine concept N91-23169
The application of neural networks to the SSME startup transient
[NASA-CR-187138] N91-23205
Theoretical prediction of vibrational infrared frequencies of tertiary amines
[AD-A232880] N91-23288
Benchmarking numerical predictions with force and moment measurements on slender, supercavitating bodies
[DE91-007066] N91-23432
Computational life prediction methodology for mechanical systems using dynamic simulation, finite element analysis, and fatigue life prediction methods N91-23494
A first-principles generic methodology for representing the knowledge base of a process diagnostic expert system
[DE90-017693] N91-23520
Bobbin stresses generated by wire winding
[DE91-009545] N91-23526

PREDICTIONS
Predictions and verification of ESD tests made with sphere injections on a flight representative telecommunication satellite: ARABSAT STM
[REPT-911-440-109] N91-23224
Microwave temperature profiler for clear air turbulence prediction
[NASA-CASE-NPO-18115-1-CU] N91-23662
A guide to the Nedwam wave model
[KNMI-WR-90-04] N91-23688
Maintenance Resource Prediction Model (MRPM) user's manual
[AD-A232019] N91-23762

PREFORMS
A simulation of the draping and a model of the consolidation of commingled fabrics N91-23239

PREMIXED FLAMES
An experimental study of flamelet surfaces in turbulent combustion
[AD-A232342] N91-23284

PREPREGS
The development and evaluation of an alternative powder prepregging technique for use with LaRC-TPI/graphite composites
[NASA-CR-188184] N91-23242

PRESIDENTIAL REPORTS
Aeronautics and space report of the President N91-24085

PRESSING (FORMING)
Unipunch capability study
[DE91-008825] N91-23498

PRESSURE DISTRIBUTION
Simulation of probabilistic wind loads and building analysis
[NASA-TM-103744] N91-23549

PRESSURE EFFECTS
Real time analysis systems of the physical parameters of the environment and the state of a human organism for a long term exposure at different gas mixtures and pressure up to 100 bar N91-23568
Pressure dynamics modeling for the design of the advanced neutron source reactor
[DE91-007860] N91-23883

PRESSURE GRADIENTS
Two-phase flow patterns and frictional pressure gradients in a small rectangular channel
[DE91-009652] N91-23414

PRESSURE ICE
Arctic remote autonomous measurement platform post CEAREX engineering report
[AD-A232843] N91-23471

PRESSURE MEASUREMENT
An engineering study of altitude determination deficiencies of the Service Aircraft Instrumentation Package (SAIP)
[AD-A232055] N91-23145
The VKI hypersonic wind tunnels and associated measurement techniques
[VKI-TM-46] N91-23196
Shock characterization of epoxy: Forty-two volume percent glass microballoons
[DE91-009616] N91-23314

PRESSURE VESSEL DESIGN
Stochastic micromechanical modeling of cleavage fracture in the ductile-brittle transition region N91-23533

PRESSURE VESSELS
Destructive physical analysis results of Ni/H2 cells cycled in LEO regime
[NASA-TM-104382] N91-23233
Study of static and dynamic fracture using strain measurements
[PB91-132217] N91-23524
A comparison between classical and substructuring finite-element stress analysis of a complex vacuum vessel shell
[DE91-010035] N91-23540
Buckling analysis of a complex vacuum vessel using the finite-element method
[DE91-010032] N91-23546
Evaluation of catastrophic failure risk in pressure vessels. Results of pressure vessel test with a large vessel (HC2-test)
[VTT-RR-708] N91-23551

PRESSURIZED WATER REACTORS
Potential impact of enhanced fracture-toughness data on fracture mechanics assessment of PWR vessel integrity for pressurized thermal shock
[DE91-009554] N91-23509
The CERBERUS Ver. 02 code: A parallel six-equation thermal-hydraulic-system simulation code
[DE91-010079] N91-23736

PRESTRESSING
Electromagnetic attachment mechanism
[NASA-CASE-MSC-21463-1] N91-23490

PREVENTION
Design rules and system testing methods
[REPT-911-440-107] N91-23222

PRIMITIVE EQUATIONS
Models of planetary wave propagation in the middle atmosphere N91-23639
Mechanisms of equatorial superrotation: Studies with two-level models N91-23642

PRINCIPAL COMPONENTS ANALYSIS
An observational study of arm structure in normal spiral galaxies N91-24007

PRINTED CIRCUITS
Silicon avalanche photodiode active-quenching circuit
[AD-A233633] N91-23395

PROBABILITY DENSITY FUNCTIONS
Turbulent mixing in nonreacting and reacting flows: A PDF approach at the two-point level N91-23422

PROBABILITY DISTRIBUTION FUNCTIONS
Computations, properties, and applications of matrix-valued functions to mathematical science and control systems
[AD-A232448] N91-23819

PROBABILITY THEORY
Model sensitivity in stress-strength reliability computations
[AD-A232023] N91-23554
The terminal Doppler weather radar tornadic vortex signature detection algorithm
[DOT-FAA-NR-91-5] N91-23675
Advanced methods of approximate reasoning
[AD-A232140] N91-23814
Large and moderate deviation limit theorems for arbitrary sequences of random variables with applications
[AD-A232334] N91-23817
Topics in inference and decision-making with partial knowledge
[NASA-CR-188209] N91-23821
Detection of outliers and robust estimation using fuzzy clustering
[RR-822-M] N91-23823
Measuring the effects of distributed database models on transaction availability measures N91-23973
A note on the performance analysis of static locking in distributed database systems N91-23975
Boundary conditions in quantum cosmology N91-24020

PROBLEM SOLVING
The problem of plate modeling theoretical and computational results
[AD-A232756] N91-23562
Genetic algorithms N91-24050

PROCESS CONTROL (INDUSTRY)
Control aspects of the brushless doubly-fed machine
[DE91-009707] N91-23387
Checklist for thick-film hybrid microcircuits manufacturer and line survey
[ESA-PSS-01-607-ISSUE-1] N91-23396
A first-principles generic methodology for representing the knowledge base of a process diagnostic expert system
[DE90-017693] N91-23520
On the initialization problem in the design of structurally constrained digital regulators
[REPT-90-039] N91-23749
Applications of neural networks to process control and modeling
[DE91-007389] N91-23784

PROCUREMENT
Strategic missiles: Uncertainties persist in the Advanced Cruise Missile (ACM) program
[AD-A232058] N91-23142

PROCUREMENT POLICY
Do civil flying qualities requirements address military missions for off-the-shelf procurement N91-23115

PRODUCT DEVELOPMENT
Aerospatiale industrial thermal plasma activities
[REPT-911-430-122] N91-23928
Technology 2000, volume 2
[NASA-CP-3109-VOL-2] N91-24041

PRODUCTION COSTS
Strategic missiles: Uncertainties persist in the Advanced Cruise Missile (ACM) program
[AD-A232058] N91-23142

PRODUCTION MANAGEMENT
Checklist for thick-film hybrid microcircuits manufacturer and line survey
[ESA-PSS-01-607-ISSUE-1] N91-23396
Checklist for thin-film hybrid microcircuits manufacturer and line survey
[ESA-PSS-01-611-ISSUE-1] N91-23397

PRODUCTIVITY
Steps toward environmentally compatible product and process design: A case for green engineering
[AD-A232888] N91-23633

PROGRAM VERIFICATION (COMPUTERS)
Software testing for evolutionary iterative rapid prototyping
[AD-A232555] N91-23771

PROGRAMMING LANGUAGES
Generalization of the FP2 parallel language by means of net theory
[RR-832-I-IMAG-99-LIFIA] N91-23780

PROJECT MANAGEMENT
Strategic missiles: Uncertainties persist in the Advanced Cruise Missile (ACM) program
[AD-A232058] N91-23142
Federally funded research: Decisions for a decade
[OTA-SET-490] N91-23998

PROJECT PLANNING
Technologies for aerobraking
[NASA-TM-102854] N91-23207
Small Explorer project: Submillimeter Wave Astronomy Satellite (SWAS). Mission operations and data analysis plan
[NASA-CR-186954] N91-23212
Computational needs survey of NASA automation and robotics missions. Volume 1: Survey and results
[NASA-TM-103860] N91-23341

PROJECTILES
Response of simulated propellants and explosives to projectile impact
[DE91-009777] N91-23333
Energy-efficient penetration of targets
[AD-A232227] N91-23518

PROJECTION
Possibilities for projection x ray lithography using holographic optical elements
[DE91-009770] N91-23464
PROP-FAN TECHNOLOGY
Unified aeroacoustics analysis for high speed turboprop aerodynamics and noise. Volume 3: Application of theory for blade loading, wakes, noise, and wing shielding
[NASA-CR-185193] N91-23850
Unified aeroacoustics analysis for high speed turboprop aerodynamics and noise. Volume 4: Computer user's manual for UAAP turboprop aeroacoustic code
[NASA-CR-185194] N91-23851
Unified aeroacoustics analysis for high speed turboprop aerodynamics and noise. Volume 5: Propagation of propeller tone noise through a fuselage boundary layer
[NASA-CR-185195] N91-23852
PROPELLANT ADDITIVES
Diagnostic measurements on an aluminized propellant plume during spin and nonspin testing
[AD-A232031] N91-23235
PROPELLANT CHEMISTRY
Material processing with hydrogen and carbon monoxide on Mars
[NASA-TM-104405] N91-23616
PROPELLANT TANKS
Superplastic forming of Al-Li alloys for lightweight, low-cost structures N91-24065
PROPELLER FANS
Unified aeroacoustics analysis for high speed turboprop aerodynamics and noise. Volume 4: Computer user's manual for UAAP turboprop aeroacoustic code
[NASA-CR-185194] N91-23851
PROPELLER NOISE
Unified aeroacoustics analysis for high speed turboprop aerodynamics and noise. Volume 5: Propagation of propeller tone noise through a fuselage boundary layer
[NASA-CR-185195] N91-23852
PROPELLERS
An experimental study of an axisymmetric turbulent boundary layer disturbed by a periodic freestream N91-23078
Unified aeroacoustics analysis for high speed turboprop aerodynamics and noise. Volume 2: Development of theory for wing shielding
[NASA-CR-185192] N91-23849
Unified aeroacoustics analysis for high speed turboprop aerodynamics and noise. Volume 5: Propagation of propeller tone noise through a fuselage boundary layer
[NASA-CR-185195] N91-23852
PROPULSION SYSTEM CONFIGURATIONS
NASA aeropropulsion research in support of propulsion systems of the 21st century
[NASA-TM-104403] N91-23083
Engine technology challenges for a 21st century high speed civil transport
[NASA-TM-104363] N91-23098
Airbreathing propulsion for space transport: New concepts, special problems and attempts at solutions N91-23154
Turbojet potential for hypersonic flight N91-23155
Compact heat exchanger for an inverse components engine N91-23157
Design considerations for combined air breathing-rocket propulsion systems
[AIAA-90-0098] N91-23158
Supersonic-hypersonic inlet studies for aerospaceplane N91-23160
Design considerations of a high expansion ratio hydrogen turbine N91-23163
Highly integrated ducted rocket propulsion modules for future hypersonic tactical missiles N91-23171
New developments in composites for space applications
[REPT-911-430-104] N91-23250
PROPULSION SYSTEM PERFORMANCE
NASA aeropropulsion research in support of propulsion systems of the 21st century
[NASA-TM-104403] N91-23083
Airbreathing propulsion for space transport: New concepts, special problems and attempts at solutions N91-23154
Turbojet potential for hypersonic flight N91-23155
Airbreathing propulsion for transatmospheric flight N91-23156
Compact heat exchanger for an inverse components engine N91-23157
Design considerations for combined air breathing-rocket propulsion systems
[AIAA-90-0098] N91-23158
Cryogenic hydrogen-induced air-liquefaction technologies N91-23159
Supersonic-hypersonic inlet studies for aerospaceplane N91-23160
Design considerations of a high expansion ratio hydrogen turbine N91-23163
Performance characteristics of hypersonic detonation wave ramjets N91-23168
Analytical and experimental investigations of the oblique detonation wave engine concept N91-23169
Highly integrated ducted rocket propulsion modules for future hypersonic tactical missiles N91-23171
The certification of the aircraft integrated propulsive system
[REPT-911-111-102] N91-23188
Temperature measurements of ET plasmas using atomic emission spectroscopy
[AD-A232498] N91-23930
PROPULSIVE EFFICIENCY
Integration of propulsive systems: Selection and compromise
[REPT-911-111-101] N91-23187
The certification of the aircraft integrated propulsive system
[REPT-911-111-102] N91-23188
PROSTHETIC DEVICES
Simulation of blood flow through an artificial heart N91-24056
PROTECTIVE CLOTHING
Effectiveness of a prototype microclimate cooling system for use with chemical protective clothing
[AD-A231572] N91-23717
Heat strain and work tolerance times with varying levels of Canadian Forces NBC protective clothing, ambient temperature, physical work intensity, and work/rest schedules
[AD-A232653] N91-23720
PROTECTIVE COATINGS
Point defect effects on hot corrosion of zirconia-based coatings
[AD-A232662] N91-23326
A tribological study of sliding contact interaction N91-23489
Flexible fluoropolymer filled protective coatings N91-24062
A conformal oxidation-resistant, plasma-polymerized coating N91-24063
PROTEIN CRYSTAL GROWTH
Protein crystal growth tray assembly
[NASA-CASE-MFS-28507-1] N91-23933
PROTOCOL (COMPUTERS)
The TurboLAN project. Phase 1: Protocol choices for high speed local area networks. Phase 2: TurboLAN Intelligent Network Adapter Card, (TINAC) architecture
[NASA-CR-188175] N91-23776
PROTON BEAMS
Recent results and future prospects for the polarized beam at Fermilab
[DE91-010590] N91-23862
PROTONS
Infrared focal plane performance in the South Atlantic anomaly
[NASA-CR-186197] N91-23458
PROTOTYPES
Integration of the execution support system for the Computer-Aided Prototyping System (CAPS)
[AD-A232015] N91-23761
Software testing for evolutionary iterative rapid prototyping
[AD-A232555] N91-23771
Building a generalized distributed system model N91-23971
PROVING
Predictions and verification of ESD tests made with sphere injections on a flight representative telecommunication satellite: ARABSAT STM
[REPT-911-440-109] N91-23224
Building real-time simulators for space applications N91-23587
PSEUDORANDOM SEQUENCES
A method of constructing a pair of pseudorandom sequences with a useful crosscorrelation function
[IAITIC-87-1001] N91-23345
PSYCHOLOGICAL FACTORS
Individual differences underlying pilot cockpit error
[DOT/FAA/RD-91/13] N91-23710
Spatiotemporal characteristics of visual localization
[AD-A232734] N91-23715
PSYCHOLOGICAL TESTS
Psychological selection of astronauts: Recent developments at the DLR testing centre in Hamburg (Fed. Republic of Germany) N91-23565
Human Performance Assessment Methods. Addendum
[AGARD-AG-308-ADD] N91-23711
PSYCHOMETRICS
Human Performance Assessment Methods. Addendum
[AGARD-AG-308-ADD] N91-23711
PSYCHOMOTOR PERFORMANCE
Ship roll stabilization and human performance
[AD-A232721] N91-23721
PSYCHOPHYSICS
Spatiotemporal characteristics of visual localization
[AD-A232734] N91-23715
PULSAR MAGNETOSPHERES
Magnetospheric structure of rotation powered pulsars
[DE91-007622] N91-24028
PULSARS
The supernova remnant G109.1-1.0 and the x-ray pulsar 1E2259+586 N91-24002
Phenomenological aspects of scalar fields in astrophysics, cosmology and particle physics N91-24014
Magnetospheric structure of rotation powered pulsars
[DE91-007622] N91-24028
The Black Widow pulsar PSR 1957+20: A potential VHE gamma-ray source N91-24038
PULSE AMPLITUDE
Infrared focal plane performance in the South Atlantic anomaly
[NASA-CR-186197] N91-23458
PULSE COMMUNICATION
SZ series GaAs super high-speed logic gate: Optimum choice. High tech; high speed; high quality
[AD-A232819] N91-23962
PULSE COMPRESSION
Digital beamforming and pulse compression in an adaptive array radar system
[AD-A232713] N91-23377
Pulse compression of 100 picosecond pulses at 1.319 microns
[AD-A232552] N91-23901
PULSE RADAR
Radar target discrimination and identification using extinction-pulses and single-mode extraction pulses
[AD-A232162] N91-23368
PULSED LASERS
Optical parametric oscillators pumped by excimer lasers N91-23473
Spatial dynamics of picosecond CO2 laser pulses produced by optical switching in Ge
[DE91-010368] N91-23476
High-power performance of a copper laser pumped dye master-oscillator-power-amplifier chain
[DE91-010460] N91-23478
PULSES
Conceptual design and system studies for a 600 kW repetitive pulse transformer
[DE91-010585] N91-23389
PUNCHES
Unipunch capability study
[DE91-008825] N91-23498
PYRIMIDINES
AFRRI reports, October - December 1990
[AD-A232236] N91-23283
PYROLYSIS
Atrane and quadroped frameworks in early transition metal and silicon GRO stereochemistry: Monomers and oligomers
[AD-A232837] N91-23331
Low-temperature laser-induced selective area growth of compound semiconductor N91-23932
PYROTECHNICS
Pyrotechnical safety of Aerospatiale tactical missiles: Application to conventional warhead
[REPT-911-320-101] N91-23139

Q

Q VALUES
Q-splines
[RR-830-M] N91-23808
QUADRATIC EQUATIONS
Error probabilities of frequency hopped MFSK with self-normalization combining in a fading channel with partial-band interference
[AD-A232467] N91-23376
Q-splines
[RR-830-M] N91-23808
QUADRUPOLES
Magnet cable manufacturing
[DE91-010210] N91-23935
QUALITY CONTROL
Improved quality acceptance procedure for interlaminar shear strength
[IAITIC-87-1005] N91-23238
Checklist for thick-film hybrid microcircuits manufacturer and line survey
[ESA-PSS-01-607-ISSUE-1] N91-23396
Checklist for thin-film hybrid microcircuits manufacturer and line survey
[ESA-PSS-01-611-ISSUE-1] N91-23397
Steps toward environmentally compatible product and process design: A case for green engineering
[AD-A232888] N91-23633

QUANTUM CHEMISTRY
Quantum chemical studies of candidate high energy density material compounds
[AD-A232393] N91-23335
QUANTUM CHROMODYNAMICS
Research in particle theory
[DE91-010749] N91-23872
QUANTUM ELECTRONICS
Exploring the mesoscopic domain where classical and quantum phenomena meet N91-23843
QUANTUM THEORY
High quality three dimensional electron gases in semiconductors
[AD-A232779] N91-23406
Theoretical studies relating to the interaction of radiation with matter
[AD-A232107] N91-23480
Exploring the mesoscopic domain where classical and quantum phenomena meet N91-23843
Intermediate/high energy nuclear physics
[DE91-010702] N91-23868
Quantum extension of Child-Langmuir law
[AD-A232407] N91-23878
Molecular dynamics simulator for optimal control of molecular motion
[AD-A232801] N91-23881
Nonequilibrium Green's functions and quantum transport theory for semiconductor microstructures N91-23937
Boundary conditions in quantum cosmology N91-24020
QUANTUM WELLS
Strained quantum well leaky-mode diode laser arrays
[DE91-009982] N91-23477
Vertical emitting, ring geometry, ultra-low threshold and ultra-high speed quantum well lasers for optical interconnect
[AD-A232122] N91-23481
Broad area distributed gain, distributed index profile GaAlAs semiconductor laser diodes
[AD-A232332] N91-23483
Magneto-optical properties of quantum wells with arbitrary potential profiles
[AD-A232037] N91-23897
Nonequilibrium Green's functions and quantum transport theory for semiconductor microstructures N91-23937
QUARK MODELS
Intermediate/high energy nuclear physics
[DE91-010702] N91-23868
QUARKS
Intermediate/high energy nuclear physics
[DE91-010702] N91-23868
Phenomenological aspects of scalar fields in astrophysics, cosmology and particle physics N91-24014
QUASARS
Bulletin of the Israel Physical Society, volume 33, 1987. Annual Meeting 1987: Program and Abstracts
[ITN-89-85012] N91-23832
Biased galaxy formation in the neutrino scenario N91-23839
The spectrum of massive accretion disks N91-23840
Theoretical studies of QSO absorption lines and the intergalactic medium N91-24025
QUATERNIONS
Real time estimation of aircraft angular attitude
[IAITIC-87-1004] N91-23107
Simulation and analyses of the aeroassist flight experiment attitude update method
[NASA-TM-102174] N91-23210
QUENCHING
Silicon avalanche photodiode active-quenching circuit
[AD-A233633] N91-23395
QUERY LANGUAGES
Processing problems in the IRUS queries: An empirical verification of problem coverage in the natural language sourcebook
[AD-A232780] N91-23800
Query processing for deductive databases with null values N91-23979
QUEUEING THEORY
Data type coherency in heterogeneous shared memory multiprocessors
[AD-A232114] N91-23729
Data transfer over multiplexed logical data links sharing a single physical circuit N91-23734
Mathematical techniques for the Performance Oriented Design (POD) tool
[AD-A232092] N91-23767
Building a generalized distributed system model
[NASA-CR-188181] N91-23970
Performance analysis of static locking in replicated distributed database systems N91-23974
A note on the performance analysis of static locking in distributed database systems N91-23975

R

RACKS (FRAMES)
Test on parabolic flights for stowage in weightlessness N91-23578
RADAR
An investigation of CFAR techniques for airborne radars
[AD-A232724] N91-23378
Design of inherently wide-band microwave frequency doubler and tripler in microstrip
[FEL-90-B255] N91-23392
RADAR ANTENNAS
Precision runway monitor demonstration report
[AD-A232671] N91-23198
RADAR APPROACH CONTROL
Precision runway monitor demonstration report
[AD-A232671] N91-23198
RADAR CROSS SECTIONS
Scattering from thin apertures in coated conductors using FDTD
[AD-A232125] N91-23365
RADAR DETECTION
Distributed radar sensors for aircraft detection
[DE91-009845] N91-23350
RADAR IMAGERY
SAR processor for the ERS-1 data phase 1, simple processor
[FEL-90-B033] N91-23359
An investigation of CFAR techniques for airborne radars
[AD-A232724] N91-23378
Object oriented programming in MMI: A software tool for analysis and planification of a radar imaging mission N91-23589
A search for strange attractors in the saturation of middle atmosphere gravity waves
[AD-A232468] N91-23658
Sea ice classification using synthetic aperture radar
[AD-A232248] N91-23689
RADAR SCATTERING
Scattering from thin apertures in coated conductors using FDTD
[AD-A232125] N91-23365
Backscattering by nonspherical particles, using the coupled-dipole method: An application in radar meteorology
[AD-A232371] N91-23373
Joint services electronics program
[AD-A232331] N91-23402
RADAR SIGNATURES
The terminal Doppler weather radar tornadic vortex signature detection algorithm
[DOT-FAA-NR-91-5] N91-23675
RADAR TARGETS
Radar target discrimination and identification using extinction-pulses and single-mode extraction pulses
[AD-A232162] N91-23368
RADAR TRACKING
Polarimetric radar observations of time-variant random targets
[DLR-FB-90-52] N91-23356
Investigation of micro- and macrophysical structures and processes in hail clouds with respect to their modification
[DLR-FB-90-38] N91-23677
Observation and theory of the radar aurora N91-24017
RADIAL FLOW
A three-dimensional Navier-Stokes stage analysis of the flow through a compact radial turbine
[NASA-TM-104420] N91-23186
RADIANT FLUX DENSITY
The effect of realistic antenna geometries on plasma loading predictions
[DE91-010782] N91-23353
RADIATION COUNTERS
Investigation of the muon component of EAS initiated by primary radiation from Hercules X-1 N91-24037
RADIATION DAMAGE
Solutions to current induced avalanche burnout
[DE90-013196] N91-23386
Laser hazards bibliography, January 1991
[AD-A232690] N91-23487
RADIATION DETECTORS
The Sudbury Neutrino Observatory project and the Kamiokande 2 project
[DE91-010641] N91-23863
Science requirements for Heavy Nuclei Collection (HNC) experiment on NASA Long Duration Exposure Facility (LDEF) Mission 2
[NASA-CR-187527] N91-23887
Instrumentation and data analysis for hard x ray astronomy N91-24010
RADIATION DISTRIBUTION
Studies of the diffuse background and interstellar dust at far ultraviolet wavelengths N91-24003
RADIATION EFFECTS
The Combined Release and Radiation Effects Satellite program (CRRES): A unique series of scientific experiments
[NASA-TM-104957] N91-23213
AFRRI reports, October - December 1990
[AD-A232236] N91-23283
Theoretical studies relating to the interaction of radiation with matter
[AD-A232107] N91-23480
Bulletin of the Israel Physical Society, volume 33, 1987. Annual Meeting 1987: Program and Abstracts
[ITN-89-85012] N91-23832
Investigation of neutral atom and ion emission during laser conditioning of multilayer HfO2-SiO2 coatings
[DE91-009749] N91-23860
Cold moderators for pulsed neutron sources
[DE91-010594] N91-23866
RADIATION HAZARDS
Laser hazards bibliography, January 1991
[AD-A232690] N91-23487
RADIATION MEASUREMENT
Qualification of concentrating mirror systems with the Hermes measurement system and the Helios simulation program
[ESA-TT-1213] N91-23230
Absolute calibration in vivo measurement systems
[DE91-009719] N91-23692
RADIATION SOURCES
Benchmark measurements and calculations of a 3-dimensional neutron streaming experiment
[DE91-010692] N91-23867
Hard x ray imaging telescope
[DE90-015815] N91-24013
RADIATION TOLERANCE
Evaluation of ferroelectric materials for memory applications
[AD-A232112] N91-23728
RADIATION TRANSPORT
Benchmark measurements and calculations of a 3-dimensional neutron streaming experiment
[DE91-010692] N91-23867
RADIATIVE TRANSFER
High-altitude non-equilibrium infrared emission models
[AD-A232503] N91-23659
Studies of the diffuse background and interstellar dust at far ultraviolet wavelengths N91-24003
Microwave imaging of Saturn's deep atmosphere and rings N91-24035
RADIO ASTRONOMY
Radio and infrared studies of mass-losing evolved stars N91-24026
RADIO COMMUNICATION
An analysis of MLAYER: A multilayer tropospheric propagation program
[AD-A232733] N91-23379
RADIO EMISSION
Matter in cosmic voids N91-23838
Near-infrared milliarcsecond observations by the lunar occultation technique N91-24034
RADIO FREQUENCIES
System-Level Integrated Circuit (SLIC) development for phased array antenna applications
[NASA-TM-104392] N91-23354
A controlled master frequency oscillator for the SSC low energy booster
[DE91-011004] N91-23391
RADIO FREQUENCY HEATING
ICRF heating on the Burning Plasma Experiment (BPX)
[DE91-010390] N91-23913
RADIO METEOROLOGY
Backscattering by nonspherical particles, using the coupled-dipole method: An application in radar meteorology
[AD-A232371] N91-23373
RADIO SIGNALS
A study of the end point path geometry in meteor burst systems using a microcomputer signal logger N91-24012
RADIO TRANSMISSION
A study of the end point path geometry in meteor burst systems using a microcomputer signal logger N91-24012
RADIOACTIVE DECAY
Diffusive, electrostatic concentration of disintegration products of inert gases in vortex flow
[AD-A232876] N91-23457
Research in particle theory
[DE91-010749] N91-23872
RADIOACTIVE ISOTOPES
Absolute calibration in vivo measurement systems
[DE91-009719] N91-23692

RADIOGRAPHY
Quantitative film radiography
[DE91-009718] N91-23463
RADIOMETERS
Non-mechanical optical path switching and its application to dual beam spectroscopy including gas filter correlation radiometry
[NASA-CASE-LAR-14588-1-CU] N91-23889
RADIOMETRIC CORRECTION
Correction of relief-induced radiometric distortions in Seasat-A SAR images for the example of the subscene of Bonn (Fed. Republic of Germany) and vicinities
[DLR-FB-90-54] N91-23613
RAILGUN ACCELERATORS
On the efficiency of rail accelerators
[PML-1990-64] N91-23204
Temperature measurements of ET plasmas using atomic emission spectroscopy
[AD-A232498] N91-23930
RAIN
Localised symmetric instability: An initial value problem N91-23672
RAMAN SPECTRA
A Raman spectroscopic and electrochemical study of the photoinduced crystallization of triethylenediamine triiodide upon a silver electrode
[AD-A232828] N91-23963
RAMJET ENGINES
Hypersonic Combined Cycle Propulsion
[AGARD-CP-479] N91-23147
Hypersonic propulsion: Past and present N91-23148
A study of supersonic and hypersonic ramjet engines in France from 1950 to 1974 (application on combined cycle aircraft engines) N91-23149
Trajectory optimization considerations for ramjet engines N91-23151
Airbreathing propulsion for transatmospheric flight N91-23156
Design techniques for dual mode ram-scramjet combustors N91-23166
Performance characteristics of hypersonic detonation wave ramjets N91-23168
Theoretical and experimental performance of a solid fuel ramjet combustion cycle for hypersonic flight conditions N91-23170
RANDOM PROCESSES
Realization of a randomized algorithm for the exact perfect matching problem, with a new constructive procedure
[REPT-90-056] N91-23751
RANDOM VARIABLES
Polarimetric radar observations of time-variant random targets
[DLR-FB-90-52] N91-23356
Large and moderate deviation limit theorems for arbitrary sequences of random variables with applications
[AD-A232334] N91-23817
RANGE ERRORS
Effect of atmospheric variations on electromagnetic distance measurements
[DE91-009726] N91-23349
RANGEFINDING
Automated handling and assembling of non-rigid objects
[AD-A231246] N91-23489
RANKINE-HUGONIOT RELATION
Shock characterization of epoxy: Forty-two volume percent glass microballoons
[DE91-009616] N91-23314
RANKING
Evaluation and ranking of candidate ceramic wafer engine seal materials
[NASA-TM-103795] N91-23515
RAPID QUENCHING (METALLURGY)
Modeling second-phase formation during rapid resolidification of stainless steel alloys
[DE91-008567] N91-23291
Rapidly solidified metallic alloys with unusual semmetry properties
[AD-A232384] N91-23304
RARE GASES
Monte Cario simulation of supercritical solutions in the grand canonical ensemble
[DE91-009152] N91-23859
RATINGS
Estimation of pilot ratings via pilot modeling N91-23121
Quantifying oil filtration effects on bearing life
[NASA-TM-104350] N91-23512
RATS
Hepatic metabolism of perfluorinated carboxylic acids: A nuclear magnetic resonance investigation
[AD-A232033] N91-23706
RAY TRACING
Parallel-processor-based Gaussian beam tracer for use in ocean acoustic tomography
[AD-A232420] N91-23690
Searching algorithms for the real roots of a Bezier function
[RR-834-I-AND-M] N91-23755
RAYLEIGH EQUATIONS
A two-scale solution of the forced Rayleigh-Plesset equation governing the dynamics of cavitation bubble vaporous growth
[AD-A232129] N91-23446
RAYLEIGH SCATTERING
Simulation of a backscatter lidar system
[DLR-FB-90-50] N91-23355
REACTION KINETICS
Theoretical and experimental performance of a solid fuel ramjet combustion cycle for hypersonic flight conditions N91-23170
Mixing and non-equilibrium chemical reaction in a compressible mixing layer
[NASA-CR-187084] N91-23181
Galvanic corrosion of aluminum-matrix composites
[AD-A232138] N91-23264
Deterministic analysis of processes at corroding metal surfaces and the study of electrochemical noise in these systems
[DE91-009997] N91-23297
A novel process for methanol synthesis
[DE91-009808] N91-23334
Chemical reactions in turbulent mixing flows
[AD-A232610] N91-23450
Comment on: Analytic solution of the Stochastic-Liouville model of spin-exchange
[DE91-010570] N91-23861
REACTIVITY
Reactive procedure based decision making for satellite control
[REPT-911-440-106] N91-23221
REACTOR DESIGN
Fatigue evaluation of piping systems with limited vibration test data
[DE91-007167] N91-23543
Gas core reactors for direct nuclear propulsion
[DE91-010050] N91-23884
Transport analysis of stellarator reactors
[DE91-010489] N91-23914
REACTOR MATERIALS
Potential impact of enhanced fracture-toughness data on fracture mechanics assessment of PWR vessel integrity for pressurized thermal shock
[DE91-009554] N91-23509
Cold moderators for pulsed neutron sources
[DE91-010594] N91-23866
REACTOR SAFETY
Potential impact of enhanced fracture-toughness data on fracture mechanics assessment of PWR vessel integrity for pressurized thermal shock
[DE91-009554] N91-23509
REACTOR TECHNOLOGY
Pressure dynamics modeling for the design of the advanced neutron source reactor
[DE91-007860] N91-23883
REAL TIME OPERATION
Interferometric investigation of supersonic flow fields with shock-shock interactions N91-23082
Microwave landing system modeling with application to air traffic control
[NASA-TM-102832] N91-23099
Real-time simulation of constrained dynamic systems N91-23189
Decentralized computing technology for fault-tolerant, survivable C3I systems, volume 1
[AD-A232289] N91-23369
Decentralized computing technology for fault-tolerant, survivable C3I systems, volume 2
[AD-A232290] N91-23370
Decentralized computing technology for fault-tolerant, survivable C3I systems. Volume 3: System/subsystem specification
[AD-A232291] N91-23371
Real time analysis systems of the physical parameters of the environment and the state of a human organism for a long term exposure at different gas mixtures and pressure up to 100 bar N91-23568
Building real-time simulators for space applications N91-23587
A procedural expert system for spacecraft command and control N91-23591
Three-dimensional graphical representation of objects according to movement data in realtime
[DLR-FB-90-51] N91-23725
Timed high-level nets
[REPT-90-050] N91-23750
Towards real-time GOMS
[AD-A232028] N91-23763
Real time pre-detection dynamic range compression
[NASA-CASE-NPO-18098-1-CU] N91-23890
Nonlinear real-time optical signal processing
[AD-A232889] N91-23909
Fiber Optic Tactical Local Network (FOTLAN) N91-24072
REBREATHING
A KO2 rebreather for EVA denitrogenation procedure N91-23588
RECEIVERS
A 30 GHz monolithic receive module
[NASA-CR-187085] N91-23346
Solar thermal energy receiver
[NASA-CASE-LEW-14949-1] N91-23617
RECOMBINATION REACTIONS
Low-energy collisions of multiply charged ions with electrons, atoms and surfaces
[DE91-010779] N91-23873
Electronic properties of Si-doped n-doping-intrinsic-p-doping-intrinsic (nipi) structures in GaAs
[DE91-009474] N91-23941
RED GIANT STARS
Radio and infrared studies of mass-losing evolved stars N91-24026
RED SHIFT
Matter in cosmic voids N91-23838
REDOX CELLS
Electrochemical parameterization of rhenium redox couples
[AD-A232043] N91-23279
REDUCED GRAVITY
An experimental method for studying combustion of an unsupported fuel droplet at reduced gravity N91-23273
Containerless undercooling and solidification of pure metals
[DLR-FB-90-48] N91-23301
In-Space technology experiments program. A high efficiency thermal interface (using condensation heat transfer) between a 2-phase fluid loop and heatpipe radiator: Experiment definition phase
[NASA-CR-186869] N91-23408
Payload related crew operations: From past missions to Columbus N91-23569
Neutral buoyancy and microgravity: Extravehicular activities with a humid water suit N91-23579
Transcapillary fluid shifts in head and neck tissues during and after simulated microgravity
[NASA-TM-103847] N91-23704
A non-invasive measure of minerals and electrolytes in tissue N91-24058
REDUNDANCY
Robotic control and inspection verification N91-24075
REELS
Bobbin stresses generated by wire winding
[DE91-009545] N91-23526
REENTRY VEHICLES
Ceramics in aerospace
[REPT-911-430-127] N91-23260
How to know CMC
[REPT-911-430-130] N91-23262
Aero-optics measurement system for the AEDC aero-optics test facility
[AD-A232852] N91-23908
REFERENCE SYSTEMS
Sea level and satellite techniques N91-23595
REFLECTION
Optimization of transparent and reflecting electrodes for amorphous silicon solar cells
[DE91-002132] N91-23618
A search for strange attractors in the saturation of middle atmosphere gravity waves
[AD-A232468] N91-23658
REFLECTOMETERS
The United Kingdom waveguide power standards above 40 GHz
[RSRE-90023] N91-23845
REFRACTIVITY
Effect of atmospheric variations on electromagnetic distance measurements
[DE91-009726] N91-23349
Two-channel spectroscopic polarization modulation ellipsometry
[DE91-010131] N91-23893
REFRACTORY MATERIALS
Combined thermal and bending fatigue of high-temperature metal-matrix composites: Computational simulation
[NASA-TM-104354] N91-23247
Carbon-carbon material with oxidation protection
[REPT-911-430-103] N91-23249
Nondestructive inspection for carbon-carbon with adapted coating for oxidation
[REPT-911-430-106] N91-23252

Thermostructural composites: Recent evolutions and improvements
[REPT-911-430-109] N91-23254
Materials and structure for Hermes
[REPT-911-430-117] N91-23258
High temperature composites in space planes and missiles development
[REPT-911-430-119] N91-23259
Metallic threaded composite fastener
[NASA-CASE-MSC-21580-1] N91-23491
Direct use R/D assistance
[DE91-009976] N91-23999

REFRIGERATORS
Research and development opportunities for natural gas fueled refrigeration in industrial processes
[PB91-136432] N91-23338

REGENERATION (ENGINEERING)
Fundamental research on tribology
[AD-A232446] N91-23519

REGENERATION (PHYSIOLOGY)
New research on bioregenerative air/water purification systems N91-24053

REGENERATIVE FUEL CELLS
SEI rover solar-electrochemical power system options
[NASA-TM-104402] N91-23620

REGRESSION ANALYSIS
Atmospheric circulation and poleward sensible heat flux variations associated with the recent Northern Hemisphere warming N91-23629

REGULATIONS
The certification of the aircraft integrated propulsive system
[REPT-911-111-102] N91-23188
Technology transfer in a changing national security environment
[AD-A232458] N91-24000

REGULATORS
On the initialization problem in the design of structurally constrained digital regulators
[REPT-90-039] N91-23749

REINFORCED PLASTICS
Improved quality acceptance procedure for interlaminar shear strength
[IAITIC-87-1005] N91-23238
A simulation of the draping and a model of the consolidation of commingled fabrics N91-23239
Characterization of composite materials for aerospace materials
[DLR-MITT-90-15] N91-23246
Thermoforming of in-situ reinforced thermoplastic composites
[AD-A232816] N91-23329

REINFORCING FIBERS
A simulation of the draping and a model of the consolidation of commingled fabrics N91-23239
Modelling of the impact response of fibre-reinforced composites
[AD-A232658] N91-23266

REISSNER THEORY
Linear bending of curved tubes without boundary influence
[ETN-91-99255] N91-23552

RELATIVISTIC ELECTRON BEAMS
Density channel tracking studies on Pulserad
[AD-A232649] N91-23888

RELATIVISTIC VELOCITY
Microscopic heavy-ion theory
[DE91-010739] N91-23869

RELATIVITY
Initial data for the two-body problem of general relativity N91-23965
Symmetries in general relativity N91-23966

RELIABILITY
Quantitative nondestructive evaluation: Requirements for tomorrow's reliability N91-24074
Robotic control and inspection verification N91-24075

RELIABILITY ANALYSIS
Checklist for thin-film hybrid microcircuits manufacturer and line survey
[ESA-PSS-01-611-ISSUE-1] N91-23397
Model sensitivity in stress-strength reliability computations
[AD-A232023] N91-23554
Statistical methods and neural network approaches for classification of data from multiple sources
[NASA-CR-188207] N91-23786
Robustness in replicated databases N91-23981

REMOTE CONTROL
Man-machine interactions and multimedia applied to ROV operations N91-23576
The Berlenga underwater survey project N91-23577
Space and telescience robotics: Development of concepts and reference technologies for teledetection and robotics in extreme environments N91-23580
Evaluation of multisensor fusion scheme for the localization of underwater remotely operated vehicles N91-23590

REMOTE HANDLING
Automated handling and assembling of non-rigid objects
[AD-A231246] N91-23489

REMOTE MANIPULATOR SYSTEM
Electromagnetic attachment mechanism
[NASA-CASE-MSC-21463-1] N91-23490
Research and development of future space robotics in NASDA N91-23582

REMOTE SENSING
Conference on Space Technology: Satellite Application Development
[REPT-911-440-103] N91-23219
Arctic remote autonomous measurement platform post CEAREX engineering report
[AD-A232843] N91-23471
Object oriented programming in MMI: A software tool for analysis and planification of a radar imaging mission N91-23589
Using satellite remote sensing imagery for marginal ice zone research in the ARCTEMIZ project N91-23600
Remote sensing of the sea at IROE/CNR N91-23604
Satellite and aeronautical technologies serving the management of living marine resources N91-23606
Medium Resolution Imaging Spectrometer (MERIS) N91-23608
Remote sensing performances
[REPT-911-440-101] N91-23615
Remote sensing of atmospheric temperature fields and the long wave radiation budget in the Antarctic
[ISSN-0069-5882] N91-23652
Sea ice monitoring in the east Greenland sea in May 1988 by means of remote sensing, with special emphasis on the computer-aided AVHRR-based extraction of sea ice motions
[DLR-FB-90-36] N91-23687
The integration of remote sensing, geographic information system, and expert system technologies for landcover classification N91-23733
Potential commercial uses of EOS remote sensing products N91-24055

REMOTE SENSORS
Distributed radar sensors for aircraft detection
[DE91-009845] N91-23350

REMOTELY PILOTED VEHICLES
Man-machine interactions and multimedia applied to ROV operations N91-23576
Evaluation of multisensor fusion scheme for the localization of underwater remotely operated vehicles N91-23590

RENORMALIZATION GROUP METHODS
An analysis of RNG based turbulence models for homogeneous shear flow
[NASA-CR-187552] N91-23433

REQUIREMENTS
Development of a low cost peak shaving generator set
[PB91-136374] N91-23332
Computational needs survey of NASA automation and robotics missions. Volume 1: Survey and results
[NASA-TM-103860] N91-23341
Strategy Combining Regionally Adapted Processes (SCRAP)
[AD-A232158] N91-23448
Quantitative nondestructive evaluation: Requirements for tomorrow's reliability N91-24074

RESCUE OPERATIONS
Airborne rescue system
[NASA-CASE-ARC-11909-1] N91-23095

RESEARCH
A test of the American Safety Flight Systems, Inc. prebreather/portable oxygen system
[AD-A232723] N91-23100

RESEARCH AND DEVELOPMENT
The costs and benefits of aircraft availability
[AD-A232660] N91-23076
Mechanical component diagnostic system
[AD-A232126] N91-23146
Technologies for aerobraking
[NASA-TM-102854] N91-23207
Fiber-reinforced glass-ceramic matrix composites: New class of materials for space applications
[REPT-911-430-107] N91-23253
Thermostructural composites: Recent evolutions and improvements
[REPT-911-430-109] N91-23254
CRREL research on materials in cold environments
[AD-A232133] N91-23280
Research and development opportunities for natural gas fueled refrigeration in industrial processes
[PB91-136432] N91-23338
Joint services electronics program
[AD-A232331] N91-23402
Manned diving activities in JAMSTEC N91-23572
Aerospatiale industrial thermal plasmas
[REPT-911-430-113] N91-23927
Federally funded research: Decisions for a decade
[OTA-SET-490] N91-23998
Direct use R/D assistance
[DE91-009976] N91-23999
Activities report of the DLR
[ISSN-0938-2194] N91-24086

RESEARCH FACILITIES
Recent results and future prospects for the polarized beam at Fermilab
[DE91-010590] N91-23862
Activities report of the DLR
[ISSN-0938-2194] N91-24086

RESEARCH MANAGEMENT
Direct use R/D assistance
[DE91-009976] N91-23999

RESEARCH PROJECTS
Summary of basic research in thermoacoustic heat transport: 1990
[AD-A232223] N91-23847
Recent results and future prospects for the polarized beam at Fermilab
[DE91-010590] N91-23862
Aeronautics and space report of the President N91-24085
Activities report of the DLR
[ISSN-0938-2194] N91-24086

RESIN MATRIX COMPOSITES
Rate dependent stress-strain behavior of advanced polymer matrix composites
[NASA-TM-104070] N91-23244
Flame-retardant composite materials N91-24064

RESONANCE
Mass resolved resonance ionization spectroscopy of combustion radicals
[DE91-010603] N91-23276

RESONANCE FLUORESCENCE
Multiphoton detection techniques for F and F2
[AD-A232641] N91-23286

RESONANCE LINES
Iron density measurements in polar atmosphere
[BONN-IR-90-53] N91-23654

RESONANT FREQUENCIES
An initial study into the influence of control stick characteristics on the handling qualities of a fly-by-wire helicopter N91-23122
Radar target discrimination and identification using extinction-pulses and single-mode extraction pulses
[AD-A232162] N91-23368

RESONATORS
Sensitive cryogenic transducer development and analysis for use on gravity wave detectors N91-24009

RESOURCES MANAGEMENT
Energy-related environmental issues in a global context
[DE91-009538] N91-23627
Information resources management long-range plan
[DE91-009745] N91-23984

REUSABLE SPACECRAFT
Design considerations of a high expansion ratio hydrogen turbine N91-23163

REUSE
Specifications for reusable software components
[RR-828-I-IMAG-116-LIFIA] N91-23756
Software reengineering N91-24047

REYNOLDS EQUATION
A system-approach to the elastohydrodynamic lubrication point-contact problem
[NASA-TM-104342] N91-23439

RHENIUM
Electrochemical parameterization of rhenium redox couples
[AD-A232043] N91-23279

RHEOLOGY
High shear stress rheology of liquid lubricants N91-23309
Interdisciplinary research on viscoelasticity and rheology
[AD-A232700] N91-23454

RIBONUCLEIC ACIDS
Molecular studies of cytokine induction
[AD-A232221] N91-23707

RICCATI EQUATION
Computations, properties, and applications of matrix-valued functions to mathematical science and control systems
[AD-A232448] N91-23819

RIGID STRUCTURES
Tripod operators for the interpretation of range images
[AD-A232631] N91-23344

Finite element based dynamical modeling of flexible open-loop manipulators with experimental results N91-23496
Bobbin stresses generated by wire winding [DE91-009545] N91-23526

RING LASERS
Vertical emitting, ring geometry, ultra-low threshold and ultra-high speed quantum well lasers for optical interconnect [AD-A232122] N91-23481

RISK
Near midair collisions as an indicator of general aviation collision risk N91-23096
Lateral dispersion of radioactive release. Draft for comments [CEMA-86/17] N91-23621

RIVERS
Detection of mining activities in the Yanomani Indian Reserve through LANDSAT-TM imagery [INPE-5182-RPE/638] N91-23609

ROBOT ARMS
An analytic study of general dynamic model and nonlinear feedback control of flexible robot arms N91-23497
Building real-time simulators for space applications N91-23587

ROBOT CONTROL
H-infinity approach to manipulator control N91-23495
Wave gaits, follow-the-leader gaits and gait transitions of legged robots N91-23503
Robot self-location in unknown environments [DE91-010450] N91-23505
On the control of two manipulators holding a rigid object in the presence of uncertainty [DE90-017742] N91-23508
Performance of visual and ultrasound sensing by an autonomous robot [DE91-010452] N91-23511
Time-optimal motion of robotic manipulators including nonlinear dynamics [LAAS-90403] N91-23516
Obstacle avoidance for redundant robots using configuration control [NASA-CASE-NPO-17852-1-CU] N91-23783
A Model-Based Approach to High-Level Robot Control with Visual Guidance [VTT-PUBL-71] N91-23788
A solution for the man/machine-interface in robotics: A high level control language with enhanced interaction equipment N91-23789
An interactive robot control system N91-23790
Monitoring an assembly task by perception requests N91-23791
Intelligent planning in controlling electronics assembly N91-23792
Planning of visual feedback with robot-sensor co-operation N91-23793
Robot-sensor co-operation planning for visual guidance N91-23794
A line based object localizing method for robot vision N91-23795
Object pose estimation based on one-degree-of-freedom sensor N91-23796

ROBOT DYNAMICS
Finite element based dynamical modeling of flexible open-loop manipulators with experimental results N91-23496
An analytic study of general dynamic model and nonlinear feedback control of flexible robot arms N91-23497
Wave gaits, follow-the-leader gaits and gait transitions of legged robots N91-23503
Articulation of spatial robots N91-23504
On the control of two manipulators holding a rigid object in the presence of uncertainty [DE90-017742] N91-23508
Time-optimal motion of robotic manipulators including nonlinear dynamics [LAAS-90403] N91-23516

ROBOT SENSORS
Performance of visual and ultrasound sensing by an autonomous robot [DE91-010452] N91-23511
Planning of visual feedback with robot-sensor co-operation N91-23793
Robot-sensor co-operation planning for visual guidance N91-23794
A line based object localizing method for robot vision N91-23795
Object pose estimation based on one-degree-of-freedom sensor N91-23796

ROBOTICS
Shape-memory alloy tactical feedback actuator, phase 1 [AD-A231389] N91-23289
Thermoforming of in-situ reinforced thermoplastic composites [AD-A232816] N91-23329
Computational needs survey of NASA automation and robotics missions. Volume 1: Survey and results [NASA-TM-103860] N91-23341
Performance of visual and ultrasound sensing by an autonomous robot [DE91-010452] N91-23511
Space and Sea [ESA-SP-312] N91-23563
The Berlenga underwater survey project N91-23577
Space and telescience robotics: Development of concepts and reference technologies for teledetection and robotics in extreme environments N91-23580
Telerobotics: A key area for possible technology transfer from underwater to space N91-23581
Research and development of future space robotics in NASDA N91-23582
EVA/robotics integration for Space Station Freedom N91-23583
Multisensory telerobotic concepts for space and underwater applications N91-23584
Building real-time simulators for space applications N91-23587
Robotics for recombinant DNA and human genetics research [DE90-016440] N91-23697
Quantifying performance degradation due to the human-machine interface of telemanipulators [AD-A232814] N91-23723
A line based object localizing method for robot vision N91-23795
Object pose estimation based on one-degree-of-freedom sensor N91-23796
Robotic control and inspection verification N91-24075

ROBOTS
On kinematic design of serial link manipulators [DE91-009414] N91-23499
Wave gaits, follow-the-leader gaits and gait transitions of legged robots N91-23503
Articulation of spatial robots N91-23504
Robot self-location in unknown environments [DE91-010450] N91-23505
Obstacle avoidance for redundant robots using configuration control [NASA-CASE-NPO-17852-1-CU] N91-23783
Robotic control and inspection verification N91-24075

ROBUSTNESS (MATHEMATICS)
H-infinity approach to manipulator control N91-23495
Use of a genetic algorithm to analyze robust stability problems [DE91-005895] N91-23742
On the initialization problem in the design of structurally constrained digital regulators [REPT-90-039] N91-23749
On locking and robustness in the finite element method [AD-A232245] N91-23815
Robustness in replicated databases N91-23981

ROCKET ENGINE DESIGN
Design considerations for combined air breathing-rocket propulsion systems [AIAA-90-0098] N91-23158

ROCKET ENGINES
Automatic particle sizing from rocket motor holograms [AD-A232553] N91-23236

RODS
Preloaded latching device [NASA-CASE-MSC-21730-1] N91-23493

ROLL
Metrics for roll response flying qualities N91-23118
An initial study into the influence of control stick characteristics on the handling qualities of a fly-by-wire helicopter N91-23122
Ship roll stabilization and human performance [AD-A232721] N91-23721

ROLLER BEARINGS
Quantifying oil filtration effects on bearing life [NASA-TM-104350] N91-23512

ROLLERS
Magnetostrictive roller drive motor [NASA-CASE-GSC-13369-1] N91-23380

ROOM TEMPERATURE
Low heat rejection diesel ceramic coupon tests [DE91-006274] N91-23318

ROOTS OF EQUATIONS
Searching algorithms for the real roots of a Bezier function [RR-834-I-AND-M] N91-23755

ROSAT MISSION
ROSAT: An international mission exploring the high energy universe [NASA-TM-104958] N91-23214

ROTARY WING AIRCRAFT
An investigation into the use of side-arm control for civil rotorcraft applications N91-23123
Technology needs for high-speed rotorcraft [NASA-CR-177578] N91-23136
Mechanical component diagnostic system [AD-A232126] N91-23146

ROTATING BODIES
Dynamic study of cyclically symmetric structures: Application to rotating a wheel of a centrifugal compressor [ISAL-91-0004] N91-23844

ROTATING CYLINDERS
Flow between eccentric rotating cylinders N91-23417

ROTATING DISKS
Incorporating finite element analysis into component life and reliability [NASA-TM-104400] N91-23550

ROTATION
The coordinate-free representation of rotational motions [RSRE-MEMO-4445] N91-23846
Magnetospheric structure of rotation powered pulsars [DE91-007622] N91-24028

ROTOR AERODYNAMICS
Model rotor icing tests in the NASA Lewis icing research tunnel [NASA-TM-104351] N91-23184

ROTORS
Mechanical component diagnostic system [AD-A232126] N91-23146
Control aspects of the brushless doubly-fed machine [DE91-009707] N91-23387
Modal analysis of multistage gear systems coupled with gearbox vibrations [NASA-TM-103797] N91-23513

RUBBER
Determination of the deviatoric material response functions for prestrained rubbers [FFA-TN-1990-29] N91-23321

RUBY LASERS
A 43 watt CW Ti:Sapphire laser [DE91-010468] N91-23479

RULES
European stakes and measures permitting the management of geometric dimensions N91-23573

RUN TIME (COMPUTERS)
Strategy Combining Regionally Adapted Processes (SCRAP) [AD-A232158] N91-23448
SZ series GaAs super high-speed logic gate: Optimum choice. High tech; high speed; high quality [AD-A232819] N91-23962

RUNWAYS
Precision runway monitor demonstration report [AD-A232671] N91-23198
Literature review on geotextiles to improve pavements for general aviation airports [AD-A232871] N91-23199

RUPTURING
Low heat rejection diesel ceramic coupon tests [DE91-006274] N91-23318

S

SAAB AIRCRAFT
Long time measurements of landing gear loads on SAAB SF-340 commuter aircraft [FFA-TN-1990-53] N91-23138

SAFETY
A test of the American Safety Flight Systems, Inc. prebreather/portable oxygen system [AD-A232723] N91-23100
Pyrotechnical safety of Aerospatiale tactical missiles: Application to conventional warhead [REPT-911-320-101] N91-23139
Laser hazards bibliography, January 1991 [AD-A232690] N91-23487
Real time analysis systems of the physical parameters of the environment and the state of a human organism for a long term exposure at different gas mixtures and pressure up to 100 bar N91-23568
Quantitative nondestructive evaluation: Requirements for tomorrow's reliability N91-24074

SAFETY FACTORS
Airborne rescue system [NASA-CASE-ARC-11909-1] N91-23095

SAFETY MANAGEMENT
The certification of the aircraft integrated propulsive system [REPT-911-111-102] N91-23188

SAMPLED DATA SYSTEMS
Decentralized computing technology for fault-tolerant, survivable C3I systems. Volume 3: System/subsystem specification
[AD-A232291] N91-23371
SAMPLING
A field-deployable digital acoustic measurement system N91-24078
SATELLITE ALTIMETRY
Space and Sea
[ESA-SP-312] N91-23563
Satellite data utilization in ocean circulation models N91-23593
Extraction of mesoscale ocean currents information from Geosat altimeter data N91-23594
Sea level and satellite techniques N91-23595
Satellite data utilization for modeling sea states N91-23598
Wind and sea state local climatology by means of satellite radar altimeter measurements N91-23599
Collection and processing of oceanographic data at CLS N91-23603
SATELLITE COMMUNICATION
Characteristics of a future aeronautical satellite communications system
[NASA-TM-104389] N91-23102
Recent advances in coding theory for near error-free communications N91-24068
SATELLITE CONFIGURATIONS
Communication and broadcasting satellites payload reconfiguration technologies
[REPT-911-440-102] N91-23218
SATELLITE CONTROL
Reactive procedure based decision making for satellite control
[REPT-911-440-106] N91-23221
A procedural expert system for spacecraft command and control N91-23591
SATELLITE DESIGN
The Eutelsat 2 programme
[REPT-911-440-108] N91-23223
SATELLITE IMAGERY
ISOCAM: The ISO's satellite infra-red camera
[REPT-911-440-104] N91-23468
Using satellite remote sensing imagery for marginal ice zone research in the ARCTEMIZ project N91-23600
Medium Resolution Imaging Spectrometer (MERIS) N91-23608
Detection of mining activities in the Yanomani Indian Reserve through LANDSAT-TM imagery
[INPE-5182-RPE/638] N91-23609
Observational study of the above-inversion structure and marine stratocumulus cloud clearing episodes during FIRE N91-23666
Surface cloud observations for radiation, climatology and incorporation into satellite-based nephanalyses N91-23671
Quantitative processing of Meteosat data: Implementation at KNMI: Applications
[KNMI-TR-127] N91-23678
Sea ice monitoring in the east Greenland sea in May 1988 by means of remote sensing, with special emphasis on the computer-aided AVHRR-based extraction of sea ice motions
[DLR-FB-90-36] N91-23687
The integration of remote sensing, geographic information system, and expert system technologies for landcover classification N91-23733
SATELLITE OBSERVATION
Energy exchange study at the ocean surface by satellite observation N91-23597
Validation requirements for the Topex/Poseidon altimeter mission N91-23602
Remote sensing of the sea at IROE/CNR N91-23604
Signal detection of MERIS in oceanographic applications N91-23605
Satellite and aeronautical technologies serving the management of living marine resources N91-23606
Infrared and visible studies of Pakistan portion of Arabian Sea using INSAT geostationary satellite N91-23611
Surface cloud observations for radiation, climatology and incorporation into satellite-based nephanalyses N91-23671
Initialization of cloud and radiation in the Florida State University global spectral model
[AD-A232425] N91-23682
SATELLITE ORBITS
Satellite maneuver evaluation tool
[AD-A232016] N91-23226
SATELLITE TRACKING
Precision orbit determination of global positioning system satellites N91-23202
High precision applications of the global positioning system N91-24073
SATELLITE-BORNE INSTRUMENTS
ISOCAM: The ISO's satellite infra-red camera
[REPT-911-440-104] N91-23468
ATSR: Precise sea surface temperature from the ERS-1 satellite N91-23601
Validation requirements for the Topex/Poseidon altimeter mission N91-23602
Remote sensing of the sea at IROE/CNR N91-23604
Medium Resolution Imaging Spectrometer (MERIS) N91-23608
SATELLITE-BORNE RADAR
SAR processor for the ERS-1 data phase 1, simple processor
[FEL-90-B033] N91-23359
SATURN ATMOSPHERE
Microwave imaging of Saturn's deep atmosphere and rings N91-24035
SATURN RINGS
Saturn's F ring: Imaging and simulation N91-24032
Microwave imaging of Saturn's deep atmosphere and rings N91-24035
SAUDI ARABIA
SWANEA (Southwest Asia-Northeast Africa): A climatological study. Volume 2: The Middle East Peninsula
[AD-A232776] N91-23684
SCALARS
Phenomenological aspects of scalar fields in astrophysics, cosmology and particle physics N91-24014
SCALE MODELS
A novel process for methanol synthesis
[DE91-009808] N91-23334
Computation of inlet reference plane flow-field for a subscale free-jet forebody/inlet model and comparison to experimental data
[AD-A232101] N91-23445
SCATTERING
Microwave landing system modeling with application to air traffic control
[NASA-TM-102832] N91-23099
The statistical properties of electromagnetic fields with application to radiation and scattering
[DE91-007467] N91-23351
High quality three dimensional electron gases in semiconductors
[AD-A232779] N91-23406
Studies of the diffuse background and interstellar dust at far ultraviolet wavelengths N91-24003
Observation and theory of the radar aurora N91-24017
SCATTEROMETERS
Characteristics and performance of an operational windscatterometer N91-23607
SCHEDULES
On the use of genetic algorithms to solve the time-table problem
[REPT-90-060] N91-23752
Proceedings of the 1991 American Association for the Advancement of Science Annual Meeting Program N91-23969
SCHEDULING
On the use of genetic algorithms to solve the time-table problem
[REPT-90-060] N91-23752
SCINTILLATION COUNTERS
Computed secondary-particle energy spectra following nonelastic neutron interactions with C-12 for E(n) between 15 and 60 MeV: Comparisons of results from two calculational methods
[DE91-010454] N91-23864
SEA ICE
Using satellite remote sensing imagery for marginal ice zone research in the ARCTEMIZ project N91-23600
Sea ice monitoring in the east Greenland sea in May 1988 by means of remote sensing, with special emphasis on the computer-aided AVHRR-based extraction of sea ice motions
[DLR-FB-90-36] N91-23687
Sea ice classification using synthetic aperture radar
[AD-A232248] N91-23689
SEA LEVEL
Sea level and satellite techniques N91-23595
SEA STATES
Satellite data utilization for modeling sea states N91-23598
Wind and sea state local climatology by means of satellite radar altimeter measurements N91-23599
SEA SURFACE TEMPERATURE
ATSR: Precise sea surface temperature from the ERS-1 satellite N91-23601
Infrared and visible studies of Pakistan portion of Arabian Sea using INSAT geostationary satellite N91-23611
The annual march of convection, sea surface temperature, and surface winds in the tropics N91-23667
SEA WATER
Effects of weightlessness (sea water immersion) on body fluid balance and CNS functions N91-23566
SEARCHING
An expert system for searching in full-text N91-23983
SEAS
Satellite and aeronautical technologies serving the management of living marine resources N91-23606
Effects of the northeast monsoon on the equatorial westerlies over Indonesia
[AD-A232106] N91-23681
SEASAT SATELLITES
Correction of relief-induced radiometric distortions in Seasat-A SAR images for the example of the subscene of Bonn (Fed. Republic of Germany) and vicinities
[DLR-FB-90-54] N91-23613
SECONDARY RADAR
Airborne Collision Avoidance System (ACAS) in controlled air traffic. Aspects of reciprocal influence in Secondary Surveillance Radar (SSR) radio loads
[ETN-91-99253] N91-23105
SECURITY
Security aspects of database management systems
[DE91-010677] N91-23987
Technology transfer in a changing national security environment
[AD-A232458] N91-24000
SEDIMENTS
Primary ocean production: Carbon and particle flux N91-23596
Detection of mining activities in the Yanomani Indian Reserve through LANDSAT-TM imagery
[INPE-5182-RPE/638] N91-23609
SEISMIC WAVES
Propagation of seismic waves in nonelastic media
[REPT-90-065] N91-23651
SEISMOLOGY
Some remarks on compliance testing
[AD-A231936] N91-23635
SELECTION
Psychological selection of astronauts: Recent developments at the DLR testing centre in Hamburg (Fed. Republic of Germany) N91-23565
SELECTIVE DISSEMINATION OF INFORMATION
Technology transfer in a changing national security environment
[AD-A232458] N91-24000
SELF ORGANIZING SYSTEMS
Information dynamics of self-programmable matter
[DE91-009954] N91-23740
Classification using multi-layered perceptrons
[AD-A232810] N91-23802
SELF TESTS
Basic properties of strongly code disjoint checkers
[RR-824-I] N91-23393
SEMANTICS
Generalized disjunctive well-founded semantics for logic programs
[AD-A232064] N91-23765
Software reverse engineering
[AD-A232644] N91-23773
Null values in definite programs
[AD-A232065] N91-23992
SEMICONDUCTOR DEVICES
Recent advances with quiescent power supply current (I(sub DDQ)) testing at Sandia using the HP82000
[DE91-009254] N91-23382
High power light activated semiconductor switches with sub-nanosecond rise time
[DE91-009250] N91-23939
Advances in silicon carbide Chemical Vapor Deposition (CVD) for semiconductor device fabrication
[NASA-TM-104410] N91-23946
Silicon carbide, an emerging high temperature semiconductor N91-24061
SEMICONDUCTOR DIODES
Study of phase-locked diode laser array and DFB/DBR surface emitting laser diode N91-23474
Broad area distributed gain, distributed index profile GaAlAs semiconductor laser diodes
[AD-A232332] N91-23483
Theory of novel nonlinear optics
[AD-A232659] N91-23903
SEMICONDUCTOR JUNCTIONS
Solutions to current induced avalanche burnout
[DE90-013196] N91-23386
SEMICONDUCTOR LASERS
Study of phase-locked diode laser array and DFB/DBR surface emitting laser diode N91-23474
Strained quantum well leaky-mode diode laser arrays
[DE91-009982] N91-23477

Vertical emitting, ring geometry, ultra-low threshold and ultra-high speed quantum well lasers for optical interconnect
[AD-A232122] N91-23481
Broad area distributed gain, distributed index profile GaAlAs semiconductor laser diodes
[AD-A232332] N91-23483
Studies of noise in semiconductor laser arrays
[AD-A232411] N91-23485
Theory of novel nonlinear optics
[AD-A232659] N91-23903

SEMICONDUCTORS (MATERIALS)
High quality three dimensional electron gases in semiconductors
[AD-A232779] N91-23406
Evaluation of ferroelectric materials for memory applications
[AD-A232112] N91-23728
Theory of novel nonlinear optics
[AD-A232659] N91-23903
Low-temperature laser-induced selective area growth of compound semiconductor N91-23932
Structural and electronic properties of the ordered ternary 3-5 semiconductors N91-23936
Nonequilibrium Green's functions and quantum transport theory for semiconductor microstructures N91-23937
Electronic properties of Si-doped n-doping-intrinsic-p-doping-intrinsic (nipi) structures in GaAs
[DE91-009474] N91-23941
Optoelectronic III-V heterostructures on SI substrates
[AD-A232035] N91-23950
Research and development on advanced silicon carbide thin film growth techniques and fabrication of high power and microwave frequency silicon carbide-based device structures
[AD-A232160] N91-23955
Silicon carbide, an emerging high temperature semiconductor N91-24061

SENSITIVITY
Model sensitivity in stress-strength reliability computations
[AD-A232023] N91-23554
Quantifying improved visual performance through vision training
[AD-A232799] N91-23716
Presentation of a computer program for analysing results of one shot device sensitivity tests: Application to the case of a one shot degenerated sequence
[REPT-911-430-126] N91-23758

SENSORY PERCEPTION
Human short-latency somatosensory evoked potentials in impact acceleration research: Equipment, procedures, and techniques
[AD-A232732] N91-23709
Monitoring an assembly task by perception requests N91-23791

SEPARATED FLOW
Simulation of brush insert for leading-edge-passage convective heat transfer
[NASA-TM-103801] N91-23409
A computationally efficient modelling of laminar separation bubbles N91-23411
Numerical simulation and topological analysis of the separated flow around a sphere
[DLR-FB-90-43] N91-23435
Simulation of blood flow through an artificial heart N91-24056

SEQUENCING
Large and moderate deviation limit theorems for arbitrary sequences of random variables with applications
[AD-A232334] N91-23817

SEQUENTIAL COMPUTERS
Specifications for reusable software components
[RR-828-I-IMAG-116-LIFIA] N91-23756

SERUMS
Three-dimensional structure of human serum albumin N91-24057

SERVICE LIFE
MHD channel gas-side element erosion-corrosion studies
[DE91-008561] N91-23911

SERVICE MODULES
EVA servicing: The Hermes capability N91-23575

SET THEORY
Timed high-level nets
[REPT-90-050] N91-23750

SEYFERT GALAXIES
High resolution imaging for Brackett gamma and H2 1-0 S(1) emission in the Seyfert galaxy NGC 1068
[MPE-PREPRINT-192] N91-23104

SHAFTS (MACHINE ELEMENTS)
Magnetostrictive roller drive motor
[NASA-CASE-GSC-13369-1] N91-23380

SHALLOW WATER
Riemann problems and the WAF method for the two-dimensional shallow water equations
[CRANFIELD-AERO-9005] N91-23443
Parallelizing the spectral transform method, part 1
[DE91-010453] N91-23805

SHAPE MEMORY ALLOYS
Shape-memory alloy tactical feedback actuator, phase 1
[AD-A231389] N91-23289

SHAPES
Strategy Combining Regionally Adapted Processes (SCRAP)
[AD-A232158] N91-23448

SHEAR FLOW
Thermodynamically consistent formulations for rapid granular and turbulent multiphase flows N91-23420
Hairpin vortices, singularities, and transition to turbulence in three-dimensional shear flows
[DE91-002792] N91-23430
An analysis of RNG based turbulence models for homogeneous shear flow
[NASA-CR-187552] N91-23433
Interdisciplinary research on viscoelasticity and rheology
[AD-A232700] N91-23454

SHEAR STRENGTH
Improved quality acceptance procedure for interlaminar shear strength
[IAITIC-87-1005] N91-23238

SHEAR STRESS
High shear stress rheology of liquid lubricants N91-23309
Finite element analysis of the lateral buckling of a cantilevered I Beam
[DE91-010123] N91-23527
Strain release in GaAs/Ga(1-x)/In(x)As strained layer superlattices grown on (112) substrates
[DE91-009972] N91-23944

SHELL THEORY
Tensor transformations and failure criteria for the analysis of fiber composite materials
[AD-A232238] N91-23265

SHIELDING
Design rules and system testing methods
[REPT-911-440-107] N91-23222
Experimental study of narrow slot, cavity-backed apertures with finite wall conductivity
[DE91-009039] N91-23352
The effect of realistic antenna geometries on plasma loading predictions
[DE91-010782] N91-23353
Unified aeroacoustics analysis for high speed turboprop aerodynamics and noise. Volume 2: Development of theory for wing shielding
[NASA-CR-185192] N91-23849
Unified aeroacoustics analysis for high speed turboprop aerodynamics and noise. Volume 3: Application of theory for blade loading, wakes, noise, and wing shielding
[NASA-CR-185193] N91-23850

SHOCK ABSORBERS
Energy dissipator
[NASA-CASE-MSC-21555-1] N91-23492

SHOCK WAVE INTERACTION
Interferometric investigation of supersonic flow fields with shock-shock interactions N91-23082
Some aspects of shock-wave boundary layer interaction relevant to intake flows N91-23161
Computational modeling and validation for hypersonic inlets N91-23162
Non-linear interaction of a detonation/vorticity wave
[NASA-CR-187550] N91-23434

SHOCK WAVES
Reacting shock waves in hypersonic propulsion applications N91-23174
A three-dimensional free-Lagrange code for multimaterial flow simulations
[DE91-002309] N91-23428
Relativistic shock waves and the excitation of plerions
[DE91-007623] N91-24027

SHORT TAKEOFF AIRCRAFT
The handling qualities of the STOL and maneuver technology demonstrator from specification to flight test N91-23117

SHUTTERS
Optical shutter switching matrix N91-24071

SIALON
Mechanistic studies of pressure-assisted superplasticity of structural ceramics
[AD-A232034] N91-23322

SIDELOBE REDUCTION
Implications of adaptive cancellation array processing for design of a space-based surveillance radar
[RSRE-MEMO-4410] N91-23364

SIGNAL ANALYSIS
A method of constructing a pair of pseudorandom sequences with a useful crosscorrelation function
[IAITIC-87-1001] N91-23345
A method for machinery condition monitoring of transient phenomena using the pseudo Wigner-Ville distribution
[AD-A232014] N91-23760

SIGNAL ANALYZERS
The 2-D acousto-optic signal processors for simultaneous spectrum analysis and direction finding
[AD-A232148] N91-23367
Frequency domain laser velocimeter signal processor N91-24077

SIGNAL DETECTION
Signal detection of MERIS in oceanographic applications N91-23605
Real time pre-detection dynamic range compression
[NASA-CASE-NPO-18098-1-CU] N91-23890
Frequency domain laser velocimeter signal processor N91-24077

SIGNAL ENCODING
Error control coding for multi-frequency modulation
[AD-A232421] N91-23374
A study of PC-Based HF ionospheric propagation predictions for use in naval communications
[AD-A232466] N91-23375
Digital CODEC for real-time processing of broadcast quality video signals at 1.8 bits/pixel N91-24067
Recent advances in coding theory for near error-free communications N91-24068

SIGNAL FADING
Error probabilities of frequency hopped MFSK with self-normalization combining in a fading channel with partial-band interference
[AD-A232467] N91-23376
A study of the end point path geometry in meteor burst systems using a microcomputer signal logger N91-24012

SIGNAL MIXING
Theory of novel nonlinear optics
[AD-A232659] N91-23903

SIGNAL PROCESSING
SAR processor for the ERS-1 data phase 1, simple processor
[FEL-90-B033] N91-23359
The 2-D acousto-optic signal processors for simultaneous spectrum analysis and direction finding
[AD-A232148] N91-23367
An analysis of MLAYER: A multilayer tropospheric propagation program
[AD-A232733] N91-23379
A controlled master frequency oscillator for the SSC low energy booster
[DE91-011004] N91-23391
Background simulation and filter design using iterated function systems
[AD-A232632] N91-23405
Mapping an adaptable Eigenstructure technique onto the topologix hypercube
[AD-A232032] N91-23764
Synergetic multisensor fusion
[AD-A232089] N91-23766
Image wavelet decomposition and applications
[NASA-CR-188217] N91-23787
Soviet atmospheric acoustics research N91-23848
The Sudbury Neutrino Observatory project and the Kamiokande 2 project
[DE91-010641] N91-23863
Real time pre-detection dynamic range compression
[NASA-CASE-NPO-18098-1-CU] N91-23890
Pulse compression of 100 picosecond pulses at 1.319 microns
[AD-A232552] N91-23901
Nonlinear real-time optical signal processing
[AD-A232889] N91-23909
Observation and theory of the radar aurora N91-24017
High precision applications of the global positioning system N91-24073
Frequency domain laser velocimeter signal processor N91-24077

SIGNAL RECEPTION
A method of constructing a pair of pseudorandom sequences with a useful crosscorrelation function
[IAITIC-87-1001] N91-23345

SIGNAL TO NOISE RATIOS
Studies of noise in semiconductor laser arrays
[AD-A232411] N91-23485
Functional approximation by feed-forward networks: A least squares approach to generalisation
[RSRE-MEMO-4453] N91-23811

SIGNAL TRANSMISSION
Recent advances in coding theory for near error-free communications N91-24068

SIGNATURE ANALYSIS
Initialization of cloud and radiation in the Florida State University global spectral model
[AD-A232425] N91-23682
SIGNS AND SYMPTOMS
Molecular studies of cytokine induction
[AD-A232221] N91-23707
SIKORSKY AIRCRAFT
Model rotor icing tests in the NASA Lewis icing research tunnel
[NASA-TM-104351] N91-23184
SILICATES
Cryomagmatism in the outer solar system N91-24019
SILICON
Silicon avalanche photodiode active-quenching circuit
[AD-A233633] N91-23395
SILICON CARBIDES
A study of the critical factors controlling the synthesis of ceramic matrix composites from preceramic polymers
[AD-A232686] N91-23327
A preliminary investigation of acousto-ultrasonic NDE of metal matrix composite test specimens
[NASA-TM-104339] N91-23521
Advances in silicon carbide Chemical Vapor Deposition (CVD) for semiconductor device fabrication
[NASA-TM-104410] N91-23946
Research and development on advanced silicon carbide thin film growth techniques and fabrication of high power and microwave frequency silicon carbide-based device structures
[AD-A232160] N91-23955
Silicon carbide, an emerging high temperature semiconductor N91-24061
SILICON DIOXIDE
Flexible fluoropolymer filled protective coatings N91-24062
SILICON NITRIDES
Mechanical behavior and failure phenomenon of an in situ-toughened silicon nitride
[NASA-TM-103741] N91-23311
Mechanistic studies of pressure-assisted superplasticity of structural ceramics
[AD-A232034] N91-23322
SILICON OXIDES
Solid-phase equilibria for Metal-Silicon-Oxygen ternary systems. Part 2: Sc, Y, and La
[AD-A232150] N91-23281
Investigation of neutral atom and ion emission during laser conditioning of multilayer HfO2-SiO2 coatings
[DE91-009749] N91-23860
SILOXANES
Stress-density variations in alumina sediments: Effects of polymer chemistry
[DE91-009055] N91-23313
SILVER
In-situ surface x ray scattering measurements of electrochemically deposited bismuth on silver (III): Structure, compressibility, and comparison with ex-situ leed measurements
[AD-A232624] N91-23880
Surface x ray scattering measurements of the substrate induced spatial modulation of an incommensurate adsorbed monolayer
[AD-A232625] N91-23959
A Raman spectroscopic and electrochemical study of the photoinduced crystallization of triethylenediamine triiodide upon a silver electrode
[AD-A232828] N91-23963
SILVER HALIDES
Optical and mechanical properties of mixed silver halide crystals N91-23837
SIMD (COMPUTERS)
The CERBERUS Ver. 02 code: A parallel six-equation thermal-hydraulic-system simulation code
[DE91-010079] N91-23736
SIMULATION
Simulation of iced wing aerodynamics
[NASA-TM-104362] N91-23086
Predictions and verification of ESD tests made with sphere injections on a flight representative telecommunication satellite: ARABSAT STM
[REPT-911-440-109] N91-23224
A simulation of the draping and a model of the consolidation of commingled fabrics N91-23239
Materials and structure for Hermes
[REPT-911-430-117] N91-23258
An event-activation record approach to simulation modeling in Ada: User's guide
[AD-A232093] N91-23768
Performance analysis of static locking in replicated distributed database systems N91-23974
A note on the performance analysis of static locking in distributed database systems N91-23975
SIMULATORS
Space and telescience robotics: Development of concepts and reference technologies for teledetection and robotics in extreme environments N91-23580
Building real-time simulators for space applications N91-23587
Molecular dynamics simulator for optimal control of molecular motion
[AD-A232801] N91-23881
Building a generalized distributed system model N91-23971
SINGLE CRYSTALS
Development of a micromechanic theory of constitutive relations of polycrystalline solids
[AD-A232697] N91-23559
SINGULARITY (MATHEMATICS)
Hairpin vortices, singularities, and transition to turbulence in three-dimensional shear flows
[DE91-002792] N91-23430
SINTERING
High-temperature alloys for high-power thermionic systems
[DE91-009292] N91-23299
Mechanical behavior and failure phenomenon of an in situ-toughened silicon nitride
[NASA-TM-103741] N91-23311
Stress-density variations in alumina sediments: Effects of polymer chemistry
[DE91-009055] N91-23313
Sintering and hot isostatic pressing of Bi2Sr2CaCu2O(x)
[DE91-010797] N91-23945
SKEWNESS
Use of secondary flows for rapid mixing in scramjet combustors N91-23167
SKIN (ANATOMY)
Laser hazards bibliography, January 1991
[AD-A232690] N91-23487
The transfer of technology to measure skin burn depth in humans N91-24076
SKIN FRICTION
Viscous three-dimensional analyses for nozzles for hypersonic propulsion N91-23175
SKY SURVEYS (ASTRONOMY)
ROSAT: An international mission exploring the high energy universe
[NASA-TM-104958] N91-23214
SLEEP
Some problems of desynchronisation of sleep-wakefulness and circadian rhythms for long duration spaceflights N91-23570
SLEEP DEPRIVATION
Some problems of desynchronisation of sleep-wakefulness and circadian rhythms for long duration spaceflights N91-23570
Strategies to sustain and enhance performance in stressful environments
[AD-A232698] N91-23714
SLENDER BODIES
Benchmarking numerical predictions with force and moment measurements on slender, supercavitating bodies
[DE91-007066] N91-23432
SLIDING FRICTION
A tribological study of sliding contact interaction N91-23488
SLOPES
The solidification of a molten droplet on an inclined plane
[NPL-DMM(A)-20] N91-23438
SLOTS
Experimental study of narrow slot, cavity-backed apertures with finite wall conductivity
[DE91-009039] N91-23352
SMOKE DETECTORS
Aircraft Command in Emergency Situations (ACES). Phase 1: Concept development
[DOT/FAA/CT-90/21] N91-23097
SMOOTHING
Two dimensional optimization of smoothing properties of multistage schemes applied to hyperbolic equations
[VKI-TN-173] N91-23807
SNOW COVER
The application of equilibrium climate models to questions of glaciation at high latitudes N91-23669
SOCIAL FACTORS
The changing face of the environmental issue
[PB91-138081] N91-23624
SODAR
A one dimensional wind profile model with stability and eddy viscosity estimations from sodar data
[DM-56] N91-23680
SODIUM COMPOUNDS
Study of the response of a crystal ball made of NaI(Tl) for heavy ions experiments
[NOTA-INTERNA-957] N91-23874
SODIUM SULFUR BATTERIES
SEI rover solar-electrochemical power system options
[NASA-TM-104402] N91-23620
SOFTWARE ENGINEERING
CESAR operating system
[FFI-91/7002] N91-23754
Specifications for reusable software components
[RR-828-I-IMAG-116-LIFIA] N91-23756
Software testing for evolutionary iterative rapid prototyping
[AD-A232555] N91-23771
Software reverse engineering
[AD-A232644] N91-23773
CLIPS: A tool for the development and delivery of expert systems N91-24043
Software reengineering N91-24047
SOFTWARE TOOLS
NAS operational test and evaluation/integration of the Maintenance Management System (MMS) test plan
[DOT/FAA/CT-TN90/41] N91-23075
Object oriented programming in MMI: A software tool for analysis and planification of a radar imaging mission N91-23589
Quantitative processing of Meteosat data: Implementation at KNMI: Applications
[KNMI-TR-127] N91-23678
Hypermedia 1990 structured Hypertext tutorial
[NASA-CR-187921] N91-23731
NODEN user's guide and installation manual
[RSRE-MEMO-4438] N91-23753
Software testing for evolutionary iterative rapid prototyping
[AD-A232555] N91-23771
Building a generalized distributed system model N91-23971
CLIPS: A tool for the development and delivery of expert systems N91-24043
Genetic algorithms N91-24050
SOIL MECHANICS
Review of finite element procedures for earth retaining structures
[AD-A232230] N91-23343
SOILS
Detection of mining activities in the Yanomani Indian Reserve through LANDSAT-TM imagery
[INPE-5182-RPE/638] N91-23609
Surface layer transfer processes over vegetation: A micrometeorological field experiment of long duration N91-23664
SOLAR ATMOSPHERE
Soft x ray/extreme ultraviolet images of the solar atmosphere with normal incidence multilayer optics N91-24006
SOLAR CELLS
Optimization of transparent and reflecting electrodes for amorphous silicon solar cells
[DE91-002132] N91-23618
PV concentrators today and tomorrow
[DE91-010577] N91-23619
SEI rover solar-electrochemical power system options
[NASA-TM-104402] N91-23620
SOLAR COLLECTORS
Qualification of concentrating mirror systems with the Hermes measurement system and the Helios simulation program
[ESA-TT-1213] N91-23230
SOLAR CORONA
Soft x ray/extreme ultraviolet images of the solar atmosphere with normal incidence multilayer optics N91-24006
SOLAR ENERGY
Infrared and visible studies of Pakistan portion of Arabian Sea using INSAT geostationary satellite N91-23611
Solar thermal energy receiver
[NASA-CASE-LEW-14949-1] N91-23617
SOLAR ENERGY CONVERSION
Component technology for stirling power converters
[NASA-TM-104387] N91-23234
SOLAR GENERATORS
PV concentrators today and tomorrow
[DE91-010577] N91-23619
SOLAR NEUTRINOS
The Sudbury Neutrino Observatory project and the Kamiokande 2 project
[DE91-010641] N91-23863
SOLAR OBSERVATORIES
The Sudbury Neutrino Observatory project and the Kamiokande 2 project
[DE91-010641] N91-23863
SOLAR RADIATION
Qualification of concentrating mirror systems with the Hermes measurement system and the Helios simulation program
[ESA-TT-1213] N91-23230

Applications of energetic particles in improving coating adhesion properties
[DE91-008833] N91-23312

SOLAR REFLECTORS
Qualification of concentrating mirror systems with the Hermes measurement system and the Helios simulation program
[ESA-TT-1213] N91-23230

SOLAR ROTATION
Auroral boundary index from 1983 to 1990
[AD-A232845] N91-23660

SOLAR SPECTRA
High resolution imaging for Brackett gamma and H2 1-0 S(1) emission in the Seyfert galaxy NGC 1068
[MPE-PREPRINT-192] N91-23104
The molecular interstellar medium and the near-infrared continuum of the barred liner NGC 6764
[MPE-PREPRINT-193] N91-24029

SOLAR SYSTEM
Cryomagmatism in the outer solar system N91-24019

SOLAR WIND
Geomagnetic storms: Potential economic impacts on electric utilities
[DE91-009523] N91-24036

SOLID CRYOGENS
Ionic solid hydrogen fuel: Experimental investigation of cluster-impact fusion
[AD-A232642] N91-23336

SOLID ELECTROLYTES
Solid polymer electrolytes for rechargeable batteries
[DE91-010231] N91-23384

SOLID LUBRICANTS
Fundamental research on tribology
[AD-A232446] N91-23519

SOLID PHASES
Solid-phase equilibria for Metal-Silicon-Oxygen ternary systems. Part 2: Sc, Y, and La
[AD-A232150] N91-23281

SOLID ROCKET PROPELLANTS
Response of simulated propellants and explosives to projectile impact
[DE91-009777] N91-23333

SOLID SOLUTIONS
Phase transformations and microstructural evolution in aged Mn-Cu-based alloys
[AD-A232473] N91-23305

SOLID STATE
Oxygen production using solid-state zirconia electrolyte technology N91-24059

SOLID STATE LASERS
Contract crystal growth and fabrication services
[AD-A232120] N91-23952

SOLID-SOLID INTERFACES
A study of the micromechanics of the fiber-matrix interphase in monofilament composites, in monotonic loading, and cyclic fatigue N91-23241

SOLIDIFICATION
Phase equilibria and solidification of Al-Li and Al-Li-Cu alloys N91-23290
Modeling second-phase formation during rapid resolidification of stainless steel alloys
[DE91-008567] N91-23291
The solidification behavior of an alloy 625/718 variant
[DE91-009544] N91-23294
Containerless undercooling and solidification of pure metals
[DLR-FB-90-48] N91-23301
Rapidly solidified metallic alloys with unusual semmetry properties
[AD-A232384] N91-23304
The solidification of a molten droplet on an inclined plane
[NPL-DMM(A)-20] N91-23438

SOLIDS FLOW
Development and utilization of new diagnostics for dense-phase pneumatic transport
[DE91-008947] N91-23339

SOLUTES
Eureca 1 AMF 117 experiment: An analysis of thermal and solutal transfer during the crystal growth of CdTe by the THM process
[REPT-911-430-118] N91-23947
Eureca 1 AMF 117 experience: Thermal and solutal transfer analysis for CdTe in tellurium during crystal growth by the THM method
[REPT-911-430-120] N91-23948

SOLVENTS
Electrodeposited coatings for diamond turning applications
[DE91-009950] N91-23315

SONAR
Control of biosonar behavior by the auditory cortex
[AD-A232699] N91-23708

SOOT
Computer modeling of soot formation comparing free radical and ionic mechanisms
[AD-A232820] N91-23287

SOUND PROPAGATION
Unified aeroacoustics analysis for high speed turboprop aerodynamics and noise. Volume 2: Development of theory for wing shielding
[NASA-CR-185192] N91-23849

SOUND WAVES
Investigation of Roe's 2D wave decomposition models for the Euler equations
[VKI-TN-172] N91-23436
Arctic remote autonomous measurement platform post CEAREX engineering report
[AD-A232843] N91-23471
Soviet atmospheric acoustics research N91-23848

SOUNDING ROCKETS
Echo 7: Magnetospheric properties determined by artificial electron beams N91-23644

SOUTHERN HEMISPHERE
Maintenance of short-term subtropical wind maxima in the Southern Hemisphere: Observational and modeling study N91-23665

SOUTHERN OSCILLATION
Atmospheric teleconnections: Emphasis on the El Nino/Southern Oscillation and monsoons N91-23636

SPACE BASED RADAR
Characteristics and performance of an operational windscatterometer N91-23607

SPACE CHARGE
Quantum extension of Child-Langmuir law
[AD-A232407] N91-23878

SPACE COMMERCIALIZATION
Survey: Potential of the Israeli industry for space technology
[CEMA-86-17] N91-23967

SPACE COMMUNICATION
A 30 GHz monolithic receive module
[NASA-CR-187085] N91-23346
Unattended network operations technology assessment study. Technical support for defining advanced satellite systems concepts
[NASA-CR-187080] N91-24030
Microwave integrated circuits for space applications N91-24069

SPACE ENVIRONMENT SIMULATION
Subsea habitats and space simulation N91-23567
Long duration hyperbaric confinement: Hydra 9 N91-23571
Comparisons between underwater and space working environments for on board activities optimization (Columbus space programme) N91-23574

SPACE EXPLORATION
America at the threshold N91-23201
ROSAT: An international mission exploring the high energy universe
[NASA-TM-104958] N91-23214
An assessment of technology alternatives for telecommunications and information management for the space exploration initiative
[NASA-TM-103783] N91-23347
Government/industry response to questionnaire on space mechanisms/tribology technology needs
[NASA-TM-104358] N91-23501
Unattended network operations technology assessment study. Technical support for defining advanced satellite systems concepts
[NASA-CR-187080] N91-24030

SPACE MISSIONS
Large space structures fielding plan
[AD-A232097] N91-23227
Government/industry response to questionnaire on space mechanisms/tribology technology needs
[NASA-TM-104358] N91-23501
Optical communication for space missions N91-24070

SPACE NAVIGATION
High precision applications of the global positioning system N91-24073

SPACE PLASMAS
Thermal ion upwelling in the high-altitude ionosphere
[AD-A232372] N91-23657
A method for solving Poisson's equation in geophysical and astrophysical plasma
[AERONOMICA-ACTA-A-357-1990] N91-23925

SPACE PLATFORMS
Large space structures fielding plan
[AD-A232097] N91-23227
Distributed radar sensors for aircraft detection
[DE91-009845] N91-23350
Research and development of future space robotics in NASDA N91-23582

SPACE POWER REACTORS
A comparison between classical and substructuring finite-element stress analysis of a complex vacuum vessel shell
[DE91-010035] N91-23540

SPACE PROCESSING
Containerless undercooling and solidification of pure metals
[DLR-FB-90-48] N91-23301

SPACE PROGRAMS
Large space structures fielding plan
[AD-A232097] N91-23227
Remote sensing performances
[REPT-911-440-101] N91-23615
Aeronautics and space report of the President N91-24085

SPACE SHUTTLE MAIN ENGINE
The application of neural networks to the SSME startup transient
[NASA-CR-187138] N91-23205
A simplified dynamic model of the Space Shuttle main engine
[NASA-TM-104421] N91-23340
Parametric study in weld mismatch of longitudinally welded SSME HPFTP inlet
[NASA-TM-103534] N91-23502

SPACE SHUTTLE ORBITERS
Simulation and analyses of the aeroassist flight experiment attitude update method
[NASA-TM-102174] N91-23210

SPACE SHUTTLES
Atmospheric turbulence review of space shuttle launches
[NASA-TM-4289] N91-23215
Localized corrosion of high performance metal alloys in an acid/salt environment N91-24066

SPACE STATION PAYLOADS
Astromag phase A assembly and servicing operations report
[NASA-CR-186262] N91-23206
Astromag data system concept
[NASA-CR-186341] N91-23211

SPACE STATION POLAR PLATFORMS
Medium Resolution Imaging Spectrometer (MERIS) N91-23608

SPACE STATIONS
Astromag phase A assembly and servicing operations report
[NASA-CR-186262] N91-23206

SPACE STORAGE
Test on parabolic flights for stowage in weightlessness N91-23578

SPACE SUITS
Neutral buoyancy and microgravity: Extravehicular activities with a humid water suit N91-23579
EVA/robotics integration for Space Station Freedom N91-23583

SPACE SURVEILLANCE (SPACEBORNE)
Implications of adaptive cancellation array processing for design of a space-based surveillance radar
[RSRE-MEMO-4410] N91-23364

SPACE TRANSPORTATION
Activities report of the DLR
[ISSN-0938-2194] N91-24086

SPACE TRANSPORTATION SYSTEM
Problems of hypersonic aerothermodynamics
[MBB-FE202/5/PUB/436] N91-23090
Airbreathing propulsion for space transport: New concepts, special problems and attempts at solutions N91-23154

SPACE-TIME FUNCTIONS
Symmetries in general relativity N91-23966

SPACEBORNE ASTRONOMY
Small Explorer project: Submillimeter Wave Astronomy Satellite (SWAS). Mission operations and data analysis plan
[NASA-CR-186954] N91-23212

SPACEBORNE EXPERIMENTS
Feasibility study of the Superconducting Gravity Gradiometer (SGG) flight test on the European Retrievable Carrier (EURECA)
[NASA-CR-184157] N91-23229
In-Space technology experiments program. A high efficiency thermal interface (using condensation heat transfer) between a 2-phase fluid loop and heatpipe radiator: Experiment definition phase
[NASA-CR-186869] N91-23408

SPACECRAFT
Aerocoat thermal protections
[REPT-911-430-102] N91-23217

SPACECRAFT CHARGING
Design rules and system testing methods
[REPT-911-440-107] N91-23222

Predictions and verification of ESD tests made with sphere injections on a flight representative telecommunication satellite: ARABSAT STM
[REPT-911-440-109] N91-23224

SPACECRAFT COMPONENTS
Government/industry response to questionnaire on space mechanisms/tribology technology needs
[NASA-TM-104358] N91-23501

SPACECRAFT CONSTRUCTION MATERIALS
Materials for hypersonic engines N91-23177
Laboratory study of the thermochemical properties of materials used in spacecraft
[AD-A232124] N91-23228
Characterization of composite materials for aerospace materials
[DLR-MITT-90-15] N91-23246
Carbon-carbon material with oxidation protection
[REPT-911-430-103] N91-23249
New developments in composites for space applications
[REPT-911-430-104] N91-23250
Oxidation resistant carbon/carbon materials
[REPT-911-430-105] N91-23251
Fiber-reinforced glass-ceramic matrix composites: New class of materials for space applications
[REPT-911-430-107] N91-23253
Ceramics in aerospace
[REPT-911-430-127] N91-23260
How to know CMC
[REPT-911-430-130] N91-23262

SPACECRAFT CONTROL
An artificial neural network control system for spacecraft attitude stabilization
[AD-A232013] N91-23225

SPACECRAFT ELECTRONIC EQUIPMENT
The Combined Release and Radiation Effects Satellite program (CRRES): A unique series of scientific experiments
[NASA-TM-104957] N91-23213

SPACECRAFT LAUNCHING
Design considerations of a high expansion ratio hydrogen turbine N91-23163
Atmospheric turbulence review of space shuttle launches
[NASA-TM-4289] N91-23215

SPACECRAFT MANEUVERS
Satellite maneuver evaluation tool
[AD-A232016] N91-23226

SPACECRAFT POWER SUPPLIES
Liquid-metal MHD power conversion for space electric systems
[SER-S/27] N91-23231

SPACECRAFT PROPULSION
Mars manned fusion spaceship
[NASA-CR-188215] N91-23232
Ionic solid hydrogen fuel: Experimental investigation of cluster-impact fusion
[AD-A232642] N91-23336
Gas core reactors for direct nuclear propulsion
[DE91-010050] N91-23884

SPACECRAFT RADIATORS
A new generation of radiators
[REPT-911-440-105] N91-23220
In-Space technology experiments program. A high efficiency thermal interface (using condensation heat transfer) between a 2-phase fluid loop and heatpipe radiator: Experiment definition phase
[NASA-CR-186869] N91-23408

SPACECRAFT STRUCTURES
Materials for hypersonic engines N91-23177
High temperature composites in space planes and missiles development
[REPT-911-430-119] N91-23259

SPACECRAFT TEMPERATURE
A new generation of radiators
[REPT-911-440-105] N91-23220

SPATIAL DISTRIBUTION
Spatiotemporal characteristics of visual localization
[AD-A232734] N91-23715

SPECIFIC IMPULSE
Ionic solid hydrogen fuel: Experimental investigation of cluster-impact fusion
[AD-A232642] N91-23336
Gas core reactors for direct nuclear propulsion
[DE91-010050] N91-23884

SPECIFICATIONS
Transition space
[AD-A231404] N91-23732

SPECIMENS
Experimentation facilities for thermomechanical static tests with analytic test specimens at Aerospatiale
[REPT-911-430-108] N91-23197

SPECKLE INTERFEROMETRY
Applications of speckle interferometry and speckle photometry to the Hyades cluster N91-24001

SPECTRA
Re-analysis of photoemission data for CuO: Revision of the configuration-energy scheme for cuprate materials
[DE91-009952] N91-23296

SPECTRAL EMISSION
The high energy spectrum of the 1983, August 1b gamma-ray burst
[MPE-PREPRINT-194] N91-24040

SPECTRAL METHODS
Design of an enhanced global spectral model
[AD-A232123] N91-23655
On 2+1-dimensional nonlinear integrable systems of Loewner-type
[MATHS-REPT-A-140] N91-23813

SPECTRAL REFLECTANCE
The applicability of thematic mapper data to the classification of tree species and natural age classes
[DLR-FB-90-44] N91-23612

SPECTRAL SENSITIVITY
Scattering in electron spectrometers
[NPL-DMM(A)-19] N91-23467

SPECTRAL THEORY
Initialization of cloud and radiation in the Florida State University global spectral model
[AD-A232425] N91-23682

SPECTROMETERS
Astromag phase A assembly and servicing operations report
[NASA-CR-186262] N91-23206
Astromag data system concept
[NASA-CR-186341] N91-23211
Scattering in electron spectrometers
[NPL-DMM(A)-19] N91-23467
Light particle emissions in heavy ion reactions
[DE91-010746] N91-23871

SPECTROSCOPIC ANALYSIS
Hardening mechanisms and analysis of the structure of the TGDDM/DDS epoxy resin system
[ESA-TT-1202] N91-23319

SPECTROSCOPY
High-precision Fourier transform spectroscopy of atmospheric molecules N91-23637
Excited state structure, energy and electron transfer dynamics of photosynthetic reaction centers: A hole burning study
[DE91-010181] N91-23693
Hepatic metabolism of perfluorinated carboxylic acids: A nuclear magnetic resonance investigation
[AD-A232033] N91-23706
Non-mechanical optical path switching and its application to dual beam spectroscopy including gas filter correlation radiometry
[NASA-CASE-LAR-14588-1-CU] N91-23889
Two-channel spectroscopic polarization modulation ellipsometry
[DE91-010131] N91-23893
Advanced diagnostics for reacting flows
[AD-A232609] N91-23902
Applications of speckle interferometry and speckle photometry to the Hyades cluster N91-24001

SPECTRUM ANALYSIS
The 2-D acousto-optic signal processors for simultaneous spectrum analysis and direction finding
[AD-A232148] N91-23367
A smoothing algorithm for upper-air soundings
[AD-A232853] N91-23661
Research and development involved in creating a quantitative EEG cartography wide band analysis system
[LAAS-91002] N91-23705

SPEED REGULATORS
Control aspects of the brushless doubly-fed machine
[DE91-009707] N91-23387

SPHERES
Numerical simulation and topological analysis of the separated flow around a sphere
[DLR-FB-90-43] N91-23435
The drag of spheres at porosites ranging from an isolated sphere to a packed bed
[CRANFIELD-AERO-9012] N91-23444
Study of the response of a crystal ball made of NaI(Tl) for heavy ions experiments
[NOTA-INTERNA-957] N91-23874

SPHERICAL SHELLS
The direct correlation function of a mixture of hard ions in the mean spherical approximation
[AD-A232452] N91-23879

SPIN DYNAMICS
Comment on: Analytic solution of the Stochastic-Liouville model of spin-exchange
[DE91-010570] N91-23861

SPIN EXCHANGE
Comment on: Analytic solution of the Stochastic-Liouville model of spin-exchange
[DE91-010570] N91-23861

SPIN TESTS
Diagnostic measurements on an aluminized propellant plume during spin and nonspin testing
[AD-A232031] N91-23235

SPIRAL GALAXIES
An observational study of arm structure in normal spiral galaxies N91-24007

SPLINE FUNCTIONS
Q-splines
[RR-830-M] N91-23808
Microscopic heavy-ion theory
[DE91-010739] N91-23869

SPOOLS
Airborne rescue system
[NASA-CASE-ARC-11909-1] N91-23095
Mechanical stress states in heterogeneous, wound rolls
[DE91-009257] N91-23537

SPRAYED COATINGS
Measurement of particle size, velocity and temperature in the plasma spray coating process
[DE91-006208] N91-23317

SPRAYERS
Measurement of particle size, velocity and temperature in the plasma spray coating process
[DE91-006208] N91-23317

SPREADING
Gravity spreading in the dispersion of dense gas plumes
[DE91-010155] N91-23628

SPUTTERING
Applications of energetic particles in improving coating adhesion properties
[DE91-008833] N91-23312
Flexible fluoropolymer filled protective coatings N91-24062

STABILIZATION
An initial study into the influence of control stick characteristics on the handling qualities of a fly-by-wire helicopter N91-23122
Aerodynamics and stabilization of combustion of hydrogen jets injected into subsonic airflow N91-23164
Mixing and non-equilibrium chemical reaction in a compressible mixing layer
[NASA-CR-187084] N91-23181
Rapidly solidified metallic alloys with unusual semmetry properties
[AD-A232384] N91-23304

STAINLESS STEELS
Modeling second-phase formation during rapid resolidification of stainless steel alloys
[DE91-008567] N91-23291
Evaluation of filler metals for high-strength stainless steels
[DE91-009931] N91-23295
The strength and toughness of stainless steels at cryogenic temperature
[DE91-009771] N91-23300

STANDARD DEVIATION
Presentation of a computer program for analysing results of one shot device sensitivity tests: Application to the case of a one shot degenerated sequence
[REPT-911-430-126] N91-23758

STANDARDS
Committee draft for an ISO standard on the acquisition and presentation of multipoint data for plastics
[NPL-DMM(A)-24] N91-23320
Image data compression in JPEG standard
[DLR-FB-90-59] N91-23746
The United Kingdom waveguide power standards above 40 GHz
[RSRE-90023] N91-23845

STAR CLUSTERS
Applications of speckle interferometry and speckle photometry to the Hyades cluster N91-24001
H II regions and young star clusters in the magellanic clouds N91-24004
Near-infrared milliarcsecond observations by the lunar occultation technique N91-24034

STAR FORMATION
H II regions and young star clusters in the magellanic clouds N91-24004
Recent star formation and the galaxy collisions in NGC 520 N91-24021
Studies of molecular excitation in star formation regions N91-24023

STAR FORMATION RATE
Recent star formation and the galaxy collisions in NGC 520 N91-24021

STAR TRACKERS
Simulation and analyses of the aeroassist flight experiment attitude update method
[NASA-TM-102174] N91-23210

STATE ESTIMATION
Real time estimation of aircraft angular attitude
[IAITIC-87-1004] N91-23107

STATIC LOADS
Static feed water electrolysis subsystem development [NASA-CASE-MSC-21577-1-SB] N91-23271
STATIC PRESSURE
An engineering study of altitude determination deficiencies of the Service Aircraft Instrumentation Package (SAIP) [AD-A232055] N91-23145
STATIC TESTS
Experimentation facilities for thermomechanical static tests with analytic test specimens at Aerospatiale [REPT-911-430-108] N91-23197
Computerized system for static and fatigue large scale structural tests: A case study [IAITIC-87-1007] N91-23522
STATISTICAL ANALYSIS
The statistical properties of electromagnetic fields with application to radiation and scattering [DE91-007467] N91-23351
Range reference atmosphere, Shemya [AD-A232813] N91-23685
Range reference atmosphere, Thule [AD-A232831] N91-23686
Statistical models and inference procedures for structural and materials reliability [AD-A232634] N91-23827
Sufficient comparison and modeling of forecasts N91-23829
An observational study of arm structure in normal spiral galaxies N91-24007
STATISTICAL DISTRIBUTIONS
The statistical properties of electromagnetic fields with application to radiation and scattering [DE91-007467] N91-23351
Some remarks on compliance testing [AD-A231936] N91-23635
Statistical methods and neural network approaches for classification of data from multiple sources [NASA-CR-188207] N91-23786
STATISTICAL MECHANICS
The thermodynamic stability of systems containing black holes N91-24022
STATISTICAL TESTS
Model sensitivity in stress-strength reliability computations [AD-A232023] N91-23554
Some remarks on compliance testing [AD-A231936] N91-23635
STEADY STATE
Models of planetary wave propagation in the middle atmosphere N91-23639
Localised symmetric instability: An initial value problem N91-23672
STEADY STATE CREEP
Rate dependent stress-strain behavior of advanced polymer matrix composites [NASA-TM-104070] N91-23244
STEELS
Study of static and dynamic fracture using strain measurements [PB91-132217] N91-23524
Stochastic micromechanical modeling of cleavage fracture in the ductile-brittle transition region N91-23533
STEEPEST DESCENT METHOD
Supersymmetric matter at finite temperature N91-23836
STEERING
Laser optical disk position encoder with active heads N91-24079
STELLAR ENVELOPES
The envelopes of RV Tauri variables N91-24008
STELLAR EVOLUTION
H II regions and young star clusters in the magellanic clouds N91-24004
Primordial lithium, stellar evolution, and cosmology: Lithium in halo stars from standard, diffusive, and rotational stellar evolution and implications for cosmology N91-24024
Radio and infrared studies of mass-losing evolved stars N91-24026
Near-infrared milliarcsecond observations by the lunar occultation technique N91-24034
STELLAR LUMINOSITY
H II regions and young star clusters in the magellanic clouds N91-24004
STELLAR MAGNETIC FIELDS
Relativistic shock waves and the excitation of plerions [DE91-007623] N91-24027
Magnetospheric structure of rotation powered pulsars [DE91-007622] N91-24028
STELLAR MASS
H II regions and young star clusters in the magellanic clouds N91-24004
STELLAR MASS EJECTION
Radio and infrared studies of mass-losing evolved stars N91-24026
STELLAR MODELS
The supernova remnant G109.1-1.0 and the x-ray pulsar 1E2259+586 N91-24002
STELLAR RADIATION
Investigation of the muon component of EAS initiated by primary radiation from Hercules X-1 N91-24037
STELLAR ROTATION
Primordial lithium, stellar evolution, and cosmology: Lithium in halo stars from standard, diffusive, and rotational stellar evolution and implications for cosmology N91-24024
STELLAR SPECTRA
H II regions and young star clusters in the magellanic clouds N91-24004
The envelopes of RV Tauri variables N91-24008
STELLAR SPECTROPHOTOMETRY
The envelopes of RV Tauri variables N91-24008
STELLARATORS
Transport analysis of stellarator reactors [DE91-010489] N91-23914
Inversion of chordal data from the ATF torsatron [DE91-010490] N91-23915
STEREOCHEMISTRY
Atrane and quadroped frameworks in early transition metal and silicon GRO stereochemistry: Monomers and oligomers [AD-A232837] N91-23331
STIFFNESS MATRIX
Analysis of truss frames by method of the stiffness matrix [AD-A232053] N91-23555
STIMULATION
Shape-memory alloy tactical feedback actuator, phase 1 [AD-A231389] N91-23289
STIRLING CYCLE
Component technology for stirling power converters [NASA-TM-104387] N91-23234
STIRLING ENGINES
Solar thermal energy receiver [NASA-CASE-LEW-14949-1] N91-23617
STOCHASTIC PROCESSES
Signals and noise in lasers and atom-field interactions N91-23475
Stochastic micromechanical modeling of cleavage fracture in the ductile-brittle transition region N91-23533
Duality methods for infinite dimensional optimization problems [AD-A232605] N91-23772
On the many-on-one stochastic duel [CEMA-86/11] N91-23828
Comment on: Analytic solution of the Stochastic-Liouville model of spin-exchange [DE91-010570] N91-23861
STOPPING
Obstacle avoidance for redundant robots using configuration control [NASA-CASE-NPO-17852-1-CU] N91-23783
STORAGE BATTERIES
Evaluation of cathode materials for high energy lithium secondary batteries [DE91-764240] N91-23385
STORAGE RINGS (PARTICLE ACCELERATORS)
Constant of motion and dynamic equations for one-dimensional autonomous system and radiation damping [DE91-011002] N91-23547
Lectures on accelerator physics [DE91-010376] N91-23886
STORAGE TANKS
Superplastic forming of Al-Li alloys for lightweight, low-cost structures N91-24065
STRAIN DISTRIBUTION
Study of static and dynamic fracture using strain measurements [PB91-132217] N91-23524
STRAIN HARDENING
Approximating the dynamic response of strain-hardening structures [DE91-006392] N91-23534
STRAIN MEASUREMENT
Long time measurements of landing gear loads on SAAB SF-340 commuter aircraft [FFA-TN-1990-53] N91-23138
Study of static and dynamic fracture using strain measurements [PB91-132217] N91-23524
STRAIN RATE
Strain rate sensitivity of polymer-matrix composites under mode I delamination [AD-A232761] N91-23268
Time rates of generalized strain tensors. Part 1: Component formulas [AD-A232497] N91-23469
STRANGE ATTRACTORS
A search for strange attractors in the saturation of middle atmosphere gravity waves [AD-A232468] N91-23658
STRANGENESS
The birth of the 'strange' particle physics [NOTA-INTERNA-958] N91-23875
STRATEGY
Information plan study: A strategy model [ISBN-90-6233-638-8] N91-23988
STRATIFIED FLOW
A numerical study of the stratified turbulent Ekman layer N91-23421
STRATOCUMULUS CLOUDS
Observational study of the above-inversion structure and marine stratocumulus cloud clearing episodes during FIRE N91-23666
STRATOSPHERE
Atmospheric turbulence review of space shuttle launches [NASA-TM-4289] N91-23215
STREAMS
Detection of mining activities in the Yanomani Indian Reserve through LANDSAT-TM imagery [INPE-5182-RPE/638] N91-23609
National stream survey database guide [PB91-141804] N91-23625
STRESS (PHYSIOLOGY)
Cultural parameters of stress [AD-A232526] N91-23713
Effectiveness of a prototype microclimate cooling system for use with chemical protective clothing [AD-A231572] N91-23717
STRESS (PSYCHOLOGY)
Human Performance Assessment Methods. Addendum [AGARD-AG-308-ADD] N91-23711
Cultural parameters of stress [AD-A232526] N91-23713
Strategies to sustain and enhance performance in stressful environments [AD-A232698] N91-23714
STRESS ANALYSIS
High shear stress rheology of liquid lubricants N91-23309
Time rates of generalized strain tensors. Part 1: Component formulas [AD-A232497] N91-23469
A tribological study of sliding contact interaction N91-23488
Computational life prediction methodology for mechanical systems using dynamic simulation, finite element analysis, and fatigue life prediction methods N91-23494
Bobbin stresses generated by wire winding [DE91-009545] N91-23526
Stress analysis of a double-doubler joint in composite structure N91-23530
Mechanical states in wound heterogeneous tapes by the finite element method [DE91-009255] N91-23536
Mechanical stress states in heterogeneous, wound rolls [DE91-009257] N91-23537
A comparison between classical and substructuring finite-element stress analysis of a complex vacuum vessel shell [DE91-010035] N91-23540
Linear bending of curved tubes without boundary influence [ETN-91-99255] N91-23552
Elastic/plastic fracture mechanics. Part 2: Marine structural applications [AD-A232560] N91-23557
STRESS DISTRIBUTION
A tribological study of sliding contact interaction N91-23488
Stress analysis of a double-doubler joint in composite structure N91-23530
ACLICO: A computer aided design system for bonded joints [REPT-911-430-101] N91-23757
STRESS INTENSITY FACTORS
A moving boundary algorithm for the solution of contact problems in linear elasticity. Part 1: Basic theory and model examples [FFA-TN-1991-08-PT-1] N91-23759
STRESS RELAXATION
Rate dependent stress-strain behavior of advanced polymer matrix composites [NASA-TM-104070] N91-23244

STRESS TENSORS
Tensor transformations and failure criteria for the analysis of fiber composite materials
[AD-A232238] N91-23265
Time rates of generalized strain tensors. Part 1: Component formulas
[AD-A232497] N91-23469
STRESS-STRAIN RELATIONSHIPS
Experimentation facilities for thermomechanical static tests with analytic test specimens at Aerospatiale
[REPT-911-430-108] N91-23197
Rate dependent stress-strain behavior of advanced polymer matrix composites
[NASA-TM-104070] N91-23244
Combined thermal and bending fatigue of high-temperature metal-matrix composites: Computational simulation
[NASA-TM-104354] N91-23247
Mechanistic studies of pressure-assisted superplasticity of structural ceramics
[AD-A232034] N91-23322
Review of finite element procedures for earth retaining structures
[AD-A232230] N91-23343
STRESSES
Boundary stability under nonequilibrium conditions
[DE91-009262] N91-23293
Stress-density variations in alumina sediments: Effects of polymer chemistry
[DE91-009055] N91-23313
STRIATION
An experimental investigation of vortex pair interaction with a clean or contaminated free surface N91-23419
STRING THEORY
Microscopic heavy-ion theory
[DE91-010739] N91-23869
STRONGLY COUPLED PLASMAS
High quality three dimensional electron gases in semiconductors
[AD-A232779] N91-23406
STRONTIUM COMPOUNDS
Sintering and hot isostatic pressing of Bi2Sr2CaCu2O(x)
[DE91-010797] N91-23945
STRUCTURAL ANALYSIS
Hypersonic numerical simulation: Problems and perspectives. Hypersonic vehicles and numerical simulation in structural analysis
[REPT-911-111-106] N91-23091
Rapidly solidified metallic alloys with unusual semmetry properties
[AD-A232384] N91-23304
Quantum chemical studies of candidate high energy density material compounds
[AD-A232393] N91-23335
Review of finite element procedures for earth retaining structures
[AD-A232230] N91-23343
Parametric study in weld mismatch of longitudinally welded SSME HPFTP inlet
[NASA-TM-103534] N91-23502
Reduced vector basis for dynamic analysis of large damped structures N91-23525
Analysis of truss frames by method of the stiffness matrix
[AD-A232053] N91-23555
STRUCTURAL BASINS
Near-equatorial deep circulation in the Indian and Pacific oceans
[AD-A232635] N91-23691
STRUCTURAL DESIGN
Design techniques for dual mode ram-scramjet combustors N91-23166
Development of a quiet supersonic wind tunnel with a cryogenic adaptive nozzle
[NASA-CR-186769] N91-23195
Elastic/plastic fracture mechanics. Part 2: Marine structural applications
[AD-A232560] N91-23557
Pressure dynamics modeling for the design of the advanced neutron source reactor
[DE91-007860] N91-23883
AGARD highlights 91/1, March 1991
[AGARD-HIGHLIGHTS-91/1] N91-24084
STRUCTURAL FAILURE
Evaluation of catastrophic failure risk in pressure vessels. Results of pressure vessel test with a large vessel (HC2-test)
[VTT-RR-708] N91-23551
Quantitative nondestructive evaluation: Requirements for tomorrow's reliability N91-24074
STRUCTURAL RELIABILITY
Statistical models and inference procedures for structural and materials reliability
[AD-A232634] N91-23827
STRUCTURAL STABILITY
Finite element analysis of the lateral buckling of a cantilevered I Beam
[DE91-010123] N91-23527
A theory for fluidelastic instability of tube-support-plate inactive modes
[DE91-006001] N91-23542
STRUCTURAL VIBRATION
A method for machinery condition monitoring of transient phenomena using the pseudo Wigner-Ville distribution
[AD-A232014] N91-23760
STYRENES
The effect of post-cure and antimony trioxide addition on the glass transition of polyester and vinyl ester resin systems
[AD-A232523] N91-23325
SUBMERGED BODIES
A two-scale solution of the forced Rayleigh-Plesset equation governing the dynamics of cavitation bubble vaporous growth
[AD-A232129] N91-23446
SUBMERGING
Effects of weightlessness (sea water immersion) on body fluid balance and CNS functions N91-23566
SUBMILLIMETER WAVES
Small Explorer project: Submillimeter Wave Astronomy Satellite (SWAS). Mission operations and data analysis plan
[NASA-CR-186954] N91-23212
SUBROUTINE LIBRARIES (COMPUTERS)
An event-activation record approach to simulation modeling in Ada: User's guide
[AD-A232093] N91-23768
SUBROUTINES
Computer programs for simulation of electrodeposition
[DE91-010203] N91-23741
SUBSONIC FLOW
Procedure for determination of three-dimensional wind tunnel wall interferences and wall adaptation in compressible subsonic flow using measured wall pressures
[DLR-FB-90-46] N91-23088
Flow field study of a rectangular jet N91-23423
SUBSTITUTES
Nonlinear real-time optical signal processing
[AD-A232889] N91-23909
SUBSTRATES
Electrodeposited coatings for diamond turning applications
[DE91-009950] N91-23315
Advances in silicon carbide Chemical Vapor Deposition (CVD) for semiconductor device fabrication
[NASA-TM-104410] N91-23946
X ray diffraction and electron spectroscopy of epitaxial molecular C60 films
[AD-A232152] N91-23954
SULFATES
Composition and distribution of carbonates, sulfates, and hydrates on the Martian surface from earth-based spectroscopy between 3-5 microns N91-24033
SULFIDATION
Point defect effects on hot corrosion of zirconia-based coatings
[AD-A232662] N91-23326
SULFONES
Hardening mechanisms and analysis of the structure of the TGDDM/DDS epoxy resin system
[ESA-TT-1202] N91-23319
SULFUR
Forecasting atmospheric particulate sulfur concentrations using national weather service synoptic charts
[AD-A231634] N91-23622
SULFUR DIOXIDES
High temperature membranes for H2S and SO2 separations
[DE91-008534] N91-23275
SULFURIC ACID
Structure of electrochemically deposited copper on gold (III) alloy
[AD-A232345] N91-23303
SUPERCAVITATING FLOW
Benchmarking numerical predictions with force and moment measurements on slender, supercavitating bodies
[DE91-007066] N91-23432
SUPERCOMPUTERS
Decentralized computing technology for fault-tolerant, survivable C3I systems, volume 1
[AD-A232289] N91-23369
Decentralized computing technology for fault-tolerant, survivable C3I systems, volume 2
[AD-A232290] N91-23370
Computer center reference manual, volume 2
[AD-A232370] N91-23781
SUPERCONDUCTING FILMS
Microstructure of epitaxial YBa2Cu3O7 thin films
[DE91-009951] N91-23942
SUPERCONDUCTING MAGNETS
Astromag phase A assembly and servicing operations report
[NASA-CR-186262] N91-23206
Astromag data system concept
[NASA-CR-186341] N91-23211
The strength and toughness of stainless steels at cryogenic temperature
[DE91-009771] N91-23300
Magnet cable manufacturing
[DE91-010210] N91-23935
SUPERCONDUCTING POWER TRANSMISSION
Magnet cable manufacturing
[DE91-010210] N91-23935
SUPERCONDUCTING SUPER COLLIDER
A controlled master frequency oscillator for the SSC low energy booster
[DE91-011004] N91-23391
Magnet cable manufacturing
[DE91-010210] N91-23935
SUPERCONDUCTIVITY
Feasibility study of the Superconducting Gravity Gradiometer (SGG) flight test on the European Retrievable Carrier (EURECA)
[NASA-CR-184157] N91-23229
Re-analysis of photoemission data for CuO: Revision of the configuration-energy scheme for cuprate materials
[DE91-009952] N91-23296
S-parameter measurements and applications of superconducting flux flow transistors
[DE91-009763] N91-23388
Effect of transition metal dopants on high T(sub c) superconductivity
[PB91-130138] N91-23934
Sensitive cryogenic transducer development and analysis for use on gravity wave detectors N91-24009
Aerospace applications of high temperature superconductivity N91-24080
Superconducting microwave electronics at Lewis Research Center N91-24081
SUPERCONDUCTORS
Solid-phase equilibria for Metal-Silicon-Oxygen ternary systems. Part 2: Sc, Y, and La
[AD-A232150] N91-23281
Melt-processed bulk superconductors: Fabrication and characterization for power and space applications N91-24082
SUPERCOOLING
Containerless undercooling and solidification of pure metals
[DLR-FB-90-48] N91-23301
SUPERCRITICAL FLUIDS
Monte Carlo simulation of supercritical solutions in the grand canonical ensemble
[DE91-009152] N91-23859
SUPERFLUIDITY
A cosmic superfluid phase
[NASA-CR-188171] N91-24016
SUPERGRAVITY
Research in particle theory
[DE91-010749] N91-23872
SUPERHIGH FREQUENCIES
Design of inherently wide-band microwave frequency doubler and tripler in microstrip
[FEL-90-B255] N91-23392
SUPERLATTICES
Bromination of carbon fibers and carbon-carbon composites N91-23240
Structural and electronic properties of the ordered ternary 3-5 semiconductors N91-23936
Nonequilibrium Green's functions and quantum transport theory for semiconductor microstructures N91-23937
Strain release in GaAs/Ga(1-x)/In(x)As strained layer superlattices grown on (112) substrates
[DE91-009972] N91-23944
SUPERNOVA REMNANTS
The supernova remnant G109.1-1.0 and the x-ray pulsar 1E2259+586 N91-24002
Relativistic shock waves and the excitation of plerions
[DE91-007623] N91-24027
SUPERPLASTICITY
Mechanistic studies of pressure-assisted superplasticity of structural ceramics
[AD-A232034] N91-23322
Superplastic forming of Al-Li alloys for lightweight, low-cost structures N91-24065
SUPERROTATION
Mechanisms of equatorial superrotation: Studies with two-level models N91-23642
SUPERSONIC COMBUSTION
Hypersonic propulsion: Past and present N91-23148

SUPERSONIC COMBUSTION RAMJET ENGINES
Comparative study of different systems of combined cycle propulsion N91-23152
Hypersonic propulsion: Status and challenge N91-23153
Design techniques for dual mode ram-scramjet combustors N91-23166
Use of secondary flows for rapid mixing in scramjet combustors N91-23167
SUPERSONIC FLIGHT
Trajectory optimization considerations for ramjet engines N91-23151
SUPERSONIC FLOW
Interferometric investigation of supersonic flow fields with shock-shock interactions N91-23082
SUPERSONIC INLETS
Supersonic-hypersonic inlet studies for aerospaceplane N91-23160
SUPERSONIC NOZZLES
The 2-D supersonic nozzle design N91-23176
SUPERSONIC SPEED
Interferometric investigation of supersonic flow fields with shock-shock interactions N91-23082
A study of supersonic and hypersonic ramjet engines in France from 1958 to 1974 (application on combined cycle aircraft engines) N91-23149
Theoretical and experimental performance of a solid fuel ramjet combustion cycle for hypersonic flight conditions N91-23170
Pitot surveys of two moderately under-expanded jets N91-23172
SUPERSONIC TRANSPORTS
Engine technology challenges for a 21st century high speed civil transport
[NASA-TM-104363] N91-23098
Application of multidisciplinary optimization methods to the design of a supersonic transport
[NASA-TM-104073] N91-23135
SUPERSONIC WIND TUNNELS
Interferometric investigation of supersonic flow fields with shock-shock interactions N91-23082
Development of a quiet supersonic wind tunnel with a cryogenic adaptive nozzle
[NASA-CR-186769] N91-23195
SUPERSYMMETRY
Bulletin of the Israel Physical Society, volume 33, 1987. Annual Meeting 1987: Program and Abstracts
[ITN-89-85012] N91-23832
Supersymmetric matter at finite temperature N91-23836
SURFACE CRACKS
Application of elastic and elastic-plastic fracture mechanics methods to surface flaws
[NASA-TM-104964] N91-23539
SURFACE DEFECTS
Application of elastic and elastic-plastic fracture mechanics methods to surface flaws
[NASA-TM-104964] N91-23539
SURFACE ENERGY
A study of the micromechanics of the fiber-matrix interphase in monofilament composites, in monotonic loading, and cyclic fatigue N91-23241
SURFACE FINISHING
Applications of energetic particles in improving coating adhesion properties
[DE91-008833] N91-23312
SURFACE LAYERS
Fundamental studies of electronic packaging materials and structures: Surface and interfaces
[AD-A232336] N91-23403
Surface layer transfer processes over vegetation: A micrometeorological field experiment of long duration N91-23664
SURFACE PROPERTIES
Applications of energetic particles in improving coating adhesion properties
[DE91-008833] N91-23312
The application of equilibrium climate models to questions of glaciation at high latitudes N91-23669
SURFACE STABILITY
Fundamental research on tribology
[AD-A232446] N91-23519
SURFACE TEMPERATURE
Simulation of brush insert for leading-edge-passage convective heat transfer
[NASA-TM-103801] N91-23409
Surface layer transfer processes over vegetation: A micrometeorological field experiment of long duration N91-23664
SURFACE VEHICLES
Computational life prediction methodology for mechanical systems using dynamic simulation, finite element analysis, and fatigue life prediction methods N91-23494
Raybot: A practical implementation of a hierarchical control system for telerobotic land vehicles
[DE90-017029] N91-23507
SURGES
Effects of the northeast monsoon on the equatorial westerlies over Indonesia
[AD-A232106] N91-23681
SURVEILLANCE RADAR
Airborne Collision Avoidance System (ACAS) in controlled air traffic. Aspects of reciprocal influence in Secondary Surveillance Radar (SSR) radio loads
[ETN-91-99253] N91-23105
SURVEYS
Pitot surveys of two moderately under-expanded jets N91-23172
Checklist for thick-film hybrid microcircuits manufacturer and line survey
[ESA-PSS-01-607-ISSUE-1] N91-23396
SUSPENSION SYSTEMS (VEHICLES)
Rule-based motion coordination for the adaptive suspension vehicle on ternary-type terrain
[AD-A232224] N91-23517
SWEDEN
Observation and theory of the radar aurora N91-24017
SWEPT FORWARD WINGS
Flying qualities of the X-29 forward swept wing aircraft N91-23127
SWEPT WINGS
Block implicit multigrid solution of the Euler equations N91-23413
SWITCHES
Photoresponse studies of ion-damaged germanium for optoelectronic switch applications
[AD-A232091] N91-23400
Design and implementation of a packet switched routing chip
[AD-A232286] N91-23401
A non-contacting velocity measurement system
[NASA-CASE-LAR-14466-1] N91-23461
High power light activated semiconductor switches with sub-nanosecond rise time
[DE91-009250] N91-23939
SWITCHING CIRCUITS
A non-contacting velocity measurement system
[NASA-CASE-LAR-14466-1] N91-23461
Optical shutter switching matrix N91-24071
SYMMETRY
Supersymmetric matter at finite temperature N91-23836
Symmetries in general relativity N91-23966
SYNCHRONISM
Transport and nucleation processes in the vapor growth of diamond
[AD-A232135] N91-23953
SYNCHROTRONS
Magnetospheric structure of rotation powered pulsars
[DE91-007622] N91-24028
SYNOPTIC METEOROLOGY
Forecasting atmospheric particulate sulfur concentrations using national weather service synoptic charts
[AD-A231634] N91-23622
SYNTHESIS (CHEMISTRY)
Poly(1,3,4-oxadiazoles) via aromatic nucleophilic displacement
[NASA-CASE-LAR-14427-1] N91-23237
Stress-density variations in alumina sediments: Effects of polymer chemistry
[DE91-009055] N91-23313
Chain propagation/step propagation polymerization. Regular thermoplastic elastomers
[AD-A232356] N91-23324
A novel process for methanol synthesis
[DE91-009808] N91-23334
Synthesis and characterization of indium-arsenic compounds containing a four-membered In-Ad-In-As or In-As-In-Cl ring: Crystal structures of ((Me3SiCH2)2 InAs(SiMe3)2)2 and (Me3SiCH2)2 InAs(SiMe3)2 In(CH2SiMe3)2Cl
[AD-A232368] N91-23956
SYNTHESIZERS
A controlled master frequency oscillator for the SSC low energy booster
[DE91-011004] N91-23391
SYNTHETIC APERTURE RADAR
SAR processor for the ERS-1 data phase 1, simple processor
[FEL-90-B033] N91-23359
Correction of relief-induced radiometric distortions in Seasat-A SAR images for the example of the subscene of Bonn (Fed. Republic of Germany) and vicinities
[DLR-FB-90-54] N91-23613
Sea ice classification using synthetic aperture radar
[AD-A232248] N91-23689
SYNTHETIC APERTURES
Atmospheric optical turbulence measurements taken at Anderson Mesa, Flagstaff, Arizona between 13-19 November 1989
[AD-A232222] N91-23656
SYSTEM EFFECTIVENESS
Statistical process allocation in a parallel processing architecture
[RR-833-I] N91-23779
Abridged USAF STINFO program manager's overview manual
[AD-A232483] N91-23995
SYSTEM FAILURES
Robustness in replicated databases N91-23981
SYSTEMS ANALYSIS
Aerodynamic preliminary analysis system 2. Part 2: User's manual
[NASA-CR-182077] N91-23081
SYSTEMS ENGINEERING
EVA servicing: The Hermes capability N91-23575
How to design efficient MMI for space N91-23586
SYSTEMS INTEGRATION
Application of multidisciplinary optimization methods to the design of a supersonic transport
[NASA-TM-104073] N91-23135
CLIPS: A tool for the development and delivery of expert systems N91-24043
SYSTEMS SIMULATION
An event-activation record approach to simulation modeling in Ada: User's guide
[AD-A232093] N91-23768
SYSTOLIC ARRAYS
Optimal systolic network for Gaussian elimination
[RR-837-I] N91-23822

T

TAIL ASSEMBLIES
Design and construction of a composite airframe for UAV research
[AD-A232422] N91-23143
TAIL ROTORS
Model rotor icing tests in the NASA Lewis icing research tunnel
[NASA-TM-104351] N91-23184
TAKEOFF
Microwave landing system modeling with application to air traffic control
[NASA-TM-102832] N91-23099
Design considerations of a high expansion ratio hydrogen turbine N91-23163
TANDEM MIRRORS
Mars manned fusion spaceship
[NASA-CR-188215] N91-23232
TARGET RECOGNITION
Radar target discrimination and identification using extinction-pulses and single-mode extraction pulses
[AD-A232162] N91-23368
Joint services electronics program
[AD-A232331] N91-23402
TARGETS
Target maneuver models for improved homing guidance N91-23101
Polarimetric radar observations of time-variant random targets
[DLR-FB-90-52] N91-23356
TASKS
Quantifying performance degradation due to the human-machine interface of telemanipulators
[AD-A232814] N91-23723
A user-oriented synthetic workload generator
[NASA-CR-188197] N91-23739
Monitoring an assembly task by perception requests N91-23791
Intelligent planning in controlling electronics assembly N91-23792
TECHNOLOGY ASSESSMENT
Technology needs for high-speed rotorcraft
[NASA-CR-177578] N91-23136
Development of a quiet supersonic wind tunnel with a cryogenic adaptive nozzle
[NASA-CR-186769] N91-23195
Technologies for aerobraking
[NASA-TM-102854] N91-23207
Communication and broadcasting satellites payload reconfiguration technologies
[REPT-911-440-102] N91-23218
An assessment of technology alternatives for telecommunications and information management for the space exploration initiative
[NASA-TM-103783] N91-23347
Federally funded research: Decisions for a decade
[OTA-SET-490] N91-23998

Unattended network operations technology assessment study. Technical support for defining advanced satellite systems concepts
[NASA-CR-187080] N91-24030

TECHNOLOGY TRANSFER
Survey: Potential of the Israeli industry for space technology
[CEMA-86-17] N91-23967
Direct use R/D assistance
[DE91-009976] N91-23999
Technology transfer in a changing national security environment
[AD-A232458] N91-24000
Technology 2000, volume 2
[NASA-CP-3109-VOL-2] N91-24041
Robotic control and inspection verification N91-24075
The transfer of technology to measure skin burn depth in humans N91-24076

TECHNOLOGY UTILIZATION
Design and construction of a composite airframe for UAV research
[AD-A232422] N91-23143
Aerospatiale industrial thermal plasma activities
[REPT-911-430-122] N91-23928
Technology 2000, volume 2
[NASA-CP-3109-VOL-2] N91-24041
Microwave integrated circuits for space applications N91-24069
Optical communication for space missions N91-24070
Aerospace applications of high temperature superconductivity N91-24080

TEETERING
Model rotor icing tests in the NASA Lewis icing research tunnel
[NASA-TM-104351] N91-23184

TELECOMMUNICATION
Conference on Space Technology: Satellite Application Development
[REPT-911-440-103] N91-23219
Eastern Europe: Please stand by
[PB91-14336] N91-23348
A study of PC-Based HF ionospheric propagation predictions for use in naval communications
[AD-A232466] N91-23375
Satellite and aeronautical technologies serving the management of living marine resources N91-23606
Fiber optic sensors for the military
[AD-A232100] N91-23898
Analysis of polarizing optical systems for digital optical computing with symmetric self electrooptic devices
[AD-A232768] N91-23906
Five-year plan for meeting the automatic data processing and telecommunications needs of the Federal Government
[PB91-103549] N91-23982

TELECONNECTIONS (METEOROLOGY)
Atmospheric teleconnections: Emphasis on the El Nino/Southern Oscillation and monsoons N91-23636

TELEOPERATORS
Space and Sea
[ESA-SP-312] N91-23563
Space and telescience robotics: Development of concepts and reference technologies for teledetection and robotics in extreme environments N91-23580
Telerobotics: A key area for possible technology transfer from underwater to space N91-23581
Research and development of future space robotics in NASDA N91-23582
EVA/robotics integration for Space Station Freedom N91-23583
Multisensory telerobotic concepts for space and underwater applications N91-23584
Telemanipulation system assisted by computer for under water applications N91-23585
Robotic control and inspection verification N91-24075

TELEROBOTICS
Raybot: A practical implementation of a hierarchical control system for telerobotic land vehicles
[DE90-017029] N91-23507
Evaluation of multisensor fusion scheme for the localization of underwater remotely operated vehicles N91-23590

TELEVISION EQUIPMENT
Visual presentation and computer animation
[DE91-010599] N91-23745

TELEVISION TRANSMISSION
Digital CODEC for real-time processing of broadcast quality video signals at 1.8 bits/pixel N91-24067

TEMPERATE REGIONS
Effects of the northeast monsoon on the equatorial westerlies over Indonesia
[AD-A232106] N91-23681

TEMPERATURE CONTROL
A new generation of radiators
[REPT-911-440-105] N91-23220
Thermal control system for the investigation of specific absorption rates for specimens exposed to electromagnetic radiation
[AD-A231329] N91-23459
A first-principles generic methodology for representing the knowledge base of a process diagnostic expert system
[DE90-017693] N91-23520

TEMPERATURE DEPENDENCE
Temperature dependence of ultraviolet absorption cross-sections of alternative chlorofluoroethanes
[AERONOMICA-ACTA-A-358-1991] N91-23647
MHD channel gas-side element erosion-corrosion studies
[DE91-008561] N91-23911

TEMPERATURE DISTRIBUTION
Water-cooling technique of high temperature gas turbine blade
[DE91-764238] N91-23506
Infrared and visible studies of Pakistan portion of Arabian Sea using INSAT geostationary satellite N91-23611
Remote sensing of atmospheric temperature fields and the long wave radiation budget in the Antarctic
[ISSN-0069-5882] N91-23652
Temperature distribution and thermal damage during tissue ablation by CO2 laser irradiation: Model and experiment N91-23833

TEMPERATURE EFFECTS
High temperature deformation processes and strengthening mechanisms in intermetallic particulate composites
[AD-A232737] N91-23267
Strain rate sensitivity of polymer-matrix composites under mode I delamination
[AD-A232761] N91-23268
Evaluation of filler metals for high-strength stainless steels
[DE91-009931] N91-23295
High shear stress rheology of liquid lubricants N91-23309
Atmospheric leakage and condensate production in NASA's biomass production chamber. Effect of diurnal temperature cycles
[NASA-TM-103819] N91-23718
Heat strain and work tolerance times with varying levels of Canadian Forces NBC protective clothing, ambient temperature, physical work intensity, and work/rest schedules
[AD-A232653] N91-23720
Temperature distribution and thermal damage during tissue ablation by CO2 laser irradiation: Model and experiment N91-23833

TEMPERATURE GRADIENTS
Experience with conventional inelastic analysis procedures in very high temperature applications
[DE91-009937] N91-23545
Evaluation of generalized thresholds in an objective multispectral satellite cloud analysis
[AD-A232716] N91-23683

TEMPERATURE MEASUREMENT
The VKI hypersonic wind tunnels and associated measurement techniques
[VKI-TM-46] N91-23196
Temperature measurements of ET plasmas using atomic emission spectroscopy
[AD-A232498] N91-23930

TEMPERATURE PROBES
Characterization of the glass transition using a microindenter
[AD-A232154] N91-23282

TEMPERATURE PROFILES
Thermal control system for the investigation of specific absorption rates for specimens exposed to electromagnetic radiation
[AD-A231329] N91-23459
Determination of the temperature profile of the troposphere with a two frequency lidar
[EXAMENARBEIT-8] N91-23653
Microwave temperature profiler for clear air turbulence prediction
[NASA-CASE-NPO-18115-1-CU] N91-23662

TEMPORAL DISTRIBUTION
Spatiotemporal characteristics of visual localization
[AD-A232734] N91-23715

TENSILE STRENGTH
Rapidly solidified metallic alloys with unusual semmetry properties
[AD-A232384] N91-23304

TENSILE TESTS
The development and evaluation of an alternative powder prepregging technique for use with LaRC-TPI/graphite composites
[NASA-CR-188184] N91-23242
A preliminary investigation of acousto-ultrasonic NDE of metal matrix composite test specimens
[NASA-TM-104339] N91-23521

TENSOR ANALYSIS
Tensor transformations and failure criteria for the analysis of fiber composite materials
[AD-A232238] N91-23265
Time rates of generalized strain tensors. Part 1: Component formulas
[AD-A232497] N91-23469

TERMINAL BALLISTICS
Energy-efficient penetration of targets
[AD-A232227] N91-23518

TERMINAL GUIDANCE
Target maneuver models for improved homing guidance N91-23101

TERMINAL VELOCITY
Energy-efficient penetration of targets
[AD-A232227] N91-23518

TERNARY SYSTEMS
Solid-phase equilibria for Metal-Silicon-Oxygen ternary systems. Part 2: Sc, Y, and La
[AD-A232150] N91-23281
Structural and electronic properties of the ordered ternary 3-5 semiconductors N91-23936

TEST CHAMBERS
Joint services electronics program
[AD-A232331] N91-23402

TEST EQUIPMENT
Laboratory study of the thermochemical properties of materials used in spacecraft
[AD-A232124] N91-23228

TEST FACILITIES
Hypersonic propulsion: Status and challenge N91-23153
The VKI hypersonic wind tunnels and associated measurement techniques
[VKI-TM-46] N91-23196
Experimentation facilities for thermomechanical static tests with analytic test specimens at Aerospatiale
[REPT-911-430-108] N91-23197
SIMOUN: A high temperature and low pressure testing facility for material characterization
[REPT-911-430-121] N91-23208
SIMOUN: A .ew test appliance for the development of Hermes thermal protections
[REPT-911-430-129] N91-23209
CRREL research on materials in cold environments
[AD-A232133] N91-23280
Aero-optics measurement system for the AEDC aero-optics test facility
[AD-A232852] N91-23908

TEST FIRING
Pyrotechnical safety of Aerospatiale tactical missiles: Application to conventional warhead
[REPT-911-320-101] N91-23139
The application of neural networks to the SSME startup transient
[NASA-CR-187138] N91-23205

TEST PILOTS
The art of flying qualities testing N91-23109

TEXTS
An expert system for searching in full-text N91-23983

THALLIUM
Surface x ray scattering measurements of the substrate induced spatial modulation of an incommensurate adsorbed monolayer
[AD-A232625] N91-23959

THEMATIC MAPPING
Detection of mining activities in the Yanomani Indian Reserve through LANDSAT-TM imagery
[INPE-5182-RPE/638] N91-23609
The applicability of thematic mapper data to the classification of tree species and natural age classes
[DLR-FB-90-44] N91-23612

THEOREM PROVING
On locking and robustness in the finite element method
[AD-A232245] N91-23815
Symmetries in general relativity N91-23966

THEOREMS
Software reverse engineering
[AD-A232644] N91-23773

THERMAL ANALYSIS
The solidification behavior of an alloy 625/718 variant
[DE91-009544] N91-23294
ISOCAM: The ISO's satellite infra-red camera
[REPT-911-440-104] N91-23468

THERMAL CONDUCTIVITY
Mechanics/heat-transfer relation for particulate materials
[DE91-008356] N91-23424
Evaluation and ranking of candidate ceramic wafer engine seal materials
[NASA-TM-103795] N91-23515

THERMAL CONTROL COATINGS
Point defect effects on hot corrosion of zirconia-based coatings
[AD-A232662] N91-23326
THERMAL CYCLING TESTS
A preliminary investigation of acousto-ultrasonic NDE of metal matrix composite test specimens
[NASA-TM-104339] N91-23521
THERMAL ENERGY
Solar thermal energy receiver
[NASA-CASE-LEW-14949-1] N91-23617
THERMAL FATIGUE
Ion beam testing of the Aerolor X-point dump plate for the Joint European Torus
[DE91-010719] N91-23245
Combined thermal and bending fatigue of high-temperature metal-matrix composites: Computational simulation
[NASA-TM-104354] N91-23247
Boundary stability under nonequilibrium conditions
[DE91-009262] N91-23293
THERMAL INSULATION
Aerocoat thermal protections
[REPT-911-430-102] N91-23217
THERMAL PLASMAS
Thermal ion upwelling in the high-altitude ionosphere
[AD-A232372] N91-23657
Aerospatiale industrial thermal plasmas
[REPT-911-430-113] N91-23927
THERMAL PROTECTION
SIMOUN: A high temperature and low pressure testing facility for material characterization
[REPT-911-430-121] N91-23208
SIMOUN: A new test appliance for the development of Hermes thermal protections
[REPT-911-430-129] N91-23209
Aerocoat thermal protections
[REPT-911-430-102] N91-23217
Carbon/carbon inox thermostructural composites: Mechanical and tectonic behavior of anti-oxidation protection
[REPT-911-430-115] N91-23257
Materials and structure for Hermes
[REPT-911-430-117] N91-23258
THERMAL SHOCK
Potential impact of enhanced fracture-toughness data on fracture mechanics assessment of PWR vessel integrity for pressurized thermal shock
[DE91-009554] N91-23509
THERMAL SIMULATION
Hypersonic numerical simulation: Problems and perspectives. Hypersonic vehicles and numerical simulation in structural analysis
[REPT-911-111-106] N91-23091
THERMAL STABILITY
A study of the critical factors controlling the synthesis of ceramic matrix composites from preceramic polymers
[AD-A232686] N91-23327
The thermodynamic stability of systems containing black holes N91-24022
THERMAL STRESSES
Water-cooling technique of high temperature gas turbine blade
[DE91-764238] N91-23506
Experience with conventional inelastic analysis procedures in very high temperature applications
[DE91-009937] N91-23545
THERMIONIC CONVERTERS
High-temperature alloys for high-power thermionic systems
[DE91-009292] N91-23299
THERMOCHEMICAL PROPERTIES
Laboratory study of the thermochemical properties of materials used in spacecraft
[AD-A232124] N91-23228
THERMOCOUPLES
Method of producing a plug type heat flux gauge
[NASA-CASE-LEW-14967-2] N91-23460
THERMODYNAMIC CYCLES
Advanced working fluids: Thermodynamic properties
[PB91-136465] N91-23964
THERMODYNAMIC EFFICIENCY
Research and development opportunities for natural gas fueled refrigeration in industrial processes
[PB91-136432] N91-23338
THERMODYNAMIC EQUILIBRIUM
Phase equilibria and solidification of Al-Li and Al-Li-Cu alloys N91-23290
The thermodynamic stability of systems containing black holes N91-24022
THERMODYNAMIC PROPERTIES
Ion beam testing of the Aerolor X-point dump plate for the Joint European Torus
[DE91-010719] N91-23245
Thermostructural composites: Recent evolutions and improvements
[REPT-911-430-109] N91-23254
Committee draft for an ISO standard on the acquisition and presentation of multipoint data for plastics
[NPL-DMM(A)-24] N91-23320
Summary of basic research in thermoacoustic heat transport: 1990
[AD-A232223] N91-23847
Epitaxial iron films
[AD-A232419] N91-23958
Advanced working fluids: Thermodynamic properties
[PB91-136465] N91-23964
The thermodynamic stability of systems containing black holes N91-24022
THERMODYNAMICS
Thermo-viscoelastic behavior of composite materials N91-23243
Carbon/carbon inox thermostructural composites: Mechanical and tectonic behavior of anti-oxidation protection
[REPT-911-430-115] N91-23257
Solid-phase equilibria for Metal-Silicon-Oxygen ternary systems. Part 2: Sc, Y, and La
[AD-A232150] N91-23281
Thermodynamically consistent formulations for rapid granular and turbulent multiphase flows N91-23420
Treatment of denser-than-air releases in an advection-diffusion model: Thermodynamic effects
[DE91-010152] N91-23632
Monte Carlo simulation of supercritical solutions in the grand canonical ensemble
[DE91-009152] N91-23859
The thermodynamic stability of systems containing black holes N91-24022
THERMOELASTICITY
Approximation methods for the identification and control of distributed parameter systems with applications to flexible structures
[AD-A232805] N91-23801
Lunar volcanism and the thermal evolution of the moon N91-24031
THERMOMECHANICAL TREATMENT
Experimentation facilities for thermomechanical static tests with analytic test specimens at Aerospatiale
[REPT-911-430-108] N91-23197
Data-reduction and analysis procedures used in NIST's thermomechanical processing research
[PB91-132282] N91-23523
THERMONUCLEAR REACTIONS
Intense light-ion beams provide a robust, common-driver path towards ignition, gain and commercial fusion energy
[DE91-010584] N91-23919
Experimental and theoretical research in applied plasma physics
[DE91-010657] N91-23920
THERMOPLASTIC FILMS
Generation of continuous liquid crystalline polymer reinforcements in thermoplastics by a novel blending process
[AD-A232824] N91-23330
THERMOPLASTIC RESINS
The development and evaluation of an alternative powder prepregging technique for use with LaRC-TPI/graphite composites
[NASA-CR-188184] N91-23242
Strain rate sensitivity of polymer-matrix composites under mode I delamination
[AD-A232761] N91-23268
Chain propagation/step propagation polymerization. Regular thermoplastic elastomers
[AD-A232356] N91-23324
Generation of continuous liquid crystalline polymer reinforcements in thermoplastics by a novel blending process
[AD-A232824] N91-23330
THERMOPLASTICITY
Chain propagation/step propagation polymerization. Regular thermoplastic elastomers
[AD-A232356] N91-23324
Thermoforming of in-situ reinforced thermoplastic composites
[AD-A232816] N91-23329
THERMOSPHERE
Neutral wind vortices in the high-latitude thermosphere N91-23673
THICK FILMS
Dissolution of Poly(p-hydroxystyrene): Molecular weight effects
[AD-A232155] N91-23323
Checklist for thick-film hybrid microcircuits manufacturer and line survey
[ESA-PSS-01-607-ISSUE-1] N91-23396
THICKNESS
Nondestructive measurement of thickness and density of composite materials by Compton backscattering
[REPT-911-430-112] N91-23255
Examination of the microstructure of 7050 aluminum alloy samples
[AD-A232544] N91-23306
Dissolution of Poly(p-hydroxystyrene): Molecular weight effects
[AD-A232155] N91-23323
Effects of rim thickness on spur gear bending stress
[NASA-TM-104388] N91-23500
THIN FILMS
Oxidation studies of fluorine containing diamond films
[AD-A232696] N91-23328
Checklist for thin-film hybrid microcircuits manufacturer and line survey
[ESA-PSS-01-611-ISSUE-1] N91-23397
Electronic GaAs-on-silicon material for advanced high-speed optoelectronic devices
[AD-A232088] N91-23399
Evaluation of ferroelectric materials for memory applications
[AD-A232112] N91-23728
Metal thin-film optical polarizers for space applications, phase 2
[NASA-CR-188202] N91-23891
Research and development on advanced silicon carbide thin film growth techniques and fabrication of high power and microwave frequency silicon carbide-based device structures
[AD-A232160] N91-23955
Flexible fluoropolymer filled protective coatings N91-24062
A conformal oxidation-resistant, plasma-polymerized coating N91-24063
Superconducting microwave electronics at Lewis Research Center N91-24081
THIN PLATES
Birefringent filter design
[NASA-CASE-LAR-13887-1] N91-23472
THREE DIMENSIONAL BODIES
Automated handling and assembling of non-rigid objects
[AD-A231246] N91-23489
A moving boundary algorithm for the solution of contact problems in linear elasticity. Part 1: Basic theory and model examples
[FFA-TN-1991-08-PT-1] N91-23759
THREE DIMENSIONAL BOUNDARY LAYER
A study of three dimensional turbulent boundary layer separation and vortex flow control using the reduced Navier Stokes equations
[NASA-TM-104407] N91-23089
Numerical simulation of transition in three dimensional boundary layers
[ESA-TT-1203] N91-23442
THREE DIMENSIONAL COMPOSITES
Tensor transformations and failure criteria for the analysis of fiber composite materials
[AD-A232238] N91-23265
THREE DIMENSIONAL FLOW
Procedure for determination of three-dimensional wind tunnel wall interferences and wall adaptation in compressible subsonic flow using measured wall pressures
[DLR-FB-90-46] N91-23088
Block implicit multigrid solution of the Euler equations N91-23413
A numerical study of the stratified turbulent Ekman layer N91-23421
Flow field study of a rectangular jet N91-23423
A three-dimensional free-Lagrange code for multimaterial flow simulations
[DE91-002309] N91-23428
Hairpin vortices, singularities, and transition to turbulence in three-dimensional shear flows
[DE91-002792] N91-23430
Numerical simulation of incompressible inhomogeneous turbulence in a plane channel flow
[ESA-TT-1199] N91-23441
Effects of three-dimensional imposed disturbance on bluff-body near wake flows
[AD-A232137] N91-23447
Vortex system evolution in 2- and 3-D swept trailing edge flows
[AD-A232692] N91-23453
THREE DIMENSIONAL MODELS
Flow between eccentric rotating cylinders N91-23417
The problem of plate modeling theoretical and computational results
[AD-A232756] N91-23562
Digital data registration and differencing compression system
[NASA-CASE-SSC-00010-1] N91-23976

Three-dimensional structure of human serum albumin N91-24057

THREE DIMENSIONAL MOTION
Tripod operators for the interpretation of range images [AD-A232631] N91-23344
Hairpin vortices, singularities, and transition to turbulence in three-dimensional shear flows [DE91-002792] N91-23430
Three-dimensional graphical representation of objects according to movement data in realtime [DLR-FB-90-51] N91-23725
Benchmark measurements and calculations of a 3-dimensional neutron streaming experiment [DE91-010692] N91-23867

TIDES
Sea level and satellite techniques N91-23595

TILT WING AIRCRAFT
Technology needs for high-speed rotorcraft [NASA-CR-177578] N91-23136

TIME
Control synthesis based upon a game theoretic approach N91-23831

TIME DEPENDENCE
Thermo-viscoelastic behavior of composite materials N91-23243
Adaptive methods for compressible fluid dynamics [AD-A232786] N91-23455

TIME LAG
SZ series GaAs super high-speed logic gate: Optimum choice. High tech; high speed; high quality [AD-A232819] N91-23962

TIME OF FLIGHT SPECTROMETERS
Microbeam titanium isotopic analysis by resonance ionization mass spectrometry [DE91-010799] N91-23277

TIME SIGNALS
A method for machinery condition monitoring of transient phenomena using the pseudo Wigner-Ville distribution [AD-A232014] N91-23760

TISSUES (BIOLOGY)
Temperature distribution and thermal damage during tissue ablation by CO2 laser irradiation: Model and experiment N91-23833
A non-invasive measure of minerals and electrolytes in tissue N91-24058

TITANIUM
Microbeam titanium isotopic analysis by resonance ionization mass spectrometry [DE91-010799] N91-23277

TITANIUM ALLOYS
High temperature ordered intermetallic alloys [AD-A232769] N91-23308

TITANIUM COMPOUNDS
Radioluminescent (RL) lighting system development program [DE91-009743] N91-23381

TITANIUM ISOTOPES
Microbeam titanium isotopic analysis by resonance ionization mass spectrometry [DE91-010799] N91-23277

TITANIUM OXIDES
Measurements of passive-scalar spectra for grid turbulence using a nonlinear optical technique [DE91-005310] N91-23892
The envelopes of RV Tauri variables N91-24008

TOKAMAK DEVICES
Inversion of chordal data from the ATF torsatron [DE91-010490] N91-23915
Ion confinement and radiation losses in the advanced toroidal facility [DE91-010382] N91-23916
Heavy ion beam probe measurements of ECH method plasma in the advanced toroidal facility [DE91-010391] N91-23917
Comparison of drift wave models with fluctuation data from the interior of the TEXT tokamak [DE91-010424] N91-23918
Hall effects on anomalous heat, particle and helicity transports through tearing-mode turbulence [DE91-010730] N91-23924

TOMOGRAPHY
Parallel-processor-based Gaussian beam tracer for use in ocean acoustic tomography [AD-A232420] N91-23690

TOPEX
Validation requirements for the Topex/Poseidon altimeter mission N91-23602

TOPOLOGY
Numerical simulation and topological analysis of the separated flow around a sphere [DLR-FB-90-43] N91-23435

TORNADOES
The terminal Doppler weather radar tornadic vortex signature detection algorithm [DOT-FAA-NR-91-5] N91-23675

TOROIDAL PLASMAS
Inversion of chordal data from the ATF torsatron [DE91-010490] N91-23915
Ion confinement and radiation losses in the advanced toroidal facility [DE91-010382] N91-23916
Heavy ion beam probe measurements of ECH method plasma in the advanced toroidal facility [DE91-010391] N91-23917

TORQUE
Metallic threaded composite fastener [NASA-CASE-MSC-21580-1] N91-23491

TOUCH
Shape-memory alloy tactical feedback actuator, phase 1 [AD-A231389] N91-23289

TOUGHNESS
The strength and toughness of stainless steels at cryogenic temperature [DE91-009771] N91-23300
Stochastic micromechanical modeling of cleavage fracture in the ductile-brittle transition region N91-23533

TOXIC HAZARDS
Region 10 environmental indicators [PB91-136580] N91-23623
Treatment of denser-than-air releases in an advection-diffusion model: Thermodynamic effects [DE91-010152] N91-23632

TOXICITY
Hepatic metabolism of perfluorinated carboxylic acids: A nuclear magnetic resonance investigation [AD-A232033] N91-23706

TRACE CONTAMINANTS
Tropospheric sampling with aircraft [DE91-009472] N91-23626

TRACKING (POSITION)
The handling qualities of the STOL and maneuver technology demonstrator from specification to flight test N91-23117

TRACKING PROBLEM
H-infinity approach to manipulator control N91-23495

TRADEOFFS
Characteristics of a future aeronautical satellite communications system [NASA-TM-104389] N91-23102

TRAILING EDGES
An experimental investigation of vortex pair interaction with a clean or contaminated free surface N91-23419
Vortex system evolution in 2- and 3-D swept trailing edge flows [AD-A232692] N91-23453

TRAINING DEVICES
Manned diving activities in JAMSTEC N91-23572
Intelligent computer-aided training and tutoring N91-24042

TRAJECTORY ANALYSIS
A vortex panel method for calculating aircraft downwash on parachute trajectories [DE91-009764] N91-23085

TRAJECTORY OPTIMIZATION
Navigation, guidance, and trajectory optimization for hypersonic vehicles N91-23150
Trajectory optimization considerations for ramjet engines N91-23151

TRAJECTORY PLANNING
Articulation of spatial robots N91-23504

TRANSATMOSPHERIC VEHICLES
Airbreathing propulsion for transatmospheric flight N91-23156

TRANSDUCERS
A submicron resolution monolithic capacitive displacement sensor with digital output [DE91-009765] N91-23465
Sensitive cryogenic transducer development and analysis for use on gravity wave detectors N91-24009

TRANSFER FUNCTIONS
A simple solution to the singular linear minimum-variance estimation problem [IAITIC-87-1002-REV] N91-23804

TRANSFER ORBITS
Mars manned fusion spaceship [NASA-CR-188215] N91-23232

TRANSFORMATIONS (MATHEMATICS)
Tensor transformations and failure criteria for the analysis of fiber composite materials [AD-A232238] N91-23265
On 2+1-dimensional nonlinear integrable systems of Loewner-type [MATHS-REPT-A-140] N91-23813

TRANSFORMERS
Conceptual design and system studies for a 600 kW repetitive pulse transformer [DE91-010585] N91-23389

TRANSIENT RESPONSE
The application of neural networks to the SSME startup transient [NASA-CR-187138] N91-23205
Theoretical studies relating to the interaction of radiation with matter [AD-A232107] N91-23480
The transient response of heavily fluid-loaded elastic plates and cylindrical shells N91-23528
A method for machinery condition monitoring of transient phenomena using the pseudo Wigner-Ville distribution [AD-A232014] N91-23760

TRANSISTORS
S-parameter measurements and applications of superconducting flux flow transistors [DE91-009763] N91-23388

TRANSITION FLOW
Hairpin vortices, singularities, and transition to turbulence in three-dimensional shear flows [DE91-002792] N91-23430

TRANSITION METALS
Atrane and quadroped frameworks in early transition metal and silicon GRO stereochemistry: Monomers and oligomers [AD-A232837] N91-23331
First principles calculation of the crystal structures in the 4d transition metals N91-23835

TRANSITION TEMPERATURE
Theory of the new high-temperature superconductors N91-23842

TRANSLATING
Software reverse engineering [AD-A232644] N91-23773
On a phonetic and structural encoding of Chinese characters in Chinese texts [RR-835-I] N91-23989

TRANSMISSION LINES
A transmission line method for the measurement of microwave permittivity and permeability [RSRE-MEMO-4450] N91-23394

TRANSMITTANCE
SZ series GaAs super high-speed logic gate: Optimum choice. High tech; high speed; high quality [AD-A232819] N91-23962

TRANSONIC FLOW
A study of the noise mechanisms of transonic blade-vortex interactions [NASA-CR-188199] N91-23084
Block implicit multigrid solution of the Euler equations N91-23413
The propagation of acoustic disturbances in the transonic flow fields of wings [ESA-TT-1126] N91-23854

TRANSONIC FLUTTER
The propagation of acoustic disturbances in the transonic flow fields of wings [ESA-TT-1126] N91-23854

TRANSONIC NOZZLES
Aero-thermal investigation of a highly loaded transonic linear turbine guide vane cascade. A test case for inviscid and viscous flow computations [VKI-TN-174] N91-23437

TRANSPARENCE
Optimization of transparent and reflecting electrodes for amorphous silicon solar cells [DE91-002132] N91-23618

TRANSPORT AIRCRAFT
Handling qualities guidelines for the design of fly-by-wire flight control systems for transport aircraft N91-23119
Observatory of new materials. Evolution perspectives for the materials used in civil transportation aircraft [REPT-911-111-107] N91-23248

TRANSPORT PROPERTIES
Computer programs for simulation of electrodeposition [DE91-010203] N91-23741
Transport analysis of stellarator reactors [DE91-010489] N91-23914
Hall effects on anomalous heat, particle and helicity transports through tearing-mode turbulence [DE91-010730] N91-23924
Theoretical and numerical study of anomalous turbulent transport in plasmas [AD-A232688] N91-23931
Effect of transition metal dopants on high T(sub c) superconductivity [PB91-130138] N91-23934

TRANSPORT THEORY
On standard forms for transport equations and fluxes, part 2 [DE91-010421] N91-23912
Nonequilibrium Green's functions and quantum transport theory for semiconductor microstructures N91-23937

TRANSPUTERS
Three-dimensional graphical representation of objects according to movement data in realtime [DLR-FB-90-51] N91-23725

TRANSVERSE WAVES
Hydromagnetic wave coupling in the magnetosphere N91-23638
TRAPPED PARTICLES
Infrared focal plane performance in the South Atlantic anomaly
[NASA-CR-186197] N91-23458
TRAYS
Protein crystal growth tray assembly
[NASA-CASE-MFS-28507-1] N91-23933
TREES
Analysis on forest decline classification of the beech using airborne multispectral scanner data
[DLR-FB-90-56] N91-23614
TREES (MATHEMATICS)
An in-depth analysis of concurrent B-tree algorithms
[AD-A232287] N91-23770
A survey of decision tree classifier methodology
[NASA-CR-188208] N91-23806
TREES (PLANTS)
The applicability of thematic mapper data to the classification of tree species and natural age classes
[DLR-FB-90-44] N91-23612
TRIANGULATION
Robot self-location in unknown environments
[DE91-010450] N91-23505
TRIBOLOGY
Materials and material systems for combined cycle engines N91-23178
A tribological study of sliding contact interaction N91-23488
Government/industry response to questionnaire on space mechanisms/tribology technology needs
[NASA-TM-104358] N91-23501
Fundamental research on tribology
[AD-A232446] N91-23519
TRIGGER CIRCUITS
High power light activated semiconductor switches with sub-nanosecond rise time
[DE91-009250] N91-23939
TRIGONOMETRIC FUNCTIONS
A fast algorithm for the evaluation of trigonometric series
[AD-A232848] N91-23775
TRIPODS
Tripod operators for the interpretation of range images
[AD-A232631] N91-23344
TRITIUM
Measurement control for calorimetric assay
[DE91-009445] N91-23274
Transport analysis of stellarator reactors
[DE91-010489] N91-23914
TROPICAL REGIONS
Maintenance of short-term subtropical wind maxima in the Southern Hemisphere: Observational and modeling study N91-23665
The annual march of convection, sea surface temperature, and surface winds in the tropics N91-23667
TROPOSPHERE
Tropospheric sampling with aircraft
[DE91-009472] N91-23626
Mechanisms of equatorial superrotation: Studies with two-level models N91-23642
Determination of the temperature profile of the troposphere with a two frequency lidar
[EXAMENARBEIT-8] N91-23653
Effects of the northeast monsoon on the equatorial westerlies over Indonesia
[AD-A232106] N91-23681
TROPOSPHERIC SCATTERING
An analysis of MLAYER: A multilayer tropospheric propagation program
[AD-A232733] N91-23379
TROUGHS
Theoretical studies of large-scale features of the Earth's mid- to high-latitude ionosphere N91-23641
Effects of the northeast monsoon on the equatorial westerlies over Indonesia
[AD-A232106] N91-23681
TRUNCATION ERRORS
Real-time simulation of constrained dynamic systems N91-23189
TRUSSES
Analysis of truss frames by method of the stiffness matrix
[AD-A232053] N91-23555
TUBE HEAT EXCHANGERS
A theory for fluidelastic instability of tube-support-plate inactive modes
[DE91-006001] N91-23542
TUNABLE LASERS
Multiphoton detection techniques for F and F2
[AD-A232641] N91-23286
Birefringent filter design
[NASA-CASE-LAR-13887-1] N91-23472
Optical parametric oscillators pumped by excimer lasers N91-23473
Signals and noise in lasers and atom-field interactions N91-23475
TUNGSTEN ALLOYS
High-temperature alloys for high-power thermionic systems
[DE91-009292] N91-23299
TUNING
Mechanical component diagnostic system
[AD-A232126] N91-23146
Birefringent filter design
[NASA-CASE-LAR-13887-1] N91-23472
TURBINE BLADES
Water-cooling technique of high temperature gas turbine blade
[DE91-764238] N91-23506
TURBINE ENGINES
Multi-heat addition turbine engine
[NASA-CASE-LEW-15094-1] N91-23180
TURBINE PUMPS
Parametric study in weld mismatch of longitudinally welded SSME HPFTP inlet
[NASA-TM-103534] N91-23502
TURBINE WHEELS
A three-dimensional Navier-Stokes stage analysis of the flow through a compact radial turbine
[NASA-TM-104420] N91-23186
TURBINES
Design considerations of a high expansion ratio hydrogen turbine N91-23163
A three-dimensional Navier-Stokes stage analysis of the flow through a compact radial turbine
[NASA-TM-104420] N91-23186
Mechanical behavior and failure phenomenon of an in situ-toughened silicon nitride
[NASA-TM-103741] N91-23311
TURBOFAN ENGINES
NASA aeropropulsion research in support of propulsion systems of the 21st century
[NASA-TM-104403] N91-23083
TURBOJET ENGINES
Comparative study of different systems of combined cycle propulsion N91-23152
Turbojet potential for hypersonic flight N91-23155
TURBOMACHINERY
Fundamental hydrodynamics research
[AD-A232650] N91-23451
TURBOPROP AIRCRAFT
Unified aeroacoustics analysis for high speed turboprop aerodynamics and noise. Volume 2: Development of theory for wing shielding
[NASA-CR-185192] N91-23849
Unified aeroacoustics analysis for high speed turboprop aerodynamics and noise. Volume 3: Application of theory for blade loading, wakes, noise, and wing shielding
[NASA-CR-185193] N91-23850
Unified aeroacoustics analysis for high speed turboprop aerodynamics and noise. Volume 4: Computer user's manual for UAAP turboprop aeroacoustic code
[NASA-CR-185194] N91-23851
Unified aeroacoustics analysis for high speed turboprop aerodynamics and noise. Volume 5: Propagation of propeller tone noise through a fuselage boundary layer
[NASA-CR-185195] N91-23852
TURBORAMJET ENGINES
Comparative study of different systems of combined cycle propulsion N91-23152
TURBOROCKET ENGINES
Comparative study of different systems of combined cycle propulsion N91-23152
TURBULENCE
Atmospheric turbulence review of space shuttle launches
[NASA-TM-4289] N91-23215
Flow field study of a rectangular jet N91-23423
Numerical simulation of incompressible inhomogeneous turbulence in a plane channel flow
[ESA-TT-1199] N91-23441
Ocean modeling for climate study N91-23592
Large scale turbulence in the equatorial electrojet N91-23643
Measurements of passive-scalar spectra for grid turbulence using a nonlinear optical technique
[DE91-005310] N91-23892
On standard forms for transport equations and fluxes, part 2
[DE91-010421] N91-23912
A cosmic superfluid phase
[NASA-CR-188171] N91-24016
TURBULENCE MODELS
Computational modeling and validation for hypersonic inlets N91-23162
Thermodynamically consistent formulations for rapid granular and turbulent multiphase flows N91-23420
An analysis of RNG based turbulence models for homogeneous shear flow
[NASA-CR-187552] N91-23433
Simulation of blood flow through an artificial heart N91-24056
TURBULENT BOUNDARY LAYER
An experimental study of an axisymmetric turbulent boundary layer disturbed by a periodic freestream N91-23078
A study of three dimensional turbulent boundary layer separation and vortex flow control using the reduced Navier Stokes equations
[NASA-TM-104407] N91-23089
A numerical study of the stratified turbulent Ekman layer N91-23421
TURBULENT FLOW
An experimental study of an axisymmetric turbulent boundary layer disturbed by a periodic freestream N91-23078
Theoretical and experimental performance of a solid fuel ramjet combustion cycle for hypersonic flight conditions N91-23170
An experimental study of flamelet surfaces in turbulent combustion
[AD-A232342] N91-23284
Flows with strongly anisotropic turbulence-dynamic and heat transfer aspects
[SER-20/P] N91-23407
Low Reynolds number two-equation modeling of turbulent flows
[NASA-TM-104368] N91-23416
Thermodynamically consistent formulations for rapid granular and turbulent multiphase flows N91-23420
A numerical study of the stratified turbulent Ekman layer N91-23421
Numerical modeling of turbulent dispersion around structures using a particle-in-cell method
[DE91-009757] N91-23426
An analysis of RNG based turbulence models for homogeneous shear flow
[NASA-CR-187552] N91-23433
Numerical simulation of incompressible inhomogeneous turbulence in a plane channel flow
[ESA-TT-1199] N91-23441
Fractal image compression of Rayleigh, Raman, LIF and LDV data in turbulent reacting flows
[AD-A232237] N91-23449
Chemical reactions in turbulent mixing flows
[AD-A232610] N91-23450
High resolution measurements of strained diffusion and reaction layer structure and extinction in turbulent flows
[AD-A232794] N91-23456
Turbulence and the feasibility of self-cooled liquid-metal blankets for fusion reactors
[SER-10/P-REV] N91-23910
TURBULENT JETS
An experimental study of flamelet surfaces in turbulent combustion
[AD-A232342] N91-23284
Chemical reactions in turbulent mixing flows
[AD-A232610] N91-23450
TURBULENT MIXING
Pitot surveys of two moderately under-expanded jets N91-23172
Turbulent mixing in nonreacting and reacting flows: A PDF approach at the two-point level N91-23422
Numerical simulation of a viscous vortex ring interaction with a density interface
[DE91-002790] N91-23429
Chemical reactions in turbulent mixing flows
[AD-A232610] N91-23450
High resolution measurements of strained diffusion and reaction layer structure and extinction in turbulent flows
[AD-A232794] N91-23456
TWO BODY PROBLEM
Initial data for the two-body problem of general relativity N91-23965
TWO DIMENSIONAL BODIES
Automated handling and assembling of non-rigid objects
[AD-A231246] N91-23489
On the structure of polynomial models of 2-D systems
[MATHS-REPT-A-139] N91-23812
TWO DIMENSIONAL FLOW
The 2-D supersonic nozzle design N91-23176
Riemann problems and the WAF method for the two-dimensional shallow water equations
[CRANFIELD-AERO-9005] N91-23443
Effects of three-dimensional imposed disturbance on bluff-body near wake flows
[AD-A232137] N91-23447
Vortex system evolution in 2- and 3-D swept trailing edge flows
[AD-A232692] N91-23453
TWO DIMENSIONAL MODELS
Flow between eccentric rotating cylinders N91-23417

Non-linear interaction of a detonation/vorticity wave
[NASA-CR-187550] N91-23434
Investigation of Roe's 2D wave decomposition models for the Euler equations
[VKI-TN-172] N91-23436
Canonical vs. micro-canonical sampling methods in a 2D Ising model
[DE91-010204] N91-23737

TWO PHASE FLOW
Two-phase flow patterns and frictional pressure gradients in a small rectangular channel
[DE91-009652] N91-23414
Particle-fluid two-phase flow modeling
[DE91-010102] N91-23415
Thermodynamically consistent formulations for rapid granular and turbulent multiphase flows N91-23420
Interphase transport and multistage separations
[DE91-009627] N91-23425
Interfacial characteristic measurements in horizontal bubbly two-phase flow
[DE91-009803] N91-23427
A three-dimensional free-Lagrange code for multimaterial flow simulations
[DE91-002309] N91-23428

U

UBV SPECTRA
H II regions and young star clusters in the magellanic clouds N91-24004

ULTRAHIGH FREQUENCIES
Analysis of the VHF-UHF electromagnetic radiation of lightning: Application to a model of the negative stepped leader propagation
[ESA-TT-1172] N91-23363
Design of inherently wide-band microwave frequency doubler and tripler in microstrip
[FEL-90-B255] N91-23392

ULTRASONIC TESTS
A preliminary investigation of acousto-ultrasonic NDE of metal matrix composite test specimens
[NASA-TM-104339] N91-23521

ULTRASONICS
Performance of visual and ultrasound sensing by an autonomous robot
[DE91-010452] N91-23511

ULTRAVIOLET ABSORPTION
Temperature dependence of ultraviolet absorption cross-sections of alternative chlorofluoroethanes
[AERONOMICA-ACTA-A-358-1991] N91-23647
Ultraviolet gas absorption and dust extinction toward M8 and the outer galactic disk N91-24018

ULTRAVIOLET RADIATION
Studies of the diffuse background and interstellar dust at far ultraviolet wavelengths N91-24003

UNDERWATER ACOUSTICS
Parallel-processor-based Gaussian beam tracer for use in ocean acoustic tomography
[AD-A232420] N91-23690

UNDERWATER ENGINEERING
Telerobotics: A key area for possible technology transfer from underwater to space N91-23581
Telemanipulation system assisted by computer for under water applications N91-23585

UNDERWATER PHOTOGRAPHY
The Berlenga underwater survey project N91-23577

UNDERWATER TESTS
Comparisons between underwater and space working environments for on board activities optimization (Columbus space programme) N91-23574

UNDERWATER VEHICLES
Evaluation of multisensor fusion scheme for the localization of underwater remotely operated vehicles N91-23590

UNIFORM FLOW
The transient response of heavily fluid-loaded elastic plates and cylindrical shells N91-23528

UNITED STATES
The changing face of the environmental issue
[PB91-138081] N91-23624
National stream survey database guide
[PB91-141804] N91-23625
Access and efficiency in Reagan-era information policy: A case study of the attempt to privatize the National Technical Information Service N91-23977
Technology transfer in a changing national security environment
[AD-A232458] N91-24000
Aeronautics and space report of the President N91-24085

UNSTEADY AERODYNAMICS
The propagation of acoustic disturbances in the transonic flow fields of wings
[ESA-TT-1126] N91-23854

UNSTEADY FLOW
Unsteady flow structure from swept edges subjected to controlled motion
[AD-A232714] N91-23094
Numerical simulation of incompressible inhomogeneous turbulence in a plane channel flow
[ESA-TT-1199] N91-23441
Riemann problems and the WAF method for the two-dimensional shallow water equations
[CRANFIELD-AERO-9005] N91-23443
A theory for fluidelastic instability of tube-support-plate inactive modes
[DE91-009676] N91-23538

UPPER ATMOSPHERE
High-altitude non-equilibrium infrared emission models
[AD-A232503] N91-23659
A smoothing algorithm for upper-air soundings
[AD-A232853] N91-23661
Range reference atmosphere, Shemya
[AD-A232813] N91-23685
Range reference atmosphere, Thule
[AD-A232831] N91-23686

URETHANES
Isolation, cloning and expression of the genes for microbial polyurethane degradation
[AD-A232108] N91-23699

USER MANUALS (COMPUTER PROGRAMS)
Aerodynamic preliminary analysis system 2. Part 2: User's manual
[NASA-CR-182077] N91-23081
NODEN user's guide and installation manual
[RSRE-MEMO-4438] N91-23753
Maintenance Resource Prediction Model (MRPM) user's manual
[AD-A232019] N91-23762
Unified aeroacoustics analysis for high speed turboprop aerodynamics and noise. Volume 4: Computer user's manual for UAAP turboprop aeroacoustic code
[NASA-CR-185194] N91-23851
Life cycle management automation user's manual, version 1.1
[AD-A232096] N91-23968
Active Design Database (ADDB) user's manual
[DE91-010431] N91-23985

USER REQUIREMENTS
National stream survey database guide
[PB91-141804] N91-23625
The Land Analysis System (LAS) N91-24054

UTILITIES
Geomagnetic storms: Potential economic impacts on electric utilities
[DE91-009523] N91-24036

UTILIZATION
Conference on Space Technology: Satellite Application Development
[REPT-911-440-103] N91-23219

V

V/STOL AIRCRAFT
AGARD highlights 91/1, March 1991
[AGARD-HIGHLIGHTS-91/1] N91-24084

VACUUM
Supersymmetric matter at finite temperature N91-23836
Non-mechanical optical path switching and its application to dual beam spectroscopy including gas filter correlation radiometry
[NASA-CASE-LAR-14588-1-CU] N91-23889

VACUUM SYSTEMS
A comparison between classical and substructuring finite-element stress analysis of a complex vacuum vessel shell
[DE91-010035] N91-23540
Buckling analysis of a complex vacuum vessel using the finite-element method
[DE91-010032] N91-23546

VALVES
Simulation of blood flow through an artificial heart N91-24056

VANADIUM OXIDES
Evaluation of cathode materials for high energy lithium secondary batteries
[DE91-764240] N91-23385

VAPOR DEPOSITION
Investigations of oxidation protection systems for carbon-carbon composites formed by chemical vapor deposition and plasma-assisted chemical vapor deposition techniques
[AD-A232800] N91-23269
Optimization of transparent and reflecting electrodes for amorphous silicon solar cells
[DE91-002132] N91-23618
Metal thin-film optical polarizers for space applications, phase 2
[NASA-CR-188202] N91-23891
Advances in silicon carbide Chemical Vapor Deposition (CVD) for semiconductor device fabrication
[NASA-TM-104410] N91-23946
Transport and nucleation processes in the vapor growth of diamond
[AD-A232135] N91-23953
Laser assisted CVD growth of AlN and GaN
[AD-A232379] N91-23957

VARIABLE STARS
The envelopes of RV Tauri variables N91-24008

VARIANCE (STATISTICS)
Polarimetric radar observations of time-variant random targets
[DLR-FB-90-52] N91-23356
A particular linear model of variance components
[RR-827-M] N91-23824

VECTORS (MATHEMATICS)
Computerized symbolic closed-form dynamics and control analysis of hybrid rigid and elastic multibody systems N91-23532

VEGETATION
Primary ocean production: Carbon and particle flux N91-23596
Surface layer transfer processes over vegetation: A micrometeorological field experiment of long duration N91-23664

VEGETATIVE INDEX
The applicability of thematic mapper data to the classification of tree species and natural age classes
[DLR-FB-90-44] N91-23612

VELOCITY DISTRIBUTION
Viscous three-dimensional analyses for nozzles for hypersonic propulsion N91-23175
Effects of inlet distortion on the development of secondary flows in a subsonic axial inlet compressor rotor
[NASA-TM-104356] N91-23179
Turbulent mixing in nonreacting and reacting flows: A PDF approach at the two-point level N91-23422
Flow field study of a rectangular jet N91-23423

VELOCITY MEASUREMENT
A non-contacting velocity measurement system
[NASA-CASE-LAR-14466-1] N91-23461

VERY HIGH FREQUENCIES
Analysis of the VHF-UHF electromagnetic radiation of lightning: Application to a model of the negative stepped leader propagation
[ESA-TT-1172] N91-23363
A study of the end point path geometry in meteor burst systems using a microcomputer signal logger N91-24012

VERY LARGE SCALE INTEGRATION
Automatic formal verification of VHDL descriptions: A first prototype
[RR-823-I] N91-23726
Integrated Vertical Bloch Line (VBL) memory N91-24051

VHSIC (CIRCUITS)
Automatic formal verification of VHDL descriptions: A first prototype
[RR-823-I] N91-23726

VIBRATION
Modal analysis of multistage gear systems coupled with gearbox vibrations
[NASA-TM-103797] N91-23513
A theory for fluidelastic instability of tube-support-plate inactive modes
[DE91-006001] N91-23542
Fatigue evaluation of piping systems with limited vibration test data
[DE91-007167] N91-23543
Computational simulation of acoustic fatigue for hot composite structures
[NASA-TM-104379] N91-23548

VIBRATION DAMPING
Reduced vector basis for dynamic analysis of large damped structures N91-23525

VIBRATION EFFECTS
A theory for fluidelastic instability of tube-support-plate inactive modes
[DE91-009676] N91-23538

VIBRATION MODE
Theoretical prediction of vibrational infrared frequencies of tertiary amines
[AD-A232880] N91-23288

VIBRATION TESTS
Fatigue evaluation of piping systems with limited vibration test data
[DE91-007167] N91-23543

VIBRATIONAL SPECTRA
Theoretical prediction of vibrational infrared frequencies of tertiary amines
[AD-A232880] N91-23288

VIDEO EQUIPMENT
The value of STINFO
[AD-A232484] N91-23996
Interacting with DTIC
[AD-A232485] N91-23997
VIDEO SIGNALS
Digital CODEC for real-time processing of broadcast quality video signals at 1.8 bits/pixel N91-24067
VIDICONS
Visual presentation and computer animation
[DE91-010599] N91-23745
VINYL COPOLYMERS
A study of the critical factors controlling the synthesis of ceramic matrix composites from preceramic polymers
[AD-A232686] N91-23327
VINYL POLYMERS
The effect of post-cure and antimony trioxide addition on the glass transition of polyester and vinyl ester resin systems
[AD-A232523] N91-23325
VIRAL DISEASES
Molecular studies of cytokine induction
[AD-A232221] N91-23707
VIRTUAL MEMORY SYSTEMS
Designing a virtual-memory implementation using the Motorola MC68010 16-bit microprocessor with multi-processor capability interfaced to the VMEbus
[AD-A232554] N91-23730
VISCOELASTICITY
Thermo-viscoelastic behavior of composite materials N91-23243
Interdisciplinary research on viscoelasticity and rheology
[AD-A232700] N91-23454
VISCOSITY
High shear stress rheology of liquid lubricants N91-23309
Developing natural convection in a fluid layer with localized heating and large viscosity variation
[DE91-005240] N91-23431
VISCOUS FLOW
A study of the noise mechanisms of transonic blade-vortex interactions
[NASA-CR-188199] N91-23084
Some aspects of shock-wave boundary layer interaction relevant to intake flows N91-23161
Viscous three-dimensional analyses for nozzles for hypersonic propulsion N91-23175
Low Reynolds number two-equation modeling of turbulent flows
[NASA-TM-104368] N91-23416
Numerical simulation of a viscous vortex ring interaction with a density interface
[DE91-002790] N91-23429
Numerical simulation and topological analysis of the separated flow around a sphere
[DLR-FB-90-43] N91-23435
VISIBILITY
Air ambulance helicopter operational analysis
[DOT/FAA/RD-91/7] N91-23134
Simulation of a backscatter lidar system
[DLR-FB-90-50] N91-23355
An expanding grid photochemical model for visibility applications
[DE91-009947] N91-23630
VISUAL CONTROL
A Model-Based Approach to High-Level Robot Control with Visual Guidance
[VTT-PUBL-71] N91-23788
Planning of visual feedback with robot-sensor co-operation N91-23793
Robot-sensor co-operation planning for visual guidance N91-23794
A line based object localizing method for robot vision N91-23795
Object pose estimation based on one-degree-of-freedom sensor N91-23796
VISUAL DISCRIMINATION
Quantifying improved visual performance through vision training
[AD-A232799] N91-23716
VISUAL FLIGHT RULES
Air ambulance helicopter operational analysis
[DOT/FAA/RD-91/7] N91-23134
VISUAL OBSERVATION
Surface cloud observations for radiation, climatology and incorporation into satellite-based nephanalyses N91-23671
VISUAL PERCEPTION
Mechanisms of higher brain functions: A study of models of perception
[AD-A232389] N91-23712
Quantifying improved visual performance through vision training
[AD-A232799] N91-23716
VOICE CONTROL
Man-machine interactions and multimedia applied to ROV operations N91-23576
VOICE DATA PROCESSING
High-quality 800-b/s voice processing algorithm
[AD-A232352] N91-23372
VOIDS
Matter in cosmic voids N91-23838
Benchmark measurements and calculations of a 3-dimensional neutron streaming experiment
[DE91-010692] N91-23867
VOLCANOES
Cryomagmatism in the outer solar system N91-24019
VOLCANOLOGY
Cryomagmatism in the outer solar system N91-24019
Lunar volcanism and the thermal evolution of the moon N91-24031
VOLT-AMPERE CHARACTERISTICS
Phase transitions at liquid solid interfaces: Pade approximant for adsorption isotherms and voltammograms
[AD-A232623] N91-23285
VOLTAGE REGULATORS
Control aspects of the brushless doubly-fed machine
[DE91-009707] N91-23387
VORTEX BREAKDOWN
Mechanisms of equatorial superrotation: Studies with two-level models N91-23642
VORTEX FILAMENTS
A vortex panel method for calculating aircraft downwash on parachute trajectories
[DE91-009764] N91-23085
VORTEX FLAPS
The performance of 60 deg delta wings: The effects of leading edge radius on vortex flaps and the wing
[CRANFIELD-AERO-9004] N91-23092
The performance of 60 deg delta wings: The effects of leading edge radius and vortex flaps
[CRANFIELD-AERO-9002] N91-23140
VORTEX GENERATORS
The effects of controlling vortex formation on the performance of a dump combustor N91-23270
An experimental investigation of vortex pair interaction with a clean or contaminated free surface N91-23419
VORTEX RINGS
Numerical simulation of a viscous vortex ring interaction with a density interface
[DE91-002790] N91-23429
VORTEX SHEDDING
Experimental investigations on the transition from stable to unstable combustion by means of active instability control N91-23165
The effects of controlling vortex formation on the performance of a dump combustor N91-23270
VORTICES
Aircraft wake vortices: An assessment of the current situation
[AD-A231658] N91-23079
A study of the noise mechanisms of transonic blade-vortex interactions
[NASA-CR-188199] N91-23084
A vortex panel method for calculating aircraft downwash on parachute trajectories
[DE91-009764] N91-23085
A study of three dimensional turbulent boundary layer separation and vortex flow control using the reduced Navier Stokes equations
[NASA-TM-104407] N91-23089
The effects of controlling vortex formation on the performance of a dump combustor N91-23270
An experimental investigation of vortex pair interaction with a clean or contaminated free surface N91-23419
Flow field study of a rectangular jet N91-23423
Vortex system evolution in 2- and 3-D swept trailing edge flows
[AD-A232692] N91-23453
Diffusive, electrostatic concentration of disintegration products of inert gases in vortex flow
[AD-A232876] N91-23457
Observed changes in the activity of baroclinic waves and their feedbacks during the life cycles of low-frequency circulation anomalies in the Northern Hemisphere winter N91-23668
Neutral wind vortices in the high-latitude thermosphere N91-23673
The terminal Doppler weather radar tornadic vortex signature detection algorithm
[DOT-FAA-NR-91-5] N91-23675
VORTICITY
The effects of controlling vortex formation on the performance of a dump combustor N91-23270
Passive laminar flow control of crossflow vorticity
[NASA-CASE-LAR-13563-1] N91-23410
Non-linear interaction of a detonation/vorticity wave
[NASA-CR-187550] N91-23434

W

WAFERS
Dissolution of Poly(p-hydroxystyrene): Molecular weight effects
[AD-A232155] N91-23323
Evaluation and ranking of candidate ceramic wafer engine seal materials
[NASA-TM-103795] N91-23515
Advances in silicon carbide Chemical Vapor Deposition (CVD) for semiconductor device fabrication
[NASA-TM-104410] N91-23946
WAKEFULNESS
Some problems of desynchronisation of sleep-wakefulness and circadian rhythms for long duration spaceflights N91-23570
WAKES
Aerodynamics and stabilization of combustion of hydrogen jets injected into subsonic airflow N91-23164
Unified aeroacoustics analysis for high speed turboprop aerodynamics and noise. Volume 3: Application of theory for blade loading, wakes, noise, and wing shielding
[NASA-CR-185193] N91-23850
WALKING MACHINES
Wave gaits, follow-the-leader gaits and gait transitions of legged robots N91-23503
Rule-based motion coordination for the adaptive suspension vehicle on ternary-type terrain
[AD-A232224] N91-23517
WALL FLOW
Low Reynolds number two-equation modeling of turbulent flows
[NASA-TM-104368] N91-23416
WALL PRESSURE
Procedure for determination of three-dimensional wind tunnel wall interferences and wall adaptation in compressible subsonic flow using measured wall pressures
[DLR-FB-90-46] N91-23088
WALLS
Review of finite element procedures for earth retaining structures
[AD-A232230] N91-23343
Experimental study of narrow slot, cavity-backed apertures with finite wall conductivity
[DE91-009039] N91-23352
WARNING SYSTEMS
Aircraft Command in Emergency Situations (ACES). Phase 1: Concept development
[DOT/FAA/CT-90/21] N91-23097
WASTE HEAT
In-Space technology experiments program. A high efficiency thermal interface (using condensation heat transfer) between a 2-phase fluid loop and heatpipe radiator: Experiment definition phase
[NASA-CR-186869] N91-23408
WASTE TREATMENT
Physical/chemical closed-loop water-recycling N91-24052
WASTE WATER
Physical/chemical closed-loop water-recycling N91-24052
New research on bioregenerative air/water purification systems N91-24053
WATER
Gas evolution and bubble formation on electrodes
[ESA-TT-1191] N91-23278
Detection of mining activities in the Yanomani Indian Reserve through LANDSAT-TM imagery
[INPE-5182-RPE/638] N91-23609
WATER CIRCULATION
Ocean modeling for climate study N91-23592
Satellite data utilization in ocean circulation models N91-23593
Validation requirements for the Topex/Poseidon altimeter mission N91-23602
WATER FLOW
Interfacial characteristic measurements in horizontal bubbly two-phase flow
[DE91-009803] N91-23427
WATER MODERATED REACTORS
Potential impact of enhanced fracture-toughness data on fracture mechanics assessment of PWR vessel integrity for pressurized thermal shock
[DE91-009554] N91-23509
WATER POLLUTION
Remote sensing of the sea at IROE/CNR N91-23604
National stream survey database guide
[PB91-141804] N91-23625

WATER QUALITY
Physical/chemical closed-loop water-recycling N91-24052
WATER RECLAMATION
Physical/chemical closed-loop water-recycling N91-24052
WATER SPLITTING
Static feed water electrolysis subsystem development [NASA-CASE-MSC-21577-1-SB] N91-23271
WATER TREATMENT
Physical/chemical closed-loop water-recycling N91-24052
New research on bioregenerative air/water purification systems N91-24053
WATER TUNNEL TESTS
Benchmarking numerical predictions with force and moment measurements on slender, supercavitating bodies [DE91-007066] N91-23432
WATER VAPOR
Surface layer transfer processes over vegetation: A micrometeorological field experiment of long duration N91-23664
WATER WAVES
A guide to the Nedwam wave model [KNMI-WR-90-04] N91-23688
WAVE DEGRADATION
Investigation of Roe's 2D wave decomposition models for the Euler equations [VKI-TN-172] N91-23436
WAVE DIFFRACTION
Joint services electronics program [AD-A232331] N91-23402
WAVE FRONTS
Analog processing of optical wavefronts using integrated guided-wave optics [AD-A232703] N91-23904
WAVE FUNCTIONS
Theory of the new high-temperature superconductors N91-23842
Boundary conditions in quantum cosmology N91-24020
WAVE INTERACTION
Hydromagnetic wave coupling in the magnetosphere N91-23638
WAVE PACKETS
Large scale turbulence in the equatorial electrojet N91-23643
WAVE PROPAGATION
Effect of atmospheric variations on electromagnetic distance measurements [DE91-009726] N91-23349
An analysis of MLAYER: A multilayer tropospheric propagation program [AD-A232733] N91-23379
Models of planetary wave propagation in the middle atmosphere N91-23639
Propagation of seismic waves in nonelastic media [REPT-90-065] N91-23651
The propagation of acoustic disturbances in the transonic flow fields of wings [ESA-TT-1126] N91-23854
Measurements of passive-scalar spectra for grid turbulence using a nonlinear optical technique [DE91-005310] N91-23892
WAVEFORMS
Pulsed power performance of the new RLA (Recirculating Linear Accelerator) [DE91-004723] N91-23885
WAVEGUIDE LASERS
Strained quantum well leaky-mode diode laser arrays [DE91-009982] N91-23477
Vertical emitting, ring geometry, ultra-low threshold and ultra-high speed quantum well lasers for optical interconnect [AD-A232122] N91-23481
WAVEGUIDES
A transmission line method for the measurement of microwave permittivity and permeability [RSRE-MEMO-4450] N91-23394
The United Kingdom waveguide power standards above 40 GHz [RSRE-90023] N91-23845
WEAR
Electrodeposited coatings for diamond turning applications [DE91-009950] N91-23315
MHD channel gas-side element erosion-corrosion studies [DE91-008561] N91-23911
WEATHER
Air ambulance helicopter operational analysis [DOT/FAA/RD-91/7] N91-23134
SWANEA (Southwest Asia-Northeast Africa): A climatological study. Volume 2: The Middle East Peninsula [AD-A232776] N91-23684
WEATHER FORECASTING
Forecasting atmospheric particulate sulfur concentrations using national weather service synoptic charts [AD-A231634] N91-23622
Technical description of the high-resolution air mass transformation model at KNMI [KNMI-TR-125] N91-23646
The terminal Doppler weather radar tornadic vortex signature detection algorithm [DOT-FAA-NR-91-5] N91-23675
WEIBULL DENSITY FUNCTIONS
Mechanical behavior and failure phenomenon of an in situ-toughened silicon nitride [NASA-TM-103741] N91-23311
Stochastic micromechanical modeling of cleavage fracture in the ductile-brittle transition region N91-23533
WEIGHT REDUCTION
Materials for hypersonic engines N91-23177
WEIGHTING FUNCTIONS
A smoothing algorithm for upper-air soundings [AD-A232853] N91-23661
WEIGHTLESSNESS
Effects of weightlessness (sea water immersion) on body fluid balance and CNS functions N91-23566
Test on parabolic flights for stowage in weightlessness N91-23578
A non-invasive measure of minerals and electrolytes in tissue N91-24058
WEIGHTLESSNESS SIMULATION
Neutral buoyancy and microgravity: Extravehicular activities with a humid water suit N91-23579
Transcapillary fluid shifts in head and neck tissues during and after simulated microgravity [NASA-TM-103847] N91-23704
WELDABILITY
Gas contents and weldability of aluminum die castings [ETN-91-99188] N91-23302
WELDED JOINTS
Evaluation of filler metals for high-strength stainless steels [DE91-009931] N91-23295
Parametric study in weld mismatch of longitudinally welded SSME HPFTP inlet [NASA-TM-103534] N91-23502
Stochastic micromechanical modeling of cleavage fracture in the ductile-brittle transition region N91-23533
Reduction factors for creep strength and fatigue life of modified 9 Cr-1 Mo steel weldments [DE91-009919] N91-23544
WELDED STRUCTURES
Parametric study in weld mismatch of longitudinally welded SSME HPFTP inlet [NASA-TM-103534] N91-23502
WHEELS
Dynamic study of cyclically symmetric structures: Application to rotating a wheel of a centrifugal compressor [ISAL-91-0004] N91-23844
WINCHES
Airborne rescue system [NASA-CASE-ARC-11909-1] N91-23095
WIND (METEOROLOGY)
Characteristics and performance of an operational windscatterometer N91-23607
Maintenance of short-term subtropical wind maxima in the Southern Hemisphere: Observational and modeling study N91-23665
On the airflow over the Alps during south Foehn [DLR-FB-90-30] N91-23676
Effects of the northeast monsoon on the equatorial westerlies over Indonesia [AD-A232106] N91-23681
WIND DIRECTION
Lateral dispersion of radioactive release. Draft for comments [CEMA-86/17] N91-23621
SWANEA (Southwest Asia-Northeast Africa): A climatological study. Volume 2: The Middle East Peninsula [AD-A232776] N91-23684
WIND EFFECTS
The annual march of convection, sea surface temperature, and surface winds in the tropics N91-23667
WIND PRESSURE
Simulation of probabilistic wind loads and building analysis [NASA-TM-103744] N91-23549
WIND PROFILES
Numerical modeling of turbulent dispersion around structures using a particle-in-cell method [DE91-009757] N91-23426
A one dimensional wind profile model with stability and eddy viscosity estimations from sodar data [DM-56] N91-23680
WIND SHEAR
Atmospheric turbulence review of space shuttle launches [NASA-TM-4289] N91-23215
Models of planetary wave propagation in the middle atmosphere N91-23639
WIND TUNNEL TESTS
Interferometric investigation of supersonic flow fields with shock-shock interactions N91-23082
The performance of 60 deg delta wings: The effects of leading edge radius on vortex flaps and the wing [CRANFIELD-AERO-9004] N91-23092
The performance of 60 deg delta wings: The effects of leading edge radius and vortex flaps [CRANFIELD-AERO-9002] N91-23140
A study of supersonic and hypersonic ramjet engines in France from 1950 to 1974 (application on combined cycle aircraft engines) N91-23149
The VKI hypersonic wind tunnels and associated measurement techniques [VKI-TM-46] N91-23196
WIND TUNNEL WALLS
Procedure for determination of three-dimensional wind tunnel wall interferences and wall adaptation in compressible subsonic flow using measured wall pressures [DLR-FB-90-46] N91-23088
WIND TUNNELS
Measurements of passive-scalar spectra for grid turbulence using a nonlinear optical technique [DE91-005310] N91-23892
WINDING
Mechanical states in wound heterogeneous tapes by the finite element method [DE91-009255] N91-23536
Mechanical stress states in heterogeneous, wound rolls [DE91-009257] N91-23537
WINDS ALOFT
Neutral wind vortices in the high-latitude thermosphere N91-23673
WINGS
Simulation of iced wing aerodynamics [NASA-TM-104362] N91-23086
Application of multidisciplinary optimization methods to the design of a supersonic transport [NASA-TM-104073] N91-23135
Integrated multidisciplinary optimization of actively controlled fiber composite wings N91-23190
Unified aeroacoustics analysis for high speed turboprop aerodynamics and noise. Volume 2: Development of theory for wing shielding [NASA-CR-185192] N91-23849
Unified aeroacoustics analysis for high speed turboprop aerodynamics and noise. Volume 3: Application of theory for blade loading, wakes, noise, and wing shielding [NASA-CR-185193] N91-23850
The propagation of acoustic disturbances in the transonic flow fields of wings [ESA-TT-1126] N91-23854
WINTER
Observed changes in the activity of baroclinic waves and their feedbacks during the life cycles of low-frequency circulation anomalies in the Northern Hemisphere winter N91-23668
WIRE WINDING
Bobbin stresses generated by wire winding [DE91-009545] N91-23526
WORKING FLUIDS
Advanced working fluids: Thermodynamic properties [PB91-136465] N91-23964
WORKLOADS (PSYCHOPHYSIOLOGY)
A user-oriented synthetic workload generator [NASA-CR-188197] N91-23739

X

X RAY ASTRONOMY
The supernova remnant G109.1-1.0 and the x-ray pulsar 1E2259+586 N91-24002
Instrumentation and data analysis for hard x ray astronomy N91-24010
X RAY BINARIES
A search for very high-energy gamma rays from Cygnus X-3 N91-24039

X RAY DIFFRACTION
X ray diffraction and electron spectroscopy of epitaxial molecular C60 films
[AD-A232152] N91-23954
X RAY IMAGERY
Instrumentation and data analysis for hard x ray astronomy N91-24010
Hard x ray imaging telescope
[DE90-015815] N91-24013
X RAY SCATTERING
Nondestructive measurement of thickness and density of composite materials by Compton backscattering
[REPT-911-430-112] N91-23255
In-situ surface x ray scattering measurements of electrochemically deposited bismuth on silver (III): Structure, compressibility, and comparison with ex-situ leed measurements
[AD-A232624] N91-23880
Surface x ray scattering measurements of the substrate induced spatial modulation of an incommensurate adsorbed monolayer
[AD-A232625] N91-23959
X RAY SOURCES
Possibilities for projection x ray lithography using holographic optical elements
[DE91-009770] N91-23464
X RAY SPECTRA
A high resolution study of the Cu K alpha(sub 1,2) x-ray emission lines N91-23841
Surface electron emission induced by slow multicharged ions
[DE91-010469] N91-23865
X RAY SPECTROSCOPY
Structure of electrochemically deposited copper on gold (III) alloy
[AD-A232345] N91-23303
Structural studies of manganese and halide in the photosynthetic oxygen evolving complex
[DE91-009071] N91-23698
X RAY TELESCOPES
Structural materials for space mirrors
[REPT-911-430-128] N91-23261
Instrumentation and data analysis for hard x ray astronomy N91-24010
Hard x ray imaging telescope
[DE90-015815] N91-24013
X RAYS
ROSAT: An international mission exploring the high energy universe
[NASA-TM-104958] N91-23214
Quantitative film radiography
[DE91-009718] N91-23463
Digital data registration and differencing compression system
[NASA-CASE-SSC-00010-1] N91-23976
Soft x ray/extreme ultraviolet images of the solar atmosphere with normal incidence multilayer optics N91-24006
Instrumentation and data analysis for hard x ray astronomy N91-24010
X-29 AIRCRAFT
Flying qualities of the X-29 forward swept wing aircraft N91-23127
Buffet induced structural/flight-control system interaction of the X-29A aircraft
[NASA-TM-101735] N91-23133
XENON CHLORIDE LASERS
Optical parametric oscillators pumped by excimer lasers N91-23473

Y

YIELD STRENGTH
The strength and toughness of stainless steels at cryogenic temperature
[DE91-009771] N91-23300
YTTRIUM OXIDES
Point defect effects on hot corrosion of zirconia-based coatings
[AD-A232662] N91-23326
S-parameter measurements and applications of superconducting flux flow transistors
[DE91-009763] N91-23388
Effect of transition metal dopants on high T(sub c) superconductivity
[PB91-130138] N91-23934
Microstructure of epitaxial YBa2Cu3O7 thin films
[DE91-009951] N91-23942
Fermi surface of YBCO by DHVA
[DE91-009963] N91-23943

Z

ZERO POINT ENERGY
Supersymmetric matter at finite temperature N91-23836
ZIRCONIUM OXIDES
Applications of energetic particles in improving coating adhesion properties
[DE91-008833] N91-23312
Mechanistic studies of pressure-assisted superplasticity of structural ceramics
[AD-A232034] N91-23322
Point defect effects on hot corrosion of zirconia-based coatings
[AD-A232662] N91-23326
Oxygen production using solid-state zirconia electrolyte technology N91-24059

PERSONAL AUTHOR INDEX

Typical Personal Author Index Listing

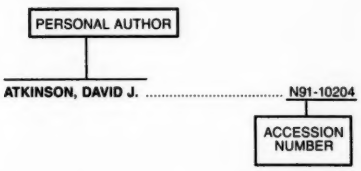

Listings in this index are arranged alphabetically by personal author. The accession number denotes the number by which the citation is identified.

A

ABDALLAH, S. A. N91-23451
ABIGADOL, NOOMI N91-23621
ABRAMS, MARK N91-23637
ABU-ZAID, SAMEER A. N91-23420
ACCENSI, A. N91-23575
ACETO, S. C. N91-23917
ADAMS, GEORGE F. N91-23335
ADELMAN, HENRY G. N91-23169
AGGARWAL, J. K. N91-23766
AGUTTES, J. P. N91-23589
AHMAD, MAOBOOL N91-23934
AKSAY, I. A. N91-23313
AKSELROD, S. N91-23833
N91-23834
ALBRIGHT, RICK N91-23623
ALBUGUES, F. N91-23262
ALEKHIN, S. I. N91-23856
ALKHATIB, HASAN S. N91-23776
ALLEN, S. M. N91-23291
ALLIA, MOURAD N91-23727
ALTERESCU, SIDNEY N91-24082
ALUKO, M. N91-23957
ALVANIPOUR, A. N91-23956
ALVERMANN, KLAUS N91-23725
AMBROSIUS, B. A. C. N91-23594
AMIDIEU, M. N91-23220
AMIET, R. K. N91-23849
ANDERSON, BERNHARD H. N91-23089
ANDERSON, CHARLES D. N91-23097
ANDERSON, D. E. N91-23583
ANDERSON, T. L. N91-23557
ANDERSSON, BOERJE N91-23759
ANDRE, G. N91-23580
ANDREI, G. N91-23156
ANGUS, JOHN C. N91-23953
ANTONIADIS, A. N91-23825
ANZ, SAMIR J. N91-23954
ARATOW, M. N91-23704
ARMSTRONG, JOHN N91-23623
ARNALL, DAVID N91-23722
ARNAUD, SARA B. N91-24058
ARNAULT, S. N91-23602
ARNOLD, JAMES O. N91-23207
ARONS, J. N91-24027
N91-24028
ARQUIS, ERIC N91-23947
N91-23948
ARTS, T. N91-23437
ASHKENAZI, J. N91-23835
N91-23842
ATAMANCHUK, T. M. N91-23168
ATCHLEY, ANTHONY A. N91-23847
ATHINIOTIS, N. N91-23306
ATIF, KARIM N91-23778
ATTAWAY, S. N91-23526
ATTIAS, ANDRE-JEAN N91-23319
ATTIYA, HAGIT N91-23774
AUGUST, RICHARD N91-23550
AVELLINI, BARBARA A. N91-23717
AVIDOR, A. N91-23833

B

BABOT, D. N91-23255
BABUSKA, IVO N91-23560
N91-23561
N91-23562
N91-23815
N91-23816
BAE, YOUNG K. N91-23336
BAEK, WOON KYUNG N91-23494
BAILEY, RANDALL E. N91-23120
BAILLIE, S. W. N91-23123
N91-23124
BAIN, B. N91-23720
BAIR, CLAYTON H. N91-23472
BAIR, SCOTT N91-23309
BAIRD, D. G. N91-23329
N91-23330
BAITY, F. W. N91-23353
BAJAJ, KRISHAN K. N91-23897
BAJCSY, R. N91-23787
BAKER, KARL W. N91-23617
BALLANCE, JOHN B. N91-23308
BALUT, STEPHEN J. N91-23077
BANKS, BRUCE A. N91-24062
BAR-CHAIM, NADAV N91-23481
BARAK, G. N91-23835
BARAKAT, A. N91-23925
BARAL, CHITTA N91-23765
N91-23993
BARDEY, P. N91-23605
BARDSLEY, J. N. N91-23865
BARKATT, AARON N91-24082
BARKAY, N. N91-23837
BARLEY, STEVEN KEITH N91-24037
BARNES, C. W. N91-23784
BARNES, P. R. N91-24036
BARNETT, D. A., JR. N91-23867
BARNETT, D. L. N91-23511
BARNIER, B. N91-23593
BARRICK, ELAINE N91-23623
BARSON, S. L. N91-23173
BARTELS, D. M. N91-23861
BARTER, S. A. N91-23306
BARTHELEMY, J.-F. M. N91-23135
BASKETT, R. L. N91-23631
BASS, H. E. N91-23848
BASS, I. L. N91-23478
N91-23479
BATCHELOR, D. B. N91-23353
N91-23913
BATTISTE, R. L. N91-23544
BAUDIN, G. N91-23608
BAUHAHN, P. N91-23346
BAUMGARTEN, RALF N91-23614
BAYER, STEVEN E. N91-24050
BAYER, THOMAS N91-23613
BAYLOR, L. R. N91-23915
N91-23916
BAYNE, FRANCES M. N91-23075
BAZEEVA, V. V. N91-23856
BEALE, K. S. N91-23235
BEARMAN, PETER N91-23447
BEAURAIN, A. N91-23178
BECKERMAN, M. N91-23511
BEIER, BERNHARD N91-23246
BEIER, E. W. N91-23863
BELL, J. B. N91-23429
N91-23430
BELMESK, Z. N91-23780
BEN-JACOB, ESHEL N91-23843
BENARY, V. N91-23834
BENEDIKTSSON, JON ATLI N91-23786
BENNETT, L. F. N91-23885
BENSHALOM, URI N91-23522
BENTS, DAVID J. N91-23620
BENZ, JOACHIM N91-23990
BERGAN, T. N91-23566
BERGER, J. R. N91-23524
BERGER, MARSHA J. N91-23455
BERGMAN, L. A. N91-24072
BERLIOZ, ALAIN N91-23844
BERMAN, P. R. N91-23480
BERNARD, R. N91-23601
BERNASCONI, GIANCARLO N91-23651
BERODIAS, G. N91-23255
BERRY, ROGER P. N91-23193
BERT, DIDIER N91-23756
BERTHON, V. N91-23220
BERTON, PIERRE N91-23149
BESSUDO, R. N91-23608
BEUGELSDIJK, T. J. N91-23697
BEYER, RICHARD A. N91-23930
BEZY, J. L. N91-23608
BEZY, J.-L. N91-23605
BHASIN, KUL B. N91-24081
BIBEL, G. D. N91-23500
BIENKOWSKI, P. R. N91-23859
BILLIG, F. S. N91-23166
BISCHEL, WILLIAM K. N91-23286
BISHOP, IVAN STUART N91-24023
BLACK, G. THOMAS N91-23111
N91-23115
BLADOS, WALTER R. N91-23995
N91-23996
N91-23997
BLANEY, DIANA LEE N91-24033
BLASS, J. J. N91-23544
BLISS, E. S. N91-23478
BLOCH, JEAN JACQUES N91-23219
BLOM, A. F. N91-23138
BLUM, L. N91-23285
N91-23303
N91-23879
BLUMENAU, L. N91-23231
BOEMAN, R. G. N91-23535
BOER, M. N91-24040
BOEZER, GORDON L. N91-24000
BOGGS, DONALD REESE N91-24018
BOITET, C. N91-23989
BOLLE, G. N91-23895
BOLLING, COREY N91-23075
BOLSTAD, PAUL VICTOR N91-23733
BONANNO, R. E. N91-23478
BOND, THOMAS H. N91-23183
N91-23184
BONNER, E. N91-23080
BOOKER, M. K. N91-23298
BORCHARDT, GARY C. N91-23732
BORGES, GARY L. N91-23880
N91-23959
BORIO, U. N91-23156
BORRIONE, DOMINIQUE N91-23726
BOUAMAR, MOHAMED N91-23705
BOUCHE, V. N91-23876
BOUCHERIE, JOEL N91-23947
N91-23948
BOUKTHIR, M. N91-23593
BOURY, D. N91-23178
BOWERS-IRONS, GAIL L. N91-23699
BOYER, J. H. N91-23484
BOYES, J. D. N91-23919
BRABBS, THEODORE A. N91-23180
BRACKENS, ANDRE N. N91-23227
BRADBURY, E. M. N91-23695
BRAGG, M. B. N91-23086
BRAINARD, GEORGE N91-23722
BRAMLETT, R. D. N91-23315
BRANDOW, B. H. N91-23296
BRANOVER, HERMAN N91-23231
N91-23407
N91-23910
BRAUN, EREZ N91-23839
BRAUN, M. J. N91-23409
BRAVENEC, R. V. N91-23918
BRENOT, JEAN-MARC N91-23591
BREWE, DAVID E. N91-23439
BRIERE, DOMINIQUE N91-23192
BRIGGS, L. L. N91-23520
BRINKMAN, C. R. N91-23298
N91-23318
BRISKE, MICHAEL W. N91-23376
BRITTON, RANDALL K. N91-23184
BROADWELL, JAMES E. N91-23450

BROSCH, N. N91-23838
BROWN, S. K. N91-23784
BRUESKE, STEPHEN L. N91-23622
BRUNAIR, R. M. N91-23502
BRUNNER, B. N91-23584
BUCHACKER, E. N91-23114
BUCHHOLTZ, BRENT N91-23232
BUCKLEY, W. M. N91-23986
BUI, JAMES N91-23077
BUNTE, STEVEN W. N91-23930
BURBECK, CHRISTINA A. N91-23715
BURGERS, GERRIT N91-23688
BURGIO, CLAUDE N91-23223
BURKE, EDWARD J. N91-23369
N91-23370
N91-23371
BURNETT, J. W. N91-23277
BURROUGHS, M. N91-23377
BUTTRAM, M. T. N91-23939
BYRNE, R. N91-23507

C

CABANEL, D. N91-23250
CABREZA, JOAN N91-23623
CAGLIOTI, VINCENZO N91-23751
CAI, Y. N91-23538
N91-23542
CAI, ZHI-XIONG N91-23940
CAIN, T. M. N91-23172
CALAWAY, W. F. N91-23277
CALCOTE, ROY K. N91-23799
CAMBIER, JEAN-LUC N91-23169
CAMBRIDGE, VIVIEN J. N91-23976
CAMERON, M. N91-23104
N91-24029
CAMPBELL, C. S. N91-23424
CANACCI, V. N91-23409
CANAVAN, G. H. N91-23350
CANNATA, RICHARD W. N91-23657
CANTRELL, JOHN H. N91-24076
CAPITANIO, C. N91-23261
CARLIN, JAYNE N91-23623
CARPENTER, J. M. N91-23866
CARPENTER, J. R. N91-23210
CARTER, C. B. N91-23403
CARTER, DANIEL C. N91-23933
N91-24057
CARTER, M. D. N91-23913
CARTON, CHARLES N91-23219
N91-23615
CASALE, ELENA N91-24057
CASE, A. M. N91-23150
CASSELL, P. N91-24072
CASTILLO, S. P. N91-23352
CASTLE, P. M. N91-23478
CASTRO, DANIEL E. N91-23553
CATALANO, L. A. N91-23807
CAYSON, STEPHEN C. N91-23193
CECCHI, GIOVANNA N91-23604
CEDERWALL, R. T. N91-23631
CERVAY, RUSSELL R. N91-23307
CHABALOWSKI, CARY F. N91-23335
CHAGANTY, NARASINGA R. N91-23817
CHAMBERLIN, J. L. N91-23619
CHAMIS, CHRISTOS C. N91-23548
N91-23549
CHAMPIGNY, P. N91-23160
CHANDRA, S. N91-23538
N91-23542
CHANG, CIUTER N91-23488
CHANG, I-DEE N91-24056
CHANG, R. P. N91-23328
CHARPENTIER, P. N91-23209
CHARYULU, USHA N91-23699
CHASE, L. L. N91-23860
CHAU, PAK SHING N91-23465
CHAUTARD, J. C. N91-23221
CHEN, BOR-LING N91-23299
CHEN, CHIH-LYEU N91-23681
CHEN, GUOTING N91-23809
CHEN, I-WEI N91-23322
CHEN, KUN-MU N91-23368
CHEN, LUNG ALBERT N91-23978
CHEN, MARGARET WEIN-MEI N91-23645
CHEN, S. S. N91-23538
N91-23542
CHEN, SINN-WEN N91-23290
CHEN, WENPING N91-24034
CHENAULT, DAVID B. N91-23906
CHENG, CHIEH-SAN N91-23211
CHENG, YI-WEN N91-23523
CHENIN, PATRICK N91-23755
CHERNIN, D. N91-23878
CHEUNG, K.-M. N91-24068
CHEVALLIER, J. N91-23575
CHIANG, DING-AN N91-23979
CHIPMAN, RUSSELL A. N91-23906
CHO, CHANG HO N91-23495
CHOATE, L. M. N91-23386
CHOI, BENJAMIN BYOUNG-SOO N91-23503
CHOI, SUNG R. N91-23311
CHOI, YONG JE N91-23504
CHOY, F. K. N91-23513
CHRISTENSEN, RICHARD M. N91-23265
CHU, TZE YAO N91-23431
CHUNG, KOO-DON N91-23734
CIESLAK, M. J. N91-23294
CITURS, KEVIN D. N91-23117
CLARK, DOUGLAS J. N91-24059
CLARK, E. L. N91-23432
CLARK, RAYMOND K. N91-23369
N91-23370
N91-23371
CLARK, VERNESSA R. N91-23713
CLARKE, ROBERT N91-23133
CLAUSER, M. J. N91-23919
CLAYTON, R. N. N91-23277
CLEMENT, G. N91-23585
CLEVER, W. N91-23080
COCHRAN, H. D. N91-23859
CODASTEFANO, P. N91-23895
COE, H. H. N91-23514
COEN, P. G. N91-23135
COHEN, P. I. N91-23958
COLCHIN, R. J. N91-23916
COLE, J. K. N91-23432
COLEMAN, GARY NEIL N91-23421
COLEMAN, JAMES J. N91-23483
COLOMBANT, D. G. N91-23878
COLORNI, ALBERTO N91-23752
COLOZZA, ANTHONY J. N91-23620
COMER, GREGORY LEE N91-24022
COMET, M. N91-23571
CONNELL, JOHN W. N91-23237
CONNOLLY, D. J. N91-24080
CONNOR, K. A. N91-23917
CONTOLATIS, T. N91-23346
COOK, D. L. N91-23919
COOK, D. M. N91-23674
COOK, GREGORY BROWN N91-23965
COON, S. R. N91-23277
COOPER, DAVID M. N91-23207
COOPER, N. G. N91-23855
CORDA, S. N91-23166
CORDON, JOSEPH G. N91-23959
COX, L. B. N91-23382
COY, J. J. N91-23514
CRANDALL, MICHAEL G. N91-23820
CRAWFORD, MARK R. N91-23117
CRENSHAW, A. N91-23704
CROSSWY, F. L. N91-23908
CROWLEY, T. P. N91-23917
N91-23918
CULVER, G. N91-23999
CURRENT, W. N91-23465
CUTTER, M. A. N91-23608

D

DAHLBERG, E. D. N91-23958
DAHLQUIST, HANS N91-23680
DAHM, WERNER J. N91-23456
DALLY, J. W. N91-23524
DARROY, J. M. N91-23591
DATTA, A. N91-23329
N91-23330
DAUM, P. H. N91-23626
DAVIDSON, N. N91-23835
DAVIES, SIMON ROBERT N91-24002
DAVIS, A. M. N91-23277
DAVIS, DAVID N91-24082
DAVIS, EDWARD V., JR. N91-23771
DAVIS, GLORIA J. N91-23341
DAVIS, ROBERT F. N91-23955
DAVIS, VIRGIL LEON N91-24075
DAWSON, D. N91-23508
DAY, R. D. N91-23315
DCRUZ, L. N91-23299
DEAN, G. D. N91-23320
DEBOER, W. P. N91-23119
DEBRUIJN, E. I. F. N91-23646
DECH, STEFAN WERNER N91-23687
DECONINCK, H. N91-23436
N91-23807
DECRAMER, L. N91-23579
DEKEL, AVISHAI N91-23839
DELAFUENTE, HORACIO M. N91-23492
DELAUZE, H. G. N91-23571
DELECLUSE, P. N91-23592
DELIYANNIS, CONSTANTINE PLATO N91-24024
DELLA-DORA, JEAN N91-23809
DELUCCHI, A. N91-23986
DEMAREST, KENNETH D. N91-23365
DEMPSEY, BRIAN P. N91-23408
DEPALMA, P. N91-23436
DEROSE, V. J. N91-23698
DESA, L. N91-23468
DESCHAMPS, VERONIQUE N91-23441
DESOUZA, J. P. N91-23329
DEUTSCH, L. J. N91-24068
DEUTSCH, MOSHE N91-23841
DEVINE, G. N91-23463
DEVRIES, F. P. P. N91-23359
DEZEEUW, W. A. N91-23204
DICKENS, J. K. N91-23864
DICKSON, T. L. N91-23509
DIDIER, MURIEL N91-23586
DIEFFENBACH, CARL W. N91-23707
DIETRICH, J. N91-23584
DIJKSTRA, P. N91-23170
DIMOTAKIS, PAUL E. N91-23450
DING, J. L. N91-23298
DING, XURU N91-23497
DINI, PAOLO N91-23411
DINKELACKER, MICHAEL N91-23278
DIPIPPO, SIMONETTA N91-23581
DIVAN, P. N91-23081
DOBIE, D. N91-23463
DOBIE, T. G. N91-23721
DODDS, H. L. N91-23883
DODI, DANIEL N91-23222
N91-23224
DOLINAR, S. J. N91-24068
DOLLINS, ANDREW B. N91-23714
DOMBROWSKI, EDMUND GERARD N91-24001
DON, J. N91-23269
DONG, QIMIN N91-23417
DORIGO, MARCO N91-23752
DORRER, M. N91-23602
DOUBLIER, MICHEL N91-23152
DOUGAN, A. D. N91-23986
DOUGAN, D. L. N91-23348
DOVI, AUGUSTINE R. N91-23135
DRAKE, J. B. N91-23805
DRAPATZ, S. N91-23104
DRESE, JOHN H. N91-23718
DRESSLER, RAINER A. N91-23228
DRUFUCA, GIUSEPPE N91-23651
DUCHENE, B. N91-23590
DUMESNIL, JEAN-JACQUES N91-23223
DUNGEY, CLIFTON E. N91-23373
DUNN, G. H. N91-23873
DUNN, K. N91-23080
DUNN, THOMAS J. N91-23491
DURHAM, STEPHEN D. N91-23827
DUSTIN, MILES O. N91-23617
DUTT, A. N91-23775
DUTTA, PIYUSH K. N91-23280
DUVAUCHELLE, P. N91-23255
DUVEAU, P. N91-23160
DUYAR, AHMET N91-23340
DWYER, J. G. N91-23325
DYER, MARK J. N91-23286

E

EAGAR, T. W. N91-23291
EASTBURG, STEVEN R. N91-23145
EBELING, ROBERT M. N91-23343
EBENEZER, DURAISINGH DIAMOND N91-23528
EBRAHIMZADEH, MAJID N91-23473
ECKART, A. N91-24029
ECKSTROM, D. J. N91-23466
EDENS, ELEANA S. N91-23710
EDER, ANDREAS N91-23990
EDGAR, G. N91-24072
EICKHOFF, H. N91-23164
EINERSON, C. J. N91-23510
EL-BOHER, A. N91-23231
ELANDS, P. J. M. N91-23170
ELBERN, HENDRIK N91-23648
ELDEM, VASFI N91-23340
ELLENDER, R. D. N91-24053
ELLWOOD, JEFFREY L. N91-23143
ELMER, J. W. N91-23291
ENDLER, J. L. N91-23721
ENGLAND, A. N91-23916
ENKAOUA, D. N91-23238
ERBERT, G. V. N91-23479
ERMAK, D. L. N91-23628
N91-23632
ERNEUX, THOMAS N91-23486
ERNST, H. A. N91-23539
ESCHER, WILLIAM J. D. N91-23159

ESSMAN, DOUGLAS J. N91-23155
EVANS, C. J. N91-23315
EVANS, K. C. N91-23987
EYLON, D. N91-23834
EYMARD, LAURENCE N91-23597
N91-23601
EZHELA, V. V. N91-23856
EZRATY, R. N91-23599

F

FABRE, M. N91-23573
FAIRHEAD, A. C. N91-23364
FAMINI, G. R. N91-23288
FARIS, GREGORY W. N91-23286
FARMER, ERIC N91-23711
FAROKHI, SAEED N91-23089
FARRAR, L. C. N91-23911
FASSBENDER, C. N91-23565
FAUBERT, DENIS N91-23378
FELDBERG, R. N91-23740
FELDMAN, M. N91-23478
FELDMAN, R. N91-23238
FENIMORE, E. E. N91-24040
FENSKE, G. R. N91-23312
FERBER, M. K. N91-23310
FERENDECI, ALTAN M. N91-23470
FERRAN, A. N91-23248
FERRARINI, LUCA N91-23747
N91-23748
FERRISS, D. H. N91-23438
FILHO, PEDRO HERNANDEZ N91-23609
FILIMONOV, B. B. N91-23856
FILIP, PAVEL N91-23746
FILY, M. N91-23600
FINCKE, J. R. N91-23317
FINKLER, RONALD A. N91-24000
FINLEY, JOHN PATRICK N91-24038
FINLEY, TOM D. N91-23461
FINNERTY, ANTHONY E. N91-23342
FIRTMAURICE, M. N91-24070
FISCHER, R. D. N91-23564
FISHER, A. S. N91-23476
FISHER, MICHAEL LYNN N91-24025
FISHER, TIM E. N91-23724
FITZMAURICE, NESSAN N91-23433
FLAKE, G. W. N91-23784
FLEMMING, ROBERT J. N91-23184
FLIFLET, ARNE W. N91-23398
FONG, C. Y. N91-23941
FORREST, S. N91-23742
FOSS, ERLING J. N91-24000
FOUDRIAT, E. C. N91-23971
FOURQUET, JEAN-YVES N91-23516
FOWLER, C. M. N91-23943
FOWLER, R. H. N91-23916
FRANC, O. N91-23251
N91-23258
FRANCE, D. M. N91-23414
FRANCISCUS, LEO C. N91-23180
FRANK, KONRAD N91-23518
FRANSEN, L. J. N91-23372
FRAZIER, THOMAS P. N91-23077
FREDERICK, R. A. N91-23235
FREEDMAN, MARC R. N91-23311
FREEMAN, B. L. N91-23943
FRENCH, JONATHAN N91-23722
FRENKLACH, MICHAEL N91-23287
FREUH, JIM N91-23232
FRI, R. W. N91-23627
FRIDGE, ERNEST M., III N91-24047
FRIED, ELIOT N91-23558
FROGGET, B. C. N91-23894
FRYE, JOAN M. N91-23957
FUGINA, J. N91-23463
FULLERTON, T. L. N91-23085
FUSARO, ROBERT L. N91-23501

G

GAIONI, STEPHEN N91-23708
GAITONDE, DATTA N91-23093
GALLANT, Y. A. N91-24027
GALLEITHNER, H. N91-23114
GALLUP, R. F. N91-23941
GARCIA, ALAIN N91-23187
GARCIA, FRANK W., JR. N91-23689
GARDETTE, B. N91-23571
GARMIRE, ELSA N91-23485
GARY, BRUCE L. N91-23662
GASCARD, J. C. N91-23600
GATES, THOMAS S. N91-23244
GATH, ISAK N91-23823
GATSKI, THOMAS B. N91-23433
GAUCH, SUSAN EVALYN N91-23983
GEDDES, J. N91-23346
GENTRY, JAMES A. N91-23802
GENZEL, R. N91-23104
N91-24029
GERING, KEVIN L. N91-23964
GHOSH, A. N91-23310
GIAKOUMAKIS, GEORGIOS H. N91-23375
GIBSON, J. C. N91-23113
GIBSON, WILLIAM N91-23722
GILFORD, MICHAEL T. N91-23684
GILLOTAY, D. N91-23647
GINATEMPO, B. N91-23292
GINLEY, D. S. N91-23388
GINOVART, C. N91-23160
GINSBURG, ARTHUR P. N91-23716
GIUNTA, C. N91-23618
GLASSER, A. N91-23921
GLEIS, S. N91-23165
GLIMM, JAMES N91-23452
GLYNN, M. S. N91-23674
GOEING, MICHAEL N91-23176
GOEL, P. N91-23173
GOETERS, K. M. N91-23565
GOLD, STEVEN H. N91-23398
GOLDBERG, MATTHEW S. N91-23076
GOLDBERG, ROB N91-23623
GOLDSTON, R. J. N91-23913
GOLOD, A. N91-23967
GOLUB, MORTON A. N91-24063
GOOD, SHARON E. N91-23781
GOODMAN, ALAN HOWARD N91-23671
GOODWIN, G. M. N91-23295
GORDON, JOSEPH G. N91-23303
N91-23880
GORDON, R. G. N91-23618
GORETTA, K. C. N91-23945
GORTAN, C. N91-23571
N91-23579
GOSSARD, ARTHUR C. N91-23406
GOTSIS, PASCAL K. N91-23247
GOULAIN, M. N91-23853
GOULDIN, F. C. N91-23284
GOULDING, R. H. N91-23353
N91-23913
GOURDEAU, L. N91-23602
GRADWOHL, BEN-AMI N91-24016
GRADY, WALTER A. N91-23115
GRAFTON, D. A. N91-23894
GRANNEN, K. J. N91-23328
GRASSL, H. N91-23203
GRAVE, ALAIN N91-23139
GRAVES, R. L. N91-23318
GRAY, DAVID L. N91-24078
GRAY, H. L. N91-23635
GREENLY, G. D., JR. N91-23744
GREENSPAN, E. N91-23231
N91-23910
GREGOIRE, G. N91-23825
GREGORY, D. C. N91-23873
GREGORY, DON A. N91-23899
GREVELING, NORBERT JOHANNES WIEGER
N91-23988
GRIGGER, DAVID J. N91-23271
GRILLI, M. N91-23875
GRIMSTAD, GREGORY E. N91-23097
GROOM, NELSON J. N91-24083
GROSSIN, M. J. N91-23216
GROSSMAN, ARIE WILLIAM N91-24035
GROVE, CHARLES H. N91-24071
GRUEN, D. M. N91-23277
GRUSH, D. J. N91-23674
GUILLAUME, A. N91-23598
GUO, TEN-HUEI N91-23340
GUSSENHOVEN, M. S. N91-23660
GUSTAVSSON, A. I. N91-23138
GUY, R. WAYNE N91-23153
GYORFFY, B. L. N91-23292

H

HACKEL, R. P. N91-23478
N91-23479
HACKNEY, S. A. N91-23293
HADLEY, G. R. N91-23477
HAFF, K. W. N91-23381
HAHN, CHARLES D. N91-23141
HAILEY, C. E. N91-23432
HALES, STEPHEN J. N91-24065
HALL, D. J. N91-23389
HALL, KEN G. N91-23141
HALL, L. E. N91-23135
HALL, STEPHEN W. N91-23233
HALLADA, MARC R. N91-23482
HALLOCK, J. N. N91-23079
HALLORAN, S. D. N91-23173
HALME, ARNE N91-23789
N91-23790
HALPERN, JOSHUA B. N91-23957
HAMEIRI, E. N91-23924
HAMEKA, H. F. N91-23268
HAMMOND, P. R. N91-23478
HAMZA, A. V. N91-23860
HANDSCHUH, R. F. N91-23500
HANKO, JAMES G. N91-23369
N91-23370
N91-23371
HANNON, PATRICK N91-23722
HANSELKA, HOLGER N91-23246
HANSON, D. B. N91-23850
N91-23852
HANSON, R. K. N91-23902
HARDING, J. N91-23266
HARGENS, ALAN R. N91-23704
HARJES, H. C. N91-23389
HARLOFF, G. J. N91-23175
HARRIS, A. I. N91-24029
HARRIS, GARY N91-23957
HARTH, ERICH N91-23712
HARTMAYER, R. N91-24072
HASELBERGER, GIL N91-23623
HASLIM, LEONARD A. N91-23095
HAUENSTEIN, R. J. N91-23961
HAVENER, A. G. N91-23908
HAVENER, C. C. N91-23873
HAYTON, G. E. N91-23812
HE, J. N91-23269
HE, XIAO-MIN N91-24057
HEARD, J. W. N91-23917
N91-23918
HEATH, M. T. N91-23735
HEDRICK, JAMES N91-23232
HEIBA, A. A. N91-23167
HEIDMANN, JAMES D. N91-23186
HEIKKILA, TAPIO N91-23788
N91-23789
N91-23790
N91-23791
N91-23792
N91-23793
N91-23794
N91-23795
N91-23796
HEILBRONN, Y. N91-23834
HEINEN, V. O. N91-24080
HELGESON, W. D. N91-23939
HELMERSSON, L. N91-23138
HENDRICKS, R. C. N91-23409
HENDRICKSON, MARK R. N91-23994
HENKUS, J. C. N91-23392
HENSHAW, PHILIP D. N91-23905
HEPP, ALOYSIUS F. N91-23616
HERBER, ANDREAS N91-23105
HERBST, W. B. N91-23131
HERGENROTHER, PAUL M. N91-23237
HERLACH, DIETER M. N91-23301
HERLIHY, ALAN T. N91-23625
HERNANDEZ, J. N91-23463
HEROLD, LEROY M. N91-23408
HERRMANN, CAL C. N91-24052
HERSCHMAN, ARTHUR N91-23969
HETHERINGTON, DICK N91-23623
HEYMAN, JOSEPH S. N91-24074
HEYSE, JOERG N91-23176
HICKMAN, D. P. N91-23692
HICKOK, R. L. N91-23917
N91-23918
HICKOX, C. E. N91-23431
HICKS, S. E. N91-23987
HIETALA, V. M. N91-23388
HIHARA, L. H. N91-23264
HIROE, S. N91-23915
N91-23916
HIRSA, AMIR HOSSEIN N91-23419
HIRSCHEL, E. H. N91-23090
HIRSINGER, FRANCIS N91-23149
HIRZINGER, G. N91-23584
HO, CHI-TING N91-23240
HO, CHING-SHUN N91-23202
HO, P. T. N91-23878
HOAGLAND, J. N91-23348
HOEFFNER, JOSEF N91-23654
HOELLER, HARTMUT N91-23677
HOFFMAN, D. C. N91-23882
HOFFMAN, D. J. N91-23353
N91-23913
HOFFMAN, M. J. N91-23150
HOFFMAN, M. M. N91-23882
HOFFMAN, R. N. N91-23655
HOFLER, THOMAS J. N91-23847
HOH, ROGER H. N91-23124

HOHIMER, J. P. N91-23477
HOINKA, KLAUS-PETER N91-23676
HOJAJI, HAMID N91-24082
HOLDEMAN, J. D. N91-23185
HOLDRIDGE, MARK N91-24030
HOLLAND, C. R. N91-23782
HOLMES, A. T. N91-23163
HOLMES, BRUCE J. N91-23410
HOLST, HARMUT N91-23088
HOLSTEN, GUY V. N91-23305
HOLT, M. W. N91-23672
HOLTSLAG, A. A. M. N91-23646
HONNORAT, C. N91-23221
HONNORAT, Y. N91-23178
HOOGSTRATEN, J. A. N91-23587
HOPE, A. N91-23566
HORDONNEAU, ALAIN N91-23260
HORNET, D. N91-23579
HORWITZ, G. N91-23836
HOSHINO, MASAHIRO N91-24027
HOWARD, RICHARD A. N91-23799
HOWELL, SUSAN E. N91-23624
HOWELLS, M. R. N91-23464
HSIN, WEI N91-23474
HU, B. K. N91-23092
N91-23140
HU, JIANHUA N91-23618
HU, SHOUXIANG N91-24082
HUANG, S. N. N91-23543
HUANG, W. D. N91-23427
HUANG, XIANG-YU N91-23679
HUCKABY, D. A. N91-23285
HUDSON, TRACY D. N91-23899
HUEBNER, WERNER N91-23552
HUESTIS, DAVID L. N91-23286
HULTS, W. L. N91-23943
HURLEY, K. N91-24040
HURRELL, JAMES WILSON N91-23665
HURWITZ, MARK VIGLINO N91-24003
HUSSAINI, M. Y. N91-23434
HUYNH, H. T. N91-23119
HWANG, IN HEE N91-23243
HYER, MICHAEL W. N91-23242

I

IDE, P. J. N91-23845
IIZUKA, MASARU N91-23826
IKEYA, T. N91-23385
IMBERT, JEAN-PIERRE N91-23574
INNOCENTI, MARIO N91-23118
INOUE, S. N91-23182
IRANI, FRED M. N91-24054
IRISH, DONALD E. N91-23963
ISAACSON, MICHAEL N91-23896
ISHIHARA, OSAMU N91-23931
ISLER, R. C. N91-23916
ITO, NOBUO N91-23572
IVERSON, J. R. N91-23332
IVES, ROBERT W. N91-23374
IWAHORI, T. N91-23385
IWATA, TSUTOMU N91-23582

J

JACHONTOV, B. O. N91-23568
JACKSON, J. M. N91-24029
JACKSON, T. L. N91-23434
JACOBI, L. Y. N91-23194
JACOBS, I. N91-23720
JACOBSEN, C. N91-23464
JACOBSON, D. L. N91-23299
JAEGER, E. F. N91-23913
JAGODA, JECHIEL I. N91-23449
JAMET, JEAN F. N91-23250
N91-23253
N91-23254
N91-23259
JANI, YASHVANT N91-24049
JAWORSKI, ALLAN N91-24030
JEDLICKA, R. P. N91-23352
JELLISON, G. E., JR. N91-23893
JENDRZEJCZYK, J. A. N91-23414
JENG, J. N91-24072
JENKINS, J. T. N91-23339
JENKINS, M. G. N91-23310
JENKINS, MICHAEL G. N91-23311
JENKINS, S. N91-23479
JENSEN, E. D. N91-23369
N91-23370
N91-23371
JENSEN, ERIC N91-23232
JENTINK, THOMAS NEIL N91-23440
JEPSEN, C. N91-23566
JIANG, TAI-LUN N91-23422
JOERG, CHRISTOPHER F. N91-23401
JOHANSSON, AAKE N91-23991
JOHN, BONNIE E. N91-23763
JOHNS, STEVEN T. N91-23901
JOHNSON, A. D. N91-23289
JOHNSON, ANNE H. N91-24053
JOHNSON, D. D. N91-23292
JOHNSON, D. L. N91-23919
JOHNSON, D. R. N91-23316
JOHNSON, D. S. N91-23812
JOHNSON, GREGORY C. N91-23691
JOHNSON, J. SCOTT N91-23731
JOHNSON, S. A. N91-23478
JONES, L. J. N91-23956
JONES, R. N91-23395
JONES, R. D. N91-23784
JONES, T. V. N91-23172
JONHSON, M. N91-23395
JORDON, K. G. N91-23741
JORSTAD, NORMAN D. N91-24000
JOSEFSON, CARL E. N91-23728
JOSEPH, ROBERT A. N91-23659
JUDAY, RICHARD D. N91-23462
N91-23724
JUNGA, FRANK A. N91-23458

K

KALBERMANN, G. N91-23836
KANG, G. S. N91-23372
KANZ, K. N91-23479
KAO, WEI-LUN N91-23739
KAPLAN, B. Z. N91-23345
KARGEL, JEFFREY STUART N91-24019
KARKKAINEN, PAAVO N91-23791
N91-23792
KASPI, T. N91-23834
KASS, JAMES R. N91-23569
KASTNER, JOEL HARVEY N91-24026
KATTI, R. R. N91-24051
KATZIR, A. N91-23833
N91-23837
KAU, L. S. N91-23303
KAUFMANN, PHILIP R. N91-23625
KAUTZ, HAROLD E. N91-23521
KAZI, LABEED IQBAL N91-23611
KEENAN, DRU N91-23623
KEGELMAN, JEROME T. N91-23453
KEINANEN, HEIKKI N91-23551
KEOUGH, I. A. N91-23325
KEPNER, J. N91-23737
KERELIUK, S. N91-23123
N91-23124
KERGOMARD, C. N91-23600
KERMATH, DON N91-23769
N91-23968
KHAYAT, M. I. N91-23883
KHELAIF, JASER N91-23664
KHOSLA, P. K. N91-23499
KIBENS, VALDIS N91-23453
KICHINSKI, R. N91-23478
KIM, D.-H. N91-23326
KIM, KEVIN DONGHUAN N91-23101
KING, J. C. N91-23943
KING, J. F. N91-23295
KIRBY, GEORGE C., III N91-23556
KIRIS, CETIN N91-24056
KISTNER, M. D. N91-23268
KJENNERUD, EIVIND N91-23576
KLAASEN, J. J. A. N91-23358
KLATTE, R. J. N91-23850
KLAVERS, H. W. N91-23338
KLEBESADEL, R. W. N91-24040
KLEIH, JUERGEN N91-23230
KLOESEL, KEVIN ARLYN N91-23666
KNOTT, WILLIAM M. N91-24060
KNOX, FRANCIS S. N91-23100
KNUDSEN, C. N91-23740
KNUPP, KEVIN R. N91-23670
KOCAMUSTAFAOGULLARI, G. N91-23427
KOCH-PETERS, DOROTHEA N91-23103
KOEHLER, J. N91-23348
KOEHLER, R. N91-23114
KOHLSTEDT, D. L. N91-23403
KOHOUT, LISA L. N91-23620
KOLBERT, W. J. N91-23204
KOLVOORD, ROBERT ANDREW N91-24032
KONOPELCHENKO, B. G. N91-23813
KOODALATTUPURAM, CHITHRABHANU N91-23078
KOOPMAN, J. N91-23164
KORJACK, THOMAS A. N91-23457
KORS, DAVID L. N91-23158
KORSAH, K. N91-23785
KORTING, P. A. O. G. N91-23170
KOURTIDES, DEMETRIUS A. N91-24064
KRABBE, A. N91-23104
KRAL, LAURIE N91-23623
KRAMER, E. J. N91-23403
KRAUS, SARIT N91-23993
KREMER, FRANS G. J. N91-23151
KRESS, MOSHE N91-23828
KRISHNAN, S. N91-23387
KROL, MARK F. N91-23901
KROUSE, CHERYL N91-23075
KRUCHTEN, D. A. N91-23692
KRUSE, RONALD L. N91-23555
KUANG, YINGHONG N91-23974
N91-23975
KUENKLER, H. N91-23154
KULKARNI, REKHA N91-23808
KUPER, C. G. N91-23842
KURENKOV, G. I. N91-23568
KUZNETSOV, A. V. N91-24040
KWAK, DOCHAN N91-24056
KWAK, S. H. N91-23517
KWON, O. J. N91-23086

L

LABORIE N91-23757
LABROT, MAXIME N91-23927
N91-23928
LACOSS, R. T. N91-23848
LADDEN, R. M. N91-23850
N91-23851
LAI, H. T. N91-23175
LAM, JUAN F. N91-23903
LAMBERT, J. N91-24072
LAMBERTDEROUVROIT, M. N91-23437
LAMBRIANIDIS, L. N91-23306
LANDEAU, JOCELYNE N91-23563
LANDERS, T. E. N91-23848
LANDGREBE, DAVID N91-23806
N91-23821
LANDIS, GEOFFREY A. N91-23616
LANGDON, A. BRUCE N91-24027
LANGE, R. N91-23632
LANNELONGUE, N. N91-23607
LANUTTI, J. J. N91-23313
LAOR, ARI N91-23840
LAROS, J. G. N91-24040
LASALMONIE, A. N91-23178
LASKA, SHIRLEY N91-23624
LASSEIGNE, D. G. N91-23434
LATANISION, R. M. N91-23264
N91-23297
LATHROP, B. W. N91-23446
LAU, Y. Y. N91-23878
LAUER, JAMES L. N91-23519
LAUNAY, JEAN-CLAUDE N91-23947
N91-23948
LAURENT, PIERRE-JEAN N91-23808
LAUW, H. K. N91-23387
LAVERGNE, CHRISTIAN N91-23824
LAWLER, R. G. N91-23861
LEA, ROBERT N. N91-24049
LECOUAT, FRANCOIS N91-23591
LEDERER, P. G. N91-23394
LEE, DONG-HUN N91-23638
LEE, FREDERICK W. N91-23377
LEE, J. K. N91-23293
LEE, JIM P. N91-23367
LEE, JUI-TINE N91-23769
LEE, LLOYD L. N91-23964
LEE, MYUNG GYOON N91-24004
LEE, R. L. N91-23426
LEE, Y. C. N91-23784
LEE, YOUNG JAE N91-23531
LEFLOCH, C. N91-23252
N91-23255
LEGALL, J. Y. N91-23606
LEGGETT, DAVID B. N91-23111
LEHMAN, T. H. N91-23351
LEI, FAN N91-24005
LELEVIER, A. N91-23568
LEMAIRE, J. N91-23925
LEONARD, ANTHONY N91-23450
LEONARD, REGIS F. N91-24069
N91-24081
LEONE, J. M., JR. N91-23426
LEONG, D. J. N91-23382
LEONHARDT, M. H. N91-23764
LEPECHON, JEAN CLAUDE N91-23567
N91-23588
LEPROVOST, C. N91-23595
LEQUERTIER, J. M. N91-23197
N91-23257
LERCH, BRAD A. N91-23521
LERNER, NARCINDA R. N91-24063

LEROUX, R. N91-23208
N91-23209
LESCEUX, J. M. N91-23925
LETRAON, PIERRE-YVES N91-23603
LEVEQUE, C. N91-23585
LEVER, A. B. N91-23279
LI, C-Y. N91-23403
LI, L. N91-23560
N91-23561
N91-23562
N91-23816
LI, Y. L. N91-23266
LICHTEN, STEPHEN M. N91-24073
LIEBERT, CURT H. N91-23460
LIEH, JUNGHSEN N91-23532
LIENAU, P. J. N91-23999
LIM, HONG S. N91-23233
LIM, SANG GYU N91-23439
LIN, TUNG-HUA N91-23559
LINDBLOM, JOAKIM FREDRIK N91-24006
LINNE, DIANE L. N91-23616
LIS, STEVEN A. N91-23905
LIU, CHAN CHIANG N91-23609
LIU, HUA-KUANG N91-23890
LIU, K. C. N91-23318
LIU, XIN-TAO N91-23871
LIU, YUAN N91-23992
LIVNE, ELIEZER N91-23190
LLAMES, RENE LIM N91-23738
LLEWELLYN-JONES, D. N91-23601
LOBB, D. N91-23608
LOBO, JORGE N91-23765
LOCATELLI, ARTURO N91-23749
LOFTIN, R. BOWEN N91-24042
LOGAN, C. N91-23463
LONG, DOU N91-23829
LONG, TREVA N91-23282
N91-23323
LOOMIS, MARK PAUL N91-23082
LOOS, ALFRED C. N91-23242
LOPEZ, G. N91-23547
LORENTS, D. C. N91-23336
LORENZ, B. N91-23566
LOUBRIEL, G. M. N91-23939
LOUGE, M. Y. N91-23339
LOUIS, J.-F. N91-23655
LOVEJOY, S. C. N91-23527
LOVENGUTH, MARC N91-23136
LOZAR, CHARLES C. N91-23227
LU, YUN-CHI N91-24054
LUBIN, P. N91-24013
LUCCIO, A. N91-23886
LUGOVSKY, S. B. N91-23856
LUNDIN, C. D. N91-23295
LUO, ANHUA N91-23299
LUTZ, HANS-JOACHIM N91-23652
LUTZE, PETER N91-23302
LYNCH, HARRY J. N91-23714
LYNCH, JAMES D. N91-23827
LYNCH, NANCY N91-23774
LYON, J. F. N91-23914
N91-23916
LYRINTZIS, ANASTASIOS S. N91-23084

M

MA, C. H. N91-23915
N91-23916
MA, CHUNG-CHUN N91-23639
MACDONALD, D. D. N91-23384
MACDOWELL, L. G. N91-24066
MACHELL, R. M. N91-23583
MACIAZSEK, T. N91-23220
MACKULIN, M. J. N91-23514
MACRET, JEAN-LUC N91-23249
N91-23251
N91-23258
MADDEN, D. N91-23660
MAFFEZZONI, C. N91-23747
MAGLIOZZI, B. N91-23852
MAGRI, CHRISTOPHER N91-24007
MAIORANA, CHARLIE N91-23995
N91-23996
N91-23997
MAISH, A. B. N91-23619
MAIURANO, M. N91-23156
MAKOWITZ, H. N91-23736
MALLAT, S. N91-23787
MALLET, R. H. N91-23545
MALLWITZ, ROLAND N91-23105
MALONE, R. M. N91-23894
MANATT, D. R. N91-23986
MANCINI, R. N91-24072
MANGOLD, PETER N91-23125
MANIEZZO, VITTORIO N91-23752
MANN, J. A., JR. N91-23953
MANN, L. N91-23921
MANSOURI, F. N91-23872
MANUKIAN, NARBIK N91-23529
MANZEY, D. N91-23565
MARCH-LEUBA, J. N91-23883
MARCHAND, M. N91-23114
MARCHEPOIL, DENIS N91-23755
MARCOVALDI, R. N91-23874
MARCUS, D. L. N91-23429
N91-23430
MARCUS, J. T. N91-23703
MARGUET, ROGER N91-23149
MARQUET, D. N91-23607
MARSHALL, T. N91-23348
MARTENS, J. S. N91-23388
MARTIN, CHRISTOPHER N91-23136
MARTIN, KEVIN P. N91-23684
MARTIN, PHILIPPE N91-23188
MASKIL, NISSAN N91-23841
MATHER, J. L. N91-23364
MATIC, PETER N91-23556
MATSON, DAVID N91-23709
MATSUSHITA, TOSHIO N91-23793
N91-23794
N91-23795
MATTHEWS, WILLIAM T. N91-23554
MATUS, LAWRENCE G. N91-23946
N91-24061
MATZEN, M. K. N91-23919
MAUK, MICHAEL G. N91-23399
MAUL, WILLIAM A. N91-23205
MAX, C. E. N91-24027
MAYER, A. N91-23315
MAZARAKIS, M. G. N91-23885
MAZZA, C. J. N91-23129
MCCABE, D. E. N91-23539
MCCLUNG, R. W. N91-23316
MCCLURE, M. D. N91-23445
MCCOLGAN, C. J. N91-23850
N91-23851
MCCOWAN, ROBERT B. N91-23398
MCDONALD, DANN C. N91-23115
MCDONALD, J. M. N91-23245
MCDOWALL, R. L. N91-23674
MCELIECE, R. J. N91-24068
MCEWAN, K. J. N91-23949
MCGHEE, R. B. N91-23517
MCGILL, T. C., JR. N91-23960
MCGREGOR, W. K. N91-23235
MCKAY, K. N91-23130
MCKIERNAN, JOHN N91-23900
MCLAREN, P. E. N91-23917
MCLAUGHLIN, D. L. N91-23939
MCLELLAN, T. N91-23720
MCMANUS, KEITH ROBERT N91-23270
MCNEELY, JAMES B. N91-23399
MCPHAIL, A. T. N91-23956
MCRUER, DUANE N91-23121
MEGER, R. A. N91-23888
MEHLHORN, T. A. N91-23919
MEILUNAS, R. J. N91-23328
MEISCHNER, PETER N91-23677
MELLO, F. N91-23526
MELNICK, GARY J. N91-23212
MENARD, Y. N91-23602
MENEES, GENE P. N91-23169
MENENDEZ-VALDES, PEDRO N91-23485
MENSAH, PATRICE EDOETE N91-23830
MENTHE, R. W. N91-23851
MERRILL, WALTER N91-23340
MESANDER, GEERT A. N91-23183
MESTHA, L. K. N91-23391
METIVAUD, GUY N91-23217
METZINGER, K. N91-23526
MEYER, CLAUDIA M. N91-23205
MEYER, F. W. N91-23873
MEYER, FRIEDRICH N91-23442
MEYERS, JAMES F. N91-24077
MICHELASSI, V. N91-23416
MILLER, E. K. N91-23351
MILLER, TERESA Y. N91-23933
MILNER, A. M. N91-23634
MIN, J. B. N91-23502
MINKER, JACK N91-23765
N91-23992
N91-23993
MINODA, M. N91-23182
MIRTICH, MICHAEL J. N91-24062
MITCH, MARK E. N91-23625
MITCHELL, CLARK N91-23136
MITCHELL, F. R. N91-23894
MITCHELL, ROBERT A. N91-23100
MITCHELL, T. E. N91-23942
N91-23944
MITCHELL, TODD PORTER N91-23667
MITTELSTEIN, MICHAEL N91-23481
MOHR, P. N91-23463
MOLINES, J. M. N91-23602
MOLTZ, D. M. N91-24015
MONDAL, J. N91-23346
MONFORD, LEO G., JR. N91-23490
MOORHOUSE, DAVID J. N91-23117
MORCHAT, R. M. N91-23325
MOREL, ANDRE N91-23596
MOREL, M. N91-23605
MORGAN, HERBERT K. N91-24030
MORGAN, J. MURRAY N91-23122
MORRIS, J. W., JR. N91-23300
MORRIS, P. J. N91-23451
MORRISON, T. R. N91-23721
MORSE, CHANNING S. N91-23110
MORTENSEN, G. A. N91-23415
MOSER, F. N91-23837
MOSS, R. N91-23463
MUELLER, F. M. N91-23943
MUKKAMALA, RAVI N91-23970
N91-23971
N91-23972
N91-23973
N91-23974
N91-23975
MULLEN, R. L. N91-23409
MULLER, S. N91-23926
MULLER, SARA H. N91-23678
MULLIS, ANDREW MARTIN N91-24031
MUMM, H. N91-23768
MUNTEAN, TRAIAN N91-23779
N91-23822
MURAD, EDMOND N91-23228
MURDOCK, T. M. N91-23742
MURNOCK, DONALD N91-23968
MURPHY, D. P. N91-23888
MURPHY, R. JAY N91-24077
MURTHY, PAPPU L. N. N91-23548
MUSHER, J. N91-23618
MUSSO, G. N91-23578
MUTCH, PATRICIA N91-23800
MYLES, GREGORY N91-23684

N

NAEIJE, M. C. N91-23594
NAGPAL, VINOD K. N91-23548
NAGY, KORNEL N91-23492
N91-23493
NAHRA, HENRY N91-24062
NAKAMURA, HISASHI N91-23668
NAKAMURA, TAICHI N91-23582
NARANG, S. C. N91-23384
NASH, A. S. N91-23945
NASH, P. N91-23945
NATH, NITYA N91-23211
NATIONS, J. A. N91-23985
NAVINCHANDRA, D. N91-23633
NEAL, D. R. N91-23892
NEAL, DONALD M. N91-23554
NEATHAMMER, ROBERT D. N91-23762
NEEB, K. P. N91-23478
NEEDELMAN, WILLIAM M. N91-23512
NEELY, EDGAR S. N91-23762
NEHRKORN, T. N91-23655
NELSON, J. S. N91-23941
NEMZEK, ROBERT JAMES N91-23644
NEU, THOMAS J. N91-23683
NEUMANN, MICHAEL N91-23818
NEWELL, ALLEN N91-23763
NEWMAN, J. C., JR. N91-23539
NEWMAN, ROBERT N91-23134
NEWSOME, PENNY N91-23211
NICHOLAS, O. P. N91-23119
NICHOLSON, D. M. N91-23292
NICOLAIDIS, M. N91-23393
NIEL, M. N91-24040
NIELSEN, MOGENS N91-23591
NIEUWPOORT, ANTON M. H. N91-23191
NIKOLAEV, A. S. N91-23856
NIX, WILLIAM D. N91-23267
NOHEL, JOHN A. N91-23454
NOOK, MARK ALLEN N91-24008
NORIEGA, CARLOS I. N91-23226
NORTHCUTT, J. D. N91-23369
N91-23370
N91-23371
NORTHEY, M. D. N91-23541
NOSE, H. N91-23182
NOVARA, M. N91-23571
NYQUIST, DENNIS P. N91-23368

O

OBERACKER, V. E. N91-23869
OBERG, TERO N91-23551
OBOT, N. T. N91-23414
OCONNELL, SUSAN M. N91-23969
OCONNOR, D. G. N91-23544
ODA, MITSUSHIGE N91-23582
ODUBIYI, JIDE N91-24030
OGDEN, ANDREA L. N91-23242
OGLESBY, ROBERT JAMES N91-23669
OGURA, YUKIO N91-23826
OHERN, T. J. N91-23892
OHLBERG, DOUGLAS A. N91-23954
OLLERTON, R. N91-23768
OLSON, C. L. N91-23919
OLSON, W. R. N91-23885
OMALLEY, M. W. N91-23939
ONOFRI, M. N91-23174
ONTIVEROS, C. N91-24066
OROURKE, M. K. N91-23784
OROURKE, MATTHEW N91-23136
OSBORNE, ERIC P. N91-24079
OSTROUCHOV, L. S. N91-23735
OUROUA, A. N91-23917
OVERBURY, S. H. N91-23873
OVERTON, W. SCOTT N91-23625
OWEN, ALBERT K. N91-23179
OZEK, TORU N91-23963

P

PABOOJIAN, ARMAND J. N91-23659
PADGETT, WILLIAM J. N91-23827
PAINTER, S. L. N91-23914
PAISNER, J. A. N91-23479
PALAZZO, FRANK V. N91-23761
PALKA, EDWARD N91-23075
PAN, YUNG N91-23769
N91-23968
PANDOLFINI, P. P. N91-23166
PANTANI, LUCA N91-23604
PARAZYNSKI, S. E. N91-23704
PARDO, C. N91-24072
PAREDIS, C. J. J. N91-23499
PAREKH, DAVID E. N91-23453
PARIKH, LINK A. N91-23206
PARISH, MARK V. N91-23951
PARK, MYUNG-KYUN N91-23530
PARKIN, B. R. N91-23446
PASCHALI, PASCHALIS GEORGE N91-24020
PASTRONE, D. N91-23578
PATEL, VADANKUMAR M. N91-23100
PAUSDER, HEINZ-JUERGEN N91-23128
PAVLIK, D. N91-23389
PEAL, K. R. N91-23471
PECHACEK, R. E. N91-23888
PEIX, G. N91-23255
PELLIN, M. J. N91-23277
PENETRANTE, B. M. N91-23865
PERES, P. N91-23256
N91-23262
PEREZ, GONZALO N91-23769
N91-23968
PERSELLO, L. F. N91-23106
PERVAIZ, M. M. N91-23448
PETERS, HANNS-JUERGEN N91-23137
PETERS, LEON, JR. N91-23402
PETIT, JEREMY B. N91-23946
PETITT, G. A. N91-23871
PETRIE, H. L. N91-23451
PETROVA, N. L. N91-23856
PEUSSA, J. T. N91-23310
PEZZANITI, J. L. N91-23906
PHANEUF, R. A. N91-23857
N91-23873
PHILLIPS, J. M. N91-23388
PIESKA, SAKARI N91-23791
N91-23792
PIKE, J. N91-23444
PILLAI, RAMADAS N91-23485
PIMENTAL, NANCY A. N91-23717
PINEAU, DIDIER N91-23929
PINGREE, JOSEPH ELLSWORTH N91-23640
PIPITONE, FRANK N91-23344
PIPPI, IVAN N91-23604
PIRAMUTHU, SELWYN N91-23802
PLATEAU, BRIGITTE N91-23362
N91-23778
PLICHTA, M. R. N91-23293
PLOTARD, P. N91-23252
POEPPEL, R. B. N91-23945
POGORELSKY, I. N91-23476
POHNER, JOHN A. N91-23408
POINTKOWSKI, JOSEPH N91-23075
POLLARA, F. N91-24068
POLLINA, R. J. N91-23911
POLVANI, R. S. N91-23315
POLYANSKI, STANLEY N91-23342
PONCHAK, DENISE S. N91-23347
POON, S. J. N91-23304
POPE, DAVID P. N91-23308
PORKOLAB, M. N91-23920
POTAPCZUK, M. G. N91-23086
N91-23087
POULOSE, M. M. N91-23099
POVINELLI, LOUIS A. N91-23162
POWELL, A. N91-23848
POWELL, J. ANTHONY N91-23946
N91-24061
POWERS, JOHN P. N91-23236
PRAKASH, RAMESH K. N91-23699
PRENDIN, WALTER N91-23581
PRESTWICH, K. R. N91-23919
PRICE, KENT M. N91-24030
PRICE, P. BUFORD N91-23887
PRUETT, D. J. N91-23381
PRYOR, ROBERT N91-23699
PRYWES, NOAH S. N91-23773
PUGH, A. C. N91-23812
PUJARA, L. R. N91-23144
PYGOTT, C. H. N91-23753

Q

QIAO, C. Y. P. N91-23295
QUEGAN, SHAUN N91-23641

R

RABADI, ELSALEM N91-23664
RABINOWITZ, PAUL H. N91-23820
RABITZ, HERSCHEL N91-23881
RACHNER, M. N91-23164
RADICATI, BRUNO N91-23604
RADZISZEWSKI, E. N91-23588
RAFFERTY, K. N91-23999
RAKEL, D. A. N91-23274
RAMACHANDRAN, R. S. N91-23498
RAMETTE, PHILIPPE N91-23152
RAMEY, D. W. N91-23381
RAMIREZ, J. J. N91-23919
RAMON, L. V. N91-23583
RAMSBOTHAM, A. J. N91-24000
RANDALL, K. L. N91-23858
RANDLES, M. H. N91-23952
RANSFORD, GARY A. N91-23976
RANSOM, V. H. N91-23415
RAO, G. V. R. N91-23167
RAPHAEL, MARILYN NOREEN N91-23629
RAQUET, C. A. N91-23354
RASMUSSEN, S. N91-23740
RASPET, R. N91-23848
RAST, M. N91-23605
RAU, W. N91-23165
RAVID, ITZHAK N91-23621
REBER, CHRISTIAN N91-23900
REDDY, D. R. N91-23175
REDDY, S. K. N91-23500
REDEY, L. N91-23390
REDIKER, ROBERT H. N91-23904
REDING, GREGORY J. N91-23661
REED, R. A. N91-23235
REIDY, R. N91-23326
REIFMAN, J. N91-23520
REINHOLD, BRIAN N91-23991
REINMANN, J. J. N91-23087
REMIS, STEVEN J. N91-23723
RENZO, BAVA N91-23112
REO, NICHOLAS V. N91-23706
REPPERGER, DANIEL W. N91-23723
REUTER, LAURIE N91-23405
REUTER, R. C., JR. N91-23537
REVELL, J. D. N91-23848
REYNOLDS, THOMAS L. N91-23097
REZVANI, M. A. N91-23540
RHEE, IHNSEOK N91-23831
RIBAUD, YVES N91-23157
RIBEIRO, DINIS AFONSO N91-23577
RICE, J. K. N91-23919
RICHARDS, B. G. N91-23272
RIGAUD, V. N91-23590
RIGHTER, A. W. N91-23382
RILEY, GARY N91-24043
RILEY, M. F. N91-23135
RINGERTZ, ULF N91-23759
RINKER, JACK N. N91-23610
RINTAMAA, RAUNO N91-23551
RITTI, M. H. N91-23256
RITZ, C. P. N91-23918
ROACH, J. F. N91-23389
ROBERDS, D. W. N91-23235
ROBERTS, B. A. N91-23877
ROBEY, H. F. N91-23892
ROBINSON, ANITA N91-23487
ROBINSON, GARY Y. N91-23950
ROCKWELL, DONALD N91-23094
RODRIGUEZ, FERDINAND N91-23282
N91-23323
ROGERS, C. N91-23813
ROGERS, STUART E. N91-24056
ROMANOFSKY, ROBERT R. N91-24069
ROME, J. A. N91-23916
ROMINE, C. H. N91-23735
RONALD, TERENCE M. F. N91-23177
RONCHI, CORRADO N91-23643
ROOS, DARRELL N91-23211
ROOS, FREDERICK W. N91-23453
ROSEN, I. G. N91-23801
ROSENFELD, YAAKOV N91-23879
ROSENTHAL, H. N91-23238
ROSS, D. W. N91-23912
N91-23918
ROSSANO, GRAHAM W. N91-23760
ROTACIUC, V. N91-23104
ROTHWELL, EDWARD J. N91-23368
ROWLAND, WAYNE D. N91-24078
ROYET, J. N91-23935
ROZHKOV, A. V. N91-23568
RUAN, Y. F. N91-23513
RUIZ, C. N91-23266
RUOFF, A. L. N91-23403
RUSPINI, ENRIQUE H. N91-23814
RUSSELL, P. N91-23476
RUSSELL, S. D. N91-23400
RUTHERFORD, A. W. N91-23437
RUTHERFORD, JOHN N91-23136
RUTLEDGE, SHARON K. N91-24062
RYAN, P. M. N91-23353
N91-23913

S

SAAR, A. N91-23837
SAARENHEIMO, ARJA N91-23551
SABASTIANI, F. N91-23875
SACHSE, GLEN W. N91-23889
SAFAVIAN, S. RASOUL N91-23806
N91-23821
SAGER, JOHN C. N91-23718
N91-24060
SAGI, A. N91-23833
SAHOTA, M. S. N91-23428
SAHR, JOHN DAVID N91-24017
SAINTE-MARIE, MARTINE N91-23188
SAKHO, IBRAHIMA N91-23822
SAKUMA, T. N91-23506
SALE, MICHAEL J. N91-23625
SALEIN, MARIANNE N91-23103
SALEM, ASHRAF N91-23726
SALEM, JONATHAN A. N91-23311
SALMONSON, J. C. N91-23245
SALTER, RICHARD H. N91-23228
SAMANT, MAHESH G. N91-23303
N91-23880
N91-23959
SAMPSELL, JEFFREY B. N91-23724
SANCHEZTARIFA, C. N91-23148
SANGOUARD, D. N91-23585
SANKAR, L. N. N91-23086
SANS, C. N91-23160
SARAFIAN, G. N91-23345
SARAVANAN, R. N91-23642
SARGENT, CHRISTIAN L. N91-23523
SARKIMO, MATTI N91-23551
SARRAZIN, P. N91-23255
SATO, TOMOMASA N91-23793
N91-23794
N91-23795
SAUBADE, C. N91-23758
SAUTHOFF, N. N91-23921
SAVAGE, M. N91-23500
N91-23514
SAVELY, ROBERT T. N91-24042
SAWCHUK, A. A. N91-23909
SCHADLER, LINDA SUE N91-23241
SCHAFHAUSER, ERICH N91-23569
SCHARDT, MATHIAS N91-23612
SCHARROO, R. N91-23594
SCHAUS, C. F. N91-23477
SCHEIDLER, MICHAEL J. N91-23469
SCHERRER, DOMINIQUE N91-23152
SCHIAVONI, NICOLA N91-23749

SCHILDBACH, M. N91-23860
SCHILLING, C. H. N91-23313
SCHLOTZHAUER, GERALD N91-23746
SCHMIDT, FRED N91-23102
SCHMITENDORF, W. E. N91-23742
SCHNEIDER, HANS N91-23818
SCHNITZLER, B. G. N91-23884
SCHNOEBELEN, P. N91-23780
N91-23810
SCHOCH, P. M. N91-23918
SCHOLL, MARIJA S. N91-24046
SCHUBERT, FRANZ H. N91-23271
SCHULTE-WERNING, BURKHARD N91-23435
SCHULTZ, F. J. N91-23381
SCHULTZ, R. L. N91-23150
SCHUMACHER, B. N91-23463
SCHWARTZ, IRA B. N91-23405
N91-23486
SCHWARZ, R. L. N91-23985
SCHWELBERGER, J. G. N91-23917
SCOTT, RODERICK S. N91-23690
SEAH, M. P. N91-23467
SEGURA, CLEMENT M. N91-23225
SEKULOW, E. N91-23348
SENDEK, DAVID M. N91-23730
SERABIAN, STEVEN M. N91-23263
SERAJI, HOMAYOUN N91-23783
SEWERSKY, R. A. N91-23146
SHADMON, G. N91-23107
SHAFRANEK, D. N91-23119
SHAGAM, R. N. N91-23892
SHAH, ASHWIN R. N91-23549
SHAH, TASNEEM MOHAMMAD N91-23418
SHAH, V. M. N91-23859
SHAHSHAHANI, M. N91-24068
SHAKED, U. N91-23804
SHALKHAUSER, K. A. N91-23354
SHALKHAUSER, MARY JO N91-24067
SHAPIRO, PAUL R. N91-23839
SHARF, YARON N91-23337
SHAVIT, NIR N91-23774
SHAW, MICHAEL J. N91-23802
N91-23803
SHAW, ROBERT J. N91-23098
SHEIKH, S. I. N91-23150
SHENG, YUEJIAN N91-23980
SHIAU, T. H. N91-23477
SHIEH, LEANG S. N91-23819
SHIFLET, G. J. N91-23304
SHIH, T.-H. N91-23416
SHIH, W. H. N91-23313
SHIN, JAIWON N91-23183
SHIN, KWANG S. N91-23299
SHIZGAL, B. N91-23925
SHOENFELT, NANETTE M. N91-23898
SHUCH, H. PAUL N91-23096
SHURRAB, M. S. N91-23546
SIFFRE, MICHEL N91-23570
SIKIVIE, P. N91-24015
SIKORA, RIYAZ N91-23803
SILVER, BURTON N91-24058
SIMCIC, V. J. N91-23917
SIMEONIDES, G. N91-23196
SIMKOVICH, G. N91-23326
SIMON, PAUL C. N91-23647
SIMONS, DOUGLAS ANTHONY N91-24011
SIMPSOM, W. N91-23911
SINGHAL, SURENDRA N. N91-23548
SINNIS, CONSTANTINE N91-24039
SIOMACCO, EDWARD M. N91-23404
SIRBAUGH, J. R. N91-23445
SISLIAN, J. P. N91-23168
SKOOG, I. N91-23575
SLABOSPITSKY, S. R. N91-23856
SLINEY, DAVID H. N91-23487
SLOAN, M. L. N91-23918
SLOCUM, ROBERT E. N91-23891
SMARTT, H. B. N91-23510
SMATHERS, J. N91-23871
SMITH, ALVIN N91-23227
SMITH, C. E. N91-23185
SMITH, D. L. N91-23885
SMITH, J. L. N91-23943
SMITH, ROGERS E. N91-23127
SMITHRICK, JOHN J. N91-23233
SMOLENSKI, D. M. N91-23459
SOBOTA, MARK S. N91-23126
SOEGAARD, SVEIN-ERIK N91-23754
SOETRISNO, MOELJO N91-23412
SOHN, PHILIP Y. N91-23102
SOKOLOFF, JASON P. N91-23901
SOKOLOV, V. N91-23346
SOLOMON, O. M., JR. N91-23349
SOLOMONSON, NORBERT DANIEL N91-24009
SOMMER, DAVID V. N91-23781
SORENSEN, LARRY B. N91-23959
SOROKA, E. N91-23804
SOVA, G. N91-23081
SOVEY, JAMES S. N91-24062
SPACHT, L. N91-23081
SPANYER, K. L. N91-23502
SPARKS, SHAWN N91-23487
SPERO, E. N91-23231
SPEZIALE, CHARLES G. N91-23433
SPIEGEL, D. R. N91-23277
SPLITT, GEORG N91-23357
SPRINGSTON, S. R. N91-23626
SRINIVASMURTHY, S. N91-23427
ST.CLAIR, TERRY L. N91-23242
STACY, JOHN L. N91-23901
STADLER, H. L. N91-24051
STALDER, K. R. N91-23336
N91-23466
STANFORD, SPENCER ADAM N91-24021
STEELE, JOHN D. N91-23966
STEINBERGER, CRAIG J. N91-23181
STEINETZ, BRUCE M. N91-23515
STEPHENS, ROBERT L. N91-23100
STERN, ALAN N91-23102
STERNBERG, A. N91-23104
STERRETT, A. N91-23767
STERRETT, M. E. N91-23498
STEWART, ROBERT KEITH N91-23977
STEWART, W. E. N91-23425
STIEGLER, JAMES O. N91-23308
STIENSTRA, DAVID I. AUEN N91-23533
STIRN, JAMES R. N91-23762
STOCKS, G. M. N91-23292
STOLLERY, J. L. N91-23092
N91-23140
N91-23161
STOREY, J. W. V. N91-23104
STRAHLE, WARREN C. N91-23449
STRAKA, J. N91-23203
STRAUSS, H. R. N91-23924
STRECKERT, H. H. N91-23327
STREICHER, JUERGEN N91-23355
STREIT, G. N91-23630
STREVELL, MICHAEL W. N91-23729
STRICKER, JEFFREY M. N91-23155
STRICKLAND, J. H. N91-23085
STRIFE, J. R. N91-23327
STRIGANOV, S. I. N91-23856
STROGANOV, Y. G. N91-23856
STRUIJS, R. N91-23436
STUCK, E. R. N91-23505
STYF, J. N91-23704
SUBRAHMANIAN, V. S. N91-23993
SUBRAHMANYAM, M. B. N91-23797
SUGA, NOBUO N91-23708
SUITOR, JERRY W. N91-24059
SUKHADIA, A. M. N91-23330
SUKORIANSKY, SEMION N91-23231
N91-23407
N91-23910
SULLIVAN, CAROL A. N91-23398
SULLIVAN, N. S. N91-24015
SUN, S. N91-23477
SUN, T. N91-23329
SUNDBERG, W. D. N91-23085
SUNDLAND, H. N91-23566
SUNKARA, MAHENDRA N91-23953
SUNYAEV, R. A. N91-24040
SURANYI, P. N91-23872
SURI, MANIL N91-23815
SUSKO, MICHAEL N91-23215
SUTJAHJO, EDHI N91-23548
SWAIN, D. W. N91-23913
SWAIN, PHILIP H. N91-23786
SWAN, DAVID HERMAN N91-23423
SWANK, W. D. N91-23317
SWANSON, L. N91-24068
SWINDEMAN, R. W. N91-23295
N91-23545
SZCZUR, MARTHA R. N91-24048
SZEWCZYK, ALBIN A. N91-23447

T

TAGGART, D. P. N91-23888
TAILHADES, J. N91-23580
TAKAI, MASAMI N91-23132
TAKEI, K. N91-23385
TALBI, E.-G. N91-23779
TALJA, HELI N91-23551
TALMAGE, G. N91-23910
TALPALLIKAR, M. V. N91-23185
TANG, DE-MING N91-23693
TANG, PING TAK PETER N91-23743
TANGUAY, ARMAND R., JR. N91-23907
TANNER, D. B. N91-24015
TARDIN, ANTONIO TEBALDI N91-23609
TARIDE, S. N91-23468
TAUDIERE, ISABELLE N91-23363
TCHEOU, F. X. N91-23989
TEAL, WALTER B. N91-23717
TEBOULLE, MARC N91-23772
TENG, DAN N91-23936
TERADA, N. N91-23385
TEREKHOV, O. V. N91-24040
TERRIBILE, ANTONIO N91-23581
TEWARI, RAJIV N91-23981
THAKOOR, ANIL N91-24045
THAYER, JEFFREY PAUL N91-23673
THEISS, T. J. N91-23509
THEOPOLD, FELIX A. N91-23653
THIEM, TERRY L. N91-23228
THIEME, LANNY G. N91-23234
THOMAS, DIETER N91-23109
THOMAS, J. M. N91-23091
THOMAS, R. K. N91-23536
THOMAS, RICHARD W. N91-23117
THOMPSON, J. M. N91-23545
THOMPSON, J. R. N91-23918
THOMPSON, J. S. N91-23873
THOMPSON, LESLIE L. N91-24055
THORPE, ARTHUR N. N91-24082
THRASHER, D. L. N91-23200
TIERNEY, J. W. N91-23334
TIGGES, C. P. N91-23388
TIMME, ADALBERT N91-23103
TIRKAS, PANAYIOTIS A. N91-23365
TOBIAS, C. W. N91-23741
TOLLIVER, J. S. N91-23353
N91-23913
TOMPKINS, J. A. N91-23381
TONEY, MICHAEL F. N91-23880
N91-23959
TONG, WILLIAM M. N91-23954
TORCZYNSKI, J. R. N91-23892
TORO, E. F. N91-23443
TORVIKOSKI, TIMO N91-23789
N91-23790
TOUGH, R. J. A. N91-23846
TOURNADRE, J. N91-23599
TOUZENE, ABDEREZAK N91-23362
TOWNSEND, D. P. N91-23513
TRAGL, KARL N91-23356
TRAPP, J. A. N91-23415
TRAVERSE, PASCAL N91-23192
TRAYBAR, JOSEPH J. N91-23124
TREASE, H. E. N91-23428
TREIL, N. N91-23787
TRUBIAN, MARCO N91-23750
TRUSZKOWSKI, WALT N91-24044
TSO, HUM CHI N91-23937
TSU, D. V. N91-23328
TU, Y. K. N91-23513
TUCKER, B. N91-23704
TUELL, JASON P. N91-23658
TURNER, MICHAEL S. N91-24015
TWARDY, HARALD N91-23246
TWIGG, PAMELA D. N91-24057
TYK, R. N91-23842
TYSON, KAREN W. N91-23076

U

UHRIG, R. E. N91-23785
UMAR, A. S. N91-23869
UNAL, O. N91-23944
UNSEREN, M. A. N91-23508
UPDIKE, E. N91-23463
UPPILI, SUDARSAN N91-23932
USAB, WILLIAM J., JR. N91-23440
USUI, H. N91-23182

V

VAERNES, R. N91-23566
VANBIBBER, KARL N91-24015
VANCUTSEM, BERNARD N91-23823
VANDYKE, J. W. N91-24036
VANENGELEN, J. A. J. N91-23119
VANGEL, MARK G. N91-23554
VANWEST, BARRY PAUL N91-23239
VARDI, MOSHE Y. N91-23798
VARVILL, R. N91-23163
VASILOFF, STEVEN V. N91-23675
VAUCHER, CHRISTOPHER A. N91-23656
VAUCHER, GAIL T. N91-23656
VEDRENNE, G. N91-24040
VELIGDAN, J. N91-23476
VEMURI, GAUTAM N91-23475
VERA, ALONSO H. N91-23763

VERAAR, R. G. N91-23170
VERKADE, J. G. N91-23331
VERRON, J. N91-23593
VERWEY, W. B. N91-23719
VETERAN, J. L. N91-23961
VIBERTI, CARLO N91-23569
N91-23574
N91-23578
VINCENT, P. N91-23602
VIZIER, PHILIPPE N91-23218
N91-23219
VOGEL, M. H. N91-23360
N91-23361
VOGT, L. N91-23564
VOIGT, KRISTINA N91-23990
VOJTESAK, MICHAEL J. N91-23684
VONGRUENHAGEN, WOLFGANG N91-23128
VORACEK, DAVID F. N91-23133
VORTMEYER, D. N91-23165
VOSS, RALPH N91-23854
VRANISH, JOHN M. N91-23380
VRCKOVNIK, GARY E. N91-23378

W

WAAHLIN, E. K. N91-23873
WADE, M. R. N91-23916
WAGENBLAST, G. R. N91-23541
WAGENER, K. B. N91-23324
WAGNER, JOHN A. N91-24065
WAIT, J. R. N91-23366
WAKKER, K. F. N91-23594
WALCHLI, LAWRENCE A. N91-23127
WALKER, M. J. N91-23130
WALTERS, DONALD L. N91-23656
WAMBSGANSS, M. W. N91-23414
WANG, HAI N91-23287
WANG, HUA N91-23745
WANG, LIANG-GUO N91-23889
WANG, LUI N91-24050
WANG, PAUL N91-23770
WANG, YAXIN N91-23953
WANG, Z. N91-23427
WARD, PAUL N91-23232
WARDEN, M. P. N91-23364
WARE, MATTHEW F. N91-24082
WARNCKE, M. N91-23566
WARNE, L. K. N91-23352
WARNER, JOSEPH D. N91-24081
WASHLOCK, PAUL A. N91-23953
WATKINS, A. D N91-23510
WATKINS, J. A. N91-23510
WATKINS, J. G. N91-23245
WATKINS, PAUL J. N91-24053
WATSON, LYN R. N91-23228
WATSON, R. D. N91-23245
WATSON, R. L. N91-23870
WEBB, ANDREW R. N91-23811
WEI, T. Y. C. N91-23520
WEINER, ALLAN M. N91-23682
WEINREICH, HERMANN-L. N91-23171
WEIRICK, L. J. N91-23314
WEIRUP, D. N91-23463
WEISS, D. N91-23967
WELCH, D. O. N91-23940
WELLS, R. L. N91-23956
WENDER, I. N91-23334
WENZEL, J. N91-23564
WENZEL, WOLFGANG N91-23938
WESSELSKI, CLARENCE J. N91-23492
N91-23493
WESSON, J. P. N91-23327
WEST, B. H. N91-23318
WEYER, THOMAS H. N91-24086
WHEADON, JOE N91-23591
WHEELER, RAYMOND M. N91-23718
WHITE, DEWEY W., JR. N91-23199
WHYTE, WAYNE A. N91-24067
WIEGAND, H. N91-23164
WIESLER, DAVID G. N91-23880
WIJEWARDHANA, L. C. R. N91-23872
WILD, W. N91-24029
WILHELM, KNUT N91-23191
WILKES, GARTH L. N91-23242
WILLEBEEK-LEMAIR, MARC HUBERT N91-23777
WILLEMS, G. C. N91-23721
WILLES, E. H., JR. N91-23986
WILLIAMS, DANIEL W. N91-23496
WILLIAMS, M. D. N91-23630
WILLIAMS, M. S. N91-23466
WILLIAMS, R. S. N91-23281
N91-23900
N91-23954
WILLIS, EDWARD A. N91-23083
WINNICK, J. N91-23275
WINTERSTEINER, PETER P. N91-23659
WIPPLER, J. L. N91-23589
WITHROW, COLLEEN A. N91-23620
WITT, ARTHUR N91-23675
WITTEN, L. N91-23872
WLEZIEN, RICHARD W. N91-23453
WOLF, PETER N91-23237
WOLF, STEPHEN D. N91-23195
WOOD, J. D., JR. N91-23634
WOODWARD, WAYNE A. N91-23635
WOOTTON, A. J. N91-23918
WORCESTER, R. K. N91-23899
WORLEY, P. H. N91-23805
WORSNOP, JOHN C. N91-24012
WRENN, GREGORY A. N91-23135
WRIGHT, KENNETH D., II N91-24078
WRIGHT, M. A. N91-23269
WROBEL, T. F. N91-23386
WU, J. C. N91-24051
WU, W. H. N91-24072
WU, XIANGQIAN N91-23663
WU, XIAO-QIANG N91-23559
WUENNENBERG, HORST N91-23116
WURTMAN, RICHARD J. N91-23714
WYDEVEN, THEODORE N91-24052
N91-24063

X

XUE, Y. N91-23084
XZYDLOWSKI, EDWARD N91-23075

Y

YADLIN, YORAM N91-23413
YANG, JIANN CHYUAN N91-23273
YANG, SONG N91-23636
YEE, LAWRENCE N91-23900
YEOH, LEAN-WENG N91-23379
YIU, YAU-CHEUNG N91-23525
YOKOSAWA, A. N91-23862
YOON, SUGJOON N91-23189
YOSHIDA, Z. N91-23924
YOST, WILLIAM T. N91-24076
YOU, HONG K. N91-23954
YOUNG, C. E. N91-23277
YOUNG, M. H. N91-23961
YOUNG, S. N91-23336
N91-23949
YOUNGDAHL, C. K. N91-23534
YUAN, HAOJIE N91-23281
YUAN, W. N91-23333
YUGO, J. J. N91-23913

Z

ZAGLAUER, HELMUT WALTER N91-24014
ZAKRAJSEK, J. J. N91-23513
ZARETSKY, ERWIN V. N91-23512
N91-23550
ZDUNEK, ADAM N91-23321
ZEHNER, D. M. N91-23873
ZEIJLMANSVANEMMICHOVEN, P. A. N91-23873
ZELTER, GABRIELA R. N91-23233
ZHANG, SHUANG NAN N91-24010
ZHANG, ZIANG N91-23871
ZHENG, K. N91-23477
ZHENG, YUAN F. N91-23489
ZHONG, WEI N91-23559
ZIADA, H. H. N91-23540
N91-23546
ZIELINSKI, ALEXANDER E. N91-23930
ZIELINSKI, J. J. N91-23917
ZIEMIANSKI, JOSEPH A. N91-23083
ZILBERMAN, M. N91-23194
ZINK, JEFFREY I. N91-23900
ZINNECKER, H. N91-24029
ZIPPERIAN, T. E. N91-23388
ZOOK, JOHN A. N91-23518
ZUTAVERN, F. J. N91-23939
ZUZEK, JOHN E. N91-23347

Typical Corporate Source Index Listing

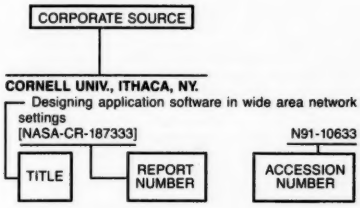

Listings in this index are arranged alphabetically by corporate source. The title of the document provides the user with a brief description of the subject matter. The report number helps to indicate the type of document cited (e.g., NASA report, translation, NASA contractor report). The accession number denotes the number by which the citation is identified. The titles are arranged under each corporate source in ascending accession number order.

A

ABERDEEN UNIV. (SCOTLAND).
Symmetries in general relativity
[REPT-911-440-105] N91-23966

ADVISORY GROUP FOR AEROSPACE RESEARCH AND DEVELOPMENT, NEUILLY-SUR-SEINE (FRANCE).
Flying Qualities
[AGARD-CP-508] N91-23108
Hypersonic Combined Cycle Propulsion
[AGARD-CP-479] N91-23147
Human Performance Assessment Methods. Addendum
[AGARD-AG-308-ADD] N91-23711
AGARD highlights 91/1, March 1991
[AGARD-HIGHLIGHTS-91/1] N91-24084

AERITALIA S.P.A., TURIN (ITALY).
Flying qualities experience on the AMX aircraft
N91-23112

AEROJET TECHSYSTEMS CO., SACRAMENTO, CA.
Design considerations for combined air breathing-rocket propulsion systems
[AIAA-90-0098] N91-23158

AERONAUTICAL RESEARCH INST. OF SWEDEN, STOCKHOLM.
Long time measurements of landing gear loads on SAAB SF-340 commuter aircraft
[FFA-TN-1990-53] N91-23138
Determination of the deviatoric material response functions for prestrained rubbers
[FFA-TN-1990-29] N91-23321
A moving boundary algorithm for the solution of contact problems in linear elasticity. Part 1: Basic theory and model examples
[FFA-TN-1991-08-PT-1] N91-23759

AERONAUTICAL RESEARCH LABS., MELBOURNE (AUSTRALIA).
Examination of the microstructure of 7050 aluminum alloy samples
[AD-A232544] N91-23306

AERONAUTICAL SYSTEMS DIV., WRIGHT-PATTERSON AFB, OH.
Do civil flying qualities requirements address military missions for off-the-shelf procurement N91-23115

AEROSPACE MEDICAL RESEARCH LABS., WRIGHT-PATTERSON AFB, OH.
Quantifying performance degradation due to the human-machine interface of telemanipulators
[AD-A232814] N91-23723

AEROSPATIALE, CANNES (FRANCE).
Communication and broadcasting satellites payload reconfiguration techniologies
[REPT-911-440-102] N91-23218
Conference on Space Technology: Satellite Application Development
[REPT-911-440-103] N91-23219
A new generation of radiators
[REPT-911-440-105] N91-23220
Reactive procedure based decision making for satellite control
[REPT-911-440-106] N91-23221
Design rules and system testing methods
[REPT-911-440-107] N91-23222
The Eutelsat 2 programme
[REPT-911-440-108] N91-23223
Predictions and verification of ESD tests made with sphere injections on a flight representative telecommunication satellite: ARABSAT STM
[REPT-911-440-109] N91-23224
ISOCAM: The ISO's satellite infra-red camera
[REPT-911-440-104] N91-23468
Medium Resolution Imaging Spectrometer (MERIS)
N91-23608
Remote sensing performances
[REPT-911-440-101] N91-23615

AEROSPATIALE, CHATILLON (FRANCE).
Pyrotechnical safety of Aerospatiale tactical missiles: Application to conventional warhead
[REPT-911-320-101] N91-23139

AEROSPATIALE, TOULOUSE (FRANCE).
Hypersonic numerical simulation: Problems and perspectives. Hypersonic vehicles and numerical simulation in structural analysis
[REPT-911-111-106] N91-23091
Integration of propulsive systems: Selection and compromise
[REPT-911-111-101] N91-23187
The certification of the aircraft integrated propulsive system
[REPT-911-111-102] N91-23188
The electrical flight control system of A320 Airbus: A fault tolerant system
[REPT-911-111-103] N91-23192
Satellite utilization by civil aviation
[REPT-911-111-105] N91-23216
Observatory of new materials. Evolution perspectives for the materials used in civil transportation aircraft
[REPT-911-111-107] N91-23248
Noise inside aircraft fuselages subjected to airborne excitations
[REPT-911-111-104] N91-23853

AEROSPATIALE AQUITAINE, SAINT-MEDARD EN JALLES (FRANCE).
Experimentation facilities for thermomechanical static tests with analytic test specimens at Aerospatiale
[REPT-911-430-108] N91-23197
SIMOUN: A high temperature and low pressure testing facility for material characterization
[REPT-911-430-121] N91-23208
SIMOUN: A new test appliance for the development of Hermes thermal protections
[REPT-911-430-129] N91-23209
Aerocoat thermal protections
[REPT-911-430-102] N91-23217
Carbon-carbon material with oxidation protection
[REPT-911-430-103] N91-23249
New developments in composites for space applications
[REPT-911-430-104] N91-23250
Oxidation resistant carbon/carbon materials
[REPT-911-430-105] N91-23251
Nondestructive inspection for carbon-carbon with adapted coating for oxidation
[REPT-911-430-106] N91-23252
Fiber-reinforced glass-ceramic matrix composites: New class of materials for space applications
[REPT-911-430-107] N91-23253
Thermostructural composites: Recent evolutions and improvements
[REPT-911-430-109] N91-23254
Nondestructive measurement of thickness and density of composite materials by Compton backscattering
[REPT-911-430-112] N91-23255
Mechanical characterisation of fibre-matrix interface in ceramic composites by an instrumented indentation test
[REPT-911-430-114] N91-23256
Carbon/carbon inox thermostructural composites: Mechanical and tectonic behavior of anti-oxidation protection
[REPT-911-430-115] N91-23257
Materials and structure for Hermes
[REPT-911-430-117] N91-23258
High temperature composites in space planes and missiles development
[REPT-911-430-119] N91-23259
Ceramics in aerospace
[REPT-911-430-127] N91-23260
Structural materials for space mirrors
[REPT-911-430-128] N91-23261
How to know CMC
[REPT-911-430-130] N91-23262
ACLICO: A computer aided design system for bonded joints
[REPT-911-430-101] N91-23757
Presentation of a computer program for analysing results of one shot device sensitivity tests: Application to the case of a one shot degenerated sequence
[REPT-911-430-126] N91-23758
Plasma torches dimensioning and optimization
[REPT-911-430-111] N91-23926
Aerospatiale industrial thermal plasmas
[REPT-911-430-113] N91-23927
Aerospatiale industrial thermal plasma activities
[REPT-911-430-122] N91-23928
Plasma on a foundry cupola
[REPT-911-430-125] N91-23929
Eureca 1 AMF 117 experiment: An analysis of thermal and solutal transfer during the crystal growth of CdTe by the THM process
[REPT-911-430-118] N91-23947
Eureca 1 AMF 117 experience: Thermal and solutal transfer analysis for CdTe in tellurium during crystal growth by the THM method
[REPT-911-430-120] N91-23948

AIR FORCE ENVIRONMENTAL TECHNICAL APPLICATIONS CENTER, SCOTT AFB, IL.
A smoothing algorithm for upper-air soundings
[AD-A232853] N91-23661
SWANEA (Southwest Asia-Northeast Africa): A climatological study. Volume 2: The Middle East Peninsula
[AD-A232776] N91-23684
Range reference atmosphere, Shemya
[AD-A232813] N91-23685
Range reference atmosphere, Thule
[AD-A232831] N91-23686

AIR FORCE FLIGHT DYNAMICS LAB., WRIGHT-PATTERSON AFB, OH.
MIL-STD-1797 is not a cookbook N91-23111

AIR FORCE GEOPHYSICS LAB., HANSCOM AFB, MA.
Laboratory study of the thermochemical properties of materials used in spacecraft
[AD-A232124] N91-23228
Auroral boundary index from 1983 to 1990
[AD-A232845] N91-23660

AIR FORCE INST. OF TECH., WRIGHT-PATTERSON AFB, OH.
Backscattering by nonspherical particles, using the coupled-dipole method: An application in radar meteorology
[AD-A232371] N91-23373
A numerical model of laser induced fluorescence in a hydrogen plasma
[AD-A232240] N91-23482
Analysis of truss frames by method of the stiffness matrix
[AD-A232053] N91-23555
Forecasting atmospheric particulate sulfur concentrations using national weather service synoptic charts
[AD-A231634] N91-23622
Thermal ion upwelling in the high-altitude ionosphere
[AD-A232372] N91-23657
A search for strange attractors in the saturation of middle atmosphere gravity waves
[AD-A232468] N91-23658

Initialization of cloud and radiation in the Florida State University global spectral model
[AD-A232425] N91-23682
Data type coherency in heterogeneous shared memory multiprocessors
[AD-A232114] N91-23729
SZ series GaAs super high-speed logic gate: Optimum choice. High tech; high speed; high quality
[AD-A232819] N91-23962

AIR FORCE MATERIALS LAB., WRIGHT-PATTERSON AFB, OH.
Materials for hypersonic engines N91-23177

ALABAMA UNIV., HUNTSVILLE.
Analysis and modeling of summertime convective cloud and precipitation structure over the Southeastern United States
[NASA-CR-188119] N91-23670
Analysis of polarizing optical systems for digital optical computing with symmetric self electrooptic devices
[AD-A232768] N91-23906

ALCATEL ESPACE, TOULOUSE (FRANCE).
Characteristics and performance of an operational windscatterometer N91-23607

AMERICAN ASSOCIATION FOR THE ADVANCEMENT OF SCIENCE, WASHINGTON, DC.
Proceedings of the 1991 American Association for the Advancement of Science Annual Meeting Program N91-23969

AMES LAB., IA.
Excited state structure, energy and electron transfer dynamics of photosynthetic reaction centers: A hole burning study
[DE91-010181] N91-23693

APPLIED RESEARCH LAB., STATE COLLEGE, PA.
A two-scale solution of the forced Rayleigh-Plesset equation governing the dynamics of cavitation bubble vaporous growth
[AD-A232129] N91-23446

ARCON CORP., WALTHAM, MA.
High-altitude non-equilibrium infrared emission models
[AD-A232503] N91-23659

ARGONNE NATIONAL LAB., IL.
Microbeam titanium isotopic analysis by resonance ionization mass spectrometry
[DE91-010799] N91-23277
Applications of energetic particles in improving coating adhesion properties
[DE91-008833] N91-23312
Characterization of active materials and electrodes for battery R and D
[DE91-010758] N91-23390
Two-phase flow patterns and frictional pressure gradients in a small rectangular channel
[DE91-009652] N91-23414
A first-principles generic methodology for representing the knowledge base of a process diagnostic expert system
[DE90-017693] N91-23520
Approximating the dynamic response of strain-hardening structures
[DE91-006392] N91-23534
A theory for fluidelastic instability of tube-support-plate inactive modes
[DE91-009676] N91-23538
A theory for fluidelastic instability of tube-support-plate inactive modes
[DE91-006001] N91-23542
Table-lookup algorithms for elementary functions and their error analysis
[DE91-006047] N91-23743
Visual presentation and computer animation
[DE91-010599] N91-23745
Comment on: Analytic solution of the Stochastic-Liouville model of spin-exchange
[DE91-010570] N91-23861
Recent results and future prospects for the polarized beam at Fermilab
[DE91-010590] N91-23862
Cold moderators for pulsed neutron sources
[DE91-010594] N91-23866
Sintering and hot isostatic pressing of Bi2Sr2CaCu2O(x)
[DE91-010797] N91-23945

ARIZONA STATE UNIV., TEMPE.
High-temperature alloys for high-power thermionic systems
[DE91-009292] N91-23299
Magneto-optical properties of quantum wells with arbitrary potential profiles
[AD-A232037] N91-23897

ARIZONA UNIV., TUCSON.
Pulse compression of 100 picosecond pulses at 1.319 microns
[AD-A232552] N91-23901
Cryomagmatism in the outer solar system N91-24019

ARMED FORCES RADIOBIOLOGY RESEARCH INST., BETHESDA, MD.
AFRRI reports, October - December 1990
[AD-A232236] N91-23283

ARMY AEROMEDICAL RESEARCH LAB., FORT RUCKER, AL.
A test of the American Safety Flight Systems, Inc. prebreather/portable oxygen system
[AD-A232723] N91-23100

ARMY ARMAMENT RESEARCH AND DEVELOPMENT COMMAND, DOVER, NJ.
Fiber optic sensors for the military
[AD-A232100] N91-23898

ARMY AVIATION SYSTEMS COMMAND, CLEVELAND, OH.
Effects of inlet distortion on the development of secondary flows in a subsonic axial inlet compressor rotor
[NASA-TM-104356] N91-23179
Maximum life spur gear design
[NASA-TM-104361] N91-23514

ARMY COLD REGIONS RESEARCH AND ENGINEERING LAB., HANOVER, NH.
CRREL research on materials in cold environments
[AD-A232133] N91-23280

ARMY CONSTRUCTION ENGINEERING RESEARCH LAB., CHAMPAIGN, IL.
Large space structures fielding plan
[AD-A232097] N91-23227
Maintenance Resource Prediction Model (MRPM) user's manual
[AD-A232019] N91-23762
Life cycle management automation programmer's manual
[AD-A232247] N91-23769
Life cycle management automation user's manual, version 1.1
[AD-A232096] N91-23968

ARMY ENGINEER TOPOGRAPHIC LABS., FORT BELVOIR, VA.
Hyperspectral imagery: What is it, what can it do
[AD-A231164] N91-23610

ARMY ENGINEER WATERWAYS EXPERIMENT STATION, VICKSBURG, MS.
Analytical study of the effects of weight on Light Helicopter (LH) exposure to ground-based weapons
[AD-A232024] N91-23141
Literature review on geotextiles to improve pavements for general aviation airports
[AD-A232871] N91-23199
Review of finite element procedures for earth retaining structures
[AD-A232230] N91-23343

ARMY ENVIRONMENTAL HYGIENE AGENCY, ABERDEEN PROVING GROUND, MD.
Laser hazards bibliography, January 1991
[AD-A232690] N91-23487

ARMY LAB. COMMAND, WATERTOWN, MA.
An experimental and finite element investigation into the nonlinear material behavior of pin-loaded composite laminates
[AD-A232098] N91-23263
Model sensitivity in stress-strength reliability computations
[AD-A232023] N91-23554

ARMY MISSILE COMMAND, REDSTONE ARSENAL, AL.
Analysis of the flutter characteristics of the advanced kinetic energy missile (ADKEM) control surface
[AD-A232377] N91-23193
Evaluation of a ferroelectric liquid crystal spatial light modulator
[AD-A232117] N91-23899

ARNOLD ENGINEERING DEVELOPMENT CENTER, ARNOLD AIR FORCE STATION, TN.
Diagnostic measurements on an aluminized propellant plume during spin and nonspin testing
[AD-A232031] N91-23235
Computation of inlet reference plane flow-field for a subscale free-jet forebody/inlet model and comparison to experimental data
[AD-A232101] N91-23445
Aero-optics measurement system for the AEDC aero-optics test facility
[AD-A232852] N91-23908

ASSISTANT SECRETARY OF THE AIR FORCE, WASHINGTON, DC.
Abridged USAF STINFO program manager's overview manual
[AD-A232483] N91-23995
The value of STINFO
[AD-A232484] N91-23996
Interacting with DTIC
[AD-A232485] N91-23997

ASTROPOWER, INC., NEWARK, DE.
Electronic GaAs-on-silicon material for advanced high-speed optoelectronic devices
[AD-A232088] N91-23399

ATLANTIC COUNCIL OF THE UNITED STATES, WASHINGTON, DC.
Energy-related environmental issues in a global context
[DE91-009538] N91-23627

ATMOSPHERIC AND ENVIRONMENTAL RESEARCH, INC., CAMBRIDGE, MA.
Design of an enhanced global spectral model
[AD-A232123] N91-23655

AVCO-EVERETT RESEARCH LAB., MA.
MHD channel gas-side element erosion-corrosion studies
[DE91-008561] N91-23911

B

BALLISTIC RESEARCH LABS., ABERDEEN PROVING GROUND, MD.
Quantum chemical studies of candidate high energy density material compounds
[AD-A232393] N91-23335
Power packs: A passive approach to extinguishing fire in combat vehicles
[AD-A232020] N91-23342
Diffusive, electrostatic concentration of disintegration products of inert gases in vortex flow
[AD-A232876] N91-23457
Time rates of generalized strain tensors. Part 1: Component formulas
[AD-A232497] N91-23469
Energy-efficient penetration of targets
[AD-A232227] N91-23518
Temperature measurements of ET plasmas using atomic emission spectroscopy
[AD-A232498] N91-23930

BAR-ILAN UNIV., RAMAT-GAN (ISRAEL).
A high resolution study of the Cu K alpha(sub 1,2) x-ray emission lines N91-23841

BATTELLE MEMORIAL INST., COLUMBUS, OH.
Theoretical prediction of vibrational infrared frequencies of tertiary amines
[AD-A232880] N91-23288

BELL COMMUNICATIONS RESEARCH, INC., MORRISTOWN, NJ.
Background simulation and filter design using iterated function systems
[AD-A232632] N91-23405

BEN GURION UNIV. OF THE NEGEV, BEERSHEVA (ISRAEL).
Liquid-metal MHD power conversion for space electric systems
[SER-S/27] N91-23231
Flows with strongly anisotropic turbulence-dynamic and heat transfer aspects
[SER-20/P] N91-23407
Turbulence and the feasibility of self-cooled liquid-metal blankets for fusion reactors
[SER-10/P-REV] N91-23910

BETA POWER, INC., SALT LAKE CITY, UT.
Conceptual design study of high-performance sodium/metal chloride batteries for electric vehicle applications
[DE91-009618] N91-23383

BOEING AEROSPACE CO., HUNTSVILLE, AL.
Piloted rover technology study
[NASA-CR-186989] N91-23200

BOEING COMMERCIAL AIRPLANE CO., SEATTLE, WA.
Aircraft Command in Emergency Situations (ACES). Phase 1: Concept development
[DOT/FAA/CT-90/21] N91-23097

BONN UNIV. (GERMANY, F.R.).
Iron density measurements in polar atmosphere
[BONN-IR-90-53] N91-23654

BRITISH AEROSPACE PUBLIC LTD. CO., PRESTON (ENGLAND).
The development of alternate criteria for FBW handling qualities N91-23113
A review of high angle of attack requirements for combat aircraft N91-23130

BROOKHAVEN NATIONAL LAB., UPTON, NY.
Spatial dynamics of picosecond CO2 laser pulses produced by optical switching in Ge
[DE91-010368] N91-23476
Tropospheric sampling with aircraft
[DE91-009472] N91-23626
Lectures on accelerator physics
[DE91-010376] N91-23886
Theory of the critical current density in YBa2Cu3O7 ceramics
[DE91-009443] N91-23940

C

CALIFORNIA INST. OF BIOLOGICAL RESEARCH, LA JOLLA.
New hosts and vectors for genome cloning
[DE91-009996] N91-23696
CALIFORNIA INST. OF TECH., PASADENA.
Chemical reactions in turbulent mixing flows
[AD-A232610] N91-23450
On the construction of two-phase equilibria in a non-elliptic hyperelastic material
[AD-A232628] N91-23558
In based III-V microstructures with novel electronic properties
[AD-A232695] N91-23960
Microwave imaging of Saturn's deep atmosphere and rings N91-24035
CALIFORNIA UNIV., BERKELEY.
Interferometric investigation of supersonic flow fields with shock-shock interactions N91-23082
Near midair collisions as an indicator of general aviation collision risk N91-23096
Study of phase-locked diode laser array and DFB/DBR surface emitting laser diode N91-23474
Reduced vector basis for dynamic analysis of large damped structures N91-23525
High-precision Fourier transform spectroscopy of atmospheric molecules N91-23637
Science requirements for Heavy Nuclei Collection (HNC) experiment on NASA Long Duration Exposure Facility (LDEF) Mission 2
[NASA-CR-187527] N91-23887
Knowledge-based retrieval of information as a process of evidential reasoning N91-23978
Studies of the diffuse background and interstellar dust at far ultraviolet wavelengths N91-24003
CALIFORNIA UNIV., BERKELEY. LAWRENCE BERKELEY LAB.
The strength and toughness of stainless steels at cryogenic temperature
[DE91-009771] N91-23300
Possibilities for projection x ray lithography using holographic optical elements
[DE91-009770] N91-23464
Structural studies of manganese and halide in the photosynthetic oxygen evolving complex
[DE91-009071] N91-23698
Canonical vs. micro-canonical sampling methods in a 2D Ising model
[DE91-010204] N91-23737
Computer programs for simulation of electrodeposition
[DE91-010203] N91-23741
A guide to experimental elementary particle physics literature, 1985-1989
[DE91-010209] N91-23856
Investigation of neutral atom and ion emission during laser conditioning of multilayer HfO2-SiO2 coatings
[DE91-009749] N91-23860
Calculation of cross sections for binary reactions between heavy ion projectiles and heavy actinide targets
[DE91-010222] N91-23882
Magnet cable manufacturing
[DE91-010210] N91-23935
CALIFORNIA UNIV., DAVIS.
A submicron resolution monolithic capacitive displacement sensor with digital output
[DE91-009765] N91-23465
CALIFORNIA UNIV., LOS ANGELES.
Integrated multidisciplinary optimization of actively controlled fiber composite wings N91-23190
Solid-phase equilibria for Metal-Silicon-Oxygen ternary systems. Part 2: Sc, Y, and La
[AD-A232150] N91-23281
A statistical model of fractures N91-23529
Development of a micromechanic theory of constitutive relations of polycrystalline solids
[AD-A232697] N91-23559
The polar wind and ionospheric outflow N91-23645
Processing problems in the IRUS queries: An empirical verification of problem coverage in the natural language sourcebook
[AD-A232780] N91-23800
Luminescence and absorption spectra of C60 films
[AD-A232153] N91-23900
X ray diffraction and electron spectroscopy of epitaxial molecular C60 films
[AD-A232152] N91-23954
Radio and infrared studies of mass-losing evolved stars N91-24026
CALIFORNIA UNIV., SANTA BARBARA.
High quality three dimensional electron gases in semiconductors
[AD-A232779] N91-23406
CALSPAN ADVANCED TECHNOLOGY CENTER, BUFFALO, NY.
The flying qualities influence of delay in the fighter pilot's cuing environment N91-23120
CALSPAN-BUFFALO UNIV. RESEARCH CENTER, NY.
Pulse compression of 100 picosecond pulses at 1.319 microns
[AD-A232552] N91-23901
CALSPAN CORP., ARNOLD AFS, TN.
Aero-optics measurement system for the AEDC aero-optics test facility
[AD-A232852] N91-23908
CARNEGIE-MELLON UNIV., PITTSBURGH, PA.
Decentralized computing technology for fault-tolerant, survivable C3I systems, volume 1
[AD-A232289] N91-23369
Decentralized computing technology for fault-tolerant, survivable C3I systems, volume 2
[AD-A232290] N91-23370
Decentralized computing technology for fault-tolerant, survivable C3I systems. Volume 3: System/subsystem specification
[AD-A232291] N91-23371
On kinematic design of serial link manipulators
[DE91-009414] N91-23499
Steps toward environmentally compatible product and process design: A case for green engineering
[AD-A232888] N91-23633
Towards real-time GOMS
[AD-A232028] N91-23763
Classification using multi-layered perceptrons
[AD-A232810] N91-23802
A distributed problem-solving approach to rule induction: Learning in distributed artificial intelligence systems
[AD-A232822] N91-23803
CASE WESTERN RESERVE UNIV., CLEVELAND, OH.
High energy dense ribbon beams and high harmonic gyrotron at millimeter wavelengths
[AD-A232839] N91-23470
Transport and nucleation processes in the vapor growth of diamond
[AD-A232135] N91-23953
CATERPILLAR TRACTOR CO., PEORIA, IL.
Direct gas injection with glow plug ignition
[PB91-136390] N91-23272
CENTER FOR INDUSTRIAL RESEARCH, OSLO (NORWAY).
Man-machine interactions and multimedia applied to ROV operations N91-23576
CENTRAL RESEARCH INST. OF ELECTRIC POWER INDUSTRY, TOKYO (JAPAN).
Evaluation of cathode materials for high energy lithium secondary batteries
[DE91-764240] N91-23385
Water-cooling technique of high temperature gas turbine blade
[DE91-764238] N91-23506
CENTRE D'ETUDES ET DE RECHERCHES DE CHRONOBIOLOGIE HUMAINE, NICE (FRANCE).
Some problems of desynchronisation of sleep-wakefulness and circadian rhythms for long duration spaceflights N91-23570
CENTRE NATIONAL D'ETUDES DES TELECOMMUNICATIONS, ISSY-LES-MOULINEAUX (FRANCE).
Energy exchange study at the ocean surface by satellite observation N91-23597
CENTRE NATIONAL D'ETUDES SPATIALES, TOULOUSE (FRANCE).
Validation requirements for the Topex/Poseidon altimeter mission N91-23602
CINCINNATI UNIV., OH.
Research in particle theory
[DE91-010749] N91-23872
CLARKSON UNIV., POTSDAM, NY.
Thermodynamically consistent formulations for rapid granular and turbulent multiphase flows N91-23420
CLEMSON UNIV., SC.
On the control of two manipulators holding a rigid object in the presence of uncertainty
[DE90-017742] N91-23508
Computerized symbolic closed-form dynamics and control analysis of hybrid rigid and elastic multibody systems N91-23532
CLS ARGOS, TOULOUSE (FRANCE).
Collection and processing of oceanographic data at CLS N91-23603
COLOGNE UNIV. (GERMANY, F.R.).
Energy partition of free Rossby waves in global atmospheric oscillations
[MITT-74] N91-23648
Remote sensing of atmospheric temperature fields and the long wave radiation budget in the Antarctic
[ISSN-0069-5882] N91-23652
COLORADO STATE UNIV., FORT COLLINS.
Optoelectronic III-V heterostructures on Si substrates
[AD-A232035] N91-23950
COMPAGNIE MARITIME D'EXPERTISES, MARSEILLE (FRANCE).
Long duration hyperbaric confinement: Hydra 9 N91-23571
Comparisons between underwater and space working environments for on board activities optimization (Columbus space programme) N91-23574
Neutral buoyancy and microgravity: Extravehicular activities with a humid water suit N91-23579
COMPANHIA ESPACIAL PORTUGUESA LTD., LISBON.
The Berlenga underwater survey project N91-23577
COMPUTER RESOURCES INTERNATIONAL A/S (DENMARK).
A procedural expert system for spacecraft command and control N91-23591
COMPUTER TECHNOLOGY ASSOCIATES, INC., ROCKVILLE, MD.
Astromag phase A assembly and servicing operations report
[NASA-CR-186262] N91-23206
Astromag data system concept
[NASA-CR-186341] N91-23211
CONSIGLIO NAZIONALE DELLE RICERCHE, FLORENCE (ITALY).
Remote sensing of the sea at IROE/CNR N91-23604
CORNELL UNIV., ITHACA, NY.
An experimental method for studying combustion of an unsupported fuel droplet at reduced gravity N91-23273
Mass resolved resonance ionization spectroscopy of combustion radicals
[DE91-010603] N91-23276
Characterization of the glass transition using a microindenter
[AD-A232154] N91-23282
An experimental study of flamelet surfaces in turbulent combustion
[AD-A232342] N91-23284
Dissolution of Poly(p-hydroxystyrene): Molecular weight effects
[AD-A232155] N91-23323
Development and utilization of new diagnostics for dense-phase pneumatic transport
[DE91-008947] N91-23339
Fundamental studies of electronic packaging materials and structures: Surface and interfaces
[AD-A232336] N91-23403
Block implicit multigrid solution of the Euler equations N91-23413
Incoherent scatter measurements and inferred energy fluxes in the equatorial F-region ionosphere N91-23640
Large scale turbulence in the equatorial electrojet N91-23643
Dynamic load balancing on highly parallel multicomputer systems N91-23777
Wavelength independent optical lithography and microscopy
[AD-A232036] N91-23896
An observational study of arm structure in normal spiral galaxies N91-24007
Observation and theory of the radar aurora N91-24017
Saturn's F ring: Imaging and simulation N91-24032
CORVALLIS ENVIRONMENTAL RESEARCH LAB., OR.
National stream survey database guide
[PB91-141804] N91-23625
COUNCIL FOR NATIONAL ACADEMIC AWARDS (ENGLAND).
A study of the end point path geometry in meteor burst systems using a microcomputer signal logger N91-24012
CPS SUPERCONDUCTORS, INC., MILFORD, MA.
Composite ceramic superconducting wires for electric motor applications
[AD-A232074] N91-23951
CRANFIELD INST. OF TECH., BEDFORD (ENGLAND).
The performance of 60 deg delta wings: The effects of leading edge radius on vortex flaps and the wing
[CRANFIELD-AERO-9004] N91-23092
The performance of 60 deg delta wings: The effects of leading edge radius and vortex flaps
[CRANFIELD-AERO-9002] N91-23140
Some aspects of shock-wave boundary layer interaction relevant to intake flows N91-23161
Riemann problems and the WAF method for the two-dimensional shallow water equations
[CRANFIELD-AERO-9005] N91-23443
The drag of spheres at porosites ranging from an isolated sphere to a packed bed
[CRANFIELD-AERO-9012] N91-23444
CYBERNETIX, MARSEILLE (FRANCE).
Telemanipulation system assisted by computer for under water applications N91-23585

D

DAVID TAYLOR RESEARCH CENTER, BETHESDA, MD.
Computer center reference manual, volume 2
[AD-A232370] N91-23781
DAYTON UNIV., OH.
Post-overload fatigue crack recovery in powder metal aluminum-lithium AL-905XL forging
[AD-A232550] N91-23307
Studies of noise in semiconductor laser arrays
[AD-A232411] N91-23485
DEFENCE AND CIVIL INST. OF ENVIRONMENTAL MEDICINE, DOWNSVIEW (ONTARIO).
Heat strain and work tolerance times with varying levels of Canadian Forces NBC protective clothing, ambient temperature, physical work intensity, and work/rest schedules
[AD-A232653] N91-23720
DEFENCE RESEARCH ESTABLISHMENT ATLANTIC, DARTMOUTH (NOVA SCOTIA).
The effect of post-cure and antimony trioxide addition on the glass transition of polyester and vinyl ester resin systems
[AD-A232523] N91-23325
DEFENCE RESEARCH ESTABLISHMENT, OTTAWA (ONTARIO).
The 2-D acousto-optic signal processors for simultaneous spectrum analysis and direction finding
[AD-A232148] N91-23367
An investigation of CFAR techniques for airborne radars
[AD-A232724] N91-23378
DELAWARE UNIV., NEWARK.
A simulation of the draping and a model of the consolidation of commingled fabrics N91-23239
DEPARTMENT OF ENERGY, WASHINGTON, DC.
Computing for magnetic fusion energy research: The next five years
[DE91-010686] N91-23921
Information resources management long-range plan
[DE91-009745] N91-23984
DEUTSCHE FORSCHUNGSANSTALT FUER LUFT- UND RAUMFAHRT, BRUNSWICK (GERMANY, F.R.).
Development of MIL-8785C into a handling qualities specification for a new European fighter aircraft N91-23114
Handling qualities evaluation for highly augmented helicopters N91-23128
Evaluation techniques for highly augmented aircraft
[DLR-FB-90-35] N91-23191
Characterization of composite materials for aerospace materials
[DLR-MITT-90-15] N91-23246
Three-dimensional graphical representation of objects according to movement data in realtime
[DLR-FB-90-51] N91-23725
DEUTSCHE FORSCHUNGSANSTALT FUER LUFT- UND RAUMFAHRT, COLOGNE (GERMANY, F.R.).
Flight mechanics/air navigation research field. A 1990 Scientific report of the German Air and Space Research Organization
[ISSN-0720-7808] N91-23103
The limits of the landing process of aircraft
[DLR-FB-90-49] N91-23137
Trajectory optimization considerations for ramjet engines N91-23151
Aerodynamics and stabilization of combustion of hydrogen jets injected into subsonic airflow N91-23164
Containerless undercooling and solidification of pure metals
[DLR-FB-90-48] N91-23301
Simulation of a backscatter lidar system
[DLR-FB-90-50] N91-23355
The diving laboratory as a simulation environment for manned spaceflight N91-23564
Sea ice monitoring in the east Greenland sea in May 1988 by means of remote sensing, with special emphasis on the computer-aided AVHRR-based extraction of sea ice motions
[DLR-FB-90-36] N91-23687
Activities report of the DLR
[ISSN-0938-2194] N91-24086
DEUTSCHE FORSCHUNGSANSTALT FUER LUFT- UND RAUMFAHRT, GOETTINGEN (GERMANY, F.R.).
Procedure for determination of three-dimensional wind tunnel wall interferences and wall adaptation in compressible subsonic flow using measured wall pressures
[DLR-FB-90-46] N91-23088
Numerical simulation and topological analysis of the separated flow around a sphere
[DLR-FB-90-43] N91-23435
DEUTSCHE FORSCHUNGSANSTALT FUER LUFT- UND RAUMFAHRT, HAMBURG (GERMANY, F.R.).
Psychological selection of astronauts: Recent developments at the DLR testing centre in Hamburg (Fed. Republic of Germany) N91-23565
DEUTSCHE FORSCHUNGSANSTALT FUER LUFT- UND RAUMFAHRT, OBERPFAFFENHOFEN (GERMANY, F.R.).
Polarimetric radar observations of time-variant random targets
[DLR-FB-90-52] N91-23356
Efficient numerical techniques for the analysis of complex microstrip-antennas and microstrip arrays
[DLR-FB-90-53] N91-23357
Multisensory telerobotic concepts for space and underwater applications N91-23584
The applicability of thematic mapper data to the classification of tree species and natural age classes
[DLR-FB-90-44] N91-23612
Correction of relief-induced radiometric distortions in Seasat-A SAR images for the example of the subscene of Bonn (Fed. Republic of Germany) and vicinities
[DLR-FB-90-54] N91-23613
Analysis on forest decline classification of the beech using airborne multispectral scanner data
[DLR-FB-90-56] N91-23614
On the airflow over the Alps during south Foehn
[DLR-FB-90-30] N91-23676
Investigation of micro- and macrophysical structures and processes in hail clouds with respect to their modification
[DLR-FB-90-38] N91-23677
Image data compression in JPEG standard
[DLR-FB-90-59] N91-23746
DIRECTION DE LA METEOROLOGIE NATIONALE, PARIS (FRANCE).
Satellite data utilization for modeling sea states N91-23598
DIRECTION DES CONSTRUCTIONS ET ARMES NAVALES, TOULON (FRANCE).
A KO2 rebreather for EVA denitrogenation procedure N91-23588
DORNIER SYSTEM G.M.B.H., FRIEDRICHSHAFEN (GERMANY, F.R.).
Handling qualities of highly augmented unstable aircraft summary of an AGARD-FMP working group effort N91-23116
Integration of handling quality aspects into the aerodynamic design of modern unstable fighters N91-23125
DUKE UNIV., DURHAM, NC.
Synthesis and characterization of indium-arsenic compounds containing a four-membered In-Ad-In-As or In-As-In-Cl ring: Crystal structures of ((Me3SiCH2)2 InAs(SiMe3)2)2 and (Me3SiCH2)2 InAs(SiMe3)2 In(CH2SiMe3)2Cl
[AD-A232368] N91-23956

E

EDGERTON, GERMESHAUSEN AND GRIER, INC., IDAHO FALLS, ID.
Measurement of particle size, velocity and temperature in the plasma spray coating process
[DE91-006208] N91-23317
Particle-fluid two-phase flow modeling
[DE91-010102] N91-23415
Heat and mass transfer in the gas tungsten and gas metal arc welding processes
[DE91-010089] N91-23510
Implementation of the FAA research and development electromagnetic database
[DE91-010063] N91-23674
The CERBERUS Ver. 02 code: A parallel six-equation thermal-hydraulic-system simulation code
[DE91-010079] N91-23736
Gas core reactors for direct nuclear propulsion
[DE91-010050] N91-23884
EDGERTON, GERMESHAUSEN AND GRIER, INC., LOS ALAMOS, NM.
Design of a twenty-element long focal length zoom lens
[DE91-010770] N91-23894
EG AND G MOUND APPLIED TECHNOLOGIES, MIAMISBURG, OH.
Measurement control for calorimetric assay
[DE91-009445] N91-23274
Unipunch capability study
[DE91-008825] N91-23498
ENVIRONMENTAL PROTECTION AGENCY, SEATTLE, WA.
Region 10 environmental indicators
[PB91-136580] N91-23623
ESPACE STUDIO, TURIN (ITALY).
Test on parabolic flights for stowage in weightlessness N91-23578
EUROPEAN SPACE AGENCY, PARIS (FRANCE).
Qualification of concentrating mirror systems with the Hermes measurement system and the Helios simulation program
[ESA-TT-1213] N91-23230
Gas evolution and bubble formation on electrodes
[ESA-TT-1191] N91-23278
Hardening mechanisms and analysis of the structure of the TGDDM/DDS epoxy resin system
[ESA-TT-1202] N91-23319
Analysis of the VHF-UHF electromagnetic radiation of lightning: Application to a model of the negative stepped leader propagation
[ESA-TT-1172] N91-23363
Numerical simulation of incompressible inhomogeneous turbulence in a plane channel flow
[ESA-TT-1199] N91-23441
Numerical simulation of transition in three dimensional boundary layers
[ESA-TT-1203] N91-23442
Threshold for fatigue crack propagation at simulated operating loads
[ESA-TT-1187] N91-23553
Space and Sea
[ESA-SP-312] N91-23563
The propagation of acoustic disturbances in the transonic flow fields of wings
[ESA-TT-1126] N91-23854
EUROPEAN SPACE AGENCY. EUROPEAN SPACE RESEARCH AND TECHNOLOGY CENTER, ESTEC, NOORDWIJK (NETHERLANDS).
Checklist for thick-film hybrid microcircuits manufacturer and line survey
[ESA-PSS-01-607-ISSUE-1] N91-23396
Checklist for thin-film hybrid microcircuits manufacturer and line survey
[ESA-PSS-01-611-ISSUE-1] N91-23397
EVA servicing: The Hermes capability N91-23575
How to design efficient MMI for space N91-23586
Signal detection of MERIS in oceanographic applications N91-23605
EXECUTIVE OFFICE OF THE PRESIDENT, WASHINGTON, DC.
America at the threshold N91-23201

F

FEDERAL AVIATION ADMINISTRATION, ATLANTIC CITY, NJ.
NAS operational test and evaluation/integration of the Maintenance Management System (MMS) test plan
[DOT/FAA/CT-TN90/41] N91-23075
Differential GPS terminal area test results
[AD-A232668] N91-23106
An investigation into the use of side-arm control for civil rotorcraft applications N91-23123
Determination of decision-height windows for decelerating IMC approaches in helicopters N91-23124
FEDERAL AVIATION ADMINISTRATION, CAMBRIDGE, MA.
Aircraft wake vortices: An assessment of the current situation
[AD-A231658] N91-23079
FEDERAL AVIATION ADMINISTRATION, WASHINGTON, DC.
Precision runway monitor demonstration report
[AD-A232671] N91-23198
Individual differences underlying pilot cockpit error
[DOT/FAA/RD-91/13] N91-23710
FERMI NATIONAL ACCELERATOR LAB., BATAVIA, IL.
A proposed search for dark-matter axions in the 0.6-16 micro-eV range
[NASA-CR-188173] N91-24015
A cosmic superfluid phase
[NASA-CR-188171] N91-24016
FIAT AVIAZIONE S.P.A., TURIN (ITALY).
Airbreathing propulsion for transatmospheric flight N91-23156
FLORIDA UNIV., GAINESVILLE.
Chain propagation/step propagation polymerization. Regular thermoplastic elastomers
[AD-A232356] N91-23324
Articulation of spatial robots N91-23504
Stress analysis of a double-doubler joint in composite structure N91-23530
FOKKER SPACE AND SYSTEMS, AMSTERDAM (NETHERLANDS).
Building real-time simulators for space applications N91-23587

G

GENERAL ACCOUNTING OFFICE, WASHINGTON, DC.
Strategic missiles: Uncertainties persist in the Advanced Cruise Missile (ACM) program
[AD-A232058] N91-23142

GENERAL ATOMIC CO., SAN DIEGO, CA.
Applied plasma physics
[DE91-010696] N91-23922
Fusion technology development
[DE91-010697] N91-23923

GENERAL ELECTRIC CO., PHILADELPHIA, PA.
Feasibility study of the Superconducting Gravity Gradiometer (SGG) flight test on the European Retrievable Carrier (EURECA)
[NASA-CR-184157] N91-23229

GENERAL ELECTRIC CO., SCHENECTADY, NY.
Benchmark measurements and calculations of a 3-dimensional neutron streaming experiment
[DE91-010692] N91-23867

GEORGE WASHINGTON UNIV., WASHINGTON, DC.
Background simulation and filter design using iterated function systems
[AD-A232632] N91-23405

GEORGIA INST. OF TECH., ATLANTA.
High temperature membranes for H2S and SO2 separations
[DE91-008534] N91-23275
High shear stress rheology of liquid lubricants N91-23309
Fractal image compression of Rayleigh, Raman, LIF and LDV data in turbulent reacting flows
[AD-A232237] N91-23449
Signals and noise in lasers and atom-field interactions N91-23475
Data transfer over multiplexed logical data links sharing a single physical circuit N91-23734

GEORGIA STATE UNIV., ATLANTA.
Light particle emissions in heavy ion reactions
[DE91-010746] N91-23871
Applications of speckle interferometry and speckle photometry to the Hyades cluster N91-24001

GESELLSCHAFT FUER STRAHLEN- UND UMWELTFORSCHUNG M.B.H., MUNICH (GERMANY, F.R.).
Information system for environmental chemicals
[GSF-BER-21/90] N91-23990

GKSS-FORSCHUNGSZENTRUM GEESTHACHT (GERMANY, F.R.).
Higher accuracy requirements for the satisfactory position calculation of an artificial satellite
[GKSS-90/E/25] N91-23203

GRENOBLE-1 UNIV. (FRANCE).
Optimal multinode broadcast on a mesh connected graph with reduced bufferization
[RR-825-I] N91-23362
Basic properties of strongly code disjoint checkers
[RR-824-I] N91-23393
Automatic formal verification of VHDL descriptions: A first prototype
[RR-823-I] N91-23726
Searching algorithms for the real roots of a Bezier function
[RR-834-I-AND-M] N91-23755
Specifications for reusable software components
[RR-828-I-IMAG-116-LIFIA] N91-23756
A method for handling complex Markov models of parallel systems
[RR-826-I] N91-23778
Statistical process allocation in a parallel processing architecture
[RR-833-I] N91-23779
Generalization of the FP2 parallel language by means of net theory
[RR-832-I-IMAG-99-LIFIA] N91-23780
Q-splines
[RR-830-M] N91-23808
Nilpotent normal form via Carleman linearization (for systems of ordinary differential equations)
[RR-838-M] N91-23809
Congruence properties of the process equivalence induced by temporal logic
[RR-831-I-IMAG-118-LIFIA] N91-23810
Optimal systolic network for Gaussian elimination
[RR-837-I] N91-23822
Detection of outliers and robust estimation using fuzzy clustering
[RR-822-M] N91-23823
A particular linear model of variance components
[RR-827-M] N91-23824
Nonparametric estimation in change-point hazard rate models for censored data: A counting process approach
[RR-836-I-AND-M] N91-23825
On a phonetic and structural encoding of Chinese characters in Chinese texts
[RR-835-I] N91-23989

H

HAMILTON STANDARD, WINDSOR LOCKS, CT.
Unified aeroacoustics analysis for high speed turboprop aerodynamics and noise. Volume 3: Application of theory for blade loading, wakes, noise, and wing shielding
[NASA-CR-185193] N91-23850
Unified aeroacoustics analysis for high speed turboprop aerodynamics and noise. Volume 4: Computer user's manual for UAAP turboprop aeroacoustic code
[NASA-CR-185194] N91-23851
Unified aeroacoustics analysis for high speed turboprop aerodynamics and noise. Volume 5: Propagation of propeller tone noise through a fuselage boundary layer
[NASA-CR-185195] N91-23852

HARVARD UNIV., CAMBRIDGE, MA.
Optimization of transparent and reflecting electrodes for amorphous silicon solar cells
[DE91-002132] N91-23618

HAWAII UNIV., HONOLULU.
A near-infrared search for brown dwarfs in the Pleiades N91-24011
Composition and distribution of carbonates, sulfates, and hydrates on the Martian surface from earth-based spectroscopy between 3-5 microns N91-24033
A search for very high-energy gamma rays from Cygnus X-3 N91-24039

HEBREW UNIV., JERUSALEM (ISRAEL).
Supersymmetric matter at finite temperature N91-23836

HELSINKI UNIV. OF TECHNOLOGY, ESPOO (FINLAND).
An interactive robot control system N91-23790

HONEYWELL, INC., BLOOMINGTON, MN.
A 30 GHz monolithic receive module
[NASA-CR-187085] N91-23346

HONEYWELL, INC., MINNEAPOLIS, MN.
Navigation, guidance, and trajectory optimization for hypersonic vehicles N91-23150

HOUSTON UNIV., CLEAR LAKE, TX.
Hypermedia 1990 structured Hypertext tutorial
[NASA-CR-187921] N91-23731

HOUSTON UNIV., TX.
Computations, properties, and applications of matrix-valued functions to mathematical science and control systems
[AD-A232448] N91-23819

HOWARD UNIV., WASHINGTON, DC.
Laser assisted CVD growth of AlN and GaN
[AD-A232379] N91-23957

HUGHES RESEARCH LABS., MALIBU, CA.
Theory of novel nonlinear optics
[AD-A232659] N91-23903
Development of Si/SiGe heterostructures
[AD-A232747] N91-23961

I

IBM RESEARCH LAB., SAN JOSE, CA.
In-situ surface x ray scattering measurements of electrochemically deposited bismuth on silver (III): Structure, compressibility, and comparison with ex-situ leed measurements
[AD-A232624] N91-23880
Surface x ray scattering measurements of the substrate induced spatial modulation of an incommensurate adsorbed monolayer
[AD-A232625] N91-23959

IFREMER, PARIS (FRANCE).
Satellite and aeronautical technologies serving the management of living marine resources N91-23606

ILLINOIS UNIV., CHICAGO.
Wave gaits, follow-the-leader gaits and gait transitions of legged robots N91-23503

ILLINOIS UNIV., URBANA.
Broad area distributed gain, distributed index profile GaAlAs semiconductor laser diodes
[AD-A232332] N91-23483

ILLINOIS UNIV., URBANA-CHAMPAIGN.
Performance analysis of garbage collection and dynamic reordering in a Lisp system
[NASA-CR-188205] N91-23738
A user-oriented synthetic workload generator
[NASA-CR-186197] N91-23739

INDUSTRIEANLAGEN-BETRIEBSGESELLSCHAFT M.B.H., OTTOBRUNN (GERMANY, F.R.).
Airbreathing propulsion for space transport: New concepts, special problems and attempts at solutions N91-23154

INFO/TEK, WASHINGTON, DC.
The value of STINFO
[AD-A232484] N91-23996
Interacting with DTIC
[AD-A232485] N91-23997

INSTITUT D'AERONOMIE SPATIALE DE BELGIQUE, BRUSSELS.
Temperature dependence of ultraviolet absorption cross-sections of alternative chlorofluoroethanes
[AERONOMICA-ACTA-A-358-1991] N91-23647
A method for solving Poisson's equation in geophysical and astrophysical plasma
[AERONOMICA-ACTA-A-357-1990] N91-23925

INSTITUT DE MECANIQUE DE GRENOBLE (FRANCE).
Satellite data utilization in ocean circulation models N91-23593
Sea level and satellite techniques N91-23595

INSTITUT FRANCAIS DE RECHERCHE POUR L'EXPLOITATION DE LA MER, BREST (FRANCE).
Wind and sea state local climatology by means of satellite radar altimeter measurements N91-23599

INSTITUT FRANCAIS DE RECHERCHE POUR L'EXPLOITATION DE LA MER, LA SEYNE SUR MER.
Evaluation of multisensor fusion scheme for the localization of underwater remotely operated vehicles N91-23590

INSTITUT NATIONAL DES SCIENCES APPLIQUEES, LYON (FRANCE).
Dynamic study of cyclically symmetric structures: Application to rotating a wheel of a centrifugal compressor
[ISAL-91-0004] N91-23844

INSTITUTE FOR COMPUTER APPLICATIONS IN SCIENCE AND ENGINEERING, HAMPTON, VA.
An analysis of RNG based turbulence models for homogeneous shear flow
[NASA-CR-187552] N91-23433
Non-linear interaction of a detonation/vorticity wave
[NASA-CR-187550] N91-23434

INSTITUTE FOR DEFENSE ANALYSES, ALEXANDRIA, VA.
The costs and benefits of aircraft availability
[AD-A232660] N91-23076
Estimating fixed and variable costs of airframe manufacturers
[AD-A232661] N91-23077
Technology transfer in a changing national security environment
[AD-A232458] N91-24000

INSTITUTE FOR PERCEPTION RVO-TNO, SOESTERBERG (NETHERLANDS).
Otolith responses in man during parabolic flight
[IZF-1990-A-32] N91-23703
The development of highly practiced skills: A starting point for driver modelling
[IZF-1990-B-16] N91-23719

INSTITUTO DE PESQUISAS ESPACIAIS, SAO JOSE DOS CAMPOS (BRAZIL).
Detection of mining activities in the Yanomani Indian Reserve through LANDSAT-TM imagery
[INPE-5182-RPE/638] N91-23609

INTERNATIONAL BUSINESS MACHINES CORP., SAN JOSE, CA.
Conference on Theoretical Aspects of Reasoning About Knowledge
[AD-A232657] N91-23798

IOWA STATE UNIV. OF SCIENCE AND TECHNOLOGY, AMES.
Atrane and quadroped frameworks in early transition metal and silicon GRO stereochemistry: Monomers and oligomers
[AD-A232837] N91-23331
Intermediate/high energy nuclear physics
[DE91-010702] N91-23868

IOWA UNIV., IOWA CITY.
Computational life prediction methodology for mechanical systems using dynamic simulation, finite element analysis, and fatigue life prediction methods N91-23494
H-infinity approach to manipulator control N91-23495

ISRAEL AIRCRAFT INDUSTRIES LTD., BEN-GURION AIRPORT.
Real time estimation of aircraft angular attitude
[IAITIC-87-1004] N91-23107
IAI hypersonic wind tunnel
[IAITIC-87-1006] N91-23194
Improved quality acceptance procedure for interlaminar shear strength
[IAITIC-87-1005] N91-23238
MIK-guided bomb simulation
[IAITIC-87-1003] N91-23337
A method of constructing a pair of pseudorandom sequences with a useful crosscorrelation function
[IAITIC-87-1001] N91-23345

Computerized system for static and fatigue large scale structural tests: A case study
[IAITIC-87-1007] N91-23522
A simple solution to the singular linear minimum-variance estimation problem
[IAITIC-87-1002-REV] N91-23804

J

JAPAN MARINE SCIENCE AND TECHNOLOGY CENTER, TOKYO.
Manned diving activities in JAMSTEC N91-23572
JCLP HYPERBARIE, PARIS (FRANCE).
Subsea habitats and space simulation N91-23567
JET PROPULSION LAB., CALIFORNIA INST. OF TECH., PASADENA.
Microwave temperature profiler for clear air turbulence prediction
[NASA-CASE-NPO-18115-1-CU] N91-23662
Obstacle avoidance for redundant robots using configuration control
[NASA-CASE-NPO-17852-1-CU] N91-23783
Real time pre-detection dynamic range compression
[NASA-CASE-NPO-18098-1-CU] N91-23890
Electronic neuroprocessors N91-24045
Intelligent vision system for autonomous vehicle operations N91-24046
Integrated Vertical Bloch Line (VBL) memory N91-24051
Oxygen production using solid-state zirconia electrolyte technology N91-24059
Recent advances in coding theory for near error-free communications N91-24068
Fiber Optic Tactical Local Network (FOTLAN) N91-24072
High precision applications of the global positioning system N91-24073
JOHNS HOPKINS UNIV., LAUREL, MD.
Design techniques for dual mode ram-scramjet combustors N91-23166

K

KANSAS UNIV. CENTER FOR RESEARCH, INC., LAWRENCE.
Scattering from thin apertures in coated conductors using FDTD
[AD-A232125] N91-23365
KENT UNIV., CANTERBURY (ENGLAND).
Studies of molecular excitation in star formation regions N91-24023

L

LABORATOIRE D'AUTOMATIQUE ET D'ANALYSE DES SYSTEMES, TOULOUSE (FRANCE).
Time-optimal motion of robotic manipulators including nonlinear dynamics
[LAAS-90403] N91-23516
Research and development involved in creating a quantitative EEG cartography wide band analysis system
[LAAS-91002] N91-23705
Saturation and vote for the fault tolerance in distributed systems
[LAAS-90390] N91-23727
LAWRENCE LIVERMORE NATIONAL LAB., CA.
Tensor transformations and failure criteria for the analysis of fiber composite materials
[AD-A232238] N91-23265
Modeling second-phase formation during rapid resolidification of stainless steel alloys
[DE91-008567] N91-23291
Response of simulated propellants and explosives to projectile impact
[DE91-009777] N91-23333
Numerical modeling of turbulent dispersion around structures using a particle-in-cell method
[DE91-009757] N91-23426
Numerical simulation of a viscous vortex ring interaction with a density interface
[DE91-002790] N91-23429
Hairpin vortices, singularities, and transition to turbulence in three-dimensional shear flows
[DE91-002792] N91-23430
Quantitative film radiography
[DE91-009718] N91-23463
A submicron resolution monolithic capacitive displacement sensor with digital output
[DE91-009765] N91-23465
High-power performance of a copper laser pumped dye master-oscillator-power-amplifier chain
[DE91-010460] N91-23478
A 43 watt CW Ti:Sapphire laser
[DE91-010468] N91-23479
Finite element analysis of the lateral buckling of a cantilevered I Beam
[DE91-010123] N91-23527
Gravity spreading in the dispersion of dense gas plumes
[DE91-010155] N91-23628
Sensitivity of numerical dispersion modeling to explosive source parameters
[DE91-009476] N91-23631
Treatment of denser-than-air releases in an advection-diffusion model: Thermodynamic effects
[DE91-010152] N91-23632
Absolute calibration in vivo measurement systems
[DE91-009719] N91-23692
Problems in understanding the organization, structure and function of chromosomes
[DE91-009939] N91-23695
Scientific visualization software for your PC: Free and available now
[DE91-010156] N91-23744
Magnetic substates populated by double electron capture in slow ion atom collisions
[DE91-010122] N91-23858
Surface electron emission induced by slow multicharged ions
[DE91-010469] N91-23865
The intelligent database: Using INGRES to manage the external analysis of your data
[DE91-010465] N91-23986
Hard x ray imaging telescope
[DE90-015815] N91-24013
Relativistic shock waves and the excitation of plerions
[DE91-007623] N91-24027
Magnetospheric structure of rotation powered pulsars
[DE91-007622] N91-24028
LEHIGH UNIV., BETHLEHEM, PA.
Unsteady flow structure from swept edges subjected to controlled motion
[AD-A232714] N91-23094
LINNHOFF MARCH, INC., SAN MATEO, CA.
Research and development opportunities for natural gas fueled refrigeration in industrial processes
[PB91-136432] N91-23338
LITTON SYSTEMS, INC., CHARLOTTE, NC.
Contract crystal growth and fabrication services
[AD-A232120] N91-23952
LIVERPOOL UNIV. (ENGLAND).
Surface cloud observations for radiation, climatology and incorporation into satellite-based nephanalyses N91-23671
LOCKHEED MISSILES AND SPACE CO., PALO ALTO, CA.
Infrared focal plane performance in the South Atlantic anomaly
[NASA-CR-186197] N91-23458
LOS ALAMOS NATIONAL LAB., NM.
Re-analysis of photoemission data for CuO: Revision of the configuration-energy scheme for cuprate materials
[DE91-009952] N91-23296
Electrodeposited coatings for diamond turning applications
[DE91-009950] N91-23315
Distributed radar sensors for aircraft detection
[DE91-009845] N91-23350
The statistical properties of electromagnetic fields with application to radiation and scattering
[DE91-007467] N91-23351
A three-dimensional free-Lagrange code for multimaterial flow simulations
[DE91-002309] N91-23428
An expanding grid photochemical model for visibility applications
[DE91-009947] N91-23630
Robotics for recombinant DNA and human genetics research
[DE90-016440] N91-23697
Information dynamics of self-programmable matter
[DE91-009954] N91-23740
Use of a genetic algorithm to analyze robust stability problems
[DE91-005895] N91-23742
Applications of neural networks to process control and modeling
[DE91-007389] N91-23784
Los Alamos Science, Number 19, 1990
[DE91-009371] N91-23855
Microstructure of epitaxial YBa2Cu3O7 thin films
[DE91-009951] N91-23942
Fermi surface of YBCO by DHVA
[DE91-009963] N91-23943
Strain release in GaAs/Ga(1-x)/In(x)As strained layer superlattices grown on (112) substrates
[DE91-009972] N91-23944
LOUGHBOROUGH UNIV. OF TECHNOLOGY (ENGLAND).
On the structure of polynomial models of 2-D systems
[MATHS-REPT-A-139] N91-23812
On 2+1-dimensional nonlinear integrable systems of Loewner-type
[MATHS-REPT-A-140] N91-23813
LOUISIANA STATE UNIV., BATON ROUGE.
Database constraint enforcement: A decompositional approach N91-23980
Sensitive cryogenic transducer development and analysis for use on gravity wave detectors N91-24009

M

MARYLAND UNIV., COLLEGE PARK.
Hierarchic modeling of plates
[AD-A232754] N91-23560
Accuracy of the Reissner-Mindlin and the (1,1,2) model for the clamped-in plate problem
[AD-A232755] N91-23561
The problem of plate modeling theoretical and computational results
[AD-A232756] N91-23562
Generalized disjunctive well-founded semantics for logic programs
[AD-A232064] N91-23765
On locking and robustness in the finite element method
[AD-A232245] N91-23815
The H-P version of the finite element method in the plate modelling problem
[AD-A232246] N91-23816
Null values in definite programs
[AD-A232065] N91-23992
Combining knowledge bases consisting of first order theories
[AD-A232090] N91-23993
MARYLAND UNIV. BALTIMORE COUNTY, CATONSVILLE.
Duality methods for infinite dimensional optimization problems
[AD-A232605] N91-23772
MASSACHUSETTS INST. OF TECH., CAMBRIDGE.
Galvanic corrosion of aluminum-matrix composites
[AD-A232138] N91-23264
Deterministic analysis of processes at corroding metal surfaces and the study of electrochemical noise in these systems
[DE91-009997] N91-23297
Design and implementation of a packet switched routing chip
[AD-A232286] N91-23401
Strategies to sustain and enhance performance in stressful environments
[AD-A232698] N91-23714
Transition space
[AD-A231404] N91-23732
An in-depth analysis of concurrent B-tree algorithms
[AD-A232287] N91-23770
Are wait-free algorithms fast
[AD-A232829] N91-23774
Analog processing of optical wavefronts using integrated guided-wave optics
[AD-A232703] N91-23904
Experimental and theoretical research in applied plasma physics
[DE91-010657] N91-23920
MATERIALS RESEARCH SOCIETY, PITTSBURG, PA.
High temperature ordered intermetallic alloys
[AD-A232769] N91-23308
MATRA ESPACE, TOULOUSE (FRANCE).
Space and telescience robotics: Development of concepts and reference technologies for teledetection and robotics in extreme environments N91-23580
MAX-PLANCK-INST. FUER METEOROLOGIE, HAMBURG (GERMANY, F.R.).
Determination of the temperature profile of the troposphere with a two frequency lidar
[EXAMENARBEIT-8] N91-23653
MAX-PLANCK-INST. FUER PHYSIK UND ASTROPHYSIK, GARCHING (GERMANY, F.R.).
High resolution imaging for Brackett gamma and H2 1-0 S(1) emission in the Seyfert galaxy NGC 1068
[MPE-PREPRINT-192] N91-23104
The molecular interstellar medium and the near-infrared continuum of the barred liner NGC 6764
[MPE-PREPRINT-193] N91-24029
The high energy spectrum of the 1983, August 1b gamma-ray burst
[MPE-PREPRINT-194] N91-24040
MCAT INST., SAN JOSE, CA.
Development of a quiet supersonic wind tunnel with a cryogenic adaptive nozzle
[NASA-CR-186769] N91-23195

MCDONNELL-DOUGLAS HELICOPTER CO., MESA, AZ.
ADFCS and NOTAR (trademark): Two ways to fix flying qualities N91-23110
Technology needs for high-speed rotorcraft [NASA-CR-177578] N91-23136
MCDONNELL-DOUGLAS RESEARCH LABS., SAINT LOUIS, MO.
Vortex system evolution in 2- and 3-D swept trailing edge flows [AD-A232692] N91-23453
MCDONNELL-DOUGLAS SPACE SYSTEMS CO., HOUSTON, TX.
EVA/robotics integration for Space Station Freedom N91-23583
MESSERSCHMITT-BOELKOW-BLOHM G.M.B.H., MUNICH (GERMANY, F.R.).
Problems of hypersonic aerothermodynamics [MBB-FE202/5/PUB/436] N91-23090
X-31A at first flight N91-23131
Highly integrated ducted rocket propulsion modules for future hypersonic tactical missiles N91-23171
MIAMI UNIV., CORAL GABLES, FL.
Infrared and visible studies of Pakistan portion of Arabian Sea using INSAT geostationary satellite N91-23611
MICHIGAN STATE UNIV., EAST LANSING.
Radar target discrimination and identification using extinction-pulses and single-mode extraction pulses [AD-A232162] N91-23368
MICHIGAN TECHNOLOGICAL UNIV., HOUGHTON.
Boundary stability under nonequilibrium conditions [DE91-009262] N91-23293
MICHIGAN UNIV., ANN ARBOR.
Real-time simulation of constrained dynamic systems N91-23189
Mechanistic studies of pressure-assisted superplasticity of structural ceramics [AD-A232034] N91-23322
An experimental investigation of vortex pair interaction with a clean or contaminated free surface N91-23419
High resolution measurements of strained diffusion and reaction layer structure and extinction in turbulent flows [AD-A232794] N91-23456
Neutral wind vortices in the high-latitude thermosphere N91-23673
MIDWEST RESEARCH INST., GOLDEN, CO.
Optimization of transparent and reflecting electrodes for amorphous silicon solar cells [DE91-002132] N91-23618
MINISTRY OF DEFENCE, HAIFA (ISRAEL).
Lateral dispersion of radioactive release. Draft for comments [CEMA-86/17] N91-23621
On the many-on-one stochastic duel [CEMA-86/11] N91-23828
MINNESOTA UNIV., MINNEAPOLIS.
A study of the noise mechanisms of transonic blade-vortex interactions [NASA-CR-188199] N91-23084
A tribological study of sliding contact interaction N91-23488
Hydromagnetic wave coupling in the magnetosphere N91-23638
Echo 7: Magnetospheric properties determined by artificial electron beams N91-23644
Epitaxial iron films [AD-A232419] N91-23958
MITRE CORP., BEDFORD, MA.
Antenna performance influenced by the finite extent and conductivity of ground planes: A collection of reprints [AD-A232132] N91-23366
MOREHOUSE COLL., ATLANTA, GA.
Cultural parameters of stress [AD-A232526] N91-23713
MOTOREN- UND TURBINEN-UNION MUENCHEN G.M.B.H. (GERMANY, F.R.).
The 2-D supersonic nozzle design N91-23176

N

NATIONAL AERONAUTICAL ESTABLISHMENT, OTTAWA (ONTARIO).
An initial study into the influence of control stick characteristics on the handling qualities of a fly-by-wire helicopter N91-23122
An investigation into the use of side-arm control for civil rotorcraft applications N91-23123
Determination of decision-height windows for decelerating IMC approaches in helicopters N91-23124
NATIONAL AERONAUTICS AND SPACE ADMINISTRATION, WASHINGTON, DC.
Aeronautical engineering: A cumulative index to a continuing bibliography (supplement 261) [NASA-SP-7037(261)] N91-23073
Aeronautical engineering: A continuing bibliography with indexes (supplement 262) [NASA-SP-7037(262)] N91-23074
Cryogenic hydrogen-induced air-liquefaction technologies N91-23159
The Combined Release and Radiation Effects Satellite program (CRRES): A unique series of scientific experiments [NASA-TM-104957] N91-23213
ROSAT: An international mission exploring the high energy universe [NASA-TM-104958] N91-23214
Space life sciences: A status report [NASA-NP-120] N91-23694
Aerospace medicine and biology: A continuing bibliography with indexes (supplement 346) [NASA-SP-7011(346)] N91-23700
Aerospace medicine and biology: A continuing bibliography with indexes (supplement 347) [NASA-SP-7011(347)] N91-23701
Aerospace medicine and biology: A continuing bibliography with indexes (supplement 348) [NASA-SP-7011(348)] N91-23702
Technology 2000, volume 2 [NASA-CP-3109-VOL-2] N91-24041
Aeronautics and space report of the President N91-24085
NATIONAL AERONAUTICS AND SPACE ADMINISTRATION. AMES RESEARCH CENTER, MOFFETT FIELD, CA.
Airborne rescue system [NASA-CASE-ARC-11909-1] N91-23095
Microwave landing system modeling with application to air traffic control [NASA-TM-102832] N91-23099
Analytical and experimental investigations of the oblique detonation wave engine concept N91-23169
Technologies for aerobraking [NASA-TM-102854] N91-23207
Computational needs survey of NASA automation and robotics missions. Volume 1: Survey and results [NASA-TM-103860] N91-23341
Transcapillary fluid shifts in head and neck tissues during and after simulated microgravity [NASA-TM-103847] N91-23704
Physical/chemical closed-loop water-recycling N91-24052
Simulation of blood flow through an artificial heart N91-24056
A non-invasive measure of minerals and electrolytes in tissue N91-24058
A conformal oxidation-resistant, plasma-polymerized coating N91-24063
Flame-retardant composite materials N91-24064
NATIONAL AERONAUTICS AND SPACE ADMINISTRATION. GODDARD SPACE FLIGHT CENTER, GREENBELT, MD.
Magnetostrictive roller drive motor [NASA-CASE-GSC-13369-1] N91-23380
Distributed, cooperating knowledge-based systems N91-24044
Transportable Applications Environment (TAE) Plus: A NASA user interface development and management system N91-24048
The Land Analysis System (LAS) N91-24054
Potential commercial uses of EOS remote sensing products N91-24055
Optical communication for space missions N91-24070
Laser optical disk position encoder with active heads N91-24079
Melt-processed bulk superconductors: Fabrication and characterization for power and space applications N91-24082
NATIONAL AERONAUTICS AND SPACE ADMINISTRATION. HUGH L. DRYDEN FLIGHT RESEARCH FACILITY, EDWARDS, CA.
Flying qualities of the X-29 forward swept wing aircraft N91-23127
Buffet induced structural/flight-control system interaction of the X-29A aircraft [NASA-TM-101735] N91-23133
NATIONAL AERONAUTICS AND SPACE ADMINISTRATION. JOHN C. STENNIS SPACE CENTER, BAY SAINT LOUIS, MS.
Digital data registration and differencing compression system [NASA-CASE-SSC-00010-1] N91-23976
New research on bioregenerative air/water purification systems N91-24053
NATIONAL AERONAUTICS AND SPACE ADMINISTRATION. JOHN F. KENNEDY SPACE CENTER, COCOA BEACH, FL.
Atmospheric leakage and condensate production in NASA's biomass production chamber. Effect of diurnal temperature cycles [NASA-TM-103819] N91-23718
Monitoring and control technologies for bioregenerative life support systems/CELSS N91-24060
Localized corrosion of high performance metal alloys in an acid/salt environment N91-24066
Optical shutter switching matrix N91-24071
Robotic control and inspection verification N91-24075
NATIONAL AERONAUTICS AND SPACE ADMINISTRATION. LYNDON B. JOHNSON SPACE CENTER, HOUSTON, TX.
Simulation and analyses of the aeroassist flight experiment attitude update method [NASA-TM-102174] N91-23210
Static feed water electrolysis subsystem development [NASA-CASE-MSC-21577-1-SB] N91-23271
Two dimensional vernier [NASA-CASE-MSC-21700-1] N91-23462
Electromagnetic attachment mechanism [NASA-CASE-MSC-21463-1] N91-23490
Metallic threaded composite fastener [NASA-CASE-MSC-21580-1] N91-23491
Energy dissipator [NASA-CASE-MSC-21555-1] N91-23492
Preloaded latching device [NASA-CASE-MSC-21730-1] N91-23493
Programmable remapper for image processing [NASA-CASE-MSC-21350-1] N91-23724
Intelligent computer-aided training and tutoring N91-24042
CLIPS: A tool for the development and delivery of expert systems N91-24043
Software reengineering N91-24047
Applications of fuzzy logic to control and decision making N91-24049
Genetic algorithms N91-24050
NATIONAL AERONAUTICS AND SPACE ADMINISTRATION. LANGLEY RESEARCH CENTER, HAMPTON, VA.
Application of multidisciplinary optimization methods to the design of a supersonic transport [NASA-TM-104073] N91-23135
Hypersonic propulsion: Status and challenge N91-23153
Poly(1,3,4-oxadiazoles) via aromatic nucleophilic displacement [NASA-CASE-LAR-14427-1] N91-23237
Rate dependent stress-strain behavior of advanced polymer matrix composites [NASA-TM-104070] N91-23244
Passive laminar flow control of crossflow vorticity [NASA-CASE-LAR-13563-1] N91-23410
A non-contacting velocity measurement system [NASA-CASE-LAR-14466-1] N91-23461
Birefringent filter design [NASA-CASE-LAR-13887-1] N91-23472
Application of elastic and elastic-plastic fracture mechanics methods to surface flaws [NASA-TM-104964] N91-23539
Non-mechanical optical path switching and its application to dual beam spectroscopy including gas filter correlation radiometry [NASA-CASE-LAR-14586-1-CU] N91-23889
Superplastic forming of Al-Li alloys for lightweight, low-cost structures N91-24065
Quantitative nondestructive evaluation: Requirements for tomorrow's reliability N91-24074
The transfer of technology to measure skin burn depth in humans N91-24076
Frequency domain laser velocimeter signal processor N91-24077
A field-deployable digital acoustic measurement system N91-24078
Description of the Large Gap Magnetic Suspension System (LGMSS) ground-based experiment N91-24083
NATIONAL AERONAUTICS AND SPACE ADMINISTRATION. LEWIS RESEARCH CENTER, CLEVELAND, OH.
NASA aeropropulsion research in support of propulsion systems of the 21st century [NASA-TM-104403] N91-23083
Simulation of iced wing aerodynamics [NASA-TM-104362] N91-23086
Icing simulation: A survey of computer models and experimental facilities [NASA-TM-104366] N91-23087
A study of three dimensional turbulent boundary layer separation and vortex flow control using the reduced Navier Stokes equations [NASA-TM-104407] N91-23089

Engine technology challenges for a 21st century high speed civil transport
[NASA-TM-104363] N91-23098
Characteristics of a future aeronautical satellite communications system
[NASA-TM-104389] N91-23102
Computational modeling and validation for hypersonic inlets N91-23162
Effects of inlet distortion on the development of secondary flows in a subsonic axial inlet compressor rotor
[NASA-TM-104356] N91-23179
Multi-heat addition turbine engine
[NASA-CASE-LEW-15094-1] N91-23180
Advanced ice protection systems test in the NASA Lewis icing research tunnel
[NASA-TM-103757] N91-23183
Model rotor icing tests in the NASA Lewis icing research tunnel
[NASA-TM-104351] N91-23184
A CFD study of jet mixing in reduced flow areas for lower combustor emissions
[NASA-TM-104411] N91-23185
A three-dimensional Navier-Stokes stage analysis of the flow through a compact radial turbine
[NASA-TM-104420] N91-23186
Destructive physical analysis results of Ni/H2 cells cycled in LEO regime
[NASA-TM-104382] N91-23233
Component technology for stirling power converters
[NASA-TM-104387] N91-23234
Combined thermal and bending fatigue of high-temperature metal-matrix composites: Computational simulation
[NASA-TM-104354] N91-23247
Mechanical behavior and failure phenomenon of an in situ-toughened silicon nitride
[NASA-TM-103741] N91-23311
A simplified dynamic model of the Space Shuttle main engine
[NASA-TM-104421] N91-23340
An assessment of technology alternatives for telecommunications and information management for the space exploration initiative
[NASA-TM-103783] N91-23347
System-Level Integrated Circuit (SLIC) development for phased array antenna applications
[NASA-TM-104392] N91-23354
Simulation of brush insert for leading-edge-passage convective heat transfer
[NASA-TM-103801] N91-23409
Low Reynolds number two-equation modeling of turbulent flows
[NASA-TM-104368] N91-23416
A system-approach to the elastohydrodynamic lubrication point-contact problem
[NASA-TM-104342] N91-23439
Method of producing a plug type heat flux gauge
[NASA-CASE-LEW-14967-2] N91-23460
Effects of rim thickness on spur gear bending stress
[NASA-TM-104388] N91-23500
Government/industry response to questionnaire on space mechanisms/tribology technology needs
[NASA-TM-104358] N91-23501
Quantifying oil filtration effects on bearing life
[NASA-TM-104350] N91-23512
Modal analysis of multistage gear systems coupled with gearbox vibrations
[NASA-TM-103797] N91-23513
Maximum life spur gear design
[NASA-TM-104361] N91-23514
Evaluation and ranking of candidate ceramic wafer engine seal materials
[NASA-TM-103795] N91-23515
A preliminary investigation of acousto-ultrasonic NDE of metal matrix composite test specimens
[NASA-TM-104339] N91-23521
Computational simulation of acoustic fatigue for hot composite structures
[NASA-TM-104379] N91-23548
Simulation of probabilistic wind loads and building analysis
[NASA-TM-103744] N91-23549
Incorporating finite element analysis into component life and reliability
[NASA-TM-104400] N91-23550
Material processing with hydrogen and carbon monoxide on Mars
[NASA-TM-104405] N91-23616
Solar thermal energy receiver
[NASA-CASE-LEW-14949-1] N91-23617
SEI rover solar-electrochemical power system options
[NASA-TM-104402] N91-23620
Advances in silicon carbide Chemical Vapor Deposition (CVD) for semiconductor device fabrication
[NASA-TM-104410] N91-23946
Silicon carbide, an emerging high temperature semiconductor N91-24061
Flexible fluoropolymer filled protective coatings N91-24062
Digital CODEC for real-time processing of broadcast quality video signals at 1.8 bits/pixel N91-24067
Microwave integrated circuits for space applications N91-24069
Aerospace applications of high temperature superconductivity N91-24080
Superconducting microwave electronics at Lewis Research Center N91-24081

NATIONAL AERONAUTICS AND SPACE ADMINISTRATION. MARSHALL SPACE FLIGHT CENTER, HUNTSVILLE, AL.
Atmospheric turbulence review of space shuttle launches
[NASA-TM-4289] N91-23215
Parametric study in weld mismatch of longitudinally welded SSME HPFTP inlet
[NASA-TM-103534] N91-23502
Protein crystal growth tray assembly
[NASA-CASE-MFS-28507-1] N91-23933
Three-dimensional structure of human serum albumin N91-24057

NATIONAL AERONAUTICS AND SPACE ADMINISTRATION. PASADENA OFFICE, CA.
Microwave temperature profiler for clear air turbulence prediction
[NASA-CASE-NPO-18115-1-CU] N91-23662
Obstacle avoidance for redundant robots using configuration control
[NASA-CASE-NPO-17852-1-CU] N91-23783
Real time pre-detection dynamic range compression
[NASA-CASE-NPO-18098-1-CU] N91-23890

NATIONAL AEROSPACE LAB., TOKYO (JAPAN).
Research on aerodynamic control of blade tip clearance flow in air-cooled turbine
[DE91-764223] N91-23182

NATIONAL INST. OF STANDARDS AND TECHNOLOGY, BOULDER, CO.
Data-reduction and analysis procedures used in NIST's thermomechanical processing research
[PB91-132282] N91-23523
Study of static and dynamic fracture using strain measurements
[PB91-132217] N91-23524

NATIONAL PARK SERVICE, ANCHORAGE, AK.
Proceedings of the Second Glacier Bay Science Symposium
[PB91-110163] N91-23634

NATIONAL PHYSICAL LAB., TEDDINGTON (ENGLAND).
Committee draft for an ISO standard on the acquisition and presentation of multipoint data for plastics
[NPL-DMM(A)-24] N91-23320
The solidification of a molten droplet on an inclined plane
[NPL-DMM(A)-20] N91-23438
Scattering in electron spectrometers
[NPL-DMM(A)-19] N91-23467

NATIONAL SEVERE STORMS LAB., NORMAN, OK.
The terminal Doppler weather radar tornadic vortex signature detection algorithm
[DOT-FAA-NR-91-5] N91-23675

NATIONAL SPACE DEVELOPMENT AGENCY, IBARAKI (JAPAN).
Research and development of future space robotics in NASDA N91-23582

NAVAL AIR DEVELOPMENT CENTER, WARMINSTER, PA.
Agility: A rational development of fundamental metrics and their relationship to flying qualities N91-23129
Worst-case design of optimal controliers over a finite horizon
[AD-A232353] N91-23797

NAVAL BIODYNAMICS LAB., NEW ORLEANS, LA.
Human short-latency somatosensory evoked potentials in impact acceleration research: Equipment, procedures, and techniques
[AD-A232732] N91-23709
Ship roll stabilization and human performance
[AD-A232721] N91-23721

NAVAL OCEAN RESEARCH AND DEVELOPMENT ACTIVITY, BAY SAINT LOUIS, MS.
Portable intelligent diagnostic aids
[AD-A230883] N91-23782

NAVAL OCEAN SYSTEMS CENTER, SAN DIEGO, CA.
Photoresponse studies of ion-damaged germanium for optoelectronic switch applications
[AD-A232091] N91-23400
Mathematical techniques for the Performance Oriented Design (POD) tool
[AD-A232092] N91-23767
An event-activation record approach to simulation modeling in Ada: User's guide
[AD-A232093] N91-23768

NAVAL POSTGRADUATE SCHOOL, MONTEREY, CA.
Design and construction of a composite airframe for UAV research
[AD-A232422] N91-23143
An engineering study of altitude determination deficiencies of the Service Aircraft Instrumentation Package (SAIP)
[AD-A232055] N91-23145
An artificial neural network control system for spacecraft attitude stabilization
[AD-A232013] N91-23225
Satellite maneuver evaluation tool
[AD-A232016] N91-23226
Automatic particle sizing from rocket motor holograms
[AD-A232553] N91-23236
Phase transformations and microstructural evolution in aged Mn-Cu-based alloys
[AD-A232473] N91-23305
Error control coding for multi-frequency modulation
[AD-A232421] N91-23374
A study of PC-Based HF ionospheric propagation predictions for use in naval communications
[AD-A232466] N91-23375
Error probabilities of frequency hopped MFSK with self-normalization combining in a fading channel with partial-band interference
[AD-A232467] N91-23376
An analysis of MLAYER: A multilayer tropospheric propagation program
[AD-A232733] N91-23379
Parametric modeling and estimation of pulse propagation on microwave integrated circuit interconnections
[AD-A232465] N91-23404
Rule-based motion coordination for the adaptive suspension vehicle on ternary-type terrain
[AD-A232224] N91-23517
Atmospheric optical turbulence measurements taken at Anderson Mesa, Flagstaff, Arizona between 13-19 November 1989
[AD-A232222] N91-23658
Effects of the northeast monsoon on the equatorial westerlies over Indonesia
[AD-A232106] N91-23681
Evaluation of generalized thresholds in an objective multispectral satellite cloud analysis
[AD-A232716] N91-23683
Sea ice classification using synthetic aperture radar
[AD-A232248] N91-23689
Parallel-processor-based Gaussian beam tracer for use in ocean acoustic tomography
[AD-A232420] N91-23690
Evaluation of ferroelectric materials for memory applications
[AD-A232112] N91-23728
Designing a virtual-memory implementation using the Motorola MC68010 16-bit microprocessor with multi-processor capability interfaced to the VMEbus
[AD-A232554] N91-23730
A method for machinery condition monitoring of transient phenomena using the pseudo Wigner-Ville distribution
[AD-A232014] N91-23760
Integration of the execution support system for the Computer-Aided Prototyping System (CAPS)
[AD-A232015] N91-23761
Software testing for evolutionary iterative rapid prototyping
[AD-A232555] N91-23771
User interface to an ICAI system that teaches discrete math
[AD-A232693] N91-23799
Summary of basic research in thermoacoustic heat transport: 1990
[AD-A232223] N91-23847
A methodology for handling data errors and inconsistencies in database conversions
[AD-A232113] N91-23994

NAVAL RESEARCH LAB., WASHINGTON, DC.
Tripod operators for the interpretation of range images
[AD-A232631] N91-23344
High-quality 800-b/s voice processing algorithm
[AD-A232352] N91-23372
Digital beamforming and pulse compression in an adaptive array radar system
[AD-A232713] N91-23377
Observation of harmonic gyro-backward-wave oscillation in a 100 GHz CARM oscillator experiment
[AD-A232063] N91-23398
Background simulation and filter design using iterated function systems
[AD-A232632] N91-23405
A new asymptotic theory for the periodically forced laser
[AD-A232633] N91-23486

A complex systems approach to metallic fracture surface characterization
[AD-A232546] N91-23556
Quantum extension of Child-Langmuir law
[AD-A232407] N91-23878
Density channel tracking studies on Pulserad
[AD-A232649] N91-23888

NAVAL UNDERWATER SYSTEMS CENTER, NEW LONDON, CT.
Mapping an adaptable Eigenstructure technique onto the topologix hypercube
[AD-A232032] N91-23764

NAVY CLOTHING AND TEXTILE RESEARCH FACILITY, NATICK, MA.
Effectiveness of a prototype microclimate cooling system for use with chemical protective clothing
[AD-A231572] N91-23717

NEW ORLEANS UNIV., LA.
Bimanes and related heterocycles as laser dyes
[AD-A232335] N91-23484
The changing face of the environmental issue
[PB91-136081] N91-23624

NEW YORK UNIV., NEW YORK.
Adaptive methods for compressible fluid dynamics
[AD-A232786] N91-23455
Theoretical studies relating to the interaction of radiation with matter
[AD-A232107] N91-23480
Hall effects on anomalous heat, particle and helicity transports through tearing-mode turbulence
[DE91-010730] N91-23924

NORTH CAROLINA STATE UNIV., RALEIGH.
Research and development on advanced silicon carbide thin film growth techniques and fabrication of high power and microwave frequency silicon carbide-based device structures
[AD-A232160] N91-23955

NORTH CAROLINA UNIV., CHAPEL HILL.
Convergence of one-dimensional diffusion processes to a jump process related to population genetics
[AD-A232121] N91-23826
Initial data for the two-body problem of general relativity N91-23965
An expert system for searching in full-text N91-23983
The thermodynamic stability of systems containing black holes N91-24022

NORTHWESTERN UNIV., EVANSTON, IL.
Oxidation studies of fluorine containing diamond films
[AD-A232696] N91-23328
A new asymptotic theory for the periodically forced laser
[AD-A232633] N91-23486

NORWEGIAN DEFENCE RESEARCH ESTABLISHMENT, KJELLER.
CESAR operating system
[FFI-91/7002] N91-23754

NORWEGIAN UNDERWATER TECHNOLOGY CENTER LTD., LAKSEVAAG.
Effects of weightlessness (sea water immersion) on body fluid balance and CNS functions N91-23566

NOTRE DAME UNIV., IN.
Effects of three-dimensional imposed disturbance on bluff-body near wake flows
[AD-A232137] N91-23447
Structural and electronic properties of the ordered ternary 3-5 semiconductors N91-23936

NOTTINGHAM UNIV. (ENGLAND).
Investigation of the muon component of EAS initiated by primary radiation from Hercules X-1 N91-24037

O

OAK RIDGE K-25 SITE, TN.
Active Design Database (ADDB) user's manual
[DE91-010431] N91-23985
Security aspects of database management systems
[DE91-010677] N91-23987

OAK RIDGE NATIONAL LAB., TN.
Order and disorder in metallic alloys
[DE91-009120] N91-23292
Evaluation of filler metals for high-strength stainless steels
[DE91-009931] N91-23295
Creep and creep-rupture behavior of Alloy 718
[DE91-007706] N91-23298
NDE (Nondestructive Examination) development for ceramics for advanced heat engines
[DE91-005516] N91-23316
Low heat rejection diesel ceramic coupon tests
[DE91-006274] N91-23318
The effect of realistic antenna geometries on plasma loading predictions
[DE91-010782] N91-23353
Radioluminescent (RL) lighting system development program
[DE91-009743] N91-23381
Robot self-location in unknown environments
[DE91-010450] N91-23505
On the control of two manipulators holding a rigid object in the presence of uncertainty
[DE90-017742] N91-23508
Potential impact of enhanced fracture-toughness data on fracture mechanics assessment of PWR vessel integrity for pressurized thermal shock
[DE91-009554] N91-23509
Performance of visual and ultrasound sensing by an autonomous robot
[DE91-010452] N91-23511
Interlaminar strains at the free-edge of a hole for thick composites in compression
[DE91-008883] N91-23535
Reduction factors for creep strength and fatigue life of modified 9 Cr-1 Mo steel weldments
[DE91-009919] N91-23544
Experience with conventional inelastic analysis procedures in very high temperature applications
[DE91-009937] N91-23545
Modeling speedup in parallel sparse matrix factorization
[DE91-010215] N91-23735
Analysis of neutron noise spectra using neural networks
[DE91-007676] N91-23785
Parallelizing the spectral transform method, part 1
[DE91-010453] N91-23805
Few-body problems, electron-correlation effects, and beyond
[DE91-010030] N91-23857
Monte Carlo simulation of supercritical solutions in the grand canonical ensemble
[DE91-009152] N91-23859
Computed secondary-particle energy spectra following nonelastic neutron interactions with C-12 for E(n) between 15 and 60 MeV: Comparisons of results from two calculational methods
[DE91-010454] N91-23864
Low-energy collisions of multiply charged ions with electrons, atoms and surfaces
[DE91-010779] N91-23873
Pressure dynamics modeling for the design of the advanced neutron source reactor
[DE91-007860] N91-23883
Two-channel spectroscopic polarization modulation ellipsometry
[DE91-010131] N91-23893
ICRF heating on the Burning Plasma Experiment (BPX)
[DE91-010390] N91-23913
Transport analysis of stellarator reactors
[DE91-010489] N91-23914
Inversion of chordal data from the ATF torsatron
[DE91-010490] N91-23915
Ion confinement and radiation losses in the advanced toroidal facility
[DE91-010382] N91-23916
Heavy ion beam probe measurements of ECH method plasma in the advanced toroidal facility
[DE91-010391] N91-23917
Geomagnetic storms: Potential economic impacts on electric utilities
[DE91-009523] N91-24036

OBSERVATORIO DEL EBRO, ROQUETAS (SPAIN).
Ionosphere 1984, volume 72
[ISSN-0211-5166] N91-23649
Ionosphere 1985, volume 73
[ISSN-0211-5166] N91-23650

OFFICE NATIONAL D'ETUDES ET DE RECHERCHES AEROSPATIALES, MODANE (FRANCE).
A study of supersonic and hypersonic ramjet engines in France from 1950 to 1974 (application on combined cycle aircraft engines) N91-23149

OFFICE NATIONAL D'ETUDES ET DE RECHERCHES AEROSPATIALES, PARIS (FRANCE).
Compact heat exchanger for an inverse components engine N91-23157
Supersonic-hypersonic inlet studies for aerospaceplane N91-23160

OFFICE OF MANAGEMENT AND BUDGET, WASHINGTON, DC.
Five-year plan for meeting the automatic data processing and telecommunications needs of the Federal Government
[PB91-103549] N91-23982

OFFICE OF TECHNOLOGY ASSESSMENT, WASHINGTON, DC.
Federally funded research: Decisions for a decade
[OTA-SET-490] N91-23998

OHB-SYSTEM G.M.B.H., BREMEN (GERMANY, F.R.).
Payload related crew operations: From past missions to Columbus N91-23569

OHIO STATE UNIV., COLUMBUS.
Joint services electronics program
[AD-A232331] N91-23402
Automated handling and assembling of non-rigid objects
[AD-A231246] N91-23489
Atmospheric circulation and poleward sensible heat flux variations associated with the recent Northern Hemisphere warming N91-23629
Mean-field theories of the Hubbard model and periodic orbits in chaotic maps N91-23938
Theoretical studies of QSO absorption lines and the intergalactic medium N91-24025

OKLAHOMA UNIV., NORMAN.
Advanced working fluids: Thermodynamic properties
[PB91-136465] N91-23964

OLD DOMINION UNIV., NORFOLK, VA.
An experimental study of an axisymmetric turbulent boundary layer disturbed by a periodic freestream N91-23078
Large and moderate deviation limit theorems for arbitrary sequences of random variables with applications
[AD-A232334] N91-23817
Building a generalized distributed system model
[NASA-CR-188181] N91-23970
Building a generalized distributed system model N91-23971
Effects of distributed database modeling on evaluation of transaction rollbacks N91-23972
Measuring the effects of distributed database models on transaction availability measures N91-23973
Performance analysis of static locking in replicated distributed database systems N91-23974
A note on the performance analysis of static locking in distributed database systems N91-23975

ONAN CORP., MINNEAPOLIS, MN.
Development of a low cost peak shaving generator set
[PB91-136374] N91-23332

OREGON GRADUATE INST. OF SCIENCE AND TECHNOLOGY, BEAVERTON.
Low-temperature laser-induced selective area growth of compound semiconductor N91-23932

OREGON INST. OF TECH., KLAMATH FALLS.
Direct use R/D assistance
[DE91-009976] N91-23999

OREGON STATE UNIV., CORVALLIS.
Control aspects of the brushless doubly-fed machine
[DE91-009707] N91-23387

ORTEL CORP., ALHAMBRA, CA.
Vertical emitting, ring geometry, ultra-low threshold and ultra-high speed quantum well lasers for optical interconnect
[AD-A232122] N91-23481

OXFORD UNIV. (ENGLAND).
Pitot surveys of two moderately under-expanded jets N91-23172
Modelling of the impact response of fibre-reinforced composites
[AD-A232658] N91-23266
Analysis of the multigrid method N91-23418

P

PACIFIC NORTHWEST LAB., RICHLAND, WA.
Stress-density variations in alumina sediments: Effects of polymer chemistry
[DE91-009055] N91-23313

PARIS VI UNIV. (FRANCE).
Ocean modeling for climate study N91-23592

PARIS VI UNIV., VILLEFRANCHE-SUR-MER (FRANCE).
Primary ocean production: Carbon and particle flux N91-23596

PENNSYLVANIA STATE UNIV., UNIVERSITY PARK.
Computer modeling of soot formation comparing free radical and ionic mechanisms
[AD-A232820] N91-23287
Point defect effects on hot corrosion of zirconia-based coatings
[AD-A232662] N91-23326
A computationally efficient modelling of laminar separation bubbles N91-23411
Fundamental hydrodynamics research
[AD-A232650] N91-23451
Atmospheric teleconnections: Emphasis on the El Nino/Southern Oscillation and monsoons N91-23636
Surface layer transfer processes over vegetation: A micrometeorological field experiment of long duration N91-23664
Observational study of the above-inversion structure and marine stratocumulus cloud clearing episodes during FIRE N91-23666

Boundary conditions in quantum cosmology N91-24020

PENNSYLVANIA UNIV., PHILADELPHIA.
A study of the micromechanics of the fiber-matrix interphase in monofilament composites, in monotonic loading, and cyclic fatigue N91-23241
Theoretical prediction of vibrational infrared frequencies of tertiary amines
[AD-A232880] N91-23288
Software reverse engineering
[AD-A232644] N91-23773
Image wavelet decomposition and applications
[NASA-CR-188217] N91-23787
The Sudbury Neutrino Observatory project and the Kamiokande 2 project
[DE91-010641] N91-23863

PHILIPS DISPLAY COMPONENTS CO., ANN ARBOR, MI.
Chevron-notched, flexure tests for measuring the elevated temperature fracture resistance of structural ceramics
[DE91-009117] N91-23310

PHYSICS AND ELECTRONICS LAB. TNO, THE HAGUE (NETHERLANDS).
Time-domain analysis of one-dimensional electromagnetic scattering by Lossy media
[FEL-90-A211] N91-23358
SAR processor for the ERS-1 data phase 1, simple processor
[FEL-90-B033] N91-23359
Calculation of near-field scattering using the plane-wave formulation and the physical optics method
[FEL-90-B215] N91-23360
Calculation of electromagnetic fields in the near-field region of a moving scattering object
[FEL-90-B216] N91-23361
Design of inherently wide-band microwave frequency doubler and tripler in microstrip
[FEL-90-B255] N91-23392

PISA UNIV. (ITALY).
Metrics for roll response flying qualities N91-23118

PITTSBURGH UNIV., PA.
A novel process for methanol synthesis
[DE91-009808] N91-23334
Flow between eccentric rotating cylinders N91-23417

POLATOMIC, INC., RICHARDSON, TX.
Metal thin-film optical polarizers for space applications, phase 2
[NASA-CR-188202] N91-23891

POLITECNICO DI MILANO (ITALY).
Propagation of seismic waves in nonelastic media
[REPT-90-065] N91-23651
Designing logic controllers with Petri nets
[REPT-90-029] N91-23747
An incremental approach to logic controllers design with Petri nets
[REPT-90-030] N91-23748
On the initialization problem in the design of structurally constrained digital regulators
[REPT-90-039] N91-23749
Timed high-level nets
[REPT-90-050] N91-23750
Realization of a randomized algorithm for the exact perfect matching problem, with a new constructive procedure
[REPT-90-056] N91-23751
On the use of genetic algorithms to solve the time-table problem
[REPT-90-060] N91-23752

PRINCETON UNIV., NJ.
Models of planetary wave propagation in the middle atmosphere N91-23639
Mechanisms of equatorial superrotation: Studies with two-level models N91-23642
Molecular dynamics simulator for optimal control of molecular motion
[AD-A232801] N91-23881

PRINS MAURITS LAB. TNO, RIJSWIJK (NETHERLANDS).
Theoretical and experimental performance of a solid fuel ramjet combustion cycle for hypersonic flight conditions N91-23170
On the efficiency of rail accelerators
[PML-1990-64] N91-23204

PUERTO RICO UNIV., RIO PIEDRAS.
Phase transitions at liquid solid interfaces: Pade approximant for adsorption isotherms and voltammograms
[AD-A232623] N91-23285
Structure of electrochemically deposited copper on gold (III) alloy
[AD-A232345] N91-23303
The direct correlation function of a mixture of hard ions in the mean spherical approximation
[AD-A232452] N91-23879
In-situ surface x ray scattering measurements of electrochemically deposited bismuth on silver (III): Structure, compressibility, and comparison with ex-situ leed measurements
[AD-A232624] N91-23880
Surface x ray scattering measurements of the substrate induced spatial modulation of an incommensurate adsorbed monolayer
[AD-A232625] N91-23959

PURDUE UNIV., WEST LAFAYETTE, IN.
Formulation of boundary conditions for the multigrid acceleration of the Euler and Navier Stokes equations
[NASA-CR-188234] N91-23440
Maintenance of short-term subtropical wind maxima in the Southern Hemisphere: Observational and modeling study N91-23665
Statistical methods and neural network approaches for classification of data from multiple sources
[NASA-CR-188207] N91-23786
A survey of decision tree classifier methodology
[NASA-CR-188208] N91-23806
Topics in inference and decision-making with partial knowledge
[NASA-CR-188209] N91-23821

Q

QUAID-I-AZAM UNIV., ISLAMABAD (PAKISTAN).
Effect of transition metal dopants on high T(sub c) superconductivity
[PB91-130138] N91-23934

QUESTECH, INC., FALLS CHURCH, VA.
Thermal control system for the investigation of specific absorption rates for specimens exposed to electromagnetic radiation
[AD-A231329] N91-23459

R

READING UNIV. (ENGLAND).
Localised symmetric instability: An initial value problem N91-23672

RENSSELAER POLYTECHNIC INST., TROY, NY.
Fundamental research on tribology
[AD-A232446] N91-23519

RHODE ISLAND UNIV., KINGSTON.
The transient response of heavily fluid-loaded elastic plates and cylindrical shells N91-23528

ROCKWELL INTERNATIONAL CORP., CANOGA PARK, CA.
Use of secondary flows for rapid mixing in scramjet combustors N91-23167
The effect of combustor flow nonuniformity on the performance of hypersonic nozzles N91-23173

ROCKWELL INTERNATIONAL CORP., LOS ANGELES, CA.
Aerodynamic preliminary analysis system 2. Part 1: Theory
[NASA-CR-182076] N91-23080
Aerodynamic preliminary analysis system 2. Part 2: User's manual
[NASA-CR-182077] N91-23081

ROLLS-ROYCE LTD., BRISTOL (ENGLAND).
Design considerations of a high expansion ratio hydrogen turbine N91-23163

ROME UNIV. (ITALY).
Reacting shock waves in hypersonic propulsion applications N91-23174
Study of the response of a crystal ball made of NaI(Tl) for heavy ions experiments
[NOTA-INTERNA-957] N91-23874
The birth of the 'strange' particle physics
[NOTA-INTERNA-958] N91-23875
Experiments on Frank-Hertz setup
[NOTA-INTERNA-961] N91-23876
Development of a digital correlator to measure the semi-elastic scattering of light
[NOTA-INTERNA-955] N91-23895

ROYAL AEROSPACE ESTABLISHMENT, BEDFORD (ENGLAND).
Handling qualities guidelines for the design of fly-by-wire flight control systems for transport aircraft N91-23119

ROYAL NETHERLANDS METEOROLOGICAL INST., DE BILT.
Technical description of the high-resolution air mass transformation model at KNMI
[KNMI-TR-125] N91-23646
Quantitative processing of Meteosat data: Implementation at KNMI: Applications
[KNMI-TR-127] N91-23678
A guide to the Nedwam wave model
[KNMI-WR-90-04] N91-23688

ROYAL SIGNALS AND RADAR ESTABLISHMENT, MALVERN (ENGLAND).
Implications of adaptive cancellation array processing for design of a space-based surveillance radar
[RSRE-MEMO-4410] N91-23364
A transmission line method for the measurement of microwave permittivity and permeability
[RSRE-MEMO-4450] N91-23394
Silicon avalanche photodiode active-quenching circuit
[AD-A233633] N91-23395
NODEN user's guide and installation manual
[RSRE-MEMO-4438] N91-23753
Functional approximation by feed-forward networks: A least squares approach to generalisation
[RSRE-MEMO-4453] N91-23811
The United Kingdom waveguide power standards above 40 GHz
[RSRE-90023] N91-23845
The coordinate-free representation of rotational motions
[RSRE-MEMO-4445] N91-23846
Liquid-crystal characterization using the Z-scan technique
[RSRE-MEMO-4451] N91-23949

RUTGERS - THE STATE UNIV., NEWARK, NJ.
Robustness in replicated databases N91-23981

RUTHERFORD APPLETON LAB., CHILTON (ENGLAND).
ATSR: Precise sea surface temperature from the ERS-1 satellite N91-23601

RUTHERFORD HIGH ENERGY LAB., CHILTON (ENGLAND).
Particle physics experiments, 1990
[RAL-91-001] N91-23877

S

SAINT ANDREW'S UNIV. (SCOTLAND).
Optical parametric oscillators pumped by excimer lasers N91-23473

SANDIA NATIONAL LABS., ALBUQUERQUE, NM.
A vortex panel method for calculating aircraft downwash on parachute trajectories
[DE91-009764] N91-23085
Ion beam testing of the Aerolor X-point dump plate for the Joint European Torus
[DE91-010719] N91-23245
The solidification behavior of an alloy 625/718 variant
[DE91-009544] N91-23294
Shock characterization of epoxy: Forty-two volume percent glass microballoons
[DE91-009616] N91-23314
Effect of atmospheric variations on electromagnetic distance measurements
[DE91-009726] N91-23349
Experimental study of narrow slot, cavity-backed apertures with finite wall conductivity
[DE91-009039] N91-23352
Recent advances with quiescent power supply current (I(sub DDQ)) testing at Sandia using the HP82000
[DE91-009254] N91-23382
Solutions to current induced avalanche burnout
[DE90-013196] N91-23386
S-parameter measurements and applications of superconducting flux flow transistors
[DE91-009763] N91-23388
Conceptual design and system studies for a 600 kW repetitive pulse transformer
[DE91-010585] N91-23389
Developing natural convection in a fluid layer with localized heating and large viscosity variation
[DE91-005240] N91-23431
Benchmarking numerical predictions with force and moment measurements on slender, supercavitating bodies
[DE91-007066] N91-23432
Strained quantum well leaky-mode diode laser arrays
[DE91-009982] N91-23477
Raybot: A practical implementation of a hierarchical control system for telerobotic land vehicles
[DE90-017029] N91-23507
Bobbin stresses generated by wire winding
[DE91-009545] N91-23526
Mechanical states in wound heterogeneous tapes by the finite element method
[DE91-009255] N91-23536
Mechanical stress states in heterogeneous, wound rolls
[DE91-009257] N91-23537
PV concentrators today and tomorrow
[DE91-010577] N91-23619
Pulsed power performance of the new RLA (Recirculating Linear Accelerator)
[DE91-004723] N91-23885

Measurements of passive-scalar spectra for grid turbulence using a nonlinear optical technique
[DE91-005310] N91-23892
Intense light-ion beams provide a robust, common-driver path towards ignition, gain and commercial fusion energy
[DE91-010584] N91-23919
High power light activated semiconductor switches with sub-nanosecond rise time
[DE91-009250] N91-23939
Electronic properties of Si-doped n-doping-intrinsic-p-doping-intrinsic (nipi) structures in GaAs
[DE91-009474] N91-23941

SANTA CLARA UNIV., CA.
The TurboLAN project. Phase 1: Protocol choices for high speed local area networks. Phase 2: TurboLAN Intelligent Network Adapter Card, (TINAC) architecture
[NASA-CR-188175] N91-23776

SCIENCE APPLICATIONS INTERNATIONAL CORP., MCLEAN, VA.
Soviet atmospheric acoustics research N91-23848

SENER S.A., MADRID (SPAIN).
Hypersonic propulsion: Past and present N91-23148

SHEFFIELD UNIV. (ENGLAND).
Theoretical studies of large-scale features of the Earth's mid- to high-latitude ionosphere N91-23641

SMITHSONIAN ASTROPHYSICAL OBSERVATORY, CAMBRIDGE, MA.
Small Explorer project: Submillimeter Wave Astronomy Satellite (SWAS). Mission operations and data analysis plan
[NASA-CR-186954] N91-23212

SOCIETE D'ARCHITECTURES EN MILIEUX EXTREMES, PARIS (FRANCE).
European stakes and measures permitting the management of geometric dimensions N91-23573

SOCIETE D'ETUDES DES SYSTEMES D'AUTOMATION, TOULOUSE (FRANCE).
Object oriented programming in MMI: A software tool for analysis and planification of a radar imaging mission N91-23589

SOCIETE EUROPEENNE DE PROPULSION, SAINT-MEDARD-EN-JALLES (FRANCE).
Materials and material systems for combined cycle engines N91-23178

SOCIETE EUROPEENNE DE PROPULSION, SURESNES (FRANCE).
Comparative study of different systems of combined cycle propulsion N91-23152

SOUTH CAROLINA UNIV., COLUMBIA.
Statistical models and inference procedures for structural and materials reliability
[AD-A232634] N91-23827

SOUTHAMPTON UNIV. (ENGLAND).
The supernova remnant G109.1-1.0 and the x-ray pulsar 1E2259+586 N91-24002
Imaging and background in low-energy gamma ray astronomy N91-24005
Instrumentation and data analysis for hard x ray astronomy N91-24010

SOUTHERN METHODIST UNIV., DALLAS, TX.
Some remarks on compliance testing
[AD-A231936] N91-23635

SOVIET-FRENCH JOINT VENTURE, MOSCOW (USSR).
Real time analysis systems of the physical parameters of the environment and the state of a human organism for a long term exposure at different gas mixtures and pressure up to 100 bar N91-23568

SPACE SYSTEMS/LORAL, PALO ALTO, CA.
Unattended network operations technology assessment study. Technical support for defining advanced satellite systems concepts
[NASA-CR-187080] N91-24030

SPARTA, INC., LEXINGTON, MA.
Ultra-dense optical mass storage
[AD-A232767] N91-23905

SPECTRAL SCIENCES, INC., BURLINGTON, MA.
Strategy Combining Regionally Adapted Processes (SCRAP)
[AD-A232158] N91-23448

SRI INTERNATIONAL CORP., MENLO PARK, CA.
Multiphoton detection techniques for F and F2
[AD-A232641] N91-23286
Ionic solid hydrogen fuel: Experimental investigation of cluster-impact fusion
[AD-A232642] N91-23336
Solid polymer electrolytes for rechargeable batteries
[DE91-010231] N91-23384
Channel diagnostics for the multi-pulse-propagation experiments at ATA
[DE91-009772] N91-23466
Spatiotemporal characteristics of visual localization
[AD-A232734] N91-23715
Advanced methods of approximate reasoning
[AD-A232140] N91-23814

STANFORD UNIV., CA.
A new architecture and expert system for aircraft design synthesis N91-23132
High temperature deformation processes and strengthening mechanisms in intermetallic particulate composites
[AD-A232737] N91-23267
The effects of controlling vortex formation on the performance of a dump combustor N91-23270
A numerical study of the stratified turbulent Ekman layer N91-23421
Advanced diagnostics for reacting flows
[AD-A232609] N91-23902
Soft x ray/extreme ultraviolet images of the solar atmosphere with normal incidence multilayer optics N91-24006

STATE DEPT., WASHINGTON, DC.
Eastern Europe: Please stand by
[PB91-14336] N91-23348

STATE UNIV. OF NEW YORK, BUFFALO.
Mixing and non-equilibrium chemical reaction in a compressible mixing layer
[NASA-CR-187084] N91-23181
Bromination of carbon fibers and carbon-carbon composites N91-23240

STATE UNIV. OF NEW YORK, STONY BROOK.
Turbulent mixing in nonreacting and reacting flows: A PDF approach at the two-point level N91-23422
Nonlinear waves in real materials
[AD-A232654] N91-23452
Near-infrared milliarcsecond observations by the lunar occultation technique N91-24034

STEVENS INST. OF TECH., HOBOKEN, NJ.
Nonequilibrium Green's functions and quantum transport theory for semiconductor microstructures N91-23937

STOCKHOLM UNIV. (SWEDEN).
Grouping of clouds and internal gravity waves in a non-hydrostatic model of moist convection
[DM-55] N91-23679
A one dimensional wind profile model with stability and eddy viscosity estimations from sodar data
[DM-56] N91-23680
The reduced version of the DERF 2 data set on a WORM optical disk
[DM-54] N91-23991

SUPERCONDUCTING SUPER COLLIDER LAB., DALLAS, TX.
A controlled master frequency oscillator for the SSC low energy booster
[DE91-011004] N91-23391
Constant of motion and dynamic equations for one-dimensional autonomous system and radiation damping
[DE91-011002] N91-23547

SVERDRUP TECHNOLOGY, INC., ARNOLD AFS, TN.
Computation of inlet reference plane flow-field for a subscale free-jet forebody/inlet model and comparison to experimental data
[AD-A232101] N91-23445

SVERDRUP TECHNOLOGY, INC., BROOK PARK, OH.
The application of neural networks to the SSME startup transient
[NASA-CR-187138] N91-23205

SVERDRUP TECHNOLOGY, INC., CLEVELAND, OH.
Viscous three-dimensional analyses for nozzles for hypersonic propulsion N91-23175

SYNTHESIS GROUP, ARLINGTON, VA.
America at the threshold N91-23201

SYRACUSE UNIV., NY.
Mechanisms of higher brain functions: A study of models of perception
[AD-A232389] N91-23712

SYSTEMS CONTROL TECHNOLOGY, INC., ARLINGTON, VA.
Air ambulance helicopter operational analysis
[DOT/FAA/RD-91/7] N91-23134

SYSTEMS TECHNOLOGY, INC., HAWTHORNE, CA.
Estimation of pilot ratings via pilot modeling N91-23121

T

TECHNICAL RESEARCH ASSOCIATES, SALT LAKE CITY, UT.
Isolation, cloning and expression of the genes for microbial polyurethane degradation
[AD-A232108] N91-23699

TECHNICAL RESEARCH CENTRE OF FINLAND, ESPOO.
Evaluation of catastrophic failure risk in pressure vessels. Results of pressure vessel test with a large vessel (HC2-test)
[VTT-RR-708] N91-23551
A Model-Based Approach to High-Level Robot Control with Visual Guidance
[VTT-PUBL-71] N91-23788

TECHNICAL RESEARCH CENTRE OF FINLAND, OULU.
A solution for the man/machine-interface in robotics: A high level control language with enhanced interaction equipment N91-23789
Monitoring an assembly task by perception requests N91-23791
Intelligent planning in controlling electronics assembly N91-23792
Planning of visual feedback with robot-sensor co-operation N91-23793
Robot-sensor co-operation planning for visual guidance N91-23794
A line based object localizing method for robot vision N91-23795
Object pose estimation based on one-degree-of-freedom sensor N91-23796

TECHNION - ISRAEL INST. OF TECH., HAIFA.
First principles calculation of the crystal structures in the 4d transition metals N91-23835
Theory of the new high-temperature superconductors N91-23842
Survey: Potential of the Israeli industry for space technology
[CEMA-86-17] N91-23967

TECHNISCHE UNIV., BRUNSWICK (GERMANY, F.R.).
Airborne Collision Avoidance System (ACAS) in controlled air traffic. Aspects of reciprocal influence in Secondary Surveillance Radar (SSR) radio loads
[ETN-91-99253] N91-23105
Gas contents and weldability of aluminum die castings
[ETN-91-99188] N91-23302

TECHNISCHE UNIV., DELFT (NETHERLANDS).
Extraction of mesoscale ocean currents information from Geosat altimeter data N91-23594

TECHNISCHE UNIV., EINDHOVEN (NETHERLANDS).
Information plan study: A strategy model
[ISBN-90-6233-638-8] N91-23988

TECHNISCHE UNIV., MUNICH (GERMANY, F.R.).
Experimental investigations on the transition from stable to unstable combustion by means of active instability control N91-23165

TECNOMARE S.P.A. (ITALY).
Telerobotics: A key area for possible technology transfer from underwater to space N91-23581

TEL-AVIV UNIV. (ISRAEL).
Bulletin of the Israel Physical Society, volume 33, 1987. Annual Meeting 1987: Program and Abstracts
[ITN-89-85012] N91-23832
Temperature distribution and thermal damage during tissue ablation by CO2 laser irradiation: Model and experiment N91-23833
An on-line computerized system for blood-flow measurements N91-23834
Optical and mechanical properties of mixed silver halide crystals N91-23837
The spectrum of massive accretion disks N91-23840
Exploring the mesoscopic domain where classical and quantum phenomena meet N91-23843

TEST SQUADRON (6510TH), EDWARDS AFB, CA.
B-1B high AOA testing in the evaluation of a stall inhibitor system N91-23126

TEXAS A&M UNIV., COLLEGE STATION.
Flow field study of a rectangular jet N91-23423
Stochastic micromechanical modeling of cleavage fracture in the ductile-brittle transition region N91-23533
Elastic/plastic fracture mechanics. Part 2: Marine structural applications
[AD-A232560] N91-23557
Excitation of atoms and molecules in collisions with highly charged ions
[DE91-010740] N91-23870

TEXAS CHRISTIAN UNIV., FORT WORTH.
Phase transitions at liquid solid interfaces: Pade approximant for adsorption isotherms and voltammograms
[AD-A232623] N91-23285

TEXAS TECHNOLOGICAL UNIV., LUBBOCK.
Theoretical and numerical study of anomalous turbulent transport in plasmas
[AD-A232688] N91-23931

TEXAS UNIV., AUSTIN.
Target maneuver models for improved homing guidance N91-23101
Precision orbit determination of global positioning system satellites N91-23202
System modeling and identification of flexible structures N91-23531
Synergetic multisensor fusion
[AD-A232089] N91-23766
Control synthesis based upon a game theoretic approach N91-23831

On standard forms for transport equations and fluxes, part 2
[DE91-010421] N91-23912
Comparison of drift wave models with fluctuation data from the interior of the TEXT tokamak
[DE91-010424] N91-23918

THOMAS (DIETER), FUERSTENFELDBRUCK (GERMANY, F.R.).
The art of flying qualities testing N91-23109

TINI ALLOY CO., OAKLAND, CA.
Shape-memory alloy tactical feedback actuator, phase 1
[AD-A231389] N91-23289

TORONTO UNIV., DOWNSVIEW (ONTARIO).
Performance characteristics of hypersonic detonation wave ramjets N91-23168

TRW SPACE TECHNOLOGY LABS., REDONDO BEACH, CA.
In-Space technology experiments program. A high efficiency thermal interface (using condensation heat transfer) between a 2-phase fluid loop and heatpipe radiator: Experiment definition phase
[NASA-CR-186869] N91-23408

U

UNIFORMED SERVICES UNIV. OF THE HEALTH SCIENCES, BETHESDA, MD.
Molecular studies of cytokine induction
[AD-A232221] N91-23707

UNITED TECHNOLOGIES CORP., WEST PALM BEACH, FL.
Mechanical component diagnostic system
[AD-A232126] N91-23146

UNITED TECHNOLOGIES RESEARCH CENTER, EAST HARTFORD, CT.
A study of the critical factors controlling the synthesis of ceramic matrix composites from preceramic polymers
[AD-A232686] N91-23327
Unified aeroacoustics analysis for high speed turboprop aerodynamics and noise. Volume 2: Development of theory for wing shielding
[NASA-CR-185192] N91-23849

UNIVERSAL ENERGY SYSTEMS, INC., DAYTON, OH.
Computation of viscous shock/shock hypersonic interactions with an implicit flux split scheme
[AD-A232405] N91-23093

UNIVERSITAET DER BUNDESWEHR MUENCHEN, NEUBIBERG (GERMANY, F.R.).
Linear bending of curved tubes without boundary influence
[ETN-91-99255] N91-23552

UNIVERSITE DES SCIENCES ET TECHNIQUES DE LILLE (FRANCE).
Using satellite remote sensing imagery for marginal ice zone research in the ARCTEMIZ project N91-23600

UNIVERSITY OF NORTHERN ARIZONA, FLAGSTAFF.
Effects of bright illumination on oral temperature and cognitive performance in humans during nighttime hours
[AD-A232787] N91-23722

UNIVERSITY OF SOUTHERN CALIFORNIA, LOS ANGELES.
Mechanics/heat-transfer relation for particulate materials
[DE91-008356] N91-23424
Studies of noise in semiconductor laser arrays
[AD-A232411] N91-23485
Approximation methods for the identification and control of distributed parameter systems with applications to flexible structures
[AD-A232805] N91-23801
Photonic materials and devices for optical information processing and computing applications
[AD-A232771] N91-23907
Nonlinear real-time optical signal processing
[AD-A232889] N91-23909

UNIVERSITY OF SOUTHERN ILLINOIS, CARBONDALE.
Investigations of oxidation protection systems for carbon-carbon composites formed by chemical vapor deposition and plasma-assisted chemical vapor deposition techniques
[AD-A232800] N91-23269

UNIVERSITY OF SOUTHWESTERN LOUISIANA, LAFAYETTE.
Query processing for deductive databases with null values N91-23979

V

VANDERBILT UNIV., NASHVILLE, TN.
Microscopic heavy-ion theory
[DE91-010739] N91-23869

VIRGINIA POLYTECHNIC INST. AND STATE UNIV., BLACKSBURG.
The development and evaluation of an alternative powder prepregging technique for use with LaRC-TPI/graphite composites
[NASA-CR-188184] N91-23242
Thermoforming of in-situ reinforced thermoplastic composites
[AD-A232816] N91-23329
Generation of continuous liquid crystalline polymer reinforcements in thermoplastics by a novel blending process
[AD-A232824] N91-23330

VIRGINIA UNIV., CHARLOTTESVILLE.
Rapidly solidified metallic alloys with unusual semmetry properties
[AD-A232384] N91-23304
Sufficient comparison and modeling of forecasts N91-23829

VISION SCIENCES RESEARCH CORP., SAN RAMON, CA.
Quantifying improved visual performance through vision training
[AD-A232799] N91-23716

VON KARMAN INST. FOR FLUID DYNAMICS, RHODE-SAINT-GENESE (BELGIUM).
The VKI hypersonic wind tunnels and associated measurement techniques
[VKI-TM-46] N91-23196
Investigation of Roe's 2D wave decomposition models for the Euler equations
[VKI-TN-172] N91-23436
Aero-thermal investigation of a highly loaded transonic linear turbine guide vane cascade. A test case for inviscid and viscous flow computations
[VKI-TN-174] N91-23437
Two dimensional optimization of smoothing properties of multistage schemes applied to hyperbolic equations
[VKI-TN-173] N91-23807

W

WASHINGTON UNIV., SAINT LOUIS, MO.
An analytic study of general dynamic model and nonlinear feedback control of flexible robot arms N91-23497
Control of biosonar behavior by the auditory cortex
[AD-A232699] N91-23708
Degeneration of linear multivariable systems under high gain and dynamic compensation N91-23830

WASHINGTON UNIV., SEATTLE.
Thermo-viscoelastic behavior of composite materials N91-23243
Numerical simulations of instabilities in compressible mixing layers N91-23412
The annual march of convection, sea surface temperature, and surface winds in the tropics N91-23667
Observed changes in the activity of baroclinic waves and their feedbacks during the life cycles of low-frequency circulation anomalies in the Northern Hemisphere winter N91-23668
In-situ surface x ray scattering measurements of electrochemically deposited bismuth on silver (III): Structure, compressibility, and comparison with ex-situ leed measurements
[AD-A232624] N91-23880
Surface x ray scattering measurements of the substrate induced spatial modulation of an incommensurate adsorbed monolayer
[AD-A232625] N91-23959
Access and efficiency in Reagan-era information policy: A case study of the attempt to privatize the National Technical Information Service N91-23977
H II regions and young star clusters in the magellanic clouds N91-24004
Phenomenological aspects of scalar fields in astrophysics, cosmology and particle physics N91-24014
Ultraviolet gas absorption and dust extinction toward M8 and the outer galactic disk N91-24018

WATERLOO UNIV. (ONTARIO).
A Raman spectroscopic and electrochemical study of the photoinduced crystallization of triethylenediamine triiodide upon a silver electrode
[AD-A232828] N91-23963

WEIZMANN INST. OF SCIENCE, REHOVOTH (ISRAEL).
Biased galaxy formation in the neutrino scenario N91-23839

WESTINGHOUSE HANFORD CO., RICHLAND, WA.
A comparison between classical and substructuring finite-element stress analysis of a complex vacuum vessel shell
[DE91-010035] N91-23540
Use of personal computers in performing a linear modal analysis of a large finite-element model
[DE91-010112] N91-23541
Fatigue evaluation of piping systems with limited vibration test data
[DE91-007167] N91-23543
Buckling analysis of a complex vacuum vessel using the finite-element method
[DE91-010032] N91-23546

WISCONSIN UNIV., MADISON.
Mars manned fusion spaceship
[NASA-CR-188215] N91-23232
Phase equilibria and solidification of Al-Li and Al-Li-Cu alloys N91-23290
Interphase transport and multistage separations
[DE91-009627] N91-23425
Interdisciplinary research on viscoelasticity and rheology
[AD-A232700] N91-23454
Finite element based dynamical modeling of flexible open-loop manipulators with experimental results N91-23496
Assimilation of ERBE data with nonlinear programming technique to improve cloud cover diagnosis N91-23663
The integration of remote sensing, geographic information system, and expert system technologies for landcover classification N91-23733
Principal components of minus M-matrices
[AD-A232354] N91-23818
Some problems in nonlinear analysis
[AD-A232701] N91-23820
The envelopes of RV Tauri variables N91-24008
Recent star formation and the galaxy collisions in NGC 520 N91-24021
The Black Widow pulsar PSR 1957 + 20: A potential VHE gamma-ray source N91-24038

WISCONSIN UNIV., MILWAUKEE.
Interfacial characteristic measurements in horizontal bubbly two-phase flow
[DE91-009803] N91-23427

WISE OBSERVATORY, TEL AVIV (ISRAEL).
Matter in cosmic voids N91-23838

WOODS HOLE OCEANOGRAPHIC INST., MA.
Arctic remote autonomous measurement platform post CEAREX engineering report
[AD-A232843] N91-23471
Near-equatorial deep circulation in the Indian and Pacific oceans
[AD-A232635] N91-23691

WRIGHT RESEARCH DEVELOPMENT CENTER, WRIGHT-PATTERSON AFB, OH.
The handling qualities of the STOL and maneuver technology demonstrator from specification to flight test N91-23117
Turbojet potential for hypersonic flight N91-23155
Strain rate sensitivity of polymer-matrix composites under mode I delamination
[AD-A232761] N91-23268

WRIGHT STATE UNIV., DAYTON, OH.
A computer aided multivariable control systems design technique with application to aircraft flying qualities
[AD-A232549] N91-23144
Hepatic metabolism cf perfluorinated carboxylic acids: A nuclear magnetic resonance investigation
[AD-A232033] N91-23706

Y

YALE UNIV., NEW HAVEN, CT.
The application of equilibrium climate models to questions of glaciation at high latitudes N91-23669
A fast algorithm for the evaluation of trigonometric series
[AD-A232848] N91-23775
Primordial lithium, stellar evolution, and cosmology: Lithium in halo stars from standard, diffusive, and rotational stellar evolution and implications for cosmology N91-24024

YORK UNIV., DOWNSVIEW (ONTARIO).
Electrochemical parameterization of rhenium redox couples
[AD-A232043] N91-23279

YORK UNIV. (ENGLAND).
Lunar volcanism and the thermal evolution of the moon N91-24031

Typical Contract Number Index Listing

Listings in this index are arranged alphanumerically by contract number. Under each contract number the accession numbers denoting documents that have been produced as a result of research done under that contract are arranged in ascending order. The accession number denotes the number by which the citation is identified.

AERO-0003-C N91-23436
N91-23807
AF PROJ. 2301 ..... N91-23470
N91-23931
AF PROJ. 2302 ..... N91-23266
N91-23559
AF PROJ. 2304 ..... N91-23452
N91-23455
N91-23772
N91-23773
N91-23801
AF PROJ. 2305 ..... N91-23308
N91-23406
N91-23906
N91-23909
AF PROJ. 2306 ..... N91-23267
N91-23269
N91-23322
N91-23896
N91-23897
N91-23950
N91-23958
N91-23960
AF PROJ. 2307 ..... N91-23094
AF PROJ. 2308 ..... N91-23287
N91-23449
N91-23450
N91-23456
N91-23902
AF PROJ. 2312 ..... N91-23706
N91-23714
N91-23722
AF PROJ. 2313 ..... N91-23708
AF PROJ. 7231 ..... N91-23723
AF PROJ. 7601 ..... N91-23660
AF-AFOSR-0001-88 ..... N91-23449
AF-AFOSR-0047-88 ..... N91-23818
AF-AFOSR-0067-89 ..... N91-23902
AF-AFOSR-0072-88 ..... N91-23287
AF-AFOSR-0075-90 ..... N91-23452
AF-AFOSR-0081-88 ..... N91-23331
AF-AFOSR-0096-89 ..... N91-23559
AF-AFOSR-0099-88 ..... N91-23406
AF-AFOSR-0114-86 ..... N91-23470
AF-AFOSR-0116-88 ..... N91-23773
AF-AFOSR-0125-90 ..... N91-23714
AF-AFOSR-0129-87 ..... N91-23266
AF-AFOSR-0130-88 ..... N91-23269
AF-AFOSR-0148-86 ..... N91-23455
AF-AFOSR-0148-90 ..... N91-23706
AF-AFOSR-0155-88 ..... N91-23450
AF-AFOSR-0156-86 ..... N91-23931
AF-AFOSR-0177-86 ..... N91-23094
AF-AFOSR-0181-84 ..... N91-23909
AF-AFOSR-0201-89 ..... N91-23267
AF-AFOSR-0218-88 ..... N91-23772
AF-AFOSR-0248-89 ..... N91-23958
AF-AFOSR-0250-87 ..... N91-23708
AF-AFOSR-0252-89 ..... N91-23815
AF-AFOSR-0289-87 ..... N91-23322
AF-AFOSR-0305-90 ..... N91-23722
AF-AFOSR-0306-86 ..... N91-23960
AF-AFOSR-0356-87 ..... N91-23801
AF-AFOSR-0367-90 ..... N91-23308
AF-AFOSR-0381-87 ..... N91-23896
AF-AFOSR-0513-89 ..... N91-23950
AF-AFOSR-0534-89 ..... N91-23897
AF-AFOSR-0541-89 ..... N91-23456
AF-AFOSR-0542-89 ..... N91-23906
ARPA ORDER 4395 ..... N91-23878
A86/K/012 ..... N91-23358
A88/M/318 ..... N91-23703
BMFT-07KF2112-1 ..... N91-23648
DA PROJ. 1C1-62622-A-553 ..... N91-23288
DA PROJ. 1L1-61101-AH-45 ..... N91-23439
DA PROJ. 1L1-61102-AH-45 ..... N91-23179
DA PROJ. 1L1-62105-AH-84 ..... N91-23263
DA PROJ. 1L1-62211-A-47-A N91-23500
N91-23513
DA PROJ. 1L1-62211-37-A N91-23514
DA PROJ. 1L1-62601-AH-91 ..... N91-23342
DA PROJ. 1L1-62618-AH-80 ..... N91-23265
N91-23518
N91-23930
DA PROJ. 3E1-62787-A-878 ..... N91-23100
DA PROJ. 4A1-62731-AT-41 ..... N91-23227
DA PROJ. 4A7-62730-AT-42 ..... N91-23280
DAAG29-84-K-0061 ..... N91-23787
DAAG29-84-9-0027 ..... N91-23787
DAAG29-85-K-0177 ..... N91-23765
N91-23993
DAAJ02-87-C-0015 ..... N91-23146
DAAL03-86-D-0001 ..... N91-23288
N91-23713
DAAL03-86-K-0050 ..... N91-23324
DAAL03-86-K-0076 ..... N91-23519
DAAL03-87-K-0001 ..... N91-23819
DAAL03-87-K-0034 ..... N91-23712
DAAL03-87-K-0036 ..... N91-23454
DAAL03-87-K-0039 ..... N91-23284
DAAL03-87-K-0043 ..... N91-23820
DAAL03-87-K-0057 ..... N91-23304
DAAL03-87-K-0089 ..... N91-23766
DAAL03-87-K-0101 ..... N91-23827
DAAL03-87-K-0104 ..... N91-23403
DAAL03-88-C-0023 ..... N91-23399
DAAL03-88-K-0076 ..... N91-23817
DAAL03-88-K-0087 ..... N91-23992
DAAL03-88-K-0104 ..... N91-23329
N91-23330
DAAL03-89-K-0156 ..... N91-23814
DAAL03-89-K-0161 ..... N91-23484
DAAL03-89-K-0173 ..... N91-23881
DAAL03-90-C-0014 ..... N91-23448
DARPA ORDER 6140 ..... N91-23961
DARPA ORDER 6325 ..... N91-23481
DE-AC02-76CH-00016 ..... N91-23476
N91-23626
N91-23886
N91-23940
DE-AC02-83CH-10093 ..... N91-23618
DE-AC02-89CH-10408 ..... N91-23383
DE-AC02-89ER-40486 ..... N91-23391
N91-23547
DE-AC03-76SF-00098 ..... N91-23300
N91-23384
N91-23464
N91-23698
N91-23737
N91-23741
N91-23856
N91-23882
N91-23935
DE-AC03-87SF-17170 ..... N91-23299
DE-AC03-89ER-52153 ..... N91-23923
DE-AC03-89ER-53277 ..... N91-23922
DE-AC04-76DP-00789 ..... N91-23085
N91-23245
N91-23294
N91-23314
N91-23349
N91-23352
N91-23382
N91-23386
N91-23388
N91-23389
N91-23431
N91-23432
N91-23477
N91-23507
N91-23526
N91-23536
N91-23537
N91-23619
N91-23885
N91-23892
N91-23919
N91-23939
N91-23941
DE-AC04-88DP-43495 ..... N91-23274
N91-23498
DE-AC05-84OR-21400 ..... N91-23292
N91-23295
N91-23298
N91-23310
N91-23316
N91-23318
N91-23353
N91-23381
N91-23505
N91-23508
N91-23509
N91-23511
N91-23535
N91-23539
N91-23544
N91-23545
N91-23625
N91-23735
N91-23785
N91-23805
N91-23857
N91-23859
N91-23864
N91-23873
N91-23883
N91-23893
N91-23913
N91-23914
N91-23915
N91-23916
N91-23917
N91-24036
DE-AC05-84OT-21400 ..... N91-23985
N91-23987
DE-AC06-76RL-01830 ..... N91-23313
DE-AC06-83ER-40129 ..... N91-23476
DE-AC06-87RL-10930 ..... N91-23540
N91-23541
N91-23543
N91-23546
DE-AC07-76ID-01570 ..... N91-23317
N91-23415
N91-23510
N91-23674
N91-23736
N91-23884
DE-AC08-88NV-10617 ..... N91-23631
N91-23894
DE-AC12-76SN-00052 ..... N91-23867
DE-AC22-87PC-90274 ..... N91-23911
DE-AC22-88PC-88947 ..... N91-23339
DE-AI05-87OR-21749 ..... N91-23311
DE-BI79-85BP-24332 ..... N91-23387
DE-FG01-89IE-10763 ..... N91-23627
DE-FG02-84ER-13291 ..... N91-23425
DE-FG02-84ER-40153 ..... N91-23872
DE-FG02-86ER-13508 ..... N91-23276
DE-FG02-86ER-53223 ..... N91-23924
DE-FG02-87ER-13764 ..... N91-23427
DE-FG02-87ER-40371 ..... N91-23868
DE-FG02-87ER-45315 ..... N91-23293
DE-FG02-88ER-40479 ..... N91-23863
DE-FG02-89ER-14042 ..... N91-23499
DE-FG02-89ER-45388 ..... N91-23297
DE-FG02-90ER-40560 ..... N91-24015
DE-FG02-91ER-54109 ..... N91-23920

DE-FG03-86ER-53225 ..... N91-23918
DE-FG03-88ER-60673 ..... N91-23695
DE-FG03-90ER-60997 ..... N91-23696
DE-FG05-84ER-13262 ..... N91-23870
DE-FG05-84ER-40162 ..... N91-23871
DE-FG05-86ER-40272 ..... N91-24015
DE-FG05-87ER-40376 ..... N91-23869
DE-FG05-88ER-53266 ..... N91-23912
N91-23918
DE-FG05-88ER-53267 ..... N91-23918
DE-FG07-87ID-12693 ..... N91-23999
DE-FG22-84PC-71257 ..... N91-23334
DE-FG22-88PC-88913 ..... N91-23424
DE-FG22-88PC-88928 ..... N91-23911
DE-FG22-89PC-89786 ..... N91-23334
DE-FG22-90PC-90293 ..... N91-23275
DFG-EM-29/2-2 ..... N91-23552
DTCG23-88-C-20037 ..... N91-23557
DTFA01-80-Y-10524 ..... N91-23675
DTFA01-87-C-00014 ..... N91-23134
DTFA03-89-C-00061 ..... N91-23097
EPA-68-C8-0006 ..... N91-23625
EPA-68-02-3889 ..... N91-23625
EPA-68-02-3994 ..... N91-23625
EPA-68-03-3246 ..... N91-23625
EPA-68-03-3249 ..... N91-23625
ESA-7627/88/NL/DG N91-23591
F19628-86-C-0118 ..... N91-23659
F19628-88-K-0042 ..... N91-23635
F19628-89-C-0112 ..... N91-23655
F30602-85-C-0274 ..... N91-23369
N91-23370
N91-23371
F30602-88-D-0026 ..... N91-23901
F30602-88-D-0027 ..... N91-23365
F30602-88-D-0028 ..... N91-23485
F33615-83-C-3603 ..... N91-23120
F33615-87-C-3615 ..... N91-23144
F33615-87-D-0650 ..... N91-23459
F33615-88-C-0541 ..... N91-23289
F33615-88-C-2908 ..... N91-23093
F33615-88-C-5437 ..... N91-23307
F33657-87-C-2214 ..... N91-23173
F49620-85-C-0144 ..... N91-23826
F49620-85-K-0018 ..... N91-23787
F49620-86-C-0090 ..... N91-23453
F49620-87-C-0043 ..... N91-23904
F49620-87-C-0056 ..... N91-23907
F49620-87-C-0093 ..... N91-23327
F49620-87-C-0104 ..... N91-23961
F49620-88-C-0042 ..... N91-23903
F49620-88-K-0003 ..... N91-23286
F49620-88-K-0008 ..... N91-23715
F49620-89-C-0108 ..... N91-23957
F49620-90-C-0020 ..... N91-23798
F49620-90-C-0048 ..... N91-23336
F49620-90-C-0056 ..... N91-23905
F49620-90-C-0063 ..... N91-23716
GRI-5086-293-1663 ..... N91-23272
GRI-5087-233-1461 ..... N91-23338
GRI-5087-233-1616 ..... N91-23964
GRI-5087-298-1508 ..... N91-23332
MDA905-89-C-0014 ..... N91-23707
MIPR-F04611-87-X-0059 ..... N91-23335
MIPR-F04611-88-C-0067 ..... N91-23335
MIPR-F04611-90-X-0057 ..... N91-23236
MIPR-133-90 ..... N91-23235
NAGW-925 ..... N91-23786
N91-23821
NAGW-1340 ..... N91-24015
N91-24016
NAG1-343 ..... N91-23242
NAG1-613 ..... N91-23738
N91-23739
NAG1-1114 ..... N91-23970
N91-23974
NAG1-1122 ..... N91-23181
NAG1-1154 ..... N91-23974
NAG2-588 ..... N91-23084
NAG2-646 ..... N91-23084
NAG3-875 ..... N91-23440
NAG3-1011 ..... N91-23181
NAG3-1047 ..... N91-23514
NAG3-1200 ..... N91-23232
NAG5-1017 ..... N91-24082
NAG5-1045 ..... N91-23787
NAG8-654 ..... N91-23670
NASA ORDER C-99066-G N91-23416
NAS1-17806 ..... N91-23887
NAS1-18015 ..... N91-23080
N91-23081
NAS1-18605 ..... N91-23433
N91-23434
NAS2-12898 ..... N91-23458
NAS2-13070 ..... N91-23136
NAS3-22238 ..... N91-23233
NAS3-23356 ..... N91-23346
NAS3-23720 ..... N91-23849
N91-23850
N91-23851
N91-23852
NAS3-25092 ..... N91-24030
NAS3-25266 ..... N91-23205
N91-23548
N91-23550
N91-23620
NAS3-25967 ..... N91-23185
NAS5-30357 ..... N91-23408
NAS5-30546 ..... N91-23206
N91-23211
NAS5-30702 ..... N91-23212
NAS7-918 ..... N91-23662
N91-23783
N91-23890
NAS7-1037 ..... N91-23891
NAS8-37857 ..... N91-23200
NAS8-38138 ..... N91-23229
NAS10-11624 ..... N91-23718
NA85AA-D-SG141 ..... N91-23624
NCC2-604 ..... N91-23195
NCC2-621 ..... N91-23776
NCC9-16 ..... N91-23731
NFR-G-GU-1705-311 ..... N91-23679
NIH-NS-10939-11 ..... N91-23787
NR PROJ. RR0-4206 ..... N91-23800
NSF CCR-88-20279 ..... N91-23561
N91-23562
N91-23616
NSF DMC-85-17315 ..... N91-23787
NSF DMR-86-08305 ..... N91-23843
NSF DMS-80-07030 ..... N91-23818
NSF DMS-87-01971 ..... N91-23818
NSF DMS-89-01445 ..... N91-23818
NSF DMS-90-12751 ..... N91-23775
NSF ECS-85-07405 ..... N91-23806
N91-23821
NSF INT-85-14199 ..... N91-23787
NSF IRI-84-10413 ..... N91-23787
NSF IRI-89-07122 ..... N91-23993
NSF MCS-81-19196 ..... N91-23787
NSF MIP-86-04893 ..... N91-23738
N00014-84-G-0201 ..... N91-23279
N00014-84-K-0099 ..... N91-23401
N00014-85-K-0124 ..... N91-23732
N00014-85-K-0474 ..... N91-23282
N91-23323
N00014-85-K-0807 ..... N91-23787
N00014-86-C-0126 ..... N91-23471
N00014-86-K-0133 ..... N91-23326
N00014-86-K-0395 ..... N91-23800
N00014-87-J-1118 ..... N91-23963
N00014-87-K-0001 ..... N91-23691
N00014-87-K-0196 ..... N91-23451
N00014-87-K-0303 ..... N91-23480
N00014-87-K-0336 ..... N91-23368
N00014-88-C-0483 ..... N91-23481
N00014-88-C-0512 ..... N91-23951
N00014-88-K-0341 ..... N91-23955
N00014-88-K-0404 ..... N91-23446
N00014-88-K-2005 ..... N91-23483
N00014-89-C-2222 ..... N91-23952
N00014-89-J-1030 ..... N91-23815
N00014-89-J-1076 ..... N91-23691
N00014-89-J-1545 ..... N91-23956
N00014-89-J-1588 ..... N91-23264
N00014-89-J-1848 ..... N91-23328
N00014-89-J-1975 ..... N91-23763
N00014-89-J-1988 ..... N91-23770
N91-23774
N00014-89-J-3167 ..... N91-23953
N00014-89-K-1007 ..... N91-23402
N00014-90-C-0182 ..... N91-23699
N00014-90-J-1030 ..... N91-23560
N91-23561
N91-23562
N91-23816
N00014-90-J-1178 ..... N91-23281
N91-23900
N91-23954
N00014-90-J-1263 ..... N91-23285
N91-23303
N91-23879
N91-23680
N91-23959
N00014-90-J-1516 ..... N91-23489
N00014-90-J-1871 ..... N91-23558
N00014-90-J-4083 ..... N91-23447
STU-79-6159 ..... N91-23321
W-31-109-ENG-38 ..... N91-23277
N91-23312
N91-23390
N91-23414
N91-23520
N91-23534
N91-23538
N91-23542
N91-23743
N91-23745
N91-23861
N91-23862
N91-23866
N91-23945
W-7405-ENG-36 ..... N91-23296
N91-23315
N91-23350
N91-23351
N91-23428
N91-23630
N91-23695
N91-23697
N91-23740
N91-23742
N91-23784
N91-23855
N91-23942
N91-23943
N91-23944
W-7405-ENG-48 ..... N91-23265
N91-23291
N91-23333
N91-23426
N91-23429
N91-23430
N91-23463
N91-23465
N91-23466
N91-23478
N91-23479
N91-23527
N91-23628
N91-23631
N91-23632
N91-23692
N91-23744
N91-23858
N91-23860
N91-23865
N91-23986
N91-24013
N91-24015
N91-24027
N91-24028
W-7405-ENG-82 ..... N91-23693
199-14-12-04 ..... N91-23704
307-51-00 ..... N91-23501
316-30-19 ..... N91-23347
N91-24030
326-81-10 ..... N91-23620
505-05-10 ..... N91-23186
505-62-12 ..... N91-23083
505-62-21 ..... N91-23416
505-62-50 ..... N91-23946
505-62-52 ..... N91-23089
N91-23179
N91-23409
505-63-1B N91-23512
505-63-1M N91-23311
505-63-5A N91-23439
505-63-5B N91-23515
N91-23550
505-63-01-05 ..... N91-23244
505-63-36 ..... N91-23500
N91-23513
505-63-50 ..... N91-23135
505-63-51 ..... N91-23514
505-67-21 ..... N91-23099
505-68-10 ..... N91-23086
N91-23087
505-68-11 ..... N91-23183
N91-23184
505-90-52-01 ..... N91-23433
N91-23434
506-41-11 ..... N91-23616
506-41-21 ..... N91-23233
506-42-31 ..... N91-23205
506-49-11-01 ..... N91-23080
N91-23081
510-01-0A N91-23548
510-01-01 ..... N91-23521
510-10-01 ..... N91-23247
532-06-37 ..... N91-23136
533-02-51 ..... N91-23133
535-03-01 ..... N91-23849
N91-23850
N91-23851
N91-23852
537-02-00 ..... N91-23098
537-02-20 ..... N91-23181

537-02-21 ..... N91-23185
549-03-61 ..... N91-23341
582-01-11 ..... N91-23340
590-13-11 ..... N91-23234
591-42-00 ..... N91-23207
650-60-20 ..... N91-23354
674-23-08-17 ..... N91-24057
676-59-44 ..... N91-23229
679-40-00 ..... N91-23102
763-01-41 ..... N91-23549
871-00-00-04 ..... N91-23887

Typical Report Number Index Listing

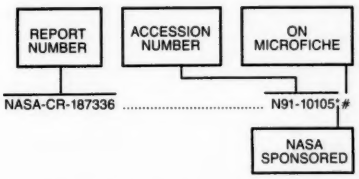

Listings in this index are arranged alphanumerically by report number. The accession number denotes the number by which the citation is identified. An asterisk (*) indicates that the item is a NASA report. A pound sign (#) indicates that the item is available on microfiche.

A-90184 ..... N91-23099* #
A-90250 ..... N91-23207* #
A-91093-VOL-1 ..... N91-23341* #
A-91096 ..... N91-23704* #

AAMRL-SR-90-510 ..... N91-23723 #

AAMRL-TR-90-039-PHASE-1 ..... N91-23289 #

AD-A230883 ..... N91-23782 #
AD-A231164 ..... N91-23610 #
AD-A231246 ..... N91-23489 #
AD-A231329 ..... N91-23459 #
AD-A231389 ..... N91-23289 #
AD-A231404 ..... N91-23732 #
AD-A231572 ..... N91-23717 #
AD-A231634 ..... N91-23622 #
AD-A231658 ..... N91-23079 #
AD-A231936 ..... N91-23635 #
AD-A232013 ..... N91-23225 #
AD-A232014 ..... N91-23760 #
AD-A232015 ..... N91-23761 #
AD-A232016 ..... N91-23226 #
AD-A232019 ..... N91-23762 #
AD-A232020 ..... N91-23342 #
AD-A232023 ..... N91-23554 #
AD-A232024 ..... N91-23141 #
AD-A232028 ..... N91-23763 #
AD-A232031 ..... N91-23235 #
AD-A232032 ..... N91-23764 #
AD-A232033 ..... N91-23706 #
AD-A232034 ..... N91-23322 #
AD-A232035 ..... N91-23950 #
AD-A232036 ..... N91-23896 #
AD-A232037 ..... N91-23897 #
AD-A232043 ..... N91-23279 #
AD-A232053 ..... N91-23555 #
AD-A232055 ..... N91-23145 #
AD-A232058 ..... N91-23142 #
AD-A232063 ..... N91-23398 #
AD-A232064 ..... N91-23765 #
AD-A232065 ..... N91-23992 #
AD-A232074 ..... N91-23951 #
AD-A232088 ..... N91-23399 #
AD-A232089 ..... N91-23766 #
AD-A232090 ..... N91-23993 #
AD-A232091 ..... N91-23400 #
AD-A232092 ..... N91-23767 #
AD-A232093 ..... N91-23768 #
AD-A232096 ..... N91-23968 #
AD-A232097 ..... N91-23227 #
AD-A232098 ..... N91-23263 #
AD-A232100 ..... N91-23898 #
AD-A232101 ..... N91-23445 #
AD-A232106 ..... N91-23681 #
AD-A232107 ..... N91-23480 #
AD-A232108 ..... N91-23699 #
AD-A232112 ..... N91-23728 #
AD-A232113 ..... N91-23994 #
AD-A232114 ..... N91-23729 #
AD-A232117 ..... N91-23899 #
AD-A232120 ..... N91-23952 #
AD-A232121 ..... N91-23826 #
AD-A232122 ..... N91-23481 #
AD-A232123 ..... N91-23655 #
AD-A232124 ..... N91-23228 #
AD-A232125 ..... N91-23365 #
AD-A232126 ..... N91-23146 #
AD-A232129 ..... N91-23446 #
AD-A232132 ..... N91-23366 #
AD-A232133 ..... N91-23280 #
AD-A232135 ..... N91-23953 #
AD-A232137 ..... N91-23447 #
AD-A232138 ..... N91-23264 #
AD-A232140 ..... N91-23814 #
AD-A232148 ..... N91-23367 #
AD-A232150 ..... N91-23281 #
AD-A232152 ..... N91-23954 #
AD-A232153 ..... N91-23900 #
AD-A232154 ..... N91-23282 #
AD-A232155 ..... N91-23323 #
AD-A232158 ..... N91-23448 #
AD-A232160 ..... N91-23955 #
AD-A232162 ..... N91-23368 #
AD-A232221 ..... N91-23707 #
AD-A232222 ..... N91-23656 #
AD-A232223 ..... N91-23847 #
AD-A232224 ..... N91-23517 #
AD-A232227 ..... N91-23518 #
AD-A232230 ..... N91-23343 #
AD-A232236 ..... N91-23283 #
AD-A232237 ..... N91-23449 #
AD-A232238 ..... N91-23265 #
AD-A232240 ..... N91-23482 #
AD-A232245 ..... N91-23815 #
AD-A232246 ..... N91-23816 #
AD-A232247 ..... N91-23769 #
AD-A232248 ..... N91-23689 #
AD-A232286 ..... N91-23401 #
AD-A232287 ..... N91-23770 #
AD-A232289 ..... N91-23369 #
AD-A232290 ..... N91-23370 #
AD-A232291 ..... N91-23371 #
AD-A232331 ..... N91-23402 #
AD-A232332 ..... N91-23483 #
AD-A232334 ..... N91-23817 #
AD-A232335 ..... N91-23484 #
AD-A232336 ..... N91-23403 #
AD-A232342 ..... N91-23284 #
AD-A232345 ..... N91-23303 #
AD-A232352 ..... N91-23372 #
AD-A232353 ..... N91-23797 #
AD-A232354 ..... N91-23818 #
AD-A232356 ..... N91-23324 #
AD-A232368 ..... N91-23956 #
AD-A232370 ..... N91-23781 #
AD-A232371 ..... N91-23373 #
AD-A232372 ..... N91-23657 #
AD-A232377 ..... N91-23193 #
AD-A232379 ..... N91-23957 #
AD-A232384 ..... N91-23304 #
AD-A232389 ..... N91-23712 #
AD-A232393 ..... N91-23335 #
AD-A232405 ..... N91-23093 #
AD-A232407 ..... N91-23878 #
AD-A232411 ..... N91-23485 #
AD-A232419 ..... N91-23958 #
AD-A232420 ..... N91-23690 #
AD-A232421 ..... N91-23374 #
AD-A232422 ..... N91-23143 #
AD-A232425 ..... N91-23682 #
AD-A232446 ..... N91-23519 #
AD-A232448 ..... N91-23819 #
AD-A232452 ..... N91-23879 #
AD-A232458 ..... N91-24000 #
AD-A232465 ..... N91-23404 #
AD-A232466 ..... N91-23375 #
AD-A232467 ..... N91-23376 #
AD-A232468 ..... N91-23658 #
AD-A232473 ..... N91-23305 #
AD-A232483 ..... N91-23995 #
AD-A232484 ..... N91-23996 #
AD-A232485 ..... N91-23997 #
AD-A232497 ..... N91-23469 #
AD-A232498 ..... N91-23930 #
AD-A232503 ..... N91-23659 #
AD-A232523 ..... N91-23325 #
AD-A232526 ..... N91-23713 #
AD-A232544 ..... N91-23306 #
AD-A232546 ..... N91-23556 #
AD-A232549 ..... N91-23144 #
AD-A232550 ..... N91-23307 #
AD-A232552 ..... N91-23901 #
AD-A232553 ..... N91-23236 #
AD-A232554 ..... N91-23730 #
AD-A232555 ..... N91-23771 #
AD-A232560 ..... N91-23557 #
AD-A232605 ..... N91-23772 #
AD-A232609 ..... N91-23902 #
AD-A232610 ..... N91-23450 #
AD-A232623 ..... N91-23285 #
AD-A232624 ..... N91-23880 #
AD-A232625 ..... N91-23959 #
AD-A232628 ..... N91-23558 #
AD-A232631 ..... N91-23344 #
AD-A232632 ..... N91-23405 #
AD-A232633 ..... N91-23486 #
AD-A232634 ..... N91-23827 #
AD-A232635 ..... N91-23691 #
AD-A232641 ..... N91-23286 #
AD-A232642 ..... N91-23336 #
AD-A232644 ..... N91-23773 #
AD-A232649 ..... N91-23888 #
AD-A232650 ..... N91-23451 #
AD-A232653 ..... N91-23720 #
AD-A232654 ..... N91-23452 #
AD-A232657 ..... N91-23798 #
AD-A232658 ..... N91-23266 #
AD-A232659 ..... N91-23903 #
AD-A232660 ..... N91-23076 #
AD-A232661 ..... N91-23077 #
AD-A232662 ..... N91-23326 #
AD-A232668 ..... N91-23106 #
AD-A232671 ..... N91-23198 #
AD-A232686 ..... N91-23327 #
AD-A232688 ..... N91-23931 #
AD-A232690 ..... N91-23487 #
AD-A232692 ..... N91-23453 #
AD-A232693 ..... N91-23799 #
AD-A232695 ..... N91-23960 #
AD-A232696 ..... N91-23328 #
AD-A232697 ..... N91-23559 #
AD-A232698 ..... N91-23714 #
AD-A232699 ..... N91-23708 #
AD-A232700 ..... N91-23454 #
AD-A232701 ..... N91-23820 #
AD-A232703 ..... N91-23904 #
AD-A232713 ..... N91-23377 #
AD-A232714 ..... N91-23094 #
AD-A232716 ..... N91-23683 #
AD-A232721 ..... N91-23721 #
AD-A232723 ..... N91-23100 #
AD-A232724 ..... N91-23378 #
AD-A232732 ..... N91-23709 #
AD-A232733 ..... N91-23379 #
AD-A232734 ..... N91-23715 #
AD-A232737 ..... N91-23267 #
AD-A232747 ..... N91-23961 #
AD-A232754 ..... N91-23560 #
AD-A232755 ..... N91-23561 #
AD-A232756 ..... N91-23562 #
AD-A232761 ..... N91-23268 #
AD-A232767 ..... N91-23905 #
AD-A232768 ..... N91-23906 #
AD-A232769 ..... N91-23308 #
AD-A232771 ..... N91-23907 #
AD-A232776 ..... N91-23684 #
AD-A232779 ..... N91-23406 #
AD-A232780 ..... N91-23800 #
AD-A232786 ..... N91-23455 #
AD-A232787 ..... N91-23722 #
AD-A232794 ..... N91-23456 #
AD-A232799 ..... N91-23716 #
AD-A232800 ..... N91-23269 #
AD-A232801 ..... N91-23881 #
AD-A232805 ..... N91-23801 #
AD-A232810 ..... N91-23802 #

AD-A232813 ..... N91-23685 #
AD-A232814 ..... N91-23723 #
AD-A232816 ..... N91-23329 #
AD-A232819 ..... N91-23962 #
AD-A232820 ..... N91-23287 #
AD-A232822 ..... N91-23803 #
AD-A232824 ..... N91-23330 #
AD-A232828 ..... N91-23963 #
AD-A232829 ..... N91-23774 #
AD-A232831 ..... N91-23686 #
AD-A232837 ..... N91-23331 #
AD-A232839 ..... N91-23470 #
AD-A232843 ..... N91-23471 #
AD-A232845 ..... N91-23660 #
AD-A232848 ..... N91-23775 #
AD-A232852 ..... N91-23908 #
AD-A232853 ..... N91-23661 #
AD-A232871 ..... N91-23199 #
AD-A232876 ..... N91-23457 #
AD-A232880 ..... N91-23288 #
AD-A232888 ..... N91-23633 #
AD-A232889 ..... N91-23909 #
AD-A233633 ..... N91-23395 #

AD-E501354 ..... N91-24000 #
AD-E501359 ..... N91-23076 #
AD-E501360 ..... N91-23077 #
AD-E951609 ..... N91-23899 #
AD-E951621 ..... N91-23193 #

AEDC-TR-90-20 ..... N91-23908 #
AEDC-TR-90-21 ..... N91-23445 #
AEDC-TR-90-28 ..... N91-23235 #

AERONOMICA-ACTA-A-357-1990 ..... N91-23925
AERONOMICA-ACTA-A-358-1991 ..... N91-23647

AFIT/CI/CIA-90-032D ..... N91-23729 #
AFIT/CI/CIA-90-035D ..... N91-23657 #
AFIT/CI/CIA-90-037D ..... N91-23482 #
AFIT/CI/CIA-90-038D ..... N91-23682 #
AFIT/CI/CIA-90-039D ..... N91-23373 #
AFIT/CI/CIA-90-127 ..... N91-23555 #
AFIT/CI/CIA-90-146 ..... N91-23622 #

AFOSR-90-0148TR ..... N91-23452 #
AFOSR-90-0855TR ..... N91-23826 #
AFOSR-91-0005TR ..... N91-23957 #
AFOSR-91-0019TR ..... N91-23950 #
AFOSR-91-0020TR ..... N91-23322 #
AFOSR-91-0021TR ..... N91-23706 #
AFOSR-91-0022TR ..... N91-23896 #
AFOSR-91-0023TR ..... N91-23897 #
AFOSR-91-0033TR ..... N91-23449 #
AFOSR-91-0046TR ..... N91-23907 #
AFOSR-91-0048TR ..... N91-23453 #
AFOSR-91-0049TR ..... N91-23904 #
AFOSR-91-0050TR ..... N91-23961 #
AFOSR-91-0053TR ..... N91-23715 #
AFOSR-91-0054TR ..... N91-23286 #
AFOSR-91-0055TR ..... N91-23327 #
AFOSR-91-0059TR ..... N91-23336 #
AFOSR-91-0064TR ..... N91-23722 #
AFOSR-91-0110TR ..... N91-23714 #
AFOSR-91-0111TR ..... N91-23456 #
AFOSR-91-0113TR ..... N91-23958 #
AFOSR-91-0116TR ..... N91-23559 #
AFOSR-91-0120TR ..... N91-23267 #
AFOSR-91-0121TR ..... N91-23906 #
AFOSR-91-0122TR ..... N91-23269 #
AFOSR-91-0123TR ..... N91-23931 #
AFOSR-91-0125TR ..... N91-23798 #
AFOSR-91-0139TR ..... N91-23094 #
AFOSR-91-0142TR ..... N91-23308 #
AFOSR-91-0145TR ..... N91-23708 #
AFOSR-91-0147TR ..... N91-23772 #
AFOSR-91-0149TR ..... N91-23773 #
AFOSR-91-0151TR ..... N91-23960 #
AFOSR-91-0152TR ..... N91-23266 #
AFOSR-91-0155TR ..... N91-23801 #
AFOSR-91-0160TR ..... N91-23470 #
AFOSR-91-0161TR ..... N91-23406 #
AFOSR-91-0168TR ..... N91-23909 #
AFOSR-91-0169TR ..... N91-23287 #
AFOSR-91-0174TR ..... N91-23331 #
AFOSR-91-0188TR ..... N91-23716 #
AFOSR-91-0195TR ..... N91-23450 #
AFOSR-91-0196TR ..... N91-23455 #

AFRRI-SR90-25 ..... N91-23283 #
AFRRI-SR90-26 ..... N91-23283 #
AFRRI-SR90-27 ..... N91-23283 #
AFRRI-SR90-30 ..... N91-23283 #
AFRRI-SR90-31 ..... N91-23283 #
AFRRI-SR90-32 ..... N91-23283 #
AFRRI-SR90-33 ..... N91-23283 #
AFRRI-SR90-34 ..... N91-23283 #
AFRRI-SR90-35 ..... N91-23283 #

AGARD-AG-308-ADD ..... N91-23711 #

AGARD-CP-479 ..... N91-23147 #
AGARD-CP-508 ..... N91-23108 #

AGARD-HIGHLIGHTS-91/1 ..... N91-24084 #

AGS/AD-91-1 ..... N91-23886 #

AI-M-1238 ..... N91-23732 #

AIAA-90-0098 ..... N91-23158 #
AIAA-91-2460 ..... N91-23185* #

AL-TR-89-055 ..... N91-23335 #

AMSMI/TR-RD-GC-90-10 ..... N91-23193 #

AMSMI/TR-RD-RE-90-6 ..... N91-23899 #

ANL-HEP-CP-91-03 ..... N91-23862 #

ANL-90/38 ..... N91-23538 #
ANL-90/46 ..... N91-23414 #

ANL/CP-71063 ..... N91-23945 #
ANL/CP-72112 ..... N91-23390 #
ANL/CP-72318 ..... N91-23277 #
ANL/CP-72530 ..... N91-23312 #
ANL/CP-72633 ..... N91-23866 #
ANL/CP-72651 ..... N91-23745 #

ANL/PP-67244 ..... N91-23861 #

ARFSD-TR-90024 ..... N91-23898 #

ARI-RN-91-29 ..... N91-23713 #

ARL-MAT-TM-403 ..... N91-23306 #

ARO-22648.19-EL ..... N91-23765 #
ARO-22648.20-EL ..... N91-23993 #
ARO-23396.16-CH ..... N91-23324 #
ARO-23525.41-EG ..... N91-23519 #
ARO-23669.29-MA ..... N91-23819 #
ARO-23932.16-MA ..... N91-23454 #
ARO-24092.15-MA ..... N91-23820 #
ARO-24111.10-LS ..... N91-23712 #
ARO-24122.15-MS ..... N91-23304 #
ARO-24417.18-EL ..... N91-23403 #
ARO-24653.20-MA ..... N91-23827 #
ARO-24693.2-EG ..... N91-23284 #
ARO-24834.4-MA ..... N91-23817 #
ARO-25021.5-PH ..... N91-23766 #
ARO-25344.9-MS ..... N91-23329 #
ARO-25344.10-MS ..... N91-23330 #
ARO-25870.29-MA ..... N91-23992 #
ARO-26207.1-EL-SBI ..... N91-23399 #
ARO-26364.2-EL ..... N91-23814 #
ARO-27529.1-CH ..... N91-23484 #
ARO-27577.1-CH ..... N91-23881 #
ARO-27961.1-EG-SBI ..... N91-23448 #
ARO-28121.1-EG-SDI ..... N91-23235 #

AVSCOM-TR-90-C-012 ..... N91-23179* #
AVSCOM-TR-90-C-024 ..... N91-23514* #
AVSCOM-TR-90-C-031 ..... N91-23439* #
AVSCOM-TR-90-C-033 ..... N91-23513* #
AVSCOM-TR-90-D-24 ..... N91-23146 #
AVSCOM-TR-91-C-015 ..... N91-23500* #

BN-1112 ..... N91-23815 #
BN-1115 ..... N91-23816 #
BN-1116 ..... N91-23562 #
BN-1117 ..... N91-23561 #
BN-1118 ..... N91-23560 #

BNL-45802 ..... N91-23476 #
BNL-45806 ..... N91-23940 #
BNL-45879 ..... N91-23626 #
BNL-45935 ..... N91-23886 #

BONN-IR-90-53 ..... N91-23654 #

BRL-CR-651 ..... N91-23265 #

BRL-MR-3885 ..... N91-23518 #

BRL-TR-3191 ..... N91-23342 #
BRL-TR-3195 ..... N91-23469 #
BRL-TR-3196 ..... N91-23930 #
BRL-TR-3207 ..... N91-23457 #
BR115906 ..... N91-23753 #
BR116237 ..... N91-23845 #
BR116334 ..... N91-23364 #
BR116433 ..... N91-23949 #
BR116434 ..... N91-23395 #
BR116507 ..... N91-23811 #
BR116535 ..... N91-23394 #
BR116612 ..... N91-23846 #

C-6734-006 ..... N91-23459 #

CA-1/90 ..... N91-23223 #
CA-2/90 ..... N91-23218 #
CA-3/90 ..... N91-23615 #
CA-4/90 ..... N91-23220 #
CA-5/90 ..... N91-23468 #
CA-7/90 ..... N91-23221 #
CA-10/90 ..... N91-23222 #

CCMS-91-08 ..... N91-23242* #

CEMA-86-17 ..... N91-23967 #
CEMA-86/11 ..... N91-23828 #
CEMA-86/17 ..... N91-23621 #

CERL-ADP-P-91/05 ..... N91-23769 #
CERL-ADP-P-91/12 ..... N91-23762 #
CERL-ADP-P-91/14 ..... N91-23968 #

CERL-TR-M-91/14 ..... N91-23227 #

CESAR-90/54 ..... N91-23511 #
CESAR-91/03 ..... N91-23505 #

CMOTT-91-01 ..... N91-23416* #

CMS-TSR-91-5 ..... N91-23818 #

CMU-CS-90-195 ..... N91-23763 #

CMU-RI-TR-90-28 ..... N91-23803 #
CMU-RI-TR-90-29 ..... N91-23802 #
CMU-RI-TR-90-34 ..... N91-23633 #

CONF-900402-13 ..... N91-23626 #
CONF-900610-2 ..... N91-23539* #
CONF-900749-1 ..... N91-23911 #
CONF-900756-60 ..... N91-23894 #
CONF-901047-2 ..... N91-23941 #
CONF-901125-11 ..... N91-23942 #
CONF-901273-3 ..... N91-23313 #
CONF-910123-18 ..... N91-23477 #
CONF-910123-22 ..... N91-23476 #
CONF-910145-3 ..... N91-23296 #
CONF-910188-1 ..... N91-23499 #
CONF-910190-2 ..... N91-23943 #
CONF-910195-1-EXC ..... N91-23886 #
CONF-910212-4 ..... N91-23945 #
CONF-910298-1 ..... N91-23940 #
CONF-910299-1 ..... N91-23274 #
CONF-910322-1 ..... N91-23944 #
CONF-910378-1 ..... N91-24036 #
CONF-910414-28 ..... N91-23736 #
CONF-910414-29 ..... N91-23415 #
CONF-910414-33 ..... N91-23867 #
CONF-910425-1 ..... N91-23619 #
CONF-910530-1 ..... N91-23628 #
CONF-910552-9 ..... N91-23390 #
CONF-910595-7 ..... N91-23479 #
CONF-910595-8 ..... N91-23478 #
CONF-910601-2 ..... N91-23316 #
CONF-910602-2 ..... N91-23542 #
CONF-910602-4 ..... N91-23534 #
CONF-910602-6 ..... N91-23543 #
CONF-910602-14 ..... N91-23509 #
CONF-910602-15 ..... N91-23545 #
CONF-910602-16 ..... N91-23544 #
CONF-910602-18 ..... N91-23540 #
CONF-910602-20 ..... N91-23546 #
CONF-910602-23 ..... N91-23541 #
CONF-910603-7 ..... N91-23785 #
CONF-910603-8 ..... N91-23883 #
CONF-910609-2 ..... N91-23916 #
CONF-910609-3 ..... N91-23917 #
CONF-910609-4 ..... N91-23913 #
CONF-910609-5 ..... N91-23353 #
CONF-910614-1 ..... N91-23298 #
CONF-910614-2 ..... N91-23294 #
CONF-910617-1 ..... N91-23318 #
CONF-910627-1 ..... N91-23386 #
CONF-910637-1 ..... N91-23697 #
CONF-910638-1 ..... N91-23507 #
CONF-910638-2 ..... N91-23508 #
CONF-910638-3 ..... N91-23742 #
CONF-910640-1 ..... N91-23885 #
CONF-910640-2 ..... N91-23389 #

CONF-910648-1 ..... N91-23520 #
CONF-910651-1 ..... N91-23430 #
CONF-910651-2 ..... N91-23429 #
CONF-910659-3 ..... N91-23631 #
CONF-910659-5 ..... N91-23426 #
CONF-910659-10 ..... N91-23630 #
CONF-910659-11 ..... N91-23744 #
CONF-910659-12 ..... N91-23632 #
CONF-910664-1 ..... N91-23428 #
CONF-910684-1 ..... N91-23892 #
CONF-910684-2 ..... N91-23431 #
CONF-910684-3 ..... N91-23317 #
CONF-910690-1 ..... N91-23939 #
CONF-910690-2 ..... N91-23388 #
CONF-9003100-5 ..... N91-23866 #
CONF-9005329-1 ..... N91-23695 #
CONF-9006105-14 ..... N91-23911 #
CONF-9008198-1 ..... N91-23740 #
CONF-9008199-1 ..... N91-23510 #
CONF-9009353-1 ..... N91-23292 #
CONF-9010287-7 ..... N91-23860 #
CONF-9011177-7 ..... N91-23862 #
CONF-9011183-1 ..... N91-23312 #
CONF-9011186-1 ..... N91-23627 #
CONF-9102102-1 ..... N91-23865 #
CONF-9103133-2 ..... N91-23745 #
CONF-9103134-2 ..... N91-23277 #
CONF-9103146-2 ..... N91-23873 #
CONF-9104163-3 ..... N91-23674 #
CONF-9104171-7 ..... N91-23085 #
CONF-9104174-1 ..... N91-23295 #
CONF-9104187-1 ..... N91-23893 #
CONF-9104198-1 ..... N91-23382 #
CONF-9104203-1 ..... N91-23464 #
CONF-9104206-1 ..... N91-23315 #
CONF-9104210-1 ..... N91-23919 #
CONF-9105137-2 ..... N91-23859 #
CONF-9105138-1 ..... N91-23310 #
CONF-9105148-1 ..... N91-23537 #
CONF-9105148-2 ..... N91-23536 #
CONF-9105148-3 ..... N91-23526 #
CONF-9105160-1 ..... N91-23986 #
CONF-9106103-1 ..... N91-23743 #
CONF-9106114-1 ..... N91-23432 #
CONF-9106117-1 ..... N91-23784 #
CONF-9106118-1 ..... N91-23351 #
CONF-9106118-2 ..... N91-23352 #
CONF-9106119-1 ..... N91-24027 #
CONF-9106119-2 ..... N91-24028 #
CONF-9106130-1 ..... N91-23291 #
CONF-9106130-2 ..... N91-23300 #
CONF-9106131-1 ..... N91-23535 #

CPSS-1290-01 ..... N91-23951 #

CRANFIELD-AERO-9002 ..... N91-23140 #
CRANFIELD-AERO-9004 ..... N91-23092 #
CRANFIELD-AERO-9005 ..... N91-23443 #
CRANFIELD-AERO-9012 ..... N91-23444 #

CRHC-91-19 ..... N91-23739* #
CRHC-91-20 ..... N91-23738* #

CRIE-T-89059 ..... N91-23506 #
CRIE-T-89074 ..... N91-23385 #

CRREL-SR-90-42 ..... N91-23280 #

CS-TR-2436 ..... N91-23765 #
CS-TR-2447 ..... N91-23992 #
CS-TR-2531 ..... N91-23993 #

DCIEM-90-51 ..... N91-23720 #

DE90-013196 ..... N91-23386 #
DE90-015815 ..... N91-24013 #
DE90-016440 ..... N91-23697 #
DE90-017029 ..... N91-23507 #
DE90-017693 ..... N91-23520 #
DE90-017742 ..... N91-23508 #
DE91-002132 ..... N91-23618 #
DE91-002309 ..... N91-23428 #
DE91-002790 ..... N91-23429 #
DE91-002792 ..... N91-23430 #
DE91-004723 ..... N91-23885 #
DE91-005240 ..... N91-23431 #
DE91-005310 ..... N91-23892 #
DE91-005516 ..... N91-23316 #
DE91-005895 ..... N91-23742 #
DE91-006001 ..... N91-23542 #
DE91-006047 ..... N91-23743 #
DE91-006208 ..... N91-23317 #
DE91-006274 ..... N91-23318 #
DE91-006392 ..... N91-23534 #
DE91-007066 ..... N91-23432 #
DE91-007167 ..... N91-23543 #
DE91-007389 ..... N91-23784 #
DE91-007467 ..... N91-23351 #
DE91-007622 ..... N91-24028 #
DE91-007623 ..... N91-24027 #
DE91-007676 ..... N91-23785 #
DE91-007706 ..... N91-23298 #
DE91-007860 ..... N91-23883 #
DE91-008356 ..... N91-23424 #
DE91-008534 ..... N91-23275 #
DE91-008561 ..... N91-23911 #
DE91-008567 ..... N91-23291 #
DE91-008825 ..... N91-23498 #
DE91-008833 ..... N91-23312 #
DE91-008883 ..... N91-23535 #
DE91-008947 ..... N91-23339 #
DE91-009039 ..... N91-23352 #
DE91-009055 ..... N91-23313 #
DE91-009071 ..... N91-23698 #
DE91-009117 ..... N91-23310 #
DE91-009120 ..... N91-23292 #
DE91-009152 ..... N91-23859 #
DE91-009250 ..... N91-23939 #
DE91-009254 ..... N91-23382 #
DE91-009255 ..... N91-23536 #
DE91-009257 ..... N91-23537 #
DE91-009262 ..... N91-23293 #
DE91-009292 ..... N91-23299 #
DE91-009371 ..... N91-23855 #
DE91-009414 ..... N91-23499 #
DE91-009443 ..... N91-23940 #
DE91-009445 ..... N91-23274 #
DE91-009472 ..... N91-23626 #
DE91-009474 ..... N91-23941 #
DE91-009476 ..... N91-23631 #
DE91-009523 ..... N91-24036 #
DE91-009538 ..... N91-23627 #
DE91-009544 ..... N91-23294 #
DE91-009545 ..... N91-23526 #
DE91-009554 ..... N91-23509 #
DE91-009616 ..... N91-23314 #
DE91-009618 ..... N91-23383 #
DE91-009627 ..... N91-23425 #
DE91-009652 ..... N91-23414 #
DE91-009676 ..... N91-23538 #
DE91-009707 ..... N91-23387 #
DE91-009718 ..... N91-23463 #
DE91-009719 ..... N91-23692 #
DE91-009726 ..... N91-23349 #
DE91-009743 ..... N91-23381 #
DE91-009745 ..... N91-23984 #
DE91-009749 ..... N91-23860 #
DE91-009757 ..... N91-23426 #
DE91-009763 ..... N91-23388 #
DE91-009764 ..... N91-23085 #
DE91-009765 ..... N91-23465 #
DE91-009770 ..... N91-23464 #
DE91-009771 ..... N91-23300 #
DE91-009772 ..... N91-23466 #
DE91-009777 ..... N91-23333 #
DE91-009803 ..... N91-23427 #
DE91-009808 ..... N91-23334 #
DE91-009845 ..... N91-23350 #
DE91-009919 ..... N91-23544 #
DE91-009931 ..... N91-23295 #
DE91-009936 ..... N91-23539* #
DE91-009937 ..... N91-23545 #
DE91-009939 ..... N91-23695 #
DE91-009947 ..... N91-23630 #
DE91-009950 ..... N91-23315 #
DE91-009951 ..... N91-23942 #
DE91-009952 ..... N91-23296 #
DE91-009954 ..... N91-23740 #
DE91-009963 ..... N91-23943 #
DE91-009972 ..... N91-23944 #
DE91-009976 ..... N91-23999 #
DE91-009982 ..... N91-23477 #
DE91-009996 ..... N91-23696 #
DE91-009997 ..... N91-23297 #
DE91-010030 ..... N91-23857 #
DE91-010032 ..... N91-23546 #
DE91-010035 ..... N91-23540 #
DE91-010050 ..... N91-23884 #
DE91-010063 ..... N91-23674 #
DE91-010079 ..... N91-23736 #
DE91-010088 ..... N91-23510 #
DE91-010102 ..... N91-23415 #
DE91-010112 ..... N91-23541 #
DE91-010122 ..... N91-23858 #
DE91-010123 ..... N91-23527 #
DE91-010131 ..... N91-23893 #
DE91-010152 ..... N91-23632 #
DE91-010155 ..... N91-23628 #
DE91-010156 ..... N91-23744 #
DE91-010181 ..... N91-23693 #
DE91-010203 ..... N91-23741 #
DE91-010204 ..... N91-23737 #
DE91-010209 ..... N91-23856 #
DE91-010210 ..... N91-23935 #
DE91-010215 ..... N91-23735 #
DE91-010222 ..... N91-23882 #
DE91-010231 ..... N91-23384 #
DE91-010368 ..... N91-23476 #
DE91-010376 ..... N91-23886 #
DE91-010382 ..... N91-23916 #
DE91-010390 ..... N91-23913 #
DE91-010391 ..... N91-23917 #
DE91-010421 ..... N91-23912 #
DE91-010424 ..... N91-23918 #
DE91-010431 ..... N91-23985 #
DE91-010450 ..... N91-23505 #
DE91-010452 ..... N91-23511 #
DE91-010453 ..... N91-23805 #
DE91-010454 ..... N91-23864 #
DE91-010460 ..... N91-23478 #
DE91-010465 ..... N91-23986 #
DE91-010468 ..... N91-23479 #
DE91-010469 ..... N91-23865 #
DE91-010489 ..... N91-23914 #
DE91-010490 ..... N91-23915 #
DE91-010570 ..... N91-23861 #
DE91-010577 ..... N91-23619 #
DE91-010584 ..... N91-23919 #
DE91-010585 ..... N91-23389 #
DE91-010590 ..... N91-23862 #
DE91-010594 ..... N91-23866 #
DE91-010599 ..... N91-23745 #
DE91-010603 ..... N91-23276 #
DE91-010641 ..... N91-23863 #
DE91-010657 ..... N91-23920 #
DE91-010677 ..... N91-23987 #
DE91-010686 ..... N91-23921 #
DE91-010692 ..... N91-23867 #
DE91-010696 ..... N91-23922 #
DE91-010697 ..... N91-23923 #
DE91-010702 ..... N91-23868 #
DE91-010719 ..... N91-23245 #
DE91-010730 ..... N91-23924 #
DE91-010739 ..... N91-23869 #
DE91-010740 ..... N91-23870 #
DE91-010746 ..... N91-23871 #
DE91-010749 ..... N91-23872 #
DE91-010758 ..... N91-23390 #
DE91-010770 ..... N91-23894 #
DE91-010779 ..... N91-23873 #
DE91-010782 ..... N91-23353 #
DE91-010797 ..... N91-23945 #
DE91-010799 ..... N91-23277 #
DE91-011002 ..... N91-23547 #
DE91-011004 ..... N91-23391 #
DE91-764223 ..... N91-23182 #
DE91-764238 ..... N91-23506 #
DE91-764240 ..... N91-23385 #

DLR-FB-88-13 ..... N91-23854 #
DLR-FB-89-12 ..... N91-23442 #
DLR-FB-89-33 ..... N91-23553 #
DLR-FB-89-35 ..... N91-23278 #
DLR-FB-89-51 ..... N91-23230 #
DLR-FB-90-30 ..... N91-23676 #
DLR-FB-90-35 ..... N91-23191 #
DLR-FB-90-36 ..... N91-23687 #
DLR-FB-90-38 ..... N91-23677 #
DLR-FB-90-43 ..... N91-23435 #
DLR-FB-90-44 ..... N91-23612 #
DLR-FB-90-46 ..... N91-23088 #
DLR-FB-90-48 ..... N91-23301 #
DLR-FB-90-49 ..... N91-23137 #
DLR-FB-90-50 ..... N91-23355 #
DLR-FB-90-51 ..... N91-23725 #
DLR-FB-90-52 ..... N91-23356 #
DLR-FB-90-53 ..... N91-23357 #
DLR-FB-90-54 ..... N91-23613 #
DLR-FB-90-56 ..... N91-23614 #
DLR-FB-90-59 ..... N91-23746 #

DLR-MITT-90-15 ..... N91-23246 #

DM-54 ..... N91-23991 #
DM-55 ..... N91-23679 #
DM-56 ..... N91-23680 #

DODA-AR-006-113 ..... N91-23306 #

DOE/AD-0005 ..... N91-23984 #

DOE/BP-24332/1 ..... N91-23387 #

DOE/CH-10406/T3 ..... N91-23383 #

DOE/ER-0493T ..... N91-23921 #
DOE/ER-13262/7 ..... N91-23870 #
DOE/ER-13291/6 ..... N91-23425 #

DOE/ER-13508/5 ..... N91-23276 #
DOE/ER-13764/T2 ..... N91-23427 #
DOE/ER-40153/7 ..... N91-23872 #
DOE/ER-40162/T5 ..... N91-23871 #
DOE/ER-40371/4 ..... N91-23868 #
DOE/ER-40376/4 ..... N91-23869 #
DOE/ER-40479/3 ..... N91-23863 #
DOE/ER-45315/15 ..... N91-23293 #
DOE/ER-45388/1 ..... N91-23297 #
DOE/ER-53223/158 ..... N91-23924 #
DOE/ER-53266/30 ..... N91-23912 #
DOE/ER-53266/36 ..... N91-23918 #
DOE/ER-54109/T1 ..... N91-23920 #
DOE/ER-60997/T1 ..... N91-23696 #

DOE/ID-12693/1 ..... N91-23999 #

DOE/PC-88913/T8 ..... N91-23424 #
DOE/PC-88947/T9 ..... N91-23339 #
DOE/PC-89786/T1 ..... N91-23334 #
DOE/PC-90293/T1 ..... N91-23275 #

DOE/SF-17170/T25 ..... N91-23299 #

DOT-FAA-NR-91-5 ..... N91-23675 #

DOT-VNTSC-FAA-90-6 ..... N91-23079 #

DOT/FAA/CT-TN90/41 ..... N91-23075 #
DOT/FAA/CT-TN90/48 ..... N91-23106 #

DOT/FAA/CT-90/21 ..... N91-23097 #

DOT/FAA/RD-90/29 ..... N91-23079 #
DOT/FAA/RD-91/5 ..... N91-23198 #
DOT/FAA/RD-91/7 ..... N91-23134 #
DOT/FAA/RD-91/13 ..... N91-23710 #

DREA-TM-90/208 ..... N91-23325 #

DREO-1049 ..... N91-23367 #
DREO-1056 ..... N91-23378 #

DTRC/CISD-90/02 ..... N91-23781 #

DU/DC/TR-18 ..... N91-23956 #

D615-10014 ..... N91-23200* #

E-5583 ..... N91-23179* #
E-5651-1 ..... N91-23521* #
E-5862 ..... N91-23512* #
E-5983 ..... N91-23311* #
E-5987 ..... N91-23549* #
E-6013 ..... N91-23183* #
E-6058 ..... N91-23347* #
E-6082 ..... N91-23515* #
E-6085 ..... N91-23513* #
E-6093 ..... N91-23409* #
E-6116 ..... N91-23439* #
E-6133 ..... N91-23340* #
E-6136 ..... N91-23184* #
E-6140 ..... N91-23247* #
E-6148 ..... N91-23501* #
E-6157 ..... N91-23514* #
E-6158 ..... N91-23086* #
E-6159 ..... N91-23098* #
E-6164 ..... N91-23087* #
E-6169 ..... N91-23416* #
E-6175 ..... N91-23234* #
E-6184 ..... N91-23548* #
E-6191 ..... N91-23233* #
E-6197 ..... N91-23500* #
E-6200 ..... N91-23102* #
E-6207 ..... N91-23354* #
E-6220 ..... N91-23550* #
E-6224 ..... N91-23620* #
E-6226 ..... N91-23083* #
E-6230 ..... N91-23616* #
E-6233 ..... N91-23089* #
E-6237 ..... N91-23946* #
E-6238 ..... N91-23185* #
E-6254 ..... N91-23186* #
E-6268 ..... N91-23205* #

EGG-M-90015 ..... N91-23510 #
EGG-M-90364 ..... N91-23674 #
EGG-M-90365 ..... N91-23736 #
EGG-M-90413 ..... N91-23415 #
EGG-M-90469 ..... N91-23317 #

EGG-NE-9087 ..... N91-23884 #

EGG-10617-411 ..... N91-23631 #
EGG-10617-5039 ..... N91-23894 #

EPA/600/8-90/005 ..... N91-23625 #
EPA/910/9-90/018 ..... N91-23623 #

ERP-1072 ..... N91-23228 #

ESA-PSS-01-607-ISSUE-1 ..... N91-23396 #
ESA-PSS-01-611-ISSUE-1 ..... N91-23397 #

ESA-SP-312 ..... N91-23563 #

ESA-TT-1126 ..... N91-23854 #
ESA-TT-1172 ..... N91-23363 #
ESA-TT-1187 ..... N91-23553 #
ESA-TT-1191 ..... N91-23278 #
ESA-TT-1199 ..... N91-23441 #
ESA-TT-1202 ..... N91-23319 #
ESA-TT-1203 ..... N91-23442 #
ESA-TT-1213 ..... N91-23230 #
ESA-TT-1259 ..... N91-23357 #
ESA-TT-1260 ..... N91-23246 #

ESL-721563-2 ..... N91-23402 #

ETL-R-151 ..... N91-23610 #

ETN-91-98876 ..... N91-23895 #
ETN-91-98878 ..... N91-23874 #
ETN-91-98879 ..... N91-23875 #
ETN-91-98882 ..... N91-23876 #
ETN-91-98908 ..... N91-23649 #
ETN-91-98909 ..... N91-23650 #
ETN-91-99049 ..... N91-23551 #
ETN-91-99061 ..... N91-23246 #
ETN-91-99062 ..... N91-23676 #
ETN-91-99063 ..... N91-23191 #
ETN-91-99064 ..... N91-23677 #
ETN-91-99065 ..... N91-23435 #
ETN-91-99066 ..... N91-23612 #
ETN-91-99067 ..... N91-23088 #
ETN-91-99068 ..... N91-23301 #
ETN-91-99069 ..... N91-23137 #
ETN-91-99070 ..... N91-23355 #
ETN-91-99071 ..... N91-23725 #
ETN-91-99072 ..... N91-23356 #
ETN-91-99073 ..... N91-23357 #
ETN-91-99074 ..... N91-23613 #
ETN-91-99075 ..... N91-23614 #
ETN-91-99076 ..... N91-23746 #
ETN-91-99078 ..... N91-23687 #
ETN-91-99079 ..... N91-23103 #
ETN-91-99080 ..... N91-23104
ETN-91-99081 ..... N91-24029
ETN-91-99082 ..... N91-24040
ETN-91-99083 ..... N91-23747
ETN-91-99084 ..... N91-23748
ETN-91-99085 ..... N91-23749
ETN-91-99088 ..... N91-23750
ETN-91-99089 ..... N91-23751
ETN-91-99090 ..... N91-23752
ETN-91-99091 ..... N91-23651
ETN-91-99092 ..... N91-23204
ETN-91-99093 ..... N91-23358
ETN-91-99094 ..... N91-23359
ETN-91-99095 ..... N91-23360
ETN-91-99096 ..... N91-23361
ETN-91-99097 ..... N91-23392
ETN-91-99098 ..... N91-23703
ETN-91-99099 ..... N91-23719
ETN-91-99101 ..... N91-23646
ETN-91-99103 ..... N91-23678
ETN-91-99105 ..... N91-23688
ETN-91-99107 ..... N91-23138 #
ETN-91-99109 ..... N91-23925
ETN-91-99110 ..... N91-23647
ETN-91-99111 ..... N91-23196 #
ETN-91-99112 ..... N91-23436 #
ETN-91-99113 ..... N91-23807 #
ETN-91-99114 ..... N91-23437 #
ETN-91-99115 ..... N91-23563 #
ETN-91-99118 ..... N91-23753 #
ETN-91-99119 ..... N91-23467
ETN-91-99120 ..... N91-23438
ETN-91-99122 ..... N91-23754 #
ETN-91-99123 ..... N91-23788 #
ETN-91-99124 ..... N91-23648 #
ETN-91-99187 ..... N91-23652 #
ETN-91-99188 ..... N91-23302 #
ETN-91-99189 ..... N91-23653 #
ETN-91-99191 ..... N91-23203 #
ETN-91-99192 ..... N91-23654 #
ETN-91-99217 ..... N91-23988 #
ETN-91-99220 ..... N91-23726 #
ETN-91-99221 ..... N91-23393 #
ETN-91-99222 ..... N91-23362 #
ETN-91-99223 ..... N91-23778 #
ETN-91-99224 ..... N91-23779 #

ETN-91-99225 ..... N91-23989 #
ETN-91-99226 ..... N91-23822 #
ETN-91-99228 ..... N91-23823 #
ETN-91-99229 ..... N91-23824 #
ETN-91-99231 ..... N91-23808 #
ETN-91-99232 ..... N91-23809 #
ETN-91-99233 ..... N91-23825 #
ETN-91-99234 ..... N91-23755 #
ETN-91-99235 ..... N91-23756 #
ETN-91-99236 ..... N91-23810 #
ETN-91-99237 ..... N91-23780 #
ETN-91-99238 ..... N91-23727 #
ETN-91-99239 ..... N91-23516 #
ETN-91-99240 ..... N91-23705 #
ETN-91-99241 ..... N91-23844 #
ETN-91-99249 ..... N91-23090 #
ETN-91-99252 ..... N91-24086 #
ETN-91-99253 ..... N91-23105 #
ETN-91-99255 ..... N91-23552 #
ETN-91-99257 ..... N91-23990 #
ETN-91-99265 ..... N91-23187 #
ETN-91-99266 ..... N91-23188 #
ETN-91-99267 ..... N91-23192 #
ETN-91-99268 ..... N91-23853 #
ETN-91-99269 ..... N91-23216 #
ETN-91-99270 ..... N91-23091 #
ETN-91-99271 ..... N91-23248 #
ETN-91-99272 ..... N91-23139 #
ETN-91-99273 ..... N91-23757 #
ETN-91-99274 ..... N91-23217 #
ETN-91-99275 ..... N91-23249 #
ETN-91-99276 ..... N91-23250 #
ETN-91-99277 ..... N91-23251 #
ETN-91-99278 ..... N91-23252 #
ETN-91-99279 ..... N91-23253 #
ETN-91-99280 ..... N91-23197 #
ETN-91-99281 ..... N91-23254 #
ETN-91-99283 ..... N91-23926 #
ETN-91-99284 ..... N91-23255 #
ETN-91-99285 ..... N91-23927 #
ETN-91-99286 ..... N91-23256 #
ETN-91-99287 ..... N91-23257 #
ETN-91-99289 ..... N91-23258 #
ETN-91-99290 ..... N91-23947 #
ETN-91-99291 ..... N91-23259 #
ETN-91-99292 ..... N91-23948 #
ETN-91-99293 ..... N91-23208 #
ETN-91-99294 ..... N91-23928 #
ETN-91-99297 ..... N91-23929 #
ETN-91-99298 ..... N91-23758 #
ETN-91-99299 ..... N91-23260 #
ETN-91-99300 ..... N91-23261 #
ETN-91-99301 ..... N91-23209 #
ETN-91-99302 ..... N91-23262 #
ETN-91-99303 ..... N91-23615 #
ETN-91-99304 ..... N91-23218 #
ETN-91-99305 ..... N91-23219 #
ETN-91-99306 ..... N91-23468 #
ETN-91-99307 ..... N91-23220 #
ETN-91-99308 ..... N91-23221 #
ETN-91-99309 ..... N91-23222 #
ETN-91-99310 ..... N91-23223 #
ETN-91-99311 ..... N91-23224 #
ETN-91-99312 ..... N91-23854 #
ETN-91-99313 ..... N91-23363 #
ETN-91-99314 ..... N91-23553 #
ETN-91-99315 ..... N91-23278 #
ETN-91-99316 ..... N91-23441 #
ETN-91-99317 ..... N91-23319 #
ETN-91-99318 ..... N91-23442 #
ETN-91-99319 ..... N91-23230 #
ETN-91-99320 ..... N91-23845 #
ETN-91-99321 ..... N91-23364 #
ETN-91-99322 ..... N91-23846 #
ETN-91-99323 ..... N91-23394 #
ETN-91-99324 ..... N91-23811 #
ETN-91-99325 ..... N91-23949 #
ETN-91-99326 ..... N91-23395 #
ETN-91-99327 ..... N91-23812 #
ETN-91-99328 ..... N91-23813 #
ETN-91-99329 ..... N91-23320
ETN-91-99330 ..... N91-23877 #
ETN-91-99332 ..... N91-23140 #
ETN-91-99333 ..... N91-23092 #
ETN-91-99334 ..... N91-23443 #
ETN-91-99335 ..... N91-23444 #
ETN-91-99336 ..... N91-23991 #
ETN-91-99337 ..... N91-23679 #
ETN-91-99338 ..... N91-23680 #
ETN-91-99339 ..... N91-23396 #
ETN-91-99340 ..... N91-23397 #
ETN-91-99341 ..... N91-23321 #
ETN-91-99342 ..... N91-23759 #

EXAMENARBEIT-8 ..... N91-23653 #

FEL-90-A211 N91-23358
FEL-90-B033 N91-23359
FEL-90-B215 N91-23360
FEL-90-B216 N91-23361
FEL-90-B255 N91-23392

FERMILAB-CONF-91/81-A N91-24015* #

FERMILAB-PUB-91/55-A N91-24016* #

FFA-TN-1990-29 N91-23321 #
FFA-TN-1990-53 N91-23138 #
FFA-TN-1991-08-PT-1 N91-23759 #

FFI-91/7002 N91-23754 #

FRCR-357-PT-2 N91-23912 #
FRCR-381 N91-23918 #

FTD-ID(RS)T-1365-90 N91-23962 #

GA-A-20362 N91-23922 #
GA-A-20363 N91-23923 #

GAO/NSIAD-91-35 N91-23142 #

GKSS-90/E/25 N91-23203 #

GL-ERP-1075 N91-23660 #

GL-TR-90-0224 N91-23228 #
GL-TR-90-0282 N91-23635 #
GL-TR-90-0309 N91-23655 #
GL-TR-90-0311 N91-23659 #
GL-TR-90-0358 N91-23660 #

GRASP-LAB-177 N91-23787* #

GRI-90/0074 N91-23338 #
GRI-90/0089 N91-23332 #
GRI-90/0102 N91-23964 #
GRI-90/0250 N91-23272 #

GSF-BER-21/90 N91-23990 #

H-1687 N91-23133* #

HAC-REF-G3658 N91-23903 #

IAITIC-87-1001 N91-23345 #
IAITIC-87-1002-REV N91-23804 #
IAITIC-87-1003 N91-23337 #
IAITIC-87-1004 N91-23107 #
IAITIC-87-1005 N91-23238 #
IAITIC-87-1006 N91-23194 #
IAITIC-87-1007 N91-23522 #

ICASE-91-34 N91-23434* #
ICASE-91-37 N91-23433* #

ICOMP-91-06 N91-23416* #

IDA-P-2401 N91-23077 #
IDA-P-2409 N91-24000 #
IDA-P-2462 N91-23076 #

IDA/HQ-90-35536 N91-23077 #
IDA/HQ-90-35599 N91-24000 #
IDA/HQ-90-35834 N91-23076 #

INPE-5182-RPE/638 N91-23609 #

IS-T-1490 N91-23693 #

ISAL-91-0004 N91-23844 #

ISBN-0-943475-03-1 N91-23634 #
ISBN-1-871564-03-4 N91-23140 #
ISBN-1-871564-05-0 N91-23092 #
ISBN-1-871564-06-9 N91-23443 #
ISBN-1-871564-12-3 N91-23444 #
ISBN-90-6233-638-8 N91-23988 #
ISBN-92-835-0594-8 N91-23147 #
ISBN-92-835-0600-6 N91-23711 #
ISBN-92-835-0602-2 N91-23108 #
ISBN-951-38-3790-4 N91-23551 #
ISBN-951-38-3942-7 N91-23788 #

ISSN-0065-3713 N91-23647
ISSN-0065-3713 N91-23925
ISSN-0069-5882 N91-23648 #
ISSN-0069-5882 N91-23652 #
ISSN-0169-1651 N91-23688
ISSN-0169-1708 N91-23646
ISSN-0169-1708 N91-23678
ISSN-0171-1342 N91-23088 #
ISSN-0171-1342 N91-23435 #
ISSN-0171-1342 N91-23612 #
ISSN-0171-1342 N91-23677 #
ISSN-0172-8741 N91-23654 #
ISSN-0211-5166 N91-23649 #
ISSN-0211-5166 N91-23650 #
ISSN-0344-9629 N91-23203 #
ISSN-0349-0467 N91-23679 #
ISSN-0349-0467 N91-23680 #
ISSN-0349-0467 N91-23991 #
ISSN-0358-5069 N91-23788 #
ISSN-0358-5077 N91-23551 #
ISSN-0379-4059 N91-23396 #
ISSN-0379-4059 N91-23397 #
ISSN-0720-7808 N91-23103 #
ISSN-0721-1694 N91-23990 #
ISSN-0802-2437 N91-23754 #
ISSN-0938-2194 N91-24086 #
ISSN-0938-5177 N91-23653 #
ISSN-0939-298X N91-23246 #
ISSN-0939-2963 N91-23137 #
ISSN-0939-2963 N91-23191 #
ISSN-0939-2963 N91-23301 #
ISSN-0939-2963 N91-23355 #
ISSN-0939-2963 N91-23356 #
ISSN-0939-2963 N91-23357 #
ISSN-0939-2963 N91-23613 #
ISSN-0939-2963 N91-23614 #
ISSN-0939-2963 N91-23676 #
ISSN-0939-2963 N91-23687 #
ISSN-0939-2963 N91-23725 #
ISSN-0939-2963 N91-23746 #
ISSN-0959-2423 N91-23438
ISSN-0959-2423 N91-23467
ISSN-0959-2426 N91-23320

ITN-88-85000 N91-23345 #
ITN-88-85001 N91-23804 #
ITN-88-85002 N91-23337 #
ITN-88-85003 N91-23107 #
ITN-88-85004 N91-23238 #
ITN-88-85005 N91-23194 #
ITN-88-85006 N91-23522 #
ITN-88-85007 N91-23910 #
ITN-88-85008 N91-23231 #
ITN-88-85009 N91-23407 #
ITN-89-85012 N91-23832 #
ITN-89-85013 N91-23828 #
ITN-89-85014 N91-23621 #
ITN-89-85015 N91-23967 #

IZF-1990-A-32 N91-23703
IZF-1990-B-16 N91-23719

K/CSD/TM-97 N91-23985 #

K/DSRD-461 N91-23987 #

KAPL-4721 N91-23867 #

KNMI-TR-125 N91-23646
KNMI-TR-127 N91-23678

KNMI-WR-90-04 N91-23688

LA-UR-90-2884 N91-23697 #
LA-UR-90-3000 N91-23855 #
LA-UR-90-3383 N91-23428 #
LA-UR-90-4168 N91-23742 #
LA-UR-91-126 N91-23784 #
LA-UR-91-226 N91-23351 #
LA-UR-91-732 N91-23695 #
LA-UR-91-847 N91-23630 #
LA-UR-91-884 N91-23315 #
LA-UR-91-887 N91-23942 #
LA-UR-91-892 N91-23296 #
LA-UR-91-896 N91-23740 #
LA-UR-91-964 N91-23943 #
LA-UR-91-1043 N91-23944 #

LA-11898-MS N91-23350 #

LAAS-90390 N91-23727 #
LAAS-90403 N91-23516 #
LAAS-91002 N91-23705 #

LBL-90-REV-11/90 N91-23856 #
LBL-29345 N91-23935 #
LBL-29502 N91-23882 #
LBL-29829 N91-23384 #
LBL-29925 N91-23741 #
LBL-30056 N91-23737 #
LBL-30057 N91-23464 #
LBL-30077 N91-23698 #
LBL-30254 N91-23300 #

LMSC-F279280 N91-23458* #

LSU-T-90-004 N91-23624 #

LTR91-005 N91-23905 #

LU-AFOSR-FR-90 N91-23094 #

L9KVAE-FR-91001 N91-23136* #

MATHS-REPT-A-139 N91-23812 #
MATHS-REPT-A-140 N91-23813 #

MBB-FE202/5/PUB/436 N91-23090 #

MD-90-14-IB N91-23815 #

MDC-QA056 N91-23453 #

MF-122 N91-23924 #

MIT/LCS/TM-442 N91-23774 #

MIT/LCS/TR-482 N91-23401 #
MIT/LCS/TR-496 N91-23770 #

MITT-74 N91-23648 #

MLM-3679 N91-23498 #
MLM-3684 N91-23274 #

MPE-PREPRINT-192 N91-23104
MPE-PREPRINT-193 N91-24029
MPE-PREPRINT-194 N91-24040

MS-CIS-89-22 N91-23787* #

MTL-TR-91-2 N91-23263 #
MTL-TR-91-3 N91-23554 #

MTR-M90-79 N91-23366 #

NADC-91005-60 N91-23797 #

NAL-TM-620 N91-23182 #

NAS 1.15:4289 N91-23215* #
NAS 1.15:101735 N91-23133* #
NAS 1.15:102174 N91-23210* #
NAS 1.15:102832 N91-23099* #
NAS 1.15:102854 N91-23207* #
NAS 1.15:103534 N91-23502* #
NAS 1.15:103741 N91-23311* #
NAS 1.15:103744 N91-23549* #
NAS 1.15:103757 N91-23183* #
NAS 1.15:103783 N91-23347* #
NAS 1.15:103795 N91-23515* #
NAS 1.15:103797 N91-23513* #
NAS 1.15:103801 N91-23409* #
NAS 1.15:103819 N91-23718* #
NAS 1.15:103847 N91-23704* #
NAS 1.15:103860 N91-23341* #
NAS 1.15:104070 N91-23244* #
NAS 1.15:104073 N91-23135* #
NAS 1.15:104339 N91-23521* #
NAS 1.15:104342 N91-23439* #
NAS 1.15:104350 N91-23512* #
NAS 1.15:104351 N91-23184* #
NAS 1.15:104354 N91-23247* #
NAS 1.15:104356 N91-23179* #
NAS 1.15:104358 N91-23501* #
NAS 1.15:104361 N91-23514* #
NAS 1.15:104362 N91-23086* #
NAS 1.15:104363 N91-23098* #
NAS 1.15:104366 N91-23087* #
NAS 1.15:104368 N91-23416* #
NAS 1.15:104379 N91-23548* #
NAS 1.15:104382 N91-23233* #
NAS 1.15:104387 N91-23234* #
NAS 1.15:104388 N91-23500* #
NAS 1.15:104389 N91-23102* #
NAS 1.15:104392 N91-23354* #
NAS 1.15:104400 N91-23550* #
NAS 1.15:104402 N91-23620* #
NAS 1.15:104403 N91-23083* #
NAS 1.15:104405 N91-23616* #
NAS 1.15:104407 N91-23089* #
NAS 1.15:104410 N91-23946* #
NAS 1.15:104411 N91-23185* #
NAS 1.15:104420 N91-23186* #
NAS 1.15:104421 N91-23340* #
NAS 1.15:104957 N91-23213* #
NAS 1.15:104958 N91-23214* #
NAS 1.15:104964 N91-23539* #
NAS 1.21:7011(346) N91-23700*
NAS 1.21:7011(347) N91-23701*

NAS 1.21:7011(348) N91-23702*
NAS 1.21:7037(261) N91-23073*
NAS 1.21:7037(262) N91-23074*
NAS 1.26:177578 ..... N91-23136* #
NAS 1.26:182076 ..... N91-23080* #
NAS 1.26:182077 ..... N91-23081* #
NAS 1.26:184157 ..... N91-23229* #
NAS 1.26:185192 ..... N91-23849* #
NAS 1.26:185193 ..... N91-23850* #
NAS 1.26:185194 ..... N91-23851* #
NAS 1.26:185195 ..... N91-23852* #
NAS 1.26:186197 ..... N91-23458* #
NAS 1.26:186262 ..... N91-23206* #
NAS 1.26:186341 ..... N91-23211* #
NAS 1.26:186769 ..... N91-23195* #
NAS 1.26:186869 ..... N91-23408* #
NAS 1.26:186954 ..... N91-23212* #
NAS 1.26:186989 ..... N91-23200* #
NAS 1.26:187080 ..... N91-24030* #
NAS 1.26:187084 ..... N91-23181* #
NAS 1.26:187085 ..... N91-23346* #
NAS 1.26:187138 ..... N91-23205* #
NAS 1.26:187527 ..... N91-23887* #
NAS 1.26:187550 ..... N91-23434* #
NAS 1.26:187552 ..... N91-23433* #
NAS 1.26:187921 ..... N91-23731* #
NAS 1.26:188119 ..... N91-23670* #
NAS 1.26:188171 ..... N91-24016* #
NAS 1.26:188173 ..... N91-24015* #
NAS 1.26:188175 ..... N91-23776* #
NAS 1.26:188181 ..... N91-23970* #
NAS 1.26:188184 ..... N91-23242* #
NAS 1.26:188197 ..... N91-23739* #
NAS 1.26:188199 ..... N91-23084* #
NAS 1.26:188202 ..... N91-23891* #
NAS 1.26:188205 ..... N91-23738* #
NAS 1.26:188207 ..... N91-23786* #
NAS 1.26:188208 ..... N91-23806 #
NAS 1.26:188209 ..... N91-23821* #
NAS 1.26:188215 ..... N91-23232* #
NAS 1.26:188217 ..... N91-23787* #
NAS 1.26:188234 ..... N91-23440* #
NAS 1.55:3109-VOL-2 ..... N91-24041* #
NAS 1.71:ARC-11909-1 ..... N91-23095* #
NAS 1.71:GSC-13369-1 ..... N91-23380* #
NAS 1.71:LAR-13563-1 ..... N91-23410* #
NAS 1.71:LAR-13887-1 ..... N91-23472* #
NAS 1.71:LAR-14427-1 ..... N91-23237* #
NAS 1.71:LAR-14466-1 ..... N91-23461* #
NAS 1.71:LAR-14588-1-CU ..... N91-23889* #
NAS 1.71:LEW-14949-1 ..... N91-23617* #
NAS 1.71:LEW-14967-2 ..... N91-23460* #
NAS 1.71:LEW-15094-1 ..... N91-23180* #
NAS 1.71:MFS-28507-1 ..... N91-23933* #
NAS 1.71:MSC-21350-1 ..... N91-23724* #
NAS 1.71:MSC-21463-1 ..... N91-23490* #
NAS 1.71:MSC-21555-1 ..... N91-23492* #
NAS 1.71:MSC-21577-1-SB ..... N91-23271* #
NAS 1.71:MSC-21580-1 ..... N91-23491* #
NAS 1.71:MSC-21700-1 ..... N91-23462* #
NAS 1.71:MSC-21730-1 ..... N91-23493* #
NAS 1.71:NPO-17852-1-CU ..... N91-23783* #
NAS 1.71:NPO-18098-1-CU ..... N91-23890* #
NAS 1.71:NPO-18115-1-CU ..... N91-23662* #
NAS 1.71:SSC-00010-1 ..... N91-23976* #
NAS 1.83:120 ..... N91-23694* #

NASA-CASE-ARC-11909-1 ..... N91-23095* #

NASA-CASE-GSC-13369-1 ..... N91-23380* #

NASA-CASE-LAR-13563-1 ..... N91-23410* #
NASA-CASE-LAR-13887-1 ..... N91-23472* #
NASA-CASE-LAR-14427-1 ..... N91-23237* #
NASA-CASE-LAR-14466-1 ..... N91-23461* #
NASA-CASE-LAR-14588-1-CU ..... N91-23889* #

NASA-CASE-LEW-14949-1 ..... N91-23617* #
NASA-CASE-LEW-14967-2 ..... N91-23460* #
NASA-CASE-LEW-15094-1 ..... N91-23180* #

NASA-CASE-MFS-28507-1 ..... N91-23933* #

NASA-CASE-MSC-21350-1 ..... N91-23724* #
NASA-CASE-MSC-21463-1 ..... N91-23490* #
NASA-CASE-MSC-21555-1 ..... N91-23492* #
NASA-CASE-MSC-21577-1-SB ..... N91-23271* #
NASA-CASE-MSC-21580-1 ..... N91-23491* #
NASA-CASE-MSC-21700-1 ..... N91-23462* #
NASA-CASE-MSC-21730-1 ..... N91-23493* #

NASA-CASE-NPO-17852-1-CU ..... N91-23783* #
NASA-CASE-NPO-18098-1-CU ..... N91-23890* #
NASA-CASE-NPO-18115-1-CU ..... N91-23662* #

NASA-CASE-SSC-00010-1 ..... N91-23976* #

NASA-CP-3109-VOL-2 ..... N91-24041* #

NASA-CR-177578 ..... N91-23136* #
NASA-CR-182076 ..... N91-23080* #
NASA-CR-182077 ..... N91-23081* #
NASA-CR-184157 ..... N91-23229* #
NASA-CR-185192 ..... N91-23849* #
NASA-CR-185193 ..... N91-23850* #
NASA-CR-185194 ..... N91-23851* #
NASA-CR-185195 ..... N91-23852* #
NASA-CR-186197 ..... N91-23458* #
NASA-CR-186262 ..... N91-23206* #
NASA-CR-186341 ..... N91-23211* #
NASA-CR-186769 ..... N91-23195* #
NASA-CR-186869 ..... N91-23408* #
NASA-CR-186954 ..... N91-23212* #
NASA-CR-186989 ..... N91-23200* #
NASA-CR-187080 ..... N91-24030* #
NASA-CR-187084 ..... N91-23181* #
NASA-CR-187085 ..... N91-23346* #
NASA-CR-187138 ..... N91-23205* #
NASA-CR-187527 ..... N91-23887* #
NASA-CR-187550 ..... N91-23434* #
NASA-CR-187552 ..... N91-23433* #
NASA-CR-187921 ..... N91-23731* #
NASA-CR-188119 ..... N91-23670* #
NASA-CR-188171 ..... N91-24016* #
NASA-CR-188173 ..... N91-24015* #
NASA-CR-188175 ..... N91-23776* #
NASA-CR-188181 ..... N91-23970* #
NASA-CR-188184 ..... N91-23242* #
NASA-CR-188197 ..... N91-23739* #
NASA-CR-188199 ..... N91-23084* #
NASA-CR-188202 ..... N91-23891* #
NASA-CR-188205 ..... N91-23738* #
NASA-CR-188207 ..... N91-23786* #
NASA-CR-188208 ..... N91-23806 #
NASA-CR-188209 ..... N91-23821* #
NASA-CR-188215 ..... N91-23232* #
NASA-CR-188217 ..... N91-23787* #
NASA-CR-188234 ..... N91-23440* #

NASA-NP-120 ..... N91-23694* #

NASA-SP-7011(346) N91-23700*
NASA-SP-7011(347) N91-23701*
NASA-SP-7011(348) N91-23702*
NASA-SP-7037(261) N91-23073*
NASA-SP-7037(262) N91-23074*

NASA-TM-4289 ..... N91-23215* #
NASA-TM-101735 ..... N91-23133* #
NASA-TM-102174 ..... N91-23210* #
NASA-TM-102832 ..... N91-23099* #
NASA-TM-102854 ..... N91-23207* #
NASA-TM-103534 ..... N91-23502* #
NASA-TM-103741 ..... N91-23311* #
NASA-TM-103744 ..... N91-23549* #
NASA-TM-103757 ..... N91-23183* #
NASA-TM-103783 ..... N91-23347* #
NASA-TM-103795 ..... N91-23515* #
NASA-TM-103797 ..... N91-23513* #
NASA-TM-103801 ..... N91-23409* #
NASA-TM-103819 ..... N91-23718* #
NASA-TM-103847 ..... N91-23704* #
NASA-TM-103860 ..... N91-23341* #
NASA-TM-104070 ..... N91-23244* #
NASA-TM-104073 ..... N91-23135* #
NASA-TM-104339 ..... N91-23521* #
NASA-TM-104342 ..... N91-23439* #
NASA-TM-104350 ..... N91-23512* #
NASA-TM-104351 ..... N91-23184* #
NASA-TM-104354 ..... N91-23247* #
NASA-TM-104356 ..... N91-23179* #
NASA-TM-104358 ..... N91-23501* #
NASA-TM-104361 ..... N91-23514* #
NASA-TM-104362 ..... N91-23086* #
NASA-TM-104363 ..... N91-23098* #
NASA-TM-104366 ..... N91-23087* #
NASA-TM-104368 ..... N91-23416* #
NASA-TM-104379 ..... N91-23548* #
NASA-TM-104382 ..... N91-23233* #
NASA-TM-104387 ..... N91-23234* #
NASA-TM-104388 ..... N91-23500* #
NASA-TM-104389 ..... N91-23102* #
NASA-TM-104392 ..... N91-23354* #
NASA-TM-104400 ..... N91-23550* #
NASA-TM-104402 ..... N91-23620* #
NASA-TM-104403 ..... N91-23083* #
NASA-TM-104405 ..... N91-23616* #
NASA-TM-104407 ..... N91-23089* #
NASA-TM-104410 ..... N91-23946* #
NASA-TM-104411 ..... N91-23185* #
NASA-TM-104420 ..... N91-23186* #
NASA-TM-104421 ..... N91-23340* #
NASA-TM-104957 ..... N91-23213* #

NASA-TM-104958 ..... N91-23214* #
NASA-TM-104964 ..... N91-23539* #

NBDL-89R001 ..... N91-23709 #
NBDL-90R007 ..... N91-23721 #

NCTRF-180 ..... N91-23717 #

NISTIR-3950 ..... N91-23523 #
NISTIR-3952 ..... N91-23524 #

NORDA-PR-90-020-252 ..... N91-23782 #

NOSC/TD-1936 ..... N91-23767 #
NOSC/TD-1944 ..... N91-23768 #
NOSC/TD-1963 ..... N91-23400 #

NOTA-INTERNA-955 ..... N91-23895 #
NOTA-INTERNA-957 ..... N91-23874 #
NOTA-INTERNA-958 ..... N91-23875 #
NOTA-INTERNA-961 ..... N91-23876 #

NPL-DMM(A)-19 ..... N91-23467
NPL-DMM(A)-20 ..... N91-23438
NPL-DMM(A)-24 ..... N91-23320

NPS-CS-91-006 ..... N91-23517 #

NPS-EC-91-003 ..... N91-23236 #

NPS-PH-91-002PR ..... N91-23847 #
NPS-PH-91-004 ..... N91-23656 #

NPS62-90-009 ..... N91-23379 #
NPS68-90-004 ..... N91-23689 #

NRL-MR-6429 ..... N91-23556 #
NRL-MR-6765 ..... N91-23398 #
NRL-MR-6770 ..... N91-23888 #
NRL-MR-6780 ..... N91-23344 #
NRL-MR-6782 ..... N91-23878 #
NRL-MR-6784 ..... N91-23405 #
NRL-MR-6787 ..... N91-23486 #
NRL-MR-6788 ..... N91-23377 #

NRL-9301 ..... N91-23372 #

NUSC-TR-8807 ..... N91-23764 #

ONERA-NT-1988-5 ..... N91-23441 #
ONERA-NT-1988-8 ..... N91-23319 #
ONERA-NT-1989-1 ..... N91-23363 #

ORNL/FTR-3875 ..... N91-23857 #

ORNL/TM-11648 ..... N91-23381 #
ORNL/TM-11718 ..... N91-23505 #
ORNL/TM-11733 ..... N91-23511 #
ORNL/TM-11747-PT-1 ..... N91-23805 #
ORNL/TM-11756 ..... N91-23914 #
ORNL/TM-11758 ..... N91-23915 #
ORNL/TM-11786 ..... N91-23735 #
ORNL/TM-11812 ..... N91-23864 #

OTA-SET-490 ..... N91-23998 #

PAPER-91-1053 ..... N91-23133* #

PB91-14336 ..... N91-23348 #
PB91-103549 ..... N91-23982 #
PB91-110163 ..... N91-23634 #
PB91-130138 ..... N91-23934 #
PB91-132217 ..... N91-23524 #
PB91-132282 ..... N91-23523 #
PB91-136374 ..... N91-23332 #
PB91-136390 ..... N91-23272 #
PB91-136432 ..... N91-23338 #
PB91-136465 ..... N91-23964 #
PB91-136580 ..... N91-23623 #
PB91-138081 ..... N91-23624 #
PB91-141804 ..... N91-23625 #

PML-1990-64 ..... N91-23204

PNL-SA-18573 ..... N91-23313 #

PSU/ARL-TR-91-002 ..... N91-23446 #

RADC-TR-90-101-VOL-1 ..... N91-23369 #
RADC-TR-90-101-VOL-1 ..... N91-23370 #
RADC-TR-90-101-VOL-3 ..... N91-23371 #
RADC-TR-90-377 ..... N91-23365 #
RADC-TR-90-389 ..... N91-23901 #
RADC-TR-90-401 ..... N91-23485 #

RAL-91-001 ..... N91-23677 #

REPT-90-029 ..... N91-23747
REPT-90-030 ..... N91-23748
REPT-90-039 ..... N91-23749
REPT-90-050 ..... N91-23750
REPT-90-056 ..... N91-23751
REPT-90-060 ..... N91-23752
REPT-90-065 ..... N91-23651
REPT-218-CA/IS/T ..... N91-23219 #
REPT-911-111-101 ..... N91-23187 #
REPT-911-111-102 ..... N91-23188 #
REPT-911-111-103 ..... N91-23192 #
REPT-911-111-104 ..... N91-23853 #
REPT-911-111-105 ..... N91-23216 #
REPT-911-111-106 ..... N91-23091 #
REPT-911-111-107 ..... N91-23248 #
REPT-911-320-101 ..... N91-23139 #
REPT-911-430-101 ..... N91-23757 #
REPT-911-430-102 ..... N91-23217 #
REPT-911-430-103 ..... N91-23249 #
REPT-911-430-104 ..... N91-23250 #
REPT-911-430-105 ..... N91-23251 #
REPT-911-430-106 ..... N91-23252 #
REPT-911-430-107 ..... N91-23253 #
REPT-911-430-108 ..... N91-23197 #
REPT-911-430-109 ..... N91-23254 #
REPT-911-430-111 ..... N91-23926 #
REPT-911-430-112 ..... N91-23255 #
REPT-911-430-113 ..... N91-23927 #
REPT-911-430-114 ..... N91-23256 #
REPT-911-430-115 ..... N91-23257 #
REPT-911-430-117 ..... N91-23258 #
REPT-911-430-118 ..... N91-23947 #
REPT-911-430-119 ..... N91-23259 #
REPT-911-430-120 ..... N91-23948 #
REPT-911-430-121 ..... N91-23208 #
REPT-911-430-122 ..... N91-23928 #
REPT-911-430-125 ..... N91-23929 #
REPT-911-430-126 ..... N91-23758 #
REPT-911-430-127 ..... N91-23260 #
REPT-911-430-128 ..... N91-23261 #
REPT-911-430-129 ..... N91-23209 #
REPT-911-430-130 ..... N91-23262 #
REPT-911-440-101 ..... N91-23615 #
REPT-911-440-102 ..... N91-23218 #
REPT-911-440-103 ..... N91-23219 #
REPT-911-440-104 ..... N91-23468 #
REPT-911-440-105 ..... N91-23220 #
REPT-911-440-106 ..... N91-23221 #
REPT-911-440-107 ..... N91-23222 #
REPT-911-440-108 ..... N91-23223 #
REPT-911-440-109 ..... N91-23224 #
REPT-93928-12/RI-62240X ..... N91-23485 #

RR-822-M ..... N91-23823 #
RR-823-I ..... N91-23726 #
RR-824-I ..... N91-23393 #
RR-825-I ..... N91-23362 #
RR-826-I ..... N91-23778 #
RR-827-M ..... N91-23824 #
RR-828-I-IMAG-116-LIFIA ..... N91-23756 #
RR-830-M ..... N91-23808 #
RR-831-I-IMAG-118-LIFIA ..... N91-23810 #
RR-832-I-IMAG-99-LIFIA ..... N91-23780 #
RR-833-I ..... N91-23779 #
RR-834-I-AND-M ..... N91-23755 #
RR-835-I ..... N91-23989 #
RR-836-I-AND-M ..... N91-23825 #
RR-837-I ..... N91-23822 #
RR-838-M ..... N91-23809 #

RSRE-MEMO-4410 ..... N91-23364 #
RSRE-MEMO-4438 ..... N91-23753 #
RSRE-MEMO-4445 ..... N91-23846 #
RSRE-MEMO-4450 ..... N91-23394 #
RSRE-MEMO-4451 ..... N91-23949 #
RSRE-MEMO-4453 ..... N91-23811 #
RSRE-MEMO-4454 ..... N91-23395 #

RSRE-90023 ..... N91-23845 #

S-623 ..... N91-23210* #

SAF/AQT-SR-90-013 ..... N91-23997 #
SAF/AQT-SR-90-014 ..... N91-23996 #
SAF/AQT-SR-90-016 ..... N91-23995 #

SAND-89-1929 ..... N91-23245 #
SAND-90-0945 ..... N91-23349 #
SAND-90-1018 ..... N91-23314 #
SAND-90-1712C ..... N91-23386 #
SAND-90-1745C ..... N91-23477 #
SAND-90-1850C ..... N91-23431 #
SAND-90-2164C ..... N91-23619 #
SAND-90-2178C ..... N91-23085 #
SAND-90-2231C ..... N91-23507 #
SAND-90-2541C ..... N91-23892 #
SAND-90-2780C ..... N91-23389 #
SAND-90-2883C ..... N91-23885 #
SAND-90-3049C ..... N91-23537 #
SAND-90-3129C ..... N91-23536 #
SAND-90-3182 ..... N91-23526 #
SAND-90-3189C ..... N91-23939 #
SAND-90-3227C ..... N91-23432 #
SAND-91-0043C ..... N91-23919 #
SAND-91-0381C ..... N91-23388 #
SAND-91-0445C ..... N91-23352 #
SAND-91-0499C ..... N91-23294 #
SAND-91-0560C ..... N91-23382 #
SAND-91-0586C ..... N91-23941 #

SER-S/27 ..... N91-23231 #

SER-10/P-REV ..... N91-23910 #
SER-20/P ..... N91-23407 #
SER-701-640 ..... N91-23146 #

SERI/TP-214-4141 ..... N91-23618 #

SR-1 ..... N91-23655 #
SR-3 ..... N91-23635 #

SRI-ECU-8139 ..... N91-23814 #

SRI-MP-90-141R ..... N91-23286 #
SRI-MP-91-005 ..... N91-23336 #

SSC-345-PT-2 ..... N91-23557 #

SSCL-308 ..... N91-23547 #
SSCL-343 ..... N91-23391 #

SSI-TR-183 ..... N91-23448 #

SSL-TR00729 ..... N91-24030* #

TD-90-1717 ..... N91-23359
TD-90-2479 ..... N91-23358
TD-90-2723 ..... N91-23204
TD-90-2771 ..... N91-23360
TD-90-2772 ..... N91-23361
TD-90-3214 ..... N91-23392
TD-90-3407 ..... N91-23703
TD-90-3409 ..... N91-23719

TR-EE-90-53 ..... N91-23821* #
TR-EE-90-54 ..... N91-23806 #
TR-EE-90-64 ..... N91-23786* #

TR-1 ..... N91-23879 #
TR-2 ..... N91-23558 #
TR-3 ..... N91-23285 #
TR-3 ..... N91-23328 #
TR-4 ..... N91-23880 #
TR-5 ..... N91-23959 #
TR-19 ..... N91-23282 #
TR-20 ..... N91-23323 #
TR-37 ..... N91-23279 #
TR-300 ..... N91-23826 #

TRW-P331.LM1.90.185 ..... N91-23408* #

TR90-14 ..... N91-23815 #
TR90-40 ..... N91-23816 #

UCRL-CR-103554 ..... N91-24013 #
UCRL-CR-105944 ..... N91-23465 #
UCRL-CR-106146 ..... N91-23291 #
UCRL-CR-106596 ..... N91-23466 #
UCRL-CR-106704 ..... N91-23333 #

UCRL-ID-106201 ..... N91-23463 #
UCRL-ID-106311 ..... N91-23692 #
UCRL-ID-106591 ..... N91-23858 #
UCRL-ID-106827 ..... N91-23527 #

UCRL-JC-105011 ..... N91-23628 #
UCRL-JC-105106 ..... N91-23860 #
UCRL-JC-105182 ..... N91-23430 #
UCRL-JC-105183 ..... N91-23429 #
UCRL-JC-105271 ..... N91-23426 #
UCRL-JC-105277 ..... N91-23631 #
UCRL-JC-105285 ..... N91-23478 #
UCRL-JC-105286 ..... N91-23479 #
UCRL-JC-105642 ..... N91-24027 #
UCRL-JC-105643 ..... N91-24028 #
UCRL-JC-105865 ..... N91-23986 #
UCRL-JC-106476 ..... N91-23865 #
UCRL-JC-106647 ..... N91-23744 #
UCRL-JC-106798 ..... N91-23632 #

UDR-TR-90-102 ..... N91-23307 #

UILU-ENG-91-2229 ..... N91-23739* #
UILU-ENG-91-2230 ..... N91-23738* #

UMIACS-TR-90-39 ..... N91-23765 #
UMIACS-TR-90-48 ..... N91-23992 #
UMIACS-TR-90-117 ..... N91-23993 #

US-PATENT-APPL-SN-331551 ..... N91-23724* #
US-PATENT-APPL-SN-418320 ..... N91-23095* #
US-PATENT-APPL-SN-591643 ..... N91-23976* #
US-PATENT-APPL-SN-601954 ..... N91-23933* #
US-PATENT-APPL-SN-608494 ..... N91-23410* #
US-PATENT-APPL-SN-615668 ..... N91-23783* #
US-PATENT-APPL-SN-615733 ..... N91-23461* #
US-PATENT-APPL-SN-618790 ..... N91-23662* #
US-PATENT-APPL-SN-633746 ..... N91-23890* #
US-PATENT-APPL-SN-636531 ..... N91-23490* #
US-PATENT-APPL-SN-640775 ..... N91-23462* #
US-PATENT-APPL-SN-645089 ..... N91-23237* #
US-PATENT-APPL-SN-645972 ..... N91-23380* #
US-PATENT-APPL-SN-647902 ..... N91-23180* #
US-PATENT-APPL-SN-648772 ..... N91-23491* #
US-PATENT-APPL-SN-653605 ..... N91-23889* #
US-PATENT-APPL-SN-656925 ..... N91-23492* #
US-PATENT-APPL-SN-660755 ..... N91-23493* #
US-PATENT-APPL-SN-676910 ..... N91-23617* #
US-PATENT-APPL-SN-681288 ..... N91-23472* #
US-PATENT-APPL-SN-685962 ..... N91-23460* #
US-PATENT-APPL-SN-748933 ..... N91-23271* #

USAARL-91-5 ..... N91-23100 #

USAF-STINFO-MANAGEMENT-90/6 ..... N91-23997 #
USAF-STINFO-MANAGEMENT-90/7 ..... N91-23996 #
USAF-STINFO-MANAGEMENT-90/9 ..... N91-23995 #

USAFETAC/PR-91/003 ..... N91-23685 #
USAFETAC/PR-91/004 ..... N91-23661 #
USAFETAC/PR-91/006 ..... N91-23686 #

USAFETAC/TN-91/002-VOL-2 ..... N91-23684 #

USAFSAM-JA-90-68 ..... N91-23459 #

USC-OMDL-2001 ..... N91-23907 #

UTRC/R90-917810-5 ..... N91-23327 #

VKI-TM-46 ..... N91-23196 #

VKI-TN-172 ..... N91-23436 #
VKI-TN-173 ..... N91-23807 #
VKI-TN-174 ..... N91-23437 #

VPI-E-91-07 ..... N91-23242* #

VTT-PUBL-71 ..... N91-23788 #

VTT-RR-708 ..... N91-23551 #

WES/MP/GL-91-3 ..... N91-23199 #

WES/MF/ITL-90-5 ..... N91-23343 #

WES/TR/EL-91-2 ..... N91-23141 #

WHC-SA-0988 ..... N91-23543 #
WHC-SA-1006 ..... N91-23541 #
WHC-SA-1007 ..... N91-23540 #
WHC-SA-1009 ..... N91-23546 #

WHOI-90-46 ..... N91-23471 #
WHOI-90-50 ..... N91-23691 #

WL-TR-91-4008 ..... N91-23307 #

WP-1 ..... N91-23624 #

WRDC-TR-90-3069 ..... N91-23144 #
WRDC-TR-90-3076 ..... N91-23093 #
WRDC-TR-90-4121 ..... N91-23268 #

YALEU/DCS/RR-841 ..... N91-23775 #

Appendix

NASA SCIENTIFIC AND TECHNICAL INFORMATION PROGRAM PRODUCTS AND SERVICES

The NASA Scientific and Technical Information (STI) Program provides for the collection and announcement of aerospace-related reports and literature obtained worldwide through agreements and exchanges. The result of the collection is the comprehensive NASA STI Database that covers aeronautics, space, and supporting disciplines.

The STI Database, documents generated or obtained by NASA, and products and services derived from or supporting the database are made available to the NASA research community and to the public. Descriptions and sources of these items are presented in the following pages.

Scientific and Technical Aerospace Reports (*STAR*) is an abstract journal, listing citations with abstracts for aerospace-related reports obtained from worldwide sources. *STAR* is issued on the 8th and 23rd of each month and announces current documents that have been entered into the NASA STI Database during the previous two weeks. The reports are of the following types:

- NASA, NASA contractor, and NASA grantee reports;
- Reports issued by other U.S. Government agencies, domestic and foreign institutions, universities, and private firms;
- Translations in report form;
- NASA-owned patents and patent applications;
- Other U.S. Government agency and foreign patents and patent applications;
- Domestic and foreign dissertations and theses.

Journal, book, and conference literature, journal translations, and certain foreign dissertations having the same subject scope as *STAR* are announced in a companion journal, *International Aerospace Abstracts* (*IAA*). *IAA* is issued on the 1st and 15th of each month and is available from the American Institute of Aeronautics and Astronautics, Technical Information Service, 555 West 57th Street, 12th Floor, New York, NY 10019.

ELIGIBILITY AND REGISTRATION FOR NASA STI PRODUCTS AND SERVICES

Organizations of the type listed below that have registered with NASA can receive products and services.

- NASA offices and installations, contractors, subcontractors, grantees, and consultants;
- Other U.S. Government agencies and their contractors;
- Libraries in the United States that have arrangements with NASA to maintain collections of NASA documents for public reference;
- Other organizations in the United States having a need for NASA documents in work related to aeronautics and space research;
- Organizations abroad that have established reciprocal documents exchange arrangements with NASA.

Only the central service points or central points of document acquisition and control within qualified organizations are eligible to register for NASA STI products and services. Domestic organizations that may be eligible to receive various classes of NASA publications and services should address their requests for registration or further information to:

NASA Center for AeroSpace Information
ATTN: Registration Services
P.O. Box 8757
BWI Airport, MD 21240
301-621-0153

Organizations abroad should direct requests to:

National Aeronautics and Space Administration
Director, Scientific and Technical Information Program
Code NTT
Washington, DC 20546
USA
703-271-5640

SUBJECT SCOPE

The subject scope of *STAR* and *IAA* includes all aspects of aeronautics and space research and development, supporting basic and applied research, and applications. Aerospace aspects of Earth resources, energy development, conservation, oceanography, environmental protection, urban transportation, and other topics of high national priority are also covered.

HOW TO USE *STAR* SUBJECT CATEGORIES

Abstracts in *STAR* are categorized by 10 major subject divisions that are divided further into 76 specific subject categories. The subject divisions and categories are listed in the Table of Contents together with a note for each that defines its scope and provides any cross-references. For example:

16 SPACE TRANSPORTATION
Includes passenger and cargo space transportation, e.g., shuttle operations; and space rescue techniques. For related information see also *03 Air Transportation and Safety* and *18 Spacecraft Design, Testing and Performance.* For space suits see *54 Man/System Technology and Life Support.*

CROSS-REFERENCES

Individual *STAR* abstracts are not ordinarily cross-referenced, except for certain conference reports or book translations that have had separate abstracts written for their component papers or chapters. Citations and abstracts of the components follow immediately after those of the parent document. When the subject content of a component differs sufficiently from the general content of the parent, a cross-reference citation also is printed at the end of the category to which it normally would have been assigned if it were independent.

DOCUMENTS ON MICROFICHE

Documents available on microfiche are designated by a pound sign (#) following the accession number.

LIMITED REPRODUCIBILITY

A note of limited reproducibility appears in the citation, if there are factors affecting the reproducibility of more than 20% of the document. These factors include faint or broken type, color photographs, black and white photographs, foldouts, dot matrix print, or some other factor that limits the reproducibility of the document. This notation also appears on the microfiche header with the specific factor checked off on a list visible in the second frame.

COLOR COPIES

An increasing number of NASA scientific and technical reports are being produced with color graphs, charts, illustrations, and photographs. An indication that a document has color pages follows the source and pricing (SAP) information in the *STAR* citation.

Registered users of the NASA Scientific and Technical Information Program will receive ordered documents with color at no additional cost, as long as stock copies of the document are available. Otherwise, an additional fee of $2.00 per color page will be charged. The NASA Center for AeroSpace Information staff will contact registered users to determine individual user's needs.

NASA PATENTS AND PATENT APPLICATIONS

Patents and patent applications owned by NASA are announced in *STAR* under appropriate subject categories and are referenced in the *STAR* indexes. In the Report/Accession Number Index, patents are indexed by the NASA Case Number, and the U.S. Patent Class. Patent applications are indexed by the NASA Case Number and the U.S. Patent Application Serial Number.

Printed copies of patents (which are not microfiched) are available for purchase from the U.S. Patent and Trademark Office.

NASA patent application specifications are sold in both paper copy and microfiche by the National Technical Information Service (NTIS). The US-Patent-Appl-SN-number should be used in ordering either paper copy or microfiche from NTIS.

When ordering patents, the U.S. Patent Number should be used, and payment must be remitted in advance, by money order or check payable to the Commissioner of Patents and Trademarks. Prepaid purchase coupons for ordering are also available from the U.S. Patent and Trademark Office.

The patents and patent applications announced in *STAR* are owned by NASA and are available for royalty-free licensing. Requests for licensing terms and further information should be addressed to:

National Aeronautics and Space Administration
Associate General Counsel for Intellectual Property
Code GP
Washington, DC 20546

SOURCES FOR DOCUMENTS

One or more sources from which a document announced in *STAR* is available to the public is given in each citation. The most commonly indicated sources and their acronyms or abbreviations are listed on page A-6. If the publication is available from a source other than those listed, the publisher and address will be displayed on the availability line or in combination with the corporate source line.

Avail: NTIS. Sold by the National Technical Information Service. Prices for hard copy (HC) and microfiche (MF) are indicated by a price code following the letters HC or MF in the *STAR* citation. Current values for the price codes are given in the tables on page A-7.

Initially distributed microfiche under the NTIS SRIM (Selected Research in Microfiche) is available at greatly reduced unit prices. For this service and for information concerning subscription to NASA printed reports, consult the NTIS Subscription Section, Springfield, VA 22161.

NOTE ON ORDERING DOCUMENTS: When ordering NASA publications (those followed by the * symbol), use the N accession number. NASA patent applications (only the specifications are offered) should be ordered by the US-Patent-Appl-SN number. Non-NASA publications (no asterisk) should be ordered by the AD, PB, or other *report number* shown on the last line of the citation, not by the N accession number. It is also advisable to cite the title and other bibliographic identification.

Avail: SOD (or GPO). Sold by the Superintendent of Documents, U.S. Government Printing Office, in hard copy. The current price and order number are given following the availability line. (NTIS will fill microfiche requests, as indicated above, for those documents identified by a # symbol.)

Avail: BLL (formerly NLL): British Library Lending Division, Boston Spa, Wetherby, Yorkshire, England. Photocopies available from this organization at the price shown. (If none is given, address inquiry to the BLL.)

Avail: DOE Depository Libraries. Organizations in U.S. cities and abroad that maintain collections of Department of Energy reports, usually in microfiche form, are listed in *Energy Research Abstracts.* Services available from the DOE and its depositories are described in a booklet, *DOE Technical Information Center - Its Functions and Services* (TID-4660), which may be obtained without charge from the DOE Technical Information Center.

Avail: ESDU. Pricing information on specific data, computer programs, and details on Engineering Sciences Data Unit (ESDU) topic categories can be obtained from ESDU International Ltd. Requesters in North America should use the Virginia address while all other requesters should use the London address, both of which are on page A-6.

Avail: Fachinformationszentrum, Karlsruhe. Sold by the Fachinformationszentrum Energie, Physik, Mathematik GMBH, Eggenstein Leopoldshafen, Federal Republic of Germany, at the price shown in deutschmarks (DM).

Avail: HMSO. Publications of Her Majesty's Stationery Office are sold in the U.S. by Pendragon House, Inc. (PHI), Redwood City, CA. The U.S. price (including a service and mailing charge) is given, or a conversion table may be obtained from PHI.

Avail: NASA Public Document Rooms. Documents so indicated may be examined at or purchased from the National Aeronautics and Space Administration, Public Documents Room (Room 126), 600 Independence Ave., S.W., Washington, DC 20546, or public document rooms located at NASA installations, and the NASA Pasadena Office at the Jet Propulsion Laboratory.

Avail: Univ. Microfilms. Documents so indicated are dissertations selected from *Dissertation Abstracts* and are sold by University Microfilms as xerographic copy (HC) and microfilm. All requests should cite the author and the Order Number as they appear in the citation.

Avail: US Patent and Trademark Office. Sold by Commissioner of Patents and Trademarks, U.S. Patent and Trademark Office, at the standard price of $1.50 each, postage free. (See discussion of NASA patents and patent applications below.)

Avail: (US Sales Only). These foreign documents are available to users within the United States from the National Technical Information Service (NTIS). They are available to users outside the United States through the International Nuclear Information Service (INIS) representative in their country, or by applying directly to the issuing organization.

Avail: USGS. Originals of many reports from the U.S. Geological Survey, which may contain color illustrations, or otherwise may not have the quality of illustrations preserved in the microfiche or facsimile reproduction, may be examined by the public at the libraries of the USGS field offices whose addresses are listed on page A-6. The libraries may be queried concerning the availability of specific documents and the possible utilization of local copying services, such as color reproduction.

Avail: Issuing Activity, or Corporate Author, or no indication of availability. Inquiries as to the availability of these documents should be addressed to the organization shown in the citation as the corporate author of the document.

FEDERAL DEPOSITORY LIBRARIES: To provide the general public with greater access to U.S. Government publications, Congress established the Federal Depository Library Program under the Government Printing Office (GPO), with 52 regional depositories responsible for permanent retention of material, inter-library loan, and reference services. (These libraries are not sales outlets.) At least one copy of nearly every NASA and NASA-sponsored publication, either in printed or microfiche format, is received and retained by the 52 regional depositories. A list of the regional GPO libraries, appears on page A-8. A local library can contact a regional depository library to help locate specific reports, or direct contact may be made by an individual.

PUBLIC COLLECTION OF NASA DOCUMENTS

An extensive collection of NASA and NASA-sponsored publications is maintianed by the British Library Lending Divison, Boston Spa, Wetherby, Yorkshire, England, for public access. The British Library Lending Division also has available many of the non-NASA publications cited in *STAR*.

European requesters may purchase facsimile copy or microfiche of NASA and NASA-sponsored documents, those identified by both the symbols # and * from ESA—Information Retrieval Service, European Space Agency, 8-10 rue Mario-Nikis, 75738 Paris CEDEX 15, France.

SUBMITTING DOCUMENTS

All users of this abstract service are urged to forward reports to be considered for announcement in *STAR*. This will aid NASA in its efforts to provide the fullest possible coverage of all scientific and technical publications that might support aeronautics and space research and development. If you have prepared relevant reports (other than those you will transmit to NASA, DOD, or DOE through the usual contract- or grant-reporting channels), please send them for consideration to the NASA Center for AeroSpace Information, P.O. Box 8757, BWI Airport, MD 21240.

Reprints of journal articles, book chapters, and conference papers are also welcome. These will be considered for announcement in *STAR*'s companion journal, *IAA*.

You may specify a particular source to be included in a report announcement if you wish; otherwise the report will be placed on a public sale at the National Technical Information Service. Copyrighted publications will be announced but not distributed or sold.

PURCHASE OF *STAR*

STAR is publicly available on annual subscription from the Superintendent of Documents, U.S. Government Printing Office, Washington, DC 20402.

STAR is available to registered users on annual subscription from the NASA Center for AeroSpace Information, ATTN: Registration Services, P.O. Box 8757, BWI Airport, MD 21240.

Microfiche of the abstract sections of *STAR* are available, on annual subscription only, from NTIS as PB91-911300, Attn: Subscriptions, 5285 Port Royal Road, Springfield, VA 22161. Annual subscription rates are $85.00 North America; $170.00 foreign. Abstract sections for previous years retroactive to 1964 are available at the current rates.

ADDRESSES OF ORGANIZATIONS

American Institute of Aeronautics and Astronautics
Technical Information Service
555 West 57th Street, 12th Floor
New York, New York 10019

British Library Lending Division,
Boston Spa, Wetherby, Yorkshire,
England

Commissioner of Patents and Trademarks
U.S. Patent and Trademark Office
Washington, DC 20231

Department of Energy
Technical Information Center
P.O. Box 62
Oak Ridge, Tennessee 37830

European Space Agency-Information Retrieval Service
ESRIN
Via Galileo Galilei
00044 Frascati (Rome) Italy

Engineering Sciences Data Unit International
P.O. Box 1633
Manassas, Virginia 22110

Engineering Sciences Data Unit International, Ltd.
251-259 Regent Street
London, W1R 7AD, England

Fachinformationszentrum Energie, Physik, Mathematik
GMBH
7514 Eggenstein Leopoldshafen
Federal Republic of Germany

Her Majesty's Stationery Office
P.O. Box 569, S.E. 1
London, England

NASA Center for AeroSpace Information
P.O. Box 8757
BWI Airport, Maryland 21240

National Aeronautics and Space Administration
Scientific and Technical Information Program (NTT)
Washington, DC 20546

National Technical Information Service
5285 Port Royal Road
Springfield, Virginia 22161

Pendragon House, Inc.
899 Broadway Avenue
Redwood City, California 94063

Superintendent of Documents
U.S. Government Printing Office
Washington, DC 20402

University Microfilms
A Xerox Company
300 North Zeeb Road
Ann Arbor, Michigan 48106

University Microfilms, Ltd
Tylers Green
London, England

U.S. Geological Survey Library National Center
MS 950
12201 Sunrise Valley Drive
Reston, Virginia 22092

U.S. Geological Survey Library
2255 North Gemini Drive
Flagstaff, Arizona 86001

U.S. Geological Survey
345 Middlefield Road
Menlo Park, California 94025

U.S. Geological Survey Library
Box 25046
Denver Federal Center, MS914
Denver, Colorado 80225

NTIS PRICE SCHEDULES

(Effective January 1, 1991)

Schedule A
STANDARD PRICE DOCUMENTS AND MICROFICHE**

PRICE CODE	NORTH AMERICAN PRICE	FOREIGN PRICE
A01	$ 8.00	$ 16.00
A02	11.00	22.00
A03	15.00	30.00
A04-A05	17.00	34.00
A06-A09	23.00	46.00
A10-A13	31.00	62.00
A14-A17	39.00	78.00
A18-A21	45.00	90.00
A22-A25	53.00	106.00
A99	*	*
N01	60.00	120.00
N02	59.00	118.00
N03	20.00	40.00

Schedule E
EXCEPTION PRICE DOCUMENTS AND MICROFICHE**

PRICE CODE	NORTH AMERICAN PRICE	FOREIGN PRICE
E01	$10.00	$ 20.00
E02	12.00	24.00
E03	14.00	28.00
E04	16.50	33.00
E05	18.50	37.00
E06	21.50	43.00
E07	24.00	48.00
E08	27.00	54.00
E09	29.50	59.00
E10	32.50	65.00
E11	35.00	70.00
E12	38.50	77.00
E13	41.00	82.00
E14	45.00	90.00
E15	48.50	97.00
E16	53.00	106.00
E17	57.50	115.00
E18	62.00	124.00
E19	69.00	138.00
E20	80.00	160.00
E99	*	*

* Contact NTIS for price quote.

** Effective January 1, 1991, the microfiche copy of any new document entering the NTIS collection will be priced the same as the paper copy of the document.

IMPORTANT NOTICE

NTIS Shipping and Handling Charges

U.S., Canada, Mexico — ADD $3.00 per TOTAL ORDER

All Other Countries — ADD $4.00 per TOTAL ORDER

Exceptions — Does NOT apply to:

ORDERS REQUESTING NTIS RUSH HANDLING

ORDERS FOR SUBSCRIPTION OR STANDING ORDER PRODUCTS *ONLY*

NOTE: Each additional delivery address on an order requires a separate shipping and handling charge.

FEDERAL REGIONAL DEPOSITORY LIBRARIES

ALABAMA

AUBURN UNIV. AT MONTGOMERY LIBRARY
Documents Dept.
7300 University Drive
Montgomery, AL 36117-3596
(205) 244-3650 FAX: (205) 244-0678

UNIV. OF ALABAMA
Amelia Gayle Gorgas Library
Govt. Documents
Box 870266
Tuscaloosa, AL 35487-0266
(205) 348-6046 FAX: (205) 348-8833

ARIZONA

DEPT. OF LIBRARY, ARCHIVES, AND PUBLIC RECORDS
Federal Documents
Third Floor State Capitol
1700 West Washington
Phoenix, AZ 85007
(602) 542-4121 FAX: (602) 542-4400; 542-4500

ARKANSAS

ARKANSAS STATE LIBRARY
State Library Services
One Capitol Mall
Little Rock, AR 72201
(501) 682-2869

CALIFORNIA

CALIFORNIA STATE LIBRARY
Govt. Publications Section
914 Capitol Mall - P.O. Box 942837
Sacramento, CA 94237-0001
(916) 322-4572 FAX: (916) 324-8120

COLORADO

UNIV. OF COLORADO - BOULDER
Norlin Library
Govt. Publications
Campus Box 184
Boulder, CO 80309-0184
(303) 492-8834 FAX: (303) 492-2185

DENVER PUBLIC LIBRARY
Govt. Publications Dept. BS/GPD
1357 Broadway
Denver, CO 80203
(303) 571-2135

CONNECTICUT

CONNECTICUT STATE LIBRARY
231 Capitol Avenue
Hartford, CT 06106
(203) 566-4971 FAX: (203) 566-3322

FLORIDA

UNIV. OF FLORIDA LIBRARIES
Documents Dept.
Library West
Gainesville, FL 32611-2048
(904) 392-0366 FAX: (904) 392-7251

GEORGIA

UNIV. OF GEORGIA LIBRARIES
Govt. Documents Dept.
Jackson Street
Athens, GA 30602
(404) 542-8949 FAX: (404) 542-6522

HAWAII

UNIV. OF HAWAII
Hamilton Library
Govt. Documents Collection
2550 The Mall
Honolulu, HI 96822
(808) 948-8230 FAX: (808) 956-5968

IDAHO

UNIV. OF IDAHO LIBRARY
Documents Section
Moscow, ID 83843
(208) 885-6344 FAX: (208) 885-6817

ILLINOIS

ILLINOIS STATE LIBRARY
Reference Dept.
300 South Second
Springfield, IL 62701-1796
(217) 782-7596 FAX: (217) 524-0041

INDIANA

INDIANA STATE LIBRARY
Serials/Documents Section
140 North Senate Avenue
Indianapolis, IN 46204
(317) 232-3678 FAX: (317) 232-3728

IOWA

UNIV. OF IOWA LIBRARIES
Govt. Publications Dept.
Washington & Madison Streets
Iowa City, IA 52242
(319) 335-5926 FAX: (319) 335-5830

KANSAS

UNIV. OF KANSAS
Govt. Documents & Map Library
6001 Malatt Hall
Lawrence, KS 66045-2800
(913) 864-4660 FAX: (913) 864-5380

KENTUCKY

UNIV. OF KENTUCKY LIBRARIES
Govt. Publications/Maps Dept.
Lexington, KY 40506-0039
(606) 257-3139 FAX: (606) 257-1563; 257-8379

LOUISIANA

LOUISIANA STATE UNIV.
Middleton Library
Govt. Documents Dept.
Baton Rouge, LA 70803
(504) 388-2570 FAX: (504) 388-6992

LOUISIANA TECHNICAL UNIV.
Prescott Memorial Library
Govt. Documents Dept.
305 Wisteria Street
Ruston, LA 71270-9985
(318) 257-4962 FAX: (318) 257-2447

MAINE

TRI-STATE DOCUMENTS DEPOSITORY
Raymond H. Fogler Library
Govt. Documents & Microforms Dept.
Univ. of Maine
Orono, ME 04469
(207) 581-1680

MARYLAND

UNIV. OF MARYLAND
Hornbake Library
Govt. Documents/Maps Unit
College Park, MD 20742
(301) 454-3034 FAX: (301) 454-4985

MASSACHUSETTS

BOSTON PUBLIC LIBRARY
Govt. Documents Dept.
666 Boylston Street
Boston, MA 02117
(617) 536-5400 ext. 226
FAX: (617) 267-8273; 267-8248

MICHIGAN

DETROIT PUBLIC LIBRARY
5201 Woodward Avenue
Detroit, MI 48202-4093
(313) 833-1440; 833-1409
FAX: (313) 833-5039

LIBRARY OF MICHIGAN
Govt. Documents Unit
P.O. Box 30007
Lansing, MI 48909
(517) 373-0640 FAX: (517) 373-3381

MINNESOTA

UNIV. OF MINNESOTA
Wilson Library
Govt. Publications Library
309 19th Avenue South
Minneapolis, MN 55455
(612) 624-5073 FAX: (612) 626-9353

MISSISSIPPI

UNIV. OF MISSISSIPPI
J.D. Williams Library
Federal Documents Dept.
106 Old Gym Bldg.
University, MS 38677
(601) 232-5857 FAX: (601) 232-5453

MISSOURI

UNIV. OF MISSOURI - COLUMBIA
Ellis Library
Govt. Documents
Columbia, MO 65201
(314) 882-6733 FAX: (314) 882-8044

MONTANA

UNIV. OF MONTANA
Maureen & Mike Mansfield Library
Documents Div.
Missoula, MT 59812-1195
(406) 243-6700 FAX: (406) 243-2060

NEBRASKA

UNIV. OF NEBRASKA - LINCOLN
D.L. Love Memorial Library
Documents Dept.
Lincoln, NE 68588
(402) 472-2562

NEVADA

UNIV. OF NEVADA
Reno Library
Govt. Publications Dept.
Reno, NV 89557
(702) 784-6579 FAX: (702) 784-1751

NEW JERSEY

NEWARK PUBLIC LIBRARY
U.S. Documents Div.
5 Washington Street - P.O. Box 630
Newark, NJ 07101-0630
(201) 733-7812 FAX: (201) 733-5648

NEW MEXICO

UNIV. OF NEW MEXICO
General Library
Govt. Publications Dept.
Albuquerque, NM 87131-1466
(505) 277-5441 FAX: (505) 277-6019

NEW MEXICO STATE LIBRARY
325 Don Gaspar Avenue
Santa Fe, NM 87503
(505) 827-3826 FAX: (505) 827-3820

NEW YORK

NEW YORK STATE LIBRARY
Documents/Gift & Exchange Section
Federal Depository Program
Cultural Education Center
Albany, NY 12230
(518) 474-5563 FAX: (518) 474-5786

NORTH CAROLINA

UNIV. OF NORTH CAROLINA - CHAPEL HILL
CB#3912, Davis Library
BA/SS Dept.—Documents
Chapel Hill, NC 27599
(919) 962-1151 FAX: (919) 962-0484

NORTH DAKOTA

NORTH DAKOTA STATE UNIV. LIBRARY
Documents Office
Fargo, ND 58105
(701) 237-8886 FAX: (701) 237-7138
In cooperation with Univ. of North Dakota, Chester Fritz Library
Grand Forks

OHIO

STATE LIBRARY OF OHIO
Documents Dept.
65 South Front Street
Columbus, OH 43266
(614) 644-7051 FAX: (614) 752-9178

OKLAHOMA

OKLAHOMA DEPT. OF LIBRARIES
U.S. Govt. Information Div.
200 NE 18th Street
Oklahoma City, OK 73105-3298
(405) 521-2502, ext. 252, 253
FAX: (405) 525-7804

OKLAHOMA STATE UNIV.
Edmon Low Library
Documents Dept.
Stillwater, OK 74078
(405) 744-6546 FAX: (405) 744-5183

OREGON

PORTLAND STATE UNIV.
Millar Library
934 SW Harrison - P.O. Box 1151
Portland, OR 97207
(503) 725-3673 FAX: (503) 725-4527

PENNSYLVANIA

STATE LIBRARY OF PENN.
Govt. Publications Section
Walnut St. & Commonwealth Ave. - P.O. Box 1601
Harrisburg, PA 17105
(717) 787-3752

SOUTH CAROLINA

CLEMSON UNIV.
Cooper Library
Public Documents Unit
Clemson, SC 29634-3001
(803) 656-5174 FAX: (803) 656-3025
In cooperation with Univ. of South Carolina, Thomas Cooper Library, Columbia

TENNESSEE

MEMPHIS STATE UNIV. LIBRARIES
Govt. Documents
Memphis, TN 38152
(901) 678-2586 FAX: (901) 678-2511

TEXAS

TEXAS STATE LIBRARY
United States Documents
P.O. Box 12927 - 1201 Brazos
Austin, TX 78711
(512) 463-5455 FAX: (512) 463-5436

TEXAS TECH. UNIV. LIBRARY
Documents Dept.
Lubbock, TX 79409
(806) 742-2268 FAX: (806) 742-1920

UTAH

UTAH STATE UNIV.
Merrill Library & Learning Resources Center, UMC-3000
Documents Dept.
Logan, UT 84322-3000
(801) 750-2684 FAX: (801) 750-2677

VIRGINIA

UNIV. OF VIRGINIA
Alderman Library
Govt. Documents
Charlottesville, VA 22903-2498
(804) 924-3133 FAX: (804) 924-4337

WASHINGTON

WASHINGTON STATE LIBRARY
Document Section
MS AJ-11
Olympia, WA 98504-0111
(206) 753-4027 FAX: (206) 753-3546

WEST VIRGINIA

WEST VIRGINIA UNIV. LIBRARY
Govt. Documents Section
P.O. Box 6069
Morgantown, WV 26506
(304) 293-3640

WISCONSIN

ST. HIST. SOC. OF WISCONSIN LIBRARY
Govt. Publications Section
816 State Street
Madison, WI 53706
(608) 262-2781 FAX: (608) 262-4711
In cooperation with Univ. of Wisconsin-Madison, Memorial Library

MILWAUKEE PUBLIC LIBRARY
Documents Div.
814 West Wisconsin Avenue
Milwaukee, WI 53233
(414) 278-2167 FAX: (414) 278-2137

WYOMING

WYOMING STATE LIBRARY
Supreme Court & Library Bldg.
Govt. Publications
Cheyenne, WY 82002
(307) 777-5920 FAX: (307) 777-6289

National Aeronautics and
Space Administration
Code NTT
Washington, D.C.
20546
Official Business
Penalty for Private Use, $300

SPECIAL FOURTH-CLASS RATE
POSTAGE & FEES PAID
NASA
PERMIT No. G27

POSTMASTER: If Undeliverable (Section 158
Postal Manual) Do Not Return